Biologically-Inspired Systems

Ephraim Cohen
Hans Merzendorfer
Editors

Extracellular Sugar-Based Biopolymers Matrices

Springer

Biologically-Inspired Systems

Volume 12

Series editor
Stanislav N. Gorb, Department of Functional Morphology and Biomechanics, Zoological Institute, Kiel University, Kiel, Germany

Motto: Structure and function of biological systems as inspiration for technical developments

Throughout evolution, nature has constantly been called upon to act as an engineer in solving technical problems. Organisms have evolved an immense variety of shapes and structures from macro down to the nanoscale. Zoologists and botanists have collected a huge amount of information about the structure and functions of biological materials and systems. This information can be also utilized to mimic biological solutions in further technical developments. The most important feature of the evolution of biological systems is multiple origins of similar solutions in different lineages of living organisms. These examples should be the best candidates for biomimetics. This book series will deal with topics related to structure and function in biological systems and show how knowledge from biology can be used for technical developments in engineering and materials science. It is intended to accelerate interdisciplinary research on biological functional systems and to promote technical developments. Documenting of the advances in the field will be important for fellow scientists, students, public officials, and for the public in general. Each of the books in this series is expected to provide a comprehensive, authoritative synthesis of the topic.

More information about this series at http://www.springer.com/series/8430

Ephraim Cohen • Hans Merzendorfer
Editors

Extracellular Sugar-Based Biopolymers Matrices

Springer

Editors
Ephraim Cohen
Department of Entomology,
The Robert H. Smith Faculty
of Agriculture Food and Environment
The Hebrew University of Jerusalem
Rehovot, Israel

Hans Merzendorfer
School of Science and Technology,
Institute of Biology – Molecular Biology
University of Siegen
Siegen, Germany

ISSN 2211-0593 ISSN 2211-0607 (electronic)
Biologically-Inspired Systems
ISBN 978-3-030-12918-7 ISBN 978-3-030-12919-4 (eBook)
https://doi.org/10.1007/978-3-030-12919-4

This book is dedicated to the memory of Professor John E. Casida (Berkeley, California), Outstanding Scientist, Superb Mentor and a Good Man

Preface

This book comprehensively covers multifaceted aspects of various sugar-based polysaccharides found in extracellular matrices (ECMs) as well as on cell surfaces or deposited into intercellular spaces. Biochemical and biophysical events such as polymer synthesis, excretion, deposition, final assembly, and transformations as well as genetic regulations are thoroughly addressed and discussed. The biological significance of exopolysaccharides is tightly associated *inter alia* with intercellular communication, cell proliferation, adhesion and motility, maintaining cell morphology, protecting from damage, facilitating tissue growth, and modulating the immune system. Chapters in the book cover taxa from prokaryotic bacteria, to eukaryotic organisms such as algae, plants, fungi, invertebrates, and vertebrates.

A variety of polysaccharides with different characteristics serve a plethora of biological and functional assignments. The individual book chapters focus on and exhaustively deal with amino sugars like chitin/chitosan and hyaluronan; glucose-based cellulose/hemicellulose and glucans; sulfated glycosaminoglycans (chondroitin, dermatan, heparin, keratin), peptidoglycans, pectic polysaccharides, and alginate. In addition to structural, biochemical, and functional aspects related to these exopolysaccharides, also various applicative facets in agriculture, environmental and food industry, biotechnology, and medicine are fastidiously discussed.

The first three chapters of the book are dedicated to chitin and its deacetylated (polycationic) form, chitosan. In arthropods (emphasis on insects), the highly organized chito-protein complex is the major component of the cuticular and peritrophic matrices (Chap. 1). Chitin is also present in other invertebrates such as nematodes and mollusks, and is found in fungi as an integral part of cell walls in association with other polysaccharide components. The mineralized shell of mollusks is a result of an intriguing biomineralization process, in which chitin as scaffold is complexed with a mineral component (e.g. calcium carbonate). Chapter 2 emphasizes the enzymatic mechanisms in mollusks that are implicated in forming the mineral-chitin composites and the involvement of myosin domain that contains chitin synthases. Chapter 3 focuses on chitosan as a unique polymer that is easily amenable to a plethora of chemical and graft co-polymerization modifications. Such

derivatives bestow various functionalities associated with physicochemical and biological properties for desired and tailored applications.

Several glycosaminoglycans are ubiquitous in vertebrate tissues (Chaps. 4 and 5). Like chitin, hyaluronan is a simple, non-sulfated, linear unbranched polymer but is composed of two alternating amino sugar blocks (N-acetylglucosamine and glucuronic acid). It is an anionic polymer with hydrophilic and viscoelastic properties that is synthesized on plasma membrane and extruded immediately into the cellular matrix without any protein linkage. Hyaluronan has a key role in wound healing, cell migration, and cell proliferation. Certain physiopathological disorders such as cancer, vascular diseases, or diabetes are associated with the polymer. It has become a useful tool in regenerative medicine, in drug delivery systems, and particularly in cosmetics. A family of sulfated glycosaminoglycans (like heparan, chondroitin, dermatan, and keratin) is found in extracellular matrices of vertebrate tissues. Chapter 5 addresses and discusses the biosynthesis, chemical structures, their characterization and extraction, as well as many crucial physiological and pathophysiological roles played by these four main polysaccharides. Chapter 6 focuses on peptidoglycans (PGN), which are unique, ubiquitous, and key structural component of bacterial cell walls. It comprehensively addresses the intricate chemical structure of the heteropolymer made of glycans cross-linked by short peptides, as well as its biosynthesis pathway, deposition, and turnover. Bacterial peptidoglycans serve as a rigid cell envelope that protects bacteria from osmotic and environmental challenges. However, during recycling and phases of enlargement, division, and differentiation, this bacterial sachet becomes flexible in order to accommodate such dynamic processes. Thus, the biosynthesis of PGN and its turnover have been major targets for antibacterial therapeutics.

Chapters 7, 8, 9, 10 and 11 are devoted to glucose-based exopolysaccharides (glucans) like cellulose/hemicellulose in plants, cellulose in bacteria, and various β-glucans in fungi. Cellulose and hemicellulose are major constituents of plant cell walls. Cellulose, a homopolysaccharide which consists of repeating β-1,4-linked cellobiose units is the most abundant, easily available, and renewable biopolymer on earth. Unlike cellulose that is synthesized at the plasma membrane, hemicelluloses are formed by Golgi membranes and are structurally diverse polymers that function as adhesive layers between cellulose microfibrils. Chapter 7 highlights studies aimed at understanding the mechanism of synthesis and regulation of cellulose and hemicelluloses in plants. A third major cluster of polysaccharides in plants is pectin. Chapter 12 describes the heteropolysaccaride structures of pectins, their intricate biosynthesis, which like hemicellulose is located in the Golgi, as well as their physiological functions and applications in food, bioenergy industry, and medicine.

Cellulose is also produced by bacteria, and it is hypothesized that cellulose synthase genes in plants originated in prokaryotes. Bacterial cellulose, which has been amply studied in *Komagataeibacter xylinus*, is non-modified, fine-structured nanocellulose. Its biomedical and industrial applications are summarized in Chap. 17. Recently it was found that *E. coli* and other bacteria are able to chemically modify cellulose post-synthetically by adding a phospholipid group. Chapter 8 adds a fascinating aspect to cellulose-producing bacteria – formation of biofilms. Biofilms

are tissue-like cell aggregates embedded in extracellular matrix and affixed to abiotic or biotic surfaces. *E. coli* biofilms have been shown to be shaped by modified cellulose or by a combination of this polysaccharide with curly amyloid fibers.

Other exopolysaccharides that participate in forming the structural architecture of bacterial biofilms are alginates (Chap. 13). Alginate-based bacterial biofilms can be found in various habitats like soil (plant rhizospheres) as well as in *Pseudomonas* and *Azotobacter* species which are important human pathogens. Cells in these communal aggregates are surrounded by alginate that protects and facilitates their survival under adverse environmental stresses including water scarcity, presence of antibiotics, or attack by the immune system.

Chapters 9, 10 and 11 deal with the role of β-glucans in fungal cell walls. The glucans are essential in maintaining the cell morphology and in modulating the immune system of the important human pathogenic fungus, *Candida albicans* (Chap. 9). Botryosphaeran and lasiodiplodan are two unique exocellular fungal β-glucans that represent the main theme of Chaps. 10 and 11. The in-depth studies conducted with the extracellular polymers and their chemical derivatives have opened vistas for various biological, biomedical, pharmaceutical, and industrial applications.

The last chapters of the book (Chaps. 14, 15, 16 and 17) present compelling studies on an array of possible and concrete applications of polysaccharides (cellulose, chitosan, glycosaminoglycans, and alginate), their chemical derivatives, hybrid composites and other adjuncts. The wide range of applications embrace areas of vast importance including agriculture, food, environment as well as pharmaceutical, biomedical, paper, textile, and cosmetics industries. Exopolysaccharide-based materials have gained great appeal as renewable resource for these applications due to their high abundance, low cost, efficient production, easy extractability, biocompatibility, biodergadibility, bioresorbability, chelating ability, low toxicity and low allergenic potentials, antimicrobial and antioxidant activities, as well as varied and advantageous physicochemical properties. Obtaining myriad functionalization designs has enabled the construction of numerous biomaterial molds such as hydrogels, aerogels, films, membranes, beads and fibers of various sizes, sponges, scaffolds suitable for regenerative medicine, bioengineering, and designs of biosensors.

The extracellular-based biomaterials have been tested for a variety of applications: removal of pollutants (toxic metals, industrial dyes) and micropollutants (pharmaceuticals and endocrine disruptors) from water and industrial wastewater; as bioink for 3D-bioprinting; as drug excipients, drug carrier systems for controlled and targeted delivery; as vaccine immunotherapy and vectors for gene therapy. One of the most promising applications resides in designs of biomaterials for the medical realm. Such applications include dressings for efficient wound healing and the harnessing of proper and tailored physicochemical properties to fabricate scaffolds for tissue engineering (repair of bone, cartilage, and tooth, as well as vascular and neuronal regeneration).

Gratitude is expressed to authors and coauthors who invested precious time and energy in contributing impactful state-of-the-art chapters. In this respect, the

reviewers listed below are immensely appreciated for carefully reading massive manuscripts and for providing beneficial comments, corrections and suggestions. Their seminal inputs have a remarkable impact in providing “added value” to the refereed chapters.

Marco Guerrini**,** Istituto di Ricerche Chimiche e Biochimiche G-Ronzoni, Italy; Nicholas C. Carpita**,** Purdue University, USA; Jùlio César dos Santos, University of São Paulo, Brazil; Jun-Ichi Tamura, Tottori University, Japan; Kevin J. Edgar, Virginia Tech, USA; Henrik V. Scheller, UC Berkeley, USA; Crispin Humberto Garcia Cruz, Universidade Estadual Paulista, Brazil; Mulloy Barbara, Imperial College, UK; Arianne de Agustini, Hôpitaux Universitaires de Genève, Switzerland; Suzuki Michio, University of Tokyo, Japan; Subbaratnam Muthukrishnan, Kansas State University, USA; Jochen Zimmer**,** University of Virginia, USA; Tiffany Abitbol, Research Institutes of Sweden (RISE), Sweden; Mariana Stelling, University of Rio de Janeiro, Brazil; Iñigo Lasa, Universidad Pùblica de Navara, Spain.

Rehovot, Israel Ephraim Cohen

Contents

Contributors

Rebeca Alonso-Monge Departamento de Microbiología y Parasitología, Universidad Complutense de Madrid, Madrid, Spain

Charles T. Anderson Department of Biology, Center for Lignocellulose Structure and Formation, The Pennsylvania State University, State College, PA, USA

Aneli M. Barbosa-Dekker Departamento de Química, Universidade Estadual de Londrina, Londrina, Paraná, Brazil

Patrícia Sofia Pinhanços Batista Universidade Católica Portuguesa, Porto, Portugal

Emiliano Bedini Dipartimento di Scienze Chimiche, Università degli Studi di Napoli Federico II, Napoli, Italy

Gabrielle C. Calegari Departamento de Química, Universidade Tecnológica Federal do Paraná, Pato Branco, Paraná, Brazil

Ephraim Cohen Department of Entomology, The Robert H. Smith Faculty of Agriculture Food and Environment, The Hebrew University of Jerusalem, Rehovot, Israel

Sylvia Colliec-Jouault Laboratoire Ecosystèmes Microbiens et Molécules Marines pour les Biotechnologies, Ifremer, Nantes, France

Maria Michela Corsaro Dipartimento di Scienze Chimiche, Università degli Studi di Napoli Federico II, Napoli, Italy

Mario A. A. Cunha Departamento de Química, Universidade Tecnológica Federal do Paraná, Pato Branco, Paraná, Brazil

Alcina Maria Miranda Bernardo de Morais Universidade Católica Portuguesa, Porto, Portugal

Rui Manuel Santos Costa de Morais Universidade Católica Portuguesa, Porto, Portugal

Robert F. H. Dekker Programa de Pós-graduação em Engenharia Ambiental, Universidade Tecnológica Federal do Paraná, Londrina, Paraná, Brazil

Alfonso Fernández-Mayoralas Instituto de Química Orgánica General, CSIC, Madrid, Spain

Ying Gu Department of Biochemistry and Molecular Biology, Center for Lignocellulose Structure and Formation, Pennsylvania State University, University Park, PA, USA

Regine Hengge Humboldt-Universität zu Berlin, Institut für Biologie, Mikrobiologie, Berlin, Germany

Alfonso Iadonisi Dipartimento di Scienze Chimiche, Università degli Studi di Napoli Federico II, Napoli, Italy

Doron Kam Institute of Plant Science and Genetics, The Robert H. Smith Faculty of Agriculture, Food and Environment, The Hebrew University of Jerusalem, Rehovot, Israel

Sandra L. A. Marin Universidade Federal do Paraná, Curitiba, Paraná, Brazil

Christoph Mayer IMIT – Microbiology and Biotechnology, University of Tübingen, Tübingen, Germany

Hans Merzendorfer School of Science and Technology, Institute of Biology – Molecular Biology, University of Siegen, Siegen, Germany

M. Fata Moradali Department of Oral Biology, College of Dentistry, University of Florida, Gainesville, FL, USA

Alberto Passi Department of Medicine and Surgery, University of Insubria, Varese, Italy

Maria Manuela Estevez Pintado Universidade Católica Portuguesa, Porto, Portugal

Jesús Pla Departamento de Microbiología y Parasitología, Universidad Complutense de Madrid, Madrid, Spain

Yehudit Posen PSW Ltd., Rehovot, Israel

Daniel Prieto Departamento de Microbiología y Parasitología, Universidad Complutense de Madrid, Madrid, Spain

Eveline A. I. F. Queiroz Núcleo de Pesquisa e Apoio Didático em Saúde (NUPADS), Instituto de Ciências da Saúde, Câmpus Universitário de Sinop, Universidade Federal de Mato Grosso, Sinop, MT, Brazil

Bernd H. A. Rehm Centre for Cell Factories and Biopolymers, Griffith Institute for Drug Discovery, Griffith University, Brisbane, Australia

Elvira Román Departamento de Microbiología y Parasitología, Universidad Complutense de Madrid, Madrid, Spain

William N. Sánchez Luna Universidade Federal do Paraná, Curitiba, Paraná, Brazil

Vidiany A. Q. Santos Departamento de Química, Universidade Tecnológica Federal do Paraná, Pato Branco, Paraná, Brazil

Diego O. Serra Humboldt-Universität zu Berlin, Institut für Biologie, Mikrobiologie, Berlin, Germany

Tal Ben Shalom Institute of Plant Science and Genetics, The Robert H. Smith Faculty of Agriculture, Food and Environment, The Hebrew University of Jerusalem, Rehovot, Israel

Oded Shoseyov Institute of Plant Science and Genetics, The Robert H. Smith Faculty of Agriculture, Food and Environment, The Hebrew University of Jerusalem, Rehovot, Israel

Zvi Shtein Institute of Plant Science and Genetics, The Robert H. Smith Faculty of Agriculture, Food and Environment, The Hebrew University of Jerusalem, Rehovot, Israel

Davide Vigetti Department of Medicine and Surgery, University of Insubria, Varese, Italy

Sapir Vinkler Institute of Plant Science and Genetics, The Robert H. Smith Faculty of Agriculture, Food and Environment, The Hebrew University of Jerusalem, Rehovot, Israel

Axel Walter IMIT – Microbiology and Biotechnology, University of Tübingen, Tübingen, Germany

Ingrid M. Weiss Institute of Biomaterials and Biomolecular Systems, University of Stuttgart, Stuttgart, Germany

Xiaoran Xin Department of Biochemistry and Molecular Biology, Center for Lignocellulose Structure and Formation, Pennsylvania State University, University Park, PA, USA

Jianzhen Zhang Institute of Applied Biology, Shanxi University, Taiyuan, Shanxi, China

Xiaoming Zhao Institute of Applied Biology, Shanxi University, Taiyuan, Shanxi, China

Kun Yan Zhu Department of Entomology, Kansas State University, Manhattan, Kansas, USA

Xiaoyu Zhu Department of Biochemistry and Molecular Biology, Center for Lignocellulose Structure and Formation, Pennsylvania State University, University Park, PA, USA

Agata Zykwinska Laboratoire Ecosystèmes Microbiens et Molécules Marines pour les Biotechnologies, Ifremer, Nantes, France

Part I
Aminosugar-Based Exopolysaccharides: Chitin-Based Extracellular Matrices

Chapter 1
Chito-Protein Matrices in Arthropod Exoskeletons and Peritrophic Matrices

Xiaoming Zhao, Jianzhen Zhang, and Kun Yan Zhu

Abstract The exoskeleton of an arthropod is formed by layered cuticles that are mainly composed of chitin and associated proteins in form of chito-protein matrices. Some internal organs of an arthropod, such as digestive tract and tracheal system, also contain chitin. Chitin biosynthesis is crucial for arthropod growth and development as the cuticular exoskeleton is regularly shed and replaced by a new cuticle. The biosynthesis starts by polymerizing *N*-acetylglucosamine (GlcNAc) units into a chitin polymer by chitin synthases. Chitin polymers are then translocated across the plasma membrane to form chitin microfibrils. Partial deacetylation of chitin polymers by chitin deacetylases facilitates a helicoidal arrangement of chitin layers. Numerous chitin-binding proteins are involved in the formation of chito-protein matrices both in the cuticle and peritrophic matrix (PM) of the midgut. These proteins influence the overall mechanical and physicochemical properties of the matrices. Chitin degradation is catalyzed by a two-component chitinolytic enzyme system, including the hydrolysis of chitin polymers into chitin oligomers by chitinases and the hydrolysis of the oligomers into monomeric GlcNAc by β-*N*-acetylglucosaminidases. Because chitin biosynthesis, modification, translocation, deposition, assembly, and degradation are highly complex biological processes, detailed mechanisms of many steps are still not fully understood. Nevertheless, chitin and chitosan (highly deacetylated chitin) have been commonly used as biomaterials due to their excellent properties including the biocompatibility, biodegradability, non-toxicity, and adsorption. Because plants and vertebrates including humans lack chitin biosynthesis, various approaches have been utilized for relatively safe control of arthropod pests by targeting their chitin biosynthetic and metabolic pathways.

X. Zhao · J. Zhang (✉)
Institute of Applied Biology, Shanxi University, Taiyuan, Shanxi, China
e-mail: zjz@sxu.edu.cn

K. Y. Zhu (✉)
Department of Entomology, Kansas State University, Manhattan, Kansas, USA
e-mail: kzhu@ksu.edu

E. Cohen, H. Merzendorfer (eds.), *Extracellular Sugar-Based Biopolymers Matrices*,
Biologically-Inspired Systems 12, https://doi.org/10.1007/978-3-030-12919-4_1

1.1 Introduction

1.1.1 Arthropods and their Taxonomic Groups

Arthropods belong to the largest phylum (Arthropoda) in the animal kingdom and are characterized by their exoskeleton (external skeleton) structure, segmented body, and paired and jointed appendages. Approximately 1.2 million arthropod species, accounting for more than 80% of the total animal species, have been described (Freeman et al. 2016), but scientists estimate that there may be 5–10 million arthropod species in the world (Ødegaard 2008). Arthropod bodies are *bilaterally symmetric*, a characteristic of animals that can move freely through their environments. Arthropods live in very diverse habitats including marine (ocean-based), freshwater, and terrestrial (land-based) ecosystems.

Arthropods can be classified into five subphyla: Trilobitomorpha (*Arctodus*), Chelicerata, Crustacea, Hexapoda, and Myriapoda. Trilobites constitute one of the earliest known groups of arthropods that disappeared in the end of the Permian about 252 million years ago. As a fossil group of extinct marine arthropods, trilobites are highly diverse. However, an easily fossilized exoskeleton is the only preserved body structure of trilobites, which include the head (cephalon), body (thorax), and tail (pygidium).

Cheliceratans (e.g., horseshoe crabs, sea spiders, scorpions, and spiders) are characterized by the division of their bodies into 2 parts: the anterior body part (head and thorax) that is made up of 6 segments and the posterior body part (abdomen) that has up to 12 individual segments and 1 tail segment. Chelicerata consists of three classes, including Merostomata, Arachnida, and Pycnogonida. Crustaceans (e.g., crabs, lobsters, crayfish, and shrimp) vary greatly in their morphology and life history. Their bodies are segmented and grouped into three regions (head, thorax, and abdomen). However, their head and thorax may be fused together to form a cephalothorax and covered by a single shell or carapace.

Crustaceans are composed of five classes, including Remipedia, Cephalocarida, Branchiopoda, Malacostraca, and Maxillopoda. Hexapoda (e.g., insects) constitutes the largest number of species of arthropods. The body of Hexapoda can be divided into three segments (head, thorax, and abdomen). The head possesses five pairs of appendages (antennae, upper lip, large jaw, small jaw, and lower lip) and the thorax three pairs of ambulatory legs. Their abdomen is also segmented, but there are no abdominal legs in the adult stage. Hexapoda contains four classes, including Protura, Collembola, Diplura, and Insecta. Insecta is a highly diverse class with over a million described species in 26 orders (Gullan and Craston 2005). In contrast, the body of subphylum Myriapoda (e.g., millipedes, centipedes) consists of head and torso. Myriapoda consists of four classes, including Diplopoda, Chilopoda, Pauropoda, and Symphyla.

Arthropods affect human life in many ways. Many crustaceans such as crabs, lobsters, and shrimp have long been part of human cuisine and provide a varied and balanced diet for humans. The greatest benefit of arthropods to humans is probably

their pollination of crops and fruits, which transfers pollen grains from the male anther of a flower to the female stigma to enable later fertilization and the production of seeds. It is estimated that total economic value of insect pollination is approximately 10% of the value of world agricultural production used as human foods (Gallai et al. 2009). On the other hand, arthropods are a major group of pathogen vectors for animal and human diseases. Many of such vectors are hematophagous, such as the malaria mosquito (*Anopheles gambiae*) that caused 445,000 human deaths in 2016 alone according to the World Health Organization (2017). Some blood-sucking insects infect livestock with diseases that kill many animals and greatly reduce their usefulness. Many species of arthropods, principally insects, are major agricultural and forest pests. It is estimated that arthropod pests destroy approximately 18–26% of annual crop production worldwide, at a value of more than $ 470 billion (Culliney 2014).

1.1.2 External and Internal Chitin-Containing Structures in Arthropods

Chitin, occurring as chito-protein matrices in nature, is the most abundant amino polysaccharide polymer and the second most abundant polysaccharide, next to cellulose, produced by fungi, mollusks, nematodes, and arthropods (Muthukrishnan et al. 2012). The chitinous integument (i.e., "body wall") of arthropods primarily consists of an outer noncellular structure (cuticle), a middle cellular layer (epidermis), and an inner noncellular membranous layer (basement membrane) (Fig. 1.1). The exoskeleton formed by the epidermis is a rigid body covering which supports and protects the soft tissues of arthropods. A typical arthropod cuticle is a multilayered structure consisting of three functionally distinct horizontal layers, including the outermost waxy coat envelope, the intermediate protein-enriched epicuticle, and the innermost procuticle. Such a cuticular arrangement is highly conserved among all the ecdysozoan animals (e.g., arthropods, nematodes). The procuticle can be further divided into exocuticle and endocuticle that interfaces with the epidermis. In arthropods, a vast majority of chitin is present in the procuticle as a chito-protein matrix, whereas chitin is thought to be absent or present only very low amounts in the envelope or epicuticle layers.

The main internal arthropod organs or tissues containing chitin include the digestive tract (i.e., gut) and tracheal system, where chitin is also present in form of chito-protein matrices. The digestive tract consists of an epithelial tube extending from the mouth to the anus. The insect gut is divided into three major regions (foregut, midgut, and hindgut) based on embryonic origins and physiological functions (Fig. 1.1). The foregut and hindgut originate from the ectoderm, whereas the midgut originates from the endoderm. Both the foregut and hindgut are lined with a cuticular layer and therefore shed off along with the insect exoskeleton during the molting process. On the other hand, the midgut lumen is lined with peritrophic

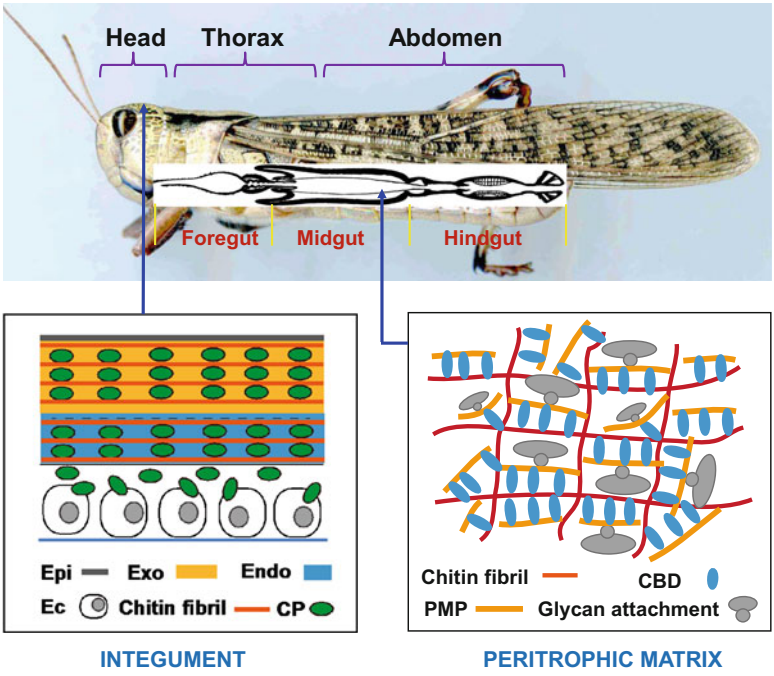

Fig. 1.1 Morphological diagram of a grasshopper to locate the integument (body wall) and the peritrophic matrix containing chitin and chitin-binding proteins. *Epi*: epicuticle; *Exo*: exocuticle; *Endo*: endocuticle; *Ec*: epidermal cell; *CP*: cuticular protein; *CBD*: chitin binding domain; and *PMP*: peritrophic matrix protein

matrix (PM), which is secreted by the intestinal cells (Hegedus et al. 2009; Merzendorfer et al. 2016) (Fig. 1.1). The PM is mainly composed of chitin, proteoglycans, and proteins (i.e., the PM proteins or PMPs). The chitin content of the PM is estimated to range between 3 and 13% (w/w) depending on the insect species, whereas the proteinaceous part (proteins, glycoproteins, and proteoglycans) accounts for 20–55% (w/w) of the total PM mass (De Mets and Jeuniaux 1962; Zimmermann et al. 1975). Chitin in the PM does not only contribute to mechanical and tensile strengths by providing a fibrillary meshwork but also is responsible for the PM permeability by tightly associating with chitin microfibrils (Tellam and Eisemann 2000; Toprak et al. 2010).

The tracheal tubes represent major respiratory system responsible for the exchange of oxygen and carbon dioxide between the internal tissues and the environment of arthropods. The tracheal system is a densely networked array of tubes known as tracheae that open to the outside through small holes called spiracles. The cuticle lining tracheae is similar to that on the insect body, but there is apparently no cement, and wax or lipid-water liquid crystals are not detectable. *Tracheoles* (about 1 μm in diameter) branch from the larger tracheae (up to several mm in diameter). Unlike tracheae, tracheoles do not shed and reform their lining membrane.

Both the tracheal and tracheolar cuticle is secreted at the plasma membrane surface of tracheal cells. Chitin is present in the wall of tracheal tubes and is utilized to reinforce the tubes by forming thickened chitin ridges (taeniidae). Such structures not only provide both the flexibility and strengths of the tubes but also prevent the tubes from collapsing under reduced air pressure.

1.1.3 Exoskeleton

1.1.3.1 Structure and Variations of Exoskeleton

As described previously, arthropod cuticle consists of three horizontal layers, including envelope, epicuticle, and procuticle. The envelope is a cement layer and composed of neutral lipids, wax, and proteins. The thickness of envelope is about 25 nm with the highest darkness observed by both transmission electron microscopy (TEM) and laser confocal microscopy. The major chemical components identified from the insect surface are free lipids including neutral lipids, such as long-chain alkanes and alkenes, long-chain alcohol, and fatty acid esters (Nelson et al. 2001, 2002, 2003; Patel et al. 2001; Nelson and Charlet 2003; Nelson and Lee 2004; Everaerts et al. 2010; Chen and Thelen 2016; Yu et al. 2016b). In the migratory locust (*Locusta migratoria*), the most abundant neutral lipids from the body surface are C29 long-chain fatty acid esters (Yu et al. 2016b).

The epicuticle is an ultrastructurally distinct layer underneath the envelope, which has a thickness of 1–4 μm (Fig. 1.1). This layer mainly contains unidentified proteins and lipids. Lipids bound to proteins possibly by covalent cross-linking appear to impregnate the inner layers of the cuticle (e.g., exocuticle). To date, however, proteins and lipids in this layer have not been identified due to technical difficulties in separating the epicuticle from the exocuticle. The procuticle is the innermost cuticle layer under the epicuticle and closely attaches to the surface of the epithelial cells. This layer is characterized by a chito-protein matrix, and there is no evidence for lipid deposition. The thickness of procuticles varies largely among species, which ranges from 10 μm to 200 μm. Unlike in fungi, the orientation of the arthropod chitin is not random. A quasicrystalline architecture of the protein-chitin extracellular matrix is described in both historical (Bouligand 1965; Neville 1965) and current literature (Zhu et al. 2016; Yu et al. 2016a).

The procuticle is divided into two sublayers including upper exocuticle and inner endocuticle. The exocuticle is formed long before insect ecdysis. Both epicuticle and the tanned exocuticle are shed off. However, deposition of the endocuticle occurs after ecdysis and ends before next apolysis, which refers to the process of separating the cuticle from the epidermis (Noh et al. 2017). In *L. migratoria*, the structural difference between the exocuticle and endocuticle can be easily recognized by TEM, because the chitin layer of the exocuticle is remarkably thinner than that of the endocuticle. In most insect wings, an additional ultrastructure, the mesocuticle, occurs between the exocuticle and endocuticle (Appel et al. 2015; Rajabi et al. 2016).

The thickness of arthropod cuticle varies significantly, from a thin and flexible membrane-like structure, such as the intersegmental membrane found in insects, to a massive rigid shell, such as that found in crabs. The hardness of various parts of the exoskeleton in different arthropods is related to the thickness and degree of tanning of the exocuticle. Tanning, also known as sclerotization, often takes place shortly after larvae/nymphs hatch from eggs or molt, or adults emerge from pupae. Insect cuticle tanning is a complex process in which specific regions of the newly produced cuticle are stabilized by the oxidative conjugation and cross-linking of cuticular proteins (CPs; i.e., structural proteins of the cuticle) by quinones, which makes the proteins insoluble and also hardens and darkens the exoskeleton (Suderman et al. 2006). Different degrees of stabilization and hardening occurring during the process of cuticle tanning contribute to different mechanical properties in different regions of the cuticle. Additionally, arthropod exoskeleton can often be mineralized with calcium carbonate or calcium phosphate and stores many nitrogen metabolites and minerals, which make them harder and stronger (Bentov et al. 2016).

Because the exoskeleton does not grow, it restricts the growth and development of arthropods. Therefore, they must periodically shed the old cuticle and produce the new one beneath the old one. The new exoskeleton is produced by the underlying single layer epidermal cells, which release enzymes that digest inner part of the old cuticle (much of the endocuticle) and then secrete a new cuticle. The exoskeleton is considered a complex metabolic library for arthropods. The substances involved in the formation of cuticle include lipids and waxes, glycosylated and non-glycosylated proteins, chitin, catecholamines, pigments, and mineral salts. Some of the metabolites can be reused, whereas others are removed in the molting process.

1.1.3.2 Functions of Exoskeleton

In arthropods, the exoskeleton formed by cuticle is a multifunctional outer covering that contributes to the stabilization of the body shape, serves as the attachment sites for muscles, and allows for the locomotion and flight. In insects, for example, all the three body parts, the appendages and the intersegmental membrane that connects different body parts and multiple segments of the abdomen contain chitin that either supports the whole exoskeleton or provides necessary plasticity of the body structures. In addition, arthropods show different body colors, some of which are contributed by the pigmentation of the cuticle. They may function as camouflage or warning signals. Arthropod exoskeleton has been known to provide good protection against microorganisms, parasitism, predation, and chemicals. The lipids and waxes associated with the cuticle also play important roles in protecting the arthropods against dehydration under hostile environmental conditions such as high temperature and low humidity (Wang et al. 2016; Yu et al. 2016b).

1.1.4 Peritrophic Matrix

1.1.4.1 Structure and Variations of Peritrophic Matrix

The PM is a noncellular, semipermeable structure that lines the midgut lumen and is composed of single layers or multilayer networks of chitin microfibrils and chitin-binding proteins (CBPs) in insects and other arthropods (Fig. 1.1). The chitin microfibrils of the PM have the same diameter as in the cuticle (Peters 1992). The microfilaments are usually arranged in parallel or more in bunches of 10 strands with the diameter of 2–6 nm (Streng 1973; Peters et al. 1979), which form 60° or 90° grid structure vertically and horizontally, or in random arrangement to form a dense mesh structure.

Based on the modes of the PM formation, the PM can be divided into two categories. Type I PM is secreted by the entire of midgut cells and is found in the majority of insect species including coleopterans, dictyopterans, ephemeropterans, hymenopterans, odonates, orthopterans, phasmids, lepidopteran larvae, and hematophagous dipteran adults (Waterhouse 1957; Peters 1992). The formation of type I PM usually starts in response to insect feeding, but it can also be formed continually. In the migratory locust (*L. migratoria migratorioides)*, for example, the formation of the PM is continuous: every 15 minutes one layer is delaminated, and the layers do not overlap (Baines 1978). On the other hand, type II PM is produced by a specialized group of cells that present on the anterior midgut and is found only in some insect groups, such as embiopterans, dipteran larvae (e.g., *A. gambiae*), some lepidopteran insects, and the insects of the primitive orders (e.g., Dermaptera and Isoptera) (Wigglesworth 1930; Peters 1992). Type II PM is more highly organized and consists of one to three laminated layers. The formation of type II PM is a continuous process regardless of the presence or absence of a food bolus. In mosquitoes, however, blood feeding can significantly stimulate the matrix production (Kato et al. 2008).

According to the arrangement of microfibrillar textures that can be visualized by ultrastructural microscopy, three structural types (orthogonal, hexagonal, and random felt-like arrangements) of the PM have been proposed (Peters 1992). In larvae of most lepidopteran species, the PM is secreted along the entire midgut, and its fibrils are organized randomly with a felt-like structure. In the tobacco hornworm (*Manduca sexta*), for example, the PM forms a thin multilayered lining in the anterior region of the midgut, but multiple layers in the middle and posterior midgut (Hopkins and Harper 2001). In the European corn borer (*Ostrinia nubilalis*), on the other hand, the single-layered PM of the anterior region of the midgut forms an orthogonal network. In the bertha armyworm (*Mamestra configurata*), the structural properties of the PM differ along the length of the midgut, and either PM turnover and/or maintenance depend upon the larval developmental stage (Toprak et al. 2014). For the orthogonal and hexagonal textures, the microvilli may determine the spacing between the microfibrils by forming a sort of a hexagonal template for the nascent PM formed between them (Mercer and Day 1952; Peters et al. 1979).

After delamination of the apical layers, a PM with orthogonal or hexagonal textures remains, which is presumably stabilized by certain types of proteins that bind to the chitin microfibrils.

1.1.4.2 Functions of Peritrophic Matrix

The PM of arthropods is an effective barrier between the midgut epithelium and ingested food and is also the first barrier for exogenous substances to enter the body of insects through the digestive tract. Following insect feeding, the food bolus is surrounded by the PM produced by midgut epithelial cells. The PM effectively separates the midgut epithelium from food particles, which prevents non-specific binding of undigested material to the epithelium wall. Due to filtration by the PM matrix via small-sized pores, only small molecules, which have been broken down by the gut enzymes, can be readily and effectively absorbed by contacting with the midgut epithelium, whereas the remaining indigestible materials will be kept in the matrix and excreted with the matrix. Thus, the presence of the PM significantly simplifies the excretion process and effectively improves the food digestion and nutrition absorption (*Bolognesi* et al. 2008*)*. Additionally, an anterior to posterior decrease in PM permeability may also facilitate digestive performance (Agrawal et al. 2014).

The second most important function of the PM is protecting the intestinal epithelial cells from the mechanical damage of intake of coarse food particles and the invasion of viruses and bacteria (Moskalyk et al. 1996). The PM is a very thin layer of structure with the maximum thicknesses of 20 μm and 2 μm for the type I and type II PMs, respectively. However, they can withstand mechanical pressure and filter out the disease-causing agents from ingested food. For example, in some lepidopteran insects, the larval PM can exhibit some biochemical composition and morphological changes to defend against the infection of different baculovirus (e.g., AcMNPV, TnSNPV, TnGV) (Derksen and Granados 1988). In the fruit fly (*Drosophila melanogaster*), the PM can prevent the damaging action of pore-forming toxins on intestinal cells (Kuraishi et al. 2011). More recently, it has been reported that the peptidoglycan recognition proteins (PGRPs) protect *Anopheles stephensi* from malaria parasite infection by regulating the structural integrity of microbiota-induced PM synthesis (Song et al. 2018).

The PM is porous, and the size of its pores varies with the insect species and can vary along the midgut within a species, which determines the PM's physical and chemical properties, and digestive efficiency (Agrawal et al. 2014). Although the pores of the PM are generally too large to impede the passage of most free chemicals, the permeability of the PM to toxic chemicals is not always proportional to the diameter of its pores (Barbehenn and Martin 1995). For example, large chemical complexes may be formed with tannic acid, proteins, lipids, and polyvalent metal cations in the insect gut fluid and be retained (Barbehenn 2001). Furthermore, some smaller toxic substances (e.g., tannins) can bind to certain surface proteins in the PM and be removed through the PM. In the desert locust (*Schistocerca gregaria*), for

example, 30% of the potential toxic substances is attached to the peritoneum and excreted with the PM (Barbehenn et al. 1996). In the forest tent caterpillar moth (*Malacosoma disstria*), because the charges of the tannins and the PM repel with each other, the tannin cannot attach to the PM, which protects the intestinal epidermal cells from toxic effects caused by tannins (Barbehenn and Martin 1994). In addition, the PM is also found to function as an effective iron-binding and radical-scavenging antioxidant that protects the midgut epithelia in the two caterpillar species, *M. disstria* and the white-marked tussock moth *(Orgyia leucostigma*) (Barbehenn and Stannard 2004).

1.2 Structure and Biosynthesis of Chitin in Arthropods

1.2.1 Chitin Structure

1.2.1.1 Chemical Compositions of Chitin

Chitin is a noncellular material and functions as a scaffold that supports the structures of the exoskeleton, trachea, and PMs (Fig. 1.1). It is synthesized from units of *N*-acetyl-D-glucosamine (GlcNAc) covalently bound by β-(1-4)-linkages (similar to the linkages between glucose units forming cellulose). However, chitin from natural sources is a heteropolymer of GlcNAc and glucosamine (GlcN) residues with various proportions (Muthukrishnan et al. 2012). After chitin chains are synthesized and transported to the extracellular site, they spontaneously assemble into microfibrils of varying diameter and length, which are deposited on the extracellular surface. Single sugar chains within the microfibrils are linked by hydrogen bonds between amine and carbonyl groups. Compared with cellulose, one hydroxyl group on each monomer in cellulose is replaced by an acetyl amine group in chitin. This specific replacement allows an increase in hydrogen bonding between adjacent polymers and enhances tensile strength of the microfibrils.

The pure chitin is uncharged, translucent, quite tough, and generally insoluble in water. In arthropods, however, chitin is often modified by chitin-modifying enzymes, such as chitin deacetylases (CDAs, EC 3.5.1.41), which modify chitin by the deacetylation of some *N*-acetyl-β-D-glucosamine units to yield β-1, 4-linked D-glucosamine units (i.e., deacetylated units) (Tsigos et al. 2000). In nature, approximately 5–20% of *N*-acetyl-β-D-glucosamine units of chitin are deacetylated (Merzendorfer 2011). Deacetylated chitin is called chitosan; however, chitosan usually refers to the modified chitin containing more than 80% of deacetylated β-1,4-linked D-glucosamine residues. Nevertheless, there is no clear distinction between chitin and chitosan based on the degree of *N*-deacetylation. Chitosan is positively charged, soft, and partially soluble in water. Partially deacetylated chitin may facilitate cross-linking with proteins to produce the chito-protein matrix with increased strength and elasticity of the cuticle in arthropods (Arakane et al. 2009b).

1.2.1.2 Structural Organization of Chitin

Chitin has a very complicated structure with multilevel constructions. After chitin polymer is synthesized, individual chitin chains assemble to form crystalline microfibrils through hydrogen bonds between the N–H and the C=O groups of adjacent polymers. In natural systems, chitin can occur in different forms including α-, β-, and γ-forms, which has been shown by X-ray diffraction analysis (Rudall and Kenchington 1973; Kramer and Koga 1986; Imai et al. 2003).

The α-form is the predominant form found in the exoskeleton of arthropods. It is characterized by its strong mechanical properties and low solubility. The three-dimensional structure of the α-form was proposed by Carlstrom (1957) and was later corrected and replenished by other researchers (Blackwell et al. 1967; Blackwell 1969). One characteristic of the α-form is that approximately 20 adjacent chitin polymers are arranged in an antiparallel manner, and the intramolecular chains in each lattice are connected by hydrogen bonds. The β-chitin is found in squid pens, spines of diatoms, tubes of giant tubeworms, and possibly the PM lining the midgut epithelial cells of insects. The β-chitin is a monoclinic lattice and contains only one type of repeated disaccharide in each lattice, and its chains are aligned in the same direction (parallel chains). In contrast, the γ-chitin is formed with the combination of parallel and antiparallel chains and is only found in the cocoon of some beetles and the PM of a few insect species, such as *S. gregaria*. However, its precise structure has not been resolved to the same extent as the other two forms of chitin. The chains of β-chitin and γ-chitin have more free NH and OH groups and can form hydrogen bonds through hydration (Saito et al. 2000; Kameda et al. 2005). More hydration and less packing tightness in the chain make β- and γ-chitin more flexible than α-chitin (Rudall and Kenchington 1973; Peters 1992).

The molecular configuration of chitin affects the water absorption capacity. A large number of hydrogen bonds make it difficult for the single chain of chitin molecules to absorb water longitudinally, whereas a small amount of water can be absorbed between the parallel axes of the two chains. Only the upper and lower chain or lamellar layer can absorb water and expand, making it possible to slip between the chains and generate some flexibility. The tight packaging of the matrix and the hydrogen bonds between the chains or within the chain of chitin molecules make the cuticle high strength, high stability, and impermeability (Giraud-Guille 1986; Kramer and Koga 1986; Lehane et al. 1996; Lehane 1997). However, the general hardness of the cuticle comes likely from *chitin*-protein interactions and their *cross-linking*. In crustaceans, the cuticle is frequently heavily mineralized with calcium or magnesium salts, further increasing its strength (Bentov et al. 2016).

1.2.1.3 Variations in Chitin Structure and Organization

Chitin structure and organization vary among insect species and within a species in different body parts and different developmental stages. Comparing the flexible

integument of a caterpillar and the stiff elytron of a beetle could help better understand the high variations in chitin structure and organization. In butterfly wing scales, chitin is organized into stacks of gyroids that produce various iridescent colors serving phenotypic signaling and communication for mating and foraging (Saranathan et al. 2010). Some beetles in the genus *Cyphochilus* also utilize chitin to form extremely thin scales and serve to scatter light. The variation of chitin structure and organization is closely related to functional requirement of the chitin-containing tissues (Merzendorfer and Zimoch 2003).

Chitin organization, which has been described by Bouligand (1965) and Neville (1965) in pioneering works in the 1960s of the last century, depends largely on the partial enzymatic modification of chitin (i.e., deacetylation) and on the interaction of chitin or chitosan fibers with respective binding proteins (Chapman 2013). In most arthropods, chitin is partially modified by deacetylation in some of the *N*-acetyl-glucosamine residues by CDAs. Unlike chitin, chitosan is better soluble in water and pliable to cross-linking with proteins. Although there is no direct evidence, the proportion between chitin and chitosan may provide a critical role in shaping tissues of various forms, sizes, and mechanical characteristics. Generally, chitin occurs largely as a component of composite materials and forms exoskeleton with different physiological properties. The exoskeleton becomes hard when compact chitin stacks with helicoidal arrangement are formed.

1.2.2 Chitin Biosynthesis, Assembly, and Deposition

1.2.2.1 Enzymes and Processes of Chitin Biosynthesis

Chitin biosynthesis is crucial for arthropod growth and development as chitin forms much of the animals' cuticular exoskeleton that is regularly shed and replaced by a new cuticle (Merzendorfer and Zimoch 2003). The formation of chitin from trehalose, a sugar consisting of two molecules of glucose, was confirmed in the southern armyworm moth (*Prodenia eridania*) by Jaworski et al. (1963). Based on the previous studies, Cohen (2001) outlined the chitin biosynthetic pathway from trehalose to chitin, which involves many enzymes, including trehalase, hexokinase, glucose-6-phosphate isomerase, glutamine-fructose-6-phosphate aminotransferase (GFAT), glucosamine-6-phosphate *N*-acetyltransferase, phosphoacetylglucosamine mutase (PAGM), UDP-*N*-acetylglucosamine pyrophosphorylase (UAP), and chitin synthase (CHS) (Fig. 1.2). The pathway can be divided into three cycles of sub-reactions. The first leads to the formation of *N*-acetylglucosamine (GlcNAc); the second follows a variant of the Leloir pathway yielding the activated amino sugar UDP-GlcNAc; and the last involves the polymerization of chitin using UDP-GlcNAc as the activated sugar donor. The first two sub-reactions occur in the cytoplasm and the third one at the specialized microdomains of the plasma membrane.

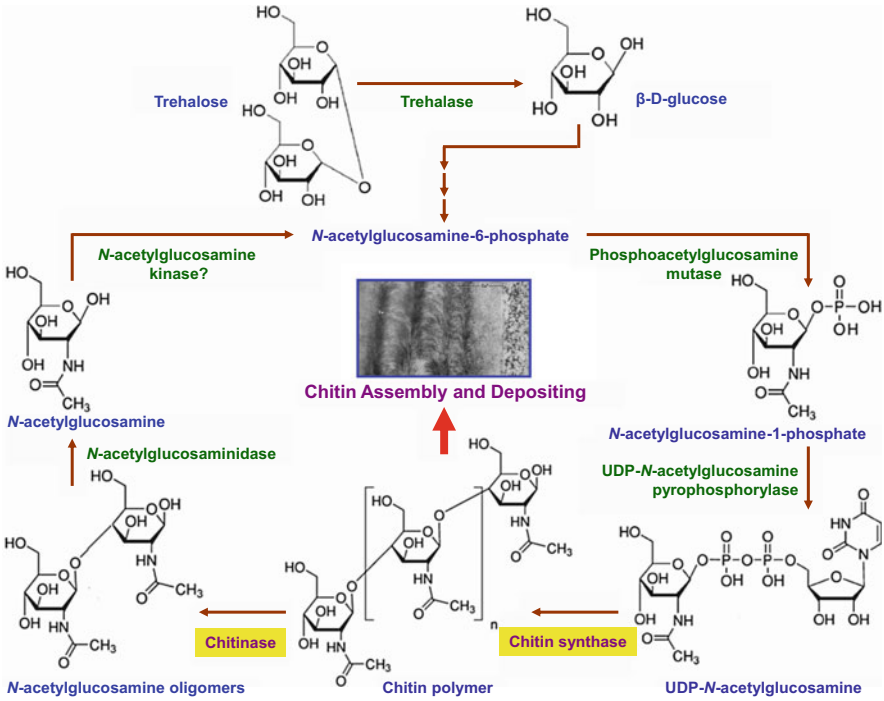

Fig. 1.2 Chitin biosynthetic and metabolic pathways. Chitin polymer is synthesized starting from trehalose. The process involves many enzymes including trehalase, hexokinase, glucose-6-phosphate isomerase, glutamine-fructose-6-phosphate aminotransferase (these steps not shown in the diagram), phosphoacetylglucosamine mutase, UDP-*N*-acetylglucosamine pyrophosphorylase, and chitin synthase. The chitin polymer is then assembled and deposited to form chitin. In chitin metabolic pathway, chitin polymer is degraded by chitinases and *N*-acetylglucosaminidase. The chitin degraded product, *N*-acetylglucosamine, can be recycled to synthesize new chitin polymer

In insects, the apical plasma membrane plaques of epidermal cells and the apical microvillar membranes of midgut cells can be considered as microdomains associated with chitin synthesis (Locke 2001; Zimoch and Merzendorfer 2002). The rate-limiting enzyme in the first cycle of sub-reactions appears to be GFAT (Durand et al. 2008), whose gene was cloned and characterized in many insect species, including *D. melanogaster*, *L. migratoria*, the yellow fever mosquito (*Aedes aegypti*), the buff-tailed bumblebee (*Bombus terrestris*), the western honey bee (*Apis mellifera*), the red flour beetle (*Tribolium castaneum*), the southern house mosquito (*Culex quinquefasciatus*), the parasitoid wasp (*Nasonia vitripennis*), and the body louse (*Pediculus humanus corporis*). The critical enzyme in the second sub-reaction is UAP, which was identified in *D. melanogaster*, *A. gambiae*, *A. aegypti*, *T. castaneum*, *C. quinquefasciatus*, *L. migratoria*, and the silkworm (*Bombyx mori*) (Liu et al. 2013, 2018).

The synthesis of chitin polymers from the activated precursor, UDP-GlcNAc, is catalyzed by the integral membrane enzyme CHS that contains a catalytic domain

and approximately 15 transmembrane helices (Tellam et al. 2000; Merzendorfer 2006; Muthukrishnan et al. 2012). It has been proposed that chitin biosynthesis involves several steps which include (1) polymerization by the catalytic domain of the CHS facing the cytoplasm, (2) translocation of the nascent chitin polymer across the membrane through the pore formed by the transmembrane helices of the CHS and release of the polymer into the extracellular space, and (3) spontaneous assembly of single polymers to form crystalline chitin microfibrils (Merzendorfer 2006). It is generally believed that CHS plays indispensable roles in chitin biosynthesis and secretion and may even participate in fibrillogenesis. However, the exact mechanisms as to how CHS plays these roles are not fully understood in arthropods (Merzendorfer and Zimoch 2003; Merzendorfer 2006).

A vast majority of insect species possess two CHS enzymes named chitin synthase 1 (CHS1, also known as CHSA) and chitin synthase 2 (CHS2, also known as CHSB). The CHS genes were first isolated from a variety of fungi such as yeast (Machida and Saito 1993; Uchida et al. 1996). The first cDNA of an insect *CHS* gene (*LcCHS1*) was identified and sequenced from the Australian sheep blowfly (*Lucilia cuprina*) approximately 20 years ago (Tellam et al. 2000). Since then, the *CHS1* cDNA sequences have been sequenced from various insect orders, including flies (Gagou et al. 2002), moths (Zhu et al. 2002), beetles (Arakane et al. 2004), grasshopper (Zhang et al. 2010a), and mosquitoes (Zhang et al. 2012). The *CHS1* is expressed in epidermal cells immediately underneath the cuticle, which is mainly responsible for biosynthesis of chitin in insect cuticle, trachea, foregut, and hindgut.

The *CHS2* is responsible for biosynthesis of chitin in the PM of the insect midgut. The first *CHS2* encoding a midgut-specific CHS enzyme was identified in *D. melanogaster*, and its expression and function were later characterized in *A. aegypti* (Ibrahim et al. 2000), *M. sexta* (Zimoch and Merzendorfer 2002), *T. castaneum* (Arakane et al. 2004), *O. nubilalis* (Khajuria et al. 2010), *A. gambiae* (Zhang et al. 2012), and *L. migratoria* (Liu et al. 2012). Ibrahim et al. (2000) first localized *AeCHS2* (*CHSB*) mRNA (i.e., transcript) at the apical site of midgut epithelial cells from female *A. aegypti* mosquitoes dissected several hours after a blood meal by using in situ hybridization. Likewise, in *M. sexta*, the transcript of *MsCHS2* (*CHSB*) was found in apical regions of the columnar cells of the anterior midgut but completely absent in the epidermis or tracheal system of larvae (Zimoch and Merzendorfer 2002).

In line with its role in the formation of the PM during insect feeding, *MsCHS2* mRNA was detected in the midgut of feeding but not of starving or molting larvae (Zimoch et al. 2005). Similar results have been obtained from the beet armyworm (*Spodoptera exigua*), the fall armyworm (*Spodoptera frugiperda*), *O. nubilalis*, and *T. castaneum* (Arakane et al. 2004; Bolognesi et al. 2005; Kumar et al. 2008; Khajuria et al. 2010). It is now clear that CHS2 is only responsible for the synthesis of chitin in the PM of the insect midgut. This is corroborated by a recent study showing the absence of CHS2 gene in hemipteran insects, such as the brown planthopper (*Nilaparvata lugens*), the small brown planthopper (*Laodelphax striatellus*), and the pea aphid (*Acyrthosiphon pisum*) as these insects lack the PM (Wang et al. 2012).

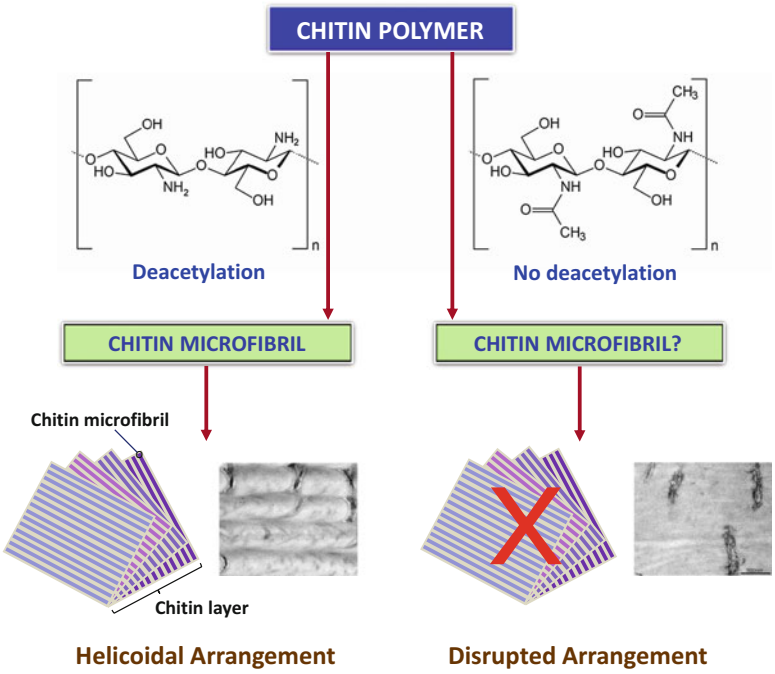

Fig. 1.3 Modification of chitin polymers by deacetylation. Chitin polymer is partially deacetylated by deacetylase to generate a heteropolysaccharide containing certain proportion of glucosamine residues. This process facilitates the cross-linking of glucosamine residues with proteins to trigger a helicoidal arrangement of chitin layers. If the chitin polymer is not deacetylated, the helicoidal structure cannot be arranged

1.2.2.2 Modification of Chitin Polymers

Chitin modification and organization are essential for the formation of exoskeleton and PM in insects. It is now known that CDAs play an important role in the modification of newly synthesized chitin during the molting process. The process facilitates the cross-linking of glucosamine residues with proteins to trigger a helicoidal arrangement of chitin layers (Fig. 1.3) (Yu et al. 2016a). Indeed, chitin deacetylation and the importance of this modification for insect growth and development has emerged as new area of research in insect molecular science (Luschnig et al. 2006; Wang et al. 2006; Arakane et al. 2009a; Yu et al. 2016a). CDAs are metalloproteins that belong to carbohydrate esterase family 4 (CE4) (Cantarel et al. 2009), a family of extracellular chitin-modifying enzymes that remove the acetyl group from chitin in arthropods.

The first cDNA (*TnCDA9*) encoding an insect CDA-like protein was characterized from the PM of the cabbage looper (*Trichoplusia ni*) (Guo et al. 2005). Since then, many genes encoding CDAs have been identified from different insect species such as *D. melanogaster*, *A. gambiae*, *A. aegypti*, *T. castaneum*, *C. quinquefasciatus*,

B. mori, *L. migratoria*, the Asian corn borer (*Ostrinia furnacalis*), and the cotton bollworm (*Helicoverpa armigera*). These proteins are encoded by a family of four to nine genes which fall into five groups (I to V) with distinct domain organizations (Xi et al. 2014; Tetreau et al. 2015a; Yu et al. 2016a). Group I comprises CDA1 and CDA2 that have a chitin-binding domain (CBD) at the *N*-terminal region, a low-density lipoprotein receptor class A domain (LDLa), and a polysaccharide deacetylase-like catalytic domain (CE4) at the *C*-terminal region. Group II is composed of CDA3 that has the same domain composition as the group I CDAs, but the overall amino acid sequence identities are only about 38% in CDA1 and CDA2. Group III and group IV include CDA4 and CDA5, respectively, which lack the LDLa domain but retain the CBD domain. Group V includes CDA6, CDA7, CDA8, and CDA9, which are only characterized by a CE-4 domain. All five groups in most insects have the CE-4 domain at the C-terminal region.

The role of CDAs has been well studied in the tracheae and the epidermis of several insect species. In *D. melanogaster*, two genes in group I, the putative CDAs Serpentine (*Serp*, *DmCDA1*) and Vermiform (*Verm*, *DmCDA2*), are expressed and secreted in the tracheal system and required for the development and formation of the tracheal tubes (Luschnig et al. 2006; Wang et al. 2006). Specifically, *DmCDA1* and *DmCDA2* mutant embryos displayed elongated and tortuous tracheal tubes (Luschnig et al. 2006). However, both CDAs contribute to chitin organization in the larval cuticle (Gangishetti et al. 2012). In *T. castaneum*, *TcCDA1* and *TcCDA2* are predominantly expressed in epidermis and tracheae. When the transcript level of *TcCDA1* or *TcCDA2* is suppressed by injection of double-stranded RNA (dsRNA) to target each specific gene, all types of insect molts are prevented, and the insects finally die during larval-larval, larvae-pupal, or pupal-adult molting (Arakane et al. 2009b). In the eastern spruce budworm (*Choristoneura fumiferana*), *CfCDA2* transcripts accumulate in the epidermis. When the expression of *CfCDA2* is downregulated, mortality increases during larval-larval and larval-pupal molting (Quan et al. 2013). In *N. lugens*, *NlCDA1* and *NlCDA2* are predominately expressed in the integument. Depletion of these transcripts by RNA interference (RNAi) results in a lethal phonotype during the nymph-nymph molting (Xi et al. 2014). In *L. migratoria*, *LmCDA2* is responsible for cuticular chitin organization and lamellar structure construction (Yu et al. 2016a).

All these results suggest that group I CDAs play critical roles in maintaining the structural integrity of the cuticular chitin laminae and the chitin fibers of the cuticle and tracheal tube. In contrast, silencing the CDAs belonging to the other four groups failed to produce any visible effects in *T. castaneum*, but resulted in molting failure except for a group IV CDA in *N. lugens* (Xi et al. 2014). Several hemimetabolous insects and even mosquitoes do not have group V CDAs. In addition, RNAi experiments targeting this group of CDA genes in insects where they are predominantly expressed in the gut tissue failed to produce any visible effect. Therefore it is speculated that the group V CDAs may be involved in digestion of chitinous material in the diet rather than the modification of endogenous chitin.

Recent studies indicate that both CDA1 and CDA2 are required for cuticle morphology, architecture, and ultrastructure, which is critical for insect molting,

growth, and development. In *T. castaneum*, TcCDA1 and TcCDA2 appear to work cooperatively to determine cuticle integrity (Noh et al. 2018b). In *D. melanogaster* and *T. castaneum*, CDA1 (Serpentine or Serp) and CDA2 (Vermiform or Verm) are mainly localized in the assembly zone (Pesch et al. 2015; Pesch et al. 2016; Noh et al. 2018b), whereas LmCDA2 from *L. migratoria* appears to be present in the outermost part of the procuticle and required for stratified structure and compactness of the cuticle (Yu et al. 2016a). LmCDA1 is predominantly localized at the apical tier of the protein-chitin matrix, but is also found in lower regions. Studies have suggested that LmCDA1 plays a role in regulating normal amounts of cuticular chitin. However, the establishment of the laminar architecture of the chitin layer seems to be independent of LmCDA1 activity, but dependent on another CDA, LmCDA2, which has no detectable effects on chitin content and deacetylation in *L. migratoria*.

The functional differentiation of group I CDAs has been confirmed in the development of *D. melanogaster* wings. DmCDA1 (Serp) and DmCDA2 (Verm) have distinct functions in differentiating the wing cuticle. Serp is the major enzyme responsible for chitin deacetylation during the formation of the wing cuticle, whereas Verm does not seem to be needed for this process. Studies based on atomic force microscopy (AFM) suggest that Serp and Verm have distinct roles in establishing the shape of the nanoscale bumps at the wing surface. These results suggest that correct differentiation of the wing cuticle involves both Serp and Verm in parallel in largely non-overlapping functions. However, researches on *L. migratoria* provided an alternative view on the organization of the quasicrystalline protein-chitin matrix during the differentiation of the insect cuticle. Furthermore, recent studies have shown that the process of protein-chitin matrix assembly occurs non-site autonomously in the assembly zone of the cuticle adjacent to the apical plasma membrane in *D. melanogaster* and *T. castaneum* (Pesch et al. 2015, 2016; Noh et al. 2018b). However, the protein-chitin matrix appears to be assembled on site in *L. migratoria*. These two alternative mechanisms may be the results of divergent evolution between the metamorphic and non-metamorphic insects.

In *D. melanogaster*, it is reported that DmCDA1 and DmCDA2 localize to the extracellular region adjacent to the apical plasma membrane of epidermal cells where they cooperate with the chitin-binding proteins Obstructor-A (Obst-A) and Knickkopf (KNK) to organize chitin fibers. The complex of Obst-A and KNK protects the newly synthesized chitin from degradation in the molting fluid and maintains the laminar structure (Chaudhari et al. 2011; Petkau et al. 2012). A chitosan protein complex, Retroactive, can be specific to transport KNK to the newly formed cuticle, thereby playing its protective effect in the new cuticle (Chaudhari et al. 2013). These proteins help to organize the chitinous cuticular layers and provide the proper rigidity and/or flexibility in different regions of the cuticle.

1.2.2.3 Regulation of Chitin Biosynthesis

The precise control of chitin content is critical not only for arthropod survival but also for optimal function of individual anatomical structures. In insects, chitin

synthesis is tightly regulated at the transcriptional level during their growth and development. *CHS1* and *CHS2* genes are expressed in different tissues and exhibit different expression patterns at different developmental stages. However, the underlying regulatory mechanisms are not yet well understood. As described above, *CHS1* gene is expressed over a wide range of developmental phases including embryonic, larval, pupal, and adult stages (Tellam et al. 2000; Gagou et al. 2002; Zhu et al. 2002). In contrast, the *CHS2* gene is not expressed in embryonic or pupal stages but is expressed in larval stages, especially during feeding in the last instar, and in the adult stage of insects, including blood-feeding mosquitoes (Ibrahim et al. 2000; Zimoch and Merzendorfer 2002; Arakane et al. 2004). These distinct developmental expression patterns of *CHS1* and *CHS2* have prompted the hypothesis that the expression of insect *CHS* genes is highly regulated in different tissues or at different developmental stages.

Arthropod molting and metamorphosis are regulated by ecdysterone (also referred to as 20-hydroxyecdysone or 20E), a steroid hormone that is secreted cyclically into the hemolymph by the prothoracic gland. During the growth and development of insects, ecdysterone regulates the molting process through activation of a series of genes including *BR-C*, *E74*, *E75*, and *HR3* by the receptor EcR/USP. So far, no factors have been identified unequivocally to act on *cis*-regulatory elements of *CHS* promoters (Moussian 2010). As transcriptional regulation of *CHS* expression during insect development appears to be complex, it has been first postulated that transcriptional regulation of *CHS* genes involves ecdysone-responsive elements in the upstream regions (Merzendorfer and Zimoch 2003). Moreover, analysis of *CHS* expression during *Drosophila* metamorphosis indicates that ecdysterone has a regulatory role on *CHS1* (*DmeChSB*) and *CHS2* (*DmeChSA*) transcript levels (Gagou et al. 2002). In addition, the consensus sequences for the ecdysone-inducible factors BR-C and E74A were predicted to be within the promoter region of *DmCHS2*. Other researchers suggest that the candidate of the transcription factor is Grainy head (Grh). The Grh triggers the activation of genes involved in sclerotization and melanization by binding to Grh element. For *DmCHS1*, five potential Grh-binding sites are in its first intron region; however, whose role in developmental control of chitin synthesis remains to be established (Moussian 2010).

In *O. furnacalis*, the core promoter of *OfCHS2* contains the binding sites of only early ecdysone-inducible elements (BR-C and E74A), but not ecdysone-response elements (EcR and USP) (Qu et al. 2011). The existence of ecdysone-inducible rather than ecdysone-response elements suggests that *OfCHS2* may be in an ecdysone-dependent regulatory pathway and not directly stimulated by ecdysone in the formation of PM. In contrast, both of the alternative promoter regions of *OfCHS1* (*OfCHS1a* and *OfCHS1b*) contain the ecdysone-response element EcR, suggesting that *OfCHS1* may be directly regulated by ecdysone (Qu et al. 2011; Qu and Yang 2012). In *S. exigua*, many binding sites of transcription factors, such as BR-C, Forkhead, and POU, have been predicted to be within the promoter region of *CHS* genes, implying that the expression of *CHS* genes may be regulated by ecdysone. After RNAi of ecdysone receptor gene *EcR* in *S. exigua*, the expression of five genes (*SeTRE1*, *SeG6PI*, *SeUAP*, *SeCHS1*, *SeCHS2*) in the chitin synthesis

pathway is downregulated, and the insects eventually die due to dysplasia (Yao et al. 2010). However, these genes can be activated again by injection of ecdysone in vivo. These results suggest that the expression of *CHS* genes could be regulated by ecdysone. In *L. migratoria*, *LmHR3*, a gene encoding the putative nuclear receptor factor was identified and characterized (Zhao et al. 2018). The expression of *LmHR3* can be upregulated by ecdysone. After injection of dsRNA for *LmHR3*, none of the locusts was able to molt normally as the synthesis of new cuticle was blocked. Furthermore, the genes involved in chitin biosynthesis (*LmUAP1* and *LmCHS1*) were significantly downregulated in the ds*LmHR3* treated insects. These results suggest that *LmHR3* is involved in the control of chitin biosynthesis by regulating the chitin synthesis genes during *L. migratoria* molting.

MicroRNAs (miRNAs) are small noncoding regulatory RNAs emerged as key posttranscriptional regulators of gene expression in multiple biological processes (Krol et al. 2010). Many studies have shown that miRNAs critically regulate the expression of the genes in chitin synthesis pathway, thus resulting in molting defect phenotypes. For example, miR-8-5p and miR-2a-3p act as molecular regulators that negatively tune membrane-bound trehalase and PAGM of the chitin biosynthesis pathway, leading to a significant reduction in survival rate along with a molting defect phenotype in the hemipteran insect *N. lugens* (Chen et al. 2013). In *L. migratoria*, depletion of Dicer-1, the enzyme catalyzing the final step of miRNA biosynthesis, can lead to molting defect (Wang et al. 2013). This finding suggests that miRNAs play a crucial role in regulating the molting process in *L. migratoria*. More recently, Yang et al. (2016) found that both *CHS* and *CHT* can be jointly regulated by miRNAs, miR-71 and miR-263, during nymph molting in *L. migratoria*. Injection of the miR-71 and miR-263 agomirs ultimately suppresses the expression of *CHS1*and *CHT10* and consequently changes the chitin production of new cuticle and the chitin metabolism of old cuticle, leading to insect molting defects.

1.2.2.4 Formation of Chitin Microfibrils

In the epidermal cuticle, chitin adopts a typical crystalline arrangement that was first described in crustaceans (Bouligand 1965) and subsequently confirmed for insects (Neville and Luke 1969). The chitin microfibrils of the insect cuticle are about 3.0 nm in diameter and about 0.3 mm long. Each microfibril consists of about 20 single chitin chains that are embedded in a protein matrix. They lie parallel to each other in the plane of the cuticle, forming a layer, but their orientation is often different in successive levels throughout the thickness of the cuticle. In most insects, the microfibrils in the outer parts of the procuticle, which subsequently becomes the exocuticle, rotate anticlockwise through a fixed angle in successive levels so that their arrangement is helicoidal and a series of thin lamellae is produced called lamellate cuticle. The inner procuticle may also be lamellate throughout, or layers with helicoidally arranged microfibrils may alternate with layers in which the

microfibrils are uniformly oriented (Neville 1965; Moussian 2010). However, how chitin or chitosan polymers interact with proteins for producing the chitin microfibrils remains largely unclear.

1.2.2.5 Deposition of Chitin in Exoskeleton and Peritrophic Matrix

The maturation of many organs and tissues is characterized by the deposition of an extracellular matrix (ECM), such as chito-protein matrix, in arthropods (Rozario and DeSimone 2010; Daley and Yamada 2013; Moussian et al. 2015; Öztürk-Çolak et al. 2016). As discussed previously, after chitin polymers are synthesized by CHS, the nascent chitin polymers are translocated across the plasma membrane to form crystalline chitin microfibrils, which allows for chitin deposition on extracellular surfaces. In arthropods, chitin is deposited in a highly organized arrangement at the apical surface of epidermal and tracheal cells to form the cuticle (Moussian 2013). Such a process is a highly complex and involves multifaceted interconnected series of biochemical and biophysical events. It starts intracellularly and ends in the inclusion of chitin in exterior supra-macromolecular structures such as the cuticles and the PM in arthropods (Cohen 2001). Nevertheless, the exact process and mechanism of chitin deposition in arthropods are still obscure.

In *Drosophila*, chitin deposition in the exoskeleton and tracheae (both are of ectodermal origin) requires the activity of the chitin synthase Krotzkopf verkehrt (Kkv) (Moussian et al. 2015). This process also requires the activity of two MH2-containing proteins, Expansion (Exp) and Rebuf (Reb). The function of Exp and Reb is the same and interchangeable, but they are absolutely required for chitin deposition. It is found that Kkv is not able to perform the task without Exp and Reb. In fact, Exp and Reb are not only required but also are sufficient to bring about early and increased chitin deposition in the presence of Kkv. In the absence of Exp and Reb, the lamellar chitin filament is not assembled, and the tracheal and epidermal cuticles are chitin-less. This phenotype is identical to that of Kkv mutants. Several lines of evidences suggest that Exp and Reb may participate in chitin polymer translocation across the membrane and/or in the formation of chitin microfibrils (Moussian et al. 2015).

Chitin is also a constituent component of the PM in arthropods as it reinforces the PM by providing a fibrillar meshwork. In *L. migratoria*, suppression of the *LmCHS2* transcript level by RNAi interrupts chitin deposition, subsequently resulting in the failure of the PM formation. Specifically, the PM from the RNAi-treated insects is amorphous and much thinner than that from the controls (Liu et al. 2012). Similarly, both silencing *T. castaneum CHS2* expression and inhibiting chitin synthesis by diflubenzuron also lead to a pronounced loss of the PM (Kelkenberg et al. 2015). These studies suggest that the chitin synthesis and deposition are closely linked but the effect may be mainly caused by reduced chitin synthesis. In *Drosophila*, *Exp* and *Reb* are not expressed in the endodermal midgut cells, suggesting that chitin deposition in the PM is independent of Exp and Reb (Moussian et al. 2015). Thus, chitin deposition in the PM may be

associated with another set of proteins (Hegedus et al. 2009). In *M. sexta*, it was proposed that chitin deposition in the midgut relies on midgut-specific CHS2 associated with a chymotrypsin-like protease (Zimoch et al. 2005).

1.3 Chitin Degradation and Recycling

1.3.1 Diversity of Chitin-Degrading Enzymes in Arthropods

Chitin content, which fluctuates throughout the life cycle of arthropods, is directly influenced not only by chitin biosynthesis but also by chitin metabolism catalyzed by chitin-degrading enzymes (Muthukrishnan et al. 2012). These enzymes digest the structural polysaccharide in their exoskeleton and gut linings during the molting process (Kramer and Koga 1986; Kramer and Muthukrishnan 1997; Fukamizo 2000). At present, biochemical and molecular studies on chitin-degrading enzymes in arthropods mainly focus on crustaceans and insects. In insects, relevant studies have been conducted using various insect species that belong to many different orders including Diptera, Lepidoptera, Coleoptera, Orthoptera, Hemiptera, and Hymenoptera (Chen et al. 2018).

The chitin-degrading enzymes can be divided into two main groups: chitinases (CHTs; EC 3.2.1.14) including both endochitinases and exochitinases and β-*N*-acetylglucosaminidases (NAGs; EC 3.2.1.52) also known as chitobiases (Fig. 1.2). Insect CHTs, which belong to family 18 glycoside hydrolase (GH18), are key enzymes that hydrolyze the linear polymer of chitin. The hydrolytic sites of endochitinases are random at the interior of chitin polymers, whose final products are soluble, low molecular weight chitooligosaccharides. Exochitinases progressively cleave off two saccharide units from the reducing or nonreducing ends of the chitin polymer to yield the disaccharides. The NAGs, on the other hand, belong to the CAZy glycoside hydrolase family 20 (GH20) enzymes that hydrolyze terminal, nonreducing β-*N*-acetylglucosamine residues of the products (i.e., chitooligosaccharides) after the action of CHTs to convert them to the monosaccharide, *N*-acetylglucosamine (Arakane and Muthkrishnan 2010; Zhu et al. 2016). Different arthropods may have different types and components of chitinases. For instance, endochitinases are found in the kuruma shrimp (*Penaeus japonicus*), but three different exochitinases with molecular weight of 66 kDa (A, B1, and B2) and two different NAGs with 116 kDa are found in the American lobster (*Homarus americanus*) (Lynn 1990). In insects, main chitin-degrading enzymes include endochitinases and NAGs. For our convenience, we refer insect endochitinases as chitinases (CHTs) in the rest of this chapter.

The first full-length cDNA encoding CHT (*MsCHT5*) was sequenced from *M. sexta* by Kramer et al. (1993). As more insect genome sequences become available in recent years, more than 100 cDNAs encoding CHT and CHT-like proteins (e.g., imaginal disk growth factors or IDGFs or related proteins) have been identified from different species such as the mealworm (*Tenebrio molitor*),

the fall webworm moth (*Hyphantria cunea*), *A. aegypti*, *A. gambiae*, *B. mori*, *D. melanogaster*, *H. armigera*, *L. migratoria*, *O. furnacalis*, *S. litura*, and *T. castaneum*. Insect CHTs are multidomain proteins that consist of three multifunctional structure regions including chitinase catalytic domain (CCD) at the *N*-terminal region, serine/threonine-rich linker (STL), and chitin-binding domain (CBD) at the *C*-terminal region. It has become clear that CHTs belong to a large family of enzymes with different expression profiles, tissue specificities, and functions in insects (Zhu et al. 2008a; Zhang et al. 2011a, b).

The insect *CHT* and *CHT*-like gene family was first systemically analyzed and classified in *T. castaneum*, when its genome sequence became available (Zhu et al. 2008a). These genes were divided into five groups (I–V) based on the sequence similarity and domain architecture. When a phylogenetic-based comparative analysis of *CHT* and *CHT*-like gene families in mosquitoes along with those from *D. melanogaster*, *T. castaneum*, and several other insect species was performed, the group number expanded to eight including three new groups (Zhang et al. 2011). Such a comparative analysis led to a uniform classification and nomenclature of the insect *CHT* and *CHT*-like genes. More recently, research in chitin metabolism enzymes in *M. sexta* revealed two new groups, which leads to a total group number of ten in insect species (Tetreau et al. 2015a). One of the two new groups, CHT-h, appears to be Lepidoptera-specific, which is consistent with its proposed bacterial origin. Table 1.1 summarizes the phylogenetics-based comparative classification of *CHT* and *CHT*-like genes from five representative insect species.

There is only one gene (*CHT5*) representing group I in most insect species known to date, but gene duplications of *CHT5* have been implicated in three mosquito species with three, four, or five *CHT5* genes (e.g., *CHT5-1*, *CHT5-2*, *CHT5-3*, *CHT5-4*, and *CHT5-5*) and in *L. migratoria* with two *CHT5* genes (*LmCHT5-1* and *LmCHT5-2*) (Zhang et al. 2011b; Li et al. 2015). The putative CHTs in group I possess typical CHT domains such as CCD, STL, and CBD, but those encoded by the duplicated *CHT5* genes in the mosquitoes and *L. migratoria* lack a CBD. RNAi to silence the group I gene *TcCHT5* at the pupal stage of *T. castaneum* resulted in a pupal-adult lethal phenotype, indicating that *TcCHT5* is required for pupal-adult molting (Zhu et al. 2008b). In *L. migratoria*, RNAi-mediated suppression of the *LmCHT5-1* transcripts led to severe molting defects and lethality, but such effects were not observed when *LmCHT5-2* was silenced (Li et al. 2015), suggesting that the newly duplicated *LmCHT5-2* plays a less important role than *LmCHT5-1* in the development and survivorship of the insect.

In group II, a single gene (*CHT10*) has been identified in the genomes of several insect species including *A. aegypti*, *A. gambiae*, *B. mori*, *D. melanogaster*, and *T. castaneum*. It encodes a large protein consisting of more than 2000 amino acid residues and containing more than four CCDs and CBDs. RNAi silencing of *TcCHT10* indicates that *TcCHT10* plays important roles in egg hatching and larval-larval, larval-pupal, and pupal-adult molting in *T. castaneum* (Zhu et al. 2008b). A single gene was also identified in each of groups III, VI, VII, VIII, IX, and X (*CHT7*, *CHT6*, *CHT2*, *CHT11*, *CHT1*, and *CHT3*, respectively) in a variety of insect species. Their putative CHTs have one or two CCD, but no CBD in CHT1,

Table 1.1 Phylogenetics-based comparative classification of chitinase and chitinase-like genes from five representative insect species

Group	Anopheles gambiae	Drosophila melanogaster	Tribolium castaneum	Manduca sexta	Locusta migratoria
IX	*AgCHT1*	*DmCHT1*	*TcCHT1*	*MsCHT1*	*LmCHT1*
VII	*AgCHT2*	*DmCHT2*	*TcCHT2*	*MsCHT2*	*LmCHT2*
X	–[a]	–	*TcCHT3*	*MsCHT3*	–
I	*AgCHT5-1*	*DmCHT5*	*TcCHT5*	*MsCHT5*	*LmCHT5-1*
	AgCHT5-2	–	–	–	*LmCHT5-2*
	AgCHT5-3	–	–	–	–
	AgCHT5-4	–	–	–	–
	AgCHT5-5	–	–	–	–
VI	*AgCHT6*	*DmCHT6*	*TcCHT6*	*MsCHT6*	*LmCHT6*
III	*AgCHT7*	*DmCHT7*	*TcCHT7*	*MsCHT7*	*LmCHT7*
II	*AgCHT10*	*DmCHT10*	*TcCHT10*	*MsCHT10*	*LmCHT10*
VIII	*AgCHT11*	*DmCHT11*	*TcCHT11*	*MsCHT11*	*LmCHT11*
V	–	*DmIDGF1*	–	*MsIDGF1*	*LmIDGF1*
	AgIDGF2	*DmIDGF2*	*TcIDGF2*	–	*LmIDGF2*
	–	*DmIDGF3*	–	–	*LmIDGF3*
	AgIDGF4	*DmIDGF4*	*TcIDGF4*	–	–
	–	*DmIDGF5*	–	–	–
	–	*DmIDGF6*	–	–	–
h				*MsCHT-h*	
IV	*AgCHT4*	*DmCHT4*	*TcCHT4*	–	*LmCHT4*
	AgCHT8	*DmCHT8*	*TcCHT8*	*MsCHT8*	*LmCHT8*
	AgCHT9	*DmCHT9*	*TcCHT9*	–	*LmCHT9*
	AgCHT12	*DmCHT12*	*TcCHT12*	–	*LmCHT12*
	AgCHT13	–	*TcCHT13*	–	*LmCHT13*
	–	–	*TcCHT14*	–	–
	–	–	*TcCHT15*	–	–
	AgCHT16	–	*TcCHT16*	–	–
	–	–	*TcCHT17*	–	–
	–	–	*TcCHT18*	–	–
	–	–	*TcCHT19*	–	–
	–	–	*TcCHT20*	–	–
	–	–	*TcCHT21*	–	–
	–	–	*TcCHT22*	–	–
	AgCHT23	–	–	–	–
	AgCHT24	–	–	–	–

[a]Putative orthologous gene not found in the giving species

CHT2, CHT11, and CHT-h. Silencing of *TcCHT7* in penultimate instar larvae by RNAi did not interfere with the larval or pupal development, but the pupae failed to contract their abdomens to the same extent as the control insects (Zhu et al. 2008b). These insects also failed to fully expand their elytra, indicating that *TcCHT7* is

required for abdominal contraction and wing extension. More recently, it was shown that *TcCHT7* is necessary for organizing chitin-containing structures in the nascent cuticle, which contributes to the rigidity of the extracellular matrix (Noh et al. 2018a). This unexpected function is distinctly different from that of other groups of epidermal CHTs that catalyze the turnover of chitin in old cuticle during the molting process. In *D. melanogaster*, the groups VII gene (i.e., *DmCHT2*) is expressed in chitin-producing organs for cuticle formation (Pesch et al. 2017).

Group IV comprises the largest number of *CHT* genes in most insect species including *A. aegypti*, *A. gambiae*, *D. melanogaster*, and *T. castaneum* (10, 8, 4, and 14 genes, respectively). No phenotypes were observed after knockdown of group IV *CHT* genes (*TcCHT8*, *TcCHT14*, and *TcCHT16*) in *T. castaneum* (Zhu et al. 2008b). On the other hand, the number of group V (i.e., *IDGF*) genes ranges from one in *A. mellifera* to as many as six in *D. melanogaster*. When dsRNA targeting *TcIDGF2* or *TcIDGF4* of group V was injected into penultimate instar and last instar larvae of *T. castaneum*, there was no effect on pupation or adult eclosion by dsRNA for *TcIDGF2*, but the insects died during adult eclosion in spite of pupation was normal by dsRNA for *TcIDGF4* (Zhu et al. 2008b).

Enzymatically active NAGs have been characterized from a variety of sources in insects, including molting fluid, hemolymph, integument, and gut (Leonard et al. 2006; Tomiya et al. 2006; Okada et al. 2007; Yang et al. 2008). Several cDNAs encoding NAGs have been sequenced in various insect species, including *B. mori* (Nagamatsu et al. 1995), *M. sexta* (Zen et al. 1996), *A. aegypti* (Filho et al. 2002), *T. castaneum* (Hogenkamp et al. 2008), *O. furnacalis* (Liu et al. 2009), and *L. migratoria* (Rong et al. 2013). NAGs are classified into five groups in insects according to phylogenetic analyses, which include chitinolytic NAGs (group I), chitinolytic NAGs (group II), *N*-glycan processing NAGs (group III), hexosaminidases (group IV), and endo-*β*-*N*-acetyl glucosaminidases (ENGs, group V) (Rong et al. 2013). All group I NAGs are predicted to be secreted proteins that were isolated mainly from molting fluid, integument, and gut (Dziadik-Turner et al. 1981). NAG1 is likely the enzyme primarily responsible for efficient degradation of cuticular chitin during insect molting process. This hypothesis is supported by studies showing that the suppression of *LmNAG1* by RNAi leads to molting defect in *L. migratoria* (Rong et al. 2013).

1.3.2 Processes of Chitin Degradation

Chitin degradation is associated with the molting process and has been carefully examined in *L. migratoria* (Zhang Lab, unpublished). As shown in Fig. 1.4, the first sign of molting is the appearance of ecdysial droplets containing enzymes, such as proteinases and CHTs, for digesting the old cuticle at the apical plasma membrane of the epidermal cell. The ecdysial droplets then separate from the apical plasma membrane and increase their size to the maximum when a new envelope is completely deposited. As new procuticle is deposited, proteins of the innermost

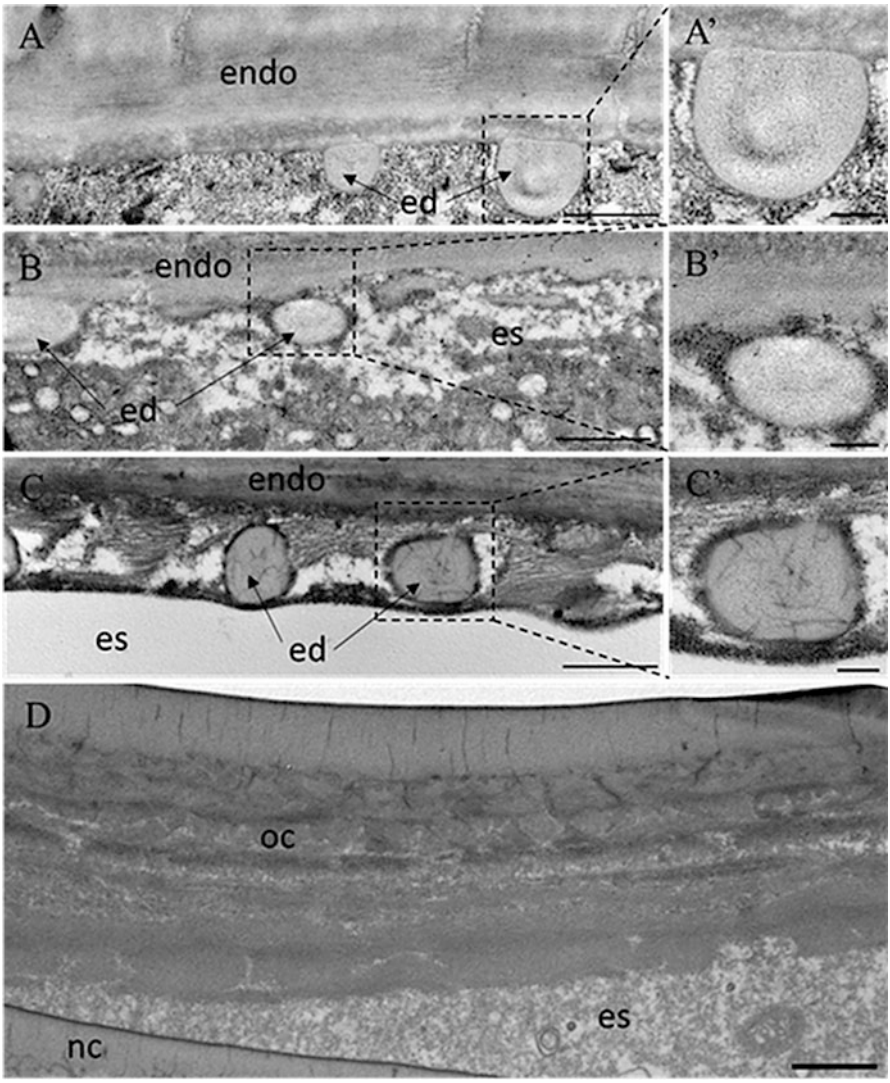

Fig. 1.4 Formation of ecdysial droplets and digestion of the old cuticle. (A-A') Appearance of ecdysial droplets containing degrading enzymes at the apical plasma membrane of the epidermis. (B-B′) Separation of ecdysial droplets from the apical plasma membrane when ecdysial space begins to emerge. (C-C′) Digestion of proteins in the innermost layer of old endocuticle with the chitin filaments remaining in or around ecdysial droplets as new procuticle is deposited. (D) Disappearance of ecdysial droplets as new cuticle is formed just before ecdysis. *ed* ecdysial droplets, *es* ecdysial space, *endo* endocuticle, *oc* old cuticle, *nc* new cuticle; A-D, scale bar = 1 μm; A'-C′, scale bar = 250 nm

layer of the old endocuticle are digested with the chitin filaments remaining in or around the ecdysial droplets. After the chitin is gradually wrapped and degraded, the ecdysial droplets are dissolved when the new exocuticle is formed. The ecdysial droplets completely disappear when the exocuticle fully matures. At this point, chitin degradation is stopped, and ecdysis is triggered.

Chitin degradation is catalyzed by a two-component chitinolytic enzyme system (Fukamizo and Kramer 1985a, b). It is first hydrolyzed by CHTs, mainly in Group I and II (i.e., CHT5 and CHT10), in a random fashion into chitin oligomers. The oligomers are subsequently hydrolyzed by NAGs from the nonreducing end into the monomeric GlcNAc (Zhu et al. 2008b). The exochitinase activity is exhibited by NAGs which often synergistically act in concert with endochitinases to depolymerize the chitin polymer in insects (Lu et al. 2002). In some cases, additional unrelated proteins, which possess one or more chitin-binding domains (CBD) but are devoid of chitinolytic activity, enhance the degradation of chitin (Vaaje-Kolstad et al. 2005).

The synergistic action of CHTs and NAGs in chitinolysis highly depends on the concentration ratio of these two enzymes, suggesting that alterations in the proportions of these enzymes could affect the rate and/or extent of chitin degradation (Fukamizo and Kramer 1985a, b). Indeed, the net effect of suppressing the expression of *CHT* and *NAG1* appears to disrupt the two-enzyme system, resulting in inefficient chitin degradation. In *T. castaneum*, the phenotype due to the suppression of *TcNAG1* expression by RNAi is strikingly similar to those by the suppression of *TcCHT5* or *TcCHT10* by RNAi (Hogenkamp et al. 2008; Zhu et al. 2008b). Insects injected with dsRNA for *TcCHT5*, *TcCHT10*, or *TcNAG1* fail to shed their old cuticle, leading to their developmental arrest. In *L. migratoria*, injection of dsRNAs of *LmNAG1*, *LmCHT5*, or *LmCHT10* led to disrupted ecdysis and insect mortality (Rong et al. 2013). These studies seem to indicate that NAG1 is the enzyme primarily responsible for efficient degradation of cuticular chitin in concert with CHT5 or CHT10 in different insect species.

The key to chitin degradation process is the elaboration of molting fluid with an assortment of CHTs and proteases that control appropriate amounts of chitin and ensure for normal molting. During the insect development and periodical molting, CHTs and NAGs are found in the molting fluid and midgut (Fukamizo and Kramer 1985b; Samuels et al. 1993). Kramer et al. (1993) found that CHT genes were not expressed in feeding larvae and only began to be expressed in a short time before larval molting, pupation, or adult emergence in the cuticle and internal organs of *M. sexta*. Meanwhile, the expression of *CHT* genes is upregulated by molting hormone but downregulated by juvenile hormone (Kramer et al. 1993). Indeed, 20E can enhance protein expression of *CfCHT5* in *C. fumiferana* (Zheng et al. 2003).

In *L. migratoria*, the expression of both *LmCHT5-1* and *LmCHT5-2* is dramatically increased from fourth-instar to fifth-instar nymphs and then to adults during a specific time prior to each molting. Such expression patterns appear to coincide with the 20E titers (Li et al. 2015), suggesting that the expression of *LmCHT5*s is under endocrine regulation. After the injection of 20E, both the *LmCHT5* transcripts sharply increased with a dramatic peak of the expression (27-fold for *LmCHT5-1* and 410-fold for *LmCHT5-2*) after 6 hours. Conversely, the injection of ds*LmEcR*

dramatically decreased the transcripts of both *LmCHT5-1* and *LmCHT5-2*. Researches also showed that the microRNA, miR-263, can negatively regulate *LmCHT10* transcript, interrupt the chitin degradation process, and finally lead to molting defect in *L. migratoria* (Yang et al. 2016). Similarly, miR-24 was identified to regulate the expression of *HaCHT5* both in vitro and in vivo in *H. armigera* (Agrawal et al. 2013). Apparently, the expression of insect CHTs is regulated by multiple factors.

In *M. sexta*, the expression of *NAG* in fifth-instar larvae was found to increase from day 5 to day 8 and positively correlate with the content of molting hormone in hemolymph (Zen et al. 1996). After the insect was injected with the molting hormone, the *NAG* mRNA level was increased in the integument by tenfold within 2 days. When *NAG* mRNA peaked at days 6 and 7, *CHT* mRNA disappeared, indicating a cross-expression pattern between *CHT* and *NAG*. In *L. migratoria*, *LmNAG1* transcript level in the integument is significantly high in the last 2 days of fourth- and fifth-instar nymphs. Silencing *LmNAG1* resulted in significant reduction of total LmNAG enzyme activity at 48 and 72 hours after the injection of *LmNAG1* dsRNA. Furthermore, 50% of the *LmNAG1* dsRNA-injected nymphs were not able to molt successfully and eventually died, suggesting that *LmNAG1* plays an essential role in molting process of *L. migratoria* (Rong et al. 2013).

1.3.3 Roles of Chitin Degradation in Cuticle Formation

Arthropods must periodically replace their old cuticle with a new one because the cuticle is too rigid to allow for their growth and development. The successful ecdysis depends on elaborated regulation of chitin degradation in the old cuticle and chitin synthesis for the formation of new cuticle. Indeed, chitin degradation of the old cuticle has been considered as an important process contributing to new cuticle formation. As described previously, ecdysial droplets emerge at the beginning of apolysis, which involves both chitin and protein degradation. The chitin degradation facilitates the formation of "apolytic space" between the newly produced cuticle and the old one and allows cuticular components secreted from epidermal cells and deposited on surface of apical plasma membrane. To form new cuticle, insects need substrate materials to synthesize chitin. Insects recycle monosaccharide from chitin degradation as substrates to produce new chitin polymer as an efficient strategy to accomplish the chitin metabolism cycle. Besides the synthesis of new chitin polymers, the complete replacement of the entire outer shell of an insect includes discarding the outer, which is highly sclerotized and includes waterproofed layers, and digesting the inner, which has more pliable layers for further recycling and resorption (Reynolds and Samuels 1996; Merzendorfer and Zimoch 2003).

Although chitin degradation is beneficial for cuticle formation by creating an apolytic space to allow for the deposition of newly produced chitin, the newly secreted chitin needs to be protected from chitin degradation as the synthesis of new cuticle and the partial degradation of the overlying old cuticle occur

concurrently. According to the long-held theory, a thin, nonchitinous envelope layer, which is deposited by the epidermal cells just before the secretion of new cuticular chitin, plays a critical role in protecting the newly synthesized cuticle from the degradation by enzymes in the molting fluid. This theory regards the envelope layer as a physical barrier to protect newly deposited chitin from contacting with molting fluid enzymes. In *T. castaneum*, however, the chitin-degrading enzyme CHT5 in the molting fluid is not excluded from the newly synthesized cuticle (Chaudhari et al. 2011). This finding challenges the conventional theory that the newly synthesized cuticle is protected by the physical barrier. Instead, the newly synthesized cuticle is protected from CHT5 action by the action of a protein called Knickkopf (TcKNK) in *T. castaneum*. TcKNK organizes chitin into laminae to confer selective protection of the new cuticle from the degradation by CHT5, but simultaneously allows the digestion of chitin in the inner layers of the old procuticle that enshrouds it (Chaudhari et al. 2011). Because KNKs are highly conserved across different invertebrates, such as insects, crustaceans, and nematodes, it has been suggested that this protein plays critical roles in the laminar ordering and protection of cuticular chitin in all these chitinous invertebrates.

1.4 Chitin-Binding Proteins in Arthropods

1.4.1 Classification and Characteristics of Chitin-Binding Proteins

Chitin is usually found in association with numerous proteins that influence the overall mechanical and physicochemical properties of the chito-protein matrix, which can range from very rigid (e.g., head capsule and mouthparts) to fully flexible (e.g., larval integument, intersegmental membrane, and wing cuticle). Since chitin is an extracellular matrix polysaccharide, the proteins that have an affinity for chitin are expected to be extracellularly secreted. Since the first insect genome was sequenced in *D. melanogaster* (Adams et al. 2000), more than 100 insect genome sequences have now become available at the *National Center for Biotechnology Information* (NCBI). Based on these genome sequences, a large number of CBPs have been identified in insects, such as *A. gambiae*, *A. mellifera*, *B. mori*, *D. melanogaster*, *N. lugens*, *N. vitripennis*, and *T. castaneum*, and from crustacean, such as the water flea (*Daphnia pulex*).

Three groups of the proteins containing sequence motifs with chitin-binding ability have been identified in insects (Willis 2010; Ioannidou et al. 2014). The first group of CBPs represents a very large number of insect CPs and CP-like proteins. The availability of fully sequenced and annotated genomes of many insect species, including *A. mellifera* (Honeybee Genome Sequencing Consortium 2006), *D. melanogaster* (Karouzou et al. 2007), *T. castaneum* (*Tribolium* Genome Sequencing Consortium 2008; Dittmer et al. 2012), *A. gambiae* (Cornman et al.

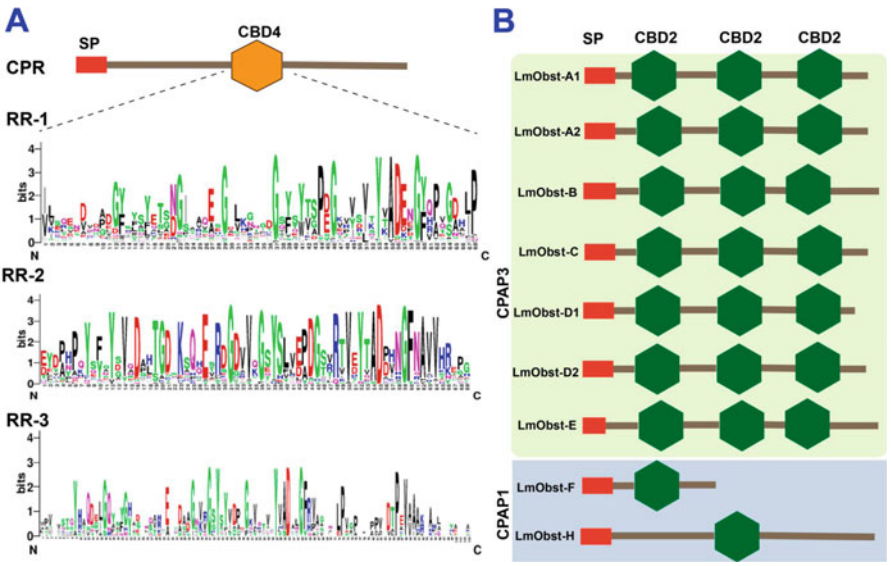

Fig. 1.5 The RR motifs of CPR family and the structure of CPAP family proteins in the migratory locust (*L. migratoria*). (**a**) The conserved sequences of the RR motifs. (**b**) The structure of CPAP family proteins. *SP* signal peptide, *CBD4* chitin-binding domain 4, and *CBD2* chitin-binding domain 2

2008), *B. mori* (Futahashi et al. 2008), *N. vitripennis* (Werren et al. 2010), and *M. sexta* (Dittmer et al. 2015), allows rapid identifications of the genes putatively encoding these proteins in recent years. More than 200 putative CP genes have been identified in *D. melanogaster* (Karouzou et al. 2007), *A. gambiae* (Ioannidou et al. 2014), and *M. sexta* (Dittmer et al. 2015). It has been estimated that these genes comprise about 2% of all predicted protein-coding genes in some insect species, such as *A. gambiae* (Willis 2010). Indeed, recent studies identified peptides from 244 of the 298 CPs in *A. gambiae* (Zhou et al. 2018).

The CPs have been divided into 13 different families as defined by their unique amino acid sequence motifs (Zhou et al. 2016). However, such classification is relatively arbitrary and subject to change (Willis 2010; Zhou et al. 2016). The largest CP family is the CPR family (Fig. 1.5). The CPRs are so named because these CPs contain a Rebers & Riddiford Consensus (R&R Consensus) of 35 amino acid residues (G-x(8)-G-x(6)-Y-x(2)-A-x-E-x-G-F-x(7)-P-x-P) identified by Rebers and Riddiford (1988). The R&R Consensus contains a CBD4 (chitin-binding domain 4) that apparently helps to coordinate the interactions between chitin fibers and the proteinaceous matrix (Rebers and Willis 2001; Togawa et al. 2004, 2007; Qin et al. 2009). Three distinct forms of the Consensus have been recognized and named by Anderson (1998, 2000), which include RR-1, RR-2, and RR-3 CPRs. The CPRs with the RR-1 and RR-2 Consensus might be associated with soft (flexible) and rigid (hard) cuticles (Willis 2010) or might predominantly form endocuticle and

exocuticle, respectively (Andersen 2000). The RR-3 CPRs are less common, and their distinctive features have not been clearly established (Willis 2010).

Many CPRs have been identified, but their number varies largely in different insect species. For example, *A. mellifera*, *B. mori*, *D. melanogaster*, *L. migratoria*, *M. sexta*, and *N. lugens* possess 28, 148, 101, 51, 207, and 96 CPRs, respectively (Willis 2010; Zhao et al. 2017; Pan et al. 2018). Phylogenetic analysis using the RR-1 and RR-2 proteins from *A. mellifera*, *B. mori*, and *D. melanogaster* suggests that CPRs may be evolved independently among insect taxa. Besides CPRs, there are other CP protein families, including CPF (with a motif of 42–44 amino acid residues), CPF-like (CPFL, like the CPFs in a conserved *C*-terminal region), CPT (with a Tweedle motif), CPG (glycine-rich), CPAP (cuticular proteins analogous to peritrophins which are a group of proteins tightly associated with the PM), CPH (hypothetical CPs), CPLC (CPs with low complexity; CPLCA, CPLCG, CPLCW, and CPLCP named after particular diagnostic features), and Apidermin (named after three *proteins* in *A. mellifera*) (Willis 2010). The CPAP family proteins have either one or three CBD2 domains but no other identifiable protein domains (Fig. 1.5). The CBD2 belongs to the carbohydrate-binding module family 14 (CBM14) binding domains also known as type 2 CBD (i.e., CBD2) with chitin-binding ability (Elvin et al. 1996). Based on the number of the CBD2 domains, CPAPs are further classified into CPAP1 and CPAP3 families with one and three CBD2 domains, respectively (Jasrapuria et al. 2010, 2012).

The second group of CBPs is peritrophic matrix proteins (PMPs) that can be extracted from insect PMs (Jasrapuria et al. 2010). PMPs contain six cysteine residues known as "peritrophin A" motif (Tellam et al. 1999), which is assumed to form three disulfide bridges. The extracted or heterologously expressed PMPs have chitin-binding activity (Elvin et al. 1996; Wijffels et al. 2001; Wang et al. 2004). *PMPs* possess CBD2 domains that can bind chitin (Elvin et al. 1996). Indeed, it has been demonstrated that even a single CBD2 domain of the CBP1, a PMP of *T. ni*, heterologously expressed in an insect cell line, has chitin-binding ability (Wang et al. 2004). PMPs are highly resistant to proteolytic degradation as potential trypsin and chymotrypsin cleavage sites reside primarily within the CBD sequences, which limits exposure of the potential cleavage sites to the digestive proteinases (Wang et al. 2004). The genes encoding the proteins with CBD2 have also been identified in cuticle-forming tissues from *D. melanogaster* (Barry et al. 1999; Behr and Hoch 2005). In *C. fumiferana*, a gene putatively encoding a protein homologous to these proteins is highly expressed in the epidermis, and the recombinant version of this protein can bind to chitin (Nisole et al. 2010). Thus, it is apparent that the proteins containing CBD2 are not only present in the PM but also in cuticle-forming tissues (e.g., integument, tracheae).

The CBPs with the CBD2 motif can be further divided into three groups, including the PM proteins, CPs analogous to peritrophins-3 (CPAP3, containing three CBD2 domains), and CPs analogous to peritrophins-1 (CPAP1, containing one CBD2 domain) (Jasrapuria et al. 2010). The number of CBD2 domains varies (with 1–19 CBD2 domains) in insect PMPs. The PMPs with multiple CBD2 domains are difficult to extract due to their strong association with the PM. Furthermore, the number of

PMPs in different species also varies largely as, for instance, 65 PMPs are predicted in *A. aegypti* and *D. melanogaster*, but only 11 are identified in *T. castaneum* (Venancio et al. 2009; Jasrapuria et al. 2010). The second group also includes enzymes of chitin metabolism such as CHTs and CDAs, some of which have the CBD2 motif (Kramer et al. 1993; Campbell et al. 2008; Dixit et al. 2008; Zhu et al. 2008a). These proteins contain one or more copies of the CBD2 motif, and the affinity of these enzymes to colloidal chitin progressively increases as the copy number of this domain in the proteins increases (Arakane et al. 2003). The third group of CBPs includes the family of antimicrobial peptides related to tachystatins from horseshoe crab (denoted as A1, A2, B1, B2, and C subfamilies) and the calcium channel antagonists, agatoxins, from spider venom. For example, tachystatin B, an antimicrobial, is a chitin-binding peptide isolated from the Japanese horseshoe crab (*Tachypleus tridentatus*). It consists of two isopeptides called tachystatin B1 and B2. This group of proteins with six cysteines and a high affinity for chitin has a triple-stranded β-sheet structure with an inhibitory cysteine knot motif (Fujitani et al. 2007).

1.4.2 Roles of Cuticular Proteins in Exoskeleton Formation

1.4.2.1 Roles of Cuticular Proteins

The CPs are the main components of exoskeleton and play a major role in determining the diverse physical properties of the cuticle depending on developmental stages as well as different body regions as a result of interactions with chitin and other CPs in arthropods (Neville 1993; Lomakin et al. 2011). Distinctly different expression patterns of the CPs in different developmental stages or in different body regions may imply the difference of their roles. For instance, 23 RR-2 CP genes are expressed at larval and pupal molting stages, whereas RR-1 CP genes are predominantly expressed in the epidermis during the larval molt and intermolt stages in *B. mori* (Okamoto et al. 2008; Liang et al. 2010). Nevertheless, functional significances of different CPs in arthropod cuticle are still not well established. It is reported that some are essential for maintaining the structural integrity of the cuticle and are found in specific locations within the cuticle.

In *B. mori*, a deletion mutation of *BmCPR2* encoding an RR-1 protein is found to be responsible for the *stony* mutant (Qiao et al. 2014). The dysfunctional BmCPR2 due to the mutation leads to significantly decreased cuticular chitin content, abnormal distribution of internode, and intersegmental fold in larvae. In *T. castaneum*, two major structural RR-2 proteins, TcCPR27 and TcCPR18, are essential for maintaining elytra rigidity of the beetle (Arakane et al. 2012). RNAi targeting *TcCPR27* or *TcCPR18* gene can cause disorganization of the laminar architecture and amorphous pore canal fibers, resulting in wrinkled and improperly expanded elytra. These results suggest that TcCPR27 and TcCPR18 play an important role in maintaining structural integrity of the elytra cuticle. In *N. lugens*, silencing of

15 CPR genes led to lethal phenotypes, indicating their essential roles in the integument structure and normal development (Pan et al. 2018).

LmACP7, a wing-specific protein that belongs to RR-2 subfamily of the CPR family, has been identified in *L. migratoria* (Zhao et al. 2017). LmACP7 occurs in the exocuticle of adult wings and is an essential structural component required for normal morphological and functional maintenance for the adult wing cuticle (unpublished data). In addition, several CPs have shown unique distribution patterns and structural functions in the organization of chitin into compact fibrils and/or laminae in procuticle. For example, in rigid cuticle of the TcCPR27-deficient adult *T. castaneum*, TcCPR4 (an RR-1 protein) uniquely distributed in the pore canals is mislocalized and distributed over the entire exocuticle, suggesting that TcCPR4 is important for determining the morphology and ultrastructure of the pore canal fibers and pore canals (Noh et al. 2015).

In *T. castnaeum*, eight CPAP3 proteins are encoded by seven different genes (Jasrapuria et al. 2012). Functional analyses of all these genes by RNAi indicate that many of these genes have distinct and non-redundant essential functions in establishing and maintaining the structural integrity of the cuticles with a wide range of physical properties. Many CPAP3 family proteins are likely to have essential functions as they are evolutionarily conserved among different insect species. In *D. melanogaster*, for example, obstructor A (orthologs of TcCPAP3 family) has been proposed to have a genetically conserved function by which it forms a matrix scaffold to coordinate trafficking and localization of proteins and enzymes in the newly deposited apical ECM. This function is critical for maturation and stabilization of the ECM as an outermost barrier in a growing and remodeling the epithelial tissue (Petkau et al. 2012; Pesch et al. 2015).

Mutants of *CPAP3-C* gene are embryo-lethal and can exhibit cuticle defects in *D. melanogaster* (Barry et al. 1999; Behr and Hoch 2005). Similar results were obtained in *N. lugens* for the genes encoding the CPAP1 and CPAP3 family proteins by RNAi (Pan et al. 2018). For the CPT family proteins, light microscope studies using fluorescently tagged proteins have shown that Tweedle proteins are incorporated into the cuticle structures in larvae, and a mutation of TweedleD gene can alter overall morphology, which confirm its role in determining body shape of *D. melanogaster* (Guan et al. 2006). In *B. mori*, transgenic overexpression of *BmCPT1*, a cuticle protein bearing a Tweedle domain, can cause upregulated expression of *BmRelish1* (a transcription factor controlled by the immune deficiency pathway) and induction of two gloverin genes (Liang et al. 2015). These findings suggest that *BmCPT1* is involved in innate immunity by participating in recognition of *Escherichia coli.*

In *A. gambiae*, four CPF genes and one CPFL gene were identified (Togawa et al. 2007). These genes are expressed just before pupal or adult ecdysis, which suggests that they may be involved in the formation of the outer layer of pupal and adult cuticles. In *B. mori*, *BmCPH24* (a member of CPH family), which is expressed in larval epidermis post ecdysis, was recently identified from a silkworm Bamboo (Bo) mutant. The RNAi-mediated knockdown and CRISPR/Cas9-mediated knockout of *BmCPH24* implies that BmCPH24 may be involved in the synthesis of

endocuticle (Xiong et al. 2017). Furthermore, the *B. mori* Bamboo (*Bo*) mutant with *BmCPH24* gene mutation is more susceptible to exposures to ultraviolet and the insecticide deltamethrin due to the deficiency in resources required to construct the cuticle (Xiong et al. 2018).

For the CPLC family, a CP with a low-complexity sequence (TcCP30) was identified from *T. castaneum*. Loss of function of TcCP30 by RNAi showed no effect on larval and pupal growth and development; however, about 70% of the adults were unable to shed their exuviae and died during adult eclosion (Mun et al. 2015). Furthermore, TcCP30 becomes cross-linked to TcCPR27, TcCPR18, and itself by the action of laccase2 (Mun et al. 2015). More recently, a gene encoding a novel ungrouped CP, NlCP21.92, was identified in *N. lugens* (Lu et al. 2018). The *NlCP21.92* gene is expressed at high levels in the integument, and RNAi-mediated silencing of the gene resulted in abnormal and lethal morphological phenotypes. Analysis with TEM suggests that this gene is essential for the formation of endocuticle. Nevertheless, still the function and mechanism in the formation of cuticle for the other CP families remain unclear.

1.4.2.2 Temporal and Spatial Variations of Cuticular Proteins

Many sequences of CPs have been identified from pre-ecdysial and post-ecdysial cuticles in different insect species. In *T. molitor*, five sequences have been identified as post-ecdysial CPs from the pupae (Baernholdt and Anderson 1998; Mathelin et al. 1998) but nine as pre-ecdysial CPs from the pupae of the same species (Andersen 1995; Haebel et al. 1995; Rondot et al. 1996; Andersen et al. 1997). In *L. migratoria*, two post-ecdysial proteins were identified from the adult cuticle (Talbo et al. 1991; Jespersen et al. 1994), two post-ecdysial proteins from the nymph cuticle, but 20 pre-ecdysial proteins from the pharate adult cuticle (Nohr et al. 1992; Andersen 1995; Jensen et al. 1998). In the desert locust (*Schistocerca gregaria*), eight sequences have been reported as post-ecdysial proteins from the adult cuticle of (Jespersen et al. 1994; Andersen 1998). On the other hand, three post-ecdysial CPs have been identified from the nymphs of the true death's head cockroach (*Blaberus craniifer*) (Jensen et al. 1997). However, some of these CPs do not have a CBD; therefore, these proteins may not be able to bind to chitin. More recently, Zhou et al. (2018) revealed that most CPs are shared among different structures and developmental stages of *A. gambiae*. Only very few are restricted to a single stage or a single adult structure.

Four major CPs (BMCP30, 22, 18, and 17) have been purified from the cuticle of *B. mori* larvae (Togawa et al. 2004). Further analysis of their binding activity has shown that the conserved R&R Consensus functions as the CBD in the formation of the two procuticle layers. The timing of expression defines the type of CPs that constructs the layer and determines the nature of each cuticular layer. In wing disks of *B. mori*, for example, 52 CP genes were examined for their expression profiles. According to the stages of peak expression of these genes, the RR-2 protein genes are expressed until the day of pupation, whereas the RR-1 protein genes are expressed before and after the pupation. Furthermore, the expression durations of

the RR-1 protein genes were longer than those of the RR-2 protein genes, suggesting different constructions of exo- and endocuticular layers (Shahin et al. 2016). Based on such expression profiles of the CP genes in *B. mori*, it has been speculated that the exocuticle is constructed with the RR-1, RR-2, and other types of CPs, whereas the endocuticle is formed with the RR-1 and other CPs (Shahin et al. 2016, 2018).

By using the *immunogold-labeling* technique with TEM, the position of several RR-1 and RR-2 proteins have been localized in the cuticle of *A. gambiae* (Vannini and Willis 2017). The RR-1 proteins are localized in the procuticle of the soft intersegmental membrane except for one protein, which is found in the hard endocuticle, whereas the RR-2 proteins are consistently found in the hard cuticle and not in the flexible cuticle. Because the histidine residues of the CPs are used for the sclerotization of cuticles (Schaefer et al. 1987; Hopkins et al. 2000; Andersen 2010), the CPs in the exocuticle contain high percentage of histidine residues. In contrast, as acidic amino acids are involved in soft cuticle, such as intersegmental membrane or larval cuticle (Cox and Willis 1987; Missios et al. 2000), acidic amino acid residues may be frequently involved in the CPs of the endocuticle. It has been recently reported that TcCP30 containing a low-complexity sequence is cross-linked with the two RR-2 CPs, TcCPR18 and TcCPR27, by laccase2, but not with the RR-1 CP, TcCPR4, in *T. castaneum* (Mun et al. 2015). TcCP30, a 19-kDa protein without the RR motif, is the third most abundant protein in the elytra of *T. castaneum.* As the RR-2 CPs, such as TcCPR18 and TcCPR27, contain high percentage of histidine residues that may allow these proteins to participate in cross-linking. In contrast, TcCP30 can undergo laccase2-mediated cross-linking with itself and its putative cross-linking partners, the RR-2 CPs, to contribute to the strength of the cuticle during cuticle maturation (Iconomidou et al. 2005; Mun et al. 2015).

1.4.3 Peritrophic Matrix-Associated Proteins

1.4.3.1 Chito-Protein Network in Peritrophic Matrix

The PM is mainly composed of chitin and proteinaceous components including glycoproteins, proteoglycans, and proteins (i.e., PMPs). The proteinaceous part is estimated to account for 20–55% (w/w) of the total PM mass (De Mets and Jeuniaux 1962; Zimmermann et al. 1975). Although the number of PMPs varies significantly in different insect species, it is estimated that the total number of PMPs ranges from 10 to 20. The highly ordered structure of the PM is thought to be maintained by the interaction of PMPs with the chitin fibrils. PMPs have one or more copies of the CBD2 motif, allowing them to bind to chitin. Different numbers of the CBD2 domains were revealed in dipteran, lepidopteran, and coleopteran species, including the Australian sheep blowfly (*Lucilia cuprina*) (Elvin et al. 1996; Tellam et al. 1999), *A. gambiae* (Shen and Jacobs-Lorena 1998, 1999), *H. armigera* (Wijffels et al. 2001), the tsetse fly (*Glossina morsitans* (Hao and Aksoy 2002), *A. aegypti* (Shao et al. 2005), *D. melanogaster* (Kuraishi et al. 2011), *T. ni* (Wang et al. 2004), and *T. castaneum* (Agrawal et al. 2014).

The number of CBDs present in the PMPs appears to be crucial in organizing the 3D meshwork of the PM. However, the precise function of individual PMPs with different numbers of CBDs in organizing chitin fibril architecture remains speculative. For example, many PMPs with a single CBD have been identified in insects that contribute to the internal stability of the PM, as this would require additional CBDs to allow the formation of cross-links (Wijffels et al. 2001; Jasrapuria et al. 2010; Tetreau et al. 2015b). PMPs with several (2–5) CBDs are thought to be PM integral proteins that largely determine the overall structure of the PM and its physicochemical properties. It is suggested that these PMPs assemble the chitin fibrils into a wide cross-hatched matrix to form water-filled pores (Dinglasan et al. 2009; Agrawal et al. 2014). On the other hand, PMPs with multiple (6–19) CBDs have been suggested to integrate into the PM after being proteolytically processed into smaller fragments by midgut proteases such as trypsin. Wang et al. (2004) described two CBPs (CBP1 and CBP2) consisting of long (10–12) multimers of CBDs in *T. ni* and proposed that they might contribute to maintaining the internal structure of the PM chitin microfibril network within the protease-rich environment of the midgut.

Insect peritrophins may also contain mucin domains (MDs). Such peritrophins are referred to as insect intestinal mucins (IIMs) (Wang and Granados 1997). IIMs have been described in both *T. ni* and the diamondback moth (*Plutella xylostella*) (Wang and Granados 1997; Sarauer et al. 2003). The IIM is composed of alternating CBD and spacer elements and portrayed with the *O*-linked glycans projecting into the interstitial space. The additional cysteine residues present in the carboxy-terminal CBD may form intermolecular disulfide bridges. Shi et al. (2004) characterized two genes encoding the two PMPs including McMUC1 (an IIM) and McPM1 (a peritrophin consisting of 19 CBDs) from *M. configurata*. McMUC1is similar in structure to other IIMs and is highly glycosylated. The authors proposed that McPM1 might interact with chitin interfibril junctions whereas McMUC1 with the extended chains in the internodal regions. Although many PMP genes have been identified from various insect species, the major question as to what features of the chitin-PMP network determine the permeability of the PM remains unanswered. Nevertheless, research has suggested that specific PMPs may be involved in the regulation of PM permeability (Agrawal et al. 2014).

1.4.3.2 Characteristics of Chito-Protein Matrix

Depending on the physiological context, the PM is composed of varying constituents that confer characteristic properties needed for its respective functions. According to the binding levels of the PMPs to the PM, PMPs are divided into four classes, including class I, the PMPs covalently attached to the PM; class II, the PMPs not covalently but closely bound to the PM; class III, the PMPs that can be removed with a mild detergent; and class IV, the PMPs that can be removed at low or high ionic concentrations (Tellam et al. 1999). PMPs often possess CBDs or peritrophin domains. Insect peritrophins contain 60–75 amino acid residues with a conserved register of cysteine residues and a number of aromatic amino acid residues (Tellam

et al. 1999). The conserved cysteine residues may be involved in the formation of intradomain disulfide bonds that enhance the peritrophin stability in the protease-rich gut environment.

The interactions between chitin microfibrils and PMPs in the PM primarily rely on the CBDs of PMPs. Indeed, PMPs identified in different insect species contain one or more CBDs with 6–10 conserved cysteine residues. Several peritrophins have been identified from dipterans such as *L. cuprina* (Tellam et al. 1999; Wijffels et al. 2001), *A. gambiae* (Shen and Jacobs-Lorena 1999), and *G. morsitans* (Hao and Aksoy 2002). Among them, three types of CBD domains (peritrophin A–C) have been identified based on the number and arrangement of conserved cysteine residues (Tellam et al. 1999). The peritrophin CBDs have been subdivided into peritrophin A domain (PAD), peritrophin B domain (PBD), and peritrophin C domain (PCD) based on the number and arrangement of conserved cysteine residues (Tellam et al. 1999). The PAD contains a register of six cysteine residues that can form three disulfide bonds between them and is common in invertebrates. However, the PBD and PCD domains have eight and ten cysteine residues, respectively (Tellam et al. 1999). The PAD, which belongs to type II CBD, is the most common CBD in PMPs and is the only type found in lepidopteran peritrophins (Shi et al. 2004; Wang et al. 2004; Campbell et al. 2008; Toprak et al. 2016).

The IIMs are rich in threonine, serine, and proline residues with a high *O*-glycosylation potential (Toprak et al. 2010) and contribute to certain functional attributes such as barrier formation, protection from digestive enzymes, and lubrication (Wang and Granados 1997; Sarauer et al. 2003). In *M. configurata*, several PMPs including IIMs (McIIM1, McIIM2, and McIIM4) and nonmucin peritrophins (containing only CBDs, McPM1, McPPAD1) have been characterized (Shi et al. 2004). These proteins bind to chitin microfilaments in the form of covalent or non-covalent bonds, which constitute the framework of the PM. In *T. ni*, a highly *O*-glycosylated IIM consisting of 807 or 788 amino acid residues is identified (Wang and Granados 1998). The IIM is similar to human intestinal mucin (MUC2) and tightly binds to chitinous reticular matrix through disulfide bonds in the PM. Such a unique structure of the chito-protein matrix may greatly enhance the PM's physical strength to provide a protective barrier against particles and infectious agents in insect midgut.

1.5 Utilities of Chitin and Its Derivatives and Chitin Metabolic Pathway

1.5.1 Applications of Arthropod Chitin and Chitin-Derived Products

Chitin and chitosan are used in a wide range of applications due to their many excellent properties, including the biocompatibility, biodegradability, non-toxicity,

and adsorption. They are used in biomedical and pharmaceutical industries (Muzzarelli et al. 1997; Ravi Kumar 1999; Kato et al. 2003; Singh et al. 2017), drug delivery and controlled release (Huang et al. 2017; Ahsan et al. 2018; Ali and Ahmed 2018), food processing and packaging (Romanazzi et al. 2017; Verlee et al. 2017; Wang et al. 2018), environmental engineering and waste management (Peniche-Covas et al. 2010; Olivera et al. 2016; Kanmani et al. 2017), and cosmetics and cosmeceutical applications (Aranaz et al. 2018). Because Chap. 20 provides a comprehensive review on the applications of chitosan, this section gives only a brief survey.

Beschitin-F (chitin-coated gauze) is a nonwoven, chitosan-based material developed by the UNITIKA Company in Japan. Previous studies have shown that Beschitin-F is an excellent nasal filler material for mucous membrane irritation in nasal packing (Zheng et al. 2017). In addition, chitosan may be also used to inhibit fibroplasia in wound healing and to promote tissue growth and differentiation in tissue culture (Muzzarelli et al. 1999). The antimicrobial and wound-healing properties of chitosan along with an excellent film capability make chitosan suitable for development of ocular bandage lenses (Elieh-Ali-Komi and Hamblin 2016). In tissue engineering, the diversity and availability of chitosan-based materials and increased clinical demand for safe scaffolds lead to an increased interest in fabricating scaffolds and have achieved fruitful progress, such as hydrogels, bioceramics, and composite (biocomposites/nanocomposites) (Ulery et al. 2011; Ahmed et al. 2018; Guo and Ma 2018). Chitosan and its derivatives have also been used as vehicles for drug delivery to achieve the purpose of sustained release and controlled release for drugs, improve the stability of drugs, and reduce adverse drug reactions. Similarly, in insect science, chitosan has been used to generate dsRNA/chitosan nanoparticles to effectively deliver dsRNA to suppress the expression of insect target genes (Zhang et al. 2010b). Many recent reviews have highlighted the popularity of chitosan and its derivatives for their use as a matrix molecule for drug delivery and their upcoming utilities in the pharmaceutical industry (Ahsan et al. 2018; Huang et al. 2017; Ali and Ahmed 2018).

In the food industry, chitin and its derivatives are mainly used as food additives, preservatives, and packaging materials, such as diet food, health food for hypertension, and cardiovascular diseases. Chitosan-based films can be used as food packaging materials and extend the shelf life of food, in the form of pure chitosan films, chitosan/biopolymer films, chitosan/synthetic polymer films, and chitosan derivative films (Romanazzi et al. 2017; Verlee et al. 2017). Indeed, different chitosan-based films have already been developed and applied in the field of food packaging, such as antibacterial films, barrier films, and sensing films (Wang et al. 2018). Chitin is also widely used to immobilize enzymes such as clarification of fruit juices and processing of milk when α- and β-amylases or invertase are grafted on chitin (Krajewska 2004).

Because chitosan and its derivatives have strong adsorption on metal ions, they can be used to treat industrial wastewater or remove heavy metals from wastewater, such as Hg^{2+}, Cd^{2+}, Cu^{2+}, Ni^{2+}, and Zn^{2+} (Peniche-Covas et al. 2010; Kanmani et al. 2017). Due to its unique molecular structure, chitosan has an extremely high affinity

for many classes of toxic dyes and has application in wastewater treatment (Olivera et al. 2016). Chitin has also been applied in fermentation industry and bioengineering. Due to a positive charge and a strong adsorption, chitosan can be used to separate proteins and amino acids and prepare affinity chromatography column to isolate and purify lectins and determine their structure (Datta et al. 1984).

For cosmetics and cosmeceutical applications, chitin and chitosan have been used as cosmetic ingredients because of their biodegradable, biocompatible, viscosity, and moisture-holding properties. Chitosan is the only natural cationic gum that becomes sticky when neutralized with acid. These materials are used in creams, lotions, and permanent waving lotions. Some commercial products are hair care products containing chitosan, skin care products containing carboxymethyl chitosan, and chitin suture absorbable in tissues (Aranaz et al. 2018).

1.5.2 Chitin Metabolic Pathway as Target for Arthropod Pest Management

The absence of chitin in vertebrate animals and plants has led to the development of new strategies to manage arthropod pest species by targeting their enzymes involved in the synthesis, modification, and degradation of chitin, which has been comprehensively reviewed by Cohen (2010) and Doucet and Retnakaran (2016). Indeed, many genes responsible for chitin biosynthesis and metabolism have been examined as potential targets for arthropod pest management. First, the chitin biosynthetic pathway can be blocked or disrupted to result in an incomplete and deformed molt that consequently leads to lethality. Commonly used chitin synthesis inhibitors as insecticides belong to the group of benzoylphenylurea (BPU) insecticides that cause molt deformities in intoxicated arthropods. BPUs adversely interfere with chitin biosynthesis in arthropods and manifest their effects during the molting process. The first compound in the BPU group is diflubenzuron discovered by the scientists at the Philips-Duphar company in 1970 (Palli and Retnakaran 1999). Mulder and Gijswijk (1973) first reported that diflubenzuron (PH6038) was able to affect the normal deposition of chitin in the cabbage white butterfly (*Pieris rapae*). Since then it has spawned the development of a whole array of new insecticide analogs (Palli and Retnakaran 1999).

Currently, at least 14 BPUs are available for arthropod pest management with an annual global market value of $441 million (Sparks and Nauen 2015). For example, hexaflumuron has been used for the control of the western subterranean termite (*Reticulitermes hesperus*) (Haagsma and Rust 2005) and many lepidopteran pests, notably *H. armigera* (Darvishzadeh et al. 2014). Novaluron is useful in controlling mosquitoes such as *A. aegypti*, *C. quinquefasciatus*, the Asian tiger mosquito (*Aedes albopictus*), the new world malaria mosquito (*Anopheles albimanus*), and *Anopheles pseudopunctipennis* (Arredondo-Jiménez and Valdez-Delgado 2006). Novaluron also provides excellent control of subterranean termites in Texas (Keefer et al.

2015). Although BPUs have been used to control arthropod pests for many years, their molecular mode of action was recently unraveled according to the resistance mutations of CHS1 in both insects and spider mites (Douris et al. 2016).

Other chemical groups of chitin synthesis inhibitors have been developed, which include thiadiazines (buprofezin), oxazolines (etoxazole), tetrazines (clofentezine, diflovidazin), thiazolidines (flubenzimine, hexythiazox), and triazines (cyromazine) (Merzendorfer 2013). Buprofezin is the only member of thiadiazines that has been commercialized as an insecticide. It is effective against plant-sucking insect pests such as *N. lugens*, the green rice leafhopper (*Nephotettix virescens*), the silverleaf whitefly (*Bemisia tabaci*), the whitebacked planthopper (*Sogatella furcifera*), and mealybug species (Heinrichs et al. 1984).

Several chitin synthesis inhibitors (e.g., polyoxins and nikkomycins) have been isolated and purified from natural sources including fungus and bacterium (Jackson et al. 2013). They act as inhibitors of chitin biosynthesis and deposition (Vardanis 1978; Binnington 1985). The insecticidal activity of polyoxin has been tested in *T. castaneum* and *S. litura* (Arakawa et al. 2008). However, very few have been developed commercially as agricultural fungicides, and none have been used to control arthropod pests due to their charged nature with limited penetration across cell membrane (Merzendorfer 2013). Several chitinase inhibitors, such as allosamidin, argadin, and argifin, have also been identified from the natural products (Spindler and Spindler-Barth 1999). Among them, allosamidin is a well-characterized chemical isolated from *Streptomyces* sp. and can inhibit larval-larval or larval-pupal ecdysis when it is injected in *B. mori* (Sakuda et al. 1987). Allosamidin mimics the carbohydrate substrate (Rao et al. 2003), whereas argadin and argifin isolated from cultures of fungi are cyclic peptides (Houston et al. 2002). However, the chitinase inhibitory activity of argadin and argifin are lower than that of allosamidin when an *L. cuprina* chitinase inhibition assay is performed (Hirose et al. 2010).

Chitinases have also been utilized to improve the efficacy of microbial insect control agents, such as bacteria, viruses, and fungi, in arthropod pest management programs as chitinases hydrolyze the chitin in the cuticle or in the gut to facilitate the penetration of the microbials (Kramer and Muthukrishnan 1997; Gooday 1999). For example, the combination of *Bacillus thuringiensis* (Bt) raw material and exogenous chitinase has been used to prevent *C. fumiferana* larvae (Smirnoff 1974). Results show that the addition of chitinase can considerably increase the septicemia enterotoxinosis provoked by Bt and consequently decrease larval feeding. In the cotton leafworm (*Spodoptera littoralis*), the addition of exogenous chitinases can also enhance the action of Bt as chitinases may weaken the insect PM, allowing more ready access of the Bt toxins to the gut epithelia (Sampson and Gooday 1998).

Besides the application of chemical inhibitors to target chitin biosynthetic and metabolic pathways, and the use of exogenous chitinases to enhance the efficacy of microbial insect control agents for managing arthropod pests, recent research has extended to explore possible molecular and biotechnological approaches to manage arthropod pests by targeting these pathways (Zhang et al. 2010a; Kola et al. 2015). When *S. frugiperda* larvae are treated with the recombinant virus *Autographa*

californica multicapsid NPV (AcMNPV) from the construct containing a chitinase gene, the larval LT_{50} is shortened from 88 h to 65 h. Furthermore, it is reported that AcMNPV has gut-permeating activity in the PM of the tobacco budworm (*Heliothis virescens*), which can make possible uses of AcMNPV to synergize the activity of other ingested biopesticides (Fiandra et al. 2010).

More recently, RNAi, which is a highly conserved posttranscriptional gene regulatory mechanism controlling gene expression at the mRNA level in eukaryotic organisms, has been proven for its great potential in insect pest management (Zhu 2013). For chitin synthases, RNAi experiments have been conducted to suppress the transcript levels of their coding genes in *T. castaneum* (*TcCHS1* and *TcCHS2*) (Arakane et al. 2005), *S. exigua* (*SeCHS1*) (Chen et al. 2008), *A. gambiae* (*AgCHS1* and *AgCHS2*) (Zhang et al. 2010b), and *A. aegypti* (*AeCHS1* and *AeCHS2*) (Singh et al. 2013). Many of these studies showed the larval-pupal or pupal-adult molt failures as the synthesis of chitin was suppressed in the insects. Scientists have also performed several studies to suppress the transcript levels of different chitinase genes in several insect species, including *T. castaneum* (*TcCHT5* and *TcCHT10*), *O. nubilalis* (*OnCHT*), and *H. armigera* (*HaCHI*) (Zhu et al. 2008b; Khajuria et al. 2010; Mamta et al. 2016). All these studies suggest that the use of RNAi to suppress the expression of the genes involved in chitin biosynthetic and metabolic pathways could be a viable approach. These genes can serve as potential targets for developing RNAi-based approaches for managing arthropod pests (Zhu et al. 2016).

1.6 Concluding Remarks

Chitin biosynthesis, modification, translocation, deposition, assembly, and degradation are highly complex biological processes and involve many enzymes and structural proteins acting in a cooperative and precise manner (Moussian et al. 2007; Muthukrishnan et al. 2012). As a result of technological advances in genome sequencing and functional genomics, a vast amount of new information on these processes has been generated, particularly on identification and characterization of the genes or proteins involved in chitin biosynthesis (CHS), modification (CDA), degradation (CHT, NAG), binding (CBP), and protection/organization (KNK) in the last two decades. However, detailed mechanisms conferring the translocation, assembly and deposition of chitin, the formation of different chitin types, and the integration of various CBPs to chitin in the formation of chito-protein matrices are still not fully understood.

Muthukrishnan et al. (2018) have recently identified 12 critical research questions in order to better understand these processes. These areas of research include (1) fundamental biochemical differences between CHS1 for cuticular chitin synthesis and CHS2 for PM chitin synthesis, (2) organization of CHS in plasma membrane, (3) mechanism to transport chitin polymers across the plasma membrane, (4) mechanism to release chitin polymers from CHS, (5) mechanism to form α-chitin

crystallites, (6) roles of CDA in chitin organization within the cuticle, (7) biochemical reactions in the assembly zone, (8) further modifications of chitin in other parts of the cuticle, (9) reasons to have so many different CBPs or CPs, (10) timing and/or order of appearance of CBPs or CPs for different types of cuticle being formed, (11) regulations of the cuticle type by epidermal cells at different anatomical positions, and (12) mechanism to allow the same epidermal cell for elaborating different types of cuticle at different times during the arthropod development. These questions are indeed important but are not easy to be addressed as many of these questions deal with very complicated biological processes. Nevertheless, given the current rapid paces in identifying the genes and proteins, and understanding their roles in chitin transport, assembly, and formation of chito-protein matrices, it is expected that rapid progresses to address these questions will be made in the near future.

Acknowledgments We would like to thank Weimin Liu in the Research Institute of Applied Biology at Shanxi University, Taiyuan, China, for her contribution of Fig. 1.4. Relevant research conducted in the authors' laboratories was supported by the grants from the National Natural Science Foundation of China (Grant Nos. 31702067, 31672364) and the Kansas Agricultural Experiment Station, Manhattan, Kansas (KS 362, KS471).

References

Adams M, Celniker S, Holt R, Evans C, Gocayne J, Amanatides P, Scherer S, Li P, Hoskins R, Galle R, George R et al (2000) The genome sequence of *Drosophila melanogaster*. Science 287:2185–2195

Agrawal N, Sachdev B, Rodrigues J, Sree KS, Bhatnagar RK (2013) Development associated profiling of chitinase and microRNA of *Helicoverpa armigera* identified chitinase repressive microRNA. Sci Rep 3:2292. https://doi.org/10.1038/srep02292

Agrawal S, Kelkenberg M, Begum K, Steinfeld L, Williams CE, Kramer KJ, Beeman RW, Park Y, Muthukrishnan S, Merzendorfer H (2014) Two essential peritrophic matrix proteins mediate matrix barrier functions in the insect midgut. Insect Biochem Mol Biol 49:24–34

Ahmed S, Annu n AA, Sheikh J (2018) A review on chitosan centred scaffolds and their applications in tissue engineering. Int J Biol Macromol 116:849–862

Ahsan S, Thomas M, Reddy K, Sooraparaju S, Asthana A, Bhatnagar I (2018) Chitosan as biomaterial in drug delivery and tissue engineering. Int J Biol Macromol 110:97–109

Ali A, Ahmed S (2018) A review on chitosan and its nanocomposites in drug delivery. Int J Biol Macromol 109:273–286

Andersen SO (1995) Insect cuticular proteins. Insect Biochem Mol Biol 25:153–176

Andersen SO (1998) Amino acid sequence studies on endocuticular proteins from the desert locust, *Schistocerca gregaria*. Insect Biochem Mol Biol 28:421–434

Andersen SO (2000) Studies on proteins in post-ecdysial nymphal cuticle of locust, *Locusta migratoria*, and cockroach, *Blaberus craniifer*. Insect Biochem Mol Biol 30:569–577

Andersen SO (2010) Insect cuticular sclerotization: a review. Insect Biochem Mol Biol 40:166–178

Andersen SO, Rafn K, Roepstorff P (1997) Sequence studies of proteins from larval and pupal cuticle of the yellow meal worm, *Tenebrio molitor*. Insect Biochem Mol Biol 27:121–131

Appel E, Heepe L, Lin CP, Gorb SN (2015) Ultrastructure of dragonfly wing veins: composite structure of fibrous material supplemented by resilin. J Anat 227:561–582

Arakane Y, Muthukrishnan S (2010) Insect chitinase and chitinase-like proteins. Cell Mol Life Sci 67:201–216

Arakane Y, Zhu Q, Matsumiya M, Muthukrishnan S, Kramer KJ (2003) Properties of catalytic, linker and chitin-binding domains of insect chitinase. Insect Biochem Mol Biol 33:631–648

Arakane Y, Hogenkamp DG, Zhu YC, Kramer KJ, Specht CA, Beeman RW, Kanost MR, Muthukrishnan S (2004) Characterization of two chitin synthase genes of the red flour beetle, *Tribolium castaneum*, and alternate exon usage in one of the genes during development. Insect Biochem Mol Biol 34:291–304

Arakane Y, Muthukrishnan S, Kramer KJ, Specht CA, Tomoyasu Y, Lorenzen MD, Kanost M, Beeman RW (2005) The *Tribolium* chitin synthase genes *TcCHS1* and *TcCHS2* are specialized for synthesis of epidermal cuticle and midgut peritrophic matrix. Insect Mol Biol 14:453–463

Arakane Y, Dixit R, Begum K, Park Y, Specht CA, Merzendorfer H, Kramer KJ, Muthukrishnan S, Beeman RW (2009a) Analysis of functions of the chitin deacetylase gene family in *Tribolium castaneum*. Insect Biochem Mol Biol 39:355–365

Arakane Y, Lomakin J, Beeman RW, Muthukrishnan S, Gehrke SH, Kanost MR, Kramer KJ (2009b) Molecular and functional analyses of amino acid decarboxylases involved in cuticle tanning in *Tribolium castaneum*. J Biol Chem 284:16584–16594

Arakane Y, Lomakin J, Gehrke SH, Hiromasa Y, Tomich JM, Muthukrishnan S, Beeman RW, Kramer KJ, Kanost MR (2012) Formation of rigid, non-flight forewings (elytra) of a beetle requires two major cuticular proteins. PLoS Genet 8:e1002682

Arakawa T, Yukuhiro F, Noda H (2008) Insecticidal effect of a fungicide containing polyoxin B on the larvae of *Bombyx mori* (Lepidoptera: Bombycidae), *Mamestra brassicae*, *Mythimna separata*, and *Spodoptera litura* (Lepidoptera: Noctuidae). Appl Entomol Zool 43:173–181

Aranaz I, Acosta N, Civera C, Elorza B, Mingo J, Castro C, Gandía M, Caballero AH (2018) Cosmetics and cosmeceutical applications of chitin, chitosan and their derivatives. Polymers 10:213. https://doi.org/10.3390/polym10020213

Arredondo-Jiménez J, Valdez-Delgado K (2006) Effect of Novaluron (Rimon 10 EC) on the mosquitoes *Anopheles albimanus*, *Anopheles pseudopunctipennis*, *Aedes aegypti*, *Aedes albopictus* and *Culex quinquefasciatus* from Chiapas, Mexico. Med Vet Entomol 20:377–387

Baernholdt D, Anderson S (1998) Sequence studies on post-ecdysial cuticular proteins from pupae of the yellow mealworm, *Tenebrio molitor*. Insect Biochem Mol Biol 28:517–526

Baines DM (1978) Observations on the peritrophic membrane of *Locusta migratoria migratorioides* (R. and F.) nymphs. Acrida 7:11–21

Barbehenn RV (2001) Roles of peritrophic membranes in protecting herbivorous insects from ingested plant allelochemicals. Arch Insect Biochem Physiol 47:86–99

Barbehenn RV, Martin MM (1994) Tannin sensitivity in larvae of *Malacosoma disstria* (Lepidoptera): roles of the peritrophic envelope and midgut oxidation. J Chem Ecol 20:1985–2001

Barbehenn RV, Martin MM (1995) Peritrophic envelope permeability in herbivorous insects. J Insect Physiol 41:303–311

Barbehenn RV, Stannard J (2004) Antioxidant defense of the midgut epithelium by the peritrophic envelope in caterpillars. J Insect Physiol 50:783–790

Barbehenn RV, Martin MM, Hagerman AE (1996) Reassessment of the roles of the peritrophic envelope and hydrolysis in protecting polyphagous grasshoppers from ingested hydrolyzable tannins. J Chem Ecol 22:1901–1919

Barry M, Triplett A, Christensen A (1999) A peritrophin-like protein expressed in the embryonic tracheae of *Drosophila melanogaster*. Insect Biochem Mol Biol 29:319–327

Behr M, Hoch M (2005) Identification of the novel evolutionary conserved obstructor multigene family in invertebrates. FEBS Lett 579:6827–6833

Bentov S, Aflalo ED, Tynyakov J, Glazer L, Sagi A (2016) Calcium phosphate mineralization is widely applied in crustacean mandibles. Sci Rep 6:22118. https://doi.org/10.1038/srep22118

Binnington K (1985) Ultrastructural changes in the cuticle of the sheep blowfly, *Lucilia*, induced by certain insecticides and biological inhibitors. Tissue Cell 17:131–140

Blackwell J (1969) Structure of beta-chitin or parallel chain systems of poly-beta-(1-4)-*N*-acetyl-D-glucosamine. Biopolymers 7:281–298

Blackwell J, Parker KD, Rudall KM (1967) Chitin fibres of the diatoms *Thalassiosira fluviatilis* and *Cyclotella cryptica*. J Mol Biol 28:383–385

Bolognesi R, Arakane Y, Muthukrishnan S, Kramer KJ, Terra WR, Ferreira C (2005) Sequences of cDNAs and expression of genes encoding chitin synthase and chitinase in the midgut of *Spodoptera frugiperda*. Insect Biochem Mol Biol 35:1249–1259

Bolognesi R, Terra W, Ferreira C (2008) Peritrophic membrane role in enhancing digestive efficiency. J Insect Physiol 54:1413–1422

Bouligand Y (1965) On a twisted fibrillar arrangement common to several biologic structures. C R Acad Sci Hebd Seances Acad Sci D 261:4864–4867

Campbell PM, Cao AT, Hines ER, East PD, Gordon KH (2008) Proteomic analysis of the peritrophic matrix from the gut of the caterpillar, *Helicoverpa armigera*. Insect Biochem Mol Biol 38:950–958

Cantarel BL, Coutinho PM, Rancurel C, Bernard T, Lombard V, Henrissat B (2009) The Carbohydrate-Active EnZymes database (CAZy): an expert resource for Glycogenomics. Nucleic Acids Res 37:233–238

Carlstrom D (1957) The crystal structure of alpha-chitin (poly-*N*-acetyl-D-glucosamine). J Biophys Biochem Cytol 3:669–683

Chapman RF (2013) The insects-structure and function, 5th edn. Cambridge University Press, Cambridge

Chaudhari SS, Arakane Y, Specht CA, Moussian B, Boyle DL, Park Y, Kramer KJ, Beeman RW, Muthukrishnan S (2011) Knickkopf protein protects and organizes chitin in the newly synthesized insect exoskeleton. Proc Natl Acad Sci USA 108:17028–17033

Chaudhari SS, Arakane Y, Specht CA, Moussian B, Kramer KJ, Muthukrishnan S, Beeman RW (2013) Retroactive maintains cuticle integrity by promoting the trafficking of Knickkopf into the procuticle of *Tribolium castaneum*. PLoS Genet 9:e1003268. https://doi.org/10.1371/journal.pgen.1003268

Chen M, Thelen JJ (2016) Acyl-lipid desaturase 1 primes cold acclimation response in *Arabidopsis*. Physiol Plant 158:11–22

Chen X, Tian H, Zou L, Tang B, Hu J, Zhang W (2008) Disruption of *Spodoptera exigua* larval development by silencing chitin synthase gene A with RNA interference. Bull Entomol Res 98:613–619

Chen J, Liang Z, Liang Y, Pang R, Zhang W (2013) Conserved microRNAs miR-8-5p and miR-2a-3p modulate chitin biosynthesis in response to 20-hydroxyecdysone signaling in the brown planthopper, *Nilaparvata lugens*. Insect Biochem Mol Biol 43:839–848

Chen W, Qu M, Zhou Y, Yang Q (2018) Structural analysis of group II chitinase (ChtII) catalysis completes the puzzle of chitin hydrolysis in insects. J Biol Chem 293:2652–2660

Cohen E (2001) Chitin synthesis and inhibition: a revisit. Pest Manag Sci 57:946–950

Cohen E (2010) Chitin biochemistry: synthesis, hydrolysis and inhibition. Adv Insect Physiol 38:5–74

Cornman RS, Togawa T, Dunn WA, He N, Emmons AC, Willis JH (2008) Annotation and analysis of a large cuticular protein family with the R&R Consensus in *Anopheles gambiae*. BMC Genomics 9:22. https://doi.org/10.1186/1471-2164-9-22

Cox D, Willis J (1987) Analysis of the cuticular proteins of *Hyalophora cecropia* with two dimensional electrophoresis. Insect Biochem 17:457–468

Culliney TW (2014) Chapter 8: Crop losses to arthropods. In: Pimentel D, Peshin R (eds) Integrated pest management: pesticide problems, vol 3, Springer Netherlands, pp 201–225

Daley WP, Yamada KM (2013) ECM-modulated cellular dynamics as a driving force for tissue morphogenesis. Curr Opin Genet Dev 23:408–414

Darvishzadeh A, Salimian-Rizi S, Katoulinezhad A (2014) Effect of biolep, permethrin and hexaflumuron on mortality of cotton bollworm, *Helicoverpa armigera* (Noctuidae: Lepidoptera). Arthropods 3:161–165

Datta P, Basu P, Datta T (1984) Isolation and characterization of *Vicia faba* lectin affinity purified on chitin column. Prep Biochem 14:373–387

De Mets R, Jeuniaux C (1962) On the organic substances constituting the peritrophic membrane of insects. Arch Int Physiol Biochim 70:93–96

Derksen AC, Granados RR (1988) Alteration of a lepidopteran peritrophic membrane by baculoviruses and enhancement of viral infectivity. Virology 167:242–250

Dinglasan R, Devenport M, Florens L, Johnson J, McHugh C, Donnelly-Doman M, Carucci D, Yates J, Jacobs-Lorena M (2009) The *Anopheles gambiae* adult midgut peritrophic matrix proteome. Insect Biochem Mol Biol 39:125–134

Dittmer NT, Hiromasa Y, Tomich JM, Lu N, Beeman RW, Kramer KJ, Kanost MR (2012) Proteomic and transcriptomic analyses of rigid and membranous cuticles and epidermis from the elytra and hindwings of the red flour beetle, *Tribolium castaneum*. J Proteome Res 11:269–278

Dittmer N, Tetreau G, Cao X, Jiang H, Wang P, Kanost M (2015) Annotation and expression analysis of cuticular proteins from the tobacco hornworm, *Manduca sexta*. Insect Biochem Mol Biol 62:100–113

Dixit R, Arakane Y, Specht CA, Richard C, Kramer KJ, Beeman RW, Muthukrishnan S (2008) Domain organization and phylogenetic analysis of proteins from the chitin deacetylase gene family of *Tribolium castaneum* and three other species of insects. Insect Biochem Mol Biol 38:440–451

Doucet D, Retnakaran A (2016) Targeting cuticular components for pest control. In: Cohen E, Moussian B (eds) Extracellular composite matrices in arthropods. Springer, Cham, pp 369–407

Douris V, Steinbach D, Panteleri R, Livadaras I, Pickett JA, Van Leeuwen T, Nauen R, Vontas J (2016) Resistance mutation conserved between insects and mites unravels the benzoylurea insecticide mode of action on chitin biosynthesis. Proc Natl Acad Sci USA 113:14692–14697

Durand P, Golinelli-Pimpaneau B, Mouilleron S, Badet B, Badet-Denisot MA (2008) Highlights of glucosamine-6P synthase catalysis. Arch Biochem Biophys 474:302–317

Dziadik-Turner C, Koga D, Mai MS, Kramer KJ (1981) Purification and characteristics of two beta-*N*-acetylhexosaminidases from the tobacco hornworm, *Manduca sexta* (L.) (Lepidoptera: Sphingidae). Arch Biochem Biophys 212:546–560

Elieh-Ali-Komi D, Hamblin M (2016) Chitin and chitosan: production and application of versatile biomedical nanomaterials. Int J Adv Res 4:411–427

Elvin CM, Vuocolo T, Pearson RD, East IJ, Riding GA, Eisemann CH, Tellam RL (1996) Characterization of a major peritrophic membrane protein, peritrophin-44, from the larvae of *Lucilia cuprina*. cDNA and deduced amino acid sequences. J Biol Chem 271:8925–8935

Everaerts C, Farine JP, Cobb M, Ferveur JF (2010) *Drosophila* cuticular hydrocarbons revisited: mating status alters cuticular profiles. PLoS One 5:e9607. https://doi.org/10.1371/journal.pone.0009607

Fiandra L, Terracciano I, Fanti P, Garonna A, Ferracane L, Fogliano V, Casartelli M, Giordana B, Rao R, Pennacchio F (2010) A viral chitinase enhances oral activity of TMOF. Insect Biochem Mol Biol 40:533–540

Filho BP, Lemos FJ, Secundino NF, Pascoa V, Pereira ST, Pimenta PF (2002) Presence of chitinase and beta-N-acetylglucosaminidase in the *Aedes aegypti:* a chitinolytic system involving peritrophic matrix formation and degradation. Insect Biochem Mol Biol 32:1723–1729

Freeman S, Quillin K, Allison L (2016) Biological science, 5th edn. Pearson Education Limited, Harlow, p 1494

Fujitani N, Kouno T, Nakahara T, Takaya K, Osaki T, Kawabata S, Mizuguchi M, Aizawa T, Demura M, Nishimura S, Kawano K (2007) The solution structure of horseshoe crab antimicrobial peptide tachystatin B with an inhibitory cystine-knot motif. J Pept Sci 13:269–279

Fukamizo T (2000) Chitinolytic enzymes: catalysis, substrate binding, and their application. Curr Protein Pept Sci 1:105–124

Fukamizo T, Kramer KJ (1985a) Mechanism of chitin hydrolysis by the binary chitinase system in insect moulting fluid. Insect Biochem 15:141–145

Fukamizo T, Kramer KJ (1985b) Mechanism of chitin oligosaccharide hydrolysis by the binary enzyme chitinase system in insect moulting fluid. Insect Biochem 15:141–145
Futahashi R, Okamoto S, Kawasaki H, Zhong Y-S, Iwanaga M, Mita K, Fujiwara H (2008) Genome-wide identification of cuticular protein genes in the silkworm, *Bombyx mori*. Insect Biochem Mol Biol 38:1138–1146
Gagou ME, Kapsetaki M, Turberg A, Kafetzopoulos D (2002) Stage-specific expression of the chitin synthase *DmeChSA* and *DmeChSB* genes during the onset of *Drosophila* metamorphosis. Insect Biochem Mol Biol 32:141–146
Gallai N, Salles J-M, Settele J, Vaissière BE (2009) Economic valuation of the vulnerability of world agriculture confronted with pollinator decline. Ecol Econ 68:810–821
Gangishetti U, Veerkamp J, Bezdan D, Schwarz H, Lohmann I, Moussian B (2012) The transcription factor Grainy head and the steroid hormone ecdysone cooperate during differentiation of the skin of *Drosophila melanogaster*. Insect Mol Biol 21:283–295
Giraud-Guille MM (1986) Direct visualization of microtomy artefacts in sections of twisted fibrous extracellular matrices. Tissue Cell 18:603–620
Gooday GW (1999) Aggressive and defensive roles for chitinases. EXS 87:157–169
Guan X, Middlebrooks BW, Alexander S, Wasserman SA (2006) Mutation of TweedleD, a member of an unconventional cuticle protein family, alters body shape in *Drosophila*. Proc Natl Acad Sci USA 103:16794–16799
Gullan PJ, Craston PS (2005) The insects: an outline of entomology, 3rd edn. Blackwell, Publishing Ltd, Hoboken. 505pp
Guo B, Ma P (2018) Conducting polymers for tissue engineering. Biomacromolecules 19:1764–1782
Guo W, Li G, Pang Y, Wang P (2005) A novel chitin-binding protein identified from the peritrophic membrane of the cabbage looper, *Trichoplusia ni*. Insect Biochem Mol Biol 35:1224–1234
Haagsma K, Rust M (2005) Effect of hexaflumuron on mortality of the western subterranean termite (Isoptera: Rhinotermitidae) during and following exposure and movement of hexaflumuron in termite groups. Pest Manag Sci 61:517–531
Haebel S, Jensen C, Andersen S, Roepstorff P (1995) Isoforms of a cuticular protein from larvae of the meal beetle, *Tenebrio molitor*, studied by mass spectrometry in combination with Edman degradation and two-dimensional polyacrylamide gel electrophoresis. Protein Sci 4:394–404
Hao Z, Aksoy S (2002) Proventriculus-specific cDNAs characterized from the tsetse, *Glossina morsitans* morsitans. Insect Biochem Mol Biol 32:1663–1671
Hegedus D, Erlandson M, Gillott C, Toprak U (2009) New insights into peritrophic matrix synthesis, architecture, and function. Annu Rev Entomol 54:285–302
Heinrichs E, Basilio R, Valencia S (1984) Buprofezin, a selective insecticide for the management of rice planthoppers (Homoptera: Delphacidae) and leafhoppers (Homoptera: Cicadellidae). Environ Entomol 13:515–521
Hirose T, Sunazuka T, Omura S (2010) Recent development of two chitinase inhibitors, Argifin and Argadin, produced by soil microorganisms. Proc Jpn Acad Ser B Phys Biol Sci 86:85–102
Hogenkamp D, Arakane Y, Kramer K, Muthukrishnan S, Beeman R (2008) Characterization and expression of the beta-*N*-acetylhexosaminidase gene family of *Tribolium castaneum*. Insect Biochem Mol Biol 38:478–489
Honeybee Genome Sequencing Consortium (2006) Insights into social insects from the genome of the honeybee *Apis mellifera*. Nature 443:931–949
Hopkins TL, Harper MS (2001) Lepidopteran peritrophic membranes and effects of dietary wheat germ agglutinin on their formation and structure. Arch Insect Biochem Physiol 47:100–109
Hopkins TL, Krchma LJ, Ahmad SA, Kramer KJ (2000) Pupal cuticle proteins of *Manduca sexta*: characterization and profiles during sclerotization. Insect Biochem Mol Biol 30:19–27
Houston DR, Eggleston I, Synstad B, Eijsink VG, van Aalten DM (2002) The cyclic dipeptide CI-4 [cyclo-(l-Arg-d-Pro)] inhibits family 18 chitinases by structural mimicry of a reaction intermediate. Biochem J 368:23–27

Huang G, Liu Y, Chen L (2017) Chitosan and its derivatives as vehicles for drug delivery. Drug Deliv 24:108–113

Ibrahim GH, Smartt CT, Kiley LM, Christensen BM (2000) Cloning and characterization of a chitin synthase cDNA from the mosquito *Aedes aegypti*. Insect Biochem Mol Biol 30:1213–1222

Iconomidou VA, Willis JH, Hamodrakas SJ (2005) Unique features of the structural model of 'hard' cuticle proteins: implications for chitin-protein interactions and cross-linking in cuticle. Insect Biochem Mol Biol 35:553–560

Imai T, Watanabe T, Yui T, Sugiyama J (2003) The directionality of chitin biosynthesis: a revisit. Biochem J 374:755–760

Ioannidou ZS, Theodoropoulou MC, Papandreou NC, Willis JH, Hamodrakas SJ (2014) CutProtFam-Pred: detection and classification of putative structural cuticular proteins from sequence alone, based on profile hidden Markov models. Insect Biochem Mol Biol 52:51–59

Jackson K, Pogula P, Patterson S (2013) Polyoxin and nikkomycin analogs: recent design and synthesis of novel peptidyl nucleosides. Heterocycl Commun 19:375–386

Jasrapuria S, Arakane Y, Osman G, Kramer KJ, Beeman RW, Muthukrishnan S (2010) Genes encoding proteins with peritrophin A-type chitin-binding domains in *Tribolium castaneum* are grouped into three distinct families based on phylogeny, expression and function. Insect Biochem Mol Biol 40:214–227

Jasrapuria S, Specht C, Kramer K, Beeman R, Muthukrishnan S (2012) Gene families of cuticular proteins analogous to peritrophins (CPAPs) in *Tribolium castaneum* have diverse functions. PLoS One 7:e49844. https://doi.org/10.1371/journal.pone.0049844

Jaworski E, Wang L, Margo G (1963) Synthesis of chitin in cell-free extracts of *Prodenia eridania*. Nature 198:790–790

Jensen UG, Rothmann A, Skou L, Andersen SO, Roepstorff P, Hojrup P (1997) Cuticular proteins from the giant cockroach, *Blaberus craniifer*. Insect Biochem Mol Biol 27:109–120

Jensen C, Andersen SO, Roepstor P (1998) Primary structure of two major cuticular proteins from the migratory locust, *Locusta migratoria*, and their identification in polyacrylamide gels by mass spectrometry. Biochim Biophys Acta 1429:151–162

Jespersen S, Hojrup P, Andersent SO, Roepstorff P (1994) The primary structure of an endocuticular protein from two locust species, *Locusta migratoria* and *Schistocerca gregaria*, determined by a combination of mass spectrometry and automatic Edman degradation. Comp Biochem Physiol B Biochem Mol Biol 109:125–138

Kameda T, Miyazawa M, Ono H, Yoshida M (2005) Hydrogen bonding structure and stability of alpha-chitin studied by 13C solid-state NMR. Macromol Biosci 5:103–106

Kanmani P, Aravind J, Kamaraj M, Sureshbabu P, Karthikeyan S (2017) Environmental applications of chitosan and cellulosic biopolymers: a comprehensive outlook. Bioresour Technol 242:295–303

Karouzou MV, Spyropoulos Y, Iconomidou VA, Cornman RS, Hamodrakas SJ, Willis JH (2007) *Drosophila* cuticular proteins with the R&R Consensus: annotation and classification with a new tool for discriminating RR-1 and RR-2 sequences. Insect Biochem Mol Biol 37:754–760

Kato Y, Onishi H, Machida Y (2003) Application of chitin and chitosan derivatives in the pharmaceutical field. Curr Pharm Biotechnol 4:303–309

Kato N, Mueller CR, Fuchs JF, McElroy K, Wessely V, Higgs S, Christensen BM (2008) Evaluation of the function of a type I peritrophic matrix as a physical barrier for midgut epithelium invasion by mosquito-borne pathogens in *Aedes aegypti*. Vector Borne Zoonot 8:701–712

Keefer T, Puckett R, Brown K, Gold R (2015) Field trials with 0.5% novaluron insecticide applied as a bait to control subterranean termites (*Reticulitermes* sp. and *Coptotermes formosanus* [Isoptera: Rhinotermitidae]) on structures. J Econ Entomol 108:2407–2413

Kelkenberg M, Odman-Naresh J, Muthukrishnan S, Merzendorfer H (2015) Chitin is a necessary component to maintain the barrier function of the peritrophic matrix in the insect midgut. Insect Biochem Mol Biol 56:21–28

Khajuria C, Buschman LL, Chen MS, Muthukrishnan S, Zhu KY (2010) A gut-specific chitinase gene essential for regulation of chitin content of peritrophic matrix and growth of *Ostrinia nubilalis* larvae. Insect Biochem Mol Biol 40:621–629

Kola V, Renuka P, Madhav M, Mangrauthia S (2015) Key enzymes and proteins of crop insects as candidate for RNAi based gene silencing. Front Physiol 6:119. https://doi.org/10.3389/fphys.2015.00119

Krajewska B (2004) Application of chitin- and chitosan-based materials for enzyme immobilizations: a review. Enzyme Microb Technol 35:126–135

Kramer KJ, Koga D (1986) Insect chitin: Physical state, synthesis, degradation and metabolic regulation. Insect Biochem 16:851–877

Kramer KJ, Muthukrishnan S (1997) Insect chitinases: molecular biology and potential use as biopesticides. Insect Biochem Mol Biol 27:887–900

Kramer KJ, Corpuz L, Choi HK, Muthukrishnan S (1993) Sequence of a cDNA and expression of the gene encoding epidermal and gut chitinases of *Manduca sexta*. Insect Biochem Mol Biol 23:691–701

Krol J, Loedige I, Filipowicz W (2010) The widespread regulation of microRNA biogenesis, function and decay. Nat Rev Genet 11:597–610

Kumar NS, Tang B, Chen X, Tian H, Zhang W (2008) Molecular cloning, expression pattern and comparative analysis of chitin synthase gene B in *Spodoptera exigua*. Comp Biochem Physiol B Biochem Mol Biol 149:447–453

Kuraishi T, Binggeli O, Opota O, Buchon N, Lemaitre B (2011) Genetic evidence for a protective role of the peritrophic matrix against intestinal bacterial infection in *Drosophila melanogaster*. Proc Natl Acad Sci USA 108:15966–15971

Lehane MJ (1997) Peritrophic matrix structure and function. Annu Rev Entomol 42:525–550

Lehane M, Allingham P, Weglicki P (1996) Composition of the peritrophic matrix of the tsetse fly, *Glossina morsitans* morsitans. Cell Tissue Res 283:375–384

Leonard R, Rendic D, Rabouille C, Wilson IB, Preat T, Altmann F (2006) The *Drosophila* fused lobes gene encodes an *N*-acetylglucosaminidase involved in *N*-glycan processing. J Biol Chem 281:4867–4875

Li D, Zhang J, Wang Y, Liu X, Ma E, Sun Y, Li S, Zhu KY, Zhang J (2015) Two chitinase 5 genes from *Locusta migratoria*: molecular characteristics and functional differentiation. Insect Biochem Mol Biol 58:46–54

Liang J, Zhang L, Xiang Z, He N (2010) Expression profile of cuticular genes of silkworm, *Bombyx mori*. BMC Genomics 11:173. https://doi.org/10.1186/1471-2164-11-173

Liang J, Wang T, Xiang Z, He N (2015) Tweedle cuticular protein BmCPT1 is involved in innate immunity by participating in recognition of *Escherichia coli*. Insect Biochem Mol Biol 58:76–88

Liu T, Liu F, Yang Q, Yang J (2009) Expression, purification and characterization of the chitinolytic beta-*N*-acetyl-D-hexosaminidase from the insect *Ostrinia furnacalis*. Protein Expr Purif 68:99–103

Liu X, Zhang H, Li S, Zhu KY, Ma E, Zhang J (2012) Characterization of a midgut-specific chitin synthase gene (*LmCHS2*) responsible for biosynthesis of chitin of peritrophic matrix in *Locusta migratoria*. Insect Biochem Mol Biol 42:902–910

Liu X, Li F, Li D, Ma E, Zhang W, Zhu KY, Zhang J (2013) Molecular and functional analysis of UDP-*N*-acetylglucosamine pyrophosphorylases from the migratory locust, *Locusta migratoria*. PLoS One 8:e71970. https://doi.org/10.1371/journal.pone.0071970

Liu XJ, Sun YW, Li DQ, Li S, Ma EB, Zhang JZ (2018) Identification of *LmUAP1* as a 20-hydroxyecdysone response gene in the chitin biosynthesis pathway from the migratory locust, *Locusta migratoria*. Insect Sci 25:211–221

Locke M (2001) The Wigglesworth Lecture: insects for studying fundamental problems in biology. J Insect Physiol 47:495–507

Lomakin J, Huber P, Eichler C, Arakane Y, Kramer K, Beeman R, Kanost M, Gehrke S (2011) Mechanical properties of the beetle elytron, a biological composite material. Biomacromolecules 12:321–335

Lu Y, Zen K, Muthukrishnan S, Kramer K (2002) Site-directed mutagenesis and functional analysis of active site acidic amino acid residues D142, D144 and E146 in *Manduca sexta* (tobacco hornworm) chitinase. Insect Biochem Mol Biol 32:1369–1382

Lu J, Luo X, Zhang X, Pan P, Zhang C (2018) An ungrouped cuticular protein is essential for normal endocuticle formation in the brown planthopper. Insect Biochem Mol Biol 100:1–9

Luschnig S, Batz T, Armbruster K, Krasnow MA (2006) Serpentine and vermiform encode matrix proteins with chitin binding and deacetylation domains that limit tracheal tube length in *Drosophila*. Curr Biol 16:186–194

Lynn K (1990) Chitinases and chitobiases from the american lobster (*Homarus americanus*). Comp Biochem Physiol B 96:761–766

Machida S, Saito M (1993) Purification and characterization of membrane-bound chitin synthase. J Biol Chem 268:1702–1707

Mamta, Reddy KRK, Rajam MV (2016) Targeting chitinase gene of *Helicoverpa armigera* by host-induced RNA interference confers insect resistance in tobacco and tomato. Plant Mol Biol 90:281–292

Mathelin J, Quennedey B, Bouhin H, Delachambre J (1998) Characterization of two new cuticular genes specifically expressed during the post-ecdysial molting period in *Tenebrio molitor*. Gene 211:351–359

Mercer EH, Day MF (1952) The fine structure of the peritrophic membrane of certain insects. Biol Bull 103:384–394

Merzendorfer H (2006) Insect chitin synthases: a review. J Comp Physiol B 176:1–15

Merzendorfer H (2011) The cellular basis of chitin synthesis in fungi and insects: common principles and differences. Eur J Cell Biol 90:759–769

Merzendorfer H (2013) Chitin synthesis inhibitors: old molecules and new developments. Insect Sci 20:121–138

Merzendorfer H, Zimoch L (2003) Chitin metabolism in insects: structure, function and regulation of chitin synthases and chitinases. J Exp Biol 206:4393–4412

Merzendorfer H, Kelkenberg M, Muthukrishnan S (2016) Peritrophic matrices. In: Cohen E, Moussian B (eds) Extracellular composite matrices in arthropods. Springer, Cham, pp 255–324

Missios S, Davidson H, Linder D, Mortimer L, Okobi A, Doctor J (2000) Characterization of cuticular proteins in the red flour beetle, *Tribolium castaneum*. Insect Biochem Mol Biol 30:47–56

Moskalyk LA, Oo MM, Jacobs-Lorena M (1996) Peritrophic matrix proteins of *Anopheles gambiae* and *Aedes aegypti*. Insect Mol Biol 5:261–268

Moussian B (2010) Recent advances in understanding mechanisms of insect cuticle differentiation. Insect Biochem Mol Biol 40:363–375

Moussian B (2013) The apical plasma membrane of chitin-synthesizing epithelia. Insect Sci 20:139–146

Moussian B, Veerkamp J, Muller U, Schwarz H (2007) Assembly of the *Drosophila* larval exoskeleton requires controlled secretion and shaping of the apical plasma membrane. Matrix Biol 26:337–347

Moussian B, Letizia A, Martinez-Corrales G, Rotstein B, Casali A, Llimargas M (2015) Deciphering the genetic programme triggering timely and spatially-regulated chitin deposition. PLoS Genet 11:e1004939. https://doi.org/10.1371/journal.pgen.1004939

Mulder R, Gijswijk M (1973) The laboratory evaluation of two promising new insecticides which interfere with cuticle formation. Pestic Sci 4:737–745

Mun S, Young Noh M, Dittmer NT, Muthukrishnan S, Kramer KJ, Kanost MR, Arakane Y (2015) Cuticular protein with a low complexity sequence becomes cross-linked during insect cuticle sclerotization and is required for the adult molt. Sci Rep 5:10484. https://doi.org/10.1038/srep10484

Muthukrishnan S, Merzendorfer H, Arakane Y, Kramer KJ (2012) Chitin metabolism in insects. In: Gilbert LI (ed) Insect molecular biology and biochemistry. Academic Press, London, pp 193–235

Muthukrishnan S, Arakane Y, Yang Q, Zhang C-X, Zhang J, Zhang W, Moussian B (2018) Future questions in insect chitin biology: a microreview. Arch Insect Biochem Physiol 98:e21454. https://doi.org/10.1002/arch.21454

Muzzarelli R, Muzzarelli C, Terbojevich M (1997) Chitin chemistry, upgrading a renewable source. Carbohydr Eur 19:10–17

Muzzarelli R, Mattioli-Belmonte M, Pugnaloni A, Biagini G (1999) Biochemistry, histology and clinical uses of chitins and chitosans in wound healing. EXS 87:251–264

Nagamatsu Y, Yanagisawa I, Kimoto M, Okamoto E, Koga D (1995) Purification of a chitooligosaccharidolytic beta-*N*-acetylglucosaminidase from *Bombyx mori* larvae during metamorphosis and the nucleotide sequence of its cDNA. Biosci Biotechnol Biochem 59:219–225

Nelson DR, Charlet LD (2003) Cuticular hydrocarbons of the sunflower beetle, *Zygogramma exclamationis*. Comp Biochem Physiol B 135:273–284

Nelson DR, Lee RE Jr (2004) Cuticular lipids and desiccation resistance in overwintering larvae of the goldenrod gall fly, *Eurosta solidaginis* (Diptera: Tephritidae). Comp Biochem Physiol B 138:313–320

Nelson DR, Tissot M, Nelson LJ, Fatland CL, Gordon DM (2001) Novel wax esters and hydrocarbons in the cuticular surface lipids of the red harvester ant, *Pogonomyrmex barbatus*. Comp Biochem Physiol B 128:575–595

Nelson DR, Olson DL, Fatland CL (2002) Cuticular hydrocarbons of the flea beetles, *Aphthona lacertosa* and *Aphthona nigriscutis*, biocontrol agents for leafy spurge (*Euphorbia esula*). Comp Biochem Physiol B 133:337–350

Nelson DR, Adams TS, Fatland CL (2003) Hydrocarbons in the surface wax of eggs and adults of the Colorado potato beetle, *Leptinotarsa decemlineata*. Comp Biochem Physiol B Biochem Mol Biol 134:447–466

Neville AC (1965) Chitin lamellogenesis in locust cuticle. Q J Microsc Sci 106:269–286

Neville AC (1993) Biology of fibrous composites: development beyond the cell membrane. Cambridge University Press, New York

Neville AC, Luke BM (1969) Molecular architecture of adult locust cuticle at the electron microscope level. Tissue Cell 1:355–366

Nisole A, Stewart D, Bowman S, Zhang D, Krell PJ, Doucet D, Cusson M (2010) Cloning and characterization of a Gasp homolog from the spruce budworm, *Choristoneura fumiferana*, and its putative role in cuticle formation. J Insect Physiol 56:1427–1435

Noh MY, Muthukrishnan S, Kramer KJ, Arakane Y (2015) *Tribolium castaneum* RR-1 cuticular protein TcCPR4 is required for formation of pore canals in rigid cuticle. PLoS Genet 11: e1004963. https://doi.org/10.1371/journal.pgen.1004963

Noh MY, Muthukrishnan S, Kramer KJ, Arakane Y (2017) Development and ultrastructure of the rigid dorsal and flexible ventral cuticles of the elytron of the red flour beetle, *Tribolium castaneum*. Insect Biochem Mol Biol 91:21–33

Noh MY, Muthukrishnan S, Kramer KJ, Arakane Y (2018a) A chitinase with two catalytic domains is required for organization of the cuticular extracellular matrix of a beetle. PLoS Genet 14: e1007307. https://doi.org/10.1371/journal.pgen.1007307

Noh MY, Muthukrishnan S, Kramer KJ, Arakane Y (2018b) Group I chitin deacetylases are essential for higher order organization of chitin fibers in beetle cuticle. J Biol Chem 293:6985–6995

Nohr C, Hojrup P, Andersen SO (1992) Primary structure of two low molecular weight proteins isolated from cuticle of fifth instar nymphs of the migratory locust, *Locusta migratoria*. Insect Biochem Mol Biol 22:19–24

Ødegaard F (2008) How many species of arthropods? Erwin's estimate revised. Biol J Linnean Soc 71:583–597

Okada T, Ishiyama S, Sezutsu H, Usami A, Tamura T, Mita K, Fujiyama K, Seki T (2007) Molecular cloning and expression of two novel beta-*N*-acetylglucosaminidases from silkworm *Bombyx mori*. Biosci Biotechnol Biochem 71:1626–1635

Okamoto S, Futahashi R, Kojima T, Mita K, Fujiwara H (2008) Catalogue of epidermal genes: genes expressed in the epidermis during larval molt of the silkworm *Bombyx mori*. BMC Genomics 9:396. https://doi.org/10.1186/1471-2164-9-396

Olivera S, Muralidhara H, Venkatesh K, Guna V, Gopalakrishna K, Kumar KY (2016) Potential applications of cellulose and chitosan nanoparticles/composites in wastewater treatment: a review. Carbohydr Polym 153:600–618

Öztürk-Çolak A, Moussian B, Araújo SJ (2016) *Drosophila* chitinous aECM and its cellular interactions during tracheal development. Dev Dyn 245:259–267

Palli SR, Retnakaran A (1999) Molecular and biochemical aspects of chitin synthesis inhibition. EXS 87:85–98

Pan P, Ye Y, Lou Y, Lu J, Cheng C, Shen Y, Moussian B, Zhang C (2018) A comprehensive omics analysis and functional survey of cuticular proteins in the brown planthopper. Proc Natl Acad Sci USA 115:5175–5180

Patel S, Nelson DR, Gibbs AG (2001) Chemical and physical analyses of wax ester properties. J Insect Sci 1:1–7

Peniche-Covas C, Alvarez L, Argüelles-Monal W (2010) The adsorption of mercuric ions by chitosan. J Appl Polym Sci 46:1147–1150

Pesch YY, Riedel D, Behr M (2015) Obstructor A organizes matrix assembly at the apical cell surface to promote enzymatic cuticle maturation in *Drosophila*. J Biol Chem 290:10071–10082

Pesch YY, Riedel D, Patil KR, Loch G, Behr M (2016) Chitinases and Imaginal disc growth factors organize the extracellular matrix formation at barrier tissues in insects. Sci Rep 6:18340. https://doi.org/10.1038/srep18340

Pesch YY, Riedel D, Behr M (2017) *Drosophila* chitinase 2 is expressed in chitin producing organs for cuticle formation. Arthropod Struct Dev 46:4–12

Peters W (1992) Peritrophic membranes. Springer, Berlin, p 238

Peters W, Heitmann S, Haese DJ (1979) Formation and fine structure of peritrophic membranes in the earwig, *Forficula auricularia* (Dermaptera: Forficulidae). Entomol Gen 5:241–254

Petkau G, Wingen C, Jussen LC, Radtke T, Behr M (2012) Obstructor-A is required for epithelial extracellular matrix dynamics, exoskeleton function, and tubulogenesis. J Biol Chem 287:21396–21405

Qiao L, Xiong G, Wang RX, He SZ, Chen J, Tong XL, Hu H, Li CL, Gai TT, Xin YQ, Liu XF, Chen B, Xiang ZH, Lu C, Dai FY (2014) Mutation of a cuticular protein, BmorCPR2, alters larval body shape and adaptability in silkworm, *Bombyx mori*. Genetics 196:1103–1115

Qin G, Lapidot S, Numata K, Hu X, Meirovitch S, Dekel M, Podoler I, Shoseyov O, Kaplan DL (2009) Expression, cross-linking, and characterization of recombinant chitin binding resilin. Biomacromolecules 10:3227–3234

Qu M, Yang Q (2012) Physiological significance of alternatively spliced exon combinations of the single-copy gene class a chitin synthase in the insect *Ostrinia furnacalis* (Lepidoptera). Insect Mol Biol 21:395–404

Qu MB, Liu TA, Yang J, Yang Q (2011) The gene, expression pattern and subcellular localization of chitin synthase B from the insect *Ostrinia furnacalis*. Biochem Biophys Res Commun 404:302–307

Quan G, Ladd T, Duan J, Wen F, Doucet D, Cusson M, Krell PJ (2013) Characterization of a spruce budworm chitin deacetylase gene: stage- and tissue-specific expression, and inhibition using RNA interference. Insect Biochem Mol Biol 43:683–691

Rajabi H, Shafiei A, Darvizeh A, Dirks JH, Appel E, Gorb SN (2016) Effect of microstructure on the mechanical and damping behaviour of dragonfly wing veins. R Soc Open Sci 3:160006. https://doi.org/10.1098/rsos.160006

Rao FV, Houston DR, Boot RG, Aerts JM, Sakuda S, van Aalten DM (2003) Crystal structures of allosamidin derivatives in complex with human macrophage chitinase. J Biol Chem 278:20110–20116

Ravi Kumar MNV (1999) Chitin and chitosan fibres: a review. B Mater Sci 22:905–915

Rebers JE, Riddiford LM (1988) Structure and expression of a Manduca sexta larval cuticle gene homologous to *Drosophila* cuticle genes. J Mol Biol 203:411–423

Rebers JE, Willis JH (2001) A conserved domain in arthropod cuticular proteins binds chitin. Insect Biochem Mol Biol 31:1083–1093

Reynolds S, Samuels R (1996) Physiology and biochemistry of insect moulting fluid, Advances in insect physiology, vol 26. Academic, London, pp 157–232

Romanazzi G, Feliziani E, Baños S, Sivakumar D (2017) Shelf life extension of fresh fruit and vegetables by chitosan treatment. Crit Rev Food Sci Nutr 57:579–601

Rondot I, Quennedey B, Courrent A, Lemoine A, Delachambre J (1996) Cloning and sequencing of a cDNA encoding a larval-pupal-specific cuticular protein in *Tenebrio molitor* (Insecta, Coleoptera). Developmental expression and effect of a juvenile hormone analogue. Eur J Biochem 235:138–143

Rong S, Li DQ, Zhang XY, Li S, Zhu KY, Guo YP, Ma EB, Zhang JZ (2013) RNA interference to reveal roles of beta-*N*-acetylglucosaminidase gene during molting process in *Locusta migratoria*. Insect Sci 20:109–119

Rozario T, DeSimone DW (2010) The extracellular matrix in development and morphogenesis: a dynamic view. Dev Biol 341:126–140

Rudall KM, Kenchington W (1973) The chitin system. Biol Rev 48:597–636

Saito Y, Okano T, Gaill F, Chanzy H, Putaux JL (2000) Structural data on the intra-crystalline swelling of beta-chitin. Int J Biol Macromol 28:81–88

Sakuda S, Isogai A, Matsumoto S, Suzuki A (1987) Search for microbial insect growth regulators. II. Allosamidin, a novel insect chitinase inhibitor. J Antibiot 40:296–300

Sampson MN, Gooday GW (1998) Involvement of chitinases of *Bacillus thuringiensis* during pathogenesis in insects. Microbiology 144:2189–2194

Samuels RI, Charnley AK, Reynolds SE (1993) A cuticle-degrading proteinase from the moulting fluid of the tobacco hornworm, *Manduca sexta*. Insect Biochem Mol Biol 23:607–614

Saranathan V, Osuji CO, Mochrie SG, Noh H, Narayanan S, Sandy A, Dufresne ER, Prum RO (2010) Structure, function, and self-assembly of single network gyroid (I4132) photonic crystals in butterfly wing scales. Proc Natl Acad Sci USA 107:11676–11681

Sarauer B, Gillott C, Hegedus D (2003) Characterization of an intestinal mucin from the peritrophic matrix of the diamondback moth, *Plutella xylostella*. Insect Mol Biol 12:333–343

Schaefer J, Kramer KJ, Garbow JR, Jacob GS, Stejskal EO, Hopkins TL, Speirs RD (1987) Aromatic cross-links in insect cuticle: detection by solid-state 13C and 15N NMR. Science 235:1200–1204

Shahin R, Iwanaga M, Kawasaki H (2016) Cuticular protein and transcription factor genes expressed during prepupal-pupal transition and by ecdysone pulse treatment in wing discs of *Bombyx mori*. Insect Mol Biol 25:138–152

Shahin R, Iwanaga M, Kawasaki H (2018) Expression profiles of cuticular protein genes in wing tissues during pupal to adult stages and the deduced adult cuticular structure of *Bombyx mori*. Gene 646:181–194

Shao L, Devenport M, Fujioka H, Ghosh A, Jacobs-Lorena M (2005) Identification and characterization of a novel peritrophic matrix protein, Ae-Aper50, and the microvillar membrane protein, AEG12, from the mosquito, *Aedes aegypti*. Insect Biochem Mol Biol 35:947–959

Shen Z, Jacobs-Lorena M (1998) A type I peritrophic matrix protein from the malaria vector *Anopheles gambiae* binds to chitin. Cloning, expression, and characterization. J Biol Chem 273:17665–17670

Shen Z, Jacobs-Lorena M (1999) Evolution of chitin-binding proteins in invertebrates. J Mol Evol 48:341–347

Shi X, Chamankhah M, Visal-Shah S, Hemmingsen S, Erlandson M, Braun L, Alting-Mees M, Khachatourians G, O'grady M, Hegedus D (2004) Modeling the structure of the type I peritrophic matrix: characterization of a *Mamestra configurata* intestinal mucin and a novel peritrophin containing 19 chitin binding domains. Insect Biochem Mol Biol 34:1101–1115

Singh A, Wong S, Ryan C, Whyard S (2013) Oral delivery of double-stranded RNA in larvae of the yellow fever mosquito, *Aedes aegypti*: implications for pest mosquito control. J Insect Sci 13:1–7

Singh R, Shitiz K, Singh A (2017) Chitin and chitosan: biopolymers for wound management. Int Wound J 14:1276–1289

Smirnoff WA (1974) The symptoms of infection by *Bacillus thuringiensis* + Chitinase formulation in larvae of *Choristoneura fumiferana*. J Invertebr Pathol 23:397–399

Song X, Wang M, Dong L, Zhu H, Wang J (2018) PGRP-LD mediates *A. stephensi* vector competency by regulating homeostasis of microbiota-induced peritrophic matrix synthesis. PLoS Pathog 14:e1006899. https://doi.org/10.1371/journal.ppat.1006899

Sparks T, Nauen R (2015) IRAC: mode of action classification and insecticide resistance management. Pestic Biochem Physiol 121:122–128

Spindler KD, Spindler-Barth M (1999) Inhibitors of chitinases. EXS 87:201–209

Streng R (1973) Die erzeugung eines chitinigen kokonfadens aus peritrophischer membran bei der larve von *Rhynchaenus fagi* L. (Coleoptera, Curculionidae). Zeitschrift Für Morphologie Der Tiere 75:137–164

Suderman RJ, Dittmer NT, Kanost MR, Kramer KJ (2006) Model reactions for insect cuticle sclerotization: cross-linking of recombinant cuticular proteins upon their laccase-catalyzed oxidative conjugation with catechols. Insect Biochem Mol Biol 36:353–365

Talbo G, Højrup P, Rahbek-Nielsen H, Andersen SO, Roepstorff P (1991) Determination of the covalent structure of an N- and C-terminally blocked glycoprotein from endocuticle of *Locusta migratoria*. Eur J Biochem 195:495–504

Tellam RL, Eisemann C (2000) Chitin is only a minor component of the peritrophic matrix from larvae of *Lucilia cuprina*. Insect Biochem Mol Biol 30:1189–1201

Tellam RL, Wijffels G, Willadsen P (1999) Peritrophic matrix proteins. Insect Biochem Mol Biol 29:87–101

Tellam RL, Vuocolo T, Johnson SE, Jarmey J, Pearson RD (2000) Insect chitin synthase cDNA sequence, gene organization and expression. Eur J Biochem 267:6025–6043

Tetreau G, Cao X, Chen YR, Muthukrishnan S, Jiang H, Blissard GW, Kanost MR, Wang P (2015a) Overview of chitin metabolism enzymes in *Manduca sexta*: identification, domain organization, phylogenetic analysis and gene expression. Insect Biochem Mol Biol 62:114–126

Tetreau G, Dittmer NT, Cao X, Agrawal S, Chen YR, Muthukrishnan S, Haobo J, Blissard GW, Kanost MR, Wang P (2015b) Analysis of chitin-binding proteins from *Manduca sexta* provides new insights into evolution of peritrophin A-type chitin-binding domains in insects. Insect Biochem Mol Biol 62:127–141

Togawa T, Nakato H, Izumi S (2004) Analysis of the chitin recognition mechanism of cuticle proteins from the soft cuticle of the silkworm, *Bombyx mori*. Insect Biochem Mol Biol 34:1059–1067

Togawa T, Augustine Dunn W, Emmons AC, Willis JH (2007) CPF and CPFL, two related gene families encoding cuticular proteins of *Anopheles gambiae* and other insects. Insect Biochem Mol Biol 37:675–688

Tomiya N, Narang S, Park J, Abdul-Rahman B, Choi O, Singh S, Hiratake J, Sakata K, Betenbaugh MJ, Palter KB, Lee YC (2006) Purification, characterization, and cloning of a *Spodoptera frugiperda* Sf9 beta-*N*-acetylhexosaminidase that hydrolyzes terminal *N*-acetylglucosamine on the *N*-glycan core. J Biol Chem 281:19545–19560

Toprak U, Baldwin D, Erlandson M, Gillott C, Hegedus DD (2010) Insect intestinal mucins and serine proteases associated with the peritrophic matrix from feeding, starved and moulting *Mamestra configurata* larvae. Insect Mol Biol 19:163–175

Toprak U, Hegedus DD, Baldwin D, Coutu C, Erlandson M (2014) Spatial and temporal synthesis of *Mamestra configurata* peritrophic matrix through a larval stadium. Insect Biochem Mol Biol 54:89–97

Toprak U, Erlandson M, Baldwin D, Karcz S, Wan L, Coutu C, Gillott C, Hegedus DD (2016) Identification of the *Mamestra configurata* (Lepidoptera: Noctuidae) peritrophic matrix proteins and enzymes involved in peritrophic matrix chitin metabolism. Insect Sci 23:656–674

Tribolium Genome Sequencing Consortium (2008) The genome of the model beetle and pest *Tribolium castaneum*. Nature 452:949–955

Tsigos I, Martinou A, Kafetzopoulos D, Bouriotis V (2000) Chitin deacetylases: new, versatile tools in biotechnology. Trends Biotechnol 18:305–312

Uchida Y, Shimmi O, Sudoh M, Arisawa M, Yamada-Okabe H (1996) Characterization of chitin synthase 2 of *Saccharomyces cerevisiae*. II: both full size and processed enzymes are active for chitin synthesis. J Biochem 119:659–666

Ulery BD, Nair LS, Laurencin CT (2011) Biomedical applications of biodegradable polymers. J Polym Sci B Polym Phys 49:832–864

Vaaje-Kolstad G, Horn SJ, van Aalten DM, Synstad B, Eijsink VG (2005) The non-catalytic chitin-binding protein CBP21 from Serratia marcescens is essential for chitin degradation. J Biol Chem 280:28492–28497

Vannini L, Willis JH (2017) Localization of RR-1 and RR-2 cuticular proteins within the cuticle of *Anopheles gambiae*. Arthropod Struct Dev 46:13–29

Vardanis A (1978) Polyoxin fungicides: demonstration of insecticidal activity due to inhibition of chitin synthesis. Experientia 34:228–229

Venancio TM, Cristofoletti PT, Ferreira C, Verjovski-Almeida S, Terra WR (2009) The *Aedes aegypti* larval transcriptome: a comparative perspective with emphasis on trypsins and the domain structure of peritrophins. Insect Mol Biol 18:33–44

Verlee A, Mincke S, Stevens C (2017) Recent developments in antibacterial and antifungal chitosan and its derivatives. Carbohydr Polym 164:268–283

Wang P, Granados R (1997) Molecular cloning and sequencing of a novel invertebrate intestinal mucin cDNA. J Biol Chem 272:16663–16669

Wang P, Granados RR (1998) Observations on the presence of the peritrophic membrane in larval *Trichoplusia ni* and its role in limiting baculovirus infection. J Invertebr Pathol 72:57–62

Wang P, Li G, Granados R (2004) Identification of two new peritrophic membrane proteins from larval *Trichoplusia ni*: structural characteristics and their functions in the protease rich insect gut. Insect Biochem Mol Biol 34:215–227

Wang S, Jayaram SA, Hemphala J, Senti KA, Tsarouhas V, Jin H, Samakovlis C (2006) Septate-junction-dependent luminal deposition of chitin deacetylases restricts tube elongation in the *Drosophila* trachea. Curr Biol 16:180–185

Wang Y, Fan H, Huang H, Xue J, Wu WJ, Bao YY, Xu HJ, Zhu ZR, Cheng JA, Zhang C-X (2012) Chitin synthase 1 gene and its two alternative splicing variants from two sap-sucking insects, *Nilaparvata lugens* and *Laodelphax striatellus* (Hemiptera: Delphacidae). Insect Biochem Mol Biol 42:637–646

Wang YL, Yang ML, Jiang F, Zhang JZ, Kang L (2013) MicroRNA-dependent development revealed by RNA interference-mediated gene silencing of *LmDicer1* in the migratory locust. Insect Sci 20:53–60

Wang Y, Yu Z, Zhang J, Moussian B (2016) Regionalization of surface lipids in insects. Proc Biol Sci 283:20152994

Wang H, Qian J, Ding F (2018) Emerging chitosan-based films for food packaging applications. J Agric Food Chem 66:395–413

Waterhouse DF (1957) Digestion in insects. Annu Rev Entomol 2:1–18

Werren JH, Richards S, Desjardins CA, Niehuis O, Gadau J, Colbourne JK, Nasonia Genome Working G, Werren JH, Richards S et al (2010) Functional and evolutionary insights from the genomes of three parasitoid *Nasonia* species. Science 327:343–348

Wigglesworth VB (1930) The formation of the peritrophic membrane in insects, with special reference to the larvae of mosquitoes. Q J Microscop Sci 73:583–616

Wijffels G, Eisemann C, Riding G, Pearson R, Jones A, Willadsen P, Tellam R (2001) A novel family of chitin-binding proteins from insect type 2 peritrophic matrix. cDNA sequences, chitin binding activity, and cellular localization. J Biol Chem 276:15527–15536

Willis JH (2010) Structural cuticular proteins from arthropods: annotation, nomenclature, and sequence characteristics in the genomics era. Insect Biochem Mol Biol 40:189–204

World Health Organization (2017) World malaria report 2017. World Health Organization, Geneva, p 160

Xi Y, Pan PL, Ye YX, Yu B, Zhang CX (2014) Chitin deacetylase family genes in the brown planthopper, *Nilaparvata lugens* (Hemiptera: Delphacidae). Insect Mol Biol 23:695–705

Xiong G, Tong X, Gai T, Li C, Qiao L, Monteiro A, Hu H, Han M, Ding X, Wu S, Xiang Z, Lu C, Dai F (2017) Body shape and coloration of silkworm larvae are influenced by a novel cuticular protein. Genetics 207:1053–1066

Xiong G, Tong X, Yan Z, Hu H, Duan X, Li C, Han M, Lu C, Dai F (2018) Cuticular protein defective Bamboo mutant of *Bombyx mori* is sensitive to environmental stresses. Pestic Biochem Physiol 148:111–115

Yang Q, Liu T, Liu F, Qu M, Qian X (2008) A novel beta-N-acetyl-D-hexosaminidase from the insect *Ostrinia furnacalis* (Guenee). FEBS J 275:5690–5702

Yang M, Wang Y, Jiang F, Song T, Wang H, Liu Q, Zhang J, Zhang J, Kang L (2016) miR-71 and miR-263 jointly regulate target genes chitin synthase and chitinase to control locust molting. PLoS Genet 12:e1006257. https://doi.org/10.1371/journal.pgen.1006257

Yao Q, Zhang D, Tang B, Chen J, Chen J, Lu L, Zhang W (2010) Identification of 20-hydroxyecdysone late-response genes in the chitin biosynthesis pathway. PLoS One 5: e14058. https://doi.org/10.1371/journal.pone.0014058

Yu R, Liu W, Li D, Zhao X, Ding G, Zhang M, Ma E, Zhu KY, Li S, Moussian B, Zhang J (2016a) Helicoidal organization of chitin in the cuticle of the migratory locust requires the function of the chitin deacetylase 2 enzyme (LmCDA2). J Biol Chem 291:24352

Yu Z, Zhang X, Wang Y, Moussian B, Zhu KY, Li S, Ma E, Zhang J (2016b) LmCYP4G102: an oenocyte-specific cytochrome P450 gene required for cuticular waterproofing in the migratory locust, *Locusta migratoria*. Sci Rep 6:29980. https://doi.org/10.1038/srep29980

Zen K, Choi H, Krishnamachary N, Muthukrishnan S, Kramer K (1996) Cloning, expression, and hormonal regulation of an insect beta-N-acetylglucosaminidase gene. Insect Biochem Mol Biol 26:435–444

Zhang J, Liu X, Zhang J, Li D, Sun Y, Guo Y, Ma E, Zhu KY (2010a) Silencing of two alternative splicing-derived mRNA variants of chitin synthase 1 gene by RNAi is lethal to the oriental migratory locust, *Locusta migratoria* manilensis (Meyen). Insect Biochem Mol Biol 40:824–833

Zhang X, Zhang J, Zhu KY (2010b) Chitosan/double-stranded RNA nanoparticle-mediated RNA interference to silence chitin synthase genes through larval feeding in the African malaria mosquito (*Anopheles gambiae*). Insect Mol Biol 19:683–693

Zhang J, Zhang X, Arakane Y, Muthukrishnan S, Kramer K, Ma E, Zhu K (2011a) Comparative genomic analysis of chitinase and chitinase-like genes in the African malaria mosquito (*Anopheles gambiae*). PLoS One 6:e19899. https://doi.org/10.1371/journal.pone.0019899

Zhang J, Zhang X, Arakane Y, Muthukrishnan S, Kramer K, Ma E, Zhu K (2011b) Identification and characterization of a novel chitinase-like gene cluster (*AgCht5*) possibly derived from tandem duplications in the African malaria mosquito, *Anopheles gambiae*. Insect Biochem Mol Biol 41:521–528

Zhang X, Zhang J, Park Y, Zhu KY (2012) Identification and characterization of two chitin synthase genes in African malaria mosquito, *Anopheles gambiae*. Insect Biochem Mol Biol 42:674–682

Zhao X, Gou X, Qin Z, Li D, Wang Y, Ma E, Li S, Zhang J (2017) Identification and expression of cuticular protein genes based on *Locusta migratoria* transcriptome. Sci Rep 7:45462. https://doi.org/10.1038/srep45462

Zhao X, Qin Z, Liu W, Liu X, Moussian B, Ma E, Li S, Zhang J (2018) Nuclear receptor HR3 controls locust molt by regulating chitin synthesis and degradation genes of *Locusta migratoria*. Insect Biochem Mol Biol 92:1–11

Zheng YP, Retnakaran A, Krell PJ, Arif BM, Primavera M, Feng QL (2003) Temporal, spatial and induced expression of chitinase in the spruce budworm, *Choristoneura fumiferana*. J Insect Physiol 49:241–247

Zheng XL, Zhao YX, Xu M (2017) Efficacy and safety of 3 nasal packing materials used after functional endoscopic sinus surgery for chronic rhinosinusitis: a comparative study in China. Med Sci Monit 23:1992–1998

Zhou Y, Badgett MJ, Bowen JH, Vannini L, Orlando R, Willis JH (2016) Distribution of cuticular proteins in different structures of adult *Anopheles gambiae*. Insect Biochem Mol Biol 75:45–57

Zhou Y, Badgett MJ, Orlando R, Willis JH (2018) Proteomics reveals localization of cuticular proteins in *Anopheles gambiae*. Insect Biochem Mol Biol. [Epub ahead of print]

Zhu KY (2013) RNA interference: a powerful tool in entomological research and a novel approach for insect pest management. Insect Sci 20:1–3

Zhu YC, Specht CA, Dittmer NT, Muthukrishnan S, Kanost MR, Kramer KJ (2002) Sequence of a cDNA and expression of the gene encoding a putative epidermal chitin synthase of *Manduca sexta*. Insect Biochem Mol Biol 32:1497–1506

Zhu Q, Arakane Y, Banerjee D, Beeman RW, Kramer KJ, Muthukrishnan S (2008a) Domain organization and phylogenetic analysis of the chitinase-like family of proteins in three species of insects. Insect Biochem Mol Biol 38:452–466

Zhu Q, Arakane Y, Beeman RW, Kramer KJ, Muthukrishnan S (2008b) Functional specialization among insect chitinase family genes revealed by RNA interference. Proc Natl Acad Sci USA 105:6650–6655

Zhu KY, Merzendorfer H, Zhang W, Zhang J, Muthukrishnan S (2016) Biosynthesis, turnover, and functions of chitin in insects. Annu Rev Entomol 61:177–196

Zimmermann A, Grabner F, Truss F (1975) Glucose consumption test in the urine for the demonstration of urinary tract infections. Med Welt 26:61–65. PMID: 1113658

Zimoch L, Merzendorfer H (2002) Immunolocalization of chitin synthase in the tobacco hornworm. Cell Tissue Res 308:287–297

Zimoch L, Hogenkamp DG, Kramer KJ, Muthukrishnan S, Merzendorfer H (2005) Regulation of chitin synthesis in the larval midgut of *Manduca sexta*. Insect Biochem Mol Biol 35:515–527

Chapter 2
Mineral-Chitin Composites in Molluscs

Ingrid M. Weiss

Chitin mineralization is just one of the many challenging aspects of biomineralization, the process by which living organisms produce minerals. The ability to form genetically determined mineralized skeletons must have existed for the past 550 million years. However, key molecular and evolutionary mechanisms which led to this ability remain enigmatic. Our understanding of enzymatic and biosynthetic aspects of mineralized chitinous exoskeletons is still in its infancy. The chitin synthases of molluscs differ from chitin synthases of all other organisms mainly in two aspects: A myosin domain and highly conserved, mollusc-specific patterns of charged amino acids. The latter bear the potential to interact in a pH-dependent manner, either with themselves or with mineral phases and/or with highly charged soluble or insoluble biomineralization proteins. The molecular diversity of these so-called biomineralization proteins is enormous, perhaps one of the reasons for deflecting attention away from mollusc chitin synthases until today. This chapter aims at closing conceptual gaps related to the biological dynamics of transmembrane myosin chitin synthases, with their cytoskeleton-based signaling potential for regulating microvilli and extracellular pattern formation on multi-scale levels.

2.1 Introduction

In 1972, W. Peters reported on the "occurrence of chitin in mollusca" (Peters 1972). He and contemporary scientists (Jeuniaux 1963) were astonished because the "mollusca" are usually famous for their fantastic abilities to form mineralized shells (Carter 1979; Carter 1989). Molluscs have certainly not been a first choice model

I. M. Weiss (✉)
Institute of Biomaterials and Biomolecular Systems, University of Stuttgart, Stuttgart, Germany
e-mail: ingrid.weiss@bio.uni-stuttgart.de

E. Cohen, H. Merzendorfer (eds.), *Extracellular Sugar-Based Biopolymers Matrices*,
Biologically-Inspired Systems 12, https://doi.org/10.1007/978-3-030-12919-4_2

system to investigate chitin, but rather invertebrate anatomy and physiology in general (Saleuddin and Wilbur 1983). However, the shell is macroscopically visible by eye, and it remains after the animal dies. Shells are used for systematically classifying many of the members of the phylum Mollusca. In terms of shape, size, growth mode, color, mineral composition, and microstructure, mollusc shells are species-specific in many subphyla (Lowenstam and Weiner 1989). Mollusc shells often retain some of their internal microstructures in fossils, which helps us to recognize that the mollusc's ability to form shells dates back to the era of the Cambrian diversification, about 542 million years ago (Runnegar and Jell 1976; Knoll 2003). Today we know that the shell's nano- and microstructure is responsible for this extraordinary mechanical stability and strength, specifically in terms of hardness and toughness. Did those early shells already contain chitin? How much chitin would they contain? Did all of them contain chitin? These are some relevant questions we should ask ourselves when trying to put mineral-chitin composites in molluscs into a broader and perhaps predominantly evolutionary context.

Meantime it is well established that molluscs do form chitin (Grégoire 1967; Peters 1972; Hunt and Nixon 1981; Furuhashi et al. 2009). Chitin produced by various organisms can become mineralized but may stay also non-mineralized (Hunt and El Sherief 1990; Falini and Fermani 2004), and there are transitions in between that have been observed in squid beaks (Miserez et al. 2008). Chitin is contained in larval mollusc shells which have to accommodate significant variations in terms of shape and composition of the interfacial tissue and "shell gland," before it differentiates into the so-called mantle epithelium later in development (Kniprath 1981; Weiss et al. 2002b; Weiss and Schönitzer 2006; Miyazaki et al. 2010; Liu et al. 2015). Chitin is also associated with adult shells and with species-specific combinations of ultrastructures such as prismatic calcite and nacreous aragonite, for example, found in the mother-of-pearl composite (Addadi et al. 2006; Nudelman et al. 2007; Suzuki et al. 2007; Furuhashi et al. 2009; Schneider et al. 2012; Suzuki and Nagasawa 2013) (Fig. 2.1).

Chitinous devices in molluscs usually perform a certain function in the body plan of the animal: They are used as hinges, shields, armor, teeth (so-called radula) (Okafor 1965; Baxter and Jones 1981; Sone et al. 2007; Butterfield 2008; Smith 2012; Sutton et al. 2012; Gnyubkin 2015), or endoskeletal "pen" of the squid (*Mollusca*: *Cephalopoda*); the latter became a well-studied research system (Hunt and Nixon 1981; Hunt and El Sherief 1990). Obviously, the performance of chitin as a structural scaffold was good enough to use it as a "construction material" for functional devices with advantageous properties. A clever trick "invented" by molluscs and species from many other phyla (Lowenstam and Weiner 1992) was to combine biopolymers (e.g., polysaccharides, proteins) and various minerals, mainly calcium carbonates and iron oxides, into composite materials, so-called controlled "biominerals" (Lowenstam 1981) with nano- and micron-scale textures (Nudelman et al. 2008). Mollusc shells are therefore natural "nanomaterials" by definition (Gao et al. 2003; Ashby 2005; Fleck et al. 2010). The hardness of the material increases with an increasing mineral content (Fratzl et al. 2004; Fratzl and Weinkamer 2007). Molluscs achieved producing stable and tough (non-brittle)

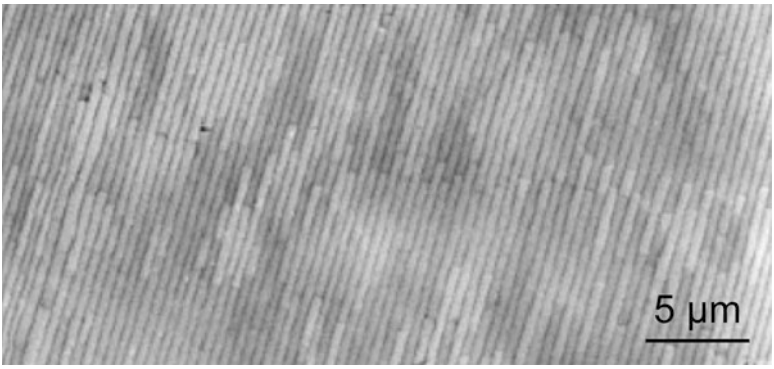

Fig. 2.1 Ultrastructure of nacre, a biogenic calcium carbonate chitin-nanocomposite. Individual nacre "tablets" are shown in cross section with dimensions of 0.5–1 µm in thickness and ~5–10 µm in diameter. The 5% (w/w) fraction of chitin/protein is distributed in between the ~95% mineral tablets as invisibly thin layers. (Courtesy of Andreas Schneider; Schneider et al. 2012)

composites with a mineral phase fraction of up to ~95% (w/w). Such a high value is difficult, if not impossible, to achieve by synthetic bulk processing of nanomaterials (Dickerson et al. 2008; Ashby et al. 2009). The 5% (w/w) fraction of the organic phase in a mollusc shell composite consists mainly of chitin and/or chitosan (Falini and Fermani 2004). Protein compounds of species-specific composition are associated with the carbohydrate parts (Weiss et al. 2002a; Jackson et al. 2006; Marin et al. 2007; Weiss and Marin 2008; Dauphin et al. 2013; McDougall and Degnan 2018). In terms of mass fraction, their contribution is minor (Lowenstam and Weiner 1989). However, in terms of fine-tuning of shell and mineral crystal properties, they are of major importance (Falini et al. 1996; Levi et al. 1998; Gotliv et al. 2003). From a chemical point of view, chitin can be directly mineralized without protein additives (Manoli et al. 1997; Falini et al. 2001).

The key concepts on which our understanding of mollusc shell biomineralization is based changed drastically over the years (Addadi et al. 2006; Cartwright and Checa 2007; Marin et al. 2012; Suzuki and Nagasawa 2013; Nudelman 2015). Concepts changed because not always were suitable experimental techniques at hand that would clarify the mineralization process on different length and time scales and especially not with respect to the role of chitin in the shell (Levi-Kalisman et al. 2001; Pérez-Huerta and Cusack 2008; Schmahl et al. 2008; Pérez-Huerta et al. 2011). Chitin is certainly a biomineralization scaffold which poses analytical challenges. As chitin is tightly associated with the so-called insoluble matrix, nondestructive analysis of biomolecular interactions with other components of the biomineralization scaffold poses challenges. One would aim at elucidating the co-orientation of mineral crystals and biomolecules in a nondestructive manner (Weiner and Traub 1980; Weiner et al. 1983; Iijima and Moriwaki 1990; Cusack et al. 2008; MacDonald et al. 2010). The insoluble matrix (Falini et al. 2003; Nudelman et al. 2006; Keene et al. 2010) remains after the calcium carbonate is removed from a mollusc shell by either complexation, low pH, or ion exchange treatment (Gotliv et al. 2003; Mann et al. 2012). It took many years until proteins

associated with the "insoluble matrix" were identified (Marin et al. 2007; Weiss and Marin 2008). Once high-throughput techniques for proteome, transcriptome, and genome analysis of complex samples and whole organisms became affordable, it turned out that only few members of the shell-forming repertoire seem to play a significantly conserved role across species (Table 2.1)

For many of them, it remains unclear how they guide the formation of fundamental arrangements of the nano- to micron-sized mineral building blocks in the observed long-range order. It also remains unclear which phyla developed basic forms of this type of exoskeletons. Possibly medusozoa (Cnidaria) have developed an early form of a biomineralized chitin skeleton, as recently suggested by Mendoza-Becerril et al. (2016). Several groundbreaking studies were published in 2001 and 2003 by the group of Steve Weiner and Lia Addadi: A cryo-TEM study revealed that it is actually chitin which is the ordered compound that provides the structural framework for the mineralization site (Levi-Kalisman et al. 2001). An in vitro study demonstrated that calcium carbonate polymorph-specific proteins, which induce either aragonite or calcite, fulfill their respective function only in the presence of a matrix that consists of silk and chitin (Falini et al. 1996; Levi et al. 1998; Gotliv et al. 2003). Speculation about the underlying principal mechanisms was at least partly ruled out in 2009, when the Pif protein complex was isolated from the shells of pearl oysters (Suzuki et al. 2009). This protein complex consists of two individual Pif polypeptides, Pif 97 and Pif 80, which interact with each other. One of them, Pif80, induces the formation of oriented aragonite. The other one contains a chitin-binding domain, in addition to some other regulatory regions with more or less conserved functions (Suzuki et al. 2009; Chang and Evans 2015). Taken together, these seminal studies suggest that chitin is intimately linked to the mineral phases and involved in their organization, starting from mineral nucleation up to species-specific shaping of macroscopic shells. The direct link between chitin and the mineral phase by means of biological factors such as the Pif protein complex is – all of a sudden – shifting the problem of control over mineral orientation on a superstructural level toward the orientation of the chitin framework. Thereby, both the integrity on different length scales (from "meso-" to micron-scale) and the integrity within the anatomical "Bauplan" play pivotal roles (Wilt et al. 2003; Schneider et al. 2012). Chitin is most likely not just a "passive" supporting matrix, which provides mechanical strength, but together with incorporated minerals a scaffold for achieving stiffness and order. It could be seen as an active member in exerting molecular and biological control over the deposition and orientation of the mineral phase.

The topic of chitin in mollusc shells is excellently covered in some previous reviews, as far as structural and certain functional details are concerned (Falini and Fermani 2004; Weiss 2010). Nevertheless, it is the enzymatic viewpoint, which is an emerging topic and which is still in its infancy (Weiss 2012). For this reason, this review will focus predominantly on the enzymatic and molecular-biological views on chitin in molluscs. It will put especially more emphasis on the challenges, which mineral-chitin composites pose on elucidating the enzymatic mechanism. One central theme will be current hypotheses about the regulation of chitin formation

Table 2.1 Biomineralization-related database resources for molluscs

Year	References	Phylum	Class/subphylum	Species	Source	Type
2006	Jackson et al. (2006)	Mollusc	Gastropod	*Haliotis*, *Lottia*	Mantle	Secretome, genome
2010	Miyazaki et al. (2010)	Mollusc	Bivalve	*Pinctada*	Developmental tissue	Transcriptome
2012	Mann et al. (2012)	Mollusc	Gastropod	*Lottia*	Shell	Proteome
2012	Zhang et al. (2012)	Mollusc	Bivalve	Oyster	n/a	Genome
2013	Miyamoto et al. (2013)	Mollusc	Bivalve	*Pinctada*	n/a	Genome
2014	Osuna-Mascaró et al. (2014)	Mollusc	Gastropod	*Strombus*	Crossed-lamellar	Proteome
2014	Mann and Jackson (2014)	Mollusc	Gastropod	*Cepaea*	Shell	Proteome
2015	Luo et al. (2015)	Brachiopod		*Lingula*	n/a	Genome
2015	Liu et al. (2015)	Mollusc	Bivalve	*Pinctada*	Larval microarray	Transcriptome
2015	Sun et al. (2015)	Mollusc	Bivalve	*Patinopecten*	Adult mantle?	Transcriptome
2015	Glazer et al. (2015)	*Arthropoda*	Crustacean	*Procambarus*	Gastrolith	Proteome
2017	Marie et al. (2017)	Mollusc	Bivalve (*Unionoida*)	*Elliptio/Villosa*	Nacre matrix	Proteome
2018	Mann et al. (2018)	Mollusc	Gastropod	*Haliotis*	Nacre/prismatic	Proteome

Overview and origin of comprehensive database information, analyzed with respect to mollusc shell formation and selected other biomineralizing model systems. The number of identified gene products is impressive, raising the question how common regulatory mechanisms could have evolved

at mineralizing interfaces by means of mollusc myosin chitin synthases. Cellular regulation at a mineralizing tissue interface comprises some additional aspects, as compared to a non-mineralized extracellular matrix. This sub-chapter aims at highlighting what makes chitin synthesis in molluscs special, as compared to chitin synthesis in representatives of other invertebrate phyla (Cohen 2009; Merzendorfer 2011; Abehsera et al. 2015). Some hypotheses claim that, at least in molluscs, chitin synthesis is part of a molecular and mechanical cross-talk mechanism between material precursors and cells (Weiss and Marin 2008; Weiss 2010, 2012). Mollusc shell formation, according to the hypothesis, is not based on the "by chance" long-range order deposition of a biopolymer in the extracellular space, eventually followed by short-range order hardening via the incorporation of proteins, ions, and minerals. There could be active control mechanisms in place on several hierarchical levels.

2.2 Limitations of the Structural Approach

2.2.1 Properties of Chitosan and Chitin in Biominerals

There are two extreme experimental approaches to investigate a ~5% fraction of chitin in the complex composite materials that molluscs form. The first one is based on nondestructive techniques such as X-ray and electron diffraction methods, which largely maintain the material's structural integrity. Based on these techniques, it has been proposed that, depending on the source and the mollusc species, mineral phases occur in composites aligned with the fiber orientations of chitin and protein beta sheets (Weiner et al. 1983). However, these techniques are clearly limited. For example, it is impossible to determine in one sample chemical compositions, functional interactions, and near-range order of the molecules involved. Therefore, the second "extreme" approach is based on differential physical and chemical extraction methods, which in the case of chitin-mineral composites always include a demineralization step. Particularly this step introduces a significant change in sample composition and structure, meaning that any result may not necessarily reflect the situation in the original composite material. One of the harshest chemical treatments of a gastropod (*Haliotis*) shell matrix allowed researchers to identify chitin by means of liquid NMR (Weiss et al. 2002a). Other mineralized tissues including silicate biominerals were later investigated also by solid-state NMR (Goobes et al. 2006, 2007; Brunner et al. 2009). This is one of the currently most promising ways to elucidate potential direct relationships between the minerals and the organic phases in biominerals on the level of individual molecular bonds. Another approach was based on the idea to extract chitinous polymers by means of volatile reagents, which would then leave an organic fraction with a minimum of artificially introduced impurities that is suitable for mass spectroscopic investigations. In fact, the chitinous biopolymer fractions were subjected to fragmentation into chitooligosaccharides. This step was necessary to achieve solubility, which decreases substantially with increasing chain length in "native" chitin samples that

retain their high degree of acetylation. It turned out that chitin samples extracted from adult and larval *Mytilus* shells differed from commercially available chitin reference samples. Mass spectrometry data then suggested that mollusc chitin has, in addition to *N*-acetylation, some further "silklike" covalent modifications, which influence the surface active properties of the compound (Weiss et al. 2009).

Generally speaking, it is extremely difficult to extrapolate from such fragmented evidence how chitin and most likely enzymatically modified chitin derivatives influence and aid the assembly process of mineral-chitin composites with short-range and long-range order, with their internally and externally curved textures posing experimental limitations for conventional material testing. All the evidences we have are based on complementary experiments, most of them using adult shell materials as starting point. On the other hand, the formation process includes precursor materials such as amorphous mineral precursors, which transform with time into crystals that are ordered also with respect to the highly curved larval shell (Weiss et al. 2002b).

Historically, biochemical pathways were elucidated by characterizing the involved enzymes (Sumper et al. 1969; Cantarel et al. 2009; Park et al. 2010; Yonezawa et al. 2016; Steven et al. 2016; Nelson et al. 2017; The UniProt Consortium 2017). The enzymes are localized either in the cytosol, in the lumen of organelles, or within the cellular membranes which separate the cytosol from the lumen of compartments. Altogether, they form a complex system which is cross-regulated by a network of signals to ensure constant flow of information between the status of gene regulation and the structural and functional integrity of cells, tissues, organs, and organisms (Nelson et al. 2017). The biochemistry of mineral-chitin composites was similarly approached: Shells were simply demineralized, and individual protein fractions were analyzed with respect to compounds tested for their ability to transform mineral phases. One of the most spectacular findings was the identification of factors that induce aragonite and calcite formation (Falini et al. 1996; Levi et al. 1998). Here, the difference between biochemical enzymes and "structural" enzymes becomes clear: A biochemical enzyme catalyzes a chemical reaction, and the product is already an educt for the next steps in a cascade of reactions – most of them taking place in the liquid state. A "structural" enzyme (Weiss and Marin 2008) is involved in phase transitions between a liquid and a solid state, and even the gas phase plays a role, at least in $CaCO_3$ systems, which are in equilibrium with HCO_3^- and CO_2 (Miyamoto et al. 1996). The problems associated with this fact have been extensively reviewed in Weiss and Marin (2008) and references therein.

Nevertheless, the recent availability of genomic, transcriptomic, and proteomic resources for various biomineralizing organisms including brachiopods, gastropods, and bivalves (Table 2.1) is certainly useful for pushing forward the complex field of biomineralization proteins. On the other hand, besides a tremendous treasure trough of biogenic additives in mollusc shells (Marin et al. 2007; McDougall and Degnan 2018), there could be just one individual key protein, which possesses the highest level of biological capabilities to interfere with minerals, namely, to gain control over so-called lattice distortions (Weber et al. 2014). Depending on the environment, even individual amino acids have the potential to induce lattice distortions to an

extent depending on the particular properties of side chains (Borukhin et al. 2012). These phenomena raise additional questions regarding the central coordinating center of the system. How did the ancestors of molluscs and brachiopods acquire the means to not only manipulate mineral phases by experimenting with organic additives but taking advantage of distinct manipulation capabilities for constructing coherent and mechanically stable, hierarchical composites with species-specific long-range order? Crack resistance could then become an evolutionary relevant selection criterion for the composite materials (Gao et al. 2003).

Assuming that mainly the 5% fraction containing chitin is responsible for stopping crack formation and supposing that this chitin fraction also interferes with the orientation of inorganic crystals – by the way with major implications for taking evolutionary advantage of their anisotropic optical properties (Kintsu et al. 2017) – it is well justified to take a closer look at the enzymatic formation of chitin in molluscs. Let us have a look which features cause the mollusc chitin synthase being a unique type of "molecular machine":

Next to motifs that are conserved in all chitin synthases, the chitin synthase involved in marine bivalve mollusc shell formation contains a myosin domain (Weiss et al. 2006).

The UniProtKB database (accessed 18-07-27; (The UniProt Consortium 2017)) lists currently six entries of mollusc myosin chitin synthases with a length of >2200 aa (with evidence on the transcript level). They originate from five bivalves (Fig. 2.2, line 1) Mediterranean mussel *Mytilus galloprovincialis*, (Fig. 2.2, line 2) Malaysian cockle *Tegillarca granosa*, (Fig. 2.2, line 3) Stiff penshell *Atrina rigida* (*Pinna rigida*), (Fig. 2.2, line 4) Akoya pearl oyster *Pinctada fucata*, (Fig. 2.2, line 5) Triangle sail mussel *Hyriopsis cumingii* (*Unio cumingii*), and one polyplacophora chiton: (Fig. 2.2, line 6) *Leptochiton asellus*.

It is characteristic for the group of mollusc myosin chitin synthases that their sequence similarity is extremely high over the whole length of the molecule (Fig. 2.2). The overall phylogenetic relationship between the six mollusc myosin chitin synthases (Fig. 2.2) is shown in Fig. 2.3.

The sequence alignment in Fig. 2.2 suggests that the following domains are essential for mollusc biomineralization-specific chitin synthesis processes:

1. A myosin domain, which is supposed to reside intracellularly because of the necessity to interact with the intracellular and/or microvilli actin cytoskeleton.
2. Five highly conserved transmembrane (TM) domains TM-01 to TM-05, interspaced with highly conserved extracellular and intracellular amino acid residues in between.
3. A highly conserved extracellular domain, spanning a conserved sequence range from ~ aa1050 to ~ aa1120.
4. Two highly conserved TM domains TM-06 to TM-07 found in the bivalve chitin synthase sequences and in the polyplacophora chitin synthase sequence.
5. An arrangement of n TM domains ($n = 1–3$), located N-terminal to the catalytic center. The respective n can be species-specific and variable. However, it must accommodate the correct localization of the catalytic center. This means that nucleotide-binding domains with D/E ("D180"), DXD ("D246/D248"), and

Fig. 2.2 Multiple alignment (Larkin et al. 2007) based on UniProtKB (accessed 18-07-27; (The UniProt Consortium 2017)) entries of mollusc myosin chitin synthases with a length of >2200 aa (with evidence on the transcript level) originating from five bivalves (1) Mediterranean mussel *Mytilus galloprovincialis* [UniProtKB – A5HKN1_MYTGA; 2281 aa], (2) Malaysian cockle *Tegillarca granosa* [UniProtKB – A0A1C9CX60_TEGGR; 2281 aa], (3) Stiff penshell *Atrina rigida* (*Pinna rigida*) [UniProtKB – Q288C6_ATRRI; 2286 aa], (4) Akoya pearl oyster *Pinctada fucata* [UniProtKB – A7BIC0_PINFU; 2276 aa], (5) Triangle sail mussel *Hyriopsis cumingii* (*Unio cumingii*) [UniProtKB – A0A141GE43_HYRCU; 2300 aa], and one polyplacophora chiton: (6) *Leptochiton asellus* [UniProtKB – A0A023PPX9_9MOLL; 2407 aa]

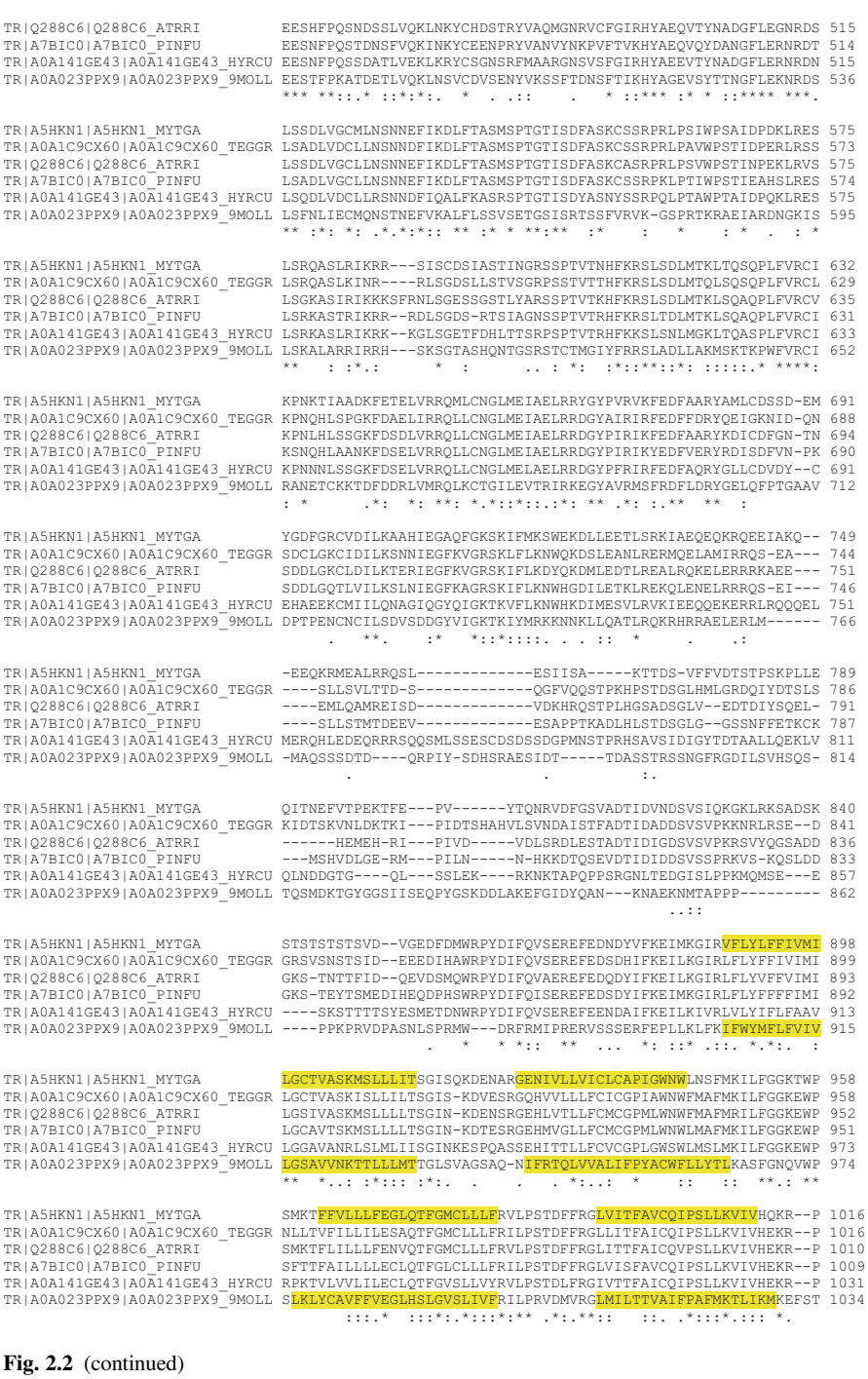

Fig. 2.2 (continued)

Fig. 2.2 (continued)

Fig. 2.2 (continued)

```
TR|A0A1C9CX60|A0A1C9CX60_TEGGR I---------QKYEPLSLMFLSVFAIAISLQFVSMFIHRWGTFLHLMSTTRVDWFKKIAT 2126
TR|Q288C6|Q288C6_ATRRI         I---------NKYEPLSLVFLSVFAIAITLQFLSMFIHRWGTFLHLMSSTRIDWFKKVHT 2118
TR|A7BIC0|A7BIC0_PINFU         I---------NKYEPLSLIFLSIFAIAISLQFLSMFMHRWGTFLHLMSSTRIDWLKKMHT 2118
TR|A0A141GE43|A0A141GE43_HYRCU I---------AKYEPLSLVFLSVFAFCITLQFLSMFIHRWGTFLHLMSSTHIDWFKNSST 2143
TR|A0A023PPX9|A0A023PPX9_9MOLL ALPHVEEGKQNHLEPLGFVFLFLFGLLLVSQFLAMLIHRWGTLLHLLSITEVPLVGKKHG 2214
                                     : ***.::** :*.: :  **.:*::*****:***:* *.:  . .

TR|A5HKN1|A5HKN1_MYTGA         EEDFVRFVVNEAQRLQRMEPAPDYDDLPPDYDDDDTTTTTY-NMPDEPYDELPSLPPTPD 2185
TR|A0A1C9CX60|A0A1C9CX60_TEGGR EEDFVRFVVNEAQRLQRMEPAADYDDMPPDYDDDDTTD-VT-NNGSEQYDELPSLPATPI 2184
TR|Q288C6|Q288C6_ATRRI         EEDFVRFVVNEAQRLQRLEPEPDYDDLPPDYDDDGFTS-SI-ETPSEQYDELPSLPASPG 2176
TR|A7BIC0|A7BIC0_PINFU         EEDFVRFVVSEAQRLQRLEPEPDYDDLPPDYEDDETT---A-TTPSEQYDELPSLPATPR 2174
TR|A0A141GE43|A0A141GE43_HYRCU EEDFVRFVVSEAQRLQRMEPAADYDEMPTDYDDNEYEDTVTAINDSEAYDILPTPPGSNH 2203
TR|A0A023PPX9|A0A023PPX9_9MOLL IQDAARDAIEKTKQLQRLRDIEFEPEPDPDYPTDEDMNEPYPDYDSEYESSLTS---SPS 2271
                                :* .* .:.::::::*:.      :   **  :           .*  . * :   :

TR|A5HKN1|A5HKN1_MYTGA         GTIKSEPKNRK---RHSGPSDPNIPLLQQIFEDRLENIHRKWKQGTLAFRNS---DKRRF 2239
TR|A0A1C9CX60|A0A1C9CX60_TEGGR DTFGRQRRGHG----PHHNGHDDVPILQQIFENRLENIHRKWKQGTLAFRYNNNNNNRRL 2240
TR|Q288C6|Q288C6_ATRRI         ATCRKISRSKSHKERSKNNFNKNVPVLQQIFENRLENIHRKWKQGTLAFRPN-----YRF 2231
TR|A7BIC0|A7BIC0_PINFU         ETFSRSVRRRYGT--MRDHENTDIPLLQQIFEDRLENIHRKWKRGTLAFRPN-----HLF 2227
TR|A0A141GE43|A0A141GE43_HYRCU NTHR---HGFPQRDKKNSPTDKDMPLLQQIFEDRLENIHRKLKRGTFAFRHQD----GPF 2256
TR|A0A023PPX9|A0A023PPX9_9MOLL DSVLSDIPP---------SYHSDEDYYQQVYDKKDKKK-RK---RRSVF----------- 2307
                                :                  . :    **:::.: ::  **      .*

TR|A5HKN1|A5HKN1_MYTGA         NRFDDNRFSQKDDIMREKMFKRSFKKNSTEENIHT-------------------------- 2274
TR|A0A1C9CX60|A0A1C9CX60_TEGGR NRHDSNRFSQRDNIMRQQMFKRSFKKYSGDEEA-------------PK------------ 2275
TR|Q288C6|Q288C6_ATRRI         DRTESHRFSEKEHIMRQKMFKRSFRRINSKEDNKNHSDDFLDHRDMPQ------------ 2279
TR|A7BIC0|A7BIC0_PINFU         TRTDSHRVSEKEQEMRQKMFKRSFRRIHSREDKSLEQN--------GQ------------ 2267
TR|A0A141GE43|A0A141GE43_HYRCU QRNDSKRYSNKISNMRQRMFKRSFKNRGRDDQHDE-----------PA------------ 2293
TR|A0A023PPX9|A0A023PPX9_9MOLL ---NDRGFST--GHTLQQAFIRRFRRMQLEEQDRQASVRSGSHTSRPSLFTAFNISREAT 2362
                                  :..  *       :: * * *:.    ::

TR|A5HKN1|A5HKN1_MYTGA         --------------------AIKIDT------------I------ 2281
TR|A0A1C9CX60|A0A1C9CX60_TEGGR --------------------SIRIDI------------------- 2281
TR|Q288C6|Q288C6_ATRRI         --------------------SIKIDM------------H------ 2286
TR|A7BIC0|A7BIC0_PINFU         --------------------SIIIDM------------HKL---- 2276
TR|A0A141GE43|A0A141GE43_HYRCU --------------------EIKIEE------------I------ 2300
TR|A0A023PPX9|A0A023PPX9_9MOLL EAGDSRPETDAEAGPSRASSAMSLSAMGTTPAPHAYMSHEFPVSS 2407
                                          : :.
```

Fig. 2.2 (continued)

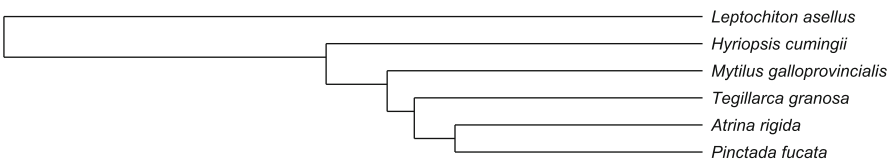

Fig. 2.3 Relationship between mollusc myosin chitin synthases (Fig. 2.2): *Leptochiton asellus* (Polyplacophora), triangle sail mussel *Hyriopsis cumingii*, Mediterranean mussel *Mytilus galloprovincialis*, Malaysian cockle *Tegillarca granosa*, Stiff penshell *Atrina rigida*, and Akoya pearl oyster *Pinctada fucata*.

GE**D**R ("D343") Mg^{2+}/UDP-binding motifs as well as the polymer guiding/channeling motif QRRRW ("W383") of the GT-domain (GT, glycosyltransferase) are accessible from the cytosolic reservoir for supply of UDP-GlcNAc. The "aa numbers" in brackets refer to the BcsA glycosyltransferase, a cellulose synthase for which a crystal structure has been determined (Morgan et al. 2016).

6. A well-defined number of TM domains, which are rich in aromatic amino acids, located C-terminal to the catalytic center. They may contribute to the "template-free" translocation by triggering a hypothetical "molecular clutch" mechanism, although the occurrence of TM movements during the translocation of the chitin polymer through the TM channel is still unclear. The sequence alignment (Fig. 2.2) shows that the five TM helices located next to the NQRRRW motif

are highly conserved, in terms of both TM sequences and the notably short interspace sequences.
7. The exact number of five TM domains next to the GT motifs leaves almost no doubt that a highly conserved domain starting at aa position ~ 1875 with a SWGTRE signature motif is located in the extracellular space.
8. At least two more TM helices are predicted for all molluscan myosin chitin synthases identified in the databases. The C-terminal extracellular domain is also conserved to a certain extent in bivalve molluscs.

Apparently, there is a significant problem of predicting the topology of some transmembrane domains. For example, the sequence motif "WSQVMYMYYLLGYKLFG" was clearly identified as a transmembrane domain in the chitin synthase of *Mytilus* (uniprot ID: A5HKN1_MYTGA, aa1473 – aa1491). In spite of its high degree of conservation, even shared by the distantly related polyplacophoran *Leptochiton* sequence (A0A023PPX9_9MOLL), this motif was not predicted as a TM domain in other sequences shown in Fig. 2.2.

The following list (Table 2.2) provides ID numbers, selected from different invertebrates according to phylogenetically representative species and respective positions of sequence motifs which share similarity with the abovementioned "problematic" WSQVMYMYYLLGYKLFG sequence motif. The presence or absence of N-terminal myosin domain, TM architecture of individual "TM clusters" as documented in the UniProt database (The UniProt Consortium 2017):

The relationship of some selected chitin synthases of the phylum mollusca to chitin synthases of other taxa that include biomineralizing organisms such as crustaceans is shown in Fig. 2.4.

The tree of chitin synthases shown in Fig. 2.4 reflects to some extent also the phylogenetic relationships. The extracellular domains, which are supposed to regulate the biomineralizing interface, are not specifically conserved between crustaceans and molluscs, both of which mineralize their exoskeletons or shells, respectively (Lowenstam and Weiner 1989). The picture may change once additional sequences of myosin domain containing chitin synthases become available, for example, from crustaceans. The gastropod *Lottia*, for example, contains several chitin synthases according to genome data (Jackson et al. 2006; Mann et al. 2012), and some of them do not possess any myosin domain at all.

So far, there is no 3D structure available for chitin synthases which resemble the topography of the mollusc myosin chitin synthases. The PDB entry 4P00 reports the structural model of the bacterial cellulose synthase (McNamara et al. 2015). According to this model, the polymer chain is translocated through a membrane-embedded channel. The channel's inner surface is decorated smoothly with aromatic residues (W, F, Y), their side chains matching the distances between the sugar monomers within the sugar chain. It is, however, important to note that there are several major differences between cellulose- and chitin-synthesizing systems. Especially the synthesis of cellulose in bacteria requires additional factors (e.g., BcsB) (Lairson et al. 2008; Bi et al. 2015; McNamara et al. 2015; Du et al. 2016), which are separate polypeptide chains located in the inner and outer membranes as well as in

Table 2.2 "Hidden" TM domain <WSQVMYMYYLLGYKLFG>

ID	Taxonomy	MMD	TM topology	Pos. WSQ... motif
A5HKN1_MYTGA	Bivalvia	+	9 + 1 + 5 + 2	1473–1491
W5J6T6_ANODA	Diptera	−	n/a	781–793
A0A0M9AB39_9HYME	Hymenoptera	−	8 + 4 + 2	682–694
A0A0C9RP55_9HYME	Hymenoptera	−	8 + 5 + 2	673–685
A0A059Q3J8_PANJP	Crustacea	−	9 + 4 + 2	712–726
A0A1S3IM62_LINUN	Brachiopoda	−	8 + 5 + 2	
A0A0L8HN41_OCTBM	Cephalopoda	−	9 + 5 + 2	
A0A023PPX9_9MOLL	Polyplacophora	+	9 + 5 + 2	1531–1546
V4B5K3_LOTGI	Gastropoda (m)	+	10 + 5 + 2	1473–1489
A0A2C9JZL6_BIOGL	Gastropoda (f)	−	9 + 5 + 2	1069–1085
A0A210QNC5_MIZYE	Bivalvia	MyoIIIB	8 + 5 + 3	1511–1523

ID	Taxonomy	UniProtKB entry
A5HKN1_MYTGA	*Mytilus galloprovincialis*	A5HKN1
W5J6T6_ANODA	*Anopheles darlingi*	W5J6T6
A0A0M9AB39_9HYME	*Melipona quadrifasciata*	A0A0M9AB39
A0A0C9RP55_9HYME	*Fopius arisanus*	A0A0C9RP55
A0A059Q3J8_PANJP	*Pandalopsis japonica*	A0A059Q3J8
A0A1S3IM62_LINUN	*Lingula unguis*	A0A1S3IM62
A0A0L8HN41_OCTBM	*Octopus bimaculoides*	A0A0L8HN41
A0A023PPX9_9MOLL	*Leptochiton asellus*	A0A023PPX9
V4B5K3_LOTGI	*Lottia gigantea*	V4B5K3
A0A2C9JZL6_BIOGL	*Biomphalaria glabrata*	A0A2C9JZL6
A0A210QNC5_MIZYE	*Mizuhopecten yessoensis*	A0A210QNC5

m marine, *f* freshwater

Selected invertebrate chitin synthases were retrieved from UniProt by similarity with the WSQVMYMYYLLGYKLFG sequence motif, which demonstrates the problem of TM topology prediction in chitin synthases. Note that there is still no ultimate proof for the absence (−) of a myosin motor domain (MMD), and cytoskeletal interaction could as well be maintained by an indirect coupling mechanism

the periplasmic space. For example, there is sound experimental evidence that BcsB is necessary to promote active template-free translocation of the cellulose polymer through the membrane channel (Morgan et al. 2016). In contrast, no template-free translocation seems to occur in the process of DNA synthesis, and several "molecular clutch mechanisms" are currently explored with respect to the role of the template (Morin et al. 2015).

Fig. 2.4 Relationship between chitin synthases that contain WSQVMYMYYLLGYKLFG domains. ID numbers: *Atrina rigida*, Q288C6; *Leptochiton asellus*, A0A023PPX9; *Pandalopsis japonica*, A0A059Q3J8; *Lingula unguis*, A0A1S3IM62; *Lottia gigantea*, V4B5K3; *Octopus bimaculoides*, A0A0L8HN41

For molluscs, we face a completely different situation. The entire process, starting from UDP-GlcNAc binding via the formation of the glycosidic bond to the translocation through a sophisticated membrane pore, also could be triggered by mechanical and/or topological forces which originate from actin-myosin interactions. Membranes are curved to some extent, especially at the tip region of a microvillus, where the chitin synthase could dynamically reside. One must therefore take into account that especially the transmembrane regions are actively molded and that conventional membrane topology predictions will never give the full picture. Any mechanistic insight, which could be derived from other glycosyltransferase systems, can only give rise to speculation about chitin formation in molluscs. Nevertheless, the molecular machinery in molluscs is conserved at least on the primary structure level to an amazingly high extent. The myosin domain of those mollusc chitin synthases, which do contain an N-terminal motor protein domain, has highest similarity to MyoIII from the Japanese scallop (Fig. 2.5).

Apparently, molecular evolution was not able to accommodate much variation when there is need to control the formation of mechanically stable chitin-mineral nanocomposites. This raises a number of questions to which we will come back, especially to implications related to the MyoIII and its relation to the shell-forming tissue architecture, in the last section of this sub-chapter.

The recent theory about a flexible gating loop (Dorfmueller et al. 2014; Morgan et al. 2016) located in the transmembrane region of glycosyltransferases such as the BcsA-B complex (Omadjela et al. 2013; McNamara et al. 2015) is still worth considering as a potential mechanism, which could be similar in both cellulose and chitin synthesis. Let us recall the basic structural facts about bacterial cellulose synthesis: The nascent glycan chain is arrested by the QXXRW motif within the channel. The UDP-activated sugar nucleotide is put on stage via Mg^{2+} and DXD motifs. Bacteria need an extra transmembrane (pericellular) BcsB complex for unknown reasons but perhaps also for triggering the translocation mechanism externally. The question arises whether the formation of the glycosidic bond induces conformational changes that directly induce the mechanical translocation of the glycan chain by a distance corresponding to one sugar subunit. For the bacterial BcsA subunit, which – like the mollusc chitin synthases – belongs to family 2 of glycosyltransferases (GT2) possessing an inverting mechanism exerted by a GT-A fold, Morgan and colleagues (McNamara et al. 2015; Morgan et al. 2016) reported a

Fig. 2.5 Phylogenetic tree based on myosin motor domain (MMD) sequences (Fig. 2.2, Table 2.2), highlighting the relationships between chitin synthases and MyoIII, the chitin synthase of the Japanese scallop, *Mizuhopecten* (Bivalvia). UniProtKB – ID numbers: *Lottia gigantea*, V4B5K3; *Biomphalaria glabrata*, A0A2C9JZL6; *Mizuhopecten yessoensis,* A0A210QNC5; *Leptochiton asellus*, A0A023PPX9; *Hyriopsis cumingii* (*Unio cumingii*), A0A141GE43; *Mytilus galloprovincialis*, A5HKN1; *Atrina rigida*, Q288C6

mechanism which couples the formation of the glycosidic bond with a movement of the interfacial "finger helix." Presumably, the catalytic aspartate takes actively part in the conformational change, depending on the protonation state (Forood et al. 1993; Dirr et al. 2005; Scharnagl et al. 2014). Frequent cycles of stabilization and destabilization of the alpha-helical secondary structure of the "finger motif" are intimately coupled to the status of the formation of the glycosidic bond and, at the same time, the position of C4-OH of the cellulose chain with respect to the newly added sugar unit. Figure 2.6 shows an alignment of *Mytilus* CS-1 (uniprot ID: A5HKN1) with BcsA (uniprot ID: Q3J125), aiming at identifying the status of conservation of the amino acid sequence of the "finger helix" in mollusc chitin synthases (Weiss et al. 2006). In fact, D1657 and Y1673 of the *Mytilus* CS-1 can be aligned with the D343 and Y359 of the BcsA subunit, the flanking amino acids, which mark the N- and C-terminus of the "finger helix," respectively.

The team of Jochen Zimmer (Morgan et al. 2016) also claims experimental evidence for a novel concept, which puts emphasis on a gating loop. This loop changes position as a function of individual steps that are taken during UDP-cleavage from the sugar, associated with phosphate release and formation of the glycosidic bond. An additional "finger" is postulated, which holds the chain in the pre-elongation step in place, while it changes position after chain elongation (=pre-translocation). Actually, it "snaps" back into its original place, still connected with the newly added sugar, which then marks the new nonreducing acceptor state being ready for the next cycle (=post-translocation).

The isoleucine I340 marks the "finger helix" in BcsA. There is also an Ile in aa position 1650 ± 5 aa for mollusc chitin synthases, with the one of *Leptochiton* being less conserved. This "Ile1650" is followed by an extremely conserved motif containing the "ED" doublet, which is shared between BcsA and mollusc chitin synthases. Although the role of a "finger helix" could be taken over by other domains, the fact that D-terminated domains are switchable in a pH-dependent manner (Forood et al. 1993; Dirr et al. 2005; Scharnagl et al. 2014) is appealing especially for biomineralizing systems, in which ion gradients across membranes might play an active role in the control mechanism at the mineralizing interface

Fig. 2.6 CLUSTAL O (1.2.4) (Larkin et al. 2007) sequence alignment of the bivalve myosin chitin synthase CS1 of *Mytilus galloprovincialis* (UniProtKB – A5HKN1) and the bacterial cellulose synthase BcsA of *Rhodobacter sphaeroides* (UniProtKB – Q3J125). Mechanistic models based on X-ray crystallographic investigations exist so far only for BcsA, see text for details. TM regions are highlighted in yellow (dark yellow, *Mytilus* CS-1; light yellow, BcsA), suggesting that arrangements of "finger helix" motifs (shaded in blue) are better conserved than hypothetical "gating loops" (green), which may recruit different TM helices in eukaryotes and prokaryotes. Low complexity regions (underlined) may fulfill additional regulatory functions and mediate cross-talk with the extracellular matrix in the case of mollusc chitin synthases

Fig. 2.6 (continued)

```
TR|A5HKN1|A5HKN1_MYTGA NNVVFIYCMINFLWTVITLQLQSMEDELKNRYIIEKYEPLSLIFLSIFAIAITLQFFSMF 2102
TR|Q3J125|Q3J125_RHOS4 ETVAYLIFGESAHWRTMREA--------------TMRPI-------------------- 707
                       :.*.::    .  * .:                . .*:

TR|A5HKN1|A5HKN1_MYTGA MHRWGTFLHLMSSTRIDWLKTVQTEEDFVRFVVNEAQRLQRMEPAPDYDDLPPDYDDDDT 2162
TR|Q3J125|Q3J125_RHOS4 -------GLLHGMARILWMAAASLPKTARDFMDEPARRRRRHEEPKEKQAHLLAFGTDFS 760
                             * . :** *: :..  :    *: : *:* :* *   : :     :. * :

TR|A5HKN1|A5HKN1_MYTGA TTTTYNMPDEPYDELPSLPPTPDGTIKSEPKNRKRHSGPSDPNIPLLQQIFEDRLENIHR 2222
TR|Q3J125|Q3J125_RHOS4 TEPDW--AGEL------LDP--TAQVSARPNTV-------------------------- 783
                       *   :   .*       * *   . :.:.*:.

TR|A5HKN1|A5HKN1_MYTGA KWKQGTLAFRNSDKRRFNRFDDNRFSQKDDIMREKMFKRSFKKNSTEENIHTAIKIDTI 2281
TR|Q3J125|Q3J125_RHOS4 AWGSN------------------------------------------------------ 788
                        * ..
```

Fig. 2.6 (continued)

(Jackson et al. 2006; Weiss 2010) and refs. in Table 2.1. Let us summarize the features of BcsA and potential equivalent domains in the molluscan enzymes:

1. W383 holding the cellulose polymer chain in position is present in molluscs (~1691).
2. D246/343 put the glucose derivative in position, also present in molluscs (~1552/~1657).
3. The "FxVTxK loop" responds to mechanical stress by conformational change. This loop may have an equivalent counterpart in molluscs, which is not obvious due to the significant rearrangements and higher number of TM helices within the C-terminal region of the enzymes. Only one domain, presumably located intracellularly between TM-16 and TM-17, shares key amino acids present in the BcsA motif EDELKN**FYIIEK**YE, the Phe (F), and the lysine (K), which are flanking the hexapeptide.
4. The "finger helix" changes position while translocating the polymer chain into the channel. The channel "inner" (cytosolic) entrance motif NQRRRW, which is also highly conserved among molluscs, represents a defined "landmark" for the topology of TM helices.
5. The "fifth-pack" of C-terminal TM helices in molluscs are, in a conserved manner, interspaced by 5 aa (intracellularly) and 11 aa (extracellularly), leaving not much room for speculation about the orientation and a presumably tight packing of the five helices. In another context, there are 5 aa and 11 aa interspaces in BcsA, which occur in the C-terminal "4th-pack" of transmembrane domains (11aa at TM04-05 and 5 aa at TM06-07). Domain shuffling should at least be taken into consideration, which suggest different regulatory mechanisms of not only translocating cellulose and chitin polymers in bacteria and in invertebrate animals but also exerting influence on the level of final textures and perhaps even the properties of fiber and/or composite materials.
6. Finally, the enzyme retains its original state and is ready for a new cycle.

2.2.2 *Hypotheses About the Role of Myosin Domains in Mollusc Chitin Synthases*

The myosin domains of the mollusc chitin synthases are also highly conserved. According to BLAST and FASTA searches, they share highest similarity to molecular motors of myosin class III. The class III myosins comprise two subtypes, MYO3A and MYO3B (Quintero et al. 2013; Raval et al. 2016; Pinkoviezky and Gov 2017). Among them are cytoskeletal transporters, but some of them are involved in the regulation of actin-based ultrastructures (Mooseker and Foth 2007; Orly et al. 2014; Masters et al. 2016; McGrath et al. 2017). Important examples are the stereocilia in the inner ear and stable actin protrusions, which are essential for eye vision (Ebrahim et al. 2016; Krey et al. 2016; Lelli et al. 2016; Liu et al. 2016; Tarchini et al. 2016; Vélez-Ortega et al. 2017). There are subtle differences between MYO3A and MYO3B, mainly related to their autophosphorylation capacity and the length and regulatory functions of the tail domain (Manor et al. 2012; Merritt et al. 2012). One could speculate how, in the course of mollusc evolution, the function of this tail domain was expanded, if not replaced, by the chitin synthase domain. Recent investigations provide experimental evidence that class III myosins enhance the formation and elongation of actin protrusions (An et al. 2014; Peña et al. 2016; Raval et al. 2016; Pinkoviezky and Gov 2017). Assuming that mollusc myosin chitin synthases also possess this "structural activity" on the tissue level, one would expect to find actin protrusions at the shell-forming interface. In fact, packed "brush border" microvilli were described at nacre-forming interfaces already many years back (Bevelander and Nakahara 1969; Phillips 1979; Jongebloed et al. 1999; Lundin and Schander 2001; Álvarez Nogal and Molist García 2015; Molist et al. 2016). Hardly anybody has paid attention to this phenomenon in respect to seminal reports on mollusc chitin synthases with similarity to class III myosins (Weiss et al. 2006; Schönitzer et al. 2011; Morozov and Likhoshway 2016). Model systems were established based on *Dictyostelium* expression hosts for testing the ability of mollusc myosin chitin synthases to induce the formation of actin protrusions. First evidence was provided by Schönitzer and colleagues who used AFM to investigate the surface roughness of the cells (Schönitzer et al. 2011). They found that the mollusc chitin synthase-expressing cells were extremely difficult to measure by AFM, namely, because of limited cell adhesion on the one hand but, on the other hand, because of "spines" extruding from the cell surface, which usually produce "mirror images" of the AFM tip on top of the cells. Therefore, it was not possible to determine the dimensions of individual spines accurately (Schönitzer et al. 2011). In summary, there is a line of evidence both on the primary structure level and based on nanoscale structural data from heterologous expression systems, which favor a microvilli-inducing function of the mollusc myosin chitin synthase.

The localization of transmembrane enzymes is in itself a mechanism for regulation. For example, the ATP synthase is arranged in dimers along the tips or edges of cristae formed by the inner membrane of the mitochondria (Steven et al. 2016). This arrangement allows pairing of two enzymes in a defined angle toward each other, which has a strong impact on the intra- and intermolecular motions of the assemblies, and at the same time ensures proper localization of the enzymatic domains with

respect to ion gradients maintained and exploited for ATP synthesis across the inner mitochondrial membrane. This "higher-order" arrangement makes the catalytic performance of the enzyme much more efficient (Steven et al. 2016).

2.2.3 *Challenges in Elucidating Mechanistic Relationships Between Myosin Chitin Synthases and Mollusc Shell Formation*

Mechanical signal transduction is a relatively young subdiscipline in life sciences. Cells interact differently with hard or soft materials (Shemesh et al. 2005; Geiger et al. 2009). Stem cells differentiate differently during their exposure to hard or soft materials (Engler et al. 2006; Lee-Thedieck and Spatz 2014). The phenomenon of cell adhesion and the dynamic formation and regulation of focal adhesion complexes involves many different factors (Cohen et al. 2003; Geiger et al. 2009; Steven et al. 2016). The model system *Dictyostelium* has 13 myosins, which generally belong to class I, class II, and class V (Gulick et al. 2000). Animal phylogeny is reflected in the evolutionary tree of myosin classes (Houdusse et al. 1999; Haszprunar and Anninger 2000; Hasegawa and Araki 2002; Mooseker and Foth 2007; Heissler and Sellers 2016; Brunet and King 2017; Kollmar and Mühlhausen 2017). The myosin chitin synthases of molluscs were previously discussed in this context (Schönitzer et al. 2011; Weiss 2012). The first occurrence of myosin class III (myosin III) is metazoan specific (Kambara et al. 2006; Heissler et al. 2014; Kollmar and Mühlhausen 2017): Anthozoa including *Nematostella vectensis* do have a myo3, whereas *Monosiga brevicollis* (Choanoflagellida) lack the one (Odronitz and Kollmar 2007). The situation is similar for classes myosin 9 and myosin 18 (Odronitz and Kollmar 2007; Kollmar and Mühlhausen 2017). Therefore, we have to answer at least two questions if we want to understand the relationship between metazoan-specific myosins (class 3, 9, 18) and the biomineralization of hard-soft interfaces, which does not only lead to "simply" depositing mollusc shells but to evolutionary conserved formation of sophisticated textures (Schäffer et al. 1997; Beedham and Trueman 2009a, b):

(Q1):
Which levels of hierarchy can be targeted by chitin synthesis under the control of myo3 at interfaces between epithelial cells and materials?

(Q2):
Which minimal structural features would enable a "chitin synthase receptor" to fulfill its hypothetical function in transducing extracellular signals of material gradients in the range of disordered or ordered, organic or inorganic, soft or hard, tough or brittle interfaces?

The answers to these questions must accommodate the likelihood that a huge diversity of shells exists, which all contain chitin that is formed by a highly conserved enzymatic machinery. Currently available sequence relationships indicate

that the myosin domains of chitin synthases of brachiopods, polyplacophoran molluscs, gastropods, and bivalves act similar to class III (myo3) myosins in terms of tip localization in actin protrusions. Under which circumstances such actin protrusions are stabilized, and how microvilli could contribute to the CHS localization and regulation of chitin framework formation remains subject to further investigations.

Additional levels of regulation and fine-tuning could occur via calmodulin-like light chains which could further modify the activity of the myo3 domain (Heissler and Sellers 2016). It could happen also by means of mineralization-inducing chitin-binding proteins (Suzuki et al. 2009; Weiss 2010; references in Table 2.1), chitinases, or chitin deacetylases, which induce the hardening or softening of the extracellular matrix (e.g., a chitin/chitosan framework) and, thus, rapidly change the settings for mechanotransduction by some orders of magnitude (e.g., kPa ← MPa → GPa). This may close the circle of materials formation, materials "testing," and materials reception, which accommodates gradual adaptation toward favorable textures, both from ontogeny and phylogeny points of view.

2.3 Some Notes with Relevance to Understand Structure and Dynamics of Chitin Formation in Molluscs

The phylum mollusca has never been really positioned at the forefront of model systems for studying functional morphology in a physiological and genomic context (Bevelander and Nakahara 1969; Saleuddin and Wilbur 1983; Cartwright and Checa 2007). Nevertheless, one should take a closer look at a few well-studied exceptions, which demonstrate that recent molluscs do possess a broad range of regulatory networks (Emery 1992; Fabbri and Capuzzo 2010). We may never know for sure whether or not these regulatory networks existed already in Cambrian shell-forming animals. However, seeing the individual pieces from a distance will eventually help to recognize the messages and contents of a bigger mosaic picture.

Mosaic piece 1 – 1992 (Bevelander and Nakahara 1969; Emery 1992; Cartwright and Checa 2007; Checa et al. 2009, 2014, 2016): The presence of microvilli at external interfaces is a widespread and presumably fundamental phenomenon in different mollusc tissues, as evidenced by the analysis of the fine structure of olfactory epithelia of gastropods.

Mosaic piece 2 – 1998 (Siegman et al. 1998; Galler 2008): The phosphorylation of a twitchin-related protein controls catch state and calcium sensitivity of force production in invertebrate smooth muscle. This is a strong indication that mechanical signaling pathways are in place, and forces within tissues are under molecular control, particularly in molluscs.

Mosaic piece 3 – 2010 (Fabbri and Capuzzo 2010): Molluscs rely on signaling pathways, which are interconnected by cAMP. This also highlights the relationship between cilia for respiration and feeding, especially in gill tissue.

Coordination occurs via neuronal networks. There is experimental evidence that manipulation of colloidal graphite or metal ions is achieved even by isolated gill tissue fractions. Unfortunately, there is still not much information how these signaling pathways interfere with shell formation. Interference between gonad activation and the physiology of the mantle tissue is just briefly mentioned.

Mosaic piece 4 – 2012 (Manor et al. 2012; Pinkoviezky and Gov 2017): With respect to explore the bioarchitectures in molluscs, the role of the respective myosin chitin synthases must be characterized in view of functional differences between the related types of MMDs. For example, freely diffusing and processively walking and stalled myosins convert into each other. The respective reaction coefficients and boundary conditions with respect to actin treadmilling must be determined.

Mosaic piece 5 – 2015 (Álvarez Nogal and Molist García 2015; Molist et al. 2016): In the shell-forming mantle tissue of *Haliotis tuberculata*, microvilli are rather short (250 nm in length) and tightly packed in different modes (60–80 nm in diameter). Depending on the mantle region, they contain different amounts of "poorly developed" actin bundles, although care must be taken for as that conventional TEM sample preparations may cause artifacts. The authors differentiate between outer and inner mantle epithelial cells, which do contain prominent "brush border microvilli." However, the outer mantle contains two other cell types of secretory cells, which lack microvilli (type B and type G). The latter produce electron dense granules which are secreted, and vesicle fusion (alternatively, fusion of their content) occurs in the extracellular space. In this context, myosin chitin synthases must be investigated with respect to inner and outer mantle regions, which produce different shell textures in terms of both chitin organization and the mineral phase. A myosin chitin synthase's cross-talk with the microvillar architecture could explain different textures of chitin, which provide different frameworks for mineralization.

Mosaic piece 6 – 2016 (Weck et al. 2016): The MMD of mollusc chitin synthases shares similarity with either myo3a, myo3b, or myo7b. The latter is associated with bundling of microvilli. *Drosophila* myo7b has a high duty ratio of 0.8. It is localized and involved in enrichment of IMAC complexes at distal ends of microvillar actin bundles. IMAC complexes interconnect microvilli and regulate cadherin activity to maintain brush border architecture. Overall, myo7b provides mechanistic insight in apical morphogenesis in a variety of epithelial contexts. Barbed-end directed processive motility of "unconventional" myosins is a prerequisite. In general, a single microvillus is supported by a core of actin bundles of about 20–30 parallel filaments 0.5–5 μm in length, with the barbed ends oriented toward the distal tips, and the pointed ends anchored in a mesh of intermediate filaments and spectrin referred to as the terminal web (Mooseker 1975). Capping proteins (Avenarius et al. 2017) prevent actin polymerization but also control access to filaments, prevent depolymerization, and interfere with elongation and widening at intermediate stages of bundle development.

Mosaic piece 7 – 2016 (Peña et al. 2016): There is evidence that microvilli evolved early in the prehistory of modern animals and have been repurposed to serve

myriad functions in different cellular contexts. Microvilli-associated proteins were analyzed according to phylogenetic relationships, emphasizing the roles of myosins, mainly classes myo3 and myo15 for length regulation of microvilli. Associated proteins such as ezrin and calmodulin serve for membrane interconnections. Furthermore, actin-bundling proteins such as fimbrin, espin, and fascin are important. Cadherins, Fas2 (Halberg et al. 2016), and myo7 act as intermicrovillar bundle formers.

Mosaic piece 8 – 2017 (Merritt et al. 2012; Ebrahim et al. 2016; Krey et al. 2016; Raval et al. 2016; Yu et al. 2017): Understanding molecular control of the packing of actin filaments requires sophisticated experimental techniques. For example, myo3 with genetically engineered architectures revealed specific domain activities of myo3 in actin bundle formation. Stereocilia staircase regulation requires espin-1 and espin-like associated proteins. The full range of biophysical, biochemical, and cell biological experimental requirements are reviewed in Weck et al. (2017), focusing on actin-based and fingerlike membrane protrusions: (a) filopodia, (b) microvilli, and (c) stereocilia. The localization of relevant MyTH4-FERM myosins and their cargoes are highlighted for Myo7a, 7b, 10, and 15b. Potential adaptor proteins in molluscs remain to be identified.

Mosaic piece 9 – 2017 (Vélez-Ortega et al. 2017): A so-called mechanotransduction current, based on mechanoresponsive Ca^{2+} channels, is essential for stability of the transducing stereocilia in mammalian auditory hair cells, as demonstrated with benzamil inhibitors. This finding is of considerable interest to understand mollusc biomineralization, where Ca^{2+} homeostasis and calcification play a major role.

2.4 Conclusions from the "Mosaic Picture"

What happens, if mollusc myosin chitin synthases share several features mentioned before? Mollusc myosin chitin synthases possess unique and highly preserved extracellular domains (e.g., ECM motif, see Table 2.3, Fig. 2.7), which still remain to be characterized in more detail (Sengupta Ghatak et al. 2013; Weiss et al. 2013; Pohl and Weiss 2014). All hypothetical features, taken together, enable mollusc myosin chitin synthase enzymes to cover an additional extracellular cross-talk with biomineral interfaces at different stages of "inorganic development." The regulatory links to the cytoskeleton and the specific role of hierarchical topologies of enzyme complexes, especially when arranged at the tips of closely packed microvilli arrays, have most likely consequences for transducing shear forces and adhesive forces between the inorganic/organic composite and the material forming cells.

1. Mollusc chitin synthases are more similar to each other than to chitin synthases of other organisms, forming a unique group.
2. Within mollusc chitin synthases, there is a group which contains the *N*-terminal myosin domain.
3. The myosin domains of mollusc chitin synthases are similar to myo3.

Table 2.3 Features of myosin motors with chitin synthase-specific motifs

Species	MMD	Transition between MMD and GT-domain	GT motif – – – QGEDRW – – – NQRRRW – – –	ECM motif – – – SWGTRE – – – KEEEEELK – – – EEKKKKKE – – -
Atrina rigida	Myo3b (?)	LC	+/+	+/+/+
Lingula anatina	Myo3b, Myo3a	+	+/+	+/+/+
Octopus bimaculoides	Myo3b, Myo3a	+	+/+	+/−/−
Biomphalaria glabrata	Myo3a, Myo7a	n.a.	+/+	+/+/+
Aplysia californica	Myo7a	n.a.	+/+	+/+/+
Yesso scallop	Myo3b, (Myo3a)	+	+/+	+/+/+
Pacific oyster	Myo3b, (Myo3a)	(?)	+/+	+/+/+
Eastern oyster	Myo3b	(?)	+/+	+/+/+
Dictyostelium discoideum	Myo7a	−	−/−	−/−/−

Species	Sequence ID	ORF length, aa
Atrina rigida	DQ081727.1	2286
Lingula anatina	XP_013415035.1	2687
Octopus bimaculoides	XP_014772462.1	2049
Biomphalaria glabrata	XP_013060602.1	1031
	XP_013085899.1	2054
Aplysia californica	XP_012946756.1	963
	XP_012935486.1	1694
Yesso scallop *Mizuhopecten yessoensis*	XP_021346055.1	2272
Pacific oyster	XP_011423725.1	2340
Crassostrea gigas	XP_011425699.1	1067
Eastern oyster	XP_022307205.1	2337
Crassostrea virginica	XP_022323224.1	1489
Dictyostelium discoideum	XP_644171.1	2357

The presence and/or similarity of four conserved myosin chitin synthase domains (MMD, myosin motor domain; LC, region of low complexity; GT, glycosyltransferase; ECM, hypothetical extracellular matrix interface) was identified by stepwise FASTA/BLAST analyses using the following UniProt (The UniProt Consortium 2017) databank resources. Note that no chitin synthase domain is present in typical myosins, e.g., Myo7a of *D. discoideum*. The NCBI Genome Data Viewer was used for data processing [https://www.ncbi.nlm.nih.gov/genome/gdv/]

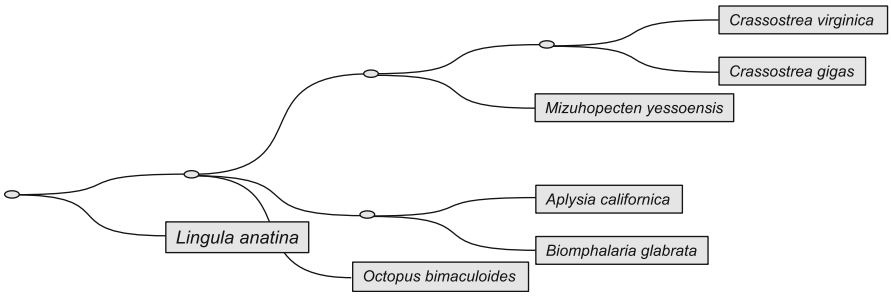

Fig. 2.7 Phylogenetic tree based on myo3 sequence features (Table 2.3)

4. Characteristic for myo3a is a *N*-terminal kinase domain for autocatalytic phosphorylation and concentration-dependent inactivation of actin binding; characteristic for myo3b is lack of the kinase domain and indirect coupling to actin bundles depending on cargos such as ezrin (see also "InterPro": https://www.ebi.ac.uk/interpro/entry/IPR001609).

2.5 Summary, Novel Hypotheses, and Outlook

As outlined in this sub-chapter, chitin mineralization in molluscs seems to be based on a chitin-synthesizing machinery which bears a significant potential for acting as a coordinator for mechanical and structural integrity transduction (Schönitzer and Weiss 2007; Weiss 2010, 2012). The fact that "unconventional" myosin motor domains are highly conserved within the class of mollusc myosin chitin synthases has several implications.

Firstly, there is a high sequence similarity to myosins associated with the formation and stabilization of microvilli (myo3) (An 2014) (An et al. 2014) and/or the interconnection of microvilli into ordered arrays (myo7). The exact functionalities of the mollusc myosins remain to be elucidated.

Secondly, the presumed localization of mollusc myosin chitin synthases in mantle epithelial tissues and their activity toward the tips of different types of microvilli suggest – in view of the hypothesis that task sharing between microvilli-bearing and secretory cells occurs – that control over chitin formation occurs right at the forefront of materials precursor deposition, whereas intracellular chitosomal precursor vesicles (well-known in yeast and other fungi; Bartnicki-Garcia 2006), their fusion/association with mineral precursor vesicles, and subsequent phase separations after secretion are presumably less relevant.

Thirdly, the localization of chitin synthases at the tip of microvilli draws attention to supramolecular assemblies at curved membrane interfaces, similar to additional levels of control in mitochondrial ATPase dimers (Steven et al. 2016). Oligomerization of yeast chitin synthases is reported (Gohlke et al. 2017), and residence of chitin synthases in microvilli-bearing midgut epithelia has also been shown (Maue

et al. 2009). It remains to be demonstrated how the highly conserved extracellular domains of the mollusc myosin chitin synthases interact with each other, either:

- Within the same microvillus.
- With other chitin synthases located at neighboring microvilli.
- Directly with the mineral composite interface, while it is either before, or in, or right after the process of structuring (by means of many other biopolymer complexes).

Materials processing-driven control represents a challenging hypothesis for mollusc shell formation. Nevertheless, the most intriguing question to answer would be whether brush border microvillar interfaces are essential to either accommodate mechanical circuits in relation to materials such as nacre with hardness parameters in the GPa range, or to minimize cell adhesion, or to exert shear forces which ensure minimization of surface roughness and coherent textures, regardless of the exact positioning and dynamics of the shell-forming tissue which seems to tolerate frequent interruptions during mineralization.

2.6 Concluding Remarks

Several lines of evidence suggest that control over chitin mineralization in molluscs is based on biochemical and tissue circuits, which involve myosin chitin synthases and other chitin modification systems including mineral nucleating lectins, chitinases, and many others. Sophisticated chitin-mineral composites are developed stepwise and with species-specific architectures, especially in the adult stage. Nevertheless, comparative studies at various levels of complexity are needed to elucidate the relevance of microvillar contributions to chitin formation in molluscs. For this purpose, novel analytical tools and significant model systems for chitin formation in molluscs are waiting to be developed.

Acknowledgments Hans Merzendorfer and Stefan Kaufmann are acknowledged for fruitful discussions and for sharing their enthusiasm about chitin synthesis in exotic model systems.

References

Abehsera S, Glazer L, Tynyakov J, Plaschkes I, Chalifa-Caspi V, Khalaila I, Aflalo ED, Sagi A (2015) Binary gene expression patterning of the molt cycle: the case of chitin metabolism Ed K. Y. Zhu. PLoS One 10:e0122602. https://doi.org/10.1371/journal.pone.0122602

Addadi L, Joester D, Nudelman F, Weiner S (2006) Mollusk shell formation: a source of new concepts for understanding biomineralization processes. Chem Eur J 12:980–987

Álvarez Nogal R, Molist García P (2015) The outer mantle epithelium of *Haliotis tuberculata* (Gastropoda Haliotidae): an ultrastructural and histochemical study using lectins. Acta Zool 96:452–459

An BC, Sakai T, Komaba S, Kishi H, Kobayashi S, Kim JY, Ikebe R, Ikebe M (2014) Phosphorylation of the kinase domain regulates autophosphorylation of myosin IIIA and its translocation in microvilli. Biochemistry 53:7835–7845

Ashby MF (2005) Hybrids to fill holes in material property space. Philos Mag 85:3235–3257

Ashby MF, Ferreira PJ, Schodek D (2009) Nanomaterials, nanotechnologies and design: an introduction for engineers and architects. Elsevier/Butterworth Heinemann, Amsterdam

Avenarius MR, Krey JF, Dumont RA, Morgan CP, Benson CB, Vijayakumar S, Cunningham CL, Scheffer DI, Corey DP, Müller U, Jones SM, Barr-Gillespie PG (2017) Heterodimeric capping protein is required for stereocilia length and width regulation. J Cell Biol 216:3861–3881

Bartnicki-Garcia S (2006) Chitosomes: past, present and future. FEMS Yeast Res 6:957–965. https://doi.org/10.1111/j.1567-1364.2006.00158.x

Baxter JM, Jones AM (1981) Valve structure and growth in the chiton *Lepidochitona cinereus* (Polyplacophora: Ischnochitonidae). J Mar Biol Assoc UK 61:65. https://doi.org/10.1017/S0025315400045914

Beedham GE, Trueman ER (2009a) The cuticle of the Aplacophora and its evolutionary significance in the Mollusca. J Zool 154:443–451

Beedham GE, Trueman ER (2009b) The relationship of the mantle and shell of the Polyplacophora in comparison with that of other Mollusca. J Zool 151:215–231

Bevelander G, Nakahara H (1969) An electron microscope study of the formation of the nacreous layer in the shell of certain bivalve molluscs. Calcif Tissue Res 3:84–92

Bi Y, Hubbard C, Purushotham P, Zimmer J (2015) Insights into the structure and function of membrane-integrated processive glycosyltransferases. Curr Opin Struct Biol 34:78–86

Borukhin S, Bloch L, Radlauer T, Hill AH, Fitch AN, Pokroy B (2012) Screening the incorporation of amino acids into an inorganic crystalline host: the case of calcite. Adv Funct Mater 22:4216–4224

Brunet T, King N (2017) The origin of animal multicellularity and cell differentiation. Dev Cell 43:124–140

Brunner E, Richthammer P, Ehrlich H, Paasch S, Simon P, Ueberlein S, van Pée K-H (2009) Chitin-based organic networks: an integral part of cell wall biosilica in the diatom *Thalassiosira pseudonana*. Angew Chem Int Ed 48:9724–9727

Butterfield NJ (2008) An early Cambrian radula. J Paleontol 82:543–554

Cantarel BL, Coutinho PM, Rancurel C, Bernard T, Lombard V, Henrissat B (2009) The carbohydrate-active EnZymes database (CAZy): an expert resource for Glycogenomics. Nucleic Acids Res 37:D233–D238

Carter JG (1979) Comparative shell microstructure of the mollusca, brachiopoda and bryozoa. Scan Electron Microsc 2:439–446

Carter JG (1989) Skeletal biomineralization: patterns, processes and evolutionary trends. American Geophysical Union, Washington, DC. https://doi.org/10.1029/SC005

Cartwright JHE, Checa AG (2007) The dynamics of nacre self-assembly. J R Soc Interface 4:491–504

Chang EP, Evans JS (2015) Pif97, a von Willebrand and Peritrophin biomineralization protein, organizes mineral nanoparticles and creates intracrystalline nanochambers. Biochemistry 54:5348–5355

Checa AG, Cartwright JHE, Willinger M-G (2009) The key role of the surface membrane in why gastropod nacre grows in towers. Proc Natl Acad Sci USA 106:38–43

Checa AG, Salas C, Harper EM, de Dios Bueno-Pérez J (2014) Early stage biomineralization in the Periostracum of the 'living fossil' bivalve *Neotrigonia* Ed M. Yamamoto. PLoS One 9:e90033. https://doi.org/10.1371/journal.pone.0090033

Checa AG, Macías-Sánchez E, Harper EM, Cartwright JHE (2016) Organic membranes determine the pattern of the columnar prismatic layer of mollusc shells. Proc R Soc B Biol Sci 283:20160032. https://doi.org/10.1098/rspb.2016.0032

Cohen E (2009) Chitin. In: Encyclopedia of insects. Elsevier, Amsterdam, pp 156–157

Cohen M, Klein E, Geiger B, Addadi L (2003) Organization and adhesive properties of the hyaluronan pericellular coat of chondrocytes and epithelial cells. Biophys J 85:1996–2005

Cusack M, Dauphin Y, Chung P, Pérez-Huerta A, Cuif J-P (2008) Multiscale structure of calcite fibres of the shell of the brachiopod *Terebratulina retusa*. J Struct Biol 164:96–100

Dauphin Y, Ball AD, Castillo-Michel H, Chevallard C, Cuif J-P, Farre B, Pouvreau S, Salomé M (2013) In situ distribution and characterization of the organic content of the oyster shell *Crassostrea gigas* (Mollusca, Bivalvia). Micron 44:373–383

Dickerson MB, Sandhage KH, Naik RR (2008) Protein- and peptide-directed syntheses of inorganic materials. Chem Rev 108:4935–4978

Dirr HW, Little T, Kuhnert DC, Sayed Y (2005) A conserved N-capping motif contributes significantly to the stabilization and dynamics of the C-terminal region of class alpha glutathione *S* -transferases. J Biol Chem 280:19480–19487

Dorfmueller HC, Ferenbach AT, Borodkin VS, van Aalten DMF (2014) A structural and biochemical model of processive chitin synthesis. J Biol Chem 289:23020–23028

Du J, Vepachedu V, Cho SH, Kumar M, Nixon BT (2016) Structure of the cellulose synthase complex of Gluconacetobacter hansenii at 23.4 Å resolution Ed H.-C. Lai. PLoS One 11: e0155886. https://doi.org/10.1371/journal.pone.0155886

Ebrahim S, Avenarius MR, Grati M, Krey JF, Windsor AM, Sousa AD, Ballesteros A, Cui R, Millis BA, Salles FT, Baird MA, Davidson MW, Jones SM, Choi D, Dong L, Raval MH, Yengo CM, Barr-Gillespie PG, Kachar B (2016) Stereocilia-staircase spacing is influenced by myosin III motors and their cargos espin-1 and espin-like. Nat Commun 7:10833. https://doi.org/10.1038/ncomms10833

Emery DG (1992) Fine structure of olfactory epithelia of gastropod molluscs. Microsc Res Tech 22:307–324

Engler AJ, Sen S, Sweeney HL, Discher DE (2006) Matrix elasticity directs stem cell lineage specification. Cell 126:677–689

Fabbri E, Capuzzo A (2010) Cyclic AMP signaling in bivalve molluscs: an overview. J Exp Zool A Ecol Genet Physiol 313A:179–200. https://doi.org/10.1002/jez.592

Falini G, Fermani S (2004) Chitin mineralization. Tissue Eng 10:1–6

Falini G, Albeck S, Weiner S, Addadi L (1996) Control of aragonite or calcite polymorphism by mollusk Shell macromolecules. Science 271:67–69

Falini G, Fermani S, Ripamonti A (2001) Oriented crystallization of octacalcium phosphate into beta-chitin scaffold. J Inorg Biochem 84:255–258

Falini G, Weiner S, Addadi L (2003) Chitin-silk fibroin interactions: relevance to calcium carbonate formation in invertebrates. Calcif Tissue Int 72:548–554

Fleck NA, Deshpande VS, Ashby MF (2010) Micro-architectured materials: past, present and future. Proc R Soc A Math Phys Eng Sci 466:2495–2516

Forood B, Feliciano EJ, Nambiar KP (1993) Stabilization of alpha-helical structures in short peptides via end capping. Proc Natl Acad Sci USA 90:838–842

Fratzl P, Weinkamer R (2007) Nature's hierarchical materials. Prog Mater Sci 52:1263–1334

Fratzl P, Burgert I, Gupta HS (2004) On the role of interface polymers for the mechanics of natural polymeric composites. Phys Chem Chem Phys 6:5575. https://doi.org/10.1039/b411986j

Furuhashi T, Beran A, Blazso M, Czegeny Z, Schwarzinger C, Steiner G (2009) Pyrolysis GC/MS and IR spectroscopy in chitin analysis of molluscan shells. Biosci Biotechnol Biochem 73:93–103

Galler S (2008) Molecular basis of the catch state in molluscan smooth muscles: a catchy challenge. J Muscle Res Cell Motil 29:73–99

Gao H, Ji B, Jager IL, Arzt E, Fratzl P (2003) Materials become insensitive to flaws at nanoscale: lessons from nature. Proc Natl Acad Sci USA 100:5597–5600

Geiger B, Spatz JP, Bershadsky AD (2009) Environmental sensing through focal adhesions. Nat Rev Mol Cell Biol 10:21–33

Glazer L, Roth Z, Weil S, Aflalo ED, Khalaila I, Sagi A (2015) Proteomic analysis of the crayfish gastrolith chitinous extracellular matrix reveals putative protein complexes and a central role for GAP 65. J Proteome 128:333–343

Gnyubkin VF (2015) The valve-movement model for the mediterranean mussel, *Mytilus galloprovincialis* Lamarck, 1819 (Bivalvia: Mytilidae). Russ J Mar Biol 41:40–50

Gohlke S, Muthukrishnan S, Merzendorfer H (2017) In vitro and in vivo studies on the structural organization of Chs3 from *Saccharomyces cerevisiae*. Int J Mol Sci 18:702. https://doi.org/10.3390/ijms18040702

Goobes G, Goobes R, Schueler-Furman O, Baker D, Stayton PS, Drobny GP (2006) Folding of the C-terminal bacterial binding domain in statherin upon adsorption onto hydroxyapatite crystals. Proc Natl Acad Sci USA 103:16083–16088

Goobes G, Stayton PS, Drobny GP (2007) Solid state NMR studies of molecular recognition at protein–mineral interfaces. Prog Nucl Magn Reson Spectrosc 50:71–85

Gotliv B-A, Addadi L, Weiner S (2003) Mollusk Shell acidic proteins: in search of individual functions. Chem Bio Chem 4:522–529

Grégoire C (1967) On the structure of organic matrixes of molluscan shells. Biol Rev Camb Philos Soc 42:653–688

Gulick AM, Bauer CB, Thoden JB, Pate E, Yount RG, Rayment I (2000) X-ray structures of the *Dictyostelium discoideum* myosin motor domain with six non-nucleotide analogs. J Biol Chem 275:398–408

Halberg KA, Rainey SM, Veland IR, Neuert H, Dornan AJ, Klämbt C, Davies S-A, Dow JAT (2016) The cell adhesion molecule Fasciclin 2 regulates brush border length and organization in *Drosophila* renal tubules. Nat Commun 7:11266. https://doi.org/10.1038/ncomms11266

Hasegawa Y, Araki T (2002) Identification of a novel unconventional myosin from scallop mantle tissue. J Biochem 131:113–119

Haszprunar G, Anninger A (2000) Molluscan muscle systems in development and evolution. J Zool Syst Evol Res 38:157–163

Heissler SM, Sellers JR (2016) Various themes of myosin regulation. J Mol Biol 428:1927–1946

Heissler SM, Billington N, Sellers JR (2014) Myosin-3B and its light chains. Biophys J 106:178a. https://doi.org/10.1016/j.bpj.2013.11.1007

Houdusse A, Kalabokis VN, Himmel D, Szent-Györgyi AG, Cohen C (1999) Atomic structure of scallop myosin subfragment S1 complexed with MgADP. Cell 97:459–470

Hunt S, El Sherief A (1990) A periodic structure in the 'pen' chitin of the squid *Loligo vulgaris*. Tissue Cell 22:191–197

Hunt S, Nixon M (1981) A comparative study of protein composition in the chitin-protein complexes of the beak, pen, sucker disc, radula and oesophageal cuticle of cephalopods. Comp Biochem Physiol B Comp Biochem 68:535–546

Iijima M, Moriwaki Y (1990) Orientation of apatite and organic matrix in *Lingula unguis* shell. Calcif Tissue Int 47:237–242

Jackson DJ, McDougall C, Green K, Simpson F, Wörheide G, Degnan BM (2006) A rapidly evolving secretome builds and patterns a sea shell. BMC Biol 4:40. https://doi.org/10.1186/1741-7007-4-40

Jeuniaux C (1963) Chitine et chitinolyse. Un chapitre de la Biologie moléculaire. Masson et Cie, Paris

Jongebloed, Stokroos, van der Want, Kalicharan (1999) Non-coating fixation techniques or redundancy of conductive coating, low kV FE-SEM operation and combined SEM/TEM of biological tissues. J Microsc 193:158–170

Kambara T, Komaba S, Ikebe M (2006) Human myosin III is a motor having an extremely high affinity for actin. J Biol Chem 281:37291–37301

Keene EC, Evans JS, Estroff LA (2010) Matrix interactions in biomineralization: aragonite nucleation by an intrinsically disordered nacre polypeptide, n16N, associated with a β-chitin substrate. Cryst Growth Des 10:1383–1389

Kintsu H, Okumura T, Negishi L, Ifuku S, Kogure T, Sakuda S, Suzuki M (2017) Crystal defects induced by chitin and chitinolytic enzymes in the prismatic layer of *Pinctada fucata*. Biochem Biophys Res Commun 489:89–95

Kniprath E (1981) Ontogeny of the molluscan shell field: a review. Zool Scr 10:61–79

Knoll AH (2003) Biomineralization and evolutionary history. Rev Mineral Geochem 54:329–356

Kollmar M, Mühlhausen S (2017) Myosin repertoire expansion coincides with eukaryotic diversification in the Mesoproterozoic era. BMC Evol Biol 17. https://doi.org/10.1186/s12862-017-1056-2

Krey JF, Krystofiak ES, Dumont RA, Vijayakumar S, Choi D, Rivero F, Kachar B, Jones SM, Barr-Gillespie PG (2016) Plastin 1 widens stereocilia by transforming actin filament packing from hexagonal to liquid. J Cell Biol 215:467–482

Lairson LL, Henrissat B, Davies GJ, Withers SG (2008) Glycosyltransferases: structures, functions, and mechanisms. Annu Rev Biochem 77:521–555

Larkin MA, Blackshields G, Brown NP, Chenna R, McGettigan PA, McWilliam H, Valentin F, Wallace IM, Wilm A, Lopez R, Thompson JD, Gibson TJ, Higgins DG (2007) Clustal W and Clustal X version 2.0. Bioinformatics 23:2947–2948

Lee-Thedieck C, Spatz JP (2014) Biophysical regulation of hematopoietic stem cells. Biomater Sci 2:1548–1561

Lelli A, Michel V, Boutet de Monvel J, Cortese M, Bosch-Grau M, Aghaie A, Perfettini I, Dupont T, Avan P, El-Amraoui A, Petit C (2016) Class III myosins shape the auditory hair bundles by limiting microvilli and stereocilia growth. J Cell Biol 212:231–244

Levi Y, Albeck S, Brack A, Weiner S, Addadi L (1998) Control over aragonite crystal nucleation and growth: an in vitro study of biomineralization. Chem Eur J 4:389–396

Levi-Kalisman Y, Falini G, Addadi L, Weiner S (2001) Structure of the nacreous organic matrix of a bivalve mollusk Shell examined in the hydrated state using Cryo-TEM. J Struct Biol 135:8–17

Liu J, Yang D, Liu S, Li S, Xu G, Zheng G, Xie L, Zhang R (2015) Microarray: a global analysis of biomineralization-related gene expression profiles during larval development in the pearl oyster, *Pinctada fucata*. BMC Genomics 16. https://doi.org/10.1186/s12864-015-1524-2

Liu H, Li J, Raval MH, Yao N, Deng X, Lu Q, Nie S, Feng W, Wan J, Yengo CM, Liu W, Zhang M (2016) Myosin III-mediated cross-linking and stimulation of actin bundling activity of Espin. eLife 5. https://doi.org/10.7554/eLife.12856

Lowenstam HA (1981) Minerals formed by organisms. Science (New York, NY) 211:1126–1131

Lowenstam HA, Weiner S (1989) On biomineralization. Oxford University Press, New York

Lowenstam HA, Weiner S (1992) Phosphatic shell plate of the barnacle *Ibla* (Cirripedia): a bone-like structure. Proc Natl Acad Sci USA 89:10573–10577

Lundin K, Schander C (2001) Ciliary ultrastructure of polyplacophorans (Mollusca, Amphineura, Polyplacophora). J Submicrosc Cytol Pathol 33:93–98

Luo Y-J, Takeuchi T, Koyanagi R, Yamada L, Kanda M, Khalturina M, Fujie M, Yamasaki S, Endo K, Satoh N (2015) The *Lingula* genome provides insights into brachiopod evolution and the origin of phosphate biomineralization. Nat Commun 6. https://doi.org/10.1038/ncomms9301

MacDonald J, Freer A, Cusack M (2010) Alignment of crystallographic *c* -Axis throughout the four distinct microstructural layers of the oyster *Crassostrea gigas*. Cryst Growth Des 10:1243–1246

Mann K, Jackson D (2014) Characterization of the pigmented shell-forming proteome of the common grove snail *Cepaea nemoralis*. BMC Genomics 15:249. https://doi.org/10.1186/1471-2164-15-249

Mann K, Edsinger-Gonzales E, Mann M (2012) In-depth proteomic analysis of a mollusc shell: acid-soluble and acid-insoluble matrix of the limpet *Lottia gigantea*. Proteome Sci 10:28. https://doi.org/10.1186/1477-5956-10-28

Mann K, Cerveau N, Gummich M, Fritz M, Mann M, Jackson DJ (2018) In-depth proteomic analyses of *Haliotis laevigata* (greenlip abalone) nacre and prismatic organic shell matrix. Proteome Sci 16. https://doi.org/10.1186/s12953-018-0139-3

Manoli F, Koutsopoulos S, Dalas E (1997) Crystallization of calcite on chitin. J Cryst Growth 182:116–124

Manor U, Grati M, Yengo CM, Kachar B, Gov NS (2012) Competition and compensation: dissecting the biophysical and functional differences between the class 3 myosin paralogs, myosins 3a and 3b. Bio Arch 2:171–174

Marie B, Arivalagan J, Mathéron L, Bolbach G, Berland S, Marie A, Marin F (2017) Deep conservation of bivalve nacre proteins highlighted by shell matrix proteomics of the Unionoida *Elliptio complanata* and *Villosa lienosa*. J R Soc Interface 14:20160846. https://doi.org/10.1098/rsif.2016.0846

Marin F, Luquet G, Marie B, Medakovic D (2007) Molluscan Shell proteins: primary structure, origin, and evolution. In: Current topics in developmental biology. Elsevier, San Diego, pp 209–276

Marin F, Le Roy N, Marie B (2012) The formation and mineralization of mollusk shell. Front Biosci (Schol Ed) 4:1099–1125

Masters TA, Kendrick-Jones J, Buss F (2016) Myosins: domain organisation, motor properties, physiological roles and cellular functions. In Jockusch BM (ed) The actin cytoskeleton. Springer, Cham, pp. 77–122

Maue L, Meissner D, Merzendorfer H (2009) Purification of an active, oligomeric chitin synthase complex from the midgut of the tobacco hornworm. Insect Biochem Mol Biol 39:654–659

McDougall C, Degnan BM (2018) The evolution of mollusc shells. Wiley Interdiscip Rev Dev Biol 7:e313. https://doi.org/10.1002/wdev.313

McGrath J, Roy P, Perrin BJ (2017) Stereocilia morphogenesis and maintenance through regulation of actin stability. Semin Cell Dev Biol 65:88–95

McNamara JT, Morgan JLW, Zimmer J (2015) A molecular description of cellulose biosynthesis. Annu Rev Biochem 84:895–921

Mendoza-Becerril MA, Maronna MM, Pacheco MLAF, Simões MG, Leme JM, Miranda LS, Morandini AC, Marques AC (2016) An evolutionary comparative analysis of the medusozoan (Cnidaria) exoskeleton. Zool J Linnean Soc 178:206–225

Merritt RC, Manor U, Salles FT, Grati M, Dose AC, Unrath WC, Quintero OA, Yengo CM, Kachar B (2012) Myosin IIIB uses an actin-binding motif in its Espin-1 cargo to reach the tips of actin protrusions. Curr Biol 22:320–325

Merzendorfer H (2011) The cellular basis of chitin synthesis in fungi and insects: common principles and differences. Eur J Cell Biol 90:759–769

Miserez A, Schneberk T, Sun C, Zok FW, Waite JH (2008) The transition from stiff to compliant materials in squid beaks. Science 319:1816–1819

Miyamoto H, Miyashita T, Okushima M, Nakano S, Morita T, Matsushiro A (1996) A carbonic anhydrase from the nacreous layer in oyster pearls. Proc Natl Acad Sci USA 93:9657–9660

Miyamoto H, Endo H, Hashimoto N, Limura K, Isowa Y, Kinoshita S, Kotaki T, Masaoka T, Miki T, Nakayama S, Nogawa C, Notazawa A, Ohmori F, Sarashina I, Suzuki M, Takagi R, Takahashi J, Takeuchi T, Yokoo N, Satoh N, Toyohara H, Miyashita T, Wada H, Samata T, Endo K, Nagasawa H, Asakawa S, Watabe S (2013) The diversity of Shell matrix proteins: genome-wide investigation of the pearl oyster, *Pinctada fucata*. Zool Sci 30:801–816

Miyazaki Y, Nishida T, Aoki H, Samata T (2010) Expression of genes responsible for biomineralization of *Pinctada fucata* during development. Comp Biochem Physiol B: Biochem Mol Biol 155:241–248

Molist P, Álvarez Nogal R, Collado GA (2016) Morphological, ultrastructural and histochemical investigation of epipodial sensory structures of *Haliotis tuberculata* (Gastropoda: Haliotidae). Acta Zool 97:67–75

Mooseker MS (1975) Organization of an actin filament-membrane complex. Filament polarity and membrane attachment in the microvilli of intestinal epithelial cells. J Cell Biol 67:725–743

Mooseker MS, Foth BJ (2007) The structural and functional diversity of the myosin family of actin-based molecular motors. In: Myosins. Springer, Dordrecht, pp 1–34

Morgan JLW, McNamara JT, Fischer M, Rich J, Chen H-M, Withers SG, Zimmer J (2016) Observing cellulose biosynthesis and membrane translocation in crystallo. Nature 531:329–334

Morin JA, Cao FJ, Lázaro JM, Arias-Gonzalez JR, Valpuesta JM, Carrascosa JL, Salas M, Ibarra B (2015) Mechano-chemical kinetics of DNA replication: identification of the translocation step of a replicative DNA polymerase. Nucleic Acids Res 43:3643–3652

Morozov AA, Likhoshway YV (2016) Evolutionary history of the chitin synthases of eukaryotes. Glycobiology 26:635–639

Nelson DL, Cox MM, Lehninger AL (2017) Lehninger principles of biochemistry, 7th edn. W.H. Freeman, New York

Nudelman F (2015) Nacre biomineralisation: a review on the mechanisms of crystal nucleation. Semin Cell Dev Biol 46:2–10

Nudelman F, Gotliv BA, Addadi L, Weiner S (2006) Mollusk shell formation: mapping the distribution of organic matrix components underlying a single aragonitic tablet in nacre. J Struct Biol 153:176–187

Nudelman F, Chen HH, Goldberg HA, Weiner S, Addadi L (2007) Spiers memorial lecture: lessons from biomineralization: comparing the growth strategies of mollusc shell prismatic and nacreous layers in *Atrina rigida*. Faraday Discuss 136:9. https://doi.org/10.1039/b704418f

Nudelman F, Shimoni E, Klein E, Rousseau M, Bourrat X, Lopez E, Addadi L, Weiner S (2008) Forming nacreous layer of the shells of the bivalves *Atrina rigida* and *Pinctada margaritifera*: an environmental- and cryo-scanning electron microscopy study. J Struct Biol 162:290–300

Odronitz F, Kollmar M (2007) Drawing the tree of eukaryotic life based on the analysis of 2,269 manually annotated myosins from 328 species. Genome Biol 8:R196. https://doi.org/10.1186/gb-2007-8-9-r196

Okafor N (1965) Isolation of chitin from the shell of the cuttlefish, *Sepia officinalis* L. Biochim et Biophysica Acta (BBA) – Mucoproteins and Mucopolysaccharides 101:193–200

Omadjela O, Narahari A, Strumillo J, Melida H, Mazur O, Bulone V, Zimmer J (2013) BcsA and BcsB form the catalytically active core of bacterial cellulose synthase sufficient for *in vitro* cellulose synthesis. Proc Natl Acad Sci USA 110:17856–17861

Orly G, Naoz M, Gov NS (2014) Physical model for the geometry of actin-based cellular protrusions. Biophys J 107:576–587

Osuna-Mascaró A, Cruz-Bustos T, Benhamada S, Guichard N, Marie B, Plasseraud L, Corneillat M, Alcaraz G, Checa A, Marin F (2014) The shell organic matrix of the crossed lamellar queen conch shell (*Strombus gigas*). Comp Biochem Physiol B: Biochem Mol Biol 168:76–85

Park BH, Karpinets TV, Syed MH, Leuze MR, Uberbacher EC (2010) CAZymes analysis toolkit (CAT): web service for searching and analyzing carbohydrate-active enzymes in a newly sequenced organism using CAZy database. Glycobiology 20:1574–1584

Peña JF, Alié A, Richter DJ, Wang L, Funayama N, Nichols SA (2016) Conserved expression of vertebrate microvillar gene homologs in choanocytes of freshwater sponges. EvoDevo 7. https://doi.org/10.1186/s13227-016-0050-x

Pérez-Huerta A, Cusack M (2008) Common crystal nucleation mechanism in shell formation of two morphologically distinct calcite brachiopods. Zoology 111:9–15

Pérez-Huerta A, Dauphin Y, Cuif JP, Cusack M (2011) High resolution electron backscatter diffraction (EBSD) data from calcite biominerals in recent gastropod shells. Micron 42:246–251

Peters W (1972) Occurrence of chitin in mollusca. Comp Biochem Physiol B: Comp Biochem 41:541–550

Phillips DW (1979) Ultrastructure of sensory cells on the mantle tentacles of the gastropod *Notoacmea scutum*. Tissue Cell 11:623–632

Pinkoviezky I, Gov NS (2017) Exclusion and hierarchy of time scales Lead to spatial segregation of molecular motors in cellular protrusions. Phys Rev Lett 118. https://doi.org/10.1103/PhysRevLett.118.018102

Pohl A, Weiss IM (2014) Real-time monitoring of calcium carbonate and cationic peptide deposition on carboxylate-SAM using a microfluidic SAW biosensor. Beilstein J Nanotechnol 5:1823–1835

Quintero OA, Unrath WC, Stevens SM, Manor U, Kachar B, Yengo CM (2013) Myosin 3A kinase activity is regulated by phosphorylation of the kinase domain activation loop. J Biol Chem 288:37126–37137

Raval MH, Quintero OA, Weck ML, Unrath WC, Gallagher JW, Cui R, Kachar B, Tyska MJ, Yengo CM (2016) Impact of the motor and tail domains of class III Myosins on regulating the formation and elongation of actin protrusions. J Biol Chem 291:22781–22792

Runnegar B, Jell PA (1976) Australian middle Cambrian molluscs and their bearing on early molluscan evolution. Alcheringa 1:109–138

Saleuddin ASM, Wilbur KM (1983) The Mollusca. Elsevier. https://doi.org/10.1016/C2013-0-11705-9

Schäffer TE, Ionescu-Zanetti C, Proksch R, Fritz M, Walters DA, Almqvist N, Zaremba CM, Belcher AM, Smith BL, Stucky GD, Morse DE, Hansma PK (1997) Does abalone nacre form by Heteroepitaxial nucleation or by growth through mineral bridges? Chem Mater 9:1731–1740

Scharnagl C, Pester O, Hornburg P, Hornburg D, Götz A, Langosch D (2014) Side-chain to main-chain hydrogen bonding controls the intrinsic backbone dynamics of the amyloid precursor protein transmembrane Helix. Biophys J 106:1318–1326

Schmahl WW, Griesshaber E, Merkel C, Kelm K, Deuschle J, Neuser RD, Göetz AJ, Sehrbrock A, Mader W (2008) Hierarchical fibre composite structure and micromechanical properties of phosphatic and calcitic brachiopod shell biomaterials – an overview. Mineral Mag 72:541–562

Schneider AS, Heiland B, Peter NJ, Guth C, Arzt E, Weiss IM (2012) Hierarchical super-structure identified by polarized light microscopy, electron microscopy and nanoindentation: implications for the limits of biological control over the growth mode of abalone sea shells. BMC Biophys 5:19. https://doi.org/10.1186/2046-1682-5-19

Schönitzer V, Weiss IM (2007) The structure of mollusc larval shells formed in the presence of the chitin synthase inhibitor Nikkomycin Z. BMC Struct Biol 7:71. https://doi.org/10.1186/1472-6807-7-71

Schönitzer V, Eichner N, Clausen-Schaumann H, Weiss IM (2011) Transmembrane myosin chitin synthase involved in mollusc shell formation produced in Dictyostelium is active. Biochem Biophys Res Commun 415:586–590

Sengupta Ghatak A, Koch M, Guth C, Weiss I (2013) Peptide induced crystallization of calcium carbonate on wrinkle patterned substrate: implications for chitin formation in Molluscs. Int J Mol Sci 14:11842–11860

Shemesh T, Geiger B, Bershadsky AD, Kozlov MM (2005) Focal adhesions as mechanosensors: a physical mechanism. Proc Natl Acad Sci USA 102:12383–12388

Siegman MJ, Funabara D, Kinoshita S, Watabe S, Hartshorne DJ, Butler TM (1998) Phosphorylation of a twitchin-related protein controls catch and calcium sensitivity of force production in invertebrate smooth muscle. Proc Natl Acad Sci USA 95:5383–5388

Smith MR (2012) Mouthparts of the burgess shale fossils *Odontogriphus* and *Wiwaxia*: implications for the ancestral molluscan radula. Proc R Soc B Biol Sci 279:4287–4295

Sone ED, Weiner S, Addadi L (2007) Biomineralization of limpet teeth: a cryo-TEM study of the organic matrix and the onset of mineral deposition. J Struct Biol 158:428–444

Steven AC, Baumeister W, Johnson DLN, Perham RN (2016) Molecular biology of assemblies and machines. Garland Science/Taylor & Francis Group, New York/London

Sumper M, Riepertinger C, Lynen F, Oesterhelt D (1969) Die Synthese verschiedener Carbonsäuren durch den Multienzymkomplex der Fettsäuresynthese aus Hefe und die Erklärung ihrer Bildung. Eur J Biochem 10:377–387

Sun X, Yang A, Wu B, Zhou L, Liu Z (2015) Characterization of the mantle transcriptome of yesso scallop (*Patinopecten yessoensis*): identification of genes potentially involved in biomineralization and pigmentation Ed A. Roulin. PLoS One 10:e0122967. https://doi.org/10.1371/journal.pone.0122967

Sutton MD, Briggs DEG, Siveter DJ, Siveter DJ, Sigwart JD (2012) A Silurian armoured aplacophoran and implications for molluscan phylogeny. Nature 490:94–97
Suzuki M, Nagasawa H (2013) Mollusk shell structures and their formation mechanism. Can J Zool 91:349–366
Suzuki M, Sakuda S, Nagasawa H (2007) Identification of chitin in the prismatic layer of the Shell and a chitin synthase gene from the Japanese pearl oyster, *Pinctada fucata*. Biosci Biotechnol Biochem 71:1735–1744
Suzuki M, Saruwatari K, Kogure T, Yamamoto Y, Nishimura T, Kato T, Nagasawa H (2009) An acidic matrix protein, Pif, is a key macromolecule for nacre formation. Science 325:1388–1390
Tarchini B, Tadenev ALD, Devanney N, Cayouette M (2016) A link between planar polarity and staircase-like bundle architecture in hair cells. Development 143:3926–3932
The Uni Prot Consortium (2017) Uni Prot: the universal protein knowledgebase. Nucleic Acids Res 45:D158–D169
Vélez-Ortega AC, Freeman MJ, Indzhykulian AA, Grossheim JM, Frolenkov GI (2017) Mechanotransduction current is essential for stability of the transducing stereocilia in mammalian auditory hair cells. eLife 6. https://doi.org/10.7554/eLife.24661
Weber E, Bloch L, Guth C, Fitch AN, Weiss IM, Pokroy B (2014) Incorporation of a recombinant biomineralization fusion protein into the crystalline lattice of calcite. Chem Mater 26:4925–4932
Weck ML, Crawley SW, Stone CR, Tyska MJ (2016) Myosin-7b promotes distal tip localization of the intermicrovillar adhesion complex. Curr Biol 26:2717–2728
Weck ML, Grega-Larson NE, Tyska MJ (2017) MyTH4-FERM myosins in the assembly and maintenance of actin-based protrusions. Curr Opin Cell Biol 44:68–78
Weiner S, Traub W (1980) X-ray diffraction study of the insoluble organic matrix of mollusk shells. FEBS Lett 111:311–316
Weiner S, Talmon Y, Traub W (1983) Electron diffraction of mollusc shell organic matrices and their relationship to the mineral phase. Int J Biol Macromol 5:325–328
Weiss IM (2010) Jewels in the pearl. Chem Bio Chem 11:297–300
Weiss IM (2012) Species-specific shells: chitin synthases and cell mechanics in molluscs. Z Krist – Cryst Mater 227:723–738
Weiss IM, Marin F (2008) The role of enzymes in biomineralization processes. In: Sigel A, Sigel H, Sigel RKO (eds) Biomineralization. Wiley, Chichester, pp 71–126
Weiss IM, Schönitzer V (2006) The distribution of chitin in larval shells of the bivalve mollusk *Mytilus galloprovincialis*. J Struct Biol 153:264–277
Weiss IM, Renner C, Strigl MG, Fritz M (2002a) A simple and reliable method for the determination and localization of chitin in abalone nacre. Chem Mater 14:3252–3259
Weiss IM, Tuross N, Addadi L, Weiner S (2002b) Mollusc larval shell formation: amorphous calcium carbonate is a precursor phase for aragonite. J Exp Zool 293:478–491
Weiss IM, Schönitzer V, Eichner N, Sumper M (2006) The chitin synthase involved in marine bivalve mollusk shell formation contains a myosin domain. FEBS Lett 580:1846–1852
Weiss IM, Kaufmann S, Heiland B, Tanaka M (2009) Covalent modification of chitin with silk-derivatives acts as an amphiphilic self-organizing template in nacre biomineralisation. J Struct Biol 167:68–75
Weiss IM, Lüke F, Eichner N, Guth C, Clausen-Schaumann H (2013) On the function of chitin synthase extracellular domains in biomineralization. J Struct Biol 183:216–225
Wilt FH, Killian CE, Livingston BT (2003) Development of calcareous skeletal elements in invertebrates. Differentiation 71:237–250
Yonezawa M, Sakuda S, Yoshimura E, Suzuki M (2016) Molecular cloning and functional analysis of chitinases in the fresh water snail, *Lymnaea stagnalis*. J Struct Biol 196:107–118

Yu I-M, Planelles-Herrero VJ, Sourigues Y, Moussaoui D, Sirkia H, Kikuti C, Stroebel D, Titus MA, Houdusse A (2017) Myosin 7 and its adaptors link cadherins to actin. Nat Commun 8:15864. https://doi.org/10.1038/ncomms15864

Zhang G, Fang X, Guo X, Li L, Luo R, Xu F, Yang P, Zhang L, Wang X, Qi H, Xiong Z, Que H, Xie Y, Holland PWH, Paps J, Zhu Y, Wu F, Chen Y, Wang J, Peng C, Meng J, Yang L, Liu J, Wen B, Zhang N, Huang Z, Zhu Q, Feng Y, Mount A, Hedgecock D, Xu Z, Liu Y, Domazet-Lošo T, Du Y, Sun X, Zhang S, Liu B, Cheng P, Jiang X, Li J, Fan D, Wang W, Fu W, Wang T, Wang B, Zhang J, Peng Z, Li Y, Li N, Wang J, Chen M, He Y, Tan F, Song X, Zheng Q, Huang R, Yang H, Du X, Chen L, Yang M, Gaffney PM, Wang S, Luo L, She Z, Ming Y, Huang W, Zhang S, Huang B, Zhang Y, Qu T, Ni P, Miao G, Wang J, Wang Q, Steinberg CEW, Wang H, Li N, Qian L, Zhang G, Li Y, Yang H, Liu X, Wang J, Yin Y, Wang J (2012) The oyster genome reveals stress adaptation and complexity of shell formation. Nature 490:49–54

Chapter 3
Chitosan Derivatives and Grafted Adjuncts with Unique Properties

Hans Merzendorfer

Abstract Chitosan is a naturally occurring polysaccharide of D-glucosamine, which has opened vista of possible applications in the chemical, environmental, agricultural, pharmaceutical, and biomedical industry. Due to the presence of functional hydroxyl and amine groups in the parent backbone, chitosan is easily amenable to chemical modification to convey distinct physicochemical and biochemical properties to the polymer without changing the basic structure. In the past four decades, copious protocols have been established and employed to generate chitosan derivatives with different physicochemical properties. Chemical modifications that have been performed include acylation, alkylation, carboxyalkylation, quaternization, thiolation, sulfation, phosphorylation, attachment of carbohydrates and dendrimers, and graft copolymerization with assorted modifications. In this article, we will review the large variety of studies that have engineered chitosan derivatives and discuss how the specific chemical modification has improved the characteristics of the polymer to meet the requirements of the desired application. This review outlines the chemical foundations of chitosan modifications, which will help to explore the plethora of suggested and accomplished application summarized in Chap. 14. Beyond that, it will hopefully bring forth new ideas and set further impulses in this important field of polymer science.

3.1 Introduction

Chitin is a natural polymer of β(1,4)-linked *N*-acetylglucosamine [2-(acetylamino)-2-deoxy-D-glucose], which is used as a starting material to develop polymers with novel functions for industrial and biomedical applications. It is found in very large amounts in marine ecosystems and is obtained commercially from shrimp and crab fishery utilizing waste shells as the source for chitin extraction by treatments of

H. Merzendorfer (✉)
School of Science and Technology, Institute of Biology – Molecular Biology, University of Siegen, Siegen, Germany
e-mail: merzendorfer@chemie-bio.uni-siegen.de

E. Cohen, H. Merzendorfer (eds.), *Extracellular Sugar-Based Biopolymers Matrices*, Biologically-Inspired Systems 12, https://doi.org/10.1007/978-3-030-12919-4_3

mechanically disrupted materials with hot sodium hydroxide for deproteination, hydrochloric acid solutions for demineralization, and acetone for decolorization (Kurita 2006). The solubility of chitin in basic and neutral aqueous and common organic solvents, however, is extremely poor due to extensive inter- and intramolecular hydrogen bonding between the hydroxyl groups and the *N*-acetamino groups. As there are numerous problems associated with solubilization of chitin, e.g., partial degradation in acidic solvents, chitin is usually chemically modified not only to increase solubility but also to obtain (multi)functional polymers with new properties. Alkaline (or enzymatic) deacetylations are probably the easiest approaches to increase the solubility of the polymer. Deacetylation results in chitosan which is predominantly made of β(1,4)-linked glucosamine (2-amino-2-deoxy-O-glucose). The free primary amino group can undergo nucleophilic substitution reactions frequently used for further derivatization. Chitosan is soluble in acidic aqueous solutions and easy to modify under controlled conditions. Next to the primary amino group, chemical modification can also be achieved by reactions involving the primary and secondary hydroxyl groups at the C2, C3, and C6 positions. To increase solubility of chitosan in physiological liquids; to improve its biocompatibility, mucoadhesiveness, and adsorption properties; and to add new functionalities, many different chitosan derivatives have been synthesized or formulated over the past decades without diminishing their overall beneficial attributes in physiological environments. Here, we will review the main chemical strategies that have been applied to modify chitosan (see also Fig. 3.1, Table 3.1).

3.2 Hydrophobic Modifications

3.2.1 N/O-*Acyl Chitosans*

Acylation of chitosan facilitates the introduction of hydrophobic side moieties at amino and/or alcohol groups, which provides high flexibility for chemical modification (Fig. 3.1). *N*-Acylation can be easily achieved by the reaction of chitosan with anhydrides or acyl halides in various aqueous and organic solvents or by coupling reactions. These reactions can be specifically controlled due to different reactivities of the amino and hydroxyl groups. In this way, many chitosan derivatives with amphiphilic characteristics have been synthesized. By the attachment of hydrophobic side groups, the physicochemical properties of the polymers are altered significantly. It results in various chitosan-based macromolecular assemblies such as hydrogels, liquid crystals, membranes, films, vesicles, and fibers with various biomedical and technical applications in chemical and pharmaceutical industry. Various acyl derivatives have been synthesized from anhydrides. A prominent example is *N*-succinyl-chitosan (NSCS), which is obtained by the reaction of chitosan with succinic anhydride under acidic conditions. NSCS is nontoxic and biocompatible, and it accumulates in mice tumors, as revealed by injecting fluorescein-labeled NSCS into tumor-bearing mice (Kato et al. 2000a). Therefore,

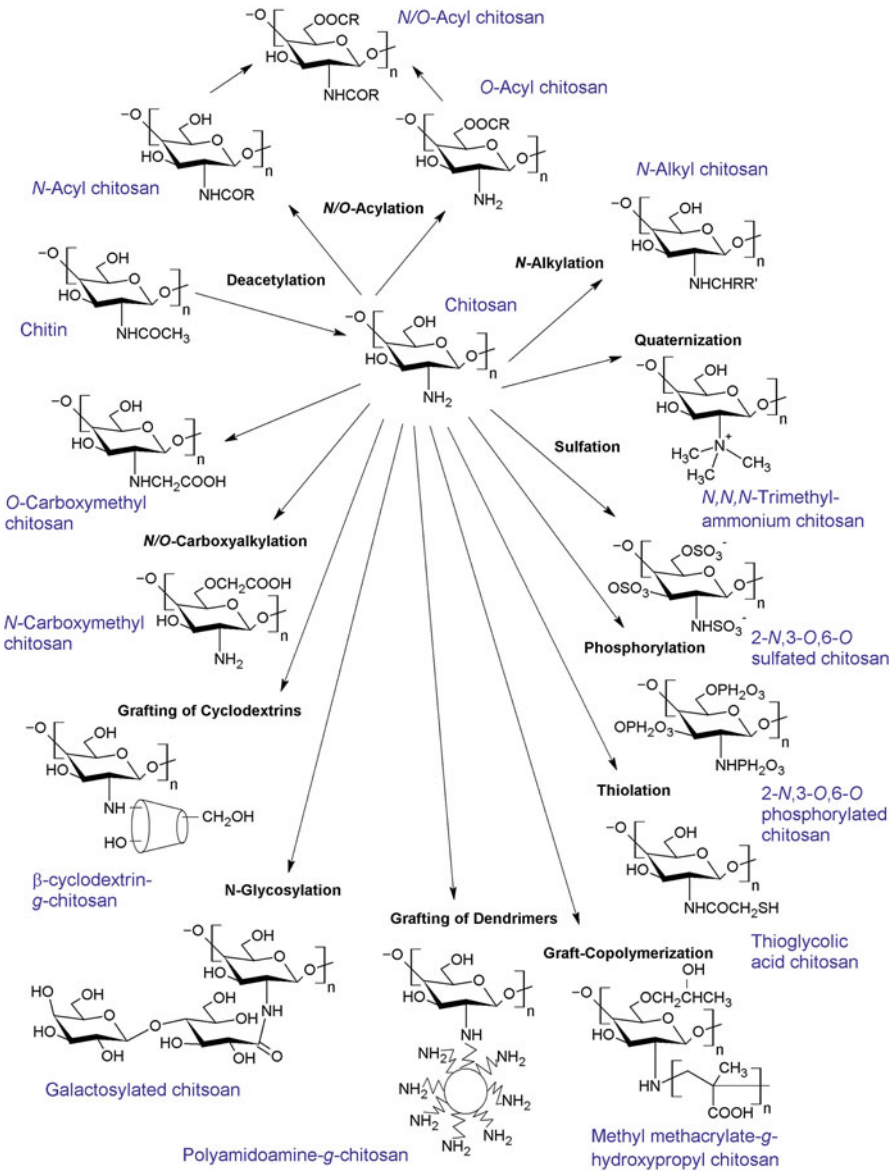

Fig. 3.1 Overview on chemical modifications to alter chitosan properties

NSCS and NSCS derivatives were tested as chemotherapeutic drug carriers and conjugated with cytostatic agents such as mitomycin C (Kato et al. 2000b), 5-fluorouracil (Yan et al. 2006), or anticancer oligonucleotides such as OGX-011 (Yan et al. 2017). *N*-Acylation of chitosan with fatty acids of various lengths (C6 to C16)

Table 3.1 Modifications of chitosan

Family	Molecule	References
Amines	Ethylenediamine	Zhou et al. (2011) and Chethan and Vishalakshi (2013)
Organochlorines	Epichlorohydrin	Nakano et al. (2004) and Silva et al. (2018)
Amino acids	Arginine	Wu et al. (2016) and Lin et al. (2017)
	Glutamine	Choi et al. (2015) and Tao et al. (2016)
Organic acids	Folic acid	Mathew et al. (2010) and Sahu et al. (2010)
	Glacial acetic acid	Xing et al. (2016b)
	Glutamic acid	Yan et al. (2013)
	Glycolic acid	Zhou et al. (2010)
	Lactic acid	Qu et al. (1999), Cai et al. (2002), Feng and Dong (2007) and Zhou et al. (2018)
	Maleic acid	Hasiploglu et al. (2005), Yang et al. (2007) and Gopal Reddi et al. (2017)
	Salicylic acid	Sin et al. (2012)
	Succinic acid	Kato et al. (2001a) and Yan et al. (2006, 2017)
Complex organics	Algal biomass	Sargın et al. (2016a) and Sunkireddy et al. (2016)
	Beeswax	Nguyen et al. (2012)
	Cotton fibers	Phongying et al. (2006) and Ferrero et al. (2014)
	Dentin	Xu et al. (2011)
	Emu eggshells	Anantha and Kota (2016)
	Fungal spores	Sargın et al. (2016b)
	Genipin (natural cross-linker)	Lin et al. (2013) and Song et al. (2018)
	Green tea extract	Qin et al. (2013)
	Humic substances	Chang and Juang (2004)
Nucleic Acids	DNA	Mansouri et al. (2004) and Baghdan et al. (2018)
	siRNA	Guzman-Villanueva et al. (2014), Choi et al. (2015) and Eivazy et al. (2017)
Proteins	Bovine albumin	Li et al. (2017a)
	Collagen	Hayashi et al. (2012) and Michalska-Sionkowska et al. (2018)
	Fibroin	Ramya and Sudha (2013), Rattanamanee et al. (2015) and Zeng et al. (2015)
	Gelatin	Liu et al. (2013) and Song et al. (2018)
	Soy proteins	Teng et al. (2013) and Wang et al. (2016)
Monosaccharides	Galactose	Park et al. (2000, 2003, 2004a) and Yu et al. (2014)
	Glucose	Gullon et al. (2016)
	Fucose	Lin et al. (2013)
Disaccharides	Cellobiose	Yang et al. (2005)
	Lactose	Ishihara et al. (2006) and Phongying et al. (2006)
	Maltose	Kurita et al. (2003), Yang et al. (2005) and Phongying et al. (2006)

(continued)

Table 3.1 (continued)

Family	Molecule	References
Polysaccharides	Alginate	El-Kamel et al. (2002), Chen et al. (2004b), El Badawy et al. (2016) and Lim and Ahmad (2017)
	Carboxymethylcellulose	Dong et al. (2012) and Spera et al. (2017)
	Carrageenan	Mahdavinia et al. (2017 and Yu et al. (2018a, b)
	Cellulose	Silva Mdos et al. (2011), Azevedo et al. (2013), Duri and Tran (2013) and Wu et al. (2014b)
	Chondroitin sulfate	Denuziere et al. (1998), Muzzarelli et al. (2012) and Silva et al. (2013)
	Cyclodextrins	Chen et al. (2013), Duri and Tran (2013) and Campos et al. (2017, 2018)
	Dextran sulfate	Delair (2011), Chaiyasan et al. (2015) and Yucel Falco et al. (2017)
	Heparin	Shan (2004)
	Hyaluronic acid	Muzzarelli et al. (2012)
	Locust bean gum	Vijayaraghavan et al. (2008) and Jana and Sen (2017)
	Pectin	Grabnar and Kristl (2010)
	Starch	Saboktakin et al. (2011), Perez and Francois (2016) and Baghaie et al. (2017)
	Xanthan	Melaj and Daraio (2013), Caddeo et al. (2014) and Westin et al. (2017)
Fatty molecules	Essential oils	Perez-Recalde et al. (2018)
	Linolenic acid	Liu et al. (2005b)
	Phosphocholine (lecithin)	Al-Remawi et al. (2017)
	Ricinoleic acid	Chitkara et al. (2006)
Carbons	Activated carbons	Wan Ngah et al. (2011) and Li et al. (2017c)
	Carbon nanotubes	Zhang et al. (2004), Tkac et al. (2007) and Shahdost-fard et al. (2013)
	Graphene oxide	Bao et al. (2011), Singh et al. (2013) and Wang et al. (2018a)
	Graphite oxide	Pauliukaite et al. (2010), Travlou et al. (2013) and Palanisamy et al. (2016)
Clay and ceramic minerals	Attapulgite	Cohen et al. (2003), Wang et al. (2009) and Wang and Wang (2016)
	Bentonite	Li et al. (2012a, 2015) and Moussout et al. (2018)
	Bioglass ceramic	Deepthi et al. (2016)
	Ceramic aluminum	Steenkamp et al. (2002)
	Hydroxyapatite	Deepthi et al. (2016)
	Kaolinite	Cohen et al. (2003)
	Montmorillonite	Cohen et al. (2003), Katti et al. (2008), Wang et al. (2014) and Kar et al. (2016)
	Perlite	Swayampakula et al. (2009)
	Silicon dioxide	Deepthi et al. (2016)
	Smectite	Puspita et al. (2017)

(continued)

Table 3.1 (continued)

Family	Molecule	References
	Titanium dioxide	Deepthi et al. (2016), Al-Mokaram et al. (2017), Mahmoud et al. (2018) and Radmansouri et al. (2018)
	Zeolite	Yu et al. (2013, Deepthi et al. (2016), Djelad et al. (2016) and Yang et al. (2018)
	Zirconium oxide	Deepthi et al. (2016) and Teimouri et al. (2016)
Inorganic monomers	Acrylic acid	Huacai et al. (2006) and Benamer et al. (2011)
	Acrylamide	Berkovich et al. (1983) and Siafu (2017)
	Hydroxyethyl methacrylate	El-Tahlawy and Hudson (2001)
	Methyl acrylate	Liu et al. (2003)
	Vinylcaprolactam	Kudyshkin et al. (2014)
Polymers	Polyacrylamide	Yazdani-Pedram et al. (2002), Li et al. (2005), Joshi and Sinha (2007) and Mukhopadhyay et al. (2014)
	Polyamidoamine	Klaykruayat et al. (2010), Tsubokawa and Takayama (2000), Leng et al. (2013) and Prabhu and Meenakshi (2015)
	Polyaniline	Cheng et al. (2005) and Abbasian et al. (2017)
	Polyaspartic acid	Zheng et al. (2007)
	Polyethylenimine	Wong et al. (2006) and Pezzoli et al. (2012)
	Polyethylene glycol	Jiang et al. (2008) and Jeong et al. (2010)
	Polyethylene oxide	Zupančič et al. (2016)
	Poly(hydroxyethyl methacrylate)	Bayramoglu et al. (2003), Subramanian and Vijayakumar (2012)
	Polylactic acid	Zhou et al. (2010, 2018)
	Polylysine	Mingyu et al. (2004), Yu et al. (2007) and Jiang et al. (2017)
	Polystyrene	Pengfei et al. (2001)
	Polyvinyl acetate	Don et al. (2002b)
	Polyvinyl alcohol	Takei et al. (2013) and Wang and Wang (2016)
	Polyvinyl chloride	Liu et al. (2003)
	Polyvinylpyrrolidone	Bian et al. (2009) and Wang et al. (2018b)

resulted in different physicochemical properties due to structural alterations. While chitosan with short-chain fatty acids exhibited similar properties as the non-modified chitosan (except for increased swelling), chitosans with longer fatty acids showed higher degrees of order and compressive strength but lower swelling than non-modified chitosan (Le Tien et al. 2003). Sulfated *N*-acyl-chitosans have amphiphilic characteristics and tend to form micellar aggregates with surfactant-like properties. While short-chain *N*-acyl-chitosans form conventional micelles, longer-chain *N*-acyl-chitosans can form so-called polymer micelles of increased stability due to the self-assembly formation of higher-ordered (helical or rodlike) micellar

structures (Yoshioka et al. 1995). Some of them have been explored as micellar drug delivery polymers.

In a number of studies, *N*-acylation has been achieved by the reaction of chitosan with acyl halides such as oleoyl chloride. In the latter case, the resulting oleoyl-chitosans (OCS) were converted into nanoparticles (Li et al. 2007), which were nontoxic to mouse embryonic fibroblasts and suitable as carriers for hydrophobic cancer therapeutic drugs such as doxorubicin (Zhang et al. 2007). Moreover, fluorescein OCS derivatives were efficiently taken up by cells derived from human lung carcinoma (Zhang et al. 2008). In addition, the OCS-based nanoparticles of about 300 nm diameter have been reported to possess antifungal activity against plant pathogenic fungi so that they may be useful in agriculture to prevent fungal-borne plant diseases (Xing et al. 2016a).

Another strategy to generate amphiphilic chitosan derivatives involves coupling reagents such as 1-ethyl-3-(3-dimethylaminopropyl) carbodiimide (EDC). Using this chemistry, Liu et al. (2005b) have covalently conjugated linoleic acid (LA) to chitosan and determined the critical aggregation concentration. Transmission electron microscopy revealed the formation of spherical nanoparticles, which had a mean diameter of about 200 nm as determined by quasi-elastic laser light scattering. The particles bound bovine serum albumin sufficiently suggesting that they may be useful as carriers for soluble proteins. LA chitosan beads of 1.25 μm in diameter have been successfully tested for one-step purification of immunoglobulin G from human plasma using a batch system (Uygun et al. 2009). In another study, trypsin was bound to LA chitosan nanoparticles of 200 to 600 nm in diameter, and the effects of pH, ionic strength, and denaturing agents were tested (Liu et al. 2005a). Notably, the thermal stability of trypsin was increased after binding to LA chitosan nanoparticles. LA chitosan nanoparticles were also modified by the incorporation of 12 nm-sized superparamagnetic iron oxide nanocrystals (SPIONs) with the aim to generate polymeric magnetic nanoprobes for increasing contrast in magnetic resonance imaging of inner organs such as the liver (Lee et al. 2009). The capsulation of the SPIONs diminished their cytotoxicity, increased their dispersion ability in water, and improved the signal-to-noise ratio in the liver after intravascular injection. The SPION-LA chitosan nanoparticles were found to be taken up effectively by hepatocytes, and it was suggested that they could be used as a contrast agent for the diagnosis of hepatic diseases.

Another example is the synthesis of stearic acid (SA)-grafted chitosan oligosaccharides resulting from EDC-mediated coupling (Hu et al. 2006b). These chitosan derivatives form micelles in aqueous solutions and were shown to bind DNA due to their cationic properties. They were tested to have a low cytotoxicity and successfully used as an effective DNA condensation carrier to transfect human lung carcinoma cells (A594). SA-grafted chitosan oligosaccharides and their derivatives are suitable carriers for cancer drugs such as paclitaxel and 10-hydroxycamptothecin (HCPT) as well (Hu et al. 2006a; You et al. 2008; Zhou et al. 2010). To improve the stability of the shells, Hu et al. (2006a) cross-linked the micelles by glutaraldehyde, which resulted in higher entrapment efficiencies of the paclitaxel. In another approach, Zhou et al. (2010) synthesized SA- and poly(lactic-co-glycolic acid)

(PLGA)-grafted chitosan oligosaccharide tripolymers and showed that HCPT-loaded micelles had a higher cytotoxicity in A549, MCF-7 (breast cancer), and HepG-2 (liver cancer) cells than if only HCPT was applied. You et al. (2008) modified SA-grafted chitosan oligosaccharides by conjugating folate and showed that the cytotoxicity of paclitaxel-loaded micelles was significantly increased. SA-grafted chitosan oligosaccharides were also modified to produce lipo-polymerosomes composed of glycol chitosan-SA copolymer and cholesterol, which was surface-functionalized with lectin by EDC and *N*-hydroxysuccinimide (NHS) coupling (Gupta et al. 2014). As shown in this study, amphotericin B-loaded lipo-polymerosomes specifically target macrophages and hence are useful for the management of intramacrophage diseases such as visceral leishmaniasis.

In comparison to *N*-acylation, *O*-acylation is less widely used to modify chitosan oligosaccharides, because the hydroxyl groups are less reactive than the amino groups, which therefore need to be protected and deprotected during synthesis. In this way, amphiphilic chitosans have been synthesized using *N*-phthaloyl chitosan as an intermediate (Nishimura et al. 1992). *O*-Acylation of chitosan can be achieved in the presence of methanesulfonic acid as a solvent and catalyst, which allows selective substitution on the hydroxyl groups (Sashiwa et al. 2002). Using this strategy, acryloyl chitosans have been synthesized and characterized by scanning electron microscopy, Fourier-transformed infrared (FTIR) and circular dichroism spectrometry (Dong et al. 2006a, b). Pavinatto et al. (2014) incorporated *O*,*O*-′-diacetyl chitosan and *O*,*O*′-dipropionyl chitosan into monolayers of zwitterionic and negatively charged phospholipids. Interestingly, the *O*,*O*′-acylated chitosan derivatives were incorporated into the hydrophobic chains of the phospholipids. It was suggested that hydrophobic derivatives should be more effective if the activity depends on the interaction with the cell membrane. Recently, *O*-acylation of chitosan nanofibers by fatty acids has been reported using pyridine as a catalyst and short- (C2–C6) and long (C8, C12)-chained fatty acid anhydrates as acylation agents (Zhang et al. 2017). Modification of chitosan nanofibers by *O*-acylation effectively controlled fiber structure and increased stability in moist environments. Hence, it can be used to improve fiber properties and expand potential applications.

As *O*-acyl chitosans are soluble in *N,N*-dimethylacetamide, further *N*-acylation can be performed using this solvent to obtain *N,O*-acylated chitosans. Many chitosan derivatives have been synthesized using this technique including *O*-octanoyl-/*N*-cinnamate and *N,O*-hexanoyl chitosans. The latter derivative showed no deleterious effects on dermal fibroblasts and exhibited a favorable tissue response in vivo with less inflammation and fibrosis when compared, for instance, to poly(lactide-co-glycolide) or unmodified chitosan (Wu et al. 2007; Xu et al. 2008). Amphiphilic *N,O*-acylated chitosan derivatives containing *N*-phthaloyl side groups can be easily obtained by coupling reactions in the presence of dicyclohexylcarbodiimide. As an example, Bian et al. (2009) reported the synthesis of an amphiphilic copolymer, ***N*-**phthaloylchitosan-g-polyvinylpyrrolidone, by grafting polyvinylpyrrolidone onto a chitosan derivative whose amino groups were protected by phthaloyl groups. When prednisone acetate was loaded onto the resulting micelles, their mean size increased from about 90 nm to about 140 nm. The micelles released prednisone continuously with no initial burst.

3.2.2 N-*Alkyl Chitosans*

N-Alkylation involves the primary amino group of chitosan (Fig. 3.1), which reacts with aldehydes and ketones to give an intermediate reaction product (e.g., a carbinolamine). The intermediate dehydrates to yield Schiff bases (aldimines and ketimines) that are converted into *N*-alkyl-derivatives when treated with proper reducing agents, such as sodium cyanoborohydride, which allows selective reduction of imines but is highly toxic. In one pioneering study, alkylated chitosans differing in the length of the alkyl chains and the degree of grafting have been systematically analyzed to achieve optimal physical gelation (Rinaudo et al. 2005). The authors found that the optimal chain length is C12 and the optimal degree of grafting is 5% and that cross-linking is highly dependent on the salt concentration. Thus, the chemical structure is critically linked with the physical properties. In addition, the role of alkyl chains on the bulk and interfacial properties in relation to the environment and the interaction with cyclodextrins (see below) in relation to alkyl chain aggregation were tested in this study.

In a more recent study, Kurita and Isogai (2012) reported the reaction of chitosan with different alkyl halides in the presence of sodium hydrogen carbonate using aqueous conditions and determined the chemical structures as well as degrees of grafting and polymerization. They showed that selective *N*-carboxymethylation, *N*-benzylation, and *N*-hydroxyethylation at the C2-amine groups of chitosan could be achieved at high yields using sodium hydrogen carbonate as the *N*-alkylation promoter. Interestingly, *N*-alkylation of chitosans may improve blood clotting. Wang and Guan (2018) synthesized *N*-alkylated chitosans with various carbon chain lengths and used this material to fabricate nanofiber membranes by an electrospinning process. Different tests to evaluate biocompatibility and blood coagulation properties revealed that the membranes derived from *N*-alkylated chitosan nanofibers were not cytotoxic and exhibited satisfactory blood clotting capabilities by activating coagulation factors and platelets. Among the various tested *N*-alkylated chitosan membranes, those made of *N*-octadecane chitosan had the best blood clotting performance, though it exhibited the weakest mechanical properties. Nevertheless, it may be a good candidate for a hemostatic agent.

3.2.3 *Further Modifications to Yield Amphiphilic Polymers, Micelles, and Liposomes*

Hydrophobic moieties have been attached to various hydrophilic chitosan derivatives (mostly carboxymethyl chitosan) to yield amphiphilic polymers that are able to generate micellar structures used as nanocarrier systems for the targeted delivery of drugs (Fig. 3.2). The addition of hydrophobic moieties to chitosan or its more

hydrophilic derivatives is expected to increase surface activity and/or may lead to an improved stability of the polymer micelles (Elsabee et al. 2009). Furthermore, hydrophobic modifications should lower the critical concentrations for aggregation and micellization.

Besides various acyl and alkyl moieties such as lauryl aldehyde (Miwa et al. 1998), hexanoyl anhydride (Liu et al. 2008a), linoleic acid (Tan and Liu 2009), stearic acid (Thotakura et al. 2017), and gallic acid (Thotakura et al. 2017), a large variety of other hydrophobic compounds have been used for this purpose. Such compounds include cholesterol (Yinsong et al. 2007), deoxycholic acid (Jin et al. 2012), or nonionic surfactants like Pluronic F127 (Westerink et al. 2001; Pepic et al. 2010); Pluronic F68 (Bueno et al. 2014); monolaurate, monooleate, or trioleate (Grant et al. 2006); polysorbate 40 (Tween 40) (Li et al. 2013); and polysorbate 80 (Tween 80) (Yadav et al. 2017). Alternatively, chitosan can be converted into amphiphilic assemblies by the attachment of anionic or cationic surfactants such as dodecyl sulfate (Pal and Pal 2017) or cetyltrimethylammonium bromide (Zhang et al. 2018a) or by the combination with lipids such as phosphatidylcholine (Mertins et al. 2005; Hong and Kim 2011; Al-Remawi et al. 2017) or lysophosphatidylcholine (Westerink et al. 2001). In the latter case, nanosized chitosan/lipid assemblies are formed that either carry the chitosan chains on the surface of lipid nanoparticles and vesicles (i.e., liposomes) or within the lumen of liposomes (lipid-coated chitosan nanoparticles termed lipochitoplexes; see Fig. 3.2) (Bugnicourt and Ladavière 2017). Chitosan/lipid assemblies exhibit superior properties for drug and DNA delivery. Recently, Baghdan et al. (2018) employed liposomal encapsulation for chitosan nanoparticles loaded with pDNA. They examined cytotoxicity and transfection efficiency using HEK293 cells and a chorioallantoic membrane in vivo model. The lipochitoplexes efficiently protected the pDNA against degradation, reduced cytotoxic effects, and significantly increased transfection efficiency under physiological conditions.

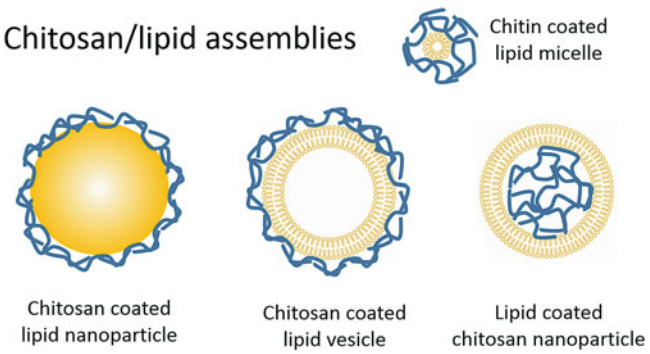

Fig. 3.2 Chitin/lipid assemblies used as drug delivery systems

3.3 Hydrophilic Modifications

3.3.1 N/O-*Carboxyalkyl Chitosans*

Carboxyalkyl chitosans have been synthesized in numerous variations and studied extensively for their potential applications in biomedicine and industry. Most of them are derivatives of carboxymethyl chitosan (CMCS; see Fig. 3.1), which can be synthesized as *N*-, *O*-, *N,O*-, or *N,N*-CMCS depending on the reaction conditions and the reagents used (Fonseca-Santos and Chorilli 2017). *O*-CMCS is mainly obtained, when the reaction is carried out at cool to ambient temperatures in a mixture of isopropanol and water containing monochloroacetic acid and sodium hydroxide (Chen and Park 2003). *O*-CMCS has been synthesized in numerous studies and tested as carrier for the delivery of various drugs such as doxorubicin (Shi et al. 2006), methotrexate (Wang et al. 2011), tetracycline (Martins et al. 2011; Maya et al. 2012), metformin (Snima et al. 2012), gentamycin and salicylic acid (Ji et al. 2012), and diltiazem (Bresolin et al. 2014).

If carried out at higher temperatures, the reaction yields mixtures of *N*- and *N,O*-CMCS (Chen et al. 2004b). *N*- and *N,N*-CMCS can either be prepared by the reaction with glyoxylic acid with subsequent reduction by cyanoborohydride (Miranda et al. 2006) or by direct alkylation using monochloroacetic acid under moderately alkaline conditions (An et al. 2008). In all cases, the reactions introduced acidic groups into the backbone of the chitosan polymer resulting in amphoteric polyelectrolytes. By controlling the degree of substitution, the charge density can be adjusted, which confers pH-dependent properties to the polymer. *N*-CMCS has valuable properties that allow a broad spectrum of applications in food and cosmetic industry (Pavlov et al. 1998). It is soluble in aqueous solutions, has a high viscosity, and forms large hydrodynamic films and gels. *N*-CMCS cross-linked with tripolyphosphate yielded polymeric nanoparticles that were useful as protective carriers for the antioxidant idebenone preserving its activity (Amorim et al. 2010). ***N*-**CMCS-based films have a compact structure, with a crossing arrangement of ***N*-**CMCS fibers (Miranda et al. 2006). *N,N*-CMCS in combination with alginate cross-linked by genipin exhibits pH-dependent swelling characteristics and proved suitable as a carrier for drug delivery in the intestine (Chen et al. 2004b). Moreover, superporous, pH-sensitive, and cross-linked hydrogels can be generated from *N,O*-CMCS, which has been used to create drug delivery systems that, for instance, allow oral administration of insulin (Chen et al. 2004a; Lin et al. 2005; Yin et al. 2007, 2010). Many further derivatives of *N,O*-CMCS have been synthesized and characterized over the past years including *N*-phthaloyl-CMCS as carrier for levofloxacin (Peng and Zhang 2007, 2009), methoxy poly(ethylene glycol)-grafted or folic acid-modified CMCS for doxorubicin (Jeong et al. 2010; Sahu et al. 2010), folate-conjugated CMCS-manganese-doped zinc sulfide nanoparticles for 5-fluorouracil (Mathew et al. 2010), and CMCS-soy protein complexes for vitamin D3 (Teng et al. 2013).

3.3.2 *Quaternized Chitosan Derivatives*

Chitosan is practically insoluble in aqueous solutions with a neutral or alkaline pH and becomes soluble only below pH 5.6. To facilitate applications in tissues at a normal physiological pH, it is essential to derivatize chitosan in a way that substantially increases solubility. One efficient method is quaternization of chitosan or its derivatives, which converts the primary amino group into a quaternary ammonium ion and hence adds positive charges to the polymer. Next to its increased solubility, quaternized chitosans exhibit enhanced antimicrobial activity and possesses improved mucoadhesiveness, epithelial absorption, and drug/DNA delivery properties than unmodified chitosan (Mourya and Inamdar 2009; Tan et al. 2013). Quaternization can be achieved either by reacting chitosan with alky halides such as iodomethane in one- or two-step procedures, or dimethyl sulfate, or by reacting chitosan with compounds that contain the quaternary ammonium itself.

Quaternization by iodomethane results in the nucleophilic substitution of the primary amino group at the C2 position of chitosan with methyl groups using sodium iodide as a catalyst. Several protocols have been established for this reaction, which differ in the starting chemicals and reaction buffers. Muzzarelli and Tanfani (1985) were the first to produce quaternized chitosan by reacting chitosan with formaldehyde followed by the reduction with sodium borohydride yielding *N,N*-dimethyl chitosan (DMC), which was then converted into *N,N,N*-trimethyl chitosan (TMC; see Fig. 3.1) by the treatment with iodomethane in acetonitrile. One year later, Domard et al. (1986) published an alternative method for chitosan quaternization. They dissolved chitosan in *N*-methyl pyrrolidinone and reacted it with iodomethane in the presence of sodium hydroxide. Both methods resulted in quaternization of chitosan with efficiencies of about 60 to 65%. However, it was noted that not only the primary amino group at C2 but also the hydroxyl groups are methylated by this procedure (Domard et al. 1987). Substantial water solubility is obtained at degrees of quaternization of larger than 25%. Repeated reaction cycles to increase the degree of quaternization to more than 85%, however, are counterproductive, as the number of hydrophobic *O*-methylated groups increases, which lessens water solubility (Sieval et al. 1998).

In the subsequent years, several variations and combinations of the basic methods were tested to improve polymer stability, chemosensitivity, and water solubility (Hamman and Kotze 2001; Snyman et al. 2002; Curti et al. 2003; Polnok et al. 2004). One promising approach to reduce the extent of *O*-methylation while preserving high degrees of quaternization is to perform the reaction in a mixture of *N,N*-dimethylformamide (DMF)/water (50:50) omitting any catalysts such as sodium iodide (Runarsson et al. 2007, 2008). Finally, several strategies have been developed to avoid *O*-methylation completely. Verheul et al. (2008) developed a two-step procedure to generate *O*-methyl-free TMC. Starting with DMC, they obtained TMC in the presence of an excess amount of iodomethane.

Another possibility to avoid *O*-methylation is to start with *O*-protected chitosan precursors carrying, for instance, *tert*-butyldimethylsilyl moieties at the C3 and C6

hydroxyl groups. These precursors can be prepared by the reaction of chitosan with *tert*-butyldimethylsilyl chloride in *N*-methyl-2-pyrrolidone or DMF/imidazole (Rúnarsson et al. 2008). Quaternization can be achieved by the reaction of the *O*-protected chitosan with iodomethane (Benediktsdottir et al. 2011).

To avoid expensive alkyl halides for the synthesis of quaternized chitosans, which are, in addition, difficult to remove from the reaction product, de Britto and Assis (2007) used dimethyl sulfate as the methylation reagent. This method turned out to be more efficient than that based on iodomethane and resulted in a highly hydrophilic product with a degree of quaternization of about 52%. However, dimethyl sulfate is toxic, and the reaction is not selective for the preferred amino group (Tundo and Selva 2002). *O*-Methylation was found to be favored over *N*-methylation with increasing temperatures, rapidly degrading chitosan.

A general disadvantage of the methods described so far is that alkyl halides and dimethyl sulfate have toxic and carcinogenic properties, which raised some concerns regarding the use of quaternized chitosan synthesized as described above. Therefore, in a recently published article, a novel strategy was presented to synthesize TMC in an ionic liquid using dimethyl carbonate as a methylation reagent (Wu et al. 2017). The quaternized chitosan essentially lacked *O*-methylation but exhibited only a low degree of quaternization of about 9%. Quaternization can also be achieved with reactants that carry a quaternary ammonium group themselves. For instance, when the primary amino group of chitosan is reacted with glycidyl trimethylammonium chloride [i.e., (2,3-epoxypropyl)trimethylammonium chloride], a quaternized, *N*-monoalkylated chitosan is obtained with an extended positively charged side chain at the amino group as revealed by nuclear magnetic resonance (NMR) spectroscopy (Loubaki et al. 1991). This synthesis strategy yields *N*-(2-hydroxy)-propyl-3-trimethylammonium chitosan. This derivative has been extensively tested for its antioxidant (Xing et al. 2008), immuno-stimulatory (Tao et al. 2017a, 2017b), and antibacterial activities as a complex with iodine (Tang et al. 2015), as well as for its efficacy as a carrier for gene delivery in human cells (Xiao et al. 2012; Li et al. 2015a). In addition, various derivatives of *N*-(2-hydroxy)-propyl-3-trimethylammonium chitosan have been synthesized, characterized, and analyzed with regard to cytotoxicity and uptake by cancer cells (Yen et al. 2018). Moreover, insulin-loaded nanoparticles made of quaternized chitosan with cholic acid groups on their surface evidently target the liver and enhance the hypoglycemic effect of insulin (Zhang et al. 2016). Quaternization can also be performed by the reaction of chitosan with 3-chloro-2-hydroxypropyl trimethylammonium chloride known as Quat-188, a commercially available quaternization reagent (Daly and Manuszak-Guerrini 2001). This reagent was also used to synthesize quaternized *N*-aryl chitosan using iodine as a catalyst (Sajomsang et al. 2009b). However, this method is less specific than *O*-alkylation, which occurs even at ambient temperatures. Very recently, Raik et al. (2018) synthesized *N*-[4-(*N,N,N*-trimethylammonium)benzyl] chitosan chloride by the chemoselective reaction of 4-formyl-*N,N,N*-trimethylanilinium iodide with the primary amino group of chitosan. Using NMR and FTIR spectrometry, turbidimetric titration, and dynamic light scattering measurements, the authors showed that the resulting polyplexes had a good solubility in

water over a wide pH range, even at lower degrees of substitution. They exhibited a high binding capacity depending on the degree of substitution and were good carriers for the efficient transfection of plasmid DNA into HEK293 cells.

Alkylation of quaternized chitosan yields amphiphilic polymers due to the simultaneous presence of charged and hydrophobic side groups. Various synthesis protocols have been developed which result in different chitosan derivatives, which frequently exhibit antimicrobial properties. Such derivatives include quaternized *N*-alkyl chitosan with different chain lengths of the alkyl substituent (Kim and Choi 2002), trimethylated and triethylated 6-NH_2-6-deoxy chitosans (Sadeghi et al. 2008), chitosan *N*-betainates (Holappa et al. 2004, 2006a), *N*-chloroacyl-6-*O*-triphenylmethyl chitosan (Holappa et al. 2006c), quaternary piperazine derivatives of chitosan (Holappa et al. 2006b; Másson et al. 2008), methylated *N*-(4-*N,N*-dimethylaminocinnamyl) chitosan (Sajomsang et al. 2009a), *N*-(4-*N,N*-dimethylaminobenzyl) or *N*-(4-pyridylmethyl) chitosan (Sajomsang et al. 2008), and methylated *N*-(3-pyridylmethyl) chitosan (Sajomsang et al. 2010). The latter quaternized chitosan derivative forms a nanocomplex with DNA and is an efficient transfection agent as tested in hepatocyte-derived cancer cells (Sajomsang et al. 2014). The cytotoxicity of the nanocomplexes was dependent on the *N*-pyridinium position of the methylated *N*-pyridylmethyl chitosan. Methylated *N*-(4-*N,N*-dimethylaminobenzyl), methylated *N*-(4-pyridyl), and methylated *N*-(benzyl) chitosan nanoparticles were also tested as drug carriers for insulin (Mahjub et al. 2011, 2014). Finally, Naberezhnykh et al. (2013) examined the interactions of lipopolysaccharides with different *N*-acyl and *N*-alkyl chitosans and their quaternized derivatives. They found that an increase in chitosan hydrophobicity strengthens the interaction with liposomes, while an increase in molecular weight reduces the inclusion of chitosan in the liposomal membrane.

3.3.3 Phosphorylated, Sulfated, and Thiolated Chitosan

The chemical modification of chitosan by phosphorylation is known to improve chelating properties and is expected to increase biocompatibility. Several methods have been developed to synthesize phosphorylated derivatives of chitosan (e.g., 2-*N*,3-*O*,6-*O* phosphorylated chitosan, Fig. 3.1), which were summarized by Jayakumar et al. (2008). In brief, phosphorylated chitosan can be prepared by the reaction with orthophosphoric acid in ***DMF*** using urea as a reaction-promoting agent or phosphorous pentoxide in methanesulfonic acid (Sakaguchi et al. 1981; Nishi et al. 1986, 1987). An alternative method is the reaction of chitin with orthophosphoric acid, tris(ethyl) phosphate, and phosphorous pentoxide in hexanol, which allows the adjustment of any desired degree of substitution by changing the molar ratio of chitosan and phosphorous pentoxide (Jayakumar and Tamura 2006). Another preparative method is grafting by the use of mono(2-methacryloyl oxyethyl) acid phosphate, which results in amphiphilic polymers with antimicrobial

properties (Jung et al. 1999), or by graft copolymerization reacting chitosan with 2-carboxyethyl phosphonic acid using EDC as catalyst (Jayakumar et al. 2006).

Incorporation of *N*-methylene phosphonic groups into chitosan can also be achieved according to the Moedritzer-Irani reaction (Moedritzer and Irani 1961) by converting chitosan with phosphorous acid and formaldehyde (Heras et al. 2001). This preparative method yields *N*-methylene phosphonic chitosan, which is soluble at a neutral pH. It is a powerful chelating agent of transition metal and calcium ions (Ramos et al. 2003a). Furthermore, *N*-methylene phosphonic chitosan has been alkylated by attaching lauryl moieties, which results in amphiphilic properties with surfactant-like activities (Ramos et al. 2003b). More recently, Ma et al. (2010) provided a simple and efficient method for the preparation of *N*-phosphoryl chitosan derivatives using the Atherton-Todd reaction of chitosan with diethyl phosphite. Both crystallinity and thermal stability of the resulting *N*-phosphoryl chitosan were found to be increased when compared to unmodified chitosan in this case.

Reacting chitosan with 2-chloro ethyl phosphonic acid in KOH/methanol results in chitosan-*O*-ethyl phosphonate with potential plant growth regulation properties due to the release of ethylene (Palma et al. 2005). To incorporate a phenyl groups into the chitosan backbone, chitosan can be further reacted with formaldehyde and phenylphosphonic acid resulting in *N*-methylene phenylphosphonic chitosan, which exhibits higher water solubility but a lower thermal stability than chitosan (Jayakumar et al. 2007b).

Chitosan and chitosan copolymers grafted with phosphorylcholine have been analyzed for their potential as drug carriers (Wu et al. 2014a) and gene delivery vectors (Li et al. 2015b; Picola et al. 2016), as well as a matrix for cellular adhesion (Zhu et al. 2002; Tardif et al. 2011; Qi et al. 2015a; Oktay et al. 2017), because they mimic the surface of the plasma membranes of cells (Gong et al. 2011). As phosphorylated chitosan has a greater ability to bind calcium ions than unmodified chitosan (Yokogawa et al. 1997), matrices from this material are ideal substrates for bone cells. In line with this statement, phosphorylated chitosan reinforced with calcium phosphate cements have been shown to improve bone regeneration in rabbits. They can be used in bone repair as they are biocompatible and possess osteoinductive properties (Wang et al. 2002). In addition, phosphorylated chitosan evidently improves biomimetic remineralization of enamel and dentin (Xu et al. 2011; Zhang et al. 2014b) and may reinforce the dentin surface resistance to erosive challenges (Beltrame et al. 2018).

The extracellular matrices in all human tissues contain sulfated polysaccharides such as heparan sulfate, keratin sulfate, or chondroitin sulfate. Hence, biocompatibility of chitosan is expected to be increased upon sulfatation, and due to the presence of additional negative charges, the sulfated polymer absorbs metal ions. Sulfated chitosans, such as 2-*N*,3-*O*,6-*O*-sulfated chitosan (Fig. 3.1), have numerous potential applications in medicine including their use as anticoagulants, hemagglutinin inhibitors, and antimicrobial and antiviral drugs (Jayakumar et al. 2007a). There are ample of techniques to synthesize sulfated chitin and chitosan using different combinations of sulfating agents (Cushing et al. 1954; Wolfrom and Han 1959; Horton and Just 1973; Nishimura et al. 1986; Terbojevich et al. 1989;

Gamzazade et al. 1997; Holme and Perlin 1997; Drozd et al. 2001; Vongchan et al. 2002). The transformation of chitosan and other polysaccharides in concentrated sulfuric acid was examined by Nagasawa et al. (1971), who treated chitosan with concentrated sulfuric acid at 0 ° C. After gelation and washing the precipitate in ether, it was dissolved in water, and the solution was adjusted to pH 7.6 using NaOH. The sulfated chitosan was further purified by dialysis and washing in ethanol and ether. In contrast to chitin, chitosan was very resistant to depolymerization as expected from the stabilizing effect of the free amino group. Gamzazade et al. (1997) reported four different methods to synthesize sulfated chitosans, which showed structural heterogeneity and considered as copolymers composed of random alternated mono-, di-, and trisubstituted units of chitosan.

Sulfoethyl chitosan is an alternative amphoteric chitosan derivative. It can be obtained by the reaction of chitosan with 2-chloroethane sulfate or 2-bromoethane sulfate under alkaline conditions without using additional reagents and organic solvents (Nudga et al. 1974; Petrova et al. 2014). Another possibility to introduce a sulfonic acid function into the chitosan backbone is through the Schiff reaction with the sodium salt of 5-formyl-2-furansulfonoic acid using mild conditions to prevent *O*-substitution and polymer degradation (Muzzarelli 1992). This reaction yields *N*-sulfofurfuryl chitosan sodium salt with a degree of substitution of 26%. In the same study, sulfoethyl *N*-carboxymethyl chitosan was prepared by reacting 2-chloroethanesulfonic acid, sodium salt, with *N*-carboxymethyl chitosan, which was suspended before in a solution of isopropanol and NaOH. The modified chitosan contains about 4% sulfur. Hirano et al. (1985) investigated anticoagulant activities for *O*-sulfated *N*-acetyl chitosan, *N,O*-sulfated chitosan, and sulfated *O*-carboxymethyl chitosan. To prepare *N,O*-sulfated chitosan and sulfated *O*-carboxymethyl chitosan, they reacted chitosan and *O*-carboxymethyl chitosan with sulfur trioxide in DMF, respectively. In a similar approach, *O*-sulfated *N*-hexanoyl chitosan was synthesized from *N*-hexanoyl chitosan and tested together with the just mentioned sulfated chitosans for their ability to release lipoprotein lipase from apolipoprotein C2, which is an unwanted side effect of anticoagulants (Hirano and Kinugawa 1986). Nishimura et al. (1998) considered the use of specifically protected intermediates such as 6-*O*-tritylchitin or 6-*O*-tritylchitosan for the synthesis of novel chitin or chitosan sulfates that were selectively sulfated at the *O*-3 or *O*-2/*O*-3 positions. They prepared chitin/chitosan sulfate by treating these intermediate with a sulfur trioxide-pyridine complex in dry pyridine. In comparison to a 6-*O*-sulfated derivative, *O*-3 or *O*-2/*O*-3 sulfated had little anticoagulant activity, but a strong anti-HIV activity. In recent years, 2-*N*,6-*O*-sulfated chitosan nanoparticles loaded with bone morphogenetic protein-2 (BMP-2) have been intensively examined with regard to their effects in vascularization and bone regeneration, and 2-*N*,6-*O*-sulfated chitosan-immobilized poly(lactide-co-glycolide) scaffolds with an without BMP-2 have been studied for cell attachment, proliferation, and osteogenic differentiation (Kong et al. 2014). Moreover, Yu et al. (2018b) have exploited the affinity of 2-*N*,6-*O*-sulfated chitosan to the vascular endothelial growth factor (VEGF) and evaluated its pro-angiogenic activity. They found that VEGF was efficiently bound by the sulfated chitosan and that the combination of both promoted

angiogenesis. Finally, Pan et al. (2018) reported that 2-*N*,6-*O*- sulfated chitosans can improve the angiogenetic effects of BMP-2 stimulating bone regeneration.

Other sulfated derivatives that have been synthesized include sulfated-6-*O*-carboxymethyl chitin and chitosan using chlorosulfonic acid and DMF (Ishihara et al. 1995; Hagiwara et al. 1999); sulfated β-chitosan derivatives using *N*-(2,3-dihydroxy)propyl chitosan, DMF, sulfuric acid, and dicyclohexylcarbodiimide (Youn et al. 2004); sulfated heterochitosans using sodium carbonate anhydrous and trimethylamine-sulfur trioxide (Park et al. 2004b); low-molecular-weight sulfated chitosan using oleum and DMF (Vikhoreva et al. 2005); high-molecular-weight sulfated chitosan using sulfur trioxide, dichloroacetic or formic acid, and DMF (Xing et al. 2005); and *N*-alkyl-*O*-sulfated chitosan using *N*-octyl-chitosan, chlorosulfonic acid, and DMF (Zhang et al. 2003).

In an interesting study published by Wang et al. (2012), four different types of polymeric micelles based on hydrophobically modified sulfated chitosans differing in the degree of substitution and kind of hydrophobic moieties were synthesized and used to encapsulate doxorubicin. The hydrophobic moieties that were attached to the sulfated chitosan were glycyrrhetinic acid (GA; recognized by receptors of hepatic cells), cholic acid, stearic acid, and lauric aldehyde. Encapsulation was found to depend on several parameters, including the degree of substitution of the sulfate group and the hydrophobic group and the type of hydrophobic group. The highest loading efficiency was found for GA-modified sulfated chitosan. Using 6-*O*-sulfated chitosan as a starting material, which was prepared according to a method described by Terbojevich et al. (1989), Tian et al. (2012) produced sulfated chitosan nanoparticles functionalized with GA using 3-*O*-hemisuccinate GA, EDC, NHS, and DMF. The GA adds a hydrophobic group for micelle formation and targets the nanoparticles to the liver. As the nanoparticles can be efficiently loaded with doxorubicin, they were tested as carriers for chemotherapeutics to treat liver cancer. Yang et al. (2013a) reported a different method to obtain highly sulfated chitosan with a high anticoagulant activity, which was dependent on the degree of sulfation. They used trimethylsilylated chitosan (Kurita et al. 2004) as a starting material for sulfation in dry dimethylsulfoxide (DMS) and reacted it with a sulfur trioxide-pyridine complex (Yang et al. 2003).

Another possibility to deal with the poor water solubility of chitosan is to introduce thiol groups to obtain a thiolated polymer, also known as thiomer. Thiolation is a highly efficient method to increase mucoadhesiveness of chitosan, which is due to formation of covalent disulfide bonds between thiol groups and mucus glycoproteins (Albrecht and Bernkop-Schnurch 2007). Thiolated chitosans have been developed into carriers for drug delivery due to their excellent gelling properties. Moreover, they possess enzyme and efflux pump inhibitory activities and improved permeation properties. Therefore, they have been specifically used to develop mucosal drug delivery systems for oral, nasal, ocular, and vaginal administration of various therapeutics, including insulin, cancer drugs, antibiotics, and antiretroviral substances (Zhu et al. 2012; Saremi et al. 2013; Millotti et al. 2014; Meng et al. 2017; Arif et al. 2018). The primary amino group at the C2 position of the glucosamine subunits of chitosan is the main target for covalently linking

sulfhydryl-bearing groups via formation of amidine or amide bonds. Cationic amidine conjugates are, for instance, formed by the reaction of chitosan with 2-iminothiolane (Traut's reagent) to yield chitosan-4-thiobutylamidine (Bernkop-Schnurch et al. 2003) or with isopropyl-S-acetylthioacetimidate to yield chitosan-thioethylamidine (Kafedjiiski et al. 2005b). Amide bonds are formed by the reaction of the carboxylic acid group of ligands such as cysteine (Bernkop-Schnurch et al. 1999), *N*-acetylcysteine (Schmitz et al. 2008), glutathione (Kafedjiiski et al. 2005a), or thioglycolic acid (Kast and Bernkop-Schnurch 2001) (Fig. 3.1) with the primary amino group of chitosan in the presence of water-soluble carbodiimides. During synthesis, disulfide bond formation by oxidation can be prevented by using inert conditions and S-protected ligands or performing the reaction at a pH $\leq$ 5, which reduces the concentration of thiolate anions required for oxidation essentially. Thiolated chitosans exhibit strongly pH-dependent reactivities, which peak at a moderate alkaline pH where the concentration of reactive thiolate anions is highest. To overcome this pH dependence, Millotti et al. (2009) developed a chitosan-6-mercaptonicotinic acid conjugate, which can form disulfide bonds independent from the presence of thiolate anions due to the formation of reactive thione tautomers. Thiolation of chitosans with hydrophobic side groups leads to amphiphilic chitosan conjugates that form micelles, which can be loaded with therapeutic agents for mucosal drug delivery. For instance, Mahmood et al. (2017) synthesized a chitosan-stearic acid-thioglycolic acid conjugate. When the authors of this study tested these conjugates in porcine mucus, they found an increase in dynamic viscosity, elastic modulus, and viscous modulus, when comparing the thiolated with non-thiolated chitosan-stearic acid conjugates.

3.3.4 Carbohydrate-Modified Chitosan

In alternative attempts to increase water solubility and provide additional biological functionalities, hydrophilic sugar moieties have been covalently attached to the backbone of the polymer by reductive *N*-alkylation. In this way, various chitosan derivatives have been synthesized bearing aldehydes (e.g., glycolaldehyde, DL-glyceraldehyde), monosaccharides (e.g., D-glucose; Gullon et al. 2016), D-galactose (Lou et al. 2016; Fig. 3.1), D-mannose, D-fructose (Wang and Hon 2003), D-fucose (Lin et al. 2013), L-fucose, *N*-acetylglucosamine (Morimoto et al. 2001), gluconic acid (Takei et al. 2013), as well as disaccharides such as sucrose, lactose, and maltose (Kurita et al. 2003; Wang and Hon 2003; Phongying et al. 2006). Carbohydrate-modified chitosan derivatives have also attracted interest, because they can be used for the development of carriers that specifically target certain cell types. For instance, Kato et al. (2001a) reported the preparation of a lactosaminated derivative of *N*-succinyl-chitosan, which specifically accumulates in mouse liver cells by interacting with the asialoglycoprotein receptor. In a subsequent study, the same authors suggested that lactosaminated *N*-succinyl-chitosan has some potential as a carrier for anticancer drugs to prevent liver metastatic cancer (Kato

et al. 2001b, 2002). Selective targeting to hepatic cells was also reported for potential cancer drug carriers made of galactosylated chitosan derivatives including chitosan-graft-dextran copolymers (Park et al. 2000), galactosylated glycol chitosan micelles (Yu et al. 2014), galactosylated chitosan-grafted multiwall carbon nanotubes (Qi et al. 2015b), and galactosylated chitosan/graphene oxide nanoparticles (Wang et al. 2018a). In addition, galactosylated chitosan obtained from the reaction of lactobionic acid and chitosan in the presence of EDC or NHS facilitates the attachment of hepatocytes making this material a suitable matrix for tissue engineering (Park et al. 2003). Furthermore, galactosylated chitosan-graft-poly(vinyl pyrrolidone) and galactosylated poly(ethylene glycol)-chitosan-graft-polyethylenimine were developed as DNA carriers for the transfection of hepatocytes in vitro and in vivo (Park et al. 2004a; Jiang et al. 2008).

In comparison to galactosylated chitosans, fewer chitosan derivatives have been generated that are branched with sialic acids (i.e., *N*-acetylneuraminic acid), although this sugar is highly abundant on the surface of mammalian cells. In addition, sialic acid is recognized by the receptors on the surface of many viral pathogens, such as the influenza virus, and hence important for infectivity (Matrosovich et al. 2015). Accordingly, sialylglycopolymers with a chitosan backbone and chitosan-sialyloligosaccharides possess potent inhibitory activities to prevent influenza virus infection and virus-induced hemagglutination (Makimura et al. 2006; Umemura et al. 2008; Cheng et al. 2014). Chitosans modified by sialic acid branching were first synthesized by Sashiwa et al. (2000a) via reductive *N*-alkylation of *p*-formylphenyl α-sialoside. To improve solubility, non-substituted amino groups were reacted with succinic anhydride. Apart from its antiviral activity, sialic acid-modified chitosans have also been examined for their efficiency as carriers for drug delivery and as neuroprotective agents. To evaluate the therapeutic efficacies of dexamethasone and methotrexate, Zhang et al. (2014a) encapsulated these drugs within quaternized polysialic acid-chitosan nanoparticles and tested their anti-inflammatory effects in a synovial cell line, which was immuno-stimulated. Both drugs were shown to retain their anti-inflammatory activity when applied via the quaternized sialic acid-chitosan particles. Using EDC again, different sialic acid-modified chitosans have been synthesized and shown to attenuate Aβ toxicity, which is associated with neurodegeneration in Alzheimer disease, using a neuroblastoma cell line. Notably, the protective properties of these chitosans were dependent on the degree of *O*-substitution in the ring structure (Dhavale and Henry 2012).

Chitosan can also be modified by attaching more complex sugars such as cyclodextrins (CDs; Fig. 3.1), which are formed during the enzymatic degradation of starch. CDs are cyclic oligosaccharides made of six (α-CDs), seven (β-CDs), or eight (γ-cDs) α(1-4)-linked D-glucose units that build a toroidal structure with a hydrophilic outer surface and a central more hydrophobic cavity, which is frequently used for the inclusion of apolar organic compounds (Duchêne and Bochot 2016). Grafting chitosan with CDs synergistically combines the advantages of both molecules resulting in molecular carriers with improved stability, size specificity, and transport and drug releasing properties. Grafting is a method in which monomers of a polymer are covalently bonded to the backbone of a parent polymer (Bhattacharya

and Misra 2004). This results in modified polymers with altered surface properties while maintaining the bulk properties of the parent polymer (Yang et al. 2007). Different grafting techniques to link CDs onto chitosan have been developed which are chemically based on Schiff base formation and reductive amination, amide formation, "click" reactions, nucleophilic substitution reactions, or photoinitiation (Campos et al. 2017). Here, we will consider only a few selected examples to illustrate the chemistry of synthesizing CD-modified chitosans. Using a Schiff base reaction, a β-cyclodextrin-modified chitosan was generated by reacting 6-*O*-(4-formylphenyl)-β-cyclodextrin with chitosan in a mixture of acetic acid and methanol at pH 5.0 (Liu et al. 2008b). The CD-modified chitosan was used to generate supramolecular assemblies by the inclusion of adamantane-modified pyrene into the CD cavity and the wrapping of chitosan chain around multiwalled carbon nanotubes. Grafting by amide formation was employed to synthesize glycol chitosan-graft-carboxymethyl-β-CD (Tan et al. 2012). In this case, EDC was used to facilitate amide formation between carboxylic groups of carboxymethyl-β-CD and the primary amine groups of glycol chitosan. The glycol chitosan-graft-carboxymethyl-β-CD was analyzed for its potential as a pH-sensitive anticancer drug carrier in this study. Chen et al. (2013) synthesized chitosan 6-OH immobilized CD derivatives by click chemistry. For this purpose, they first reacted 6-tosylated-2-benzaldehyde chitosan with sodium azide in DMF to obtain a Schiff base protected chitosan, which was then linked to (2-propargyl)-amino-deoxo-β-cyclodextrin using Cu (I) as a catalyst. Finally, the protecting group was removed. Using the fact that chitosan is a potent nucleophile, Chen et al. (2012) first synthesized chitin with tosylated 6-OH groups, which are good electrophiles and leaving groups. In a second step, they displaced the tosyl group by a monoamino β-cyclodextrin derivative via nucleophilic substitution to obtain 6-OH substituted cyclodextrin derivatives. Electromagnetic radiation is frequently employed for chitosan grafting (see also below), which can be achieved with gamma, ultraviolet, or microwave radiation with or without photosensitizers. Employing electromagnetic radiation, Sharma and Rajesh (2017) published a simple microwave-assisted method to prepare β-cyclodextrin-grafted chitosan using glutaraldehyde as a cross-linker. For this purpose, they treated chitosan, β-cyclodextrin, and glutaraldehyde in a microwave synthesis reactor for a few minutes at 750 W, precipitated the product with NaOH, and washed it with acetone. Finally, they analyzed the capability of the resultant polymer to adsorb palladium (II).

In addition, numerous polysaccharides have been attached to or mixed with chitosan for the purpose of drug delivery, wound healing, and tissue engineering. The resulting hybrid composites include alginate/chitosan microparticles (Lacerda et al. 2014); cellulose/chitosan nanocomposite films (Azevedo et al. 2013; Wu et al. 2014b); carboxymethylcellulose/chitosan films and polyelectrolyte complexes (Cerchiara et al. 2016; Spera et al. 2017); hyaluronic acid/chitosan nanoparticles, coacervate-based scaffolds, and hydrogels (Kaderli et al. 2015; Zhang et al. 2015a; Karabiyik Acar et al. 2018); starch/(carboxymethyl)chitosan films and magnetic nanoparticles (Saboktakin et al. 2011; Saikia et al. 2015; Baghaie et al. 2017); chitosan/xanthan gum microparticles, polyelectrolyte complexes, and scaffolds

(Caddeo et al. 2014; Dehghan and Marzuka 2014; Westin et al. 2017); chitosan/locust bean gum nanocomposites (Vijayaraghavan et al. 2008; Jana and Sen 2017); chitosan/fucoidan hydrogels (Sezer et al. 2008; Lin et al. 2017); carrageenan/chitosan hydrogel films and complexes (Mahdavinia et al. 2017; Yu et al. 2018a, b); pectin/chitosan polyelectrolyte complexes (Macleod et al. 1999; Grabnar and Kristl 2010; Neufeld and Bianco-Peled 2017); heparin/chitosan complexes, nanoparticles, and scaffolds (Kratz et al. 1997; Thomas et al. 2014; Li et al. 2017b); and chitosan/dextran sulfate hydrogels, (superparamagnetic) nanoparticles (Chaiyasan et al. 2015; Perumal et al. 2017; Yucel Falco et al. 2017; Shevtsov et al. 2018).

3.4 Graft Copolymerized Chitosan

Graft copolymerization is one of the most frequently used methods for the introduction of various types of side chains to achieve polymers with specific characteristics such as antibacterial, antioxidant, adsorption, chelating, or complexation properties. Grafting can involve the primary amino groups or the hydroxyl groups at the C3 and C6 carbons. The physicochemical properties of the resulting polymers are largely determined by the number and characteristics of the side chains that have been attached to the chitosan backbone. There are three main techniques for grafting copolymerization, i.e., "grafting from," "grafting onto," and "grafting through" (Argüelles-Monal et al. 2018). The latter technique means grafting during main chain polymerization, which is not relevant for chitosan, as the polysaccharide backbone is already formed. In the "grafting from" method, polymerization of the graft monomer is initiated directly from the main chain, while in the "grafting onto" method, functional side groups of the backbone chain react with end-functional groups of preformed polymers. In contrast to the "grafting from" method, which does not yield defined macromolecular structures, the "grafting onto" method allows the generation of polymer systems with a well-defined structure; it is frequently used to prepare comb and bottlebrush polymers. Various reaction types have been employed to initiate graft copolymerization of chitosan (Jayakumar et al. 2005). Next to free radical formation, copolymerization has been achieved by the use of radiation, enzymes, polycondensation, living cations and radicals, oxidative coupling, as well as cyclic monomers (Fig. 3.3). Grafting percentage and efficiency are mainly controlled by the type and concentration of the initiator, the concentration of monomers, as well as the reaction temperature and time.

3.4.1 Free-Radical-Initiated Graft Copolymerization

Graft polymerization initiated by free radicals has been reported in numerous studies. Using ammonium persulfate as an initiator acrylamide was grafted onto

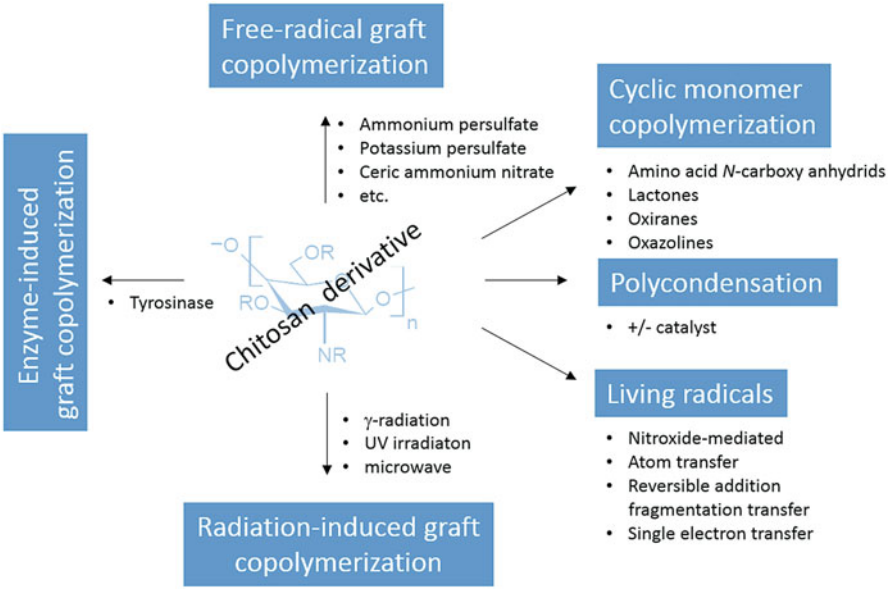

Fig. 3.3 Reaction types to initiate graft copolymerization of chitosan

maleilated chitosan (Berkovich et al. 1983), maleic acid sodium onto hydroxypropyl chitosan (Fig. 3.1) or carboxymethyl chitosan (Xie et al. 2002; Sun et al. 2004), methacrylic acid onto carboxymethyl chitosan (Sun et al. 2003), (*N,N*-dimethylamino)ethyl methacrylate onto *N*-carboxymethyl chitosan (Kang et al. 2006), acrylamide onto *N*-succinyl-chitosan (Mukhopadhyay et al. 2014), methyl methacrylate onto chitosan (Zheng et al. 2016), and *N*-vinyl-2-pyrrolidone onto chitosan (Sutirman et al. 2018). Similarly, potassium persulfate was frequently used as an initiator for chitosan graft copolymerization using 2-hydroxyethyl acrylate (Mun et al. 2008), acrylonitrile and/or methyl methacrylate (Hsu et al. 2002; Prashanth and Tharanathan 2003; Sabaa et al. 2018), acrylic acid and/or acrylamide (Yazdani-Pedram et al. 2000; Yazdani-Pedram et al. 2002; Mahdavinia et al. 2004), 4-acrylamidobenzenesulfonamide (Al-Sagheer et al. 2017), maleic acid (Hasiploglu et al. 2005), 2-acrylamido-2-methylpropane-sulfonic acid (Najjar et al. 2000), vinylpyrrolidone (YazdaniPedram and Retuert 1997), 4-vinylpyridine (Khalil and Al-Matar 2013), 2-hydroxyethyl methacrylate-co-itaconic acid (Subramanian and Vijayakumar 2012), and *N*-vinylcaprolactam (Kudyshkin et al. 2014) (see also Table 3.1).

Ceric ammonium nitrate is another inducer for generating graft copolymers of chitosan. It has been used to produce chitosan graft copolymers with acrylonitrile (Pourjavadi et al. 2003), *N*-isopropylacrylamide (Kim et al. 2000), acrylic acid (Huacai et al. 2006), methyl methacrylate (Liu et al. 2011), 2-hydroxyethyl methacrylate (Radhakumary et al. 2003), vinyl acetate (Don et al. 2002a b), 4-vinylpyridine (Caner et al. 1998), *N,NO*-dimethyl-*N*-methacryloxyethyl-*N*-

(3-sulfopropyl)ammonium, (dimethylamino)ethyl methacrylate (Liang et al. 2004), 3-(trimethoxysilyl)propyl methacrylate (Prabaharan and Mano 2007), acrylamide (Joshi and Sinha 2007), triethylene glycol dimethacrylate (Yilmaz et al. 2007) and *N*-vinylimidazole (Caner et al. 2007), or chitosan-g-maleic anhydride copolymers with ethylene dimethacrylate (Gopal Reddi et al. 2017).

Other initiators employed for grafting methyl methacrylic acid, 2-hydroxyethyl methacrylate, and acrylonitrile onto chitosan include thiocarbonate-potassium bromate (El-Tahlawy and Hudson 2001), potassium diperiodatocuprate (III) (Liu et al. 2003), potassium diperiodatonickelate (IV) (Liu et al. 2002), potassium ditelluratocuprate (III) (Liu et al. 2005d), 2,2-azobisisobutyro nitrile (Bayramoglu et al. 2003), 2,2-azobis(2-methylpropionitrile) (El-Tahlawy et al. 2006), ferrous ammonium sulfate/H_20_2 (Fenton's reagent) (Lagos and Reyes 1988), and tributyl borane (Kojima et al. 1979).

3.4.2 Radiation-Induced Graft Copolymerization

Graft polymerization induced by radiation is a powerful technique to introduce desirable side chains into polymers, which can be achieved by radiation with different wavelengths. It has many benefits in comparison to conventional techniques, such as chemical graft polymerization. For instance, the method is relatively simple as no catalyst or further additives are required for initiating the reaction.

3.4.2.1 γ-Radiation-Induced Graft Copolymerization

^{60}Co γ-irradiation was used in several studies to create chitosan copolymers with various properties. Grafting percentage and efficiency mainly depend on the radiation dose, the monomer concentration, the reaction temperature, and in some cases also on the solvent. In a study published in 1982 by Shigeno et al. (1982), styrene was grafted successfully onto chitin and chitosan by ^{60}Co γ-irradiation, whereby the grafting yield increased with radiation dose. However, this technique resulted in different kinds of chitosan graft copolymers and polystyrenes depending on the precise grafting conditions (Pengfei et al. 2001). ^{60}Co γ-radiation-induced grafting of *N,N*-dimethylaminoethyl methacrylate onto chitosan was reported by Singh and Ray (1997). They observed that the composition of the solvent has a striking effect on the degree of grafting. Graft copolymerization of butyl acrylate onto chitosan in acetic acid aqueous solution was investigated by Yu et al. (2003) using ^{60}Co γ-irradiation. In this study, the effects of different reaction conditions on graft copolymerization were discussed considering grafting efficiency, grafting percentage, and homopolymer percentage. Grafting percentages were found to increase with growing monomer concentration and total dose and decrease with increasing chitosan concentration and reaction temperature. When they compared pure chitosan films with chitosan graft poly(butyl acrylate) films, they found that the grafted

copolymers exhibited enhanced hydrophobicity and impact strength. Another study reported γ-radiation-mediated grafting of 3-hydroxybutyrate onto chitosan (Torres et al. 2015), with a particular focus on the effects of different solvents. Huang et al. (2005) used ^{60}Co γ-irradiation to graft butyl acrylate onto *N*-maleamic acid-chitosan and determined the thermal stabilities of the graft copolymer by thermal gravimetric analysis. Similar findings were published by Cai et al. (2005), who grafted *N*-isopropylacrylamide onto chitin via γ-radiation.

Using a one-pot γ-radiation-assisted reaction strategy mucoadhesive, thermo-responsive chitosan-graft-poly(*N*-isopropylacrylamide) copolymers were prepared, which self-assembled into polymeric micelles (Sosnik et al. 2015). To design a chitosan-based flocculant, Wang et al. (2008) prepared a chitosan graft copolymer using acrylamide as monomeric units by γ-radiation. Acetic acid concentration had a negligible effect on the grafting percentage, while grafting percentage increased with increasing total irradiation dose. However, in this case, a lower irradiation dose rate was in favor of grafting percentage at a fixed total irradiation dose, whereas a higher monomer concentration resulted in an increase in grafting percentage. With the aim to specifically support membrane peptides, a biocompatible polymeric assembly was developed by Zhou et al. (2015). For this purpose, the authors grafted poly (sulfobetaine methacrylate) onto chitosan via controlled polymerization under γ-irradiation and then analyzed the interaction of alamethicin, an antimicrobial peptide, with the resulting micelles. They found that the helical peptide penetrated the shell reaching the hydrophobic core. Very recently, Jeong et al. (2018) reported a one-step protocol for grafting 2-aminoethyl methacrylate-onto chitosan using γ-radiation for two purposes, synthesis and sterilization. The water-soluble copolymer effectively condensed plasmid DNA to form polyplexes with sizes ranging from 170 to 280 nm. Using different cell lines, the authors demonstrated that the formed copolymer is able to transfect colon cancer cells and hence is a suitable candidate for gene delivery.

3.4.2.2 UV-Induced Graft Copolymerization

In addition, different methods based on UV irradiation have been reported to graft chitosan. For instance, Ng et al. (2001) grafted hydroxyethyl methacrylate onto chitosan by ultraviolet light illumination. *p*-Benzoquinone was then coupled to the resulting chitosan-poly(hydroxyethyl methacrylate) for activation of the copolymer to immobilize sulfite oxidase for the development of an enzyme-based electrochemical biosensor. More recently, polyacrylamide-grafted chitosan was synthesized by the copolymerization of acrylamide and chitosan by ultraviolet irradiation using 2-hydroxy-4′-(2-hydroxyethoxy)-2-methylpropiophenone as photoinitiator (Ma et al. 2016). The resulting chitosan graft-polyacrylamide nanoparticles were found to be effective in the flocculation of both kaolin suspension and Cu^{2+} simulated wastewater.

3.4.2.3 Microwave-Induced Graft Copolymerization

Microwave-assisted modification of chitosan has been used in a number of studies and was found to be a convenient way for the production of a wide range of products with different degrees of substitution and molecular weight, only by varying reaction time and/or radiation dose. It has also been used to deacetylate chitin for the rapid synthesis of chitosan (Sahu et al. 2009), degrade chitosan in the presence of hydrogen peroxide (Li et al. 2012b), introduce *N*-sulfo and *O*-sulfo groups into chitosan (Xing et al. 2004), graft polyacrylonitrile onto chitosan (Singh et al. 2005), and synthesize carboxymethyl chitosan (Ge and Luo 2005; Wongpanit et al. 2005). Further microwave-assisted methods have been employed to synthesize chitosan-modified multiwalled carbon nanotubes (Yu et al. 2009), crown ether-cross-linked chitosan as a chelating agent for heavy metal ions (Radwan et al. 2010), chitosan-hydroxyapatite superporous hydrogel composites (Beskardes et al. 2015), *N*-butylacrylate-grafted chitosan as adsorbent for Cr(IV) (Santhana Krishna Kumar et al. 2014), magnetic chitosan microparticles for the immobilization of fungal cells (Safarik et al. 2015), 6-*O*-poly(ethyleneglycol)-*graft*-chitosan-*N*-cysteine tri-block copolymers (Badhe et al. 2015), *N*-methylene phosphonic chitosan (Dadhich et al. 2015), amphiphilic chitosans grafted with alkyl chains (Petit et al. 2015), and porous montmorillonite-hydroxyapatite-grafted chitosan composite scaffolds (Kar et al. 2016). Also antibacterial chitosan or carboxymethyl chitosan-silver nanocomposites (Huang et al. 2016; Raghavendra et al. 2016), gelatin cross-linked with chitosan and polyvinylpyrrolidone using an ultrasonic-assisted approach (Wang et al. 2018b), and antibacterial graft copolymers consisting of acrylic acid, acrylonitrile, and chitosan (Kumar et al. 2018) were fabricated using microwave radiation. Very recently, Mahmoud et al. (2018) reported microwave-assisted functionalization of titanium oxide nanoparticles with a chitosan nanolayer for the removal of trace concentration of metal ions.

3.4.3 Enzyme-Induced Graft Copolymerization

Graft polymerization can also be achieved in biomimetic reactions catalyzed by enzymes, which has several advantages over the use of chemical catalysts. They are highly selective and environmentally safe, and they can easily be inactivated and removed. Tyrosinase was used by several groups to graft chitosan with different phenolic compounds in a reaction which mimics sclerotization of arthropod cuticles involving the formation of highly reactive *O*-chinones (Kumar et al. 1999; Chen et al. 2000; Vachoud et al. 2001; Muzzarelli and Muzzarelli 2002; Muzzarelli et al. 2003; Freddi et al. 2006). Tyrosinase grafting was furthermore used to graft peptides onto chitosan resulting in bioconjugates with novel functionalities (Anghileri et al. 2007; Demolliens et al. 2008). Notably, chitosan nanoparticles carrying tyrosinase have been also developed into biosensors for the electrochemical detection of

phenolic compounds (Abdullah et al. 2006; Lu et al. 2010; Yang et al. 2012; Han et al. 2015; Fartas et al. 2017).

3.4.4 Other Graft Copolymerization Techniques

The grafting techniques discussed hereafter are less widely used to modify chitosan. Polycondensation has been used for grafting D,L-lactic acid onto chitosan or phthaloyl chitosan in the absence or presence of a catalyst, respectively, which results in pH-sensitive hydrogels in both cases (Qu et al. 1999; Feng and Dong 2007). Grafting of poly(D,L-lactic acid) onto chitosan has also been achieved using EDC as a catalyst (Cai et al. 2002). Living polymerization is a special form of chain growth polymerization in polymer chemistry without chain termination and chain transfer reactions resulting in more constant growth rates. It is frequently used to synthesize block copolymers, because the polymer can be built in successive steps using different monomers. Living cationic polymerization involves cationic propagating species. Using this technique, Yoshikawa et al. (1998) grafted living poly (isobutyl vinyl ether) and poly(2-methyl-2-oxazoline) cations onto chitosan resulting in copolymers of controlled molecular weight and narrow molecular weight distribution. Interestingly, the mole number of grafted polymer chain on chitosan decreased with increasing molecular weights of the living polymer cation due to growing steric hindrance of the functional groups of chitosan. An oxidative coupling reaction was used by Cheng et al. (2005) to graft polyaniline onto chitosan with the aim to generate a conductive copolymer. The resulting nanocomposites had rice-grain morphologies when analyzed by transmission electron microscopy and a maximal electrical conductivity of about 0.25 S cm^{-1} when high amount of polyaniline were used for grafting.

Cyclic monomer copolymerization via ring opening is another option for grafting polysaccharides. Cyclic monomers that have been used for graft copolymerization are α-amino acid *N*-carboxy anhydrides, lactones, oxiranes, and 2-alkyl oxazolines. For instance, using L-tryptophan *N*-carboxy anhydride and water-soluble chitosan, a chitosan-poly(L-tryptophan) copolymer with secondary structural side chains has been synthesized by ring-opening polymerization (Xiang et al. 2008). Strikingly, spectrometric analyses indicated that the secondary structure of the side chains changes from β-sheets to α-helices with their lengthening. Cationic ring-opening polymerization was described by Aoi et al. (1994). They grafted poly(2-oxazoline) prepolymers onto partially deacetylated chitin in DMS. In this case, ring-opening polymerization of the 2-acyloxazoline was performed in acetonitrile using methyl trifluoromethanesulfonate as an initiator, and termination of living polyoxazolines was found to be due to the free amino groups of the partially deacetylated chitin. Similarly, living poly(2-methyl-2-oxazoline) and poly(isobutyl vinyl ether) were terminated by surface amino groups on chitosan powder when synthesizing the corresponding block copolymer (Aoi et al. 1999). Using tin(II) 2-ethylhexanoate as catalyst and toluene as a swelling agent, Liu et al. (2005c) produced chitosan-g-

polycaprolactone by ring-opening graft copolymerization of ε-caprolactone onto phthaloyl-protected chitosan. To improve cellular uptake, solubility, and stability in aqueous media, Duan et al. (2010) generated amphiphilic brushlike polycations to obtain cationic nanomicelles as carrier for 7-ethyl-10-hydroxycamptothecin. For this purpose, they synthesized cationic chitosan-graft-polycaprolactone copolymers by ring-opening polymerization of polycaprolactone onto the hydroxyl groups of chitosan in the presence of methanesulfonic acid used as solvent and catalyst. Electrospinning of mixed solutions of poly(ε-caprolactone) and chitosan-graft-poly (ε-caprolactone) yielded cationic nanofibrous materials with properties rendering them suitable as scaffolds for skin tissue engineering (Chen et al. 2011). Furthermore, different micelle-forming derivatives of chitosan-graft-poly(ε-caprolactone) copolymers produced by ring-opening polymerization were developed for the delivery of drugs such as 5-fluorouracil (Gu et al. 2014), ganciclovir (Sawdon and Peng 2015), or rifampicin (Praphakar et al. 2017).

The development of graft copolymerization based on living radical polymerization has progressed significantly over the last years. Frequently, they are based on nitroxide-mediated polymerization (Nicolas et al. 2006; Lefay et al. 2013), atom transfer radical polymerization (Li et al. 2005; Ping et al. 2010), and reversible addition fragmentation transfer (Mayadunne et al. 1999; Abbasian and Mahmoodzadeh 2017). Also single-electron transfer living radical polymerization was used to functionalize chitosan in order to increase its antimicrobial activity (Lin et al. 2015). In this study, chitosan was functionalized with methacryloyloxyethyl trimethylammonium chloride in a ionic liquid system using Cu^0/*N,N,N′,N″,N″*-pentamethyldiethylenetriamine as a catalyst.

3.5 Chitosan-Based Poly(Amidoamine) Dendrimers

Poly(amidoamine) (PAMAM) dendrimers comprise polymers that are highly branched and exhibit three-dimensional structures that are well-defined. The core is made of tertiary amines, whereas the surface exposes primary amines that are linked to the core via an amide backbone (Fig. 3.1). Due to their multifunctional properties and conformational flexibility, dendrimers offer ample of possibilities for diverse applications in supramolecular polymer chemistry, medical chemistry, and catalysis (Bosman et al. 1999). The first chitosan-dendrimer hybrids were synthesized almost 20 years ago. Synthesis of a hyperbranched chitosan-sialic acid dendrimer hybrid with a tetraethylene glycol spacer by reductive *N*-alkylation was reported by Sashiwa et al. (2000b). However, the possibilities to create reactive dendrimers are limited for steric reasons in this case. Therefore, the authors developed a second method to bind chitosan to the dendrimer surface, which allows the use of commercially available amino-dendrimers such as PAMAM or poly (ethyleneimine). Tsubokawa and Takayama (2000) investigated the grafting of dendritic PAMAM onto the surface of chitosan powder. Successful grafting was achieved when two processes were repeated: Michael addition of methyl acrylate to

the surface amino groups and amidation of the resulting ester moieties with ethylendiamine (Tomalia et al. 1985). Since then, several chitosan-based PAPAM dendrimers have been developed for different applications. Klaykruayat et al. (2010) grafted cationic hyperbranched dendritic PAMAM onto chitosan, as described above, with the aim to prepare a water-soluble chitosan-dendrimer hybrid with a high antimicrobial activity. Wen et al. (2012) synthesized quaternized carboxymethyl chitosan/poly(amidoamine) dendrimers with antibacterial activity, which showed a stronger activity against gram-negative bacteria than *N*-[(2-hydroxy-3-trimethylammonium) propyl] chitosan chloride. Later, they showed that the nanoparticles exerted the antibacterial activity in a sequential event-driven mechanism leading to the disorganization of the outer membrane and cell death (Wen et al. 2015). Moreover, chitosan hydrogels were prepared by grafting PAMAM dendrimers onto chitosan using glutaraldehyde as a cross-linking agent (He et al. 2016). The hydrogel was reported to have antibacterial activities against gram-negative and gram-positive bacteria. Other chitosan-based dendrimers were tested for their ability to adsorb fluoride and heavy metals (Prabhu and Meenakshi 2015; Zarghami et al. 2016) or to deliver drugs such as dexamethasone (Oliveira et al. 2010), methotrexate (Leng et al. 2013), albendazole (Mansuri et al. 2016), or ofloxacin (Maheshwari et al. 2015).

3.6 Further Chitosan Modifications and Hybrid Materials

Next to chemical derivatization and copolymerization described so far, chitosan was modified by a variety of non-related chemical compounds to add specific properties, some of which will be discussed in more details in subsequent chapters. Not mentioned so far is, for instance, chemical modification by epichlorohydrin or ethylenediamine, which adds improved sorption properties to the resulting material (Nakano et al. 2004; Zhou et al. 2011; Chethan and Vishalakshi 2013; Silva et al. 2018). In addition, fatty acids, phospholipids, and oils have been used to generate chitosan-based hybrid composites for applications in biomedicine, pest management, and food industry. For instance, carboxymethyl chitosan carrying ricinoleic functions has been used as an emulsifier for the botanical pesticide azadirachtin (Feng and Peng 2012) and chitosan/phosphatidylcholine hybrid films as vehicles for the delivery of the anticancer drug paclitaxel (Grant et al. 2005), and chitosan coatings enriched with different essential oils have been used in plant protection and food industry (Xing et al. 2011; Guerra et al. 2015; Yuan et al. 2016). The latter chitosan hybrids have also potential applications in wound healing (Perez-Recalde et al. 2018).

Hybrid composites of chitosan and clay minerals or ceramic materials are other modifications worthy of being mentioned here, as they have been used as adsorptive materials (Chang and Juang 2004; Prakash et al. 2013; Azzam et al. 2016), as scaffolds for tissue engineering (Bhowmick et al. 2018), and as platform for biocatalysts (Dincer et al. 2012; Sun et al. 2016) (see also Table 1). Chitosan-

based adsorptive materials and flocculants used in water treatment have been reported for clinoptilolite and saponite (Budnyak et al. 2016), bentonite (Liu et al. 2015; Kumar and Viswanathan 2017; Moussout et al. 2018), attapulgite (Wang et al. 2009; Zhang et al. 2011), kaolinite (Agbovi and Wilson 2018), hydroxyapatite (Sairam Sundaram et al. 2008; Pandi and Viswanathan 2015), montmorillonite (Pereira et al. 2013; Wang et al. 2014), perlite (Swayampakula et al. 2009), and zeolite (Zhang et al. 2015b; Teimouri et al. 2016). Chitosan-based composites proposed or used as scaffolds for tissue engineering comprise hydroxyapatite, montmorillonite, bioglass ceramic, silicon dioxide, titanium dioxide, zirconium oxide, and zeolite (Katti et al. 2008; Pighinelli and Kucharska 2013; Yu et al. 2013; Deepthi et al. 2016; Kar et al. 2016).

3.7 Nanosized Chitosan-Based Materials

Nanosized metals have been used in many cases to add antimicrobial, chelating, or magnetic properties to the resulting chitosan composites (see also Table 3.1). Copper/chitosan complexes have been tested with regard to their antimicrobial and antitumor activities (Zheng et al. 2006; Arjunan et al. 2017) and copper/chitosan chelate gels as food additive for cattle nutrition (Duffy et al. 2018). Iron oxide/chitosan composites, some containing magnetite (Fe_3O_4) or maghemite (Fe_2O_3), have been examined as materials for the removal of arsenic, chromium, mercury, phosphate, fluoride, and ammonium ions (Liu et al. 2000; Gupta et al. 2009; Su et al. 2016; Lu et al. 2017; Pandi et al. 2017; Kim et al. 2018; Sun et al. 2018). In addition, iron oxide chitosan nanoparticles have significant antimicrobial activities (Nehra et al. 2018), and they have been developed into sensor platforms for the electrochemical or chemiluminescent detection of various analytes including pesticides (Prabhakar et al. 2016; Shirazi et al. 2016; Sun et al. 2017). Silk fibroin/chitosan/iron oxide scaffolds with superparamagnetic responsiveness and tunable pore structures have been fabricated and analyzed for potential applications in bone tissue engineering (Aliramaji et al. 2017). Finally, silver/chitosan composites with nanoscale surface structures have been extensively examined as antimicrobial biomaterials and anti-infectious wound dressings (Ishihara et al. 2015).

To improve the mechanical properties of chitosan-based composites, Wang et al. (2005) prepared multiwalled carbon nanotubes with a high number of surface hydroxyl groups that allow homogenous dispersion in the chitosan matrix. An important characteristic of such type of three-dimensional chitosan-carbon nanotube scaffolds is their conductivity (Lau et al. 2008). It allows a broad range of biosensor applications using immobilized biomolecules such as horseradish peroxidase or cytochrome c for the determination of hydrogen peroxide (Xiang et al. 2007; Chen et al. 2008), antibodies to detect carcinoembryonic antigen (Gao et al. 2011), tyrosinase for the detection of catechol (Yang et al. 2012), lactate oxidase for the detection of L-lactate (Hernandez-Ibanez et al. 2016), and specific ssDNA aptamers for the detection of adenosine and streptomycin (Shahdost-fard et al. 2013; Aghajari

and Azadbakht 2018). Moreover, chitosan/carbon film electrodes were loaded with hydrochinone for the detection of ascorbic acid (Jirimali et al. 2013), and β-glucosidase was immobilized on chitosan-carbon composites in a two-phase system to efficiently hydrolyze isoflavone glycoside for industrial applications (Chang et al. 2013). Hydroxyapatite/chitosan/carbon composites have further been characterized in tissue engineering as scaffolds for bone regeneration (Venkatesan et al. 2012; Long et al. 2014) and electrically conductive chitosan/carbon nanocomposites for the renewal of cardiac muscle cells (Martins et al. 2014). Chitosan/graphene oxide nanocomposites have been extensively examined with regard to their adsorptive properties (Hosseinzadeh and Ramin 2018; Qi et al. 2018; Zhang et al. 2018b; Zhou et al. 2018), their application as drug delivery systems (Bao et al. 2011; Justin and Chen 2014; Shi et al. 2016; Saeednia et al. 2017; Wang et al. 2018a), their use as three-dimensional scaffolds in tissue engineering (Fan et al. 2010; Dinescu et al. 2014; Cao et al. 2017; Hermenean et al. 2017; Sivashankari et al. 2018), and their suitability as platform for biosensors for the specific detection of various compounds in medicine and environmental monitoring (Wu et al. 2009; Yang et al. 2013b; Bao et al. 2015; Fartas et al. 2017; Tabasi et al. 2017). Chitosan/graphite nanocomposites have mainly found applications as sensor platform for the detection of organic compounds such as dipyrone (Pauliukaite et al. 2010), vitamin B12 (Kuralay et al. 2011), DNA hybrids (Erdem et al. 2012), or dopamine (Palanisamy et al. 2016).

Finally, chitosan at nanoscaled dimensions can be obtained by electrospinning or wet spinning (Ignatova et al. 2013; Yudin et al. 2014). Such nanofibers and nanofibrous films are frequently used in textiles (see Sect. 14.4.4). Different biomaterials have been used to generate chitosan-based nanocomposites and nanofibers, which frequently are blended with additional components. Such materials include fibroin (Zeng et al. 2015; Li et al. 2017d), gelatin (Gomes et al. 2017; Park 2017; Song et al. 2018), cotton fabrics (Liu et al. 2013; Ferrero et al. 2014), algal material (Sunkireddy et al. 2016), green tea polyphenols (Qin et al. 2013), collagen (Hayashi et al. 2012; Michalska-Sionkowska et al. 2018), soy protein (Teng et al. 2013; Wang et al. 2016), bovine serum albumin (Li et al. 2017a), nucleic acids (Mansouri et al. 2004), or glycosaminoglycans such as heparin, hyaluronan, and chondroitin sulfate (Muzzarelli et al. 2012; Shan 2004; Li et al. 2017b). In addition, carboxy-cellulose nanocrystals were grafted with chitooligosaccharides, which were used as stabilizer to fabricate Ag nanoparticles with high antibacterial activity and low cytotoxicity (Ni et al. 2018).

3.8 Concluding Remarks

As outlined in this review, chitosan is an enormously versatile polymer from a chemical perspective as it can be easily modified at various positions, and the cationic properties allow chitosan to form electrostatic complexes or multilayered structures with other negatively charged synthetic or natural polymers. Chitosan

exhibits favorable characteristics such as biocompatibility, biodegradability, nontoxicity, and a low allergenic potential. Moreover, many studies reported that chitosan has antimicrobial, antitumor, and antioxidant activities, and in many cases, these properties appear to be maintained or even increased after chemical modification. The large variety of chemical modifications that have been developed to derivatize chitosan prove that it is not only possible to increase chitosan solubility at a pH required for the respective applications but also conceivable to develop derivatives with specific characteristic for the safe and reliable use in different technical and biomedical applications. In Chap. 14, we provide an overview on the plethora of promising developments and already existing applications of chitosan-based materials in water treatment, food industry, plant protection, and medical therapies.

Acknowledgments The author is grateful to Subbaratnam Muthukrishnan and Ephraim Cohen for critically reading the manuscript.

References

Abbasian M, Jaymand M, Niroomand P, Farnoudian-Habibi A, Karaj-Abad SG (2017) Grafting of aniline derivatives onto chitosan and their applications for removal of reactive dyes from industrial effluents. Int J Biol Macromol 95:393–403

Abbasian M, Mahmoodzadeh F (2017) Synthesis of antibacterial silver–chitosan-modified bionanocomposites by RAFT polymerization and chemical reduction methods. J Elastomers Plast 49:173–193

Abdullah J, Ahmad M, Heng LY, Karuppiah N, Sidek H (2006) Chitosan-based tyrosinase optical phenol biosensor employing hybrid nafion/sol-gel silicate for MBTH immobilization. Talanta 70:527–532

Agbovi HK, Wilson LD (2018) Design of amphoteric chitosan flocculants for phosphate and turbidity removal in wastewater. Carbohydr Polym 189:360–370

Aghajari R, Azadbakht A (2018) Amplified detection of streptomycin using aptamer-conjugated palladium nanoparticles decorated on chitosan-carbon nanotube. Anal Biochem 547:57–65

Al-Mokaram AMAAA, Yahya R, Abdi MM, Mahmud HNME (2017) The development of non-enzymatic glucose biosensors based on electrochemically prepared polypyrrole-chitosan-titanium dioxide nanocomposite films. Nano 7:pii E129. https://doi.org/10.3390/nano7060129

Al-Remawi M, Elsayed A, Maghrabi I, Hamaidi M, Jaber N (2017) Chitosan/lecithin liposomal nanovesicles as an oral insulin delivery system. Pharm Dev Technol 22:390–398

Al-Sagheer F, Khalil K, Mahmoud H, Elassar AZ, Ibrahim E (2017) Chitosan-g-poly (4-acrylamidobenzenesulfonamide) copolymers: synthesis, characterization, and bioactivity. J Polym Res 24:230

Albrecht K, Bernkop-Schnurch A (2007) Thiomers: forms, functions and applications to nanomedicine. Nanomedicine 2:41–50

Aliramaji S, Zamanian A, Mozafari M (2017) Super-paramagnetic responsive silk fibroin/chitosan/magnetite scaffolds with tunable pore structures for bone tissue engineering applications. Mater Sci Eng C 70:736–744

Amorim CM, Couto AG, Netz DJA, de Freitas RA, Bresolin TMB (2010) Antioxidant idebenone-loaded nanoparticles based on chitosan and *N*-carboxymethylchitosan. Nanomedicine 6:745–752

An NT, Dung PL, Thien DT, Dong NT, Nhi TTY (2008) An improved method for synthesizing *N*, *N*′-dicarboxymethylchitosan. Carbohydr Polym 73:261–264

Anantha RK, Kota S (2016) An evaluation of the major factors influencing the removal of copper ions using the egg shell (*Dromaius novaehollandiae*): chitosan (*Agaricus bisporus*) composite. 3 Biotech 6:83. https://doi.org/10.1007/s13205-016-0381-2

Anghileri A, Lantto R, Kruus K, Arosio C, Freddi G (2007) Tyrosinase-catalyzed grafting of sericin peptides onto chitosan and production of protein-polysaccharide bioconjugates. J Biotechnol 127:508–519

Aoi K, Takasu A, Okada M (1994) Synthesis of novel chitin derivatives having poly(2-alkyl-2-oxazoline) side-chains. Macromol Chem Phys 195:3835–3844

Aoi K, Takasu A, Okada M, Imae T (1999) Synthesis and assembly of novel chitin derivatives having amphiphilic polyoxazoline block copolymer as a side chain. Macromol Chem Phys 200:1112–1120

Argüelles-Monal W, Lizardi-Mendoza J, Fernández-Quiroz D, Recillas-Mota M, Montiel-Herrera M (2018) Chitosan derivatives: introducing new functionalities with a controlled molecular architecture for innovative materials. Polymers 10:342. https://doi.org/10.3390/polym10030342

Arif M, Dong QJ, Raja MA, Zeenat S, Chi Z, Liu CG (2018) Development of novel pH-sensitive thiolated chitosan/PMLA nanoparticles for amoxicillin delivery to treat *Helicobacter pylori*. Mater Sci Eng C 83:17–24

Arjunan N, Singaravelu CM, Kulanthaivel J, Kandasamy J (2017) A potential photocatalytic, antimicrobial and anticancer activity of chitosan-copper nanocomposite. Int J Biol Macromol 104:1774–1782

Azevedo EP, Retarekar R, Raghavan ML, Kumar V (2013) Mechanical properties of cellulose: chitosan blends for potential use as a coronary artery bypass graft. J Biomater Sci Polym Ed 24:239–252

Azzam EM, Eshaq G, Rabie AM, Bakr AA, Abd-Elaal AA, El Metwally AE, Tawfik SM (2016) Preparation and characterization of chitosan-clay nanocomposites for the removal of cu(II) from aqueous solution. Int J Biol Macromol 89:507–517

Badhe RV, Nanda RK, Chejara DR, Choonara YE, Kumar P, du Toit LC, Pillay V (2015) Microwave-assisted facile synthesis of a new tri-block chitosan conjugate with improved mucoadhesion. Carbohydr Polym 130:213–221

Baghaie S, Khorasani MT, Zarrabi A, Moshtaghian J (2017) Wound healing properties of PVA/starch/chitosan hydrogel membranes with nano zinc oxide as antibacterial wound dressing material. J Biomater Sci Polym Ed 28:2220–2241

Baghdan E, Pinnapireddy SR, Strehlow B, Engelhardt KH, Schafer J, Bakowsky U (2018) Lipid coated chitosan-DNA nanoparticles for enhanced gene delivery. Int J Pharm 535:473–479

Bao H, Pan Y, Ping Y, Sahoo NG, Wu T, Li L, Li J, Gan LH (2011) Chitosan-functionalized graphene oxide as a nanocarrier for drug and gene delivery. Small 7:1569–1578

Bao J, Hou C, Chen M, Li J, Huo D, Yang M, Luo X, Lei Y (2015) Plant esterase-chitosan/gold nanoparticles-graphene nanosheet composite-based biosensor for the ultrasensitive detection of organophosphate pesticides. J Agric Food Chem 63:10319–10326

Bayramoglu G, Yilmaz M, Arica MY (2003) Affinity dye-ligand poly(hydroxyethyl methacrylate)/chitosan composite membrane for adsorption lysozyme and kinetic properties. Biochem Eng J 13:35–42

Beltrame A, Suchyta D, Abd Alraheam I, Mohammed A, Schoenfisch M, Walter R, Almeida ICS, Souza LC, Miguez PA (2018) Effect of phosphorylated chitosan on dentin erosion: an *in vitro* study. Caries Res 52:378–386

Benamer S, Mahlous M, Tahtat D, Nacer-Khodja A, Arabi M, Lounici H, Mameri N (2011) Radiation synthesis of chitosan beads grafted with acrylic acid for metal ions sorption. Radiat Phys Chem 80:1391–1397

Benediktsdottir BE, Gaware VS, Runarsson OV, Jonsdottir S, Jensen KJ, Masson M (2011) Synthesis of *N,N,N*-trimethyl chitosan homopolymer and highly substituted *N*-alkyl-*N*,*N*-dimethyl chitosan derivatives with the aid of di-*tert*-butyldimethylsilyl chitosan. Carbohydr Polym 86:1451–1460

Berkovich LA, Tsyurupa MP, Davankov VA (1983) The synthesis of crosslinked co-polymers of maleilated chitosan and acrylamide. J Polym Sci A 21:1281–1287

Bernkop-Schnurch A, Brandt UM, Clausen AE (1999) Synthesis and *in vitro* evaluation of chitosan-cysteine conjugates. Sci Pharm 67:197–208

Bernkop-Schnurch A, Hornof M, Zoidl T (2003) Thiolated polymers-thiomers: synthesis and *in vitro* evaluation of chitosan-2-iminothiolane conjugates. Int J Pharm 260:229–237

Beskardes IG, Demirtas TT, Durukan MD, Gumusderelioglu M (2015) Microwave-assisted fabrication of chitosan-hydroxyapatite superporous hydrogel composites as bone scaffolds. J Tissue Eng Regen Med 9:1233–1246

Bhattacharya A, Misra BN (2004) Grafting: a versatile means to modify polymers: techniques, factors and applications. Prog Polym Sci 29:767–814

Bhowmick A, Banerjee SL, Pramanik N, Jana P, Mitra T, Gnanamani A, Das M, Kundu PP (2018) Organically modified clay supported chitosan/hydroxyapatite-zinc oxide nanocomposites with enhanced mechanical and biological properties for the application in bone tissue engineering. Int J Biol Macromol 106:11–19

Bian F, Jia L, Yu W, Liu M (2009) Self-assembled micelles of N-phthaloylchitosan-g-polyvinylpyrrolidone for drug delivery. Carbohydr Polym 76:454–459

Bosman AW, Janssen HM, Meijer EW (1999) About dendrimers: structure, physical properties, and applications. Chem Rev 99:1665–1688

Bresolin JR, Largura M-CT, Dalri CC, Hoffer G, Rodrigues CA, Lucinda-Silva RM (2014) Spray-dried *O*-carboxymethyl chitosan as potential hydrophilic matrix tablet for sustained release of drug. Drug Dev Ind Pharm 40:503–510

Budnyak TM, Yanovska ES, Kichkiruk OY, Sternik D, Tertykh VA (2016) Natural minerals coated by biopolymer chitosan: synthesis, physicochemical, and adsorption properties. Nanoscale Res Lett 11:492. https://doi.org/10.1186/s11671-016-1696-y

Bueno CZ, Dias AM, de Sousa HJ, Braga ME, Moraes AM (2014) Control of the properties of porous chitosan-alginate membranes through the addition of different proportions of Pluronic F68. Mater Sci Eng C 44:117–125

Bugnicourt L, Ladavière C (2017) A close collaboration of chitosan with lipid colloidal carriers for drug delivery applications. J Control Release 256:121–140

Caddeo C, Nacher A, Diez-Sales O, Merino-Sanjuan M, Fadda AM, Manconi M (2014) Chitosan-xanthan gum microparticle-based oral tablet for colon-targeted and sustained delivery of quercetin. J Microencapsul 31:694–699

Cai H, Zhang ZP, Sun PC, He BL, Zhu XX (2005) Synthesis and characterization of thermo- and pH-sensitive hydrogels based on chitosan-grafted *N*-isopropylacrylamide via gamma-radiation. Radiat Phys Chem 74:26–30

Cai KY, Yao K, Cui Y, Lin S, Yang Z, Li X, Xie H, Qing T, Luo J (2002) Surface modification of poly (D,L-lactic acid) with chitosan and its effects on the culture of osteoblasts *in vitro*. J Biomed Mater Res 60:398–404

Campos EVR, Oliveira JL, Fraceto LF (2017) Poly(ethylene glycol) and cyclodextrin-grafted chitosan: from methodologies to preparation and potential biotechnological applications. Front Chem 5:93

Campos EVR, Proença PLF, Oliveira JL, Melville CC, Della Vechia JF, de Andrade DJ, Fraceto LF (2018) Chitosan nanoparticles functionalized with β-cyclodextrin: a promising carrier for botanical pesticides. Sci Rep 8:2067. https://doi.org/10.1038/s41598-018-20602-y

Caner H, Hasipoglu H, Yilmaz O, Yilmaz E (1998) Graft copolymerization of 4-vinylpyridine on to chitosan - I. By ceric ion initiation. Eur Polym J 34:493–497

Caner H, Yilmaz E, Yimaz O (2007) Synthesis, characterization and antibacterial activity of poly (*N*-vinylimidazole) grafted chitosan. Carbohydr Polym 69:318–325

Cao L, Zhang F, Wang Q, Wu X (2017) Fabrication of chitosan/graphene oxide polymer nanofiber and its biocompatibility for cartilage tissue engineering. Mater Sci Eng C 79:697–701

Cerchiara T, Abruzzo A, Parolin C, Vitali B, Bigucci F, Gallucci MC, Nicoletta FP, Luppi B (2016) Microparticles based on chitosan/carboxymethylcellulose polyelectrolyte complexes for colon delivery of vancomycin. Carbohydr Polym 143:124–130

Chaiyasan W, Srinivas SP, Tiyaboonchai W (2015) Crosslinked chitosan-dextran sulfate nanoparticle for improved topical ocular drug delivery. Mol Vis 21:1224–1234
Chang J, Lee YS, Fang SJ, Park DJ, Choi YL (2013) Hydrolysis of isoflavone glycoside by immobilization of beta-glucosidase on a chitosan-carbon in two-phase system. Int J Biol Macromol 61:465–470
Chang MY, Juang RS (2004) Adsorption of tannic acid, humic acid, and dyes from water using the composite of chitosan and activated clay. J Colloid Interface Sci 278:18–25
Chen H, Huang J, Yu J, Liu S, Gu P (2011) Electrospun chitosan-graft-poly (epsilon -caprolactone)/poly (epsilon-caprolactone) cationic nanofibrous mats as potential scaffolds for skin tissue engineering. Int J Biol Macromol 48:13–19
Chen L, Tian Z, Du Y (2004a) Synthesis and pH sensitivity of carboxymethyl chitosan-based polyampholyte hydrogels for protein carrier matrices. Biomaterials 25:3725–3732
Chen S-C, Wu Y-C, Mi F-L, Lin Y-H, Yu L-C, Sung H-W (2004b) A novel pH-sensitive hydrogel composed of N,O-carboxymethyl chitosan and alginate cross-linked by genipin for protein drug delivery. J Control Release 96:285–300
Chen T, Kumar G, Harris MT, Smith PJ, Payne GF (2000) Enzymatic grafting of hexyloxyphenol onto chitosan to alter surface and rheological properties. Biotechnol Bioeng 70:564–573
Chen X-G, Park H-J (2003) Chemical characteristics of O-carboxymethyl chitosans related to the preparation conditions. Carbohydr Polym 53:355–359
Chen X, Chen X, Li C, Liu Y, Du Z, Xu S, Li L, Zhang M, Wang T (2008) Electrocatalytic activity of horseradish peroxidase/chitosan/carbon microsphere microbiocomposites to hydrogen peroxide. Talanta 77:37–41
Chen Y, Ye Y, Li R, Guo Y, Tan H (2013) Synthesis of chitosan 6-OH immobilized cyclodextrin derivates via click chemistry. Fiber Polym 14:1058–1065
Chen Y, Ye Y, Wang L, Guo Y, Tan H (2012) Synthesis of chitosan C6-substituted cyclodextrin derivatives with tosyl-chitin as the intermediate precursor. J Appl Polym Sci 125:E378–E383
Cheng D, Xia H, Chan HS (2005) Synthesis and characterization of surface-functionalized conducting polyaniline-chitosan nanocomposite. J Nanosci Nanotechnol 5:466–473
Cheng S, Zhao H, Xu Y, Yang Y, Lv X, Wu P, Li X (2014) Inhibition of influenza virus infection with chitosan-sialyloligosaccharides ionic complex. Carbohydr Polym 107:132–137
Chethan PD, Vishalakshi B (2013) Synthesis of ethylenediamine modified chitosan and evaluation for removal of divalent metal ions. Carbohydr Polym 97:530–536
Chitkara D, Shikanov A, Kumar N, Domb AJ (2006) Biodegradable injectable in situ depot-forming drug delivery systems. Macromol Biosci 6:977–990
Choi B, Cui ZK, Kim S, Fan J, Wu BM, Lee M (2015) Glutamine-chitosan modified calcium phosphate nanoparticles for efficient siRNA delivery and osteogenic differentiation. J Mater Chem B 3:6448–6455
Cohen E, Joseph T, Kahana F, Magdassi S (2003) Photostabilization of an entomopathogenic fungus using composite clay matrices. Photochem Photobiol 77:180–185
Curti E, de Britto D, Campana-Filho SP (2003) Methylation of chitosan with iodomethane: effect of reaction conditions on chemoselectivity and degree of substitution. Macromol Biosci 3:571–576
Cushing IB, Davis RV, Kratovil EJ, Maccorquodale DW (1954) The sulfation of chitin in chlorosulfonic acid and dichloroethane. J Am Chem Soc 76:4590–4591
Dadhich P, Das B, Dhara S (2015) Microwave assisted rapid synthesis of *N*-methylene phosphonic chitosan via Mannich-type reaction. Carbohydr Polym 133:345–352
Daly WH, Manuszak-Guerrini MA (2001) Biocidal chitosan derivatives for cosmetics and pharmaceuticals. USA Patent 6306835
de Britto D, Assis OBG (2007) A novel method for obtaining a quaternary salt of chitosan. Carbohydr Polym 69:305–310
Deepthi S, Venkatesan J, Kim SK, Bumgardner JD, Jayakumar R (2016) An overview of chitin or chitosan/nano ceramic composite scaffolds for bone tissue engineering. Int J Biol Macromol 93:1338–1353

Dehghan GMH, Marzuka M (2014) Lyophilized chitosan/xanthan polyelectrolyte complex based mucoadhesive inserts for nasal delivery of promethazine hydrochloride. Iranian J Pharm Res 13:769–784

Delair T (2011) Colloidal polyelectrolyte complexes of chitosan and dextran sulfate towards versatile nanocarriers of bioactive molecules. Eur J Pharm Biopharm 78:10–18

Demolliens A, Boucher C, Durocher Y, Jolicoeur M, Buschmann MD, De Crescenzo G (2008) Tyrosinase-catalyzed synthesis of a universal coil-chitosan bioconjugate for protein immobilization. Bioconjug Chem 19:1849–1854

Denuziere A, Ferrier D, Damour O, Domard A (1998) Chitosan-chondroitin sulfate and chitosan-hyaluronate polyelectrolyte complexes: biological properties. Biomaterials 19:1275–1285

Dhavale D, Henry JE (2012) Evaluation of sialic acid-analogs for the attenuation of amyloid-beta toxicity. Biochim Biophys Acta 1820:1475–1480

Dincer A, Becerik S, Aydemir T (2012) Immobilization of tyrosinase on chitosan-clay composite beads. Int J Biol Macromol 50:815–820

Dinescu S, Dinescu S, Ionita M, Pandele AM, Galateanu B, Iovu H, Ardelean A, Costache M, Hermenean A (2014) *In vitro* cytocompatibility evaluation of chitosan/graphene oxide 3D scaffold composites designed for bone tissue engineering. Biomed Mater Eng 24:2249–2256

Djelad A, Morsli A, Robitzer M, Bengueddach A, di Renzo F, Quignard F (2016) Sorption of cu (II) ions on chitosan-zeolite X composites: impact of gelling and drying conditions. Molecules 21:E109. https://doi.org/10.3390/molecules21010109

Domard A, Gey C, Rinaudo M, Terrassin C (1987) C-13 and H-1-NMR spectroscopy of chitosan and *N*-trimethyl chloride derivatives. Int J Biol Macromol 9:233–237

Domard A, Rinaudo M, Terrassin C (1986) New method for the quaternization of chitosan. Int J Biol Macromol 8:105–107

Don TM, King CF, Chiu WY (2002a) Preparation of chitosan-graft-poly(vinyl acetate) copolymers and their adsorption of copper ion. Polym J 34:418–425

Don TM, King CF, Chiu WY (2002b) Synthesis and properties of chitosan-modified poly(vinyl acetate). J Appl Polym Sci 86:3057–3063

Dong H, Li F, Li J, Li Y (2012) Characterizations of blend gels of carboxymethylated polysaccharides and their use for the controlled release of herbicide. J Macromol Sci A 49:235–241

Dong Y-m, Mao W, H-w W, Y-q Z, Bi D-x, L-l Y, Ge Q, Z-q O (2006a) Electron microscopic studies on planar texture and disclination of cholesteric mesophases in acyloyl chitosan/acrylic acid composite films. Carbohydr Polym 65:42–48

Dong Y-m, Mao W, H-w W, Y-q Z, Li X-j, Bi D-x, L-l Y, Ge Q, Fang X (2006b) Measurement of critical concentration for mesophase formation of chitosan derivatives in both aqueous and organic solutions. Polym Int 55:1444–1449

Drozd NN, Sher AI, Makarov VA, Galbraikh LS, Vikhoreva GA, Gorbachiova IN (2001) Comparison of antithrombin activity of the polysulphate chitosan derivatives in *in vivo* and *in vitro* system. Thromb Res 102:445–455

Duan K, Zhang X, Tang X, Yu J, Liu S, Wang D, Li Y, Huang J (2010) Fabrication of cationic nanomicelle from chitosan-graft-polycaprolactone as the carrier of 7-ethyl-10-hydroxy-camptothecin. Colloid Surf B 76:475–482

Duchêne D, Bochot A (2016) Thirty years with cyclodextrins. Int J Pharm 514:58–72

Duffy C, O'Riordan D, O'Sullivan M, Jacquier JC (2018) *In vitro* evaluation of chitosan copper chelate gels as a multimicronutrient feed additive for cattle. J Sci Food Agric 98:4177–4183

Duri S, Tran CD (2013) Supramolecular composite materials from cellulose, chitosan and cyclodextrin: facile preparation and their selective inclusion complex formation with endocrine disruptors. Langmuir 29:5037–5049

Eivazy P, Atyabi F, Jadidi-Niaragh F, Aghebati Maleki L, Miahipour A, Abdolalizadeh J, Yousefi M (2017) The impact of the codelivery of drug-siRNA by trimethyl chitosan nanoparticles on the efficacy of chemotherapy for metastatic breast cancer cell line (MDA-MB-231). Artif Cells Nanomed Biotechnol 45:889–896

El-Kamel A, Sokar M, Naggar V, Al Gamal S (2002) Chitosan and sodium alginate-based bioadhesive vaginal tablets. AAPS PharmSci 4:E44. https://doi.org/10.1208/ps040444
El-Tahlawy K, Hudson SM (2001) Graft copolymerization of hydroxyethyl methacrylate onto chitosan. J Appl Polym Sci 82:683–702
El-Tahlawy KF, El-Rafie SM, Aly AS (2006) Preparation and application of chitosan/poly (methacrylic acid) graft copolymer. Carbohydr Polym 66:176–183
El Badawy M, Taktak NEM, Awad OM, Elfiki SA, Abou El-Ela NE (2016) Evaluation of released malathion and spinosad from chitosan/alginate/gelatin capsules against *Culex pipiens* larvae. Res Rep Trop Med 7:23–38
Elsabee MZ, Morsi RE, Al-Sabagh AM (2009) Surface active properties of chitosan and its derivatives. Colloids Surf B: Biointerfaces 74:1–16
Erdem A, Muti M, Karadeniz H, Congur G, Canavar E (2012) Electrochemical monitoring of indicator-free DNA hybridization by carbon nanotubes-chitosan modified disposable graphite sensors. Colloids Surf B: Biointerfaces 95:222–228
Fan H, Wang L, Zhao K, Li N, Shi Z, Ge Z, Jin Z (2010) Fabrication, mechanical properties, and biocompatibility of graphene-reinforced chitosan composites. Biomacromolecules 11:2345–2351
Fartas FM, Abdullah J, Yusof NA, Sulaiman Y, Saiman MI (2017) Biosensor based on tyrosinase immobilized on graphene-decorated gold nanoparticle/chitosan for phenolic detection in aqueous. Sensors 17. https://doi.org/10.3390/s17051132
Feng B-H, Peng L-F (2012) Synthesis and characterization of carboxymethyl chitosan carrying ricinoleic functions as an emulsifier for azadirachtin. Carbohydr Polym 88:576–582
Feng H, Dong CM (2007) Synthesis and characterization of phthaloyl-chitosan-g-poly(L-lactide) using an organic catalyst. Carbohydr Polym 70:258–264
Ferrero F, Periolatto M, Vineis C, Varesano A (2014) Chitosan coated cotton gauze for antibacterial water filtration. Carbohydr Polym 103:207–212
Fonseca-Santos B, Chorilli M (2017) An overview of carboxymethyl derivatives of chitosan: their use as biomaterials and drug delivery systems. Mater Sci Eng C 77:1349–1362
Freddi G, Anghileri A, Sampaio S, Buchert J, Monti P, Taddei P (2006) Tyrosinase-catalyzed modification of Bombyx mori silk fibroin: grafting of chitosan under heterogeneous reaction conditions. J Biotechnol 125:281–294
Gamzazade A, Sklyar A, Nasibov S, Sushkov I, Shashkov A, Knirel Y (1997) Structural features of sulfated chitosans. Carbohydr Polym 34:113–116
Gao X, Zhang Y, Wu Q, Chen H, Chen Z, Lin X (2011) One step electrochemically deposited nanocomposite film of chitosan-carbon nanotubes-gold nanoparticles for carcinoembryonic antigen immunosensor application. Talanta 85:1980–1985
Ge HC, Luo DK (2005) Preparation of carboxymethyl chitosan in aqueous solution under microwave irradiation. Carbohydr Res 340:1351–1356
Gomes S, Rodrigues G, Martins G, Henriques C, Silva JC (2017) Evaluation of nanofibrous scaffolds obtained from blends of chitosan, gelatin and polycaprolactone for skin tissue engineering. Int J Biol Macromol 102:1174–1185
Gong M, Wang YB, Li M, Hu BH, Gong YK (2011) Fabrication and hemocompatibility of cell outer membrane mimetic surfaces on chitosan by layer by layer assembly with polyanion bearing phosphorylcholine groups. Colloids Surf B: Biointerfaces 85:48–55
Gopal Reddi MR, Gomathi T, Saranya M, Sudha PN (2017) Adsorption and kinetic studies on the removal of chromium and copper onto chitosan-g-maliec anhydride-g-ethylene dimethacrylate. Int J Biol Macromol 104:1578–1585
Grabnar PA, Kristl J (2010) Physicochemical characterization of protein-loaded pectin-chitosan nanoparticles prepared by polyelectrolyte complexation. Pharmazie 65:851–852
Grant J, Blicker M, Piquette-Miller M, Allen C (2005) Hybrid films from blends of chitosan and egg phosphatidylcholine for localized delivery of paclitaxel. J Pharm Sci 94:1512–1527
Grant J, Cho J, Allen C (2006) Self-assembly and physicochemical and rheological properties of a polysaccharide-surfactant system formed from the cationic biopolymer chitosan and nonionic sorbitan esters. Langmuir 22:4327–4335

Gu C, Le V, Lang M, Liu J (2014) Preparation of polysaccharide derivates chitosan-graft-poly (varepsilon-caprolactone) amphiphilic copolymer micelles for 5-fluorouracil drug delivery. Colloids Surf B: Biointerfaces 116:745–750

Guerra ICD, de Oliveira PDL, de Souza Pontes AL, ASSC L, Tavares JF, Barbosa-Filho JM, Madruga MS, de Souza EL (2015) Coatings comprising chitosan and Mentha piperita L. or Mentha x villosa Huds essential oils to prevent common postharvest mold infections and maintain the quality of cherry tomato fruit. Int J Food Microbiol 214:168–178

Gullon B, Montenegro MI, Ruiz-Matute AI, Cardelle-Cobas A, Corzo N, Pintado ME (2016) Synthesis, optimization and structural characterization of a chitosan-glucose derivative obtained by the Maillard reaction. Carbohydr Polym 137:382–389

Gupta A, Chauhan VS, Sankararamakrishnan N (2009) Preparation and evaluation of iron-chitosan composites for removal of as(III) and as(V) from arsenic contaminated real life groundwater. Water Res 43:3862–3870

Gupta PK, Asthana S, Jaiswal AK, Kumar V, Verma AK, Shukla P, Dwivedi P, Dube A, Mishra PR (2014) Exploitation of lectinized lipo-polymerosome encapsulated amphotericin B to target macrophages for effective chemotherapy of visceral leishmaniasis. Bioconjug Chem 25:1091–1102

Guzman-Villanueva D, El-Sherbiny IM, Vlassov AV, Herrera-Ruiz D, Smyth HD (2014) Enhanced cellular uptake and gene silencing activity of siRNA molecules mediated by chitosan-derivative nanocomplexes. Int J Pharm 473:579–590

Hagiwara K, Kuribayashi Y, Iwai H, Azuma I, Tokura S, Ikuta K, Ishihara C (1999) A sulfated chitin inhibits hemagglutination by *Theileria sergenti* merozoites. Carbohydr Polym 39:245–248

Hamman JH, Kotze AF (2001) Effect of the type of base and number of reaction steps on the degree of quaternization and molecular weight of *N*-trimethyl chitosan chloride. Drug Dev Ind Pharm 27:373–380

Han E, Yang Y, He Z, Cai J, Zhang X, Dong X (2015) Development of tyrosinase biosensor based on quantum dots/chitosan nanocomposite for detection of phenolic compounds. Anal Biochem 486:102–106

Hasiploglu HN, Yilmaz E, Yilmaz O, Caner H (2005) Preparation and characterization of maleic acid grafted chitosan. Int J Polym Anal Charact 10:313–327

Hayashi Y, Yamada S, Yanagi Guchi K, Koyama Z, Ikeda T (2012) Chitosan and fish collagen as biomaterials for regenerative medicine. Adv Food Nutr Res 65:107–120

He G, Zhu C, Ye S, Cai W, Yin Y, Zheng H, Yi Y (2016) Preparation and properties of novel hydrogel based on chitosan modified by poly(amidoamine) dendrimer. Int J Biol Macromol 91:828–837

Heras A, Rodriguez NM, Ramos VM, Agullo E (2001) *N*-methylene phosphonic chitosan: a novel soluble derivative. Carbohydr Polym 44:1–8

Hermenean A, Codreanu A, Herman H, Balta C, Rosu M, Mihali CV, Ivan A, Dinescu S, Ionita M, Costache M (2017) Chitosan-graphene oxide 3D scaffolds as promising tools for bone regeneration in critical-size mouse calvarial defects. Sci Rep 7:16641

Hernandez-Ibanez N, Garcia-Cruz L, Montiel V, Foster CW, Banks CE, Iniesta J (2016) Electrochemical lactate biosensor based upon chitosan/carbon nanotubes modified screen-printed graphite electrodes for the determination of lactate in embryonic cell cultures. Biosens Bioelectron 77:1168–1174

Hirano S, Kinugawa J (1986) Effect of sulfated derivatives of chitosan on lipoprotein-lipase activity of rabbit plasma after their intravenous-injection. Carbohydr Res 150:295–299

Hirano S, Tanaka Y, Hasegawa M, Tobetto K, Nishioka A (1985) Effect of sulfated derivatives of chitosan on some blood coagulant factors. Carbohydr Res 137:205–215

Holappa J, Hjálmarsdóttir M, Másson M, Rúnarsson Ö, Asplund T, Soininene P, Nevalainen T, Järvinen T (2006a) Antimicrobial activity of chitosan *N*-betainates. Carbohydr Polym 65:114–118

Holappa J, Nevalainen T, Safin R, Soininen P, Asplund T, Luttikhedde T, Másson M, Järvinen T (2006b) Novel water-soluble quaternary piperazine derivatives of chitosan: synthesis and characterization. Macromol Biosci 6:139–144

Holappa J et al (2004) Synthesis and characterization of chitosan *N*-betainates having various degrees of substitution. Macromolecules 37:2784–2789

Holappa J, Nevalainen T, Soininen P, Masson M, Jarvinen T (2006c) Synthesis of novel quaternary chitosan derivatives via *N*-chloroacyl-6-O-triphenylmethylchitosans. Biomacromolecules 7:407–410

Holme KR, Perlin AS (1997) Chitosan *N*-sulfate. A water-soluble polyelectrolyte. Carbohydr Res 302:7–12

Hong YJ, Kim JC (2011) Egg phosphatidylcholine liposomes incorporating hydrophobically modified chitosan: pH-sensitive release. J Nanosci Nanotechnol 11:204–209

Horton D, Just EK (1973) Preparation from chitin of (1-4)-2-amino-2-deoxy-beta-D-glucopyranuronan and its 2-sulfoamino analog having blood anticoagulant properties. Carbohydr Res 29:173–179

Hosseinzadeh H, Ramin S (2018) Effective removal of copper from aqueous solutions by modified magnetic chitosan/graphene oxide nanocomposites. Int J Biol Macromol 113:859–868

Hsu SC, Don TM, Chiu WY (2002) Synthesis of chitosan-modified poly(methyl methacrylate) by emulsion polymerization. J Appl Polym Sci 86:3047–3056

Hu FQ, Ren GF, Yuan H, Du YZ, Zeng S (2006a) Shell cross-linked stearic acid grafted chitosan oligosaccharide self-aggregated micelles for controlled release of paclitaxel. Colloids Surf B: Biointerfaces 50:97–103

Hu FQ, Zhao MD, Yuan H, You J, Du YZ, Zeng S (2006b) A novel chitosan oligosaccharide-stearic acid micelles for gene delivery: properties and *in vitro* transfection studies. Int J Pharm 315:158–166

Huacai G, Wan P, Dengke L (2006) Graft copolymerization of chitosan with acrylic acid under microwave irradiation and its water absorbency. Carbohydr Polym 66:372–378

Huang M, Shen X, Sheng Y, Fang Y (2005) Study of graft copolymerization of *N*-maleamic acid-chitosan and butyl acrylate by gamma-ray irradiation. Int J Biol Macromol 36:98–102

Huang S, Wang J, Zhang Y, Yu Z, Qi C (2016) Quaternized carboxymethyl chitosan-based silver nanoparticles hybrid: microwave-assisted synthesis, characterization and antibacterial activity. Nano 6. https://doi.org/10.3390/nano6060118

Ignatova M, Manolova N, Rashkov I (2013) Electrospun antibacterial chitosan-based fibers. Macromol Biosci 13:860–872

Ishihara C, Shimakawa S, Tsuji M, Arikawa J, Tokura S (1995) A sulfated chitin, Scm-chitin-iii, inhibits the clearance of human erythrocytes from the blood-circulation in erythrocyte-transfused scid mice. Immunopharmacology 29:65–71

Ishihara M, Nguyen VQ, Mori Y, Nakamura S, Hattori H (2015) Adsorption of silver nanoparticles onto different surface structures of chitin/chitosan and correlations with antimicrobial activities. Int J Mol Sci 16:13973–13988

Ishihara M et al (2006) Chitosan hydrogel as a drug delivery carrier to control angiogenesis. J Artif Organs 9:8–16

Jana S, Sen KK (2017) Chitosan - locust bean gum interpenetrating polymeric network nanocomposites for delivery of aceclofenac. Int J Biol Macromol 102:878–884

Jayakumar R, Nwe N, Tokura S, Tamura H (2007a) Sulfated chitin and chitosan as novel biomaterials. Int J Biol Macromol 40:175–181

Jayakumar R, Prabaharan M, Reis RL, Mano JF (2005) Graft copolymerized chitosan—present status and applications. Carbohydr Polym 62:142–158

Jayakumar R, Reis RL, Mano JF (2006) Phosphorous containing chitosan beads for controlled oral drug delivery. J Bioact Compat Polym 21:327–340

Jayakumar R, Reis RL, Mano JF (2007b) Synthesis and characterization of *N*-methylenephenyl phosphonic chitosan. J Macromol Sci A 44:271–275

Jayakumar R, Selvamurugan N, Nair SV, Tokura S, Tamura H (2008) Preparative methods of phosphorylated chitin and chitosan - An overview. Int J Biol Macromol 43:221–225

Jayakumar R, Tamura H (2006) New synthesis procedure of phosphoryl chitin. Paper presented at the 55th SPSJ Annual Meeting, Nagoya, Japan

Jeong SI, Park SC, Park SJ, Kim EJ, Heo H, Park JS, Gwon HJ, Lim YM, Jang MK (2018) One-step synthesis of gene carrier via gamma irradiation and its application in tumor gene therapy. Intl J Nanomed 13:525–536

Jeong Y-I, Jin SG, Kim IY, Pei J, Wen M, Jung TY, Moon KS, Jung S (2010) Doxorubicin-incorporated nanoparticles composed of poly(ethylene glycol)-grafted carboxymethyl chitosan and antitumor activity against glioma cells *in vitro*. Colloids Surf B: Biointerfaces 79:149–155

Ji J, Hao S, Dong J, Wu D, Yang B, Xu Y (2012) Preparation, evaluation, and *in vitro* release study of *O*-carboxymethyl chitosan nanoparticles loaded with gentamicin and salicylic acid. J Appl Polym Sci 123:1684–1689

Jiang D, Zhang X, Yu D, Xiao Y, Wang T, Su Z, Liu Y, Zhang N (2017) Tumor-microenvironment relaxivity-changeable gd-loaded poly(l-lysine)/carboxymethyl chitosan nanoparticles as cancer-recognizable magnetic resonance imaging contrast agents. J Biomed Nanotechnol 13:243–254

Jiang HL et al (2008) Galactosylated poly(ethylene glycol)-chitosan-graft-polyethylenimine as a gene carrier for hepatocyte-targeting. J Control Release 131:150–157

Jin Y-H, Hu HY, Qiao MX, Zhu J, Qi JW, Hu CJ, Zhang Q, Chen DW (2012) pH-sensitive chitosan-derived nanoparticles as doxorubicin carriers for effective anti-tumor activity: preparation and *in vitro* evaluation. Colloids Surf B: Biointerfaces 94:184–191

Jirimali HD, Nagarale RK, Saravanakumar D, Lee JM, Shin W (2013) Hydroquinone modified chitosan/carbon film electrode for the selective detection of ascorbic acid. Carbohydr Polym 92:641–644

Joshi JM, Sinha VK (2007) Ceric ammonium nitrate induced grafting of polyacrylamide onto carboxymethyl chitosan. Carbohydr Polym 67:427–435

Jung B-O, Kim C-H, Choi K-S, Lee YM, Kim J-J (1999) Preparation of amphiphilic chitosan and their antimicrobial activities. J Appl Polym Sci 72:1713–1719

Justin R, Chen B (2014) Characterisation and drug release performance of biodegradable chitosan-graphene oxide nanocomposites. Carbohydr Polym 103:70–80

Kaderli S, Boulocher C, Pillet E, Watrelot-Virieux D, Rougemont AL, Roger T, Viguier E, Gurny R, Scapozza L, Jordan O (2015) A novel biocompatible hyaluronic acid-chitosan hybrid hydrogel for osteoarthrosis therapy. Int J Pharm 483:158–168

Kafedjiiski K, Foger F, Werle M, Bernkop-Schnurch B (2005a) Synthesis and *in vitro* evaluation of a novel chitosan-glutathione conjugate. Pharm Res 22:1480–1488

Kafedjiiski K, Krauland AH, Hoffer MH, Bernkop-Schnurch A (2005b) Synthesis and *in vitro* evaluation of a novel thiolated chitosan. Biomaterials 26:819–826

Kang HM, Cai YL, Liu PS (2006) Synthesis, characterization and thermal sensitivity of chitosan-based graft copolymers. Carbohydr Res 341:2851–2857

Kar S, Kaur T, Thirugnanam A (2016) Microwave-assisted synthesis of porous chitosan-modified montmorillonite-hydroxyapatite composite scaffolds. Int J Biol Macromol 82:628–636

Karabiyik Acar O, Kayitmazer AB, Torun Kose G (2018) Hyaluronic acid/chitosan coacervate-based scaffolds. Biomacromolecules 19:1198–1211

Kast CE, Bernkop-Schnurch A (2001) Thiolated polymers - thiomers: development and *in vitro* evaluation of chitosan-thioglycolic acid conjugates. Biomaterials 22:2345–2352

Kato Y, Onishi H, Machida Y (2000a) Biological fate of highly-succinylated *N*-succinyl-chitosan and antitumor characteristics of its water-soluble conjugate with mitomycin C at i.V. And i.P. Administration into tumor-bearing mice. Biol Pharm Bull 23:1497–1503

Kato Y, Onishi H, Machida Y (2000b) Evaluation of *N*-succinyl-chitosan as a systemic long-circulating polymer. Biomaterials 21:1579–1585

Kato Y, Onishi H, Machida Y (2001a) Biological characteristics of lactosaminated *N*-succinyl-chitosan as a liver-specific drug carrier in mice. J Control Release 70:295–307

Kato Y, Onishi H, Machida Y (2001b) Lactosaminated and intact *N*-succinyl-chitosans as drug carriers in liver metastasis. Int J Pharm 226:93–106

Kato Y, Onishi H, Machida Y (2002) Efficacy of lactosaminated and intact *N*-succinylchitosan-mitomycin C conjugates against M5076 liver metastatic cancer. J Pharm Pharmacol 54:529–537

Katti KS, Katti DR, Dash R (2008) Synthesis and characterization of a novel chitosan/montmorillonite/hydroxyapatite nanocomposite for bone tissue engineering. Biomed Mater 3:034122

Khalil KD, Al-Matar HM (2013) Chitosan based heterogeneous catalyses: chitosan-grafted-poly (4-vinylpyridne) as an efficient catalyst for Michael additions and alkylpyridazinyl carbonitrile oxidation. Molecules 18:5288–5305

Kim CH, Choi KS (2002) Synthesis and antibacterial activity of quaternized chitosan derivatives having different methylene spacers. J Ind Eng Chem 8:71–76

Kim JH, Kim SB, Lee SH, Choi JW (2018) Laboratory and pilot-scale field experiments for application of iron oxide nanoparticle-loaded chitosan composites to phosphate removal from natural water. Environ Technol 39:770–779

Kim SY, Cho SM, Lee YM, Kim SJ (2000) Thermo- and pH-responsive behaviors of graft copolymer and blend based on chitosan and *N*-isopropylacrylamide. J Appl Polym Sci 78:1381–1391

Klaykruayat B, Siralertmukul K, Srikulkit K (2010) Chemical modification of chitosan with cationic hyperbranched dendritic polyamidoamine and its antimicrobial activity on cotton fabric. Carbohydr Polym 80:197–207

Kojima K, Yoshikuni M, Suzuki T (1979) Tributylborane-initiated grafting of methyl-methacrylate onto chitin. J Appl Polym Sci 24:1587–1593

Kong X, Wang J, Cao L, Yu Y, Liu C (2014) Enhanced osteogenesis of bone morphology protein-2 in 2-*N*,6-*O*-sulfated chitosan immobilized PLGA scaffolds. Colloids Surf B: Biointerfaces 122:359–367

Kratz G, Arnander C, Swedenborg J, Back M, Falk C, Gouda I, Larm O (1997) Heparin-chitosan complexes stimulate wound healing in human skin. Scand J Plast Reconstr Surg Hand Surg 31:119–123

Kudyshkin VO, Futoryanskaya AM, Milusheva RY, Kareva ND, Rashidova SS (2014) Graft copolymerization of *N*-vinyl caprolactame onto chitosan. Intl J Mater Chem 3:65–68

Kumar D, Pandey J, Kumar P (2018) Synthesis and characterization of modified chitosan via microwave route for novel antibacterial application. Int J Biol Macromol 107:1388–1394

Kumar G, Smith PJ, Payne GF (1999) Enzymatic grafting of a natural product onto chitosan to confer water solubility under basic conditions. Biotechnol Bioeng 63:154–165

Kumar IA, Viswanathan N (2017) Development of multivalent metal ions imprinted chitosan biocomposites for phosphate sorption. Int J Biol Macromol 104:1539–1547

Kuralay F, Vural T, Bayram C, Denkbas EB, Abaci S (2011) Carbon nanotube-chitosan modified disposable pencil graphite electrode for vitamin B12 analysis. Colloids Surf B: Biointerfaces 87:18–22

Kurita K (2006) Chitin and chitosan: functional biopolymers from marine crustaceans. Mar Biotechnol 8:203–226

Kurita K, Akao H, Yang J, Shimojoh M (2003) Nonnatural branched polysaccharides: synthesis and properties of chitin and chitosan having disaccharide maltose branches. Biomacromolecules 4:1264–1268

Kurita K, Hirakawa M, Kikuchi S, Yamanaka H, Yang J (2004) Trimethylsilylation of chitosan and some properties of the product. Carbohydr Polym 56:333–337

Kurita Y, Isogai A (2012) *N*-Alkylations of chitosan promoted with sodium hydrogen carbonate under aqueous conditions. Int J Biol Macromol 50:741–746

Lacerda L, Parize AL, Fávere V, Laranjeira MCM, Stulzer HK (2014) Development and evaluation of pH-sensitive sodium alginate/chitosan microparticles containing the antituberculosis drug rifampicin. Mater Sci Eng C 39:161–167

Lagos A, Reyes J (1988) Grafting onto chitosan.1. Graft-copolymerization of methyl-methacrylate onto chitosan with Fenton reagent (Fe^{2+}-H_2O_2) as a redox initiator. J Polym Sci A Polym Chem 26:985–991

Lau C, Cooney MJ, Atanassov P (2008) Conductive macroporous composite chitosan-carbon nanotube scaffolds. Langmuir 24:7004–7010

Le Tien C, Lacroix M, Ispas-Szabo P, Mateescu MA (2003) *N*-acylated chitosan: hydrophobic matrices for controlled drug release. J Control Release 93:1–13

Lee C-M, Jeong HJ, Kim SL, Kim EM, Kim DW, Lim ST, Jang KY, Jeong YY, Nah JW, Sohn MH (2009) SPION-loaded chitosan–linoleic acid nanoparticles to target hepatocytes. Int J Pharm 371:163–169

Lefay C et al (2013) Heterogeneous modification of chitosan via nitroxide-mediated polymerization. Polym Chem 4:322–328

Leng ZH, Zhuang QF, Li YC, He Z, Chen Z, Huang SP, Jia HY, Zhou JW, Liu Y, Du LB (2013) Polyamidoamine dendrimer conjugated chitosan nanoparticles for the delivery of methotrexate. Carbohydr Polym 98:1173–1178

Li G, Huang J, Chen T, Wang X, Zhang H, Chen Q (2017a) Insight into the interaction between chitosan and bovine serum albumin. Carbohydr Polym 176:75–82

Li G, Xiao Q, Zhang L, Zhao Y, Yang Y (2017b) Nerve growth factor loaded heparin/chitosan scaffolds for accelerating peripheral nerve regeneration. Carbohydr Polym 171:39–49

Li GF, Wang JC, Feng XM, Liu ZD, Jiang CY, Yang JD (2015a) Preparation and testing of quaternized chitosan nanoparticles as gene delivery vehicles. Appl Biochem Biotechnol 175:3244–3257

Li J, Jiang B, Liu Y, Qiu C, Hu J, Qian G, Guo W, Ngo HH (2017c) Preparation and adsorption properties of magnetic chitosan composite adsorbent for Cu^{2+} removal. J Clean Prod 158:51–58. https://doi.org/10.1016/j.jclepro.2017.04.156

Li J, Wang Q, Gu Y, Zhu Y, Chen L, Chen Y (2017d) Production of composite scaffold containing silk fibroin, chitosan, and gelatin for 3d cell culture and bone tissue regeneration. Med Sci Monit 23:5311–5320

Li J, Yao J, Li Y, Shao Y (2012a) Controlled release and retarded leaching of pesticides by encapsulating in carboxymethyl chitosan/bentonite composite gel. J Environ Sci Health B 47:795–803

Li K, Xing R, Liu S, Qin Y, Meng X, Li P (2012b) Microwave-assisted degradation of chitosan for a possible use in inhibiting crop pathogenic fungi. Int J Biol Macromol 51:767–773

Li L, Zhao F, Zhao B, Zhang J, Li C, Qiao R (2015b) Chitosan grafted with phosphorylcholine and macrocyclic polyamine as an effective gene delivery vector: preparation, characterization and *in vitro* transfection. Macromol Biosci 15:912–926

Li N, Bai R, Liu C (2005) Enhanced and selective adsorption of mercury ions on chitosan beads grafted with polyacrylamide via surface-initiated atom transfer radical polymerization. Langmuir 21:11780–11787

Li Y, Ai L, Yokoyama W, Shoemaker CF, Wei D, Ma J, Zhong F (2013) Properties of chitosan-microencapsulated orange oil prepared by spray-drying and its stability to detergents. J Agric Food Chem 61:3311–3319

Li YY, Chen XG, Liu CS, Cha DS, Park HJ, Lee CM (2007) Effect of the molecular mass and degree of substitution of oleoylchitosan on the structure, rheological properties, and formation of nanoparticles. J Agric Food Chem 55:4842–4847

Liang J, Ni P, Zhang M, Yu Z (2004) Graft copolymerization of (dimethylamino)ethyl methacrylate onto chitosan initiated by ceric ammonium nitrate. J Macromol Sci A 41:685–696

Lim G-P, Ahmad MS (2017) Development of ca-alginate-chitosan microcapsules for encapsulation and controlled release of imidacloprid to control dengue outbreaks. J Ind Eng Chem 56:382–393

Lin C, Liu D, Luo W, Liu Y, Zhu M, Li X, Liu M (2015) Functionalization of chitosan via single electron transfer living radical polymerization in an ionic liquid and its antimicrobial activity. J Appl Polym Sci 132:42754

Lin YH, Liang HF, Chung CK, Chen MC, Sung HW (2005) Physically crosslinked alginate/*N*,*O*-carboxymethyl chitosan hydrogels with calcium for oral delivery of protein drugs. Biomaterials 26:2105–2113

Lin YH, Lu KY, Tseng CL, Wu JY, Chen CH, Mi FL (2017) Development of genipin-crosslinked fucoidan/chitosan-*N*-arginine nanogels for preventing *Helicobacter* infection. Nanomedicine. https://doi.org/10.2217/nnm-2017-0055

Lin YH, Tsai SC, Lai CH, Lee CH, He ZS, Tseng GC (2013) Genipin-cross-linked fucose-chitosan/heparin nanoparticles for the eradication of *Helicobacter pylori*. Biomaterials 34:4466–4479

Liu C-G, Chen X-G, Park H-J (2005a) Self-assembled nanoparticles based on linoleic-acid modified chitosan: stability and adsorption of trypsin. Carbohydr Polym 62:293–298

Liu C, Honda H, Ohshima A, Shinkai M, Kobayashi T (2000) Development of chitosan-magnetite aggregates containing *Nitrosomonas europaea* cells for nitrification enhancement. J Biosci Bioeng 89:420–425

Liu CG, Desai KG, Chen XG, Park HJ (2005b) Linolenic acid-modified chitosan for formation of self-assembled nanoparticles. J Agric Food Chem 53:437–441

Liu J, Liu C, Liu Y, Chen M, Hu Y, Yang Z (2013) Study on the grafting of chitosan-gelatin microcapsules onto cotton fabrics and its antibacterial effect. Colloids Surf B: Biointerfaces 109:103–108

Liu K-H, Chen S-Y, Liu D-M, Liu T-Y (2008a) Self-assembled hollow nanocapsule from amphiphatic carboxymethyl-hexanoyl chitosan as drug carrier. Macromolecules 41:6511–6516

Liu L, Chen XW, Wang P, Wang C (2011) Studies on methyl methacrylate grafted onto chitosan by ceric ion initiation. Adv Mater Res 284-286:1713–1716

Liu L, Wang Y, Shen X, Fang Y (2005c) Preparation of chitosan-g-polycaprolactone copolymers through ring-opening polymerization of epsilon-caprolactone onto phthaloyl-protected chitosan. Biopolymers 78:163–170

Liu Q, Yang B, Zhang L, Huang R (2015) Adsorption of an anionic azo dye by cross-linked chitosan/bentonite composite. Int J Biol Macromol 72:1129–1135

Liu Y, Li Y, Lv J, Wu G, Li J (2005d) Graft copolymerization of methyl methacrylate onto chitosan initiated by potassium Ditelluratocuprate(III). J Macromol Sci A 42:1169–1180

Liu Y, Liu Z, Zhang Y, Deng K (2002) Graft copolymerization of methyl acrylate onto chitosan initiated by potassium diperiodatonickelate (IV). J Macromol Sci A 39:129–143

Liu Y, Liu Z, Zhang Y, Deng K (2003) Graft copolymerizaztion of methyl acrylate onto chitosan initiated by potassium diperiodatocuprate (III). J Appl Polym Sci 89:2283–2289

Liu Y, Yu Z-L, Zhang Y-M, Guo D-S, Liu Y-P (2008b) Supramolecular architectures of β-cyclodextrin-modified chitosan and pyrene derivatives mediated by carbon nanotubes and their DNA condensation. J Am Chem Soc 130:10431–10439

Long T, Liu YT, Tang S, Sun JL, Guo YP, Zhu ZA (2014) Hydrothermal fabrication of hydroxyapatite/chitosan/carbon porous scaffolds for bone tissue engineering. J Biomed Mater Res B 102:1740–1748

Lou R, Xie H, Zheng H, Ren Y, Gao M, Guo X, Song Y, Yu W, Liu X, Ma X (2016) Alginate-based microcapsules with galactosylated chitosan internal for primary hepatocyte applications. Int J Biol Macromol 93:1133–1140

Loubaki E, Ourevitch M, Sicsic S (1991) Chemical modification of chitosan by glycidyl trimethylammonium chloride. Characterization of modified chitosan by 13C- and 1H-NMR spectroscopy. Eur Polym J 27:311–317

Lu J, Xu K, Yang J, Hao Y, Cheng F (2017) Nano iron oxide impregnated in chitosan bead as a highly efficient sorbent for Cr(VI) removal from water. Carbohydr Polym 173:28–36

Lu L, Zhang L, Zhang X, Huan S, Shen G, Yu R (2010) A novel tyrosinase biosensor based on hydroxyapatite-chitosan nanocomposite for the detection of phenolic compounds. Anal Chim Acta 665:146–151

Ma J, Fu K, Shi J, Sun Y, Zhang X, Ding L (2016) Ultraviolet-assisted synthesis of polyacrylamide-grafted chitosan nanoparticles and flocculation performance. Carbohydr Polym 151:565–575

Ma L, Li G, Li L, Liu P (2010) Synthesis and characterization of diethoxy phosphoryl chitosan. Int J Biol Macromol 47:578–581

Macleod GS, Collett JH, Fell JT (1999) The potential use of mixed films of pectin, chitosan and HPMC for bimodal drug release. J Control Release 58:303–310

Mahdavinia GR, Mosallanezhad A, Soleymani M, Sabzi M (2017) Magnetic- and pH-responsive kappa-carrageenan/chitosan complexes for controlled release of methotrexate anticancer drug. Int J Biol Macromol 97:209–217

Mahdavinia GR, Pourjavadi A, Hosseinzadeh H, Zohuriaan MJ (2004) Modified chitosan 4. Superabsorbent hydrogels from poly(acrylic acid-co-acrylamide) grafted chitosan with salt- and pH-responsiveness properties. Eur Polym J 40:1399–1407

Maheshwari RGS, Thakur S, Singhal S, Patel RP, Tekade M, Tekade RK (2015) Chitosan encrusted nonionic surfactant based vesicular formulation for topical administration of Ofloxacin. Sci Adv Mater 7:1163–1176

Mahjub R, Dorkoosh FA, Amini M, Khoshayand MR, Rafiee-Tehrani M (2011) Preparation, statistical optimization, and *in vitro* characterization of insulin nanoparticles composed of quaternized aromatic derivatives of chitosan. AAPS PharmSciTech 12:1407–1419

Mahjub R, Radmehr M, Dorkoosh FA, Ostad SN, Rafiee-Tehrani M (2014) Lyophilized insulin nanoparticles prepared from quaternized *N*-aryl derivatives of chitosan as a new strategy for oral delivery of insulin: *in vitro, ex vivo* and *in vivo* characterizations. Drug Dev Ind Pharm 40:1645–1659

Mahmood A, Lanthaler M, Laffleur F, Huck CW, Bernkop-Schnurch A (2017) Thiolated chitosan micelles: highly mucoadhesive drug carriers. Carbohydr Polym 167:250–258

Mahmoud ME, Abou Ali SAA, Elweshahy SMT (2018) Microwave functionalization of titanium oxide nanoparticles with chitosan nanolayer for instantaneous microwave sorption of cu(II) and cd(II) from water. Int J Biol Macromol 111:393–399

Makimura Y, Watanabe S, Suzuki T, Suzuki Y, Ishida H, Kiso M, Katayama T, Kumagai H, Yamamoto K (2006) Chemoenzymatic synthesis and application of a sialoglycopolymer with a chitosan backbone as a potent inhibitor of human influenza virus hemagglutination. Carbohydr Res 341:1803–1808

Mansouri S, Lavigne P, Corsi K, Benderdour M, Beaumont E, Fernandes JC (2004) Chitosan-DNA nanoparticles as non-viral vectors in gene therapy: strategies to improve transfection efficacy. Eur J Pharm Biopharm 57:1–8

Mansuri S, Kesharwani P, Tekade RK, Jain NK (2016) Lyophilized mucoadhesive-dendrimer enclosed matrix tablet for extended oral delivery of albendazole. Eur J Pharm Biopharm 102:202–213

Martins AM, Eng G, Caridade SG, Mano JF, Reis RL, Vunjak-Novakovic G (2014) Electrically conductive chitosan/carbon scaffolds for cardiac tissue engineering. Biomacromolecules 15:635–643

Martins P, Daga M, Zandonai CF, Grandi BS, Cruz AB, Lucinda Silva RM, Rodrigues CA (2011) Release of tetracycline from *O*-carboxymethylchitosan films. Pharm Dev Technol 16:179–186

Másson M, Holappa J, Hjálmarsdóttir M, Rúnarsson ÖV, Nevalainen T, Järvinen T (2008) Antimicrobial activity of piperazine derivatives of chitosan. Carbohydr Polym 74:566–571

Mathew ME, Mohan JC, Manzoor K, Nair SV, Tamura H, Jayakumar R (2010) Folate conjugated carboxymethyl chitosan–manganese doped zinc sulphide nanoparticles for targeted drug delivery and imaging of cancer cells. Carbohydr Polym 80:442–448

Matrosovich M, Herrler G, Klenk HD (2015) Sialic acid receptors of viruses. Top Curr Chem 367:1–28

Maya S, Indulekha S, Sukhithasri V, Smitha KT, Nair SV, Jayakumar R, Biswas R (2012) Efficacy of tetracycline encapsulated *O*-carboxymethyl chitosan nanoparticles against intracellular infections of *Staphylococcus aureus*. Int J Biol Macromol 51:392–399

Mayadunne RTA, Rizzardo E, Chiefari J, Chong YK, Moad G, Thang SH (1999) Living radical polymerization with reversible addition−fragmentation chain transfer (RAFT polymerization) using dithiocarbamates as chain transfer agents. Macromolecules 32:6977–6980

Melaj MA, Daraio ME (2013) Preparation and characterization of potassium nitrate controlled-release fertilizers based on chitosan and xanthan layered tablets. J Appl Polym Sci 130:2422–2428

Meng J, Agrahari V, Ezoulin MJ, Purohit SS, Zhang T, Molteni A, Dim D, Oyler NA, Youan BC (2017) Spray-dried thiolated chitosan-coated sodium alginate multilayer microparticles for vaginal HIV microbicide delivery. AAPS J 19:692–702

Mertins O, Sebben M, Pohlmann AR, da Silveira NP (2005) Production of soybean phosphatidylcholine-chitosan nanovesicles by reverse phase evaporation: a step by step study. Chem Phys Lipids 138:29–37

Michalska-Sionkowska M, Kaczmarek B, Walczak M, Sionkowska A (2018) Antimicrobial activity of new materials based on the blends of collagen/chitosan/hyaluronic acid with gentamicin sulfate addition. Mater Sci Eng C 86:103–108

Millotti G, Laffleur F, Perera G, Vigl C, Pickl K, Sinner F, Bernkop-Schnurch A (2014) *In vivo* evaluation of thiolated chitosan tablets for oral insulin delivery. J Pharm Sci 103:3165–3170

Millotti G, Samberger C, Frohlich E, Bernkop-Schnurch A (2009) Chitosan-graft-6-mercaptonicotinic acid: synthesis, characterization, and biocompatibility. Biomacromolecules 10:3023–3027

Mingyu C, Kai G, Jiamou L, Yandao G, Nanming Z, Xiufang Z (2004) Surface modification and characterization of chitosan film blended with poly-L-lysine. J Biomater Appl 19:59–75

Miranda MES, Marcolla C, Rodrígues CA, Wilhelm HM, Sierakowski MR, Bresolin TMB, de Freitas RA (2006) Chitosan and *N*-carboxymethylchitosan: I. The role of *N*-carboxymethylation of chitosan in the thermal stability and dynamic mechanical properties of its films. Polym Int 55:961–969

Miwa A, Ishibe A, Nakano M, Yamahira T, Itai S, Jinno S, Kawahara H (1998) Development of novel chitosan derivatives as micellar carriers of Taxol. Pharm Res 15:1844–1850

Moedritzer K, Irani RR (1961) Synthesis and properties of mono-methylene-and poly-methylene-Diphosphonic acids and esters. J Inorg Nucl Chem 22:297–304

Morimoto M, Saimoto H, Usui H, Okamoto Y, Minami S, Shigemasa Y (2001) Biological activities of carbohydrate-branched chitosan derivatives. Biomacromolecules 2:1133–1136

Mourya VK, Inamdar NN (2009) Trimethyl chitosan and its applications in drug delivery. J Mater Sci Mater Med 20:1057–1079

Moussout H, Ahlafi H, Aazza M, El Akili C (2018) Performances of local chitosan and its nanocomposite 5%bentonite/chitosan in the removal of chromium ions (Cr(VI)) from wastewater. Int J Biol Macromol 108:1063–1073

Mukhopadhyay P, Sarkar K, Bhattacharya S, Bhattacharyya A, Mishra R, Kundu PP (2014) pH sensitive *N*-succinyl chitosan grafted polyacrylamide hydrogel for oral insulin delivery. Carbohydr Polym 112:627–637

Mun GA, Nurkeeva ZS, Dergunov SA, Nam IK, Maimakov TP, Shaikhutdinov EM, Lee SC, Park K (2008) Studies on graft copolymerization of 2-hydroxyethyl acrylate onto chitosan. React Funct Polym 68:389–395

Muzzarelli C, Muzzarelli RAA (2002) Reactivity of quinones towards chitosans. Trends Glycosci Glycotechnol 14:223–229

Muzzarelli RA, Greco F, Busilacchi A, Sollazzo V, Gigante A (2012) Chitosan, hyaluronan and chondroitin sulfate in tissue engineering for cartilage regeneration: a review. Carbohydr Polym 89:723–739

Muzzarelli RAA (1992) Modified chitosans carrying sulfonic-acid groups. Carbohydr Polym 19:231–236

Muzzarelli RAA, Littarrua G, Muzzarelli C, Tosi G (2003) Selective reactivity of biochemically relevant quinones towards chitosans. Carbohydr Polym 53:109–115

Muzzarelli RAA, Tanfani F (1985) The *N*-Permethylation of chitosan and the preparation of *N*-Trimethyl chitosan iodide. Carbohydr Polym 5:297–307

Naberezhnykh GA, Gorbach VI, Likhatskaya GN, Bratskaya SY, Solov'eva TF (2013) Interaction of *N*-acylated and *N*-alkylated chitosans included in liposomes with lipopolysaccharide of gram-negative bacteria. Biochemistry (Mosc) 78:301–308

Nagasawa K, Tohira Y, Inoue Y, Tanoura N (1971) Reaction between carbohydrates and sulfuric acid: Part I Depolymerization and sulfation of polysaccharides by sulfuric acid. Carbohydr Res 18:95–102

Najjar AMK, Yunus WMZW, Ahmad MB, Rahman MZA (2000) Preparation and characterization of poly(2-acrylamido-2-methylpropane-sulfonic acid) grafted chitosan using potassium persulfate as redox initiator. J Appl Polym Sci 77:2314–2318

Nakano T, Ikawa N, Ozimek L (2004) Use of epichlorohydrin-treated chitosan resin as an adsorbent to isolate kappa-casein glycomacropeptide from sweet whey. J Agric Food Chem 52:7555–7560

Nehra P, Chauhan RP, Garg N, Verma K (2018) Antibacterial and antifungal activity of chitosan coated iron oxide nanoparticles. Br J Biomed Sci 75:13–18

Neufeld L, Bianco-Peled H (2017) Pectin-chitosan physical hydrogels as potential drug delivery vehicles. Int J Biol Macromol 101:852–861

Ng LT, Guthrie JT, Yuan YJ, Zha HJ (2001) UV-cured natural polymer-based membrane for biosensor application. J Appl Polym Sci 79(3):466

Nguyen HM, Hwang IC, Park JW, Park HJ (2012) Photoprotection for deltamethrin using chitosan-coated beeswax solid lipid nanoparticles. Pest Manag Sci 68:1062–1068

Ni X, Wang J, Yue Y, Cheng W, Wang D, Han G (2018) Enhanced antibacterial performance and cytocompatibility of silver nanoparticles stabilized by cellulose nanocrystal grafted with chito-oligosaccharides. Materials 11. https://doi.org/10.3390/ma11081339

Nicolas J, Dire C, Mueller L, Belleney J, Charleux B (2006) Living character of polymer chains prepared via nitroxide-mediated controlled free-radical polymerization of methyl methacrylate in the presence of a small amount of styrene at low temperature. Macromolecules 39:8274–8282

Nishi N, Ebina A, S-i N, Tsutsumi A, Hasegawa O, Tokura S (1986) Highly phosphorylated derivatives of chitin, partially deacetylated chitin and chitosan as new functional polymers: preparation and characterization. Int J Biol Macromol 8:311–317

Nishi N, Maekita Y, S-i N, Hasegawa O, Tokura S (1987) Highly phosphorylated derivatives of chitin, partially deacetylated chitin and chitosan as new functional polymers: metal binding property of the insolubilized materials. Int J Biol Macromol 9:109–114

Nishimura S, Kai H, Shinada K, Yoshida T, Tokura S, Kurita K, Nakashima H, Yamamoto N, Uryu T (1998) Regioselective syntheses of sulfated polysaccharides: specific anti-HIV-1 activity of novel chitin sulfates. Carbohydr Res 306:427–433

Nishimura S, Kohgo O, Ishii S, Hurita K, Mochida K, Kuzuhara H (1992) New trends in bioactive chitosan derivatives: use of 'standardized intermediates' with excellent solubility in common organic solvents. In: Brine CJ, Sandford PA, Zikakis JP (eds) Advances in chitin and chitosan. Elsevier, London, pp 533–542

Nishimura SI, Nishi N, Tokura S, Okiei W, Somorin O (1986) Inhibition of the hydrolytic activity of thrombin by chitin heparinoids. Carbohydr Res 156:286–292

Nudga LA, Plisko EA, Danilov SN (1974) Synthesis and properties of sulfoethylchitosan. J Appl Chem-USSR 47:872–875

Oktay B, Kayaman-Apohan N, Suleymanoglu M, Erdem-Kuruca S (2017) Zwitterionic phosphorylcholine grafted chitosan nanofiber: preparation, characterization and *in-vitro* cell adhesion behavior. Mater Sci Eng C 73:569–578

Oliveira JM, Kotobuki N, Tadokoro M, Hirose M, Mano JF, Reis RL, Ohgushi H (2010) *Ex vivo* culturing of stromal cells with dexamethasone-loaded carboxymethylchitosan/poly (amidoamine) dendrimer nanoparticles promotes ectopic bone formation. Bone 46:1424–1435

Pal P, Pal A (2017) Surfactant-modified chitosan beads for cadmium ion adsorption. Int J Biol Macromol 104:1548–1555

Palanisamy S, Thangavelu K, Chen SM, Gnanaprakasam P, Velusamy V, Liu XH (2016) Preparation of chitosan grafted graphite composite for sensitive detection of dopamine in biological samples. Carbohydr Polym 151:401–407

Palma G, Casals P, Cardenas G (2005) Synthesis and characterization of new chitosan-*O*-ethyl phosphonate. J Chil Chem Soc 50:719–724

Pan Y, Chen J, Yu Y, Dai K, Wang J, Liu C (2018) Enhancement of BMP-2-mediated angiogenesis and osteogenesis by 2-*N*,6-*O*-sulfated chitosan in bone regeneration. Biomater Sci 6:431–439

Pandi K, Periyasamy S, Viswanathan N (2017) Remediation of fluoride from drinking water using magnetic iron oxide coated hydrotalcite/chitosan composite. Int J Biol Macromol 104:1569–1577

Pandi K, Viswanathan N (2015) Synthesis and applications of eco-magnetic nano-hydroxyapatite chitosan composite for enhanced fluoride sorption. Carbohydr Polym 134:732–739
Park I-K, Yang J, Jeong HJ, Bom HS, Harada I, Akaike T, Kim SI, Cho CS (2003) Galactosylated chitosan as a synthetic extracellular matrix for hepatocytes attachment. Biomaterials 24:2331–2337
Park IK, Jiang HL, Cook SE, Cho MH, Kim SI, Jeong HJ, Akaike T, Cho CS (2004a) Galactosylated chitosan (GC)-graft-poly(vinyl pyrrolidone) (PVP) as hepatocyte-targeting DNA carrier: *in vitro* transfection. Arch Pharm Res 27:1284–1289
Park IK, Park YH, Shin BA, Choi ES, Kim YR, Akaike T, Cho CS (2000) Galactosylated chitosan-graft-dextran as hepatocyte-targeting DNA carrier. J Control Release 69:97–108
Park K (2017) Chitosan-gelatin-platelet gel composite scaffold for bone regeneration. J Control Release 254:137
Park PJ, Je JY, Jung WK, Ahn CB, Kim SK (2004b) Anticoagulant activity of heterochitosans and their oligosaccharide sulfates. Eur Food Res Technol 219:529–533
Pauliukaite R, Ghica ME, Fatibello-Filho O, Brett CM (2010) Graphite-epoxy electrodes modified with functionalised carbon nanotubes and chitosan for the rapid electrochemical determination of dipyrone. Comb Chem High Throughput Screen 13:590–598
Pavinatto A, Souza AL, Delezuk JA, Pavinatto FJ, Campana-Filho SP, Oliveira ON Jr (2014) Interaction of O-acylated chitosans with biomembrane models: probing the effects from hydrophobic interactions and hydrogen bonding. Colloids Surf B: Biointerfaces 114:53–59
Pavlov GM, Korneeva EV, Harding SE, Vichoreva GA (1998) Dilute solution properties of carboxymethylchitins in high ionic-strength solvent. Polymer 39:6951–6961
Peng X, Zhang L (2007) Formation and morphologies of novel self-assembled micelles from chitosan derivatives. Langmuir 23:10493–10498
Peng X, Zhang L (2009) Self-assembled micelles of *N*-phthaloyl-carboxymethychitosan for drug delivery. Colloids Surf A Physicochem Eng Asp 337:21–25
Pengfei L, Maolin Z, Jilan W (2001) Study on radiation-induced grafting of styrene onto chitin and chitosan. Radiat Phys Chem 61:149–153
Pepic I, Hafner A, Lovric J, Pirkic B, Filipovic-Grcic J (2010) A nonionic surfactant/chitosan micelle system in an innovative eye drop formulation. J Pharm Sci 99:4317–4325
Pereira FA, Sousa KS, Cavalcanti GR, Fonseca MG, de Souza AG, Alves AP (2013) Chitosan-montmorillonite biocomposite as an adsorbent for copper (II) cations from aqueous solutions. Int J Biol Macromol 61:471–478
Perez-Recalde M, Ruiz Arias IE, Hermida EB (2018) Could essential oils enhance biopolymers performance for wound healing? A systematic review. Phytomedicine 38:57–65
Perez JJ, Francois NJ (2016) Chitosan-starch beads prepared by ionotropic gelation as potential matrices for controlled release of fertilizers. Carbohydr Polym 148:134–142
Perumal V, Arfuso F, Chen Y, Fox S, Dharmarajan AM (2017) Delivery of expression constructs of secreted frizzled-related protein 4 and its domains by chitosan-dextran sulfate nanoparticles enhances their expression and anti-cancer effects. Mol Cell Biochem 443:205–213
Petit C, Reynaud S, Desbrieres J (2015) Amphiphilic derivatives of chitosan using microwave irradiation. Toward an eco-friendly process to chitosan derivatives. Carbohydr Polym 116:26–33
Petrova YS, Neudachina LK, Mekhaev AV, Pestov AV (2014) Simple synthesis and chelation capacity of *N*-(2-sulfoethyl)chitosan, a taurine derivative. Carbohydr Polym 112:462–468
Pezzoli D, Olimpieri F, Malloggi C, Bertini S, Volonterio A, Candiani G (2012) Chitosan-graft-branched polyethylenimine copolymers: influence of degree of grafting on transfection behavior. PLoS One 7:e34711. https://doi.org/10.1371/journal.pone.0034711
Phongying S, Aiba S, Chirachanchai S (2006) A novel soft and cotton-like chitosan-sugar nanoscaffold. Biopolymers 83:280–288
Picola IP, Shi Q, Fernandes JC, Petronio MS, Lima AM, de Oliveira Tiera VA, Tiera MJ (2016) Chitosan derivatives for gene transfer: effect of phosphorylcholine and diethylaminoethyl grafts on the *in vitro* transfection efficiency. J Biomater Sci Polym Ed 27:1611–1630

Pighinelli L, Kucharska M (2013) Chitosan-hydroxyapatite composites. Carbohydr Polym 93:256–262

Ping Y, Liu CD, Tang GP, Li JS, Li J, Yang WT, Xu FJ (2010) Functionalization of chitosan via atom transfer radical polymerization for gene delivery. Adv Funct Mater 20:3106–3116

Polnok A, Borchard G, Verhoef JC, Sarisuta N, Junginger HE (2004) Influence of methylation process on the degree of quaternization of *N*-trimethyl chitosan chloride. Eur J Pharm Biopharm 57:77–83

Pourjavadi A, Mahdavinia GR, Zohuriaan-Mehr MJ, Omidian H (2003) Modified chitosan. I. Optimized cerium ammonium nitrate-induced synthesis of chitosan-graft-polyacrylonitrile. J Appl Polym Sci 88:2048–2054

Prabaharan M, Mano JF (2007) Synthesis and characterization of chitosan-graft-poly (3-(trimethoxysilyl)propyl methacrylate) initiated by ceric (IV) ion. J Macromol Sci A 44:489–494

Prabhakar N, Thakur H, Bharti A, Kaur N (2016) Chitosan-iron oxide nanocomposite based electrochemical aptasensor for determination of malathion. Anal Chim Acta 939:108–116

Prabhu SM, Meenakshi S (2015) A dendrimer-like hyper branched chitosan beads toward fluoride adsorption from water. Int J Biol Macromol 78:280–286

Prakash N, Latha S, Sudha PN, Renganathan NG (2013) Influence of clay on the adsorption of heavy metals like copper and cadmium on chitosan. Environ Sci Pollut Res Int 20:925–938

Praphakar RA, Munusamy MA, Rajan M (2017) Development of extended-voyaging anti-oxidant linked amphiphilic polymeric nanomicelles for anti-tuberculosis drug delivery. Int J Pharm 524:168–177

Prashanth KVH, Tharanathan RN (2003) Studies on graft copolymerization of chitosan with synthetic monomers. Carbohydr Polym 54:343–351

Puspita A, Prawati G, Fatimah I (2017) Chitosan-modified smectite clay and study on adsorption-desorption of urea. Chem Eng Trans 56:1645–1650

Qi B, Kujawa P, Toita S, Beaune G, Winnik FM (2015a) Phosphorylcholine-modified chitosan films as effective promoters of cell aggregation: correlation between the films properties and cellular response. Macromol Biosci 15:490–500

Qi C, Zhao L, Lin Y, Wu D (2018) Graphene oxide/chitosan sponge as a novel filtering material for the removal of dye from water. J Colloid Interface Sci 517:18–27

Qi X, Rui Y, Fan Y, Chen H, Ma N, Wu Z (2015b) Galactosylated chitosan-grafted multiwall carbon nanotubes for pH-dependent sustained release and hepatic tumor-targeted delivery of doxorubicin *in vivo*. Colloids Surf B: Biointerfaces 133:314–322

Qin Y, Guo XW, Li L, Wang HW, Kim W (2013) The antioxidant property of chitosan green tea polyphenols complex induces transglutaminase activation in wound healing. J Med Food 16:487–498. https://doi.org/10.1089/jmf.2012.2623

Qu X, Wirsen A, Albertsson AC (1999) Synthesis and characterization of pH-sensitive hydrogels based on chitosan and D,L-lactic acid. J Appl Polym Sci 74:3193–3202

Radhakumary C, Divya G, Nair PD, Mathew S, Reghunadhan Nair CP (2003) Graft copolymerization of 2-hydroxy ethyl methacrylate onto chitosan with cerium (IV) ion. I. Synthesis and characterization. J Macromol Sci A 40:715–730

Radmansouri M, Bahmani E, Sarikhani E, Rahmani K, Sharifianjazi F, Irani M (2018) Doxorubicin hydrochloride - loaded electrospun chitosan/cobalt ferrite/titanium oxide nanofibers for hyperthermic tumor cell treatment and controlled drug release. Int J Biol Macromol 116:378–384

Radwan AA, Alanazi FK, Alsarra IA (2010) Microwave irradiation-assisted synthesis of a novel crown ether crosslinked chitosan as a chelating agent for heavy metal ions (M(+n)). Molecules 15:6257–6268

Raghavendra GM, Jung J, Kim D, Seo J (2016) Microwave assisted antibacterial chitosan-silver nanocomposite films. Int J Biol Macromol 84:281–288

Raik SV, Poshina DN, Lyalina TA, Polyakov DS, Vasilyev VB, Kritchenkov AS, Skorik YA (2018) *N*-[4-(*N,N,N*-trimethylammonium)benzyl]chitosan chloride: synthesis, interaction with DNA and evaluation of transfection efficiency. Carbohydr Polym 181:693–700

Ramos VM, Rodriguez NM, Diaz MF, Rodriguez MS, Heras A, Agullo E (2003a) *N*-methylene phosphonic chitosan. Effect of preparation methods on its properties. Carbohydr Polym 52:39–46

Ramos VM, Rodriguez NM, Rodriguez MS, Heras A, Agullo E (2003b) Modified chitosan carrying phosphonic and alkyl groups. Carbohydr Polym 51:425–429

Ramya R, Sudha PN (2013) Adsorption of cadmium (II) and copper (II) ions from aqueous solution using chitosan composite. Polym Compos 34:233–240

Rattanamanee A, Niamsup H, L-o S, Punyodom W, Watanesk R, Watanesk S (2015) Role of chitosan on some physical properties and the urea controlled release of the silk fibroin/gelatin hydrogel. J Polym Environ 23:334–340

Rinaudo M, Auzely R, Vallin C, Mullagaliev I (2005) Specific interactions in modified chitosan systems. Biomacromolecules 6:2396–2407

Runarsson OV, Holappa J, Jonsdottir S, Steinsson H, Masson M (2008) *N*-selective 'one pot' synthesis of highly *N*-substituted trimethyl chitosan (TMC). Carbohydr Polym 74:740–744

Runarsson OV, Holappa J, Nevalainen T, Hjálmarsdóttir M, Järvinen T, Loftsson T, Einarsson JM, Jónsdóttir S, Valdimarsdóttir M, Másson M (2007) Antibacterial activity of methylated chitosan and chitooligomer derivatives: synthesis and structure activity relationships. Eur Polym J 43:2660–2671

Rúnarsson ÖV, Malainer C, Holappa J, Sigurdsson ST, Másson M (2008) Tert-Butyldimethylsilyl O-protected chitosan and chitooligosaccharides: useful precursors for *N*-modifications in common organic solvents. Carbohydr Res 343:2576–2582

Sabaa MW, Elzanaty AM, Abdel-Gawad OF, Arafa EG (2018) Synthesis, characterization and antimicrobial activity of Schiff bases modified chitosan-graft-poly(acrylonitrile). Int J Biol Macromol 109:1280–1291

Saboktakin MR, Tabatabaie RM, Maharramov A, Ramazanov MA (2011) Synthesis and *in vitro* evaluation of carboxymethyl starch-chitosan nanoparticles as drug delivery system to the colon. Int J Biol Macromol 48:381–385

Sadeghi AMM, Amini A, Avadi MR, Siedi F, Rafiee-Tehrani M, Junginger HE (2008) Synthesis, characterization, and antibacterial effects of trimethylated and triethylated 6-NH_2-6-deoxy chitosan. J Bioact Compat Polym 23:262–275

Saeednia L, Yao L, Berndt M, Cluff K, Asmatulu R (2017) Structural and biological properties of thermosensitive chitosan-graphene hybrid hydrogels for sustained drug delivery applications. J Biomed Mater Res A 105:2381–2390

Safarik I, Pospiskova K, Maderova Z, Baldikova E, Horska K, Safarikova M (2015) Microwave-synthesized magnetic chitosan microparticles for the immobilization of yeast cells. Yeast 32:239–243

Sahu A, Goswami P, Bora U (2009) Microwave mediated rapid synthesis of chitosan. J Mater Sci Mater Med 20:171–175

Sahu SK, Mallick SK, Santra S, Maiti TK, Ghosh SK, Pramanik P (2010) *In vitro* evaluation of folic acid modified carboxymethyl chitosan nanoparticles loaded with doxorubicin for targeted delivery. J Mater Sci Mater Med 21:1587–1597

Saikia C, Hussain A, Ramteke A, Sharma HK, Maji TK (2015) Carboxymethyl starch-chitosan-coated iron oxide magnetic nanoparticles for controlled delivery of isoniazid. J Microencapsul 32:29–39

Sairam Sundaram C, Viswanathan N, Meenakshi S (2008) Uptake of fluoride by nano-hydroxyapatite/chitosan, a bioinorganic composite. Bioresour Technol 99:8226–8230

Sajomsang W, Gonil P, Ruktanonchai UR, Petchsangsai M, Opanasopit P, Puttipipatkhachorn S (2014) Effect of *N*-pyridinium positions of quaternized chitosan on transfection efficiency in gene delivery system. Carbohydr Polym 104:17–22

Sajomsang W, Gonil P, Tantayanon S (2009a) Antibacterial activity of quaternary ammonium chitosan containing mono or disaccharide moieties: preparation and characterization. Int J Biol Macromol 44:419–427

Sajomsang W, Ruktanonchai UR, Gonil P, Warin C (2010) Quaternization of *N*-(3-pyridylmethyl) chitosan derivatives: effects of the degree of quaternization, molecular weight and ratio of *N*-methylpyridinium and *N,N,N*-trimethyl ammonium moieties on bactericidal activity. Carbohydr Polym 82:1143–1152

Sajomsang W, Tantayanon S, Tangpasuthadol V, Daly WH (2008) Synthesis of methylated chitosan containing aromatic moieties: chemo selectivity and effect on molecular weight. Carbohydr Polym 72:740–750

Sajomsang W, Tantayanon S, Tangpasuthadol V, Daly WH (2009b) Quaternization of *N*-aryl chitosan derivatives: synthesis, characterization, and antibacterial activity. Carbohydr Res 344:2502–2511

Sakaguchi T, Horikoshi T, Nakajima A (1981) Adsorption of uranium by chitin phosphate and chitosan phosphate. Agric Biol Chem 45:2191–2195

Santhana Krishna Kumar A, Uday Kumar C, Rajesh V, Rajesh N (2014) Microwave assisted preparation of *N*-butylacrylate grafted chitosan and its application for Cr(VI) adsorption. Int J Biol Macromol 66:135–143

Saremi S, Dinarvand R, Kebriaeezadeh A, Ostad SN, Atyabi F (2013) Enhanced oral delivery of docetaxel using thiolated chitosan nanoparticles: preparation, *in vitro* and *in vivo* studies. Biomed Res Int 2013:150478. https://doi.org/10.1155/2013/150478

Sargın İ, Arslan G, Kaya M (2016a) Efficiency of chitosan–algal biomass composite microbeads at heavy metal removal. React Funct Polym 98:38–47

Sargın İ, Arslan G, Kaya M (2016b) Microfungal spores (*Ustilago maydis* and *U. digitariae*) immobilised chitosan microcapsules for heavy metal removal. Carbohydr Polym 138:201–209

Sashiwa H et al (2002) Chemical modification of chitosan. 13.(1) synthesis of organosoluble, palladium adsorbable, and biodegradable chitosan derivatives toward the chemical plating on plastics. Biomacromolecules 3:1120–1125

Sashiwa H, Makimura Y, Shigemasa Y, Roy R (2000a) Chemical modification of chitosan: preparation of chitosan-sialic acid branched polysaccharide hybrids. Chem Commun 11:909–910. https://doi.org/10.1039/B001861I

Sashiwa H, Shigemasa Y, Roy R (2000b) Chemical modification of chitosan. 3. Hyperbranched chitosan−sialic acid dendrimer hybrid with tetraethylene glycol spacer. Macromolecules 33:6913–6915

Sawdon AJ, Peng CA (2015) Ring-opening polymerization of epsilon-caprolactone initiated by ganciclovir (GCV) for the preparation of GCV-tagged polymeric micelles. Molecules 20:2857–2867

Schmitz T, Hombach J, Bernkop-Schnurch A (2008) Chitosan-*N*-acetyl cysteine conjugates: *In vitro* evaluation of permeation enhancing and P-glycoprotein inhibiting properties. Drug Deliv 15:245–252

Sezer AD, Cevher E, Hatipoglu F, Ogurtan Z, Bas AL, Akbuga J (2008) Preparation of fucoidan-chitosan hydrogel and its application as burn healing accelerator on rabbits. Biol Pharm Bull 31:2326–2333

Shahdost-fard F, Salimi A, Sharifi E, Korani A (2013) Fabrication of a highly sensitive adenosine aptasensor based on covalent attachment of aptamer onto chitosan-carbon nanotubes-ionic liquid nanocomposite. Biosens Bioelectron 48:100–107

Shan L (2004) Glycol chitosan/heparin-immobilized gold-deposited iron oxide nanoparticles. In: Molecular imaging and contrast agent database (MICAD). National Center for Biotechnology Information (US), Bethesda

Sharma S, Rajesh N (2017) Expeditious preparation of β-cyclodextrin grafted chitosan using microwave radiation for the enhanced palladium adsorption from aqueous waste and an industrial catalyst. J Environ Chem Eng 5:1927–1935

Shevtsov M, Nikolaev B, Marchenko Y, Yakovleva L, Skvortsov N, Mazur A, Tolstoy P, Ryzhov V, Multhoff G (2018) Targeting experimental orthotopic glioblastoma with chitosan-based superparamagnetic iron oxide nanoparticles (CS-DX-SPIONs). Intl J Nanomed 13:1471–1482

Shi X, Du Y, Yang J, Zhang B, Sun L (2006) Effect of degree of substitution and molecular weight of carboxymethyl chitosan nanoparticles on doxorubicin delivery. J Appl Polym Sci 100:4689–4696

Shi Y, Xiong Z, Lu X, Yan X, Cai X, Xue W (2016) Novel carboxymethyl chitosan-graphene oxide hybrid particles for drug delivery. J Mater Sci Mater Med 27:169

Shigeno Y, Kondo K, Takemoto K (1982) Functional monomers and polymers 90. Radiation-induced graft-polymerization of styrene onto chitin and chitosan. J Macromol Sci Chem A17:571–583

Shirazi H, Ahmadi A, Darzianiazizi M, Kashanian S, Kashanian S, Omidfar K (2016) Signal amplification strategy using gold/*N*-trimethyl chitosan/iron oxide magnetic composite nanoparticles as a tracer tag for high-sensitive electrochemical detection. IET Nanobiotechnol 10:20–27

Siafu SI (2017) Silicone doped chitosan-acrylamide coencapsulated urea fertilizer: An approach to controlled release fertilizers. J Nanotechnol 2017:8490730. https://doi.org/10.1155/2017/8490730

Sieval AB, Thanou M, Kotze AF, Verhoef JE, Brussee J, Junginger HE (1998) Preparation and NMR characterization of highly substituted N-trimethyl chitosan chloride. Carbohydr Polym 36:157–165

Silva JM, Georgi N, Costa R, Sher P, Reis RL, Van Blitterswijk CA, Karperien M, Mano JF (2013) Nanostructured 3D constructs based on chitosan and chondroitin sulphate multilayers for cartilage tissue engineering. PLoS One 8:e55451. https://doi.org/10.1371/journal.pone.0055451

Silva Mdos S, Cocenza DS, Grillo R, de Melo NF, Tonello PS, de Oliveira LC, Cassimiro DL, Rosa AH, Fraceto LF (2011) Paraquat-loaded alginate/chitosan nanoparticles: preparation, characterization and soil sorption studies. J Hazard Mater 190:366–374

Silva PMO, Francisco JE, Caje JCM, Cassella RJ, Pacheco WF (2018) A batch and fixed bed column study for fluorescein removal using chitosan modified by epichlorohydrin. J Environ Sci Health A 53:55–64

Sin J-C, Lam S-M, Mohamed AR, Lee K-T (2012) Degrading endocrine disrupting chemicals from wastewater by TIO2 photocatalysis: a review international. J Photoenergy 2012:185159. https://doi.org/10.1155/2012/185159

Singh A, Sinsinbar G, Choudhary M, Kumar V, Pasricha R, Verma HN, Singh SP, Arora K (2013) Graphene oxide-chitosan nanocomposite based electrochemical DNA biosensor for detection of typhoid. Sensor Actuat B Chem 185:675–684. https://doi.org/10.1016/j.snb.2013.05.014

Singh DK, Ray AR (1997) Radiation-induced grafting of *N,N′*-dimethylaminoethylmethacrylate onto chitosan films. J Appl Polym Sci 66:869–877

Singh V, Tripathi DN, Tiwari A, Sanghi R (2005) Microwave promoted synthesis of chitosan-graft-poly(acrylonitrile). J Appl Polym Sci 95:820–825

Sivashankari PR, Moorthi A, Abudhahir KM, Prabaharan M (2018) Preparation and characterization of three-dimensional scaffolds based on hydroxypropyl chitosan-graft-graphene oxide. Int J Biol Macromol 110:522–530

Snima KS, Jayakumar R, Unnikrishnan AG, Nair SV, Lakshmanan V-K (2012) O-Carboxymethyl chitosan nanoparticles for metformin delivery to pancreatic cancer cells. Carbohydr Polym 89:1003–1007

Snyman D, Hamman JH, Kotze JS, Rollings JE, Kotze AF (2002) The relationship between the absolute molecular weight and the degree of quaternisation of N-trimethyl chitosan chloride. Carbohydr Polym 50:145–150

Song Y, Nagai N, Saijo S, Kaji H, Nishizawa M, Abe T (2018) *In situ* formation of injectable chitosan-gelatin hydrogels through double crosslinking for sustained intraocular drug delivery. Mater Sci Eng C 88:1–12

Sosnik A, Imperiale JC, Vázquez-González B, Raskin MM, Muñoz-Muñoz F, Burillo G, Cedillo G, Bucio E (2015) Mucoadhesive thermo-responsive chitosan-g-poly(*N*-isopropylacrylamide) polymeric micelles via a one-pot gamma-radiation-assisted pathway. Colloids Surf B: Biointerfaces 136:900–907

Spera MBM, Taketa TB, Beppu MM (2017) Roughness dynamic in surface growth: layer-by-layer thin films of carboxymethyl cellulose/chitosan for biomedical applications. Biointerphases 12:04E401. https://doi.org/10.1116/1.4986057

Steenkamp GC, Keizer K, Neomagus HWJP, Krieg HM (2002) Copper(II) removal from polluted water with alumina/chitosan composite membranes. J Membr Sci 197:147–156

Su F, Zhou H, Zhang Y, Wang G (2016) Three-dimensional honeycomb-like structured zero-valent iron/chitosan composite foams for effective removal of inorganic arsenic in water. J Colloid Interface Sci 478:421–429

Subramanian K, Vijayakumar V (2012) Synthesis and evaluation of chitosan-graft-poly (2-hydroxyethyl methacrylate-co-itaconic acid) as a drug carrier for controlled release of tramadol hydrochloride. Saudi Pharm J 20:263–271

Sun J, Yendluri R, Liu K, Guo Y, Lvov Y, Yan X (2016) Enzyme-immobilized clay nanotube-chitosan membranes with sustainable biocatalytic activities. Phys Chem Chem Phys 19:562–567

Sun M, Cheng G, Ge X, Chen M, Wang C, Lou L, Xu X (2018) Aqueous hg(II) immobilization by chitosan stabilized magnetic iron sulfide nanoparticles. Sci Total Environ 621:1074–1083

Sun T, Xie WM, Xu PX (2004) Superoxide anion scavenging activity of graft chitosan derivatives. Carbohydr Polym 58:379–382

Sun T, Xu PX, Liu Q, Xue JA, Xie WM (2003) Graft copolymerization of methacrylic acid onto carboxymethyl chitosan. Eur Polym J 39:189–192

Sun Y, Wang Y, Li J, Ding C, Lin Y, Sun W, Luo C (2017) An ultrasensitive chemiluminescence aptasensor for thrombin detection based on iron porphyrin catalyzing luminescence desorbed from chitosan modified magnetic oxide graphene composite. Talanta 174:809–818

Sunkireddy P, Kanwar RK, Ram J, Kanwar JR (2016) Ultra-small algal chitosan ocular nanoparticles with iron-binding milk protein prevents the toxic effects of carbendazim pesticide. Nanomedicine 11:495–511

Sutirman ZA, Sanagi MM, Abd Karim J, Abu Naim A, Wan Ibrahim WA (2018) New crosslinked-chitosan graft poly(*N*-vinyl-2-pyrrolidone) for the removal of cu(II) ions from aqueous solutions. Int J Biol Macromol 107:891–897

Swayampakula K, Boddu VM, Nadavala SK, Abburi K (2009) Competitive adsorption of cu (II), co (II) and Ni (II) from their binary and tertiary aqueous solutions using chitosan-coated perlite beads as biosorbent. J Hazard Mater 170:680–689

Tabasi A, Noorbakhsh A, Sharifi E (2017) Reduced graphene oxide-chitosan-aptamer interface as new platform for ultrasensitive detection of human epidermal growth factor receptor 2. Biosens Bioelectron 95:117–123

Takei T, Nakahara H, Tanaka S, Nishimata H, Yoshida M, Kawakami K (2013) Effect of chitosan-gluconic acid conjugate/poly(vinyl alcohol) cryogels as wound dressing on partial-thickness wounds in diabetic rats. J Mater Sci Mater Med 24:2479–2487

Tan H, Ma R, Lin C, Liu Z, Tang T (2013) Quaternized chitosan as an antimicrobial agent: antimicrobial activity, mechanism of action and biomedical applications in orthopedics. Int J Mol Sci 14:1854–1869

Tan H, Xue Y, Luan Q, Yao X (2012) Evaluation of glycol chitosan-graft-carboxymethyl [small beta]-cyclodextrin as potential pH-sensitive anticancer drug carrier by surface plasmon resonance. Anal Methods 4:2784–2790

Tan Y, Liu C-G (2009) Self-aggregated nanoparticles from linoleic acid modified carboxymethyl chitosan: synthesis, characterization and application *in vitro*. Colloids Surf B: Biointerfaces 69:178–182

Tang Y, Xie L, Sai M, Xu N, Ding D (2015) Preparation and antibacterial activity of quaternized chitosan with iodine. Mater Sci Eng C 48:1–4. https://doi.org/10.1016/j.msec.2014.11.019

Tao W, Fu T, He Z, Hu R, Jia L, Hong Y (2017a) Evaluation of immunostimulatory effects of *n*-(2-hydroxy) propyl-3-trimethylammonium chitosan chloride for improving live attenuated hepatitis a virus vaccine efficacy. Viral Immunol 30:120–126

Tao W, Zheng HQ, Fu T, He ZJ, Hong Y (2017b) *N*-(2-hydroxy) propyl-3-trimethylammonium chitosan chloride: An immune-enhancing adjuvant for hepatitis E virus recombinant polypeptide vaccine in mice. Hum Vaccin Immunother 13:1818–1822

Tao X, Li K, Yan H, Yang H, Li A (2016) Simultaneous removal of acid green 25 and mercury ions from aqueous solutions using glutamine modified chitosan magnetic composite microspheres. Environ Pollut 209:21–29

Tardif K, Cloutier I, Miao Z, Lemieux C, St-Denis C, Winnik FM, Tanguay JF (2011) A phosphorylcholine-modified chitosan polymer as an endothelial progenitor cell supporting matrix. Biomaterials 32:5046–5055

Teimouri A, Nasab SG, Vahdatpoor N, Habibollahi S, Salavati H, Chermahini AN (2016) Chitosan /zeolite Y/Nano ZrO2 nanocomposite as an adsorbent for the removal of nitrate from the aqueous solution. Int J Biol Macromol 93:254–266

Teng Z, Luo Y, Wang Q (2013) Carboxymethyl chitosan-soy protein complex nanoparticles for the encapsulation and controlled release of vitamin D(3). Food Chem 141:524–532

Terbojevich M, Carraro C, Cosani A, Focher B, Naggi AM, Torri G (1989) Solution studies of chitosan 6-*O*-sulfate. Makromol Chem 190:2847–2855

Thomas AM, Gomez AJ, Palma JL, Yap WT, Shea LD (2014) Heparin-chitosan nanoparticle functionalization of porous poly(ethylene glycol) hydrogels for localized lentivirus delivery of angiogenic factors. Biomaterials 35:8687–8693

Thotakura N, Dadarwal M, Kumar P, Sharma G, Guru SK, Bhushan S, Raza K, Katare OP (2017) Chitosan-stearic acid based polymeric micelles for the effective delivery of tamoxifen: cytotoxic and pharmacokinetic evaluation. AAPS PharmSciTech 18:759–768

Tian Q, Wang XH, Wang W, Zhang CN, Wang P, Yuan Z (2012) Self-assembly and liver targeting of sulfated chitosan nanoparticles functionalized with glycyrrhetinic acid. Nanomedicine 8:870–879

Tkac J, Whittaker JW, Ruzgas T (2007) The use of single walled carbon nanotubes dispersed in a chitosan matrix for preparation of a galactose biosensor. Biosens Bioelectron 22:1820–1824

Tomalia DA, Baker H, Dewald J, Hall M, Kallos G, Martin S, Roeck J, Ryder J, Smith P (1985) A new class of polymers: starburst-dendritic macromolecules. Polym J 17:117. https://doi.org/10.1295/polymj.17.117

Torres MG, Muñoz SV, Rosales SG, Carreón-Castro Mdel P, Muñoz RA, González RO, González MR, Talavera RR (2015) Radiation-induced graft polymerization of chitosan onto poly (3-hydroxybutyrate). Carbohydr Polym 133:482–492

Travlou NA, Kyzas GZ, Lazaridis NK, Deliyanni EA (2013) Graphite oxide/chitosan composite for reactive dye removal. Chem Eng J 217:256–265

Tsubokawa N, Takayama T (2000) Surface modification of chitosan powder by grafting of 'dendrimer-like' hyperbranched polymer onto the surface. React Funct Polym 43:341–350

Tundo P, Selva M (2002) The chemistry of dimethyl carbonate accounts. Chem Res 35:706–716

Umemura M, Itoh M, Makimura Y, Yamazaki K, Umekawa M, Masui A, Matahira Y, Shibata M, Ashida H, Yamamoto K (2008) Design of a sialylglycopolymer with a chitosan backbone having efficient inhibitory activity against influenza virus infection. J Med Chem 51:4496–4503

Uygun DA, Uygun M, Karagozler A, Ozturk N, Akgol S, Denizli A (2009) A novel support for antibody purification: fatty acid attached chitosan beads. Colloids Surf B: Biointerfaces 70:266–270

Vachoud L, Chen T, Payne GF, Vazquez-Duhalt R (2001) Peroxidase catalyzed grafting of gallate esters onto the polysaccharide chitosan. Enzym Microb Technol 29:380–385

Venkatesan J, Ryu B, Sudha PN, Kim SK (2012) Preparation and characterization of chitosan-carbon nanotube scaffolds for bone tissue engineering. Int J Biol Macromol 50:393–402

Verheul RJ, Amidi M, van der Wal S, van Riet E, Jiskoot W, Hennink WE (2008) Synthesis, characterization and *in vitro* biological properties of *O*-methyl free *N,N,N*-trimethylated chitosan. Biomaterials 29:3642–3649

Vijayaraghavan C, Vasanthakumar S, Ramakrishnan A (2008) *In vitro* and *in vivo* evaluation of locust bean gum and chitosan combination as a carrier for buccal drug delivery. Pharmazie 63:342–347

Vikhoreva G, Bannikova G, Stolbushkina P, Panov A, Drozd N, Makarov V, Varlamov V, Gal'braikh L (2005) Preparation and anticoagulant activity of a low-molecular-weight sulfated chitosan. Carbohydr Polym 62:327–332

Vongchan P, Sajomsang W, Subyen D, Kongtawelert P (2002) Anticoagulant activity of a sulfated chitosan. Carbohydr Res 337:1239–1242

Wan Ngah WS, Teong LC, Hanafiah MAKM (2011) Adsorption of dyes and heavy metal ions by chitosan composites: a review. Carbohydr Polym 83:1446–1456

Wang C, Zhang Z, Chen B, Gu L, Li Y, Yu S (2018a) Design and evaluation of galactosylated chitosan/graphene oxide nanoparticles as a drug delivery system. J Colloid Interface Sci 516:332–341

Wang H, Tang H, Liu Z, Zhang X, Hao Z, Liu Z (2014) Removal of cobalt(II) ion from aqueous solution by chitosan-montmorillonite. J Environ Sci (China) 26:1879–1884

Wang J-P, Chen Y-Z, Zhang S-J, Yu H-Q (2008) A chitosan-based flocculant prepared with gamma-irradiation-induced grafting. Bioresour Technol 99:3397–3402

Wang JW, Hon MH (2003) Sugar-mediated chitosan/poly(ethylene glycol)-beta-dicalcium pyrophosphate composite: mechanical and microstructural properties. J Biomed Mater Res A 64:262–272

Wang SF, Shen L, Zhang WD, Tong YJ (2005) Preparation and mechanical properties of chitosan/carbon nanotubes composites. Biomacromolecules 6:3067–3072

Wang X, Guan J (2018) Exploration of blood coagulation of *N*-alkyl chitosan nanofiber membrane *in vitro*. Biomacromolecules 19:731–739

Wang X et al (2016) Improvement in physical and biological properties of chitosan/soy protein films by surface grafted heparin. Int J Biol Macromol 83:19–29

Wang X, Ma J, Wang Y, He B (2002) Bone repair in radii and tibias of rabbits with phosphorylated chitosan reinforced calcium phosphate cements. Biomaterials 23:4167–4176

Wang X, Wang C (2016) Chitosan-poly(vinyl alcohol)/attapulgite nanocomposites for copper (II) ions removal: pH dependence and adsorption mechanisms. Colloids Surf A Physicochem Eng Asp 500:186–194

Wang X, Zheng Y, Wang A (2009) Fast removal of copper ions from aqueous solution by chitosan-g-poly(acrylic acid)/attapulgite composites. J Hazard Mater 168:970–977

Wang XH, Tian Q, Wang W, Zhang CN, Wang P, Yuan Z (2012) *In vitro* evaluation of polymeric micelles based on hydrophobically-modified sulfated chitosan as a carrier of doxorubicin. J Mater Sci Mater Med 23:1663–1674

Wang Y, Yang X, Yang J, Wang Y, Chen R, Wu J, Liu Y, Zhang N (2011) Self-assembled nanoparticles of methotrexate conjugated O-carboxymethyl chitosan: preparation, characterization and drug release behavior *in vitro*. Carbohydr Polym 86:1665–1670

Wang Y, Zhang X, Qiu D, Li Y, Yao L, Duan J (2018b) Ultrasonic assisted microwave synthesis of poly (chitosan-co-gelatin)/polyvinyl pyrrolidone IPN hydrogel. Ultrason Sonochem 40:714–719

Wen Y, Tan Z, Sun F, Sheng L, Zhang X, Yao F (2012) Synthesis and characterization of quaternized carboxymethyl chitosan/poly(amidoamine) dendrimer core–shell nanoparticles. Mater Sci Eng C 32:2026–2036

Wen Y, Yao F, Sun F, Tan Z, Tian L, Xie L, Song Q (2015) Antibacterial action mode of quaternized carboxymethyl chitosan/poly(amidoamine) dendrimer core-shell nanoparticles against *Escherichia coli* correlated with molecular chain conformation. Mater Sci Eng C 48:220–227

Westerink MA, Smithson SL, Srivastava N, Blonder J, Coeshott C, Rosenthal GJ (2001) ProJuvant (Pluronic F127/chitosan) enhances the immune response to intranasally administered tetanus toxoid. Vaccine 20:711–723

Westin CB, Trinca RB, Zuliani C, Coimbra IB, Moraes AM (2017) Differentiation of dental pulp stem cells into chondrocytes upon culture on porous chitosan-xanthan scaffolds in the presence of kartogenin. Mater Sci Eng C 80:594–602

Wolfrom ML, Han TMS (1959) The sulfonation of chitosan. J Am Chem Soc 81:1764–1766

Wong K, Sun G, Zhang X, Dai H, Liu Y, He C, Leong KW (2006) PEI-g-chitosan, a novel gene delivery system with transfection efficiency comparable to polyethylenimine *in vitro* and after liver administration *in vivo*. Bioconjug Chem 17:152–158

Wongpanit P, Sanchavanakit N, Pavasant P, Supaphol P, Tokura S, Rujiravanit R (2005) Preparation and characterization of microwave-treated carboxymethyl chitin and carboxymethyl chitosan films for potential use in wound care application. Macromol Biosci 5:1001–1012

Wu H, Wang J, Kang X, Wang C, Wang D, Liu J, Aksay IA, Lin Y (2009) Glucose biosensor based on immobilization of glucose oxidase in platinum nanoparticles/graphene/chitosan nanocomposite film. Talanta 80:403–406

Wu M, Guo K, Dong H, Zeng R, Tu M, Zhao J (2014a) *In vitro* drug release and biological evaluation of biomimetic polymeric micelles self-assembled from amphiphilic deoxycholic acid-phosphorylcholine-chitosan conjugate. Mater Sci Eng C 45:162–169

Wu M, Long Z, Xiao H, Dong C (2017) Preparation of *N,N,N*-trimethyl chitosan via a novel approach using dimethyl carbonate. Carbohydr Polym 169:83–91

Wu T, Farnood R, O'Kelly K, Chen B (2014b) Mechanical behavior of transparent nanofibrillar cellulose-chitosan nanocomposite films in dry and wet conditions. J Mech Behav Biomed Mater 32:279–286

Wu Y, Hisada K, Maeda S, Sasaki T, Sakurai K (2007) Fabrication and structural characterization of the Langmuir–Blodgett films from a new chitosan derivative containing cinnamate chromophores. Carbohydr Polym 68:766–772

Wu Z-C, Wang Z-Z, Liu J, Yin J-H, Kuang S-P (2016) Removal of cu(II) ions from aqueous water by l-arginine modifying magnetic chitosan. Colloids Surf A Physicochem Eng Asp 499:141–149

Xiang C, Zou Y, Sun LX, Xu F (2007) Direct electrochemistry and electrocatalysis of cytochrome c immobilized on gold nanoparticles-chitosan-carbon nanotubes-modified electrode. Talanta 74:206–211

Xiang Y, Si J, Zhang Q, Liu Y, Guo H (2008) Homogeneous graft copolymerization and characterization of novel artificial glycoprotein: chitosan-poly(L-tryptophan) copolymers with secondary structural side chains. J Polym Sci A 47:925–934

Xiao B, Wan Y, Wang X, Zha Q, Liu H, Qiu Z, Zhang S (2012) Synthesis and characterization of *N*-(2-hydroxy)propyl-3-trimethyl ammonium chitosan chloride for potential application in gene delivery. Colloids Surf B: Biointerfaces 91:168–174

Xie WM, Xu PX, Wang W, Liu Q (2002) Preparation and antibacterial activity of a water-soluble chitosan derivative. Carbohydr Polym 50:35–40

Xing K, Shen X, Zhu X, Ju X, Miao X, Tian J, Feng Z, Peng X, Jiang J, Qin S (2016a) Synthesis and *in vitro* antifungal efficacy of oleoyl-chitosan nanoparticles against plant pathogenic fungi. Int J Biol Macromol 82:830–836

Xing R, Liu S, Guo Z, Yu H, Zhong Z, Ji X, Li P (2008) Relevance of molecular weight of chitosan-*N*-2-hydroxypropyl trimethyl ammonium chloride and their antioxidant activities. Eur J Med Chem 43:336–340

Xing R, Liu S, Yu H, Guo Z, Li Z, Li P (2005) Preparation of high-molecular weight and high-sulfate content chitosans and their potential antioxidant activity *in vitro*. Carbohydr Polym 61:148–154

Xing R, Liu S, Yu H, Zhang Q, Li Z, Li P (2004) Preparation of low-molecular-weight and high-sulfate-content chitosans under microwave radiation and their potential antioxidant activity *in vitro*. Carbohydr Res 339:2515–2519

Xing Y, Xu Q, Che Z, Li X, Li W (2011) Effects of chitosan-oil coating on blue mold disease and quality attributes of jujube fruits. Food Funct 2:466–474

Xing Y, Xu Q, Li X, Chen C, Ma L, Li S, Che Z, Lin H (2016b) Chitosan-based coating with antimicrobial agents: preparation, property, mechanism, and application effectiveness on fruits and vegetables. Intl J Polym Sci 2016:24. https://doi.org/10.1155/2016/4851730

Xu C, Pan H, Jiang H, Tang G, Chen W (2008) Biocompatibility evaluation of *N,O*-hexanoyl chitosan as a biodegradable hydrophobic polycation for controlled drug release. J Mater Sci Mater Med 19:2525–2532

Xu Z, Neoh KG, Lin CC, Kishen A (2011) Biomimetic deposition of calcium phosphate minerals on the surface of partially demineralized dentine modified with phosphorylated chitosan. J Biomed Mater Res B 98:150–159

Yadav M, Parle M, Sharma N, Dhingra S, Raina N, Jindal DK (2017) Brain targeted oral delivery of doxycycline hydrochloride encapsulated tween 80 coated chitosan nanoparticles against ketamine induced psychosis: behavioral, biochemical, neurochemical and histological alterations in mice. Drug Deliv 24:1429–1440

Yan C, Chen D, Gu J, Qin J (2006) Nanoparticles of 5-fluorouracil (5-FU) loaded *N*-succinyl-chitosan (Suc-Chi) for cancer chemotherapy: preparation, characterization--*in-vitro* drug release and anti-tumour activity. J Pharm Pharmacol 58:1177–1181

Yan C, Gu J, Jing H, Taishi J, Lee RJ (2017) Tat-tagged and folate-modified *N*-succinyl-chitosan (tat-Suc-FA) self-assembly nanoparticle for therapeutic delivery OGX-011 to A549 cells. Mol Pharm 14:1898–1905

Yan H, Li H, Yang H, Li A, Cheng R (2013) Removal of various cationic dyes from aqueous solutions using a kind of fully biodegradable magnetic composite microsphere. Chem Eng J 223:402–411

Yang F, Wen X, Ke QF, Xie XT, Guo YP (2018) pH-responsive mesoporous ZSM-5 zeolites/chitosan core-shell nanodisks loaded with doxorubicin against osteosarcoma. Mater Sci Eng C 85:142–153

Yang J, Luo K, Li D, Yu S, Cai J, Chen L, Du Y (2013a) Preparation, characterization and *in vitro* anticoagulant activity of highly sulfated chitosan. Int J Biol Macromol 52:25–31

Yang J, Yu JH, Rudi Strickler J, Chang WJ, Gunasekaran S (2013b) Nickel nanoparticle-chitosan-reduced graphene oxide-modified screen-printed electrodes for enzyme-free glucose sensing in portable microfluidic devices. Biosens Bioelectron 47:530–538

Yang JH, Du YM, Wen Y, Li TY, Hu L (2003) Sulfation of Chinese lacquer polysaccharides in different solvents. Carbohydr Polym 52:397–403

Yang L, Xiong H, Zhang X, Wang S (2012) A novel tyrosinase biosensor based on chitosan-carbon-coated nickel nanocomposite film. Bioelectrochemistry 84:44–48

Yang Q, Wang L, Xiang W, Zhou J, Li J (2007) Grafting polymers onto carbon black surface by trapping polymer radicals. Polymer 48:2866–2873

Yang TC, Chou CC, Li CF (2005) Antibacterial activity of *N*-alkylated disaccharide chitosan derivatives. Int J Food Microbiol 97:237–245

Yazdani-Pedram M, Lagos A, Retuert PJ (2002) Study of the effect of reaction variables on grafting of polyacrylamide onto chitosan. Polym Bull 48:93–98

Yazdani-Pedram M, Retuert J, Quijada R (2000) Hydrogels based on modified chitosan, 1 - synthesis and swelling behavior of poly(acrylic acid) grafted chitosan. Macromol Chem Phys 201:923–930

YazdaniPedram M, Retuert J (1997) Homogeneous grafting reaction of vinyl pyrrolidone onto chitosan. J Appl Polym Sci 63:1321–1326

Yen HJ, Young YA, Tsai TN, Cheng KM, Chen XA, Chen YC, Chen CC, Young JJ, Hong PD (2018) Positively charged gold nanoparticles capped with folate quaternary chitosan: synthesis, cytotoxicity, and uptake by cancer cells. Carbohydr Polym 183:140–150

Yilmaz E, Adali T, Yilmaz O, Bengisu M (2007) Grafting of poly(triethylene glycol dimethacrylate) onto chitosan by ceric ion initiation. React Funct Polym 67:10–18

Yin L, Ding J, Zhang J, He C, Tang C, Yin C (2010) Polymer integrity related absorption mechanism of superporous hydrogel containing interpenetrating polymer networks for oral delivery of insulin. Biomaterials 31:3347–3356

Yin L, Fei L, Cui F, Tang C, Yin C (2007) Superporous hydrogels containing poly(acrylic acid-co-acrylamide)/O-carboxymethyl chitosan interpenetrating polymer networks. Biomaterials 28:1258–1266

Yinsong W, Lingrong L, Jian W, Zhang Q (2007) Preparation and characterization of self-aggregated nanoparticles of cholesterol-modified *O*-carboxymethyl chitosan conjugates. Carbohydr Polym 69:597–606

Yokogawa Y, Paz Reyes J, Mucalo MR, Toriyama M, Kawamoto Y, Suzuki T, Nishizawa K, Nagata F, Kamayama T (1997) Growth of calcium phosphate on phosphorylated chitin fibres. J Mater Sci Mater M 8:407–412

Yoshikawa S, Takayama T, Tsubokawa N (1998) Grafting reaction of living polymer cations with amino groups on chitosan powder. J Appl Polym Sci 68:1883–1889

Yoshioka H, Nonaka K, Fukuda K, Kazama S (1995) Chitosan-derived polymer-surfactants and their micellar properties. Biosci Biotechnol Biochem 59:1901–1904

You J, Li X, de Cui F, Du YZ, Yuan H, Hu FQ (2008) Folate-conjugated polymer micelles for active targeting to cancer cells: preparation, *in vitro* evaluation of targeting ability and cytotoxicity. Nanotechnology 19:045102

Youn RG, Ryual RS, Doung JH, Uk JB (2004) Synthesis and characterization of beta-poly(glucose-amine)*N*-(2,3-dihydroxypropyl) derivatives as medical care and biological joint material. Family 2. Tri or tetra-sulfated beta-chitosan. Macromol Symp 216:47–54

Yu H, Chen X, Lu T, Sun J, Tian H, Hu J, Wang Y, Zhang P, Jing X (2007) Poly(L-lysine)-graft-chitosan copolymers: synthesis, characterization, and gene transfection effect. Biomacromolecules 8:1425–1435

Yu HC, Zhang H, Ren K, Z Y, Zhu F, Qian J, Ji J, Wu ZL, Zheng Q (2018a) Ultrathin kappa-carrageenan/chitosan hydrogel films with high toughness and antiadhesion property. ACS Appl Mater Interfaces 10:9002–9009

Yu JG, Huang KL, Tang JC, Yang Q, Huang DS (2009) Rapid microwave synthesis of chitosan modified carbon nanotube composites. Int J Biol Macromol 44:316–319

Yu JM et al (2014) Preparation and characterization of galactosylated glycol chitosan micelles and its potential use for hepatoma-targeting delivery of doxorubicin. J Mater Sci Mater Med 25:691–701

Yu L, Gong J, Zeng C, Zhang L (2013) Preparation of zeolite-a/chitosan hybrid composites and their bioactivities and antimicrobial activities. Mater Sci Eng C 33:3652–3660

Yu L, He Y, Bin L, Yue'e F (2003) Study of radiation-induced graft copolymerization of butyl acrylate onto chitosan in acetic acid aqueous solution. J Appl Polym Sci 90:2855–2860

Yu Y, Chen R, Sun Y, Pan Y, Tang W, Zhang S, Cao L, Yuan Y, Wang J, Liu C (2018b) Manipulation of VEGF-induced angiogenesis by 2-*N*, 6-*O*-sulfated chitosan. Acta Biomater 71:510–521

Yuan G, Chen X, Li D (2016) Chitosan films and coatings containing essential oils: the antioxidant and antimicrobial activity, and application in food systems. Food Res Int 89:117–128

Yucel Falco C, Falkman P, Risbo J, Cardenas M, Medronho B (2017) Chitosan-dextran sulfate hydrogels as a potential carrier for probiotics. Carbohydr Polym 172:175–183

Yudin VE, Dobrovolskaya IP, Neelov IM, Dresvyanina EN, Popryadukhin PV, Ivan'kova EM, Elokhovskii VY, Kasatkin IA, Okrugin BM, Morganti P (2014) Wet spinning of fibers made of chitosan and chitin nanofibrils. Carbohydr Polym 108:176–182

Zarghami Z, Akbari A, Latifi AM, Amani MA (2016) Design of a new integrated chitosan-PAMAM dendrimer biosorbent for heavy metals removing and study of its adsorption kinetics and thermodynamics. Bioresour Technol 205:230–238

Zeng S, Liu L, Shi Y, Qiu J, Fang W, Rong M, Guo Z, Gao W (2015) Characterization of silk fibroin/chitosan 3d porous scaffold and *in vitro* cytology. PLoS One 10:e0128658

Zhang B, Yang X, Li P, Guo C, Ren X, Li J (2018a) Preparation of chitosan sulfate and vesicle formation with a conventional cationic surfactant. Carbohydr Polym 183:240–245

Zhang C, Chen Z, Guo W, Zhu C, Zou Y (2018b) Simple fabrication of chitosan/graphene nanoplates composite spheres for efficient adsorption of acid dyes from aqueous solution. Int J Biol Macromol 112:1048–1054

Zhang C, Ping QN, Zhang HJ, Jian S (2003) Preparation of *N*-alkyl-O-sulfate chitosan derivatives and micellar solubilization of taxol. Carbohydr Polym 54:137–141

Zhang J, Chen XG, Li YY, Liu CS (2007) Self-assembled nanoparticles based on hydrophobically modified chitosan as carriers for doxorubicin. Nanomedicine 3:258–265

Zhang J, Chen XG, Peng WB, Liu CS (2008) Uptake of oleoyl-chitosan nanoparticles by A549 cells. Nanomedicine 4:208–214

Zhang J, Jin Y, Wang A (2011) Rapid removal of Pb(II) from aqueous solution by chitosan-g-poly (acrylic acid)/attapulgite/sodium humate composite hydrogels. Environ Technol 32:523–531
Zhang L, Liu T, Xiao Y, Yu D, Zhang N (2015a) Hyaluronic acid-chitosan nanoparticles to deliver gd-dtpa for mr cancer imaging. Nano 5:1379–1396
Zhang MG, Smith A, Gorski W (2004) Carbon nanotube-chitosan system for electrochemical sensing based on dehydrogenase enzymes. Anal Chem 76:5045–5050
Zhang N, Wardwell PR, Bader RA (2014a) *In vitro* efficacy of polysaccharide-based nanoparticles containing disease-modifying antirheumatic drugs. Pharm Res 31:2326–2334
Zhang X, Li Y, Sun X, Kishen A, Deng X, Yang X, Wang H, Cong C, Wang Y, Wu M (2014b) Biomimetic remineralization of demineralized enamel with nano-complexes of phosphorylated chitosan and amorphous calcium phosphate. J Mater Sci Mater Med 25:2619–2628
Zhang Y, Yan W, Sun Z, Pan C, Mi X, Zhao G, Gao J (2015b) Fabrication of porous zeolite/chitosan monoliths and their applications for drug release and metal ions adsorption. Carbohydr Polym 117:657–665
Zhang Z, Cai H, Liu Z, Yao P (2016) Effective enhancement of hypoglycemic effect of insulin by liver-targeted nanoparticles containing cholic acid-modified chitosan derivative. Mol Pharm 13:2433–2442
Zhang Z, Jin F, Wu Z, Jin J, Li F, Wang Y, Wang Z, Tang S, Wu C, Wang Y (2017) *O*-acylation of chitosan nanofibers by short-chain and long-chain fatty acids. Carbohydr Polym 177:203–209
Zheng XF, Lian Q, Yang H, Wang X (2016) Surface molecularly imprinted polymer of chitosan grafted poly(methyl methacrylate) for 5-fluorouracil and controlled release. Sci Rep 6:21409. https://doi.org/10.1038/srep21409
Zheng Y, Yang W, Wang C, Hu J, Fu S, Dong L, Wu L, Shen X (2007) Nanoparticles based on the complex of chitosan and polyaspartic acid sodium salt: preparation, characterization and the use for 5-fluorouracil delivery. Eur J Pharm Biopharm 67:621–631
Zheng Y, Yi Y, Qi Y, Wang Y, Zhang W, Du M (2006) Preparation of chitosan-copper complexes and their antitumor activity. Bioorg Med Chem Lett 16:4127–4129
Zhou G, Wang KP, Liu HW, Wang L, Xiao XF, Dou DD, Fan YB (2018) Three-dimensional polylactic acid@graphene oxide/chitosan sponge bionic filter: highly efficient adsorption of crystal violet dye. Int J Biol Macromol 113:792–803
Zhou L, Jin J, Liu Z, Liang X, Shang C (2011) Adsorption of acid dyes from aqueous solutions by the ethylenediamine-modified magnetic chitosan nanoparticles. J Hazard Mater 185:1045–1052
Zhou Y, Dong P, Wei Y, Qian J, Hua D (2015) Synthesis of poly(sulfobetaine methacrylate)-grafted chitosan under gamma-ray irradiation for alamethicin assembly. Colloids Surf B: Biointerfaces 132:132–137
Zhou YY, Du YZ, Wang L, Yuan H, Zhou JP, Hu FQ (2010) Preparation and pharmacodynamics of stearic acid and poly (lactic-co-glycolic acid) grafted chitosan oligosaccharide micelles for 10-hydroxycamptothecin. Int J Pharm 393:143–151
Zhu A, Wang S, Yuan Y, Shen J (2002) Cell adhesion behavior of chitosan surface modified by bonding 2-methacryloyloxyethyl phosphorylcholine. J Biomater Sci Polym Ed 13:501–510
Zhu X, Su M, Tang S, Wang L, Liang X, Meng F, Hong Y, Xu Z (2012) Synthesis of thiolated chitosan and preparation nanoparticles with sodium alginate for ocular drug delivery. Mol Vis 18:1973–1982
Zupančič Š, Potrč T, Baumgartner S, Kocbek P, Kristl J (2016) Formulation and evaluation of chitosan/polyethylene oxide nanofibers loaded with metronidazole for local infections. Eur J Pharm Sci 95:152–160

Part II
Aminosugar-Based Exopolysaccharides: Glucosaminoglycans

Chapter 4
Hyaluronan: Structure, Metabolism, and Biological Properties

Alberto Passi and Davide Vigetti

Abstract The unique role of hyaluronan (HA) in mammal life can be easily understood considering that the first reaction in mammals involves this molecule. In fact, the spermatozoa, before fertilization, use a specific hyaluronidase to digest a large stratum of HA surrounding the oocyte in order to reach it. HA is an extracellular matrix polymer with extraordinary structure and functions: it is a simple, linear, and unbranched polymer chain without sulfate or phosphate groups. Nevertheless, it has a key role in several physiological and pathophysiological processes in mammals. HA is ubiquitous in mammalian tissues with several specific functions, such as influencing cell proliferation and migration, angiogenesis, and inflammation. Considering the simple structure of HA, to exert several important functions in tissues, this polymer can only be modified in its concentration and size. Hence, HA content in tissues is carefully controlled by different mechanisms, including covalent modification of the synthetic enzymes and epigenetic control of their gene expression. HA function is also critical in several diseases including cancer, diabetes, and chronic inflammation. Among these biological roles, the biophysical properties of HA allow its use as a hydrogel in regenerative medicine, cosmetics, and drug delivery. HA takes advantage from its capacity to form gels even at the concentration of 1% producing non-immunogenic scaffolds with very intriguing mechanical properties. The HA hydrogels are useful tools in regenerative medicine as biocompatible material for advanced therapeutic uses, also as drug delivery system.

4.1 Introduction

4.1.1 Structure

Hyaluronan (HA) is the simplest glycosaminoglycan (GAG) present in nature. Even though characterized by a simple linear chain, it has several important biomechanical

A. Passi (✉) · D. Vigetti
Department of Medicine and Surgery, University of Insubria, Varese, Italy
e-mail: alberto.passi@uninsubria.it

E. Cohen, H. Merzendorfer (eds.), *Extracellular Sugar-Based Biopolymers Matrices*,
Biologically-Inspired Systems 12, https://doi.org/10.1007/978-3-030-12919-4_4

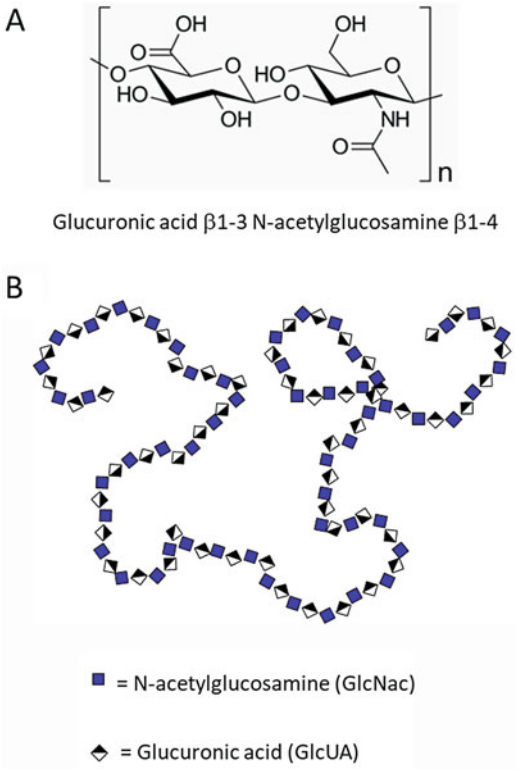

Fig. 4.1 HA chemical structure. (**a**) The hyaluronan disaccharide is composed of D-glucuronic acid and D-*N*-acetylglucosamine linked together with β-1-3 and β-1-4 glycosidic bonds, respectively. This disaccharide can be repeated up to thousands of times to give high molecular mass HA. (**b**) Schematic representation of HA disaccharide by using the symbol nomenclature for graphical representations of glycans (Varki et al. 2015)

properties. First it has terrific hydrophilic properties, in fact, 1 g of this polymer can interact with several liters of water, and this influences most of the biomechanical properties of the polymer (Laurent and Fraser 1992). HA is a polymer constituted by disaccharide units of D-glucuronic acid (GlcUA) linked to *N*-acetyl-D-glucosamine (GlcNAc) with a glucuronic beta 1–3 linkage between GlcUA and GlcNAc and a hexosaminidic bond beta 1–4 between GlcNAc and GlcUA (Fig. 4.1, panel A). The disaccharide unit can interact with 25 water molecules and is repeated till 25,000 times; hence, the HA chain reaches a molecular mass of millions of Dalton generating a linear polymer with a molecular mass ranging from 5×0^5 to 5×0^6 Da and more (Fig. 4.1, panel B) (Fraser et al. 1997; Viola et al. 2015b). The synthesis of HA is peculiar: it is the only GAG produced on the cell membrane and immediately extruded in the extracellular matrix (ECM) without any protein linkage. The other GAGs are produced inside the Golgi and secreted in the ECM or exposed on the cell membrane linked to the protein core constituting proteoglycans.

The enzymes involved in HA synthesis are located on the cellular membrane and are structurally organized to extrude the polymer outside of the cell in the ECM. These enzymes are called hyaluronan synthases (HASes) and in mammals are present as three different isoforms: HAS1, 2, and 3. The isoforms are coded on different chromosomes, and these genes could be a product of an ancestral gene duplication, which can explain the specific evolutionary path of this molecule

(Spicer and McDonald 1998). Until now, scarce information is available on the structure of these enzymes, as they have never been crystallized. HA is widely distributed in mammals and in few bacteria and considering the other GAGs or structural-related carbohydrate polymers as chitin and cellulose, interestingly, appeared late in the evolution (Csoka and Stern 2013).

HASes use the UDP-sugar precursors (UDP-GlcUA and UDP-GlcNAc) to produce HA chain picking up these molecules from the cytoplasm. In these enzymes, the presence of a double catalytic domain to interact with the two different substrates generating the disaccharide units necessary to create the polymer is of remarkable interest. The kinetic of the HASes has been extensively studied, even though, without crystallography information, all kinetic explanations are still hypothetical (Weigel and DeAngelis 2007).

The presence of three different enzymes to produce HA raised the question if each specific enzyme shows unique kinetic properties, and it has been proposed that the different enzymes can produce polymers with different length and at different rates (Itano and Kimata 2002; Viola et al. 2015a, b; Vigetti et al. 2015). Beside the chain length, a large body of evidences supports the idea that the HASes also differ between each other in the regulation of their catalytic activity. Only HAS2 has several covalent regulations, as phosphorylation (Suzuki et al. 1995; Vigetti et al. 2011a), O-GlcNAcylation (Vigetti et al. 2012), and ubiquitination (Karousou et al. 2010). Indeed, in the case of HAS3, its activity is regulated by its sorting to the cell membrane by interaction with Rab10 (Deen et al. 2014).

To exert its biological properties, HA requires specific interactions with receptors which not only regulate the cell-ECM interactions but trigger intracellular signaling. Beside receptors, other proteins can interact with HA and regulate tridimensional ECM structure. In general, all proteins that interact with HA are defined "hyaloadherins" including not only receptors but also proteoglycans and other ECM molecules (Tammi et al. 2011). Proteoglycans as aggrecan, neurocan, brevican, and versican can be included among these ECM molecules interacting with HA-forming networks that act as an architectural scaffold (Laurent and Fraser 1992). The biological functions of HA in tissues are due to its interactions with these "hyaloadherins." Such proteins are receptors (i.e., CD44, RHAMM, LYVE-1, Layilin, Stabilin 1, and HARE) and, in fact, can trigger specific intracellular signaling (for a review on this issue, see (Day and Prestwich 2002)) or receptors that mediate endocytosis and degradation of HA. Proteins can interact with HA by using the LINK module or Bx7B motif (Day and Prestwich 2002; Baggenstoss et al. 2017). Interestingly, TLR2/4 was recently described as an HA-binding receptor, even though it does contain neither the LINK module nor the BX7B motif. TLR2/4 is necessary to trigger the response after LMW-HA stimulation; however this process is still controversial (Cyphert et al. 2015). Although the physical direct interaction between TLR and HA is still not experimentally demonstrated, it is reasonable that the polyanionic nature of HA mimics the canonical ligands of TLR2/4 as lipopolysaccharides. HA and PG LiNk protein family (HAPLN1–4) has been described to interact with HA and PG stabilizing such multicomponent complexes (Day and Prestwich 2002).

The most common HA receptor is CD44, a proteoglycan widely distributed in different cells and particularly concentrated on the membranes of inflammatory and cancer cells (Toole 2004). Another important HA receptor related to cell motility is RHAMM. RHAMM is an acronym for *r*eceptor for *h*yaluronan-*m*ediated *m*otility; the receptor is also known as CD168. RHAMM has been found in several cell types, including cancer and endothelial cells (Hardwick et al. 1992; Savani et al. 2001). Interaction between HA and RHAMM triggers a signaling pathway not completely described which includes ras oncogene activity (Hall and Turley 1995; Hofmann et al. 1998; Tolg et al. 2006). It is also known that RHAMM and CD44 share ERK1/2 phosphorylation cascade activation (Tolg et al. 2006).

Even though HA is typically present in mammalian ECM, it is also described in few bacteria, which probably imported the genes from mammals during evolution. It is noteworthy that HA-producing bacteria use three genes, which encode UDP-glucose pyrophosphorylase (*hasC*), UDP-glucose dehydrogenase (*hasB*), and HA synthase (*hasA*), and these genes are arranged in an operon (Weigel and DeAngelis 2007; Weigel et al. 2013).

Interestingly, microorganisms such as *Streptococcus uberis*, *Streptococcus equisimilis*, *Streptococcus pyogenes*, and *Pasteurella multocida* (pathogens for humans and other vertebrates) evolved with the capacity to produce a HA capsule which acts as a shield-protecting bacteria from the immune system (Lee and Spicer 2000). Bacterial and vertebrate HA present the same structure with the same biomechanical properties and absence of immunogenic activity, which represents a major advantage in medical applications.

In the last decade, HA started to be considered more than a passive molecule, characterized by remarkable mechanical properties, including space filler and molecular sieving. Due to its biological properties, this GAG emerged among the most biologically active relevant molecules in the body. HA plays a key role in several physiological processes including development (Vigetti et al. 2006), wound healing (Motolese et al. 2013), cell migration (Vigetti et al. 2009b), and proliferation (Vigetti et al. 2011b). It is also involved in several pathologies, such as cancer (Toole 2004), vascular diseases (Merrilees et al. 2011; Bollyky et al. 2012; Vigetti et al. 2014d), and diabetes (Bollyky et al. 2012).

4.1.2 Discovery of Hyaluronan

The first description of HA was done by Carl Meyer (Meyer and Palmer 1934), who purified the polymer from corpus vitreous of the eye. In the next years, HA was found in other tissues, and today it is known to be present in almost all mammalian tissues. The first described property for HA is its dramatic capacity to interact with water, and, because of that, most of the initial hypotheses for HA role in tissues were related to this hydrophilic characteristic. Hence, the main function attributed to HA is ECM space filler and organizer. HA presence in synovial fluid suggested its role as a lubricant in the joints. This observation is based on the first clinical application of

HA in visco-supplementation in joint disease. Until now, this therapy represents one of the most common HA applications in humans. The polymer rheology is strongly dependent on its size and concentration, and pharmaceutical companies are induced to produce specific HA solutions with defined rheology for specific applications. The use of bioreactors with genetically modified bacteria for the production of highly pure HA opened the field to HA-focused biotechnology. This technology dramatically changed the field and is now considered obsolete for the presence of tissue contaminants.

The human body contains more than 15 g HA, mainly located in the dermis. HA turnover is fast; about 30% of the molecule is replaced daily (Stern 2004). The human body finely regulates HA production, and the polymer is mainly removed through the lymphatic system to the liver. Polymer size is critical for HA biological function. In healthy tissues, a typical HA size is, approximately, 1×10^3 kDa, and this is considered high molecular weight HA (HMWHA). The relationship between size and biological functions is confirmed by recent literature describing a very HMWHA in naked mole rat (Tian et al. 2013), an animal with an incredible longevity and cancer resistance.

HA fast degradation rate is due to the activity of a class of enzymes called hyaluronidases, hydrolases which degrade HA in small fragments, named oligosaccharides (Stern 2004; Stern et al. 2007). It was recently demonstrated that HA oligosaccharides exert important biological functions in tissues (Stern et al. 2006). HA fragments are usually internalized into cells and destroyed within lysosomes. When oligosaccharide concentration exceeds the cell capacity to properly remove these fragments from ECM, they accumulate and trigger important biological processes, inducing angiogenesis and inflammation and changing cell behavior (Bohaumilitzky et al. 2017). Besides hyaluronidase activity, there are other processes of HA depolymerization, including exposure to UV radiation and free radicals. Moreover, tissue HA content is critical, and its reduction, such as in aging, dramatically influences the viscoelastic properties of the tissues. Several years ago, it was described that HA decrease in synovial fluid represents joint disease marker (Dicker et al. 2014). Figure 4.2 summarizes HA metabolic roles.

4.1.3 Biological Properties of Hyaluronan

HA presents a simple linear structure and exerts several functions by the sole modification of its size and concentration (Stern et al. 2006; Dicker et al. 2014). As previously described, high molecular weight and concentration can protect animals from aging and cancer development (Tian et al. 2013). Interestingly, HA fragments present biological relevance and often an opposite effect compared to the high molecular weight intact molecule (Erickson and Stern 2012).

The presence of HA oligos in specific conditions gained great interest, producing an increasing body of literature that describes HA fragments as ligands for toll-like receptors (TLR), triggering specific inflammatory pathways (Jiang et al. 2005, 2011;

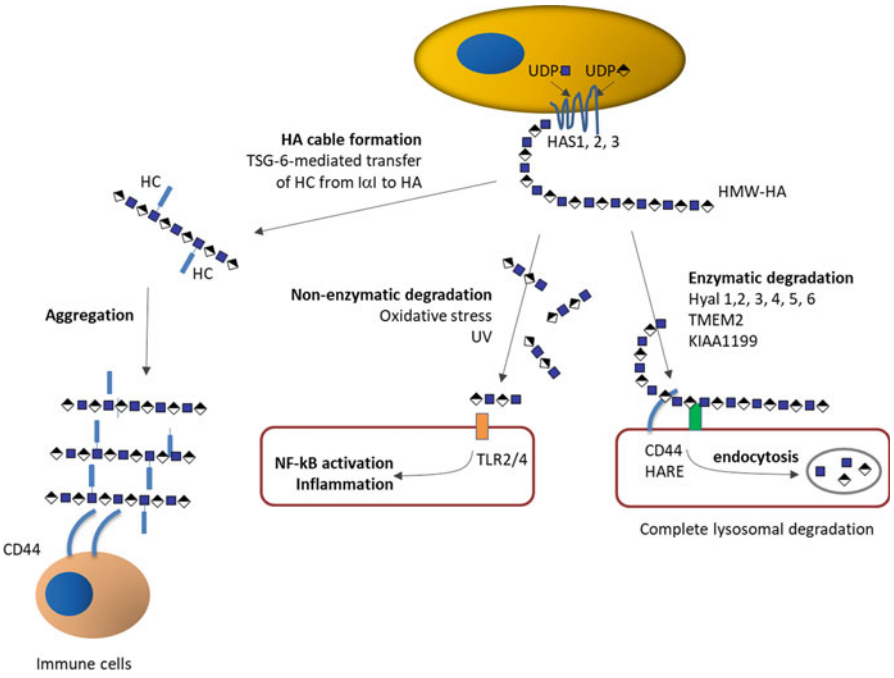

Fig. 4.2 Schematic representation of HA metabolism. HA is synthesized by HAS1, 2, or 3, located in the plasma membrane that uses cytosolic UDP-GlcUA and UDP-GlcNAc as precursors. HASes catalyze the formation of a high molecular weight HA (HMWHA) that can remain associated to the enzyme (contributing to form the pericellular coat) or can be released in to ECM. During inflammation HA can be covalently bond with the heavy chains (HC) of inter-alpha-inhibitor (I-alpha-I). TSG6 catalyzes the transfer reaction of HC to the hydroxyl group of C6 of GlcNAc. Modified HA can form aggregates that under microscopy look like cables that possess the ability to interact and recruit monocytes via CD44. HA can be fragmented both via enzymatic reactions (catalyzed by different HA-degrading enzymes) and via nonenzymatic reactions (i.e., UV and ROS). Low molecular weight HA can be further internalized in the cell and completely degraded in lysosomes throughout receptor CD44 and HARE. Alternatively, LMW-HA can also trigger inflammation via activation of TLRs and NF-kB

Iijima et al. 2011). In an opposite way, HMWHA shows anti-angiogenic, immune-suppressive, and anti-inflammatory activities, inducing tissue-reparative processes, as described in wound healing (Jiang et al. 2011; Motolese et al. 2013). HA oligosaccharides below 200 kDa show the capacity to induce inflammatory processes, as well as, angiogenesis through the interactions with specific receptors (Day and Prestwich 2002; Iijima et al. 2011). Considering the latter properties, HA oligosaccharides can be considered part of the alarmin protein family (Gariboldi et al. 2008).

The biological activities of both HMWHA and oligosaccharides are mediated by cell-surface receptors (Sherman et al. 1994). HA functions depend on its structural properties. Hydrophilic properties mediate water content control in all tissues. One of the most important HA biological functions is to maintain a well-hydrated ECM

and a perfect environment for cell migration and proliferation (Vigetti et al. 2006). The presence of a well-hydrated and soft ECM is critical for embryo development; in fact, oocytes' microenvironment is mainly constituted of HA (Fenderson et al. 1993). The unique viscoelastic properties of HA have critical roles in the biomechanical functions of various tissues, from corpus vitreous to derma (Fraser et al. 1997). It is of remarkable importance to consider that HA presents a gel form when its concentration is above 1%, a concentration often reached in mammalian tissues. The space between epidermal keratinocytes, the synovial fluid, and the Wharton jelly from umbilical cords are examples of gel-like structures formed by high HA concentration, in which this polymer plays the role of space filler and shock-absorbing macromolecule (Raio et al. 2005; Viola et al. 2015b).

HMWHA and HA oligosaccharides' biological activities are mediated by their specific receptors. CD44, the most abundant HA receptor, triggers ERK 1/2 activation (Itano 2008; Jeyapalan et al. 2011). CD44/HA interactions have been studied in inflammatory cells, where HA is able to interact with inflammatory cell receptors (CD44) to block cells in the inflamed area (Jiang et al. 2005, 2007, 2011). The signaling cascade triggered by CD44/HA includes PI3K/PDK1/Akt activation and Ras phosphorylation, which involves RAF1, MEK, and, eventually, Erk1/2 (Vigetti et al. 2008b). CD44/HA complexes recruit other cytoplasmic proteins, such as ezrin, merlin, and erbB1/2 (Toole 2004).

HA binding to CD44 is critical for cell adhesiveness, triggering the phosphorylation of CD44 cytoplasmic domain, which is also required for cell migration and infiltration (Jiang et al. 2007). CD44 signaling also participates in wound healing, influencing fibroblast migration into the wounded area from perilesional stroma (Clark et al. 2004). It is evident that CD44 does not directly regulate cell migration; however, its activation by HMWHA promotes the wound healing process. Moreover, the directionality of cell migration is strongly dependent on CD44 expression and on HA gradient in the ECM environment (Acharya et al. 2008).

RHAMM has been described in cancer cells and in endothelial cells (Hardwick et al. 1992; Savani et al. 2001). Several studies report that RHAMM plays a critical role in cell migration and inflammation and in tissue healing (Tolg et al. 2003; Zaman et al. 2005).

Stabilin 2, also known as HARE, an acronym for "hyaluronan receptor for endocytosis," was initially described in endothelial cells in lymph nodes, the spleen, and the liver (Zhou et al. 2000; Nonaka et al. 2007). More recently, HARE has been described in the eye, brain, kidney, and heart. HARE also interacts with other GAGs, such as chondroitin sulfates (A, B, C, D, and E) (Harris et al. 2007). HARE is mainly implicated in HA endocytosis and localizes close to clathrin clusters in the cell membrane. Finally, HARE in endocytosis is well reported; however, its involvement in lysosomal pathways is still not clear, and information on its activity at molecular level is scarce (Zhou et al. 2002, 2003).

Lymphatic vessel endothelial hyaluronan receptor 1 (LYVE 1) is a HA receptor specifically expressed on lymphatic endothelial cells, also found in lymph nodes and sinusoidal endothelial cells in the liver (Prevo et al. 2001; Mouta Carreira et al. 2001; Wróbel et al. 2005). Due to this peculiar cell distribution, LYVE 1 is generally

considered a molecular marker for lymphatic endothelial cells (Akishima et al. 2004). LYVE 1 interacts with HA, and the resulting complex receptor/HA can be internalized and digested in lysosomes (Johnson et al. 2007). LYVE 1 main function is HA absorption and transfer from tissues to the lymph acting as a regulator of tissue hydration. LYVE 1 abrogation from lymphatics generated animals with normal physiology, indicating that other still unknown receptors may rescue LYVE 1 activity in mammals (Gale et al. 2007).

A large body of evidence supports the role of toll-like receptors (TLRs) in HA signaling. TLRs belong to the innate immunity system and are expressed on the plasma membrane of all mammalian cells (Aderem and Ulevitch 2000; Takeda et al. 2003). Humans produce ten TLRs, and those involved in HA signaling are TLR2 and 4 (Jiang et al. 2011), TLR2 being able to interact with mycobacteria and Gram-positive bacteria, whereas TLR4 recognizes lipopolysaccharide (LPS). In macrophages, HA triggers, via TLR2 or TLR4, a signaling cascade that promotes expression of chemokine genes, and this process is strongly dependent on MyD88 (Jiang et al. 2011). The signaling triggered by TLR/HA strongly depends on HA size. TLR clustering on the cell membrane is promoted by interaction with HMWHA, and this complex induces cell survival. In an opposite fashion, HA oligosaccharides induce inflammatory stress and cell death (Jiang et al. 2011). It is important to note that the direct interaction between HA and TLR is not completely resolved and further experiments must be performed. HA oligosaccharides also induce dendritic cell maturation and TNF-alpha synthesis through the phosphorylation of MAPK and NF-kB nuclear translocation. HA oligosaccharides are also involved in transplant rejection demonstrating their involvement in alloimmunity (Tesar et al. 2006). The synthesis of IL-8 and MMP2 is also stimulated by HA/TLR4 interaction (Voelcker et al. 2008). Moreover, during osteoclast differentiation, HA/TLR4 interaction blocks the signaling triggered by macrophage colony-stimulating factor (M-CSF) (Chang et al. 2007). The role of HA oligosaccharides in the gut has been recently described as inducers of beta-defensin-2 synthesis in intestinal epithelium (Hill et al. 2012). HA oligosaccharide role in defensin synthesis has remarkable importance in tissue metabolism and wound healing. In fact, defensins are a family of small proteins with antibiotic properties and capacity to stimulate tissue regeneration (Gariboldi et al. 2008; Hill et al. 2012).

In tissues, HA degradation rate regulates HA concentration. Mammals present six hyaluronidases (Hyal-1, -2, -3, -4, P1, and PH20) which catalyze the hydrolysis of linkage bonds beta1-4 between hexosamine and glucuronic acid residues. The hyaluronidases (Hyals) are classified as endo-beta-*N*-acetylglucosaminidases according to their hydrolytic mechanisms (Csoka et al. 2001; Stern et al. 2007). All six Hyals in human are β, 1–4 endogalactosaminidases. The genes HYAL1, HYAL2, and HYAL3 code for the enzymes Hyal-1, Hyal-2, and Hyal-3 (Csoka et al. 2001; Soltés et al. 2006). These genes are tightly clustered on chromosome 3p21.3. Hyal-1 and -2 are the major hyaluronidases found in tissues. Hyal-1 is found in lysosomes, whereas Hyal-2 is a GPI-anchored protein with extracellular activity (Csoka et al. 2001). Hyal-2 produces HA fragments with a size of about 20 kDa. Hyal-1 appears to be a lysosomal protein which cleaves HA into small disaccharides. The role and activities of Hyal-3

are still elusive, and few information is available on this enzyme, such as its report from KO mice-based experiments (Dumaresq-Doiron et al. 2012).

Other three genes HYAL4, HYAL1, and SPAM1 (sperm adhesion molecule1) are clustered on chromosome 7q31.3. Hyal-4 is a pseudogene transcribed, but not translated, in the human, and PH-20 is the enzyme that digests oocyte-surrounding HA, facilitating ovum fertilization (Cherr et al. 2001). The Hyals (1–4) can work in acidic environment (about pH 3 and 4), whereas PH-20 and other hyaluronidases from insects and snakes' venoms are active at neutral pH (Girish and Kemparaju 2007). Hyal 1, common in mammalian tissues, is active intracellularly. Finally, Hyal-1 deficiency leads to a genetic disease called mucopolysaccharidosis type IX (Martin et al. 2008).

Hyaluronidase 2 (Hyal 2) is a GPI-anchored receptor operating in acidic microenvironment (Bourguignon et al. 2004). This enzyme degrades HMWHA into low molecular weight HA (LMW-HA) (about 20 kDa) (Stern 2004) which is internalized and further digested to smaller HA oligosaccharides (oligo-HA) by Hyal 1.

Interestingly, bacteria present several hyaluronidases which act as lyases (Csoka et al. 2001; Csoka and Stern 2013). In mammals, Hyal 1 and 2 activities are synergic; in fact, Hyal 2 degrades HA to fragments of 20 kDa, and, then, Hyal 1 degrades these fragments into smaller fragments of about 800 Da. HA polymer degradation could also be due to the action of free radicals that break HA polymer in fragments of unspecific size (Soltés et al. 2006). HA minimal size able to trigger cell response has been extensively addressed. It has been reported that 4-6 disaccharide units (4-6mers) oligomers are responsible for NF-kB signaling and metalloprotease synthesis (Voelcker et al. 2008); oligomers ranging from 4 to 16 disaccharides are able to activate dendritic cells via TLR receptors (Taylor et al. 2004; Takahashi et al. 2005).

Recently, a new hyaluronidase has been described: TMEM2, which is a transmembrane protein with strong hyaluronidase activity (Yamamoto et al. 2017; Yamaguchi et al. 2018). TMEM2 specifically degrades HMWHA into ~5-kDa fragments. Another hyaluronidase called CEMIP/KIAA1199 (also known as HYBID) has been recently identified with HA-degrading activity (Nagaoka et al. 2015; Yoshida et al. 2018). Interestingly, this enzyme has a key role in cancer development, in skin biology, and in cell senescence (Zhang et al. 2014b; Yoshida et al. 2018).

4.2 The Magic Glue: Hyaluronan and Its Oligosaccharide Chemical Structure

HA is a GAG polymer constituted by disaccharide units of D-glucuronic acid (GlcUA) linked to *N*-acetyl-D-glucosamine (GlcNAc) with a glucuronic beta 1–3 linkage between GlcUA and GlcNAc and a hexosaminidic beta bond 1-4 between GlcNAc and GlcUA. These units are repeated, approximately, 25,000 times to a molecular mass of millions of Daltons ranging from 5×10^5 to 5×10^6 Da and more

(Fraser et al. 1997; Viola et al. 2015b). The biotechnological properties of HA are unique and dependent on the structure of the polymer. HA structure is based on the presence of beta linkages which allows HA bulky groups (the hydroxyls, the carboxylate moiety, and the anomeric carbon on the adjacent sugar) to be in sterically favorable equatorial positions, favoring chemical modification. All axial positions, less favorable for chemical derivatization, are occupied by simple hydrogen atoms (Tamer 2013). When the polymer is in aqueous solution, a network of hydrogen bonds is established and maintains HA stiffness. The axial small hydrogens form a relatively hydrophobic environment, whereas the equatorial groups are more hydrophilic and interact with solvent, creating a twisting ribbon structure. In solution, HA forms an extended random coil structure, which can interact with other chains. Even at very low concentrations, soluble HA chains can entangle in each other. This phenomenon starts at 1 mg/mL and is a spontaneous process (Morris et al. 1980). HA helical chain in solution can bind 1000 times its weight in water (Cowman and Matsuoka 2005). At 1% HA forms a hydrogel with soft properties which allows handling using syringe with needles; it can be defined as a "quasi-plastic material" (Narins et al. 2003). Moreover, HA chains in solution can form double helices after and during entanglement (Scott et al. 1991). These physical aspects indicate HA hydrogel a perfect product with lubricant properties that can be used for replacing synovial fluid or in surgery to prevent postsurgical adhesion formation after abdominal surgery procedures.

HA hydrogel formation represents the most important property, allowing this molecule to be used as an innovative biocompatible product in several applications (Burdick and Prestwich 2011). HA solution viscosity increases with concentration, and its elasticity increases with polymer size. The relationship between elasticity and viscosity is two critical parameters used in commercial hyaluronan gel preparation (Edsman et al. 2012). The organ surface takes advantage from the rheological properties of HA, as in cartilage and in muscle bundles acting as osmotic buffer regulating the water content in the tissues (Simkovic 2013). From these viscoelastic properties arise the biomechanical characteristics for hydrogel medical applications (Jha et al. 2009; Bonafè et al. 2014). HA gels are useful tools for scaffold preparations in regenerative medicine. They are biodegradable, biocompatible, and bioresorbable. HA scaffolds induce cell differentiation and growth (Itano 2008) and improve wound healing without nonspecific absorption of proteins enhancing tissue growth and repair (Seyfried et al. 2005a, b; Damodarasamy et al. 2014). Preparation of highly purified HA is based on the applications of modern biotechnology procedures using bioreactors with genetically modified bacteria. The availability of large amounts of highly pure HA polymer introduces the possibility to treat arthritic joints, restoring lubrication and replacing the rheological properties of synovial fluid. HA chains can be chemically modified using adipic hydrazide, tyramide, benzyl ester, glycidyl methacrylate, thiopropionyl hydrazide, or bromoacetate, either at carboxylic acid of glucuronic acid or at the C-6 hydroxyl group of the *N*-acetylglucosamine (Darr and Calabro 2009). HA hydrogels can be used as drug delivery systems, as proposed in ophthalmology and otolaryngology (Lim et al. 2002; Välimäki 2015). HA hydrogels' main function is to facilitate in situ

drug release by HA degradation (Yang et al. 2012). In other in vivo models, the reabsorption of HA matrix is the mechanism used to produce new tissue in situ, stimulating cells with growth factors, such as BMP2 in cartilage (Jha et al. 2009).

4.3 Hyaluronan Biosynthesis Control

HA has a peculiar distribution in the human body with a rapid turnover. HA content is strictly regulated by cells in a finely tuned balance between synthetic and catabolic activities. Part of the polymer could also be removed from tissues by lymphatic system, which transport HA to liver for final degradation. Most oligosaccharides produced by hyaluronidase digestion are removed by cells through receptor-mediated internalization.

4.3.1 Formation of UDP-GlcNAc and UDP-Glucuronic Acid

The regulation of the HA synthesis includes mechanisms still poorly understood. One of them is substrate availability. It was demonstrated that substrate availability (UDP-sugars) influences HA synthesis. Altering UDP-sugars' availability in cytoplasm influenced HA production as well as expression of HAS2 and 3 (Vigetti et al. 2003b, 2006).

UDP-sugar precursors are molecules with a high-energy cost, competing with glycolysis and other catabolic pathways for their synthesis (see Fig. 4.3, panel A). Hence, GAG synthesis is possible in tissues with a good oxygen supply, as oxygen allows the two oxidative reactions necessary for UDP-GlcUA synthesis (Fig. 4.3, panel B). The synthesis of UDP-GlcUA is a critical step for all GAGs, except keratan sulfate (KS), which does not contain uronic acid. In fact, KS is usually common in tissues with poor oxygen supply or even without vascularization. The synthesis of UDP-GlcUA requires the action of the UDP-glucose dehydrogenase (UGDH), which produces UDP-GlcUA from precursor UDP-Glc (Fig. 4.3, panel B). This reaction is possible in the presence of NAD, which is transformed in NADH during the double oxidation of the C-6 of UDP-Glc. This uncommon reaction has a remarkable role in terms of cell energy balance. From this point of view, the costs of UDP-GlcUA synthesis are completely balanced by the re-oxidation in mitochondria of the two NADH molecules produced by the UDP-GlcUA synthesis. HA synthesis reaction stoichiometry indicates that the disaccharide units contain one molecule of GlcUA and one GlcNAc with a ratio of 1:1. The five ATP obtained by the re-oxidation of two NADH molecules in mitochondria balance the energy cost of HA-unsulfated backbone synthesis.

The modulation of UDP-GlcUA availability by overexpressing or silencing UGDH in cytoplasm can dramatically influence HA production, as well as expression of HAS2 and 3 (Vigetti and Passi 2014; Vigetti et al. 2003b, 2006, 2014b, c).

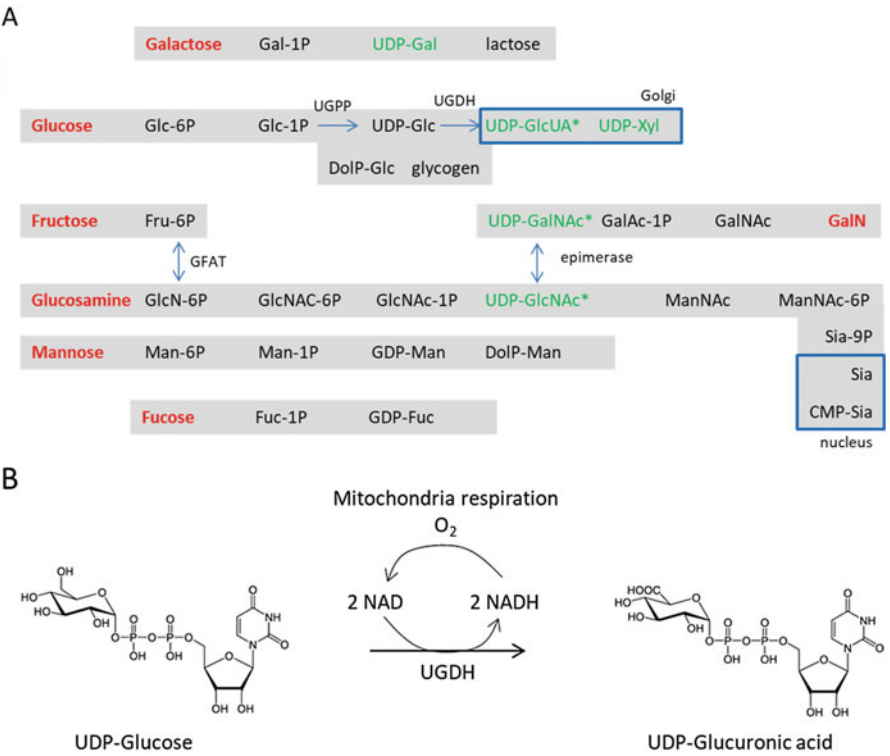

Fig. 4.3 (**a**) Schematic representation of the metabolism of dietary monosaccharides (in red) in the formation of activated sugar nucleotides used in biosynthesis of various glycans. UDP-sugars used for GAG and PG biosynthesis are shown in green. All reactions take place in the cytosol except for reaction boxed in blue. In this scheme almost all the enzymes have been omitted except for the critical enzymes involved in UDP-GlcUA synthesis (UGPP and UGDH), UDP-GlcNAc synthesis through the hexosamine biosynthetic pathway (GFAT), and UDP-GalNAc (epimerase) synthesis. These latter UDP-sugars will be further chemically modified in HS/heparin, CS, and KS biosynthesis. (**b**) Conversion of UDP-glucose to UDP-glucuronic acid by UGDH. In the scheme is highlighted the involvement of 2 NAD in the oxidation of the C6 of glucose with the generation of 2 NADH. The regeneration of NAD via the mitochondrial metabolism is critical to supply energy. The big red arrows highlight the double oxidation on C6

4-methylumbelliferone confirmed this aspect as it binds UDP-GlcUA, reducing the availability of this precursor (Viola et al. 2008; Vigetti et al. 2009b; Piccioni et al. 2012). Another way to regulate HA synthesis involves the activity of adenosine monophosphate-activated protein kinase (AMPK), the cell's energy level sensor. It was demonstrated that the activation of AMPK can phosphorylate HAS2 threonine 110 residue, blocking enzyme activity (Vigetti et al. 2011a). It is remarkable that this kind of regulation is specific only for HAS2 and does not influence the other two enzymes. Moreover, this regulation only affects HA production, leaving other GAGs' synthesis unaltered. This observation correlates a cell's energy level with its specific capacity to produce HA.

4.3.2 Regulation of the UDP-Sugar Precursors Concentration in Cytoplasm

As discussed previously the first HA synthesis regulation level is UDP-sugar availability in cytoplasm. The substrate for glycosyltransferases used to synthesize all the glycans (i.e., GAGs, as well as, glycoproteins and glycolipids) is nucleotide-activated sugars. UDP is the most common nucleotide used to activate sugars in animal cells, as it is found linked to glucose (Glc), galactose (Gal), *N*-acetylated glucosamine (GlcNAc), *N*-acetylated galactosamine (GalNAc), glucuronic acid (GlcA), and xylose (Xyl). Only two additional nucleotides are used in animals, GDP that is linked to mannose (Man) and fucose (Fuc) and CMP that is linked to sialic acid (Sia) (Fig. 4.3, panel A) (Yarema and Bertozzi 2001). It is to be noted that all the substrates for glycoconjugate reactions are sugar nucleotides generated mainly in the cytosol, with the exception for the synthesis of UDP-Xyl and CMP-Sia that take place in the Golgi and in the nucleus, respectively (Fig. 4.3, panel A). Further, these sugar-nucleotide precursors are transported in the ER/Golgi by specialized transporters (Gerardy-Schahn et al. 2001; Hadley et al. 2014). This point is crucial, as it allows the creation of two precursor pools: one in the cytosol and the other inside the ER/Golgi. Although the real concentration of the sugar nucleotides in these two pools is not easily measurable, it is reasonable to suppose that ER/Golgi precursors would be in higher concentration than in the cytosol, as transporters have low Km values, ensuring an efficient supply of such precursors in the ER/Golgi lumen. On the other hand, the cytosolic pool could be directly affected by nutrients, as clearly described for the concentration of UDP-GlcNAc (Marshall et al. 2004).

4-methylumbelliferone, a drug that binds the UDP-GlcUA reducing the availability of this precursor, is another way to confirm this metabolic aspect (Vigetti et al. 2009a; Piccioni et al. 2012). The activation of AMPK by AICAR induces the phosphorylation of a threonine (Thr 110) in HAS2, blocking enzyme activity (Vigetti et al. 2011a). AMPK activity acts only on HAS2 and not on HAS1 and 3, confirming the specific regulation of HASes. Moreover, AMPK activity plays a role only for HA synthesis, and not for the synthesis of other GAGs, indicating that HA is the only GAG affected by energy modulation mechanisms, correlating cell energy level with HA synthesis.

The concentration of the second UDP-sugar precursor of HA synthesis (UDP-GlcNAc) has an important role in this context; however, it participates in a different mechanism. UDP-GlcNAc influences HA synthesis not only as precursor but also because HAS2 itself is a target of O-GlcNAcylation, a protein covalent modification described by Torres and Hart in 1984 (Torres and Hart 1984). The cytosolic levels of UDP-GlcNAc are finely regulated by the hexosamine pathway. When UDP-GlcNAc is elevated in the cytoplasm, it induces the activity of the enzyme O-GlcNAc transferase (OGT), which catalyzes the β-O-linkage of one residue of N-acetylglucosamine (GlcNAc) to serine 221 of HAS2 (Vigetti et al. 2012). As previously discussed for the AMPK regulation, the O-GlcNAcylation is a covalent regulation specific for HAS2 and does not affect other HASes and the synthesis of

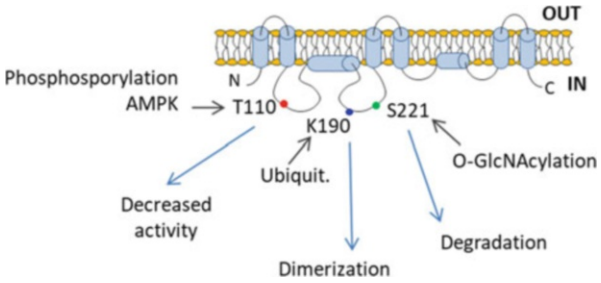

Fig. 4.4 Schematic representation of human HAS2. HAS2 protein, which belongs to Class I HASes, is schematized in the plasma membrane and the eight transmembrane helices represented as cylinders. The large intracellular loop between transmembrane helices two and four contains the catalytic site. Moreover, the three critical residues modified by phosphorylation, O-GlcNAcylation, and ubiquitination that modulate protein activity, stability, and dimerization are shown in different colors

the other GAGs. O-GlcNAcylation is a protein covalent modification widely described in several physiological and pathological conditions including cancer and chronic diseases (Dias and Hart 2007; Hart et al. 2007). It is interesting to note that protein O-GlcNAcylation is related to general metabolic conditions, and UDP-GlcNAc is defined as a "general sensor" of energy level in mammalian cells (Lewis and Hanover 2014). In the case of HAS2, the mechanism used by cells to regulate HA synthesis through O-GlcNAcylation affects enzyme stability on the membrane. HAS2 is usually active on the cell membrane for 17 min, whereas after O-GlcNAcylation, the enzyme can remain active on the cell membrane for more than 5 h, increasing HA content in the ECM (Vigetti et al. 2012). The regulation sites of the enzyme are reported in Fig. 4.4.

4.3.3 Hyaluronan Synthases

HASes are classified in two classes. Class I HASes are multiple transmembrane proteins that are present in bacteria and animals. Typically, bacterial enzymes contain six membrane-associated helices, whereas animals' HASes have eight transmembrane domains (Fig. 4.4). *Pasteurella multocida* expresses a peculiar HAS that belongs to Class II family; it has only one transmembrane domain at the C-terminal of the protein and has a completely different mechanism of catalysis (for a review see (Weigel and DeAngelis 2007)).

The literature suggests that several growth factors and cytokines regulate the expression of the HASes (Jacobson et al. 2000; Pienimaki et al. 2001; Karvinen et al. 2003; Pasonen-Seppänen et al. 2003) by signaling pathways triggered by specific receptors (Wang et al. 2005).

4.3.4 Epigenetic Regulation of Hyaluronan Synthase

Besides direct covalent modification of enzymes, HAS2 gene transcription epigenetic control has been described involving a long noncoding RNA. It was recently described a HAS2 antisense (HAS2-A1) which can increase HAS2 transcription acting as a gene activator in cis (Vigetti et al. 2014a, d). The presence of antisense transcript is common in different cell models. This epigenetic regulation was described in an in vivo approach based on murine and human tissue specimen (Vigetti et al. 2014c). Noteworthy, HAS2-A1 activity involves NF-kB signaling cascade through P65. The interaction of this nucleoprotein with antisense promoter may explain the correlation between inflammatory signals and HAS2 expression.

Even if several aspects of HASes activity are still elusive, it is evident that the complexity of activity regulation depends on the general metabolic conditions of the cells. HA synthesis regulation is carried out by direct and different covalent modifications at protein level, as well as by epigenetic modifications at gene expression level (Vigetti et al. 2014d).

4.4 Biological Role of Hyaluronan in Mammalian Tissues

4.4.1 Hyaluronan in Musculoskeletal Tissue

One of the first HA medical applications is in intra-articular injections to attenuate damage to cartilage in inflamed joints (Plaas et al. 2011). The complete mechanism of action is not fully understood, probably due to the combination of lubricant and anti-inflammatory properties of HMWHA (Jiang et al. 2011). HA could stimulate chondrocyte metabolism, restoring cartilage ECM to physiological deposition; nevertheless, this hypothesis should be confirmed by more robust experimental and clinical data. Alternative approaches foresee to use of stem cells with the aim to regenerate damaged tissues. Interestingly many scaffolds used to maintain stem cells in the affected area and to increase stem cell viability are HA hydrogels that probably trigger stem cells specific signals, favoring survival and proliferation. A similar approach is used for skin regeneration with interesting results (Burdick and Prestwich 2011).

4.4.2 Hyaluronan in the Skin

The skin contains the largest amount of HA in human body, particularly concentrated in the dermis. A dramatic reduction of HA is common in aging. HA decrease implies a diminished skin thickness and hydration (Meyer and Stern 1994; Tigges et al. 2014). Interestingly, the naked mole rat, the only rodent with the exceptional

life span of about 30 years, produces an extremely large HA of over 20 million Dalton within the skin that protects this animal from cancers (Tian et al. 2013). Moreover, these animals are active and fertile for a very long time. On the other hand, HA in the skin is not always protective; in fact Chinese Shar-Pei dogs' characteristic of wrinkled skin derives from mutations in HAS2 promoter that greatly increase HAS2 expression. These animals suffer from periodic fever syndrome (Olsson et al. 2011).

In epidermis, HA has a critical role in keratinocyte differentiation and is also involved in the scarless wound healing process, stimulating keratinocyte migration (Aya and Stern 2014). It is of remarkable importance to note that oligosaccharides have a dramatic effect on skin beta-defensin-2 secretion both in mice and in human (Gariboldi et al. 2008).

4.4.3 Hyaluronan in Cardiovascular Tissue

HA is critical in several pathophysiological conditions of the cardiovascular system. Normally, HA is present mainly in artery adventitia; nevertheless, in early stages of atherosclerosis, HA accumulates in the media layer, favoring migration and proliferation of smooth muscle cells and contributing to vessel thickening (Viola et al. 2015a). HA can, therefore, participate in immune cell recruitment to the vessel wall, favoring inflammation. HA is the major component of the endothelial glycocalyx, and when its content is reduced, immune cell adhesion increases and favors shear stress (Nagy et al. 2010; Fischer 2018). During acute inflammation, as well as angioplasty or, in animal models, after wire or balloon injuries, HA is involved in neointima ECM formation, and the inhibition of HA synthesis dramatically reduces neointima formation, as demonstrated in conditional HAS2 KO mice (Kashima et al. 2013).

4.4.4 Hyaluronan in Neural Tissue

The central nervous system has a HA-rich ECM that contributes to brain hydration in physiological conditions (Perkins et al. 2017). HA is present in the perineuronal net where it, in collaboration with other sulfated GAGs, such as chondroitin 4-sulfate, regulates neuron excitability via binding with divalent cations (Vigetti et al. 2008a). Recent findings showed that lack of HA in the brain causes reduced extracellular space volume, increasing the concentration of neurotransmitters and affecting normal synapsis function, as described in a mouse model of epilepsy (Arranz et al. 2014).

4.4.5 HA in Respiratory System

HA present in the lungs contributes to the mechanical and viscoelastic properties of the tissues influencing stiffness and elasticity. In asthmatic patients or after cigarette smoking, HA fragmentation is evident and can be involved in chronic inflammation via the TLR2/4 and NF-kB pathway and macrophage recruitment that eventually contribute to fibrosis (Lauer et al. 2015; Tighe and Garantziotis 2018). HA receptor RHAMM (but not CD44) has been described to have a pivotal role in hyperoxia-mediated neonatal lung injury, disrupting alveolar development (Liao et al. 2015).

4.4.6 Hyaluronan in Development

During development, gut rotation is a critical event. ECM and HA play a pivotal role in controlling such gut movements that take place in fetal development (Kurpios et al. 2008). In adult, patients with chronic intestinal inflammation (i.e., Crohn's disease and ulcerative colitis) accumulate HA in colon nonvascular space dramatically increasing the recruitment of immune cells, contributing to the infiltration of leukocytes (Rieder et al. 2011; de la Motte 2011). In a rat model of inflammatory bowel disease, HA is altered not only in the mucosa but also in neurons of the enteric nervous system, where it could regulate physiological functions, such as cell motility (Filpa et al. 2017). HA is also involved in liver fibrosis representing a key molecule for therapy in pathophysiology (Neuman et al. 2016). HA has a critical role in development. Silencing of the main enzyme HAS2 in mouse leads to severe cardiac malformation that causes embryo death (Camenisch et al. 2000). The conditional abrogation of Has2 in different tissues also revealed its importance in skeletal growth, patterning, chondrocyte maturation, and joint formation in the developing limb (Matsumoto et al. 2009). HAS1 and HAS3 knockout mice do not show defects and have no effect on development. Recent data on HAS1 and HAS3 KO mice are investigated to detect specific HAS isoform functions, as reported, for instance, in the skin (Wang et al. 2014) or in hematopoiesis (Goncharova et al. 2012). In other model organisms, as the amphibian *Xenopus laevis*, lack of HAS3 impairs gastrulation (Vigetti et al. 2003a). In recent years, zebrafish has been used as a convenient model to study development and human pathologies, and HA has been described as a critical molecule for organogenesis and, interestingly, necessary for tail regeneration (Bakkers et al. 2004; Chanmee et al. 2015, 2016); Ouyang et al. 2017).

4.5 Hyaluronan in Pathology

4.5.1 Hyaluronan in Tumors

Aggressive malignancies present an increased HA content surrounding cells and inside them as well (Tammi et al. 2008; Chanmee et al. 2016). Upregulation of HASes and Hyals has been described in several malignancies, as well as an increased activity of HA receptors (Udabage et al. 2005). In many animal models, the inhibition of HA synthesis via 4-MU reduced tumor growth and metastasis, suggesting that HA metabolism could represent a good target for new therapeutic strategies (Nagy et al. 2015; Edelman et al. 2017).

Many tumors present an increased HA UDP-sugar precursor concentration, which is in accordance with an augmented HA synthesis (Oikari et al. 2018). Moreover, UDP-GlcUA is used in the liver to detoxify chemotherapy drugs, such as epirubicin, and, for this reason, an increased HA synthesis reducing UDP-GlcUA availability could favor drug resistance.

4.5.2 New Insights into Hyaluronan Role in Human Pathology

The use of hyaluronidases in therapy is a recent evidence that shows interesting application in the treatment of solid tumors where hyaluronidase treatment improves chemotherapy bioactivity (Infante et al. 2018). Hyaluronidase role in human pathology and in cancer is still not clear, and several controversial data are reported in literature. However, these contradictory data indicate that Hyal 1 and Hyal 2 might promote or suppress tumor development, suggesting that Hyals activity might be part of a finely tuned system which includes HA synthesis and degradation (McAtee et al. 2014).

It was previously discussed that HA is normally present in healthy tissue in high molecular weight. However, in some specific pathological conditions, such as inflammation or reactive oxygen species (ROS) production (Jiang et al. 2005, 2011), the amount of HA fragments with different low molecular weights increase, and these fragments show diverse biological activities (Stern et al. 2006).

ROS degrade HA chains generating biologically active fragments. Usually, ROS are present in injured tissues, in inflamed areas and in tumor microenvironment. They may provide a mechanism for generating HA fragments in vivo and may further exaggerate the inflammatory state.

The accumulation of the HA fragments should be carefully avoided, as they could trigger an inflammatory response. This is the reason why the removal of digested fragments from the ECM through internalization after their interactions with receptors, such as CD44, is a critical step for inflammation development. In fact, HA fragments can be recognized by specific receptors that could influence cell behavior

according to their size (Iijima et al. 2011). From this point of view, HA oligosaccharides could be classified as matrikines (Maquart et al. 1999) as they have all characteristics of ECM active fragments. Oligosaccharides produced by the catabolic activity of hyaluronidase, if not rapidly internalized by the cells, can diffuse through tissues and bind to HA receptors on adjacent cells, acting as intracellular signals such as NF-kB and Erk.

4.6 Hyaluronan as Drug Delivery System and in Cosmetics

4.6.1 Hyaluronan as Drug Delivery System

HA is involved in several therapies in regenerative medicine and in cosmetics. In wound healing or in surgery as anti-adherence agent (Tsai et al. 2005), HA shows an effective activity due to its capacity to improve cell growth and angiogenesis.

HA hydrogel can be also used as a drug delivery system (Hsu et al. 2018; Jiang et al. 2018). The polymer chain chemistry can be easily modified with adipic hydrazide, tyramide, benzyl ester, glycidyl methacrylate, thiopropionyl hydrazide, or bromoacetate, either at carboxylic acid of glucuronic acid or at the C-6 hydroxyl group of the *N*-acetylglucosamine (Darr and Calabro 2009).

HA has attracted significant interest in development of drug delivery systems because of its intrinsic physicochemical and biological properties. As previously described, HA water solubility, viscoelasticity, non-immunogenicity, biocompatibility, and biodegradability are key aspects for consideration when applying this polymer as a vehicle for drug delivery (Saravanakumar et al. 2014). HA interacts with specific receptors (e.g., CD44) on disease-related cells, such as cancer cells and activated macrophages, followed by receptor-mediated endocytosis. With these unique features, HA has been extensively used for development of the targetable carriers to deliver therapeutic and imaging agents (Huang and Huang 2018). Many reports present an extensive use of HA in the controlled release and targeted drug delivery systems. However, most studies are performed only in vitro, and in vivo data are scarce (Huang and Huang 2018).

As previously discussed, HA presents hydroxyl, carboxyl, and *N*-acetyl groups suitable for chemical modification. Therefore, HA and its derivatives act as drug carriers; contribute to drug concentration, sustained release, and transdermal absorption; and improve drug targeting. The chemical coupling of cytotoxic drug to HA improves drug pharmacokinetic profile, prolongs drug distribution, and reduces time for drug effect (Zhang et al. 2014a). Basically, HA allows low plasma drug concentration increasing drug concentration in affected tissue (Ossipov 2010; Ossipov et al. 2010). HA and its derivatives have been widely used in various drug delivery systems, such as nanoparticle drug delivery system, gel drug delivery system, cationic polymer gene carrier system, nano-emulsion delivery system, polyelectrolyte microcapsule drug delivery system, microsphere drug delivery system, and film delivery system, and these various techniques enhanced flexibility

(Saravanakumar et al. 2014). HA hydrogels are methods of gene delivery and have been widely used, especially in tissue engineering as HA forms a system that controls gene delivery for tissue regeneration.

One of the first drug delivery systems based on HA was the creation of an amphipathic vector with polyethyleneimine (PEI). The hyaluronic acid-PEI (HAP) for gene delivery by periodic acid oxidation is one of the first systems developed in this context (Yao et al. 2010). This vector protects DNA from nuclease degradation, isolates DNA from the complex, and is less toxic. The high transfection rate of HAP in cancerous HepG2 cells promoted more effective cell drug uptake. Another molecule coupled with HA was spermine, developed to improve transfection efficiency of encapsulated DNA. Synthetic hyaluronic acid-polylysine (PLL) conjugate is recognized by HARE receptor in the sinusoidal epithelium of liver cells (Asayama et al. 1998; Rosso et al. 2013). This complex was designed to induce the ε-amino group of HA-terminal PLL to form a comb-type copolymer by reducing the amino group. This copolymer has been used to form a complex with DNA after intravenous injection in the animal model. This system showed that the copolymer was mainly concentrated in the sinusoidal cells of the liver affecting gene expression. The first HA gene delivery application was HA-adipic acid dihydrazide (ADH) hydrogels used to protect DNA from enzyme degradation and for sustained release of DNA (Shoham et al. 2013). This injectable HA/ADH hydrogel worked as a vessel for protecting preadipocytes during and at short term after delivery to native tissues. This system was used in research toward regenerative medicine in tissue reconstructions. Therefore, HA can act as a non-viral vector for gene drugs and could be targeted to tumor cells through CD44 receptor-mediated endocytosis working as antitumor delivering gene drug (Huang and Huang 2018).

HA was also tested for siRNA delivery. HA cross-linking could be formed by disulfide bonds, which can be degraded by glutathione in the cytoplasm (Lee et al. 2007). Moreover, to confirm the mechanism of internalization, the efficiency of cell absorption and gene silencing was much higher in the CD44-overexpressed cell lines compared to cell lines with lower CD44 expression (Lee et al. 2007; Jang et al. 2014). The HAP conjugate was also developed to deliver siRNA through LYVE-1-mediated targeting cells (Jang et al. 2014).

A recent achievement is the production of complex polyethylene glycol (PEG) and HA, which resulted in a very useful tool for its pharmacokinetic properties. In fact, in physiological conditions, PEGylated HA nanoparticles (HA-NPs) formed self-assembled nanoparticles (217–269 nm in diameter) with negatively charged surfaces (Choi et al. 2011). The nanoparticles uptake is mediated by CD44, resulting in a high tumor targetability of PEGylated HA-NPs. These data were obtained in vitro and in vivo modes, supported by intravital tumor imaging. In these experiments, rapid extravasation into the tumor tissue was observed, indicating that PEGylated HA-NPs can be useful as a means for cancer therapy and diagnosis (Choi et al. 2011). PEGylation presents advantages in terms of biodistribution but may present some problems associated with long-term therapies. HA emerged as a

good vehicle for drug delivery; in fact, each individual HA chain conjugates with several different peptides, making it possible for polypeptide drugs to exert multiple effects (Jiang et al. 2012). The coupling procedures for HA are very mild and use the carboxylic group as acceptor. This strongly supports the use of HA as drug delivery carrier. To prolong release time of protein drugs, HA hydrogels have been extensively studied producing hybrid hydrogel system showing both simple drug loading and controlled release with no denaturation of the protein drugs (Hirakura et al. 2010). One example of HA use in protein release by a cross-linked HA hydrogel was the product generated to release erythropoietin (EPO) (Motokawa et al. 2006). HA-drug conjugates are widely tested as they can improve drug solubility and change drug distribution and its half-life in vivo. These events can increase drug concentration in tumor tissue by enhancing the osmotic retention effect augmenting the efficacy of therapy (Fan et al. 2015; Dosio et al. 2016). The antitumor complex HA-paclitaxel was developed to improve the antitumor effect of this compound, and in vivo and in vitro tests proved the concept identifying CD44 as a receptor for this complex. HA-paclitaxel can effectively inhibit tumor growth in human cancer xenografts via HA-mediated mechanism (Galer et al. 2011). HA was also tested with liposomes (El Kechai et al. 2015), HA-modified polylactic acid-glycolic acid copolymer nanoparticles (HCDs) were prepared to increase drug uptake in breast cancer cells (Park et al. 2011). From these examples, HA has several advantages in cancer therapy and in drug release in general; these aspects are related to its good biocompatibility, easily chemically modifiable groups, and targeting of tumor cells via CD44. Nevertheless, some problems are still present in HA application in therapy, for instance, the number of molecules linked to the chain has to be carefully controlled as an excess of linking material can modify HA solubility and interaction with HA receptors. Moreover, as HA receptor is largely present in the liver, in intravenous treatment a great part of the complex can be blocked in this organ. These aspects limit widespread use of HA as a drug delivery system and require an improved tumor active targeting to ameliorate efficacy. The preliminary data from clinical trials indicate that industrialization and wide clinical application of HA as drug delivery system are still to be properly developed.

4.6.2 Hyaluronan in Cosmetics

In cosmetics HA polymer is commonly present in the products commercially available, and this is due to HA activity as a moisturizing agent. It has been demonstrated that elastic properties of the skin have been improved by the regular application of HA on skin even though the biological effects on keratinocytes are not completely understood at molecular level (Gariboldi et al. 2008). Nevertheless, even robust scientific data are still necessary to completely understand HA role in topic cutaneous application, several sunscreen products containing HA showed important

anti-free radicals' action with a protective activity against ultraviolet irradiation (Manuskiatti and Maibach 1996). In plastic surgery HA gels with entanglements or chemical linkages between chains are widely used as filler to treat facial lines and wrinkles (Maytin 2016; Fallacara et al. 2017). The success of this application is due to the greater tolerability of HA filler compared to collagen products (Duranti et al. 1998; Narins et al. 2003; Pao and Mancini 2014). Even the use of HA as filler is largely diffused in aesthetic medicine, it must be considered that HA is not only a filler (Maytin 2016). The filler technology addressed mainly the problem related to the HA integrity and the viscoelastic properties of the hydrogels used. In the market there are several formulations of HA filler that have chemical bonds between chains (cross-linkers) or natural entanglements between HA chains. HA concentration, the number of HA bonds, and polymer size influence hydrogel viscoelastic properties and gave the producers the possibility to develop dozens of different fillers. Duration, filler effect, syringe application, and skin rejuvenation are all aspects that characterize different filler products. HA filler advantages are its easy modulation considering the skin area, the effect target, and the possibility to be rapidly digested by hyaluronidases if the product generates adverse reactions (inflammation, granuloma).

Eventually, HA is also present in nutraceutical market, as beverages, food, and confectioneries which have been approved as health food material worldwide. Nevertheless, its use is still unclear as these macromolecules are completely digested in the gut.

4.7 Concluding Remarks

HA represents a key molecule in the ECM from the beginning of embryo development to advanced age. The aging of mammals is characterized by a marked reduction of HA content in tissues. In other acute and chronic pathologies, HA role emerged as a critical aspect in disease outcome. Randomized controlled trials have successfully proved the remarkable HA properties. Trials currently in progress approach various therapeutic strategies, including healing burns, surgery, and chronic wound healing (Voigt and Driver 2012). In diabetes, in chronic inflammatory diseases and in pulmonary and kidney fibrosis, HA represents a potential therapeutic target (Rieder et al. 2011; Wang et al. 2011; Petrey and de la Motte 2014; Hascall et al. 2014). The HA interactome and viscoelastic properties indicate that HA will be more than an ECM molecule. HA synergistic activity with bioactive molecules and drugs is close to be ready for clinical applications, even if few technical questions remain to be addressed. From this point of view, the HA hydrogels will be a common tool in engineered tissues and in regenerative medicine.

References

Acharya PS, Majumdar S, Jacob M, Hayden J, Mrass P, Weninger W et al (2008) Fibroblast migration is mediated by CD44-dependent TGF beta activation. J Cell Sci 121 (Pt 9):1393–1402

Aderem A, Ulevitch RJ (2000) Toll-like receptors in the induction of the innate immune response. Nature 406(6797):782–787

Akishima Y, Ito K, Zhang L, Ishikawa Y, Orikasa H, Kiguchi H et al (2004) Immunohistochemical detection of human small lymphatic vessels under normal and pathological conditions using the LYVE-1 antibody. Virchows Arch 444:153–157

Arranz AM, Perkins KL, Irie F, Lewis DP, Hrabe J, Xiao F et al (2014) Hyaluronan deficiency due to Has3 knock-out causes altered neuronal activity and seizures via reduction in brain extracellular space. J Neurosci 34:6164–6176

Asayama S, Nogawa M, Takei Y, Akaike T, Maruyama A (1998) Synthesis of novel polyampholyte comb-type copolymers consisting of a poly(L-lysine) backbone and hyaluronic acid side chains for a DNA carrier. Bioconjug Chem 9:476–481

Aya KL, Stern R (2014) Hyaluronan in wound healing: rediscovering a major player. Wound Repair Regen 22:579–593

Baggenstoss BA, Harris EN, Washburn JL, Medina AP, Nguyen L, Weigel PH (2017) Hyaluronan synthase control of synthesis rate and hyaluronan product size are independent functions differentially affected by mutations in a conserved tandem B-X7-B motif. Glycobiology 27:154–164

Bakkers J, Kramer C, Pothof J, Quaedvlieg NE, Spaink HP, Hammerschmidt M (2004) Has2 is required upstream of Rac1 to govern dorsal migration of lateral cells during zebrafish gastrulation. Development 131:525–537

Bohaumilitzky L, Huber AK, Stork EM, Wengert S, Woelfl F, Boehm H (2017) A trickster in disguise: hyaluronan's ambivalent roles in the matrix. Front Oncol 7:242. https://doi.org/10.3389/fonc.2017.00242

Bollyky PL, Bogdani M, Bollyky JB, Hull RL, Wight TN (2012) The role of hyaluronan and the extracellular matrix in islet inflammation and immune regulation. Curr Diab Rep 12:471–480

Bonafè F, Govoni M, Giordano E, Caldarera CM, Guarnieri C, Muscari C (2014) Hyaluronan and cardiac regeneration. J Biomed Sci 21:100. https://doi.org/10.1186/s12929-014-0100-4

Bourguignon LY, Singleton PA, Diedrich F (2004) Hyaluronan-CD44 interaction with Rac1-dependent protein kinase N-gamma promotes phospholipase Cgamma1 activation, Ca(2+) signaling, and cortactin-cytoskeleton function leading to keratinocyte adhesion and differentiation. J Biol Chem 279:29654–29669

Burdick JA, Prestwich GD (2011) Hyaluronic acid hydrogels for biomedical applications. Adv Mater 23:H41–H56

Camenisch TD, Spicer AP, Brehm-Gibson T, Biesterfeldt J, Augustine ML, Calabro A et al (2000) Disruption of hyaluronan synthase-2 abrogates normal cardiac morphogenesis and hyaluronan-mediated transformation of epithelium to mesenchyme. J Clin Invest 106:349–360

Chang EJ, Kim HJ, Ha J, Ryu J, Park KH, Kim UH et al (2007) Hyaluronan inhibits osteoclast differentiation via Toll-like receptor 4. J Cell Sci 120(Pt 1):166–176

Chanmee T, Ontong P, Kimata K, Itano N (2015) Key roles of hyaluronan and its CD44 receptor in the stemness and survival of cancer stem cells. Front Oncol 5:180. https://doi.org/10.3389/fonc.2015.00180

Chanmee T, Ontong P, Itano N (2016) Hyaluronan: a modulator of the tumor microenvironment. Cancer Lett 375:20–30

Cherr GN, Yudin AI, Overstreet JW (2001) The dual functions of GPI-anchored PH-20: hyaluronidase and intracellular signaling. Matrix Biol 20:515–525
Choi KY, Min KH, Yoon HY, Kim K, Park JH, Kwon IC et al (2011) PEGylation of hyaluronic acid nanoparticles improves tumor targetability in vivo. Biomaterials 32:1880–1889
Clark RA, Lin F, Greiling D, An J, Couchman JR (2004) Fibroblast invasive migration into fibronectin/fibrin gels requires a previously uncharacterized dermatan sulfate-CD44 proteoglycan. J Invest Dermatol 122:266–277
Cowman MK, Matsuoka S (2005) Experimental approaches to hyaluronan structure. Carbohydr Res 340:791–809
Csoka AB, Stern R (2013) Hypotheses on the evolution of hyaluronan: a highly ironic acid. Glycobiology 23:398–411
Csoka AB, Frost GI, Stern R (2001) The six hyaluronidase-like genes in the human and mouse genomes. Matrix Biol 20:499–508
Cyphert JM, Trempus CS, Garantziotis S (2015) Size matters: molecular weight specificity of hyaluronan effects in cell biology. Int J Cell Biol 2015:1–8
Damodarasamy M, Johnson RS, Bentov I, MacCoss MJ, Vernon RB, Reed MJ (2014) Hyaluronan enhances wound repair and increases collagen III in aged dermal wounds. Wound Repair Regen 22:521–526
Darr A, Calabro A (2009) Synthesis and characterization of tyramine-based hyaluronan hydrogels. J Mater Sci Mater Med 20:33–44
Day AJ, Prestwich GD (2002) Hyaluronan-binding proteins: tying up the giant. J Biol Chem 277:4585–4588
de la Motte CA (2011) Hyaluronan in intestinal homeostasis and inflammation: implications for fibrosis. Am J Physiol Gastrointest Liver Physiol 301:G945–G949
Deen AJ, Rilla K, Oikari S, Kärnä R, Bart G, Häyrinen J et al (2014) Rab10-mediated endocytosis of the hyaluronan synthase HAS3 regulates hyaluronan synthesis and cell adhesion to collagen. J Biol Chem 289:8375–8389
Dias WB, Hart GW (2007) O-GlcNAc modification in diabetes and Alzheimer's disease. Mol BioSyst 3:766–772
Dicker KT, Gurski LA, Pradhan-Bhatt S, Witt RL, Farach-Carson MC, Jia X (2014) Hyaluronan: a simple polysaccharide with diverse biological functions. Acta Biomater 10:1558–1570
Dosio F, Arpicco S, Stella B, Fattal E (2016) Hyaluronic acid for anticancer drug and nucleic acid delivery. Adv Drug Deliv Rev 97:204–236
Dumaresq-Doiron K, Edjekouane L, Orimoto AM, Yoffou PH, Gushulak L, Triggs-Raine B et al (2012) Hyal-1 but not Hyal-3 deficiency has an impact on ovarian folliculogenesis and female fertility by altering the follistatin/activin/Smad3 pathway and the apoptotic process. J Cell Physiol 227:1911–1922
Duranti F, Salti G, Bovani B, Calandra M, Rosati ML (1998) Injectable hyaluronic acid gel for soft tissue augmentation. A clinical and histological study. Dermatol Surg 24:1317–1325
Edelman R, Assaraf YG, Levitzky I, Shahar T, Livney YD (2017) Hyaluronic acid-serum albumin conjugate-based nanoparticles for targeted cancer therapy. Oncotarget 8:24337–24353
Edsman K, Nord LI, Ohrlund A, Lärkner H, Kenne AH (2012) Gel properties of hyaluronic acid dermal fillers. Dermatol Surg 38:1170–1179
El Kechai N, Bochot A, Huang N, Nguyen Y, Ferrary E, Agnely F (2015) Effect of liposomes on rheological and syringeability properties of hyaluronic acid hydrogels intended for local injection of drugs. Int J Pharm 487:187–196
Erickson M, Stern R (2012) Chain gangs: new aspects of hyaluronan metabolism. Biochem Res Int 2012:1–9
Fallacara A, Manfredini S, Durini E, Vertuani S (2017) Hyaluronic acid fillers in soft tissue regeneration. Facial Plast Surg 33:87–96
Fan X, Zhao X, Qu X, Fang J (2015) pH sensitive polymeric complex of cisplatin with hyaluronic acid exhibits tumor-targeted delivery and improved in vivo antitumor effect. Int J Pharm 496:644–653

Fenderson BA, Stamenkovic I, Aruffo A (1993) Localization of hyaluronan in mouse embryos during implantation, gastrulation and organogenesis. Differentiation 54:85–98

Filpa V, Bistoletti M, Caon I, Moro E, Grimaldi A, Moretto P et al (2017) Changes in hyaluronan deposition in the rat myenteric plexus after experimentally-induced colitis. Sci Rep 7. https://doi.org/10.1038/s41598-017-18020-7

Fischer JW (2018) Role of hyaluronan in atherosclerosis: current knowledge and open questions. Matrix Biol. https://doi.org/10.1016/j.matbio.2018.03.003

Fraser JR, Laurent TC, Laurent UB (1997) Hyaluronan: its nature, distribution, functions and turnover. J Intern Med 242:27–33

Gale NW, Prevo R, Espinosa J, Ferguson DJ, Dominguez MG, Yancopoulos GD et al (2007) Normal lymphatic development and function in mice deficient for the lymphatic hyaluronan receptor LYVE-1. Mol Cell Biol 27:595–604

Galer CE, Sano D, Ghosh SC, Hah JH, Auzenne E, Hamir AN et al (2011) Hyaluronic acid-paclitaxel conjugate inhibits growth of human squamous cell carcinomas of the head and neck via a hyaluronic acid-mediated mechanism. Oral Oncol 47:1039–1047

Gariboldi S, Palazzo M, Zanobbio L, Selleri S, Sommariva M, Sfondrini L et al (2008) Low molecular weight hyaluronic acid increases the self-defense of skin epithelium by induction of beta-defensin 2 via TLR2 and TLR4. J Immunol 181:2103–2110

Gerardy-Schahn R, Oelmann S, Bakker H (2001) Nucleotide sugar transporters: biological and functional aspects. Biochimie 83:775–782

Girish KS, Kemparaju K (2007) The magic glue hyaluronan and its eraser hyaluronidase: a biological overview. Life Sci 80:1921–1943

Goncharova V, Serobyan N, Iizuka S, Schraufstatter I, de Ridder A, Povaliy T et al (2012) Hyaluronan expressed by the hematopoietic microenvironment is required for bone marrow hematopoiesis. J Biol Chem 287:25419–25433

Hadley B, Maggioni A, Ashikov A, Day CJ, Haselhorst T, Tiralongo J (2014) Structure and function of nucleotide sugar transporters: current progress. Comput Struct Biotechnol J 10:23–32

Hall CL, Turley EA (1995) Hyaluronan: RHAMM mediated cell locomotion and signaling in tumorigenesis. J Neuro-Oncol 26:221–229

Hardwick C, Hoare K, Owens R, Hohn HP, Hook M, Moore D et al (1992) Molecular cloning of a novel hyaluronan receptor that mediates tumor cell motility. J Cell Biol 117:1343–1350

Harris EN, Kyosseva SV, Weigel JA, Weigel PH (2007) Expression, processing, and glycosaminoglycan binding activity of the recombinant human 315-kDa hyaluronic acid receptor for endocytosis (HARE). J Biol Chem 282:2785–2797

Hart GW, Housley MP, Slawson C (2007) Cycling of O-linked beta-N-acetylglucosamine on nucleocytoplasmic proteins. Nature 446:1017–1022

Hascall VC, Wang A, Tammi M, Oikari S, Tammi R, Passi A et al (2014) The dynamic metabolism of hyaluronan regulates the cytosolic concentration of UDP-GlcNAc. Matrix Biol 35:14–17

Hill DR, Kessler SP, Rho HK, Cowman MK, de la Motte CA (2012) Specific-sized hyaluronan fragments promote expression of human β-defensin 2 in intestinal epithelium. J Biol Chem 287:30610–30624

Hirakura T, Yasugi K, Nemoto T, Sato M, Shimoboji T, Aso Y et al (2010) Hybrid hyaluronan hydrogel encapsulating nanogel as a protein nanocarrier: new system for sustained delivery of protein with a chaperone-like function. J Control Release 142:483–489

Hofmann M, Assmann V, Fieber C, Sleeman JP, Moll J, Ponta H et al (1998) Problems with RHAMM: a new link between surface adhesion and oncogenesis? Cell 95:592–593

Hsu MF, Tyan YS, Chien YC, Lee MW (2018) Hyaluronic acid-based nano-sized drug carrier-containing Gellan gum microspheres as potential multifunctional embolic agent. Sci Rep 8 (1):731. https://doi.org/10.1038/s41598-018-19191-7

Huang G, Huang H (2018) Application of hyaluronic acid as carriers in drug delivery. Drug Deliv 25:766–772

Iijima J, Konno K, Itano N (2011) Inflammatory alterations of the extracellular matrix in the tumor microenvironment. Cancers (Basel) 3:3189–3205

Infante JR, Korn RL, Rosen LS, LoRusso P, Dychter SS, Zhu J et al (2018) Phase 1 trials of PEGylated recombinant human hyaluronidase PH20 in patients with advanced solid tumours. Br J Cancer 118(2):e3. https://doi.org/10.1038/bjc.2017.438

Itano N (2008) Simple primary structure, complex turnover regulation and multiple roles of hyaluronan. J Biochem 144:131–137

Itano N, Kimata K (2002) Mammalian hyaluronan synthases. IUBMB Life 54:195–199

Jacobson A, Brinck J, Briskin MJ, Spicer AP, Heldin P (2000) Expression of human hyaluronan synthases in response to external stimuli. Biochem J 348(Pt 1):29–35

Jang YL, Ku SH, Jin S, Park JH, Kim WJ, Kwon IC et al (2014) Hyaluronic acid-siRNA conjugate/reducible polyethylenimine complexes for targeted siRNA delivery. J Nanosci Nanotechnol 14:7388–7394

Jeyapalan Z, Deng Z, Shatseva T, Fang L, He C, Yang BB (2011) Expression of CD44 3-′-untranslated region regulates endogenous microRNA functions in tumorigenesis and angiogenesis. Nucleic Acids Res 39:3026–3041

Jha AK, Hule RA, Jiao T, Teller SS, Clifton RJ, Duncan RL et al (2009) Structural analysis and mechanical characterization of hyaluronic acid-based doubly cross-linked networks. Macromolecules 42:537–546

Jiang D, Liang J, Fan J, Yu S, Chen S, Luo Y et al (2005) Regulation of lung injury and repair by Toll-like receptors and hyaluronan. Nat Med 11:1173–1179

Jiang D, Liang J, Noble PW (2007) Hyaluronan in tissue injury and repair. Annu Rev Cell Dev Biol 23:435–461

Jiang D, Liang J, Noble PW (2011) Hyaluronan as an immune regulator in human diseases. Physiol Rev 91:221–264

Jiang T, Zhang Z, Zhang Y, Lv H, Zhou J, Li C et al (2012) Dual-functional liposomes based on pH-responsive cell-penetrating peptide and hyaluronic acid for tumor-targeted anticancer drug delivery. Biomaterials 33:9246–9258

Jiang Z, Dong X, Yan X, Liu Y, Zhang L, Sun Y (2018) Nanogels of dual inhibitor-modified hyaluronic acid function as a potent inhibitor of amyloid β-protein aggregation and cytotoxicity. Sci Rep 8(1):3505. https://doi.org/10.1038/s41598-018-21933-6

Johnson LA, Prevo R, Clasper S, Jackson DG (2007) Inflammation-induced uptake and degradation of the lymphatic endothelial hyaluronan receptor LYVE-1. J Biol Chem 282:33671–33680

Karousou E, Kamiryo M, Skandalis SS, Ruusala A, Asteriou T, Passi A et al (2010) The activity of hyaluronan synthase 2 is regulated by dimerization and ubiquitination. J Biol Chem 285:23647–23654

Karvinen S, Pasonen-Seppänen S, Hyttinen JM, Pienimäki JP, Törrönen K, Jokela TA et al (2003) Keratinocyte growth factor stimulates migration and hyaluronan synthesis in the epidermis by activation of keratinocyte hyaluronan synthases 2 and 3. J Biol Chem 278:49495–49504

Kashima Y, Takahashi M, Shiba Y, Itano N, Izawa A, Koyama J et al (2013) Crucial role of hyaluronan in neointimal formation after vascular injury. PLoS One 8(3):e58760. https://doi.org/10.1371/journal.pone.0058760

Kurpios NA, Ibañes M, Davis NM, Lui W, Katz T, Martin JF et al (2008) The direction of gut looping is established by changes in the extracellular matrix and in cell:cell adhesion. Proc Natl Acad Sci USA 105:8499–8506

Lauer ME, Dweik RA, Garantziotis S, Aronica MA (2015) The rise and fall of hyaluronan in respiratory diseases. Int J Cell Biol 2015:1–15

Laurent TC, Fraser JR (1992) Hyaluronan. FASEB J 6:2397–2404

Lee JY, Spicer AP (2000) Hyaluronan: a multifunctional, megaDalton, stealth molecule. Curr Opin Cell Biol 12:581–586

Lee H, Mok H, Lee S, Oh YK, Park TG (2007) Target-specific intracellular delivery of siRNA using degradable hyaluronic acid nanogels. J Control Release 119:245–252

Lewis BA, Hanover JA (2014) O-GlcNAc and the epigenetic regulation of gene expression. J Biol Chem 289:34440–34448

Liao J, Kapadia VS, Brown LS, Cheong N, Longoria C, Mija D et al (2015) The NLRP3 inflammasome is critically involved in the development of bronchopulmonary dysplasia. Nat Commun 6:8977. https://doi.org/10.1038/ncomms9977

Lim ST, Forbes B, Berry DJ, Martin GP, Brown MB (2002) In vivo evaluation of novel hyaluronan/chitosan microparticulate delivery systems for the nasal delivery of gentamicin in rabbits. Int J Pharm 231:73–82

Manuskiatti W, Maibach HI (1996) Hyaluronic acid and skin: wound healing and aging. Int J Dermatol 35:539–544

Maquart FX, Siméon A, Pasco S, Monboisse JC (1999) Regulation of cell activity by the extracellular matrix: the concept of matrikines. J Soc Biol 193:423–428

Marshall S, Nadeau O, Yamasaki K (2004) Dynamic actions of glucose and glucosamine on hexosamine biosynthesis in isolated adipocytes: differential effects on glucosamine 6-phosphate, UDP-N-acetylglucosamine, and ATP levels. J Biol Chem 279:35313–35319

Martin DC, Atmuri V, Hemming RJ, Farley J, Mort JS, Byers S et al (2008) A mouse model of human mucopolysaccharidosis IX exhibits osteoarthritis. Hum Mol Genet 17:1904–1915

Matsumoto K, Li Y, Jakuba C, Sugiyama Y, Sayo T, Okuno M et al (2009) Conditional inactivation of Has2 reveals a crucial role for hyaluronan in skeletal growth, patterning, chondrocyte maturation and joint formation in the developing limb. Development 136:2825–2835

Maytin EV (2016) Hyaluronan: more than just a wrinkle filler. Glycobiology 26:553–559

McAtee CO, Barycki JJ, Simpson MA (2014) Emerging roles for hyaluronidase in cancer metastasis and therapy. Adv Cancer Res 123:1–34

Merrilees MJ, Beaumont BW, Braun KR, Thomas AC, Kang I, Hinek A et al (2011) Neointima formed by arterial smooth muscle cells expressing versican variant V3 is resistant to lipid and macrophage accumulation. Arterioscler Thromb Vasc Biol 31:1309–1316

Meyer K, Palmer JW (1934) The polysaccharide of the vitreous humor. J Biol Chem 107:629–634

Meyer LJ, Stern R (1994) Age-dependent changes of hyaluronan in human skin. J Invest Dermatol 102:385–389

Morris ER, Rees DA, Welsh EJ (1980) Conformation and dynamic interactions in hyaluronate solutions. J Mol Biol 138:383–400

Motokawa K, Hahn SK, Nakamura T, Miyamoto H, Shimoboji T (2006) Selectively crosslinked hyaluronic acid hydrogels for sustained release formulation of erythropoietin. J Biomed Mater Res A 78:459–465

Motolese A, Vignati F, Brambilla R, Cerati M, Passi A (2013) Interaction between a regenerative matrix and wound bed in nonhealing ulcers: results with 16 cases. Biomed Res Int 2013:1–5

Mouta Carreira C, Nasser SM, di Tomaso E, Padera TP, Boucher Y, Tomarev SI et al (2001) LYVE-1 is not restricted to the lymph vessels: expression in normal liver blood sinusoids and down-regulation in human liver cancer and cirrhosis. Cancer Res 61:8079–8084

Nagaoka A, Yoshida H, Nakamura S, Morikawa T, Kawabata K, Kobayashi M et al (2015) Regulation of Hyaluronan (HA) metabolism mediated by HYBID (Hyaluronan-binding protein involved in HA depolymerization, KIAA1199) and HA synthases in growth factor-stimulated fibroblasts. J Biol Chem 290:30910–30923

Nagy N, Freudenberger T, Melchior-Becker A, Röck K, Ter Braak M, Jastrow H et al (2010) Inhibition of hyaluronan synthesis accelerates murine atherosclerosis: novel insights into the role of hyaluronan synthesis. Circulation 122:2313–2322

Nagy N, Kuipers HF, Frymoyer AR, Ishak HD, Bollyky JB, Wight TN et al (2015) 4-methylumbelliferone treatment and hyaluronan inhibition as a therapeutic strategy in inflammation, autoimmunity, and cancer. Front Immunol 6:123. https://doi.org/10.3389/fimmu.2015.00123

Narins RS, Brandt F, Leyden J, Lorenc ZP, Rubin M, Smith S (2003) A randomized, double-blind, multicenter comparison of the efficacy and tolerability of Restylane versus Zyplast for the correction of nasolabial folds. Dermatol Surg 29:588–595

Neuman MG, Cohen LB, Nanau RM (2016) Hyaluronic acid as a non-invasive biomarker of liver fibrosis. Clin Biochem 49:302–315

Nonaka H, Tanaka M, Suzuki K, Miyajima A (2007) Development of murine hepatic sinusoidal endothelial cells characterized by the expression of hyaluronan receptors. Dev Dyn 236:2258–2267

Oikari S, Kettunen T, Tiainen S, Häyrinen J, Masarwah A, Sudah M et al (2018) UDP-sugar accumulation drives hyaluronan synthesis in breast cancer. Matrix Biol 67:63–74

Olsson M, Meadows JR, Truvé K, Rosengren Pielberg G, Puppo F, Mauceli E et al (2011) A novel unstable duplication upstream of HAS2 predisposes to a breed-defining skin phenotype and a periodic fever syndrome in Chinese Shar-Pei dogs. PLoS Genet 7(3):e1001332. https://doi.org/10.1371/journal.pgen.1001332

Ossipov DA (2010) Nanostructured hyaluronic acid-based materials for active delivery to cancer. Expert Opin Drug Deliv 7:681–703

Ossipov DA, Piskounova S, Varghese OP, Hilborn J (2010) Functionalization of hyaluronic acid with chemoselective groups via a disulfide-based protection strategy for in situ formation of mechanically stable hydrogels. Biomacromolecules 11:2247–2254

Ouyang X, Panetta NJ, Talbott MD, Payumo AY, Halluin C, Longaker MT et al (2017) Hyaluronic acid synthesis is required for zebrafish tail fin regeneration. PLoS One 12(2):e0171898. https://doi.org/10.1371/journal.pone.0171898

Pao KY, Mancini R (2014) Nonsurgical periocular rejuvenation: advanced cosmetic uses of neuromodulators and fillers. Curr Opin Ophthalmol 25:461–469

Park JK, Shim JH, Kang KS, Yeom J, Jung HS, Kim JY et al (2011) Solid free-form fabrication of tissue-engineering scaffolds with a poly(lactic-co-glycolic acid) grafted hyaluronic acid conjugate encapsulating an intact bone morphogenetic protein-2/poly(ethylene glycol) complex. Adv Funct Mater 21:2906–2912

Pasonen-Seppänen S, Karvinen S, Törrönen K, Hyttinen JM, Jokela T, Lammi MJ et al (2003) EGF upregulates, whereas TGF-beta downregulates, the hyaluronan synthases Has2 and Has3 in organotypic keratinocyte cultures: correlations with epidermal proliferation and differentiation. J Invest Dermatol 120:1038–1044

Perkins KL, Arranz AM, Yamaguchi Y, Hrabetova S (2017) Brain extracellular space, hyaluronan, and the prevention of epileptic seizures. Rev Neurosci 28:869–892

Petrey AC, de la Motte CA (2014) Hyaluronan, a crucial regulator of inflammation. Front Immunol 5:101. https://doi.org/10.3389/fimmu.2014.00101

Piccioni F, Malvicini M, Garcia MG, Rodriguez A, Atorrasagasti C, Kippes N et al (2012) Antitumor effects of hyaluronic acid inhibitor 4-methylumbelliferone in an orthotopic hepatocellular carcinoma model in mice. Glycobiology 22:400–410

Pienimaki JP, Rilla K, Fulop C, Sironen RK, Karvinen S, Pasonen S et al (2001) Epidermal growth factor activates hyaluronan synthase 2 in epidermal keratinocytes and increases pericellular and intracellular hyaluronan. J Biol Chem 276:20428–20435

Plaas A, Li J, Riesco J, Das R, Sandy JD, Harrison A (2011) Intraarticular injection of hyaluronan prevents cartilage erosion, periarticular fibrosis and mechanical allodynia and normalizes stance time in murine knee osteoarthritis. Arthritis Res Ther 13:R46. https://doi.org/10.1186/ar3286

Prevo R, Banerji S, Ferguson DJ, Clasper S, Jackson DG (2001) Mouse LYVE-1 is an endocytic receptor for hyaluronan in lymphatic endothelium. J Biol Chem 276:19420–19430

Raio L, Cromi A, Ghezzi F, Passi A, Karousou E, Viola M et al (2005) Hyaluronan content of Wharton's jelly in healthy and down syndrome fetuses. Matrix Biol 24:166–174

Rieder F, Kessler SP, West GA, Bhilocha S, de la Motte C, Sadler TM et al (2011) Inflammation-induced endothelial-to-mesenchymal transition: a novel mechanism of intestinal fibrosis. Am J Pathol 179:2660–2673

Rosso F, Quagliariello V, Tortora C, Di Lazzaro A, Barbarisi A, Iaffaioli RV (2013) Cross-linked hyaluronic acid sub-micron particles: in vitro and in vivo biodistribution study in cancer xenograft model. J Mater Sci Mater Med 24:1473–1481

Saravanakumar G, Deepagan VG, Jayakumar R, Park JH (2014) Hyaluronic acid-based conjugates for tumor-targeted drug delivery and imaging. J Biomed Nanotechnol 10:17–31

Savani RC, Cao G, Pooler PM, Zaman A, Zhou Z, DeLisser HM (2001) Differential involvement of the hyaluronan (HA) receptors CD44 and receptor for HA-mediated motility in endothelial cell function and angiogenesis. J Biol Chem 276:36770–36778

Scott JE, Cummings C, Brass A, Chen Y (1991) Secondary and tertiary structures of hyaluronan in aqueous solution, investigated by rotary shadowing-electron microscopy and computer simulation. Hyaluronan is a very efficient network-forming polymer. Biochem J 274(Pt 3):699–705

Seyfried NT, Blundell CD, Day AJ, Almond A (2005a) Preparation and application of biologically active fluorescent hyaluronan oligosaccharides. Glycobiology 15:303–312

Seyfried NT, McVey GF, Almond A, Mahoney DJ, Dudhia J, Day AJ (2005b) Expression and purification of functionally active hyaluronan-binding domains from human cartilage link protein, aggrecan and versican: formation of ternary complexes with defined hyaluronan oligosaccharides. J Biol Chem 280:5435–5448

Sherman L, Sleeman J, Herrlich P, Ponta H (1994) Hyaluronate receptors: key players in growth, differentiation, migration and tumor progression. Curr Opin Cell Biol 6:726–733

Shoham N, Sasson AL, Lin FH, Benayahu D, Haj-Ali R, Gefen A (2013) The mechanics of hyaluronic acid/adipic acid dihydrazide hydrogel: towards developing a vessel for delivery of preadipocytes to native tissues. J Mech Behav Biomed Mater 28:320–331

Simkovic I (2013) Unexplored possibilities of all-polysaccharide composites. Carbohydr Polym 95:697–715

Soltés L, Mendichi R, Kogan G, Schiller J, Stankovska M, Arnhold J (2006) Degradative action of reactive oxygen species on hyaluronan. Biomacromolecules 7:659–668

Spicer AP, McDonald JA (1998) Characterization and molecular evolution of a vertebrate hyaluronan synthase gene family. J Biol Chem 273:1923–1932

Stern R (2004) Hyaluronan catabolism: a new metabolic pathway. Eur J Cell Biol 83:317–325

Stern R, Asari AA, Sugahara KN (2006) Hyaluronan fragments: an information-rich system. Eur J Cell Biol 85:699–715

Stern R, Kogan G, Jedrzejas MJ, Soltés L (2007) The many ways to cleave hyaluronan. Biotechnol Adv 25:537–557

Suzuki M, Asplund T, Yamashita H, Heldin CH, Heldin P (1995) Stimulation of hyaluronan biosynthesis by platelet-derived growth factor-BB and transforming growth factor-beta 1 involves activation of protein kinase C. Biochem J 307(Pt 3):817–821

Takahashi Y, Li L, Kamiryo M, Asteriou T, Moustakas A, Yamashita H et al (2005) Hyaluronan fragments induce endothelial cell differentiation in a CD44- and CXCL1/GRO1-dependent manner. J Biol Chem 280:24195–24204

Takeda K, Kaisho T, Akira S (2003) Toll-like receptors. Annu Rev Immunol 21:335–376

Tamer TM (2013) Hyaluronan and synovial joint: function, distribution and healing. Interdiscip Toxicol 6:111–125

Tammi RH, Kultti A, Kosma VM, Pirinen R, Auvinen P, Tammi MI (2008) Hyaluronan in human tumors: pathobiological and prognostic messages from cell-associated and stromal hyaluronan. Semin Cancer Biol 18:288–295

Tammi RH, Passi AG, Rilla K, Karousou E, Vigetti D, Makkonen K et al (2011) Transcriptional and post-translational regulation of hyaluronan synthesis. FEBS J 278:1419–1428

Taylor KR, Trowbridge JM, Rudisill JA, Termeer CC, Simon JC, Gallo RL (2004) Hyaluronan fragments stimulate endothelial recognition of injury through TLR4. J Biol Chem 279:17079–17084

Tesar BM, Jiang D, Liang J, Palmer SM, Noble PW, Goldstein DR (2006) The role of hyaluronan degradation products as innate alloimmune agonists. Am J Transplant 6:2622–2635

Tian X, Azpurua J, Hine C, Vaidya A, Myakishev-Rempel M, Ablaeva J et al (2013) High-molecular-mass hyaluronan mediates the cancer resistance of the naked mole rat. Nature 499:346–349

Tigges J, Krutmann J, Fritsche E, Haendeler J, Schaal H, Fischer JW et al (2014) The hallmarks of fibroblast ageing. Mech Ageing Dev 138:26–44

Tighe RM, Garantziotis S (2018) Hyaluronan interactions with innate immunity in lung biology. Matrix Biol. https://doi.org/10.1016/j.matbio.2018.01.027

Tolg C, Poon R, Fodde R, Turley EA, Alman BA (2003) Genetic deletion of receptor for hyaluronan-mediated motility (Rhamm) attenuates the formation of aggressive fibromatosis (desmoid tumor). Oncogene 22:6873–6882

Tolg C, Hamilton SR, Nakrieko KA, Kooshesh F, Walton P, McCarthy JB et al (2006) Rhamm-/- fibroblasts are defective in CD44-mediated ERK1,2 motogenic signaling, leading to defective skin wound repair. J Cell Biol 175:1017–1028

Toole BP (2004) Hyaluronan: from extracellular glue to pericellular cue. Nat Rev Cancer 4:528–539

Torres CR, Hart GW (1984) Topography and polypeptide distribution of terminal N-acetylglucosamine residues on the surfaces of intact lymphocytes. Evidence for O-linked GlcNAc. J Biol Chem 259:3308–3317

Tsai SW, Fang JF, Yang CL, Chen JH, Su LT, Jan SH (2005) Preparation and evaluation of a hyaluronate-collagen film for preventing post-surgical adhesion. J Int Med Res 33:68–76

Udabage L, Brownlee GR, Nilsson SK, Brown TJ (2005) The over-expression of HAS2, Hyal-2 and CD44 is implicated in the invasiveness of breast cancer. Exp Cell Res 310:205–217

Välimäki JO (2015) Pilot study of glaucoma drainage implant surgery supplemented with reticulated hyaluronic acid gel in severe glaucoma. Eur J Ophthalmol 25:140–144

Varki A, Cummings RD, Aebi M, Packer NH, Seeberger PH, Esko JD et al (2015) Symbol nomenclature for graphical representations of glycans. Glycobiology 25:1323–1324

Vigetti D, Passi A (2014) Hyaluronan synthases posttranslational regulation in cancer. In: Simpson MA, Heldin P (eds) Hyaluronan signaling and turnover, pp 95–119

Vigetti D, Viola M, Gornati R, Ori M, Nardi I, Passi A et al (2003a) Molecular cloning, genomic organization and developmental expression of the *Xenopus laevis* hyaluronan synthase 3. Matrix Biol 22:511–517

Vigetti D, Viola M, Gornati R, Ori M, Nardi I, Passi A et al (2003b) Molecular cloning, genomic organization and developmental expression of the *Xenopus laevis* hyaluronan synthase 3. Matrix Biol 22:511–517

Vigetti D, Ori M, Viola M, Genasetti A, Karousou E, Rizzi M et al (2006) Molecular cloning and characterization of UDP-glucose dehydrogenase from the amphibian Xenopus laevis and its involvement in hyaluronan synthesis. J Biol Chem 281:8254–8263

Vigetti D, Andrini O, Clerici M, Negrini D, Passi A, Moriondo A (2008a) Chondroitin sulfates act as extracellular gating modifiers on voltage-dependent ion channels. Cell Physiol Biochem 22:137–146

Vigetti D, Viola M, Karousou E, Rizzi M, Moretto P, Genasetti A et al (2008b) Hyaluronan-CD44-ERK1/2 regulate human aortic smooth muscle cell motility during aging. J Biol Chem 283:4448–4458

Vigetti D, Genasetti A, Karousou E, Viola M, Clerici M, Bartolini B et al (2009a) Modulation of hyaluronan synthase activity in cellular membrane fractions. J Biol Chem 284:30684–30694

Vigetti D, Rizzi M, Viola M, Karousou E, Genasetti A, Clerici M et al (2009b) The effects of 4-methylumbelliferone on hyaluronan synthesis, MMP2 activity, proliferation, and motility of human aortic smooth muscle cells. Glycobiology 19:537–546

Vigetti D, Clerici M, Deleonibus S, Karousou E, Viola M, Moretto P et al (2011a) Hyaluronan synthesis is inhibited by adenosine monophosphate-activated protein kinase through the regulation of HAS2 activity in human aortic smooth muscle cells. J Biol Chem 286:7917–7924

Vigetti D, Rizzi M, Moretto P, Deleonibus S, Dreyfuss JM, Karousou E et al (2011b) Glycosaminoglycans and glucose prevent apoptosis in 4-Methylumbelliferone-treated human aortic smooth muscle cells. J Biol Chem 286:34497–34503

Vigetti D, Deleonibus S, Moretto P, Karousou E, Viola M, Bartolini B et al (2012) Role of UDP-N-Acetylglucosamine (GlcNAc) and O-GlcNAcylation of hyaluronan synthase 2 in the control of chondroitin sulfate and hyaluronan synthesis. J Biol Chem 287:35544–35555

Vigetti D, Deleonibus S, Moretto P, Bowen T, Fischer JW, Grandoch M et al (2014a) Natural antisense transcript for hyaluronan synthase 2 (HAS2-AS1) induces transcription of HAS2 via protein O-GlcNAcylation. J Biol Chem 289:28816–28826

Vigetti D, Karousou E, Viola M, Deleonibus S, De Luca G, Passi A (2014b) Hyaluronan: biosynthesis and signaling. Biochim Biophys Acta, Gen Subj 1840:2452–2459

Vigetti D, Viola M, Karousou E, De Luca G, Passi A (2014c) Metabolic control of hyaluronan synthases. Matrix Biol 35:8–13

Vigetti D, Viola M, Karousou E, Deleonibus S, Karamanou K, De Luca G et al (2014d) Epigenetics in extracellular matrix remodeling and hyaluronan metabolism. FEBS J 281:4980–4992

Vigetti D, Karousou E, Viola M, Passi A (2015) Analysis of hyaluronan synthase activity. Methods Mol Biol 1229:201–208

Viola M, Vigetti D, Genasetti A, Rizzi M, Karousou E, Moretto P et al (2008) Molecular control of the hyaluronan biosynthesis. Connect Tissue Res 49:111–114

Viola M, Karousou E, D'Angelo ML, Caon I, De Luca G, Passi A et al (2015a) Regulated hyaluronan synthesis by vascular cells. Int J Cell Biol 2015:1–8

Viola M, Vigetti D, Karousou E, D'Angelo ML, Caon I, Moretto P et al (2015b) Biology and biotechnology of hyaluronan. Glycoconj J 32:93–103

Voelcker V, Gebhardt C, Averbeck M, Saalbach A, Wolf V, Weih F et al (2008) Hyaluronan fragments induce cytokine and metalloprotease upregulation in human melanoma cells in part by signalling via TLR4. Exp Dermatol 17:100–107

Voigt J, Driver VR (2012) Hyaluronic acid derivatives and their healing effect on burns, epithelial surgical wounds, and chronic wounds: a systematic review and meta-analysis of randomized controlled trials. Wound Repair Regen 20:317–331

Wang HS, Tung WH, Tang KT, Wong YK, Huang GJ, Wu JC et al (2005) TGF-beta induced hyaluronan synthesis in orbital fibroblasts involves protein kinase C betaII activation in vitro. J Cell Biochem 95:256–267

Wang KC, Yang YW, Liu B, Sanyal A, Corces-Zimmerman R, Chen Y et al (2011) A long noncoding RNA maintains active chromatin to coordinate homeotic gene expression. Nature 472:120–124

Wang Y, Lauer ME, Anand S, Mack JA, Maytin EV (2014) Hyaluronan synthase 2 protects skin fibroblasts against apoptosis induced by environmental stress. J Biol Chem 289:32253–32265

Weigel PH, DeAngelis PL (2007) Hyaluronan synthases: a decade-plus of novel glycosyltransferases. J Biol Chem 282:36777–36781

Weigel PH, Padgett-McCue AJ, Baggenstoss BA (2013) Methods for measuring Class I membrane-bound hyaluronan synthase activity. Methods Mol Biol 1022:229–247

Wróbel T, Dziegiel P, Mazur G, Zabel M, Kuliczkowski K, Szuba A (2005) LYVE-1 expression on high endothelial venules (HEVs) of lymph nodes. Lymphology 38:107–110

Yamaguchi Y, Yamamoto H, Tobisawa Y, Irie F (2018) TMEM2: a missing link in hyaluronan catabolism identified? Matrix Biol. https://doi.org/10.1016/j.matbio.2018.03.020

Yamamoto H, Tobisawa Y, Inubushi T, Irie F, Ohyama C, Yamaguchi Y (2017) A mammalian homolog of the zebrafish transmembrane protein 2 (TMEM2) is the long-sought-after cell-surface hyaluronidase. J Biol Chem 292:7304–7313

Yang JA, Kim ES, Kwon JH, Kim H, Shin JH, Yun SH et al (2012) Transdermal delivery of hyaluronic acid – human growth hormone conjugate. Biomaterials 33:5947–5954

Yao J, Fan Y, Du R, Zhou J, Lu Y, Wang W et al (2010) Amphoteric hyaluronic acid derivative for targeting gene delivery. Biomaterials 31:9357–9365

Yarema KJ, Bertozzi CR (2001) Characterizing glycosylation pathways. Genome Biol 2: REVIEWS0004

Yoshida H, Nagaoka A, Komiya A, Aoki M, Nakamura S, Morikawa T et al (2018) Reduction of hyaluronan and increased expression of HYBID (KIAA1199) correlate with clinical symptoms in photoaged skin. Br J Dermatol 179:136–144

Zaman A, Cui Z, Foley JP, Zhao H, Grimm PC, Delisser HM et al (2005) Expression and role of the hyaluronan receptor RHAMM in inflammation after bleomycin injury. Am J Respir Cell Mol Biol 33:447–454

Zhang X, Wang H, Ma Z, Wu B (2014a) Effects of pharmaceutical PEGylation on drug metabolism and its clinical concerns. Expert Opin Drug Metab Toxicol 10:1691–1702

Zhang Y, Jia S, Jiang WG (2014b) KIAA1199 and its biological role in human cancer and cancer cells (review). Oncol Rep 31:1503–1508

Zhou B, Weigel JA, Fauss L, Weigel PH (2000) Identification of the hyaluronan receptor for endocytosis (HARE). J Biol Chem 275:37733–37741

Zhou B, Weigel JA, Saxena A, Weigel PH (2002) Molecular cloning and functional expression of the rat 175-kDa hyaluronan receptor for endocytosis. Mol Biol Cell 13:2853–2868

Zhou B, McGary CT, Weigel JA, Saxena A, Weigel PH (2003) Purification and molecular identification of the human hyaluronan receptor for endocytosis. Glycobiology 13:339–349

Chapter 5
Chondroitin, Dermatan, Heparan, and Keratan Sulfate: Structure and Functions

Emiliano Bedini, Maria Michela Corsaro, Alfonso Fernández-Mayoralas, and Alfonso Iadonisi

Abstract Sulfated glycosaminoglycans (heparan sulfate, chondroitin sulfate, dermatan sulfate, and keratan sulfate) are a family of complex polysaccharides ubiquitously, but not exclusively, distributed among mammals, found both in extracellular matrices and on cell surfaces. They play key roles in a myriad of physiological and pathological processes, including, among others, angiogenesis, cancer, immunity, and infectious diseases. Here the main issues concerning their chemical structure, biosynthesis, extraction, and purification from natural sources, structural characterization, as well as their most important biological functions are discussed.

5.1 Introduction

The class of proteoglycans (PGs) is one of the major and critically important components of the extracellular matrix (ECM) as well as of cell surfaces. PGs play several essential roles in a variety of biological events. They are involved both in ECM structure, by governing ECM assembly and its physical properties, and in regulating signaling pathways by interacting with other ECM components, directing tissue growth and development, cell proliferation, adhesion, and motility. This leads to key roles for PGs in several physiological and pathological processes, for example, angiogenesis, cancer, immunity, and infectious diseases (Iozzo and Karamanos 2010).

E. Bedini (✉) · M. M. Corsaro · A. Iadonisi
Dipartimento di Scienze Chimiche, Università degli Studi di Napoli Federico II, Napoli, Italy
e-mail: ebedini@unina.it

A. Fernández-Mayoralas
Instituto de Química Orgánica General, CSIC, Madrid, Spain

E. Cohen, H. Merzendorfer (eds.), *Extracellular Sugar-Based Biopolymers Matrices*, Biologically-Inspired Systems 12, https://doi.org/10.1007/978-3-030-12919-4_5

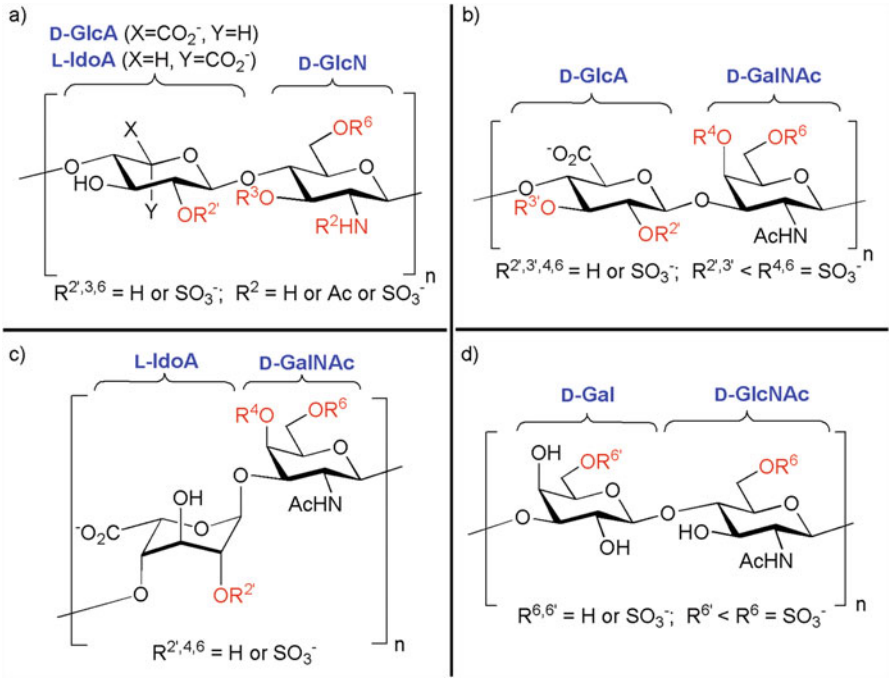

Fig. 5.1 Structure of sulfated GAGs: (**a**) heparan sulfate, (**b**) chondroitin sulfate, (**c**) dermatan sulfate, and (**d**) keratan sulfate

From a structural point of view, PGs are very complex macromolecular glycoconjugates, composed of a protein core and highly negatively charged, linear polysaccharide chains, termed glycosaminoglycans (GAG), which are covalently linked through their reducing ends to the side chains of serine – or more rarely threonine or asparagine – residues in the protein. GAGs can be distinguished into five main different types: hyaluronic acid (HA), heparan sulfate (HS), chondroitin sulfate (CS), dermatan sulfate (DS), and keratan sulfate (KS). Except for HA, the only GAG that is non-sulfated and non-covalently linked to a protein core, all the other GAG polysaccharides of PGs are extensively decorated with sulfate groups (Fig. 5.1). The distribution of such sulfate groups along the polymeric chain (sulfation pattern) can be theoretically arranged in an extremely huge number of different combinations. Together with the different possibilities of GAG chains anchoring on the protein core of PGs, it creates an enormous structural diversity and potential variation in biological activity (Lindahl et al. 2017). Nonetheless, sulfation pattern seems to be strictly regulated in vivo and able to encode a variety of information, in line with the central role played by sulfated GAGs in many biological events. This "GAG sulfation code" is still very poorly understood in detail, even if in the last years, some of its roles have been deciphered (Gama et al. 2006; Swarup et al. 2013).

5.2 Structural Features and Biosynthesis of Sulfated Glycosaminoglycans

5.2.1 Heparan Sulfate

Heparan sulfate (HS) is a type of glycosaminoglycan composed of repeating units of D-glucuronic (GlcA) or L-iduronic (IdoA) acid linked to 2-amino-2-deoxy-D-glucopyranose (glucosamine, GlcN) (Fig. 5.1a). These disaccharide units may be sulfated at *C*-3 and *C*-6 of GlcN and at *C*-2 of the uronic acid, and the GlcN amine function may be changed to sulfamate, acetamide, or unsubstituted. HS polysaccharides do not usually occur as free molecules but rather form covalent species with proteins presenting the so-called heparan sulfate proteoglycans (HSPG, Fig. 5.2). HSPGs are present in the ECM or on the cell surface of essentially all animals, from simple invertebrates to humans. Syndecans and glypicans are the two main cell surface HSPGs, whereas agrin and perlecan are found in the extracellular matrix. The anticoagulant heparin is commonly considered as a highly sulfated variant of HS, which was first discovered in 1916 and derives its name from its abundance in hepatic tissue (Howell and Holt 1918). In fact, HS was originally called heparitin sulfate since it was initially identified as an impurity of heparin (Linker et al. 1958). Actually, the higher sulfate content of heparin with respect to HS is true for most but not all cases. Recently, it was demonstrated that HS extracted from rabbit cartilage chondrocytes in rabbits has a sulfation degree very similar to heparin (Parra et al. 2012). The major difference between HS and heparin rather lies in a biosynthetic aspect: heparin is produced exclusively in the Golgi of vertebrate mast cells, whereas HS is found ubiquitously to the cell surface of both vertebrate and invertebrate species (Sampaio et al. 2006).

Although a huge number of combinations could derive from the abovementioned modifications at the different positions of the disaccharide unit, the biosynthetic process imposes some restrictions, and the fine structure of the chains is eventually

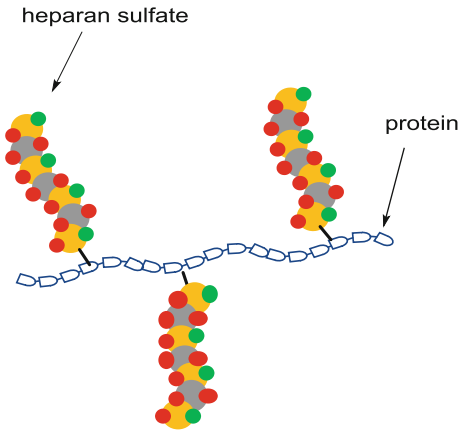

Fig. 5.2 Typical assembly of heparan sulfate proteoglycans

regulated by the expression and action of a variety of enzymes. HS biosynthesis is a multi-step process that takes place in the Golgi (Esko and Selleck 2002; Johan and Lena 2012). The process is initiated with the xylosylation of specific serine residues of the triplet sequence (serine-glycine-acidic amino acid) of the core protein, followed by the formation of a linkage tetrasaccharide, glucuronic acid-galactose-galactose-xylose (Fig. 5.3). This fragment may be phosphorylated at the xylose moiety and sulfated at the two galactose units. These modifications seem to influence the catalytic activity of the enzyme glucuronyltransferase-I (GlcAT-1) that completes the synthesis of this linkage region (Tone et al. 2008). This part of the biosynthesis is shared by HS and chondroitin sulfate (CS), but the pathways diverge after formation of the tetrasaccharide linkage. The addition of a 2-acetamido-2-deoxy-D-glucopyranose (*N*-acetylglucosamine, GlcNAc) unit to the chain by the action of EXTL family of glycosyltransferases initiates HS chain formation. There is a competition between this reaction and the addition of a 2-acetamido-2-deoxy-D-galactopyranose (*N*-acetylgalactosamine, GalNAc) unit catalyzed by a different enzyme, and when the latter glycosidation occurs, the formation of CS takes place. In a study using cultures of genetically engineered cells unable to produce HS, it was shown that the cells gave instead a twofold increase in CS biosynthesis as compared to wild-type ones (Jan et al. 2012). Since HS and CS biosynthesis competes for the same tetrasaccharide intermediate, the reduction of HS biosynthesis results in more available substrate for CS biosynthesis, which explains the increase in CS levels. A different local environment around the glycosylated serine residue of the core protein could determine the presence of HS or CS chain in the proteoglycan. In particular, a series of serine-glycine dipeptides flanked by a cluster of acidic amino acids allows HS chain assembly, whereas CS formation requires a serine-glycine-acidic amino acid-glycine tetrapeptide sequence (Kokenyesi and Bernfield 1994). Nonetheless, also portions of the core protein far away from the glycosylation sites can influence HS vs. CS chain formation (Chen and Lander 2001).

After the EXTL-mediated attachment of the first GlcNAc unit, HS polymer formation proceeds by the stepwise alternating addition of GlcA and GlcNAc residues to the growing polymer (chain polymerization step, Fig. 5.3). During or immediately following the assembly process, the chains are subjected to a series of structural modifications in which a number of GlcNAc units become *N*-deacetylated and sulfamated at *C*-2, the adjacent glucuronic acids are epimerized to IdoA, and finally sulfation of uronic acid residues at *C*-2 and of GlcNAc and GlcNS units at *C*-6 takes place with 3′-phosphoadenosine-5′-phosphosulfate (PAPS) cofactor as sulfate donor (El Masri et al. 2017). Occasionally, the *C*-3 of GlcN residues may also be sulfated. These modifications are catalyzed by the enzymes NDST (*N*-deacetylase *N*-sulfotransferase), epimerase, and 2OST, 6OST, and 3OST (2-*O*-, 6-*O*-, and 3-*O*-sulfotransferases), respectively. Since these modification reactions do not reach completion, the mature HS chain contains three types of domains that give rise to another way to describe its structure: contiguous sulfamated regions (NS domains), regions of alternating *N*-acetylated and sulfamated disaccharide units (NA/NS domains), and unmodified *N*-acetylated regions (NA domains). The degrees of modification and the sulfation pattern can vary widely between different tissues

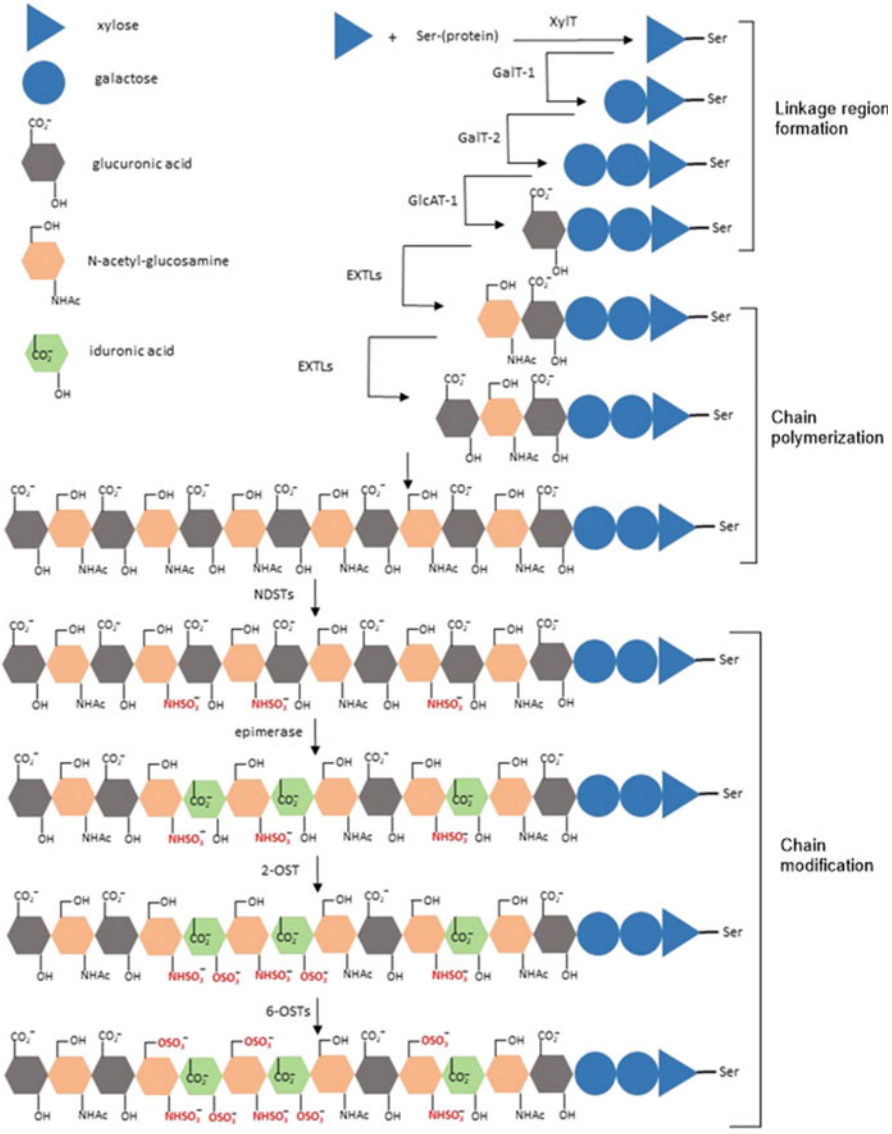

Fig. 5.3 Scheme of HS biosynthesis. The different steps and enzymes involved are shown. The nascent polysaccharide chains are partially modified by GlcNAc *N*-deacetylase/*N*-sulfotransferase (NDST). Some GlcA units are epimerized to IdoA, and sulfation occurs at different positions. Please note that, for sake of figure simplicity, chain modification reactions are depicted as occurring exclusively following the polymerization process, even if the events can also be simultaneous

and during developmental stages due to specific expression of enzyme isoforms having different specificities (Safaiyan et al. 2000; Esko and Lindahl 2001; Yabe et al. 2005; Warda et al. 2006). Furthermore, it has been also hypothesized that

differently composed macromolecular assemblies of HS (as well as other sulfated GAGs) biosynthetic enzymes (termed GAGOSOMEs) in different regions of Golgi apparatus are able to finely coordinate and tune polymerization and structural modifications of the nascent polysaccharide chain (Chua and Kuberan 2017). In addition to the structural variations produced during biosynthesis, the sulfation and sulfamation pattern of HS may be modified extracellularly by the action of sulfatases (Nagamine et al. 2012). This structural variability generates different protein-binding HS sequences that regulate a diversity of biological processes (see Paragraph 5.4.1).

5.2.2 *Chondroitin Sulfate*

CS is a type of glycosaminoglycan found in both vertebrates and invertebrates, composed of GlcA and GalNAc linked together through alternating β-1→3 and β-1→4 glycosidic bond. The resulting →4)-β-GlcA-(1→3)-β-GalNAc-(1→ disaccharide repeating unit can be sulfated to various extents (Fig. 5.1b). Interestingly, sulfation decoration of chondroitin polysaccharides seems to be a result of evolution, in order to let CS play key roles in some special functions typical of higher animals (e.g., central nervous system development: see Paragraph 5.4.2). Indeed, chondroitin isolated from simple and evolutionary more ancient organisms such as bacteria and nematodes shows only or mostly unsulfated GlcA and GalNAc units (Yamada et al. 2007), whereas CS with different sulfation patterns can be extracted from arthropods up to mammals. A list of the sulfation patterns found in CSs is depicted in Fig. 5.4. The differently sulfated disaccharide subunits are commonly identified with a letter (e.g., CS-A means a →4)-β-GlcA-(1→3)-β-GalNAc4S-(1→ disaccharide with a single sulfate group on *C*-4 hydroxy of GalNAc).

Interestingly, sulfate groups are almost exclusively found at position *C*-4 and/or *C*-6 of GalNAc units in CS from terrestrial animal sources, whereas CS from marine species usually shows oversulfated disaccharide units along the polysaccharide backbone, with additional sulfate groups on GlcA units at *C*-2 (shark, ray) (Nadanaka and Sugahara 1997; Takeda et al. 2016) or *C*-3 (invertebrates such as crab, squid, octopus) (Sugahara et al. 1996; Kumar Shetty et al. 2009; Higashi et al. 2015), or, very rarely (shrimp), at both *C*-2 and *C*-3 positions (Cavalcante et al.

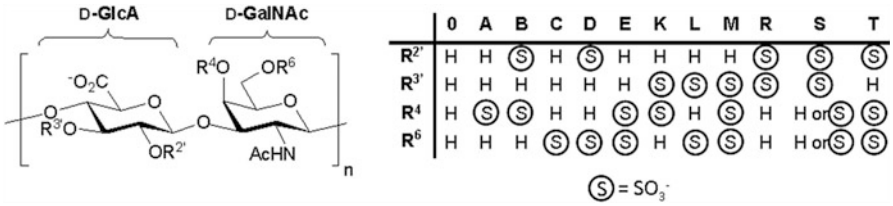

Fig. 5.4 Distribution of sulfation pattern in CS

2018). However, it is worth noting that sulfation pattern is not only varying with the animal species but also with the tissue source. Furthermore, in higher animals it can be subjected to variations also due to different physiopathological conditions, such as aging, inflammation, and tumor formation (Collin et al. 2017).

Some marine invertebrates possess unique CS polysaccharides, with neutral or negatively charged mono- or disaccharide branches, linked predominantly but not exclusively to *C*-3 of GlcA units (Kinoshita-Toyoda et al. 2004; Higashi et al. 2016). Among these branched CSs, fucosylated chondroitin sulfate (fCS) has been the focus of much attention in the last decade, due to its highly interesting potential application as orally deliverable anticoagulant drug alternative to heparin (Pomin 2014). fCS has been found up to now exclusively in sea cucumbers; its structure usually shows variously sulfated L-fucose monosaccharides or, much more rarely, oligosaccharide branches (Chen et al. 2011; Myron et al. 2014; Li et al. 2018; Soares et al. 2018) linked through an α-configured glycosidic bond at *C*-3 of GlcA units or, in very few cases, at *C*-6 of GalNAc residues (Yang et al. 2015; Ustyuzhanina et al. 2016; Li et al. 2018). Figure 5.5 summarizes the variability of fCS structures.

CS in animals is ubiquitously found in the ECM and on cell surfaces as CS proteoglycans (CSPGs), in which the CS polysaccharide is covalently anchored to a core protein through the tetrasaccharide linker region common to both HSPGs and CSPGs, as discussed in Paragraph 5.2.1. CSPGs are usually large biomacromolecules containing from 1 up to 100 CS side chains departing from the core protein. The main CSPG found in cartilaginous tissues is aggrecan, a giant biomacromolecule with about 100 CS polysaccharide branches anchored on the central domain of a 220 kDa protein core, which carries also some keratan sulfate

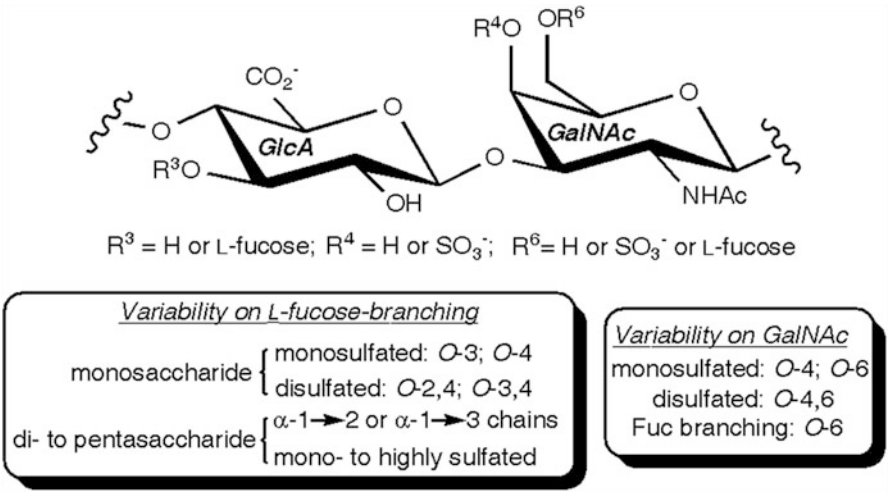

Fig. 5.5 Structural variability of fCS from sea cucumbers

chains (see also Paragraph 5.2.4) (Iozzo 1998). CS chains are similar in length and so closely packed to each other (their spacing is approx. 3–4 nm) that they have almost no conformational freedom, and therefore the whole PG is forced to adopt a highly extended 3D structure. Interestingly, it has been shown that aggrecans from different cartilaginous tissues can differ in the length and number of CS chains, in order to bestow a higher or lower stiffness to its brush-like structure affording different levels of mechanical strength to, for example, load-bearing or non-load-bearing cartilages (Ng et al. 2003).

Aggrecan and three other CSPGs with lower numbers of CS chains (versican, neurocan, and brevican with 10–30, 3–7, and 1–3 polysaccharide branches, respectively) are together named as hyalectans (hyaluronic- and lectin-binding proteoglycans), as the *N*-terminal domain of the core protein binds to hyaluronic acid non-covalently, and at the same time, the *C*-terminal domain can bind lectins. The so-formed huge aggregates are considered to serve as frameworks for construction of the ECM in the brain (Maeda 2015). Decorin and biglycan are instead examples of CSPGs (or more precisely CS/DS proteoglycans (CS/DSPGs): see also Paragraph 5.2.3), which are not aggregated on a hyaluronic acid backbone. They are also named as small leucine-rich CSPGs, with only 1–2 CS (or DS) chains attached on terminal domains of a leucine-rich protein. Other CSPGs displaying a low number of CS chains are phosphacan, bamacan, neuroglycan C, leprecan, thrombomodulin, epiphycan, and bikunin (Ly et al. 2010). The last one is the smallest PG discovered up to now, with a single CS chain on a small (approx. 16 kDa) protein. Interestingly, the nonreducing region of the CS chain is composed exclusively of non-sulfated GlcA-GalNAc subunits (see also Paragraph 5.3.3.2) (Ly et al. 2011) and is linked through ester bonds involving GalNAc *C*-6 positions to two proteins (HC1 and HC2) (Enghild et al. 1999). Such unique covalent assemblage with CS acting as bridging unit between three proteins seems to have an essential role in ECM formation in the context of inflammatory diseases and ovulation (Rugg et al. 2005).

The biosynthesis of CS has been already described in part in Paragraph 5.2.1, since the tetrasaccharide linkage to serine units of CSPGs core protein is shared with HS. By action of a GalNAc- instead of a GlcNAc-transferase, the biosynthesis then diverges to CS instead of HS assembly (see Paragraph 5.2.1 for CS vs. HS biosynthesis regulating factors). The polymerization process consists of a stepwise alternating transfer of GlcA and GalNAc residues from activated precursor to the nonreducing terminal of the nascent polymer chain through the action of GalNAc- and GlcA-transferases, respectively. Interestingly, the transfer of exclusively the first GalNAc unit on the tetrasaccharide linkage region and of all the other ones on the growing polymer chain is catalyzed by two different GalNAc-transferases (CS-GalNAcT-1 and CS-GalNAcT-2). The concomitant action of a variety of highly specific sulfotransferases is devoted to the decoration of the growing chain with sulfate groups at specific positions (Habuchi 2000). It is worth noting that the machinery involved in the biosynthesis of the branched CSs found in some invertebrates, such as fCS from sea cucumbers, is still completely unknown.

5.2.3 *Dermatan Sulfate*

Dermatan sulfate (DS) is a glycosaminoglycan composed of repeating disaccharide units of IdoA and GalNAc. The iduronic acid residues display an α-configuration and are attached to *O*-3 of the *N*-acetylgalactosamine units which in turn are linked, as β-glycosides, to *O*-4 of the subsequent IdoA residues (Fig. 5.1c). This polysaccharide is one of the most abundant GAGs in eukaryotes and is typically found conjugated to a core protein as a proteoglycan. It is present in the skin, cartilage, central nervous system, and blood vessels, mainly as a component of ECM.

DS shares with CS the first stages of the biosynthetic pathway where a tetrasaccharide primer is generated through *O*-glycosidation of lateral chains of serine residues within the core protein (see Paragraph 5.2.1); a chondroitin chain is created from the primer (see Paragraphs 5.2.2), and then the DS sequences are generated through epimerization of the D-glucuronic acid units into L-iduronic acid residues, with subsequent sulfation steps (Malmström et al. 2012). Unlike CS, DS is almost always sulfated at *C*-4 of the GalNAc units (Fig. 5.6); residues of GalNAc sulfated only at *C*-6 are quite unusual (iC subunit), whereas the *C*-6 sulfation of a residue previously sulfated at *C*-4 could be detected (iE subunit), in view of the existence of an enzyme devoted to this specific process (see below). Iduronic acid residues can also be sulfated at position *C*-2, to give iB and iD subunits. Interestingly, in spite of its low occurrence in DS (approximately 5%), iB subunit has an important biological role (see Paragraph 5.4.2.), as the repeat of three of such subunits gives a hexasaccharide with a high affinity for heparin cofactor II (HCII) (Tollefsen 1992).

As for the key epimerization step, two different epimerases, namely, dermatan sulfate epimerase 1 and 2 (DS-epi1 and DS-epi2), are known. They are differentiated in the chromosomal origin and in the relative distribution in the body (Pacheco et al. 2009a). The epimerization steps are not quantitative, and the final polysaccharide chain is indeed a hybrid of CS and DS tracts with the specific content being dependent on several factors. The distribution of DS motifs within the chain can also be variable, with the possible generation of IdoA blocks (relatively long DS

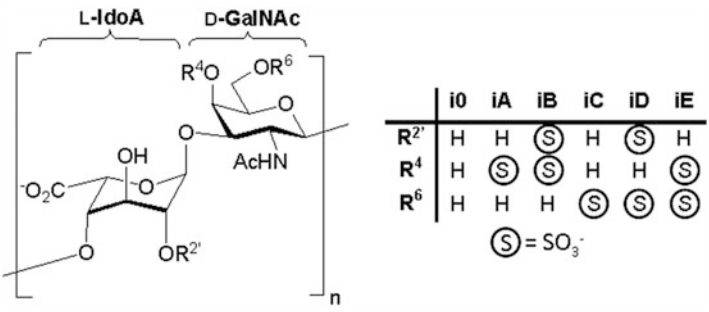

Fig. 5.6 Sulfation pattern distribution in DS

sequences with consecutive L-iduronic acid residues) as found in CS/DSPGs such as decorin and biglycan, or sequences bearing isolated IdoA units (as in versican CS/DSPG), or tracts with alternating of D-gluco- and L-iduronic acid residues, as found in decorin and biglycan again. Experiments with mutants have shown that the epimerization process likely entails an initial β-elimination mechanism induced by deprotonation at *C*-5 of a GlcA residue and detachment of the GalNAc residue as an hemiacetal; the resulting α,β-unsaturated acid then undergoes an addition process ultimately leading to reattachment of the GalNAc hemiacetal to the *C*-4 position (with retention of the initial configuration at *C*-4), and reprotonation at *C*-5 from the top face of the ring, to cause the change of configuration at that position (Pacheco et al. 2009b). The initial elimination step in this mechanism is analogous to that occurring in the lyase catalyzed GAG chain fragmentation (see Paragraph 5.3.2) and not surprisingly DS-epimerases, and some lyases feature some structural similarities. It has been recently demonstrated that epimerization mechanism of DS-epi1 requires a sufficiently long oligosaccharide chain as the substrate, with the process starting from a random uronic acid residue and proceeding toward the nonreducing terminus (Tykesson et al. 2016).

As for CS and HS, sulfation of the DS skeleton entails PAPS as the sulfo-transfer activated reagent. *C*-4 sulfation is catalyzed by a single sulfotransferase, dermatan sulfate 4-*O*-sulfotransferase 1, indicated as D4ST1. Interestingly, this enzyme was found to critically influence the extent of generation of IdoA blocks in the GAG chain, in spite of not being directly involved in the epimerization process (the sulfation step catalyzed by this enzyme follows the epimerization) (Pacheco et al. 2009c). This is just one of the numerous examples of the regulatory aspects governing GAG biosynthesis which has yet to be unveiled.

Further sulfation events can occur in DS blocks; the enzyme GalNAc(4S)-6ST specifically catalyzes sulfation at GalNAc *C*-6 position of a residue previously sulfated at *C*-4; alternatively, IdoA *C*-2 sulfation can be catalyzed by uronosyl sulfotransferase (UST), the same enzyme involved in the *C*-2 sulfation of GlcA residues in CS.

5.2.4 Keratan Sulfate

Keratan sulfate (KS) is a glycosaminoglycan consisting of the repeating disaccharide unit →3)-β-Gal-(1→4)-β-GlcNAc-(1→ (Fig. 5.1d). This is the only GAG that does not contain any acidic residue (Funderburgh 2000, 2002). The amount of substitution of the saccharide portion with sulfate groups is highly variable and depends on the localization of the KS proteoglycan (KSPG). Sulfate groups usually decorate the *C*-6 position of GlcNAc residues, although Gal units can also be sulfated at the same position.

A KSPG was firstly identified in the cornea by Suzuki (1939), who suggested only a compositional structure. Later, the structural analysis indicated the linkage of the polysaccharide to a protein moiety (Bray et al. 1967; Bhavanandan and Meyer

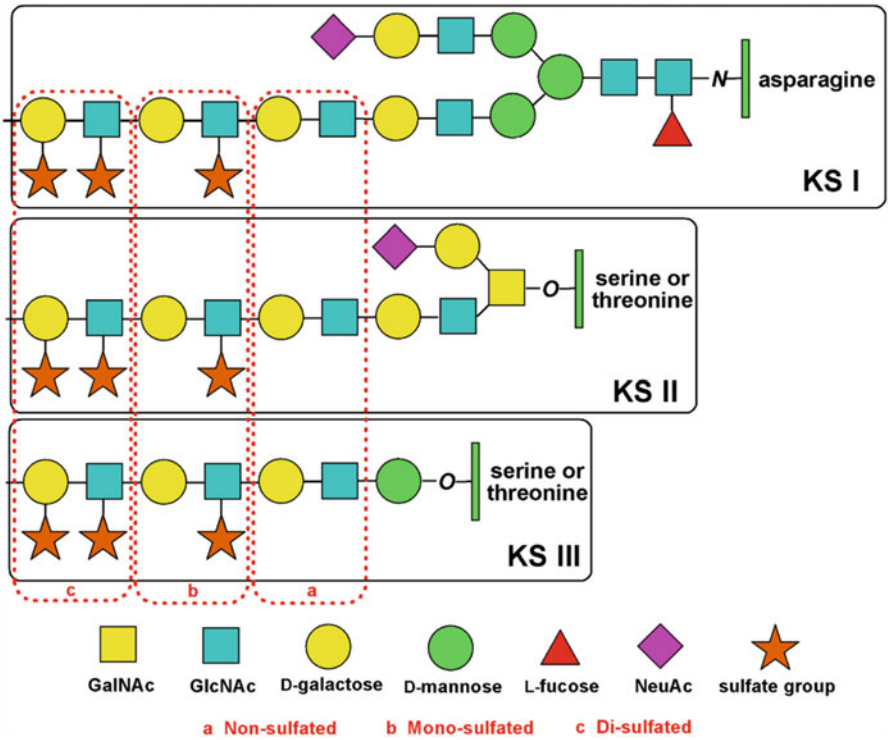

Fig. 5.7 Schematic representation of KS-I, KS-II, and KS-III structure

1968; Choi and Meyer 1975; Brown et al. 1996), revealing that in the cornea, the KS chain is anchored to an asparagine residue of the protein through a *N*-glycosidic linkage. As for the linkage to the protein core, KS is the only sulfated GAG not attached via the tetrasaccharide linker found in PGs carrying CS, DS, and HS chains (see Paragraphs 5.2.1, 5.2.2, and 5.2.3). In particular, today we know that at least three types of KS, namely, types I, II, and III, exist in nature. The classification depends on the tissue where the KS was firstly isolated and on the kind of linkage to the protein core. All these KS structures comprise segments with unsulfated disaccharide subunits, as well as regions showing mono-sulfated and disulfated disaccharides. KS-I has been mainly isolated from the cornea, even if it has also been found from small leucine-rich proteoglycans in tissues different from the cornea. The linkage of KS-I to the core protein involves a complex-type biantennary oligosaccharide, which is linked in turn to an asparagine residue through a *N*-glycosidic bond (Fig. 5.7). The second core branch is substituted by a single lactosamine disaccharide (2-acetamido-2-deoxy-4-*O*-β-D-galactopyranosyl-D-glucopyranose) capped with a *N*-acetylneuraminic acid (NeuAc) (Fig. 5.7) (Funderburgh 2000). Corneal KSPGs such as lumican, keratocan, and osteoglycin/mimecan have 2–3 KS chains with a 10–15 kDa molecular weight each (Hassell et al. 1979; Funderburgh et al. 1997; Dunlevy et al. 1998). Instead, in KS-I from non-corneal tissues, such as in

fibromodulin KSPG from human articular cartilage, the polysaccharide chain is relatively shorter and more heavily sulfated with respect to that of the cornea (Lauder et al. 1997). Fibromodulin aside, KS-I can be found in cartilage tissues in lumican and keratocan KSPGs (Plaas et al. 1990; Lauder et al. 1996).

KS-II appears in aggrecan, the most abundant proteoglycan in cartilage, which mainly contains CS chains (see Paragraph 5.2.2). The linkage to the protein core in bovine articular cartilage is, for most of the KS chains, through an *O*-glycosidic bond. KS chains in aggrecan can be found in five different domains, namely, in the hyaluronan-binding region (HABR), in the interglobular domain (IGD), in the G2 globular domain, in the KS-rich region, and interspersed throughout the CS1 and CS2 domains of the CS-rich region (Caterson and Melrose 2018). The nonreducing ends of the chains are capped by NeuAc substituting the terminal GlcNAc at the *O*-3 or *O*-6 position. A residue of α-fucose can be also present at the position *O*-3 of sulfated GlcNAc (Brown et al. 1996). Conversely, KS-II chains from non-load-bearing nasal and tracheal cartilage are not fucosylated, nor do they contain a NeuAc linked at *O*-6 position of the terminal GlcNAc (Nieduszynski et al. 1990; Dickenson et al. 1991).

KS-III, first isolated from mouse brain tissues (Krusius et al. 1986), has been recognized to be *O*-linked to a Ser/Thr unit of the protein core through a single mannose residue. Proteoglycans such as phosphacan, synapse vesicle proteoglycan-2 (SV-2), and abakan in brain tissues are rich in KS-III chains (Caterson and Melrose 2018).

Although KS is found in many kinds of tissues, only a few proteins in each tissue type are modified with KS. Consequently, there should be a fine recognition of protein amino acid sequence to specifically insert the KS chains, and some studies report indeed on the relationships between the consensus sequence and KS decoration (Barry et al. 1994; Dunlevy et al. 1998). KS biosynthesis occurs through alternating addition of Gal and GlcNAc residues to the growing chain. The Gal unit is transferred by a β-(1-4)-galactosyltransferase (β4GalT-1) (Funderburgh 2002). Interestingly, two types of β4GalT-1 have been identified up to now, of which one is able to catalyze the transfer of Gal to a nonreducing terminal GlcNAc acceptor, producing the non-sulfated poly-*N*-acetyl-lactosamine (Brew et al. 1968; Schanbacher and Ebner 1970), whereas the other recognizes the nonreducing terminal GlcNAc-6-sulfate as acceptor (Seko et al. 2003) and is responsible for the production of mono- and disulfated disaccharide subunits in the KS chain.

As for the β-(1-3)-*N*-acetylglucosaminyl transferases, many enzymes capable to transfer GlcNAc to Gal/GalNAc residues have been identified (β3GnT-1, 2, 3, 4, 5, 6, 7), even if only β3GnT-7 is clearly reported to be involved in KS chain elongation (Seko and Yamashita 2004; Uchimura 2015). After the transfer of a residue of GlcNAc, a GlcNAc-6-*O*-sulfotransferase-1 (GlcNAc6ST1) transfers a sulfo group to the *C*-6 position of GlcNAc at the nonreducing end (Uchimura et al. 1998, 2002). Finally, sulfation of the Gal residue at position *C*-6 can occur through a KS galactose 6-*O*-sulfotransferase (KSGal6ST) after the formation of the polysaccharide chain (Uchimura 2015). The biosynthesis of KS can start either in the ER as for KS-I or directly in the Golgi, as for KS-II (Hassell et al. 1986).

5.3 Structural Characterization of Sulfated Glycosaminoglycans

5.3.1 Isolation and Purification from Natural Sources

The isolation of sulfated GAGs from animal tissues firstly requires their detachment from the core protein of PGs. This can be done through a β-elimination reaction like for *O*-linked glycoproteins, nonetheless the requirement for strong alkaline conditions can result in polysaccharide structural modifications (Conrad 2001). A nonselective peptidase digestion with a proteolytic enzyme under denaturing conditions, or a stepwise treatment with different proteases, followed by purification by iterative precipitations (Garnjanagoonchorn et al. 2007; Vázquez et al. 2013), is often preferred to obtain the intact sulfated GAG chain, which in this case is still attached to the serine primer through the tetrasaccharide linkage region. Very often the polysaccharide purity achieved after the precipitations is not satisfying for a detailed structural characterization, and therefore sulfated GAG is further purified by ultrafiltration/diafiltration/dialysis techniques and/or chromatography (typically anion exchange or size exclusion techniques). Lyases – enzymes able to cleave the polysaccharide chain of GAGs (see Paragraph 5.3.2) – are also often employed in combination with molecular weight-based separation techniques, in order to avoid the contamination of the sample with other GAGs.

5.3.2 Chemical and Enzymatic Methods

Several reactions have been developed as useful tools for the analysis of sulfated GAGs structure. For example, the reaction of sulfated GAGs with 1,9-dimethylmethylene blue (DMMB) dye produces a visible light absorption with a blue shift, which is more or less pronounced depending upon the type of GAG being analyzed, thus giving a preliminary and rapid clue to the identity of the investigated GAG (Stone et al. 1994). Degradative reactions cleaving the glycosidic bonds of GAG polysaccharides (typically acid-catalyzed hydrolysis or alcoholysis) are employed for obtaining a mixture of their monosaccharide components. They can be then separated and analyzed by several chromatographic techniques as themselves or after further derivatizations. It is worth noting that such unselective depolymerization methods cause also the cleavage of sulfate groups (Toida et al. 2009). For this reason, many efforts have been devoted toward the optimization of selective degradation reactions able to cleave only a specific kind of glycosidic bond within the GAG structure, leaving the other ones as well as sulfate esters untouched. Examples include β-elimination reaction at uronic acid sites (Gao et al. 2015), deaminative cleavage on the amino sugar residues (Bienkowski and Conrad 1985), free radical or photochemical-promoted oxidative depolymerization preferentially degrading IdoA units (Nagasawa et al. 1992; Ofman et al. 1997; Panagos et al.

2016), and mild acid hydrolysis selective for L-fucose branches in fCS (Santos et al. 2017a). After extensive and suitably optimized separation of the reaction mixtures, pure sulfated GAG oligosaccharides can be obtained in this way. They are useful not only to gain some insights into subtle details of the native GAG structure, such as the determination of short sequence (4–12 saccharides) of monosaccharide constituents, but also for precise structure-activity relationship investigations.

The mildest and most selective depolymerizations of sulfated GAG chains can be achieved through enzymatic reactions. For example, endolytic enzymes such as CS/DS lyases AC I, B and ABC, heparin lyases, and hyaluronan hydrolase have been used to obtain a mixture of differently sulfated disaccharides, which can be easily separated into its single components by liquid chromatographic techniques, for example, ion-pairing reversed-phase high-pressure liquid chromatography (IPRP-HPLC) (Grøndahl et al. 2011). The obtained data allow a qualitative-quantitative determination of the sulfation pattern in the original CS/DS polysaccharide. Investigators have also reported the possibility of obtaining sulfated CS and DS oligosaccharides longer than disaccharides through non-exhaustive depolymerizations under controlled lyase digestion conditions, followed by extensive multi-step chromatographic separations (Yang et al. 2000; Deepa et al. 2007; Pomin et al. 2012b). The same approach was also used for sequencing heparin blocks through enzymatic reaction with heparin lyases (Liu et al. 1995; Mourier et al. 2015). It is worth noting that, even if enzymatic cleavage of sulfated GAG chains has a much higher specificity with respect to chemical reactions, some limitations have to be considered. Apart from the cost of such methods, some structural features of sulfated GAGs have been demonstrated to be resistant to enzymatic cleavage, as, for example, CS branching at GlcA *O*-3 position in fCS extracted from sea cucumbers. It has been proposed indeed that such branching serves to prevent digestion of the sea cucumber body wall, which is rich in fCS polysaccharide, by sea microorganisms (Vieira et al. 1991).

Another kind of enzymes useful for sulfated GAG structural characterization are sulfatases from microorganisms. They are able to cleave sulfate groups at selective positions and/or on specific units of the GAG polysaccharide chain (Ulmer et al. 2014; Wang et al. 2015). This can be exploited for confirming or refuting the presence of sulfate groups on specific sites of the studied GAG (Chi et al. 2009).

5.3.3 Physical Methods

5.3.3.1 Nuclear Magnetic Resonance (NMR) Spectroscopy

Solution NMR spectroscopy has become one of the preferred analytical techniques for structural characterization of sulfated GAGs in the last 25 years. Indeed, confirmation of data inferred from monosaccharide composition analysis (Paragraph 5.3.2) and, in addition, the determination of the positions involved in glycosidic bonds connecting the monosaccharide units and the stereochemistry of such linkages

as well as sulfation and other decoration (acetylation, fucosylation) patterns can be obtained. First, ^{1}H and ^{13}C-NMR chemical shift assignment is performed, usually exploiting homo-correlated (COSY, TOCSY, NOESY) and hetero-correlated (DEPT-HSQC, HSQC-TOCSY, HMBC) two-dimensional experiments, due to the crowd of superimposed signals in mono-dimensional spectra – especially ^{1}H-NMR – of GAGs; thereafter, comparison between the observed chemical shift values and literature data (Mucci et al. 2000; Mulloy et al. 2000; Huckerby et al. 2005; Pomin 2015) allows the elucidation of many structural details. In particular, a 0.7–1.2 ppm downfield shift for ^{1}H chemical shifts with respect to normal values, with a concomitant 5–10 ppm downfield shift for ^{13}C carbon signals, is typically informative for sulfation at the related carbinolic position. Similarly, a 8–12 ppm downfield shift of the sole ^{13}C chemical shift is indicative of a carbinolic group involved in a glycosylation linkage. $^{3}J_{H1,H2}$ and $^{1}J_{C1,H1}$ coupling constant values can be exploited for confirming the anomeric configuration expected for the monosaccharide constituents of sulfated GAGs.

The peaks of a 2D-NMR experiment such as HSQC or DEPT-HSQC can be integrated, if specific constraints are satisfied, in order to furnish a quantitative estimation of the GAG sulfation pattern in terms of the relative proportion of disaccharide subunit in the polysaccharide (Guerrini et al. 2005; Gargiulo et al. 2009; Mauri et al. 2017). It is worth noting that this is a nondestructive method for the quali-quantitative determination of sulfation pattern on GAG polysaccharide chains (Fig. 5.8), as an alternative to enzymatic hydrolysis followed by chromatographic separation of the obtained disaccharides and their comparison with standards (see Paragraph 5.3.2).

NMR spectroscopy was employed also for unveiling subtle but often crucial structural details of sulfated GAGs (e.g., the different conformations of IdoA that depend on the sulfation pattern of adjacent residues in HS chains: Ferro et al. 1990; Hsieh et al. 2016) and GAG mixtures. In the latter case, a very illustrative example is the use of NMR spectroscopy for determining the etiological agent of the "heparin contamination crisis" in 2008, with hundreds of serious adverse events, including 149 deaths, in the USA and Europe (Kishimoto et al. 2008). Indeed, a combination of ^{13}C 1D-NMR and DEPT-HSQC and HMBC 2D-NMR techniques allowed the identification of a contamination of some heparin lots with per-sulfated chondroitin (Guerrini et al. 2008), a GAG polysaccharide able to induce strong allergic-type responses (Greinacher et al. 1992). Thereafter, such 1D- and 2D-NMR techniques were indicated as an effective routine method for determining the structural differences between pharmaceutical grade heparins from different animal sources as well as for assessing their purity (Tovar et al. 2016). Diffusion-Ordered Spectroscopy (DOSY), a very powerful NMR technique for analyzing mixtures of chemical species, was also proposed for unveiling the presence of polysaccharide impurities in heparin lots (Sitkovski et al. 2008). Analogously to the heparin case, 1D- and 2D-NMR spectroscopy was shown to be an effective analytical tool also for the determination of mono- and polysaccharide ingredients and contaminants (mainly KS: Pomin et al. 2012a) present in pharmaceutical grade CS formulations (Santos et al. 2017b).

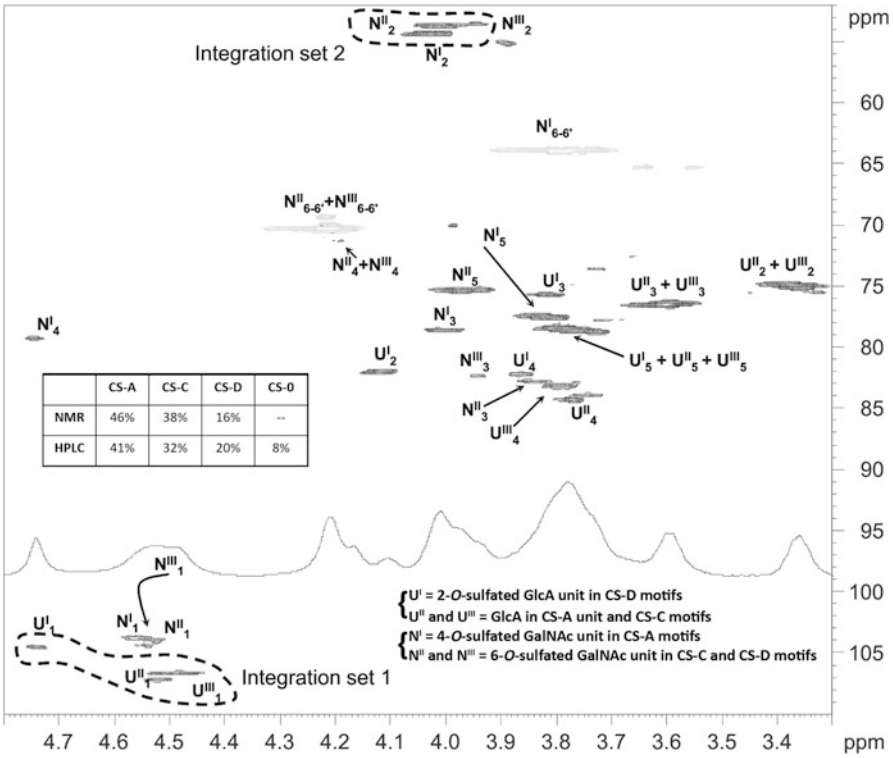

Fig. 5.8 Structural characterization of CS from dogfish and comparison between disaccharide subunit relative proportion evaluation by DEPT-HSQC 2D-NMR spectroscopy and by chondroitinase ABC chain cleavage followed by HPLC separation. (adapted with permission from Gargiulo et al. 2009; ©2009 Oxford University Press)

5.3.3.2 Mass Spectrometry

Analytical methods based on mass spectrometry (MS) are in general highly desirable for applications involving low amounts of sample and/or heterogeneous mixtures, due to its very high sensitivity and the possibility, depending upon the kind of ionization method, to detect any single component in sample mixtures or to connect the mass spectrometer online with a liquid chromatography instrument. In the case of the analysis of a pure sulfated GAG oligosaccharide or a mixture thereof, coming from chemical or enzymatic hydrolysis of the polysaccharide (see Paragraph 5.3.2), MS methods involving a matrix-assisted laser desorption ionization (MALDI) or electrospray ionization (ESI) were reported, often enhanced with tandem MS and sometimes also MS^3 techniques (Juhasz and Biemann 1995; Chai et al. 1998; Zaia and Costello 2003; Laremore et al. 2006; Nimptsch et al. 2009; Bielik and Zaia 2011). These methods were employed not only for the fine structural characterization of sulfated GAGs but also for the rapid detection, identification, and quantification of

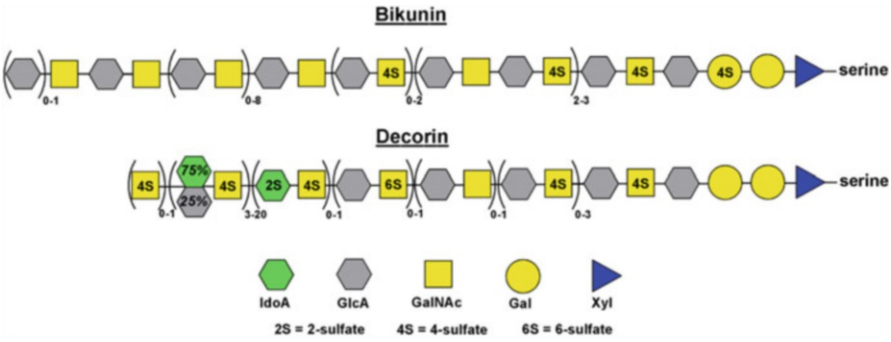

Fig. 5.9 Sequence of monosaccharide components in sulfated GAG chain of bikunin and porcine skin decorin

impurities and adulterants in pharmaceutical grade heparin and CS lots (Saad et al. 2005). Nonetheless, there is a serious limitation to the analysis of complex sulfated GAG oligosaccharides by mass spectrometric methods. It is the difficulty to gain accurate identification of the sulfation pattern as sulfate groups are labile and therefore easily lost upon collisional activation. A strategy to overcome this limitation consists in subjecting the GAG oligosaccharide mixture, coming from a controlled chemical or enzymatic hydrolysis, to a standardized chemical protocol with the aim to convert the labile sulfate groups into stable acetyl esters, while maintaining the information on the original sulfation sites (Huang et al. 2011). Furthermore, some advanced MS techniques, such as negative electron transfer dissociation (NETD) for ion trap MS and Fourier transform ion cyclotron resonance mass spectrometers (FTICR-MS), as well as collision-induced detachment (CID) or electron detachment dissociation (EDD) for FTICR-MS, have been recently applied to sulfated GAGs. They demonstrated the possibility of analyzing intact sulfated GAG oligosaccharides, by minimizing sulfate group loss and contemporarily enhancing structurally relevant glycosidic and cross-ring fragment ions, to be revealed in tandem MS or MS^n experiments (Wolff et al. 2007, 2010; Huang et al. 2013; Kailemia et al. 2014; Agyekum et al. 2018). The great potential of FTICR-MS techniques has been very well exemplified in the full sequence analysis of CS chain in bikunin, the smallest CSPG discovered up to now. Its molecular size-based fractionation through electrophoresis gave picomolar quantities of serine-linked polysaccharides with a degree of polymerization from 27 to 43. Then, the complete structure of each of them was determined by CID-FTICR-MS, and the integrated data analysis not only demonstrated unequivocally that CS chain of bikunin possesses a defined sequence but also unveiled it (Fig. 5.9) (Ly et al. 2011).

The same approach was successfully applied also on the CS/DS chain of a more complex proteoglycan such as decorin from porcine skin (Figs. 5.9 and 5.10), even if a slightly less precise sequencing output could be gained (Yu et al. 2017). Since the biosynthetic pathway is common to all natural proteoglycans, these results strongly suggest that all sulfated GAG chains of PGs, even the more structurally complex ones, such as HS, have a single or small number of sequences among the extremely huge amount of possible ones.

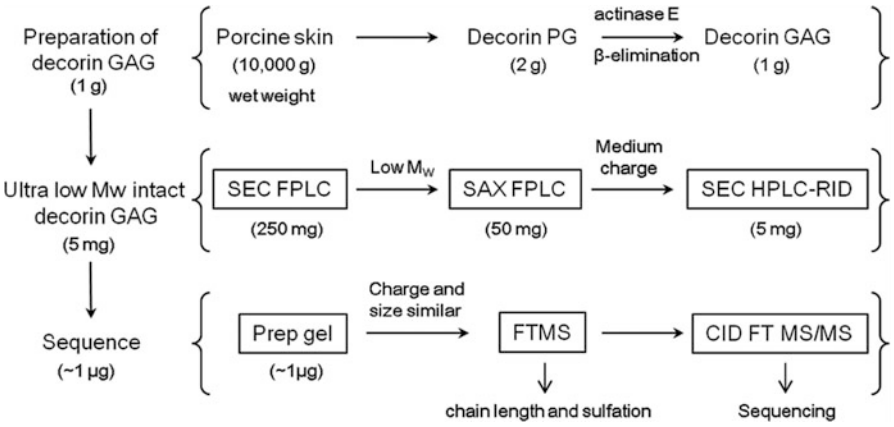

Fig. 5.10 Protocol flowchart for solving GAG chain structure of decorin. (reprinted with permission from Yu et al. 2017; ©2017 American Chemical Society)

An alternative method for sequencing sulfated GAG chains was very recently reported through an original combination of mass spectrometry and gas-phase infrared (IR) ion spectroscopy. Even if this method has been applied up to now for discriminating between IdoA and GlcA as well as determining the sulfation pattern only on short sulfated GAG oligosaccharides (Schindler et al. 2017; Renois-Predelus et al. 2018), it appears very promising as a valuable alternative to MS/MS and MS^n technique in the cases where no conditions can be found for collecting a satisfying amount of structurally informative fragment ions. The usually low resolution of IR spectra can be improved by performing the vibrational analysis on cryogenically cooled ions. Indeed, a combination of cryogenic IR spectroscopy and MS spectrometry, together with an ion mobility-based gas-phase separation, has been very recently proposed as a technique able to distinguish and sequence sulfated GAGs using very low quantity of biological samples (Khanal et al. 2017).

Recently, a MS technique has been reported that employs direct analysis in real-time (DART) pyrolysis ion source for the very rapid (approx. 30 s/sample), nanogram scale discrimination of sulfated GAGs from biological or pharmaceutical sample (Nemes et al. 2013).

5.4 Biological Functions of Sulfated Glycosaminoglycans

Sulfated proteoglycans are key molecules in a variety of physiological and pathological processes. This research field has expanded so far in the last two decades that here it is impossible to cover all aspects of sulfated GAG biology. Therefore, only a global overview of the most investigated biological processes in which HSPGs, CS/DSPGs, and KSPGs play a key role is presented here below. For more details, the reader is referred to the several, recently published, excellent reviews covering the

specific fields (Malmström et al. 2012; Xu and Esko 2014; Mizumoto et al. 2015; Mulloy et al. 2016; Caterson and Melrose 2018; Karamanos et al. 2018).

5.4.1 Heparan Sulfate

Heparan sulfate, normally in the form of heparan sulfate proteoglycans, is present in the ECM or on the cell surface of essentially all animal cells. HS has structural functions and is involved in numerous biological processes (Lindahl and Li 2009; Sarrazin et al. 2011; Xu and Esko 2014). As a component of ECM, HS contributes to its structural integrity through binding with other ECM components, such as collagen I and IV, fibronectin, and laminin. HS in the ECM can also bind cytokines, chemokines, growth factors, and morphogens, creating a protecting depot of these proteins from protease degradation and environmental damage. The proteins are released by selective degradation of the heparan sulfate chains. In addition, HS can modulate the function of the extracellular proteins acting to increase their range of diffusion and local concentration or to present the proteins to their high-affinity receptors. The highly sulfated chain of HS binds to proteins mainly through electrostatic interactions between its sulfate groups and positively charged groups of the protein, typically lysine/arginine residues aligned in "Cardin-Weintraub" sequences (Cardin and Weintraub 1989). Some nonionic interactions are also present and they do not occur randomly. The specificity and the affinity of a protein for HS chains depends largely on the sulfation profile and chain length of HS (Capila and Linhardt 2002; Lindahl and Li 2009). Some examples of HS-binding proteins with their biological activity are reported in Table 5.1. A comprehensive list can be found in Mulloy et al. 2016.

One of the most relevant aspects of HSPGs located in the ECM or inserted in the cell membrane is that they can act as scaffold bringing two proteins into close proximity to facilitate their interactions. A ternary complex is formed between the two proteins and the HS chain. This property of HSs is possible owing to their long-chain length, flexibility, and structural diversity. A very well-documented system in which HS serves as molecular scaffold is the antithrombin/thrombin interaction, which results in the inhibition of blood coagulation cascade (van Boeckel and Petitou 1993; Desai et al. 1998). Thrombin is an enzyme that converts fibrinogen into soluble strands of fibrins, which is a main step in the blood coagulation cascade. Antithrombin by itself is not an efficient inhibitor of thrombin. However, its inhibitory activity increases up to several thousand-fold in the presence of heparin, due to the ability of the polysaccharide to bring antithrombin and thrombin into close proximity. The binding of antithrombin to heparin induces a conformational change in the protein which results in the inhibitory activation of antithrombin. While a specific sulfated pentasaccharide fragment is sufficient for antithrombin and a sulfated hexasaccharide is required for thrombin binding (Desai et al. 1998), a longer octadecasaccharide containing the sulfated pentasaccharide fragment at the reducing

Table 5.1 Examples of HS-binding proteins and their biological activity

Class	Examples	Physiological function	Pathophysiology
Growth factors	FGF2, $VEGF_{165}$, neuropilin-1	Mitogenesis, development, wound healing, angiogenesis, axon guidance	Cancer
ECM proteins	Collagen, fibrinogen, laminin	Cell adhesion, migration, differentiation, blood coagulation	Cancer, Knobloch syndrome
Cell adhesion proteins	P-selection, L-selectin, integrins	Cell adhesion, inflammation	Cancer
Morphogens	Activin, BMP-2, sonic hedgehog	Development, regeneration, bone formation	Multiple hereditary exostoses, osteoarthritis
Chemokines	Platelet factor 4, IL-8, TNF-α, CXCL12	Chemotaxis, cell migration, immune response, angiogenesis	Inflammation, arteriosclerosis, cancer
Blood coagulation factors	Antithrombin III, factor Xa, leuserpin-2	Regulation of clotting cascade	Heparin-induced thrombocytopenia
Lipoproteins	ApoE, ApoB, lipoprotein lipase	Lipid metabolism, cell membrane functions	Atherosclerosis, Alzheimer's disease, AA amyloidosis
Nuclear proteins	Histones, transcription factors	Unknown	Cancer
Amyloid proteins	App, Aβ, tau protein, α-synuclein, PrP^{Sc}	Synapse organization, brain development, memory, circadian rhythm	Alzheimer's/Parkinson's disease, prion disease
Viral proteins	gB, gC, gD, gp120, Tat, E protein, L1 capsid protein	–	Viral attachment and invasion
Microbial proteins	M protein, PfEMP1, Opa, circumsporozoite protein	–	Bacterial/parasite infection, inflammation

Reprinted with permission from Weiss et al. 2017; ©2017 Royal Society of Chemistry

end is the minimal sequence able to form the ternary antithrombin-thrombin-heparin complex (Lane et al. 1984; Petitou and van Boeckel 2004).

A large number of studies on the ternary complex model involving HS, growth factors, and their high-affinity receptors have also been reported. Commercial heparin and fragments derived from its partial enzymatic hydrolysis have been frequently used to investigate this model. Thus, it has long been known that fibroblast growth factor (FGF) signaling requires the formation of a FGF/FGFR/HS ternary complex (Rapraeger et al. 1991; Kan et al. 1993). The FGF/FGFR complexes tend to dissociate under size exclusion chromatography conditions. However, in the presence of heparin, the ternary complex is much more stable and can be purified by chromatography, indicating that heparin increases the affinity of FGF toward FGFR (Schlessinger et al. 2000). The binding to heparin might induce a conformational change in FGF to generate a molecular structure that better fits into

the FGFR binding site. Structural studies have shown different complex stoichiometries, and two ternary complex models have been suggested: a symmetrical 2:2:2 FGF/FGFR/HS complex with two saccharide chains and a 2:2:1 complex with a single saccharide (Goodger et al. 2008). An octasaccharide seemed to be the shortest heparin fragment that formed 2:2:1 complexes, while very short heparin fragments (tetra- and hexasaccharides) would form symmetrical 2:2:2 complexes (Robinson et al. 2005; Goodger et al. 2008). Similar mechanisms based on ternary complexes were also proposed for other signaling pathways, such as those for bone morphogenetic protein (BMP) (Ruppert et al. 1996), wingless-type MMTV integration site family (WNT) (Reichsman et al. 1996), and vascular endothelial growth factor (VEGF) (Gengrinovitch et al. 1999). As a result of these interactions with proteins, many of them involved in cell signaling pathways, HSs are able to modulate a variety of processes that are important in the regulation of cell, tissue, and organ development in health and disease (Whitelock and Iozzo 2005; Xu and Esko 2014), which is discussed next.

Several studies have shown that HSPGs are key regulators of stem cell biology (Mikami and Kitagawa 2017). Stem cells are defined by their ability to self-renew and their capacity for differentiation into specialized cells. The decision of stem cells to self-renew or undergo differentiation is regulated at multiple levels. Several growth factors that regulate signaling pathways in cellular proliferation and differentiation are HS-dependent. Because the interaction with these proteins depends on the structure and sulfation profile of the HS chain, the cellular biosynthetic machinery for HS production participates in the regulation of stem cell fate. Thus, it has been shown that the biosynthesis of HS increased and its composition changed during the transition of embryonic stem cells from self-renewal to differentiation (Johnson et al. 2007; Nairn et al. 2007; Smith et al. 2011). This switch seems to be dependent on specific sulfation motifs on HS chain, since differentiation is accompanied with expression of specific sulfotransferases that modified HS sulfation profile (Johnson et al. 2007; Nairn et al. 2007). On the other hand, when the stem cells are deficient in the HS polymerase EXT-1 and are unable to synthesize HS chains, these cells are maintained in a pluripotent state and are unable to differentiate.

Some relevant biological functions of HS are played in the central nervous system together with CS. In contrast to other organs and tissues, the ECM of the central nervous system (CNS) shows relatively low content of fibrous matrix proteins such as collagens and fibronectin. Instead, it is particularly rich in proteoglycans that are synthesized by neurons and astrocytes (Ruoslahti 1996). HS and CS proteoglycans of the ECM and on the surface of neural cells play relevant roles in brain development, axon growth and guidance, formation and function of synapses, and also response of the CNS to injury (Maeda 2015; Smith et al. 2015).

When the nervous system is forming, the neurons connect with other neurons by fibers, dendrites, and axons to form complex neuronal networks. During this process, the axons extend over long distances to connect with other brain cells. In order to reach their targeted brain regions, some chemical substances act as guidance cues, by attracting or repelling axons. These molecules with key roles in neural wiring are

classified into four major families: netrins, semaphorins, slits, and ephrins. A critical role for HS in axon guidance was demonstrated in mutant embryonic mouse brain cells that are unable to synthesize HS (Inatani et al. 2003). The EXT1-null brain displayed severe guidance errors in major commissural tracts. In another study with two HS sulfotransferase mutant embryos lacking the capacity to catalyze sulfation at *C*-2 of uronic acid and at *C*-6 of glucosamine, it was shown that the sulfation pattern of HS was important in the navigation of retinal ganglion cell (RGC) axons (Pratt et al. 2006). The author demonstrated that the response of RGC axons to slit2 depended on the 6-*O*-sulfotransferase synthesized by the RGC. Similarly, by manipulating extracellular sulfation pattern of HS, the axonal projection of motor neurons was redirected upon misexpression of the HS 6-*O*-sulfotransferase (Bülow et al. 2008). In another study that focused on the family of ephrins, which induce repulsive responses such as growth cone collapse, it was shown that in mutant cells, which are defective in HS synthesis, the ephrin-A3-dependent EphA receptor activation was reduced, which indicates that HS modulates this signaling pathway (Irie et al. 2008). These examples, illustrating the role of HS and the influence of their sulfation profile on axon guidance, use gene knockout experiments of HS biosynthetic enzymes. The results from these experiments, however, must be taken with caution since there may exist compensation mechanisms with an increase in other sulfation types (Kamimura et al. 2006). In order to study the structure-function relationships of HS, the availability of HS structures with defined sulfation motifs is of great value. Using a microarray-based approach, Shipp and Hsieh-Wilson showed the importance of the sulfation profile of HS in the interaction with a number of axon guidance proteins such as slit, netrin, ephrin, and semaphoring (Shipp and Hsieh-Wilson 2007). They used heparins that had been previously desulfated selectively at certain positions using chemical tools. A strong preference of slit2 for 6-sulfated heparin and 2-desulfated heparin was observed. They also found that netrin1 requires sulfation at *C*-2 and *C*-6 and sulfamation at *C*-2. In the case of ephrinA1 and ephrinA5, they exhibited preference for HS having both 2-sulfated and 2-sulfamated motifs.

HSPGs are strongly involved in cancer proliferation, invasion, and tumor metastasis (Afratis et al. 2012). Certain cancer cells show an increased expression of HSPG on the cell surface, which results in an enhancement of the proliferative response to growth factors (Knelson et al. 2014). In the ECM, on the other hand, HSPGs play a crucial role in cancer progression. For tumor cells invading surrounding normal tissue and spreading via the circulatory system, degradation by heparanase of HSPGs in the ECM is an important step. The growth factors that bind HS in the extracellular matrix include the proteins that regulate angiogenesis and vasculogenesis, such as the VEGF and FGF families. Therefore, the disruption of HS chains of the ECM catalyzed by heparanase will lead to the release of proteins that stimulate proliferation of tumor cells, angiogenesis, and vascularization of the tumor. Angiogenesis is a prerequisite for the growth of tumors, and hence the enzyme heparanase produced by tumor cells is considered a pro-angiogenic factor.

Heparanase is an endo-D-glucuronidase that cleaves heparin and HS. The enzyme catalyzes hydrolysis of the glycosidic bond between anomeric carbon of D-glucuronic acid and *O*-4 of D-glucosamine. The enzyme, however, does not

cleave all the glucuronide bonds, but there is a selectivity depending on the presence of sulfate groups around the glycosidic bond. Therefore, hydrolysis of HS by heparanase generates fragments of variable size, between 10 and 20 monosaccharide units. The existence of heparanase activity has been known for more than 30 years. However, the structures of free human heparanase and heparanase associated with several heparan sulfate ligands have recently been described (Wu et al. 2015). Expression of heparanase in normal tissues is relatively low. In contrast, the enzyme is overexpressed in many tumor cells, and some studies have confirmed a correlation between heparanase expression and increased mortality (Sato et al. 2004). Several causes for tumor aggressiveness have been proposed. In addition to releasing proteins that promote proliferation and angiogenesis, some fragments of HS generated by heparanase-catalyzed hydrolysis may also activate intracellular signaling pathways (Goodall et al. 2014). Also, when the structural integrity of the ECM and of the basement membrane is lost, mobility and invasion of neighboring tissues is facilitated; furthermore, tumor cells may enter the bloodstream and lead to metastasis. Destruction of blood vessels is another consequence of overexpression of heparanase, which potentiates metastasis. HSPGs are important components in the structural integrity of blood vessels. Excessive rupture of HS from blood vessels and capillaries by the action of heparanase weakens their structure and facilitates extravasation of tumor cells (Jin-Ping 2008).

There is only one heparanase enzyme activity in humans, which is expressed at very low levels in normal cells. Animals with knock-out of the gene encoding heparanase did not show any type of deficiency or phenotype change, which suggests that the inhibition of heparanase will cause minimal side effects in patients with cancer. Altogether, this makes the enzyme a highly attractive target for cancer therapy (Vlodavsky et al. 2016).

Heparin has been evaluated in clinical trials against various types of cancer. The properties of heparin as an anticancer agent were discovered indirectly in patients with cancer who developed venous thrombosis (Jin-Ping 2008). When these patients were treated with heparin, they showed a reduction in mortality compared to those not treated with the anticoagulant. Epidemiological studies and subsequent clinical trials with heparin and other anticoagulants demonstrated its protective and therapeutic effect in treatment of metastatic tumors (Tagalakis et al. 2007). Several factors may contribute to the antitumor activity of heparin. A main line of study focuses on its activity as a heparanase inhibitor. Although heparin can be a substrate for heparanase, since it is a large molecule, its hydrolysis can generate fragments that act as inhibitors of the enzyme. Heparin might also associate and sequester growth factors that stimulate proliferation of tumor cells. Concerning its antimetastatic activity, some studies have focused on its ability to inhibit the interaction of tumor cells with adhesion proteins (P- and L-selectins) expressed in the endothelial cells of blood vessels and involved in the extravasation process during metastasis (Stevenson et al. 2005). P- and L-selectin are also involved in inflammatory processes, and hence heparin has been studied as an anti-inflammatory agent.

The use of heparin as an anticancer drug, however, is restricted by its anticoagulant activity. In addition, its highly negative charge density (heparin is a highly

sulfated HS) allows its interaction with a variety of proteins in a non-specific way and therefore affects many other functions. For this reason, more specific heparin analogs without anticoagulant activity are being studied as anticancer agents (Afratis et al. 2012; Vlodavsky et al. 2016). Four compounds with anti-heparanase activity have been approved for clinical trials with cancer patients (PI-88, Roneparstat, M402, and PG545). All of them are heparin analogs/mimetics, which presumably block the active center of the enzyme by interacting with the heparin-binding domains flanking the catalytic center. PI-88, also called Muparfostat, is the most extensively studied HS mimetic in clinical trials. It has reached stage III in the treatment of patients with hepatocarcinoma (Vlodavsky et al. 2016). PI-88 is a sulfated derivative of a phosphomannopentaose, which inhibits heparanase activity with an IC_{50} value of 1.7 μM and exhibits anti-angiogenic and antimetastatic activity. In addition to heparin and structural analogs, other non-sugar molecules have been studied to inhibit heparanase activity, including small molecules, anti-heparanase antibodies, or nucleic acid-based inhibitors (Rivara et al. 2016). In conclusion, a substantial amount of knowledge concerning heparanase function comes from studies on its role in cancer progression. The current interest in development of clinically relevant heparanase inhibitors for cancer therapy is, after all, a direct consequence of the important roles of heparan sulfate in the ECM.

Cell surface HSs are exploited by several bacteria, parasites, and viruses as mediators for infecting animals. HSPGs are used by microbial pathogens not only to achieve adherence and colonization but also in the invasion, internalization, dissemination, and toxicity processes. A comprehensive list of human pathogenic microorganisms that are known to recognize HS (and in some cases also CS and DS) as cell surface receptors can be found in García et al. (2016). The interactions have been inferred to be non-specific, driven by the highly negative charge density of HS chains, even if in some cases unique chain sequences appear to be involved in the adherence process, as demonstrated for the interaction of HS with herpes simplex virus type-1 (HSV-1) proteins (Shukla and Spear 2001) and suggested for the binding of HS with human immunodeficiency virus (HIV) envelope glycoprotein gp120 (Connell and Lortat-Jacob 2013).

5.4.2 Chondroitin and Dermatan Sulfate

CS/DSPGs have been demonstrated to interact with a plethora of key proteins for important biological functions, such as cell proliferation, differentiation and migration, cytokinesis, tissue morphogenesis and wound repair, and infection. A schematic, non-comprehensive picture of CS/DSPG functions is reported in Fig. 5.11.

CS has profound effects on the synthesis, activity, and turnover of key structural components of the ECM in connective tissues, such as type-II collagen and hyaluronic acid. For example, the synthesis of such macromolecules is fostered by TGF-β1 and HAS-2 growth factors, respectively, the expression of which is enhanced by CS binding to integrins (Bishnoi et al. 2016). Loss of CS from cartilage

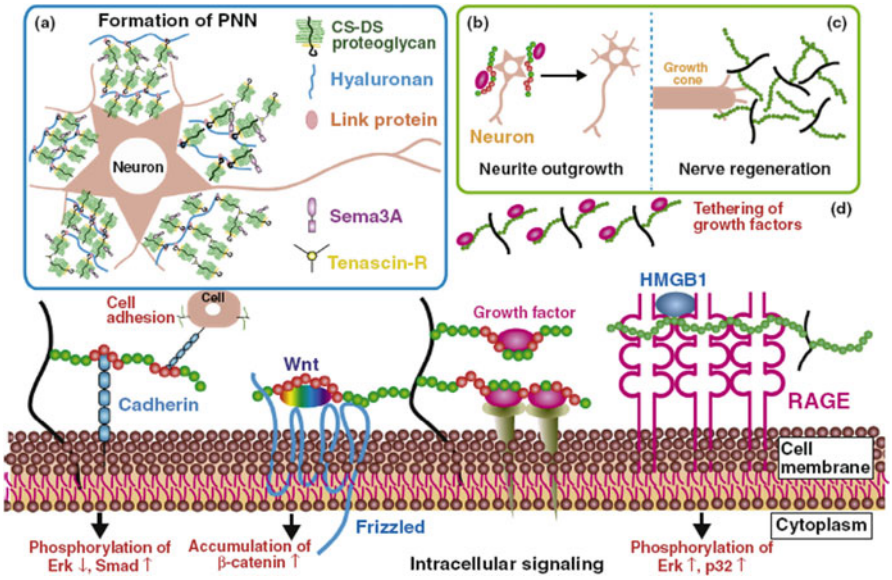

Fig. 5.11 Various functions of CS/DSPGs: (**a**) formation of perineuronal nets (PNN), (**b**) neurite outgrowth activity, (**c**) inhibition of nerve cone growth after spinal cord injury, and (**d**) regulation of signal transduction, osteogenesis, and tumor metastasis through interaction of cell surface CS/DSPGs with growth factors and signaling proteins. (reprinted with permission from Mizumoto et al. 2015; ©2015 Elsevier)

tissues leads to osteochondral angiogenesis, one of the major cause of osteoarthritis (Bara et al. 2012), a very common disease of the aged population for which the administration of exogenous CS represents indeed a first-line therapy. Therapeutic efficiency of CS for osteoarthritis treatment is related not only to structural roles but also to an anti-inflammatory effect. The latter is due to the inhibition of signal transduction pathways, activated by damage-derived fragments of the ECM components in chondrocytes, synoviocytes, osteocytes, and osteoblasts and leading to a diminished translocation of pro-inflammatory transcription factors. In particular, CS oligosaccharides engage chondrocyte membrane receptors such as CD44 and ICAM1, to release IRAK-M, an IRAK inhibitor, and MPK-1, a MAPK dephosphorylating agent, both causing a reduction of nuclear translocation of NF-κB and therefore alleviating the inflammatory reaction. Furthermore, CS diminishes the proteolytic cleavage of kininogen to bradykinin, which induces the desensitization and internalization of B2R (du Souich 2014).

CS and DS are involved in hepatocellular proliferation and differentiation, by interaction with hepatocyte growth factors (HGF and HB-EGF). In particular, it seems that highly sulfated variants of CS and DS are involved in physiological processes (Lyon et al. 1998; Li et al. 2007), whereas in rat models with fibrous lesions due to liver cirrhosis, a decrease of the sulfation degree and an increase in CS

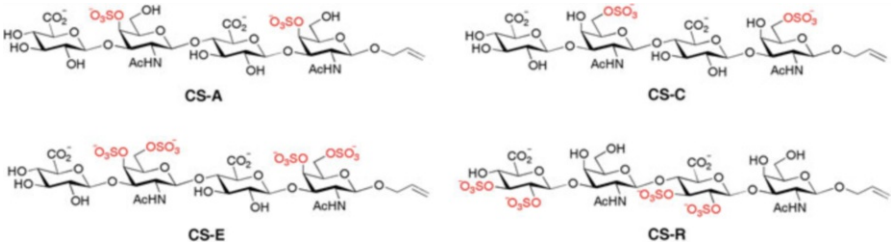

Fig. 5.12 Chemical structure of CS-E, CS-C, CS-A, and CS-R tetrasaccharides assayed for their interaction with protein growth factors (Gama et al. 2006)

to DS ratio have been detected (Koshiishi et al. 1999). Furthermore, a deficiency in xylosyltransferase 2 (one of the enzymes initiating HS and CS/DS biosynthesis: see Paragraph 5.2.1) results in significant abnormalities of liver structure such as fibrosis, biliary tract hyperplasia, and cysts (Condac et al. 2007).

Like HSPGs, CSPGs play a significant role in CNS development (Silver and Silver 2014; Miller and Hsieh-Wilson 2015; Hayes et al. 2018). They are essential for FGF-2-mediated proliferation and maintenance of neural stem cells (Sirko et al. 2010) and interact with different growth factors (Rogers et al. 2011). The interaction with proteins is also determined by specific sulfation motifs in the CS chain. To define the sequence of sulfate groups and study the structure-function relationship of CSs, chemically synthesized CS tetrasaccharides (CS-A, CS-C, CS-E, and CS-R: Fig. 5.12; see also Fig. 5.4 for nomenclature of CS subunits) were assayed for their interaction with protein growth factors (Gama et al. 2006). A selective binding of midkine and neurotrophin BDNF to the CS-E tetrasaccharide was found, while none of the tetrasaccharides showed appreciable interaction with fibroblast growth factor FGF-1. Although CSPGs are known to repel extending axons, some sulfation variants of CS have been found in growth permissive regions of the CNS. Therefore, the authors investigated the effect of the sulfation patterns on the neurite outgrowth of hippocampal, dopaminergic, and dorsal root ganglion neuron cultures. Only the tetrasulfated CS-E stimulated the neurite outgrowth of the different cell types. Altogether, the results suggest that CS sulfation motifs can function as molecular recognition elements for growth factors and facilitate activation of the corresponding signaling pathways.

The fact that CS chains can stimulate or inhibit neuronal outgrowth depending on the sulfation sequence has been utilized to fabricate neuron-guiding substrates (Swarup et al. 2013). In particular, four major CS sulfation variants (CS-A, CS-C, CS-D, and CS-E) and DS found in mammalian brain were printed in stripes on preactivated poly-L-lysine-coated substrates. Hippocampal neurons were then cultured on printed CS stripes. Neurites preferred growing over CS-A, CS-E, and DS lanes and avoided penetrating into the CS-C containing lanes. The binary combination containing alternate lanes of neurite repelling (CS-C) and attracting (CS-A, CS-E, and DS) polysaccharide chains led to a significant alignment of neurites on the attracting lanes (Fig. 5.13).

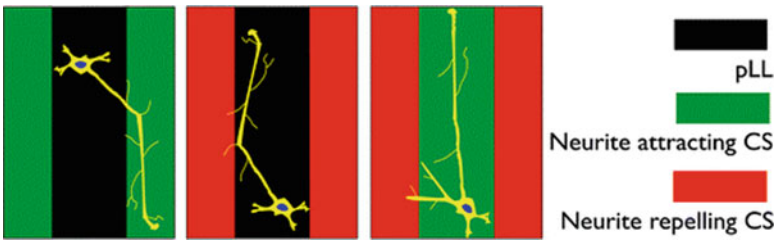

Fig. 5.13 Fluorescent images of effect on neurite growth of poly-L-lysine (pLL)-coated glass surface printed with CSs having different sulfation patterns. (reprinted with permission from Swarup et al. 2013; ©2013 American Chemical Society)

CSPGs are involved in the control of neural plasticity, the ability of the brain to rewire the neural circuits in response to new experiences. In the mammalian CNS, there is a postnatal limited time window, which is called the critical period, during which neuroplasticity is at a high level. When the critical period ends, reticular structures, known as perineuronal nets (PNNs), deposit around the cell bodies and dendrites of neurons helping to stabilize the newly established synapses but restricting plasticity. PPNs contain components of the ECM with high concentration of CSPGs, which play an important role in maintaining stability and restricting plasticity (Bartus et al. 2012; Miyata and Kitagawa 2017). As an illustrative experiment to show that CS can suppress neuronal plasticity, it was reported that the injection of chondroitinase ABC, which catalyzes the eliminative degradation of CS, into the adult visual cortex of rats led to a reactivation of ocular dominance plasticity, even after the end of the critical period (Pizzorusso et al. 2002). In line with this study, Gogolla et al. (2009) showed that CSPGs of PNNs could be responsible for the resistance of fear memories to erasure by extinction in adult rats. In contrast to adult animals, extinction in young rats leads to erasure of fear memories. When adult mice were injected in the amygdala with chondroitinase ABC, the subsequently acquired fear memory was susceptible to erasure (Gogolla et al. 2009). Therefore, degradation of CSPGs in adult rats reenabled erasure of fear memories by extinction that is typical in young rodents.

The influence of specific sulfation patterns of CS on cortical plasticity was shown in transgenic mice that overexpress human C6ST-1 enzyme, which catalyzes the sulfation of CS chains at position 6 (Miyata et al. 2012). The authors found that the increase in GalNAc 4- vs. 6-*O*-sulfonation of CSPGs of the brain ECM leads to the termination of the critical period for ocular dominance plasticity in the mouse visual cortex. Consequently, they observed that the mice with upregulated 6-*O*-sulfonation had reduced PNN formation, and they retained juvenile-like plasticity as adults. The results suggest that the temporal shift of the 4S/6S ratio may be developmentally programmed to regulate the critical period for cortical plasticity.

CS plays a central role in traumatic injury of the brain and spinal cord, which is a major health problem worldwide and is associated with long-term physical difficulties. After injury in the CNS, there is a reaction which results in recruitment of glial cells and formation of a scar surrounding the injury site. Although these responses

could be beneficial since isolating the injury can minimize the damage, some ECM components produced by these glial cells can inhibit regeneration and thus retard functional recovery. It is well known that CSPGs released by reactive astrocytes are major impediments to axonal regeneration and the inhibitory activity depends upon CS sulfation pattern (Smith et al. 2015). In addition to increased expression of CSPG by astrocytes, there are also changes in the sulfation pattern of the CS chains (George and Geller 2018). Expression of 4- and 6-sulfotransferases, which modify the GalNAc unit, is upregulated. Although the exact mechanisms by which these CSPGs affect axonal regeneration are not entirely known yet, one possibility is that they interact with transmembrane receptors on the neuron cell surface. It was reported that a transmembrane protein tyrosine phosphatase, PTPσ, is a receptor for CS chains that mediates the inhibitory effect of CSPGs in the glial scar (Shen et al. 2009). The identification of this receptor provided a new target for therapeutic approaches. Thus, administration of a peptide that binds to PTPσ was reported to restore axon regeneration and facilitate functional recovery after spinal cord injury (Lang et al. 2014). A widely used approach tested in many injury models that can neutralize the inhibitory effect of CSPGs is treatment with chondroitinase ABC, which degrades the CS chains (Bradbury and Carter 2011).

Interestingly, CS and HS have been shown to have antagonistic effects in some biological functions. Thus, while CSPG restricts neuronal plasticity by stabilizing the existing synaptic connections, HSPG syndecan-2 was shown to induce dendritic spine formation in hippocampal neurons (Ethell et al. 2001). The opposite functions were described in neuronal polarization, in which CS stabilizes and the HS destabilizes the growth of axons (Nishimura et al. 2010). In another example, CS interacts with transmembrane receptors RPTPσ during inhibition of axon growth after injury, as discussed above, while HSPGs binding to this receptor promotes axonal growth (Aricescu et al. 2002). An interesting antagonistic activity was found for TβRIII transmembrane proteoglycan that exists with HS and/or CS chains linked to the protein core (Jenkins et al. 2016). This proteoglycan regulates Wnt signaling in cells with roles in development and cancer. HS chains result in inhibition of Wnt signaling, whereas CS chains promote the signaling cascade. The authors suggested that TβRIII proteoglycan state (HS and/or CS) may be regulated by the expression of the glycosyltransferases which initiate the synthesis of HS or CS chains. The final balance of HS and CS determines the ligand responses.

As illustrated in the above examples focused on the nervous system, the variety of processes in which HS and CS are involved depend largely on the distribution of sulfate groups along the sugar chain. This sulfation pattern is determined in a dynamic way by the enzymatic synthesis and modification of HS and CS. Evidence accumulated in the last two decades indicates that during development and damage repair, the nervous system makes use of spatial and temporal expression of sulfotransferases and sulfatases, which modify the sulfation profile of HS and CS, to regulate a number of biological processes. Considering the high molecular diversity that can potentially exist in HS and CS chains, it is not surprising that a "sulfation code" hypothesis has been proposed, whereby HS and CS encode functional information in a manner similar to those of nucleic acids and proteins (Bülow and Hobert 2004; Holt and Dickson 2005).

As well as HS, CS and DS have been also found to play pivotal roles in the biology of tumors. Tumor progression has been associated with several cases with accumulation and structural modification of CS/DSPGs (Wegrowski and Maquart 2004). For example, by comparing the structural characteristics of versican and decorin in human colon adenocarcinoma vs. normal tissues, a noticeable increase of CS vs. DS subunit content and a profound change of the sulfation pattern – from about 75% of iA subunits (see Paragraph 5.3.3.1 and Fig. 5.9) to approx. 65% of C subunits – were observed, together with a slight decrease in the length of the polysaccharide chain (Theocharis 2002). Overexpression and altered sulfation patterns of CS chains with respect to tissue from healthy organs were similarly reported for various phenotypes of breast, prostate, testicular, lung, gastric, and pancreatic malignant cancers (Theocharis et al. 2000, 2003; Li et al. 2008; Svensson et al. 2011). Structural alterations of CS chains in carcinoma cells result in various activities with respect to binding with growth factors, selectins, CD44 receptor, and metalloproteinases, all involved in tumor formation, progression, spreading, and metastasis (Afratis et al. 2012). In some cases, the specificity of CS sulfation patterns leading to enhanced binding has been revealed. For example, an enhanced level of A subunits specifically favors the complexation of CS with metalloproteinases in melanoma cells, leading to activation of the metastatic cascade (Iida et al. 2007), or affects integrin signaling pathways governing tumor cell motility (Clausen et al. 2016). In several cases CS-E subunits have been detected to give a specific interaction with growth factors involved in tumor growth and spreading. For example, expression of CS-E in ovarian adenocarcinoma ECM mediates VEGF binding, which promotes signaling pathways related to tumor progression, whereas in the physiological case, such kind of CS subunit is absent (Ten Dam et al. 2007). Analogously, in CD44-expressing pancreatic tumor cells, partially depolymerized CS-E chains specifically enhance CD44 receptor cleavage, a process involved in tumor cell motility (Sugahara et al. 2008). The overexpression and structural modification of CS and DS in tumors are currently under investigation also for exploiting them in targeting malignant cells or tissues. In particular, liposome or nanostructured delivery systems of anticancer drugs or genes have been formulated for the selective release to CS-overexpressing tumor cells (Lee et al. 2002). Antibodies against specific CS sequences blocking their action in tumor progression have been reported too (Afratis et al. 2012). Furthermore, chemical and/or enzymatic synthesis of CS oligosaccharides with tailored, well-defined structures has been exploited to inhibit interaction of CS chains overexpressed in tumor cells with their receptors (Mizumoto et al. 2012; Poh et al. 2015).

As already mentioned for HS, CS located on cell surfaces can be exploited by some microorganisms for adhering to and then entering animal cells (Yamada and Sugahara 2008). In particular, Lyme disease spirochete, HSV-1, and malarial parasite are known to interact with cell surface CS (Banfield et al. 1995; Alkhalil et al. 2000; Mårdberg et al. 2002). Concerning malaria, it has been demonstrated that CS sulfation pattern found on the placental syncytium is strictly related to the high susceptibility of pregnant women to *Plasmodium falciparum*, even despite previous immunity. Indeed, placental CS is different from CS present in other organ tissues, with the higher content of blocks of continuous CS-A disaccharide subunits in the

former allowing a stronger interaction with the unique protein VAR2CSA present on *P. falciparum* infected erythrocyte membranes (Sugiura et al. 2016).

The flexibility related to the presence of IdoA, a monosaccharide featuring several conformations such as $^{1}C_{4}$ and $^{4}C_{1}$ chairs, and $^{2}S_{O}$ skew-boat, whereas GlcA essentially displays only a $^{4}C_{1}$ chair conformation (Ferro et al. 1990), is usually invoked for explaining some special biological functions associated with DS or hybrid CS/DS chains, as discussed here below.

Collagen 3D structure formation is a really complex phenomenon entailing the engagement of a large number of collagen ligands, including several PGs (Kadler et al. 2008); the core protein of decorin CS/DSPG seems to be implicated in interaction with collagen through multiple binding domains (Schonherr et al. 1995), whereas the single GAG chain of decorin was shown to play an important role in collagen fibril formation at the early stages of fibrillogenesis (Rühland et al. 2007). In addition, DS can mediate the linkage of collagen with other macromolecules, for example, tenascin-X, an ECM protein important for the properties of connective tissues (Elefteriou et al. 2001). The specific nature of the GAG structures can influence the diameter of collagen fibers; for example, in tendons the highest diameters are observed in tissues more enriched with DS, whereas decreasing values are detected in tissues with higher amounts of CS and HA (Ryan et al. 2015).

There are several pieces of evidence about possible interactions of DS sequences with growth factors, events with relevant biological implications. For example, relatively short DS sequences can bind with high affinity to hepatocyte growth factor/scatter factor (HGF/SF) (Deakin et al. 2009), secreted by mesenchymal cells and implicated in the regulation of cell growth, motility, and morphogenesis. Endocan, a CS/DSPG specifically secreted by endothelial cells, was found to interact with HGF/SF, thereby stimulating mitogenic activity (Bechard et al. 2001). DS can potentiate the response of fibroblast growth factor type 2 (FGF-2) on skeletal muscle satellite cell proliferation and migration (Villena and Brandan 2004). GAG chains of syndecan-4 and glypican-4 PGs are directly involved in the activation of FGF in early stages of embryo development through initial formation of a GP-FGF complex and subsequent degradation of the proteoglycan core protein performed by a protease overexpressed at this stage, with consequent release of an active DS-FGF complex that stimulates long-range FGF signaling (Hou et al. 2007).

DS also plays a role by interacting with several mediators of coagulation, as typically ascribed to heparin structures. For example, decorin binds to von Willebrand factor, a protein implicated in platelet adhesion in wounded sites, through its single CS/DS chain. The affinity in this case is less influenced by IdoA content but, rather, by sulfation degree (Guidetti et al. 2004). DS chains, even if not especially long, can bind with high affinity to HCII, accelerating the inhibitory action of this protein toward thrombin (Maimone and Tollefsen 1990; Sarilla et al. 2010). In particular, a DS hexasaccharide fragment composed of three iB subunits (see Fig. 5.6) has been recognized as responsible for an approximately 1000-fold increase of the rate of HCII-mediated inhibition of thrombin by providing a template to which both HCII and thrombin bind (Tollefsen 1992).

DS is able to bind to α-defensin, a small neutrophil-derived peptide, and this interaction results in neutralization of the bactericidal action of α-defensin. This is a protective mechanism developed by some pathogenic bacteria such as *Pseudomonas aeruginosa*, *Enterococcus faecalis*, and *Streptococcus pyogenes*. This process is triggered by the secretion of extracellular proteinases whose hydrolytic action leads to core protein degradation of PGs and liberation of the corresponding GAG chains (Schmidtchen et al. 2001).

DS is involved in the development of esophageal squamous cell carcinoma, as demonstrated by the reduced migration and invasiveness recorded for tumor cells with downregulated DS epimerase 1 (DS-epi1). This downregulation reduces the IdoA content and, consequently, the activation of pERK-1/2 signaling mediated by growth factors that has a critical role for tumor invasion (Thelin et al. 2012).

Genetic disorders associated with defective expression of sulfatase or epimerase enzymes engaged in the biosynthesis of DS chains in PGs are known. A deficient activity of the sulfotransferase DS4-1 has implications, as previously discussed (Paragraph 5.2.3), in the content of iduronic acid residues in the GAG chain (Pacheco et al. 2009c), and the altered functionality of the PGs, thus obtained, is manifested by an irregular assembly of collagen fibrils leading to connective tissue disorders (Zhang et al. 2010). Altered expression of DS-epi2, relatively abundant in the brain in healthy individuals, is the cause of bipolar disorders (Goossens et al. 2003).

5.4.3 Keratan Sulfate

KSPGs are biomacromolecules with multifunctional biological activities, localized in the cornea, brain, and cartilages. Several papers report on the connection of sulfate distribution to activity (Saito et al. 2008; Liles et al. 2010; Nakayama et al. 2013). Relatively little is known about their functional properties in comparison with the other sulfated GAGs. In the cornea membrane, KS short chains are mainly localized in keratocan, lumican, mimecan, and fibromodulin, KSPGs that are included in class II small leucine-rich proteoglycans (Iozzo and Schaefer 2015). KS chains have been also found interspersed within the CS-rich region of the aggrecan PG in many tissues, but their function has not been elucidated yet. Instead, KS chains located in the aggrecan G1 domain are reported to inhibit immune responses to this domain. Indeed, patients with rheumatoid arthritis showed enhanced immune reactivity toward the G1 domain only when KS chains were removed (Leroux et al. 1996; Guerassimov et al. 1998).

KSPGs display a significant role in regulating corneal transparency, also by controlling collagen fibril architecture (Ho et al. 2014). In addition, corneal KS binds with high affinity to FGF-2 and sonic hedgehog (Weyers et al. 2013), indicating that KSPGs regulate growth factor activity and morphogen gradient formation. One pathology involving KS in the cornea is keratoconus, a disorder of the eye leading to a progressive thinning of the cornea. People suffering from this pathology display

double and blurry vision, high myopia (nearsightedness), astigmatism, and light sensitivity (Funderburgh et al. 1989; Edrington et al. 1995; Espandar and Meyer 2010). It has been suggested that the changed KS antigenicity found in the cornea extracts from surgical patients of keratoplasty can be due to a decrease in the number of KS chains per proteoglycan molecule, a decreased or altered KS sulfation pattern, or reduction of KS chain length (Funderburgh et al. 1989).

Brain tissues are the second richest source of KS in the human body after the cornea. Highly sulfated KS-III chains are displayed by numerous large KSPGs in the brain, among which the SV-2 plays significant neuronal and synaptic regulatory roles (Scranton et al. 1993). The negative charges on KS chains of SV2 distributed around a synaptic vesicle interact with Ca^{2+} ions and with neurotransmitters such as dopamine, thus forming a smart gel proteoglycan delivery complex (Caterson and Melrose 2018). It has been found that the interruption of SV2 functionality is connected to epilepsy (Wan et al. 2010).

Variation in the sulfation of KS chains has been revealed to be a marker for the presence of tumor cells. In podocalyxin, a cell surface mucin-like KSPG marker of human embryonic and induced pluripotent stem cells, the low sulfate content of KS chains has been detected by monoclonal antibody R-10G (Kawabe et al. 2013). In contrast, antibodies such as 5D4 or MZ14 (Caterson et al. 1983) revealed that tumor cells produce highly sulfated KS. In addition, podocalyxin has been found overexpressed in a variety of cancers. In particular, in high-grade serous ovarian carcinomas, it decreases adhesion of β-integrins at the cell surface either by altering their availability or their stability, contributing to the initial transperitoneal diffusion of metastasis (Cipollone et al. 2012).

Another report about the involvement of KS chains in diseases describes modified KS glycans in Alzheimer pathology (Lindahl et al. 1996; Zhang et al. 2017). The sulfotransferase GlcNAc6ST1 was found to be upregulated in the brains of transgenic mouse models (J20 and Tg2576) and of patients with Alzheimer disease (Zhang et al. 2017). KS chains have also been found to play key roles in the early phase of amyotrophic lateral sclerosis (ALS) (Hirano et al. 2013), a motor neuron-degenerative disease that leads to progressive muscle weakness and complete paralysis within 1 to 5 years after disease onset. Finally, it is worth noting that abundance of cell-associated KS in the endometrial lining varies markedly during the menstrual cycle, reaching a peak at the time at which embryo implantation occurs (Graham et al. 1994).

5.5 Outlook and Future Perspectives

Sulfated GAGs are the carbohydrate portion of PGS, a family of complex biomacromolecules ubiquitously found in the ECM and on cell surfaces and playing critical roles in a plethora of physiological and pathological events. In this chapter the chemical structure and biosynthesis of the four main sulfated GAG types are

firstly described, and then the most commonly employed isolation and purification methods as well as the spectroscopic and spectrometric techniques for their structural analysis are discussed, with a focus on the most recent advancements in the field. Lastly, an overview of the most important biological functions of the different sulfated GAGs is reported, with special attention to the molecular features – sulfation pattern above all – that have been revealed to play significant roles in the discussed biological events.

In spite of a myriad studies on sulfated GAG chemistry and biochemistry, especially in the last 25 years, structure-biological function relationships have been elucidated in detail up to now only in few cases. This is mainly due to the complexity of sulfated GAGs, showing structural heterogeneity that makes their profiling in cells, tissues, and biological fluids as well as the precise understanding of their interaction with proteins and other biomolecules very challenging (Ricard-Blum and Lisacek 2017).

We foresee that in the next years, many efforts in the field will be devoted to fill these gaps and in particular to unveil the details of the roles played by GAG sulfation code in as more biological events as possible.

Essential prerequisite for solving these issues are at least (Mizumoto et al. 2015):

(i) The development of methods and technical solutions for the streamlined sequence determination of sulfated GAG chain more complex than bikunin and decorin – the two simplest CSPGs for which the full structure could be sequenced (Ly et al. 2011; Yu et al. 2017)
(ii) An access to (semi)-synthetic sulfated GAG oligo- and polysaccharides (as well as analogs thereof: Lane et al. 2017; Gao and Edgar 2019) with a very well-defined structure through chemical and/or chemo-enzymatic procedures, which would be easier, cheaper, and more efficient than the procedures described up to now (Bedini and Parrilli 2012; Dulaney and Huang 2012; DeAngelis et al. 2013; Liu and Linhardt 2014; Mende et al. 2016)
(iii) The improvement of the biochemical efforts toward a more precise and complete comprehension of the regulatory aspects governing sulfated GAG biosynthesis
(iv) The implementation of computational tools for mining sulfated GAG-protein interactions and fully exploring the topology of ECM and surface interaction networks involving sulfated GAGs

Another urgent gap concerning sulfated GAGs to be filled in the next years is the development of multi-analytical methods for the rapid and efficient screening of purity and titer of sulfated GAGs employed as ingredients of drugs and nutraceuticals, due to the lack of robust data on this issue.

Acknowledgment Ministero dell'Istruzione, dell'Università e della Ricerca (MIUR) is acknowledged for funding to EB (FFABR 2017, "Fondo per il finanziamento delle attività base di ricerca"). AFM thanks the support of the Spanish Ministerio de Economía y Competitividad (Grant MAT2015-65184-C2-2-R).

References

Afratis N, Gialeli C, Nikitovic D, Tsegenidis T, Karousou E, Theocharis AD, Pavão MS, Tzanakakis GN, Karamanos NK (2012) Glycosaminoglycans: key players in cancer cell biology and treatment. FEBS J 279:1177–1197

Agyekum I, Pepi L, Yu Y, Li J, Yan L, Linhardt RJ, Chen S, Amster IJ (2018) Structural elucidation of fucosylated chondroitin sulfates from sea cucumber using FTICR-MS/MS. Eur J Mass Spectrom 24:157–167

Alkhalil A, Achur RN, Valiyaveettil M, Ockenhouse CF, Gowda DC (2000) Structural requirements for the adherence of Plasmodium falciparum-infected erythtocytes to chondroitin sulfate proteoglycans of human placenta. J Biol Chem 275:40357–40364

Aricescu AR, McKinnell IW, Halfter W, Stoker AW (2002) Heparan sulfate proteoglycans are ligands for receptor protein tyrosine phosphatase σ. Mol Cell Biol 22:1881–1892

Banfield BW, Leduc Y, Esford L, Visalli RJ, Brandt CR, Tufaro F (1995) Evidence fora n interaction of herpes simplex virus with chondroitin sulfate proteoglycans during infection. Virology 208:531–539

Bara JJ, Johnson WE, Caterson B, Roberts S (2012) Articular cartilage glycosaminoglycans inhibit the adhesion of endothelial cells. Connect Tissue Res 53:220–228

Barry FP, Neame PJ, Sasse J, Pearson D (1994) Length variation in the keratan sulfate domain of mammalian aggrecan. Matrix Biol 14:323–328

Bartus K, James ND, Bosch KD, Bradbury EJ (2012) Chondroitin sulphate proteoglycans: key modulators of spinal cord and brain plasticity. Exp Neurol 235:5–17

Bechard D, Gentina T, Delehedde M, Scherpereel A, Lyon M, Aumercier M, Vazeux R, Richet C, Degand P, Jude B, Janin A, Fernig DG, Tonnel AB, Lassalle P (2001) Endocan is a novel chondroitin sulfate/dermatan sulfate proteoglycan that promotes hepatocyte growth factor/scatter factor mitogenic activity. J Biol Chem 276:48341–48349

Bedini E, Parrilli M (2012) Synthetic and semi-synthetic chondroitin sulfate oligosaccharides, polysaccharides, and glycomimetics. Carbohydr Res 356:75–85

Bhavanandan VP, Meyer K (1968) Studies on keratosulfates. Methylation, desulfation, and acid hydrolysis studies on old human rib cartilage keratosulfate. J Biol Chem 243:1052–1059

Bielik AM, Zaia J (2011) Multistage tandem mass spectrometry of chondroitin sulfate and dermatan sulfate. Int J Mass Spectrom 305:131–137

Bienkowski MJ, Conrad HE (1985) Structural characterization of the oligosaccharides formed by depolymerization of heparin with nitrous acid. J Biol Chem 260:356–365

Bishnoi M, Jain A, Hurkat P, Jain SK (2016) Chondroitin sulfate: a focus on osteoarthritis. Glycoconj J 33:693–705

Bradbury EJ, Carter LM (2011) Manipulating the glial scar: chondroitinase ABC as a therapy for spinal cord injury. Brain Res Bull 84:306–316

Bray BA, Lieberman R, Meyer K (1967) Structure of human skeletal keratosulfate. The linkage region. J Biol Chem 242:3373–3380

Brew K, Vanaman TC, Hill RL (1968) The role of alpha-lactalbumin and the A protein in lactose synthetase: a unique mechanism for the control of a biological reaction. Proc Natl Acad Sci USA 59:491–497

Brown GM, Huckerby TN, Abram BL, Nieduszynski IA (1996) Characterization of a non-reducing terminal fragment from bovine articular cartilage keratan sulphates containing alpha(2-3)-linked sialic acid and alpha(1-3)-linked fucose. A sulphated variant of the VIM-2 epitope. Biochem J 319:137–141

Bülow HE, Hobert O (2004) Differential sulfations and epimerization define heparan sulfate specificity in nervous system development. Neuron 41:723–736

Bülow HE, Tjoe N, Townley RA, Didiano D, van Kuppevelt TH, Hobert O (2008) Extracellular sugar modifications provide instructive and cell-specific information for axon-guidance choices. Curr Biol 18:1978–1985

Capila I, Linhardt RJ (2002) Heparin–protein interactions. Angew Chem Int Ed 41:390–412
Cardin AD, Weintraub HJ (1989) Molecular modeling of protein-glycosaminoglycan interactions. Arterioscl Throm Vas Biol 9:21–32
Caterson B, Melrose J (2018) Keratan sulfate, a complex glycosaminoglycan with unique functional capability. Glycobiology 28:182–206
Caterson B, Christner JE, Baker JR (1983) Identification of a monoclonal antibody that specifically recognizes corneal and skeletal keratan sulfate. Monoclonal antibodies to cartilage proteoglycan. J Biol Chem 258:8848–8854
Cavalcante RS, Brito AS, Palhares LCGF, Lima MA, Cavalheiro RP, Nader HB, Sassaki G, Chavante SF (2018) 2,3-Di-*O*-sulfo glucuronic acid: an unmodified and unusual residue in a highly sulfated chondroitin sulfate from *Litopenaeus vannamei*. Carbohydr Polym 183:192–200
Chai W, Luo J, Lim CK, Lawson AM (1998) Characterization of heparin oligosaccharide mixtures as ammonium salts using electrospray mass spectrometry. Anal Chem 70:2060–2066
Chen RL, Lander AD (2001) Mechanisms underlying preferential assembly of heparan sulfate on glypican-1. J Biol Chem 276:7507–7517
Chen S, Xue C, Yin L, Tang Q, Yu G, Chai W (2011) Comparison of structures and anticoagulant activities of fucosylated chondroitin sulfates from different sea cucumbers. Carbohydr Polym 83:688–696
Chi L, Wolff JJ, Laremore TN, Restaino OF, Xie J, Schiraldi C, Toida T, Amster IJ, Linhardt RJ (2009) Structural analysis of bikunin glycosaminoglycan. J Am Chem Soc 130:2617–2625
Choi HU, Meyer K (1975) The structure of keratan sulphates from various sources. Biochem J 151:543–553
Chua JS, Kuberan B (2017) Synthetic xylosides: probing the glycosaminoglycan biosynthetic machinery for biomedical applications. Acc Chem Res 50:2693–2705
Cipollone JA, Graves ML, Kobel M, Kalloger SE, Poon T, Gilks CB, McNagny KM, Roskelley CD (2012) The anti-adhesive mucin podocalyxin may help initiate the transperitoneal metastasis of high grade serous ovarian carcinoma. Clin Exp Metastasis 29:239–252
Clausen TM, Pereira MA, Al Nakouzi N, Oo H, Agerbæk MØ, Lee S, Ørum-Madsen MS, Kristensen AR, El-Naggar A, Grandgenett PM, Grem JL, Hollingsworth MA, Holst PJ, Theander T, Sorensen PH, Daugaard M, Salanti A (2016) Oncofetal chondroitin sulfate glycosaminoglycans are key players in integrin signaling and tumor cell motility. Mol Cancer Res 14:1288–1299
Collin EC, Carroll O, Kilcoyne M, Peroglio M, See E, Hendig D, Alini M, Grad S, Pandit A (2017) Ageing affects chondroitin sulfates and their synthetic enzymes in the intervertebral disc. Signal Transduction Targeted Ther 2:e17049
Condac E, Silasi-Mansat R, Kosanke S, Schoeb T, Towner R, Lupu F, Cummings RD, Hinsdale ME (2007) Polycistic disease caused by deficiency in xylosyltransferase 2, an initiating enzyme of glycosaminoglycan biosynthesis. Proc Natl Acad Sci USA 104:9416–9421
Connell BJ, Lortat-Jacob H (2013) Human immunodeficiency virus and heparan sulfate: from attachment to entry inhibition. Front Immunol 4:385
Conrad HS (2001) Beta-elimination for release of O-linked glycosaminoglycans from proteoglycans. Curr Protoc Mol Biol 17:15.1–15.3
Deakin JA, Blaum BS, Gallagher JT, Uhrin D, Lyon M (2009) The binding properties of minimal oligosaccharides reveal a common heparan sulfate/dermatan sulfate-binding site in hepatocyte growth factor/scatter factor that can accommodate a wide variety of sulfation patterns. J Biol Chem 284:6311–6321
DeAngelis P, Liu J, Linhardt RJ (2013) Chemoenzymatic synthesis of glycosaminoglycans: re-creating, re-modeling and re-designing nature's longest or most complex carbohydrate chains. Glycobiology 23:764–777
Deepa SS, Yamada S, Fukui S, Sugahara K (2007) Structural determination of novel sulfated octasaccharides isolated from chondroitin sulfate of shark cartilage and their application for characterizing monoclonal antibody epitopes. Glycobiology 17:631–645

Desai UR, Petitou M, Björk I, Olson ST (1998) Mechanism of heparin activation of antithrombin: role of individual residues of the pentasaccharide activating sequence in the recognition of native and activated states of antithrombin. J Biol Chem 273:7478–7487

Dickenson JM, Huckerby TN, Nieduszynski IA (1991) A non-reducing terminal fragment from tracheal cartilage keratan sulphate chains contains alpha (2-3)-linked *N*-acetylneuraminic acid. Biochem J 278:779–785

du Souich P (2014) Absorption, distribution and mechanism of action of SYSADOAS. Pharmacol Ther 142:362–374

Dulaney SB, Huang X (2012) Strategies in synthesis of heparin/heparan sulfate oligosaccharides: 2000-present. Adv Carbohydr Chem Biochem 67:95–136

Dunlevy JR, Neame PJ, Vergnes JP, Hassell JR (1998) Identification of the *N*-linked oligosaccharide sites in chick corneal lumican and keratocan that receive keratan sulfate. J Biol Chem 273:9615–9621

Edrington TB, Zadnik K, Barr JT (1995) Keratoconus. Optom Clin 4:65–73

El Masri R, Seffouh A, Lortat-Jacob H, Vivès RR (2017) The "in and out" of glucosamine 6-O-sulfation: the 6th sense of heparan sulfate. Glycoconj J 34:285–298

Elefteriou F, Exposito JY, Garrone R, Lethias C (2001) Binding of tenascin-X to decorin. FEBS Lett 495:44–47

Enghild J, Thøgersen IB, Cheng F, Fransson LA, Roepstorff P, Rahbek-Nielsen H (1999) Organization of the inter-α-inhibitor heavy chains on the chondroitin sulfate originating from Ser10 of bikunin: posttranslational modification of IαI-derived bikunin. Biochemistry 38:11804–11813

Esko JD, Lindahl U (2001) Molecular diversity of heparan sulfate. J Clin Invest 108:169–173

Esko JD, Selleck SB (2002) Order out of chaos: assembly of ligand binding sites in heparan sulfate. Annu Rev Biochem 71:435–471

Espandar L, Meyer J (2010) Keratoconus: overview and update on treatment. Middle East Afr J Ophthalmol 17:15–20

Ethell IM, Irie F, Kalo MS, Couchman JR, Pasquale EB, Yamaguchi Y (2001) EphB/syndecan-2 signalling in dendritic spine morphogenesis. Neuron 31:1001–1013

Ferro DR, Provasoli A, Ragazzi M, Casu B, Torri G, Bossennec V, Perly B, Sinay P, Petitou M, Choay J (1990) Conformer populations of L-iduronic acid residues in glycosaminoglycan sequences. Carbohydr Res 195:157–167

Funderburgh JL (2000) Keratan sulfate: structure, biosynthesis and function. Glycobiology 10:951–958

Funderburgh JL (2002) Keratan sulfate biosynthesis. IUBMB Life 54:187–194

Funderburgh JL, Panjwani N, Conrad GW, Baum J (1989) Altered keratan sulfate epitopes in keratoconus. Invest Ophthalmol Vis Sci 30:2278–2281

Funderburgh JL, Corpuz LM, Roth MR, Funderburgh ML, Tasheva ES, Conrad GW (1997) Mimecan, the 25-kDa corneal keratan sulfate proteoglycan, is a product of the gene producing osteoglycin. J Biol Chem 272:28089–28095

Gama CI, Tully SE, Sotogaku N, Clark PM, Rawat M, Vaidehi N, Goddard Iii WA, Nishi A, Hsieh-Wilson LC (2006) Sulfation patterns of glycosaminoglycans encode molecular recognition and activity. Nat Chem Biol 2:467–473

Gao C, Edgar KJ (2019) Efficient synthesis of glycosaminoglycan analogs. Biomacromolecules 20:608–617

Gao N, Lu F, Xiao C, Yang L, Chen J, Zhou K, Wen D, Li Z, Wu M, Jiang J, Liu G, Zhao J (2015) β-Eliminative depolymerization of the fucosylated chondroitin sulfate and anticoagulant activities of resulting fragments. Carbohydr Polym 127:427–437

García B, Merayo-Lloves J, Martin C, Alcalde I, Quirós LM, Vazquez F (2016) Surface proteoglycans as mediators in bacterial pathogens infections. Front Microbiol 7:220

Gargiulo V, Lanzetta R, Parrilli M, De Castro C (2009) Structural analysis of chondroitin sulfate from *Scyliorhinus canicula*: a useful source of this polysaccharide. Glycobiology 19:1485–1491

Garnjanagoonchorn W, Wongekalak L, Engkagul A (2007) Determination of chondroitin sulfate from different sources of cartilage. Chem Eng Proc 46:465–471

Gengrinovitch S, Berman B, David G, Witte L, Neufeld G, Ron D (1999) Glypican-1 Is a VEGF165 Binding proteoglycan that acts as an extracellular chaperone for VEGF165. J Biol Chem 274:10816–10822

George N, Geller HM (2018) Extracellular matrix and traumatic brain injury. J Neurosci Res 96:573–588

Gogolla N, Caroni P, Lüthi A, Herry C (2009) Perineuronal nets protect fear memories from erasure. Science 325:1258–1261

Goodall KJ, Poon IKH, Phipps S, Hulett MD (2014) Soluble heparan sulfate fragments generated by heparanase trigger the release of pro-Inflammatory cytokines through TLR-4. PLoS One 9: e109596

Goodger SJ, Robinson CJ, Murphy KJ, Gasiunas N, Harmer NJ, Blundell TL, Pye DA, Gallagher JT (2008) Evidence that heparin saccharides promote FGF2 mitogenesis through two distinct mechanisms. J Biol Chem 283:13001–13008

Goossens D, Van Gestel S, Claes S, De Rijk P, Souery D, Massat I, Van den Bossche D, Backhovens H, Mendlewicz J, Van Broeckhoven C, Del-Favero J (2003) A novel CpG-associated brain-expressed candidate gene for chromosome 18q-linked bipolar disorder. Mol Psychiatry 8:83–89

Graham RA, Li TC, Cooke ID, Aplin JD (1994) Keratan sulphate as a secretory product of human endometrium: cyclic expression in normal women. Hum Reprod 9:926–930

Greinacher A, Michels I, Schäfer M, Kiefel V, Mueller-Eckhardt C (1992) Heparin-associated thrombocytopenia in a patient treated with polysulphated chondroitin sulphate: evidence for immunological crossreactivity between heparin and polysulphated glycosaminoglycan. Br J Haematol 81:252–254

Grøndahl F, Tveit H, Akslen-Hoel LK, Prydz K (2011) Easy HPLC-based separation and quantitation of chondroitin sulphate and hyaluronan disaccharides after chondroitinase ABC treatment. Carbohydr Res 346:50–57

Guerassimov A, Zhang Y, Banerjee S, Cartman A, Leroux JY, Rosenberg LC, Esdaile J, Fitzcharles MA, Poole AR (1998) Cellular immunity to the G1 domain of cartilage proteoglycan aggrecan is enhanced in patients with rheumatoid arthritis but only after removal of keratan sulfate. Arthritis Rheum 41:1019–1025

Guerrini M, Naggi A, Guglieri S, Santarsiero R, Torri G (2005) Complex glycosaminoglycans: profiling substitution patterns by two-dimensional nuclear magnetic resonance spectroscopy. Anal Biochem 337:35–47

Guerrini M, Beccati D, Shriver Z, Naggi A, Viswanathan K, Bisio A, Capila I, Lansing JC, Guglieri S, Fraser B, Al-Hakim A, Gunay NS, Zhang Z, Robinson L, Buhse LF, Nasr M, Woodcock J, Langer R, Venkataraman G, Linhardt RJ, Casu B, Torri G, Sasisekharan R (2008) Oversulfated chondroitin sulfate is a contaminant in heparin associated with adverse clinical events. Nat Biotechnol 26:669–675

Guidetti GF, Bartolini B, Bernardi B, Tiraa ME, Berndt MC, Balduinia C, Torti M (2004) Binding of von Willebrand factor to the small proteoglycan decorin. FEBS Lett 574:95–100

Habuchi O (2000) Diversity and functions of glycosaminoglycan sulfotransferases. Biochim Biophys Acta 1474:115–127

Hassell JR, Newsome DA, Hascall VC (1979) Characterization and biosynthesis of proteoglycans of corneal stroma from rhesus monkey. J Biol Chem 254:12346–12354

Hassell JR, Kimura JH, Hascall VC (1986) Proteoglycan core protein families. Annu Rev Biochem 55:539–567

Hayes A, Sugahara K, Farrugia B, Whitelock JM, Caterson B, Melrose J (2018) Biodiversity of CS–proteoglycan sulphation motifs: chemical messenger recognition modules with roles in information transfer, control of cellular behaviour and tissue morphogenesis. Biochem J 475:587–620

Higashi K, Okamoto Y, Mukuno A, Wakai J, Hosoyama S, Linhardt RJ, Toida T (2015) Functional chondroitin sulfate from *Enteroctopus dofleini* containing a 3-O-sulfo glucuronic acid residue. Carbohydr Polym 134:557–565

Higashi K, Takeda K, Mukuno A, Okamoto Y, Masuko S, Linhardt RJ, Toida T (2016) Identification of keratan sulfate disaccharide at C-3 position of glucuronate of chondroitin sulfate from *Mactra chinensis*. Biochem J 473:4145–4148

Hirano K, Ohgomori T, Kobayashi K, Tanaka F, Matsumoto T, Natori T, Matsuyama Y, Uchimura K, Sakamoto K, Takeuchi H, Hirakawa H, Suzumura A, Sobue G, Ishiguro N, Imagama S, Kadomatsu K (2013) Ablation of keratan sulfate accelerates early phase pathogenesis of ALS. PLoS One 8:e66969

Ho LT, Harris AM, Tanioka H, Yagi N, Kinoshita S, Caterson B, Quantock AJ, Young RD, Meek KM (2014) A comparison of glycosaminoglycan distributions, keratan sulphate sulphation patterns and collagen fibril architecture from central to peripheral regions of the bovine cornea. Matrix Biol 38:59–68

Holt CE, Dickson BJ (2005) Sugar codes for axons? Neuron 46:169–172

Hou S, Maccarana M, Min TH, Strate I, Pera EM (2007) The secreted serine protease xHtrA1 stimulates long-range FGF signalling in the early *Xenopus* embryo. Dev Cell 13:226–241

Howell WH, Holt E (1918) Two new factors in blood coagulation—Heparin and pro-antithrombin. Am J Physiol-Legacy Content 47:328–341

Hsieh PH, Thieker DF, Guerrini M, Woods RJ, Liu J (2016) Uncovering the relationship between sulphation patterns and conformation of iduronic acid in heparan sulphate. Sci Rep 6:29602

Huang R, Pomin VH, Sharp JS (2011) LC-MS^n analysis of isomeric chondroitin sulfate oligosaccharides using a chemical derivatization strategy. J Am Soc Mass Spectrom 22:1577–1587

Huang H, Yu X, Mao Y, Costello CE, Zaia J, Lin C (2013) De novo sequencing of heparan sulfate oligosaccharides by electron-activated dissociation. Anal Chem 85:11979–11986

Huckerby TN, Nieduszynski IA, Giannopoulos M, Weeks SD, Sadler IH, Lauder RM (2005) Characterization of oligosaccharides from the chondroitin/dermatan sulfate. ^{1}H-NMR and ^{13}C-NMR studies of reduced trisaccharides and hexasaccharides. FEBS J 272:6276–6286

Iida J, Wilhelmson KL, Ng J, Lee P, Morrison C, Tam E, Overall CM, McCarthy JB (2007) Cell surface chondroitin sulfate glycosaminoglycan in melanoma: role in the activation of pro-MMP-2 (progelatinase A). Biochem J 403:553–563

Inatani M, Irie F, Plump AS, Tessier-Lavigne M, Yamaguchi Y (2003) Mammalian brain morphogenesis and midline axon guidance require heparan sulfate. Science 302:1044–1046

Iozzo RV (1998) Matrix proteoglycans: from molecular design to cellular function. Annu Rev Biochem 67:609–652

Iozzo RV, Karamanos N (2010) Proteoglycans in health and disease: emerging concepts and future directions. FEBS J 277:3863

Iozzo RV, Schaefer L (2015) Proteoglycan form and function: a comprehensive nomenclature of proteoglycans. Matrix Biol 42:11–55

Irie F, Okuno M, Matsumoto K, Pasquale EB, Yamaguchi Y (2008) Heparan sulfate regulates ephrin-A3/EphA receptor signalling. Proc Natl Acad Sci USA 105:12307–12312

Jan SL, Hayashi M, Kasza Z, Eriksson I, Bishop JR, Weibrecht I, Heldin J, Holmborn K, Jakobsson L, Söderberg O, Spillmann D, Esko JD, Claesson-Welsh L, Kjellén L, Kreuger J (2012) Functional overlap between chondroitin and heparan sulfate proteoglycans during VEGF-induced sprouting angiogenesis. Arterioscl Throm Vas Biol 32:1255–1263

Jenkins LM, Singh P, Varadaraj A, Lee NY, Shah S, Flores HV, O'Connell K, Mythreye K (2016) Altering the proteoglycan state of transforming growth factor β type III receptor (TβRIII)/betaglycan modulates Ccnonical Wnt/β-catenin signalling. J Biol Chem 291:25716–25728

Jin-Ping L (2008) Heparin, heparan sulfate and heparanase in cancer: remedy for metastasis? Anti-Cancer Agents Med Chem 8:64–76

Johan K, Lena K (2012) Heparan sulfate biosynthesis: regulation and variability. J Histochem Cytochem 60:898–907

Johnson CE, Crawford BE, Stavridis M, ten Dam G, Wat AL, Rushton G, Ward CM, Wilson V, van Kuppevelt TH, Esko JD, Smith A, Gallagher JT, Merry CLR (2007) Essential alterations of heparan sulfate during the differentiation of embryonic stem cells to Sox1-enhanced green fluorescent protein-rxpressing neural progenitor cells. Stem Cells 25:1913–1923

Juhasz P, Biemann K (1995) Utility of noncovalent complexes in the matrix-assisted laser desorption ionization mass spectrometry of heparin-derived oligosaccharides. Carbohydr Res 270:131–147

Kadler KE, Hill A, Canty-Laird EG (2008) Collagen fibrillogenesis: fibronectin, integrins, and minor collagens as organizers and nucleators. Curr Opin Cell Biol 20:495–501

Kailemia MJ, Park M, Kaplan DA, Venot A, Boons GJ, Li L, Linhardt RJ, Amster IJ (2014) High-field asymmetric-waveform ion mobility spectrometry and electron detachment dissociation of isobaric mixtures of glycosaminoglycans. J Am Soc Mass Spectrom 25:258–268

Kamimura K, Koyama T, Habuchi H, Ueda R, Masu M, Kimata K, Nakato H (2006) Specific and flexible roles of heparan sulfate modifications in *Drosophila* FGF signalling. J Cell Biol 174:773–778

Kan M, Wang F, Xu J, Crabb J, Hou J, McKeehan W (1993) An essential heparin-binding domain in the fibroblast growth factor receptor kinase. Science 259:1918–1921

Karamanos NK, Piperigkou Z, Theocharis AD, Watanabe H, Franchi M, Baud S, Brézillon S, Götte M, Passi A, Vigetti A, Ricard-Blum S, Sanderson RD, Neill T, Iozzo RV (2018) Proteoglycan chemical diversity drives multifunctional cell regulation and therapeutics. Chem Rev 118:9152–9232

Kawabe K, Tateyama D, Toyoda H, Kawasaki N, Hashii N, Nakao H, Matsumoto S, Nonaka M, Matsumura H, Hirose Y, Morita A, Katayama M, Sakuma M, Kawasaki N, Furue MK, Kawasaki T (2013) A novel antibody for human induced pluripotent stem cells and embryonic stem cells recognizes a type of keratan sulfate lacking oversulfated structures. Glycobiology 23:322–336

Khanal N, Masellis C, Kamrath MZ, Clemmer DE, Rizzo TR (2017) Glycosaminoglycan analysis by cryogenic messenger-tagging IR spectroscopy combined with IMS-MS. Anal Chem 89:7601–7606

Kinoshita-Toyoda A, Yamada S, Haslam SM, Khoo KH, Sugiura M, Morris HR, Dell A, Sugahara K (2004) Structural determination of five novel tetrasaccharides containing 3-*O*-sulfated D-glucuronic acid and two rare oligosaccharides containing a β-D-glucose branch isolated from squid cartilage chondroitin sulfate. Biochemistry 43:11063–11074

Kishimoto TK, Viswanathan K, Ganguly T, Elankumaran S, Smith S, Pelzer K, Lansing JC, Sriranganathan N, Zhao G, Galcheva-Gargova Z, Al-Hakim A, Bailey GS, Fraser B, Roy S, Rogers-Cotrone T, Buhse LF, Whary M, Fox J, Nasr M, Dal Pan GJ, Shriver Z, Langer RS, Venkataraman G, Austen KF, Woodcock J, Sasisekharan R (2008) Contaminated heparin associated with adverse clinical events and activation of the contact system. New Engl J Med 358:2457–2467

Knelson EH, Nee JC, Blobe GC (2014) Heparan sulfate signalling in cancer. Trends Biochem Sci 39:277–288

Kokenyesi R, Bernfield M (1994) Core protein structure and sequence determine the site and presence of heparan sulfate and chondroitin sulfate on syndecan-1. J Biol Chem 269:12304–12309

Koshiishi I, Takenouchi M, Imanari T (1999) Structural characteristics of oversulfated chondroitin/dermatan sulfates in the fibrous lesions of the liver with cirrhosis. Arch Biochem Biophys 370:151–155

Krusius T, Finne J, Margolis RK, Margolis RU (1986) Identification of an *O*-glycosidic mannose-linked sialylated tetrasaccharide and keratan sulfate oligosaccharides in the chondroitin sulfate proteoglycan of brain. J Biol Chem 261:8237–8242

Kumar Shetty A, Kobayashi T, Mizumoto S, Narumi M, Kudo Y, Yamada S, Sugahara K (2009) Isolation and characterization of a novel chondroitin sulfate from squid liver integument rich in N-acetylgalactosamine(4,6-disulfate) and glucuronate(3-sulfate) residues. Carbohydr Res 344:1526–1532

Lane DA, Denton J, Flynn AM, Thunberg L, Lindahl U (1984) Anticoagulant activities of heparin oligosaccharides and their neutralization by platelet factor 4. Biochem J 218:725–732

Lane RS, St Ange K, Zolghadr B, Liu X, Schäffer C, Linhardt RJ, DeAngelis PL (2017) Expanding glycosaminoglycan chemical space: towards the creation of sulfated analogs, novel polymers and chimeric constructs. Glycobiology 27:646–656

Lang BT, Cregg JM, DePaul MA, Tran AP, Xu K, Dyck SM, Madalena KM, Brown BP, Weng Y-L, Li S, Karimi-Abdolrezaee S, Busch SA, Shen Y, Silver J (2014) Modulation of the proteoglycan receptor PTPσ promotes recovery after spinal cord injury. Nature 518:404–408

Laremore TN, Murugesan S, Park TJ, Avci FU, Zagorevski D, Linhardt RJ (2006) Matrix-assisted laser desorption/ionization mass spectrometric analysis of uncomplexed highly sulfated oligosaccharides using ionic liquid matrices. Anal Chem 78:1774–1779

Lauder RM, Huckerby TN, Nieduszynski IA (1996) The structure of the keratan sulphate chains attached to fibromodulin isolated from articular cartilage. Eur J Biochem 242:402–409

Lauder RM, Huckerby TN, Nieduszynski IA (1997) The structure of the keratan sulphate chains attached to fibromodulin from human articular cartilage. Glycoconj J 14:651–660

Lee CM, Tanaka T, Murai T, Kondo M, Kimura J, Su W, Kitagawa T, Ito T, Matsuda H, Miyasaka M (2002) Novel chondroitin sulfate-binding cationic liposomes loaded with cisplatin efficiently suppress the local growth and liver metastasis of tumor cells *in vivo*. Cancer Res 62:4282–4288

Leroux JY, Guerassimov A, Cartman A, Delaunay N, Webber C, Rosenberg LC, Banerjee S, Poole AR (1996) Immunity to the G1 globular domain of the cartilage proteoglycan aggrecan can induce inflammatory erosive polyarthritis and spondylitis in BALB/c mice but immunity to G1 is inhibited by covalently bound keratan sulfate in vitro and in vivo. J Clin Invest 97:621–632

Li F, Kumar Shetty A, Sugahara K (2007) Neuritogenic activity of chondroitin/dermatan sulfate hybrid chains of embryonic pig brain and their mimicry from shark liver. Involvement of the pleiotrophin and hepatocyte growth factor signaling pathways. J Biol Chem 282:2956–2966

Li F, ten Dam GB, Murugan S, Yamada S, Hashiguchi T, Mizumoto S, Oguri K, Okayama M, van Kuppevelt TH, Sugahara K (2008) Involvement of highly sulfated chondroitin sulfate in the metastasis of the Lewis lung carcinoma cells. J Biol Chem 283:34294–34304

Li Q, Cai C, Chang Y, Zhang F, Linhardt RJ, Xue C, Li G, Yu G (2018) A novel structural fucosylated chondroitin sulfate from *Holothuria mexicana* and its effects on growth factors binding and anticoagulation. Carbohydr Polym 181:1160–1168

Liles M, Palka BP, Harris A, Kerr B, Hughes C, Young RD, Meek KM, Caterson B, Quantock AJ (2010) Differential relative sulfation of keratan sulfate glycosaminoglycan in the chick cornea during embryonic development. Invest Ophthalmol Vis Sci 51:1365–1372

Lindahl U, Li JP (2009) Chapter 3: Interactions between heparan sulfate and proteins—Design and functional implications. In: Jeon KW (ed) International review of cell and molecular biology, vol 276. Academic Press, New York, pp 105–159

Lindahl B, Eriksson L, Spillmann D, Caterson B, Lindahl U (1996) Selective loss of cerebral keratan sulfate in Alzheimer's disease. J Biol Chem 271:16991–16994

Lindahl U, Couchman J, Kimata K, Esko JD (2017) Chapter 17: Proteoglycans and sulfated glycosaminoglycans. In: Varki AK, Esko JD, Stanley P, Hart GW, Aebi M, Darvill AG, Kinoshita T, Packer NH, Prestegard JH, Schnaar RL, Seeberger PH (eds) Essential of glycobiology, 3rd edn. Cold Spring Harbor Laboratory Press, Cold Spring Harbor

Linker A, Hoffman P, Sampson P, Meyer K (1958) Heparitin sulfate. Biochim Biophys Acta 29:443–444

Liu J, Linhardt RJ (2014) Chemoenzymatic synthesis of heparan sulfate and heparin. Nat Prod Res 31:1676–1685

Liu J, Desai UR, Han XJ, Toida T, Linhardt RJ (1995) Strategy for the sequence analysis of heparin. Glycobiology 5:775–764

Ly M, Laremore TN, Linhardt RJ (2010) Proteoglycomics: recent progress and future challenges. OMICS 14:389–399

Ly M, Leach FE III, Laremore TN, Toida T, Amster IJ, Linhardt RJ (2011) The proteoglycan bikunin has a defined sequence. Nat Chem Biol 7:827–833

Lyon M, Deakin JA, Rahmoune H, Fernig DG, Nakamura T, Gallagher JT (1998) Hepatocyte growth factor/scatter factor binds with high affinity to dermatan sulfate. J Biol Chem 273:271–278

Maeda N (2015) Proteoglycans and neuronal migration in the cerebral cortex during development and disease. Front Neurosci 9:98

Maimone MM, Tollefsen DM (1990) Structure of a dermatan sulfate hexasaccharide that binds to heparin cofactor II with high affinity. J. Biol. Chem 265:18263–18271

Malmström A, Bartolini B, Thelin MA, Pacheco B, Maccarana M (2012) Iduronic acid in chondroitin/dermatan sulfate: biosynthesis and biological function. J Histochem Cytochem 60:916–925

Mårdberg K, Trybala E, Tufaro F, Bergström T (2002) Herpes simplex virus type I glycoprotein C is necessary for efficient infection of chondroitin sulfate-expressing gro2C cells. J Gen Virol 83:291–300

Mauri L, Boccardi G, Torri G, Karfunkle M, Macchi E, Muzi L, Keire D, Guerrini M (2017) Qualification of HSQC methods for quantitative composition of heparin and low molecular weight heparins. J Pharm Biomed Anal 136:92–105

Mende M, Bednarek C, Wawryszyn M, Sauter P, Biskup MB, Schepers U, Bräse S (2016) Chemical synthesis of glycosaminoglycans. Chem Rev 116:8193–8255

Mikami T, Kitagawa H (2017) Sulfated glycosaminoglycans: their distinct roles in stem cell biology. Glycoconj J 34:725–735

Miller GM, Hsieh-Wilson LC (2015) Sugar-dependent modulation of neuronal development, regeneration, and plasticity by chondroitin sulfate proteoglycans. Exp Neurol 274:115–125

Miyata S, Kitagawa H (2017) Formation and remodeling of the brain extracellular matrix in neural plasticity: roles of chondroitin sulfate and hyaluronan. Biochim Biophys Acta 1861:2420–2434

Miyata S, Komatsu Y, Yoshimura Y, Taya C, Kitagawa H (2012) Persistent cortical plasticity by upregulation of chondroitin 6-sulfation. Nat Neurosci 15:414–422

Mizumoto S, Takahashi J, Sugahara K (2012) Receptor for advanced glycation end products (RAGE) functions as receptor for specific sulfated glycosaminoglycans, and anti-RAGE antibody or sulfated glycosaminoglycans delivered *in vivo* inhibit pulmonary metastasis of tumor cells. J Biol Chem 287:18985–18994

Mizumoto S, Yamada S, Sugahara K (2015) Molecular interactions between chondroitin-dermatan sulfate and growth factors/receptors/matrix proteins. Curr Opin Struct Biol 34:35–42

Mourier P, Anger P, Martinez C, Herman F, Viskov C (2015) Quantitative compositional analysis of heparin using exhaustive heparinase digestion and strong anion exchange chromatography. Anal Chem Res 3:46–53

Mucci A, Schenetti L, Volpi N (2000) ^{1}H and ^{13}C nuclear magnetic resonance identification and characterization of components of chondroitin sulfates of various origin. Carbohydr Polym 41:37–45

Mulloy B, Mourão PAS, Gray E (2000) Structure/function studies of anticoagulant sulphated polysaccharides using NMR. J Biotechnol 77:123–135

Mulloy B, Hogwood J, Gray E, Lever R, Page CP (2016) Pharmacology of heparin and related drugs. Pharmacol Rev 68:76–141

Myron P, Siddiquee S, Al Azad S (2014) Fucosylated chondroitin sulfate diversity in sea cucumbers: a review. Carbohydr Polym 112:173–178

Nadanaka S, Sugahara K (1997) The unusual tetrasaccharide sequence GlcA beta 1-3GalNAc (4-sulfate)beta 1-4GlcA(2-sulfate)beta 1-3GalNAc(6-sulfate) found in the hexasaccharides prepared by testicular hyaluronidase digestion of shark cartilage chondroitin sulfate D. Glycobiology 7:253–263

Nagamine S, Tamba M, Ishimine H, Araki K, Shiomi K, Okada T, Ohto T, Kunita S, Takahashi S, Wismans RGP, van Kuppevelt TH, Masu M, Keino-Masu K (2012) Organ-specific sulfation patterns of heparan sulfate generated by extracellular sulfatases Sulf1 and Sulf2 in mice. J Biol Chem 287:9579–9590

Nagasawa K, Uchiyama H, Sato N, Hatano A (1992) Chemical change involved in the oxidative-reductive depolymerization of heparin. Carbohydr Res 236:165–180

Nairn AV, Kinoshita-Toyoda A, Toyoda H, Xie J, Harris K, Dalton S, Kulik M, Pierce JM, Toida T, Moremen KW, Linhardt RJ (2007) Glycomics of proteoglycan biosynthesis in murine embryonic stem cell differentiation. J Proteome Res 6:4374–4387

Nakayama F, Umeda S, Ichimiya T, Kamiyama S, Hazawa M, Yasuda T, Nishihara S, Imai T (2013) Sulfation of keratan sulfate proteoglycan reduces radiation-induced apoptosis in human Burkitt's lymphoma cell lines. FEBS Lett 587:231–237

Nemes P, Hoover WJ, Keire DA (2013) High-throughput differentiation of heparin from other glycosaminoglycans by pyrolysis mass spectrometry. Anal Chem 85:7405–7412

Ng L, Grodzinsky AJ, Patwari P, Sandy J, Plaas A, Ortiz C (2003) Individual cartilage aggrecan macromolecules and their constituent glycosaminoglycans visualized via atomic force microscopy. J Struct Biol 143:242–257

Nieduszynski IA, Huckerby TN, Dickenson JM, Brown GM, Tai GH, Morris HG, Eady S (1990) There are two major types of skeletal keratan sulphates. Biochem J 271:243–245

Nimptsch A, Schibur S, Schnabelrauch M, Fuchs B, Huster D, Schiller J (2009) Characterization of the quantitative relationship between signal-to-noise (S/N) ratio and sample amount on-target by MALDI-TOF MS: determination of chondroitin sulfate subsequent to enzymatic digestion. Anal Chim Acta 635:175–182

Nishimura K, Ishii M, Kuraoka M, Kamimura K, Maeda N (2010) Opposing functions of chondroitin sulfate and heparan sulfate during early neuronal polarization. Neuroscience 169:1535–1547

Ofman D, Slim GC, Watt DK, Yorke SC (1997) Free radical induced oxidative depolymerisation of chondroitin sulphate and dermatan sulphate. Carbohydr Polym 33:47–56

Pacheco B, Maccarana M, Malmström A (2009a) Two dermatan sulfate epimerases form iduronic acid domains in dermatan sulfate. J Biol Chem 284:9788–9795

Pacheco B, Maccarana M, Goodlett DR, Malmström A, Malmström L (2009b) Identification of the active site of DS-epimerase 1 and requirement of *N*-glycosylation for enzyme function. J Biol Chem 284:1741–1747

Pacheco B, Maccarana M, Malmström A (2009c) Dermatan 4-*O*-sulfotransferase 1 is pivotal in the formation of iduronic acid blocks in dermatan sulfate. Glycobiology 19:1197–1203

Panagos CG, August DP, Jesson C, Uhrín D (2016) Photochemical depolymerization of dermatan sulfate and analysis of the generated oligosaccharides. Carbohydr Polym 140:13–19

Parra A, Veraldi N, Locatelli M, Fini M, Martini L, Torri G, Sangiorgi L, Bisio A (2012) Heparin-like heparan sulfate from rabbit cartilage. Glycobiology 22:248–257

Petitou M, van Boeckel CAA (2004) A synthetic antithrombin III binding pentasaccharide is now a drug! what comes next? Angew Chem Int Ed 43:3118–3133

Pizzorusso T, Medini P, Berardi N, Chierzi S, Fawcett JW, Maffei L (2002) Reactivation of ocular dominance plasticity in the adult visual cortex. Science 298:1248–1251

Plaas AH, Neame PJ, Nivens CM, Reiss L (1990) Identification of the keratan sulfate attachment sites on bovine fibromodulin. J Biol Chem 265:20634–20640

Poh ZW, Gan CH, Lee EJ, Guo S, Yip GW, Lam Y (2015) Divergent synthesis of chondroitin sulfate disaccharides and identification of sulfate motifs that inhibit triple negative breast cancer. Sci Rep 5:14355

Pomin VH (2014) Holothurian fucosylated chondroitin sulfate. Mar Drugs 12:232–254

Pomin VH (2015) NMR structural determination of unique invertebrate glycosaminoglycans endowed with medical properties. Carbohydr Res 413:41–50

Pomin VH, Piquet AA, Pereira MS, Mourão PAS (2012a) Residual keratan sulfate in chondroitin sulfate formulations for oral administration. Carbohydr Polym 90:839–846

Pomin VH, Park Y, Huang R, Heiss C, Sharp JS, Azadi P, Prestegard JH (2012b) Exploiting enzyme specificities in digestions of chondroitin sulfates A and C: production of well-defined hexasaccharides. Glycobiology 22:826–838

Pratt T, Conway CD, Tian NMM-L, Price DJ, Mason JO (2006) Heparan sulphation patterns generated by specific heparan sulfotransferase enzymes direct distinct aspects of retinal axon guidance at the optic chiasm. J Neurosci 26:6911–6923

Rapraeger A, Krufka A, Olwin B (1991) Requirement of heparan sulfate for bFGF-mediated fibroblast growth and myoblast differentiation. Science 252:1705–1708

Reichsman F, Smith L, Cumberledge S (1996) Glycosaminoglycans can modulate extracellular localization of the wingless protein and promote signal transduction. J Cell Biol 135:819–827

Renois-Predelus G, Schindler B, Compagnon I (2018) Analysis of sulfate patterns in glycosaminoglycan oligosaccharides by MS^n coupled to infrared ion spectroscopy: the case of GalNAc4S and GalNAc6S. J Am Soc Mass Spectrom 29:1242–1249

Ricard-Blum S, Lisacek F (2017) Glycosaminoglycanomics: where we are. Glycoconj J 34:339–349

Rivara S, Milazzo FM, Giannini G (2016) Heparanase: a rainbow pharmacological target associated to multiple pathologies including rare diseases. Fut Med Chem 8:647–680

Robinson CJ, Harmer NJ, Goodger SJ, Blundell TL, Gallagher JT (2005) Cooperative dimerization of fibroblast growth factor 1 (FGF1) upon a single heparin saccharide may drive the formation of 2:2:1 FGF1·FGFR2c·heparin ternary complexes. J Biol Chem 280:42274–42282

Rogers CJ, Clark PM, Tully SE, Abrol R, Garcia KC, Goddard WA, Hsieh-Wilson LC (2011) Elucidating glycosaminoglycan–protein–protein interactions using carbohydrate microarray and computational approaches. Proc Natl Acad Sci USA 108:9747–9752

Rugg MS, Willis AC, Mukhopadhyay D, Hascall VC, Fries E, Fülöp C, Milner CM, Day AJ (2005) Characterization of complexes formed between TSG-6 and inter-α-inhibitor that act as intermediates in the covalent transfer of heavy chains onto hyaluronan. J Biol Chem 280:25674–25686

Rühland C, Schönherr E, Robenek H, Hansen U, Iozzo RV, Bruckner P, Seidler DG (2007) The glycosaminoglycan chain of decorin plays an important role in collagen fibril formation at the early stages of fibrillogenesis. FEBS J 274:4246–4255

Ruoslahti E (1996) Brain extracellular matrix. Glycobiology 6:489–492

Ruppert R, Hoffmann E, Sebald W (1996) Human bone morphogenetic protein 2 contains a heparin-binding site which modifies Its biological activity. Eur J Biochem 237:295–302

Ryan CNM, Sorushanova A, Lomas AJ, Mullen AM, Pandit A, Zeugolis DI (2015) Glycosaminoglycans in tendon physiology, pathophysiology, and therapy. Bioconjug Chem 26:1237–1251

Saad OM, Myers RA, Castleton DL, Leary JA (2005) Analysis of hyaluronan content in chondroitin sulfate preparations by using selective enzymatic digestion and electrospray ionization mass spectrometry. Anal Biochem 344:232–239

Safaiyan F, Lindahl U, Salmivirta M (2000) Structural diversity of N-sulfated heparan sulfate domains: distinct modes of glucuronyl C5 epimerization, iduronic acid 2-O-sulfation, and glucosamine 6-O-sulfation. Biochemistry 39:10823–10830

Saito T, Nishida K, Nakayama J, Akama TO, Fukuda MN, Watanabe K, Quantock AJ, Maeda N, Watanabe H, Tano Y (2008) Sulfation patterns of keratan sulfate in different macular corneal dystrophy immunophenotypes using three different probes. Br J Ophthalmol 92:1434–1436

Sampaio LO, Tersariol ILS, Lopes CC, Bouças RI, Nascimento FD, Rocha HAO, Nader HB (2006) Heparins and heparan sulfates. Structure, distribution and protein interactions. In: Verli H (ed) Insights into carbohydrate structure and biological function. Transworld Research Network, Trivandrum

Santos GRC, Porto ACO, Soares PAG, Vilanova E, Mourão PAS (2017a) Exploring the structure of fucosylated chondroitin sulfate through bottom-up nuclear magnetic resonance and electrospray ionization-high-resolution mass spectrometry approaches. Glycobiology 27:625–634

Santos GRC, Piquet AA, Glauser BF, Tovar AMF, Pereira MS, Vilanova E, Mourão PAS (2017b) Systematic analysis of pharmaceutical preparations of chondroitin sulfate combined with glucosamine. Pharmaceuticals 10:38

Sarilla S, Habib SY, Tollefsen DM, Friedman DB, Arnett DR, Verhamme IM (2010) Glycosaminoglycan-binding properties and kinetic characterization of human heparin cofactor II expressed in *Escherichia coli*. Anal Biochem 406:166–175

Sarrazin S, Lamanna WC, Esko JD (2011) Heparan sulfate proteoglycans. Cold Spring Harb Perspect Biol 3:a004952

Sato T, Yamaguchi A, Goi T, Hirono Y, Takeuchi K, Katayama K, Matsukawa S (2004) Heparanase expression in human colorectal cancer and its relationship to tumor angiogenesis, hematogenous metastasis, and prognosis. J Surg Oncol 87:174–181

Schanbacher FL, Ebner KE (1970) Galactosyltransferase acceptor specificity of the lactose synthetase A protein. J Biol Chem 245:5057–5061

Schindler B, Renois-Predelus G, Bagdadi N, Melizi S, Barnes L, Chambert S, Allouche AR, Compagnon I (2017) MS/IR, a new MS-based hyphenated method for analysis of hexuronic acid epimers in glycosaminoglycans. Glycoconj J 34:421–425

Schlessinger J, Plotnikov AN, Ibrahimi OA, Eliseenkova AV, Yeh BK, Yayon A, Linhardt RJ, Mohammadi M (2000) Crystal structure of a ternary FGF-FGFR-heparin complex reveals a dual role for heparin in FGFR binding and dimerization. Mol Cell 6:743–750

Schmidtchen A, Frick IM, Björck L (2001) Dermatan sulphate is released by proteinases of common pathogenic bacteria and inactivates antibacterial α-defensin. Mol Microbiol 39:708–713

Schonherr E, Hausser H, Beavan L, Kresse H (1995) Decorin-type I collagen interaction. Presence of separate core protein-binding domains. J Biol Chem 270:8877–8883

Scranton TW, Iwata M, Carlson SS (1993) The SV2 protein of synaptic vesicles is a keratan sulfate proteoglycan. J Neurochem 61:29–44

Seko A, Yamashita K (2004) Beta1,3-*N*-acetylglucosaminyltransferase-7 (beta3Gn-T7) acts efficiently on keratan sulfate-related glycans. FEBS Lett 556:216–220

Seko A, Dohmae N, Takio K, Yamashita K (2003) Beta 1,4-galactosyltransferase (beta 4GalT)-IV is specific for GlcNAc 6-*O*-sulfate. Beta 4GalT-IV acts on keratan sulfate-related glycans and a precursor glycan of 6- sulfosialyl-Lewis X. J Biol Chem 278:9150–9158

Shen Y, Tenney AP, Busch SA, Horn KP, Cuascut FX, Liu K, He Z, Silver J, Flanagan JG (2009) PTPσ Is a receptor for chondroitin sulfate proteoglycan, an Inhibitor of neural regeneration. Science 326:592–596

Shipp EL, Hsieh-Wilson LC (2007) Profiling the sulfation specificities of glycosaminoglycan interactions with growth factors and chemotactic proteins using microarrays. Chem Biol 14:195–208

Shukla D, Spear BG (2001) Herpesviruses and heparan sulfate: an intimate relationship in aid of viral entry. J Clin Invest 108:503–510

Silver DJ, Silver J (2014) Contributions of chondroitin sulfate proteoglycans to neurodevelopment, injury, and cancer. Curr Opin Neurobiol 27:171–178

Sirko S, Holst AV, Weber A, Wizenmann A, Theocharidis U, Götz M, Faissner A (2010) Chondroitin sulfates Are required for fibroblast growth factor-2-dependent proliferation and maintenance in neural stem cells and for epidermal growth factor-dependent migration of their progeny. Stem Cells 28:775–787

Sitkovski J, Bednarek E, Bocian W, Kozerski L (2008) Assessment of oversulfated chondroitin sulfate in low molecular weight and unfractioned heparins diffusion ordered nuclear magnetic resonance spectroscopy method. J Med Chem 51:7663–7665

Smith RAA, Meade K, Pickford CE, Holley RJ, Merry CLR (2011) Glycosaminoglycans as regulators of stem cell differentiation. Biochem Soc Trans 39:383–387

Smith PD, Coulson-Thomas VJ, Foscarin S, Kwok JCF, Fawcett JW (2015) "GAG-ing with the neuron": the role of glycosaminoglycan patterning in the central nervous system. Exp Neurol 274:100–114

Soares PAG, Ribeiro KA, Valente AP, Capillé NV, Oliveira SNMCG, Tovar AMF, Pereira MS, Vilanova E, Mourão PAS (2018) A unique fucosylated chondroitin sulfate type II with strikingly homogeneous and neatly distributed α-fucose branches. Glycobiology 28:565–579

Stevenson JL, Choi SH, Varki A (2005) Differential metastasis inhibition by clinically relevant levels of heparins—correlation with selectin inhibition, not antithrombotic activity. Clin Cancer Res 11:7003–7011

Stone JE, Akhtar N, Botchway S, Pennock CA (1994) Interaction of 1,9-dimethylmethylene blue with glycosaminoglycans. Ann Clin Biochem 31:147–152

Sugahara K, Tanaka Y, Yamada S, Seno N, Kitagawa H, Haslam SM, Morris HR, Dell A (1996) Novel sulfated oligosaccharides containing 3-O-sulfated glucuronic acid from king crab cartilage chondroitin sulfate K. J Biol Chem 271:26745–26754

Sugahara K, Hirata T, Tanaka T, Ogino S, Takeda M, Terasawa H, Shimada I, Tamura J, ten Dam GB, van Kuppevelt TH, Miyasaka M (2008) Chondroitin sulfate E fragments enhance CD44 cleavage and CD44-dependent motility in tumor cells. Cancer Res 68:7191–7199

Sugiura N, Clausen TM, Shioiri T, Gustavsson T, Watanabe T, Salanti A (2016) Molecular dissection of placental malaria protein VAR2CSA interaction with a chemo-enzymatically synthesized chondroitin sulfate library. Glycoconj J 33:985–994

Suzuki M (1939) Biochemical studies on carbohydrates. I prosthetic group of cornea mucoid. J Biochem 30:185–191

Svensson KJ, Christianson HC, Kucharzewska P, Fagerström V, Lundstedt L, Borgquist S, Jirström K, Belting M (2011) Chondroitin sulfate expression predicts poor outcome in breast cancer. Int J Oncol 39:1421–1428

Swarup VP, Hsiao TW, Zhang J, Prestwich GD, Kuberan B, Hlady V (2013) Exploiting differential surface display of chondroitin sulfate variants for directing neuronal outgrowth. J Am Chem Soc 135:13488–13494

Tagalakis V, Blostein M, Robinson-Cohen C, Kahn SR (2007) The effect of anticoagulants on cancer risk and survival: systematic review. Cancer Treat Rev 33:358–368

Takeda N, Horai S, Tamura J (2016) Facile analysis of contents and compositions of the chondroitin sulfate/dermatan sulfate hybrid chain in shark and ray tissues. Carbohydr Res 424:54–58

Ten Dam GB, van de Westerlo EM, Purushothaman A, Stan RV, Bulten J, Sweep FC, Massuger LF, Sugahara K, van Kuppevelt TH (2007) Antibody GD3G7 selected against embryonic glycosaminoglycans defines chondroitin sulfate-E domains highly up-regulated in ovarian cancer and involved in vascular endothelial growth factor binding. Am J Pathol 171:1324–1333

Thelin MA, Svensson KJ, Shi X, Bagher M, Axelsson J, Isinger-Ekstrand A, van Kuppevelt TH, Johansson J, Nilbert M, Zaia J, Belting M, Maccarana M, Malmström A (2012) Dermatan sulfate is involved in the tumorigenic properties of esophagus squamous cell carcinoma. Cancer Res 72:1943–1952

Theocharis AD (2002) Human colon adenocarcinoma is associated with specific post-translational modifications of versican and decorin. Biochim Biophys Acta 1588:165–172

Theocharis AD, Tsara ME, Papageorgacopoulou N, Karavias DD, Theocharis DA (2000) Pancreatic carcinoma is characterized by elevated content of hyaluronan and chondroitin sulfate with altered disaccharide composition. Biochim Biophys Acta 1502:201–206

Theocharis AD, Vynios DH, Papageorgakopoulou N, Skandalis SS, Theocharis DA (2003) Altered content composition and structure of glycosaminoglycans and proteoglycans in gastric carcinoma. Int J Biochem Cell Biol 35:376–390

Toida T, Sato K, Sakamoto N, Sakai S, Hosoyama S, Linhardt RJ (2009) Solvolytic depolymerization of chondroitin and dermatan sulfates. Carbohydr Res 344:888–893

Tollefsen DM (1992) The interaction of glycosaminoglycans with heparin cofactor II: structure and activity of a high-affinity dermatan sulfate hexasaccharide. Adv Exp Med Biol 313:167–176

Tone Y, Pedersen LC, Yamamoto T, Izumikawa T, Kitagawa H, Nishihara J, Tamura J, Negishi M, Sugahara K (2008) 2-O-Phosphorylation of xylose and 6-O-sulfation of galactose in the protein linkage region of glycosaminoglycans influence the glucuronyltransferase-I activity involved in the linkage region synthesis. J Biol Chem 283:16801–16807

Tovar AMF, Santos GRC, Capillé NV, Piquet AA, Glauser BF, Pereira MS, Vilanova E, Mourão PAS (2016) Structural and haemostatic features of pharmaceutical heparins from different animal sources: challenges to define thresholds separating distinct drugs. Sci Rep 6:35619

Tykesson E, Mao Y, Maccarana M, Pu Y, Gao J, Lin C, Zaia J, Westergren-Thorsson G, Ellervik U, Malmström L, Malmström A (2016) Deciphering the mode of action of the processive polysaccharide modifying enzyme dermatan sulfate epimerase 1 by hydrogen–deuterium exchange mass spectrometry. Chem Sci 7:1447–1456

Uchimura K (2015) Keratan Sulfate: biosynthesis, structures, and biological functions. Methods Mol Biol 1229:389–400

Uchimura K, Muramatsu H, Kadomatsu K, Fan QW, Kurosawa N, Mitsuoka C, Kannagi R, Habuchi O, Muramatsu T (1998) Molecular cloning and characterization of an *N*-acetylglucosamine-6-*O*-sulfotransferase. J Biol Chem 273:22577–22583

Uchimura K, El-Fasakhany FM, Hori M, Hemmerich S, Blink SE, Kansas GS, Kanamori A, Kumamoto K, Kannagi R, Muramatsu T (2002) Specificities of *N*-acetylglucosamine-6-*O*-sulfotransferases in relation to L-selectin ligand synthesis and tumor-associated enzyme expression. J Biol Chem 277:3979–3984

Ulmer JE, Vilén EM, Namburi RB, Benidia A, Beneteau J, Malleron A, Bonnaffè D, Driguez PA, Descroix K, Lassalle G, Le Narvor C, Sandström C, Spillmann D, Berteau O (2014) Characterization of glycosaminoglycan (GAG) sulfatases from the human gut symbiont bacteroides thetaiotaomicron reveals the first GAG-specific bacterial endosulfatase. J Biol Chem 289:24289–24303

Ustyuzhanina NE, Bilan MI, Dmitrenok AS, Tsvetkova EA, Shashkov AS, Stonik VA, Nifantiev NE, Usov AI (2016) Structural characterization of fucosylated chondroitin sulfates from sea cucumbers *Apostichopus japonicus* and *Actinopyga mauritiana*. Carbohydr Polym 153:399–405

van Boeckel CAA, Petitou M (1993) The unique antithrombin III binding domain of heparin: a lead to new synthetic antithrombotics. Angew Chem Int Ed 32:1671–1690

Vázquez JA, Rodríguez-Amado I, Montemayor MI, Fraguas J, González MDP, Murado MA (2013) Chondroitin sulfate, hyaluronic acid and chitin/chitosan production using marine waste sources: characteristics, applications and eco-friendly processes: a review. Mar Drugs 11:747–774

Vieira RP, Mulloy B, Mourão PAS (1991) Structure of a fucose-branched chondroitin sulfate from sea cucumber. J Biol Chem 266:13530–13536

Villena J, Brandan E (2004) Dermatan sulfate exerts an enhanced growth factor response on skeletal muscle satellite cell proliferation and migration. J Cell Physiol 198:169–178

Vlodavsky I, Singh P, Boyango I, Gutter-Kapon L, Elkin M, Sanderson RD, Ilan N (2016) Heparanase: from basic research to therapeutic applications in cancer and inflammation. Drug Resist Update 29:54–75

Wan QF, Zhou ZY, Thakur P, Vila A, Sherry DM, Janz R, Heidelberger R (2010) SV2 acts via presynaptic calcium to regulate neurotransmitter release. Neuron 66:884–895

Wang W, Han W, Cai X, Zheng X, Sugahara K, Li F (2015) Cloning and characterization of a novel chondroitin sulfate/dermatan sulfate 4-*O*-endosulfatase from a marine bacterium. J Biol Chem 290:7823–7832

Warda M, Toida T, Zhang F, Sun P, Munoz E, Xie J, Linhardt RJ (2006) Isolation and characterization of heparan sulfate from various murine tissues. Glycoconj J 23:555–563

Wegrowski Y, Maquart FX (2004) Involvement of stromal proteoglycans in tumour progression. Crit Rev Oncol Hematol 49:259–268

Weiss R, Esko JD, Tor Y (2017) T argeting heparin and heparan sulfate protein interactions. Org Biomol Chem 15:5656–5658

Weyers A, Yang B, Solakyildirim K, Yee V, Li L, Zhang F, Linhardt RJ (2013) Isolation of bovine corneal keratan sulfate and its growth factor and morphogen binding. FEBS J 280:2285–2293

Whitelock JM, Iozzo RV (2005) Heparan sulfate: a complex polymer charged with biological activity. Chem Rev 105:2745–2764

Wolff JJ, Amster IJ, Chi L, Linhardt RJ (2007) Electron detachment dissociation of glycosaminoglycan tetrasaccharides. J Am Soc Mass Spectrom 18:234–244

Wolff JJ, Leach FE III, Laremore TN, Kaplan DA, Easterling ML, Linhardt RJ, Amster IJ (2010) Negative electron transfer dissociation of glycosaminoglycans. Anal Chem 82:3460–3466

Wu L, Viola CM, Brzozowski AM, Davies GJ (2015) Structural characterization of human heparanase reveals insights into substrate recognition. Nat Struct Mol Biol 22:1016–1022

Xu D, Esko JD (2014) Demystifying heparan sulfate–protein interactions. Ann Rev Biochem 83:129–157

Yabe T, Hata T, He J, Maeda N (2005) Developmental and regional expression of heparan sulfate sulfotransferase genes in the mouse brain. Glycobiology 15:982–993

Yamada S, Sugahara K (2008) Potential therapeutic application of chondroitin sulfate/dermatan sulfate. Curr Drug Discov Technol 5:289–301

Yamada S, Morimoto H, Fujisawa T, Sugahara K (2007) Glycosaminoglycans in *Hydra magnipapillata* (Hydrozoa, Cnidaria): demonstration of chondroitin in the developing nematocyst, the sting organelle, and structural characterization of glycosaminoglycans. Glycobiology 17:886–894

Yang HO, Gunay NS, Toida T, Kuberan B, Yu G, Kim YS, Linhardt RJ (2000) Preparation and structural determination of dermatan sulfate–derived oligosaccharides. Glycobiology 10:1033–1039

Yang J, Wang Y, Jiang T, Lv L, Zhang B, Lv Z (2015) Depolymerized glycosaminoglycan and its anticoagulant activities from sea cucumber *Apostichopus japonicus*. Int J Biol Macromol 72:699–705

Yu Y, Duan J, Leach FE III, Toida T, Higashi K, Zhang H, Zhang F, Amster IJ, Linhardt RJ (2017) Sequencing the dermatan sulfate chain of decorin. J Am Chem Soc 139:16986–16995

Zaia J, Costello CE (2003) Tandem mass spectrometry of sulfated heparin-like glycosaminoglycan oligosaccharides. Anal Chem 75:2445–2455

Zhang L, Muller T, Baenziger JU, Janecke AR (2010) Congenital disorders of glycosylation with emphasis on loss of dermatan-4-sulfotransferase. Prog Mol Biol Transl Sci 93:289–307

Zhang Z, Takeda-Uchimura Y, Foyez T, Ohtake-Niimi S, Narentuya, Akatsu H, Nishitsuji K, Michikawa M, Wyss-Coray T, Kadomatsu K, Uchimura K (2017) Deficiency of a sulfotransferase for sialic acid-modified glycans mitigates Alzheimer's pathology. Proc Natl Acad Sci USA 114:E2947–E2954

Part III
Aminosugar-Based Exopolysaccharides: Peptidoglycans

Chapter 6
Peptidoglycan Structure, Biosynthesis, and Dynamics During Bacterial Growth

Axel Walter and Christoph Mayer

Abstract The peptidoglycan is the key structural component of the bacterial cell wall that rests outside the cytoplasmic membrane and provides bacterial cells with physical strength and shape. It constitutes a huge mesh-like macromolecule composed of linear glycans held together by short peptides: the glycans consist of alternating amino sugars, *N*-acetylglucosamine (GlcNAc), and *N*-acetylmuramic acid (MurNAc), connected by β-1,4-glycosidic linkages, and the peptides include noncanonical D-amino acids and cross-link the glycan chains via binding to MurNAc. The peptidoglycan macromolecule is ubiquitous in bacteria, regardless of whether displaying a Gram-positive, Gram-negative, or complex mycobacterial cell envelope structure, and it is also highly restricted to bacteria, thereby distinguishing bacteria from eukaryotic microorganisms and archaea. In all bacteria, the peptidoglycan is synthesized from a lipid-anchored precursor that is preformed in the cytoplasm, flipped outward through the plasma membrane by channeling proteins (flippases), and is finally polymerized by membrane-bound, outward-facing synthetic enzymes (glycosyltransferases and transpeptidases) building a net-shaped covering of the entire bacterial cell, called the peptidoglycan sacculus. The peptidoglycan sacculus allows bacteria to cope with osmotic and environmental challenges, and it secures cell integrity during all stages of bacterial growth. It has to be sufficiently strong and rigid but, at the same time, flexible and dynamic to assure integrity of the cell during enlargement, division, and differentiation processes. Thus, the synthesis and integrity of the peptidoglycan are major targets of antibacterial therapeutics. We are summarizing in this chapter present knowledge including recent discoveries of peptidoglycan structure, assembly, and dynamics during bacterial growth.

A. Walter · C. Mayer (✉)
IMIT – Microbiology and Biotechnology, University of Tübingen, Tübingen, Germany
e-mail: christoph.mayer@uni-tuebingen.de

E. Cohen, H. Merzendorfer (eds.), *Extracellular Sugar-Based Biopolymers Matrices*,
Biologically-Inspired Systems 12, https://doi.org/10.1007/978-3-030-12919-4_6

6.1 Introduction

The bacterial cell is encased in a rigid cell wall containing the macromolecule peptidoglycan (PGN; synonym murein) as the critical structural component, which protects the membrane-covered protoplast and forms a barrier toward the environment (Rogers 1974; Seltmann and Holst 2002). The PGN is ubiquitous within bacteria, with only few exceptions such as the members of the phylum *Tenericutes* (e.g., mycoplasma) or conditional cell wall-less bacteria, so-called L-forms, but absent beyond this domain of life (Litzinger and Mayer 2010). The elucidation of the PGN structure went along with the discovery of the biosynthesis precursors, the "Park nucleotides" by James Theodore "Ted" Park (1922–2014) (Park and Johnson 1949; Park 1952; Park and Strominger 1957), which at that time were the first examples of nucleotide activated sugar molecules, carrying unusual amino sugars and D-amino acids, also novel back then. These findings paved the path toward the identification of the chemical structure of the PGN and its biosynthesis. Early PGN research was also closely linked with the discovery of the function of two antibacterial agents targeting cell wall integrity and synthesis, lysozyme and penicillin, both discovered by Alexander Fleming (Fleming 1955; Geddes 2008). Lysozyme is an antibacterial enzyme that specifically cleaves the PGN backbone, and penicillin is an antibacterial drug that inhibits PGN synthesis, eventually both are causing lysis of bacterial cells. Ever since, PGN synthesis is one of the most important targets for antibiotics to treat bacterial infections, as the pathways and enzymes involved in PGN biosynthesis are usually essential for bacteria but do not exist in humans. With the advent of electron microscopy, the PGN cell wall could first be visualized (Mudd et al. 1941; Salton and Horne 1951; Chapman and Hillier 1953; Kellenberger and Ryter 1958). Later on, the bag-shaped PGN structure was recognized by Wolfhard Weidel and his group at the Max Planck Institute for Biology in Tübingen, who investigated how phages lyse bacterial cells to get themselves released (Weidel and Primosigh 1958). He observed that in this process bacteria lose their rodlike shape and identified characteristic sugar peptides (muropeptides) in the medium, produced by a lysozyme-like activity of the phage and very similar to the products released from bacteria treated with penicillin (see Braun 2015). In collaboration with his colleague Helmut Pelzer, he developed the concept of the "murein sacculus" (from Latin "sacculus" for the sack and "murus" wall) (Weidel et al. 1960; Weidel and Pelzer 1964). Accordingly, the murein or PGN sacculus constitutes a huge, net-shaped macromolecule that surrounds the bacterial cell and provides a backpressure against the intracellular turgor (Rogers 1974; Höltje 1998; Seltmann and Holst 2002). Some billion years ago, when the domain *Bacteria* arose from prokaryotic progenitors, this exoskeleton-like structural element was acquired to cope with an increase in the intracellular osmotic pressure (turgor) due to the accumulation of metabolites as the cellular metabolism became more and more complex (Litzinger and Mayer 2010). The PGN is also essential for cell morphogenesis, as it allows bacterial cells to maintain their characteristic shapes (Young 2003). Although these properties of the PGN imply rigidity, this molecule has at the

same time to be highly flexible and dynamic. The steady degradation and resynthesis of the PGN allows the bacterial cell wall to continuously adapt to environmental and physiological constraints in a highly dynamic process during growth and differentiation. Despite intense research for more than 60 years now, fundamental questions regarding the architecture, temporal and spatial assembly, and dynamic remodeling of PGN are still unsolved. Recently however, new technologies, in particular new visualization techniques as well as advances in the chemical and physical analysis of bacterial cell walls, have revived the field of PGN research and allowed a new view on this versatile and complex polymer. In the first parts of this chapter, we will describe the chemical nature and structure, including recent insights into the 3D architecture, as well as compositional modifications of the PGN within bacteria. In the further part, we will review the PGN biosynthesis and assembly, which includes new observations aided by advances in fluorescence microscopy, and finally, we will elaborate the PGN as a dynamic macromolecule that undergoes a permanent turnover.

6.2 The Peptidoglycan Cell Wall and Envelope Structures of Bacteria

As the name indicates, the PGN is a complex heteropolymer made of glycans that are cross-linked via short peptides (Fig. 6.1). The glycans of the PGN are linear sugar chains of variable length that are composed of alternating β-1,4-linked amino sugars *N*-acetylglucosamine (GlcNAc) and *N*-acetylmuramic acid (MurNAc) (Fig. 6.1). MurNAc is a characteristic acidic amino sugar exclusively found within bacteria. It is a derivative of GlcNAc, carrying a D-lactic acid substituent, ether-linked via the hydroxyl group at the 3-position of GlcNAc (i.e., 3-O-D-lactic acid-GlcNAc) (Fig. 6.1). To the free carboxylic acid of the lactic acid substituent of MurNAc, short-chain peptides are amide-bound, and they partially cross-link the glycans. Thereby, a netlike macromolecular fabric is formed that is unique to bacteria and also highly restricted to bacteria, thereby distinguishing bacteria from archaea and eukaryotic microorganisms, e.g., fungi which mainly contain chitin/chitosan (see Chapters 1 to 17 within this book). Although PGN is not present in archaea, some methanogenic archaea contain pseudopeptidoglycan (pseudoPGN or pseudomurein), which is a somewhat similar polymer that instead of MurNAc contains the amino sugar *N*-acetyltalosaminuronic acid (TalNAcUA), β-1,3-linked with GlcNAc (Fig. 6.1). Thus, while the repeating subunit of the PGN polymer of bacteria is a GlcNAc-β-1,4-MurNAc-peptide, the repeating unit of the pseudoPGN is a GlcNAc-β-1,3-TalNAcUA-peptide (Fig. 6.1). Information regarding the pseudoPGN is rather limited, and therefore we focus in this chapter on the PGN of bacteria. For more information about the pseudoPGN/pseudomurein, refer to Kandler and König (1978), König et al. (1983), Kandler and König (1993), Hartmann and Konig (1994), Shockman et al. (1996), and Kandler and König (1998).

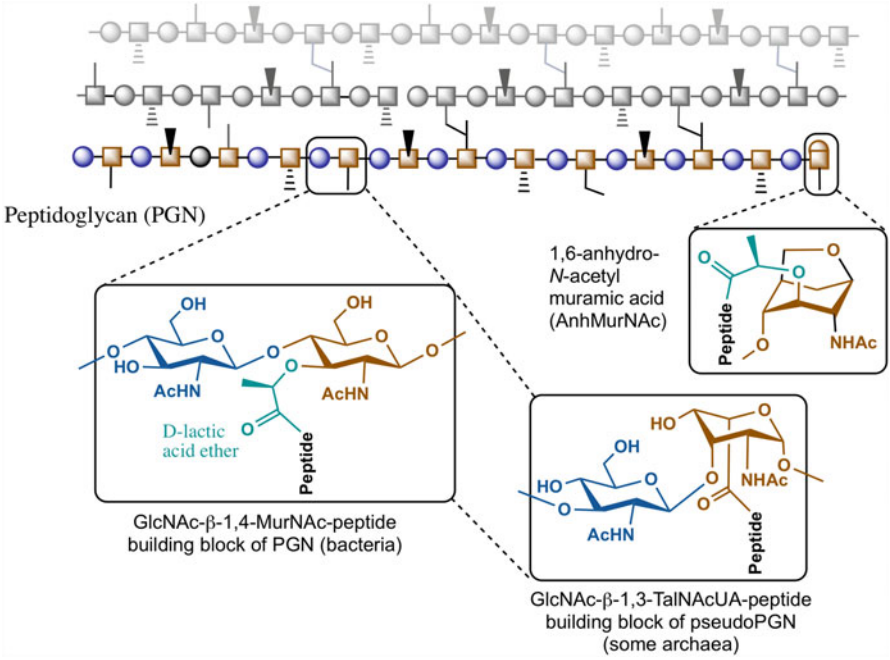

Fig. 6.1 Peptidoglycans are heteropolymers made of disaccharide-peptides building a netlike macromolecular fabric. They consist of linear glycan chains made of amino sugars and short-chain peptides that are partially interlinked. The PGN (murein) of bacteria is composed of alternating β-1,4-linked amino sugars *N*-acetyl-glucosamine (GlcNAc; blue, circles) and *N*-acetylmuramic acid (MurNAc; brown squares). Short-chain peptides (black lines), amide-linked to the D-lactic acid substituent (cyan structure) of MurNAc at C3, are used to cross-link the glycan chains yielding a 3D network. In most bacterial species, the glycan strands of the PGN terminate in 1,6-anhydro-*N*-acetylmuramic acid (AnhMurNAc) moieties, which are generated by the action of PGN-lytic transglycosylase enzymes. The pseudomurein (pseudoPGN) of some archaea is a polymer somewhat similar to PGN; however, it contains the β-1,3-linked amino sugars GlcNAc and *N*-acetyltalosaminuronic acid (TalNAcUA), which is substituted at the C6 carboxylic acid by peptides

Almost all bacteria contain PGN in their cell wall, yet they can have very distinct overall cell envelope structures (Silhavy et al. 2010). The traditional classification distinguishes Gram-positive bacteria and Gram-negative bacteria based on an ancient staining technique with the dye crystal violet developed by Hans Christian Gram in the 19th century (Gram 1884); see also Bartholomew and Mittwer (1952). The discrimination of bacteria by this technique relies, as we know now, on the retention of the dye in Gram-positive cells and the facile washing-out of the dye with organic solvents from the Gram-negative cell envelope (Popescu and Doyle 1996). Gram-positive bacteria (e.g., *Bacillus subtilis*, *Staphylococcus aureus*), which retain the dye, have a thick PGN layer that is covalently modified by secondary anionic glycopolymers (teichoic and teichuronic acid) and interweaved by lipoteichoic acids (Fig. 6.2a; see also heading 6.4.4; Chapman and Hillier 1953; Matias and Beveridge 2006). Moreover, they lack an outer membrane, which is characteristic for Gram-

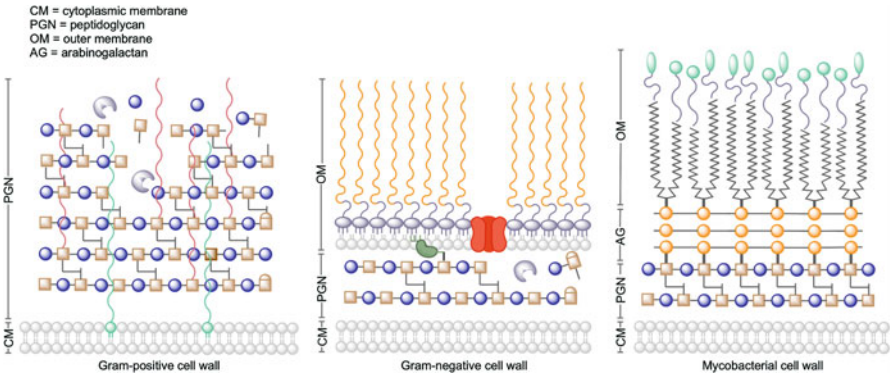

Fig. 6.2 Cell envelope structures of Gram-positive, Gram-negative, and mycobacterial cell envelopes. (**a**) The Gram-positive cell wall contains a thick layer of PGN adjacent to the cytoplasmic membrane (CM) with covalently bound secondary cell wall polymers, which include wall teichoic acids (WTA; red lines) and interweaved by lipoteichoic acids (LTA, green lines) that are membrane-bound. The PGN cell wall is rigid and at the same time flexible, to allow cell expansion: new PGN is deposited to the cell wall from below in a relaxed form, it is then stretched due to the turgor during cell expansion, and finally it is degraded in the outer regions by autolytic enzymes (violet symbols). (**b**) Gram-negative bacteria contain thin PGN connected to an additional outer membrane (OM) via lipoproteins (Braun's lipoprotein, green symbol, see heading 6.5.4). The OM includes lipopolysaccharides (LPS) (lipid part, violet; polysaccharide part, orange) in its outer leaflet, and cell wall-binding porins (red symbol). (**c**) The mycobacterial cell envelope is characterized by a PGN-arabinogalactan (AG; orange balls) complex and a lipid monolayer containing long-chain mycolic acids (MA) and glycolipids (green balloons). (This figure was modified after (Gerstmans et al. 2016))

negative bacteria (e.g., *Escherichia coli, Pseudomonas aeruginosa*) (Fig. 6.2b). Gram-negative bacteria are characterized (in most cases) by a thin PGN layer that is covered by an inner (the cytoplasmic membrane) and an additional outer membrane (Matias et al. 2003; Vollmer and Höltje 2004 and references cited within). The defined space between inner and outer membrane, in which the PGN layer is embedded, is called the periplasmic space. It is filled with a viscous gel, the periplasm, made of hydrated oligosaccharides, proteins, as well as the PGN (Hobot et al. 1984; Matias and Beveridge 2005; Silhavy et al. 2010).

The Gram classification, although generally useful, oversimplifies the variability of bacterial cell envelope structures. For example, the cyanobacteria, a large, diverse, and ancient group of bacteria, possess cell envelopes with combined features characteristic for both groups (Hoiczyk and Hansel 2000). They mostly stain "Gram-positive" despite having an outer membrane and, thus, an overall Gram-negative envelope. However, the PGN layer of cyanobacteria is considerably thicker than that of most Gram-negative bacteria and complexed with anionic secondary cell wall polymers; thus the dye can be retained. An even more complex structure of the cell envelope is found in mycobacteria (e.g., *Mycobacterium tuberculosis*). Instead of a real outer membrane, they contain surface glycolipids bound to a lipid monolayer of long-chain fatty acids (mycolic acids), and instead of a PGN-wall teichoic

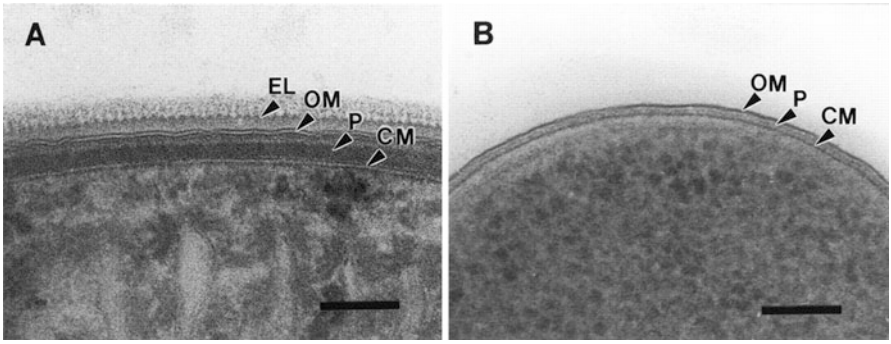

Fig. 6.3 Electron microscopic comparison of Gram-negative cell envelopes of a cyanobacterium and *E. coli*. (**a**) The cell envelope of the cyanobacterium (*Phormidium uncinatum*) reveals a thick (35 nm) PGN layer (P) that is embedded between the cytoplasmic membrane (CM) and an outer membrane (OM). In addition, an external layer (EL) composed of an S-layer and oscillin fibrils is visible. (**b**) The cell envelope of *E. coli* shows typical Gram-negative features: a thin (3–6 nm) PGN layer (P) sandwiched between the cytoplasmic membrane (CM) and outer membrane (OM). Both bacteria were identically processed using cryo-substitution, bars 100 nm. (The figures were reproduced with permission from ASM (Hoiczyk and Hansel 2000))

acid complex, they contain a PGN-arabinogalactan heteropolymeric cell wall (Fig. 6.2c; see also Sect. 6.5.5) (Brennan and Nikaido 1995; Jankute et al. 2015; Raghavendra et al. 2018). Mycobacteria and other bacteria (e.g., rickettsia and spirochetes) that do not respond to the Gram staining can be stained by the acid-fast technique (Ziehl-Neelsen stain) (Vilcheze and Kremer 2017); for a more detailed description of the mycobacterial PGN and cell envelope, refer to Sect. 6.5.5.

Classical light microscopy lacks high resolution and can barely assess the architectural differences of Gram-positive and Gram-negative cell envelopes. However, with the introduction of electron microscopy, particularly transmission electron microscopy (TEM) of thin sections in the mid-1950s, much better views on bacterial cell envelope structures were possible, and the multilayered architecture of Gram-negative cell walls was discovered (Kellenberger and Ryter 1958; Weidel et al. 1960; Murray et al. 1965; De Petris 1967). Conventional embedding and thin section techniques rely on harsh treatments, the removal of water, chemical fixation, and heavy metal staining for contrast, which may cause structural artifacts when sample preparation fails to preserve the native structural features. Recent advances in cryo-TEM avoided these difficulties and allowed to visualize the complex cell envelope structure of Gram-negative bacteria, including cyanobacteria, with a resolution as low as 1 nm (Hoiczyk and Hansel 2000; Matias et al. 2003; Chen et al. 2010; Harris 2015) (Fig. 6.3). The gentle cryo-substitution technique enables the examination of native polymeric cell wall structures in sections of hydrated, frozen cells under cryogenic conditions. Ultrarapid freezing of bacteria immobilizes the samples in non-crystalline ice (i.e., vitrification) and allows to preserve close-to-native structures

(Matias et al. 2003; Chen et al. 2010; Wolf et al. 2014). Electron cryotomography (Cryo-ET) is a specialized application of cryo-TEM that allows to reconstruct 3D images (tomograms) of high (1–4 nm) resolution (Chen et al. 2010). Very recent developments replace the sectioning by the thinning of specimens via fast ion beam milling (FIB milling) of surfaces. It is expected that in the future this technique in combination with electron microscopy or electron tomography will provide more details about the native cell wall architectures (Villa et al. 2013).

With cryo-TEM as well as atomic force microscopy (AFM), the thickness of the PGN of Gram-negative bacteria was determined to be 1.5 to 3 nm in non-hydrated form (De Petris 1967; Yao et al. 1999;) and 3 to 6 nm ((Yao et al. 1999; Matias et al. 2003) or > 6 nm in hydrated form (Hobot et al. 1984; Leduc et al. 1989). This is in agreement with earlier measurements using small-angle neutron scattering that revealed a thickness of 2.5–3 nm, attributed to one single layer of PGN, which makes up 75–80% of the *E. coli* cell wall, and the remaining being triple-layered (Labischinski et al. 1991). AFM was also used to measure the thickness of collapsed PGN sacculi: air-dried sacculi from *E. coli* had a thickness of 3.0 nm, whereas those from *P. aeruginosa* were 1.5 nm thick (Yao et al. 1999). When rehydrated, the sacculi of both bacteria swelled to double their anhydrous thickness. Thus, the thickness of the PGN depends on its state of hydration. Also bacteria themselves can vary the thickness of their cell wall during growth and differentiation and even the thickness of the Gram-negative periplasm can vary significantly and largely depends on the osmolarity of the medium (Hobot et al. 1984). Recent work revealed that the intermembrane distance of the periplasm is critical in Gram-negative bacteria and controlled by periplasmic lipoproteins that anchor the outer membrane to the periplasmic PGN polymer (Miller and Salama 2018).

An about five- to tenfold thicker cell wall (20–55 nm) was visualized in Gram-positive bacteria using cryo-TEM. Surprisingly, this technique also revealed a periplasmic-like compartment in Gram-positive bacteria, classically attributed only to Gram-negative bacteria. Cryo-TEM of frozen-hydrated sections of *Bacillus subtilis* visualized a bipartite structure above the plasma membrane consisting of a low-density, 22-nm-thick inner wall zone (IWZ), above which a higher-density 33 nm region or outer wall zone (OWZ) resides (Matias and Beveridge 2005). Similarly, *Staphylococcus aureus* revealed a bipartite wall consisting of a 16 nm IWZ, followed by a 19 nm OWZ (Fig. 6.4a) (Matias and Beveridge 2006). Intriguingly, five different zones of alternating low and high densities are present in the septal regions (Fig. 6.4b). An overall thickness of approximately 32 nm was determined for *Corynebacterium* sp., with 8.5 nm corresponding to an outer layer, 6.5 nm to an electron translucent region, and 17 nm to the PGN (Marienfeld et al. 1997). The thickness of the PGN in cyanobacteria appears to be more in the range of Gram-positives, usually >10 nm (e.g., in *Synechococcus*), 15–35 nm in filamentous species (Fig. 6.3a), and in the extreme can reach 700 nm, although they possess a Gram-negative outer membrane (Hoiczyk and Hansel 2000) (Fig. 6.3).

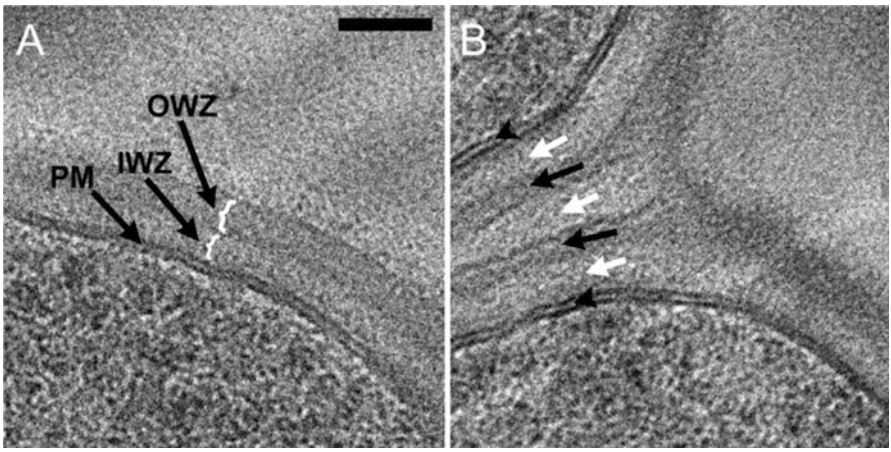

Fig. 6.4 A bipartite cell wall structure revealed by cryo-TEM images of cross sections of frozen-hydrated *S. aureus* cells (Gram-positive). (**a**) High-magnification image detailing the dipartite cell wall at non-septal regions. A low-density inner wall zone (IWZ) and an adjacent high-density outer wall zone (OWZ) are visible adjacent to the plasma membrane (PM). (**b**) At the septum, five different zones of alternating low (white arrows) and high (black arrows) densities are distinguished between the two membranes of the septum (arrowheads). Both images are shown at the same magnification, bar 50 nm. (The figures were reproduced with permission from ASM (Matias and Beveridge 2006))

6.3 The Peptidoglycan Sacculus: A Protecting Shield and Determinant of Cell Shape

Bacteria come in a multitude of different shapes (Fig. 6.5a). This had become evident already when Antonie van Leeuwenhoek in the 1660s first observed bacteria and other microbes with his newly constructed microscope and described their morphology (Porter 1976). Remarkably, he already anticipated at that time that surface structures likely are responsible for the various shapes (Salton 1994). Considerably later, a cell wall surrounding bacterial cells was identified by staining techniques and connected with osmotic stability, cell division, and growth (reviewed in Vollmer and Höltje 2004). The invention of electron microscopy not only allowed to visualize bacterial cell walls but also to demonstrate that isolated bacterial cell walls retain the shape of the bacterium (Salton and Horne 1951) (Fig. 6.5b) and that lysozyme and penicillin affect bacteria shape by interference with PGN structure and biosynthesis, respectively (Strominger and Tipper, 1965). Electron microscopy also greatly facilitated the development of purification methods of cell walls (Salton and Horne 1951) and ultimately led to the discovery of the bag-shaped PGN structure the "murein sacculus" (Weidel et al. 1960; Weidel and Pelzer 1964). The murein or PGN sacculus constitutes a giant, single bag-shaped molecule of >3 x 10^9 Da (and approximately 3.5 x 10^6 PGN building blocks, GlcNAc-MurNAc-peptides per *E. coli* cell). It is thus about the same size as the other huge macromolecule of the

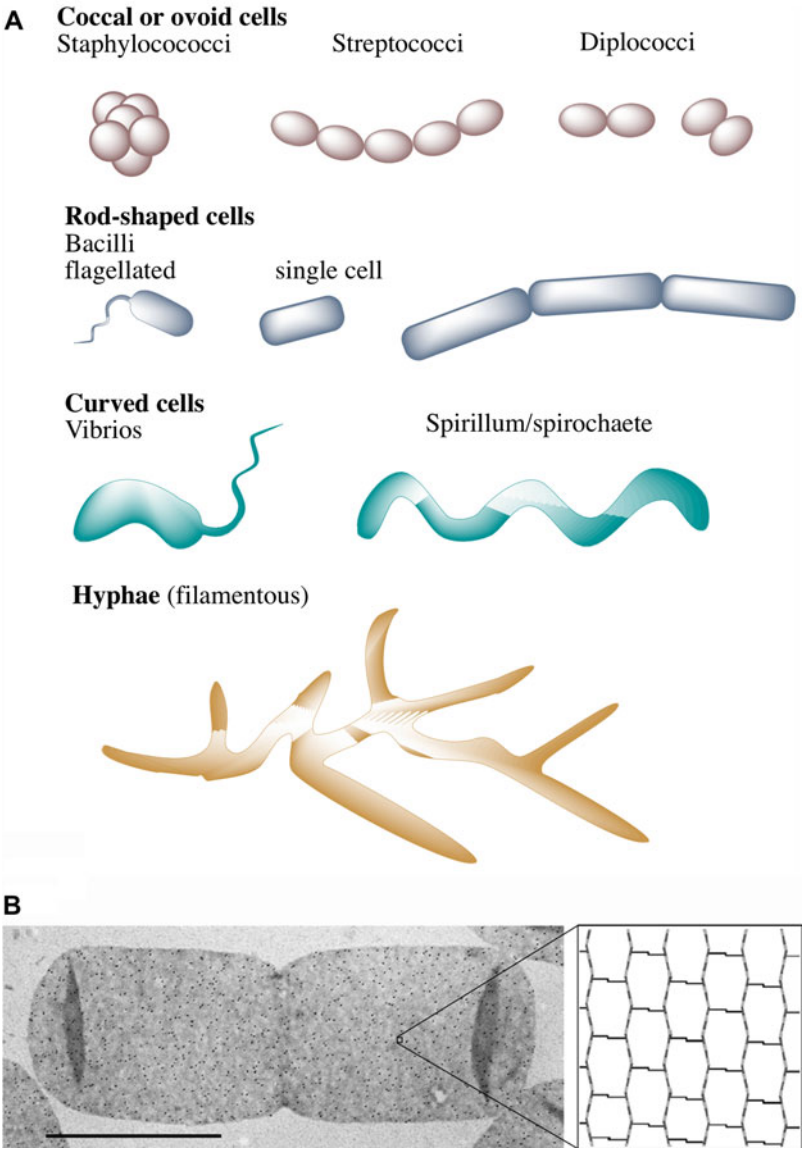

Fig. 6.5 The cell shape-maintaining PGN or murein sacculus. (**a**) The PGN allows bacteria to adapt various shapes. (**b**) The PGN sacculus can be isolated and maintains the shape of the cell it was derived from. Electron micrograph (transmission electron microscopy, TEM) of a dividing *E. coli* cell (left side). The black dots are 6 nm gold particles used to visualize an anti-murein antibody bound to the sacculus. Bar, 1 μm. The right side shows a model of the murein layer in a section of approximately 30 × 30 nm. The glycan strands (zigzag lines) are running perpendicular to the long axis, and the peptides (thin lines) connect the glycans and run in the direction of the long axis of the sacculus. The smallest hexagonal unit is termed "tessera" and has a calculated mesh width of c. 1 nm. (Figure (**b**) was reproduced with permission from Elsevier (Vollmer and Bertsche 2008))

bacterial cell, the genomic DNA (Vollmer and Höltje 2004). Isolated sacculi retain the structure of the cell they were purified from, e.g., *E. coli* cells maintain the rod shape as visualized by electron microscopy (Fig. 6.5b), demonstrating the shape-controlling function of the PGN.

The PGN confers stability to the cell, allowing to withstand the high internal turgor pressure that can reach 5 atm in Gram-negative and up to 50 atm in Gram-positive bacteria (Archibald et al. 1993; Seltmann and Holst 2002). The absence or impairment of the PGN sacculus may cause cell disruption and lysis due to increased turgor in hypoosmotic medium or may interfere with cell growth and division due to reduced cell turgor causing plasmolysis in hyperosmotic medium (Witholt and Boekhout 1978; Morbach and Kramer 2002; Rojas et al. 2014). An exception from this rule are obligate intracellular bacteria, e.g., members of the genus mycoplasma, and so-called L-forms, which are cell wall-deficient bacteria that have lost their PGN, e.g., upon treatment with cell wall-acting antibiotics or lytic substances (Errington et al. 2016; Kawai et al. 2018). These cell wall-deficient bacteria and L-forms lose their cell shape and become spheric but still are able to proliferate in osmo-protecting medium. As they are perfectly capable of growing and dividing, they distinguish from protoplasts and spheroplasts, which are viable but not propagating bacteria, Gram-positives or Gram-negatives, respectively, having their cell wall removed. Bacteria of the phylum *Tenericutes* (including *Mollicutes*, *Spiroplasma*, *Phytoplasma*) and L-forms are much more resistant to lysis by osmotic shock than were the bacterial protoplasts and spheroplasts, indicating that also other cell envelope structures participate in stabilization the cell envelope (Razin and Argaman 1963). Moreover, upregulation of lipid synthesis is associated with conversion of bacteria to stable L-forms (Strahl and Errington 2017). Notably, it was recently recognized that members of the phyla *Chlamydiae* and *Planctomycetes* do contain PGN in their cell wall, albeit only rudimentarily structured, which is not osmotically protecting and mainly synthesized during the cell division process (Liechti et al. 2014; Jeske et al. 2015; Liechti et al. 2016).

The current consensus is that the PGN sacculus maintains shape, which however is determined by the bacterial cytoskeleton directing PGN biosynthesis throughout cell expansion and division (Löwe et al. 2004; Cabeen and Jacobs-Wagner 2007; Young 2010; Fink et al. 2016) (see Sect. 6.5.4 for more details). The flexibility of PGN in the construction of different cell shapes was illustrated by an intriguing experiment described by Takeuchi et al. (2005). Single *E. coli* cells were grown in microchambers of agarose that forced the cells to adapt various shapes. The authors obtained viable *E. coli* cell that were round, spiral, or curved, as determined by the shape of the vessel they were grown in. Supposedly, the PGN synthesis can adapt different shapes and can be very flexibly adjusted in a bacterium to cope with environmental constraints. The process of biosynthesis of the PGN will be described in detail in Sect. 6.7. In the next chapter, we will first summarize still ongoing efforts to determine the structural organization of the PGN network that was boosted by recent advances in microscopic visualization techniques.

6.4 The Structural Organization of the Peptidoglycan Cell Wall

The small size of a bacterial cell and the insolubility, heterogeneity, and flexibility of the PGN network for a long time prevented the determination of its three-dimensional architecture by conventional low-resolution imaging or high-resolution structural techniques, such as X-ray crystallography and NMR spectroscopy. Thus, the topology of the PGN remained uncertain for a long time and therefore had been a subject of various theoretical considerations and speculations (Weidel and Pelzer 1964; Kelemen and Rogers 1971; Braun et al. 1973; Burge et al. 1977b; Burge et al. 1977a; Labischinski et al. 1979; Koch and Doyle 1985; Koch 1985; Koch 1995; Höltje 1998; Vollmer and Höltje 2001; Dmitriev et al. 2005). Until now, many structural views of the PGN cell wall depicted in textbooks are in part imaginations, as they are not experimentally supported. For example, the regular organization of the PGN, with twisted glycan strands oriented in parallel, forming hexagons (tessera) due to peptide cross-linkage, shown in Fig. 6.5b, clearly is an oversimplification (Vollmer and Bertsche 2008). Early X-ray diffraction studies revealed the lack of regular, semicrystalline structures within the PGN macromolecule but also recognized a not entirely disordered organisation (Formanek and Rauscher 1979; Labischinski et al. 1979). Moreover, the PGN sacculus was shown to be remarkably flexible: it can be stretched about three times the initial surface area as shown by low-angle light scattering (Koch and Woeste 1992).

In recent years, new techniques allowed to gain deeper insights into the structure and organization of the PGN, particularly cryo-TEM, Cryo-ET, and AFM, that provide structural information close to atomic resolution. These techniques helped to resolve the debate about the orientation of the glycan chains of the PGN. The "layered structural model," in which the glycan strands of the PGN run mostly perpendicular to the long axis and parallel to the cell membrane, is the classical view of the cell wall PGN (Höltje 1998; Vollmer and Bertsche 2008). It is supported by theoretical considerations based on experimentally determined PGN thickness, amount of PGN material, glycan chain length, and degree of PGN cross-linkage (Vollmer and Höltje, 2004; Vollmer and Seligman 2010). However, based on computer modeling, an axial orientation, the so-called scaffold model had been suggested (Dmitriev et al. 1999; Dmitriev et al. 2000; Dmitriev et al. 2003; Dmitriev et al. 2004; Dmitriev et al. 2005). This model proposed that the glycan chain may extend perpendicular to the cell membrane. It had attracted attention, since this prediction fits well with the process of biosynthesis, the NMR structure of a synthetic PGN fragment, and the assembly of flagella and channel proteins within the cell wall (Meroueh et al. 2006). Vollmer and Höltje argued against this view, showing that at least for *E. coli* and other gram-negative bacteria the axial orientation of the PGN is not consistent with the data, but supports the layer structural model (Vollmer and Höltje 2004). Further support for the layered model originates from measurements of elasticity and stiffness of the cell wall PGN. With the development of AFM at the end of the 1990s, the elucidation of the mechanical properties of the PGN was possible (Yao et al. 1999; Arnoldi et al. 2000; Touhami et al. 2004; Scheuring and

Dufrene 2010; Loskill et al. 2014; Mularski et al. 2015). AFM can be used either to acquire topological images of the bacterial surface and isolated sacculi or to measure adhesion forces to quantify the cell surface elasticity. With the latter method, Yao et al. (1999) determined an anisotropy of elasticity of the *E. coli*-hydrated sacculi that are 1.8 times more stretchable in the longitudinal axis than in the perpendicular axis. This likely results from the flexible peptides being oriented more or less parallel to the cell longitudinal axis, while the glycan chains would be predominantly perpendicular to it. Similar measurements were performed in *S. aureus* (Loskill et al. 2014) and revealed that the stiffness of the PGN increased with elevated percentage of cross-linkage. As a result, the cell radius and cell wall stiffness are correlated to stress and pressure, thus offering a regulatory mechanism for cell shape changes under environmental conditions. Cryo-ET experiments conducted by Grant Jensen and coworkers (Gan et al. 2008) ultimately revealed that the PGN of *E. coli* is mostly arranged in a layer roughly parallel to the membrane strands and the glycan chains, encircling the cell in a disorganized hooplike fashion (Fig. 6.6). With Cryo-ET technique as well as with sensitive radioactive assays, it was shown recently that

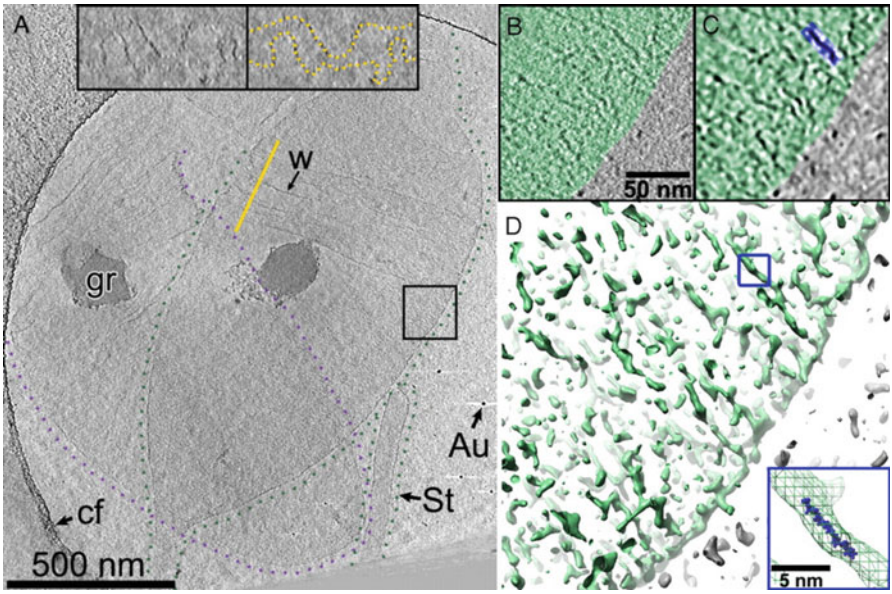

Fig. 6.6 3D-organization of *Caulobacter crescentus* (Gram-negative) PGN revealed by Cryo-ET. (**a**) Image showing the 30-nm-thick Z-slice of two overlapping *C. crescentus* cells, outlined by green and violet dotted lines. Inserts showing 30-nm-thick cross sections cut through the yellow line in the main panel. The yellow dotted line follows the "upper" and "lower" halves of the PGN. (**b** and **c**) Enlarged views (of a 4-nm-thick slice; boxed in **a**) after 3D median filtration (**b**) and image (**c**). The green-shaded region demarcates the PGN with one putative glycan strand highlighted in blue. (**d**) Iso-surface rendering; the putative glycan is boxed in blue. Blue box: Superposition of a PGN 9-mer atomic model. Abbreviations: W, wrinkle; gr, grain; St, stalk (part of the PGN-extension of *C. crescentus*); Au, gold particle; cf, carbon support film. The figure was from Gan et al. (2008), copyright (2008) National Academy of Sciences.

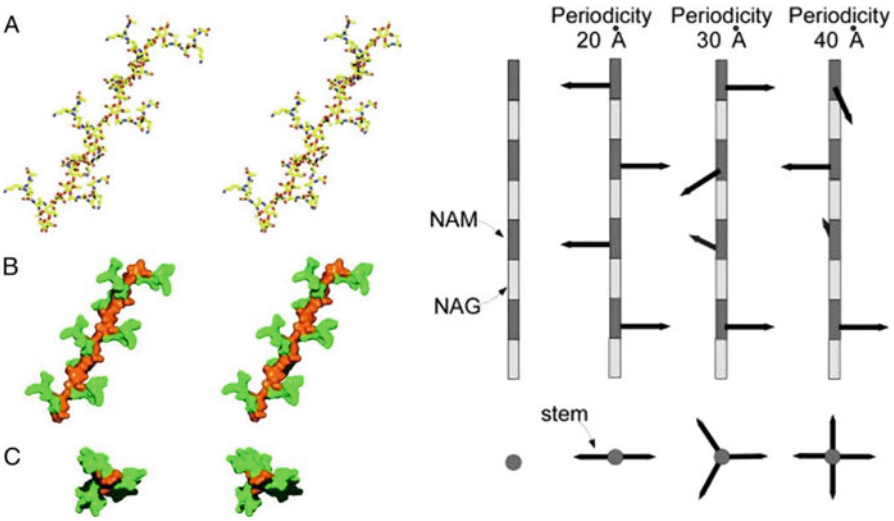

Fig. 6.7 Architecture of glycan backbone of the PGN and orientation of the peptide stems. (**a**) Stereoview of a (NAG-NAM-Peptide)$_8$ octamer construct with threefold symmetry (periodicity 30 Å) derived from the NMR structure of a synthetic fragment (Meroueh et al. 2006). The (NAG-NAM)$_8$ conformer, shown in capped-stick representation (O, N, and C are shown in red, blue, and yellow, respectively). (**b**) Solvent-accessible Connolly surface representation with the glycan backbone shown in orange and the peptide in green for the same perspective shown in **a**. (**c**) Stereoview of this construct seen from above (down the helical axis), shown as a solvent-accessible Connolly surface with the same color coding as in **b**. (**d**) Different possible glycan backbone conformations with twofold (periodicity 20 Å), threefold (40%), or fourfold (40%) symmetry (Kim et al. 2015). (The Figures **a**–**c** were from Meroueh et al. (2006), copyright (2006) National Academy of Sciences, and Figure **d** from Kim et al. (2015) reproduced with permission from Elsevier)

bacteria so far assumed to entirely lack a PGN wall, *Chlamydiales* and *Planctomycetales*, do contain PGN in the cell wall (Pilhofer et al. 2013; Liechti et al. 2014; Jeske et al. 2015; van Teeseling et al. 2015).

The glycan strands of the PGN were initially thought to adopt a chitin-like parallel (or antiparallel) orientation with a disaccharide periodicity of 20 Å and stem peptide rotated by 180° relative to the previous and next one (Vollmer and Höltje 2004; Kim et al. 2015) (Fig. 6.7). However, a solution structure of a synthetic tetrasaccharide-pentapeptide fragment was determined by NMR techniques, which revealed a right-handed helix with a periodicity of three subunits per turn and a 120° rotation symmetry (Fig. 6.7a–c) (Meroueh et al. 2006). Thus, cross-linkage of these glycans would make up a PGN network of hexagonal honeycomb-like structure with 70-Å diameter pores, since the peptide bridges could not be oriented in plane. In contrast, solid-state NMR studies using ^{13}C-labeled PGN indicated a fourfold axial symmetry (Fig. 6.7d) that would allow for a maximum of 50% cross-linkage in a single-layered PGN (Gram-negative) and up to 100% cross-linkage of densely packed glycan strands in thick Gram-positive PGN, as applied for *S. aureus* (Kim

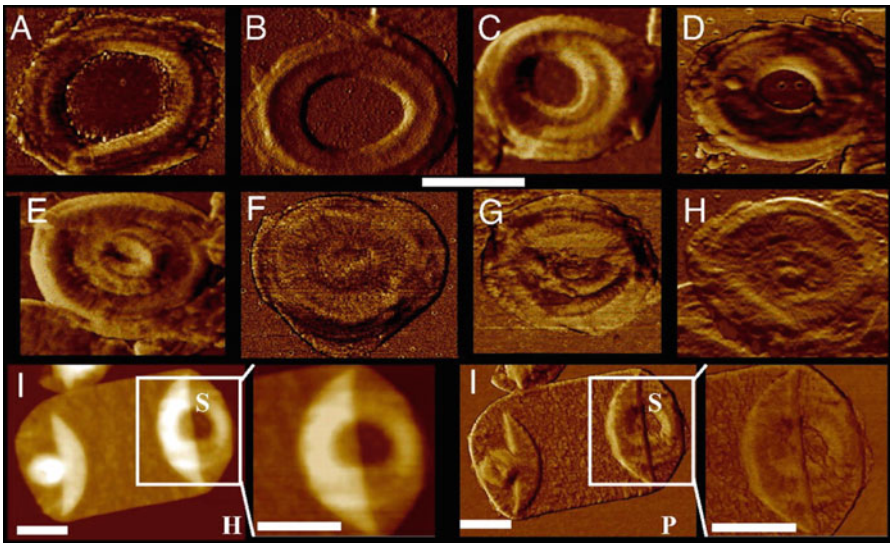

Fig. 6.8 Atomic force microscopy (AFM) analysis of *B. subtilis* sacculi and the septal architecture. The images (**a**–**h**) show the progression from early septum (**a**) to complete septum (**h**). Visible are large cables and cross-striations transversing the larger cables. All images are phase top view, scale bar, 500 nm. (I) Height (H) and phase (P) images of an entire cell with a partially completed septum (S) containing a hole and a completed septum at the other end of the sacculus that contains a small annular closing plug. (The figure was taken from Hayhurst et al. (2008), copyright (2008) National Academy of Sciences)

et al. 2015). The extent of cross-linkage however is variable in bacteria and, with the exception of *S. aureus*, usually less than 50% (see Sect. 6.5.1).

With AFM, besides assessing mechanical properties, the surface structures of bacteria, isolated cell walls, and even single chains of PGN can be mapped (Turner et al. 2016). AFM studies with *B. subtilis* sacculi resulted in surprising findings that the inner surface of cell walls has a regular macrostructure of thick, ca. 50-nm-wide cables running circumferential around the short axis of the rod-shaped cell (Hayhurst et al. 2008). If these structures, which are very different from the classical view of a layered cell wall, reveal intertwined PGN cables and how these may be synthesized is currently unknown. AFM can also visualize the PGN architecture at the septation sites (Hayhurst et al. 2008). Defined septa at all stages of septal closure can be seen in Fig. 6.8. The cable-like structures of in average 135 nm width form a spiral toward the center.

Combining AFM with size exclusion chromatography, Hayhurst et al. 2008 reported that the glycan chains in *B. subtilis* have an average length of 1.3 μm and are up to 5 μm long, which corresponds to a glycan composed of 5000 disaccharides. This finding contrasts earlier reports of glycans with an average length of 54–96 disaccharides in *B. subtilis* (Ward 1973), 25–40 disaccharides in *E. coli* (Glauner et al. 1988), and only 6–9 disaccharides in *S. aureus* (Tipper et al. 1967; Ward 1973; Boneca et al. 2000). However, the glycan chain length in these older reports is likely

an underestimation of the portion of longer chains. Harz and coauthors have already mentioned that ca. 30% of the PGN glycans that could not be separated by size exclusion have a size of >30 disaccharides (Harz et al. 1990). Although *S. aureus* has rather small-sized glycans, it was recently reported that only 30% of the glycans in this organism have a chain length of <50 disaccharides (Wheeler et al. 2015). Clearly, this long glycan chains are not consistent with the "scaffold model" of PGN architecture. Glycans in its normal rod shape are long and circumferentially oriented; however, when a spheroid shape is induced (chemically or genetically), glycans become short and disordered (Turner et al. 2018). Thus, altered cell shape is associated with substantial changes in PGN biophysical properties.

6.5 Variations of the Chemical Composition of the Peptidoglycan

Although the overall chemical composition of the PGN is very similar within bacteria, considerable variations from the general scheme exist in different species. Particularly, the chemical composition of the peptides, and whether the cross-linkage involves bridging peptides, varies significantly among different bacteria (Schleifer and Kandler 1972; Vollmer et al. 2008a; Litzinger and Mayer 2010). In their monumental work, Schleifer and Kandler distinguished over hundred different PGN chemotypes of bacteria according to their amino acid composition and mode of cross-linkage and used variations within the PGN for taxonomic classification (Schleifer and Kandler 1972). The glycan part of PGN is less variable, yet still a number of sugar modifications do occur, e.g., *O*-acetylation, *N*-deacetylation, or *N*-glycolylation (with mycobacteria), and also differences in the chain length of the glycans, as well as modification by secondary cell wall polymers (via MurNAc 6-phosphate, MurNAc 6P) and 1,6-anhydro-MurNAc end-capping (Vollmer 2008). It should be noted that bacteria are able to flexibly change their PGN structure depending on cell cycle, growth phase, and nutrient status. Moreover, they can retrieve PGN building blocks from the environment and incorporate them into their cell walls, e.g., different amino acid, including noncanonical and even nonnatural fluorogenic amino acids (see Sect. 6.7.3). Thus, the chemical composition of the bacterial PGN can be rather flexible. Nevertheless, differences between bacterial strains exist and are summarized in the following sections. The variation in the peptide part of the PGN will be addressed first, followed by the description of glycan modifications, and then three further sections will address (i) modifications that occur during spore cell wall biogenesis; (ii) attachment of proteins, secondary polysaccharides, and teichoic acids to the PGN; and (iii) special PGN modifications within mycobacteria.

6.5.1 *Variation in the Stem Peptide and Modes of Cross-Linkage*

Characteristic for the PGN peptides is that they contain noncanonical D-amino acids (D-Ala; D-Glu), besides L-amino acids (L-Ala; L-Lys; seldomly L-ornithine, L-Orn) and amino acids carrying two amino groups (diamino acids), that may thus contain both a D- and an L-stereochemical site, e.g., meso-diaminopimelic acid (m-DAP) (Fig. 6.9). These amino acids are connected in such a way that they generate peptides with alternating D,L- and L,D-peptide/amide linkages, beginning with the D-lactic acid

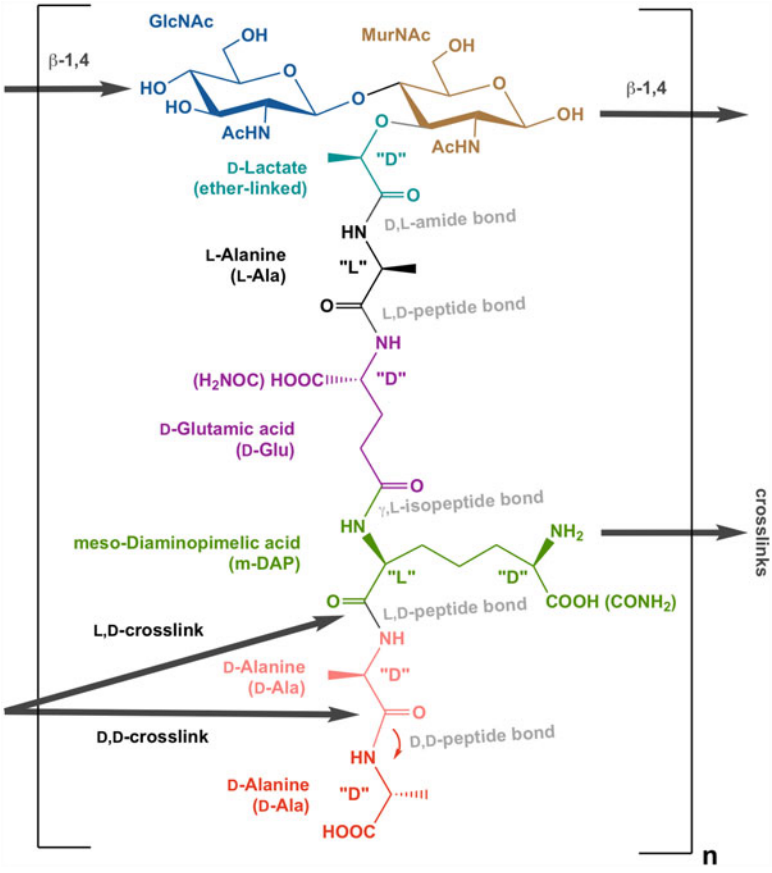

Fig. 6.9 Chemical structure of the GlcNAc-MurNAc-pentapeptide building block of the PGN and modes of cross-linkage. The stem peptide shown is the variant found in most Gram-negative bacteria and many bacilli and contains m-DAP at position 3 (green). The amino group at the stereochemical D-site of m-DAP is used to generate PGN cross-linkages with D-Ala residues of neighboring strands. These cross-linkages occur via transpeptidation reactions, energized by the cleavage of a terminal D-Ala residue (red), and yield either D,D-(4,3) or L,D-(3,3) peptide bonds. (This figure was adapted from Litzinger and Mayer (2010))

substituent of MurNAc. The last amino acids in the stem peptides, usually two D-Ala, are linked by a D,D-peptide bond. The resulting D,L,D,L,D,D-sequence of the peptides within the PGN makes them insensitive to cleavage by normal proteases/peptidases, which are specific for L,L-peptide bonds (Litzinger and Mayer 2010). In addition, it gives the peptides more flexibility by preventing the formation of alpha-helical structures and results in a compact disposition with the terminal D-Ala-D-Ala hidden in a curled peptide that can be stretched 2.5-fold from 10 Å to 25 Å (de Pedro and Cava 2015). Fig. 6.9 depicts the chemical structure of the general disaccharide-peptide building block of PGN as it is found within *E. coli* and *Bacillus subtilis* that contains a stem peptide with the general sequence L-Ala-iso-D-Glu-m-DAP-D-Ala-D-Ala (Fig. 6.9). Variations in this building block among bacteria involves primarily the presence of either meso-diaminopimelic acid (mDAP) at the third position within the stem peptide, which occurs in most Gram-negative as well as in some bacilli (e.g., *B. subtilis*), or L-Lys, which occurs in the majority of Gram-positive bacteria. However, some bacteria also contain L,L-DAP (e.g., *Actinobacteria*), L-ornithine (L-Orn), or, in some rare cases, L-2,4-diaminobutyric acid (Vollmer 2008; Litzinger and Mayer 2010). The diamino acids, mostly located at the third position in the stem peptide, contain a second amino group (diamino acids) that is used to cross-link the stem peptides in the PGN network (Fig. 6.9). Besides the free amino group of a diamino acid, the terminal D-Ala-D-Ala of the pentapeptide stem is critical for the cross-linkage of peptide via transpeptidases (penicillin-binding proteins, PBPs, involved in PGN biosynthesis; see Sect. 6.7.3). However, these enzymes that catalyze the cleavage of the D,D-peptide bond between the amino acids at the fourth and the fifth position, D-Ala(4)-D-Ala (5), do not catalyze an hydrolysis but a transpeptidation reaction. After release of D-Ala(5), the D-Ala(4) remains bound to the enzyme, and in a second reaction step, the free amino group of a diamino acid of a neighboring peptide strand attacks the D-alanyl-enzyme intermediate, thereby catalyzing the formation of a new peptide/amide bond (Fig. 6.9). Since these enzymes catalyze the cleavage as well as the reformation of a peptide/amide bond, they are called "transpeptidases." These transpeptidases are very famous enzymes since they are the targets of penicillin and other β-lactam antibiotics. They were identified by their interaction with penicillin and thus were called penicillin-binding proteins (PBPs) (Sauvage et al. 2008). Of course, the physiological function of the PBPs is not binding of penicillin; rather this is a fatal reaction for the bacterium as it interferes with its capability to cross-link the PGN. To circumvent penicillin stress or to provide themselves with immunity toward antibiotics targeting the D-Ala-D-Ala part, bacteria can instead of D,D-transpeptidases use penicillin-insensitive L,D-transpeptidases to cross-link their PGN (Mainardi et al. 2008). These enzymes cleave the DAP(3)-D-Ala(4) or L-Lys-D-Ala(4) bonds to initiate the transpeptidation reaction forming L,D- instead of D,D-cross-linkages. Enterococci use this "alternative" cross-linkage to become insensitive to β-lactam and glycopeptide antibiotics which bind to the D-Ala-D-Ala structure (Cremniter et al. 2006; Magnet et al. 2007a). It should be noted that members of the L,D-transpeptidase family also links Braun's lipoprotein with the PGN (Magnet et al. 2008) (see Sect. 6.5.4).

Amino acids at the other positions of the stem peptides are less frequently modified (Vollmer et al. 2008a). The fifth amino acid, i.e., the D-Ala(5) which is used for the transpeptidation reaction, can be substituted by glycine, D-serine, or D-lactate. These modifications are associated with vancomycin antibiotic resistance, which is a result of weaker binding of these antibiotics to the modified peptide (Boneca and Chiosis 2003). Bacteria are able to adjust stem-peptide composition (e.g., D-Ala-D-lactate instead of D-Ala-D-Ala) well as the linkage type (e.g., L,D- instead of L,D-cross-bridges) in response to treatment with vancomycin or β-lactam antibiotics, respectively (Magnet et al. 2008). However, also within the same bacterial strain, there are considerable variations in the PGN composition and structure. Bacteria generally are able to chemically adjust the PGN composition and the cross-linkage in dependence on growth condition, growth phase, or environmental and antibiotic constraints. Bacteria are also able to add unusual or even nonnatural amino acids within their cell wall. This had paved the route for fluorescent labeling of the PGN (see Fig. 6.17; Sect. 6.7.3).

The predominant cross-linkage type is the direct connection between mDAP and L-Lys at position 3 of one stem peptide with an D-Ala residue at position 4 of another peptide (direct 3–4 cross-linkage; A1γ- type; see Fig. 6.10; Schleifer and Kandler 1972). However, the cross-linkage within bacteria can vary and may involve amino acid or peptide bridges. The sizes of these bridges range from one to seven amino acids (Vollmer et al. 2008a). Most prominent is the penta-glycine (Gly_5) bridge of *S. aureus* (Fig. 6.10). Worth mentioning is also the peptide bridge of *Micrococcus luteus*, in which the peptide stem is duplicated (Fig. 6.10). Presumably, the stem peptides become detached by an amidase and is cross-bridged by an unusual transpeptidase reaction (Vollmer et al. 2008a). Bridging can also involve charged amino acids, such as in *Lactobacillus* or *Enterococcus* sp. (Fig. 6.10). The three digit code established by Schleifer and Kandler to classify the types of cross-linkages within bacteria is explained in the legend to Fig. 6.10 (Schleifer and Kandler 1972).

6.5.2 Modifications of the Glycan Backbone

The glycan part of the PGN shows less variation among different bacteria, compared to the peptide part. Nevertheless, these few variations are of great importance, since they greatly alter the susceptibility of bacteria toward lysozyme and other cell wall hydrolases and affect the recognition by the innate immune system (Vollmer 2008). This holds in particular for *N*-deacetylation and *O*-acetylation of the sugars within the PGN. *O*-Acetylation is used by *Bacillus*, *Staphylococcus*, or *Neisseria* sp. to alter its susceptibility toward lysozyme and other muramidases. Lysozyme-resistant strains of *B. cereus* and *B. anthracis* are characterized by high proportion of glucosamine (77% or 88%, respectively) and muramic acid (50% or 34%, respectively) (Araki et al. 1971; Zipperle et al. 1984). Even the lysozyme-sensitive *B. subtilis* 168 contains a significant amount of glucosamine (19%) and muramic acid (33%) in its PGN; however, *B. subtilis* strain W23 contains only glucosamine

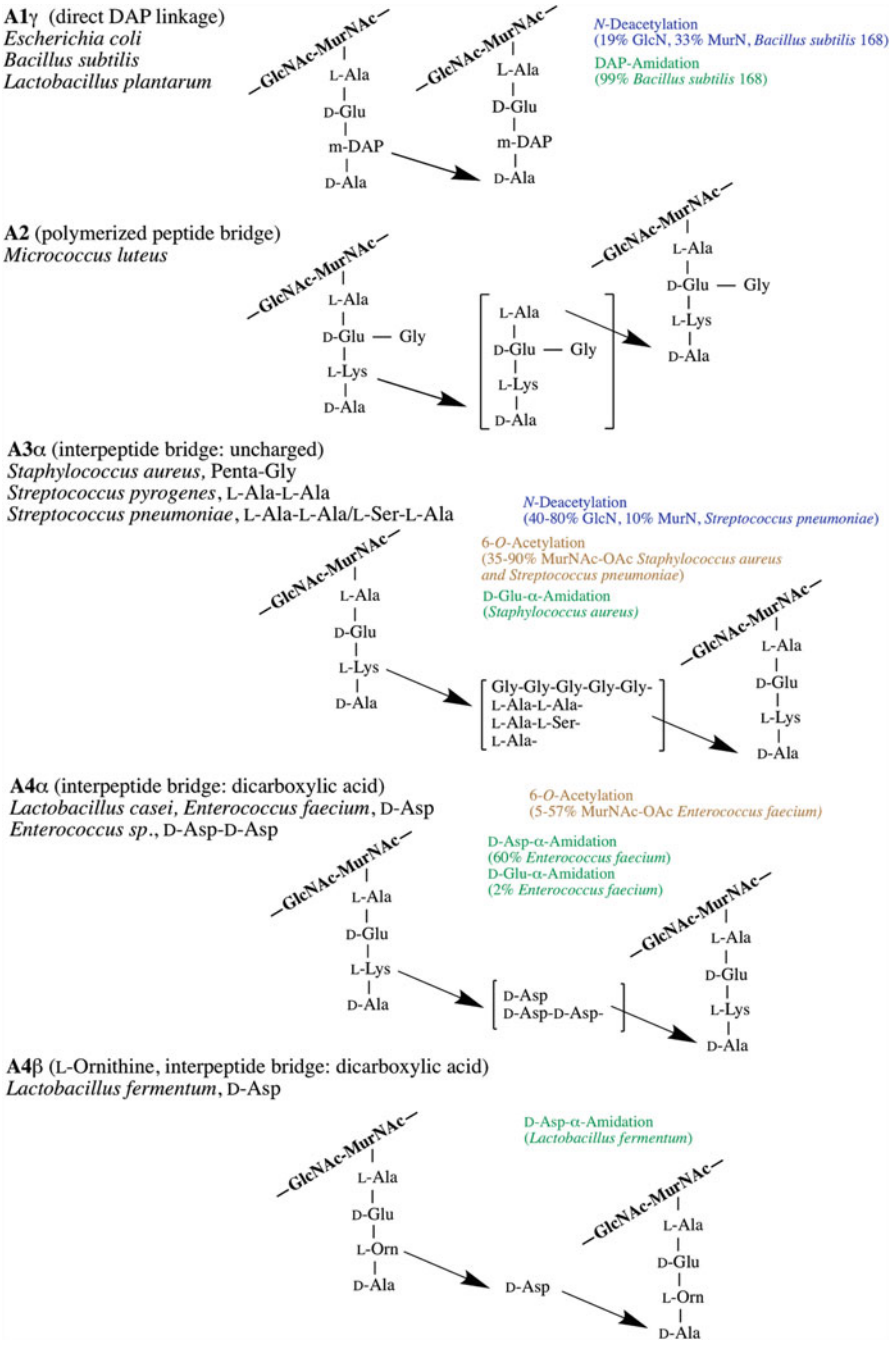

Fig. 6.10 Primary structures and cross-linkage types of PGN in different bacteria. According to Schleifer and Kandler 1972, 3–4 cross-linkages, which are the most common, are designated with the letter A. A1γ-type PGN is characterized by direct 3–4 cross-linkages involving meso-DAP and is present in *E. coli* and most other Gram-negative bacteria, as well as some bacilli (e.g., *Bacillus subtilis*, *Bacillus megaterium*, *Lactobacillus plantarum*), which however may comprise some

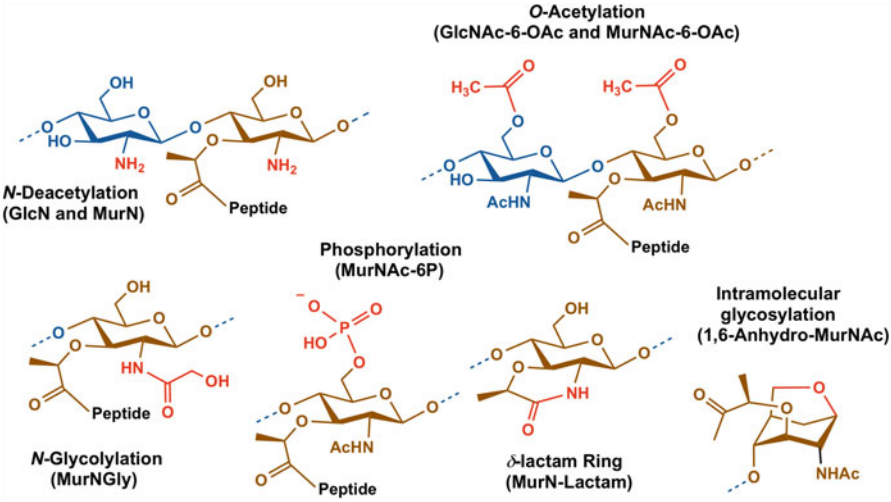

Fig. 6.11 Modifications of the PGN glycan part. The GlcNAc (blue) and/or the MurNAc (brown) within the PGN can be de-*N*-acetylated or *O*-acetylated and thereby renders resistant against PGN-glycosidases such as lysozyme. The MurNAc can be phosphorylated, which is used to covalently attach secondary cell wall polymers, such as teichoic acids. It can be *N*-glycolylated, e.g., in mycobacteria, or form a delta-lactam ring, e.g., in *Bacillus* spore PGN, or can have a 1,6-anhydro-bond, which is the product of PGN cleavage by lytic transglycosylases. Modifications are highlighted in red

(16%) and no *N*-deacetylated MurNAc (Zipperle et al. 1984; Atrih et al. 1999). *S. aureus* is characterized by a significant portion of MurNAc that is *O*-acetylated at the C-6 hydroxyl. *O*-acetylation of the GlcNAc is of only minor relevance. While all Gram-positive bacteria and most Gram-negative bacteria *O*-acetylate their PGN, the well-studied *E. coli* and *P. aeruginosa* are among the few exceptions where such modifications are absent (Moynihan et al. 2014). *N*-deacetylation and *O*-acetylation of the PGN have been implicated in PGN chain-length regulation and control of autolysins. A comprehensive survey of bacterial PGN glycan modifications can be found in Vollmer 2008 and Moynihan et al. (2014). These reviews also describe the different enzymes that catalyze these modifications. The glycan modification becomes particularly important during cell differentiations. Fig. 6.11 depicts the various observed modifications of the glycan part of the PGN. How these

Fig. 6.10 (continued) modifications such as sugar *N*-deacetylation and mDAP amidation. Three to four cross-linkages that include an interpeptide bridge can be found primarily in Gram-positive bacteria. The A2-type PGN found in *M. luteus* is characterized by stem peptide duplications; it also contains a glycine modification at position 2. A3α, A4α, and A4b types of PGN contain neutral amino acid or peptide bridges, either pentaglycine bridges as found in *Staphylococcus aureus* or L-Ala-L-Ala bridge such as in *Enterococcus faecalis*, double-charged amino acid (Asn/Asp) bridges such as in *Lactobacillus* sp. or involve D-ornitin (D-Orn) at position 3. Other possible linkage types may involve 2–4 cross-linkages (not shown)

modifications occur during *Bacillus* spore PGN synthesis will be addressed in the following section.

6.5.3 *PGN Alterations During Starvation: The* B. subtilis *Spore PGN*

Major alterations of PGN structure in most bacteria occur during differentiation under nutrient starvation. One of the most radical processes of differentiation is endospore formation in some bacteria, e.g., *Bacillus* and *Clostridium* sp. (Foster and Popham 2002; Popham 2002). Rearrangement of the vegetative PGN cell wall starts with an asymmetric cell division event, and subsequent thinning of the thick PGN of the smaller cell (the prespore or forespore) by a process called prespore engulfment. In this process, three layers of the spore wall are formed simultaneously: (1) a thin inner PGN layer adjacent to the cell membrane, known as the primordial cell wall or germ cell wall, which has the same PGN composition as the vegetative wall but its thickness is reduced (Fig. 6.12); (2) an additional membrane, covering the newly formed cell wall; and (3) a new cell wall layer, called the cortex, which is a thick PGN with a very unique structure (Fig. 6.12). In the cortex PGN, the stem peptides and the *N*-acetyl groups are removed from c. 50% of the MurNAc residues, and a special delta-lactam ring is formed in the molecule between the free carboxylic acid of the D-lactate substituent and the free amino group of the muramic acid (Fig. 6.11). Furthermore, c. 24% of the MurNAc residues contain no stem peptide that can be cross-linked but only L-Ala substitutions (Fig. 6.12). Thus, the cross-linkage of the cortex PGN is very low (cross-linkage index = 3%). The outermost layer of the spore wall is composed of the proteinous spore coat, which is most responsible for the resistant properties of the spore. During spore germination the cortex is cleaved to allow outgrowth of the spore by specialized autolytic enzymes that target the cortex PGN but keep the primordial cell wall intact.

6.5.4 *Covalent Attachments to the Peptidoglycan*

Most Gram-positive bacteria but also some Gram-negatives (e.g., cyanobacteria) are characterized by a PGN cell wall that is modified by secondary cell wall polymers (e.g., teichoic acids and capsule polysaccharides). These polymers are attached via phosphodiester bonds to the PGN, particularly to the 6-hydroxyl group of MurNAc (Fig. 6.11). The enzymatic process of transfer of the polymers to the PGN had long been enigmatic. However recently, proteins of the LCP (LytR, CpsA, Psr) family were shown to be involved in the linkage of teichoic acid, mycobacterial arabinogalactans, and capsule polysaccharides to the PGN (Kawai et al. 2011; Eberhardt et al. 2012; Chan et al. 2014; Harrison et al. 2016). Mutants lacking the

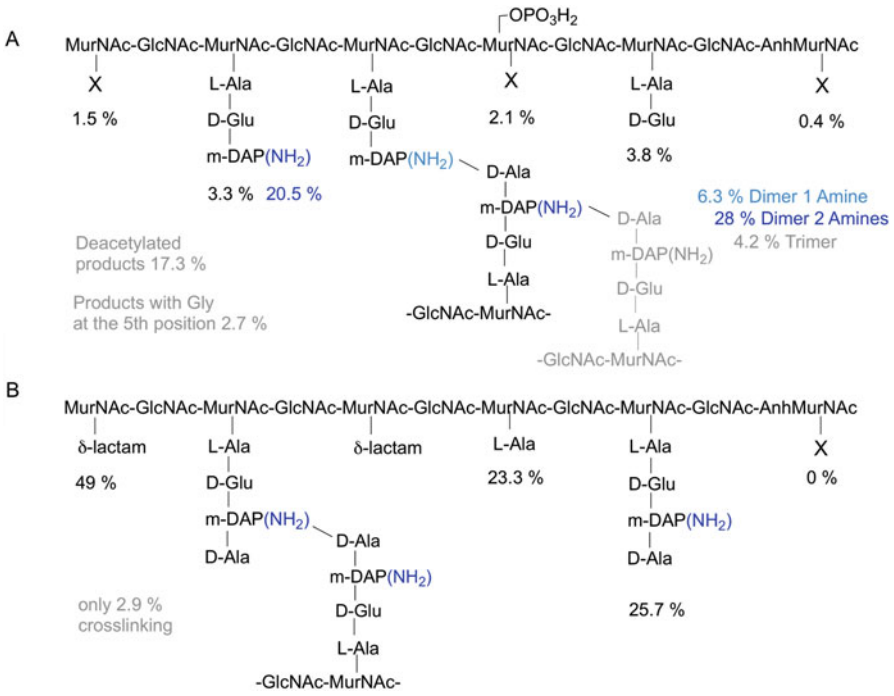

Fig. 6.12 Comparison of the structures of the *B. subtilis* PGN in the vegetative wall/primordial spore wall and in the endospore cortex. (**a**) The primordial or germ wall contains PGN that is identical to the vegetative PGN. The cross-linkage index is high (27–33%), and the main muropeptides found in cell wall analyses are shown (Atrih et al. 1999; Atrih and Foster 1999). (**b**) Profound alterations within the PGN occur in the cortex layer. The cross-linkage index of spore cortex PGN is very low (c. 3%) (Atrih et al. 1996; Atrih and Foster 1999)

LCP family proteins release wall teichoic acids into the medium, as they are preformed but cannot be attached to the PGN (Chan et al. 2013). Moreover, PGN is the anchor point for surface proteins. The covalent attachment of proteins to the PGN occurs mostly in Gram-positive bacteria, where the PGN is the outermost layer that exposes proteins and enzymes to the cell surface. The signal peptide-directed localization of proteins to the PGN is called "cell wall sorting" (Schneewind and Missiakas 2012). Secreted proteins may carry a C-terminal amino acid motif, which is the sorting signal that is cleaved by the sortase and transfers the protein to the PGN. Specific sorting signals are recognized by dedicated sortase enzymes, e.g., pilus-specific sortases. However, all Gram-positive bacteria express sortase A, a membrane-anchored transpeptidase that cleaves the C-terminal LPXTG signal peptide of proteins destined for cell wall anchoring (Mazmanian et al. 1999; Ton-That et al. 1999). Somewhat similar to the protein sorting within Gram-positives is the process by which Gram-negative bacteria connect their PGN sacculus with the outer membrane. This is crucial for Gram-negative bacteria in order to avoid the loss of

outer membrane vesicles into the medium. They carry a great number of Braun's lipoprotein (Braun and Rehn 1969; Braun (1975)). In *E. coli* approximately 10^5 lipoprotein molecules are anchored to the inner leaflet of the outer membrane by an acylated N-terminal cysteine, which is a characteristic linkage of lipoproteins, and approximately one third of them are covalently connected via the amino group of the C-terminal lysine residue of the protein to the stem peptides of the PGN via an L,D-peptide bond. *E. coli* contains five L,D-transpeptidases, which are similar to the enzymes catalyzing the PGN cross-linkage in β-lactamase-resistant strains via L,D-transpeptidation (see Fig. 6.9). In *E. coli* three of these enzymes can individually anchor of the outer membrane-bound lipoprotein to the PGN. Two other enzymes of the same family are able to generate L,D-peptide cross-linkages, connecting two m-DAPs of distinct stem peptides in the PGN (Magnet et al. 2008). The biosynthesis and connection of the Braun lipoprotein is shown in Fig. 6.13.

6.5.5 *Special Mycobacterial Peptidoglycan*

A very complex cell envelope structure is found in mycobacteria (e.g., *M. tuberculosis*), which, instead of a real outer membrane, contain a lipid layer of long-chain fatty acids (mycolic acids) and glycolipids, which is connected to a PGN-arabinogalactan heteropolymeric cell wall (Fig. 6.2c) (Raghavendra et al. 2018). Mycobacteria and other bacteria that do not respond to the Gram staining (e.g., rickettsia and spirochetes) can be stained by the acid-fast technique (Ziehl-Neelsen stain) (Vilcheze and Kremer 2017). Mycobacteria, including *M. tuberculosis*, the etiological agent of tuberculosis, are a group of bacteria characterized by a very special cell envelope structure that is distinct from the cell envelope of both Gram-negative and Gram-positive (Jankute et al. 2015) (cf. Fig. 6.2). The mycolic acids within the mycobacterial cell envelope are connected to highly branched arabinogalactan polysaccharides, which themselves are covalently bound to the PGN (Jankute et al. 2015). Additional lipoglycans (lipoarabinomannan; LAM) connected with the inner membrane and the PGN-arabinogalactan heteropolymer functionally resemble the wall and lipoteichoic acids of Gram-positives (Raghavendra et al. 2018). Although the PGN of mycobacteria is classified as the common A1y-type (Schleifer and Kandler 1972), it contains some unique features: besides MurNAc, mycobacteria as well as related actinobacteria contain *N*-glycolylmuramic acid (MurNGly) (Holt et al. 1994; Vollmer, 2008). The modification is introduced in the cytoplasm by the monooxygenase NamH (UDP-MurNAc hydroxylase), which oxidizes the acetamido group in the soluble precursor using oxygen and NADPH (Raymond et al. 2005). This modification is believed to be involved in increasing the overall strength of PGN by providing sites for hydrogen bonding, as well as in decreasing susceptibility toward lysozyme (Raymond et al. 2005). The Mur ligases of mycobacteria have a broad substrate specificity allowing to accept the *N*-glycolyl form of UDP-MurNAc-(peptides). The usual 3–4 cross-linkages between mDAP and L-Ala are predominant

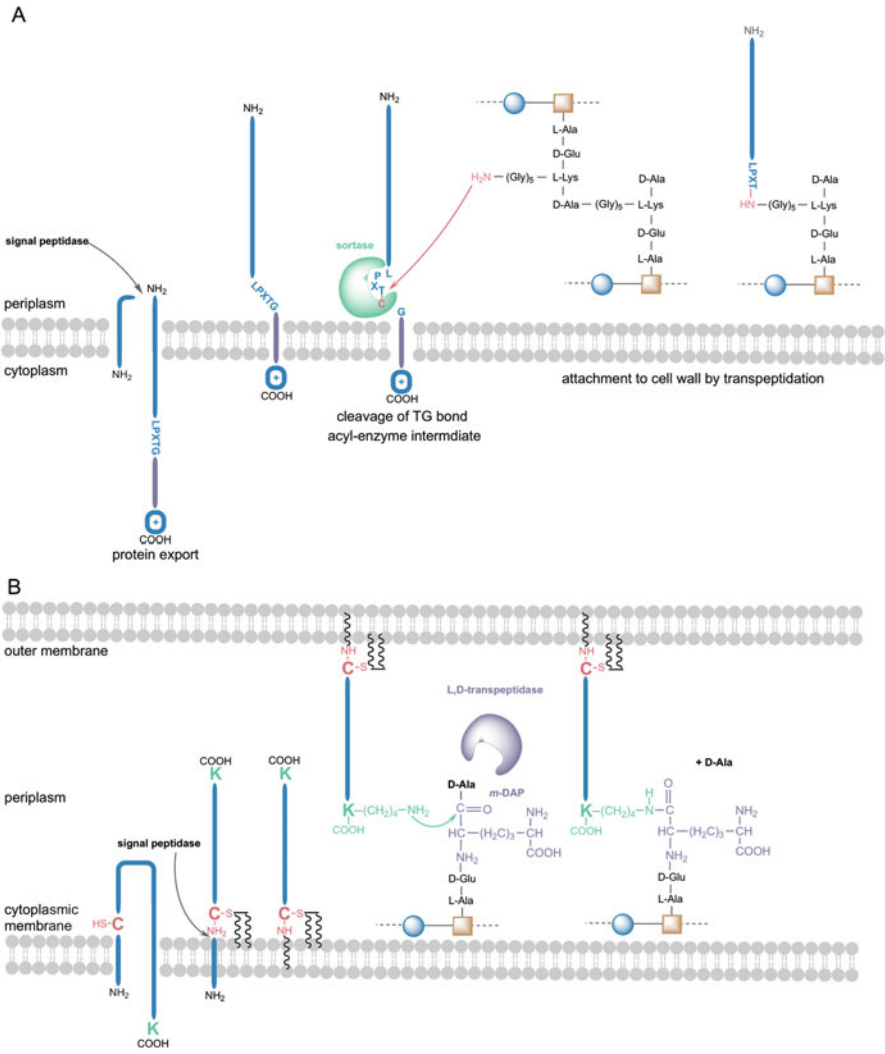

Fig. 6.13 Covalent attachment of proteins to the PGN. Linking of surface proteins by sortase enzymes (cell sorting) in Gram-positives (**a**) and attachment of Braun's lipoprotein to PGN in Gram-negatives (**b**). The proteins are synthesized in the cytoplasm as precursor polypeptides that carry an N-terminal signal sequence for the translocation through the cytoplasmic membrane via the secretion system (Sec). (**a**) Complete translocation of the polypeptide is blocked due to positively charged amino acids near the C-terminus adjacent to a hydrophobic domain (violet). Membrane-anchored sortase enzymes recognize the LPXTG amino acid motif, the sorting signal, located upstream of the hydrophobic domain of this stuck polypeptide, and cleave between the amino acids Thr and Gly. An acyl-enzyme is formed with the active site cysteine of the sortase and the threonine residue of the cleaved polypeptide. The peptidyl in then transfers from the sortase to a stem peptide within the lipid II or nascent PGN, e.g., to the pentaglycine (Gly5) in *S. aureus*. Thereby the cell wall-anchored protein is subsequently moved outward with progression of PGN synthesis. This figure was drawn based on published cartoons (Schneewind et al. 1995; Ton-That et al. 1999; Schneewind and Missiakas 2012). (**b**) The prolipoprotein is composed of 78 amino acids containing an N-terminal signal sequence and an adjacent lipobox (L,S/A,A/G,C). Signal cleavage of Braun's lipoprotein does not occur directly after secretion but only after a diacylglyceryl from

in mycobacteria. However L-Ala is often substituted by Gly, and thus mDAP-Gly crosslinkages occur and further modifications include amidation of D-Glu and DAP (Botella et al. 2017; Squeglia et al. 2018).

6.6 Compositional Analytics of Peptidoglycans

Characterization of the PGN classically involves the compositional analysis (of amino acid and amino sugars) by thin layer chromatography or gas chromatography/mass spectrometry after total or partial hydrolysis of isolated PGN with hydrochloric acid. Further analysis involves glycan chain length distribution and cross-linkage types, as well as the amount of stem-peptides undergoing cross-links (degree of cross-linkage). Characterization of a novel bacterial species, for example, necessitates the classification of the PGN-type according to Schleifer and Kandler (1972) and classification of PGN types (Ghuysen 1968; Schleifer and Kandler 1972; Litzinger and Mayer 2010) (see Sect. 6.5.1). Before conducting a PGN analysis, the sacculi need to be purified. This process of purification of intact PGN sacculi involves the instant boiling in a solution of sodium dodecyl sulfate (SDS), which simultaneously inactivates endogenic autolytic enzymes and disrupts the cell by solubilizing the membranes. Further steps involve the extensive washing to remove the SDS, which would interfere with the following enzymatic digests, and the subsequent enzymatic degradation of protein linked to the PGN, glycogen, and DNA/RNA by proteases, amylase, and nucleases, respectively (Desmarais et al. 2013; Desmarais et al. 2014). PGN purified by this procedure has a good cleanliness and can be used for compositional analyses (muropeptide analysis), which relies on a controlled enzymatic digest, generally using a lysozyme from *Streptomyces* sp., called mutanolysin or cellosyl. High-performance liquid chromatography (HPLC) is generally used to separate the muropeptide building blocks generated by chemical or enzymatic digests of isolated sacculi (Glauner 1988; Glauner et al. 1988; de Jonge et al. 1992; Atrih et al. 1999). For *E. coli*, more than 80 distinct muropeptides can be resolved by HPLC analysis, indicating an intriguing complexity of PGN chemical structure. De Pedro and Cava (2015) stressed out that even minor components of a muropeptide analytes provide significant numbers in biological terms. Complete digestion of PGN with an amidase enables the isolation of glycan strand for chain length analysis (Harz et al. 1990). Apart from radiodetection, mainly UV-detection

Fig. 6.13 (continued) phosphatidylglycerol is transferred to the SH group of the cysteine residue located within the lipobox of the protein. Thereafter, the N-terminus is cleaved, and an additional fatty acid residue is transferred to the free amino group of the cysteine. This modification is required for the recognition by the Lol system that transfers the lipoprotein to the outer membrane (Dramsi et al. 2008). After being inserted in the outer membrane, the C-terminal Lys reacts with the PGN stem peptide in a L,D-transpeptidase reaction, thereby connecting the lipoprotein with the PGN (Magnet et al. 2007b)

(200–210 nm), although not very sensitive, is generally applied for muropeptide analysis. Recently, a fast and sensitive LC-MS-based high-throughput muropeptide analysis method was reported (Kühner et al. 2014).

6.7 Peptidoglycan Biosynthesis

The synthesis of PGN in bacteria is a conserved process that can be divided into three stages occurring within different compartments. It starts in the cytoplasm with the formation of the soluble precursors, UDP-GlcNAc, UDP-MurNAc, and UDP-MurNAc-peptides (the so-called Park nucleotides). The PGN building block is then anchored to the cell membrane by transfer onto the lipid carrier, called undecaprenol-phosphate or bactoprenol-phosphate. First, MurNAc-pentapeptide from UDP-MurNAc-pentapeptide is transferred to undecaprenol-phosphate yielding lipid I (undecaprenyl-pyrophosphoryl-MurNAc-pentapeptide). Subsequently, GlcNAc is transferred from UDP-GlcNAc to lipid I to give the final substrate for PGN assembly, called lipid II (undecaprenyl-pyrophosphoryl-MurNAc-pentapeptide-GlcNAc). Lipid II is the general membrane-anchored precursor of PGN biosynthesis of bacteria that can be further modified (e.g., in *S. aureus* five glycine residues are added to the L-Lys to yield a lipid II with a pentapeptide-pentaglycine stem). The lipid II molecule is then flipped through the cell membrane, and the PGN precursors are polymerized outside of the cell by glycan synthases that are anchored within the outer leaflet of the cytoplasmic membrane. They polymerize the PGN by the action of glycosyltransferases and incorporate the newly formed PGN into the existing wall by cross-linking transpeptidases. The complete process is schematically depicted in Fig. 6.14. In the following section, the enzymatic steps of these three stages will be described in more detail. As the synthesis of PGN is unique to bacteria and mostly conserved across species but absent in humans, the pathway is an ideal target for antibiotics. Thus we will also discuss various antibiotics targeting individual steps of PGN synthesis.

6.7.1 Soluble Precursor Biosynthesis

The synthesis of the precursors UDP-GlcNAc and UDP-MurNAc, depicted in Fig. 6.15**,** starts in the cytoplasm of the bacterial cell. D-Fructose-6-phosphate (fructose-6P) derived from the glycolysis metabolic pathway is converted to D-glucosamine-6-phosphate (GlcN 6P) by the glutamine-fructose-6-phosphate-amidotransferase (GlmS) (Badet et al. 1988). The amino group originates from L-glutamine, which is hydrolyzed by the N-terminal glutaminase domain of GlmS into glutamate and ammonia; the latter is channeled to the C-terminal isomerase domain of GlmS, which conducts the isomerization and attachment of the amino group (Badet-Denisot and Badet 1992). GlmS is a critical enzyme controlling the amino

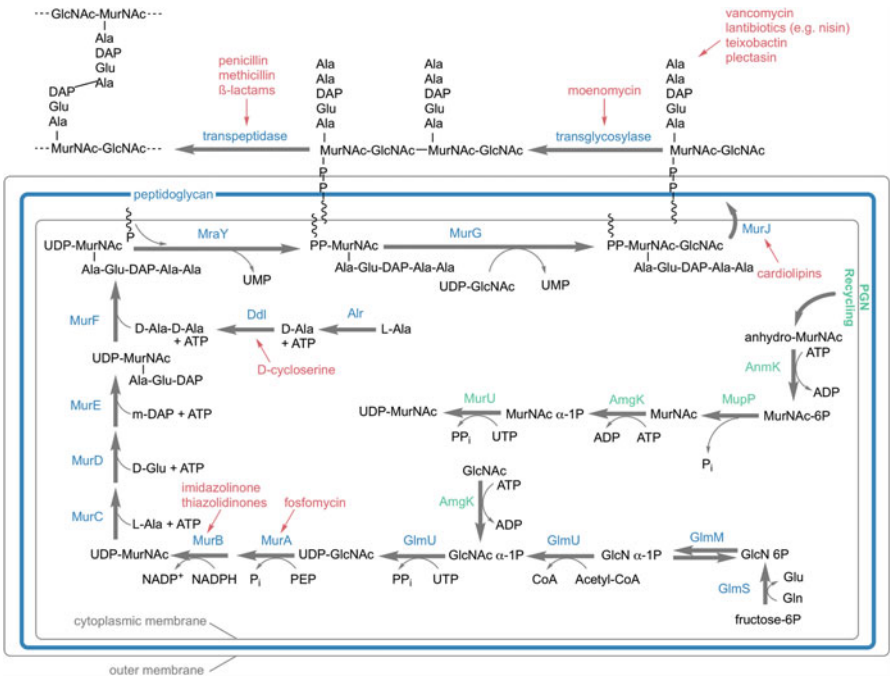

Fig. 6.14 Overview of the PGN biosynthesis occurring in three stages, within the cytoplasm, the cell membrane, and the cell wall compartment. Shown is the PGN biosynthesis pathway as it occurs in most Gram-negative bacteria and Gram-positive bacilli (blue enzymatic steps). With minor differences, the pathway also occurs in other Gram-positive bacteria or mycobacteria (for details see text). Furthermore, the recycling pathway (green enzymatic steps) as it occurs in *Pseudomonas* sp. and many other Gram-negative bacteria adds to the PGN precursor pool. Selected antibiotics inhibiting specific steps of theses pathways are indicated (red). The standard pathway (blue): GlmSMU generate UDP-GlcNAc from fructose-6P; MurA (inhibited by fosfomycin) and MurB (inhibited by imidazolinone and thiazolidinones) in a further process yield UDP-GlcNAc and UDP-MurNAc, respectively; MurCDEF successively add single amino acids forming the stem peptide; D-Ala-D-Ala is attached as a dipeptide, which is provided by Ddl (and inhibited by D-cycloserine); D-Ala is provided by the Alr racemase from L-Ala; MraY loads the MurNAc-pentapeptide onto the undecaprenyl-phosphate (undecaprenyl-P) lipid carrier, forming lipid I; and lipid II is generated by the addition of GlcNAc from UDP-GlcNAc. This is carried out by MurG, which thereby forms the β-1,4-glycosidic bond between MurNAc and GlcNAc; lipid II is subsequently flipped across the membrane by the flippase MurJ, for which cardiolipins have been found to be inhibitors; the further polymerization of lipid II in the periplasm can be inhibited by various antibiotics such as vancomycin and lantibiotics like nisin, teixobactin, and plectasin; moenomycin inhibits the transglycosylase step, whereas the transpeptidation, conducted by PBP transpeptidase domains, is inhibited by β-lactams such as methicillin and penicillin; some bacteria have developed alternative pathways for UDP-MurNAc synthesis; *Pseudomonas* (green) uses anhydro-MurNAc derived from cell wall turnover to generate UDP-MurNAc via anhydro-MurNAc kinase AnmK, MurNAc-6P phosphatase MupP, anomeric MurNAc/GlcNAc kinase AmgK, which can phosphorylate both MurNAc and GlcNAc at C1 position, and the MurNAc α-1P uridyltransferase MurU; MupP, AmgK, and MurU homologues have been identified in many Gram-negative bacteria suggesting a *Pseudomonas* like pathway (Gisin et al. 2013; Borisova et al. 2017)

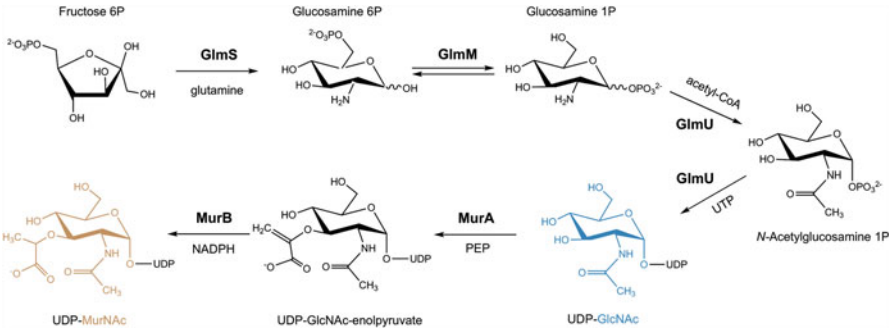

Fig. 6.15 Enzymatic steps toward the synthesis of the PGN precursors UDP-GlcNAc and UDP-MurNAc. Shown is the biosynthesis of UPD-MurNAc from fructose-6P by GlmSMU, which generates UDP-GlcNAc with an amino group derived from L-glutamine, an acetyl group derived from acetyl-CoA and UTP, and MurAB, which converts UDP-GlcNAc to UDP-MurNAc with the addition of an enolpyruvate derived from PEP followed by a reduction to form the D-lactyl residue of UDP-MurNAc

sugar metabolism and is thus delicately regulated in bacteria. In Gram-positive bacteria, a ribozyme sensing rising glucosamine-6-P levels cleaves the *glmS* mRNA, thereby repressing transcription and expression of GlmS (Winkler et al. 2004). In *E. coli* posttranscriptional regulation of *glmS* in response to GlcN 6P levels involves small regulatory RNAs (Kalamorz et al. 2007). GlcN 6P is then isomerized to α-glucosamine 1-P (GlcN α-1P) by the hexose-phosphate mutase GlmM (Mengin-Lecreulx and van Heijenoort 1996). GlmM converts GlcN 6-P to GlcN α-1P via a glucose-1,6-diphosphate intermediate. The reaction can proceed in reverse direction although at a reduced rate (Jolly et al. 1999). The next step involves the essential, bifunctional enzyme GlmU that converts GlcN α-1P to UDP-GlcNAc in a two-step process. First, it transfers an acetyl group provided by acetyl-CoA to the amino group generating α-*N*-acetylglucosamine 1-phosphate (GlcNAc α-1P), which remains bound to the enzyme. In a second step, an uridyl group from UTP is transferred to GlcNAc α-1P, while UMP and pyrophosphate (PPi) are released, and UDP-GlcNAc is generated. The first dedicated step of PGN synthesis is the formation of UDP-MurNAc from UDP-GlcNAc, and both are used directly for PGN synthesis (Gehring et al. 1996; Mengin-Lecreulx and van Heijenoort 1994). For the formation of UDP-MurNAc from UDP-GlcNAc, two steps are necessary, which are catalyzed by MurA and MurB. MurA transfers an enolpyruvyl group from phosphoenolpyruvate to the 3′ hydroxyl group of UDP-GlcNAc (Du et al. 2000). The MurA reaction proceeds through a tetrahedral intermediate of substrates, UDP-GlcNAc and phosphoenolpyruvate, followed by elimination of the phosphate to yield the enolpyruvyl product from which phosphate is released generating UDP-GlcNAc-enolpyruvate (Brown et al. 1994; Eschenburg et al. 2003; Zhu et al. 2012). The final step toward UDP-MurNAc is catalyzed by the flavoprotein MurB. FAD serves as a redox intermediate since it gets reduced by NADPH to $FADH_2$, which subsequently reduces the vinyl enol group of UDP-GlcNAc-enolpyruvate yielding

UDP-MurNAc (Benson et al. 1993; Benson et al. 1997). MurA can be inhibited by fosfomycin, an epoxide and structural analog of PEP, which covalently binds the MurA active site cysteine (Eschenburg et al. 2005). Thiazolidinones inhibit MurB by mimicking the diphosphate moiety of UDP-GlcNAc-enolpyruvate (Andres et al. 2000). Also some imidazolinone analogues that show antibacterial activity against *S. aureus* have been identified (Bronson et al. 2003). Because of their unfavorable physicochemical properties, these compounds were not further studied, and new inhibitors were not discovered for over a decade until, based on the MurB crystal structure (Chen et al. 2013), novel tetrazole inhibitors of MurB were discovered, although they do not possess in vitro antimicrobial activity against *S. aureus* or *E. coli* (Hrast et al. 2018).

To yield the final soluble PGN precursor UDP-MurNAc-pentapeptide, a pentapeptide chain needs to be attached at the lactyl residue of UDP-MurNAc. This occurs by stepwise addition of amino acids and is catalyzed by the ATP-dependent Mur ligases MurCDEF (van Heijenoort 2001; Vollmer and Bertsche 2008; Kouidmi et al. 2014). The reaction mechanism is common in all Mur ligases. The carboxyl group of UDP-MurNAc (or UDP-MurNAc-peptides) is activated by ATP resulting in an acyl phosphate intermediate and ADP. A nucleophilic attack on the amide group of the added amino acid results in an intermediate from which the phosphate group dissociates generating an amide or peptide bond (Bouhss et al. 2002). An ATP-binding consensus sequence and six invariant residues define the Mur ligases as a family of enzymes (Bouhss et al. 1997). The domain organization is similar in all Mur ligases with the UDP-precursor binding N-terminal domain, the central ATP binding domain, and the amino acid or dipeptide binding C-terminal domain (Smith 2006). L-Ala is the first amino acid added to UDP-MurNAc (Schleifer and Kandler 1972) with a stereo specificity for the L-amino acid, and D-Ala is not recognized as a substrate (Liger et al. 1995). D-Glu is the second amino acid of the peptide stem in most species (Schleifer and Kandler 1972). Although there are a variations like amidation of the α-carboxylic acid group, these modifications are introduced after incorporation of D-Glu, which is the substrate of MurD in all species (Vollmer et al. 2008a). D-Glu is provided by the glutamate racemase MurI from L-Glu in *E. coli* (Doublet et al. 1994). The third amino acid, incorporated by MurE, is in most cases either *meso*-diaminopimelic acid (*m*-DAP), such as in Gram-negatives and some bacilli, or L-Lys, such as in most Gram-positives (Schleifer and Kandler 1972; Ruane et al. 2013). MurE is highly specific for the correspondent amino acid, and false incorporation, for example, L-Lys in *E. coli*, leads to cell lysis (Mengin-Lecreulx et al. 1999). In *B. subtilis m*-DAP gets amidated by the amidotransferase AsnB. The Δ*asnB* mutant exhibits increased sensitivity to cell wall targeting antibiotics and has a disturbed balance between PGN synthesis and hydrolysis ultimately leading to cell lysis (Dajkovic et al. 2017). In *Corynebacterium glutamicum*, a *m*-DAP amidase, LtsA, has been identified as well with similar effects in the mutant such as high lysozyme and β-lactam susceptibility (Levefaudes et al. 2015). Finally, the dipeptide D-Ala-D-Ala is added by MurF, which exclusively utilizes dipeptide substrates composed of D-amino acids (Bugg and Walsh 1992). MurF is more promiscuous regarding substrates than the other Mur ligases (Anderson et al. 1996) and can also

integrate noncanonical D-amino acids such as D-Met, D-cystein, or fluorescent derivatives (see Fig. 6.17) into the PGN. D-Ala-D-Ser or D-Ala-D-Lac are used in vancomycin-resistant strains (Healy et al. 2000), for example, in *Enterococcus faecalis* via a D-Ala-D-Ser ligase (Meziane-Cherif et al. 2012). D-Ala is provided by the alanine racemases Alr and DadX (Wild et al. 1985) and used by the D-Ala-D-Ala ligase DdlA yielding the dipeptide (Zawadzke et al. 1991). The Ddl ligase can be inhibited by D-cycloserine (Batson et al. 2017). *E. coli* Mpl is a nonessential murein ligase (Mengin-Lecreulx et al. 1996) that can ligate the L-Ala-iso-D-Glu-*m*-DAP tripeptide, derived from the cell wall turnover, directly with UDP-MurNAc (Park and Uehara 2008).

6.7.2 Membrane-Bound Precursors

Lipids I and II describe undecaprenyl-pyrophosphate (undecaprenyl-PP)-bound MurNAc-pentapeptide and GlcNAc-MurNAc-pentapeptide, respectively. The first membrane associated step starts with the de novo synthesis of the C_{55}-P lipid carrier (undecaprenyl-P). UppS initially forms undecaprenyl-PP in the inner leaflet of the plasma membrane (Fujihashi et al. 2001), which is then dephosphorylated by the phosphatase UppP in the outer leaflet (Manat et al. 2014). Subsequently, the phospho-MurNAc-pentapeptide generated by the Mur ligases is loaded onto undecaprenyl-P by the membrane protein MraY, a prenyl sugar transferase (Al-Dabbagh et al. 2008) with the predicted active site in the cytoplasm and an extended hydrophobic groove which could be harboring the acyl lipid tail of the carrier (Chung et al. 2013). The antibiotic tunicamycin rearranges transmembrane helices and cytoplasmic loops of MraY thus preventing the substrate binding (Hakulinen et al. 2017). Lipid II is formed with the addition of GlcNAc by the membrane-tethered glycosyltransferase (GT) MurG (Anderson et al. 1965; Bouhss et al. 2004; van Heijenoort 2007). The MurG crystal structure revealed a common GT-B superfamily fold (Hu et al. 2003). In some Gram-positive bacteria like *S. aureus* lipid II is further modified, where five glycine residues are added to the amino group on position 3 of L-Lys (Navarre and Schneewind 1999). Also D-Glu can be amidated by the glutamine amidotransferase-like GatD and Mur ligase homologue MurT, which form a stable bi-enzyme complex. Mutants show an increased susceptibility to methicillin and are less viable (Münch et al. 2012). An antibiotic termed teixobactin was discovered by a screening of previously uncultured bacteria. It is able to bind a highly conserved motif of lipid II and even lipid III, which is the precursor for wall teichoic acids in Gram-positive bacteria. It is effective against important pathogens such as *S. aureus* and *M. tuberculosis* (Ling et al. 2015). Lipid II is also a target for the vancomycin group of glycopeptides and several lantibiotics such as nisin. The mode of action is complexation, which prevents cross-linking and incorporation into the cell wall (Bugg et al. 2011). The same mode of action has been demonstrated for the fungal defensing plectasin (Schneider et al. 2010).

After synthesis in the cytoplasm, the lipid II must be translocated across the membrane in order to get incorporated into the PGN. The translocation does not occur spontaneously. In fact, a specialized protein machinery is required for this process (van Dam et al. 2007). A candidate was identified by a reductionist bioinformatics approach suggesting MurJ (MviN) as the PGN lipid II flippase in *E. coli* (Ruiz 2008). MurJ is part of the MATE (multi-antimicrobial extrusion)-like superfamily, from which members have been shown to function as drug and sodium antiporters. MurJ-deficient cells have been shown to swell and burst (Omote et al. 2006; Inoue et al. 2008). Furthermore, the integral membrane protein FtsW of the SEDS (shape, elongation, division, and sporulation) family, which is essential in the bacterial division machinery, is able to flip lipid-linked PGN precursors across model membranes in in vitro assays (Mohammadi et al. 2011). Another hint for FtsW is that all MurJ homologues could be deleted in *B. subtilis* (Fay and Dworkin 2009) although a flippase is supposed to be essential. However, an alternative flippase, Amj, was found in *B. subtilis*. It is upregulated in the absence of MurJ via an envelope stress-response pathway (Meeske et al. 2015) and has no sequence or structural homology to MurJ (Sham et al. 2014). Another recent discovery favors MurJ as the main flippase, since variants of WzxC, a flippase involved in *E. coli* capsule (colanic acid) synthesis, were able to rescue lethal MurJ deficiency (Sham et al. 2018). MurJ can be inhibited by exogenous cardiolipins that associate with MurJ and reduce lipid II binding (Bolla et al. 2018). Furthermore, MurJ inhibitors inspired from the human microbiome, synthesized on the basis of bioinformatics predictions, have been shown to potentiate β-lactams, making the combination effective even against the infamous methicillin-resistant *S. aureus* (MRSA) and vancomycin-resistant *E. faecalis* (VRE) (Lai et al. 2017).

6.7.3 Polymerization of the Peptidoglycan Network

After the lipid II is exported, it needs to be incorporated into the existing PGN. Therefore, two types of enzymes are essential. Glycosyltransferases (GT) attach the nonreducing end of the existing PGN strand via a β-1,4-glycosidic bond to the lipid II (Lovering et al. 2007), and transpeptidases (TP) assemble the peptide cross-links (Lovering et al. 2012); both reactions are demonstrated in Fig. 6.16. Penicillin-binding proteins (PBPs), named after their susceptibility for β-lactam antibiotics, are important enzymes in this process. They can be either bifunctional GT/TP (class A, aPBPs) or monofunctional TP (class B, bPBPs). Most species possess a variety of PBPs for different conditions like growth, division, stress, and antibiotic resistance, and they are spatially and temporally regulated by protein-protein interactions (Egan et al. 2015) with activator proteins like LpoA (Sathiyamoorthy et al. 2017) and LpoB, a regulator of PBP1B (Egan et al. 2014; King et al. 2014). Even though monofunctional GT like MtgA in *E. coli* (Di Berardino et al. 1996; Vollmer and Bertsche 2008) were found, the bifunctional aPBPs were presumed to be the major GT. However, aPBPs are not the only PGN GT. It has been shown that *B. subtilis*

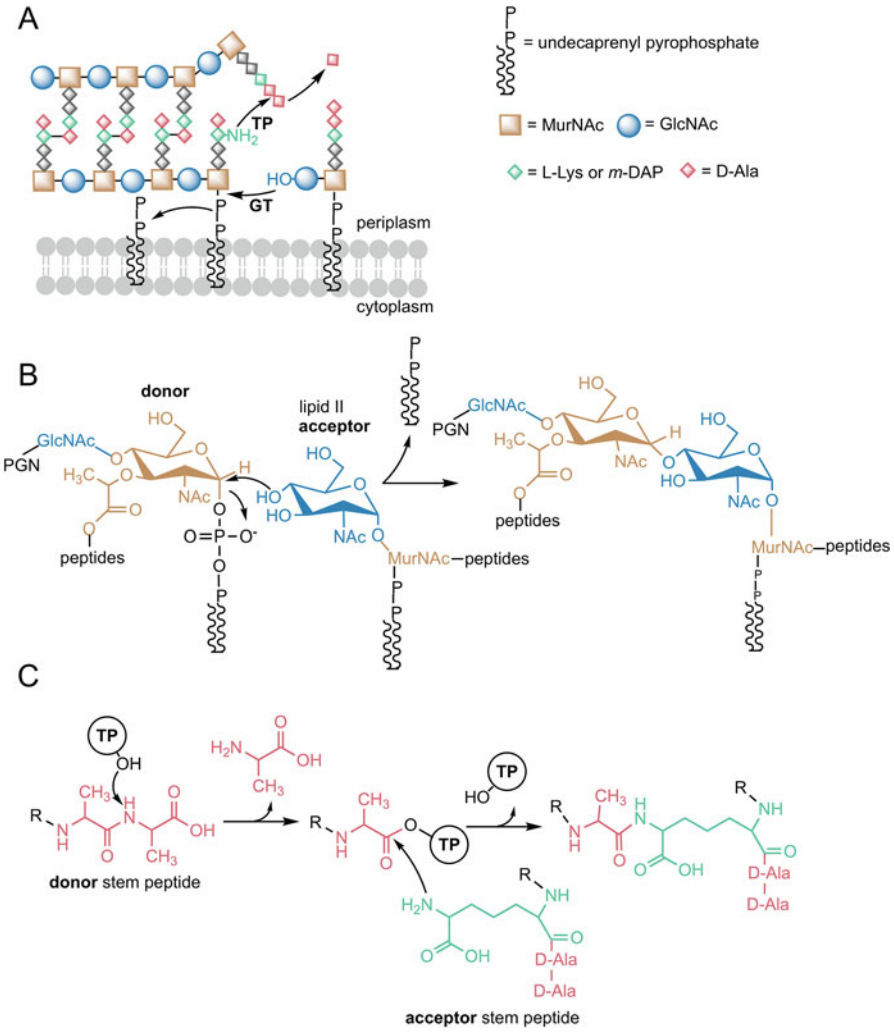

Fig. 6.16 Glycosyltransferase (GT) and transpeptidase reaction (TP). (**a**) The growing PGN chain gets transferred onto lipid II via a GT followed by peptide cross-linking between D-Ala on position 4 of the donor stem peptide L-Lys or *m*-DAP on position 3 of the acceptor stem peptide. (**b**) GT reaction in detail: the growing PGN strand is the donor for a new lipid II acceptor; the C4 hydroxyl group on the lipid II GlcNAc attacks the C1 on MurNAc of the donor releasing undecaprenyl-pyrophosphate, and a new β-1,4-glycosidic bond is formed. (**c**) TP reaction in detail: The hydroxyl group of serine in the transpeptidase attacks the peptide bond between the D-Ala-D-Ala on the donor stem peptide, releasing the terminal D-Ala and forming an enzyme substrate intermediate, which can be attacked by the free amino group of the diamino acid on position 3 of the acceptor stem peptide (in this example *m*-DAP) releasing the transpeptidase and covalently bonding the two stem peptides forming the cross-link

deficient in all aPBPs is still viable (McPherson and Popham 2003). The crucial role of SEDS (shape, elongation, division, and sporulation) family PGN polymerases has been demonstrated. The overexpression of RodA, a member of the Rod complex involved in cell elongation, can compensate aPBP deletion (Meeske et al. 2016). Also a screening with the known GT inhibitor moenomycin revealed the SEDS protein RodA as the missing GT in *B. subtilis* with a novel catalytic mechanism (van Heijenoort et al. 1987), since it was not inhibited by moenomycin (Emami et al. 2017). While RodA is necessary for cell elongation, the SEDS protein FtsW is suggested to be the GT of the divisome (Henrichfreise et al. 2016). RodA and FtsW form cognate enzyme pairs with the monofunctional PGN TP PBP2B and FtsI, making them specialized GT/TP pairs acting on their specific subcellular sites (Egan et al. 2015; van der Ploeg et al. 2015). They are also independent from the multifunctional aPBPs, which function outside of the elongasome and divisome independent from SEDS proteins (Cho et al. 2016). Instead of having one of the common GT folds (GT-A and GT-B), the murein GT of family G51 resemble lysozyme (Coutinho et al. 2003). The GT domain features an active site cleft between an α-helical head subdomain and a membrane-fixed jaw domain. Same as lysozyme, the active site cleft is occupied by six sugar moieties. Inside the jaw domain, a hydrophobic channel binds the acyl chain of lipid II (Lovering et al. 2007). After polymerization, the glycan strands can be further modified. The *O*-acetyltransferase OatA, an integral membrane protein, acetylates MurNAc at the C6 hydroxyl group conveying lysozyme resistance (Bera et al. 2005). Additionally, the C6 *O*-acetylation of GlcNAc has been described in *Lactobacillus plantarum*, which protects the cells from autolysins in a similar manner as MurNAc *O*-acetylation (Bernard et al. 2011). Also GlcNAc *N*-deacetylation by PgdA in *Streptococcus pneumonia* (Vollmer and Tomasz 2000) and MurNAc *N*-glycosylation by NamH can be observed in mycobacteria (Raymond et al. 2005).

The glycan strands polymerized by GT are incorporated into the cell wall by TP, which catalyze the cross-linking of peptide stems between adjacent glycan strands (Archibald et al. 1993; Foster and Popham 2002). The active site of TP features a catalytic serine and a general base, lysine (Goffin and Ghuysen 1998). The donor stem peptide binds non-covalently to the TP, the serine attacks the D-Ala-D-Ala peptide bond forming an acyl intermediate, and the terminal D-Ala is released. The acyl intermediate can be cross-linked with the acceptor stem peptide (McDonough et al. 2002) by a nucleophilic attack of the non-α-amino group of the dibasic amino acid (Gram-negatives and bacilli) or the last amino acid of the cross-bridge peptides (most Gram-positives) on position 3 of the acceptor stem peptide toward the C-terminus of D-Ala on position 4 of the donor stem peptide (Lovering et al. 2012; Sobhanifar et al. 2013). Even though the amino acids differ, the mechanism is conserved across species (Lupoli et al. 2011). During the reaction, undecaprenyl-PP is released and de-phosphorylated, yielding the lipid carrier bactoprenol, which is flipped back to be reused for new lipid II assembly (El Ghachi et al. 2005; van Heijenoort 2007). The enzymes with D,D-TP activity are known as PBPs, since β-lactam antibiotics like penicillin mimic the D-Ala-D-Ala dipeptide substrate (Tipper and Strominger 1965) inducing a D,D-TP active-site serine attack on the β-lactam

ring resulting in a covalent complex and impaired TP activity (Lovering et al. 2012). Some PBPs have evolved to be resistant against β-lactam antibiotics like PBP2a, which functions as an alternative to PBP2 and can be found in MRSA. The TP domain of PBP2 is rendered inactive with the TP of PBP2a being used instead (Lim and Strynadka 2002).

The 4,3-D,D-cross-links formed by the majority of transpeptidases such as PBPs can be exchanged with 3,3-L,D-cross-links under stress conditions like β-lactam antibiotics, to which L,D-TP have a much lower affinity. In *Mycobacterium* the L,D-transpeptidation is abundant even during growth without β-lactam stress (Lavollay et al. 2008). The production of the *E. coli* L,D-TP YcbB in combination with elevated ppGpp alarmone levels bypasses all D,D-TP activity and leads to broad-spectrum β-lactam resistance. YcbB uses only a tetrapeptide stem as a substrate, not a classical pentapeptide stem. D,D-carboxypeptidases like DacA are essential for subsequent L,D-TP activity, since they cleave off the D-Ala of the pentapeptide stem, providing the tetrapeptide (Hugonnet et al. 2016). Interestingly, the L,D-TP Ldt_{Mt2} of *M. tuberculosis* only cross-links stem peptides with amidated *m*-DAP, making the responsible amidotransferase AsnB an attractive target for anti-mycobacterial drugs (Ngadjeua et al. 2018).

Recently, a nifty strategy for in situ labeling of PGN with fluorescent D-amino acids (FDAAs) in combination with fluorescence microscopy has been introduced, allowing to directly visualize PGN biosynthesis within cells and to study the location of enzymes involved in cell wall deposition (Kuru et al. 2015; Hsu et al. 2017). The labeling is based on the inherent promiscuity of bacterial PBPs and L,D-TP, which, instead of catalyzing cross-linkages of PGN, performs a transpeptidation reaction that incorporate FDAAs (Fig. 6.17) (Hsu et al. 2017). The synthesis of FDAAs with different emission wavelengths spanning the entire visible spectrum (Hsu et al. 2017) (see Figs. 6.17 and 6.18) allows to add different dyes at different times to obtain a virtual time lapse labeling zones of active PGN synthesis (Fig. 6.18). This technique has emerged using an important and effective tool for studies of PGN synthesis and dynamics.

6.7.4 Peptidoglycan Deposition in Cell Walls

The different cell shapes of bacterial species require individual structural organization of the cell wall for cell growth and division. While coccoid bacteria like *S. aureus* can rely solely on PGN synthesis during cell division, rod-shaped bacteria like *E. coli* and *B. subtilis* need a synthesis machinery that is able to provide lateral cell wall growth for cell elongation. The insertion of cell wall in these rod-shaped bacteria is dispersed throughout the lateral body and mainly excludes the inert polar caps. This contrasts with the polar growth prevalent in Gram-positive *Actinomycetales*, including mycobacteria, and in Gram-negative α-proteobacteria. In these bacteria the zone of cell wall growth resides at the polar tip region. In all cases, however, bacteria need to divide, and thus, the cell wall synthesis machinery at the division site, the divisome, is widespread across bacterial species and described in detail in the next section. It uses

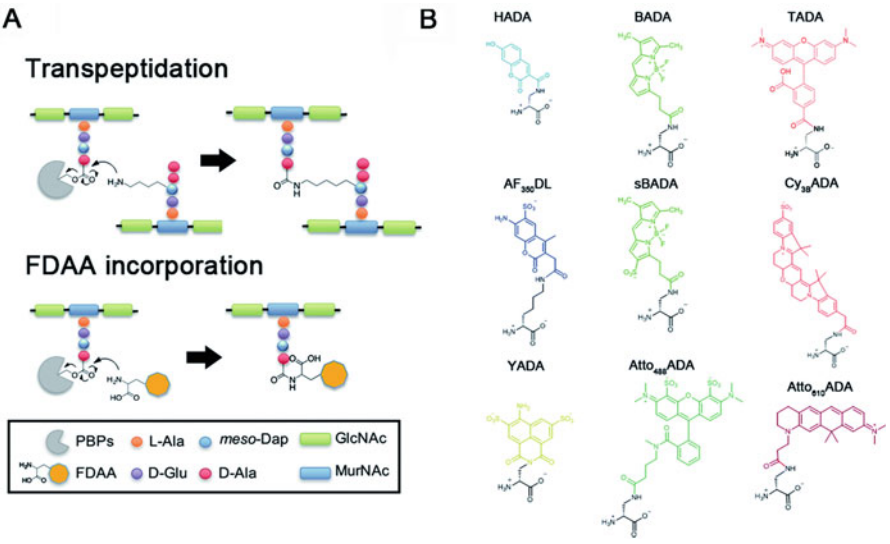

Fig. 6.17 Cell wall synthesis and labeling with fluorescent D-amino acids. (**a**) Comparison between transpeptidation (PGN cross-linking) and incorporation of FDAA, both reactions are performed by PBPs. The PBP peptide intermediate is attacked by a free amino group of *m*-DAP, resulting in cross-linking. The amino group of the fluorescently labeled lysin can attack the donor acyl group as well, resulting in FDAA incorporation. (**b**) Different fluorescence labels can enable the use of different fluorescent colors to illustrate growth dynamics. (This figure was taken from Hsu et al. (2017). Copyright (2008) National Academy of Sciences)

the protein FtsZ, a homologue to the eukaryotic tubulin, to form a contractile ring powered by its GTPase domain to constrict the cell, while new PGN is incorporated and the daughter cells are separated by hydrolases. Rod-shaped bacteria require lateral growth, for which they, among others, use a machinery named Rod complex, described in more detail in a following section. In principle the synthesis machinery circumferentially moves around the cell guided by the cytoskeleton consisting of a bacterial homologue to eukaryotic actin (such as MreB), where mature PGN is broken up by hydrolysis to incorporate a new cell wall in a "break before make"-like fashion (Zhao et al. 2017). Interestingly, some symbiotic rod-shaped bacteria, attached to their host on one cell pole, seem to divide across their longitudinal axis with their divisome spanning across the length of the cell (Pende et al. 2018). Some filamentous bacteria like *Streptomyces* grow by tip extension and initiation of new branches. The polar growth is directed by the cytoskeletal-like protein DivIVA, which acts as a polar recruitment factor to assemble the cell wall synthesis machinery named polarisome (Flärdh 2010). Recently discovered bacteria-specific factors are the bactofilins, which are polymer-forming proteins that shape elongated structures in the cell poles of *Myxococcus xanthus* and provide a scaffold for the chromosome segregation machinery (Lin et al. 2017). In the next two sections, the cell division and elongation will be discussed in more detail with a focus on the model organisms *E. coli* and *B. subtilis.*

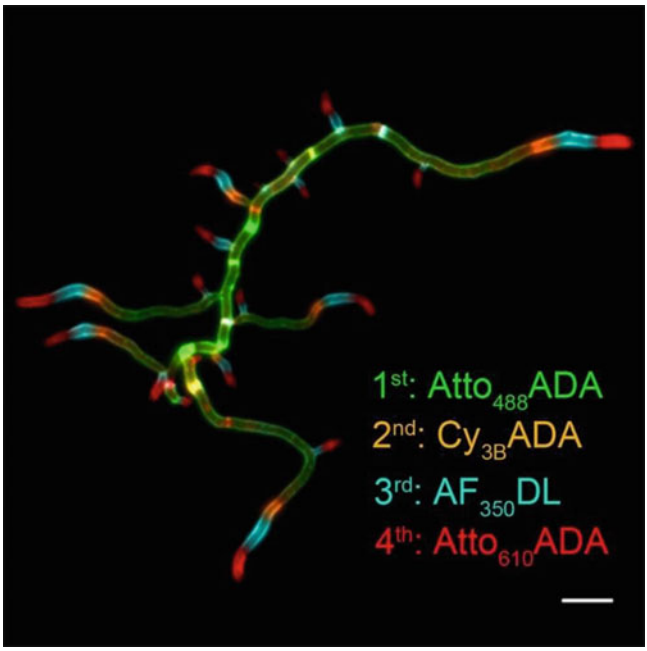

Fig. 6.18 Successive FDAA labeling in polar growing bacteria, *Streptomyces venezuelae*. This labeling method is known as virtual time-lapse labeling (Hsu et al. 2017). Labeling with different FDAA visualizes apical growth of *Streptomyces* and the formation of new branches; first labeling 3 h with $Atto_{488}$ADA (green), second labeling15 min with Cy_{3B}ADA (orange), third labeling 15 min with AF_{350}DL (cyan), and fourth labeling 15 min with $Atto_{610}$ADA (red); between every labeling step the previous FDAA were washed out. (This figure was taken from Hsu et al. (2017). Copyright (2008) National Academy of Sciences)

6.7.4.1 Cell Division

The cell division machinery is best understood in the model organisms *E. coli* and *B. subtilis*. A simplified scheme with the essential divisome components is shown in Fig. 6.19. The cell division genes in *E. coli* were discovered using thermosensitive mutants that exhibited a filamentous phenotype with cells unable to divide. Therefore, the genes were named *fts* for their filamentous temperature-sensitive phenotype (Rowlett and Margolin 2015). One of the first components discovered by immunogold labeling was FtsZ, forming a structure that is called the Z ring at the site of mid-cell division of *E. coli* (Bi and Lutkenhaus 1991). Successively, it was shown that FtsA, FtsQ, FtsW, and FtsI also localize at the division site in a FtsZ-dependent manner (Addinall and Lutkenhaus 1996; Weiss et al. 1997; Wang et al. 1998; Buddelmeijer et al. 1998). FtsN localization depends on the prior localization of FtsZ and FtsA (Small and Addinall 2003). FtsZ, the initiator of division, polymerizes at the inner face of the cytoplasmic membrane forming filaments (Michie and Lowe 2006). The Z ring anchors a dynamic multiprotein complex with structural, cell wall synthesis, and turnover proteins (Egan and Vollmer 2013). The FtsZ

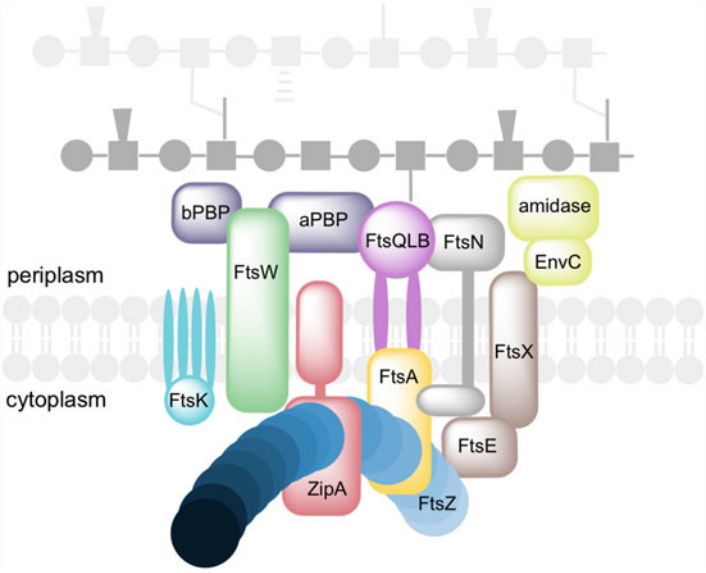

Fig. 6.19 Scheme displaying the essential divisome components. FtsZ (blue) filaments form the Z ring, which is able to contract by FtsZ GTPase activity. ZipA (red) and FtsA (yellow) anchor the Z ring to the cytoplasmic membrane. The FtsEX (brown) ATP transporter recruits EnvC (lime) to the septum, which in turn activates amidases (lime) that cleave PGN cross-links in order to separate the two daughter cells. FtsK (cyan) consists of a DNA translocase domain and four membrane-spanning segments, which might play a role in fusion of the invaginating membrane. The FtsQLB complex (purple) might function as a link between the Z ring and PGN synthesis enzymes. The role of FtsW (green) is not completely understood, being a RodA homologue TG activity is possible; however, flippase activity has been demonstrated as well. FtsW interacts with class aPBPs and bPBPs (violet). FtsN (gray) interacts with FtsQLB and FtsA initiating synthesis

filament displays a rotational, inward movement driven by its own GTPase activity. The movement coincides with the deposition of new cell wall material (Yang et al. 2017; Bisson-Filho et al. 2017). FtsZ generating its own motion, inducing cell wall synthesis in the process, might be necessary to apply enough force for cell division (Zhao et al. 2017). The two essential division proteins ZipA and FtsA interact directly with FtsZ and are required to recruit additional division proteins (Hale and de Boer 1997; Wang 1997; Pichoff 2002). ZipA possesses a N-terminal membrane-spanning domain and a C-terminal domain that binds FtsZ (Hale and de Boer 1997) and can bundle FtsZ protofilaments in vitro (Hale et al. 2000). Although FtsA, which is structurally related to eukaryotic actin, has no membrane-spanning domain, it has a conserved C-terminal amphipathic helix that targets FtsA to the membrane and to the Z ring. FtsA is much more conserved in bacteria than ZipA, suggesting it to be the main membrane anchor for the Z ring (Pichoff and Lutkenhaus 2005). After formation of the Z ring, at least nine additional proteins are recruited to this domain (Schmidt et al. 2004; Goehring and Beckwith 2005). FtsE and FtsX encode an ABC transporter homologue to the lol system in *E. coli* (Schmidt et al. 2004) with the transmembrane component FtsX and the ATPase FtsE. Interestingly, FtsEX is only

essential in low-salt media (Reddy 2007). FtsEX has been identified as a regulator of cell wall hydrolysis at the division site. Via a periplasmic loop of FtsX, EnvC is recruited to the septum. EnvC is activated by conformational changes of FtsEX, mediated by ATP hydrolysis in the cytoplasm. EnvC subsequently activates the amidase AmiB, which splits dividing cells (Yang et al. 2011). The FtsQLB enzyme complex activity is unknown; however, it seems to function as a link between the Z ring and PGN synthesis enzymes (Goehring and Beckwith 2005). FtsK consist of a DNA translocase domain and four membrane-spanning segments (Begg et al. 1995). The latter may play a role in fusing the invaginating membrane to complete cytokinesis (Fleming et al. 2010). FtsI and FtsW are orthologues of PBP2 and RodA, respectively (Typas et al. 2012), which are the major TP and TG during cell elongation as part of the Rod complex. However, FtsW has been reported to have flippase activity (Mohammadi et al. 2011), but the identification of RodA as a TG instead of a flippase suggests the same for FtsW. Moreover, both TG form cognate enzyme pairs with a TP (Henrichfreise et al. 2016). On the other hand, FtsW forms a complex with bPBP3 and aPBP1B, which as a bifunctional PBP possesses a TG domain. Intriguingly, FtsW negatively regulated aPBP1B in in vitro assay and did not exhibit TG activity in these experiments (Leclercq et al. 2017). The trigger for septation is the arrival of FtsN at the division complex (Goehring and Beckwith 2005; Gerding et al. 2009), which is a bitopic protein with a short cytoplasmic region and a large periplasmic region connected by a transmembrane domain (Dai et al. 1993). FtsN is suggested to act on both sides of the membrane inducing a conformational change in both FtsA and the FtsQLB complex de-repressing septal PGN synthesis and membrane invagination in *E. coli.* Thus, a premature start of synthesis is prevented, while the complex is not yet assembled completely (Liu et al. 2015). Cell separation is regulated differently in Gram-positive and Gram-negative bacteria (Yang et al. 2011). The septal PGN shared between the daughter cells needs to be split by hydrolases in order to complete the division (Vollmer et al. 2008b). These hydrolases need to be tightly regulated together with PGN synthesis since too much hydrolysis activity would bear the danger of cell lysis (Uehara and Bernhardt 2011). In *E. coli* the LytC-type amidases AmiA, AmiB, and AmiC are most important (Heidrich et al. 2001). The divisome-associated proteins EnvC and NlpD contain LytM domains, which usually possess endopeptidase activity against PGN cross-links (Firczuk and Bochtler 2007b). However, experiments have shown that rather than directly cleaving PGN, EnvC activates AmiA and AmiB and NlpD activates AmiC (Uehara et al. 2010). Since EnvC is activated by FtsEX, which interacts with FtsZ (Corbin et al. 2007), the amidase activation could be coupled directly with the contraction of the Z ring, enabling amidase activity only after the start of synthesis without the risk of cell lysis (Yang et al. 2011). In Gram-positive bacteria the expression of PGN hydrolase gene is controlled among others by the WalK/WalR regulon, a key player in the maintenance of cell wall homeostasis. The WalR response regulator, being phosphorylated by the WalK kinase, induces the expression of PGN hydrolases and represses the expression of their inhibitors (Dubrac et al. 2008). WalK seems to interact with components of the septal ring and needs an intact divisome in order to phosphorylate WalR (Fukushima et al. 2011). The localization

and activity of hydrolases seem to be controlled by teichoic acid distribution (Yamamoto et al. 2008; Schlag et al. 2010) as well as the acetylation status of the sugar backbone (Moynihan and Clarke 2011).

6.7.4.2 Cell Elongation

Cell elongation is conducted by a multiprotein complex (Laddomada et al. 2016; Egan et al. 2017). The essential components are depicted in Fig. 6.20. The eukaryotic actin homologue MreB, which is localized on the lateral cell wall (Jones et al. 2001), directs the spatiotemporal elongation process (van den Ent et al. 2001). A loss of MreB, which is found in most rod-shaped bacteria, leads to a reduced lateral cell wall synthesis and eventually to a loss of the rod shape. MreB localizes in areas of negative Gaussian curvature where the cell shape is dented and therefore needs strengthening. Thereby, the rod shape is initiated and maintained (Ursell et al. 2014). Interestingly, MreB orthologues have not been found in coccoid bacteria (Zapun et al. 2008). The polymerization of MreB, which happens in the presence of ATP, results in antiparallel double filaments that form a patch-like structure bound to the membrane via a

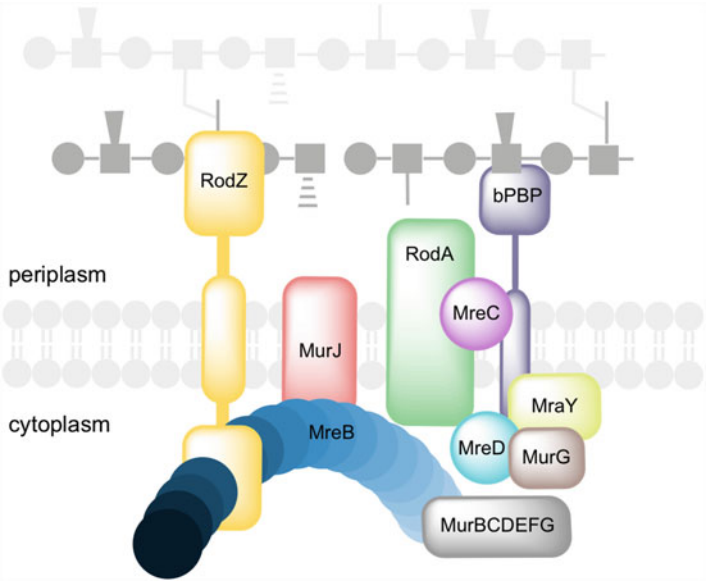

Fig. 6.20 Essential components of the Rod complex. The actin homologue MreB (blue) polymerizes in patches rotating circumferentially. RodZ (yellow) connects MreB filaments with PGN; that way PGN synthesis can drive the rotation of the Rod complex. The flippase MurJ (red) provides lipid II for the glycosyltransferase RodA (green); the peptide cross-linking is conducted by bPBPs (violet). MreC (purple) controls the spatial organization of PBPs in the periplasm. MreD (cyan) interacts with the precursor synthesis enzymes MraY (lime) and MurG (brown) as well as determining MreB location. MreB also recruits the MurBCDEF precursor synthesis enzymes (gray), providing a high amount of precursors at the Rod complex location

hydrophobic loop and N-terminal amphipathic helix (van den Ent et al. 2001; Salje et al. 2011; van den Ent et al. 2014; Errington 2015). RodZ, an integral transmembrane protein, assembles as a complex with MreB (van den Ent et al. 2010) and mediates MreB rotation by coupling MreB to the cell wall synthesis enzymes, RodA (TG) and PBP2 (TP). The rotation is required for the robustness of rod shape and growth under ~~cell wall~~ stress conditions (Morgenstein et al. 2015). This complex (MreB-RodAZ-bPBP) will be referred to as the Rod complex. Instead of forming continuous filaments, MreB rotates circumferentially around the cell in patches, the motion driven by bPBP activity and the presence of RodA. Yet at least in *E. coli*, the activity of aPBPs is not necessary (Dominguez-Escobar et al. 2011; Garner et al. 2011). Hence, the MreB movement is not driven by its own polymerization, but the periplasmic cell wall synthesis machinery, acting like a motor, pulls the MreB patches in the cytoplasm and periplasmic and cytoplasmic components connected via RodZ across the membrane (van Teeffelen et al. 2011). The location of synthesis is also coordinated by MreC, controlling the spatial orientation of the penicillin-binding proteins in the periplasm, and MreD, interacting with the precursor synthesis enzymes MurG and MraY as well as determining MreB localization. Additionally, MreB cables are required for the organization of MurBCEF (White et al. 2010) and can even recruit DapI, the enzyme required for the synthesis of *m*-DAP (Rueff et al. 2014). All in all, this leads to a concentrated precursor availability near the Rod complex. In vivo cell wall polymerase assays in *E. coli* revealed that cell wall synthesis is mediated by two distinct polymerase systems, the Rod complex and the aPBPs, the latter being active outside of the Rod complexes (Cho et al. 2016). *B. subtilis* flippase Amj can replace the *E. coli* flippase MurJ. Since Amj and MurJ are no homologues, it is unlikely for Amj to interact with either synthesis complex, suggesting that flippases work independently from both Rod complex and aPBPs (Meeske et al. 2015). RodA TG activity contributes significantly to the lateral cell wall synthesis in *E. coli* (Cho et al. 2016), but unlike in Gram-positive bacteria, where RodA is sufficient to sustain growth, the Gram-negative bacterium *Vibrio cholerae* relies on the bifunctional PBP1A during transition into stationary phase (Dörr et al. 2014). A model for a flippase providing for both RodA/bPBP and aPBP independently is shown in Fig. 6.21. PGN is a rigid molecule that needs to be broken before the insertion of new material for cell elongation (Vollmer et al. 2008b). The *B. subtilis* hydrolases LytE and CwlO are essential for cell elongation, since their inactivation blocks the process (Bisicchia et al. 2007). Both LytE, localizing at the septa, poles and the cylindrical part of the cell, and CwlO, localizing at the cylindrical part, are essential for cell proliferation and the only D,L-endopeptidases acting on the lateral cell wall. Chimeric protein assays with LytF and CwlS, which localize to the septum and hydrolyze PGN during cell division (Fukushima et al. 2006), revealed that the N-terminal domain is responsible for the localization (Hashimoto et al. 2011). Furthermore, a deletion of LytE or CwlO severely impairs transformation efficiency in *B. subtilis,* which indicates a possible role in the natural competence of *B. subtilis* (Liu et al. 2018). Remarkably, FtsX, which is known to be involved in cell division in *E. coli*, has been shown to be required for CwlO hydrolase activity during cell wall elongation in *B. subtilis* (Meisner et al. 2013; Dominguez-Cuevas et al. 2013). Prior to the incorporation of new cell wall material,

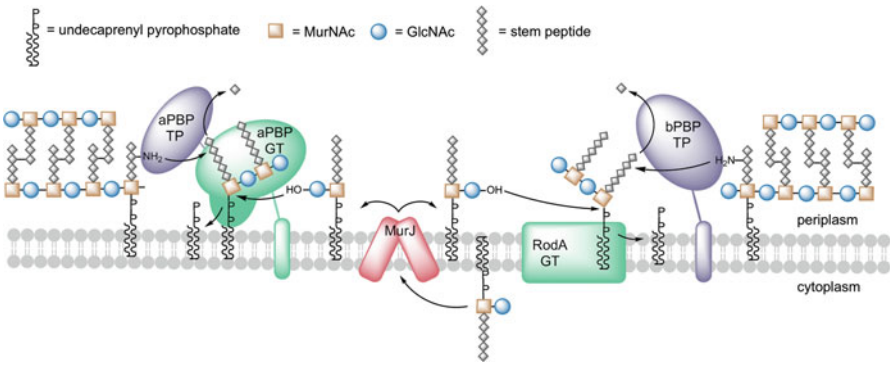

Fig. 6.21 Model for lateral cell wall synthesis by aPBPs and RodA/bPBPs during cell elongation. The MurJ flippase (red) provides lipid II for both synthesis machineries, which are either single-acting aPBPs with GT (green) and TP (violet) domains or a combination of the GT RodA (green) with bPBPs (violet) that work together as part of the Rod complex

the existing cell wall needs to be cleaved by endopeptidases (Vollmer 2012). Matching this hypothesis, MreB homologues in *B. subtilis* have been shown to direct LytE as well as CwlO (Dominguez-Cuevas et al. 2013). Based on these recent discoveries, Zhao et al. (2017) proposes a "break before make" mechanism, where endopeptidases cleave cross-links in mature PGN. Rod A then provides a template PGN strand, with the circumferentially moving Rod complex, which is attached to the sacculus by bPBPs. Subsequently, aPBPs, exhibiting a diffusive motion with prolonged persistence (Cho et al. 2016; Lee et al. 2016), generate additional strands along the template and connect them to the existing PGN (Zhao et al. 2017). However, it has also been shown in *E. coli* that endopeptidase activity increases cell wall attachment of aPBPs during bPBP2 inhibition, indicating Rod complex independent starting points of cell wall synthesis (Lai et al. 2017).

6.8 The Dynamic Cell Wall: Peptidoglycan Turnover and Recycling

The bacterial cell wall is not static but subject to constant degradation and resynthesis, in a process that is called cell wall or PGN turnover (Boothby et al. 1973; Doyle et al. 1988; Park and Uehara 2008; Reith and Mayer 2011). During cell growth (elongation), cell division, as well as various processes of adaptation, due to osmotic challenges, starvation, or exposure to antibiotics, the PGN is steadily remodeled and newly synthesized to adapt structure and shape. Thereby, the PGN is partially cleaved and renewed at a significant rate. It has been calculated that as much as 50% of cell wall material per generation is turned over (Park and Uehara 2008; Reith and Mayer 2011; Borisova et al. 2016). At the same time, old PGN is removed and degraded. Cell wall degradation and turnover are conducted by PGN hydrolases

and lytic transglycosylases (LTs), termed autolysins, as they have the potential to lyse its own cell wall (Smith et al. 2000). Thus, the PGN turnover must occur without compromising its stabilizing function in a delicately balanced manner. The tight connection between cell wall lysis and synthesis has been demonstrated by interaction of respective enzymes, stressing the significance of cell wall turnover for bacterial cell growth (Vollmer and Bertsche 2008; Egan et al. 2017). Considering the huge amounts of material, it seems reasonable that bacteria recover the released PGN fragments to save on resources. Only up to 8% of the cell wall material was found to be released to the medium in the Gram-negative bacterium *E. coli* (Goodell and Schwarz 1985); however, the major part of PGN is efficiently recycled (Goodell 1985). PGN fragments derived from the turnover process are taken up and intracellularly reused for energy metabolism or PGN de novo synthesis (Park and Uehara 2008; Johnson et al. 2013; Gisin et al. 2013). In many Gram-negative bacteria, a direct shortcut pathway exists that converts recycled amino sugars to UDP-activated PGN precursors and thus leads to intrinsic resistance to the antibiotic fosfomycin, shown in Fig. 6.15 (Gisin et al. 2013; Borisova et al. 2017). This pathway is absent in Gram-positive bacteria, but it was shown recently that *B. subtilis*, *S. aureus*, and *Streptomyces coelicolor* do recycle their PGN via a pathway that involves the use of MurNAc (Borisova et al. 2016). The following sections will briefly summarize current knowledge of the PGN turnover and recycling in the model organisms *E. coli*, *B. subtilis*, and *S. aureus.*

6.8.1 Cell Wall Hydrolases and Autolysins

Autolysins, lytic enzymes acting on the producers own cell wall, can be classified as glycosidases and amidases (Smith et al. 2000; van Heijenoort 2011). There is a specialized group of lytic enzymes for almost every bond within the bacterial cell wall (an overview is given in Fig. 6.22). The sugar backbone in general can be cleaved by exo- or endo-acting *N*-acetylglucosaminidases and *N*-acetylmuramidases (e.g., lysozyme), which target either of the two distinct glycosidic bonds within the PGN, GlcNAc-β-1,4-MurNAc or MurNAc-β-1,4-GlcNAc, respectively (Höltje 1995). A very distinct family of MurNAc-β-1,4-GlcNAc-cleaving enzymes are the lytic transglycosylases (LTs), which, unlike lysozyme and other muramidases, do not hydrolyze this bond. Instead they cleave the glycosidic bond by an intramolecular attack of the 6-hydroxyl group, thereby generating an 1,6-anhydro bond at the MurNAc residue (Scheurwater et al. 2008). By the action of lytic transglycosylases, anhydro-muropeptides (GlcNAc-anhydro-MurNAc-peptides) are released. They are subsequently recovered by a specific transporter and further reused in a process called cell wall or PGN recycling (Park and Uehara 2008). *E. coli* has a soluble Slt70 LT as well as the membrane-bound MltA, B, C, D, E, and F LTs, which are anchored in the outer membrane facing the periplasm with their catalytic domains. MtlA and MtlB are exoenzymes that cut from the reducing end of the glycan chain (Vollmer and Bertsche 2008; Scheurwater et al. 2008). *B. subtilis* has the Slt70 homologues,

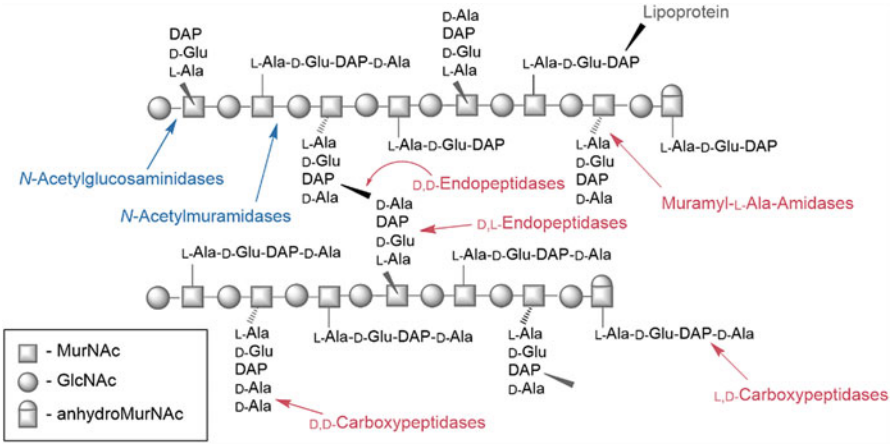

Fig. 6.22 Cleavage sites within the PGN sugar backbone PGN hydrolases, potential autolysins. *N*-acetylglucosaminidases and *N*-acetylmuramidases (blue) cleave the glycosidic bond between GlcNAc-MurNAc and MurNAc-GlcNAc, respectively. For every peptide bond within the cross-link, specialized enzymes can be found with often redundant function (red). In general, the cleavage of five different bonds is possible. The amide bond between the lactyl residue of MurNAc and L-Ala can be cleaved by muramyl-L-Ala-amidases. D,D-Endopeptidases cleave D,D-peptide bonds, e.g., between *m*-DAP and D-Ala and between cross-linked stem peptides, whereas D,L-endopeptidases cleave D,L-bonds like D-Glu-DAP. Carboxypeptidases cleave uncross-linked stem peptides between D-Ala-D-Ala (D,D-carboxypeptidases) or *m*-DAP-D-Ala (L,D-carboxypeptidases). This figures was modified after (Mayer 2012)

CwlP and CwlQ, the latter being a bifunctional enzyme with muramidase and lytic transglycosylase activity. The major autolysins during vegetative growth, however, are the *N*-acetylglucosaminidases LytD and LytG (Smith et al. 2000; Horsburgh et al. 2003; Sudiarta et al. 2010). PGN amidases are abundant and diverse with more than several enzymes for each amide linkage. This redundancy emphasizes their crucial function, since a bacterial cell cannot for instance afford their inhibition by antibiotics. Amidases can be classified by their mode of action into metallo-, serine- and cysteine-amidases and further discriminated into nine different fold groups (Firczuk and Bochtler 2007a). Metal-dependent amidases, the structurally most diverse group, represent five- out of the ninefolds. They all feature a single Zn^{2+} in their active site with the exception of the *B. subtilis* D,D-aminopeptidase DppA, which has two Zn^{2+} and cleaves the D-Ala-D-Ala peptide bond (Cheggour et al. 2000; Remaut et al. 2001). In *E. coli*, the penicillin-insensitive D,L-endopeptidase MepA (Marcyjaniak et al. 2004) and D,D-endopeptidase MpaA (Uehara and Park 2003) are examples of metallo amidases. Representative of the cysteine amidases are classified within the L,D-transpeptidases (Ldt) family, some of them acting as transpeptidases rather than amidases under physiological conditions (Magnet et al. 2007a). Serine amidases can be categorized into a L,D-carboxypeptidase and β-lactamase type (Firczuk and Bochtler 2007a). LdcA of *E. coli* belongs to the former type and is involved in PGN recycling in the cytoplasm (Templin et al. 1999).

Some β-lactamase-type members possess β-lactamase or transpeptidase rather than hydrolase activities (Scheffers and Pinho 2005). The *E. coli* PBP4 and PBP5 both have D-Ala-D-Ala carboxypeptidase activity, while PBP4 has an additional D-Ala-*m*-DAP-endopeptidase activity (Nicholas et al. 2003; Kishida et al. 2006). The membrane-associated PBP7 lacks carboxypeptidase activity and has D,D-endopeptidase activity instead that hydrolyzes the D-Ala-*m*-DAP cross-link (Romeis and Höltje 1994). The reaction mechanism of serine amidases is similar to the transpeptidation reaction with the hydroxyl group of serine attacking the amide bond and the formation of an acyl intermediate (Firczuk and Bochtler 2007a). The main four zinc-dependent Muramyl-L-Ala-amidases in *E. coli*, AmiABCD, are crucial for cell growth and separation. AmiA, B, and C deletion mutants grow in long chains unable to separate at the division site (Heidrich et al. 2001). While AmiA, B, and C are soluble enzymes in the periplasm, AmiD is an outer membrane-anchored lipoprotein (Pennartz et al. 2009). In *B. subtilis,* CwlB and CwlC possess muramyl-L-Ala-amidase function and are required for mother cell lysis during sporulation (Shida et al. 2000, 2001). The four D,L-endopeptidases LytE, LytF, CwlO, and CwlS are involved in cell morphology maintenance with varied roles in cell elongation and separation (Hashimoto et al. 2018).

6.8.2 Peptidoglycan Turnover, Scavenging, and Recycling

The turnover of PGN components in Gram-positive and Gram-negative bacteria, and the enzymes involved in this process, is summarized in Fig. 6.23. During PGN turnover in Gram-negative bacteria, the major fragments released by lytic transglycosylases and amidases are GlcNAc-anhydro-MurNAc-peptides (muropeptides) and small peptides. While the latter are small and may easily diffuse through the outer membrane, the former are mostly trapped within the periplasm, from which they have to be recovered for reutilization. In *E. coli*, the PGN-derived peptides (tri- and tetrapeptides) are taken up by the oligopeptide ABC-transporter Opp, which requires the periplasmic binding protein MppA to collect the peptides (Park 1993; Park et al. 1998). The muropeptides are almost exclusively taken up by the AmpG permease (Cheng and Park 2002; Park and Uehara 2008). Moreover, MurNAc and GlcNAc can be taken up by sugar-specific PTS transporters (Dahl et al. 2004). Muropeptides are processed intracellularly by the β-*N*-acetylglucosaminidase NagZ that cleaves off GlcNAc (Vötsch and Templin 2000; Cheng et al. 2000) and the anhydro-MurNAc-L-Ala amidase AmpD, which is highly specific for anhydro-muropeptides leaving the UDP-MurNAc-pentapeptide cell wall precursor intact (Jacobs et al. 1995). The L,D-carboxypeptidase LdcA cleaves the terminal D-Ala off the tetrapeptide, releasing the tripeptide L-Ala-D-Glu-*m*-DAP (Templin et al. 1999). The tripeptide is attached to UDP-MurNAc by the murein peptide ligase Mpl, thereby bypassing the de novo PGN biosynthesis enzymes MurCDE (Mengin-Lecreulx et al. 1996). Mpl is also able to transfer the "wrong" tetrapeptide, but this is a fatal reaction as it obviates the addition D-Ala-D-Ala by MurF (Templin et al.

1999). Anhydro-MurNAc can be further converted into MurNAc 6P by the AnmK kinase, and GlcNAc is phosphorylated by NagK (Uehara and Park 2004; Uehara et al. 2005). The etherase MurQ generates GlcNAc 6P from MurNAc 6P by cleavage of the lactyl residue. GlcNAc 6P can then be further degraded to fructose-6P by NagA and NagB and used in glycolysis or directed into PGN de

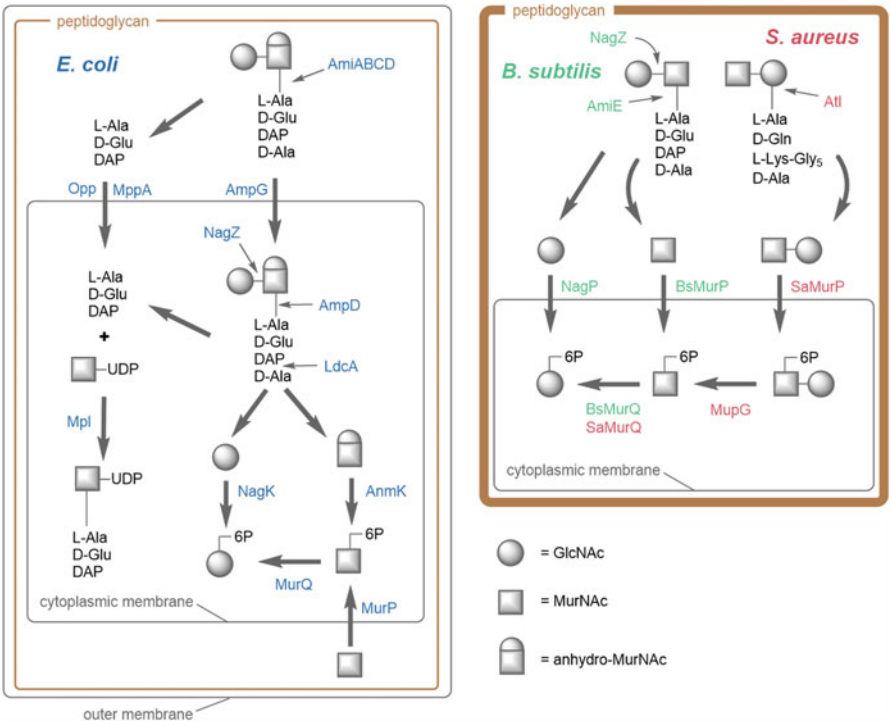

Fig. 6.23 PGN recycling in *E. coli*, *B. subtilis*, and *S. aureus*. *E. coli* PGN recycling metabolism (left panel; blue) involves the AmpG permease that transports anhydro-muropeptides derived from turnover into the cell; Opp transports tripeptides with the help of the periplasmic binding protein MppA; the anhydro-muropeptide is further processed intracellularly: NagZ cleaves off GlcNAc, which gets phosphorylated by NagK; AmpD cleaves of the stem peptide, from which D-Ala gets released by LdcA, and the tripeptide can be transferred onto UDP-MurNAc for new PGN synthesis; anhydro-MurNAc is phosphorylated by AnmK, and the lactyl residue is removed by MurQ yielding GlcNAc-6P, which can be channeled into either de novo PGN synthesis or catabolism; the phosphotransferase system PTS transporter MurP takes up and concomitantly phosphorylates MurNAc, generating MurNAc-6P. Both *B. subtilis* (right; green) and *S. aureus* (right; red) carry a MurQ orthologue (BsMurQ, SaMurQ, respectively). In *B. subtilis*, the major turnover products are processed outside of the cell by NagZ, which releases GlcNAc, and AmiE, which cuts off the peptide stem from MurNAc; MurNAc and GlcNAc are transported into the cell and phosphorylated by the individual PTS transporter MurP and NagP, respectively; intracellularly MurNAc-6P can be converted into GlcNAc-6P followed by de novo PGN synthesis or catabolism, similar to *E. coli*. In *S. aureus* the major autolysin Atl, a bifunctional amidase and *N*-acetylglucosaminidase, releases the disaccharide MurNAc-GlcNAc from the PGN. The PTS transporter SaMurP takes up this disaccharide and phosphorylates it yielding MurNAc-6P-GlcNAc, which is subsequently cleaved by a MurNAc-6P-glycosidase (MupG) and MurNAc-6P etherase (MurQ) (Kluj et al. 2018)

novo synthesis (Jaeger et al. 2005; Uehara et al. 2006). In *B. subtilis*, most of the recycling happens extracellularly followed by the uptake of the released products into the cell by specialized transporters. Most of the related genes are located in a putative MurNAc uptake and recovery pathway operon orthologous to *E. coli* (Reith and Mayer 2011). The *B. subtilis* NagZ, an orthologue to the *E. coli N*-acetylglucosaminidase, is secreted and acts on GlcNAc-MurNAc-peptide fragments, releasing GlcNAc and MurNAc-peptides, the substrate of AmiE, which cleaves the peptides from MurNAc (Litzinger et al. 2010). GlcNAc and MurNAc, released extracellularly, are taken up by the PTS transporters NagP and BsMurP, respectively, phosphorylating their substrates at C6 in the process (Reizer et al. 1988). The *B. subtilis* MurQ orthologue YbbI converts MurNAc 6P to GlcNAc 6P from which it can be utilized as a carbon source or redirected into de novo PGN biosynthesis similar to *E. coli* (Reith and Mayer 2011). Recently, a novel deviation of this pathway was recognized in *S. aureus*. The *S. aureus* PTS-transporter SaMurP, besides MurNAc, can transport and concomitantly phosphorylate MurNAc-GlcNAc, the product of PGN cleavage by Atl, the major autolysin of *S. aureus* (Kluj et al. 2018). Intracellularly, the MurNAc-6-phosphate-GlcNAc product is hydrolyzed by a novel 6-phosphomuramidase named MupG (Kluj et al. 2018).

6.9 Concluding Remarks

Research on PGN has attained a tremendous revival in the last years. It has long been considered as a completed field, yet actually nothing is farther from truth. New technologies have provided us with a surprisingly complex view of PGN structure, a stunning richness in variations of its composition, and intriguing new insights in its biosynthesis and assembly. As different as bacteria themselves, the PGN of each species has its own particularity. Thus, PGN has turned into a fascinating biological asset for advanced research, as well as for pharmaceutical strategies to develop antibacterial drugs,

Acknowledgments CM thanks Marina and Florian Alexander for their support to finish up this manuscript.

References

Addinall SG, Lutkenhaus J (1996) FtsA is localized to the septum in an FtsZ-dependent manner. J Bacteriol 178:7167–7172

Al-Dabbagh B, Henry X, El Ghachi M, Auger G, Blanot D, Parquet C, Mengin-Lecreulx D, Bouhss A (2008) Active site mapping of MraY, a member of the polyprenyl-phosphate *N*-acetylhexosamine 1-phosphate transferase superfamily, catalyzing the first membrane step of peptidoglycan biosynthesis. Biochemistry 47:8919–8928

Anderson JS, Matsuhashi M, Haskin MA, Strominger JL (1965) Lipid-phosphoacetylmuramyl-pentapeptide and lipid-phosphodisaccharide-pentapeptide: presumed membrane transport intermediates in cell wall synthesis. Proc Natl Acad Sci USA 53:881–889

Anderson MS, Eveland SS, Onishi HR, Pompliano DL (1996) Kinetic mechanism of the *Escherichia coli* UDPMurNAc-tripeptide D-alanyl- D-alanine-adding enzyme: use of a glutathione S-transferase fusion. Biochemistry 35:16264–16269

Andres CJ, Bronson JJ, D'Andrea SV, Deshpande MS, Falk PJ, Grant-Young KA, Harte WE, Ho HT, Misco PF, Robertson JG, Stock D, Sun Y, Walsh AW (2000) 4-Thiazolidinones: novel inhibitors of the bacterial enzyme MurB. Bioorg Med Chem Lett 10:715–717

Araki Y, Nakatani T, Hayashi H, Ito E (1971) Occurrence of non-*N*-substituted glucosamine residues in lysozyme-resistant peptidoglycan from *Bacillus cereus* cell walls. Biochem Biophys Res Commun 42:691–697

Archibald AR, Hancock IC, Harwood CR (1993) Cell wall structure, synthesis, and turnover. In: Sonenshein AL, Hoch JA, Losick R (eds) *Bacillus subtilis* and other Gram-positive bacteria: Biochemistry, physiology, and molecular genetics. ASM press, Washington, DC, pp 381–410

Arnoldi M, Fritz M, Bauerlein E, Radmacher M, Sackmann E, Boulbitch A (2000) Bacterial turgor pressure can be measured by atomic force microscopy. Phys Rev E Stat Phys Plasmas Fluids Relat Interdiscip Topics 62:1034–1044

Atrih A, Foster SJ (1999) The role of peptidoglycan structure and structural dynamics during endospore dormancy and germination. Antonie Van Leeuwenhoek 75:299–307

Atrih A, Zöllner P, Allmaier G, Foster SJ (1996) Structural analysis of *Bacillus subtilis* 168 endospore peptidoglycan and its role during differentiation. J Bacteriol 178:6173–6183

Atrih A, Bacher G, Allmaier G, Williamson MP, Foster SJ (1999) Analysis of peptidoglycan structure from vegetative cells of *Bacillus subtilis* 168 and role of PBP 5 in peptidoglycan maturation. J Bacteriol 181:3956–3966

Badet B, Vermoote P, Le Goffic F (1988) Glucosamine synthetase from *Escherichia coli*: kinetic mechanism and inhibition by *N*3-fumaroyl-L-2,3-diaminopropionic derivatives. Biochemistry 27:2282–2287

Badet-Denisot MA, Badet B (1992) Chemical modification of glucosamine-6-phosphate synthase by diethyl pyrocarbonate: evidence of histidine requirement for enzymatic activity. Arch Biochem Biophys 292:475–478

Bartholomew JW, Mittwer T (1952) The Gram stain. Bacteriol Rev 16:1–29

Batson S, de Chiara C, Majce V, Lloyd AJ, Gobec S, Rea D, Fulop V, Thoroughgood CW, Simmons KJ, Dowson CG, Fishwick CWG, de Carvalho LPS, Roper DI (2017) Inhibition of D-Ala:D-Ala ligase through a phosphorylated form of the antibiotic D-cycloserine. Nat Commun 8(1):1939. https://doi.org/10.1038/s41467-017-02118-7

Begg KJ, Dewar SJ, Donachie WD (1995) A new *Escherichia coli* cell division gene, *ftsK*. J Bacteriol 177:6211–6222

Benson TE, Marquardt JL, Marquardt AC, Etzkorn FA, Walsh CT (1993) Overexpression, purification, and mechanistic study of UDP-N-acetylenolpyruvylglucosamine reductase. Biochemistry 32:2024–2030

Benson TE, Walsh CT, Massey V (1997) Kinetic characterization of wild-type and S229A mutant MurB: evidence for the role of Ser 229 as a general acid. Biochemistry 36:796–805

Bera A, Herbert S, Jakob A, Vollmer W, Götz F (2005) Why are pathogenic staphylococci so lysozyme resistant? The peptidoglycan *O*-acetyltransferase OatA is the major determinant for lysozyme resistance of *Staphylococcus aureus*. Mol Microbiol 55:778–787

Bernard E, Rolain T, Courtin P, Guillot A, Langella P, Hols P, Chapot-Chartier MP (2011) Characterization of *O*-acetylation of *N*-acetylglucosamine: a novel structural variation of bacterial peptidoglycan. J Biol Chem 286:23950–23958

Bi EF, Lutkenhaus J (1991) FtsZ ring structure associated with division in *Escherichia coli*. Nature 354:161–164

Bisicchia P, Noone D, Lioliou E, Howell A, Quigley S, Jensen T, Jarmer H, Devine KM (2007) The essential YycFG two-component system controls cell wall metabolism in *Bacillus subtilis*. Mol Microbiol 65:180–200

Bisson-Filho AW, Hsu YP, Squyres GR, Kuru E, Wu F, Jukes C, Sun Y, Dekker C, Holden S, VanNieuwenhze MS, Brun YV, Garner EC (2017) Treadmilling by FtsZ filaments drives peptidoglycan synthesis and bacterial cell division. Science 355:739–743

Bolla JR, Sauer JB, Wu D, Mehmood S, Allison TM, Robinson CV (2018) Direct observation of the influence of cardiolipin and antibiotics on lipid II binding to MurJ. Nat Chem 10:363–371

Boneca IG, Chiosis G (2003) Vancomycin resistance: occurrence, mechanisms and strategies to combat it. Expert Opin Ther Targets 7:311–328

Boneca IG, Huang ZH, Gage DA, Tomasz A (2000) Characterization of *Staphylococcus aureus* cell wall glycan strands, evidence for a new β-*N*-acetylglucosaminidase activity. J Biol Chem 275:9910–9918

Boothby D, Daneo-Moore L, Higgins ML, Coyette J, Shockman GD (1973) Turnover of bacterial cell wall peptidoglycans. J Biol Chem 248:2161–2169

Borisova M, Gaupp R, Duckworth A, Schneider A, Dalugge D, Mühleck M, Deubel D, Unsleber S, Yu W, Muth G, Bischoff M, Götz F, Mayer C (2016) Peptidoglycan recycling in gram-positive bacteria is crucial for survival in stationary phase. MBio 7(5):e00923–e00916. https://doi.org/10.1128/mBio.00923-16

Borisova M, Gisin J, Mayer C (2017) The *N*-acetylmuramic acid 6-phosphate phosphatase MupP completes the *Pseudomonas* peptidoglycan recycling pathway leading to intrinsic fosfomycin resistance. MBio 8(2). https://doi.org/10.1128/mBio.00092-17

Botella H, Yang G, Ouerfelli O, Ehrt S, Nathan CF, Vaubourgeix J (2017) Distinct spatiotemporal dynamics of peptidoglycan synthesis between *Mycobacterium smegmatis* and *Mycobacterium tuberculosis*. mBio, 8(5). https://doi.org/10.1128/mBio.01183-17

Bouhss A, Mengin-Lecreulx D, Blanot D, van Heijenoort J, Parquet C (1997) Invariant amino acids in the Mur peptide synthetases of bacterial peptidoglycan synthesis and their modification by site-directed mutagenesis in the UDP-MurNAc:L-alanine ligase from *Escherichia coli*. Biochemistry 36:11556–11563

Bouhss A, Dementin S, van Heijenoort J, Parquet C, Blanot D (2002) MurC and MurD synthetases of peptidoglycan biosynthesis: borohydride trapping of acyl-phosphate intermediates. Methods Enzymol 354:189–196

Bouhss A, Crouvoisier M, Blanot D, Mengin-Lecreulx D (2004) Purification and characterization of the bacterial MraY translocase catalyzing the first membrane step of peptidoglycan biosynthesis. J Biol Chem 279:29974–29980

Braun V (1975) Covalent lipoprotein from the outer membrane of *Escherichia coli*. Biochim Biophys Acta 415:335–377

Braun V (2015) Bacterial cell wall research in Tubingen: a brief historical account. Int J Med Microbiol 305:178–182

Braun V, Rehn K (1969) Chemical characterization, spatial distribution and function of a lipoprotein (murein-lipoprotein) of the *E. coli* cell wall. The specific effect of trypsin on the membrane structure. Eur J Biochem 10:426–438

Braun V, Gnirke H, Henning U, Rehn K (1973) Model for the structure of the shape-maintaining layer of the *Escherichia coli* cell envelope. J Bacteriol 114:1264–1270

Brennan PJ, Nikaido H (1995) The envelope of mycobacteria. Annu Rev Biochem 64:29–63

Bronson JJ, DenBleyker KL, Falk PJ, Mate RA, Ho HT, Pucci MJ, Snyder LB (2003) Discovery of the first antibacterial small molecule inhibitors of MurB. Bioorg Med Chem Lett 13:873–875

Brown ED, Marquardt JL, Lee JP, Walsh CT, Anderson KS (1994) Detection and characterization of a phospholactoyl-enzyme adduct in the reaction catalyzed by UDP-N-acetylglucosamine enolpyruvoyl transferase, MurZ. Biochemistry 33:10638–10645

Buddelmeijer N, Aarsman ME, Kolk AH, Vicente M, Nanninga N (1998) Localization of cell division protein FtsQ by immunofluorescence microscopy in dividing and nondividing cells of *Escherichia coli*. J Bacteriol 180:6107–6116

Bugg TD, Walsh CT (1992) Intracellular steps of bacterial cell wall peptidoglycan biosynthesis: enzymology, antibiotics, and antibiotic resistance. Nat Prod Rep 9:199–215

Bugg TD, Braddick D, Dowson CG, Roper DI (2011) Bacterial cell wall assembly: still an attractive antibacterial target. Trends Biotechnol 29:167–173

Burge RE, Adams R, Balyuzi HH, Reaveley DA (1977a) Structure of the peptidoglycan of bacterial cell walls. II J Mol Biol 117:955–974

Burge RE, Fowler AG, Reaveley DA (1977b) Structure of the peptidoglycan of bacterial cell walls. I J Mol Biol 117:927–953

Cabeen MT, Jacobs-Wagner C (2007) Skin and bones: the bacterial cytoskeleton, cell wall, and cell morphogenesis. J Cell Biol 179:381–387

Chan YG, Frankel MB, Dengler V, Schneewind O, Missiakas D (2013) *Staphylococcus aureus* mutants lacking the LytR-CpsA-Psr family of enzymes release cell wall teichoic acids into the extracellular medium. J Bacteriol 195:4650–4659

Chan YG, Kim HK, Schneewind O, Missiakas D (2014) The capsular polysaccharide of *Staphylococcus aureus* is attached to peptidoglycan by the LytR-CpsA-Psr (LCP) family of enzymes. J Biol Chem 289:15680–15690

Chapman GB, Hillier J (1953) Electron microscopy of ultra-thin sections of bacteria I. Cellular division in *Bacillus cereus*. J Bacteriol 66:362–373

Cheggour A, Fanuel L, Duez C, Joris B, Bouillenne F, Devreese B, Van Driessche G, Van Beeumen J, Frere JM, Goffin C (2000) The *dppA* gene of *Bacillus subtilis* encodes a new D-aminopeptidase. Mol Microbiol 38:504–513

Chen S, McDowall A, Dobro MJ, Briegel A, Ladinsky M, Shi J, Tocheva EI, Beeby M, Pilhofer M, Ding HJ, Li Z, Gan L, Morris DM, Jensen GJ (2010) Electron cryotomography of bacterial cells. J Vis Exp: JoVE 39. https://doi.org/10.3791/1943

Chen MW, Lohkamp B, Schnell R, Lescar J, Schneider G (2013) Substrate channel flexibility in *Pseudomonas aeruginosa* MurB accommodates two distinct substrates. PLoS One 8(6):e66936

Cheng Q, Park JT (2002) Substrate specificity of the AmpG permease required for recycling of cell wall anhydro-muropeptides. J Bacteriol 184:6434–6436

Cheng Q, Li H, Merdek K, Park JT (2000) Molecular characterization of the β-*N*-acetylglucosaminidase of *Escherichia coli* and its role in cell wall recycling. J Bacteriol 182:4836–4840

Cho H, Wivagg CN, Kapoor M, Barry Z, Rohs PD, Suh H, Marto JA, Garner EC, Bernhardt TG (2016) Bacterial cell wall biogenesis is mediated by SEDS and PBP polymerase families functioning semi-autonomously. Nat Microbiol:16172. https://doi.org/10.1038/nmicrobiol.2016.172

Chung BC, Zhao J, Gillespie RA, Kwon DY, Guan Z, Hong J, Zhou P, Lee SY (2013) Crystal structure of MraY, an essential membrane enzyme for bacterial cell wall synthesis. Science 341:1012–1016

Corbin BD, Wang Y, Beuria TK, Margolin W (2007) Interaction between cell division proteins FtsE and FtsZ. J Bacteriol 189:3026–3035

Coutinho PM, Deleury E, Davies GJ, Henrissat B (2003) An evolving hierarchical family classification for glycosyltransferases. J Mol Biol 328:307–317

Cremniter J, Mainardi JL, Josseaume N, Quincampoix JC, Dubost L, Hugonnet JE, Marie A, Gutmann L, Rice LB, Arthur M (2006) Novel mechanism of resistance to glycopeptide antibiotics in *Enterococcus faecium*. J Biol Chem 281:32254–32262

Dahl U, Jaeger T, Nguyen BT, Sattler JM, Mayer C (2004) Identification of a phosphotransferase system of *Escherichia coli* required for growth on *N*-acetylmuramic acid. J Bacteriol 186:2385–2392

Dai K, Xu Y, Lutkenhaus J (1993) Cloning and characterization of *ftsN*, an essential cell division gene in *Escherichia coli* isolated as a multicopy suppressor of *fts*A12(Ts). J Bacteriol 175:3790–3797

Dajkovic A, Tesson B, Chauhan S, Courtin P, Keary R, Flores P, Marliere C, Filipe SR, Chapot-Chartier MP, Carballido-Lopez R (2017) Hydrolysis of peptidoglycan is modulated by

amidation of meso-diaminopimelic acid and Mg(2+) in *Bacillus subtilis*. Mol Microbiol 104:972–988

de Jonge BL, Chang YS, Gage D, Tomasz A (1992) Peptidoglycan composition of a highly methicillin-resistant *Staphylococcus aureus* strain. The role of penicillin binding protein 2A. J Biol Chem 267:11248–11254

de Pedro MA, Cava F (2015) Structural constraints and dynamics of bacterial cell wall architecture. Front Microbiol 6:449. https://doi.org/10.3389/fmicb.2015.00449

De Petris S (1967) Ultrastructure of the cell wall of *Escherichia coli* and chemical nature of its constituent layers. J Ultrastruct Res 19:45–83

Desmarais SM, De Pedro MA, Cava F, Huang KC (2013) Peptidoglycan at its peaks: how chromatographic analyses can reveal bacterial cell wall structure and assembly. Mol Microbiol 89:1–13

Desmarais SM, Cava F, de Pedro MA, Huang KC (2014) Isolation and preparation of bacterial cell walls for compositional analysis by ultra performance liquid chromatography. J Vis Exp: JoVE 83:e51183. https://doi.org/10.3791/51183

Di Berardino M, Dijkstra A, Stuber D, Keck W, Gubler M (1996) The monofunctional glycosyltransferase of *Escherichia coli* is a member of a new class of peptidoglycan-synthesising enzymes. FEBS Lett 392:184–188

Dmitriev BA, Ehlers S, Rietschel ET (1999) Layered murein revisited: a fundamentally new concept of bacterial cell wall structure, biogenesis and function. Med Microbiol Immunol 187:173–181

Dmitriev BA, Ehlers S, Rietschel ET, Brennan PJ (2000) Molecular mechanics of the mycobacterial cell wall: from horizontal layers to vertical scaffolds. Int J Med Microbiol 290:251–258

Dmitriev BA, Toukach FV, Schaper K-J, Holst O, Rietschel ET, Ehlers S (2003) Tertiary structure of bacterial murein: the scaffold model. J Bacteriol 185:3458–3468

Dmitriev BA, Toukach FV, Holst O, Rietschel ET, Ehlers S (2004) Tertiary structure of *Staphylococcus aureus* cell wall murein. J Bacteriol 186:7141–7148

Dmitriev B, Toukach F, Ehlers S (2005) Towards a comprehensive view of the bacterial cell wall. Trends Microbiol 13:569–574

Dominguez-Cuevas P, Porcelli I, Daniel RA, Errington J (2013) Differentiated roles for MreB-actin isologues and autolytic enzymes in *Bacillus subtilis* morphogenesis. Mol Microbiol 89:1084–1098

Dominguez-Escobar J, Chastanet A, Crevenna AH, Fromion V, Wedlich-Soldner R, Carballido-Lopez R (2011) Processive movement of MreB-associated cell wall biosynthetic complexes in bacteria. Science 333:225–228

Dörr T, Lam H, Alvarez L, Cava F, Davis BM, Waldor MK (2014) A novel peptidoglycan binding protein crucial for PBP1A-mediated cell wall biogenesis in Vibrio cholerae. PLoS Genet 10(6): e1004433

Doublet P, van Heijenoort J, Mengin-Lecreulx D (1994) The glutamate racemase activity from *Escherichia coli* is regulated by peptidoglycan precursor UDP-N-acetylmuramoyl-L-alanine. Biochemistry 33:5285–5290

Doyle RJ, Chaloupka J, Vinter V (1988) Turnover of cell walls in microorganisms. Microbiol Rev 52:554–567

Dramsi S, Magnet S, Davison S, Arthur M (2008) Covalent attachment of proteins to peptidoglycan. FEMS Microbiol Rev 32:307–320

Du W, Brown JR, Sylvester DR, Huang J, Chalker AF, So CY, Holmes DJ, Payne DJ, Wallis NG (2000) Two active forms of UDP-N-acetylglucosamine enolpyruvyl transferase in gram-positive bacteria. J Bacteriol 182:4146–4152

Dubrac S, Bisicchia P, Devine KM, Msadek T (2008) A matter of life and death: cell wall homeostasis and the WalKR (YycGF) essential signal transduction pathway. Mol Microbiol 70:1307–1322

Eberhardt A, Hoyland CN, Vollmer D, Bisle S, Cleverley RM, Johnsborg O, Havarstein LS, Lewis RJ, Vollmer W (2012) Attachment of capsular polysaccharide to the cell wall in *Streptococcus pneumoniae*. Microb Drug Resist 18:240–255

Egan AJ, Vollmer W (2013) The physiology of bacterial cell division. Ann N Y Acad Sci 1277:8–28

Egan AJ, Jean NL, Koumoutsi A, Bougault CM, Biboy J, Sassine J, Solovyova AS, Breukink E, Typas A, Vollmer W, Simorre JP (2014) Outer-membrane lipoprotein LpoB spans the periplasm to stimulate the peptidoglycan synthase PBP1B. Proc Natl Acad Sci USA 111:8197–8202

Egan AJ, Biboy J, van't Veer I, Breukink E, Vollmer W (2015) Activities and regulation of peptidoglycan synthases. Philos Trans R Soc Lond Ser B Biol Sci 370(1679). https://doi.org/10.1098/rstb.2015.0031

Egan AJ, Cleverley RM, Peters K, Lewis RJ, Vollmer W (2017) Regulation of bacterial cell wall growth. FEBS J 284:851–867

El Ghachi M, Derbise A, Bouhss A, Mengin-Lecreulx D (2005) Identification of multiple genes encoding membrane proteins with undecaprenyl pyrophosphate phosphatase (UppP) activity in *Escherichia coli*. J Biol Chem 280:18689–18695

Emami K, Guyet A, Kawai Y, Devi J, Wu LJ, Allenby N, Daniel RA, Errington J (2017) RodA as the missing glycosyltransferase in *Bacillus subtilis* and antibiotic discovery for the peptidoglycan polymerase pathway. Nat Microbiol 2:16253. https://doi.org/10.1038/nmicrobiol.2016.253

Errington J (2015) Bacterial morphogenesis and the enigmatic MreB helix. Nat Rev Microbiol 13:241–248

Errington J, Mickiewicz K, Kawai Y, Wu LJ (2016) L-form bacteria, chronic diseases and the origins of life. Philos Trans R Soc Lond Ser B Biol Sci 371(1707). https://doi.org/10.1098/rstb.2015.0494

Eschenburg S, Kabsch W, Healy ML, Schönbrunn E (2003) A new view of the mechanisms of UDP-N-acetylglucosamine enolpyruvyl transferase (MurA) and 5-enolpyruvylshikimate-3-phosphate synthase (AroA) derived from X-ray structures of their tetrahedral reaction intermediate states. J Biol Chem 278:49215–49222

Eschenburg S, Priestman M, Schönbrunn E (2005) Evidence that the fosfomycin target Cys115 in UDP-*N*-acetylglucosamine enolpyruvyl transferase (MurA) is essential for product release. J Biol Chem 280:3757–3763

Fay A, Dworkin J (2009) *Bacillus subtilis* homologs of MviN (MurJ), the putative *Escherichia coli* lipid II flippase, are not essential for growth. J Bacteriol 191:6020–6028

Fink G, Szewczak-Harris A, Löwe J (2016) SnapShot: The Bacterial Cytoskeleton. Cell 166:522–522. e521. https://doi.org/10.1016/j.cell.2016.06.057

Firczuk M, Bochtler M (2007a) Folds and activities of peptidoglycan amidases. FEMS Microbiol Rev 31:676–691

Firczuk M, Bochtler M (2007b) Mutational analysis of peptidoglycan amidase MepA. Biochemistry 46(1):120–128

Flärdh K (2010) Cell polarity and the control of apical growth in *Streptomyces*. Curr Opin Microbiol 13:758–765

Fleming A (1955) The story of penicillin. Bull Georgetown Univ Med Cent 8:128–132

Fleming TC, Shin JY, Lee SH, Becker E, Huang KC, Bustamante C, Pogliano K (2010) Dynamic SpoIIIE assembly mediates septal membrane fission during *Bacillus subtilis* sporulation. Genes Dev 24:1160–1172

Formanek H, Rauscher R (1979) Electron diffraction studies of the peptidoglycan of bacterial cell walls. Ultramicroscopy 3:337–342

Foster SJ, Popham DL (2002) Structure and synthesis of cell wall, spore cortex, teichoic acids, S-layers, and capsules. In: Sonenshein AL, Hoch JA, Losick R (eds) *Bacillus subtilis* and its closest relatives: From genes to cells. ASM Press, Washington, DC, pp 21–41

Fujihashi M, Zhang YW, Higuchi Y, Li XY, Koyama T, Miki K (2001) Crystal structure of cis-prenyl chain elongating enzyme, undecaprenyl diphosphate synthase. Proc Natl Acad Sci USA 9:4337–4342

Fukushima T, Afkham A, Kurosawa S, Tanabe T, Yamamoto H, Sekiguchi J (2006) A new D, L-endopeptidase gene product, YojL (renamed CwlS), plays a role in cell separation with LytE and LytF in *Bacillus subtilis*. J Bacteriol 188:5541–5550

Fukushima T, Furihata I, Emmins R, Daniel RA, Hoch JA, Szurmant H (2011) A role for the essential YycG sensor histidine kinase in sensing cell division. Mol Microbiol 79:503–522

Gan L, Chen S, Jensen GJ (2008) Molecular organization of Gram-negative peptidoglycan. Proc Natl Acad Sci USA 105:18953–18957

Garner EC, Bernard R, Wang W, Zhuang X, Rudner DZ, Mitchison T (2011) Coupled, circumferential motions of the cell wall synthesis machinery and MreB filaments in *B. subtilis*. Science 333:222–225

Geddes A (2008) 80th Anniversary of the discovery of penicillin: An appreciation of Sir Alexander Fleming. Int J Antimicrob Agents 32(5):373. https://doi.org/10.1016/j.ijantimicag.2008.06.001

Gehring AM, Lees WJ, Mindiola DJ, Walsh CT, Brown ED (1996) Acetyltransfer precedes uridylyltransfer in the formation of UDP-N-acetylglucosamine in separable active sites of the bifunctional GlmU protein of *Escherichia coli*. Biochemistry 35:579–585

Gerding MA, Liu B, Bendezu FO, Hale CA, Bernhardt TG, de Boer PA (2009) Self-enhanced accumulation of FtsN at division sites and roles for other proteins with a SPOR domain (DamX, DedD, and RlpA) in *Escherichia coli* cell constriction. J Bacteriol 191:7383–7401

Gerstmans H, Rodriguez-Rubio L, Lavigne R, Briers Y (2016) From endolysins to Artilysin(R)s: novel enzyme-based approaches to kill drug-resistant bacteria. Biochem Soc Trans 44:123–128

Ghuysen JM (1968) Use of bacteriolytic enzymes in determination of wall structure and their role in cell metabolism. Bacteriol Rev 32:425–464

Gisin J, Schneider A, Nägele B, Borisova M, Mayer C (2013) A cell wall recycling shortcut that bypasses peptidoglycan *de novo* biosynthesis. Nat Chem Biol 9:491–493

Glauner B (1988) Separation and quantification of muropeptides with high-performance liquid chromatography. Anal Biochem 172:451–464

Glauner B, Höltje JV, Schwarz U (1988) The composition of the murein of *Escherichia coli*. J Biol Chem 263:10088–10095

Goehring NW, Beckwith J (2005) Diverse paths to midcell: assembly of the bacterial cell division machinery. Curr Biol 15:R514–R526

Goffin C, Ghuysen JM (1998) Multimodular penicillin-binding proteins: an enigmatic family of orthologs and paralogs. Microbiol Mol Biol Rev 62:1079–1093

Goodell EW (1985) Recycling of murein by *Escherichia coli*. J Bacteriol 163:305–310

Goodell EW, Schwarz U (1985) Release of cell wall peptides into culture medium by exponentially growing *Escherichia coli*. J Bacteriol 162:391–397

Gram H (1884) The differential staining of Schizomycetes in tissue sections and in dried preparations. Fortschr Med 2:185–189

Hakulinen JK, Hering J, Branden G, Chen H, Snijder A, Ek M, Johansson P (2017) MraY-antibiotic complex reveals details of tunicamycin mode of action. Nat Chem Biol 13:265–267

Hale CA, de Boer PA (1997) Direct binding of FtsZ to ZipA, an essential component of the septal ring structure that mediates cell division in *E. coli*. Cell 88:175–185

Hale CA, Rhee AC, de Boer PA (2000) ZipA-induced bundling of FtsZ polymers mediated by an interaction between C-terminal domains. J Bacteriol 182:5153–5166

Harris JR (2015) Transmission electron microscopy in molecular structural biology: a historical survey. Arch Biochem Biophys 581:3–18

Harrison J, Lloyd G, Joe M, Lowary TL, Reynolds E, Walters-Morgan H, Bhatt A, Lovering A, Besra GS, Alderwick LJ (2016) Lcp1 Is a phosphotransferase responsible for ligating arabinogalactan to peptidoglycan in *Mycobacterium tuberculosis*. mBio 7(4). https://doi.org/10.1128/mBio.00972-16

Hartmann E, Konig H (1994) A novel pathway of peptide biosynthesis found in methanogenic Archaea. Arch Microbiol 162:430–432

Harz H, Burgdorf K, Höltje JV (1990) Isolation and separation of the glycan strands from murein of *Escherichia coli* by reversed-phase high-performance liquid chromatography. Anal Biochem 190:120–128

Hashimoto M, Ooiwa S, Sekiguchi J (2011) Synthetic lethality of the *lytE cwlO* genotype in *Bacillus subtilis* is caused by lack of D,L-endopeptidase activity at the lateral cell wall. J Bacteriol 194:796–803

Hashimoto M, Matsushima H, Suparthana IP, Ogasawara H, Yamamoto H, Teng C, Sekiguchi J (2018) Digestion of peptidoglycan near the cross-link is necessary for the growth of *Bacillus subtilis*. Microbiology 164:299–307

Hayhurst EJ, Kailas L, Hobbs JK, Foster SJ (2008) Cell wall peptidoglycan architecture in *Bacillus subtilis*. Proc Natl Acad Sci USA 105:14603–14608

Healy VL, Lessard IA, Roper DI, Knox JR, Walsh CT (2000) Vancomycin resistance in enterococci: reprogramming of the D-ala-D-Ala ligases in bacterial peptidoglycan biosynthesis. Chem Biol 7:R109–R119

Heidrich C, Templin MF, Ursinus A, Merdanovic M, Berger J, Schwarz H, de Pedro MA, Höltje JV (2001) Involvement of *N*-acetylmuramyl-L-alanine amidases in cell separation and antibiotic-induced autolysis of *Escherichia coli*. Mol Microbiol 41:167–178

Henrichfreise B, Brunke M, Viollier PH (2016) Bacterial surfaces: the wall that SEDS built. Curr Biol 26:R1158–R1160

Hobot JA, Carlemalm E, Villiger W, Kellenberger E (1984) Periplasmic gel: new concept resulting from the reinvestigation of bacterial cell envelope ultrastructure by new methods. J Bacteriol 160:143–152

Hoiczyk E, Hansel A (2000) Cyanobacterial cell walls: news from an unusual prokaryotic envelope. J Bacteriol 182:1191–1199

Holt JG, Krieg NR, Sneath PHA, Staley JT, Williams ST (1994) Bergey's manual of determinative bacteriology, 9th edn. Williams and Wilkins, Philadelphia

Höltje J-V (1995) From growth to autolysis: the murein hydrolases in *Escherichia coli*. Arch Microbiol 164:243–254

Höltje JV (1998) Growth of the stress-bearing and shape-maintaining murein sacculus of *Escherichia coli*. Microbiol Mol Biol Rev 62:181–203

Horsburgh GJ, Atrih A, Williamson MP, Foster SJ (2003) LytG of *Bacillus subtilis* is a novel peptidoglycan hydrolase: the major active glucosaminidase. Biochemistry 42:257–264

Hrast M, Jukic M, Patin D, Tod J, Dowson CG, Roper DI, Barreteau H, Gobec S (2018) *In silico* identification, synthesis and biological evaluation of novel tetrazole inhibitors of MurB. Chem Biol Drug Des 91:1101–1112

Hsu YP, Rittichier J, Kuru E, Yablonowski J, Pasciak E, Tekkam S, Hall E, Murphy B, Lee TK, Garner EC, Huang KC, Brun YV, VanNieuwenhze MS (2017) Full color palette of fluorescent D-amino acids for in situ labeling of bacterial cell walls. Chem Sci 8:6313–6321

Hu Y, Chen L, Ha S, Gross B, Falcone B, Walker D, Mokhtarzadeh M, Walker S (2003) Crystal structure of the MurG:UDP-GlcNAc complex reveals common structural principles of a superfamily of glycosyltransferases. Proc Natl Acad Sci USA 100:845–849

Hugonnet JE, Mengin-Lecreulx D, Monton A, den Blaauwen T, Carbonnelle E, Veckerle C, Brun YV, van Nieuwenhze M, Bouchier C, Tu K, Rice LB, Arthur M (2016) Factors essential for L, D-transpeptidase-mediated peptidoglycan cross-linking and β-lactam resistance in *Escherichia coli*. Elife:5. https://doi.org/10.7554/eLife.19469

Inoue A, Murata Y, Takahashi H, Tsuji N, Fujisaki S, Kato JI (2008) Involvement of an essential gene, *mviN*, in murein synthesis in *Escherichia coli*. J Bacteriol 190:7298–7301

Jacobs C, Joris B, Jamin M, Klarsov K, Van Beeumen J, Mengin-Lecreulx D, van Heijenoort J, Park JT, Normark S, Frere JM (1995) AmpD, essential for both β-lactamase regulation and cell wall recycling, is a novel cytosolic *N*-acetylmuramyl-L-alanine amidase. Mol Microbiol 15:553–559

Jaeger T, Arsic M, Mayer C (2005) Scission of the lactyl ether bond of *N*-acetylmuramic acid by *Escherichia coli* "etherase". J Biol Chem 280:30100–30106

Jankute M, Cox JA, Harrison J, Besra GS (2015) Assembly of the mycobacterial cell wall. Annu Rev Microbiol 69:405–423

Jeske O, Schüler M, Schumann P, Schneider A, Boedeker C, Jogler M, Bollschweiler D, Rohde M, Mayer C, Engelhardt H, Spring S, Jogler C (2015) Planctomycetes do possess a peptidoglycan cell wall. Nat Commun 6:7116. https://doi.org/10.1038/ncomms8116

Johnson JW, Fisher JF, Mobashery S (2013) Bacterial cell-wall recycling. Ann N Y Acad Sci 1277:54–75

Jolly L, Ferrari P, Blanot D, Van Heijenoort J, Fassy F, Mengin-Lecreulx D (1999) Reaction mechanism of phosphoglucosamine mutase from *Escherichia coli*. Eur J Biochem 262:202–210

Jones LJ, Carballido-Lopez R, Errington J (2001) Control of cell shape in bacteria: helical, actin-like filaments in *Bacillus subtilis*. Cell 104:913–922

Kalamorz F, Reichenbach B, Marz W, Rak B, Görke B (2007) Feedback control of glucosamine-6-phosphate synthase GlmS expression depends on the small RNA GlmZ and involves the novel protein YhbJ in *Escherichia coli*. Mol Microbiol 65:1518–1533

Kandler O, König H (1978) Chemical composition of the peptidoglycan-free cell walls of methanogenic bacteria. Arch Microbiol 118:141–152

Kandler O, König H (1993) Cell envelopes of archaea: Structure and chemistry. In: Mea K (ed) The biochemistry of Archaea (Archaebacteria). Elsevier Science Publishers B. H, Amsterdam, pp 223–259

Kandler O, König H (1998) Cell wall polymers in Archaea (Archaebacteria). Cell Mol Life Sci 54:305–308

Kawai Y, Marles-Wright J, Cleverley RM, Emmins R, Ishikawa S, Kuwano M, Heinz N, Bui NK, Hoyland CN, Ogasawara N, Lewis RJ, Vollmer W, Daniel RA, Errington J (2011) A widespread family of bacterial cell wall assembly proteins. EMBO J 30:4931–4941

Kawai Y, Mickiewicz K, Errington J (2018) Lysozyme counteracts β-lactam antibiotics by promoting the emergence of L-form bacteria. Cell 172:1038–1049

Kelemen MV, Rogers HJ (1971) Three-dimensional molecular models of bacterial cell wall mucopeptides (peptidoglycans). Proc Natl Acad Sci USA 68:992–996

Kellenberger E, Ryter A (1958) Cell wall and cytoplasmic membrane of *Escherichia coli*. J Biophys Biochem Cytol 4:323–326

Kim SJ, Chang J, Singh M (2015) Peptidoglycan architecture of Gram-positive bacteria by solid-state NMR. Biochim Biophys Acta 1848(1 Pt B):350–362

King DT, Lameignere E, Strynadka NC (2014) Structural insights into the lipoprotein outer membrane regulator of penicillin-binding protein 1B. J Biol Chem 289:19245–19253

Kishida H, Unzai S, Roper DI, Lloyd A, Park SY, Tame JR (2006) Crystal structure of penicillin binding protein 4 (*dacB*) from *Escherichia coli*, both in the native form and covalently linked to various antibiotics. Biochemistry 45:783–792

Kluj RM, Ebner P, Adamek M, Ziemert N, Mayer C, Borisova M (2018) Recovery of the peptidoglycan turnover product released by the Autolysin Atl in *Staphylococcus aureus* involves the phosphotransferase system transporter MurP and the Novel 6-phospho-*N*-acetylmuramidase MupG. Front Microbiol 9(2725). https://doi.org/10.3389/fmicb.2018.02725

Koch AL (1985) How bacteria grow and divide in spite of internal hydrostatic pressure. Can J Microbiol 31:1071–1084

Koch AL (1995) Bacterial growth and form: Evolution and biophysics. Chapman and Hall, New York

Koch AL, Doyle RJ (1985) Inside-to-outside growth and turnover of the wall of Gram-positive rods. J Theor Biol 117:137–157

Koch AL, Woeste S (1992) Elasticity of the sacculus of *Escherichia coli*. J Bacteriol 174:4811–4819

König H, Kandler O, Jensen M, Rietschel ET (1983) The primary structure of the glycan moiety of pseudomurein from *Methanobacterium thermoautotrophicum*. Hoppe Seylers Z Physiol Chem 364:627–636

Kouidmi I, Levesque RC, Paradis-Bleau C (2014) The biology of Mur ligases as an antibacterial target. Mol Microbiol 94:242–253

Kühner D, Stahl M, Demircioglu DD, Bertsche U (2014) From cells to muropeptide structures in 24 h: peptidoglycan mapping by UPLC-MS. Sci Rep 4:7494. https://doi.org/10.1038/srep07494

Kuru E, Tekkam S, Hall E, Brun YV, Van Nieuwenhze MS (2015) Synthesis of fluorescent D-amino acids and their use for probing peptidoglycan synthesis and bacterial growth in situ. Nat Protoc 10:33–52

Labischinski H, Barnickel G, Bradaczek H, Giesbrecht P (1979) On the secondary and tertiary structure of murein. Low and medium-angle X-ray evidence against chitin-based conformations of bacterial peptidoglycan. Eur J Biochem 95:147–155

Labischinski H, Goodell EW, Goodell A, Hochberg ML (1991) Direct proof of a "more-than-single-layered" peptidoglycan architecture of *Escherichia coli* W7: a neutron small-angle scattering study. J Bacteriol 173:751–756

Laddomada F, Miyachiro MM, Dessen A (2016) Structural insights into protein-protein interactions involved in bacterial cell wall biogenesis. Antibiotics (Basel) 5(2):E14. https://doi.org/10.3390/antibiotics5020014

Lai GC, Cho H, Bernhardt TG (2017) The mecillinam resistome reveals a role for peptidoglycan endopeptidases in stimulating cell wall synthesis in *Escherichia coli*. PLoS Genet 13(7): e1006934

Lavollay M, Arthur M, Fourgeaud M, Dubost L, Marie A, Veziris N, Blanot D, Gutmann L, Mainardi JL (2008) The peptidoglycan of stationary-phase *Mycobacterium tuberculosis* predominantly contains cross-links generated by L,D-transpeptidation. J Bacteriol 190:4360–4366

Leclercq S, Derouaux A, Olatunji S, Fraipont C, Egan AJ, Vollmer W, Breukink E, Terrak M (2017) Interplay between Penicillin-binding proteins and SEDS proteins promotes bacterial cell wall synthesis. Sci Rep 7:43306. https://doi.org/10.1038/srep43306

Leduc M, Frehel C, Siegel E, Van Heijenoort J (1989) Multilayered distribution of peptidoglycan in the periplasmic space of *Escherichia coli*. J Gen Microbiol 135:1243–1254

Lee TK, Meng K, Shi H, Huang KC (2016) Single-molecule imaging reveals modulation of cell wall synthesis dynamics in live bacterial cells. Nat Commun 7:13170. https://doi.org/10.1038/ncomms13170

Levefaudes M, Patin D, de Sousa-d'Auria C, Chami M, Blanot D, Herve M, Arthur M, Houssin C, Mengin-Lecreulx D (2015) Diaminopimelic acid amidation in Corynebacteriales: new insights into the role of LtsA in peptidoglycan modification. J Biol Chem 290:13079–13094

Liechti GW, Kuru E, Hall E, Kalinda A, Brun YV, VanNieuwenhze M, Maurelli AT (2014) A new metabolic cell-wall labelling method reveals peptidoglycan in *Chlamydia trachomatis*. Nature 506:507–510

Liechti G, Kuru E, Packiam M, Hsu YP, Tekkam S, Hall E, Rittichier JT, VanNieuwenhze M, Brun YV, Maurelli AT (2016) Pathogenic Chlamydia lack a classical sacculus but synthesize a narrow, mid-cell peptidoglycan ring, egulated by MreB, for cell division. PLoS Pathog 12(5): e1005590

Liger D, Masson A, Blanot D, van Heijenoort J, Parquet C (1995) Over-production, purification and properties of the uridine-diphosphate-*N*-acetylmuramate:L-alanine ligase from *Escherichia coli*. Eur J Biochem 230:80–87

Lim D, Strynadka NC (2002) Structural basis for the β-lactam resistance of PBP2a from methicillin-resistant *Staphylococcus aureus*. Nat Struct Biol 9:870–876

Lin L, Osorio Valeriano M, Harms A, Sogaard-Andersen L, Thanbichler M (2017) Bactofilin-mediated organization of the ParABS chromosome segregation system in *Myxococcus xanthus*. Nat Commun 8(1):1817. https://doi.org/10.1038/s41467-017-02015-z

Ling LL, Schneider T, Peoples AJ, Spoering AL, Engels I, Conlon BP, Mueller A, Schaberle TF, Hughes DE, Epstein S, Jones M, Lazarides L, Steadman VA, Cohen DR, Felix CR, Fetterman KA, Millett WP, Nitti AG, Zullo AM, Chen C, Lewis K (2015) A new antibiotic kills pathogens without detectable resistance. Nature 517:455–459

Litzinger S, Mayer C (2010) Chapter 1: The murein sacculus. In: König H, Claus H, Varma A (eds) Prokaryotic cell wall compounds – Structure and biochemistry. Springer, Heidelberg/Berlin/New York, pp 3–52

Litzinger S, Duckworth A, Nitzsche K, Risinger C, Wittmann V, Mayer C (2010) Muropeptide rescue in *Bacillus subtilis* involves sequential hydrolysis by β-*N*-acetylglucosaminidase and *N*-acetylmuramyl-L-alanine amidase. J Bacteriol 192:3132–3143

Liu B, Persons L, Lee L, de Boer PA (2015) Roles for both FtsA and the FtsBLQ subcomplex in FtsN-stimulated cell constriction in *Escherichia coli*. Mol Microbiol 95:945–970

Liu TY, Chu SH, Shaw GC (2018) Deletion of the cell wall peptidoglycan hydrolase gene *cwlO* or *lytE* severely impairs transformation efficiency in *Bacillus subtilis*. J Gen Appl Microbiol 64:139–144

Loskill P, Pereira PM, Jung P, Bischoff M, Herrmann M, Pinho MG, Jacobs K (2014) Reduction of the peptidoglycan crosslinking causes a decrease in stiffness of the *Staphylococcus aureus* cell envelope. Biophys J 107:1082–1089

Lovering AL, de Castro LH, Lim D, Strynadka NC (2007) Structural insight into the transglycosylation step of bacterial cell-wall biosynthesis. Science 315:1402–1405

Lovering AL, Safadi SS, Strynadka NC (2012) Structural perspective of peptidoglycan biosynthesis and assembly. Annu Rev Biochem 81:451–478

Löwe J, van den Ent F, Amos LA (2004) Molecules of the bacterial cytoskeleton. Annu Rev Biophys Biomol Struct 33:177–198

Lupoli TJ, Tsukamoto H, Doud EH, Wang TS, Walker S, Kahne D (2011) Transpeptidase-mediated incorporation of D-amino acids into bacterial peptidoglycan. J Am Chem Soc 133:10748–10751

Magnet S, Arbeloa A, Mainardi JL, Hugonnet JE, Fourgeaud M, Dubost L, Marie A, Delfosse V, Mayer C, Rice LB, Arthur M (2007a) Specificity of L,D-transpeptidases from gram-positive bacteria producing different peptidoglycan chemotypes. J Biol Chem 282:13151–13159

Magnet S, Bellais S, Dubost L, Fourgeaud M, Mainardi JL, Petit-Frere S, Marie A, Mengin-Lecreulx D, Arthur M, Gutmann L (2007b) Identification of the L,D-transpeptidases responsible for attachment of the Braun lipoprotein to *Escherichia coli* peptidoglycan. J Bacteriol 189:3927–3931

Magnet S, Dubost L, Marie A, Arthur M, Gutmann L (2008) Identification of the L, D-transpeptidases for peptidoglycan cross-linking in *Escherichia coli*. J Bacteriol 190:4782–4785

Mainardi JL, Villet R, Bugg TD, Mayer C, Arthur M (2008) Evolution of peptidoglycan biosynthesis under the selective pressure of antibiotics in Gram-positive bacteria. FEMS Microbiol Rev 32:386–408

Manat G, Roure S, Auger R, Bouhss A, Barreteau H, Mengin-Lecreulx D, Touze T (2014) Deciphering the metabolism of undecaprenyl-phosphate: the bacterial cell-wall unit carrier at the membrane frontier. Microb Drug Resist 20:199–214

Marcyjaniak M, Odintsov SG, Sabala I, Bochtler M (2004) Peptidoglycan amidase MepA is a LAS metallopeptidase. J Biol Chem 279:43982–43989

Marienfeld S, Uhlemann EM, Schmid R, Kramer R, Burkovski A (1997) Ultrastructure of the *Corynebacterium glutamicum* cell wall. Antonie Van Leeuwenhoek 72:291–297

Matias VR, Beveridge TJ (2005) Cryo-electron microscopy reveals native polymeric cell wall structure in *Bacillus subtilis* 168 and the existence of a periplasmic space. Mol Microbiol 56:240–251

Matias VR, Beveridge TJ (2006) Native cell wall organization shown by cryo-electron microscopy confirms the existence of a periplasmic space in *Staphylococcus aureus*. J Bacteriol 188:1011–1021

Matias VR, Al-Amoudi A, Dubochet J, Beveridge TJ (2003) Cryo-transmission electron microscopy of frozen-hydrated sections of *Escherichia coli* and *Pseudomonas aeruginosa*. J Bacteriol 185:6112–6118

Mayer C (2012) Bacterial cell wall recycling. eLS: https://doi.org/10.1002/9780470015902.a0021974

Mazmanian SK, Liu G, Ton-That H, Schneewind O (1999) *Staphylococcus aureus* sortase, an enzyme that anchors surface proteins to the cell wall. Science 285:760–763

McDonough MA, Anderson JW, Silvaggi NR, Pratt RF, Knox JR, Kelly JA (2002) Structures of two kinetic intermediates reveal species specificity of penicillin-binding proteins. J Mol Biol 322:111–122

McPherson DC, Popham DL (2003) Peptidoglycan synthesis in the absence of class A penicillin-binding proteins in *Bacillus subtilis*. J Bacteriol 185:1423–1431

Meeske AJ, Sham LT, Kimsey H, Koo BM, Gross CA, Bernhardt TG, Rudner DZ (2015) MurJ and a novel lipid II flippase are required for cell wall biogenesis in *Bacillus subtilis*. Proc Natl Acad Sci USA 112:6437–6442

Meeske AJ, Riley EP, Robins WP, Uehara T, Mekalanos JJ, Kahne D, Walker S, Kruse AC, Bernhardt TG, Rudner DZ (2016) SEDS proteins are a widespread family of bacterial cell wall polymerases. Nature 537:634–638

Meisner J, Montero Llopis P, Sham LT, Garner E, Bernhardt TG, Rudner DZ (2013) FtsEX is required for CwlO peptidoglycan hydrolase activity during cell wall elongation in *Bacillus subtilis*. Mol Microbiol 89:1069–1083

Mengin-Lecreulx D, van Heijenoort J (1994) Copurification of glucosamine-1-phosphate acetyltransferase and *N*-acetylglucosamine-1-phosphate uridyltransferase activities of *Escherichia coli*: characterization of the *glmU* gene product as a bifunctional enzyme catalyzing two subsequent steps in the pathway for UDP-*N*-acetylglucosamine synthesis. J Bacteriol 176:5788–5795

Mengin-Lecreulx D, van Heijenoort J (1996) Characterization of the essential gene *glmM* encoding phosphoglucosamine mutase in *Escherichia coli*. J Biol Chem 271:32–39

Mengin-Lecreulx D, van Heijenoort J, Park JT (1996) Identification of the *mpl* gene encoding UDP-*N*-acetylmuramate: L-alanyl-γ-D-glutamyl-*meso*-diaminopimelate ligase in *Escherichia coli* and its role in recycling of cell wall peptidoglycan. J Bacteriol 178(18):5347–5352

Mengin-Lecreulx D, Falla T, Blanot D, van Heijenoort J, Adams DJ, Chopra I (1999) Expression of the *Staphylococcus aureus* UDP-N-acetylmuramoyl-L-alanyl-D-glutamate:L-lysine ligase in *Escherichia coli* and effects on peptidoglycan biosynthesis and cell growth. J Bacteriol 181:5909–5914

Meroueh SO, Bencze KZ, Hesek D, Lee M, Fisher JF, Stemmler TL, Mobashery S (2006) Three-dimensional structure of the bacterial cell wall peptidoglycan. Proc Natl Acad Sci USA 103:4404–4409

Meziane-Cherif D, Saul FA, Haouz A, Courvalin P (2012) Structural and functional characterization of VanG D-Ala:D-Ser ligase associated with vancomycin resistance in *Enterococcus faecalis*. J Biol Chem 287:37583–37592

Michie KA, Lowe J (2006) Dynamic filaments of the bacterial cytoskeleton. Annu Rev Biochem 75:467–492

Miller SI, Salama NR (2018) The gram-negative bacterial periplasm: size matters. PLoS Biol 16(1): e2004935

Mohammadi T, van Dam V, Sijbrandi R, Vernet T, Zapun A, Bouhss A, Diepeveen-de Bruin M, Nguyen-Disteche M, de Kruijff B, Breukink E (2011) Identification of FtsW as a transporter of lipid-linked cell wall precursors across the membrane. EMBO J 30:1425–1432

Morbach S, Kramer R (2002) Body shaping under water stress: osmosensing and osmoregulation of solute transport in bacteria. Chembiochem 3:384–397

Morgenstein RM, Bratton BP, Nguyen JP, Ouzounov N, Shaevitz JW, Gitai Z (2015) RodZ links MreB to cell wall synthesis to mediate MreB rotation and robust morphogenesis. Proc Natl Acad Sci USA 112:12510–12515

Moynihan PJ, Clarke AJ (2011) O-Acetylated peptidoglycan: controlling the activity of bacterial autolysins and lytic enzymes of innate immune systems. Int J Biochem Cell Biol 43:1655–1659

Moynihan PJ, Sychantha D, Clarke AJ (2014) Chemical biology of peptidoglycan acetylation and deacetylation. Bioorg Chem 54:44–50

Mudd S, Polevitzky K, Anderson TF, Chambers LA (1941) Bacterial morphology as shown by the electron microscope: II. The bacterial cell-wall in the genus *Bacillus*. J Bacteriol 42:251–264

Mularski A, Wilksch JJ, Wang H, Hossain MA, Wade JD, Separovic F, Strugnell RA, Gee ML (2015) Atomic force microscopy reveals the mechanobiology of lytic peptide action on bacteria. Langmuir 31:6164–6171

Münch D, Roemer T, Lee SH, Engeser M, Sahl HG, Schneider T (2012) Identification and in vitro analysis of the GatD/MurT enzyme-complex catalyzing lipid II amidation in *Staphylococcus aureus*. PLoS Pathog 8(1):e1002509

Murray RG, Steed P, Elson HE (1965) The location of the mucopeptide in sections of the cell wall of *Escherichia coli* and other Gram-negative bacteria. Can J Microbiol 11:547–560

Navarre WW, Schneewind O (1999) Surface proteins of Gram-positive bacteria and mechanisms of their targeting to the cell wall envelope. Microbiol Mol Biol Rev 63:174–229

Ngadjeua F, Braud E, Saidjalolov S, Iannazzo L, Schnappinger D, Ehrt S, Hugonnet JE, Mengin-Lecreulx D, Patin D, Etheve-Quelquejeu M, Fonvielle M, Arthur M (2018) Critical impact of peptidoglycan precursor amidation on the activity of L,D-transpeptidases from *Enterococcus faecium* and *Mycobacterium tuberculosis*. Chemistry 24:5743–5747

Nicholas RA, Krings S, Tomberg J, Nicola G, Davies C (2003) Crystal structure of wild-type penicillin-binding protein 5 from *Escherichia coli*: implications for deacylation of the acyl-enzyme complex. J Biol Chem 278:52826–52833

Omote H, Hiasa M, Matsumoto T, Otsuka M, Moriyama Y (2006) The MATE proteins as fundamental transporters of metabolic and xenobiotic organic cations. Trends Pharmacol Sci 27:587–593

Park JT (1952) Uridine-5′-pyrophosphate derivatives. I Isolation from Staphylococcus aureus. J Biol Chem 194:877–884

Park JT (1993) Turnover and recycling of the murein sacculus in oligopeptide permease-negative strains of *Escherichia coli*: indirect evidence for an alternative permease system and for a monolayered sacculus. J Bacteriol 175:7–11

Park JT, Johnson MJ (1949) Accumulation of labile phosphate in *Staphylococcus aureus* grown in the presence of penicillin. J Biol Chem 179:585–592

Park JT, Strominger JL (1957) Mode of action of penicillin. Science 125:99–101

Park JT, Uehara T (2008) How bacteria consume their own exoskeletons (turnover and recycling of cell wall peptidoglycan). Microbiol Mol Biol Rev 72:211–227

Park JT, Raychaudhuri D, Li H, Normark S, Mengin-Lecreulx D (1998) MppA, a periplasmic binding protein essential for import of the bacterial cell wall peptide L-alanyl-gamma-D-glutamyl-*meso*-diaminopimelate. J Bacteriol 180:1215–1223

Pende N, Wang J, Weber PM, Verheul J, Kuru E, Rittmann SKR, Leisch N, VanNieuwenhze MS, Brun YV, den Blaauwen T, Bulgheresi S (2018) Host-polarized cell growth in animal symbionts. Curr Biol 28:1039–1051

Pennartz A, Genereux C, Parquet C, Mengin-Lecreulx D, Joris B (2009) Substrate-induced inactivation of the *Escherichia coli* AmiD *N*-acetylmuramoyl-L-alanine amidase highlights a new strategy to inhibit this class of enzyme. Antimicrob Agents Chemother 53:2991–2997

Pichoff S, Shen B, Sullivan B, Lutkenhaus J (2002) FtsA mutants impaired for self-interaction bypass ZipA suggesting a model in which FtsA's self-interaction competes with its ability to recruit downstream division proteins. Microbiology 83:151–167. https://doi.org/10.1111/j.1365-2958.2011.07923.x. Epub

Pichoff S, Lutkenhaus J (2005) Tethering the Z ring to the membrane through a conserved membrane targeting sequence in FtsA. Mol Microbiol 55:1722–1734

Pilhofer M, Aistleitner K, Biboy J, Gray J, Kuru E, Hall E, Brun YV, VanNieuwenhze MS, Vollmer W, Horn M, Jensen GJ (2013) Discovery of chlamydial peptidoglycan reveals bacteria with murein sacculi but without FtsZ. Nat Commun 4:2856. https://doi.org/10.1038/ncomms3856

Popescu A, Doyle RJ (1996) The Gram stain after more than a century. Biotech Histochem 71:145–151

Popham DL (2002) Specialized peptidoglycan of the bacterial endospore: the inner wall of the lockbox. Cell Mol Life Sci 59:426–433

Porter JR (1976) Antony van Leeuwenhoek: tercentenary of his discovery of bacteria. Bacteriol Rev 40:260–269

Raghavendra T, Patil S, Mukherjee R (2018) Peptidoglycan in Mycobacteria: chemistry, biology and intervention. Glycoconj J 35:421–432

Raymond JB, Mahapatra S, Crick DC, Pavelka MS Jr (2005) Identification of the *namH* gene, encoding the hydroxylase responsible for the *N*-glycolylation of the mycobacterial peptidoglycan. J Biol Chem 280:326–333

Razin S, Argaman M (1963) Lysis of Mycoplasma, bacterial protoplasts, spheroplasts and L-forms by various agents. J Gen Microbiol 30:155–172

Reddy M (2007) Role of FtsEX in cell division of *Escherichia coli*: viability of *ftsEX* mutants is dependent on functional SufI or high osmotic strength. J Bacteriol 189:98–108

Reith J, Mayer C (2011) Peptidoglycan turnover and recycling in Gram-positive bacteria. Appl Microbiol Biotechnol 92:1–11

Reizer J, Saier MH Jr, Deutscher J, Grenier F, Thompson J, Hengstenberg W (1988) The phosphoenolpyruvate:sugar phosphotransferase system in gram-positive bacteria: properties, mechanism, and regulation. Crit Rev Microbiol 15:297–338

Remaut H, Bompard-Gilles C, Goffin C, Frere JM, Van Beeumen J (2001) Structure of the *Bacillus subtilis* D-aminopeptidase DppA reveals a novel self-compartmentalizing protease. Nat Struct Biol 8:674–678

Rogers HJ (1974) Peptidoglycans (mucopeptides): structure, function, and variations. Ann N Y Acad Sci 235:29–51

Rojas E, Theriot JA, Huang KC (2014) Response of *Escherichia coli* growth rate to osmotic shock. Proc Natl Acad Sci USA 111:7807–7812

Romeis T, Höltje JV (1994) Penicillin-binding protein 7/8 of *Escherichia coli* is a DD-endopeptidase. Eur J Biochem 224:597–604

Rowlett VW, Margolin W (2015) The bacterial divisome: ready for its close-up. Philos Trans R Soc Lond Ser B Biol Sci 370(1679). https://doi.org/10.1098/rstb.2015.0028

Ruane KM, Lloyd AJ, Fulop V, Dowson CG, Barreteau H, Boniface A, Dementin S, Blanot D, Mengin-Lecreulx D, Gobec S, Dessen A, Roper DI (2013) Specificity determinants for lysine incorporation in *Staphylococcus aureus* peptidoglycan as revealed by the structure of a MurE enzyme ternary complex. J Biol Chem 288:33439–33448

Rueff AS, Chastanet A, Dominguez-Escobar J, Yao Z, Yates J, Prejean MV, Delumeau O, Noirot P, Wedlich-Soldner R, Filipe SR, Carballido-Lopez R (2014) An early cytoplasmic step of peptidoglycan synthesis is associated to MreB in *Bacillus subtilis*. Mol Microbiol 91:348–362

Ruiz N (2008) Bioinformatics identification of MurJ (MviN) as the peptidoglycan lipid II flippase in *Escherichia coli*. Proc Natl Acad Sci USA 105:15553–15557

Salje J, van den Ent F, de Boer P, Lowe J (2011) Direct membrane binding by bacterial actin MreB. Mol Cell 43:478–487

Salton MR (1994) The bacterial cell envelope – a historical perspective. In: Ghuysen J-M, Hakenbeck R (eds) Bacterial cell wall, vol 29. Elsevier, Amsterdam, pp 1–22

Salton MR, Horne RW (1951) Studies of the bacterial cell wall. II Methods of preparation and some properties of cell walls. Biochim Biophys Acta 7:177–197

Sathiyamoorthy K, Vijayalakshmi J, Tirupati B, Fan L, Saper MA (2017) Structural analyses of the *Haemophilus influenzae* peptidoglycan synthase activator LpoA suggest multiple conformations in solution. J Biol Chem 292:17626–17642

Sauvage E, Kerff F, Terrak M, Ayala JA, Charlier P (2008) The penicillin-binding proteins: structure and role in peptidoglycan biosynthesis. FEMS Microbiol Rev 32:234–258

Scheffers DJ, Pinho MG (2005) Bacterial cell wall synthesis: new insights from localization studies. Microbiol Mol Biol Rev 69:585–607

Scheuring S, Dufrene YF (2010) Atomic force microscopy: probing the spatial organization, interactions and elasticity of microbial cell envelopes at molecular resolution. Mol Microbiol 75:1327–1336

Scheurwater E, Reid CW, Clarke AJ (2008) Lytic transglycosylases: bacterial space-making autolysins. Int J Biochem Cell Biol 40:586–591

Schlag M, Biswas R, Krismer B, Kohler T, Zoll S, Yu W, Schwarz H, Peschel A, Gotz F (2010) Role of staphylococcal wall teichoic acid in targeting the major autolysin Atl. Mol Microbiol 75:864–873

Schleifer KH, Kandler O (1972) Peptidoglycan types of bacterial cell walls and their taxonomic implications. Bacteriol Rev 36:407–777

Schmidt KL, Peterson ND, Kustusch RJ, Wissel MC, Graham B, Phillips GJ, Weiss DS (2004) A predicted ABC transporter, FtsEX, is needed for cell division in *Escherichia coli*. J Bacteriol 186:785–793

Schneewind O, Missiakas DM (2012) Protein secretion and surface display in Gram-positive bacteria. Philos Trans R Soc Lond Ser B Biol Sci 367:1123–1139

Schneewind O, Fowler A, Faull KF (1995) Structure of the cell wall anchor of surface proteins in *Staphylococcus aureus*. Science 268:103–106

Schneider T, Kruse T, Wimmer R, Wiedemann I, Sass V, Pag U, Jansen A, Nielsen AK, Mygind PH, Raventos DS, Neve S, Ravn B, Bonvin AM, De Maria L, Andersen AS, Gammelgaard LK, Sahl HG, Kristensen HH (2010) Plectasin, a fungal defensin, targets the bacterial cell wall precursor Lipid II. Science 328:1168–1172

Seltmann G, Holst O (2002) Periplasmic space and rigid layer. In: Seltmann G, Holst O (eds) The bacterial cell wall. Springer-Verlag, Berlin, pp 103–132

Sham LT, Butler EK, Lebar MD, Kahne D, Bernhardt TG, Ruiz N (2014) Bacterial cell wall. MurJ is the flippase of lipid-linked precursors for peptidoglycan biogenesis. Science 345:220–222

Sham LT, Zheng S, Yakhnina AA, Kruse AC, Bernhardt TG (2018) Loss of specificity variants of WzxC suggest that substrate recognition is coupled with transporter opening in MOP-family flippases. Mol Microbiol 109:633–641

Shida T, Hattori H, Ise F, Sekiguchi J (2000) Overexpression, purification, and characterization of *Bacillus subtilis N*-acetylmuramoyl-L-alanine amidase CwlC. Biosci Biotech Bioch 64:1522–1525

Shida T, Hattori H, Ise F, Sekiguchi J (2001) Mutational analysis of catalytic sites of the cell wall lytic *N*-acetylmuramoyl-L-alanine amidases CwlC and CwlV. J Biol Chem 276:28140–28146

Shockman GD, Daneo-Moore L, Kariyama R, Massidda O (1996) Bacterial walls, peptidoglycan hydrolases, autolysins, and autolysis. Microb Drug Resist 2:95–98

Silhavy TJ, Kahne D, Walker S (2010) The bacterial cell envelope. Cold Spring Harb Perspect Biol 2(5):a000414. https://doi.org/10.1101/cshperspect.a000414

Small E, Addinall SG (2003) Dynamic FtsZ polymerization is sensitive to the GTP to GDP ratio and can be maintained at steady state using a GTP-regeneration system. Microbiology 149:2235–2242

Smith CA (2006) Structure, function and dynamics in the mur family of bacterial cell wall ligases. J Mol Biol 362:640–655

Smith TJ, Blackman SA, Foster SJ (2000) Autolysins of *Bacillus subtilis*: multiple enzymes with multiple functions. Microbiology 146:249–262

Sobhanifar S, King DT, Strynadka NC (2013) Fortifying the wall: synthesis, regulation and degradation of bacterial peptidoglycan. Curr Opin Struct Biol 23:695–703

Squeglia F, Ruggiero A, Berisio R (2018) Chemistry of peptidoglycan in *Mycobacterium tuberculosis* life cycle: an off-the-wall balance of synthesis and degradation. Chemistry 24:2533–2546

Strahl H, Errington J (2017) Bacterial membranes: structure, domains, and function. Annu Rev Microbiol 71:519–538

Strominger JL, Tipper DJ (1965) Bacterial cell wall synthesis and structure in relation to the mechanism of action of penicillins and other antibacterial agents. Am J Med 39:708–721

Sudiarta IP, Fukushima T, Sekiguchi J (2010) *Bacillus subtilis* CwlQ (previous YjbJ) is a bifunctional enzyme exhibiting muramidase and soluble-lytic transglycosylase activities. Biochem Biophys Res Commun 398:606–612

Takeuchi S, DiLuzio WR, Weibel DB, Whitesides GM (2005) Controlling the shape of filamentous cells of *Escherichia coli*. Nano Lett 5:1819–1823

Templin MF, Ursinus A, Höltje JV (1999) A defect in cell wall recycling triggers autolysis during the stationary growth phase of *Escherichia coli*. EMBO J 18:4108–4117

Tipper DJ, Strominger JL (1965) Mechanism of action of penicillins: a proposal based on their structural similarity to acyl-D-alanyl-D-alanine. Proc Natl Acad Sci USA 54:1133–1141

Tipper DJ, Strominger JL, Ensign JC (1967) Structure of the cell wall of *Staphylococcus aureus*, strain Copenhagen. VII Mode of action of the bacteriolytic peptidase from *Myxobacter* and the isolation of intact cell wall polysaccharides. Biochemistry 6:906–920

Ton-That H, Liu G, Mazmanian SK, Faull KF, Schneewind O (1999) Purification and characterization of sortase, the transpeptidase that cleaves surface proteins of *Staphylococcus aureus* at the LPXTG motif. Proc Natl Acad Sci USA 96:12424–12429

Touhami A, Jericho MH, Beveridge TJ (2004) Atomic force microscopy of cell growth and division in *Staphylococcus aureus*. J Bacteriol 186:3286–3295

Turner RD, Hobbs JK, Foster SJ (2016) Atomic force microscopy analysis of bacterial cell wall peptidoglycan architecture. Methods Mol Biol 1440:3–9

Turner RD, Mesnage S, Hobbs JK, Foster SJ (2018) Molecular imaging of glycan chains couples cell-wall polysaccharide architecture to bacterial cell morphology. Nat Commun 9(1):1263. https://doi.org/10.1038/s41467-018-03551-y

Typas A, Banzhaf M, Gross CA, Vollmer W (2012) From the regulation of peptidoglycan synthesis to bacterial growth and morphology. Nat Rev Microbiol 10:123–136

Uehara T, Bernhardt TG (2011) More than just lysins: peptidoglycan hydrolases tailor the cell wall. Curr Opin Microbiol 14:698–703

Uehara T, Park JT (2003) Identification of MpaA, an amidase in *Escherichia coli* that hydrolyzes the gamma-D-glutamyl-meso-diaminopimelate bond in murein peptides. J Bacteriol 185:679–682

Uehara T, Park JT (2004) The *N*-acetyl-D-glucosamine kinase of *Escherichia coli* and its role in murein recycling. J Bacteriol 186:7273–7279

Uehara T, Suefuji K, Valbuena N, Meehan B, Donegan M, Park JT (2005) Recycling of the anhydro-*N*-acetylmuramic acid derived from cell wall murein involves a two-step conversion to *N*-acetylglucosamine-phosphate. J Bacteriol 187:3643–3649

Uehara T, Suefuji K, Jaeger T, Mayer C, Park JT (2006) MurQ etherase is required by *Escherichia coli* in order to metabolize anhydro-*N*-acetylmuramic acid obtained either from the environment or from its own cell wall. J Bacteriol 188:1660–1662

Uehara T, Parzych KR, Dinh T, Bernhardt TG (2010) Daughter cell separation is controlled by cytokinetic ring-activated cell wall hydrolysis. EMBO J 29:1412–1422

Ursell TS, Nguyen J, Monds RD, Colavin A, Billings G, Ouzounov N, Gitai Z, Shaevitz JW, Huang KC (2014) Rod-like bacterial shape is maintained by feedback between cell curvature and cytoskeletal localization. Proc Natl Acad Sci USA 111:E1025–E1034

van Dam V, Sijbrandi R, Kol M, Swiezewska E, de Kruijff B, Breukink E (2007) Transmembrane transport of peptidoglycan precursors across model and bacterial membranes. Mol Microbiol 64:1105–1114

van den Ent F, Amos LA, Lowe J (2001) Prokaryotic origin of the actin cytoskeleton. Nature 413:39–44

van den Ent F, Johnson CM, Persons L, de Boer P, Lowe J (2010) Bacterial actin MreB assembles in complex with cell shape protein RodZ. EMBO J 29:1081–1090

van den Ent F, Izore T, Bharat TA, Johnson CM, Lowe J (2014) Bacterial actin MreB forms antiparallel double filaments. elife 3:e02634. https://doi.org/10.7554/eLife.02634

van der Ploeg R, Goudelis ST, den Blaauwen T (2015) Validation of FRET assay for the screening of growth inhibitors of *Escherichia coli* reveals elongasome assembly dynamics. Int J Mol Sci 16:17637–17654

van Heijenoort J (2001) Recent advances in the formation of the bacterial peptidoglycan monomer unit. Nat Prod Rep 18:503–519

van Heijenoort J (2007) Lipid intermediates in the biosynthesis of bacterial peptidoglycan. Microbiol Mol Biol Rev 71:620–635

van Heijenoort J (2011) Peptidoglycan hydrolases of *Escherichia coli*. Microbiol Mol Biol Rev 75:636–663

van Heijenoort Y, Leduc M, Singer H, van Heijenoort J (1987) Effects of moenomycin on *Escherichia coli*. J Gen Microbiol 133:667–674

van Teeffelen S, Wang S, Furchtgott L, Huang KC, Wingreen NS, Shaevitz JW, Gitai Z (2011) The bacterial actin MreB rotates, and rotation depends on cell-wall assembly. Proc Natl Acad Sci USA 108:15822–15827

van Teeseling MC, Mesman RJ, Kuru E, Espaillat A, Cava F, Brun YV, VanNieuwenhze MS, Kartal B, van Niftrik L (2015) Anammox Planctomycetes have a peptidoglycan cell wall. Nat Commun 6:6878. https://doi.org/10.1038/ncomms7878

Vilcheze C, Kremer L (2017) Acid-fast positive and acid-fast negative *Mycobacterium tuberculosis*: the Koch paradox. Microbiol Spectr 5(2). https://doi.org/10.1128/microbiolspec.TBTB2-0003-2015

Villa E, Schaffer M, Plitzko JM, Baumeister W (2013) Opening windows into the cell: focused-ion-beam milling for cryo-electron tomography. Curr Opin Struct Biol 23:771–777

Vollmer W (2008) Structural variation in the glycan strands of bacterial peptidoglycan. FEMS Microbiol Rev 32:287–306

Vollmer W (2012) Bacterial growth does require peptidoglycan hydrolases. Mol Microbiol 86:1031–1035

Vollmer W, Bertsche U (2008) Murein (peptidoglycan) structure, architecture and biosynthesis in *Escherichia coli*. Biochim Biophys Acta 1778:1714–1734

Vollmer W, Höltje JV (2001) Morphogenesis of *Escherichia coli*. Curr Opin Microbiol 4:625–633

Vollmer W, Höltje JV (2004) The architecture of the murein (peptidoglycan) in Gram-negative bacteria: vertical scaffold or horizontal layer(s)? J Bacteriol 186:5978–5987

Vollmer W, Seligman SJ (2010) Architecture of peptidoglycan: more data and more models. Trends Microbiol 18:59–66

Vollmer W, Tomasz A (2000) The *pgdA* gene encodes for a peptidoglycan *N*-acetylglucosamine deacetylase in *Streptococcus pneumoniae*. J Biol Chem 275:20496–20501

Vollmer W, Blanot D, de Pedro MA (2008a) Peptidoglycan structure and architecture. FEMS Microbiol Rev 32:149–167

Vollmer W, Joris B, Charlier P, Foster S (2008b) Bacterial peptidoglycan (murein) hydrolases. FEMS Microbiol Rev 32:259–286

Vötsch W, Templin MF (2000) Characterization of a β-*N*-acetylglucosaminidase of *Escherichia coli* and elucidation of its role in muropeptide recycling and β-lactamase induction. J Biol Chem 275:39032–39038

Wang X, Huang J, Mukherjee A, Cao C, Lutkenhaus J (1997) Analysis of the interaction of FtsZ with itself, GTP, and FtsA. J Bacteriol 179:5551–5559

Wang L, Khattar MK, Donachie WD, Lutkenhaus J (1998) FtsI and FtsW are localized to the septum in *Escherichia coli*. J Bacteriol 180:2810–2816

Ward JB (1973) The chain length of the glycans in bacterial cell walls. Biochem J 133:395–398

Weidel W, Pelzer H (1964) Bagshaped macromolecules − a new outlook on bacterial cell walls. Adv Enzymol 26:193–232

Weidel W, Primosigh J (1958) Biochemical parallels between lysis by virulent phage and lysis by penicillin. J Gen Microbiol 18:513–517

Weidel W, Frank H, Martin HH (1960) The rigid layer of the cell wall of *Escherichia coli* strain B. J Gen Microbiol 22:158–166

Weiss DS, Pogliano K, Carson M, Guzman L-M, Fraipont C, Nguyen-Distèche M, Losick R, Beckwith J (1997) Localization of the *Escherichia coli* cell division protein FtsI (PBP3) to the division site and cell pole. Mol Microbiol 25:671–681

Wheeler R, Turner RD, Bailey RG, Salamaga B, Mesnage S, Mohamad SA, Hayhurst EJ, Horsburgh M, Hobbs JK, Foster SJ (2015) Bacterial cell enlargement requires control of cell wall stiffness mediated by peptidoglycan hydrolases. mBio 6(4):e00660. https://doi.org/10.1128/mBio.00660-15

White CL, Kitich A, Gober JW (2010) Positioning cell wall synthetic complexes by the bacterial morphogenetic proteins MreB and MreD. Mol Microbiol 76:616–633

Wild J, Hennig J, Lobocka M, Walczak W, Klopotowski T (1985) Identification of the *dadX* gene coding for the predominant isozyme of alanine racemase in *Escherichia coli* K12. Mol Gen Genet 198:315–322

Winkler WC, Nahvi A, Roth A, Collins JA, Breaker RR (2004) Control of gene expression by a natural metabolite-responsive ribozyme. Nature 428:281–286

Witholt B, Boekhout M (1978) The effect of osmotic shock on the accessibility of the murein layer of exponentially growing *Escherichia coli* to lysozyme. Biochim Biophys Acta 508:296–305

Wolf SG, Houben L, Elbaum M (2014) Cryo-scanning transmission electron tomography of vitrified cells. Nat Methods 11:423–428

Yamamoto H, Miyake Y, Hisaoka M, Kurosawa S, Sekiguchi J (2008) The major and minor wall teichoic acids prevent the sidewall localization of vegetative DL-endopeptidase LytF in *Bacillus subtilis*. Mol Microbiol 70:297–310

Yang DC, Peters NT, Parzych KR, Uehara T, Markovski M, Bernhardt TG (2011) An ATP-binding cassette transporter-like complex governs cell-wall hydrolysis at the bacterial cytokinetic ring. Proc Natl Acad Sci USA 108:E1052–E1060

Yang X, Lyu Z, Miguel A, McQuillen R, Huang KC, Xiao J (2017) GTPase activity-coupled treadmilling of the bacterial tubulin FtsZ organizes septal cell wall synthesis. Science 355:744–747

Yao X, Jericho M, Pink D, Beveridge T (1999) Thickness and elasticity of gram-negative murein sacculi measured by atomic force microscopy. J Bacteriol 181:6865–6875

Young KD (2003) Bacterial shape. Mol Microbiol 49:571–580

Young KD (2010) Bacterial shape: two-dimensional questions and possibilities. Annu Rev Microbiol 64:223–240

Zapun A, Vernet T, Pinho MG (2008) The different shapes of cocci. FEMS Microbiol Rev 32:345–360

Zawadzke LE, Bugg TD, Walsh CT (1991) Existence of two D-alanine:D-alanine ligases in *Escherichia coli*: cloning and sequencing of the *ddlA* gene and purification and characterization of the DdlA and DdlB enzymes. Biochemistry 30:1673–1682

Zhao H, Patel V, Helmann JD, Dörr T (2017) Don't let sleeping dogmas lie: new views of peptidoglycan synthesis and its regulation. Mol Microbiol 106:847–860

Zhu JY, Yang Y, Han H, Betzi S, Olesen SH, Marsilio F, Schönbrunn E (2012) Functional consequence of covalent reaction of phosphoenolpyruvate with UDP-N-acetylglucosamine 1-carboxyvinyltransferase (MurA). J Biol Chem 287:12657–12667

Zipperle GF Jr, Ezzell JW Jr, Doyle RJ (1984) Glucosamine substitution and muramidase susceptibility in *Bacillus anthracis*. Can J Microbiol 30:553–559

Part IV
Glucose-Based Exopolysaccharides

Chapter 7
Cellulose and Hemicellulose Synthesis and Their Regulation in Plant Cells

Xiaoyu Zhu, Xiaoran Xin, and Ying Gu

Abstract As the major components in plant cell walls, cellulose and hemicelluloses have attracted many scientists long before the recent buzz of referring them as alternative resources for biofuels. Plant cells invest ~10% of their genes in the biosynthesis and regulation of cell walls. Taking biosynthesis as an example, we are still far from deciphering each enzyme's exact biochemical and biological function. Despite the challenge, many discoveries were made in the past two decades. In this chapter, we highlight recent progress toward understanding the mechanisms by which cellulose and hemicelluloses are synthesized and regulated in plants.

7.1 Introduction: Molecular and Structural Compositions of the Plant Cell Walls

All plant cells are encaged by cell walls that are mainly composed of a well-organized mixture of complex polysaccharides and a small amount of structural proteins (Cosgrove 2005). Plant cell walls not only determine the shape of cells but also play essential roles in the regulation of cell growth. Based on differences in structural compositions and physiological functions, plant cell walls are classified into two types: the primary cell walls (PCWs) and the secondary cell walls (SCWs). The PCWs are deposited during cell growth and are primarily composed of three types of polysaccharides: cellulose, hemicelluloses, and pectin. Cellulose exists in the form of crystalline cellulose microfibrils, which are cross-linked by hemicelluloses, providing the cell wall with tensile strength. The cellulose-hemicelluloses network is embedded in the pectin matrix, which serves as "glue" to hold the cell wall together and enables the cell wall to extend. In certain plant tissues, the SCWs are deposited upon the cessation of cell growth. Different from the PCWs, the SCWs

X. Zhu · X. Xin · Y. Gu (✉)
Department of Biochemistry and Molecular Biology, Center for Lignocellulose Structure and Formation, Pennsylvania State University, University Park, PA, USA
e-mail: yug13@psu.edu

E. Cohen, H. Merzendorfer (eds.), *Extracellular Sugar-Based Biopolymers Matrices*, Biologically-Inspired Systems 12, https://doi.org/10.1007/978-3-030-12919-4_7

contain lignin instead of pectin as one of the three major polymers. Not all SCWs are lignified. For example, cotton fiber SCWs are made of nearly pure cellulose (Haigler et al. 2012). Lignification represents one of the final stages of SCW synthesis as it replaces water and stiffens the cell wall.

7.2 Biosynthesis and Regulation of Cellulose

7.2.1 Structural Properties of Cellulose

Cellulose, the major component of plant cell walls, is the most abundant biopolymer on the planet. Naturally deposited cellulose is a linear, unbranched polysaccharide chain composed of D-glucose residues. The glucose residues are linked via β (1-4)-glycosidic bonds, with each neighboring glucose residue rotated 180° along the glucan chain axis. Parallel glucan chains are further stacked into crystalline cellulose microfibrils with a width of 3–5 nm, by hydrogen bonds and van der Waals forces (Nieduszy and Preston 1970; Gardner and Blackwell 1974). The length and molecular weight of cellulose microfibrils can be reflected by the degree of polymerization (DP). In different cell wall types, the DP of cellulose microfibrils can range from ~500 to up to 15,000 units (Triplett and Timpa 1995; Brett 2000).

Depending on different crystal structures, seven polymorphs of cellulose were discovered so far, namely, cellulose Iα, Iβ, II, III_I, III_{II}, IV_I, and IV_{II} (Nishiyama et al. 2002; Nishiyama 2009). Among them, only two forms are synthesized in nature: cellulose Iα and Iβ. These two native cellulose forms show differential nuclear magnetic resonance (NMR)/X-ray diffraction spectra due to different positions of glucan chains. Cellulose Iα (triclinic) is composed of identical chains, while cellulose Iβ (monoclinic) is composed of two distinct types of chains (Atalla and Vanderhart 1984; Brown 1996; Sturcova et al. 2004). Cellulose Iα can be transformed to cellulose Iβ after high temperature treatment (Wada et al. 2003). Under strong alkaline conditions, cellulose I can also be irreversibly converted to the more stable cellulose II, which is composed of antiparallel chains (Brown 1999; Brett 2000).

7.2.2 Enzymology for Cellulose Biosynthesis

7.2.2.1 Cellulose Synthase (CESA)

In higher plants, cellulose microfibrils are synthesized by plasma membrane-localized enzymes called cellulose synthases (CESAs). CESAs belong to the glycosyltransferase-2 (GT-2) superfamily that are capable of making inverted β linkages. GT-2 superfamily includes proteins from different species, ranging from bacteria to higher plants. The CESA proteins were first identified in the cellulose-producing bacterium *Acetobacter xylinum* (Saxena et al. 1990; Wong et al. 1990). The first plant CESA was discovered from cotton, based on sequence homology to

the bacterial CESA (Pear et al. 1996). Later, CESA genes from various land plant species, including *Arabidopsis*, rice, maize, and poplar, were subsequently identified and cloned (Arioli et al. 1998; Holland et al. 2000). Phylogenetic analysis of CESA sequences revealed that moss lacks orthologs of vascular plant CESA, indicating the divergence of moss and seed plants predates the diversification of CESA for primary and secondary cell wall synthesis (Roberts and Bushoven 2007; Carroll and Specht 2011).

7.2.2.1.1 Structural Features of CESA

The plant CESAs are integral membrane proteins with eight putative transmembrane domains (TMDs). TMDs are predicted to form a pore at the plasma membrane and enable the secretion of newly synthesized glucan chains (Fig. 7.1a). Two of the TMDs are located toward the N-terminus of the protein, while the rest of TMDs are at the C-terminus following a large cytosolic catalytic domain (Pear et al. 1996; Delmer 1999). Recent work showed that a conserved FxVTxK motif in the "gating loop" is misplaced between putative TMDs 5 and 6, suggesting that CESA contains 7 TMDs with the C-terminus facing extracellular side of the plasma membrane (Slabaugh et al. 2016). The plant CESAs contain a large cytoplasmic region, referred to as the central domain or the globular domain that is located between TMDs 2 and 3. In the central domain lies the catalytic core of GT2 family proteins: the glycosyltransferase (GT) domain. The GT domain contains several signature motifs, namely, three conserved aspartic acid residues (D1, D2, and D3), and a QxxRW motif. These signature motifs are predicted to be essential for the binding and catalysis of substrates (Saxena et al. 2001; Williamson et al. 2002). Supporting this hypothesis, a recent study of the secondary cell wall CESAs (CESA4, CESA7, and CESA8) showed that point mutations on individual conserved aspartic acid residues resulted in deficient cellulose biosynthesis, reflected by inhibited plant growth, reduced cellulose content, and altered cellulose structure. However, equivalent D to N mutations on different CESA isoforms led to diverse degrees of cellulose biosynthesis deficiency, indicating different catalytic activities of secondary cell wall CESAs (Kumar et al. 2018).

While the crystal structure of plant CESAs remains elusive, the atomic structure of a catalytically active complex of the bacterial cellulose synthase complex, BcsA-BcsB, was solved (Morgan et al. 2013). BcsA is the catalytically active subunit that contains a cytosolic GT domain, a transmembrane helix domain, and a C-terminal domain. BcsB does not possess GT domain and is composed of a periplasmic domain and a transmembrane domain (Fig. 7.1b). Although BcsB does not have a catalytic domain, it was shown to be required for the catalysis of the BcsA-BcsB complex (Morgan et al. 2013; Omadjela et al. 2013). BcsA and BcsB form an elongated heterodimer across the plasma membrane. BcsA's TM3-8 forms a channel to accommodate the translocation of glucan chain. Supporting the proposed model for coupling of cellulose synthesis and translocation of nascent polysaccharides, purified BcsA-BcsB complex is sufficient for the reconstitution of cellulose

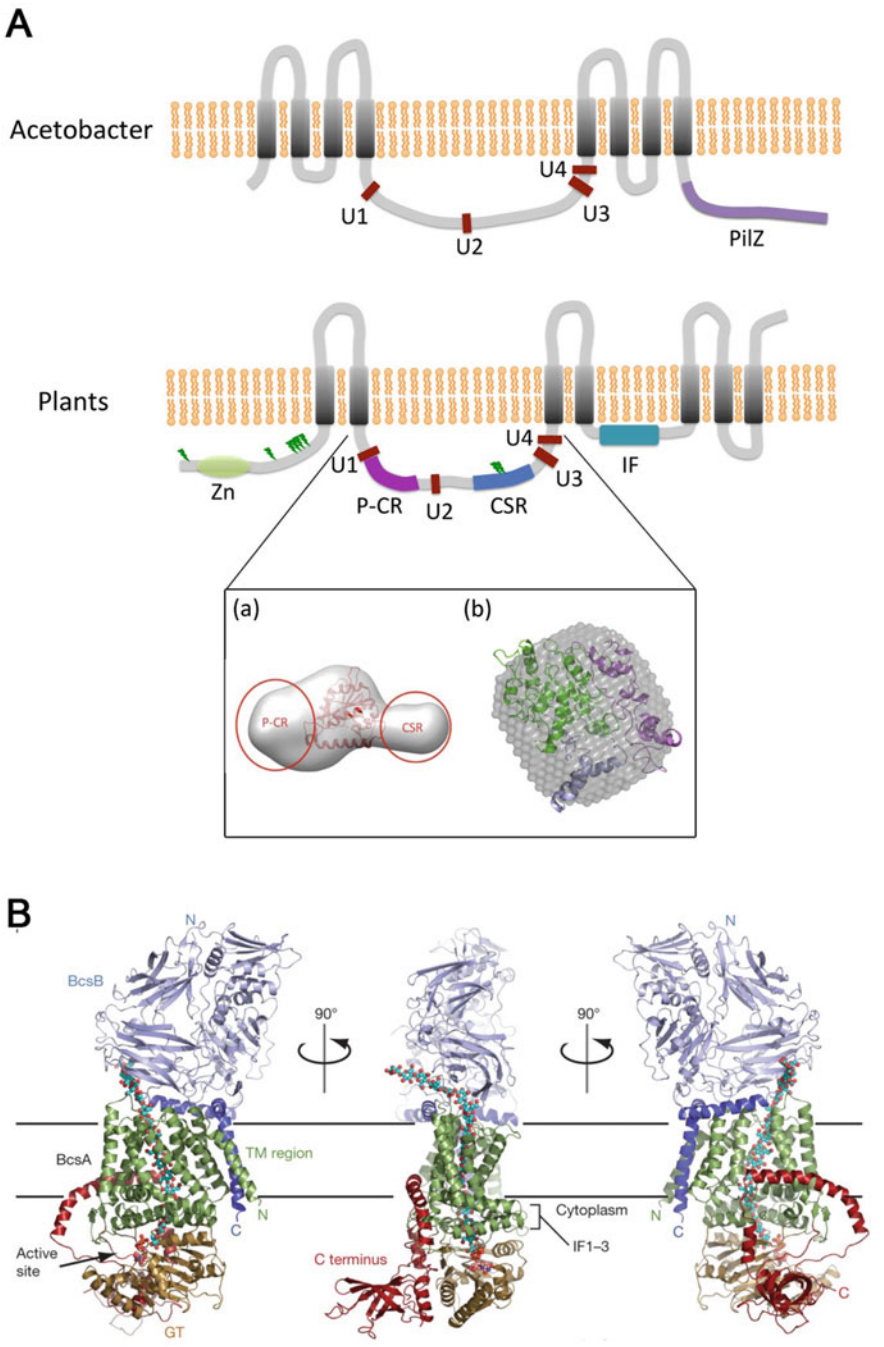

Fig. 7.1 Structures of plant and bacterial cellulose synthase. (**a**) Comparison of CESA protein structure from plants and bacteria. Domains shown by color blocks are transmembrane domains (TMD, black) and conserved regions (U1–U4, brown) present in both bacteria and plants; c-di-GMP recognition domain only present in bacteria (PiLZ, purple); domains unique for plants

synthesis in vitro (Omadjela et al. 2013). The groundbreaking discovery of crystal structure of bacterial BcsA-BcsB coincides with an effort to model plant CESAs. Modeling of the cytoplasmic catalytic domain of cotton CESA1 confirms the similarities between plant and bacterial CESAs and highlights the differences across different kingdoms (Sethaphong et al. 2013).

The N-terminal region of the CESA protein is predicted to be cytoplasmic, and it contains a short N-terminal region, a zinc finger domain that is predicted to be important for protein dimerization, and a variable region (Kurek et al. 2002). Between the second and the third TMDs lies several plant-specific signature regions. The first signature region is named the plant-conserved region (P-CR) that is highly conserved among all plant species. The second signature region was initially named hyper variable region (HVR) because of the lack of conserved sequences among few CESA genes identified at that time (Pear et al. 1996). It was later termed the class-specific region (CSR) as subgroups of CESA show strong sequence conservation in a class-specific fashion (Vergara and Carpita 2001). CSR region is highly variable among different CESA isoforms of the same species, while very conserved among CESA homologs, and is therefore suggested to control class-specific function of CESAs (Roberts and Roberts 2007). However, recent swap experiments between CSRs in distinct CESA classes in moss argue against the proposed class-specific function of CSRs (Scavuzzo-Duggan et al. 2018).

As bacterial CESAs do not have the plant-specific P-CR domain or CSR domain, recent studies have focused on these two regions (Fig. 7.1a). Molecular modeling of cotton CESA1 revealed that P-CR and CSR fold into distinct structures on the periphery of the GT domain (Sethaphong et al. 2013). The crystal structure of P-CR domain from rice CESA8 has recently been solved, which contains two antiparallel coiled-coil alpha-helices linked by a connecting loop (Rushton et al. 2017). Previous modeling of cotton CESA1 revealed that both the P-CR and CSR regions are composed of alpha helices (Sethaphong et al. 2013). A refined model of P-CR and CSR regions was presented by comparing six *Arabidopsis* CESA isoforms including AtCESA1, AtCESA3, AtCESA6, AtCESA4, AtCESA7, and AtCESA8. This study reveals a conserved structure of the P-CR region located at the periphery of the complex, while variable structures of the CSR region packed tightly in the interface of the homodimer (Sethaphong et al. 2016). Small-angle X-ray scattering study of the AtCESA1 central domain confirmed that the P-CR domain points outward to the cytosolic space and may be required for interacting with non-CESA proteins. However, the CSR region does not interact with the interfaces within the

Fig. 7.1 (continued) including zinc finger domain (Zn, light green); conserved region in plants (P-CR, pink) and class-specific region (CSR, blue); phosphorylation sites (lightning mark, green); and interfacial helix (IF, cyan) (modified from Li et al. 2012). Structures of the central domain of rice CESA8 (**a**, modified from Olek et al. 2014) and *Arabidopsis* CESA1 (**b**, modified from Vandavasi et al. 2016) were presented in the lower boxes. The P-CR and CSR regions are colored in violet and blue, respectively. (**b**) Crystallographic structure of the bacterial BcsA-BcsB complex. (Modified from Morgan et al. 2013)

homodimer. Instead, it is responsible for connecting neighbor CESA trimers to form cellulose synthase complexes (Vandavasi et al. 2016). In contrast to the trimer structure of CESA, solution structure of catalytic domain of rice CESA8 by small-angle X-ray scattering and crystallography favors the assembly of dimers (Olek et al. 2014). As CSR and P-CR domains flank the central catalytic core, the solution structure fits well with predicted model of dimerization of CESAs (Olek et al. 2014). However, both models are based on the structure of cytosolic domain excluding the TMDs; the structure of intact CESA remains to be elusive. Recent advances in single-particle cryo-electron microscopy (cryo-EM) and tomography offer unique opportunity to image larger CESA assemblies in lipid membrane.

7.2.2.1.2 Composition and Structure of the Cellulose Synthase Complexes (CSCs)

So far, the best characterized *CESA* genes are from the model plant *Arabidopsis thaliana* (Richmond 2000; Carroll and Specht 2011). The *Arabidopsis* genome encodes ten *CESA* genes (*CESA1-10*) (Richmond 2000). Genetic evidence, together with the spatial-temporal expression study of the *CESA* genes, has revealed that different *CESAs* are involved in the synthesis of different types of cell walls. It is widely accepted that *CESA1*, *CESA3*, and *CESA6* are required for the synthesis of PCWs; while *CESA4*, *CESA7*, and *CESA8* are involved in the formation of SCWs (Arioli et al. 1998; Fagard et al. 2000; Taylor et al. 2003; Persson et al. 2007b). It has also been shown that *CESA2*, *CESA5*, and *CESA9* have partially redundant functions with *CESA6*, while not much is known about the role of *CESA10* (Persson et al. 2007b; Kumar and Turner 2015). However, accumulating evidence suggests that the grouping of primary and secondary *CESAs* may not be as absolute. For instance, *CESA2*, *CESA5*, and *CESA9* are required for the secondary cell wall thickening in the radial cell walls of seed coat (Stork et al. 2010; Harpaz-Saad et al. 2011; Mendu et al. 2011). Moreover, *CESA1*, *CESA3*, and *CESA6* are important for the secondary cell wall deposition in the *Arabidopsis* shoot trichomes (Betancur et al. 2010). These results indicate that *CESAs* may play roles in either primary and/or secondary cell walls in specific cell types. Therefore, the traditional classification of primary and secondary *CESAs* may need to be modified. Further supporting the cross-functionality of primary and secondary CESAs, it has been reported that primary and secondary CESAs functionally substitutes each other in vivo. For example, CESA7 can partially rescue the growth defect of a *CESA3* mutant allele. Similarly, the *CESA8* knockout mutant phenotype can be complemented by the ectopic expression of CESA1 (Carroll et al. 2012).

CESAs, together with potential CESA-associated proteins, constitute the active unit for cellulose synthesis, namely, cellulose synthase complex (CSC). More than four decades ago, CSCs were visualized in algae by freeze-fracture electron microscopy and were described as “granules” that were attached to the end of nascent microfibrils (Robinson et al. 1972). Later, the granular structures were repeatedly observed in a variety of cellulose-producing species, including bacterium, green algae, and multiple higher plants (Herth 1983; Haigler and Brown 1986; Tsekos 1999). As they often

associated to the ends of microfibrils, these structures were therefore named "terminal complexes (TCs)" (Brown and Montezinos 1976; Brown et al. 1976). Closer visualization of the TCs revealed that they were hexameric rosette-like intramembrane compartments with diameter of 24 ± 2.5 nm (Giddings et al. 1980; Mueller and Brown 1980). Although the TCs had long been speculated as cellulose-producing complexes, their identity remained elusive until the late 1990s. Immunogold labeling of TCs using CESA antibodies confirmed that they are indeed cellulose synthase-containing complexes (Kimura et al. 1999). Composition and structure of CSCs is still hampered by difficulties in the isolation of native CSCs from plants despite the recent advance in structural determination by small-angle neutron scattering, small-angle X-ray scattering, and computational modeling. Many outstanding questions have been debated for decades and will remain to be addressed, e.g., how many CESAs does one CSC contain? Does each lobe represent homo- or hetero-CESAs? What is the arrangement pattern of CESAs within each CSC?

Based on the originally proposed 36-glucan-chain microfibril structure, the most popular CSC structural model depicts "hexamers of hexamers," where each of the six lobes contains six CESAs (Herth 1983; Perrin 2001; Doblin et al. 2002). However, accumulating evidence argues against the hexamers of hexamers model. Subsequent results from various plant species suggest that there are 18 to 24 glucan chains per elementary microfibril. Therefore, each CSC is composed of 18 to 24 CESAs, with 3 or 4 CESAs within each lobe ("hexamers of trimers" and "hexamers of tetramers," respectively) (Fernandes et al. 2011; Newman et al. 2013; Thomas et al. 2013; Oehme et al. 2015). Given that both primary and secondary cell wall CSCs hold a 1:1:1 stoichiometry (Gonneau et al. 2014; Hill et al. 2014), the "hexamers of trimers" model is preferred over the "hexamers of tetramers" model. Further supporting the hexamers of trimers model, a structural study of the *Arabidopsis* CESA1 central domain revealed self-assembly of CESAs into a stable homo-trimer (Vandavasi et al. 2016). However, the possibility of hetero-trimers cannot be ruled out. Nevertheless, triangular lobes were frequently observed by direct visualization of the *Physcomitrella* CSC rosettes using transmission electron microscopy (Nixon et al. 2016). A recent quantitative proteomic study revealed that stoichiometry varies in different plant species and/or in different tissues of the same species (Zhang et al. 2018). The stoichiometry was 1:1:1 in developing xylem of Norway spruce as previously observed in *Arabidopsis* stem. The stoichiometry in the angiosperm aspen shifted from 3:2:1 in the developing xylem to 8:3:1 in tension wood, arguing for an alternative model in addition to the hexamers of trimmers model.

7.2.2.1.3 Localization and Dynamics of the CSCs

Fluorescent protein (FP) tagging, as well as the innovative fluorescence microscopy techniques, greatly advanced the visualization and characterization of plant CSCs. Unlike the traditional electron microscopy, which requires fixation of plant tissues, confocal laser scanning microscopy enables the real-time visualization of FP-tagged CSCs in living cells. So far, multiple FP-tagged CESA proteins from different plant

species, both from the primary and secondary cell walls, have been visualized via live-cell imaging. In the epidermal cells of *Arabidopsis* hypocotyls, the FP-tagged CESAs localize in various subcellular locations, including Golgi apparatus, post-Golgi compartments, and the plasma membrane, which is consistent with previous freeze-fracture studies (Giddings et al. 1980; Haigler and Brown 1986). The observation that CSCs exist not only at the plasma membrane but also in the Golgi cisternae and vesicles is consistent with the widely accepted hypothesis that the CSCs are assembled in Golgi and then are transported from the Golgi apparatus to the plasma membrane. CSCs synthesize cellulose only after they are successfully integrated into the plasma membrane. Therefore, the dynamics of CSCs at the plasma membrane has been intensely studied in the last decade. During the synthesis of PCWs, the CSCs move bi-directionally at the plasma membrane, following linear trajectories co-aligned with the cortical microtubules (Paredez et al. 2006) (Fig. 7.2). The dynamics of primary cell wall CSCs in different plant species have been evaluated and reported by multiple research groups. In the *Arabidopsis* hypocotyls, the average velocity of moving CSC particles is between ~250 nm/min and ~350 nm/min, which is comparable to the CSC velocities in the model grass *Brachypodium distachyon* and in *Physcomitrella patens*, a moss model organism (Paredez et al. 2006; DeBolt et al. 2007; Desprez et al. 2007; Li et al. 2016; Liu et al. 2017; Tran et al. 2018). It is estimated that average velocity of CSCs corresponds to the addition of 300–1000 glucose residues per minute, roughly a third of the first estimate of cellulose synthesis rate in algae (Reiss et al. 1984).

Unlike the primary cell wall CSCs, which can be easily visualized in the epidermal cells of the *Arabidopsis* seedlings, the investigation of CSC dynamics during secondary cell wall synthesis has been hindered. Secondary cell wall synthesizing cells in vasculature and fiber cells are buried deep within plant tissues that are beyond normal working distance of confocal microscopy (Wightman et al. 2009). Recently, FP-tagged CESA7 was expressed in an in vivo inducible system, where the formation of secondary cell walls was ectopically induced in the epidermal cells (Yamaguchi et al. 2010; Watanabe et al. 2015; Li et al. 2016). It is reported that during the synthesis of secondary cell wall, the CSCs are more densely distributed at the plasma membrane and move slightly faster than that of CSCs in the primary cell walls (Watanabe et al. 2015; Li et al. 2016). The crowding of CSCs during secondary cell wall biosynthesis may be attributed by the elevated rate of CSC delivery (Li et al. 2016). Moreover, instead of evenly distributed bi-directional movement (as that in the primary cell wall), secondary cell wall CSCs exhibit directionally coherent movement along a single linear track (Li et al. 2016). The differences in the CSC distributions and dynamics possibly underline the differential microfibril organizations and mechanical characteristics between primary and secondary cell walls.

7.2.2.2 Non-CESA Proteins that Are Associated with CSCs

Aside from CESAs, multiple non-CESA proteins were identified as integral or peripheral components of CSCs (Somerville 2006; Li et al. 2014). The cellulose synthase interactive protein 1 (CSI1)/POM-POM2 is the first interactive

partner of CESAs identified in higher plants. CSI1 not only physically interacts with the central domain of multiple primary CESAs but also directly binds to in vitro-polymerized microtubules (MTs). In living cells, FP-tagged CSI1 co-localized with CSCs at the plasma membrane and moved along trajectories that were underlined by the cortical microtubules. In the *csi1* null mutants, the CSC-MT alignment was abolished, leading to swelling etiolated hypocotyls and right-handed torsion of light-grown inflorescence stems (Landrein et al. 2013). These data suggest that that CSI1 serves as a physical linker between CSCs and cortical microtubules (Gu et al. 2010; Gu and Somerville 2010; Bringmann et al. 2012; Lei et al. 2012; Li et al. 2012; Landrein et al. 2013). In addition to its plasma membrane localization, the CSI1 protein also localized in small CESA compartments (SmaCCs) or microtubule-associated cellulose synthase compartments (MASCs) (Crowell et al. 2009; Gutierrez et al. 2009; Bringmann et al. 2012; Lei et al. 2015). Further studies indicate that CSI1 is required for the formation of SmaCCs/MASCs, and this association is important for plants to regulate cellulose synthesis through fast recycling of CSCs to the plasma membrane under abiotic stress (Lei et al. 2015). A recent proteomic analysis of microtubule-associated proteins in *Arabidopsis* tracheary elements showed that CSI1 is enriched during SCW formation, indicating its role in SCW biosynthesis (Derbyshire et al. 2015). Supporting this hypothesis, CSI1 proteins associate with both secondary CSCs and microtubules during xylem vessel development. Moreover, mutation of CSI1 led to aberrant xylem vessel patterns in *Arabidopsis* (Schneider et al. 2017). However, null mutant of *csi1* had no deficiency in crystalline cellulose content in stems nor did it exhibit typical xylem defect exemplified as irregular xylem in secondary *cesa* mutants (Gu and Somerville 2010), suggesting that either xylem vessel patterns are not important for cellulose synthesis or additional players are involved in regulating cellulose synthesis in SCWs.

There are two CSI1-like genes encoded by the *Arabidopsis* genome, *CSI2* and *CSI3*, both of which share over 60% sequence similarity of CSI1 (Gu and Somerville 2010; Lei et al. 2013). There is no functional study of CSI2, as promoter-GUS analysis revealed no expression in *Arabidopsis*. In contrast, CSI3 is widely expressed in various tissues. Observation of CSI3 in living cells showed that CSI3 associated with both CSCs and microtubules and it shared about 50% of co-localization ratio with CSI1. Moreover, the *csi1 csi3* mutants show enhanced growth defect than that of the *csi1* mutants, whereas *csi3* mutants had no detectable phenotype. These data indicate that CSI3 might play a distinct role from CSI1 in the regulation of cellulose biosynthesis (Lei et al. 2013).

The cellulose synthase companion proteins (CC1 and CC2) were shown to associate with both CSCs and microtubules (Endler et al. 2015, 2016). Unlike CSI1, the CC proteins do not directly affect co-alignment between CSCs and microtubules. Loss of CC1 and CC2 function impaired the plant's resistance to adverse conditions, due to severe instability of microtubules. When treating wild-type plants with salt stress, CC1 was observed to remain associated with CSCs in SmaCCs/MASCs; and it also accompanies the delivery of CSCs to the plasma membrane. Moreover, the N-terminus of CC1 was shown to promote microtubule

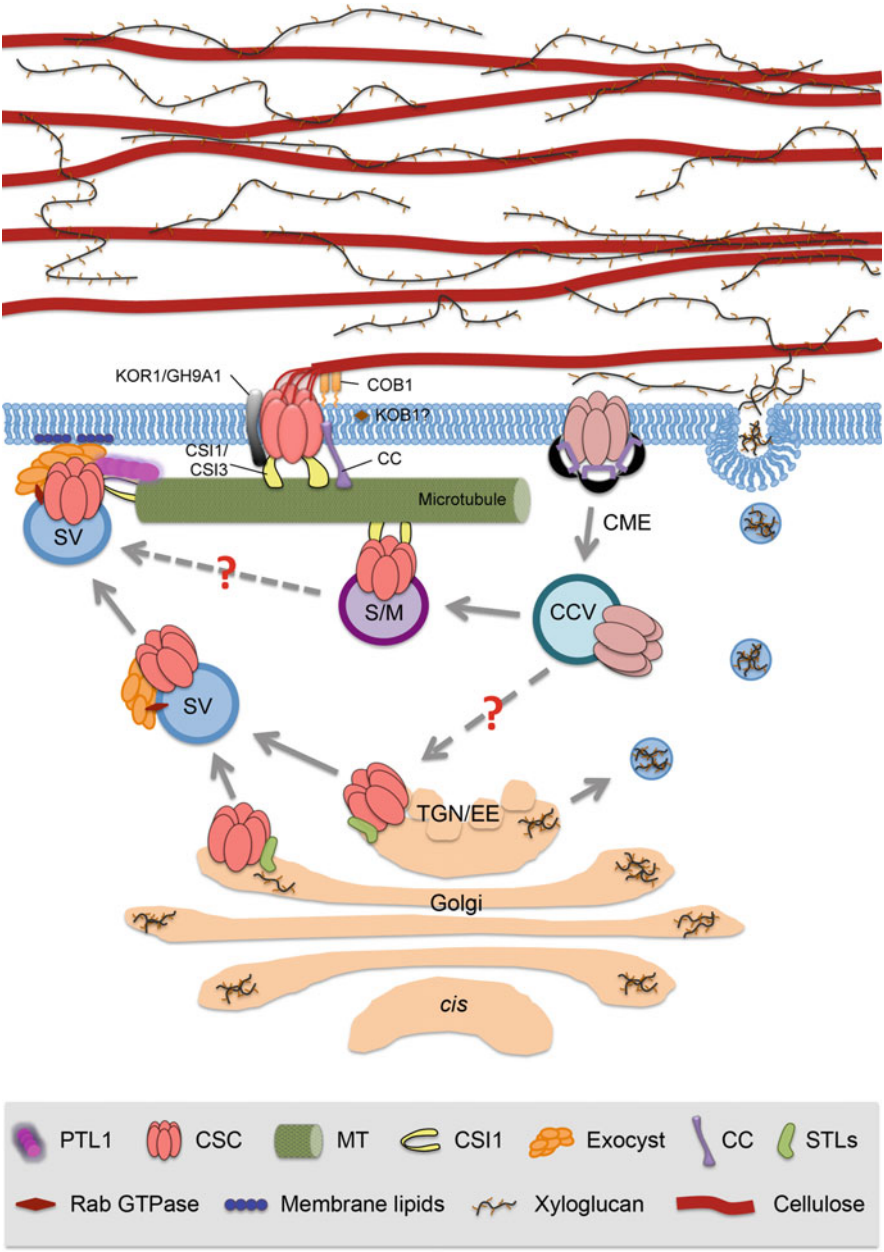

Fig. 7.2 A schematic model depicts the delivery and synthesis of cellulose and xyloglucan in primary cell walls. Cellulose microfibrils are synthesized by plasma membrane localized cellulose synthase complexes (CSCs). Proteins associated with CSCs include Companions of Cellulose synthase (CC), COBRA1 (COB1), Cellulose Synthase Interacting Protein 1/3 (CSI1/CSI3), KOBITO1 (KOB1), and KORRIGAN1/Glycosyl Hydrolase Family 9 Class A1 (KOR1/GH9A1), STELLOs (STLs). Newly synthesized CSCs are transported via Golgi- or TGN/EE-derived secretory vesicles (SVs), which are tethered to the plasma membrane by the exocyst complex and directed to the site of cortical microtubules by CSI1. PATROL1 (PTL1) facilitates the fusion of SVs with the plasma membrane, which enables incorporation of CSCs to the plasma membrane. Inactivated or faulty CSCs are internalized into clathrin-coated vesicles (CCVs) via clathrin-mediated endocytosis (CME) followed by fast recycling via SmaCCs/MASCs (S/M). Xyloglucan is synthesized in Golgi and delivered to plasma membrane via secretory vesicles derived from TGN

formation via its direct interaction with microtubules. Therefore, it is proposed that the CCs function in supporting the stability of microtubules and CSCs under stress conditions (Endler et al. 2015).

KORRIGAN1 (KOR1) encodes a putative membrane-bound β-1,4-endoglucanase (Nicol et al. 1998; Liebminger et al. 2013). Mutations of *KOR1* led to defects in both primary and secondary cell wall organization, reflected by short and swelling roots, abnormal cytokinesis, and collapsed xylem (Nicol et al. 1998; Zuo et al. 2000; Sato et al. 2001; Szyjanowicz et al. 2004; Takahashi et al. 2009). Different from CSI1, KOR1 co-localized not only with CSCs at the plasma membrane but also in Golgi and other endosomal compartments (Lei et al. 2014; Vain et al. 2014). Moreover, in vitro protein pull-down assay showed that KOR1 interacted with both primary and secondary CESAs (Lei et al. 2014). Despite the tight association with CSCs, the precise function of KOR1 remains unclear. It was proposed that KOR1 might involve in microfibril ordering/organization, cleavage of the cellulose synthesis primer, or removal of CSCs from the terminal of microfibrils (Nicol et al. 1998; Molhoj et al. 2002). A subsequent study showed that KOR1 is required for the organization of microtubules and cellulose microfibrils (Lei et al. 2014). In a *KOR1* mutant allele where the endoglucanase activity was predicted to be abolished, mutant seedlings showed disorganized cortical microtubules and abrupt kinks in cellulose microfibrils (Lei et al. 2014). As mutation in KOR1 does not affect the co-alignment between CSCs and microtubules, it is possible that the defects in both cellulose microfibrils and microtubules reflect a feedback regulation between cell wall and the cytoskeleton.

Two Golgi-localized proteins, STELLO1 and STELLO2 (STL1 and 2), were shown to interact with CESAs (Zhang et al. 2016b). Disruption of both STL1 and STL2 genes led to dwarf primary roots, etiolated hypocotyls, and adult plants. The *stl1stl2* mutant also had reduced cellulose content in both primary and secondary cell walls. Live cell imaging revealed that the Golgi localization, delivery rate, and plasma membrane motility of CESAs were significantly impaired in the *stl1stl2* mutant. Moreover, blue-native polyacrylamide gel electrophoresis analysis of microsomes from seedlings or plant stems showed that the *stl1stl2* mutant had substantially reduced protein bands at high molecular weight indicating that CSC assembly was affected by the loss of STL1 and STL2. Therefore, it is proposed that STLs impacts the secretion and activity of CSCs via regulating CSC assembly (Zhang et al. 2016b).

Additional proteins play important roles in the regulation of cellulose production, although not necessarily interact with CESAs directly. For example, COBRA1 (COB1), a glycosyl-phosphatidyl inositol-anchored protein, was found to be required for the regulation of cellulose microfibril orientation (Schindelman et al. 2001; Roudier et al. 2005). A member of COBRA family COBRA-Like 4 (COBL4) is expressed during SCW formation. Mutations in COBL4 showed a severe cellulose-deficient phenotype in *Arabidopsis* and maize, consistent with that *COBRA* gene family plays an important but as yet undetermined role in cellulose synthesis (Brown et al. 2005; Sindhu et al. 2007). Furthermore, a kinesin-like protein, named FRA1, is known to play a role in the regulation of oriented deposition

of cellulose microfibrils. The *fra1* mutants show abnormal organization of cellulose microfibrils, which resulted in reduced mechanical strength in fiber cells. It is therefore proposed that FRA1 is required for the control of cellulose microfibril organization via its interactions with microtubules (Zhong et al. 2002). Random cellulose microfibril orientation was observed in mutants of the *KOBITO1* (*KOB1*) gene, which eventually resulted in incomplete cell walls, mimicking the phenotype of *prc1-1*, a mutant allele of *CESA6*. FP-KOB1 localizes to the plasma membrane in elongated epidermal/cortical cells. However, the precise function of KOB1 requires further investigations (Pagant et al. 2002; Lertpiriyapong and Sung 2003; Brocard-Gifford et al. 2004; Kong et al. 2012).

7.2.3 Regulations of Cellulose Biosynthesis

7.2.3.1 Regulation of the CESA

7.2.3.1.1 Transcriptional Regulation of CESA Levels

As every plant cell is engaged by cell walls, *CESAs* are expressed in various cell types throughout different developmental stages (Hamann et al. 2004; Persson et al. 2005). Multiple transcription factors have been shown to function in the transcriptional regulation of cellulose synthesis-related genes. During secondary cell wall synthesis, a group of closely related NAC domain transcription factors, including the Secondary Wall-associated NAC Domain Protein (SND1), the NAC Secondary Wall Thickening Promoting Factor 1 (NST1), Vascular-related NAC-domain 6 (VND6), and Vascular-related NAC-domain 7 (VND7), function as the first-level master switches, which directly regulate the expression of downstream transcription factors (Zhong et al. 2006, 2010; Mitsuda et al. 2007; Mitsuda and Ohme-Takagi 2008). The second-level master switches include MYB46, MYB83, and their close homologs. Supporting their role in the regulation of secondary cell wall synthesis, simultaneous mutation of *MYB46* and *MYB83* led to mechanistic defect in secondary cell walls and collapse of vessel cells (Zhong et al. 2007; McCarthy et al. 2009). The complexity of transcriptional network controlling cellulose and lignin synthesis is nicely reviewed elsewhere (Wang and Dixon 2012; Zhong and Ye 2014).

The expression of *CESA* genes can also be affected by the synthesis of plant hormones. CESA genes were transcriptionally regulated by brassinosteroid (BR) (Xie et al. 2011; Schrick et al. 2012). Reduced BR level resulted in deficient cellulose deposition. Overexpression of the BR receptor, *BRI1,* partially rescued the growth defect of primary *cesa* mutants. Moreover, the chromatin immunoprecipitation (ChIP) data showed that BES1, the BR-associated transcription factor, associated with upstream elements of most *CESA* genes (Xie et al. 2011).

7.2.3.1.2 Posttranscriptional Modulations of CSCs

Phosphorylation represents the most well-studied posttranscriptional modification of CESAs. Phosphoproteomics studies of the *Arabidopsis* plasma membrane proteins in response to the bacterial elicitor flagellin revealed multiple phosphorylation sites within CESA1, CESA3, and CESA5. The majority of phosphorylation sites were located at the N-terminal cytosolic region (Nuhse et al. 2004; Benschop et al. 2007). There are six phosphorylation sites on CESA1 (S162, T165, T166, S167, S686, and S688), which are clustered in two of the hyper variable regions that are presumably not essential for CESA's catalytic activities (Nuhse et al. 2004). Phospho-ablative and phospho-mimic mutants of CESA1 resulted in abnormal cell expansion in elongating roots and hypocotyls. Moreover, in contrast to bi-directional motility of CSCs, phospho-mutants of CESA1 had asymmetric motility along microtubule tracks. Interestingly, the disruption of symmetry in CSCs motility could be rescued by the application of oryzalin, a drug that depolymerizes microtubules. This indicates that phosphorylation of CESA1 in those non-catalytic sites might be required for the CSC-microtubule coordination (Chen et al. 2010). Brassinosteroid insensitive 2 (BIN2) specifically phosphorylates CESA1 peptide containing a phosphor-primed residue pS162. The phosphorylation of CESA1 by BIN2 relies on residue T157 as BIN2 was not able to phosphorylate pS162 T157A variant peptide in vitro. Transgenic line containing T157A bypasses the BIN2-mediated negative regulation of cellulose synthesis, which supports a role of BIN2 in regulating CSC activity (Sanchez-Rodriguez et al. 2017).

CESA5 is the closest isoform of CESA6 and is a putative CESA6 redundant protein. While different from CESA6, which contains no detectable phosphorylation sites via phosphoproteomics study, CESA5 is phosphorylated at the N-terminal hypervariable region at four sites: Ser122, Ser126, Ser229, and Ser230. FP-CESA5 had reduced motility in the *CESA6* mutant line, *prc1-1*. However, the CSC motility could be rescued by a phosphor-mimic version of CESA5. Additionally, destabilization of microtubules attenuated the CSC motility defect in *prc1-1*, which further supports the hypothesis that phosphorylation of CESAs is a key factor for the CSC-microtubule interaction (Bischoff et al. 2011).

Phosphorylation sites have also been identified by mass spectrometry in secondary cell wall CESAs. CESA4 is phosphorylated at one site, and CESA7 is phosphorylated at two serine residues. All of these sites were located in the non-conserved region. Interestingly, incubation of the phosphorylation site-containing region of CESA7 with plant extracts led to its degradation via a proteasome-dependent pathway, indicating that phosphorylation of CESA7 is required for its targeted degradation, which is potentially a mechanism to regulate overall protein levels of CESAs (Taylor 2007).

Recent studies have revealed that S-acylation of CESAs is an important mechanism to regulate localization of CESAs (Kumar et al. 2016). Both CESA1 and CESA3 were shown to be S-acylated in plants (Hemsley et al. 2013). Utilizing the acyl-resin-assisted capture assay, it was shown that S-acylation occurred in both primary and secondary CESAs. Mutational analysis of CESA7 revealed that the acylation of four cysteine residues at the variable region 2 (VR2) and two cysteine

residues at the C-terminus (CT) was important. Mutations of either VR2 or CT cysteine residues led to decreased cellulose deposition. Live-cell imaging revealed that loss of acylation at these sites affected localization of CSCs at the plasma membrane. It is proposed that the S-acylation of CESAs facilitates the partitioning of CESAs into microdomains, which further promotes protein localization in the same protein complex.

7.2.3.2 Trafficking of the CSC Complex

7.2.3.2.1 Endocytosis

As cellulose is produced by the plasma membrane-localized CSCs, to allow normal cellulose deposition for plant growth, the homeostasis of CSCs on the cell surface has to be strictly regulated. Specifically, as CSCs are delivered to the plasma membrane, deactivated or faulty CSCs have to be removed from the plasma membrane via endocytic pathways (Fig. 7.2). It has been proposed that the endocytosis of CSCs is via clathrin-mediated endocytosis (CME), which is the best-characterized endocytosis pathway in eukaryotes. Via a yeast two-hybrid screen, it was discovered that the *Arabidopsis* μ2/AP2M protein, a component of the adaptor protein 2 (AP2) complex, can directly interact with CESA6. In living cells, μ2/AP2M transiently co-localizes with both clathrin light chain (CLC) and the CSCs. Further supporting its role in CSC endocytosis, loss of the μ2/AP2M function led to defect in CSC internalization, reflected by increased density of CSCs at the plasma membrane (Bashline et al. 2013, 2014).

A follow-up study revealed that the TWD40-2 protein, a putative component of the newly characterized TPLATE complex (TPC), is also required for the endocytosis of CESAs (Gadeyne et al. 2014; Bashline et al. 2015). Many TPC mutations are lethal, indicating their essential role for plant growth. A knockdown mutant allele of the *Arabidopsis TWD40-2* made functional characterization of TWD40-2 possible. More importantly, double mutant of *twd40-2-3 ap2m-1* was generated to test the genetic interaction between TPC and CME components. Simultaneous disruption of *TWD40-2* and *μ2/AP2M* led to enhanced growth defect. By live-cell imaging, it was shown that TWD40-2, μ2/AP2M, and CLC transiently co-localized in distinct punctate in cortex, indicating that they function cooperatively in the CME process. However, TWD40-2 might play a different role from that of μ2/AP2M, as mutations of *TWD40-2* and *μ2/AP2M* affected the plasma membrane CLC densities and lifetimes in different ways. Single mutants of *TWD40-2* and *μ2/AP2M* showed differential defects in plant growth and cellulose content. Moreover, the plasma membrane CSC densities were increased in both *twd40-2-3* and *ap2m-1* mutants. However the CSC motilities were decreased only in twd40-2-3 mutant, but not in *ap2m-1* mutant (Bashline et al. 2015). All these data suggest that TWD40-2 and AP2M play distinct but coordinated roles in the CME process of CSCs. Further studies are needed to decipher the precise role of TWD40-2 in CME.

7.2.3.2.2 Exocytosis

It is generally accepted that CSCs are assembled in the Golgi and are delivered to the plasma membrane via secretory vesicles. We know very little about how CSC-containing vesicles are delivered to the plasma membrane, which factors mediate the vesicle fusion process, and how CSCs are integrated into the plasma membrane. Multiple lines of evidence have shown that the cytoskeleton plays important roles in the trafficking of CSC-containing secretory vesicles (Crowell et al. 2009; Gutierrez et al. 2009; Sampathkumar et al. 2013). The cortical microtubules direct the delivery position of CSC-containing vesicles at the plasma membrane, while actin affects the regulation of CSC-containing Golgi bodies via its involvement in cytoplasmic streaming. Accumulating evidence suggests that the cortical microtubules not only guide the movement of plasma membrane CSCs but also function as landmarks for the delivery of CSCs to the plasma membrane. CSC-containing Golgi bodies are frequently observed to pause on cortical microtubules, which coordinate with CSC insertion to the plasma membrane (Crowell et al. 2009). Utilizing the fluorescence recovery after photobleaching (FRAP) technology, which enables the visualization of newly delivered CSC particles, it was shown that the CSCs were often inserted to positions underlined by cortical microtubules (Gutierrez et al. 2009). Different from microtubules, the actin filaments are not directly involved in the insertion of CSCs to the plasma membrane. However, defect of actin organization led to reduction in Golgi motility, as well as accumulation of post-Golgi compartments. This subsequently resulted in significant reduction in the delivery rate of CSCs, which caused growth defect that mimics cellulose synthesis-related mutants, reflected by abnormal cell wall morphology and reduced cellulose deposition (Sampathkumar et al. 2013).

So far, the only CSC-specific post-Golgi vesicles that have been characterized are called SmaCCs/MASCs (Crowell et al. 2009; Gutierrez et al. 2009). The SmaCCs/MASCs often associate with the depolymerization ends of microtubules, and their occurrences often associate with the delivery of CSCs to the plasma membrane. It is therefore proposed that the SmaCCs/MASCs function in assisting the delivery of CSCs to the cortical microtubules (Gutierrez et al. 2009). However, it is intriguing that the population of SmaCCs/MASCs is very small in actively elongating cells. The active cell elongation presumably requires fast delivery of large amount of newly synthesized CSCs and possibly rapid turnover of plasma membrane CSCs. In contrast, the frequency of SmaCCs/MASCs is much higher in cells that are approaching the end of their elongation. Therefore, it is possible that the SmaCCs/MASCs is only required for the secretion of specific population of CSCs under certain conditions; while the massive secretion of CSCs is via other exocytic pathways. Formation of SmaCCs/MASCs can be induced by osmotic stress or perturbation of cellulose synthesis. These observation lead to the hypothesis that SmaCCs/MASCs might function as storage vesicles for the massively internalized CSCs under stress conditions (Wightman and Turner 2010). Consistently, it has been shown that the integrity of CME machinery is required for the formation of SmaCCs/MASCs (Lei et al. 2015).

A subsequent study revealed that CSI1 is required for the fast recycling of CSCs to the plasma membrane after stress release (Lei et al. 2015). When treated with isoxaben, a herbicide that can specifically inhibit cellulose synthesis (Scheible et al. 2001; Desprez et al. 2002), the CSCs in wild-type seedlings were cleared from the plasma membrane and were temporarily retained in SmaCCs/MASCs (Crowell et al. 2009; Gutierrez et al. 2009). After washing out of isoxaben, the CSCs can be quickly recycled back to the plasma membrane. However, in the *csi1* mutants, the SmaCCs/MASCs cannot be induced by isoxaben treatment; and the plasma membrane CSCs can no longer be efficiently recovered after isoxaben is washed out (Lei et al. 2015). These observations further support that SmaCCs/MASCs act as storage vesicles for rapid internalization and recycling.

If SmaCCs/MASCs do not control massive secretion of CSCs, what other players could be involved? In eukaryotes, the central component for polarized exocytosis is a protein complex called the exocyst complex. Yeast, mammals, and plants have eight conserved exocyst complex subunits: Sec3, Sec5, Sec6, Sec8, Sec10, Sec15, Exo70, and Exo80 (Brennwald and Rossi 2007; Hala et al. 2008; He and Guo 2009; Heider and Munson 2012; Polgar and Fogelgren 2017). By interacting with downstream small GTPases, the exocyst functions in tethering the secretory vesicles to the target membranes. In plants, the genes encoding the exocyst subunits are greatly duplicated, in particular for *Exo70* gene (Cvrckova et al. 2012). The possibility of a large number of distinct exocyst complexes in plants is compatible with the versatility and plasticity of plant life. The exocyst complex has been speculated to mediate the insertion of CSCs to the plasma membrane (Bashline et al. 2014). Supporting this hypothesis, the *Exo70A1* gene has been reported to play a role in the secondary cell wall deposition by mediating vesicle trafficking in the *Arabidopsis* tracheary element (TE) (Wang et al. 2013a). In the *Arabidopsis* TEs, multiple exocyst subunits were localized to the sites of SCW thickening; and they consistently associated with cortical MTs throughout the differentiation process of TEs. Moreover, the exocyst subunit Exo84b is important for the proper localization of CESA7 (Vukasinovic et al. 2017).

Although circumstantial evidence has suggested that the CSCs could be secretory cargo of the exocyst-mediated exocytosis, how exocyst complex-mediated exocytosis is involved in cellulose synthesis remained elusive. In an affinity purification of CSCs in *Arabidopsis* plants, multiple exocyst subunits were co-precipitated with CSCs (Zhu et al. 2018). Direct interactions between CESA and exocyst subunits were confirmed via in vitro pull-down assays. Coincidently, exocyst subunits were also co-purified with CSI1 in a parallel affinity purification. Abolishment of the exocyst function significantly reduced the delivery rate of CSCs to the plasma membrane, which resulted in deficient cell growth and insufficient cellulose deposition. Moreover, FRAP assay showed that newly delivered CSCs were accompanied by the tethering of exocyst complex. All these data suggest that the secretion of CSC-containing vesicles depends on exocyst complex-mediated exocytosis.

Aside from the exocyst complex, a protein named PATROL1 (PTL1) also showed high affinity to the CSI1 protein (Zhu et al. 2018). Interestingly, PTL1 also interacted with a core subunit of the exocyst complex, Sec10. Similar to the exocyst subunits, mutation of PTL1 affected delivery of CSCs to the plasma

membrane. However mutation of CSI1 did not affect the delivery rate but affected the tethering of CSC's delivery to the MTs (Bringmann et al. 2012; Zhu et al. 2018). It is therefore proposed that the exocyst complex, PTL1, and CSI1 cooperate in the secretion of CSCs to the plasma membrane. Specifically, the exocyst and PTL1 are required for tethering/fusion of CSCs to the target membrane, while the CSI1 proteins serve as landmarks on the microtubules to define the position of secretion. PTL1 contains a MUN domain that shares limited sequence similarity (8%) to MUN domain in Munc13, a protein involved in vesicle fusion in mammals (Hashimoto-Sugimoto et al. 2013). In contrast to Munc13, PTL1 does not contain calmodulin-binding domain, C1 and C2 domain. However PTL1 has a plant-specific domain of unknown function 810 (DUF810), which is not present in animal or yeast. It remains to be determined whether PTL1 shares a similar role as Munc13 or has a plant-specific function in vesicle fusion.

7.2.4 Organization of Cellulose Microfibrils

The exact number of glucan chains within a single microfibril and the organization of glucan chains in native cellulose microfibrils have been much debated. Assuming that one CSC synthesizes an elementary microfibril and each CESA synthesizes one glucan chain, a 36-chain model is widely cited (Scheible et al. 2001). However, re-examining the structure of cellulose microfibrils using small-angle neutron scattering (SANS), wide-angle X-ray scattering (WAXS), and solid-state nuclear magnetic resonance (ssNMR) suggests a different model of either 18 chain or 24 chain. Utilizing these tools, multiple groups have examined the structure of cellulose microfibrils from a variety of species, including tunicate, *Cladophora*, *Arabidopsis*, mung bean, and spruce (Fernandes et al. 2011; Newman et al. 2013; Thomas et al. 2013; Wang and Hong 2016). As each study uses different techniques to determine the structure of cellulose microfibril from different species in two types of cell walls, no agreement has been reached. An elementary cellulose microfibril contains at least 18 glucan chains, and two 18-chain can stack to form a 36-chain microfibril (Fernandes et al. 2011; Newman et al. 2013; Thomas et al. 2013; Cosgrove 2014). SANS and WAXS data from spruce wood favor a 24-chain model, but it could not exclude an 18-chain model. Both 18-chain and 24-chain models can be fitted in the recent atomic force microscopy (AFM) measurements of native hydrated onion cell walls, which shows an average 3.5 nm diameter of single cellulose microfibril (Zhang et al. 2016a). While 24-chain model represents best-fit model, it is unlikely that the 24-chain model holds true for different plant species or different tissues of the same species.

Parallel with the debate on numbers of glucan chains within each microfibril, there has also long been a question for the composition of CSCs rosettes. Although studies of primary and secondary CSCs both suggest a 1:1:1 ratio stoichiometry, where same numbers of three different CESA isoforms exist in a single lobe of the CSC rosette, the exact number of CESAs within each lobe remains uncertain (Taylor 2008; Hill et al. 2014). A recent computational study in combination with freeze

fracture electron microscopy (FF-TEM) images of moss (*Physcomitrella patens*) rosette CSCs suggests that one CSC rosette is composed of 18 CESAs (Nixon et al. 2016). Moreover, it has been shown that heterologously expressed CESA isoforms can synthesize cellulose microfibrils in vitro in both *Physcomitrella* and *Populous*, indicating that single CESA isoform is sufficient for catalyzing the polymerization of glucan chains (Cho et al. 2015, 2017; Purushotham et al. 2016). Although to what extent the heterologously polymerized microfibrils are comparable to the native cellulose microfibrils remains to be shown, these observations, together with the 18 CESAs model, seem to favor the hypothesis that a single microfibril is composed of 18 glucan chains (Nixon et al. 2016).

7.3 Biosynthesis and Regulation of Hemicelluloses

Hemicelluloses represent an essential group of cell wall polysaccharides that can be found in both PCWs and SCWs. Hemicelluloses act as an adhesive layer between cellulose microfibrils that control microfibril movement during growth and in response to external forces. Hemicelluloses make about one-third of total dry mass of cell walls. However, the composition and distribution of hemicelluloses vary greatly in different species and cell types. In contrast to cellulose, hemicelluloses are much easier to extract. Most hemicelluloses can be extracted by alkali treatment. Therefore, both the abundance and availability of hemicelluloses enable its utilization for industrial products such as food additives and chemicals.

7.3.1 Structure and Distribution of Hemicelluloses

Unlike cellulose, which consists of repeating disaccharide unit, hemicelluloses are joint names for a group of heterogeneous polysaccharides that generally have a β-(1,4)-linked backbone. There are four major groups of hemicelluloses: xyloglucans (XyG), xylans, mannans and glucomannans, as well as mixed-linkage glucans (MLGs) (Scheller and Ulvskov 2010). As the structure, distribution, and biochemical properties vary greatly among different groups of hemicelluloses, separate discussions will be presented for each group.

7.3.1.1 Xyloglucan (XyG)

XyGs are found in all land plants and are the most abundant hemicelluloses in PCWs of dicots and non-commelinid monocots (Scheller and Ulvskov 2010). XyGs were first identified as a seed storage biopolymer (Kooiman 1957). XyG has a β-(1,4)-linked glucan backbone that is identical to cellulose (Hayashi 1989). To conveniently describe the structure of XyGs, unbranched glucose residues are denoted as "G." Frequently, the O-6 positions on the backbone are substituted by D-xylosyl residues and are denoted as "X." The xylosyl residues can be further linked with a D-galactosyl residue or L-arabinose residue at the O-2 position, which are named "L side chain" or

"S side chain," respectively. The O-2 position of the galactosyl residue can also be substituted by an L-fucosyl residue and is denoted as "F" (Tuomivaara et al. 2015). Variations in side chain compositions determine the branching patterns of XyG, which have both functional and taxonomic significance (Schultink et al. 2014; Tuomivaara et al. 2015). Differential residue substitution patterns led to great diversity of XyGs in land plants. In land plants, the most common repeating units in XyGs are XXXG or XXGG. XXXGs constitute XyGs in dicots and some non-graminaceous monocots, whereas the less branched XXGGs are mostly found in the XyGs of graminaceous monocots, the Solanales, and some mosses (Fry et al. 1993).

7.3.1.2 Xylan

Xylan is the most abundant hemicelluloses in SCWs of dicots, as well as in the PCWs of commelinid monocots. The land plant xylans are characterized by a β-(1,4)-liked xylose backbone. The diversity of xylan compositions comes from variable substitutions of the xylose residues with acetyl, glucuronic acid (GlcA), 4-*O*-methylglucuronic acid (Me-GlcA), and arabinose residues (Rennie and Scheller 2014). A common modification of xylans is residual substitution by α-(1,2)-linked GlcA and MeGlcA. Xylans with this type of modification are named glucuronoxylan (GX). Most xylans, especially those in dicot secondary cell walls, are acetylated to various degrees (Ebringerova et al. 2005). Xylans contain *O*-acetyl groups, α-(1,2) and/or α-(1,3)-linked arabinose residue substitutions, as well as GlcA/MeGlcA, and are known as glucuronoarabinoxylans (GAX). Arabinoxylan (AX) is another type of xylan, which harbors arabinose residue substitutions and acetyl groups, but lacks GlcA/MeGlcA. The constitutions of xylan variants differ among different types of cell walls from different species (Scheller and Ulvskov 2010; Cosgrove and Jarvis 2012). GAXs are the major hemicelluloses of primary walls of commelinid monocots, whereas GXs make up the majority of secondary walls of all angiosperms. One of the distinctive features of hemicellulose makeup of Type I and Type II walls is that the principle hemicelluloses GAXs interlock with cellulose in primary walls of commelinid monocots instead of xyloglucan in dicot and non-commelinid monocots (Carpita and Gibeaut 1993).

7.3.1.3 Mannan and Glucomannan

Mannans and glucomannans both refer to β-(1,4)-linked polysaccharides containing mannose (Moreira and Filho 2008). Depending on their backbone constitutions and side chain substitutions, they can be further classified into four groups: mannans, galactomannans, glucomannans, and galactoglucomannans. The backbones of mannans and galactomannans are purely composed of mannose, while the backbones of glucomannans and galactoglucomannans are composed of a mixture of mannose and glucose (Reid 1985). Moreover, glucomannans and galactoglucomannans are often decorated with α-(1,6)-linked galactosyl residues (Reid et al. 1995).

The presence of hetero-mannans in algae suggests that they evolved early from an evolutionary perspective (Popper and Fry 2003; Popper 2008; Domozych et al. 2012). They are widely distributed in different plant species, functioning as either seed storage polysaccharides or cell wall components (Ebringerova et al. 2005). In particular, hetero-mannans are the major component of hemicelluloses in gymnosperms and can also be found in some spermatophyte species with low abundance (Rodriguez-Gacio et al. 2012).

7.3.1.4 Mixed-Linkage Glucans (MLGs)

Mixed-linkage glucans (MLGs) are unbranched and unsubstituted glucose chain composed of two distinct β-(1,3) and β-(1,4)-linkage types. MLGs are only present in two distantly related groups: the "fern ally" genus *Equisetum* and a variety of Poales species of the commelinid monocots (Stone and Carke 1992; Smith and Harris 1999; Sorensen et al. 2008). The hallmark of MLG is the predominant trisaccharides G4G3G and a minority of tetrasaccharides G4G4G3G produced on digestion with *Bacillus subtilis* lichenase (Stone and Carke 1992). The function of mixed-linkage glucans has not yet determined, but it has been proposed to interact with cellulose to regulate growth and provide a source of sugars for energy needs.

7.3.2 Biosynthesis of Hemicelluloses

Unlike cellulose, which is exclusively synthesized at the plasma membrane, hemicelluloses are synthesized by Golgi-membrane localized glycosyltransferases and are transported to the cell surface via Golgi-derived vesicles, followed by integration into the cell walls. In the past two decades, significant progress has been made in understanding the biosynthesis of XyG. The biosynthetic mechanism of xylan, mannan/glucomannan, and mixed-linkage glucan has not yet been fully characterized.

7.3.2.1 Xyloglucan (XyG)

The enzyme for biosynthesis of backbone of XyG was first described in an elegant experiment showing the synthesis of heptasaccharide product (Glc_4Xyl_3) from UDP-Glc and UDP-Xyl by pea membrane (Gordon and Maclachlan 1989). The enzymes were later discovered to be the cellulose synthase-like C (CSLC) family proteins (Table 7.1). The *CSLC4* gene was firstly identified in *Tropaeolum majus* and was showed to be responsible for the massive XyG deposition in seeds. The *Arabidopsis* CSLC4 homolog shares high sequence similarity with the TmCSLC4. Supporting its role in XyG biosynthesis, AtCSLC4 is found to localize to the membrane of Golgi apparatus (Cocuron et al. 2007; Davis et al. 2010). Further topology

studies revealed that the AtCSLC4 contains approximately six transmembrane domains, and its central catalytic domain faces the cytosolic side of Golgi (Davis et al. 2010). Supporting the role of CSLC4 as a candidate for β-(1,4)-glucan synthase, its biochemical activity was shown in yeast *Pichia pastoris* (Cocuron et al. 2007).

The side chains of XyG are added by a variety of GTs including α-(1,6)-xylosyltransferases, β-(1,2)-galactosyltransferases, and α-(1,2)-fucosyltransferase. The *Arabidopsis* GT34 family contains five XyG xylosyltransferases, namely, XXT1, XXT2, XXT3, XXT4, and XXT5, with the AtXXT5 representing a separate clade of the GT34 family (Faik et al. 2002; Zabotina et al. 2008; Vuttipongchaikij et al. 2012). The biochemical xylosyltransferase activity was demonstrated for XXT1, XXT2, and XXT5 (Faik et al. 2002; Cavalier and Keegstra 2006; Culbertson et al. 2016). Simultaneous knocking out of the *XXT1 XXT2* genes resulted in drastic XyG reduction (Cavalier et al. 2008). The XyG synthesis defect in single and double mutants of *XXT2* and *XXT5* genes can be partially rescued by over-expressing *XXT3* (Cavalier et al. 2008; Zabotina et al. 2012). It has been shown that XXT1, XXT2, and XXT5 form a Golgi-localized protein complex with CSLC4 (Chou et al. 2012), which presumably enables the simultaneous backbone elongation and side chain substitutions. The crystal structure of XXT1 has recently been determined (Culbertson et al. 2018). Together with homology modeling of XXT2 and XXT5, it provides a linear model of sequential binding of XXTs and xylosylation of a glucan chain.

Further substitution of the side chains is mediated by multiple GTs of the *Arabidopsis* GT47 family. The *Arabidopsis* MURUS3 (MUR3) and the xyloglucan L-sidechain Galactosyltransferase Position 2 (XLT2) are both β-(1,2)-galactosyltransferases that are responsible for adding galactosyl residues to the xylosyl unit within the XXXG core structure of xyloglucan, respectively (Reiter et al. 1997; Madson et al. 2003; Durand et al. 2009; Jensen et al. 2012). Double mutants of *xlt2 mur3* resulted in insufficient substitution of galactosyl residues (Jensen et al. 2012). Noticeably, MUR3 and XLT2 are responsible for the galactosylation of the third and second xylosyl residue of the XXXG motif, respectively; and it therefore remains to be discussed whether the structural specificity of the acceptor motif determines the functionality of MUR3 and XLT2 proteins (Madson et al. 2003). Xyloglucan-specific Galacturonosyltransferase1 (XUT1) is a member of family GT47 glycosyltransferase that is required for side chain substitutions. XUT1 is present in *Arabidopsis* root hairs and is responsible for adding a galacturonosyl residue to the O-2 of a xylosyl residue (Pena et al. 2012). Knocking out of the *XUT1* gene had no effect on the overall plant growth but led to short root hairs, which may indicate its functional specificity in roots. In *Arabidopsis*, the GT37 family member, Fucosyltransferase1 (FUT1), is a fucosyltransferase that can add terminal fucosyl groups to the galactosyl or galacturonosyl residues (Perrin et al. 1999; Vanzin et al. 2002). Simultaneous disruption of *FUT1* and *MUR2* expression led to loss of XyG fucosylation, although no growth defect could be detected in those mutants (Durand et al. 2009).

Before being transported to the plasma membrane and incorporated into the cell walls, XyGs may undergo important modifications or trimming processes. A group of glycosidases, such as the xylosidase Altered Xyloglucan 3 (AXY3)/Xylosidase

Table 7.1 Genes involved in hemicellulose synthesis and regulation in *Arabidopsis thaliana*

Type	Gene name	Gene ID	Gene family	Enzyme activity	Mutant	Cell wall characterization	References
Xyloglucan	CSLC4	AT3G28180	GT2	β-1,4-Glucan synthase	NA	NA	Cocuron et al. (2007) and Davis et al. (2010)
	XXT1	AT3G62720	GT34	α-1,6-Xylosyltransferase	*xxt1, xxt1 xxt2*	Reduced XyG	Faik et al. (2002), Cavalier and Keegstra (2006), Cavalier et al. (2008), and Zabotina et al. (2012)
	XXT2	AT4G02500	GT34	α-1,6-Xylosyltransferase	*xxt1 xxt2, xxt2 xxt5*	Reduced XyG	Cavalier and Keegstra (2006), Cavalier et al. (2008), and Zabotina et al. (2012)
	XXT3	AT5G07720	GT35	α-1,6-Xylosyltransferase	*xxt3-1*	Reduced XyG	Faik et al. (2002), Cavalier et al. (2008), and Zabotina et al. (2012)
	XXT4	AT1G18690	GT36	α-1,6-Xylosyltransferase	*xxt4-1*	Reduced XyG	Faik et al. (2002) and Cavalier et al. (2008)
	XXT5	AT1G74380	GT37	α-1,6-Xylosyltransferase	*xxt2 xxt5, xxt1 xxt2 xxt5*	Reduced XyG	Zabotina et al. (2012) and Chou et al. (2012)
	MUR3	AT2G20370	GT47	β-1,2-Galactosyltransferase	*mur3, xlt2 mur3*	Reduced XyG fucosylation	Reiter et al. (1997), Madson et al. (2003), and Jensen et al. (2012)
	XLT2	AT5G62220	GT47	β-1,2-Galactosyltransferase	*xlt2, xlt2 mur3*	Reduced XyG fucosylation	Madson et al. (2003) and Jensen et al. (2012)
	XUT1	AT1G63450	GT47	Galacturonosyltransferase	*xut1*	ND	Pena et al. (2012)
	FUT1/ MUR2	AT2G03220	GT37	α-1,2-Fucosyltransferase	*fut1-3, mur2*	Lack of fucosylated XyG	Vanzin et al. (2002) and Pena et al. (2012)
	AXY4	AT1G70230	GT	*O*-Acetyltransferase	*axy4-1, axy4-2, axy4-3*	Reduced XyG acetylation	Gille et al. (2011b), Gille and Pauly (2012), and Zhu et al. (2014)
		AT1G68560	GH31	Xylosidase			

	AXY3/ XYL1				*xyl1, axy3-1, axy3-2, axy3-3*	Altered XyG structure	Sampedro et al. (2001, 2012) and Gunl et al. (2011)
	BGAL10	AT5G63810	GH35	Galactosidase	*bgal10, xyl1 bgal10*	ND	Sampedro et al. (2012)
	AXY8	AT4G34260	GH95	α-1,2-Fucosidase	*axy8, axy8-5, axy8-6*	Increased XyG fucosylation	Leonard et al. (2008), Gunl et al. (2011), and Wan et al. (2018)
Xylan	IRX9	AT2G37090	GT43	β-1,4-Xylan synthase	*irx9*	Reduced xylan chain length	Brown et al. (2005, 2009) and Pena et al. (2007)
	IRX14	AT4G36890	GT43	β-1,4-Xylan synthase	*irx14-1, irx14-2*	Reduced xylose content	Wu et al. (2009), Keppler and Showalter (2010), and Lee et al. (2010)
	IRX10/ GUT2	AT1G27440	GT47	β-1,4-Xylan synthase	*irx10*	Reduced xylan chain length	Brown et al. (2009) and Wu et al. (2009)
	IRX9-LIKE	AT1G27600	GT43	β-1,4-Xylan synthase	*irx9-L*	Reduced xylan chain length	Wu et al. (2009, 2010), Lee et al. 2010, and Ren et al. (2014)
	IRX14-LIKE	AT5G67230	GT43	β-1,4-Xylan synthase	*irx14-L*	Reduced xylan chain length	Wu et al. (2010), Keppler and Showalter (2010), and Ren et al. (2014)
	IRX10-LIKE	AT5G61840	GT47	β-1,4-Xylan synthase	*irx10-L*	Reduced xylan chain length	Brown et al. (2009) and Wu et al. (2009)
	IRX7/ FRA8	AT2G28110	GT47	Glucuronyltransferase	*irx7, fra8*	ND	Zhong et al. (2005) and Hu et al. (2016)
	F8H	AT5G22940	GT47	Glycosyltransferase	*f8h*	ND	Lee et al. (2009)
	IRX8/ GAUT12	AT5G54690	GT8	Galacturonosyltransferase	*irx8*	ND	Sterling et al. (2006), Persson et al. (2007a), and Pena et al. (2007)
	PARVUS	AT1G19300	GT8	Galacturonosyltransferase	*parvus*	ND	Lee et al. (2007)
	GUX1	AT3G18660	GT8	Glucuronyltransferase			

(continued)

Table 7.1 (continued)

Type	Gene name	Gene ID	Gene family	Enzyme activity	Mutant	Cell wall characterization	References
					gux1-1, gux1-2	Altered xylan property	Mortimer et al. (2010), Lee et al. (2012a), and Bromley et al. (2013)
	GUX2	AT4G33330	GT8	Glucuronyltransferase	*gux2-1, gux2-2*	Altered xylan property	Mortimer et al. (2010), Lee et al. (2012a), and Bromley et al. (2013)
	GUX3	AT1G77130	GT8	Glucuronyltransferase	NA	NA	Mortimer et al. (2010), Lee et al. (2012a), and Bromley et al. (2013)
	GUX4	AT1G54940	GT8	Glucuronyltransferase	NA	NA	Lee et al. (2012a) and Bromley et al. (2013)
	GUX5	AT1G08990	GT8	Glucuronyltransferase	NA	NA	Lee et al. (2012a) and Bromley et al. (2013)
	GXMT/ GXM3	AT1G33800	DUF579	4-*O*-Methyltransferases	*gxmt1-1, gxmt1-2*	Reduced GX methyl-etherification	Lee et al. (2012b) and Urbanowicz et al. (2012)
	GXM1	AT1G09610	DUF579	Methyltransferases	*gxm1/2/3*	Loss of GlcA methylation	Lee et al. (2012b) and Yuan et al. (2014)
	GXM2	AT4G09990	DUF579	Methyltransferases	*gxm1/2/3*	Loss of GlcA methylation	Lee et al. (2012b) and Yuan et al. (2014)
	IRX15	AT3G50220	DUF579	Methyltransferases	*irx15 irx15-L*	Reduced xylan content	Brown et al. (2011) and Jensen et al. (2011)
	IRX15-LIKE	AT5G67210	DUF579	Methyltransferases	*irx15 irx15-L*	Reduced xylan content	Brown et al. (2011) and Jensen et al. (2011)
	ESK1/ TBL29	AT3G55990	TBL	*O*-acetyltransferase	*esk1*	Reduced xylan acetylation	Xiong et al. (2013) and Yuan et al. (2013)
	TBL3	AT5G01360	TBL	*O*-acetyltransferase	*esk1 tbl3 tbl31*	Reduced xylan acetylation	Yuan et al. (2016c)
	TBL31	AT1G73140	TBL	*O*-acetyltransferase			Yuan et al. (2016c)

					esk1 tbl3 tbl31	Reduced xylan acetylation	
	TBL32	AT3G11030	TBL	*O*-acetyltransferase	*esk1 tbl32 tbl33*	Reduced xylan acetylation	Yuan et al. (2016a)
	TBL33	AT2G40320	TBL	*O*-acetyltransferase	*esk1 tbl32 tbl33*	Reduced xylan acetylation	Yuan et al. (2016a)
	TBL34	AT2G38320	TBL	*O*-acetyltransferase	*esk1 tbl34 tbl35*	Reduced xylan acetylation	Yuan et al. (2016b)
	TBL35	AT5G01620	TBL	*O*-acetyltransferase	*esk1 tbl34 tbl35*	Reduced xylan acetylation	Yuan et al. (2016b)
	AXY9	AT3G03210	NA	*O*-acetyltransferase	*axy9-1, axy9-2*	Reduced xylan acetylation	Schultink et al. (2015)
	RWA1	At5G46340	Cas1p	*O*-acetyltransferase	*rwa1/2/3/4*	Reduced xylan acetylation	Lee et al. (2011)
	RWA2	AT3G06550	Cas1p	*O*-acetyltransferase	*rwa2*	Reduced hemicellulose acetylation	Manabe et al. (2011)
	RWA3	AT2G34410	Cas1p	*O*-acetyltransferase	*rwa1/2/3/4*	Reduced xylan acetylation	Lee et al. (2011)
	RWA4	AT1G29890	Cas1p	*O*-acetyltransferase	*rwa1/2/3/4*	Reduced xylan acetylation	Lee et al. (2011)
Mannan	CSLA7	AT2G35650	GT2	Glycosyltransferase	*csla7*	ND	Goubet et al. (2003), Dhugga et al. (2004), Liepman et al. (2005), and Verhertbruggen et al. (2011)
	CSLD2	AT5G16910	GT2	Mannan synthase		Absence of mannan	

(continued)

Table 7.1 (continued)

Type	Gene name	Gene ID	Gene family	Enzyme activity	Mutant	Cell wall characterization	References
					csld2 *csld3* *csld5*		Bernal et al. (2007, 2008), Zeng and Keegstra (2008), Verhertbruggen et al. (2011), and Yin et al. (2011)
	CSLD3	AT3G03050	GT2	Mannan synthase	*csld2* *csld3* *csld5*	Absence of mannan	Bernal et al. (2007, 2008), Zeng and Keegstra (2008), Verhertbruggen et al. (2011), and Yin et al. (2011)
	CSLD5	AT1G02730	GT2	Mannan synthase	*csld2* *csld3* *csld5*	Absence of mannan	Bernal et al. (2007, 2008), Zeng and Keegstra (2008), Verhertbruggen et al. (2011), and Yin et al. (2011)
Glucomannan	CSLA2	AT5G22740	GT2	4-β-mannosyltransferase	*csla2-1*, *csla2-2*	Glucomannan reduction	Liepman et al. (2005) and Goubet et al. (2009)
	CSLA3	AT1G23480	GT2	4-β-mannosyltransferase	*csla3-1*, *csla3-2*	Glucomannan reduction	Goubet et al. (2009)
	CSLA9	AT5G03760	GT2	4-β-mannosyltransferase	*csla9-1*, *csla9-2*	Glucomannan reduction	Goubet et al. (2009)
	MSR1	AT3G21190	GT65R	Glycosyltransferase	*msr1-1.* *msr1-2*	Glucomannan reduction	Wang et al. (2012, 2013)
	MSR2	AT1G51630	GT65R	Glycosyltransferase	*msr2-1*, *msr2-2*, *msr2-3*	Glucomannan reduction	Wang et al. (2012, 2013)

1 (XYL1) (Sampedro et al. 2001), the galactosidase Beta-galactosidase 10 (BGAL10) (Sampedro et al. 2012), and the Altered Xyloglucan 8 (AXY8) (Leonard et al. 2008; Gunl et al. 2011), have been shown to involve in this process. Supporting their proposed functions, mutations of *AXY3/XYL1, AXY8,* and *BGAL10* led to increased degree of xylosylation, fucosylation, and galactosidation in *Arabidopsis* tissues, respectively (Gunl et al. 2011). Moreover, the endotransglucosylase/hydrolase (XTH) modification enzymes, which consist of the endotransglucosylase (XET) and the endohydrolase (XEH), are responsible for the cleavage and reforming of the XyG backbones in rapidly growing cells (Rose et al. 2002).

7.3.2.2 Xylan

Different from other hemicelluloses, the backbone of xylan is not synthesized by cellulose synthase-like (CSL) proteins. Instead, multiple GTs, including IRX9 and IRX14 from the GT43 family (Pena et al. 2007; Lee et al. 2010; Wu et al. 2010), and IRX10 from the GT47 family (Brown et al. 2009), have been found to be required for the elongation of xylan backbones in secondary cell walls. Mutants of these genes all showed reduced xylan chain length and GX abundance, ultimately leading to altered xylem structures. Additionally, IRX9-LIKE, IRX10-LIKE, and IRX14-LIKE proteins have also been identified and shown to play redundant roles with their corresponding counterparts in xylan elongation (Keppler and Showalter 2010; Wu et al. 2010; Chiniquy et al. 2013; Hornblad et al. 2013). The xylosyltransferase activity has been demonstrated unequivocally for IRX10 and IRX10L (Jensen et al. 2014; Urbanowicz et al. 2014).

The backbones of xylans in secondary cell walls in vascular plants are characterized by a unique reducing end polysaccharide, with a structure of β-D-Xylp-(1→4)-β-D-Xylp-(1→3)-α-L-Rhap-(1→2)-α-D-GalpA-(1→4)-D-Xylp (or denoted as Xyl-Rha-GalA-Xyl). This characteristic tetrasaccharide unit was firstly isolated in wood and then was also found in xylem in *Arabidopsis* (Pena et al. 2007). Although it remains to be validated which GTs are required for the assembly of the tetrasaccharide unit, several candidates have been proposed to function in making specific linkages. FRA8, also known as irregular xylem 7 (IRX7), belongs to the GT47 family and is proposed to transfer xylose to form the Xyl-Rha unit. Supporting this hypothesis, heterogeneously expressed AtFRA8/AtIRX7 showed xylosyltransferase activity (Zhong et al. 2005; Wu et al. 2010; Hu et al. 2016). In addition, another GT47 family member, F8H, exhibits functional redundancy with FRA8/IRX7, as overexpression of the *AtF8H* partially rescued the *fra8/irx7* mutant phenotype, and simultaneous knocking out both *AtFRA8/AtIRX7* and *AtF8H* led to enhanced defects (Lee et al. 2009; Wu et al. 2010). The GT8 family member IRX8 is a homolog of the GalA transferase, GAUT1, and IRX is therefore a candidate for transferring GalA to form the GalA-Xyl linkage (Sterling et al. 2006; Persson et al. 2007a). PARVUS is also a member of the GT8 family. Unlike the GT candidates mentioned above, which exclusively localize in Golgi, PARVUS was found to exist not only in Golgi but also in endoplasmic reticulum (ER), indicating its function in earlier steps of the tetrasaccharide formation (Lee et al. 2007). Therefore, it is

speculated that PARVUS is responsible for adding xylose to a primer at the very beginning of xylose synthesis. The biochemical activity of PARVUS has yet to be shown.

More genes have been identified and shown to have roles in side chain decorations of xylans. The *Arabidopsis* GT8 family contains five GUX proteins (GUX1–5), which are responsible for adding GlcA to the xylan backbones. Mutants of various GUX genes showed different GlcA substitution patterns of xylan (Mortimer et al. 2010; Lee et al. 2012a; Bromley et al. 2013). The rice GT61 family member, XAX1, was shown to be involved in adding xylosyl units to the side chain of xylan (Chiniquy et al. 2012). Moreover, the wheat XAT1 and XAT2 also belong to the GT61 family, while they both exhibit arabinosyl transferase activities (Anders et al. 2012). It is proposed that various GTs, either for backbone or side chain synthesis, might be organized into a functional complex and work cooperatively in the synthesis of xylan. There is growing evidence that GTs form complexes in different cisternae of the Golgi stacks (Faik 2010; Zeng et al. 2010, 2016; Jiang et al. 2016). In wheat, xylan synthase complex (XSC) has a core component consisting of three GTs, *TaGT43-4*, *TaGT47-13*, and *TaGT75-4* (Zeng et al. 2010). A similar XSC composition has been shown for *Asparagus* (Zeng et al. 2016). It is expected that biochemical assay will be developed to verify the activity of XSC and its individual components.

7.3.2.3 Mannan and Glucomannan

Like other hemicellulosic polysaccharides, mannans are synthesized in the Golgi catalyzed by at least two enzymes: mannan synthase (ManS) for backbone synthesis and galactomannan galactosyl transferase (GMGT) for side chain addition (Edwards et al. 1999; Dhugga et al. 2004; Liepman et al. 2005). ManS was first identified from guar (*Cyamopsis tetragonoloba*) as a member of the cellulose synthase-like A (CSLA) family (Dhugga et al. 2004). *CSLA* genes are present in all land plants (Yin et al. 2009). Heterologously expressed recombinant CSLA proteins from a variety of plants exhibit mannan synthase activity in vitro (Liepman et al. 2005, 2007; Suzuki et al. 2006; Gille et al. 2011a). Genetic analysis of *Arabidopsis CSLA* mutants further supported the hypothesis that CSLA proteins are responsible for glucomannan biosynthesis in vivo (Goubet et al. 2009). It has been shown that the glucomannan was substantially reduced in *csla9* mutants, and no detectable glucomannan in the stems of *csla2csla3csla9* triple mutants was observed (Goubet et al. 2009). Cellulose synthase-like D (CSLD) family has been proposed to synthesize mannans based on mannan synthase activity using tobacco microsomes isolated from plants transiently expressing *Arabidopsis* CSLD5 or co-expressing CSLD2 and CSLD3. Supporting the proposed biochemical activity, *csld2 csdl3 csld*5 triple mutants had no detectable mannan in the xylem and interfascicular fibers (Bernal et al. 2007; Yin et al. 2011). Aberrant root hair development was observed for *csld2*, *csld3*, and *csld5* (Bernal et al. 2008; Yin et al. 2011). Subsequent studies suggest that CSLD3 is involved in cellulose synthesis in root hairs (Park et al. 2011). So far, the

mannan synthase activity has not been demonstrated for purified CSLD. The biochemical activity of CSLD remains to be determined.

GMGT was first identified from fenugreek (*Trigonella foenum-graecum*) seed endosperm (Edwards et al. 1999). It was reported that GMGT catalyzed the transfer of galactose (Gal) to backbone mannose residues using UDP-Gal as substrate (Edwards et al. 1989, 2002). Two homologs of fenugreek mannan synthesis-related (MSR), AtMSR1 and AtMSR2, were subsequently identified in *Arabidopsis* (Wang et al. 2013b). *msr1* single mutant and *msr1 msr2* double mutant exhibited reductions in mannosyl levels examined by neutral monosaccharide composition analysis and immunofluorescence labeling of *Arabidopsis* stems, which indicates that MSR proteins are involved in mannan biosynthesis in *Arabidopsis* (Wang et al. 2013b).

7.3.2.4 Mixed-Linkage Glucans (MLGs)

Two groups of proteins have been shown to play roles in the synthesis of MLGs: Cellulose Synthase Like F (CSLF) and Cellulose Synthase Like H (CSLH). Multiple rice CSLF isoforms, OsCSLF2, OsCSLF4, and OsCSLF6, are implicated in the synthesis MLGs (Hazen et al. 2002; Burton et al. 2006, 2011; Vega-Sanchez et al. 2012). Heterologous expression of rice *OsCSLF2* or barley *HvCSLH1* led to MLG accumulation in transgenic *Arabidopsis* where MLG is normally absent (Burton et al. 2006; Doblin et al. 2009). Similarly, transient expression of *OsCLSF6* in tobacco led to the accumulation of MLG. Overexpression of the *HvCSLF6* led to excessive MLG production in barley, suggesting that both CSLF6 and CSLH1 have MLG synthesis function (Burton et al. 2011).

Interestingly, CSLFs and CSLHs seem to have overlapping functions. Both of them are able to produce β-(1,3)- and β-(1,4)- linkages. The site where MLG is synthesized has been debated. It was first shown by Gibeaut and Carpita that MLG from maize was synthesized using membranes isolated from Golgi (Gibeaut and Carpita 1993). Further studies with isolated Golgi suggest that the substrate concentration determines the ratio of cellotriosyl and cellotetraosyl units in the native MLG (Buckeridge et al. 1999). Consistent with the idea of synthesis of MLG in Golgi, the protease protection assays showed the topology of the catalytic domains of maize MLG glucan synthase facing the cytoplasmic face of the Golgi membrane (Urbanowicz et al. 2004). However, MLG was not detected in the Golgi or Golgi-derived vesicles, which led to the hypothesis that MLG is first synthesized as a short β-(1,4)-glucan polymer and then stitched together by transglucosylation at the plasma membrane (Wilson et al. 2006; Fincher 2009). Supporting the role of mixed-linkage glucan synthesis at the plasma membrane, catalytically active CSLF6 was detected in plasma membrane-enriched fractions (Wilson et al. 2015). In contrast to previous results, subsequent study showed that MLG was detected at the periphery of Golgi stacks and vesicles. Both in vitro and in vivo analyses demonstrated MLG activity in the Golgi fraction (Carpita and McCann 2010). Furthermore, BdCSLF6 was shown to localize to Golgi, and the Golgi localization was sufficient for MLG synthesis (Kim et al. 2015). The contradictory results in MLG detection may be due to the differences in epitope exposure. As CSLF6 alone

can make both β-(1,3)- and β-(1,4)- linkages, it is unnecessary to have a two-stage synthesis and stitching process. Consistent with this idea, recent data showed that a single amino acid within the transmembrane helix 4 controls the MLG structure (Jobling 2015).

7.3.3 Acetylation of Hemicelluloses

Hemicelluloses are composed of structural diverse polymers, many of which can be further modified to various degrees. One of the most abundant modifications is *O*-acetyl-substitution. *O*-acetyl-substitution occurs in nearly all types of hemicelluloses except mixed-linkage glucan in grasses (Lundqvist et al. 2002; Jia et al. 2005; Urbanowicz et al. 2012). Wall polymers with the *O*-acetyl-substitution can reduce saccharification yield; therefore, it has attracted attention to understand the mechanism of *O*-acetylation (Pauly et al. 2013). The first characterization of *O*-acetylation of the XyG came from an oligosaccharide mass profiling (OLIMP) coupled with matrix-assisted laser desorption ionization time of flight mass spectrometry (MALDI-TOF MS) to analyze substitution pattern in wall polymers. The analysis revealed that degree of O-acetylation varies in different tissues (Obel et al. 2009). *O*-acetylation in XyG occurs at various positions, including *O*-acetyl-substitution on galactosyl residues in the side chain and the glucosyl residues of the XyG backbone. *Trichome Birefringence (tbr)* was a EMS mutant that lacked strong birefringence under polarized light and showed reduction in cellulose deposition in SCWs (Potikha and Delmer 1995). In addition to TBR, 45 TBL make up the large plant-specific protein family of which a few have been shown to be involved in acetylation of cell wall polymers (Gille and Pauly 2012). *O*-acetyl-substitution in XyG involves the Altered Xyloglucan 4 (AXY4), a member of the Trichome Birefringence-like (TBL) protein family (Gille et al. 2011b; Gille and Pauly 2012; Zhu et al. 2014). The *O*-acetylation of XyG was completely abolished in the null mutants of *axy4*. Intriguingly, disruption of the AXY4 function had no discernable effects on the growth of plants, suggesting that acetylation of XyGs might be dispensable for plant growth under laboratory conditions (Gille et al. 2011b). Unlike AXY4, which is a XyG-specific *O*-acetyltransferase, reduced wall acetylation (RWA) has a non-specific *O*-acetyl-substitution in all wall polymers. Mutations in *RWA2* resulted in an overall 20% reduction in wall polymer acetylation levels including xylan, XyG, and pectin (Manabe et al. 2011). However, *rwa2* did not impact overall plant growth and morphology. Surprisingly, *rwa1/2/3/4* quadruple mutant resulted in 40% reduction in xylan acetylation with only a mild deformation of vessels (Lee et al. 2011). Various combinations of *rwa* triple and quadruple mutants were generated using different alleles. In contrast to mild phenotype reported by Lee et al., *rwa* quadruple mutants were extremely dwarf and completely lacked interfascicular fibers (Manabe et al. 2013). The severe growth defects were associated with more than 60% reduction in wall *O*-acetylation. These studies suggest that plants can tolerate reduction of wall polysaccharides acetylation without impairment of plant development.

ESKIMO 1/TRICHOME BIREFRINGENCE-LIKE (ESK1/TBL29) is a member of TBL family that contains 46 members with a domain of unknown function 213 (DUF213). ESK1 as well as other members of the family have been shown to mediate acetylation of xylosyl residues in xylan. ESK1/TBL29 is preferentially expressed in xylem and interfascicular fibers. Similar to typical xylan-deficient mutants, *esk1* mutants displayed collapsed xylem vessels and reduced secondary wall thickenings. However, *esk1* had no defect in xylose content. Xylan fraction analysis revealed that *esk1* had 30% reduction in xylan acetylation. Consistent with the proposed xylan acetyltransferase function, xylan acetyltransferase activity in the microsomes from *esk1* mutant was reduced (Yuan et al. 2013). Two T-DNA null mutants *tbl29-1* and *tbl29-2* showed ~50% reduction in xylan acetylation, suggesting additional genes are redundant with *ESK1/TBL29* in the regulation of xylan acetylation. It is expected that other TBL family members contribute to *O*-acetylation of xylan and/or other wall polymers (Xiong et al. 2013). Indeed, TBL3 and TBL31–TBL35 were recently shown to have redundant function with ESK1 (Yuan et al. 2016a, b, c). Both *tbl3 tbl31 esk1* and *tbl32 tbl33 esk1* resulted in more than 85% reduction in xylan acetylation. *Altered Xyloglucan9* (*AXY9*) is a single copy gene with limited protein sequence homology with domains in TBL family including GDS active site and a DXXH motif (Schultink et al. 2015). *axy9* mutants had reduced growth and collapsed xylem vessels that are similar to *esk1*. Although *axy9* mutants had reduced acetylation in both XyG and xylan, it is likely the mutant phenotype is due to reduced acetylation in xylan but not in XyG. The biochemical activity of AXY9 has not yet been determined.

The TBL family encodes more than 66 members in rice (Gao et al. 2017). The gene duplication is exemplified by 15 TBL29 homologs in rice. OsTBL1 and OsTBL2 are closely homologous to TBL34 in *Arabidopsis*. Transgenic amiRNA lines with reduced OSTBL1 and OsTBL2 resulted in reduction in xylan acetylation despite normal xylem vessels. The increased susceptibility to rice blight disease of transgenic amiRNA lines indicates that xylan modification is important for pathogen resistance. Recent discovery of xylan deacetylation by a GDSL esterase in rice adds another layer of complexity in xylan modification. *Brittle leaf sheath 1* (*bs1*) is a rice mutant that has fragile leaf sheaths (Zhang et al. 2017). *BS1* encodes a member of large family of GDSL lipases/esterases. The rice genome encodes more than 108 *GDSL esterases*. BS1 specifically cleaves acetyl group from the xylan backbone at O-2 and O-3 position. *bs1* mutants had pleotropic phenotype including reduced plant height, reduced tiller number, smaller panicle, increased pit size, and abnormal spiral patterns. It remains to be determined whether any of the above phenotype is a direct effect of excessive acetylation in xylan.

Glucuronoxylan in vascular plants are modified at O-4 of GlcA by methylation. *O*-methyl-esterification is a key feature of SCWs of vascular plants, while moss *Physcomitrella patens* lacks *O*-methyl-esterified GlcA. GXMT/GXM3, GXM1, and GXM2 are glucuronoxylan methyltransferases that are capable of transferring the methyl group to O-4 of GlcA (Lee et al. 2012b; Urbanowicz et al. 2012). Despite 75% reduction in 4-*O*-methyl-estrification, *gxmt1-1* had normal growth lacking typical collapsed xylem phenotype in xylan-deficient mutants (Urbanowicz et al. 2012). The lack of defect in pith, xylem, and interfascicular fiber cells was further

confirmed in either single or double *gxm* mutants (Lee et al. 2012b). The complete lack of GlcA methylation in *gxm* triple mutants indicates that GXM1, GXM2, and GXMT/GXM3 account for the GlcA methylation in xylan (Yuan et al. 2014). GXM belongs to a family of 10-member DUF579-containing proteins. Five of DUF579-containing proteins (GXMT/GXM3, GXM1–2, IRX15, and IRX15-LIKE) are co-expressed with CESA4, CESA7, and CESA8 in developing xylems (Brown et al. 2011). *irx15 irx15-L* had irregular inner surface in interfascicular fibers, and 65% reduced xylose levels (Brown et al. 2011; Jensen et al. 2011). The biochemical activity of IRX15 and IRX15-L has not yet been shown.

7.3.4 Secretion of Hemicelluloses

Unlike cellulose microfibrils, which are exclusively synthesized at the plasma membrane, most noncellulosic polysaccharides are synthesized in Golgi. Golgi therefore is the most important organelle that relates to regulation of hemicelluloses biosynthesis. During cell division, new cell walls are formed by fusion of Golgi-derived vesicles to the cell plate. As cell continues to grow after division, new polysaccharides are constantly delivered to cell wall from Golgi-derived vesicles. In plants, Golgi has distinct membrane compartments known as *cis*-, medial-, and *trans*-cisternae. Similar to the best-studied N-glycosylation of glycoproteins in animal and yeast, the enzymes that synthesize hemicelluloses presumably also localize to different sub-compartments within Golgi. So far, XyG represents the only and best-characterized sub-compartmentalization during complex polysaccharide biosynthesis. XyG backbone was observed primarily in *trans*-cisternae and trans-Golgi network (TGN). Fucosyl residues are proposed to occur in the *trans*-cisternae and TGN as Fuc-decorated XyG was located mostly in *trans*-cisternae and TGN (Zhang and Staehelin 1992). Enzymes involved in XyG synthesis have also been mapped to different sub-compartment within Golgi using immunogold-electron microscopy (Chevalier et al. 2010). AtXXT1-GFP was localized mainly in *cis*- and medial-cisternae, whereas AtMUR3-GFP and AtFUT1-GFP were localized predominantly in medial- and *trans*-cisternae, respectively.

TGN plays a critical role in post-Golgi trafficking in multicellular organisms. The importance of TGN in plants is manifested in distinct features that are different from those of TGN in mammals and yeast. In plant cells, TGN is either associated with *trans*-cisternae or free from Golgi association as an independent compartment. TGN is highly dynamic and acts as a central hub of secretion, endocytosis, and recycling in plants (Kang and Staehelin 2008). The unique feature of plant TGN further complicates the already challenging situation of polysaccharide secretion. Although it is generally accepted that most noncellulosic polysaccharides are transported to the cell surface via TGN-derived vesicles, it has also been shown that unconventional secretion pathway that bypasses Golgi exists in plants (Ding et al. 2014).

A protein complex, composed of YPT/RAB GTPase Interacting Protein 4a (YIP4a) and YIP4b, as well as ECHIDNA (ECH), is found to play a role in the

secretion of both pectin and XyG in *Arabidopsis*. The ECH/YPT complex is localized in the TGN. Mutations of either *ECH* or *YIP4a YIP4b* led to drastic accumulation of both pectin and XyG, indicating a defect in polysaccharide secretion, which accompanied changes in cell wall composition (Gendre et al. 2011, 2013). Moreover, the Secretory Carrier Membrane Protein 2 (SCAMP2) was proposed to mediate the TGN-derived polysaccharide-containing vesicles in tobacco. NtSCAMP2 is a plant homolog of the SCAMPs, which represent a group of transmembrane proteins that function in the vesicle trafficking from Golgi to the plasma membrane in eukaryotes (Castle and Castle 2005). Supporting this proposed function, NtSCAMP2 localized at the plasma membrane, TGN, and cell plate in the tobacco BY-2 cells. In addition, NtSCAMP2 also localized in a novel population of vesicles termed as the secretory vesicle clusters (SVCs). Antibody labeling showed that these SVCs contained a mixture of polysaccharides including pectin. It would be informative to see whether the SVCs and SCAMPs are required for the delivery of hemicelluloses (Toyooka et al. 2009; Toyooka and Matsuoka 2009).

Cell wall polysaccharide secretion was recently studied in root border cell in alfalfa (Wang et al. 2017). Electron tomographic reconstruction revealed morphological features of the Golgi stack and secretory vesicles in border cells. Golgi stacks in border cells have typical *cis*-, medial-, *trans*-cisternae, and Golgi-associated TGN (GA-TGN). Large vesicles (LVs) were detected that bud off from *trans*-cisternae, GA-TGN, and free-TGN. Immunogold labeling revealed distinct secretory pathways for different polysaccharides. Xylogalacturonan is secreted by LVs from trans-cisternae, whereas XyG and RG-I are packed into TGN-derived LVs and small vesicles (SVs).

7.4 Cellulose and Hemicelluloses Interaction

Cellulose microfibrils are linked together by non-covalent interactions with xyloglucan in PCWs. These non-covalent interactions are thought to be important for cell expansion. XyG binds to cellulose to form a strong but extensible XyG-cellulose network, further enhancing the mechanical support (Hayashi 1989; Pauly et al. 1999; Somerville et al. 2004). Meanwhile, binding of XyG is proposed to prevent hyperaggregation of cellulose microfibrils (Thompson 2005; Anderson et al. 2010). Several pieces of evidence argue against the most popular "tethered network model." *Arabidopsis* plants completely lacking XyG displayed a minor phenotype (Cavalier et al. 2008). The extensive interaction between XyG and cellulose was not detected by NMR studies (Dick-Perez et al. 2011). Moreover, XyG-specific endoglucanase failed to induce cell wall creep, which is contradictory to the idea that XyG works as load-bearing tethers to cross-link adjacent cellulose microfibrils. A small percentage of XyG-cellulose (0.3% of total XyG) accounts for large biochemical effects (Park and Cosgrove 2012). It remains to be determined as to how the XyG-cellulose network impacts cell wall mechanics and cell expansion. As XyG can interact with multiple polysaccharides such as pectin, it possibly functions

as an adaptor molecule between cellulose and other matrix polymers (Popper and Fry 2008).

Study suggests that xylan may interact with cellulose microfibrils as a twofold helical screw in SCWs (Busse-Wicher et al. 2014). Molecular dynamic simulation of xylan-cellulose interaction discovered two different domains for non-covalent interactions between xylan and cellulose microfibrils. The major domain has evenly spaced GlcA that forms stable interaction on the hydrophilic surface of cellulose microfibrils. The minor domain with randomly spaced GlcA binds to the hydrophoblic surface of cellulose microfibrils. It is hypothesized that the even acetylation pattern is important for maintaining non-covalent interactions between xylan major domain and hydrophilic surface of cellulose microfibrils. Supporting the xylan-cellulose interaction model, xylan did not interact with cellulose in *esk1* mutant, in which even pattern of acetyl esters on xylan was absent (Grantham et al. 2017). It appears to be a two-way street as cellulose is also required for xylan twofold screw conformation. The twofold screw conformation was absent in *irx3* mutants (Simmons et al. 2016). We are just beginning to understand polymer-polymer interactions. It is anticipated that the full knowledge of the molecular nature of interactions will help us understand the cell wall architecture and wall expansion.

7.5 Concluding Remarks

Despite recent progress on understanding toward cellulose and hemicellulose biosynthesis and regulation in plants, it remains challenging to isolate proteins and develop enzymatic assays for most of glycosyltransferases. The challenge has many folds: most enzymes are integral membrane proteins that are difficult to isolate or express in a heterologous system; some of the enzymes form a complex with low activity alone, but its partner is unknown; genetic redundancy interferes with the specific function assignment. There is limited knowledge about localization of enzymes, concerted action, and regulation between individual enzyme/complex enzymes and substrate transporters, not to mention the coordination between different enzymes in a time and space resolved manner. For example, do backbone synthase and the substituting glycosyltransferase operate independently or in a coordinated fashion? In the case of a relatively regular spacing of substituents along the chain, is it achieved by enzyme complex that determines the precise pattern of addition or substitution? How do plant control heterogeneity where substitution is not symmetrically distributed? There is still limited knowledge about regulation of glycosyltransferases at the plasma membrane or in the Golgi. There are many outstanding questions, such as the following: (1) How is CSC activated at the plasma membrane? (2) How is chain initiation in both cellulosic and noncellulosic polysaccharides controlled? (3) How is chain termination controlled? (4) Are noncellulosic polysaccharides delivered to the apoplastic space via distinct vesicle trafficking pathways? (5) How is complex polysaccharide assembly pathway regulated in a spatial and temporal fashion in Golgi? (6) How is abundance

of CSC controlled through endocytosis, exocytosis, and recycling in different tissues and wall types? We anticipate that answers for some of the above questions will be revealed with the innovations in the areas of cell biology, biochemistry, and computational modeling.

Acknowledgment We thank Shundai Li for critical reading of manuscripts. This work was supported by the Center for Lignocellulose Structure and Formation, an Energy Frontier Research Center funded by the DOE, Office of Science, BES under Award DE-SC0001090.

References

Anders N, Wilkinson MD, Lovegrove A, Freeman J, Tryfona T, Pellny TK, Weimar T, Mortimer JC, Stott K, Baker JM, Defoin-Platel M, Shewry PR, Dupree P, Mitchell RA (2012) Glycosyl transferases in family 61 mediate arabinofuranosyl transfer onto xylan in grasses. Proc Natl Acad Sci U S A 109:989–993

Anderson CT, Carroll A, Akhmetova L, Somerville C (2010) Real-time imaging of cellulose reorientation during cell wall expansion in *Arabidopsis* roots. Plant Physiol 152:787–796

Arioli T, Peng LC, Betzner AS, Burn J, Wittke W, Herth W, Camilleri C, Hofte H, Plazinski J, Birch R, Cork A, Glover J, Redmond J, Williamson RE (1998) Molecular analysis of cellulose biosynthesis in *Arabidopsis*. Science 279:717–720

Atalla RH, Vanderhart DL (1984) Native cellulose: a composite of two distinct crystalline forms. Science 223:283–285

Bashline L, Li SD, Anderson CT, Lei L, Gu Y (2013) The endocytosis of cellulose synthase in *Arabidopsis* is dependent on mu 2, a clathrin-mediated endocytosis adaptin. Plant Physiol 163:150–160

Bashline L, Li SD, Gu Y (2014) The trafficking of the cellulose synthase complex in higher plants. Ann Bot 114:1059–1067

Bashline L, Li SD, Zhu XY, Gu Y (2015) The TWD40-2 protein and the AP2 complex cooperate in the clathrin-mediated endocytosis of cellulose synthase to regulate cellulose biosynthesis. Proc Natl Acad Sci U S A 112:12870–12875

Benschop JJ, Mohammed S, O'Flaherty M, Heck AJR, Slijper M, Menke FLH (2007) Quantitative phosphoproteomics of early elicitor signaling in *Arabidopsis*. Mol Cell Proteomics 6:1198–1214

Bernal AJ, Jensen JK, Harholt J, Sorensen S, Moller I, Blaukopf C, Johansen B, de Lotto R, Pauly M, Scheller HV, Willats WG (2007) Disruption of *ATCSLD5* results in reduced growth, reduced xylan and homogalacturonan synthase activity and altered xylan occurrence in *Arabidopsis*. Plant J 52:791–802

Bernal AJ, Yoo CM, Mutwil M, Jensen JK, Hou G, Blaukopf C, Sorensen I, Blancaflor EB, Scheller HV, Willats WG (2008) Functional analysis of the cellulose synthase-like genes *CSLD1*, *CSLD2*, and *CSLD4* in tip-growing *Arabidopsis* cells. Plant Physiol 148:1238–1253

Betancur L, Singh B, Rapp RA, Wendel JF, Marks MD, Roberts AW, Haigler CH (2010) Phylogenetically distinct cellulose synthase genes support secondary wall thickening in *Arabidopsis* shoot trichomes and cotton fiber. J Integr Plant Biol 52:205–220

Bischoff V, Desprez T, Mouille G, Vernhettes S, Gonneau M, Hofte H (2011) Phytochrome regulation of cellulose synthesis in *Arabidopsis*. Curr Biol 21:1822–1827

Brennwald P, Rossi G (2007) Spatial regulation of exocytosis and cell polarity: yeast as a model for animal cells. FEBS Lett 581:2119–2124

Brett CT (2000) Cellulose microfibrils in plants: biosynthesis, deposition, and integration into the cell wall. Int Rev Cytol 199:161–199

Bringmann M, Li EY, Sampathkumar A, Kocabek T, Hauser MT, Persson S (2012) POM-POM2/CELLULOSE SYNTHASE INTERACTING1 is essential for the functional association of cellulose synthase and microtubules in *Arabidopsis*. Plant Cell 24:163–177

Brocard-Gifford I, Lynch TJ, Garcia ME, Malhotra B, Finkelstein RR (2004) The *Arabidopsis thaliana ABSCISIC ACID-INSENSITIVE8* locus encodes a novel protein mediating abscisic acid and sugar responses essential for growth. Plant Cell 16:406–421

Bromley JR, Busse-Wicher M, Tryfona T, Mortimer JC, Zhang Z, Brown DM, Dupree P (2013) GUX1 and GUX2 glucuronyltransferases decorate distinct domains of glucuronoxylan with different substitution patterns. Plant J 74:423–434

Brown RM (1996) The biosynthesis of cellulose. J Macromol Sci, Pure Appl Chem A33:1345–1373

Brown RM (1999) Cellulose structure and biosynthesis. Pure Appl Chem 71:767–775

Brown RM Jr, Montezinos D (1976) Cellulose microfibrils: visualization of biosynthetic and orienting complexes in association with the plasma membrane. Proc Natl Acad Sci U S A 73:143–147

Brown RM Jr, Willison JH, Richardson CL (1976) Cellulose biosynthesis in *Acetobacter xylinum*: visualization of the site of synthesis and direct measurement of the in vivo process. Proc Natl Acad Sci U S A 73:4565–4569

Brown DM, Zeef LAH, Ellis J, Goodacre R, Turner SR (2005) Identification of novel genes in *Arabidopsis* involved in secondary cell wall formation using expression profiling and reverse genetics. Plant Cell 17:2281–2295

Brown DM, Zhang Z, Stephens E, Dupree P, Turner SR (2009) Characterization of IRX10 and IRX10-like reveals an essential role in glucuronoxylan biosynthesis in *Arabidopsis*. Plant J 57:732–746

Brown D, Wightman R, Zhang Z, Gomez LD, Atanassov I, Bukowski JP, Tryfona T, McQueen-Mason SJ, Dupree P, Turner S (2011) *Arabidopsis* genes *IRREGULAR XYLEM* (*IRX15*) and *IRX15L* encode DUF579-containing proteins that are essential for normal xylan deposition in the secondary cell wall. Plant J 66:401–413

Buckeridge MS, Vergara CE, Carpita NC (1999) The mechanism of synthesis of a mixed-linkage (1–>3), (1–>4)beta-D-glucan in maize. Evidence for multiple sites of glucosyl transfer in the synthase complex. Plant Physiol 120:1105–1116

Burton RA, Wilson SM, Hrmova M, Harvey AJ, Shirley NJ, Medhurst A, Stone BA, Newbigin EJ, Bacic A, Fincher GB (2006) Cellulose synthase-like *CslF* genes mediate the synthesis of cell wall (1,3;1,4)-beta-D-glucans. Science 311:1940–1942

Burton RA, Collins HM, Kibble NA, Smith JA, Shirley NJ, Jobling SA, Henderson M, Singh RR, Pettolino F, Wilson SM, Bird AR, Topping DL, Bacic A, Fincher GB (2011) Over-expression of specific HvCslF cellulose synthase-like genes in transgenic barley increases the levels of cell wall (1,3;1,4)-beta-d-glucans and alters their fine structure. Plant Biotechnol J 9:117–135

Busse-Wicher M, Gomes TC, Tryfona T, Nikolovski N, Stott K, Grantham NJ, Bolam DN, Skaf MS, Dupree P (2014) The pattern of xylan acetylation suggests xylan may interact with cellulose microfibrils as a twofold helical screw in the secondary plant cell wall of *Arabidopsis thaliana*. Plant J 79:492–506

Carpita NC, Gibeaut DM (1993) Structural models of primary-cell walls in flowering plants - consistency of molecular-structure with the physical-properties of the walls during growth. Plant J 3:1–30

Carpita NC, McCann MC (2010) The maize mixed-linkage (1->3),(1->4)-beta-D-glucan polysaccharide is synthesized at the golgi membrane. Plant Physiol 153:1362–1371

Carroll A, Specht CD (2011) Understanding plant cellulose synthases through a comprehensive investigation of the cellulose synthase family sequences. Front Plant Sci 2(5). https://doi.org/10.3389/fpls.2011.00005

Carroll A, Mansoori N, Li SD, Lei L, Vernhettes S, Visser RGF, Somerville C, Gu Y, Trindade LM (2012) Complexes with mixed primary and secondary cellulose synthases are functional in *Arabidopsis* plants. Plant Physiol 160:726–737

Castle A, Castle D (2005) Ubiquitously expressed secretory carrier membrane proteins (SCAMPs) 1-4 mark different pathways and exhibit limited constitutive trafficking to and from the cell surface. J Cell Sci 118:3769–3780

Cavalier DM, Keegstra K (2006) Two xyloglucan xylosyltransferases catalyze the addition of multiple xylosyl residues to cellohexaose. J Biol Chem 281:34197–34207

Cavalier DM, Lerouxel O, Neumetzler L, Yamauchi K, Reinecke A, Freshour G, Zabotina OA, Hahn MG, Burgert I, Pauly M, Raikhel NV, Keegstra K (2008) Disrupting two *Arabidopsis thaliana* xylosyltransferase genes results in plants deficient in xyloglucan, a major primary cell wall component. Plant Cell 20:1519–1537

Chen SL, Ehrhardt DW, Somerville CR (2010) Mutations of cellulose synthase (CESA1) phosphorylation sites modulate anisotropic cell expansion and bidirectional mobility of cellulose synthase. Proc Natl Acad Sci U S A 107:17188–17193

Chevalier L, Bernard S, Ramdani Y, Lamour R, Bardor M, Lerouge P, Follet-Gueye ML, Driouich A (2010) Subcompartment localization of the side chain xyloglucan-synthesizing enzymes within Golgi stacks of tobacco suspension-cultured cells. Plant J 64:977–989

Chiniquy D, Sharma V, Schultink A, Baidoo EE, Rautengarten C, Cheng K, Carroll A, Ulvskov P, Harholt J, Keasling JD, Pauly M, Scheller HV, Ronald PC (2012) XAX1 from glycosyltransferase family 61 mediates xylosyltransfer to rice xylan. Proc Natl Acad Sci U S A 109:17117–17122

Chiniquy D, Varanasi P, Oh T, Harholt J, Katnelson J, Singh S, Auer M, Simmons B, Adams PD, Scheller HV, Ronald PC (2013) Three novel rice genes closely related to the *Arabidopsis IRX9*, *IRX9L*, and *IRX14* genes and their roles in xylan biosynthesis. Front Plant Sci 4(83). https://doi.org/10.3389/fpls.2013.00083

Cho SH, Du J, Sines I, Poosarla VG, Vepachedu V, Kafle K, Park YB, Kim SH, Kumar M, Nixon BT (2015) In vitro synthesis of cellulose microfibrils by a membrane protein from protoplasts of the non-vascular plant Physcomitrella patens. Biochem J 470:195–205

Cho SH, Purushotham P, Fang C, Maranas C, Diaz-Moreno SM, Bulone V, Zimmer J, Kumar M, Nixon BT (2017) Synthesis and self-assembly of cellulose microfibrils from reconstituted cellulose synthase. Plant Physiol 175:146–156

Chou YH, Pogorelko G, Zabotina OA (2012) Xyloglucan xylosyltransferases XXT1, XXT2, and XXT5 and the glucan synthase CSLC4 form Golgi-localized multiprotein complexes. Plant Physiol 159:1355–1366

Cocuron JC, Lerouxel O, Drakakaki G, Alonso AP, Liepman AH, Keegstra K, Raikhel N, Wilkerson CG (2007) A gene from the cellulose synthase-like C family encodes a beta-1,4 glucan synthase. Proc Natl Acad Sci U S A 104:8550–8555

Cosgrove DJ (2005) Growth of the plant cell wall. Nat Rev Mol Cell Biol 6:850–861

Cosgrove DJ (2014) Re-constructing our models of cellulose and primary cell wall assembly. Curr Opin Plant Biol 22:122–131

Cosgrove DJ, Jarvis MC (2012) Comparative structure and biomechanics of plant primary and secondary cell walls. Front Plant Sci 3. https://doi.org/10.3389/fpls.2012.00204

Crowell EF, Bischoff V, Desprez T, Rolland A, Stierhof YD, Schumacher K, Gonneau M, Hofte H, Vernhettes S (2009) Pausing of Golgi bodies on microtubules regulates secretion of cellulose synthase complexes in *Arabidopsis*. Plant Cell 21:1141–1154

Culbertson AT, Chou YH, Smith AL, Young ZT, Tietze AA, Cottaz S, Faure R, Zabotina OA (2016) Enzymatic activity of xyloglucan xylosyltransferase 5. Plant Physiol 171:1893–1904

Culbertson AT, Ehrlich JJ, Choe JY, Honzatko RB, Zabotina OA (2018) Structure of xyloglucan xylosyltransferase 1 reveals simple steric rules that define biological patterns of xyloglucan polymers. Proc Natl Acad Sci U S A 115:6064–6069

Cvrckova F, Grunt M, Bezvoda R, Hala M, Kulich I, Rawat A, Zarsky V (2012) Evolution of the land plant exocyst complexes. Front Plant Sci 3. ARTN 159

Davis J, Brandizzi F, Liepman AH, Keegstra K (2010) *Arabidopsis* mannan synthase CSLA9 and glucan synthase CSLC4 have opposite orientations in the Golgi membrane. Plant J 64:1028–1037

DeBolt S, Gutierrez R, Ehrhardt DW, Somerville C (2007) Nonmotile cellulose synthase subunits repeatedly accumulate within localized regions at the plasma membrane in *Arabidopsis* hypocotyl cells following 2,6-dichlorobenzonitrile treatment. Plant Physiol 145:334–338

Delmer DP (1999) Cellulose biosynthesis: exciting times for a difficult field of study. Annu Rev Plant Physiol Plant Mol Biol 50:245–276

Derbyshire P, Menard D, Green P, Saalbach G, Buschmann H, Lloyd CW, Pesquet E (2015) Proteomic analysis of microtubule interacting proteins over the course of xylem tracheary element formation in *Arabidopsis*. Plant Cell 27:2709–2726

Desprez T, Vernhettes S, Fagard M, Refregier G, Desnos T, Aletti E, Py N, Pelletier S, Hofte H (2002) Resistance against herbicide isoxaben and cellulose deficiency caused by distinct mutations in same cellulose synthase isoform CESA6. Plant Physiol 128:482–490

Desprez T, Juraniec M, Crowell EF, Jouy H, Pochylova Z, Parcy F, Hofte H, Gonneau M, Vernhettes S (2007) Organization of cellulose synthase complexes involved in primary cell wall synthesis in *Arabidopsis thaliana*. Proc Natl Acad Sci U S A 104:15572–15577

Dhugga KS, Barreiro R, Whitten B, Stecca K, Hazebroek J, Randhawa GS, Dolan M, Kinney AJ, Tomes D, Nichols S, Anderson P (2004) Guar seed beta-mannan synthase is a member of the cellulose synthase super gene family. Science 303:363–366

Dick-Perez M, Zhang Y, Hayes J, Salazar A, Zabotina OA, Hong M (2011) Structure and interactions of plant cell-wall polysaccharides by two- and three-dimensional magic-angle-spinning solid-state NMR. Biochemistry 50:989–1000

Ding Y, Robinson DG, Jiang L (2014) Unconventional protein secretion (UPS) pathways in plants. Curr Opin Cell Biol 29:107–115

Doblin MS, Kurek I, Jacob-Wilk D, Delmer DP (2002) Cellulose biosynthesis in plants: from genes to rosettes. Plant Cell Physiol 43:1407–1420

Doblin MS, Pettolino FA, Wilson SM, Campbell R, Burton RA, Fincher GB, Newbigin E, Bacic A (2009) A barley cellulose synthase-like *CSLH* gene mediates (1,3;1,4)-beta-D-glucan synthesis in transgenic *Arabidopsis*. Proc Natl Acad Sci U S A 106:5996–6001

Domozych DS, Ciancia M, Fangel JU, Mikkelsen MD, Ulvskov P, Willats WGT (2012) The cell walls of green algae: a journey through evolution and diversity. Front Plant Sci 3. https://doi.org/10.3389/fpls.2012.00082. ARTN 82

Durand C, Vicre-Gibouin M, Follet-Gueye ML, Duponchel L, Moreau M, Lerouge P, Driouich A (2009) The organization pattern of root border-like cells of *Arabidopsis* is dependent on cell wall homogalacturonan. Plant Physiol 150:1411–1421

Ebringerova A, Hromadkova Z, Heinze T (2005) Hemicellulose Polysaccharides 1: Structure, Characterization and Use 186:1–67

Edwards ME, Dickson CA, Chengappa S, Sidebottom C, Gidley MJ, Reid JS (1999) Molecular characterisation of a membrane-bound galactosyltransferase of plant cell wall matrix polysaccharide biosynthesis. Plant J 19:691–697

Edwards M, Bulpin PV, Dea ICM, Reid JSG (1989) Biosynthesis of legume-seed galactomannans invitro – cooperative interactions of a guanosine 5′-diphosphate-mannose-linked (1-]4)-beta-d-mannosyltransferase and a uridine 5′-diphosphate-galactose-linked alpha-d-galactosyltransferase in particulate enzyme preparations from developing endosperms of fenugreek (*Trigonella-Foenum-Graecum L*) and guar (Cyamopsis-Tetragonoloba [L] Taub). Planta 178:41–51

Edwards ME, Marshall E, Gidley MJ, Reid JS (2002) Transfer specificity of detergent-solubilized fenugreek galactomannan galactosyltransferase. Plant Physiol 129:1391–1397

Endler A, Kesten C, Schneider R, Zhang Y, Ivakov A, Froehlich A, Funke N, Persson S (2015) A mechanism for sustained cellulose synthesis during salt stress. Cell 162:1353–1364

Endler A, Schneider R, Kesten C, Lampugnani ER, Persson S (2016) The cellulose synthase companion proteins act non-redundantly with CELLULOSE SYNTHASE INTERACTING1/

POM2 and CELLULOSE SYNTHASE 6. Plant Signal Behav 11:e1135281. https://doi.org/10.1080/15592324.2015.1135281

Fagard M, Desnos T, Desprez T, Goubet F, Refregier G, Mouille G, McCann M, Rayon C, Vernhettes S, Hofte H (2000) PROCUSTE1 encodes a cellulose synthase required for normal cell elongation specifically in roots and dark-grown hypocotyls of *Arabidopsis*. Plant Cell 12:2409–2423

Faik A (2010) Xylan biosynthesis: news from the grass. Plant Physiol 153:396–402

Faik A, Price NJ, Raikhel NV, Keegstra K (2002) An *Arabidopsis* gene encoding an alpha-xylosyltransferase involved in xyloglucan biosynthesis. Proc Natl Acad Sci U S A 99:7797–7802

Fernandes AN, Thomas LH, Altaner CM, Callow P, Forsyth VT, Apperley DC, Kennedy CJ, Jarvis MC (2011) Nanostructure of cellulose microfibrils in spruce wood. Proc Natl Acad Sci U S A 108:E1195–E1203. https://doi.org/10.1073/pnas.1108942108

Fincher GB (2009) Revolutionary times in our understanding of cell wall biosynthesis and remodeling in the grasses. Plant Physiol 149:27–37

Fry SC, York WS, Albersheim P, Darvill A, Hayashi T, Joseleau JP, Kato Y, Lorences EP, Maclachlan GA, Mcneil M, Mort AJ, Reid JSG, Seitz HU, Selvendran RR, Voragen AGJ, White AR (1993) An unambiguous nomenclature for xyloglucan-derived oligosaccharides. Physiol Plant 89:1–3

Gadeyne A, Sanchez-Rodriguez C, Vanneste S, Di Rubbo S, Zauber H, Vanneste K, Van Leene J, De Winne N, Eeckhout D, Persiau G, De Slijke EV, Cannoot B, Vercruysse L, Mayers JR, Adamowski M, Kania U, Ehrlich M, Schweighofer A, Ketelaar T, Maere S, Bednarek SY, Friml J, Gevaert K, Witters E, Russinova E, Persson S, De Jaeger G, Van Damme D (2014) The TPLATE adaptor complex drives clathrin-mediated endocytosis in plants. Cell 156:691–704

Gao Y, He C, Zhang D, Liu X, Xu Z, Tian Y, Liu XH, Zang S, Pauly M, Zhou Y, Zhang B (2017) Two trichome birefringence-like proteins mediate xylan acetylation, which is essential for leaf blight resistance in rice. Plant Physiol 173:470–481

Gardner KH, Blackwell J (1974) Hydrogen-bonding in native cellulose. Biochim Biophys Acta 343:232–237

Gendre D, Oh J, Boutte Y, Best JG, Samuels L, Nilsson R, Uemura T, Marchant A, Bennett MJ, Grebe M, Bhalerao RP (2011) Conserved *Arabidopsis* ECHIDNA protein mediates trans-Golgi-network trafficking and cell elongation. Proc Natl Acad Sci U S A 108:8048–8053

Gendre D, McFarlane HE, Johnson E, Mouille G, Sjodin A, Oh J, Levesque-Tremblay G, Watanabe Y, Samuels L, Bhalerao RP (2013) Trans-Golgi network localized ECHIDNA/Ypt interacting protein complex is required for the secretion of cell wall polysaccharides in *Arabidopsis*. Plant Cell 25:2633–2646

Gibeaut DM, Carpita NC (1993) Synthesis of (1–>3), (1–>4)-beta-D-glucan in the Golgi apparatus of maize coleoptiles. Proc Natl Acad Sci U S A 90:3850–3854

Giddings TH, Brower DL, Staehelin LA (1980) Visualization of particle complexes in the plasma-membrane of micrasterias-denticulata associated with the formation of cellulose fibrils in primary and secondary cell-walls. J Cell Biol 84:327–339

Gille S, Cheng K, Skinner ME, Liepman AH, Wilkerson CG, Pauly M (2011a) Deep sequencing of voodoo lily (*Amorphophallus konjac*): an approach to identify relevant genes involved in the synthesis of the hemicellulose glucomannan. Planta 234:515–526

Gille S, de Souza A, Xiong G, Benz M, Cheng K, Schultink A, Reca IB, Pauly M (2011b) O-acetylation of *Arabidopsis* hemicellulose xyloglucan requires AXY4 or AXY4L, proteins with a TBL and DUF231 domain. Plant Cell 23:4041–4053

Gille S, Pauly M (2012) O-acetylation of plant cell wall polysaccharides. Front Plant Sci 3(12). https://doi.org/10.3389/fpls.2012.00012

Gonneau M, Desprez T, Guillot A, Vernhettes S, Hofte H (2014) Catalytic subunit stoichiometry within the cellulose synthase complex. Plant Physiol 166:1709–1712

Gordon R, Maclachlan G (1989) Incorporation of UDP-[C]glucose into xyloglucan by pea membranes. Plant Physiol 91:373–378

Goubet F, Misrahi A, Park SK, Zhang Z, Twell D, Dupree P (2003) AtCSLA7, a cellulose synthase-like putative glycosyltransferase, is important for pollen tube growth and embryogenesis in *Arabidopsis*. Plant Physiol 131:547–557

Goubet F, Barton CJ, Mortimer JC, Yu X, Zhang Z, Miles GP, Richens J, Liepman AH, Seffen K, Dupree P (2009) Cell wall glucomannan in *Arabidopsis* is synthesised by CSLA glycosyltransferases, and influences the progression of embryogenesis. Plant J 60:527–538

Grantham NJ, Wurman-Rodrich J, Terrett OM, Lyczakowski JJ, Stott K, Iuga D, Simmons TJ, Durand-Tardif M, Brown SP, Dupree R, Busse-Wicher M, Dupree P (2017) An even pattern of xylan substitution is critical for interaction with cellulose in plant cell walls. Nat Plants 3:859–865

Gu Y, Somerville C (2010) Cellulose synthase interacting protein: a new factor in cellulose synthesis. Plant Signal Behav 5:1571–1574

Gu Y, Kaplinsky N, Bringmann M, Cobb A, Carroll A, Sampathkumar A, Baskin TI, Persson S, Somerville CR (2010) Identification of a cellulose synthase-associated protein required for cellulose biosynthesis. Proc Natl Acad Sci U S A 107:12866–12871

Gunl M, Neumetzler L, Kraemer F, de Souza A, Schultink A, Pena M, York WS, Pauly M (2011) AXY8 encodes an alpha-fucosidase, underscoring the importance of apoplastic metabolism on the fine structure of *Arabidopsis* cell wall polysaccharides. Plant Cell 23:4025–4040

Gutierrez R, Lindeboom JJ, Paredez AR, Emons AM, Ehrhardt DW (2009) *Arabidopsis* cortical microtubules position cellulose synthase delivery to the plasma membrane and interact with cellulose synthase trafficking compartments. Nat Cell Biol 11:797–806

Haigler CH, Brown RM (1986) Transport of rosettes from the Golgi-apparatus to the plasma-membrane in isolated mesophyll-cells of zinnia-elegans during differentiation to tracheary elements in suspension-culture. Protoplasma 134:111–120

Haigler CH, Betancur L, Stiff MR, Tuttle JR (2012) Cotton fiber: a powerful single-cell model for cell wall and cellulose research. Front Plant Sci 3:104. https://doi.org/10.3389/fpls.2012.00104

Hala M, Cole R, Synek L, Drdova E, Pecenkova T, Nordheim A, Lamkemeyer T, Madlung J, Hochholdinger F, Fowler JE, Zarsky V (2008) An exocyst complex functions in plant cell growth in *Arabidopsis* and tobacco. Plant Cell 20:1330–1345

Hamann T, Osborne E, Youngs HL, Misson J, Nussaume L, Somerville C (2004) Global expression analysis of *CESA* and *CSL* genes in *Arabidopsis*. Cellulose 11:279–286

Harpaz-Saad S, McFarlane HE, Xu SL, Divi UK, Forward B, Western TL, Kieber JJ (2011) Cellulose synthesis via the FEI2 RLK/SOS5 pathway and CELLULOSE SYNTHASE 5 is required for the structure of seed coat mucilage in *Arabidopsis*. Plant J 68:941–953

Hashimoto-Sugimoto M, Higaki T, Yaeno T, Nagami A, Irie M, Fujimi M, Miyamoto M, Akita K, Negi J, Shirasu K, Hasezawa S, Iba K (2013) A Munc13-like protein in *Arabidopsis* mediates H^+-ATPase translocation that is essential for stomatal responses. Nat Commun 4. https://doi.org/10.1038/ncomms3215. ARTN 2215

Hayashi T (1989) Xyloglucans in the primary-cell wall. Annu Rev Plant Physiol Plant Mol Biol 40:139–168

Hazen SP, Scott-Craig JS, Walton JD (2002) Cellulose synthase-like genes of rice. Plant Physiol 128:336–340

He B, Guo W (2009) The exocyst complex in polarized exocytosis. Curr Opin Cell Biol 21:537–542

Heider MR, Munson M (2012) Exorcising the exocyst complex. Traffic 13:898–907

Hemsley PA, Weimar T, Lilley KS, Dupree P, Grierson CS (2013) A proteomic approach identifies many novel palmitoylated proteins in *Arabidopsis*. New Phytol 197:805–814

Herth W (1983) Arrays of plasma-membrane "rosettes" involved in cellulose microfibril formation of spirogyra. Planta 159:347–356

Hill JL Jr, Hammudi MB, Tien M (2014) The *Arabidopsis* cellulose synthase complex: a proposed hexamer of CESA trimers in an equimolar stoichiometry. Plant Cell 26:4834–4842

Holland N, Holland D, Helentjaris T, Dhugga KS, Xoconostle-Cazares B, Delmer DP (2000) A comparative analysis of the plant cellulose synthase (CesA) gene family. Plant Physiol 123:1313–1324

Hornblad E, Ulfstedt M, Ronne H, Marchant A (2013) Partial functional conservation of IRX10 homologs in physcomitrella patens and *Arabidopsis thaliana* indicates an evolutionary step contributing to vascular formation in land plants. BMC Plant Biol 13:3

Hu R, Li J, Yang X, Zhao X, Wang X, Tang Q, He G, Zhou G, Kong Y (2016) Irregular xylem 7 (IRX7) is required for anchoring seed coat mucilage in *Arabidopsis*. Plant Mol Biol 92:25–38

Jensen JK, Kim H, Cocuron JC, Orler R, Ralph J, Wilkerson CG (2011) The DUF579 domain containing proteins IRX15 and IRX15-L affect xylan synthesis in *Arabidopsis*. Plant J 66:387–400

Jensen JK, Schultink A, Keegstra K, Wilkerson CG, Pauly M (2012) RNA-Seq analysis of developing nasturtium seeds (*Tropaeolum majus*): identification and characterization of an additional galactosyltransferase involved in xyloglucan biosynthesis. Mol Plant 5:984–992

Jensen JK, Johnson NR, Wilkerson CG (2014) *Arabidopsis thaliana* IRX10 and two related proteins from psyllium and Physcomitrella patens are xylan xylosyltransferases. Plant J 80:207–215

Jia ZH, Cash M, Darvill AG, York WS (2005) NMR characterization of endogenously O-acetylated oligosaccharides isolated from tomato (*Lycopersicon esculentum*) xyloglucan. Carbohydr Res 340:1818–1825

Jiang N, Wiemels RE, Soya A, Whitley R, Held M, Faik A (2016) Composition, assembly, and trafficking of a wheat xylan synthase complex. Plant Physiol 170:1999–2023

Jobling SA (2015) Membrane pore architecture of the CslF6 protein controls (1-3,1-4)-beta-glucan structure. Sci Adv 1:e1500069. https://doi.org/10.1126/sciadv.1500069

Kang BH, Staehelin LA (2008) ER-to-Golgi transport by COPII vesicles in *Arabidopsis* involves a ribosome-excluding scaffold that is transferred with the vesicles to the Golgi matrix. Protoplasma 234:51–64

Keppler BD, Showalter AM (2010) IRX14 and IRX14-LIKE, two glycosyl transferases involved in glucuronoxylan biosynthesis and drought tolerance in *Arabidopsis*. Mol Plant 3:834–841

Kim SJ, Zemelis S, Keegstra K, Brandizzi F (2015) The cytoplasmic localization of the catalytic site of CSLF6 supports a channeling model for the biosynthesis of mixed-linkage glucan. Plant J 81:537–547

Kimura S, Laosinchai W, Itoh T, Cui X, Linder CR, Brown RM Jr (1999) Immunogold labeling of rosette terminal cellulose-synthesizing complexes in the vascular plant vigna angularis. Plant Cell 11:2075–2086

Kong D, Karve R, Willet A, Chen MK, Oden J, Shpak ED (2012) Regulation of plasmodesmatal permeability and stomatal patterning by the glycosyltransferase-like protein KOBITO1. Plant Physiol 159:156–168

Kooiman P (1957) Amyloids of plant seeds. Nature 179:107–109

Kumar M, Turner S (2015) Plant cellulose synthesis: CESA proteins crossing kingdoms. Phytochemistry 112:91–99

Kumar M, Wightman R, Atanassov I, Gupta A, Hurst CH, Hemsley PA, Turner S (2016) S-acylation of the cellulose synthase complex is essential for its plasma membrane localization. Science 353:166–169

Kumar M, Mishra L, Carr P, Pilling M, Gardner P, Mansfield SD, Turner S (2018) Exploiting CELLULOSE SYNTHASE (CESA) class specificity to probe cellulose microfibril biosynthesis. Plant Physiol 177:151–167

Kurek I, Kawagoe Y, Jacob-Wilk D, Doblin M, Delmer D (2002) Dimerization of cotton fiber cellulose synthase catalytic subunits occurs via oxidation of the zinc-binding domains. Proc Natl Acad Sci U S A 99:11109–11114

Landrein B, Lathe R, Bringmann M, Vouillot C, Ivakov A, Boudaoud A, Persson S, Hamant O (2013) Impaired cellulose synthase guidance leads to stem torsion and twists phyllotactic patterns in *Arabidopsis*. Curr Biol 23:895–900

Lee C, Zhong R, Richardson EA, Himmelsbach DS, McPhail BT, Ye ZH (2007) The *PARVUS* gene is expressed in cells undergoing secondary wall thickening and is essential for glucuronoxylan biosynthesis. Plant Cell Physiol 48:1659–1672

Lee C, Teng Q, Huang W, Zhong R, Ye ZH (2009) The F8H glycosyltransferase is a functional paralog of FRA8 involved in glucuronoxylan biosynthesis in *Arabidopsis*. Plant Cell Physiol 50:812–827

Lee C, Teng Q, Huang W, Zhong R, Ye ZH (2010) The *Arabidopsis* family GT43 glycosyltransferases form two functionally nonredundant groups essential for the elongation of glucuronoxylan backbone. Plant Physiol 153:526–541

Lee CH, Teng Q, Zhong RQ, Ye ZH (2011) The four *Arabidopsis REDUCED WALL ACETYLATION* genes are expressed in secondary wall-containing cells and required for the acetylation of xylan. Plant Cell Physiol 52:1289–1301

Lee C, Teng Q, Zhong R, Ye ZH (2012a) *Arabidopsis* GUX proteins are glucuronyltransferases responsible for the addition of glucuronic acid side chains onto xylan. Plant Cell Physiol 53:1204–1216

Lee C, Teng Q, Zhong R, Yuan Y, Haghighat M, Ye ZH (2012b) Three *Arabidopsis* DUF579 domain-containing GXM proteins are methyltransferases catalyzing 4-o-methylation of glucuronic acid on xylan. Plant Cell Physiol 53:1934–1949

Lei L, Li S, Gu Y (2012) Cellulose synthase interactive protein 1 (CSI1) mediates the intimate relationship between cellulose microfibrils and cortical microtubules. Plant Signal Behav 7:714–718

Lei L, Li S, Du J, Bashline L, Gu Y (2013) Cellulose synthase INTERACTIVE3 regulates cellulose biosynthesis in both a microtubule-dependent and microtubule-independent manner in *Arabidopsis*. Plant Cell 25:4912–4923

Lei L, Zhang T, Strasser R, Lee CM, Gonneau M, Mach L, Vernhettes S, Kim SH, Cosgrove DJ, Li SD, Gu Y (2014) The *jiaoyao1* mutant is an allele of *korrigan1* that abolishes endoglucanase activity and affects the organization of both cellulose microfibrils and microtubules in *Arabidopsis*. Plant Cell 26:2601–2616

Lei L, Singh A, Bashline L, Li SD, Yingling YG, Gu Y (2015) CELLULOSE SYNTHASE INTERACTIVE1 is required for fast recycling of cellulose synthase complexes to the plasma membrane in *Arabidopsis*. Plant Cell 27:2926–2940

Leonard R, Pabst M, Bondili JS, Chambat G, Veit C, Strasser R, Altmann F (2008) Identification of an *Arabidopsis* gene encoding a GH95 alpha1,2-fucosidase active on xyloglucan oligo- and polysaccharides. Phytochemistry 69:1983–1988

Lertpiriyapong K, Sung ZR (2003) The *elongation defective1* mutant of *Arabidopsis* is impaired in the gene encoding a serine-rich secreted protein. Plant Mol Biol 53:581–595

Li S, Lei L, Somerville CR, Gu Y (2012) Cellulose synthase interactive protein 1 (CSI1) links microtubules and cellulose synthase complexes. Proc Natl Acad Sci U S A 109:185–190

Li S, Bashline L, Lei L, Gu Y (2014) Cellulose synthesis and its regulation. *Arabidopsis* Book 12: e0169. https://doi.org/10.1199/tab.0169

Li SD, Bashline L, Zheng YZ, Xin XR, Huang SX, Kong ZS, Kim SH, Cosgrove DJ, Gu Y (2016) Cellulose synthase complexes act in a concerted fashion to synthesize highly aggregated cellulose in secondary cell walls of plants. Proc Natl Acad Sci U S A 113:11348–11353

Liebminger E, Grass J, Altmann F, Mach L, Strasser R (2013) Characterizing the link between glycosylation state and enzymatic activity of the endo-beta 1,4-glucanase KORRIGAN1 from *Arabidopsis thaliana*. J Biol Chem 288:22270–22280

Liepman AH, Wilkerson CG, Keegstra K (2005) Expression of cellulose synthase-like (Csl) genes in insect cells reveals that CslA family members encode mannan synthases. Proc Natl Acad Sci U S A 102:2221–2226

Liepman AH, Nairn CJ, Willats WG, Sorensen I, Roberts AW, Keegstra K (2007) Functional genomic analysis supports conservation of function among cellulose synthase-like a gene family members and suggests diverse roles of mannans in plants. Plant Physiol 143:1881–1893

Liu D, Zehfroosh N, Hancock BL, Hines K, Fang W, Kilfoil M, Learned-Miller E, Sanguinet KA, Goldner LS, Baskin TI (2017) Imaging cellulose synthase motility during primary cell wall synthesis in the grass Brachypodium distachyon. Sci Rep 7:15111

Lundqvist J, Teleman A, Junel L, Zacchi G, Dahlman O, Tjerneld F, Stalbrand H (2002) Isolation and characterization of galactoglucomannan from spruce (*Picea abies*). Carbohydr Polym 48:29–39

Madson M, Dunand C, Li X, Verma R, Vanzin GF, Caplan J, Shoue DA, Carpita NC, Reiter WD (2003) The *MUR3* gene of *Arabidopsis* encodes a xyloglucan galactosyltransferase that is evolutionarily related to animal exostosins. Plant Cell 15:1662–1670

Manabe Y, Nafisi M, Verhertbruggen Y, Orfila C, Gille S, Rautengarten C, Cherk C, Marcus SE, Somerville S, Pauly M, Knox JP, Sakuragi Y, Scheller HV (2011) Loss-of-function mutation of *REDUCED WALL ACETYLATION2* in *Arabidopsis* leads to reduced cell wall ACETYLATION and increased resistance to Botrytis cinerea. Plant Physiol 155:1068–1078

Manabe Y, Verhertbruggen Y, Gille S, Harholt J, Chong SL, Pawar PM, Mellerowicz EJ, Tenkanen M, Cheng K, Pauly M, Scheller HV (2013) Reduced wall acetylation proteins play vital and distinct roles in cell wall O-acetylation in *Arabidopsis*. Plant Physiol 163:1107–1117

McCarthy RL, Zhong RQ, Ye ZH (2009) MYB83 is a direct target of SND1 and acts redundantly with MYB46 in the regulation of secondary cell wall biosynthesis in *Arabidopsis*. Plant Cell Physiol 50:1950–1964

Mendu V, Griffiths JS, Persson S, Stork J, Downie AB, Voiniciuc C, Haughn GW, DeBolt S (2011) Subfunctionalization of cellulose synthases in seed coat epidermal cells mediates secondary radial wall synthesis and mucilage attachment. Plant Physiol 157:441–453

Mitsuda N, Ohme-Takagi M (2008) NAC transcription factors NST1 and NST3 regulate pod shattering in a partially redundant manner by promoting secondary wall formation after the establishment of tissue identity. Plant J 56:768–778

Mitsuda N, Iwase A, Yamamoto H, Yoshida M, Seki M, Shinozaki K, Ohme-Takagi M (2007) NAC transcription factors, NST1 and NST3, are key regulators of the formation of secondary walls in woody tissues of *Arabidopsis*. Plant Cell 19:270–280

Molhoj M, Pagant SR, Hofte H (2002) Towards understanding the role of membrane-bound endo-beta-1,4-glucanases in cellulose biosynthesis. Plant Cell Physiol 43:1399–1406

Moreira LRS, Filho EXF (2008) An overview of mannan structure and mannan-degrading enzyme systems. Appl Microbiol Biotechnol 79:165–178

Morgan JL, Strumillo J, Zimmer J (2013) Crystallographic snapshot of cellulose synthesis and membrane translocation. Nature 493:181–186

Mortimer JC, Miles GP, Brown DM, Zhang Z, Segura MP, Weimar T, Yu X, Seffen KA, Stephens E, Turner SR, Dupree P (2010) Absence of branches from xylan in *Arabidopsis gux* mutants reveals potential for simplification of lignocellulosic biomass. Proc Natl Acad Sci U S A 107:17409–17414

Mueller SC, Brown RM (1980) Evidence for an intramembrane component associated with a cellulose microfibril-synthesizing complex in higher-plants. J Cell Biol 84:315–326

Newman RH, Hill SJ, Harris PJ (2013) Wide-angle x-ray scattering and solid-state nuclear magnetic resonance data combined to test models for cellulose microfibrils in mung bean cell walls. Plant Physiol 163:1558–1567

Nicol F, His I, Jauneau A, Vernhettes S, Canut H, Hofte H (1998) A plasma membrane-bound putative endo-1,4-beta-D-glucanase is required for normal wall assembly and cell elongation in *Arabidopsis*. EMBO J 17:5563–5576

Nieduszy I, Preston RD (1970) Crystallite size in natural cellulose. Nature 225:273–274

Nishiyama Y (2009) Structure and properties of the cellulose microfibril. J Wood Sci 55:241–249

Nishiyama Y, Langan P, Chanzy H (2002) Crystal structure and hydrogen-bonding system in cellulose Ibeta from synchrotron X-ray and neutron fiber diffraction. J Am Chem Soc 124:9074–9082

Nixon BT, Mansouri K, Singh A, Du J, Davis JK, Lee JG, Slabaugh E, Vandavasi VG, O'Neill H, Roberts EM, Roberts AW, Yingling YG, Haigler CH (2016) Comparative structural and

computational analysis supports eighteen cellulose synthases in the plant cellulose synthesis complex. Sci Rep 6:28696
Nuhse TS, Stensballe A, Jensen ON, Peck SC (2004) Phosphoproteomics of the *Arabidopsis* plasma membrane and a new phosphorylation site database. Plant Cell 16:2394–2405
Obel N, Erben V, Schwarz T, Kuhnel S, Fodor A, Pauly M (2009) Microanalysis of plant cell wall polysaccharides. Mol Plant 2:922–932
Oehme DP, Downton MT, Doblin MS, Wagner J, Gidley MJ, Bacic A (2015) Unique aspects of the structure and dynamics of elementary Ibeta cellulose microfibrils revealed by computational simulations. Plant Physiol 168:3–17
Olek AT, Rayon C, Makowski L, Kim HR, Ciesielski P, Badger J, Paul LN, Ghosh S, Kihara D, Crowley M, Himmel ME, Bolin JT, Carpita NC (2014) The structure of the catalytic domain of a plant cellulose synthase and its assembly into dimers. Plant Cell 26:2996–3009
Omadjela O, Narahari A, Strumillo J, Melida H, Mazur O, Bulone V, Zimmer J (2013) BcsA and BcsB form the catalytically active core of bacterial cellulose synthase sufficient for in vitro cellulose synthesis. Proc Natl Acad Sci U S A 110:17856–17861
Pagant S, Bichet A, Sugimoto K, Lerouxel O, Desprez T, McCann M, Lerouge P, Vernhettes S, Hofte H (2002) *KOBITO1* encodes a novel plasma membrane protein necessary for normal synthesis of cellulose during cell expansion in *Arabidopsis*. Plant Cell 14:2001–2013
Paredez AR, Somerville CR, Ehrhardt DW (2006) Visualization of cellulose synthase demonstrates functional association with microtubules. Science 312:1491–1495
Park YB, Cosgrove DJ (2012) A revised architecture of primary cell walls based on biomechanical changes induced by substrate-specific endoglucanases. Plant Physiol 158:1933–1943
Park S, Szumlanski AL, Gu F, Guo F, Nielsen E (2011) A role for CSLD3 during cell-wall synthesis in apical plasma membranes of tip-growing root-hair cells. Nat Cell Biol 13:973–980
Pauly M, Albersheim P, Darvill A, York WS (1999) Molecular domains of the cellulose/xyloglucan network in the cell walls of higher plants. Plant J 20:629–639
Pauly M, Gille S, Liu L, Mansoori N, de Souza A, Schultink A, Xiong G (2013) Hemicellulose biosynthesis. Planta 238:627–642
Pear JR, Kawagoe Y, Schreckengost WE, Delmer DP, Stalker DM (1996) Higher plants contain homologs of the bacterial *celA* genes encoding the catalytic subunit of cellulose synthase. Proc Natl Acad Sci U S A 93:12637–12642
Pena MJ, Zhong R, Zhou GK, Richardson EA, O'Neill MA, Darvill AG, York WS, Ye ZH (2007) *Arabidopsis irregular xylem8* and *irregular xylem9*: implications for the complexity of glucuronoxylan biosynthesis. Plant Cell 19:549–563
Pena MJ, Kong Y, York WS, O'Neill MA (2012) A galacturonic acid-containing xyloglucan is involved in *Arabidopsis* root hair tip growth. Plant Cell 24:4511–4524
Perrin RM (2001) Cellulose: how many cellulose synthases to make a plant? Curr Biol 11:R213–R216
Perrin RM, DeRocher AE, Bar-Peled M, Zeng W, Norambuena L, Orellana A, Raikhel NV, Keegstra K (1999) Xyloglucan fucosyltransferase, an enzyme involved in plant cell wall biosynthesis. Science 284:1976–1979
Persson S, Wei HR, Milne J, Page GP, Somerville CR (2005) Identification of genes required for cellulose synthesis by regression analysis of public microarray data sets. Proc Natl Acad Sci U S A 102:8633–8638
Persson S, Caffall KH, Freshour G, Hilley MT, Bauer S, Poindexter P, Hahn MG, Mohnen D, Somerville C (2007a) The *Arabidopsis irregular xylem8* mutant is deficient in glucuronoxylan and homogalacturonan, which are essential for secondary cell wall integrity. Plant Cell 19:237–255
Persson S, Paredez A, Carroll A, Palsdottir H, Doblin M, Poindexter P, Khitrov N, Auer M, Somerville CR (2007b) Genetic evidence for three unique components in primary cell-wall cellulose synthase complexes in *Arabidopsis*. Proc Natl Acad Sci U S A 104:15566–15571
Polgar N, Fogelgren B (2017) Regulation of cell polarity by exocyst-mediated trafficking. Cold Spring Harb Perspect Biol. https://doi.org/10.1101/cshperspect.a031401

Popper ZA (2008) Evolution and diversity of green plant cell walls. Curr Opin Plant Biol 11:286–292

Popper ZA, Fry SC (2003) Primary cell wall composition of bryophytes and charophytes. Ann Bot 91:1–12

Popper ZA, Fry SC (2008) Xyloglucan-pectin linkages are formed intra-protoplasmically, contribute to wall-assembly, and remain stable in the cell wall. Planta 227:781–794

Potikha T, Delmer DP (1995) A mutant of *Arabidopsis thaliana* displaying altered patterns of cellulose deposition. Plant J 7:453–460

Purushotham P, Cho SH, Diaz-Moreno SM, Kumar M, Nixon BT, Bulone V, Zimmer J (2016) A single heterologously expressed plant cellulose synthase isoform is sufficient for cellulose microfibril formation in vitro. Proc Natl Acad Sci U S A 113:11360–11365

Reiter WD, Chapple C, Somerville CR (1997) Mutants of *Arabidopsis thaliana* with altered cell wall polysaccharide composition. Plant J 12:335–345

Ren Y, Hansen SF, Ebert B, Lau J, Scheller HV (2014) Site-directed mutagenesis of IRX9, IRX9L and IRX14 proteins involved in xylan biosynthesis: glycosyltransferase activity is not required for IRX9 function in *Arabidopsis*. PLoS One 9:e105014. https://doi.org/10.1371/journal.pone.0105014

Reid JSG (1985) Cell wall storage carbohydrates in seeds - biochemistry of the seed gums and hemicelluloses. Adv Bot Res 11:125–155

Reid JSG, Edwards M, Gidley MJ, Clark AH (1995) Enzyme specificity in galactomannan biosynthesis. Planta 195:489–495

Rennie EA, Scheller HV (2014) Xylan biosynthesis. Curr Opin Biotechnol 26:100–107

Reiss HD, Schnepf E, Herth W (1984) The plasma membrane of the *Funaria* caulonema tip cell: morphology and distribution of particle rosettes, and the kinetics of cellulose synthesis. Planta 160:428–435

Richmond T (2000) Higher plant cellulose synthases. Genome Biol 1:REVIEWS3001

Roberts AW, Bushoven JT (2007) The cellulose synthase (*CESA*) gene superfamily of the moss *Physcomitrella patens*. Plant Mol Biol 63:207–219

Roberts A, Roberts E (2007) Evolution of the cellulose synthase (*CesA*) gene family: insights from green algae and seedless plants. In: Brown RM, Saxena IM (eds) Cellulose: Molecular and Structural Biology. Springer, Dordrecht, pp 17–34

Robinson DG, Preston RD, White RK (1972) Fine-structure of swarmers of *Cladophora* and *Chaetomorpha* .3. Wall synthesis and development. Planta 107:131–144

Rodriguez-Gacio MDC, Iglesias-Fernandez R, Carbonero P, Matilla AJ (2012) Softening-up mannan-rich cell walls. J Exp Bot 63:3975–3988

Rose JK, Braam J, Fry SC, Nishitani K (2002) The XTH family of enzymes involved in xyloglucan endotransglucosylation and endohydrolysis: current perspectives and a new unifying nomenclature. Plant Cell Physiol 43:1421–1435

Roudier F, Fernandez AG, Fujita M, Himmelspach R, Borner GH, Schindelman G, Song S, Baskin TI, Dupree P, Wasteneys GO, Benfey PN (2005) COBRA, an *Arabidopsis* extracellular glycosyl-phosphatidyl inositol-anchored protein, specifically controls highly anisotropic expansion through its involvement in cellulose microfibril orientation. Plant Cell 17:1749–1763

Rushton PS, Olek AT, Makowski L, Badger J, Steussy CN, Carpita NC, Stauffacher CV (2017) Rice cellulose synthasea8 plant-conserved region is a coiled-coil at the catalytic core entrance. Plant Physiol 173:482–494

Sampathkumar A, Gutierrez R, McFarlane HE, Bringmann M, Lindeboom J, Emons AM, Samuels L, Ketelaar T, Ehrhardt DW, Persson S (2013) Patterning and lifetime of plasma membrane-localized cellulose synthase is dependent on actin organization in *Arabidopsis* interphase cells. Plant Physiol 162:675–688

Sampedro J, Sieiro C, Revilla G, Gonzalez-Villa T, Zarra I (2001) Cloning and expression pattern of a gene encoding an alpha-xylosidase active against xyloglucan oligosaccharides from *Arabidopsis*. Plant Physiol 126:910–920

Sampedro J, Gianzo C, Iglesias N, Guitian E, Revilla G, Zarra I (2012) AtBGAL10 is the main xyloglucan beta-galactosidase in *Arabidopsis*, and its absence results in unusual xyloglucan subunits and growth defects. Plant Physiol 158:1146–1157

Sanchez-Rodriguez C, Ketelaar K, Schneider R, Villalobos JA, Somerville CR, Persson S, Wallace IS (2017) BRASSINOSTEROID INSENSITIVE2 negatively regulates cellulose synthesis in *Arabidopsis* by phosphorylating cellulose synthase 1. Proc Natl Acad Sci U S A 114:3533–3538

Sato S, Kato T, Kakegawa K, Ishii T, Liu YG, Awano T, Takabe K, Nishiyama Y, Kuga S, Sato S, Nakamura Y, Tabata S, Shibata D (2001) Role of the putative membrane-bound endo-1,4-beta-glucanase KORRIGAN in cell elongation and cellulose synthesis in *Arabidopsis thaliana*. Plant Cell Physiol 42:251–263

Saxena IM, Lin FC, Brown RM (1990) Cloning and sequencing of the cellulose synthase catalytic subunit gene of *Acetobacter-Xylinum*. Plant Mol Biol 15:673–683

Saxena IM, Brown RM, Dandekar T (2001) Structure-function characterization of cellulose synthase: relationship to other glycosyltransferases. Phytochemistry 57:1135–1148

Scavuzzo-Duggan TR, Chaves AM, Singh A, Sethaphong L, Slabaugh E, Yingling YG, Haigler CH, Roberts AW (2018) Cellulose synthase 'class specific regions' are intrinsically disordered and functionally undifferentiated. J Integr Plant Biol. https://doi.org/10.1111/jipb.12637

Scheible WR, Eshed R, Richmond T, Delmer D, Somerville C (2001) Modifications of cellulose synthase confer resistance to isoxaben and thiazolidinone herbicides in *Arabidopsis Ixr1* mutants. Proc Natl Acad Sci U S A 98:10079–10084

Scheller HV, Ulvskov P (2010) Hemicelluloses. Annu Rev Plant Biol 61:263–289

Schindelman G, Morikami A, Jung J, Baskin TI, Carpita NC, Derbyshire P, McCann MC, Benfey PN (2001) COBRA encodes a putative GPI-anchored protein, which is polarly localized and necessary for oriented cell expansion in *Arabidopsis*. Genes Dev 15:1115–1127

Schneider R, Tang L, Lampugnani ER, Barkwill S, Lathe R, Zhang Y, McFarlane HE, Pesquet E, Niittyla T, Mansfield SD, Zhou Y, Persson S (2017) Two complementary mechanisms underpin cell wall patterning during xylem vessel development. Plant Cell 29:2433–2449

Schrick K, DeBolt S, Bulone V (2012) Deciphering the molecular functions of sterols in cellulose biosynthesis. Front Plant Sci 3. https://doi.org/10.3389/fpls.2012.00084. ARTN 84

Schultink A, Liu L, Zhu L, Pauly M (2014) Structural diversity and function of xyloglucan sidechain substituents. Plants (Basel) 3:526–542

Schultink A, Naylor D, Dama M, Pauly M (2015) The role of the plant-specific ALTERED XYLOGLUCAN9 protein in *Arabidopsis* cell wall polysaccharide O-acetylation. Plant Physiol 167:1271–1283

Sethaphong L, Haigler CH, Kubicki JD, Zimmer J, Bonetta D, DeBolt S, Yingling YG (2013) Tertiary model of a plant cellulose synthase. Proc Natl Acad Sci U S A 110:7512–7517

Sethaphong L, Davis JK, Slabaugh E, Singh A, Haigler CH, Yingling YG (2016) Prediction of the structures of the plant-specific regions of vascular plant cellulose synthases and correlated functional analysis. Cellulose 23:145–161

Simmons TJ, Mortimer JC, Bernardinelli OD, Poppler AC, Brown SP, deAzevedo ER, Dupree R, Dupree P (2016) Folding of xylan onto cellulose fibrils in plant cell walls revealed by solid-state NMR. Nat Commun 7:13902

Sindhu A, Langewisch T, Olek A, Multani DS, McCann MC, Vermerris W, Carpita NC, Johal G (2007) Maize *brittle stalk2* encodes a COBRA-like protein expressed in early organ development but required for tissue flexibility at maturity. Plant Physiol 145:1444–1459

Slabaugh E, Scavuzzo-Duggan T, Chaves A, Wilson L, Wilson C, Davis JK, Cosgrove DJ, Anderson CT, Roberts AW, Haigler CH (2016) The valine and lysine residues in the conserved FxVTxK motif are important for the function of phylogenetically distant plant cellulose synthases. Glycobiology 26:509–519

Smith BG, Harris PJ (1999) The polysaccharide composition of Poales cell walls: Poaceae cell walls are not unique. Biochem Syst Ecol 27:33–53

Somerville C (2006) Cellulose synthesis in higher plants. Annu Rev Cell Dev Biol 22:53–78

Somerville C, Bauer S, Brininstool G, Facette M, Hamann T, Milne J, Osborne E, Paredez A, Persson S, Raab T, Vorwerk S, Youngs H (2004) Toward a systems approach to understanding plant cell walls. Science 306:2206–2211

Sorensen I, Pettolino FA, Wilson SM, Doblin MS, Johansen B, Bacic A, Willats WG (2008) Mixed-linkage (1–>3),(1–>4)-beta-D-glucan is not unique to the Poales and is an abundant component of Equisetum arvense cell walls. Plant J 54:510–521

Sterling JD, Atmodjo MA, Inwood SE, Kumar Kolli VS, Quigley HF, Hahn MG, Mohnen D (2006) Functional identification of an *Arabidopsis* pectin biosynthetic homogalacturonan galacturonosyltransferase. Proc Natl Acad Sci U S A 103:5236–5241

Stone BA, Carke AE (1992) Chemistry and biology of (1–3)-beta-glucans. La Trobe University Press

Stork J, Harris D, Griffiths J, Williams B, Beisson F, Li-Beisson Y, Mendu V, Haughn G, DeBolt S (2010) CELLULOSE SYNTHASE9 serves a nonredundant role in secondary cell wall synthesis in *Arabidopsis* epidermal testa cells. Plant Physiol 153:580–589

Sturcova A, His I, Apperley DC, Sugiyama J, Jarvis MC (2004) Structural details of crystalline cellulose from higher plants. Biomacromolecules 5:1333–1339

Suzuki S, Li L, Sun YH, Chiang VL (2006) The cellulose synthase gene superfamily and biochemical functions of xylem-specific cellulose synthase-like genes in Populus trichocarpa. Plant Physiol 142:1233–1245

Szyjanowicz PMJ, McKinnon I, Taylor NG, Gardiner J, Jarvis MC, Turner SR (2004) The *irregular xylem 2* mutant is an allele of korrigan that affects the secondary cell wall of *Arabidopsis thaliana*. Plant J 37:730–740

Takahashi J, Rudsander UJ, Hedenstrom M, Banasiak A, Harholt J, Amelot N, Immerzeel P, Ryden P, Endo S, Ibatullin FM, Brumer H, del Campillo E, Master ER, Scheller HV, Sundberg B, Teeri TT, Mellerowicz EJ (2009) KORRIGAN1 and its aspen homolog PttCel9A1 decrease cellulose crystallinity in *Arabidopsis* stems. Plant Cell Physiol 50:1099–1115

Taylor NG (2007) Identification of cellulose synthase AtCesA7 (IRX3) in vivo phosphorylation sites - a potential role in regulating protein degradation. Plant Mol Biol 64:161–171

Taylor NG (2008) Cellulose biosynthesis and deposition in higher plants. New Phytol 178:239–252

Taylor NG, Howells RM, Huttly AK, Vickers K, Turner SR (2003) Interactions among three distinct CesA proteins essential for cellulose synthesis. Proc Natl Acad Sci U S A 100:1450–1455

Thomas LH, Forsyth VT, Sturcova A, Kennedy CJ, May RP, Altaner CM, Apperley DC, Wess TJ, Jarvis MC (2013) Structure of cellulose microfibrils in primary cell walls from collenchyma. Plant Physiol 161:465–476

Thompson DS (2005) How do cell walls regulate plant growth? J Exp Bot 56:2275–2285

Toyooka K, Matsuoka K (2009) Exo- and endocytotic trafficking of SCAMP2. Plant Signal Behav 4:1196–1198

Toyooka K, Goto Y, Asatsuma S, Koizumi M, Mitsui T, Matsuoka K (2009) A mobile secretory vesicle cluster involved in mass transport from the Golgi to the plant cell exterior. Plant Cell 21:1212–1229

Tran ML, McCarthy TW, Sun H, Wu SZ, Norris JH, Bezanilla M, Vidali L, Anderson CT, Roberts AW (2018) Direct observation of the effects of cellulose synthesis inhibitors using live cell imaging of cellulose synthase (CESA) in *Physcomitrella patens*. Sci Rep 8:735

Triplett BA, Timpa JD (1995) Characterization of cell-wall polymers from cotton ovule culture fiber cells by gel-permeation chromatography. In Vitro Cell Dev Biol Plant 31:171–175

Tsekos I (1999) The sites of cellulose synthesis in algae: diversity and evolution of cellulose-synthesizing enzyme complexes. J Phycol 35:635–655

Tuomivaara ST, Yaoi K, O'Neill MA, York WS (2015) Generation and structural validation of a library of diverse xyloglucan-derived oligosaccharides, including an update on xyloglucan nomenclature. Carbohydr Res 402:56–66

Urbanowicz BR, Rayon C, Carpita NC (2004) Topology of the maize mixed linkage (1->3),(1->4)-beta-d-glucan synthase at the Golgi membrane. Plant Physiol 134:758–768

Urbanowicz BR, Pena MJ, Ratnaparkhe S, Avci U, Backe J, Steet HF, Foston M, Li H, O'Neill MA, Ragauskas AJ, Darvill AG, Wyman C, Gilbert HJ, York WS (2012) 4-O-methylation of glucuronic acid in *Arabidopsis* glucuronoxylan is catalyzed by a domain of unknown function family 579 protein. Proc Natl Acad Sci U S A 109:14253–14258

Urbanowicz BR, Pena MJ, Moniz HA, Moremen KW, York WS (2014) Two *Arabidopsis* proteins synthesize acetylated xylan *in vitro*. Plant J 80:197–206

Vain T, Crowell EF, Timpano H, Biot E, Desprez T, Mansoori N, Trindade LM, Pagant S, Robert S, Hofte H, Gonneau M, Vernhettes S (2014) The cellulase KORRIGAN is part of the cellulose synthase complex. Plant Physiol 165:1521–1532

Vandavasi VG, Putnam DK, Zhang Q, Petridis L, Heller WT, Nixon BT, Haigler CH, Kalluri U, Coates L, Langan P, Smith JC, Meiler J, O'Neill H (2016) A structural study of CESA1 catalytic domain of *Arabidopsis* cellulose synthesis complex: evidence for CESA trimers. Plant Physiol 170:123–135

Vanzin GF, Madson M, Carpita NC, Raikhel NV, Keegstra K, Reiter WD (2002) The *mur2* mutant of *Arabidopsis thaliana* lacks fucosylated xyloglucan because of a lesion in fucosyltransferase AtFUT1. Proc Natl Acad Sci U S A 99:3340–3345

Vega-Sanchez ME, Verhertbruggen Y, Christensen U, Chen X, Sharma V, Varanasi P, Jobling SA, Talbot M, White RG, Joo M, Singh S, Auer M, Scheller HV, Ronald PC (2012) Loss of cellulose synthase-like F6 function affects mixed-linkage glucan deposition, cell wall mechanical properties, and defense responses in vegetative tissues of rice. Plant Physiol 159:56–69

Vergara CE, Carpita NC (2001) Beta-D-glycan synthases and the CesA gene family: lessons to be learned from the mixed-linkage (1 -> 3),(1 -> 4)beta-D-glucan synthase. Plant Mol Biol 47:145–160

Verhertbruggen Y, Yin L, Oikawa A, Scheller HV (2011) Mannan synthase activity in the CSLD family. Plant Signal Behav 6:1620–1623

Vukasinovic N, Oda Y, Pejchar P, Synek L, Pecenkova T, Rawat A, Sekeres J, Potocky M, Zarsky V (2017) Microtubule-dependent targeting of the exocyst complex is necessary for xylem development in *Arabidopsis*. New Phytol 213:1052–1067

Vuttipongchaikij S, Brocklehurst D, Steele-King C, Ashford DA, Gomez LD, McQueen-Mason SJ (2012) *Arabidopsis* GT34 family contains five xyloglucan alpha-1,6-xylosyltransferases. New Phytol 195:585–595

Wada M, Kondo T, Okano T (2003) Thermally induced crystal transformation from cellulose I-alpha to I-beta. Polymer J 35:155–159

Wan JX, Zhu XF, Wang YQ, Liu LY, Zhang BC, Li GX, Zhou YH, Zheng SJ (2018) Xyloglucan fucosylation modulates *Arabidopsis* cell wall hemicellulose aluminium binding capacity. Sci Rep 8:428

Wang HZ, Dixon RA (2012) On-off switches for secondary cell wall biosynthesis. Mol Plant 5:297–303

Wang Y, Alonso AP, Wilkerson CG, Keegstra K (2012) Deep EST profiling of developing fenugreek endosperm to investigate galactomannan biosynthesis and its regulation. Plant Mol Biol 79:243–258

Wang T, Hong M (2016) Solid-state NMR investigations of cellulose structure and interactions with matrix polysaccharides in plant primary cell walls. J Exp Bot 67:503–514

Wang C, Yan X, Chen Q, Jiang N, Fu W, Ma BJ, Liu JZ, Li CY, Bednarek SY, Pan JW (2013a) Clathrin light chains regulate clathrin-mediated trafficking, auxin signaling, and development in *Arabidopsis*. Plant Cell 25:499–516

Wang Y, Mortimer JC, Davis J, Dupree P, Keegstra K (2013b) Identification of an additional protein involved in mannan biosynthesis. Plant J 73:105–117

Wang P, Chen X, Goldbeck C, Chung E, Kang BH (2017) A distinct class of vesicles derived from the trans-Golgi mediates secretion of xylogalacturonan in the root border cell. Plant J 92:596–610

Watanabe Y, Meents MJ, McDonnell LM, Barkwill S, Sampathkumar A, Cartwright HN, Demura T, Ehrhardt DW, Samuels AL, Mansfield SD (2015) Visualization of cellulose synthases in *Arabidopsis* secondary cell walls. Science 350:198–203

Wightman R, Turner S (2010) Trafficking of the plant cellulose synthase complex. Plant Physiol 153:427–432

Wightman R, Marshall R, Turner SR (2009) A cellulose synthase-containing compartment moves rapidly beneath sites of secondary wall synthesis. Plant Cell Physiol 50:584–594

Williamson RE, Burn JE, Hocart CH (2002) Towards the mechanism of cellulose synthesis. Trends in Plant Sci 7:461–467

Wilson SM, Burton RA, Doblin MS, Stone BA, Newbigin EJ, Fincher GB, Bacic A (2006) Temporal and spatial appearance of wall polysaccharides during cellularization of barley (*Hordeum vulgare*) endosperm. Planta 224:655–667

Wilson SM, Ho YY, Lampugnani ER, Van de Meene AM, Bain MP, Bacic A, Doblin MS (2015) Determining the subcellular location of synthesis and assembly of the cell wall polysaccharide (1,3; 1,4)-beta-D-glucan in grasses. Plant Cell 27:754–771

Wong HC, Fear AL, Calhoon RD, Eichinger GH, Mayer R, Amikam D, Benziman M, Gelfand DH, Meade JH, Emerick AW, Bruner R, Benbassat A, Tal R (1990) Genetic organization of the cellulose synthase operon in *Acetobacter xylinum*. Proc Natl Acad Sci U S A 87:8130–8134

Wu AM, Rihouey C, Seveno M, Hornblad E, Singh SK, Matsunaga T, Ishii T, Lerouge P, Marchant A (2009) The *Arabidopsis* IRX10 and IRX10-LIKE glycosyltransferases are critical for glucuronoxylan biosynthesis during secondary cell wall formation. Plant J 57:718–731

Wu AM, Hornblad E, Voxeur A, Gerber L, Rihouey C, Lerouge P, Marchant A (2010) Analysis of the *Arabidopsis* IRX9/IRX9-L and IRX14/IRX14-L pairs of glycosyltransferase genes reveals critical contributions to biosynthesis of the hemicellulose glucuronoxylan. Plant Physiol 153:542–554

Xie LQ, Yang CJ, Wang XL (2011) Brassinosteroids can regulate cellulose biosynthesis by controlling the expression of CESA genes in *Arabidopsis*. J Exp Bot 62:4495–4506

Xiong G, Cheng K, Pauly M (2013) Xylan O-acetylation impacts xylem development and enzymatic recalcitrance as indicated by the *Arabidopsis* mutant *tbl29*. Mol Plant 6:1373–1375

Yamaguchi M, Goue N, Igarashi H, Ohtani M, Nakano Y, Mortimer JC, Nishikubo N, Kubo M, Katayama Y, Kakegawa K, Dupree P, Demura T (2010) VASCULAR-RELATED NAC-DOMAIN6 and VASCULAR-RELATED NAC-DOMAIN7 effectively induce transdifferentiation into xylem vessel elements under control of an induction system. Plant Physiol 153:906–914

Yin Y, Huang J, Xu Y (2009) The cellulose synthase superfamily in fully sequenced plants and algae. BMC Plant Biol 9:99

Yin L, Verhertbruggen Y, Oikawa A, Manisseri C, Knierim B, Prak L, Jensen JK, Knox JP, Auer M, Willats WGT, Scheller HV (2011) The cooperative activities of CSLD2, CSLD3, and CSLD5 are required for normal *Arabidopsis* development. Mol Plant 4:1024–1037

Yuan YX, Teng Q, Zhong RQ, Ye ZH (2013) The *Arabidopsis* DUF231 domain-containing protein ESK1 mediates 2-O- and 3-O-acetylation of xylosyl residues in xylan. Plant Cell Physiol 54:1186–1199

Yuan Y, Teng Q, Lee C, Zhong R, Ye ZH (2014) Modification of the degree of 4-O-methylation of secondary wall glucuronoxylan. Plant Sci 219-220:42–50

Yuan Y, Teng Q, Zhong R, Haghighat M, Richardson EA, Ye ZH (2016a) Mutations of *Arabidopsis* TBL32 and TBL33 affect xylan acetylation and secondary wall deposition. PLoS One 11:e0146460

Yuan Y, Teng Q, Zhong R, Ye ZH (2016b) Roles of *Arabidopsis* TBL34 and TBL35 in xylan acetylation and plant growth. Plant Sci 243:120–130

Yuan Y, Teng Q, Zhong R, Ye ZH (2016c) TBL3 and TBL31, two *Arabidopsis* DUF231 domain proteins, are required for 3-O-Monoacetylation of xylan. Plant Cell Physiol 57:35–45

Zabotina OA, van de Ven WT, Freshour G, Drakakaki G, Cavalier D, Mouille G, Hahn MG, Keegstra K, Raikhel NV (2008) Arabidopsis XXT5 gene encodes a putative alpha-1,6-xylosyltransferase that is involved in xyloglucan biosynthesis. Plant J 56:101–115

Zabotina OA, Avci U, Cavalier D, Pattathil S, Chou YH, Eberhard S, Danhof L, Keegstra K, Hahn MG (2012) Mutations in multiple *XXT* genes of *Arabidopsis* reveal the complexity of xyloglucan biosynthesis. Plant Physiol 159:1367–1384

Zeng W, Jiang N, Nadella R, Killen TL, Nadella V, Faik A (2010) A glucurono(arabino)xylan synthase complex from wheat contains members of the GT43, GT47, and GT75 families and functions cooperatively. Plant Physiol 154:78–97

Zeng W, Lampugnani ER, Picard KL, Song L, Wu AM, Farion IM, Zhao J, Ford K, Doblin MS, Bacic A (2016) Asparagus IRX9, IRX10, and IRX14A are components of an active xylan backbone synthase complex that forms in the Golgi apparatus. Plant Physiol 171:93–109

Zhang GF, Staehelin LA (1992) Functional compartmentation of the Golgi apparatus of plant cells : immunocytochemical analysis of high-pressure frozen- and freeze-substituted sycamore maple suspension culture cells. Plant Physiol 99:1070–1083

Zhang T, Zheng Y, Cosgrove DJ (2016a) Spatial organization of cellulose microfibrils and matrix polysaccharides in primary plant cell walls as imaged by multichannel atomic force microscopy. Plant J 85:179–192

Zhang Y, Nikolovski N, Sorieul M, Vellosillo T, McFarlane HE, Dupree R, Kesten C, Schneider R, Driemeier C, Lathe R, Lampugnani E, Yu X, Ivakov A, Doblin MS, Mortimer JC, Brown SP, Persson S, Dupree P (2016b) Golgi-localized STELLO proteins regulate the assembly and trafficking of cellulose synthase complexes in Arabidopsis. Nat Commun 7:11656. doi:10.1038/ncomms11656

Zhang BC, Zhang LJ, Li F, Zhang DM, Liu XL, Wang H, Xu ZP, Chu CC, Zhou YH (2017) Control of secondary cell wall patterning involves xylan deacetylation. Nature Plants 3. https://doi.org/10.1038/nplants.2017.17. ARTN 17017

Zhang X, Dominguez PG, Kumar M, Bygdell J, Miroshnichenko S, Sundberg B, Wingsle G, Niittyla T (2018) Cellulose synthase stoichiometry in aspen differs from *Arabidopsis* and *Norway spruce*. Plant Physiol 177:1096–1107

Zeng W, Keegstra K (2008) AtCSLD2 is an integral Golgi membrane protein with its N-terminus facing the cytosol. Planta 228:823–838

Zhong RQ, Ye ZH (2014) Complexity of the transcriptional network controlling secondary wall biosynthesis. Plant Sci 229:193–207

Zhong RQ, Burk DH, Morrison WH, Ye ZH (2002) A kinesin-like protein is essential for oriented deposition of cellulose microfibrils and cell wall strength. Plant Cell 14:3101–3117

Zhong R, Pena MJ, Zhou GK, Nairn CJ, Wood-Jones A, Richardson EA, Morrison WH 3rd, Darvill AG, York WS, Ye ZH (2005) Arabidopsis fragile fiber8, which encodes a putative glucuronyltransferase, is essential for normal secondary wall synthesis. Plant Cell 17:3390–3408

Zhong RQ, Demura T, Ye ZH (2006) SND1, a NAC domain transcription factor, is a key regulator of secondary wall synthesis in fibers of *Arabidopsis*. Plant Cell 18:3158–3170

Zhong R, Richardson EA, Ye ZH (2007) The MYB46 transcription factor is a direct target of SND1 and regulates secondary wall biosynthesis in *Arabidopsis*. Plant Cell 19:2776–2792

Zhong RQ, Lee CH, Ye ZH (2010) Evolutionary conservation of the transcriptional network regulating secondary cell wall biosynthesis. Trends Plant Sci 15:625–632

Zhu XF, Sun Y, Zhang BC, Mansoori N, Wan JX, Liu Y, Wang ZW, Shi YZ, Zhou YH, Zheng SJ (2014) TRICHOME BIREFRINGENCE-LIKE27 affects aluminum sensitivity by modulating

the O-acetylation of xyloglucan and aluminum-binding capacity in *Arabidopsis*. Plant Physiol 166:181–189

Zhu X, Li S, Pan S, Xin X, Gu Y (2018) CSI1, PATROL1, and exocyst complex cooperate in delivery of cellulose synthase complexes to the plasma membrane. Proc Natl Acad Sci U S A 115:E3578–E3587. https://doi.org/10.1073/pnas.1800182115

Zuo JR, Niu QW, Nishizawa N, Wu Y, Kost B, Chua NH (2000) KORRIGAN, an *Arabidopsis* endo-1,4-beta-glucanase, localizes to the cell plate by polarized targeting and is essential for cytokinesis. Plant Cell 12:1137–1152

Chapter 8
Cellulose in Bacterial Biofilms

Diego O. Serra and Regine Hengge

Abstract Many bacteria produce cellulose as an exopolysaccharide component of the extracellular matrix in biofilms, which are large aggregates of bacterial cells often attached to abiotic or biotic surfaces. Cellulose has been particularly well studied in two model bacteria, *Komagataeibacter xylinus* and *Escherichia coli*. The widely conserved bacterial cellulose synthase consists of a membrane-inserted core complex, whose BcsA subunit provides for a glucosyltransferase activity that is allosterically activated by the second messenger c-di-GMP and which, together with the BcsB subunit, forms a transmembrane channel for co-synthetic secretion of cellulose. Various accessory Bcs proteins further conduct cellulose to the cell surface, where glucan chains are aligned and assembled into higher order fibrils. The corresponding genes are generally organized in operons that are easily detected in genome sequences. *K. xylinus* produces highly crystalline cellulose, which alone or in technically generated composite materials is now widely used in food and paper technology or in medical applications. A surprise in the bacterial cellulose field was the recent discovery that *E. coli* and many other bacteria "decorate" their cellulose with a phospholipid-derived phosphoethanolamine (pEtN) group in a post-synthetic process catalyzed by BcsG at the outer side of the cytoplasmic membrane. This enzymatic process not only represents the first natural chemical modification of cellulose but enables pEtN-cellulose to form nanocomposites with amyloid fibers in the extracellular matrix of biofilms. The result is tissue-like cohesion and elasticity, which allow growing macrocolony or pellicle biofilms to buckle up and fold into macroscopic morphological patterns of wrinkles and high ridges. These recent discoveries hold promise that other types of modified cellulose with novel chemical and biomechanical properties are yet be found in nature or could even be generated by synthetic biology approaches.

D. O. Serra · R. Hengge (✉)
Humboldt-Universität zu Berlin, Institut für Biologie, Mikrobiologie, Berlin, Germany
e-mail: regine.hengge@hu-berlin.de

E. Cohen, H. Merzendorfer (eds.), *Extracellular Sugar-Based Biopolymers Matrices*,
Biologically-Inspired Systems 12, https://doi.org/10.1007/978-3-030-12919-4_8

8.1 Introduction

Cellulose is a linear homopolysaccharide composed of β-1,4–linked glucosyl residues. Being a key structural component of the primary and secondary cell walls of vascular plants, cellulose represents the most abundant biopolymer on Earth. Of great economic importance, cellulose is processed to produce papers and fibers and is chemically modified to yield substances used in the manufacture of such items as plastics, photographic films, and rayon. In addition to plants, many bacterial species produce cellulose (Römling and Galperin 2015). In fact, cellulose biosynthesis in plants is proposed to have a bacterial origin, with cellulose synthase genes having been acquired by plants from the cyanobacterial ancestors of their chloroplasts (Nobles et al. 2001). Bacterial cellulose serves as an alternative source to plant cellulose and is increasingly used in biotechnology and nanotechnology (Rajwade et al. 2015).

The link between the ability of bacteria to produce cellulose and to form highly structured communities now known as biofilms can be traced back to the very discovery of bacterial cellulose by Adrian Brown in the nineteenth century (Brown 1886). Brown identified cellulose as a key component of a gelatinous membrane formed on the fluid surface upon vinegar fermentation by "*Bacterium xylinum*" (Brown 1886), a bacterium currently known as *Komagataeibacter xylinus* (also formerly *Acetobacter xylinum* or *Gluconacetobacter xylinus*) that to this day serves as a model organism for studies on bacterial cellulose. In retrospective, the gelatinous membrane on the fluid surface that Brown described is no other thing than what we now know as a pellicle biofilm, i.e., a microbial community embedded in an extracellular matrix (ECM) that forms at the air/liquid interface in static cultures. Thus, along with the description of the multicellular nature of *Bacillus subtilis* cultures by Ferdinand Cohn in 1877 (Cohn 1877), Brown's study represents one of the earliest references to a bacterial biofilm. Especially noteworthy is the fact that he detected cellulose in the pellicle, which can be considered the first experimental evidence that implicates an exopolysaccharide in the formation of a bacterial multicellular community.

In retrospect, another remarkable finding in *K. xylinus* also provided an early link between cellulose production and biofilm formation: the discovery of bis-(3′-5′)-cyclic dimeric guanosine monophosphate (c-di-GMP) as an allosteric activator of cellulose synthase by Moshe Benziman and co-workers in 1987 (Ross et al. 1987). While it took years until c-di-GMP became appreciated in the biofilm field, Benziman's work on c-di-GMP and cellulose biosynthesis was seminal, and today c-di-GMP is unequivocally recognized as a key signaling molecule that ubiquitously promotes bacterial biofilm formation, in most cases by directly or indirectly stimulating the synthesis of ECM components (Römling et al. 2013; Whitney and Howell 2013; Jenal et al. 2017).

Around the time when microbiologists started to recognize biofilms as major contributors to persistent infections and hence a serious threat to public health, cellulose was identified as the second major ECM component of biofilms formed

by *Salmonella enterica* serovar Typhimurium (*S. typhimurium*) and *Escherichia coli* (Zogaj et al. 2001). The latter also includes pathogenic variants such as uropathogenic and enterohemorrhagic *E. coli* (Hung et al. 2013; Richter et al. 2014). Along with curli proteins that upon secretion assemble into amyloid fibers, cellulose was shown to provide agar-grown macrocolony biofilms with the ability to form intricate 3D structures that have been termed "wrinkled," "rugose," or "rdar" (for red, dry, and rough) (Römling 2005; Serra et al. 2013a). Since then, *E. coli* and *Salmonella* have joined *K. xylinus* in becoming extensively studied for their cellulose production. In particular, broad knowledge on the regulation of cellulose biosynthesis and on the role of cellulose as an ECM component in biofilms has been obtained in *E. coli* and *Salmonella*. Especially noteworthy is the recent finding that cellulose produced by *E. coli* and *Salmonella* is post-synthetically modified with phosphoethanolamine (pEtN) (Thongsomboon et al. 2018). Since the genes required for installing this modification appear to be absent in *K. xylinus*, this recent finding not only helps to shed light on existing differences between cellulose produced by *K. xylinus* and *E. coli* but also opens new exciting perspectives on fundamental and applied research on cellulose.

This chapter will first provide an overview of exopolysaccharides as major ECM components in bacterial biofilms, with a special focus on cellulose. It will then discuss structure, function, and c-di-GMP regulation of genes and protein subunits involved in the synthesis, excretion, and pEtN modification of the cellulose molecule, highlighting differences between *K. xylinus* and *E. coli.* This will be followed by a discussion of the supramolecular structure, assembly, and properties of cellulose fibrils, again with an emphasis on differences between *K. xylinus* and *E. coli*. Finally, this chapter will illustrate how pEtN-cellulose from *E. coli*, either in isolation or in association with amyloid curli fibers, shapes the micro- and macroarchitecture of colony biofilms.

8.2 Exopolysaccharides in Bacterial Biofilms

8.2.1 Diversity of Exopolysaccharides in the Extracellular Matrix (ECM)

To succeed in building a biofilm, bacteria must inevitably produce an ECM. The essentiality of the ECM lies mainly in its role in keeping cells attached to each other and to surfaces, which is what overall defines a biofilm as a sessile microbial community. The ECM, however, carries out several equally important functions such as protecting biofilm cells from environmental threats (e.g., the invasion of competitors, predation, biocides, etc.); promoting retention of water, enzymes, and metabolites; or even participating in genetic exchange and signaling (Dragos and Kovacs 2017). The functional attributes of the ECM are primarily dictated by its constituents, which typically include exopolysaccharides, amyloid fibers, soluble

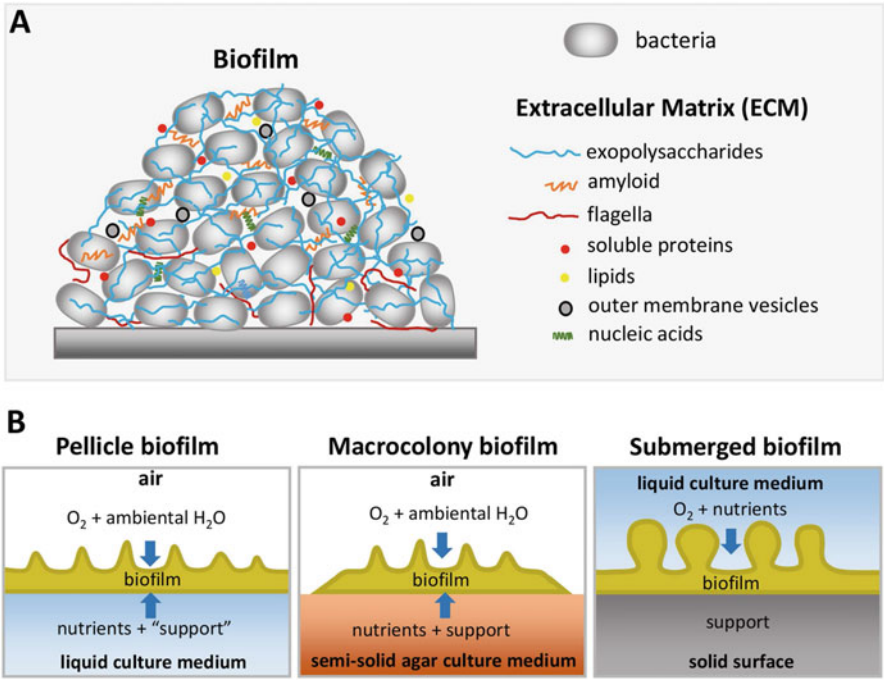

Fig. 8.1 (**a**). Schematic representation of a generic bacterial biofilm illustrating the diversity of components that constitute the extracellular matrix (ECM). (**b**). Schematic representation of three types of bacterial biofilms in which cellulose commonly occurs as a major ECM component. The scheme illustrates differences in surface support and spatial distribution of nutrients, oxygen, and water

proteins, lipids, outer-membrane vesicles, and nucleic acids (Fig. 8.1a). Among them, exopolysaccharides are the most ubiquitous and often the most abundant components (Flemming and Wingender 2010). Exopolysaccharides themselves are highly diverse, not only in their monosaccharide constituents but also in glycosidic linkages, branching, and substitutions with noncarbohydrate residues (e.g., acetate, pyruvate, succinate, phosphate), leading to a nearly unlimited range of structures.

The diversity of exopolysaccharides is easily appreciated among phylogenetically distant bacteria, but it is even common among strains of a single species. Strains of the biofilm-model microorganism *Pseudomonas aeruginosa*, for example, can produce combinations of at least three exopolysaccharides that differentially contribute to biofilm formation: alginate, which is a linear polymer of guluronic and mannuronic acid; Pel, an exopolysaccharide of partially acetylated galactosamine and glucosamine; and Psl, a repeating pentasaccharide polymer consisting of mannose, rhamnose, and glucose (Franklin et al. 2011; Jennings et al. 2015). Alginate is typically overproduced by mucoid variants that are often isolated from the lungs of chronically colonized cystic fibrosis patients, whereas Pel and Psl are variably produced by non-mucoid clinical and environmental isolates (Franklin et al. 2011).

Also single strains often produce multiple exopolysaccharides. Many *E. coli* strains, for example, can synthesize pEtN-cellulose; colanic acid, which is a polyanionic heteropolymer consisting of glucose, galactose, fucose, glucuronic acid, and pyruvate; and PGA, a linear homopolymer of β-1,6-N-acetyl-glucosamine. Interestingly, while all three exopolysaccharides contribute to *E. coli* biofilm formation (for a review, see Beloin et al. 2008), at least two of them, pEtN-cellulose and PGA, are known to be produced under opposite conditions. Thus, PGA synthesis is stimulated by glucose, NaCl, and high temperature (37 °C) (Cerca and Jefferson 2008), whereas pEtN-cellulose production is maximized under conditions of nutrient limitation, low NaCl concentration, and low temperature (<30 °C) (Römling 2005). Such inverse regulation not only reflects the ability of *E. coli* to adapt its biofilm composition to diverse environments, which is consistent with its remarkable versatility to thrive inside and outside mammalian hosts, but also shows that it is essential for the bacterium to be able not only to build a biofilm but endow its biofilms with different properties in diverse environments.

8.2.2 *Different Roles for Aggregative and Mucoid Exopolysaccharides in Bacterial Biofilm Formation*

Although a functional categorization of exopolysaccharides in biofilms is beyond the scope of this chapter, it is interesting to note that different exopolysaccharides contribute differentially to biofilm formation, e.g., by promoting aggregation or mucoidy of macrocolony biofilms. Macrocolonies are large biofilms that grow over extended times from a cell suspension (a few microliters) spotted onto a semisolid agar medium (Serra and Hengge 2017) (Fig. 8.1b). Aggregative exopolysaccharides are those that also in shaking liquid cultures promote strong cell aggregation. Examples are cellulose of *K. xylinus* (Toyosaki et al. 1995), pEtN-cellulose of *E. coli* and *Salmonella* (Zogaj et al. 2001; Serra et al. 2013a), Psl and Pel of *P. aeruginosa* (Friedman and Kolter 2004), VPS of *Vibrio cholerae* (Yildiz and Schoolnik 1999), and the exopolysaccharide of *B. subtilis* (Branda et al. 2001). When produced or overproduced in macrocolony biofilms, aggregative exopolysaccharides confer extreme cohesion and elasticity to the ECM network, which at the community-level translate into tissue-like properties. As a consequence, colonies can grow into flat and larges structures that fold into intricate 3D structures, which commonly generates a rugose or wrinkled morphology of macrocolonies (Friedman and Kolter 2004; Serra et al. 2013a; Yan et al. 2017). As discussed later in this chapter on the role of pEtN-cellulose in *E. coli* biofilms, the emergence of morphological structures in macrocolonies often relies on the ability of aggregative exopolysaccharides to interact with other ECM components, such as amyloid proteins (Romero et al. 2010; Serra et al. 2013a; Yan et al. 2017).

Unlike aggregative exopolysaccharides, mucoid exopolysaccharides, such as alginate of *P. aeruginosa* (Pritt et al. 2007), colanic acid of *E. coli* (Sutherland

1970), xanthan gum of *Xanthomonas campestris* (Harding et al. 1987), or the capsular polysaccharides of *Streptococcus pneumoniae* and *Klebsiella pneumoniae* (Hammerschmidt et al. 2005; Shon et al. 2013), lead to convex-shaped colony biofilms that are smooth and featureless in appearance, which already visually indicates that mucoid exopolysaccharides do not play the same architectural role as aggregative exopolysaccharides. Rather, mucoid exopolysaccharides form highly hydrated and viscous gel-like matrixes that, besides conferring the typical shiny appearance of mucoid colonies, are highly protective, allowing cells to resist environmental insults, including phagocytosis and antibiotic treatment (Hammerschmidt et al. 2005; Pritt et al. 2007). The primacy of aggregative exopolysaccharides over mucoid exopolysaccharides in shaping biofilm structure has also been observed in submerged biofilms of mucoid *P. aeruginosa* strains, where the mushroom-like shape of biofilms was found to be crucially dependent on Pel and Psl, but not on alginate (Yang et al. 2012).

8.2.3 Cellulose, a Widespread ECM Element

Cellulose biosynthesis has been documented in a wide variety of bacteria, most of which belong to the phylum *Proteobacteria*, particularly to the alpha and gamma classes (Römling and Galperin 2015). Prominent genera of cellulose producers include *Komagataeibacter*, *Agrobacterium*, *Rhizobium*, *Enterobacter*, *Escherichia*, *Salmonella*, *Dickeya*, and *Pseudomonas*. The actual list of cellulose producers is obviously much more extensive, considering the large number of proteobacterial genomes in which bacterial cellulose synthase (*bcs*) loci were found (Römling and Galperin 2015). Cellulose ubiquity is reflected in biofilms, where it commonly occurs as a major ECM component of pellicles, macrocolonies, and other types of biofilms (Fig. 8.1b). This makes cellulose perhaps the most common exopolysaccharide present in the ECM of bacterial biofilms.

Many cellulose producers are bacteria that exhibit symbiotic or pathogenic relationships with plants and that form cellulose-based biofilms as a means to establish efficient contact with their host (Augimeri et al. 2015) (Fig. 8.2). Thus, cellulose production by *Rhizobiaceae* species that include *Rhizobium leguminosarum*, a nitrogen-fixing plant symbiont, and *Agrobacterium tumefaciens*, a tumor-inducing phytopathogen, was shown to promote irreversible attachment and biofilm formation of both bacteria on root hairs of their respective hosts (Smit et al. 1987; Matthysse et al. 2005). Similarly, cellulose production by *K. xylinus*, which naturally inhabits the carposphere, is required for efficient colonization of the surface of apples when inoculated as pellicle biofilms (Williams and Cannon 1989). Only *K. xylinus* strains that formed cellulose-containing pellicles prevented colonization of the apple surface by fungi and other bacteria and protected cells from desiccation and the damaging effects of UV light (Williams and Cannon 1989). Interestingly, *K. xylinus* cellulose was shown to interact and even to be structurally modified by plant cell wall components such as hemicelluloses, pectin, and lignin. The hemicellulose glucomannan, for instance, prevents – at least to some extent – *K. xylinus*

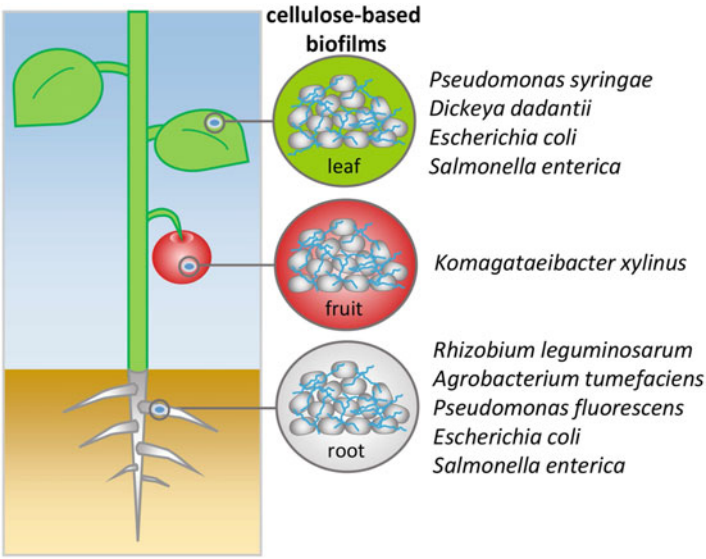

Fig. 8.2 Plant pathogenic, growth-promoting, or symbiotic bacteria as well as human pathogenic enterobacteria take advantage of cellulose production as a means to establish efficient contact with specific plant organs and tissues

cellulose from aggregating into microfibrils, which translates into decreased crystallinity (Hackney et al. 1994). This suggests that cellulose fibers present in *K. xylinus* biofilms could coalesce with hemicellulose in the fruit cell walls, which could result in increased anchoring of the bacterial community to the fruit surface.

Similar to specialized plant-interacting bacteria, important human enteric pathogens take advantage of cellulose production at relatively low temperature (<30 °C) to establish close contact with plant hosts (Fig. 8.2), including fresh produce (Yaron and Römling 2014). This ultimately contributes to the occurrence of food-borne diseases. *E. coli* O157:H7 and *S. typhimurium*, for example, were found to require cellulose for optimal adherence to tomato fruits and alfalfa sprouts, respectively (Matthysse et al. 2008; Shaw et al. 2011). Temperature control of cellulose production, which usually is co-regulated with amyloid curli, can vary among strains. Thus, several isolates of different enterobacterial genera, including *Escherichia*, *Salmonella*, *Citrobacter*, and *Enterobacter*, were shown to co-produce cellulose and curli also at 37 °C (Zogaj et al. 2003). Although the actual role of cellulose-containing biofilms in the interaction of enterobacteria with the mammalian gastrointestinal tract is not yet fully clear, a novel view of cellulose as an anti-virulence factor in *Salmonella* and *E. coli* has begun to emerge. Pontes et al. (2015) reported that preventing cellulose synthesis increases *S. typhimurium* virulence, while stimulation of cellulose synthesis inside macrophages decreases virulence. Consistent with this notion, Ahmad et al. (2016) showed that a *S. typhimurium* mutant defective in the endoglucanase BcsZ, one of the cellulose synthase components, accumulates more cellulose in the extracellular matrix and is attenuated in virulence and mice

colonization. Consistently, invasion of epithelial cells by *S. typhimurium* was effectively suppressed by deletion of c-di-GMP-degrading phosphodiesterases, which in turn could be partially relieved by deleting the cellulose synthase gene *bcsA* (Ahmad et al. 2011). In line with these evidences, cellulose was also found to counteract curli-mediated adherence to mammalian cells as well as curli's pro-inflammatory effect when *E. coli* co-expressed the two ECM components (Wang et al. 2006). Altogether, this reveals a dual commitment of cellulose in the bacterial decision to prioritize biofilm formation over acute virulence. On the one hand, it directly serves as a crucial biofilm-building element, while on the other hand, it can impede acute virulence at multiple levels. This may, however, not always be the rule, and strain- and host-specific variations can still lead to a different outcome. A recent report, for instance, revealed that pEtN-cellulose may actually contribute to uropathogenic *Escherichia coli* pathogenesis in the urinary tract by enhancing curli-mediated bacterial adhesion to bladder epithelial cells under high-shear conditions (Hollenbeck et al. 2018). The loss of ability of African invasive nontyphoidal *Salmonella* ST313 strains to synthesize pEtN-modified cellulose due to a mutation in *bcsG* has been shown to be consistent with the adaptation of these strains to a human-to-human mode of transmission (Singletary et al. 2016).

Cellulose was also reported to be produced by marine bacteria such as the gamma-proteobacterium *Vibrio fischeri* (Bassis and Visick 2010). *V. fischeri* uses biofilm formation to promote symbiotic colonization of the light organ of the Hawaiian bobtail squid, *Euprymna scolopes*, where it causes bioluminescence. In addition to cellulose, *V. fischeri* produces another exopolysaccharide called symbiosis polysaccharide (Syp) that is required for initiating squid symbiosis (Yip et al. 2005). Although the actual involvement of cellulose in biofilm formation during symbiosis is unclear, in vitro studies have shown that cellulose is required for the maturation of submerged biofilm, morphogenesis of macrocolony biofilms, and pellicle biofilm formation (Bassis and Visick 2010; Visick et al. 2013). Curiously, cellulose-containing pellicles of *V. fischeri* were found to be induced by arabinose (Visick et al. 2013). Since this sugar is plentiful in seaweed (Rao and Ramana 1991), it is conceivable that *V. fischeri* triggers cellulose-based biofilm formation upon interaction with marine algae.

8.3 Biosynthesis and Natural Modification of Cellulose in Bacteria

8.3.1 Organization of bcs *Loci in* K. xylinus *and* E. coli

While cellulose production is widespread among *Proteobacteria*, the *bcs* loci encoding the subunits of the bacterial cellulose synthase (BCS) complex display variable genetic organization across species. This diversity was recently revisited by Römling and Galperin, who proposed a classification of *bcs* loci into three

major types as found in *K. xylinus*, *E. coli*, and *A. tumefaciens* with subdivisions into subtypes based on the gene order and content (Römling and Galperin 2015). Here, we will focus on the organization of representative *bcs* loci of *K. xylinus* and *E. coli* strains.

In *K. xylinus*, the *bcs* locus includes a four-gene operon, *bcsABCD* (synonym, *acsABCD*), and three additional genes: *bcsZ* (synonym, *cmcAx*) and *bcsH* (synonyms, *ccpAx*, ORF2) upstream of the operon and *bglX* (synonym, *bglAx*) downstream of it (Fig. 8.3a). The first two genes in the operon encode the cellulose synthase subunits BcsA and BcsB, whereas the following genes encode BcsC and BcsD, two proteins proposed to be involved in exporting and assembly the glucan chains, respectively (Saxena et al. 1994). The extra genes *bcsZ* and *bglX* encode an endoglucanase and a β-glucosidase, respectively, whereas *bcsH* encodes an auxiliary protein believed to be involved in fibril assembly (Nakai et al. 2002). Similar *bcs* loci are found in certain representatives of alpha-, beta-, and gamma-proteobacteria (Römling and Galperin 2015). In some strains exhibiting this type of loci, *bcsA* and *bcsB* occur as a single fused gene that gives rise to a large BcsAB fusion protein, which in most cases is processed posttranslationally into two proteins (McManus et al. 2016).

In *E. coli* and *Salmonella*, the *bcs* locus includes two divergently arranged operons, *bcsRQABZC* and *bcsEFG* (formerly *yhjRQONML* and *yhjSTU*, respectively) (Solano et al. 2002) (Fig. 8.3a). This type of locus is widespread among the members of beta- and gamma-proteobacteria and can show some variations in gene order and content (Römling and Galperin 2015). Like *K. xylinus*, *E. coli* contains the core genes, *bcsA*, *bcsB*, *bcsC*, and *bcsZ*, with the latter gene inserted between *bcsB* and *bcsC* in *E. coli*. A distinguishing feature is the presence in *E. coli* of *bcsR* and *bcsQ*, which are the first two genes of the operon and encode a small protein and a homologue of the cell division protein MinD, respectively (Le Quéré and Ghigo 2009). The most substantial difference between both loci, however, is the presence in *E. coli* of the divergent *bcsEFG* operon (Fig. 8.3a). As discussed further below in this chapter, gene products of this operon were recently shown to be responsible for installing the pEtN modification in the cellulose molecule in *E. coli* and *Salmonella* (Thongsomboon et al. 2018). This finding now turns out to be key to understanding the differences in structure and properties between cellulose produced by *E. coli* and *K. xylinus*.

8.3.2 Components of the Bacterial Cellulose Synthase (BCS) Complex and Their Role in the Synthesis and Extrusion of Glucan Chains

Cellulose consists of a linear chain of several hundred of D-glucose units connected through β-1,4-glycosidic linkages where every glucose unit is rotated by 180 degrees with respect to its neighbor. The synthesis and extrusion of such long glucan chains represent the first crucial steps in the biogenesis of cellulose and are carried out by a membrane-inserted BCS complex – also known as the terminal complex

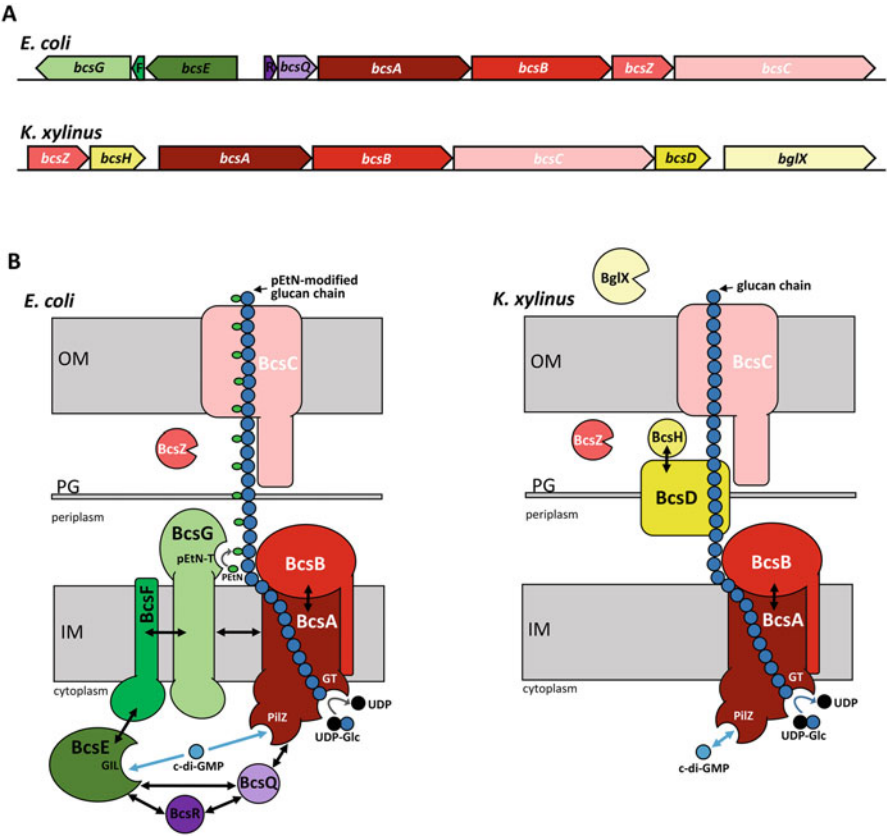

Fig. 8.3 (**a**). Organization of the *bcs* loci in *E. coli* and *K. xylinus*. (**b**). Proposed organization of components of BCS complexes from *E. coli* and *K. xylinus* (see text for details and references). All BCS components are represented as single subunits and colored the same way as their respective genes in A. Double-headed black arrows indicate direct interaction between respective components. Light blue arrows indicate c-di-GMP binding to the PilZ and GIL domains of BcsA and BcsE, respectively. Gray arrows indicate glycosyltransferase and phosphoethanolamine transferase activities of BcsA and BcsG, respectively. Abbreviations: *IM* inner membrane; *PG* peptidoglycan layer; *OM* outer membrane; *GT* glycosyltransferase domain; *PilZ* PilZ domain; *GIL* GGDEF I-site like domain; *pEtN-T* phosphoethanolamine transferase domain

(TC) subunit for *K. xylinus*. Synthesis initiates on the cytoplasmic side of the inner membrane (Bureau and Brown 1987) and requires BcsA and BcsB, which are the minimal core of the BCS complex. BcsA is an inner-membrane protein with multiple transmembrane helices and two cytoplasmic domains, a glycosyltransferase domain that catalyzes the polymerization of uridine diphospho-glucose (UDP-glucose) into the β-1,4-linked glucan (Lin et al. 1990), and a PilZ domain that, as discussed further in a later section, is involved in c-di-GMP-mediated activation of the catalytic activity of the enzyme (Fig. 8.3b). BcsB is a large mainly periplasmic protein that

is anchored to the inner membrane via a single C-terminal transmembrane region. BcsB interacts with BcsA at the periplasmic face of the inner membrane, with the two subunits forming a channel for co-synthetic translocation across the membrane of the newly formed polymer (Morgan et al. 2013). Interestingly, in *E. coli*, the core BcsA-BcsB unit was recently found present in multiple copies in a single larger complex, suggesting that various glucan chains are synthesized simultaneously (Krasteva et al. 2017). Extrusion of glucan chains from the periplasm to the extracellular environment is believed to occur through the action of BcsC, an outer-membrane porin with periplasmic scaffolding motifs (Fig. 8.3b). This export function is consistent with BcsC being essential for cellulose production in vivo and dispensable for cellulose production in vitro (Wong et al. 1990). The fourth subunit ubiquitously present in proteobacterial BCS complexes is the periplasmic endo-β-1-4-glucanase BcsZ, which is suggested to be required for degradation of cellulose if accumulated in the periplasm and/or for cleavage of nascent glucan chains to allow microfibril formation to occur outside the cell (Mazur and Zimmer 2011).

A component present in *K. xylinus* and absent in *E. coli* is BcsD (Fig. 8.3b), a periplasmic protein that is required for the production of cellulose in crystalline (i.e., highly ordered) conformation (Saxena et al. 1994; Hu et al. 2010). Although the mechanism by which BcsD operates is unclear, structural studies revealed that BcsD assembles into a cylindrical octamer with four inner passageways that are proposed to facilitate the association of four newly synthesized glucan chains and prepare them for extrusion through BcsC. In addition, *K. xylinus* possesses BcsH, a small protein found to interact and co-localize with BcsD that is also required for the production of crystalline cellulose (Nakai et al. 2002; Sunagawa et al. 2013) (Fig. 8.3b). Thus, the roles of BcsD and BcsH help to explain the highly crystalline nature of *K. xylinus* cellulose and further support the differences with *E. coli*, which lacks both proteins and produces noncrystalline cellulose fibrils and sheets. *K. xylinus* strains also produce the β-glucosidase BglX, which has been detected and purified from the extracellular medium of *K. xylinus* cultures (Tahara et al. 1998). While in addition to BcsZ, BglX was found to affect the degree of polymerization of the cellulose produced, its definitive role is still unclear (Tonouchi et al. 1997).

BcsR and BcsQ are present in *E. coli* and in many beta- and gamma-proteobacteria (Fig. 8.3b). BcsQ is homologous to the *E. coli* cell division protein MinD and was found to localize at the cell pole (Le Quéré and Ghigo 2009). Since BcsQ oligomerizes and interacts with several other BCS components, it has been suggested to be required for polar localization of the BCS complex in *E. coli* and related bacteria (Le Quéré and Ghigo 2009; Krasteva et al. 2017). Such polar localization, however, was not detected for other BCS components even though cellulose itself seems to be produced at the cell pole. Interestingly, the absence of BcsQ in *K. xylinus* is consistent with the fact that in this bacterium the BCS complexes do not localize to the cell pole, but rather organize in rows along the longitudinal cell axis. BcsR is a small protein predicted to be localized in the cytosol that, however, interacts with several BCS components. Experimental evidence indicates that BcsR is required for cellulose secretion (Serra et al. 2013a; Krasteva et al. 2017), but its precise function in the process remains elusive.

8.3.3 *Phosphoethanolamine (pEtN)-Modified Cellulose and Roles of BcsE, BcsF, and BcsG in pEtN Installation in* E. coli

A recent experimental approach using solid-state nuclear magnetic resonance spectroscopy revealed that cellulose produced by *E. coli* and *Salmonella* is actually modified with a pEtN group (Thongsomboon et al. 2018). This modification likely escaped detection in previous research because of its instability in conventional acid digestion and isolation protocols designed to specifically detect cellulose. The analysis revealed that the pEtN moiety attaches at the C6 position in the glucose residues (as in glucose-6-phosphate) and occurs in every other glucose unit in the cellulose molecule (Thongsomboon et al. 2018). Of note are the negative and positive charges introduced by the phosphate and amine groups of pEtN, respectively, which confer a zwitterionic character to pEtN-modified cellulose.

Genetic and biochemical analyses revealed that the proteins involved in the installation of the pEtN modification are encoded by the *bcsEFG* operon (Thongsomboon et al. 2018). The gene products of this operon have long been implicated in cellulose synthesis in *Salmonella* and *E. coli* and thus termed Bcs proteins (Solano et al. 2002); however, no definitive role in the synthesis process had been ascribed to any of them. The new study showed that BcsG is the enzyme responsible for installing the pEtN modification. BcsG is a 559-amino acid inner-membrane protein with its N-terminal domain exposed to the cytosol and a large C-terminal domain residing in the periplasm that contains the PEtN transferase activity, for which histidine residues (His^{396}, His^{400}, His^{443}) proposed to coordinate a metal ion were found important (Thongsomboon et al. 2018) (Fig. 8.3b). This protein architecture and transmembrane orientation of domains resemble those of known pEtN transferases that modify lipid A of LPS or subunits of flagella or type IV pili. These include EptB from *E. coli*, EptC from *Campylobacter jejuni*, and LptA from *Neisseria meningitis*, with whom BcsG has also in common the use of phosphatidylethanolamine as a substrate (Aas et al. 2006; Cullen et al. 2012). Very recent X-ray structural determination shows the periplasmic C-terminal pEtN transfer domain of BcsG to be a globular domain with a zinc ion coordinated by His, Cys, Ser, and Glu residues located within a cleft that seems to represent the active site of BcsG (Sun et al. 2018).

BcsF is a membrane-inserted peptide of 63 amino acids with a N-terminal single transmembrane region and a small C-terminal domain remaining on the cytoplasmic side of the membrane, whereas BcsE is a cytosolic protein that contains a GGDEF I-site like (GIL) domain featuring a RxGD motive that was shown to bind c-di-GMP (Fang et al. 2014) (Fig. 8.3b). The transmembrane peptide BcsF was found to interact in vivo both with BcsG and BcsE (Thongsomboon et al. 2018). In addition, since BcsG interacts with BcsA (Thongsomboon et al. 2018), the BcsE-BcsF-BcsG complex is likely to operate in close proximity to the cellulose-synthesizing BcsA-BcsB core unit. This is consistent with the observation of several copies of both the BcsA-BcsB core unit and the BcsE-BcsF-BcsG unit in a larger complex that also contains BcsR and BcsQ (Krasteva et al. 2017). Nonpolar single deletions of the

genes in the *bcsEFG* operon not only eliminate or diminish cellulose modification but also result in lower overall levels of cellulose production (Sun et al. 2018; Thongsomboon et al. 2018). Therefore, the BcsE-BcsF-BcsG unit seems to play a dual role in this large BCS complex, i.e., besides installing the pEtN modification onto cellulose emerging into the periplasm, it may also contribute to assembly and/or stability of the BcsA-BcsB core cellulose synthase.

Overall, these findings provided conclusive chemical and genetic evidence for the natural occurrence of a post-synthetically modified form of cellulose. The finding that BcsE binds c-di-GMP also suggests that this second messenger controls not only cellulose synthesis (by binding to BcsA) but also cellulose modification (see also below). Later in this chapter, it will be discussed how pEtN modification influences the amorphous conformation and properties of *E. coli* cellulose and its implications for the architectural role of cellulose in bacterial biofilms.

8.4 C-di-GMP-Mediated Regulation of Cellulose Biosynthesis and Modification

8.4.1 C-di-GMP Input Into the Bacterial Cellulose Synthase Complex

C-di-GMP is widely recognized as an ubiquitous bacterial second messenger that in many species promotes biofilm formation, often by directly or indirectly stimulating the synthesis of ECM components (Römling et al. 2013; Jenal et al. 2017). Although cellulose was the first ECM component whose synthesis was found to be stimulated by c-di-GMP (already 30 years ago), the mechanistic details of this regulation have only recently begun to be clarified with the resolution of the crystal structure of the BcsA-BcsB complex from *Rhodobacter sphaeroides* (Morgan et al. 2013, 2014).

BcsA, the catalytic subunit of the BCS complex, consists of eight transmembrane helices and two large cytoplasmic domains, a conserved family-2 glycosyltransferase domain between transmembrane helices 4 and 5 and a C-terminal fragment that contains the regulatory PilZ domain (Morgan et al. 2013). The transmembrane helices form a narrow channel approximately 8 Å wide and 33 Å long, directly above the glycosyltransferase domain, which allows accommodation of ten glucose residues of the nascent glucan chain with the assistance of BcsB (Morgan et al. 2013). The cytosolic glycosyltransferase domain of BcsA hosts the active site that binds UDP-glucose and catalyzes the transfer of the donor glucose to the 4′-hydroxyl group at the nonreducing end of the growing glucan chain (acceptor). The regulatory PilZ domain consists of a six-stranded β-barrel and a preceding linker region that harbors an RxxxR motif involved in c-di-GMP binding (Amikam and Galperin 2006; Morgan et al. 2013). This linker serves as a bridge between the preceding transmembrane domain and the six-stranded β-barrel of the PilZ domain and crucially interacts with BcsA's "gating loop," a series of about 18 residues that runs across the opening of the glycosyltransferase domain (Morgan et al. 2014).

Comparison of BcsA-BcsB structures in the non-stimulated and c-di-GMP-activated states revealed that c-di-GMP exerts its activator function by releasing BcsA from an auto-inhibited state imposed by the gating loop (Morgan et al. 2013, 2014). In the absence of c-di-GMP, a salt bridge would rigidify the gating loop, which would block the entrance to the active site, thereby keeping BcsA in a resting state (Morgan et al. 2014). Upon c-di-GMP binding to the RxxxR motif, the gating loop is displaced from the active site, allowing a large opening toward the substrate-binding pocket that is wide enough for UDP-glucose diffusion (Morgan et al. 2014). Opening and closing the active site, however, do not seem to be the only function of BcsA's gating loop. The structures also reveal that when UDP-glucose binds to the active site, the gating loop inserts deeply into the catalytic pocket and coordinates the nucleotide via conserved residues (Morgan et al. 2014). It is assumed that this action would allow initiation of catalysis and that after the glycosyl transfer reaction occurs, the gating loop may retract from the glycosyltransferase domain, thereby allowing UDP for UDP-glucose exchange.

This molecular mechanism by which c-di-GMP activates BcsA is consistent with biochemical evidence indicating that increasing c-di-GMP concentrations does not increase the affinity of BcsA for UDP-glucose (Omadjela et al. 2013), but rather increases the fraction of catalytically active enzymes. Thus, in the absence of c-di-GMP or under conditions where the concentration of c-di-GMP is rate limiting, only a fraction of the catalytic sites might be accessible, leading to a reduction in the overall reaction rate.

In *E. coli*, *Salmonella*, and related bacteria, a second binding site for c-di-GMP in the large BCS complex is present at the cytosolic protein BcsE, which is linked to the complex via its direct interactions with BcsF and BcsQ (Fang et al. 2014; Krasteva et al. 2017; Thongsomboon et al. 2018). Since the *bcsEFG* operon represents a distinct genetic unit and BcsE, BcsF, and BcsG form a subcomplex within the larger BCS complex, it is hypothesized (Thongsomboon et al. 2018) that BcsE and BcsF operate by protein-protein interaction in a transmembrane c-di-GMP signaling pathway that controls the BcsG-mediated transfer of pEtN to cellulose in the periplasm in response to c-di-GMP on the cytoplasmic side of the inner membrane (Fig. 8.3b). Structural and functional details of this novel inside-out c-di-GMP signaling pathway have yet to be elucidated.

8.4.2 Diguanylate Cyclases (DGCs) and Phosphodiesterases (PDEs) in the Control of Cellulose Biosynthesis by **K. xylinus**

C-di-GMP is synthesized from two molecules of GTP by enzymes called diguanylate cyclases (DGCs) and is degraded into 5′-phosphoguanylyl-(3′-5′)-guanosine (pGpG) and/or GMP by specific phosphodiesterases (PDEs) (Schirmer 2016; Jenal et al. 2017). These antagonistic enzymes regulate intracellular levels of

c-di-GMP, which is bound by effector components that affect the activities of target components or structures by direct interaction. While the PilZ and glycosyltransferase domains in BcsA represented the prototype of an effector/target system, a striking diversity of these systems has been found in recent years (Krasteva et al. 2012).

The first description of the enzymes that produce and degrade c-di-GMP coincides with the discovery of c-di-GMP as an activator of cellulose synthase in *K. xylinus* by Benziman and co-workers, as they also identified a membrane-associated DGC and two membrane-bound phosphodiesterases (PDEA and PDEB) as responsible for synthesizing and degrading the c-di-GMP activator, respectively (Ross et al. 1987). In a later study, following biochemical purification of DGC and PDEA, Benziman's group identified genes encoding isoforms of both enzymes that are located on three distinct operons named *cdg1*, *cdg2*, and *cdg3* (Tal et al. 1998). Within each operon, a *pde* gene lies upstream of a *dgc* gene. Strikingly, the six encoded proteins exhibit the same PAS-GGDEF-EAL domain organization, and yet the gene products were distinctively associated with either PDE or DGC activities (Tal et al. 1998). Thus, according to operon association and enzymatic activities, proteins were designated as *Ax*PDEA-1 and *Ax*DGC-1, *Ax*PDEA-2 and *Ax*DGC-2, and *Ax*PDEA-3 and *Ax*DGC-3 and were shown to control the overall DGC and PDE activities in *K. xylinus* (formerly *Acetobacter xylinum*).

Functional studies of *Ax*PDEA-1 and *Ax*DGC-2 provided novel insights into relationships between oxygen level, c-di-GMP concentration, and cellulose biosynthesis by *K. xylinus* (Chang et al. 2001; Qi et al. 2009). The PDE *Ax*PDEA-1 contains a heme-PAS type of domain, and it was found that O_2 binding by the heme cofactor suppresses the phosphodiesterase activity of the EAL domain (Chang et al. 2001). This implies that high O_2 tension impedes c-di-GMP hydrolysis by *Ax*PDEA-1, contributing to maintain a high c-di-GMP level. The DGC *Ax*DGC-2 also contains a PAS domain, but it binds the cofactor flavin adenine dinucleotide (FAD) (Qi et al. 2009). Non-covalent binding of oxidized FAD to *Ax*DGC-2 induced higher catalytic activity of the GGDEF domain compared to $FADH_2$, indicating a role of the cellular redox status in modulating c-di-GMP levels (Qi et al. 2009). Since FAD regeneration primarily occurs at the electron transport chain with O_2 as a terminal electron acceptor, it is expected that the maximal contribution of *Ax*DGC-2 to increasing cellular c-di-GMP levels occurs when O_2 in the environment is abundant. The PAS domains of *Ax*DGC-1 and *Ax*DGC-3 are also likely to function as redox and oxygen sensors as both show very high sequence similarity (>90%) to the PAS domains of *Ax*DGC-2. Altogether, these data led to propose a model (Fig. 8.4a) in which high cellular O_2 concentration will simultaneously stimulate the DGC activity of *Ax*DGC-1, *Ax*DGC-2, and *Ax*DGC-3 and suppress the PDE activity of *Ax*PDEA-1, *Ax*PDEA-2, and *Ax*PDEA-3, with the possibility that the isoenzymes substitute for each other depending on their specific expression (Qi et al. 2009). As a consequence, the cellular c-di-GMP level will be high under aerobic conditions and will allow activation of cellulose synthesis upon c-di-GMP binding to BcsA. This model is consistent with the fact that *K. xylinus* naturally colonizes the surface of fruits, an environment with direct access to O_2, and that in static cultures it

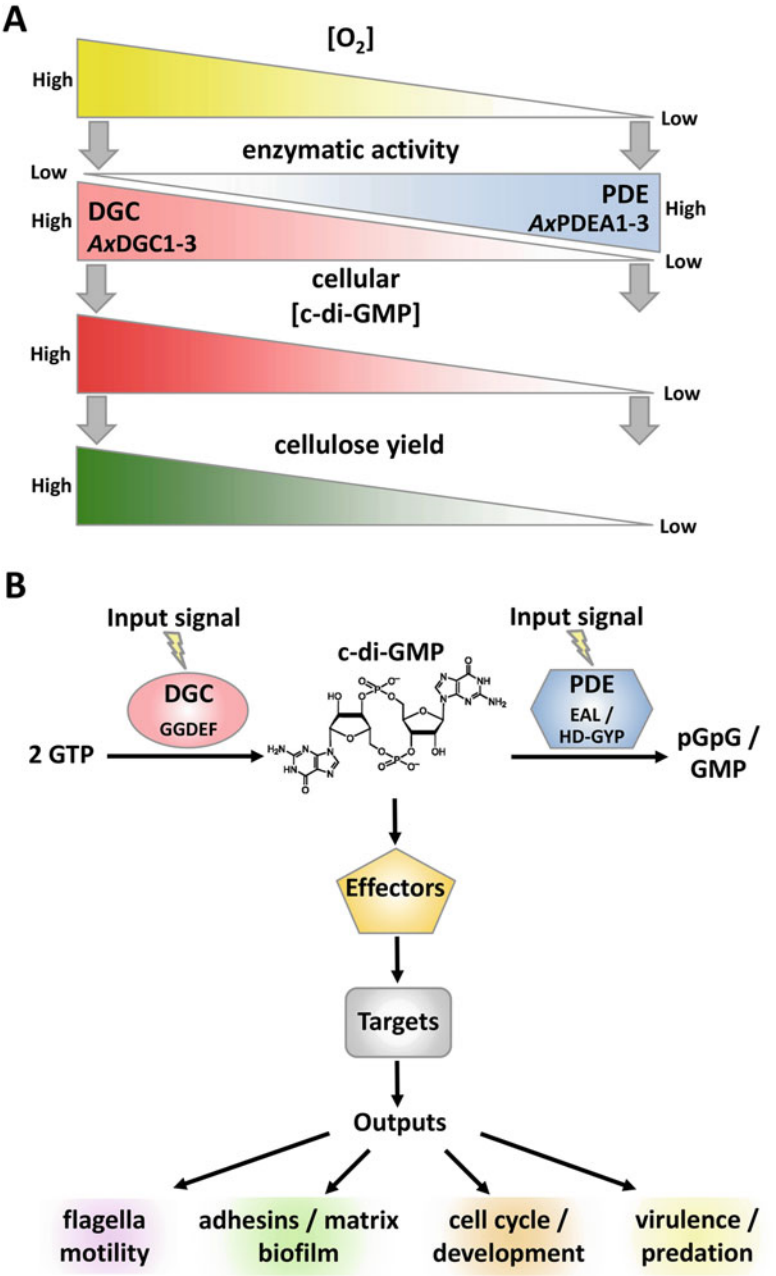

Fig. 8.4 (**a**). Schematic model illustrating the relationship between oxygen levels, cellular c-di-GMP levels, and cellulose production in *K. xylinus*. Abbreviations: DGC, diguanylate cyclase activity of *Ax*DGC1-3 enzymes; PDE, phosphodiesterase activity of *Ax*PDE1-3 enzymes. (**b**). Synthesis, degradation, mechanism of action, and physiological target processes of the second

forms cellulose-based pellicle biofilms at the O_2-rich air-liquid interface. Moreover, since cellulose production is expected to be costly, in terms of both carbon sources and energy, shutting down cellulose synthesis under low O_2, and hence low-energy efficiency, may be a way of saving resources.

C-di-GMP regulation of cellulose biosynthesis in *K. xylinus* by the antagonistic actions of several DGCs and PDEs with the cellular redox status and oxygen concentration as cellular and environmental signal input provided an early framework for studying c-di-GMP signaling in general. However, assigning DGC or PDE activities to specific domains was difficult since the c-di-GMP-controlling enzymes involved in this model system all featured GGDEF as well as EAL domains. Thus, unequivocal assignment of DGC activity with the GGDEF domain and of PDE activity with the EAL domain (Fig. 8.4b) was achieved only later with proteins from other bacterial species that carried either one or the other domain alone (Paul et al. 2004; Christen et al. 2005; Schmidt et al. 2005).

8.4.3 *Signal Input, DGCs, and PDEs Involved in C-di-GMP Control of Cellulose Biosynthesis and Modification in* E. coli

In *E. coli*, pEtN-cellulose is produced along with amyloid curli fibers when cells enter into stationary phase and have shut down flagellar expression and activity. Thus, regulation of pEtN-cellulose production is embedded in a large regulatory network that inversely controls flagellar activity and synthesis of ECM components (Serra and Hengge 2014). Within this network, c-di-GMP signaling has decisive inputs into pEtN-cellulose synthesis at three distinct regulatory levels (Fig. 8.5). This requires a specific subset of the 12 DGCs and 13 PDEs (of a total of 29 GGDEF and/or EAL domain proteins) that are encoded in the genome of the *E. coli* K-12 strain (Povolotsky and Hengge 2016).

The first layer of regulation involves the activation of expression of CsgD, the biofilm master regulator that positively controls the production of cellulose as well as of curli subunits (Römling et al. 2000; Serra and Hengge 2014) (Fig. 8.5). The backbone of the regulation of CsgD expression is a feedforward transcription factor cascade that uses the stationary phase sigma factor RpoS (σ^S) as a master regulator and the MerR-like transcription factor MlrA as a highly specific activator of

Fig. 8.4 (continued) messenger c-di-GMP. C-di-GMP signaling typically involves diguanylate cyclases, which synthesize c-di-GMP via their GGDEF domain, phosphodiesterases of the EAL or HD-GYP domain type that degrade c-di-GMP, effector components that bind c-di-GMP, and target components whose diverse output functions are controlled by the effectors upon c-di-GMP binding. Yellow bolts indicate signal inputs typically transduced via different N-terminal sensory domains of DGCs and PDEs. Abbreviations: *DGC* diguanylate cyclase; *PDE* phosphodiesterase; *pGpG* 5′-phosphoguanylyl-(3′-5′)-guanosine

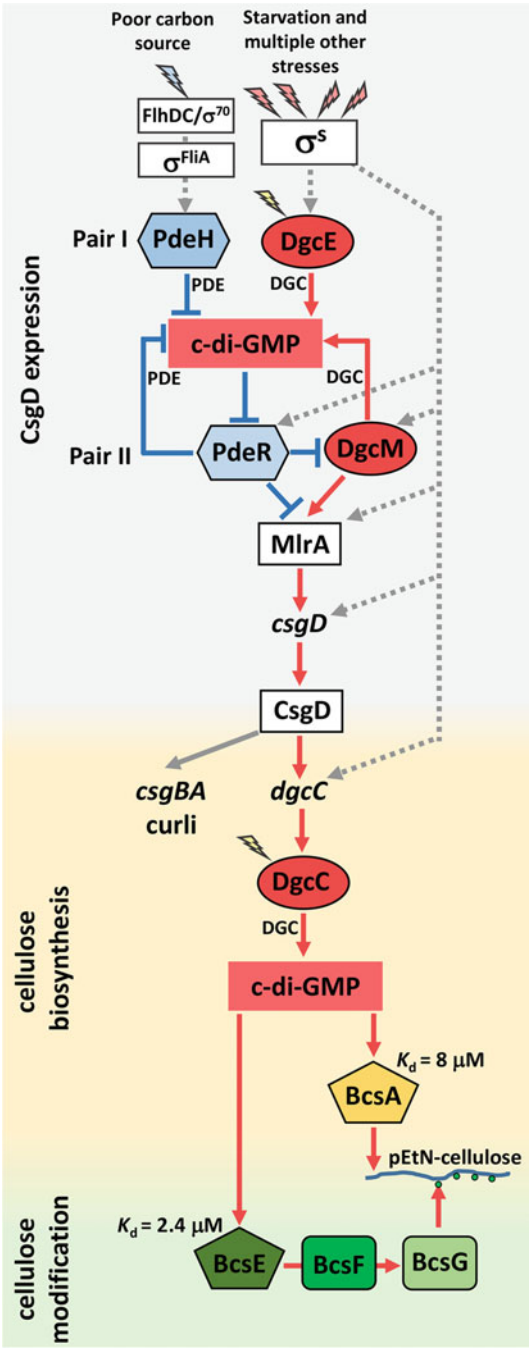

Fig. 8.5 Regulatory input of c-di-GMP into cellulose biosynthesis and modification in *E. coli*. The scheme illustrates the complex regulatory cascade controlling pEtN-cellulose production in *E. coli* (see text for details and references). Different background colors indicate the three levels at which c-di-GMP exerts its regulatory effects: activation of expression of the biofilm regulator CsgD, allosteric activation of cellulose biosynthesis by BcsA, and activation of pEtN transfer to glucan chains via the BcsE-BcsF-BcsG pathway. C-di-GMP-producing DGCs are shown as red ovals, c-di-GMP-degrading PDEs as light blue hexagons, and c-di-GMP-binding effector proteins as pentagons. Note that as a "trigger PDE," PdeR serves as both a PDE and an effector (see text for details). Dissociation constants (K*d*) of effector proteins are shown. Yellow bolts indicate additional unknown signal input via the N-terminal sensory domains of DGCs and PDEs. Transcription factors are represented by white rectangles. Blue and red bolts indicate stress signal inputs associated with post-exponential and stationary phase physiology, respectively

transcription initiation at the promoter of *csgD*. This gene in turn encodes a transcription factor that serves as a key biofilm regulator (Brown et al. 2001; Weber et al. 2006). At this level, c-di-GMP plays its decisive regulatory role by controlling the activity of MlrA via two PDE/DGC pairs: PdeH/DgcE (pair I; formerly YhjH/YegE) and PdeR/DgcM (pair II, formerly YciR/YdaM). Both enzyme pairs operate in a cascade involving multiple direct protein-protein interactions (Lindenberg et al. 2013). In this cascade, the key component is PdeR, which acts as a bifunctional trigger enzyme that links c-di-GMP as negotiated by pair I to the activity of MlrA (Lindenberg et al. 2013; Hengge 2016). In still growing cells, which contain very low c-di-GMP levels due to high activity of PdeH (*E. coli*'s master PDE), which is under the control of the flagellar regulatory cascade, PdeR inhibits both MlrA and DgcM by direct interaction. As a consequence, *csgD* is not transcribed. During entry into stationary phase, c-di-GMP production increases because the RpoS-dependent DgcE is induced and PdeH is no longer expressed and its cellular level decreases. This results in binding and cleavage of c-di-GMP by PdeR which is associated with a release of inhibition of MlrA and DgcM. This allows DgcM to also produce c-di-GMP (thereby generating a positive feedback in this switch mechanism) and, in addition, to act as a direct coactivator for MlrA, which is essential for full activation of *csgD* transcription (Lindenberg et al. 2013).

The second layer of c-di-GMP regulation is at the level of cellulose synthesis, where c-di-GMP acts as allosteric activator of the catalytic subunit BcsA upon binding to its regulatory PilZ domain (Fig. 8.5). The mechanism of BcsA activation was discussed in detail above and is presumed to be conserved among bacterial species. A crucial distinction, however, seems to be the origin of the c-di-GMP that activates BcsA, which in most *E. coli* strains is specifically attributed to DgcC (formerly YaiC; AdrA in *Salmonella*), a DGC whose expression is under the control of CsgD and RpoS-containing RNAP (Römling et al. 2000; Zogaj et al. 2001; Weber et al. 2006; Sommerfeldt et al. 2009). *dgcC/adrA* mutants do express CsgD and curli subunits normally but are specifically defective in producing cellulose (Zogaj et al. 2001; Simm et al. 2004). Although the reason for the high specificity of DgcC for activating cellulose synthase is not fully clear, one hypothesis is that DgcC, which is an inner-membrane protein, could operate in close proximity to the cellulose synthesizing BcsA-BcsB complex, thus serving as a local c-di-GMP source. Moreover, this highly specific secondary c-di-GMP input into cellulose production via DgcC – besides the co-regulation of curli and cellulose by c-di-GMP at the higher hierarchical level of CsgD expression (Fig. 8.5) – also opens the possibility to differentially control cellulose synthesis and thereby the ratio between curli and cellulose, possibly in different zones of the biofilm matrix. It is important to note that while CsgD/DgcC is the most conserved pathway regulating cellulose synthesis, several *E. coli* and *Salmonella* strains were shown to use regulatory pathways independent of CsgD and dependent on alternative DGCs (e.g., DgcQ; formerly YedQ) to control cellulose

production, depending also on the environmental conditions (Garcia et al. 2004; Da Re and Ghigo 2006).

The third level of c-di-GMP regulation, which is assumed to run parallel to BcsA activation, affects the periplasmic pEtN modification of the newly synthesized cellulose molecule by BcsG (Fig. 8.5). Here, the key regulatory component seems BcsE, which, in response to c-di-GMP binding, probably controls BcsG activity via the transmembrane BcsE-BcsF-BcsG direct interaction pathway (Thongsomboon et al. 2018). Following the hypothesis that DgcC would act as a local c-di-GMP source for BcsA, it seems logical to imagine DgcC playing an equivalent role for the equally co-localized BcsE. Such local "customized" provision of c-di-GMP to a specific effector/target system also seems necessary here, since the global cellular c-di-GMP pool remains strikingly low (approximately 100 nM) even under conditions of curli and cellulose production (Sarenko et al. 2017), despite the significantly higher K_d values for c-di-GMP binding of BcsA and BcsE (8 and 2.4 μM, respectively) (Pultz et al. 2012; Fang et al. 2014). The approximately threefold lower K_d of BcsE may also ensure that efficient pEtN modification will occur whenever c-di-GMP production by DgcC is high enough to support cellulose synthesis (Fig. 8.5). This observation together with evidence that the absence of pEtN modification leads to incomplete or defective formation of larger cellulose filaments (see below) indicates that cellulose synthesis and modification should remain coupled. On the other hand, the fact that the *bcsEFG* operon as a genetic unit is separate from the long *bcs* operon encoding the core BCS subunits (Fig. 8.3a) also leaves the possibility that under certain circumstances the two processes become uncoupled by differential regulation and non-modified cellulose is alternatively produced.

8.5 Supramolecular Structure of Bacterial Cellulose

8.5.1 From Glucan Chains to Fibrils

Cellulose biogenesis involves not only synthesis, modification – in *E. coli* and *Enterobacteria* – and extrusion of glucan chains by BCS complexes but also the subsequent hierarchical assembly of the glucan chains into fibrils. This assembly occurs in the space immediately exterior to the surface of the bacteria and essentially depends on the establishment of hydrogen bonds and van der Waals interactions within and among glucan chains (Ross et al. 1991). The events of fibril assembly have been investigated extensively in *K. xylinus*. Electron microscopy studies have shown that *K. xylinus* cells exhibit about 50 BCS complexes (or TC subunits) in their cell envelope that typically organize in rows along the longitudinal cell axis (Brown et al. 1976; Kimura et al. 2001) (Fig. 8.6). Once glucan chains begin to co-emerge from individual BCS complexes, they aggregate to form the so-called sub-elementary fibrils. It has been proposed that about 10–15 chains associate with each other

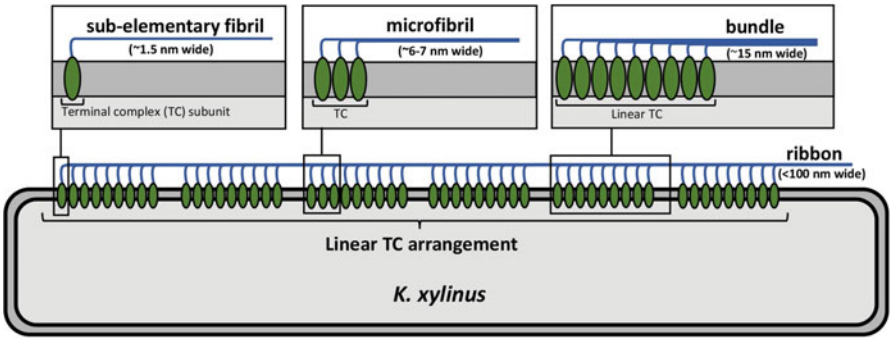

Fig. 8.6 Hierarchical assembly of glucan chains into ribbon-shaped cellulose fibrils in *K. xylinus*. The scheme has been drawn after (Mehta et al. 2015) and illustrates the organization of BCS complexes or terminal complex (TC) subunits along the longitudinal axis of a *K. xylinus* cell. Co-emerging glucan chains aggregate to form sub-elementary fibrils. Adjacent sub-elementary fibrils from neighboring TC subunits aggregate further to form microfibrils. The association and linear arrangement of TC subunits facilitate the assembly of microfibrils into bundles and of bundles into ribbon-shaped cellulose fibrils

forming 1.5-nm-wide sub-elementary fibrils (Ross et al. 1991). Subsequently, adjacent sub-elementary fibrils from neighboring complexes aggregate further to form microfibrils (6–7 nm), which thereafter assemble into bundles. Finally, bundles assemble further into flat, ribbon-shaped fibrils that usually are less than 100 nm wide (Ross et al. 1991) (Fig. 8.6). These fibrils are 200 times finer than cotton fibers and, due to their composite nature, exhibit significantly high surface area (Vitta and Thiruvengadam 2012).

In *E. coli*, the actual events that guide the assembly of pEtN-cellulose into fibrils and sheets are currently unclear. The recent finding that multiple copies of the catalytic BcsA-BcsB core occur in single BCS complexes, potentially allowing the synthesis of multiple glucan chains in parallel, leads to new hypotheses on fibril formation (Krasteva et al. 2017). Two alternative models have been proposed: one where individual glucan chains are guided and excreted through individual BcsC porins and then assembled into microfibrils at the cell surface and a second model where the glucan chains aggregate already in the periplasm and the resulting microfibril is then exported through a wider composite outer-membrane β-barrel, also formed by BcsC (Krasteva et al. 2017). It is important to note that these models were proposed shortly before *E. coli* cellulose was reported to be modified with pEtN, and therefore none of the models take this crucial aspect into consideration. Irrespective of the actual model, another significant difference with *K. xylinus* is the potential absence in *E. coli* of a collective organization of BCS complexes. BcsQ and excreted cellulose were shown to localize at the poles of *E. coli* cells (Le Quéré and Ghigo 2009), but so far no further evidence on the location and potential further assembly of BCS complexes has been reported. Overall, this further accounts for the differences in supramolecular structure that exist between cellulose produced by *E. coli* and *K. xylinus*.

8.5.2 Crystalline and Amorphous Cellulose

The spatial arrangement of the glucan chains with respect to each other (i.e., chain orientation and alignment) determines the crystalline state of cellulose. Most natural cellulose is produced as crystalline cellulose, also known as cellulose I, where glucan chains orient parallel to each other and are closely packed side by side forming a metastable sub-elementary fibril (Brett 2000). Crystalline cellulose I also occurs in two allomorphs, namely, Iα and Iβ, which differ with respect to their crystal packing, molecular conformation, and hydrogen bonding (Atalla and Vanderhart 1984). Cellulose from *K. xylinus*, for example, is rich in the metastable allomorph I_α (Atalla and Vanderhart 1984). Cellulose microfibrils can contain both allomorphs in different ratios, which impart different physicochemical properties to the final cellulose fibrils. Of much less frequent occurrence is crystalline cellulose II, which was reported to be produced also by *K. xylinus* under physical constraints (Shibazaki et al. 1998). In cellulose II the arrangement of the glucan chains is antiparallel (Kolpak and Blackwell 1976). While this arrangement would result in an additional hydrogen bond per glucose residue, making cellulose II more thermodynamically stable than other allomorphs of cellulose, it is actually unclear how glucan chains would adopt such an atypical configuration in vivo.

Cellulose also occurs in a noncrystalline or amorphous form where glucan chains show less ordered and less compact arrangements. In crystalline cellulose I, domains of amorphous cellulose are commonly found in between large crystalline domains (Larsson et al. 1997). Importantly, amorphous cellulose seems the dominant form of cellulose produced by enterobacteria such as *E. coli* and *Salmonella* and by *Sarcina* and *Rhodobacter sphaeroides* (Jonas and Farah 1998). In *E. coli* cellulose has been visualized as long and thick filaments and sheets (Serra et al. 2013a). However, the details about how glucan chains interact and organize to form these structures are unknown. With every second glucosyl residue in the glucan chain being modified with a pEtN group (Thongsomboon et al. 2018), one would expect the distance between the glucan chains to increase and, as a consequence, the hydrogen-bonding network being less extensive as in crystalline cellulose. Furthermore, the positive and negative charges of the zwitterionic pEtN groups are likely to have a drastic influence on the interaction between the glucan chains and may also allow electrostatic interactions. That pEtN modification is crucial for the supramolecular structure of *E. coli* cellulose was shown in biofilms, where a *bcsG* mutant strain that is unable to install the modification produces only short, thin, and curled cellulose fibers that clearly contrast with the long and thick filaments produced from pEtN-cellulose in the wild-type strain (Thongsomboon et al. 2018). In light of these recent findings, future work will need to focus on characterizing structural details of amorphous pEtN-cellulose and clarifying the actual role of the pEtN modification in the assembly of cellulose and its ability to form nanocomposites with other fibers such as amyloids (see also below).

8.5.3 Physicochemical and Mechanical Properties of Bacterial Cellulose

The molecular and supramolecular structure of cellulose defines its overall physicochemical and mechanical properties. In *K. xylinus* cellulose, for instance, the high number of crystalline domains correlates with a remarkably high tensile strength as well as with water insolubility (Ross et al. 1991). Since in the crystalline state the hydrogen-bonding network formed among hydroxyl groups of glucosyl residues is extensive, the glucan chains are firmly held together and able to resist high mechanical stress. At the fibril level, this translates into a stress resistance that is comparable to that of steel (Yamanaka et al. 1989). Such a compact configuration, on the other hand, makes the hydroxyl groups in glucan chains inaccessible to interact with water, thus limiting cellulose solubility. As an additional consequence, water exclusion from crystalline regions allows cellulose fibrils to maintain high stiffness, which is reflected in the very high Young's modulus (also known as elastic modulus) of crystalline cellulose from *K. xylinus* (Yamanaka et al. 1989; Guhados et al. 2005).

Water molecules can, however, diffuse into amorphous regions, where they can break intermolecular hydrogen bonds between glucan chains (Mazeau 2015). This swelling process not only increases cellulose solubility but also makes fibrils more mechanically flexible (i.e., reduces Young's modulus) as water penetration increases the distance between glucan chains (Pang et al. 2016). Thus, the occurrence of amorphous regions in crystalline cellulose plays an important role in modulating the physicochemical and mechanical properties of the final fibrils. Consistent with its proposed amorphous configuration and zwitterionic nature, purified pEtN-cellulose produced by *E. coli* dissolves – to some extent – in water resulting in a hydrogel-like suspension (unpublished data). This is in clear contrast to the behavior of crystalline cellulose from *K. xylinus*, which precipitates out of solution.

The influence of water on the physicochemical and mechanical properties of cellulose can ultimately translate into changes in the structure of cellulose-containing biofilms. In fact, this is readily visible in agar-grown *E. coli* macrocolony biofilms where differences in water content of the agar-solidified medium or even in air humidity inside the Petri dish lead to substantial changes in the wrinkling and spreading patterns of the macrocolonies (Serra and Hengge 2017), which to a great extent is the result of alterations in the elastic properties of cellulose. Thus, while environmental conditions can decisively influence cellulose-based biofilm formation by exerting regulatory effects on cellulose production at the gene expression or protein function levels, the effect of water content on biofilms serves as an example of how an environmental factor can also have a direct modulatory effect on biofilm formation by simply influencing the material properties of cellulose at the fibril level.

8.6 Supracellular Architecture, ECM Organization, and Cellular Physiology in pEtN-Cellulose-Containing *E. coli* Biofilms

8.6.1 *pEtN-Cellulose and Amyloid Curli Fibers as Building Materials of Structured* E. coli *Biofilms*

Recent advances in understanding the architectural role of cellulose in biofilms have been made through the study of macrocolony biofilms of *E. coli* (Serra et al. 2013a, 2015; Serra and Hengge 2014). By adopting specific morphological patterns as a function of ECM composition, macrocolony biofilms have served as an ideal model system to study the "building material" properties of individual ECM components (Serra and Hengge 2017). *E. coli* turned out to be a particularly suitable model system, as its macrocolony ECM usually contains two components only, i.e., pEtN-cellulose and amyloid curli fibers, whose regulation is well-understood and thus can easily be genetically manipulated.

As an aggregative exopolysaccharide, pEtN-cellulose confers strong cohesion and remarkable elasticity, which at the supracellular level translate into tissue-like properties (Serra et al. 2013a). In terms of "building material," this is comparable to the attributes that steel confers to buildings. In growing macrocolonies, tissue-like properties combine with spatial constraints generated as a consequence of cellular proliferation in the community, which leads macrocolonies to buckle up and fold into complex and large-scale 3D structures. Thus, *E. coli* macrocolonies exhibit elastic behavior with high mechanical flexibility when pEtN-cellulose is the dominant or the only ECM component. This translates into elaborate morphological patterns that typically consist of small intertwined wrinkles that become particularly dense toward the center of the macrocolony, i.e., the oldest region of the community subject to most severe spatial constraints (Serra et al. 2013a; Serra and Hengge 2017) (Fig. 8.7). This highly wrinkled pattern shows pink coloration when Congo red (CR), a diazo dye that binds to both pEtN-cellulose and amyloid curli, is supplemented to the culture medium (Serra and Hengge 2017). This CR-based pink staining is distinctive of pEtN-cellulose and hence commonly used as a readout for its presence.

Some *E. coli* strains, e.g., the commonly used K-12 laboratory strains, do not produce cellulose, but their biofilm matrix contains amyloid curli fibers only. Remarkably, amyloid fibers alone form a highly dense ECM network that exhibits "building material" attributes opposite but complementary to those of pEtN-cellulose. The curli ECM network is nonelastic, i.e., highly brittle, and, as a consequence of the biofilm internal pressure generated by cell growth and proliferation, it breaks (Serra et al. 2013a, b). In macrocolonies, these breakages occur at a certain distance behind the outer growth zone, where curli begins to accumulate, and propagate and become confluent in a circular manner, which over time replicates to give rise to a pattern of concentric rings (Serra et al. 2013a, b) (Fig. 8.7).

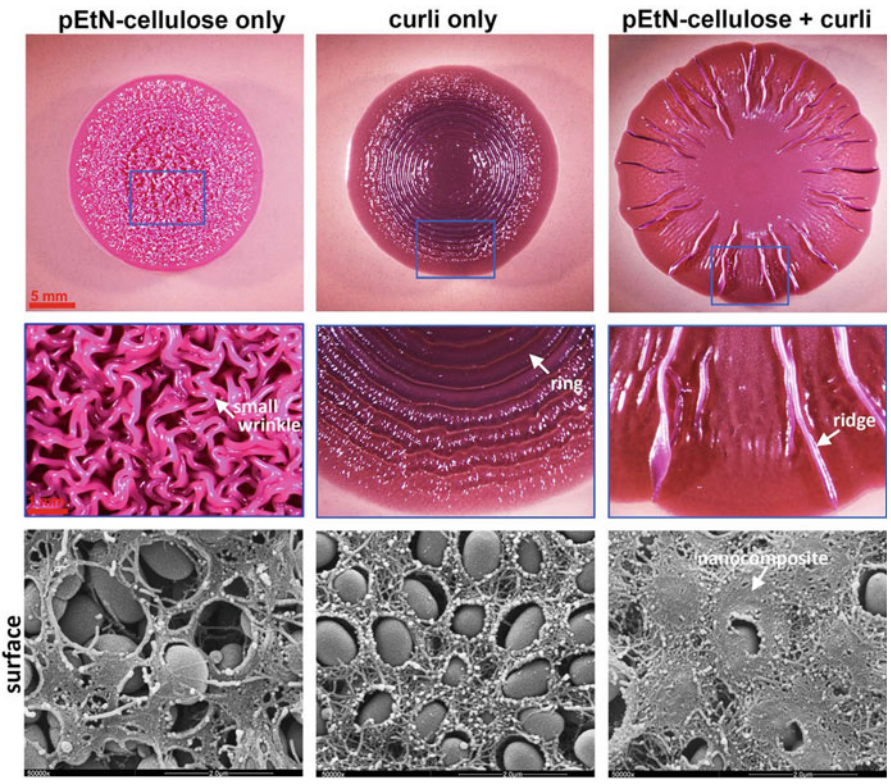

Fig. 8.7 Macrocolony biofilms of *E. coli* K-12 strains producing pEtN-cellulose and/or amyloid curli display distinctive morphologies and staining with Congo red (CR)/Coomassie brilliant blue (CM) (upper panels). Macrocolonies were grown for 5 days on CR/CB-supplemented NaCl-free LB agar plates at 28 °C. The middle panels show enlarged views of boxed areas of the respective macrocolony images in the upper panels. The bottom panels show corresponding high-resolution SEM images revealing details of the fine structure and organization of ECM components and bacterial cells at the surface of *E. coli* macrocolonies. (Images in this figure have been published before (Serra et al. 2013a; Serra and Hengge 2017) and are shown here with permission from the *Journal of Bacteriology* and Springer Nature)

In fully biofilm-proficient *E. coli* strains, however, pEtN-cellulose is co-regulated and co-produced with curli proteins (Fig. 8.5), which upon secretion assemble into amyloid fibers (Chapman et al. 2002; Zogaj et al. 2003). pEtN-cellulose and curli fibers form a nanocomposite ECM network that combines the "building material" properties of both components (Serra et al. 2013a). In this nanocomposite, amyloid curli serves as embedding material that fixes cells in place, strengthens the cohesion, and counterbalances the flexibility conferred by pEtN-cellulose, i.e., it plays a comparable role to mortar in building construction. For reasons that probably have to do with the highly complex supracellular matrix architecture further described below, macrocolonies producing both pEtN-cellulose and curli fibers grow extremely flat and expand horizontally (with diameters of >20 mm after 5–7 days).

In terms of material properties, the pEtN-cellulose/curli fiber nanocomposite in these biofilms confers not only elasticity but high mechanical strength and stability to the macrocolonies (i.e., obviously a high Young's modulus), since these wild-type biofilms can tolerate high mechanical stress associated with cellular proliferation. This allows buckling and folding of macrocolonies without breaking, which results in high ridges, which differ from the small intertwined wrinkles of pEtN-cellulose-only macrocolonies (Serra et al. 2013a) (Fig. 8.7). These ridges mostly originate at interspaced positions around the outer rim of the macrocolonies, which is an area that experiences highest growth rates and increasing geometrical constraints with increasing colony diameter (Serra et al. 2013a). Over time, the ridges are pushed up very high (up to a few millimeters) and propagate radially toward the center of the macrocolony where they intertwine and also combine with smaller wrinkles. In the presence of CR, macrocolonies containing both pEtN-cellulose and curli acquire a red coloration, which becomes dark red/purple if also Coomassie blue (CB) is added, a dye that stains proteins and thus can enhance color discrimination between curli and pEtN-cellulose (Serra and Hengge 2017) (Fig. 8.7).

8.6.2 *Physiological Stratification and Asymmetric ECM Distribution in Structured* E. coli *Biofilms*

In order to gain a deeper understanding of the architectural role of pEtN-cellulose and curli in *E. coli* biofilms, it has been crucial to successfully cope with the main obstacle that macrocolony biofilms pose to most microscopic techniques, i.e., their massive compactness. This was possible, thanks to experimental approaches that combined macrocolony cryo-sectioning, in situ staining of pEtN-cellulose and curli, and fluorescence and scanning electron microscopy, which allowed the visualization of bacterial cells and both ECM elements inside macrocolonies at remarkably high resolution (Serra et al. 2013a; Serra and Hengge 2017). Studies applying these approaches revealed that morphogenesis of macrocolonies does depend not only on the building material properties of both ECM components but also on how they distribute and organize within the 3D space of the biofilms. Notably, the distribution of pEtN-cellulose and/or curli across *E. coli* macrocolonies was found to be strikingly asymmetric, with both ECM components being generated exclusively in the upper aerobic region of the biofilm (Serra et al. 2013a, b) (Fig. 8.8, upper panels). By contrast, the lower bottom layer closer to the nutrient-providing agar is free of ECM.

Importantly, this asymmetric ECM distribution arises as a consequence of the physiological differentiation that *E. coli* cells experience in response to gradients of nutrients, oxygen, and waste products that build up across the biofilm (Serra et al. 2013b; Serra and Hengge 2014; Klauck et al. 2018). Thus, the synthesis of pEtN-cellulose and curli in the upper macrocolony layer is the result of cells being far away from the nutrient source, so that they experience nutrient limitation and enter into stationary phase. Under these conditions, cells become ovoid (Fig. 8.7, bottom

panels), which is the typical starving cell morphology, and induce the expression of stationary-phase sigma factor RpoS, which then drives global changes in gene expression redirecting the cell physiology towards optimizing maintenance and survival (Serra et al. 2013b; Serra and Hengge 2014). As discussed above (Fig. 8.5), RpoS is the master regulator of the transcription factor cascade that controls the expression of CsgD, i.e., the biofilm master regulator that activates the production of pEtN-cellulose and curli subunits (Weber et al. 2006; Lindenberg et al. 2013). In marked contrast to the upper macrocolony layer, the bottom layer is populated by rod-shaped cells that elongate and divide, which overall is consistent with cells being closer to the nutrient-supplying agar (Serra et al. 2013b). Cells in this biofilm zone feature multiple flagella which – in the densely packed biofilm – do not function as motility-providing organelles but rather form an entangled mesh that contributes to stabilizing the bottom layer (Serra et al. 2013b). The fact that flagella expression requires cAMP, i.e., a second messenger that signals nonoptimal nutrient supply, indicated that the non-matrix-producing cells in the bottom layer grow relatively slowly. A recent study indicated that this may be due to oxygen limitation which probably leads to an energy-inefficient use of nutrients by fermentation, whereas a subpopulation of cells somewhat higher up, i.e. in the middle layer where oxygen levels are higher and nutrients are still enough due to diffusion, manages to grow faster, and probably by aerobic respiration (Klauck et al. 2018).

Since the physiological response of *E. coli* to local environments, i.e., essentially to metabolic gradients, within the biofilm is what dictates the overall two-layer matrix architecture, it occurs in all types of macrocolonies, independently of which ECM components are present (Fig. 8.8). Nevertheless, whether pEtN-cellulose or curli is produced in the biofilm is highly relevant because they can differentially modulate further the physiological responses of the cells by (i) modifying the consumption rate of carbon/energy resources (as ECM production is costly) and (ii) determining the extent to which macrocolonies expand vertically and horizontally, which in turn affects nutrient and oxygen gradients generated inside the resulting biofilms with different geometry. Thus, while the overall pattern of chemical gradients – i.e., bottom-to-top and vice versa – is conserved among macrocolonies, variations in the gradients are expected between macrocolonies that produce either pEtN-cellulose or curli alone, which typically reach thicknesses in the range of 200–300 μm, and macrocolonies containing both ECM components that exhibit a strikingly constant height of 60–65 μm only (Serra et al. 2013a, b) (Fig. 8.8, upper panels). In fact, the flatness of pEtN-cellulose/curli-containing macrocolonies is suggested to be an adaptation of the community to facilitate access to oxygen, which is required as the terminal electron acceptor for aerobic respiration (Serra et al. 2013a). On the other hand, the flatness of pEtN-cellulose/curli-containing macrocolonies also helps to explain the emergence of large ridges as it is a condition that facilitates buckling of the upper layer (~40–45 μm thick) into the double-layered ridges that maintain a constant width independent of their actual height (Serra et al. 2013a) (Figs. 8.7 and 8.8). The space that opens up at the base of an emerging ridge was found to be entirely occupied by non-ECM-producing cells (Serra et al. 2013a). These cells, which rapidly colonize and fill up this new space, may originate either

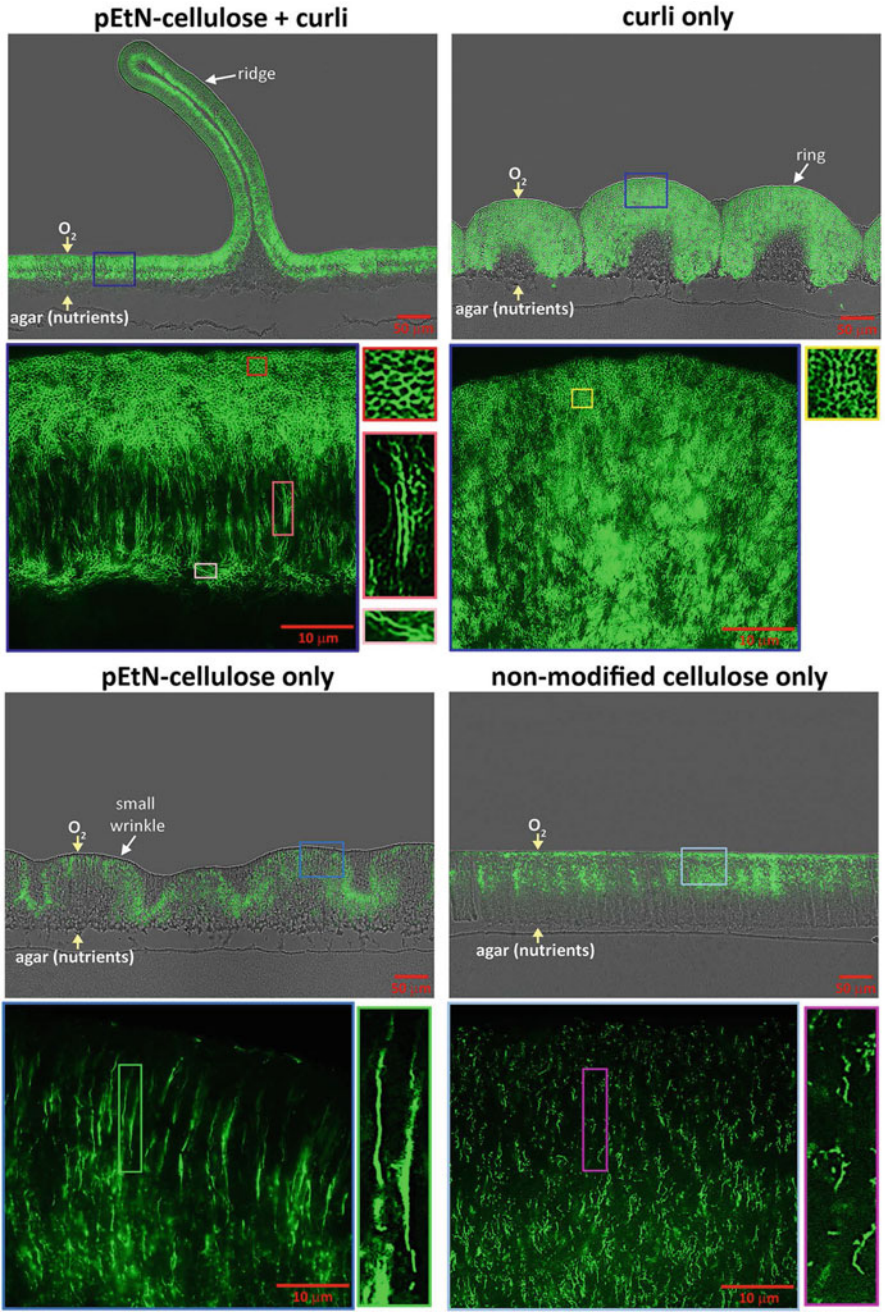

Fig. 8.8 Spatial organization and fine structure of pEtN-cellulose, amyloid curli, and non-modified cellulose in *E. coli* macrocolony biofilms. The figure presents bright-field/fluorescence merged images of thin cross-sections of 3-day-old *E. coli* macrocolonies containing pEtN-cellulose and/or

from the bottom layer or from the clusters of more rapidly growing and non-ECM-producing cells interspersed with the matrix-producing cells in the lower zone of the ECM-producing layer (Klauck et al. 2018) (see also below). Notably, the absence of ECM in the bottom layer is essential for maintaining the physical integrity of the biofilms. In macrocolonies of strains engineered to artificially produce ECM in both layers, the lower stratum turns into a rigid base platelike structure that no longer allows cells to flexibly invade the space that opens up when the upper layer buckles into ridges and wrinkles (Serra et al. 2015). As a consequence, the upper layer detaches, can no longer maintain its water content via capillary action, and therefore dries out and exfoliates literally like paper (Serra et al. 2015).

8.6.3 *Fine Structure and Organization of pEtN-Cellulose and Curli/pEtN-Cellulose Nanocomposite in the 3D Space of* E. coli *Biofilms*

The fine structure and organization of pEtN-cellulose alone or in combination with amyloid curli fibers in the upper layer of macrocolonies was also examined at cellular resolution. In the highly wrinkled pEtN-cellulose-only macrocolonies, pEtN-cellulose was observed to assemble into irregular thick filaments (up to 15 μm long) and sheet- and netlike structures that extend between or across cells (Serra et al. 2013a) (Figs. 8.7 and 8.8). Strikingly, the long pEtN-cellulose filaments arrange parallel to each other (with a separation of 1–5 μm) in vertical orientation, i.e., perpendicular to the border formed by the wrinkled surface, with this pattern found in almost the entire upper ECM-containing layer (Serra et al. 2013a). At the macrocolony surface, however, pEtN-cellulose filaments and sheets form a flat network with relatively large pores (Fig. 8.7), through which the small ovoid cells can be squeezed, in particular between the wrinkles (Fig. 8.8) (Serra et al. 2013a).

This is in marked contrast to the spatial arrangement of amyloid curli in concentric ring-shaped curli-only macrocolonies. Upon assembly at the surface of stationary-phase cells, amyloid fibers of curli are released and accumulate in the

Fig. 8.8 (continued) amyloid curli or non-modified cellulose only as indicated. Macrocolonies exhibit distinct microarchitectures but a conserved two-layer stratification with ECM components being restricted to the upper biofilm layer as visualized by Thioflavin S (TS), a green fluorescent dye that stains pEtN and non-modified cellulose as well as amyloid curli. Below bright-field/fluorescence merged images, fluorescence-only images show magnified views of the color-coded boxed areas in respective images. Insets show enlarged views of internal color-coded boxed areas in the respective images. Images and insets show the fine structure and arrangement of TS-stained pEtN-cellulose, amyloid curli and non-modified cellulose in macrocolonies. (Several images in this figure have been published before (Serra et al. 2013a; Thongsomboon et al. 2018) and are shown here with permission from the *Journal of Bacteriology and Science*)

intercellular space, where they form "basket"-like structures surrounding the ECM-producer cells in the upper macrocolony layer (Serra et al. 2013b) (Figs. 8.7 and 8.8). The confluence of "basket"-like structures gives the curli network the overall appearance of a "honeycomb" (Serra et al. 2013b).

Finally, in the upper layer of the flat and ridge-featuring pEtN-cellulose/curli-containing macrocolonies, three patterns of ECM organization can be clearly distinguished (Fig. 8.8, upper left panel) (Serra et al. 2013a; Klauck et al. 2018). First, a top zone of about 15–20 μm height features a "honeycomb"-like or "dense brickwork" ECM pattern around bacterial silhouettes. This pattern is characteristic not only for curli alone but also for the pEtN-cellulose/curli nanocomposite, indicating that the geometric arrangement of the latter is determined by the curli fiber network, whereas its biomechanical property – i.e., its elasticity, which is in pronounced contrast to the brittle curli-only matrix – is a function of pEtN-cellulose within the nanocomposite. At the macrocolony surface, the highly dense nanocomposite of both ECM elements covers essentially all bacterial cells. A second zone deeper inside the upper layer (of an approximate height of 15–20 μm) exhibits a pattern of "vertical pillars," i.e., sheathlike structures that resemble the long filaments and sheets – arranged here into cylinders around lines of cells – that pEtN-cellulose forms in isolation. This is followed further below by a narrow zone (about 5–10 μm high) where the ECM forms a loose horizontal network, which, like the vertical pillars, is likely to consist of pEtN-cellulose exclusively (Serra et al. 2013a). Notably, in the vertical pillars and loose horizontal network zones, EMC production is heterogeneous with ECM-producing and non-producing cells found side by side (Serra et al. 2013a; Klauck et al. 2018). The location and arrangement of the vertical pillars appears to be particularly important during buckling up in regions of extreme curvature such as the tip of the ridges. Here, these filaments appear in a highly stretched form that reflects not only the high mechanical stress that the curvature imposes but also the stabilizing role of the pEtN-cellulose assembly (Serra et al. 2013a), which resembles tensegrity architectures as exemplified by suspension bridges (Buckminster Fuller 1961; Ingber 2008).

Overall, these studies revealed that the spatial distribution and arrangement of pEtN-cellulose and curli in the 3D space of biofilms is not random but represents a highly functional supracellular ECM architecture. This not only confers elasticity, i.e., essentially tissue-like behavior, to a macrocolony biofilm community, but also allows it to optimize the use of each ECM component in order to achieve – in a spatially controlled manner – the proper combination of cohesion and mechanical flexibility necessary for buckling and folding, i.e., the large-scale morphogenetic movements required to build and shape its striking macroscopic 3D architecture.

8.6.4 Implications of the pEtN Modification for the Architectural Role of Cellulose

In *E. coli*, the presence of pEtN groups modifying the glucan chains was found to be essential for cellulose to fulfill its function as biofilm building material. Unlike the

hyper-wrinkled and CR-based pink macrocolonies that contain only pEtN-cellulose, macrocolonies of a *bcsG csgB* double mutant strain that produces non-modified cellulose only were unstructured and exhibited a lighter pink coloration (Thongsomboon et al. 2018). Elimination of the pEtN modification also drastically impairs the ability of cellulose to form a nanocomposite with amyloid curli fibers, which leads the macrocolonies to adopt a ring-shaped pattern as if curli were the only ECM element present (Thongsomboon et al. 2018). In fact, it has been previously observed that *bcsE/F/G* mutants produce a macrocolony morphotype similar to that of a curli-only strain (Serra et al. 2013a). This phenotype, however, was misguidedly taken as an indirect indication that no cellulose was made at all, while the new data show that cellulose production is only somewhat reduced and the main effect is the complete absence of the pEtN modification (Thongsomboon et al. 2018).

The inability of non-modified cellulose to fulfill its building material function appears to be related to major defects in its supramolecular structure. Microscopy studies showed that, unlike the long and thick filaments and sheets found in pEtN-cellulose-only macrocolonies, non-modified cellulose appears as short, thin, and partially curled filaments (Thongsomboon et al. 2018) (Fig. 8.8, bottom right panel). While these short fibers conserve the vertical orientation, they appear unable to associate into longer filaments as well as with curli fibers (Thongsomboon et al. 2018), which translates into low, if any, cellular cohesion and – at the supracellular level – an absence of the tissue-like elasticity of macrocolonies required for buckling and folding and for resisting shear stress (Thongsomboon et al. 2018).

8.7 Conclusion and Perspectives

Our current knowledge about bacterial cellulose and its function in biofilms – as outlined in this review – leads to new scientific questions as well as to new technological opportunities. In both respects, the discovery of the natural chemically modified pEtN-cellulose along with the enzymatic machinery involved in installing this modification (Thongsomboon et al. 2018) has been particularly inspiring. What is the superstructure of pEtN-cellulose produced by *E. coli* and *Salmonella* as well as obviously many other bacteria that possess the genes encoding the modification machinery? What is the structural basis for its formation of nanocomposites with amyloid curli fibers? From the perspective of its biological function, we also have to clarify how the complex supracellular ECM architecture in biofilms is generated that contains this nanocomposite as well as pEtN-cellulose alone in a specific spatial distribution. Why and how is this ECM architecture crucial for the large-scale morphogenetic movements that allow these tissue-like bacterial biofilms to fold into macroscopic "landscapes" of ridges and wrinkles? Moreover, it should be explored whether yet other natural modifications of cellulose exist in other bacterial species.

Plant-derived cellulose is the most-used material of natural origin on this planet, and its chemical modification and thereby artificial variation of its material properties have a long tradition. Non-modified and highly fine-structured nanocellulose

produced by *K. xylinus* is already used alone or in polymer composites for many applications, e.g., in food or paper technology as well as in medicine (Stanisławska 2016). Intriguingly, the unique precedent of pEtN-cellulose as a naturally occurring modified cellulose suggests that other types of modified cellulose with novel chemical and mechanical properties might be found in nature or even may be generated by synthetic biology approaches. While cellulose-based cultural techniques and practices have been with us since the dawn of mankind, new and sustainable materials based on bacterial cellulose are now opening new avenues for biotechnology and even design and architecture.

Acknowledgments Research in the Hengge lab mentioned in this review has been funded by the Deutsche Forschungsgemeinschaft (DFG grants He1556/17-1, He1556/20-1, and He1556/21-1 to RH), the European Research Council under the European Union's Seventh Framework Programme (ERC-AdG 249780 to R.H.), and the Alexander von Humboldt Foundation (postdoctoral fellowship to DOS).

References

Aas FE, Egge-Jacobsen W, Winther-Larsen HC, Lovold C, Hitchen PG, Dell A, Koomey M (2006) *Neisseria gonorrhoeae* type IV pili undergo multisite, hierarchical modifications with phosphoethanolamine and phosphocholine requiring an enzyme structurally related to lipopolysaccharide phosphoethanolamine transferases. J Biol Chem 281:27712–27723

Ahmad I, Lamprokostopoulou A, Le Guyon S, Streck E, Barthel M, Peters V et al (2011) Complex c-di-GMP signaling networks mediate transition between virulence properties and biofilm formation in *Salmonella enterica* serovar Typhimurium. PLoS One 6:e28351

Ahmad I, Rouf SF, Sun L, Cimdins A, Shafeeq S, Le Guyon S et al (2016) BcsZ inhibits biofilm phenotypes and promotes virulence by blocking cellulose production in *Salmonella enterica* serovar Typhimurium. Microb Cell Factories 15:177. https://doi.org/10.1186/s12934-016-0576-6

Amikam D, Galperin MY (2006) PilZ domain is part of the bacterial c-di-GMP binding protein. Bioinformatics 22:3–6

Atalla RH, Vanderhart DL (1984) Native cellulose: a composite of two distinct crystalline forms. Science 223:283–285

Augimeri RV, Varley AJ, Strap JL (2015) Establishing a role for bacterial cellulose in environmental interactions: lessons learned from diverse biofilm-producing Proteobacteria. Front Microbiol 6:1282. https://doi.org/10.3389/fmicb.2015.01282

Bassis CM, Visick KL (2010) The cyclic-di-GMP phosphodiesterase BinA negatively regulates cellulose-containing biofilms in *Vibrio fischeri*. J Bacteriol 192:1269–1278

Beloin C, Roux A, Ghigo JM (2008) *Escherichia coli* biofilms. Curr Top Microbiol Immunol 322:249–289

Branda SS, Gonzalez-Pastor JE, Ben-Yehuda S, Losick R, Kolter R (2001) Fruiting body formation by *Bacillus subtilis*. Proc Natl Acad Sci USA 98:11621–11626

Brett CT (2000) Cellulose microfibrils in plants: biosynthesis, deposition, and integration into the cell wall. Int Rev Cytol 199:161–199

Brown AJ (1886) XLIII.—on an acetic ferment which forms cellulose. J Chem Soc Trans 49:432–439

Brown RM Jr, Willison JH, Richardson CL (1976) Cellulose biosynthesis in *Acetobacter xylinum*: visualization of the site of synthesis and direct measurement of the in vivo process. Proc Natl Acad Sci USA 73:4565–4569

Brown PK, Dozois CM, Nickerson CA, Zuppardo A, Terlonge J, Curtiss R 3rd (2001) MlrA, a novel regulator of curli (AgF) and extracellular matrix synthesis by *Escherichia coli* and *Salmonella enterica* serovar Typhimurium. Mol Microbiol 41:349–363

Buckminster Fuller R (1961) Tensegrity. Portfolio Art News Annu 4:112–127

Bureau TE, Brown RM (1987) In vitro synthesis of cellulose II from a cytoplasmic membrane fraction of *Acetobacter xylinum*. Proc Natl Acad Sci USA 84:6985–6989

Cerca N, Jefferson KK (2008) Effect of growth conditions on poly-N-acetylglucosamine expression and biofilm formation in *Escherichia coli*. FEMS Microbiol Lett 283:36–41

Chang AL, Tuckerman JR, Gonzalez G, Mayer R, Weinhouse H, Volman G et al (2001) Phosphodiesterase A1, a regulator of cellulose synthesis in *Acetobacter xylinum*, is a heme-based sensor. Biochemistry 40:3420–3426

Chapman MR, Robinson LS, Pinkner JS, Roth R, Heuser J, Hammar M et al (2002) Role of *Escherichia coli* curli operons in directing amyloid fiber formation. Science 295:851–855

Christen M, Christen B, Folcher M, Schauerte A, Jenal U (2005) Identification and characterization of a cyclic di-GMP-specific phosphodiesterase and its allosteric control by GTP. J Biol Chem 280:30829–30837

Cohn F (1877) Untersuchungen über Bacterien. IV Beiträge zur Biologie der Bacillen Beiträge zur biologie der Pflanzen 7:249–276

Cullen TW, Madsen JA, Ivanov PL, Brodbelt JS, Trent MS (2012) Characterization of unique modification of flagellar rod protein FlgG by *Campylobacter jejuni* lipid A phosphoethanolamine transferase, linking bacterial locomotion and antimicrobial peptide resistance. J Biol Chem 287:3326–3336

Da Re S, Ghigo JM (2006) A CsgD-independent pathway for cellulose production and biofilm formation in *Escherichia coli*. J Bacteriol 188:3073–3087

Dragos A, Kovacs AT (2017) The peculiar functions of the bacterial extracellular matrix. Trends Microbiol 25:257–266

Fang X, Ahmad I, Blanka A, Schottkowski M, Cimdins A, Galperin MY et al (2014) GIL, a new c-di-GMP-binding protein domain involved in regulation of cellulose synthesis in enterobacteria. Mol Microbiol 93:439–452

Flemming HC, Wingender J (2010) The biofilm matrix. Nat Rev Microbiol 8:623–633

Franklin MJ, Nivens DE, Weadge JT, Howell PL (2011) Biosynthesis of the *Pseudomonas aeruginosa* extracellular polysaccharides, alginate, Pel, and Psl. Front Microbiol 2:167. https://doi.org/10.3389/fmicb.2011.00167

Friedman L, Kolter R (2004) Two genetic loci produce distinct carbohydrate-rich structural components of the *Pseudomonas aeruginosa* biofilm matrix. J Bacteriol 186:4457–4465

Garcia B, Latasa C, Solano C, Garcia-del Portillo F, Gamazo C, Lasa I (2004) Role of the GGDEF protein family in Salmonella cellulose biosynthesis and biofilm formation. Mol Microbiol 54:264–277

Guhados G, Wan W, Hutter JL (2005) Measurement of the elastic modulus of single bacterial cellulose fibers using atomic force microscopy. Langmuir 21:6642–6646

Hackney JM, Atalla RH, Vander Hart DL (1994) Modification of crystallinity and crystalline structure of *Acetobacter xylinum* cellulose in the presence of water-soluble beta-1,4-linked polysaccharides: 13C-NMR evidence. Int J Biol Macromol 16:215–218

Hammerschmidt S, Wolff S, Hocke A, Rosseau S, Muller E, Rohde M (2005) Illustration of pneumococcal polysaccharide capsule during adherence and invasion of epithelial cells. Infect Immun 73:4653–4667

Harding NE, Cleary JM, Cabanas DK, Rosen IG, Kang KS (1987) Genetic and physical analyses of a cluster of genes essential for xanthan gum biosynthesis in *Xanthomonas campestris*. J Bacteriol 169:2854–2861

Hengge R (2016) Trigger phosphodiesterases as a novel class of c-di-GMP effector proteins. Philos Trans R Soc Lond Ser B Biol Sci 371. https://doi.org/10.1098/rstb.2015.0498

Hollenbeck EC, Antonoplis A, Chai C, Thongsomboon W, Fuller GG, Cegelski L (2018) Phosphoethanolamine cellulose enhances curli-mediated adhesion of uropathogenic *Escherichia coli* to bladder epithelial cells. Proc Natl Acad Sci USA 115:10106–10111

Hu SQ, Gao YG, Tajima K, Sunagawa N, Zhou Y, Kawano S et al (2010) Structure of bacterial cellulose synthase subunit D octamer with four inner passageways. Proc Natl Acad Sci USA 107:17957–17961

Hung C, Zhou Y, Pinkner JS, Dodson KW, Crowley JR, Heuser J et al (2013) *Escherichia coli* biofilms have an organized and complex extracellular matrix structure. MBio 4:e00645–e00613. https://doi.org/10.1128/mBio.00645-13

Ingber DE (2008) Tensegrity-based mechanosensing from macro to micro. Prog Biophys Mol Biol 97:163–179

Jenal U, Reinders A, Lori C (2017) Cyclic di-GMP: second messenger extraordinaire. Nat Rev Microbiol 15:271–284

Jennings LK, Storek KM, Ledvina HE, Coulon C, Marmont LS, Sadovskaya I et al (2015) Pel is a cationic exopolysaccharide that cross-links extracellular DNA in the *Pseudomonas aeruginosa* biofilm matrix. Proc Natl Acad Sci USA 112:11353–11358

Jonas R, Farah LF (1998) Production and application of microbial cellulose. Polym Degrad Stab 59:101–106

Kimura S, Chen HP, Saxena IM, Brown RM Jr, Itoh T (2001) Localization of c-di-GMP-binding protein with the linear terminal complexes of *Acetobacter xylinum*. J Bacteriol 183:5668–5674

Klauck G, Serra DO, Possling A, Hengge R (2018) Spatial organization of different sigma factor activities and c-di-GMP signalling within the three-dimensional landscape of a bacterial biofilm. Open Biol 8. https://doi.org/10.1098/rsob.180066

Kolpak FJ, Blackwell J (1976) Determination of the structure of cellulose II. Macromolecules 9:273–278

Krasteva PV, Giglio KM, Sondermann H (2012) Sensing the messenger: the diverse ways that bacteria signal through c-di-GMP. Protein Sci 21:929–948

Krasteva PV, Bernal-Bayard J, Travier L, Martin FA, Kaminski PA, Karimova G et al (2017) Insights into the structure and assembly of a bacterial cellulose secretion system. Nat Commun 8:2065. https://doi.org/10.1038/s41467-017-01523-2

Larsson PT, Wickholm K, Iversen T (1997) A CP/MAS ^{13}C NMR investigation of molecular ordering in celluloses. Carbohydr Res 302:19–25

Le Quéré B, Ghigo JM (2009) BcsQ is an essential component of the *Escherichia coli* cellulose biosynthesis apparatus that localizes at the bacterial cell pole. Mol Microbiol 72:724–740

Lin FC, Brown RM Jr, Drake RR Jr, Haley BE (1990) Identification of the uridine 5'--diphosphoglucose (UDP-Glc) binding subunit of cellulose synthase in *Acetobacter xylinum* using the photoaffinity probe 5-azido-UDP-Glc. J Biol Chem 265:4782–4784

Lindenberg S, Klauck G, Pesavento C, Klauck E, Hengge R (2013) The EAL domain protein YciR acts as a trigger enzyme in a c-di-GMP signalling cascade in *E. coli* biofilm control. EMBO J 32:2001–2014

Matthysse AG, Marry M, Krall L, Kaye M, Ramey BE, Fuqua C, White AR (2005) The effect of cellulose overproduction on binding and biofilm formation on roots by *Agrobacterium tumefaciens*. Mol Plant-Microbe Interact 18:1002–1010

Matthysse AG, Deora R, Mishra M, Torres AG (2008) Polysaccharides cellulose, poly-beta-1,6-n-acetyl-D-glucosamine, and colanic acid are required for optimal binding of *Escherichia coli* O157:H7 strains to alfalfa sprouts and K-12 strains to plastic but not for binding to epithelial cells. Appl Environ Microbiol 74:2384–2390

Mazeau K (2015) The hygroscopic power of amorphous cellulose: a modeling study. Carbohydr Polym 117:585–591

Mazur O, Zimmer J (2011) Apo- and cellopentaose-bound structures of the bacterial cellulose synthase subunit BcsZ. J Biol Chem 286:17601–17606

McManus JB, Deng Y, Nagachar N, Kao TH, Tien M (2016) AcsA-AcsB: the core of the cellulose synthase complex from *Gluconacetobacter hansenii* ATCC23769. Enzym Microb Technol 82:58–65

Mehta K, Pfeffer S, Malcolm Brown RJ (2015) Characterization of an *acsD* disruption mutant provides additional evidence for the hierarchical cell-directed self-assembly of cellulose in *Gluconacetobacter xylinus*. Cellulose 22:119–137

Morgan JL, Strumillo J, Zimmer J (2013) Crystallographic snapshot of cellulose synthesis and membrane translocation. Nature 493:181–186

Morgan JL, McNamara JT, Zimmer J (2014) Mechanism of activation of bacterial cellulose synthase by cyclic di-GMP. Nat Struct Mol Biol 21:489–496

Nakai T, Nishiyama Y, Kuga S, Sugano Y, Shoda M (2002) ORF2 gene involves in the construction of high-order structure of bacterial cellulose. Biochem Biophys Res Commun 295:458–462

Nobles DR, Romanovicz DK, Brown RM Jr (2001) Cellulose in cyanobacteria. Origin of vascular plant cellulose synthase? Plant Physiol 127:529–542

Omadjela O, Narahari A, Strumillo J, Melida H, Mazur O, Bulone V, Zimmer J (2013) BcsA and BcsB form the catalytically active core of bacterial cellulose synthase sufficient for in vitro cellulose synthesis. Proc Natl Acad Sci USA 110:17856–17861

Pang J, Liu X, Yang J, Lu F, Wang B, Xu F et al (2016) Synthesis of highly polymerized water-soluble cellulose acetate by the side reaction in carboxylate ionic liquid 1-ethyl-3-methylimidazolium acetate. Sci Rep 6:33725. https://doi.org/10.1038/srep33725

Paul R, Weiser S, Amiot NC, Chan C, Schirmer T, Giese B, Jenal U (2004) Cell cycle-dependent dynamic localization of a bacterial response regulator with a novel di-guanylate cyclase output domain. Genes Dev 18:715–727

Pontes MH, Lee EJ, Choi J, Groisman EA (2015) *Salmonella* promotes virulence by repressing cellulose production. Proc Natl Acad Sci USA 112:5183–5188

Povolotsky TL, Hengge R (2016) Genome-based comparison of cyclic di-GMP signaling in pathogenic and commensal *Escherichia coli* strains. J Bacteriol 198:111–126

Pritt B, O'Brien L, Winn W (2007) Mucoid *Pseudomonas* in cystic fibrosis. Am J Clin Pathol 128:32–34

Pultz IS, Christen M, Kulasekara HD, Kennard A, Kulasekara B, Miller SI (2012) The response threshold of *Salmonella* PilZ domain proteins is determined by their binding affinities for c-di-GMP. Mol Microbiol 86:1424–1440

Qi Y, Rao F, Luo Z, Liang ZX (2009) A flavin cofactor-binding PAS domain regulates c-di-GMP synthesis in AxDGC2 from *Acetobacter xylinum*. Biochemistry 48:10275–10285

Rajwade JM, Paknikar KM, Kumbhar JV (2015) Applications of bacterial cellulose and its composites in biomedicine. Appl Microbiol Biotechnol 99:2491–2511

Rao EV, Ramana KS (1991) Structural studies of a polysaccharide isolated from the green seaweed *Chaetomorpha anteninna*. Carbohydr Res 217:163–170

Richter AM, Povolotsky TL, Wieler LH, Hengge R (2014) Cyclic-di-GMP signalling and biofilm-related properties of the Shiga toxin-producing 2011 German outbreak *Escherichia coli* O104:H4. EMBO Mol Med 6:1622–1637

Romero D, Aguilar C, Losick R, Kolter R (2010) Amyloid fibers provide structural integrity to *Bacillus subtilis* biofilms. Proc Natl Acad Sci USA 107:2230–2234

Römling U (2005) Characterization of the rdar morphotype, a multicellular behaviour in Enterobacteriaceae. Cell Mol Life Sci 62:1234–1246

Römling U, Galperin MY (2015) Bacterial cellulose biosynthesis: diversity of operons, subunits, products, and functions. Trends Microbiol 23:545–557

Römling U, Rohde M, Olsen A, Normark S, Reinkoster J (2000) AgfD, the checkpoint of multicellular and aggregative behaviour in *Salmonella typhimurium* regulates at least two independent pathways. Mol Microbiol 36:10–23

Römling U, Galperin MY, Gomelsky M (2013) Cyclic di-GMP: the first 25 years of a universal bacterial second messenger. Microbiol Mol Biol Rev 77:1–52

Ross P, Weinhouse H, Aloni Y, Michaeli D, Weinberger-Ohana P, Mayer R et al (1987) Regulation of cellulose synthesis in *Acetobacter xylinum* by cyclic diguanylic acid. Nature 325:279–281

Ross P, Mayer R, Benziman M (1991) Cellulose biosynthesis and function in bacteria. Microbiol Rev 55:35–58

Sarenko O, Klauck G, Wilke FM, Pfiffer V, Richter AM, Herbst S et al (2017) More than enzymes that make or break cyclic di-GMP-local signaling in the interactome of GGDEF/EAL domain proteins of *Escherichia coli*. MBio 8. https://doi.org/10.1128/mBio.01639-17

Saxena IM, Kudlicka K, Okuda K, Brown RM Jr (1994) Characterization of genes in the cellulose-synthesizing operon (acs operon) of *Acetobacter xylinum*: implications for cellulose crystallization. J Bacteriol 176:5735–5752

Schirmer T (2016) C-di-GMP synthesis: structural aspects of evolution, catalysis and regulation. J Mol Biol 428:3683–3701

Schmidt AJ, Ryjenkov DA, Gomelsky M (2005) The ubiquitous protein domain EAL is a cyclic diguanylate-specific phosphodiesterase: enzymatically active and inactive EAL domains. J Bacteriol 187:4774–4781

Serra DO, Hengge R (2014) Stress responses go three dimensional – the spatial order of physiological differentiation in bacterial macrocolony biofilms. Environ Microbiol 16:1455–1471

Serra DO, Hengge R (2017) Experimental detection and visualization of the extracellular matrix in macrocolony biofilms. Methods Mol Biol 1657:133–145

Serra DO, Richter AM, Hengge R (2013a) Cellulose as an architectural element in spatially structured *Escherichia coli* biofilms. J Bacteriol 195:5540–5554

Serra DO, Richter AM, Klauck G, Mika F, Hengge R (2013b) Microanatomy at cellular resolution and spatial order of physiological differentiation in a bacterial biofilm. MBio 4:e00103–e00113. https://doi.org/10.1128/mBio.00103-13

Serra DO, Klauck G, Hengge R (2015) Vertical stratification of matrix production is essential for physical integrity and architecture of macrocolony biofilms of *Escherichia coli*. Environ Microbiol 17:5073–5088

Shaw RK, Lasa I, Garcia BM, Pallen MJ, Hinton JC, Berger CN, Frankel G (2011) Cellulose mediates attachment of *Salmonella enterica* serovar Typhimurium to tomatoes. Environ Microbiol Rep 3:569–573

Shibazaki H, Saito M, Kuga S, Okano T (1998) Native cellulose II production by *Acetobacter xylinum* under physical constraints. Cellulose 5:165–173

Shon AS, Bajwa RP, Russo TA (2013) Hypervirulent (hypermucoviscous) *Klebsiella pneumoniae*: a new and dangerous breed. Virulence 4:107–118

Simm R, Morr M, Kader A, Nimtz M, Römling U (2004) GGDEF and EAL domains inversely regulate cyclic di-GMP levels and transition from sessility to motility. Mol Microbiol 53:1123–1134

Singletary LA, Karlinsey JE, Libby SJ, Mooney JP, Lokken KL, Tsolis RM et al (2016) Loss of Multicellular Behavior in Epidemic African Nontyphoidal *Salmonella enterica* Serovar Typhimurium ST313 Strain D23580. MBio 7:e02265. https://doi.org/10.1128/mBio.02265-15

Smit G, Kijne JW, Lugtenberg BJ (1987) Involvement of both cellulose fibrils and a Ca2+-dependent adhesin in the attachment of *Rhizobium leguminosarum* to pea root hair tips. J Bacteriol 169:4294–4301

Solano C, Garcia B, Valle J, Berasain C, Ghigo JM, Gamazo C, Lasa I (2002) Genetic analysis of *Salmonella enteritidis* biofilm formation: critical role of cellulose. Mol Microbiol 43:793–808

Sommerfeldt N, Possling A, Becker G, Pesavento C, Tschowri N, Hengge R (2009) Gene expression patterns and differential input into curli fimbriae regulation of all GGDEF/EAL domain proteins in *Escherichia coli*. Microbiology 155:1318–1331

Stanisławska A (2016) Bacterial nanocellulose as a microbiological derived nanomaterial. Adv Mater Sci 16:45–57

Sun L, Vella P, Schnell R, Polyakova A, Bourenkov G, Li F et al (2018) Structural and functional characterization of the BcsG subunit of the cellulose synthase in *Salmonella typhimurium*. J Mol Biol 430:3170–3189

Sunagawa N, Fujiwara T, Yoda T, Kawano S, Satoh Y, Yao M et al (2013) Cellulose complementing factor (Ccp) is a new member of the cellulose synthase complex (terminal complex) in *Acetobacter xylinum*. J Biosci Bioeng 115:607–612

Sutherland IW (1970) Structural studies on colanic acid, the common exopolysaccharide found in the *Enterobacteriaceae*, by partial acid hydrolysis. Biochem J 115:935–945

Tahara N, Tonouchi N, Yano H, Yoshinaga F (1998) Purification and Characterization of Exo-1,4-b-Glucosidase from *Acetobacter xylinum* BPR2001. J Ferment Bioeng 85:589–594

Tal R, Wong HC, Calhoon R, Gelfand D, Fear AL, Volman G et al (1998) Three cdg operons control cellular turnover of cyclic di-GMP in *Acetobacter xylinum*: genetic organization and occurrence of conserved domains in isoenzymes. J Bacteriol 180:4416–4425

Thongsomboon W, Serra DO, Possling A, Hadjineophytou C, Hengge R, Cegelski L (2018) Phosphoethanolamine cellulose: a naturally produced chemically modified cellulose. Science 359:334–338

Tonouchi N, Tahara N, Kojima Y, Nakai T, Sakai F, Hayashi T et al (1997) A beta-glucosidase gene downstream of the cellulose synthase operon in cellulose-producing *Acetobacter*. Biosci Biotechnol Biochem 61:1789–1790

Toyosaki H, Naritomi T, Seto A, Matsuoka M, Tsuchida T, Yoshinaga F (1995) Screening of bacterial cellulose-producing *Acetobacter* strains suitable for agitated culture. Biosci Biotech Biochem 59:1498–1502

Visick KL, Quirke KP, McEwen SM (2013) Arabinose induces pellicle formation by *Vibrio fischeri*. Appl Environ Microbiol 79:2069–2080

Vitta S, Thiruvengadam V (2012) Multifunctional bacterial cellulose and nanoparticle-embedded composites. Curr Sci 102:1398–1405

Wang X, Rochon M, Lamprokostopoulou A, Lunsdorf H, Nimtz M, Römling U (2006) Impact of biofilm matrix components on interaction of commensal *Escherichia coli* with the gastrointestinal cell line HT-29. Cell Mol Life Sci 63:2352–2363

Weber H, Pesavento C, Possling A, Tischendorf G, Hengge R (2006) Cyclic-di-GMP-mediated signalling within the sigma network of *Escherichia coli*. Mol Microbiol 62:1014–1034

Whitney JC, Howell PL (2013) Synthase-dependent exopolysaccharide secretion in Gram-negative bacteria. Trends Microbiol 21:63–72

Williams WS, Cannon RE (1989) Alternative environmental roles for cellulose produced by *Acetobacter xylinum*. Appl Environ Microbiol 55:2448–2452

Wong HC, Fear AL, Calhoon RD, Eichinger GH, Mayer R, Amikam D et al (1990) Genetic organization of the cellulose synthase operon in *Acetobacter xylinum*. Proc Natl Acad Sci USA 87:8130–8134

Yamanaka S, Watanabe K, Kitamura N, Iguchi M, Mitsuhashi S, Nishi Y, Uryu M (1989) The structure and mechanical properties of sheets prepared from bacterial cellulose. J Mater Sci 24:3141–3145

Yan J, Nadell CD, Stone HA, Wingreen NS, Bassler BL (2017) Extracellular-matrix-mediated osmotic pressure drives *Vibrio cholerae* biofilm expansion and cheater exclusion. Nat Commun 8:327. https://doi.org/10.1038/s41467-017-00401-1

Yang L, Hengzhuang W, Wu H, Damkiaer S, Jochumsen N, Song Z et al (2012) Polysaccharides serve as scaffold of biofilms formed by mucoid *Pseudomonas aeruginosa*. FEMS Immunol Med Microbiol 65:366–376

Yaron S, Römling U (2014) Biofilm formation by enteric pathogens and its role in plant colonization and persistence. Microb Biotechnol 7:496–516

Yildiz FH, Schoolnik GK (1999) *Vibrio cholerae* O1 El Tor: identification of a gene cluster required for the rugose colony type, exopolysaccharide production, chlorine resistance, and biofilm formation. Proc Natl Acad Sci USA 96:4028–4033

Yip ES, Grublesky BT, Hussa EA, Visick KL (2005) A novel, conserved cluster of genes promotes symbiotic colonization and sigma-dependent biofilm formation by *Vibrio fischeri*. Mol Microbiol 57:1485–1498

Zogaj X, Nimtz M, Rohde M, Bokranz W, Römling U (2001) The multicellular morphotypes of *Salmonella typhimurium* and *Escherichia coli* produce cellulose as the second component of the extracellular matrix. Mol Microbiol 39:1452–1463

Zogaj X, Bokranz W, Nimtz M, Römling U (2003) Production of cellulose and curli fimbriae by members of the family *Enterobacteriaceae* isolated from the human gastrointestinal tract. Infect Immun 71:4151–4158

Chapter 9
Role of Glucan-Derived Polymers in the Pathogenic Fungus Candida albicans

Daniel Prieto, Elvira Román, Rebeca Alonso-Monge, and Jesús Pla

Abstract The cell wall is one of the most important structures to every fungi. *Candida albicans* is the most important fungal pathogen leading to superficial but also invasive infections which are frequently life-threatening. The *C. albicans* cell wall is composed of different polysaccharides, mainly mannan, chitin, and glucan. Glucans (β-(1,3) and β-(1,6)) differ in abundance among the different cellular morphologies (yeast or hypha) of this fungus but are essential to maintain the morphology of the cells and to provide protection against external injuries and as an anchoring scaffold to other components of the wall. In *C. albicans*, glucan is normally hidden in the inner wall layer, but it may be exposed in response to different environmental conditions and/or drug treatments. Glucans may play a role in biofilm formation and, most importantly, modulate immune recognition by phagocytes via the Dectin-1 receptor, therefore influencing the outcome of colonization and infection of this important pathogen.

9.1 Introduction

The fungus *Candida albicans* is member of the human microbiota, being a frequent colonizer of the vaginal and gastrointestinal tract of humans. Although it normally remains as a commensal microorganism, it can also cause infections in immunological-deficient individuals, leading to superficial infections and, in some cases, severe systemic diseases. *C. albicans* is therefore an opportunistic pathogen, and its behavior is dependent on several virulence factors such as secreted enzymes, metabolic traits, and signaling pathways (Navarro-García et al. 2001; Mayer et al. 2013). This microbe is able to display different morphologies, and it is therefore called a polymorphic yeast (Odds 1988) (Fig. 9.1). The most common situation under laboratory conditions is the yeast unicellular form (or blastospore), while

D. Prieto · E. Román · R. Alonso-Monge · J. Pla (✉)
Departamento de Microbiología y Parasitología, Universidad Complutense de Madrid, Madrid, Spain
e-mail: jpla@ucm.es

E. Cohen, H. Merzendorfer (eds.), *Extracellular Sugar-Based Biopolymers Matrices*, Biologically-Inspired Systems 12, https://doi.org/10.1007/978-3-030-12919-4_9

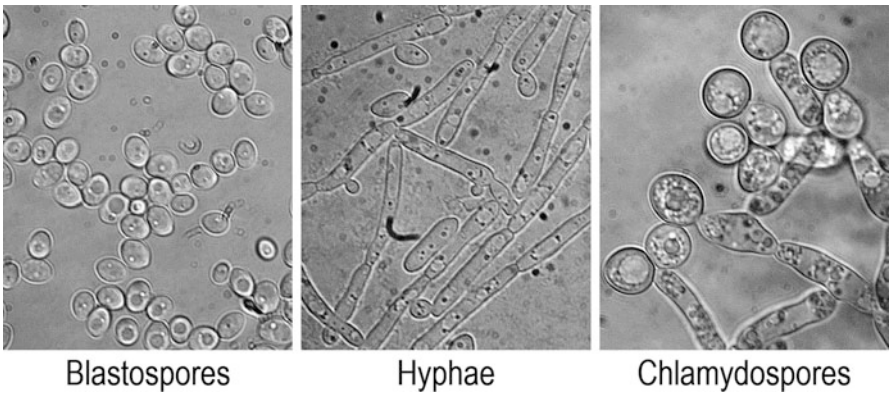

Fig. 9.1 *C. albicans* polymorphism
C. albicans is able to alternate among different morphologies. The blastospores display the characteristic unicellular budding yeast shape (left panel). Under certain conditions this fungus can develop germ tubes through bud elongation that end up forming hyphae (central panel) or pseudohyphae. Chlamydospores are large rounded cells with a dense cell wall that can be formed in the hyphae end (right panel)

within the host, it is frequently encountered as a hypha (or filament). This so-called dimorphic (or yeast-to-hypha) transition is environmentally regulated, and depending on the conditions, one form is favored over the other (Mitchell 1998; Liu 2001). The ability to switch between both morphologies has been related to virulence, since each morphology seems to play different functions during infection (Saville et al. 2003, 2008).

A most important feature of pathogenic fungi is the cell wall. Surviving in an always-changing environment (such as a mammalian host) requires this structure to be robust but also dynamic (Hall 2015). External stimuli trigger the reorganization of the wall via signal transduction pathways such as those that involve mitogen-activated protein kinase (MAPK) cascades. In *C. albicans,* this process is mainly dependent on the Mkc1- and Cek1-mediated pathways, which generates a transcriptional response that ultimately leads to adaptation to the new situation (Alonso-Monge et al. 2006; Ernst and Pla 2011). The cell wall acts as an effective barrier for different harms, protecting the cell against physical agents such as mechanical forces, desiccation, osmotic stress, UV radiation, or even temperature. It is also relevant against chemical mediators such as pH, reactive oxygen species (ROS), enzymes, immune mediators, or antimicrobial peptides.

In pathogenic fungi, however, the cell wall gains a special significance, as it is the first structure that the host detects (Arana et al. 2009; Gow and Hube 2012). It plays a critical role in adhesion to the host skin and mucosa, which is considered as the first step in colonization and infection; it also participates in the recognition by the innate immune cells, mainly phagocytes, and in evading the immune response and survival within the phagosome.

Microorganism recognition by the host is critical to develop a proper immune response against pathogens. The first step for this process is carried out by the innate

immune system that specifically recognizes some conserved microbial structures known as pathogen-associated molecular patterns (PAMPs), absent in the host cells. Importantly, these PAMPs are usually part of the polymers that conform the fungal cell wall (Jouault et al. 2009). The pattern recognition receptors (PRRs) interact with PAMPs and develop a signaling cascade in the cell in accordance with the stimuli, resulting in induction of immunological responses. Most of these PRRs are included in the Toll-like receptor (TLR), the C-type lectin receptor (CLR), or the NOD-like receptor (NLR) families (Erwig and Gow 2016). The transduction and integration of signals from different PRRs lead to a functional response after pathogen recognition. The most studied PRRs for recognizing fungi are TLR2, TLR4, TLR6, and TLR9; the CLRs Dectin-1, Dectin-2, mannose receptor (MR), and DC-SIGN; and the NLRs NOD2 and NLRP3 (Erwig and Gow 2016).

Given the role of the cell wall in the interaction with the host, the study of its composition, synthesis, and functional analysis is therefore of primary importance both in basic and applied (clinical) research. In this chapter, we will review some of the main features of glucan derived-polymers in *C. albicans*, focusing on their role in features relevant to pathogenicity.

9.2 The Fungal Cell Wall

The fungal cell wall is composed of both polysaccharide-derived polymers and cell wall proteins (CWPs), which are usually linked to skeletal polysaccharides (such as β-(1,6)-glucan; see later) via GPI remnants (glycosylphosphatidylinositol), but they are also able to bind directly to β-(1,3)-glucan due to the presence of internal repeats (named Pir CWP) (Richard and Plaine 2007). The function of these proteins includes the synthesis and remodeling of the cell wall, but they are also directly involved in adhesion and invasion of the host cells (Klis et al. 2009; Karkowska-Kuleta and Kozik 2015). Some species present also other minor – but interesting – components such as melanin-derived pigments formed by amorphous phenolic polymers (Butler and Day 1998) or lipid compounds such as phospholipomannan (PLM) (Trinel et al. 1993) which are linked among them by different types of chemical bonds.

Cell wall polysaccharides, essentially glucans, chitin, and mannans, are arranged forming a layered matrix (Chaffin 2008; Arana et al. 2009; Free 2013). These polymers, together with CWPs, are assembled and linked by different enzymes all along the cell wall after their export to the cell surface (Cabib and Arroyo 2013). The relative abundance of each component not only varies among different *Candida* species or even morphologies (Shibata et al. 2007; Lowman et al. 2014) but also in response to stress conditions and drugs (Latge and Beauvais 2014).

Chitin is a β-(1,4)-N-acetylglucosamine polymer. Although being very abundant in nature, it is a minor component of the wall representing only 1–6% of the dry mass of the wall in yeast cells. It is essential to form the deeper structural layer that acts as a robust scaffold for the rest of the components (Kollár et al. 1995). Chitin is essential in the formation of septum, bud scars, and the contractile ring between mother and bud cell during budding. Recent data suggest that this polymer, although

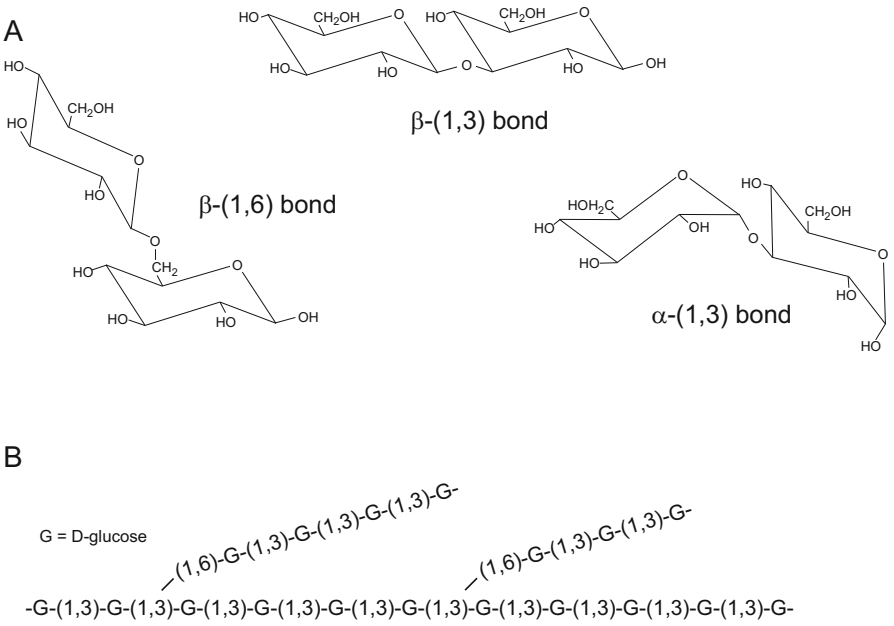

Fig. 9.2 Glucan polymer structure
(**a**) Fungal cell wall glucan polymers link D-glucose monomers mainly by β-(1,3), β-(1,6) and ∝-(1,3) bonds. (**b**) β-(1,3)-gl*u*can is composed by long linear fibers that might display branching chains connected by a β-(1,6) link

internal within the wall, has an important role in modulating the immune response of the host (Lenardon et al. 2010).

Mannans represent a 35–40% of the wall and consist of chains of mannose residues that are sequentially incorporated in CWPs in asparagine (N) or serine/threonine (O) residues (N- and O-glycosylation) (Chaffin 2008). This results in large chains of sugars with α-(1,2), α-(1,3), and α-(1,6)-mannoses (Free 2013), accounting up to 90% of the molecular mass of the CWPs.

Glucans are polymers of D-glucose monomers through β-(1,3), β-(1,4), β-(1,6), or α-(1,3) bonds (Fig. 9.2a) that account for ≈50–60% of the cell wall (Free 2013). Their role is more deeply discussed in the next sections.

9.3 β-(1,3)-Glucan

9.3.1 Cellular Function and Biosynthesis

The predominant type of glucan in the fungal cell wall is β-(1,3)-glucan. The β-(1,3) linkage forms linear fibers that are thought to be disposed forming helices with one or three strands (Laroche and Michaud 2007; Free 2013). However, some linear

β-(1,3) chains are linked through a β-(1,6) bond, generating a complex branched polymer (Klis et al. 2006; Lesage and Bussey 2006) (Fig. 9.2b). Making use of the appropriate extraction protocol, it is possible to detect two fractions of β-(1,3)-glucan in the cell wall: a high molecular mass one, linked to chitin, and an alkali soluble one (with a lower molecular mass) that would be involved in cell wall remodeling (Cabib et al. 2012). In *Aspergillus fumigatus* and *Neurospora crassa*, β-(1,4) bonds have been also detected within the β-(1,3)-glucan polymer (Fontaine et al. 2000; Maddi and Free 2010).

β-(1,3)-glucan is predominantly present in the inner layer of the cell wall, where it conforms the supporting base of the cell wall strength together with chitin (Arana et al. 2009; Orlean 2012). Therefore, β-(1,3)-glucan is usually hidden to the mammalian host cells, although some conditions may lead to an enhanced exposure of this polymer, with important consequences for immunity recognition (see below). Such conditions are alterations in certain genes related with cell wall remodeling (i.e., *PHR2*, *CEK1*, or *KRE5*), bud scars, physical treatments such as heating, drugs such as caspofungin, low pH, and some host environments during infection (Gantner et al. 2005; Wheeler and Fink 2006; Wheeler et al. 2008; Galan-Diez et al. 2010; Hopke et al. 2016; Sherrington et al. 2017).

β-(1,3)-Glucan synthesis is carried out by glucan synthases encoded by *FKS* genes. Even though there are three variants in this family (*FKS1*, *FKS2*, and *FKS3*), *FKS1* is the most important, being an essential gene in *C. albicans*. This transmembrane protein links glucose residues (from UDP-glucose) to the nonreducing terminal of a glucan chain through the reaction UDP-glucose + β-(1,3)-glucan (N) → UDP + β-(1,3)-glucan (N + 1). While elongating, the polymer is transported to the cell wall region. When needed, the activity of Fks1 can be increased over its basal capacity through the activation of the Rho1 GTPase, a member of the cell integrity MAPK pathway (Douglas et al. 1994; Frost et al. 1994; Mazur and Baginsky 1996; Free 2013).

Fks synthase activity is the target for the echinocandin antifungal family, now habitually used to treat fungal invasive diseases, that includes caspofungin, micafungin, and anidulafungin as representative compounds. These compounds are cyclic hexapeptides with a fatty acyl side chain that act as fungicidal agents in most fungi and are especially useful for treatment of invasive candidiasis (Douglas et al. 1997; Kurtz and Douglas 1997). Resistance mechanisms have arisen since the introduction of echinocandins in the clinical practice. *FKS1* mutation is the main form of resistance found in *C. albicans* (Garcia-Effron et al. 2009; Perlin 2011). Interestingly, this alteration leads to compensatory mechanisms increasing the chitin synthesis and an impairment in filamentation and vegetative growth (Ben-Ami et al. 2011). Enfumafungins, a new group of Fks inhibitors suitable for oral administration, are under study. These molecules seem to target a different part of the enzyme since they are still active in echinocandin-resistant isolates (Perlin 2011).

Some other enzymes, mainly transglycosylases, contribute to properly assemble and reconfigure the polymer in the cell wall. The Crh family includes enzymes that catalyze the link between chitin and β-(1,3) or β-(1,6)-glucan (Pardini et al. 2006; Cabib et al. 2007; Cabib 2009). There are five genes in the *PHR* family (called *GAS* in

S. cerevisiae). They encode glucan transglycosylases, also called β-(1,3)-glucan elongases, that hydrolyze and transfer small β-(1,3)-glucan chains to other parts of the polymer (Popolo et al. 2017). Moreover, they also generate ramifications in this polymer through catalyzing a β-(1,6) link (Fonzi 1999; Aimanianda et al. 2017). Interestingly, *PHR1* and *PHR2* are regulated in a pH-dependent manner through the Rim101 transcription factor. Relatively alkaline environments (pH = 7–8) promote the expression of *PHR1*, while *PHR2* is only expressed at pH < 7 (Saporito-Irwin et al. 1995; Muhlschlegel and Fonzi 1997). β-(1,6) ramifications are also performed by the endo-β-(1,3)-glucanase Bgl2 (Mrsa et al. 1993; Goldman et al. 1995). Regarding the particular links found in other fungi, it has been identified the transglycosylase Tft1 as the enzyme responsible in *A. fumigatus* for performing the specific β-(1,4) bond that appears within the β-(1,3)-glucan polymer (Samar et al. 2015).

9.3.2 Relevance During Host Interaction

β-(1,3)-glucan is involved in different important biological aspects such as the modulation of the host immune response and the development of biofilms; in fact it is considered a crucial PAMP in *C. albicans*. This was somehow unexpected some time ago, since β-(1,3)-glucan is usually masked by the rest of the cell wall components. The CLR Dectin-1 is responsible for the specific recognition of β-(1,3)-glucan (Brown and Gordon 2001). Through this interaction, Dectin-1 mediates phagocytosis of *C. albicans* cells and induces an antimicrobial pro-inflammatory response (Brown et al. 2003; Brown and Gordon 2005). In phagocytes, Dectin-1 activation is transmitted through the MAPK NF-kB pathway, triggering the production of pro-inflammatory cytokines such as TNFα, although in some cases it seems to require the contribution of TLR2 (Brown et al. 2003; Gantner et al. 2003). The recognition of the β-(1,3)-glucan is possible when the polymer is unmasked in the cell wall. All the known treatments (or genetic alterations) that enhance the exposure of β-(1,3)-glucan favor its recognition via Dectin-1. It has been proposed that, since this polymer is unmasked in bud scars, Dectin-1 recognize in vitro *C. albicans* yeast morphology more easily than hyphae, since germ tube elongation lacks these structures (Gantner et al. 2005). However, this is not necessarily the case in vivo, as certain infection conditions, or even just phagocytosis, actually favor the exposure of β-(1,3)-glucan also in filaments (Wheeler et al. 2008; Hopke et al. 2016). Therefore, under certain conditions, both *C. albicans* morphologies would expose enough β-(1,3)-glucan to interact with PRRs from the host. Interestingly, it has been reported that phagocytes are able to distinguish β-(1,3)-glucan derived from yeast or from hyphae. In this way, they activate the NLRP3 inflammasome system, responsible for the activation of the inflammation mediator IL-1β, only when the β-(1,3)-glucan detected by Dectin-1 is produced by hyphae (Joly et al. 2009; Cheng et al. 2011). It has been proposed that this occurs due to a differential chemical structure in the β-(1,3)-glucan, that displays a peculiar circular structure (Lowman et al. 2014).

Dectin-1-mediated β-(1,3)-glucan recognition also affects the adaptive immune response. This response partially relies on dendritic cells (DCs) that sense and phagocyte microorganisms and antigens initiating a consequent antigen-dependent immune response. After interaction with *C. albicans*, DCs drive CD4+ T cells to a mainly protective Th17 response via secretion of the IL-23, IL-1β, and IL-6 cytokines. The recognition of the hyphal β-(1,3)-glucan through Dectin-1 is necessary, and enough in some conditions, to trigger this specific protective response (Leibundgut-Landmann et al. 2007; Cheng et al. 2011).

Last, but not less important, Dectin-1 is involved in the control of fungal populations colonizing the gastrointestinal mucosa needed for preventing *C. albicans* invasion in a mouse model of intestinal inflammation (colitis) (Iliev et al. 2012). Moreover, this reduction of *Candida* translocation implies a decrease in the grade of inflammation and, therefore, in the colitis severity. As the gut is the most important pool for disseminated candidiasis, this finding has crucial consequences for the possible control of risk factors in immune-deficient patients.

The other feature where glucan seems to be, either directly or indirectly involved, is biofilm formation. The formation of biofilms on solid surfaces allows fungi to grow in a particular environment where cells interact more as a community than as simply individuals (Fig. 9.3). This state is certainly most prevalent in natural ecosystems than the planktonic cultures traditionally used in the laboratory to study fungi biology. The complex extracellular matrix (ECM) of biofilms is a three-dimensional structure that protects cells from external harms, including toxic compounds (antifungals or ROS) or phagocytes; it is also a source of nutrients and favors adhesion (Mitchell et al. 2016). The composition of the ECM shares normally several components with the fungal cell wall (Fig. 9.3). However, it is assumed that polysaccharide polymers suffer further modifications in the periplasmic space once they are released from the cells (Zarnowski et al. 2014).

In *C. albicans* biofilms, ECM, there are glucans, chitin, mannan, DNA (especially noncoding), and proteins, some of them presumed to be only cytosolic. The amount of each component depends on the kind of biofilm and the surrounding context, making really challenging the approaches for its analyses. Different biofilm models

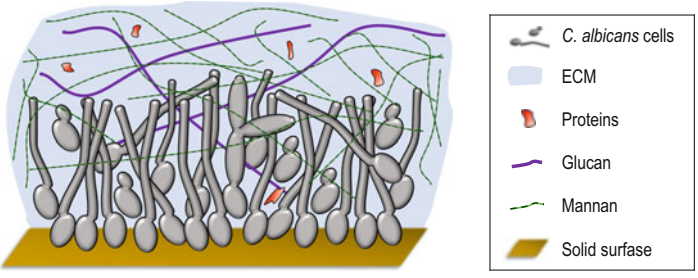

Fig. 9.3 *C. albicans* biofilm
C. albicans form submerged biofilms on solid surfaces such us catheters or mucosa. A mature stage display different cell morphologies and a prominent ECM structure that is composed mainly by glucan and mannan polymers. Proteins in the ECM contribute to the polymers assembling

have been used, showing diverse results depending on experimental conditions (Hawser et al. 1998; Nett et al. 2010a; Zarnowski et al. 2014).

The contribution of β-(1,3)-glucan to biofilms is still controversial. It has been commonly considered as one of the main components in the *C. albicans* ECM, being responsible for biofilm antifungal resistance through antifungal sequestration (Nett et al. 2007, 2010b). In fact, β-(1,3)-glucanases have been suggested as anti-biofilm agents (Tan et al. 2018). However, a recent work using a novel biochemical and nuclear magnetic resonance analysis reports an almost absence of this polymer in the ECM although drug sequestration was still observed (Zarnowski et al. 2014). Nevertheless, caution must be taken about data from mono-species biofilms and/or experiments performed strictly in vitro. Biofilm characteristics and complexity seem to change importantly when more accurate approaches such as polymicrobial or animal models are addressed (Peters et al. 2012; Nett et al. 2015). For instance, in a rat model of vascular implanted catheter, the contribution of the host to the ECM represents more than 98% of the protean fraction (Nett et al. 2015).

Since PAMPs are molecules that are absent in the host, they can be a good diagnostic marker. Detection of β-(1,3)-glucan in serum is used in the clinical practice for the diagnosis of a probable invasive fungal disease (IFD), especially in risk populations, even before symptoms are present (De Pauw et al. 2008; Mikulska et al. 2015). Since β-(1,3)-glucan is present in most fungi, its detection helps to presume a IFD from a wide range of fungal pathogens, and therefore it does not indicate the ethiologic agent. However, this kind of tests may suffer from lack of enough sensitivity and specificity (Mikulska et al. 2015).

9.4 β-(1,6)-Glucan

β-(1,6)-Glucan is an important polymer commonly found in the fungal cell walls (Aimanianda et al. 2009; Free 2013) although it is not present in some taxons (e.g., *A. fumigatus* and *N. crassa*). This highly branched polymer is distributed throughout the cell wall, linking covalently the rest of the components, i.e., chitin, β-(1,3)-glucan, and GPI mannan-CWPs (Kapteyn et al. 1996; Kollar et al. 1997). Therefore, it contributes to interconnect and organize the three-dimensional network that configures the cell wall.

Some genes have been described as relevant for the synthesis of β-(1,6)-glucan, frequently displaying redundant activities, although no catalytic activity has been yet proved (Orlean 2012). *KRE* genes have been identified as their mutations frequently lead to resistance to certain killer toxins (KT). Since β-(1,6)-glucan is the primary receptor for most of these toxins, reduction of its abundance in *kre* mutants' cell wall decreases KT interaction. Kre6 and Skn1 are thought to be redundant β-(1,6)-glucan synthases (Roemer and Bussey 1991; Roemer et al. 1993); however, this possibility is still controversial (Aimanianda et al. 2009; Kurita et al. 2011). Kre5 is one of the most critical proteins involved in β-(1,6)-glucan synthesis, although via an indirect mechanism such as GPI glycosylation of CWPs (Shahinian et al. 1998; Herrero et al.

2004; Aimanianda et al. 2009). Kre1 is a GPI-CWP that would cross-link β-(1,6)-glucan chains, therefore elongating the polymer (Boone et al. 1990; Boone et al. 1991). *KRE9* and *KNH1* are redundant enzymes present in the cell wall that are thought to cross-link the β-1,6-glucan polymer (Lesage and Bussey 2006).

In contrast to β-(1,3)-glucan, this glucan polymers does not seem to be directly recognized by PRRs, although it may contribute or interfere with the immune response. β-(1,6)-glucan appears to participate in the phagocytosis of *C. albicans* by neutrophils; in this case, the polymer is bound by the host complement protein C3d, contributing to the opsonization of the pathogen (Rubin-Bejerano et al. 2007). β-(1,6)-Glucan is also an important component of *C. albicans* biofilms. Some authors have reported that it is in fact the main glucan in the ECM, representing 13% of the total polysaccharide polymers forming a mannan-glucan complex (MGCx) (Zarnowski et al. 2014).

9.5 α-(1,3)-Glucan

Although *S. cerevisiae* and *C. albicans* lack α-(1,3)-glucan, several species present this polymer in the external cell wall layers. The α-(1,3)-glucan polymer is produced by Ags1, a α-(1,3)-glucan synthase, similar to the β-(1,3)-glucan synthase. However, in *N. crassa*, Ags1 seems to present an additional transglucanase activity in the N-terminal extracellular domain; therefore, it would not only contribute to the synthesis but also to the assembly of the produced chains (Fu et al. 2014). In *Histoplasma capsulatum*, Amy1 (an α-(1,4)-amylase) is also essential for α-(1,3)-glucan synthesis (Marion et al. 2006).

Depending on the species, α-(1,3)-glucan seems to play quite diverse functions. In *N. crassa* it has been detected just in the cell wall from the conidia (Fu et al. 2014). In *H. capsulatum* yeast cells, α-(1,3)-glucan seems to configure the outer layer, preventing the exposition of β-(1,3)-glucan and impairing a Dectin-1-mediated phagocytosis and proinflammatory interleukin response (Kanetsuna et al. 1974; Rappleye et al. 2007). Mutant strains of *A. fumigatus* with reduced amounts of α-(1,3)-glucan display higher virulence than their isogenic controls (Maubon et al. 2006). This polymer is also essential to maintain the capsule of *Cryptococcus neoformans* attached to the cell wall (Reese et al. 2007).

9.6 Concluding Remarks

Fungi, compared to other microbes, have evolved to synthesize glucan and depend on its presence in their walls. Although their amount can be partially compensated by other polymers such as chitin (so-called compensatory mechanism), their existence is an absolute requirement for many fungi to provide the necessary strength that allows growth in non-osmotically protected environments. This role is of primary

importance in pathogenic fungi such as *C. albicans*. The relatively limited amount of available antifungals and the emergence of resistance to some of them may compromise antifungal therapies in the near future. In addition, glucans are important mediators of the immune response of the host, not only as a primary antigen but also as a scaffold to other proteins that interact with the host cells. Understanding the biogenesis and function of glucans in fungal pathogens is therefore essential to develop new drugs and therapeutic approaches to their eradication.

References

Aimanianda V, Clavaud C, Simenel C, Fontaine T, Delepierre M, Latge JP (2009) Cell wall beta-(1,6)-glucan of *Saccharomyces cerevisiae*: structural characterization and *in situ* synthesis. J Biol Chem 284:13401–13412

Aimanianda V, Simenel C, Garnaud C, Clavaud C, Tada R, Barbin L, Mouyna I, Heddergott C, Popolo L, Ohya Y, Delepierre M, Latge JP (2017) The dual activity responsible for the elongation and branching of beta-(1,3)-glucan in the fungal cell wall. MBio 8(3). https://doi.org/10.1128/mBio.00619-17

Alonso-Monge R, Román E, Nombela C, Pla J (2006) The MAP kinase signal transduction network in *Candida albicans*. Microbiology 152:905–912

Arana DM, Prieto D, Román E, Nombela C, Alonso-Monge R, Pla J (2009) The role of the cell wall in fungal pathogenesis. Microb Biotechnol 2:308–320

Ben-Ami R, Garcia-Effron G, Lewis RE, Gamarra S, Leventakos K, Perlin DS, Kontoyiannis DP (2011) Fitness and virulence costs of *Candida albicans FKS1* hot spot mutations associated with echinocandin resistance. J Infect Dis 204:626–635

Boone C, Sommer SS, Hensel A, Bussey H (1990) Yeast *KRE* genes provide evidence for a pathway of cell wall beta-glucan assembly. J Cell Biol 110:1833–1843

Boone C, Sdicu A, Laroche M, Bussey H (1991) Isolation from *Candida albicans* of a functional homolog of the *Saccharomyces cerevisiae KRE1* gene, which is involved in cell wall beta-glucan synthesis. J Bacteriol 173:6859–6864

Brown GD, Gordon S (2001) Immune recognition. A new receptor for beta-glucans. Nature 413:36–37

Brown GD, Gordon S (2005) Immune recognition of fungal beta-glucans. Cell Microbiol 7:471–479

Brown GD, Herre J, Williams DL, Willment JA, Marshall AS, Gordon S (2003) Dectin-1 mediates the biological effects of beta-glucans. J Exp Med 197:1119–1124

Butler M, Day A (1998) Fungal melanins: a review. Can J Microbiol 44:1115–1136

Cabib E (2009) Two novel techniques for determination of polysaccharide cross-links show that Crh1p and Crh2p attach chitin to both beta(1-6)- and beta(1-3)glucan in the *Saccharomyces cerevisiae* cell wall. Eukaryot Cell 8:1626–1636

Cabib E, Arroyo J (2013) How carbohydrates sculpt cells: chemical control of morphogenesis in the yeast cell wall. Nat Rev Microbiol 11:648–655

Cabib E, Blanco N, Grau C, Rodriguez-Pena JM, Arroyo J (2007) Crh1p and Crh2p are required for the cross-linking of chitin to beta(1-6)glucan in the *Saccharomyces cerevisiae* cell wall. Mol Microbiol 63:921–935

Cabib E, Blanco N, Arroyo J (2012) Presence of a large beta(1-3)glucan linked to chitin at the *Saccharomyces cerevisiae* mother-bud neck suggests involvement in localized growth control. Eukaryot Cell 11:388–400

Chaffin WL (2008) *Candida albicans* cell wall proteins. Microbiol Mol Biol Rev 72:495–544

Cheng SC, van de Veerdonk FL, Lenardon M, Stoffels M, Plantinga T, Smeekens S, Rizzetto L, Mukaremera L, Preechasuth K, Cavalieri D, Kanneganti TD, Van der Meer JW, Kullberg BJ, Joosten LA, Gow NA, Netea MG (2011) The dectin-1/inflammasome pathway is responsible for the induction of protective T-helper 17 responses that discriminate between yeasts and hyphae of *Candida albicans*. J Leukoc Biol 90:357–366

De Pauw B, Walsh TJ, Donnelly JP, Stevens DA, Edwards JE, Calandra T, Pappas PG, Maertens J, Lortholary O, Kauffman CA, Denning DW, Patterson TF, Maschmeyer G, Bille J, Dismukes WE, Herbrecht R, Hope WW, Kibbler CC, Kullberg BJ, Marr KA, Munoz P, Odds FC, Perfect JR, Restrepo A, Ruhnke M, Segal BH, Sobel JD, Sorrell TC, Viscoli C, Wingard JR, Zaoutis T, Bennett JE, European Organization for R, Treatment of Cancer/Invasive Fungal Infections Cooperative G, National Institute of A, Infectious Diseases Mycoses Study Group Consensus G (2008) Revised definitions of invasive fungal disease from the European Organization for Research and Treatment of Cancer/Invasive Fungal Infections Cooperative Group and the National Institute of Allergy and Infectious Diseases Mycoses Study Group (EORTC/MSG) Consensus Group. Clin Infect Dis 46:1813–1821

Douglas CM, Foor F, Marrinan JA, Morin N, Nielsen JB, Dahl AM, Mazur P, Baginsky W, Li W, el-Sherbeini M (1994) The *Saccharomyces cerevisiae FKS1* (*ETG1*) gene encodes an integral membrane protein which is a subunit of 1,3-beta-D-glucan synthase. Proc Natl Acad Sci U S A 91:12907–12911

Douglas CM, D'Ippolito JA, Shei GJ, Meinz M, Onishi J, Marrinan JA, Li W, Abruzzo GK, Flattery A, Bartizal K, Mitchell A, Kurtz MB (1997) Identification of the *FKS1* gene of *Candida albicans* as the essential target of 1,3-beta-D-glucan synthase inhibitors. Antimicrob Agents Chemother 41:2471–2479

Ernst JF, Pla J (2011) Signaling the glycoshield: maintenance of the *Candida albicans* cell wall. Int J Med Microbiol 301:378–383

Erwig LP, Gow NA (2016) Interactions of fungal pathogens with phagocytes. Nat Rev Microbiol 14:163–176

Fontaine T, Simenel C, Dubreucq G, Adam O, Delepierre M, Lemoine J, Vorgias CE, Diaquin M, Latge JP (2000) Molecular organization of the alkali-insoluble fraction of *Aspergillus fumigatus* cell wall. J Biol Chem 275:27594–27607

Fonzi WA (1999) *PHR1* and *PHR2* of *Candida albicans* encode putative glycosidases required for proper cross-linking of beta-1,3- and beta-1,6-glucans. J Bacteriol 181:7070–7079

Free SJ (2013) Fungal cell wall organization and biosynthesis. Adv Genet 81:33–82

Frost DJ, Brandt K, Capobianco J, Goldman R (1994) Characterization of (1,3)-beta-glucan synthase in *Candida albicans*: microsomal assay from the yeast or mycelial morphological forms and a permeabilized whole-cell assay. Microbiology 140:2239–2246

Fu C, Tanaka A, Free SJ (2014) *Neurospora crassa* 1,3-alpha-glucan synthase, AGS-1, is required for cell wall biosynthesis during macroconidia development. Microbiology 160:1618–1627

Galan-Diez M, Arana DM, Serrano-Gomez D, Kremer L, Casasnovas JM, Ortega M, Cuesta-Dominguez A, Corbi AL, Pla J, Fernandez-Ruiz E (2010) *Candida albicans* beta-glucan exposure is controlled by the fungal *CEK1*-mediated mitogen-activated protein kinase pathway that modulates immune responses triggered through dectin-1. Infect Immun 78:1426–1436

Gantner BN, Simmons RM, Canavera SJ, Akira S, Underhill DM (2003) Collaborative induction of inflammatory responses by dectin-1 and Toll-like receptor 2. J Exp Med 197:1107–1117

Gantner BN, Simmons RM, Underhill DM (2005) Dectin-1 mediates macrophage recognition of *Candida albicans* yeast but not filaments. EMBO J 24:1277–1286

Garcia-Effron G, Park S, Perlin DS (2009) Correlating echinocandin MIC and kinetic inhibition of *fks1* mutant glucan synthases for *Candida albicans*: implications for interpretive breakpoints. Antimicrob Agents Chemother 53:112–122

Goldman RC, Sullivan PA, Zakula D, Capobianco JO (1995) Kinetics of beta-1,3 glucan interaction at the donor and acceptor sites of the fungal glucosyltransferase encoded by the *BGL2* gene. Eur J Biochem 227:372–378

Gow NA, Hube B (2012) Importance of the *Candida albicans* cell wall during commensalism and infection. Curr Opin Microbiol 15:406–412

Hall RA (2015) Dressed to impress: impact of environmental adaptation on the *Candida albicans* cell wall. Mol Microbiol 97:7–17

Hawser SP, Baillie GS, Douglas LJ (1998) Production of extracellular matrix by *Candida albicans* biofilms. J Med Microbiol 47:253–256

Herrero AB, Magnelli P, Mansour MK, Levitz SM, Bussey H, Abeijon C (2004) *KRE5* gene null mutant strains of *Candida albicans* are avirulent and have altered cell wall composition and hypha formation properties. Eukaryot Cell 3:1423–1432

Hopke A, Nicke N, Hidu EE, Degani G, Popolo L, Wheeler RT (2016) Neutrophil attack triggers extracellular trap-dependent *Candida* cell wall remodeling and altered immune recognition. PLoS Pathog 12(5):e1005644

Iliev ID, Funari VA, Taylor KD, Nguyen Q, Reyes CN, Strom SP, Brown J, Becker CA, Fleshner PR, Dubinsky M, Rotter JI, Wang HL, McGovern DP, Brown GD, Underhill DM (2012) Interactions between commensal fungi and the C-type lectin receptor Dectin-1 influence colitis. Science 336:1314–1317

Joly S, Ma N, Sadler JJ, Soll DR, Cassel SL, Sutterwala FS (2009) *Candida albicans* hyphae formation triggers activation of the Nlrp3 inflammasome. J Immunol 183:3578–3581

Jouault T, Sarazin A, Martinez-Esparza M, Fradin C, Sendid B, Poulain D (2009) Host responses to a versatile commensal: PAMPs and PRRs interplay leading to tolerance or infection by *Candida albicans*. Cell Microbiol 11:1007–1015

Kanetsuna F, Carbonell LM, Gil F, Azuma I (1974) Chemical and ultrastructural studies on the cell walls of the yeast-like and mycelial forms of *Histoplasma capsulatum*. Mycopathol Mycol Appl 54:1–13

Kapteyn JC, Montijn RC, Vink E, de la Cruz J, Llobell A, Douwes JE, Shimoi H, Lipke PN, Klis FM (1996) Retention of *Saccharomyces cerevisiae* cell wall proteins through a phosphodiester-linked beta-1,3−/beta-1,6-glucan heteropolymer. Glycobiology 6:337–345

Karkowska-Kuleta J, Kozik A (2015) Cell wall proteome of pathogenic fungi. Acta Biochim Pol 62:339–351

Klis FM, Boorsma A, de Groot PW (2006) Cell wall construction in *Saccharomyces cerevisiae*. Yeast 23:185–202

Klis FM, Sosinska GJ, de Groot PW, Brul S (2009) Covalently linked cell wall proteins of *Candida albicans* and their role in fitness and virulence. FEMS Yeast Res 9:1013–1028

Kollár R, Petráková E, Ashwell G, Robbins PW, Cabib E (1995) Architecture of the yeast cell wall: the linkage between chitin and ß (1-3)-glucan. J Biol Chem 3:1170–1178

Kollar R, Reinhold BB, Petrakova E, Yeh HJ, Ashwell G, Drgonova J, Kapteyn JC, Klis FM, Cabib E (1997) Architecture of the yeast cell wall. Beta(1–>6)-glucan interconnects mannoprotein, beta(1–>)3-glucan, and chitin. J Biol Chem 272:17762–17775

Kurita T, Noda Y, Takagi T, Osumi M, Yoda K (2011) Kre6 protein essential for yeast cell wall beta-1,6-glucan synthesis accumulates at sites of polarized growth. J Biol Chem 286:7429–7438

Kurtz MB, Douglas CM (1997) Lipopeptide inhibitors of fungal glucan synthase. J Med Vet Mycol 35:79–86

Laroche C, Michaud P (2007) New developments and prospective applications for beta (1,3) glucans. Recent Pat Biotechnol 1:59–73

Latge JP, Beauvais A (2014) Functional duality of the cell wall. Curr Opin Microbiol 20:111–117

Leibundgut-Landmann S, Gross O, Robinson MJ, Osorio F, Slack EC, Tsoni SV, Schweighoffer E, Tybulewicz V, Brown GD, Ruland J, Reis e S (2007) Syk- and CARD9-dependent coupling of innate immunity to the induction of T helper cells that produce interleukin 17. Nat Immunol 8:630–638

Lenardon MD, Munro CA, Gow NA (2010) Chitin synthesis and fungal pathogenesis. Curr Opin Microbiol 13:416–423

Lesage G, Bussey H (2006) Cell wall assembly in *Saccharomyces cerevisiae*. Microbiol Mol Biol Rev 70:317–343

Liu H (2001) Transcriptional control of dimorphism in *Candida albicans*. Curr Opin Microbiol 4:728–735

Lowman DW, Greene RR, Bearden DW, Kruppa MD, Pottier M, Monteiro MA, Soldatov DV, Ensley HE, Cheng SC, Netea MG, Williams DL (2014) Novel structural features in *Candida albicans* hyphal glucan provide a basis for differential innate immune recognition of hyphae versus yeast. J Biol Chem 289:3432–3443

Maddi A, Free SJ (2010) alpha-1,6-Mannosylation of N-linked oligosaccharide present on cell wall proteins is required for their incorporation into the cell wall in the filamentous fungus *Neurospora crassa*. Eukaryot Cell 9:1766–1775

Marion CL, Rappleye CA, Engle JT, Goldman WE (2006) An alpha-(1,4)-amylase is essential for alpha-(1,3)-glucan production and virulence in *Histoplasma capsulatum*. Mol Microbiol 62:970–983

Maubon D, Park S, Tanguy M, Huerre M, Schmitt C, Prevost MC, Perlin DS, Latge JP, Beauvais A (2006) AGS3, an alpha(1-3)glucan synthase gene family member of *Aspergillus fumigatus*, modulates mycelium growth in the lung of experimentally infected mice. Fungal Genet Biol 43:366–375

Mayer FL, Wilson D, Hube B (2013) *Candida albicans* pathogenicity mechanisms. Virulence 4:119–128

Mazur P, Baginsky W (1996) *In vitro* activity of 1,3-beta-D-glucan synthase requires the GTP-binding protein Rho1. J Biol Chem 271:14604–14609

Mikulska M, Furfaro E, Viscoli C (2015) Non-cultural methods for the diagnosis of invasive fungal disease. Expert Rev Anti-Infect Ther 13:103–117

Mitchell AP (1998) Dimorphism and virulence in *Candida albicans*. Curr Opin Microbiol 1:687–692

Mitchell KF, Zarnowski R, Andes DR (2016) Fungal Super Glue: The Biofilm Matrix and Its Composition, Assembly, and Functions. PLoS Pathog 12(9):e1005828

Mrsa V, Klebl F, Tanner W (1993) Purification and characterization of the *Saccharomyces cerevisiae BGL2* gene product, a cell wall endo-ß-1,3-glucanase. J Bacteriol 175:2102–2106

Muhlschlegel FA, Fonzi WA (1997) *PHR2* of *Candida albicans* encodes a functional homolog of the pH-regulated gene *PHR1* with an inverted pattern of pH-dependent expression. Mol Cell Biol 17:5960–5967

Navarro-García F, Sánchez M, Nombela C, Pla J (2001) Virulence genes in the pathogenic yeast *Candida albicans*. FEMS Microbiol Rev 25:245–268

Nett J, Lincoln L, Marchillo K, Massey R, Holoyda K, Hoff B, VanHandel M, Andes D (2007) Putative role of beta-1,3 glucans in *Candida albicans* biofilm resistance. Antimicrob Agents Chemother 51:510–520

Nett JE, Crawford K, Marchillo K, Andes DR (2010a) Role of Fks1p and matrix glucan in *Candida albicans* biofilm resistance to an echinocandin, pyrimidine, and polyene. Antimicrob Agents Chemother 54:3505–3508

Nett JE, Sanchez H, Cain MT, Andes DR (2010b) Genetic basis of *Candida* biofilm resistance due to drug-sequestering matrix glucan. J Infect Dis 202:171–175

Nett JE, Zarnowski R, Cabezas-Olcoz J, Brooks EG, Bernhardt J, Marchillo K, Mosher DF, Andes DR (2015) Host contributions to construction of three device-associated *Candida albicans* biofilms. Infect Immun 83:4630–4638

Odds FC (1988) *Candida* and candidosis, vol 2. Baillière Tindall, London

Orlean P (2012) Architecture and biosynthesis of the *Saccharomyces cerevisiae* cell wall. Genetics 192:775–818

Pardini G, de Groot PW, Coste AT, Karababa M, Klis FM, de Koster CG, Sanglard D (2006) The *CRH* family coding for cell wall glycosylphosphatidylinositol proteins with a predicted transglycosidase domain affects cell wall organization and virulence of *Candida albicans*. J Biol Chem 281:40399–40411

Perlin DS (2011) Current perspectives on echinocandin class drugs. Future Microbiol 6:441–457
Peters BM, Jabra-Rizk MA, O'May GA, Costerton JW, Shirtliff ME (2012) Polymicrobial interactions: impact on pathogenesis and human disease. Clin Microbiol Rev 25(1):193–213
Popolo L, Degani G, Camilloni C, Fonzi WA (2017) The *PHR* family: The role of extracellular transglycosylases in shaping *Candida albicans* cells. J Fungi (Basel) 3(4). https://doi.org/10.3390/jof3040059
Rappleye CA, Eissenberg LG, Goldman WE (2007) *Histoplasma capsulatum* alpha-(1,3)-glucan blocks innate immune recognition by the beta-glucan receptor. Proc Natl Acad Sci USA 104:1366–1370
Reese AJ, Yoneda A, Breger JA, Beauvais A, Liu H, Griffith CL, Bose I, Kim MJ, Skau C, Yang S, Sefko JA, Osumi M, Latge JP, Mylonakis E, Doering TL (2007) Loss of cell wall alpha(1-3) glucan affects *Cryptococcus neoformans* from ultrastructure to virulence. Mol Microbiol 63:1385–1398
Richard ML, Plaine A (2007) Comprehensive analysis of glycosylphosphatidylinositol-anchored proteins in *Candida albicans*. Eukaryot Cell 6:119–133
Roemer T, Bussey H (1991) Yeast beta-glucan synthesis: *KRE6* encodes a predicted type II membrane protein required for glucan synthesis *in vivo* and for glucan synthase activity *in vitro*. Proc Natl Acad Sci USA 88:11295–11299
Roemer T, Delaney S, Bussey H (1993) *SKN1* and *KRE6* define a pair of functional homologs encoding putative membrane proteins involved in beta-glucan synthesis. Mol Cell Biol 13:4039–4048
Rubin-Bejerano I, Abeijon C, Magnelli P, Grisafi P, Fink GR (2007) Phagocytosis by human neutrophils is stimulated by a unique fungal cell wall component. Cell Host Microbe 2:55–67
Samar D, Kieler JB, Klutts JS (2015) Identification and deletion of Tft1, a predicted glycosyltransferase necessary for cell wall beta-1,3;1,4-glucan synthesis in *Aspergillus fumigatus*. PLoS One 10(2):e0117336
Saporito-Irwin SM, Birse CE, Sypherd PS, Fonzi WA (1995) *PHR1*, a pH-regulated gene of *Candida albicans*, is required for morphogenesis. Mol Cell Biol 15:601–613
Saville SP, Lazzell AL, Monteagudo C, Lopez-Ribot JL (2003) Engineered control of cell morphology *in vivo* reveals distinct roles for yeast and filamentous forms of *Candida albicans* during infection. Eukaryot Cell 2:1053–1060
Saville SP, Lazzell AL, Chaturvedi AK, Monteagudo C, Lopez-Ribot JL (2008) Use of a genetically engineered strain to evaluate the pathogenic potential of yeast cell and filamentous forms during *Candida albicans* systemic infection in immunodeficient mice. Infect Immun 76:97–102
Shahinian S, Dijkgraaf GJ, Sdicu AM, Thomas DY, Jakob CA, Aebi M, Bussey H (1998) Involvement of protein N-glycosyl chain glucosylation and processing in the biosynthesis of cell wall beta-1,6-glucan of *Saccharomyces cerevisiae*. Genetics 149:843–856
Sherrington SL, Sorsby E, Mahtey N, Kumwenda P, Lenardon MD, Brown I, Ballou ER, MacCallum DM, Hall RA (2017) Adaptation of *Candida albicans* to environmental pH induces cell wall remodelling and enhances innate immune recognition. PLoS Pathog 13(5):e1006403
Shibata N, Suzuki A, Kobayashi H, Okawa Y (2007) Chemical structure of the cell-wall mannan of *Candida albicans* serotype A and its difference in yeast and hyphal forms. Biochem J 404:365–372
Tan Y, Ma S, Leonhard M, Moser D, Schneider-Stickler B (2018) beta-1,3-glucanase disrupts biofilm formation and increases antifungal susceptibility of *Candida albicans* DAY185. Int J Biol Macromol 108:942–946
Trinel PA, Borg-Von-Zepelin M, Lepage G, Jouault T, Mackenzie D, Poulain D (1993) Isolation and preliminary characterization of the 14- to 18-kilodalton *Candida albicans* antigen as a phospholipomannan containing beta-1,2-linked oligomannosides. Infect Immun 61:4398–4405
Wheeler RT, Fink GR (2006) A drug-sensitive genetic network masks fungi from the immune system. PLoS Pathog 2(4):e35

Wheeler RT, Kombe D, Agarwala SD, Fink GR (2008) Dynamic, morphotype-specific *Candida albicans* beta-glucan exposure during infection and drug treatment. PLoS Pathog 4(12): e1000227

Zarnowski R, Westler WM, Lacmbouh GA, Marita JM, Bothe JR, Bernhardt J, Lounes-Hadj Sahraoui A, Fontaine J, Sanchez H, Hatfield RD, Ntambi JM, Nett JE, Mitchell AP, Andes DR (2014) Novel entries in a fungal biofilm matrix encyclopedia. MBio 5(4):e01333-01314. https://doi.org/10.1128/mBio.01333-14

Chapter 10
Structure and Biological Properties of Lasiodiplodan: An Uncommon Fungal Exopolysaccharide of the (1 → 6)-β-D-Glucan Type

Mario A. A. Cunha, Vidiany A. Q. Santos, Gabrielle C. Calegari, William N. Sánchez Luna, Sandra L. A. Marin, Robert F. H. Dekker, and Aneli M. Barbosa-Dekker

Abstract Glucans find a wide range of commercial applications in different industrial sectors, food, pharmaceuticals, and fine chemicals. Commercially available β-glucans are obtained chiefly through complex extraction procedures of the cell walls of microorganisms and cereals that are time-consuming processes. Some microorganisms also produce β-glucans exocellularly, which have been exploited commercially for this purpose. In this context, exopolysaccharides such as lasiodiplodan (a linear (1 → 6) β-glucan) standout because of the greater ease of their production by submerged fermentation and recovery from the cell-free fermentation broth by precipitation methods. Lasiodiplodan from the fungus *Lasiodiplodia theobromae* MMPI was first described in 2008, and studies have since addressed its production, chemical derivatization, and chemical and biological characterization. Lasiodiplodan presents biological functions that include antioxidant, hypoglycemic, antiproliferative, and transaminase activities, as well as protective activity against doxorubicin-induced DNA damage. The different biological properties of lasiodiplodan make it a biomolecule attractive for commercial exploitation. Medicines for treatments of different conditions of human diseases, containing lasiodiplodan as one of the active or co-adjuvant principles, could be developed by

M. A. A. Cunha (✉) · V. A. Q. Santos · G. C. Calegari
Departamento de Química, Universidade Tecnológica Federal do Paraná, Pato Branco, Paraná, Brazil
e-mail: mario.utfpr@gmail.com

W. N. Sánchez Luna · S. L. A. Marin
Universidade Federal do Paraná, Curitiba, Paraná, Brazil

R. F. H. Dekker
Programa de Pós-graduação em Engenharia Ambiental, Universidade Tecnológica Federal do Paraná, Londrina, Paraná, Brazil

A. M. Barbosa-Dekker
Departamento de Química, Universidade Estadual de Londrina, Londrina, Paraná, Brazil

E. Cohen, H. Merzendorfer (eds.), *Extracellular Sugar-Based Biopolymers Matrices*, Biologically-Inspired Systems 12, https://doi.org/10.1007/978-3-030-12919-4_10

the pharmaceutical industry. Antiaging creams and ointments, as well as self-healing hydrogels, are also good possibilities for commercial applications. Another attractive possibility of use is as a prebiotic agent in food products. Chemical modifications in the lasiodiplodan structure by *O*-acetylation, carboxymethylation, phosphorylation, or sulfonylation have been shown to be a potentiating mechanism of some of its properties. This chapter addresses the studies that have been carried out with lasiodiplodan and future production perspectives and applications.

10.1 Introduction

A wide range of microbial species including bacteria, fungi, and microalgae produce exopolysaccharides (EPS) secreted into the culture media when cultivated by submerged fermentation. Exopolysaccharides comprise carbohydrate biomacromolecules of complex heterogeneous structures made up of various sugars linked by various glycosidic bonds that can be branched or unbranched, and they may be soluble or sparingly soluble in water.

Microbial polysaccharides have attracted widespread commercial attention for their peculiar properties and biological functions, with possibilities of a wide range of technological applications as bio-based products. The global trend of using bio-based products has promoted the growth of the market for natural polymers obtained by biotechnological processes, compared to traditional organic polymers derived by chemical synthesis from crude petroleum.

In fact, the so-called white biotechnology (known as industrial biotechnology) has driven the need to foster biodegradable products that require less energy for their production and generate less toxic or nontoxic effluents. In this context, microbial polysaccharides are environmentally friendly bio-based products considering the low energy cost for their production and recovery, as well as the relative ease of treatment of the effluents generated in the production process.

One highly studied group of exopolysaccharides, the β-D-glucans, is produced by fungi, and mainly by the ascomycetes, the largest phylum of fungi, for example, botryosphaeran produced by *Botryosphaeria rhodina* (Barbosa et al. 2003). The basidiomycetes (white-rot fungi) that includes macrofungi (macromycetes) producing fruiting bodies such as mushrooms, brackets, and conks also produce β-D-glucans, and they can be produced exocellularly when cultivated under submerged fermentation conditions, e.g., schizophyllan by *Schizophyllum commune* (Zhang et al. 2013) and scleroglucan by *Sclerotium rolfsii* (Castillo et al. 2015). These β-D-glucans are chiefly of the (1 → 3)-β-D-glucosidic type with branches containing D-glucose residues linked through β-(1 → 6) bonds.

The chemistry and biology of the (1 → 3)-β-D-glucans has been much studied since the late 1950s, and one excellent book was published on the topic by Bruce A. Stone (Bacic et al. 2009). Another group of fungal β-glucans that are rarer, but can also be produced extracellularly by submerged fermentation, are of the (1 → 6)-β-D-glucan kind, e.g., lasiodiplodan produced by several strains of *Lasiodiplodia theobromae* (Vasconcelos et al. 2008; Oliveira et al. 2015) and pustulan from

Guignardia citricarpa (Sassaki et al. 2002). Polysaccharides of this kind mainly exist as constituents of the fungal cell wall. Variations in the fine structure, molecular weight, extent of branching, and conformation of the β-glucans can play a crucial role in influencing their biological functions (Leung et al. 2006; Wang et al. 2017).

10.2 Developments Leading to Studies on Lasiodiplodan

In searching for a suitable source of an exopolysaccharide that could have interesting properties and biological functions for applications, we decided upon *L. theobromae*, in view of earlier studies from our research group (Saldanha et al. 2007). We observed that on cultivating this particular fungus on glucose medium, the culture fluid became viscous. This suggested that a biopolymer was being produced. At the time, there was no information in the scientific literature on exopolysaccharides produced by this fungal genus and species. This sparked our curiosity to discover the chemical nature of its biopolymer and examine its properties and biological functions. This then set the path that became the subject of a long-term investigation by our group.

10.3 Fungi Belonging to the Taxa Botryosphaeriaceae

L. theobromae is a filamentous fungus belonging to the taxa Botryosphaeriaceae, which constitutes a family of fungi with "saclike structures" representative of the order Botryosphaeriales of the phylum Ascomycota. *L. theobromae* is the anamorphic form of *Botryosphaeria rhodina*, both of which are ascomycetes.

They are phytopathogens causing devastating plant diseases that can include dieback (branch and whole tree), wilt, blight, root rot, and gummosis among others in a wide range of plant hosts. These pathogens lead to the death of various plants of agricultural and horticultural importance and cause microbial rots and spoilage in post-harvested fruits and vegetables. Altogether, these pathogens can inflict huge economic losses annually, worldwide. *L. theobromae* is a highly virulent member of this family and is widely distributed geographically in temperate and tropical climatic regions of the world.

10.4 Lasiodiplodan: An Exopolysaccharide of the (1 → 6)-β-D-Glucan Kind

L. theobromae, a well-known and widespread plant pathogen, has been described as producing various bioactive compounds exhibiting diverse biological functions. Among the bio-based products are exocellular polysaccharides such as lasiodiplodan

produced by several strains of *L. theobromae* isolated from rotting tropical fruits and first described by Vasconcelos et al. (2008) and identified as a linear, unbranched (1 → 6)-β-D-glucan. One of the strains of *L. theobromae* (MMBJ) was found to also produce an exocellular mix-linked (1 → 3)(1 → 6)-β-D-glucan, in addition to lasiodiplodan (Oliveira et al. 2015). More recently, a new exopolysaccharide named lasiosan was described that was produced by a *Lasiodiplodia* sp. (strain B2) and characterized structurally as a glucomannan (glucose to mannose ratio 1:1). This biopolymer exhibited promising biological activities (Kumar et al. 2018).

Other examples of metabolites of interest produced by *L. theobromae* include lipases (lipolytic enzymes that can be used to make biodiesel in transesterification-methanolysis catalyzed reactions) (Venkatesagowda et al. 2017); jasmonic acid (plant hormone whose derivatives serve as important ingredients in different cosmetic formulations) (Eng et al. 2016; Jackson et al. 2017); and lasiodiplodins (resorcylic acid lactones) that possess various biological functions including anticancer activity (Sultan et al. 2014; Huang et al. 2017).

It is interesting to note that some bio-based products with attractive properties and functions can be obtained by microorganisms that have some degree of pathogenicity to plant hosts. A classic example in this sense is xanthan gum (a substituted cellulose with alternate glucose residues containing a trisaccharide appendage at the C3 position) produced on an industrial scale by the phytopathogenic bacterium *Xanthomonas campestris* (causal agent of bacterial plant diseases). Xanthan is one of the most widely used bio-based products within the food and pharmaceutical sectors (García-Ochoa et al. 2000).

The *L. theobromae* strain MMPI which was used to produce lasiodiplodan was isolated from rotting pinha (sugar apple, *Annona squamosa*), a tropical fruit from the northeast of Brazil (Saldanha et al. 2007). Initial studies demonstrated that this fungal isolate produced lasiodiplodan in submerged culture on different carbon and nitrogen sources. Glucose and maltose were the carbon sources that promoted highest production of this uncommon β-glucan, but yeast extract also contributed to enhance its production (Cunha et al. 2012). Interesting rheological aspects of lasiodiplodan were also described by our group, e.g., the display of high apparent viscosity at 25 °C even under conditions of high ionic strength.

Antioxidant activity was described for lasiodiplodan (Cunha et al. 2012; Giese et al. 2015; Kagimura et al. 2015a), and some biological activities were recognized that included hypoglycemic and transaminase activities in mice (Túrmina et al. 2012). Also, protective activity against doxorubicin-induced DNA damage was described by Mello et al. (2017), as well as antiproliferative activity against MCF-7 breast cancer cells that was associated with apoptosis, necrosis, and oxidative stress (Queiroz et al. 2015). Presently, our research group studied the use of lasiodiplodan as an elicitor of resistance against phytopathogens in different plant cultures, with promising results (data not yet published).

Another relevant aspect is to introduce new functional groups in the primary structure of polysaccharides. This strategy has been employed to enhance, or produce, new chemical and biological functions of the derivatized biopolymer for technical applications (Cumpstey 2013; Chen and Huang 2018). In this respect,

chemical derivatization of lasiodiplodan has improved some properties, e.g., increased water solubility following carboxymethylation (Theis et al. 2017) and phosphorylation (Sechi et al. 2017), while sulfonylation exhibited antimicrobial activity against bacteria and yeasts (Calegari et al. 2017). Potentiation of the antioxidant capacity was demonstrated after carboxymethylation (Theis et al. 2017) and sulfonylation (Calegari et al. 2017).

In this chapter, we highlight and discuss the biotechnological production of lasiodiplodan in submerged cultivation, the chemical derivatization as a strategy for the potentiation of its biological and technological properties, and the relationship between chemical structure and biological functions. Also discussed are some aspects related to the physical properties of this uncommon biopolymer.

10.5 Production of Lasiodiplodan by Submerged Cultivation

Fungal exocellular polysaccharides are commonly produced by submerged fermentation where they are secreted into the medium. Submerged cultivations are characterized as processes where the substrates (carbon sources, nitrogen supplementation, and mineral salts) are soluble in the fermentation medium, which facilitates their assimilation by the cultivated microorganism (Mahapatra and Banerjee 2013).

Presently, most commercially available β-D-glucans are still obtained by extracting yeast cell walls (*Saccharomyces cerevisiae*) and cereals grains (barley and oats). However, the process of recovering cell wall glucans is more complex than the recovery of exocellular glucans. The major advantage of the process of obtaining exocellular glucans relative to cell wall glucans is in the downstream processing steps. The industrial process of recovering cell wall β-glucans of Brewer's yeast (*Saccharomyces cerevisiae*) commonly involves complex procedures of lysis (autolysis, enzymatic, chemical, and physical processes) and extraction. The yeast cell wall represents 15–30% of the dry weight of the yeast. Typically, the yeast cell wall contains 30–60% of polysaccharides, 15–30% of which constitutes the β-glucans of the (1 → 3)- and (1 → 6)-linked types. Other cell wall constituents include manno-oligosaccharides linked to proteins (15–30%), proteins (15–30%), lipids (5–20%), and small amounts of chitin (Huang 2008).

The separation of cell wall material from cytoplasm after lysis involves sequential extraction steps that may include organic solvents (removal of lipidic materials), cold and hot water, and alkali (NaOH) followed by neutralization with acids (HCl, acetic acid, citric acid) (Pengkumsri et al. 2017). Other methods employed in this process involve sonication and dynamic high-pressure microfluidization treatment with ionic liquids (Liu et al. 2016). On the other hand, the recovery of exopolysaccharides such as lasiodiplodan from the cell-free culture broth involves simple steps of precipitation of the biopolymer with cold ethanol and subsequent filtration/centrifugation and dialysis/ultrafiltration (Calegari et al. 2017; Theis et al.

2017). In this sense, the process of recovering exopolysaccharides besides simplicity has economic and environmental advantages over cell wall extraction methods.

Metabolites of fungal origin such as exopolysaccharides have many biotechnological applications, so optimization strategies of the processes used to obtain these biopolymers have been extensively cited in the scientific literature (Cunha et al. 2012; Mahapatra and Banerjee 2013; Vlaev et al. 2016; Zhu et al. 2016). Fermentation parameters, such as pH, temperature, aeration and dissolved oxygen, stirring speed, incubation time, composition of the nutrient medium, carbon source and concentration, nitrogen supplementation, and the presence of salts containing phosphates, have a significant influence on the production yield and purity of these biomacromolecules. Moreover, depending upon the fermentation conditions, the exopolysaccharides may exhibit variations in their physical, chemical, and biological properties (Survase et al. 2007; Cunha et al. 2012). Carbon and nitrogen sources for the biological production of lasiodiplodan by *L. theobromae* MMPI cultivated under submerged fermentation conditions were studied by Cunha et al. (2012). Carbon sources such as glucose, fructose, maltose, and sucrose, as well as different sources of nitrogen (yeast extract, peptone, urea, potassium nitrate, and ammonium sulfate) were evaluated as substrates. Glucose and maltose and yeast extract were found to be the best sources of carbon and nitrogen, resulting in the respective production of lasiodiplodan of 2.05, 2.08, and 2.46 g L^{-1}. Interestingly, urea as a nitrogen source resulted in more lasiodiplodan per unit biomass than yeast extract (0.74 vs. 0.22 g g^{-1}, respectively).

In this work, response surface methodology using a two-level complete (2^2) factorial design was used to optimize production of lasiodiplodan and mycelial growth in submerged fermentation in a stirred tank bioreactor and evaluated the variables of concentration of glucose and impeller speed. The cultivation conditions that promoted the highest production of lasiodiplodan (6.3 g L^{-1}) were 60 g L^{-1} glucose and 200 rpm impeller speed (Cunha et al. 2012). Kagimura et al. (2015a) evaluated the production of lasiodiplodan by *L. theobromae* MMPI in a stirred-tank bioreactor, using a lower concentration of glucose (20 g L^{-1}), a higher impeller speed (400 rpm), and a minimum salts medium (Vogel 1956). Maximum production and yield of lasiodiplodan (9.53 g L^{-1} and 0.58 g g^{-1}) were verified in 72 h of cultivation. Accordingly, the use of high concentrations of sugars associated with long periods of cultivation can stress the fungal isolate and induce the synthesis of dark pigments [e.g., melanins, high-molecular-weight polymers synthesized primarily from phenolic compounds (Gessler et al. 2014)], which causes the blackening of the biomass and darkens the exopolysaccharide produced. A similar amount of lasiodiplodan (9.6 g L^{-1}) could be produced in a stirred-tank bioreactor in less fermentation time (48 h) by using the same glucose concentration (20 g L^{-1}) but replaced the Vogel minimum salts medium by K_2HPO_4 (2 g L^{-1}) and $MgSO_4.7H_2O$ (2 g L^{-1}) and used yeast extract (2 g L^{-1}) as the nitrogen source (Theis et al. 2017). Normally, lasiodiplodan consists of a white-colored product when dried. The presence of pigments in exopolysaccharides is undesirable, as they may decrease their acceptance for use as ingredients in food products and pharmaceutical formulations and may interfere with the polysaccharide's properties and functions.

Considering the high market value of β-glucans and the production efficiency of lasiodiplodan by *L. theobromae* MMPI, associated with the simplicity of its recovery, the submerged fermentation process for lasiodiplodan production has much potential for commercial scale-up and production.

10.6 Structure: Biological Function Relationships of β-Glucans

The glucose residues constituting exocellular lasiodiplodan are linked to each other by (1 → 6)-β-glucosidic bonds that give rise to a high-molecular-weight, linear, unbranched chain structure that is water-soluble (Vasconcelos et al. 2008).

β-D-Glucans [(1→3)(1→6)-branched and (1→6)-linear linked β-glucosidic chains] are part of the complex structural matrix that makes up the cell wall of the kingdom of fungi, which can constitute from 65% to 90% of the total β-glucan present. Besides β-glucans, other biopolymers may also be present, such as chitin (homopolymer of β-1,4-linked *N*-acetyl-D-glucosamine residues), glycoproteins, mannoproteins, mannans, α-linked glucans, other β-glucans of different linkages, and melanin, among others (Free 2013; Gow et al. 2017).

β-Glucans are immunomodulators and are recognized by the immune system of higher organisms as microbial-associated molecular patterns that bind to pattern recognition receptors (e.g., Dectin-1, Toll-like receptors, TLRs) present on the surface of host cells (e.g., dendritic) (Stier et al. 2014). When ingested orally, the β-glucans are transported in toto (undigested; digestive enzymes degrading the β-glucans are not known to be produced in the human gut) within the human gastrointestinal tract to the small intestine where specialized epithelial cells (Peyer's patches) located in the mucosa tissue of the ileum take up the β-glucans for translocation into the lymphatic system initiating an immune response by cells of the immune system. The β-glucans can bind to specific receptors (Dectin-1, TLRs, and complement receptor CR-3) on the immune cells' surfaces and then trigger a cascade of internal cell signaling processes that manifest various biological responses to trigger gene expression and stimulation of cytokine secretion by immune cells, such as natural killer cells, macrophages, neutrophils, dendritic cells, and monocytes (Cunha et al. 2017). The immunomodulatory potential of the β-glucans has been directly related to the chemical structure of these macromolecules, which act as activators and modulators of the immune system. Smiderle et al. (2013) reported increased expression of pro-inflammatory genes *IL-1β*, *TNF-α*, and *COX-2* in THP-1 macrophages, induced by a linear (1 → 6)-β-D-glucan (similar structure to lasiodiplodan) extracted from fruiting bodies of the mushrooms *Agaricus bisporus* and *Agaricus brasiliensis*.

Other biological functions that are related to the chemical structure of β-glucans include antioxidant, antimicrobial, antitumor, antiviral, anticoagulant, hypocholesterolemic, and hypoglycemic activities (Sánchez et al. 2018).

β-Glucans can assist in the control of Alzheimer's disease (Rahar et al. 2011), among other biological functions described in the scientific literature.

Up to the present time, some properties and biological functions have been demonstrated for lasiodiplodan. They include antioxidant activity (Cunha et al. 2012; Giese et al. 2015; Kagimura et al. 2015a), protective activity against doxorubicin-induced DNA damage (Mello et al. 2017), hypoglycemic and transaminase activities (Túrmina et al. 2012), and anticancer activity in the breast cancer cell line MCF-7 (Queiroz et al. 2015).

10.7 Antioxidant Activity of Lasiodiplodan

The antioxidant ability of β-glucans is related to structural parameters such as solubility, molecular weight, monosaccharide composition, glycosidic linkages, and the extent of branching by side-chain functional groups (Wang et al. 2014). Kagimura et al. (2015a) and Giese et al. (2015) first reported through several analytical protocols the ability of lasiodiplodan to scavenge free radicals. Kagimura et al. (2015a) further described potential scavenging activity related to DPPH (2,2-Diphenyl-1-picrylhydrazyl) and ABTS (2,2′-Azino-bis (3-ethylbenzothiazoline-6-sulfonic acid) radicals and ferric ion reducing antioxidant power. These authors assessed the antioxidant activity of lasiodiplodan up to a concentration of 5000 μg mL^{-1} and found an ABTS radical scavenging activity around 5% at a concentration of 1000 μg mL^{-1}. The relatively low ABTS radical scavenging potential of native lasiodiplodan (not chemically modified) was attributed to low water solubility of the biopolymer after dehydration (lyophilization). In relation to the DPPH radical, a scavenging activity of around 10% was found at 50 μg mL^{-1} concentration, and the ferric reducing antioxidant power (FRAP) at 5000 μg mL^{-1} was 150 μM $FeSO_4.7.H_2O$ equivalent.

Giese et al. (2015) used other methods to evaluate antioxidant activity in lasiodiplodan, namely, the hydroxyl radical ($HO^{\bullet}$) and nitric oxide radical ($NO^{\bullet}$) activities, total antioxidant capacity (determined through evaluation of the capacity of the reduction of molybdate species), and reducing power. Lasiodiplodan presented HO• scavenging activity of around 14% when tested at a concentration of 3 g L^{-1}, and this concentration showed a total antioxidant activity of 10%. Nitric oxide radical (NO•) is considered a cytotoxic reactive nitrogen species (RNOS) that mediates nitrosative or oxidative stress reactions that can trigger diseases (Giese et al. 2015). Lasiodiplodan (3 g L^{-1}) showed scavenging activity corresponded to 38%, the same activity as observed with curdlan (1 → 3)-β-glucan at 2 g L^{-1} concentration. The reducing power ability was evaluated in the presence of potassium ferricyanide using ascorbic acid as an antioxidant standard, and lasiodiplodan presented reducing power capacity fivefold less than the standard (ascorbic acid). More recently, the antioxidant activity of lasiodiplodan was evaluated by the hydrogen peroxide and $OH^{\bullet}$ scavenging activities and reducing power assays. Theis et al. (2017) reported that lasiodiplodan was able to remove 5% of hydrogen peroxide at

concentrations of 1 and 2 mg mL^{-1}. In this study, lasiodiplodan was able to scavenge 33.4% of hydroxyl radicals at concentrations of 2 mg mL^{-1}, and the reducing power was assessed by capacity for potassium ferricyanide reduction, which was around 50% of the reducing power exhibited by ascorbic acid standard. Calegari et al. (2017) found no hydrogen peroxide removal potential in assays using a low concentration of lasiodiplodan (0.88 g L^{-1}) but reported 44.32% hydroxyl radical removal activity. Sánchez et al. (2018) reported 6% of hydrogen peroxide removal capacity and hydroxyl radical scavenging activity of 27.38% by lasiodiplodan at 150 mg L^{-1} concentration.

The antioxidant potential of some carbohydrates macromolecules can be considered poor compared to standard antioxidants such as Trolox (analogue of vitamin E). In this sense, chemical modifications in the macromolecule by the introduction of functional groups can promote an increase in the antioxidant activity as described below.

10.8 Biological Activities of Lasiodiplodan

A study was conducted on the toxicological effects at sub-chronic treatments with lasiodiplodan in mice and evaluated various biochemical, hematological, and histopathological parameters (Túrmina et al. 2012). Treatment of mice with lasiodiplodan administered by gavage at a concentration of 50 mg kg^{-1} b.w./day demonstrated a significant reduction in blood glucose levels (hypoglycemic effect) in the male group of the mice and transaminase activity in both genders. In addition, no hematological and histopathological alterations were found indicating no signs of any toxicity.

In vitro antiproliferative activity of lasiodiplodan against MCF-7 breast cancer cells was reported by Cunha et al. (2012). Lasiodiplodan showed an antiproliferative effect at concentration of 100 μg mL^{-1} with an IC_{50} (half maximal inhibitory concentration) that was time- and dose-dependent. Follow-up studies found that this effect was associated with apoptosis, necrosis, and oxidative stress. This study demonstrated that the apoptosis induced by lasiodiplodan was mediated by AMP-activated protein kinase and Forkhead transcription factor, FOXO3a (Queiroz et al. 2015).

The genotoxic effects and protective activity of lasiodiplodan against DNA damage induced by the antitumor drug, doxorubicin, and the impact on the expression of genes associated with DNA damage and inflammatory responses were reported by Mello et al. (2017). This study showed that lasiodiplodan did not induce disturbances in DNA stability and significantly reduced DNA damage and inflammation caused by exposure to the drug.

Intracerebroventricular administration of lasiodiplodan in rats demonstrated a protective effect against neurotoxicity induced by D-penicillamine and prevented D-penicillamine-induced (convulsive and preconvulsive) behavioral alterations. Lasiodiplodan also prevented lipoperoxidation in the cerebral cortex, and no histopathological alteration was observed (Malfatti et al. 2017). In this study,

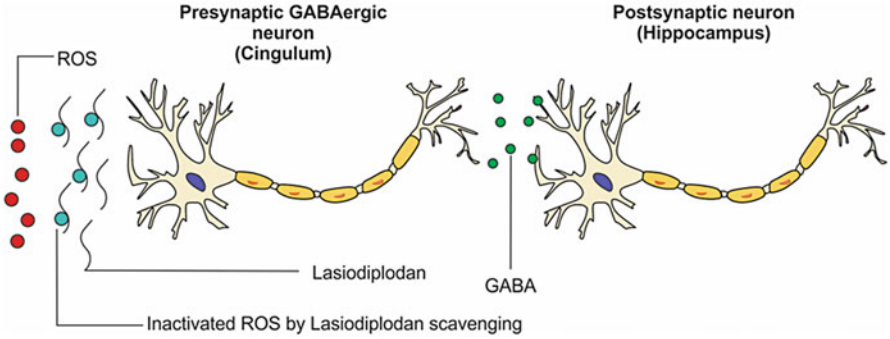

Fig. 10.1 Neuroprotective activity of lasiodiplodan related to possible protective effect against oxidative damage of GABAergic inhibition in the cingulum that projects GABAergic neurons to the hippocampus as suggested by Malfatti et al. (2017)

lasiodiplodan seems to provide a protective effect against oxidative damage of GABAergic inhibition in the cingulum that projects GABAergic neurons to the hippocampus (Fig. 10.1), a region in the brain that has a strong relationship with epilepsy (Treiman 2001).

10.9 Chemical Derivatization as a Strategy for the Potentiation of Biological Properties

Although β-glucans naturally present biological functions as antioxidant (Khan et al. 2016), immunomodulatory (Samuelsen et al. 2014), anti-inflammatory (Mello et al. 2017), and antitumor activities (Sun et al. 2009), chemical derivatization is an important strategy to intensify or even promote the emergence of new functions, thus increasing its possible biotechnological applications, especially in the pharmaceutical, chemical, and medical sectors (Calegari et al. 2017; Li et al. 2017).

Chemical derivatizations are characterized by reactions in which hydroxyl groups on the parent molecule are replaced by other functional groups according to the type of chemical modification performed, and this can affect the biological functions of the modified polysaccharides (Chen and Huang 2018). The major derivatizations reported in the literature for polysaccharides include *O*-acetylation, carboxymethylation, phosphorylation, and sulfonylation (Cumpstey 2013). Accordingly, these respective derivatization procedures were employed to modify lasiodiplodan (Kagimura et al. 2015a; Calegari et al. 2017; Sechi et al. 2017; Sánchez et al. 2018). The operational conditions involved in the process of chemical derivatization of polysaccharides such as the choice of the solubilizing agent (usually organic solvents) and the reagent responsible for introducing the chemical groups into the molecule (usually an organic acid) are essential for the success of the desired chemical modification (Kagimura et al. 2015a).

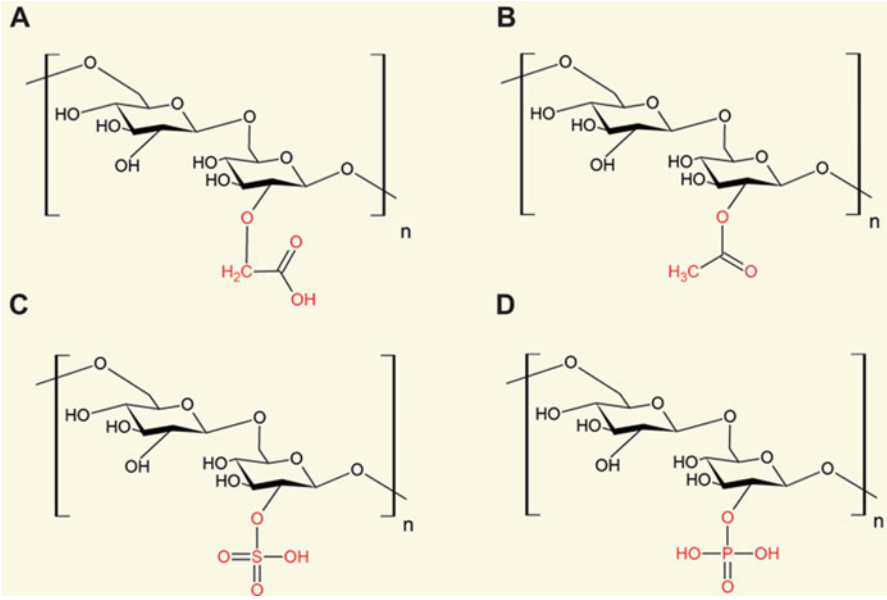

Fig. 10.2 Structural representation of lasiodiplodan derivatives by carboxymethylation (**a**), acetylation (**b**), sulfonylation (**c**), and phosphorylation (**d**)

10.9.1 Acetylation

O-Acetylation is a chemical modification procedure in which the free hydroxyl groups on the monomeric glucose units of a polysaccharide are replaced by *O*-acetyl groups (CH_3COO-; see Fig. 10.2b), and this occurs by an esterification reaction. The reaction can be influenced by factors such as temperature, reaction time, concentration of the derivatizing agent, and the types of solvents (Sánchez et al. 2018). The most commonly used derivatizing agents for *O*-acetylation are acetic acid and acetic anhydride, but in some cases, catalysts such as iodine, sulfuric acid, or perchloric acid were also being used (Biswas et al. 2009). *O*-Acetylation helped to improve some of the properties of polysaccharides, for example, by improving and controlling their solubility, water absorptivity, and hydrophobicity (Xu et al. 2010). According to Bai et al. (2014), such improvements in properties may be related to the added groups and the degree of substitution of the modified polysaccharide. *O*-Acetylation of polysaccharides can also enhance biological activities such as antioxidant, antitumor, and immune regulation. The chemical modification by *O*-acetylation enhanced the immunomodulatory activity and the antioxidant power of a polysaccharide extracted from *Ganoderma lucidum* (Chen et al. 2014; Chen and Huang 2018). Chen and Huang (2018) studied the effects of *O*-acetylation of polysaccharides on regulation of the immune system and demonstrated that the ability of dendritic cells to secrete the cytokine IL-12p70 was increased by *O*-acetylation and consequently this modification promoted IL-12p70 secretion.

O-Acetylation of lasiodiplodan (Fig. 10.2b) was first reported by Sánchez et al. (2018), in which acetic anhydride was used as the derivatizing agent and pyridine as catalyst, that resulted in *O*-acetylated derivatives of lasiodiplodan with degrees of substitution (DS) of 0.48, 0.66, 1.03, and 1.26. According to these authors, the electronic cloud along the polymer structure was increased by *O*-acetylation, which made the hydroxyls more "active," and consequently potentiating the donation of hydrogens. *O*-Acetyl groups in the main chain contributed to the weakening of the dissociation energy of the hydrogen bond, and, consequently, the hydrogen-donating ability of the macromolecules derivatives could be increased.

O-Acetylation increases the ability to remove hydroxyl radicals (45.6%, DS, 0.48) and hydrogen peroxide (36.0%, DS, 0.48), contributing to the increase of the reducing power (118.59%, DS, 0.48) of the derivatized polysaccharide. There appeared to be a correlation between the DS and the antioxidant potential of acetylated lasiodiplodan, since derivatives with a high degree of substitution did not present higher radical scavenging efficiency or greater reducing potential than derivatives with lower DS values (Sánchez et al. 2018).

From the foregoing, the *O*-acetylation of lasiodiplodan contributed to improving the biological functions of the modified parent polysaccharide making it attractive for biomedical and industrial applications.

10.9.2 Carboxymethylation

Derivatization by carboxymethylation consists of substituting the hydroxyl groups present in monomeric glucose units of the polysaccharide with carboxymethyl groups (-CH_2COOH) (Theis 2018). Some enhancements of biological functionalities in glucans were observed such as increased water solubility, reduced viscosity, and potentiation of antioxidant, antimicrobial, antitumor, and antiviral activities (Wang et al. 2009; Machová et al. 2014; Kagimura et al. 2015b; Theis et al. 2017).

The first report on carboxymethylation of lasiodiplodan used chloroacetic acid as the derivatizing agent that resulted in a carboxymethylated lasiodiplodan with DS of 1.27 (Kagimura et al. 2015b). Carboxymethylated lasiodiplodan presented higher solubility in water (60% higher) than unmodified lasiodiplodan, which is related to the reduction of intra- and intermolecular interactions in the macromolecule after the insertion of the carboxymethyl group. The antioxidant potential of carboxymethylated lasiodiplodan was also higher than that observed in the unmodified lasiodiplodan. The carboxymethylated sample (at a concentration of 10,000 μg mL^{-1}) was able to remove 36.3% of the ABTS cation-free radical, while the native sample only removed 9.6%. Carboxymethylation also demonstrated the ability to potentiate the power of reducing iron (III) to iron (II) of the sample (FRAP, 536 μM $FeSO_4.7.H_2O$ equivalent, at concentration 15,000 μg mL^{-1}). Theis et al. (2017) obtained a carboxymethylated lasiodiplodan with a DS of 0.45 using monochloroacetic acid as the donor of carboxymethyl groups. Carboxymethylation increased the antioxidant potential similarly to what was earlier reported by

Kagimura et al. (2015a). The carboxymethylated sample at a concentration of 2 mg mL^{-1} showed hydrogen peroxide removal capacity (12.7%) that was 2.5 times higher than the unmodified polysaccharide. Carboxymethylation also promoted an increase of about 37.3% in hydroxyl radical scavenging activity, achieving 33.4% radical removal at a concentration 2 mg mL^{-1}. In addition, the capacity for potassium ferricyanide reduction to potassium ferrocyanide was augmented by carboxymethylation of lasiodiplodan at 2 mg mL^{-1}. Studies conducted by others also demonstrated that carboxymethylation may be a tool to increase the biological potential of polysaccharides, especially in relation to antioxidant and immunomodulatory activities (Wang et al. 2009; Wang et al. 2012; Wang et al. 2014). A carboxymethylated (1 → 3)-β-D-glucan extracted from the fungus *Poria cocos* was evaluated for its antioxidant potential and bile acid chelation capacity (Wang et al. 2009), with similar results found by Kagimura et al. (2015b) and Theis et al. (2017). Carboxymethylation enhanced the antioxidant ability of the polysaccharide and also promoted an increase in its solubility in water (98.4%).

10.9.3 Phosphorylation

In chemical derivatization by phosphorylation, phosphate groups ($H_2PO_3^-$) are inserted into the structure of the macromolecule (Fig. 11.2d). The most commonly used phosphorylating agents are phosphoric acid, sodium di-hydrogen phosphate, sodium hexametaphosphate, sodium hydrogen phosphate, sodium trimetaphosphate, sodium tripolyphosphate, and phosphorus oxychloride (Li et al. 2016). The insertion of phosphate groups onto polysaccharides is known to promote an increase in biological activities, especially due to improved water solubility, molecular weight change, and in modifying chain conformation of the biopolymers (Li et al. 2016; Sechi et al. 2017).

The phosphorylation of lasiodiplodan was recently described by Sechi et al. (2017). In this study, lasiodiplodan was phosphorylated with sodium trimetaphosphate resulting in a derivative with a low degree of substitution (DS, 0.014). Phosphorylation promoted a significant increase in the solubility (52.4%) of lasiodiplodan in water, even though the modified polysaccharide bore a low DS. The increase in polysaccharide solubility after phosphorylation was reported in the literature. Deng et al. (2015) verified an increase in the solubility and antioxidant potential of an α-D-glucan extracted from the mushroom, *Dictyophora indusiata*, that was phosphorylated with phosphoric acid (DS, 0.206). They demonstrated antitumor activity against cell lines: MCF-7 (breast cancer) and B-16 (melanoma). Antitumor activity against S-180 sarcoma (assayed in mice) was demonstrated by the polysaccharide from the fungus, *Lachnum* YM 120, after phosphorylation (phosphate content, 6.39%) with trimetaphosphate and sodium tripolyphosphate (Ye et al. 2013).

10.9.4 Sulfonylation

Sulfonylation is a type of chemical derivatization where a nucleophilic substitution of hydroxyl groups of the macromolecule by sulfonated groups occurs (HSO_3-) (Fig. 11.2c) (Calegari et al. 2017; Li et al. 2017). Chemical modification of polysaccharides by sulfonylation has been widely explored because of the ability to confer or potentiate biotechnological functions such as anticoagulant (Murry et al. 2014), antioxidant, and antimicrobial activities (Zhang et al. 2016).

The sulfonylation reaction occurs basically by suspending the polysaccharide in a solution of formamide, dimethylformamide, or dimethyl sulfoxide, followed by the addition of a catalyst (pyridine) and the sulfonylating reagent, which can include sulfuric acid, chlorosulfonic acid, or pyridine-SO_3 complexes. Chlorosulfonic acid is the most commonly employed derivatizing agent in sulfonylation reactions of polysaccharides (Mendes et al. 2009; Zhang et al. 2011; Vasconcelos et al. 2013; Calegari et al. 2017). Vasconcelos et al. (2013) first reported the sulfonylation of lasiodiplodan produced by *L. theobromae* strain MMLR. In the sulfonylation protocol, they used formamide as solvent, pyridine as catalyst, and chlorosulfonic acid as the sulfonylating agent. Sulfonylation of the lasiodiplodan (DS, 0.95) resulted in a new biological function, anticoagulant activity in a dose-dependent manner. Anticoagulant potential was demonstrated by appropriate assays measuring thrombin time (TT), prothrombin (PT), and activated partial thromboplastin (APTT). Calegari et al. (2017) sulfonylated lasiodiplodan produced by a different strain of *L. theobromae* (MMPI) following a protocol similar to that described by Vasconcelos et al. (2013). Derivatization potentiated the antioxidant activity of lasiodiplodan (DS, 0.24), especially in relation to the hydroxyl radical removal capacity (74.32%). Another important aspect described by the authors was that sulfonylation promoted antimicrobial activity of the modified lasiodiplodan against bacteria and fungi. Inhibitory potential was demonstrated against Gram-negative bacteria *Escherichia coli* ATCC 25922 and *Salmonella enterica* Typhimurium ATCC 0028 and against the yeasts *Candida albicans* ATCC 118804 and *Candida tropicalis* ATCC 13803.

Antimicrobial activity of a sulfonated β-glucan ((1 → 3)-β-D-glucan extracted from the mycelium of *Ganoderma lucidum*) was reported by Wan-Mohtar et al. (2016). Sulfonylation was performed using sulfuric acid as the derivatizing agent. Antimicrobial activity was demonstrated against a variety of bacteria relevant to foodstuffs and human health (*E. coli*, *P. aeruginosa*, *S. enteritidis*, *L. monocytogenes*, *S. aureus*, *S. epidermidis*, and *S. aureus* strain resistant to methicillin) and was found after sulfonylation of the sample (DS, 0.9). In addition, the sulfonated-β-glucan showed no cytotoxic effect against normal prostate cells (PN2TA) and exhibited antiproliferative activity against leukemic cancer cells (U937) at concentrations below 60 μg mL^{-1}.

10.10 Nuclear Magnetic Resonance (NMR) of Derivatized Lasiodiplodans

The elucidation of the chemical structures of lasiodiplodan was studied by ^{13}C NMR. Both native lasiodiplodan (Vasconcelos et al. 2008) and different chemical derivatizations of this polysaccharide (acetylation, carboxymethylation, phosphorylation, sulfonylation) were examined by ^{13}C NMR, not only to confirm the β-configuration of the exopolysaccharide but also to indicate the carbon position of the bonding of the functional group inserted in the structure of lasiodiplodan by the derivatization reaction (Vasconcelos et al. 2013; Kagimura et al. 2015b; Calegari et al. 2017; Sánchez et al. 2018). The first ^{13}C NMR spectrum of lasiodiplodan obtained from *L. theobromae* strains MMPI and MMLR was presented in a study of Vasconcelos et al. (2008), and the spectrum of lasiodiplodan from strain MMLR was compared when this was sulfonylated (Vasconcelos et al. 2008; Kagimura et al. 2015b). The spectrum confirmed the β-type configuration of lasiodiplodan due to the chemical shift in the region of δ 105 (ppm), typical of polysaccharides with this type of chemical configuration.

The sulfonylation reaction of lasiodiplodan was confirmed in studies conducted by Calegari et al. (2017) and Vasconcelos et al. (2013) by insertion of sulfonate groups into the O-positions at carbons C-2 and C-4, and C-2, of the exopolysaccharide's primary structure, respectively. Sánchez et al. (2018) using ^{13}C NMR also confirmed the insertion of a functional group. In this case *O*-acetyl groups occurred at the C-2 carbon position in acetylated lasiodiplodan. Kagimura et al. (2015b) used the ^{13}C NMR technique to confirm that upon carboxymethylation of lasiodiplodan, the carboxymethyl groups were insertion at the C-3 and C-4 carbon positions. On the other hand, in a study by Sechi et al. (2017), upon phosphorylated lasiodiplodan at low degrees of substitution, ^{13}C NMR was not adequate to confirm the site of the derivatization. In this case, the ^{31}P NMR technique would be more appropriate to detect which regions were associated with the presence of phosphate groups in the polysaccharide.

10.11 Fourier Transform Infrared (FTIR) of the Derivatized Lasiodiplodans

The FTIR spectroscopy technique has been used for the identification of chemical bonds and monomer composition and mainly for the confirmation of acetylation, carboxymethylation, phosphorylation, and sulfonation reactions, through the identification of bands typical of the bonds of the functional groups covalently bound to the primary structure.

The first reports on the typical bonds of the chemical structure and monomeric composition of lasiodiplodan were presented by Vasconcelos et al. (2013) and Kagimura et al. (2015b). However, only in the study by Kagimura et al. (2015b), some bands characteristic of this β-glucan were described, as the band attributed to the glucose ring (1648 cm^{-1}), symmetric vibrations of C-O-C bonds that are characteristic of sugars (1075 cm^{-1}) and absorption in the region of (890 cm^{-1}) that is typical of the β-configuration in polysaccharides. In relation to the chemical derivatizations performed on lasiodiplodan, Vasconcelos et al. (2013) and Calegari et al. (2017) used FTIR to confirm the insertion of sulfonate groups, characteristic of sulfonation, into the primary structure of the exopolysaccharide. In a work related to our derivatized lasiodiplodans, we observed typical bands of vibrations: asymmetric S = O (1258 cm^{-1} and 1240 cm^{-1}), symmetric C-O-S associated with the C-O-SO_3 group (810 cm^{-1}), and unsaturated bonds characteristic of sulfonation (1631 cm^{-1}) for the sulfonated polysaccharide. Kagimura et al. (2015b) and Theis (2018) used FTIR to confirm the carboxymethylation reaction in lasiodiplodan of different degrees of substitution. These authors verified bands typical of strong absorption related to the asymmetric (1600, 1604, and 1598 cm^{-1}) and symmetric vibrations of the COO^- group (1421 and 1422 cm^{-1}) that characterized the successful insertion of carboxymethyl groups in lasiodiplodan. Phosphorylation of lasiodiplodan was also confirmed in a study by Sechi et al. (2017) using the FTIR technique, which showed characteristic bands of P-OH bonds (1041 cm^{-1}) and typical asymmetric stretching bands P=O (1228 cm^{-1}). After subjecting lasiodiplodan to *O*-acetylation, Sánchez et al. (2018) also confirmed by FTIR the insertion of *O*-acetyl groups in lasiodiplodan. The typical acetylation signals were verified with characteristic bands of acetate ester groups (– O (C=O)) in the region of 1233 cm^{-1}, C-O vibration at 1041 cm-1, and C = O carbonyl groups at the 1751 cm^{-1} region.

10.12 Physical Properties of Lasiodiplodan

In this section, the main physical properties are described for lasiodiplodan that include thermal characteristics, crystallographic parameters, structural morphology, viscosity, and water solubility.

10.12.1 Thermal Properties

Thermal analysis includes a group of techniques used to evaluate the relationship between a sample property and the temperature at which it is subjected in a controlled manner. The techniques include TGA (thermogravimetric analysis),

DTG (derivative thermogravimetric analysis), DTA (differential thermal analysis), and DSC (differential scanning calorimetry), which have been used for thermal characterization of unmodified and chemically modified lasiodiplodan. The following is an approach on the main thermal characterization results described in the scientific literature for lasiodiplodan.

Kagimura et al. (2015b) carried out DTA, TGA, and DTG of unmodified and carboxymethylated lasiodiplodan (DS, 1.27). Both lasiodiplodans demonstrated high thermal stability, presenting four stages of mass loss. The polysaccharides were subjected to the following analytical conditions: heating range between 26 and 800 °C, at a heating rate of 10 °C min^{-1} and 50 mL min^{-1} synthetic airflow. The first stage occurred at 125 °C, indicative of water loss (dehydration) of the sample, followed by two events of mass loss between 200 and 400 °C (attributed to degradation of lasiodiplodan). The final decomposition of the sample occurred at temperatures between 425 and 620 °C. In another study, Theis et al. (2017) evaluated the thermal stability of a carboxymethylated lasiodiplodan of a lower DS (DS, 0.45). The test was conducted by heating at temperatures between 30 and 500 °C, at a heating rate of 5, 10, and 20 °C min^{-1} and synthetic air, and/or nitrogen, flow of 100 mL min^{-1}. As observed by Kagimura et al. (2015b), carboxymethylated lasiodiplodan of lower DS showed similar initial decomposition temperatures, remaining stable for up to 230 °C, and did not present any relevant changes in relation to the heating rates evaluated. In an atmosphere of synthetic air, there were two stages of mass loss, which indicated the oxidative decomposition and the dehydration of the polysaccharide. On the other hand, under a nitrogen atmosphere, only one stage of mass loss was found, which was related to the dehydration of the polysaccharide.

Sechi et al. (2017) characterized phosphorylated lasiodiplodan samples (DS between 0.025 and 0.050) by TGA, DTA, and DTG, using similar conditions to that described by Kagimura et al. (2015b). The phosphorylated lasiodiplodan presented thermal stability with mass loss stages associated with dehydration, thermal degradation, and carbonization, with a mass loss stage beginning at 200 °C. Only the derivatized lasiodiplodan of lower degree of phosphorylation (DS, 0.025) showed the first stage of mass loss (dehydration) and occurred at a lower temperature (150 °C). *O*-Acetylated lasiodiplodan also demonstrated high thermal stability. Sánchez et al. (2018) evaluated the thermal stability of *O*-acetylated derivatives of lasiodiplodan of different degrees of substitution (DS, 0.48, 0.66, 1.03, and 1.26) by DTA, DTG, and DSC analysis. Analyses were conducted in an atmosphere using synthetic air (50 mL min^{-1}) with a heating rate of 5 °C min^{-1} and temperatures ranging from 25 to 800 °C. All samples tested showed high thermal stability. The *O*-acetylated lasiodiplodan of DS 0.48 presented three stages of mass loss, whereas the *O*-acetylated derivatives of higher DS (DS, 0.66, 1.03, and 1.26) presented four stages of mass loss. Compared with the parent polysaccharide, the modified lasiodiplodan demonstrated high thermal stability at temperatures commonly employed in production processes within the food or pharmaceutical industry sectors.

10.12.2 X-Ray Diffraction Profile of Lasiodiplodan

X-ray diffraction was employed to evaluate possible changes in the macromolecular structure of lasiodiplodan following modifications by the introduction of chemical groups (Kagimura et al. 2015b; Calegari et al. 2017; Sechi et al. 2017; Theis et al. 2017). Polysaccharides such as the noncellulosic β-glucans of mixed linkages present diffraction patterns typical of an amorphous matrix, but the introduction of chemical groups into the macromolecular structure may lead to small changes in their X-ray diffraction patterns.

X-ray analysis of unmodified lasiodiplodan showed broad peaks, typical of an amorphous matrix. The introduction of carboxymethyl groups promoted changes in the diffractograms of the sample, resulting in a slight shift of peaks to the right (between 5° and 15° at 2θ) (Kagimura et al. 2015b). Theis et al. (2017) reported differences in the diffractograms between the unmodified and carboxymethylated lasiodiplodan, with changes in the intensity observed for some peaks (21.1° and 23.8° at 2θ), which suggests that some changes occurred in the molecular orientation in the amorphous matrix of the exopolysaccharide through carboxymethylation. Sechi et al. (2017) reported that lasiodiplodan with a low degree of phosphorylation (DS, 0.049) maintained a typically amorphous X-ray diffraction pattern, but a peak at 29° (2θ) was observed following derivatization. They attributed this peak to possible formation of new chemical bonds in the structure of the phosphorylated polysaccharide. In sulfonated lasiodiplodan, Calegari et al. (2017) observed peaks in the regions at 11.64°, 29.15°, and 31.15° (2θ), which suggests the appearance of semicrystalline regions in the structure of the sulfonylated biopolymer. Similarly, Sánchez et al. (2018) also verified the appearance of crystalline regions evidenced by peaks at 20.9° and 23.4° (2θ) in the matrix of *O*-acetylated lasiodiplodan.

10.12.3 Morphological Characteristics

The morphological aspects of lasiodiplodan (lyophilized samples) by scanning electron microscopy was first described by Kagimura et al. (2015b). Unmodified lasiodiplodan presented spherical structures like granules with an ovoid shape (3.33 μm average diameter), and these granules ruptured following carboxymethylation of the exopolysaccharide.

Sánchez et al. (2018) reported that *O*-acetylation of lasiodiplodan promoted morphological changes in the polysaccharide according to the degree of substitution with *O*-acetyl groups. An interesting aspect on the change in surface structure was observed when lasiodiplodan was produced in stirred Erlenmeyer flasks. Under these conditions, granular structures as described by Kagimura et al. (2015a) were not present. This contrasted to the case when the exopolysaccharide was produced in a stirred-tank bioreactor of different scale dimensions and operational conditions. The morphological structure of lasiodiplodan produced in stirred flasks presented a form

of thin films with folds along their lengths and of a translucent appearance. When this produced lasiodiplodan was derivatized by *O*-acetylation, the films observed were similar to that for the unmodified polysaccharide regardless of the DS, but with notable differences in thickness and transparency of the films. Derivatization of lasiodiplodan by sulfonylation also promoted significant changes in the surface structure compared to the unmodified parent exopolysaccharide (Calegari et al. 2017). In particular, the appearance of fibrils along the microstructure of the modified polysaccharide was observed, which may possibly be related to a decrease in hydrogen bond interactions along the macromolecular structure after sulfonation. Surface regions with the presence of microfibrils were observed in phosphorylated lasiodiplodan, and this can be related to the decrease of the hydrogen interactions between the polysaccharide chains as a function of the substitution of hydrogens of some hydroxyls by phosphate groups (Sechi et al. 2017).

10.12.4 Viscosity and Solubility

The relationship between the viscosity (a liquid's resistance to flow) and the shear rate of an aqueous solution was evaluated on unmodified lasiodiplodan (2 g L^{-1}) (Cunha et al. 2012). Lasiodiplodan presented a pseudoplastic behavior at temperatures between 25 and 60 °C. The increase of the shear rate, which contributed to the reduction of the viscosity, possibly through an alignment of the polymer chains, resulted in a decrease of the resistance to flow. The apparent viscosity increased at 60 °C and also in the presence of calcium chloride. It is important to highlight the pseudoplastic nature of lasiodiplodan, which makes it possible to use in mixing processes for the elaboration of pharmaceutical and cosmetic products (creams, gels, lotions, mousses) that are stored in tubes and bottles (Bongiovani et al. 2009).

The ability of a biopolymer to be soluble in water is highlighted in the literature as an important property for biotechnological applications of biopolymers. In the case of β-glucans of the (1 → 3)- and (1 → 6)-types after lyophilization or dehydration by drying, they can have a tendency of being sparingly (low) soluble in aqueous solutions. Low solubility is interesting in relation to the microbiological stability of the product as a raw material, but it can limit its use. In this context, chemical modifications of the macromolecule can be an interesting tool to obtain more soluble derivatives of polysaccharides.

Derivatization by carboxymethylation was found to be a mechanism for increasing the solubility of lasiodiplodan. Carboxymethylated lasiodiplodan with a degree of substitution of 1.27 promoted an increase in water solubility of 60% compared to the unmodified polysaccharide. Kagimura et al. (2015b) and Theis (2018) evaluated the water solubility of five carboxymethylated derivatives of lasiodiplodan (DS, 0.32, 0.47, 0.51, 0.58, and 0.68) and found that the derivative with the lowest degree of substitution (DS, 0.32) showed highest solubility (67.99%) compared to the unmodified polysaccharide (4.02%). Similarly, phosphorylation of lasiodiplodan appeared to be an interesting mechanism for increasing water solubility. After

phosphorylation the water solubility of lasiodiplodan increased (52.8%), even at a low degree of substitution (DS, 0.014) (Sechi et al. 2017).

10.13 Advances and Future Perspectives for Lasiodiplodan

Lasiodiplodan, a (1 → 6)-β-D-glucan produced by *L. theobromae* MMPI, has been described over the last decade, and several studies on its production, chemical derivatization, and chemical and biological characterization have been published. The first biological property of lasiodiplodan along with botryosphaeran (a fungal β-glucan of (1 → 3)(1 → 6)-linkages) was demonstrated in MCF-7 breast cancer cells. Lasiodiplodan exhibited an antiproliferative effect that was associated with apoptosis, necrosis, and oxidative stress. This study demonstrated for the first time that the apoptosis induced by lasiodiplodan and botryosphaeran was mediated by AMP-activated protein kinase and Forkhead transcription factor, FOXO3a (Queiroz et al. 2015). Moderate antioxidant activity of lasiodiplodan was demonstrated in vitro through a suite of different chemical assay protocols, and further studies showed that lasiodiplodan exhibited hypoglycemic and transaminase activities in mice and demonstrated protective activity against doxorubicin-induced DNA damage.

An approach that has been proposed for potentiating biological functionalities of lasiodiplodan is through the modification of its chemical structure through the introduction of functional groups. Phosphorylation and carboxymethylation contributed an increase of their water solubility; sulfonylation, in addition, promoted microbicidal activity against different microorganisms, and all modifications contributed to an increase of the antioxidant activity of the biomacromolecules.

More recently, studies with lasiodiplodan promoted its uses as an elicitor agent of resistance in different plant cultures, including fruit crops such as grapes and herbal cultures such as basil. This unpublished finding set the pathway for further research in this field, in view of the continuous expansion of the world agricultural market. The market for elicitor-induced (defensive phytosanitary) products is eagerly looking for new products and innovative technologies that can contribute effectively to pest and disease control in crops. In addition, biologically based (naturally occurring) and therefore environmentally friendly phytosanitary products have attracted the interest of companies in the agricultural sector.

Other perspectives for future applications of lasiodiplodan include its use as an active ingredient in drug formulations and dermato-cosmetic products. Among these possibilities, the development of hydrogels with healing properties is very promising, and in this way, the development of topical skin creams with anti-herpetic and antimelanoma activities can also be a good alternative for the broader technological use of lasiodiplodan.

References

Bacic A, Fincher G, Stone B (eds) (2009) Chemistry, biochemistry and biology of (1-3)-β-Glucans and related polysaccharides. Academic Press, Cambridge

Bai N, Gu M, Zhang W, Xu W, Mai K (2014) Effects of β-glucan derivatives on the immunity of white shrimp *Litopenaeus vannamei* and its resistance against white spot syndrome virus infection. Aquaculture 426–427:66–73

Barbosa AM, Steluti RM, Dekker RFH, Cardoso MS, Corradi Da Silva ML (2003) Structural characterization of Botryosphaeran: A (1→3;1→6)-β-D-glucan produced by the ascomyceteous fungus, *Botryosphaeria* sp. Carbohydr Res 338:1691–1698

Biswas A, Selling GS, Shogren RL, Willett JL, Buchanan CM, Cheng HN (2009) Iodine-catalyzed esterification of polysaccharides. Chim Oggi 27:33–35

Bongiovani RAM, Silveira JLM, Penna ALB, Dekker RFH, Barbosa-Dekker AM, Corradi Da Silva ML (2009) Caracterização reológica dos botriosferanas produzidos pelo *Botryosphaeria rhodina* MAMB-05 em glucose, sacarose e frutose como fontes de carbono. Braz J Food Technol 12:53–59

Calegari GC, Santos VAQ, Teixeira SD, Barbosa-Dekker AM, Dekker RFH, Cunha MAA (2017) Sulfonation of (1→6)-β-D-Glucan (lasiodiplodan) and its antioxidant and antimicrobial potential. J Pharm Pharmacol 5:850–863

Castillo NA, Valdez AL, Fariña JI (2015) Microbial production of scleroglucan and downstream processing. Front Microbiol 6:1–19

Chen F, Huang G (2018) Preparation and immunological activity of polysaccharides and their derivatives. Int J Biol Macromol 112:211–216

Chen Y, Zhang H, Wang Y, Nie S, Li C, Xie M (2014) Acetylation and carboxymethylation of the polysaccharide from *Ganoderma atrum* and their antioxidant and immunomodulating activities. Food Chem 156:279–288

Cumpstey I (2013) Chemical modification of polysaccharides. ISRN Org Chem 2013:1–27

Cunha MAA, Turmina JA, Ivanov RC, Barroso RR, Marques PT, Fonseca EAI, Fortes ZB, Dekker RFH, Khaper N, Barbosa AM (2012) Lasiodiplodan, an exocellular (1→6)-β-D-glucan from *Lasiodiplodia theobromae* MMPI: production on glucose, fermentation kinetics, rheology and anti-proliferative activity. J Ind Microbiol Biotechnol 39:1179–1188

Cunha MAA, Albornoz SL, Santos VAQ, Sánchez WN, Barbosa-Dekker AM, Dekker RFH (2017) Structure and biological functions of D-glucans and their applications. In: Rahman AU (ed) Studies in natural products chemistry, 1st edn. Elsevier, Amterdã, pp 309–337

Deng C, Fu H, Xu J, Shang J, Cheng Y (2015) Physiochemical and biological properties of phosphorylated polysaccharides from *Dictyophora indusiata*. Int J Biol Macromol 72:894–899

Eng F, Haroth S, Feussner K, Meldau D, Rekhter D, Ischebeck T, Brodhun F, Feussner I (2016) Optimized jasmonic acid production by *Lasiodiplodia theobromae* reveals formation of valuable plant secondary metabolites. PLoS One 11:e0167627

Free SJ (2013) Fungal cell wall organization and biosynthesis. In: Kumar D (ed) Advances in genetics, 1st edn. Elsevier, Amterdã, pp 33–82

García-Ochoa F, Santos VE, Casas JA, Gómez E (2000) Xanthan gum: production, recovery, and properties. Biotechnol Adv 18:549–579

Gessler NN, Egorova AS, Belozerskaya TA (2014) Melanin pigments of fungi under extreme environmental conditions (Review). Appl Biochem Microbiol 50:105–113

Giese EC, Gascon J, Anzelmo G, Barbosa AM, da Cunha MAA, Dekker RFH (2015) Free-radical scavenging properties and antioxidant activities of botryosphaeran and some other β-D-glucans. Int J Biol Macromol 72:125–130

Gow NAR, Latge JP, Munro CA (2017) The fungal cell wall: structure, biosynthesis, and function. Microbiol Spectr 5:1–25

Huang GL (2008) Extraction of two active polysaccharides from the yeast cell wall. Z Naturforsch 63:919–921

Huang J, Xu J, Wang Z, Khan D, Niaz SI, Zhu Y, Lin Y, Li J, Liu LL (2017) New lasiodiplodins from mangrove endophytic fungus *Lasiodiplodia* sp. 318. Nat Prod Res 31:326–332

Jackson KM, Ponnusamy M, Uthandi S (2017) Evaluation of jasmonic acid production by *Lasiodiplodia theobromae* under Submerged fermentation. Int J Curr Microbiol App Sci 6:1635–1639

Kagimura FY, Cunha MAA, Barbosa AM, Dekker RFH, Malfatti CRM (2015a) Biological activities of derivatized D-glucans: a review. Int J Biol Macromol 72:588–598

Kagimura FY, Cunha MAA, Theis TV, Malfatti CRM, Dekker RFH, Barbosa AM, Teixeira SD, Salomé K (2015b) Carboxymethylation of (1→6)-β-glucan (lasiodiplodan): Preparation, characterization and antioxidant evaluation. Carbohydr Polym 127:390–399

Khan AA, Gani A, Masoodi FA, Amin F, Wani IA, Khanday FA, Gani A (2016) Structural, thermal, functional, antioxidant & antimicrobial properties of β-D-glucan extracted from baker's yeast (*Saccharomyces cereviseae*) - effect of gamma-irradiation. Carbohydr Polym 140:442–450

Kumar CG, Mongolla P, Pombala S (2018) Lasiosan, a new exopolysaccharide from *Lasiodiplodia* sp. strain B2 (MTCC 6000): structural characterization and biological evaluation. Process Biochem 2:1–8

Leung MYK, Liu C, Koon JCM, Fung KP (2006) Polysaccharide biological response modifiers. Immunol Lett 105:101–114

Li S, Xiong Q, Lai X, Li X, Wan M, Zhang J, Yan Y, Cao M, Lu L, Guan J, Zhang D, Lin Y (2016) Molecular modification of polysaccharides and resulting bioactivities. Compr Rev Food Sci Food Saf 15:237–250

Li S, Dai S, Shah NP (2017) Sulfonation and antioxidative evaluation of polysaccharides from pleurotus mushroom and *Streptococcus thermophilus* bacteria: a review. Compr Rev Food Sci Food Saf 16:282–294

Liu H, Li Y, Gao J, Shi A, Liu L, Hu H, Putri N, Yu H, Fan W, Wang Q (2016) Effects of microfluidization with ionic liquids on the solubilization and structure of β-D-glucan. Int J Biol Macromol 84:394–401

Machová E, Čížová A, Bystrický P (2014) Effect of carboxymethylation on antioxidant properties and radical degradation of mannans and glucans. Carbohydr Polym 112:603–607

Mahapatra S, Banerjee D (2013) Fungal exopolysaccharide: production, composition and applications. Microbiol Insights 6:1–16

Malfatti CRM, Santos FS, Wouk J, Silva LA, Michel RG, Snak AL, Czervinski T, Cunha MAA, Barbosa AM, Dekker RFH (2017) Intracerebroventricular administration of the (1→6)-β-D-glucan (lasiodiplodan) in male rats prevents D-penicillamine-induced behavioral alterations and lipoperoxidation in the cortex. Pharm Biol 55:1289–1294

Mello MB, Machado CS, Ribeiro DL, Aissa AF, Burim RV, Cunha MAA, Barcelos GRM, Antunes LMG, Bianchi MLP (2017) Protective effects of the exopolysaccharide lasiodiplodan against DNA damage and inflammation induced by doxorubicin in rats: cytogenetic and gene expression assays. Toxicology 376:66–74

Mendes SF, Santos O, Barbosa AM, Vasconcelos AFD, Aranda-Selverio G, Monteiro NK, Dekker RFH, Pereira MS, Tovar AMF, Mourão PAS, Silva MLC (2009) Sulfonation and anticoagulant activity of botryosphaeran from *Botryosphaeria rhodina* MAMB-05 grown on fructose. Int J Biol Macromol 45:305–309

Murry JP, Godoy J, Mukim A, Swann J, Bruce JW, Ahlquist P, Bosque A, Planelles V, Spina CA, Young JAT (2014) Sulfonation pathway inhibitors block reactivation of latent HIV-1. Virology 471:1–12

Oliveira KSM, Di M, Cordeiro LMC, Costa MF, Toledo KA, Iacomini M, Babosa AM, Dekker RFH, Nascimento VMG (2015) (1→6)-and (1→3)(1→6)-β-glucans from *Lasiodiplodia theobromae* MMBJ: structural characterization and pro-inflammatory activity. Carbohydr Polym 133:539–546

Pengkumsri N, Sivamaruthi BS, Sirilun S, Peerajan S, Kesika P, Chaiyasut K, Chaiyasut C (2017) Extraction of β-glucan from *Saccharomyces cerevisiae*: comparison of different extraction methods and *in vivo* assessment of immunomodulatory effect in mice. Food Sci Technol 37:124–130

Queiroz EAIF, Fortes ZB, Cunha MAA, Barbosa AM, Khaper N, Dekker RFH (2015) Antiproliferative and pro-apoptotic effects of three fungal exocellular β-glucans in MCF-7 breast cancer cells is mediated by oxidative stress, AMP-activated protein kinase (AMPK) and the Forkhead transcription factor, FOXO3a. Int J Biochem Cell Biol 67:14–24

Rahar S, Swami G, Nagpal N, Nagpal M, Singh G (2011) Preparation, characterization, and biological properties of β-glucans. J Adv Pharm Technol Res 2:94–103

Saldanha RL, Garcia JE, Dekker RFH, Vilas-Boas LA, Barbosa AM (2007) Genetic diversity among Botryosphaeria isolates and their correlation with cell wall-lytic enzyme production. Braz J Microbiol 38:259–264

Samuelsen ABC, Schrezenmeir J, Knutsen SH (2014) Effects of orally administered yeast-derived beta-glucans: a review. Mol Nutr Food Res 58:183–193

Sánchez WN, Santos VAQ, Teixeira SD, Barbosa-Dekker AM, Dekker RFH, Cunha MAA (2018) Acetylated (1→6)-β-D-Glucan (Lasiodiplodan): chemical derivatization, characterization and antioxidant activity. J Pharm Pharmacol 6:320–332

Sassaki GL, Ferreira JC, Glienke-Blanco C, Torri G, De Toni F, Gorin PAJ, Iacomini M (2002) Pustulan and branched β-galactofuranan from the phytopathogenic fungus *Guignardia citricarpa*, excreted from media containing glucose and sucrose. Carbohydr Polym 48:385–389

Sechi NM, Calegari GC, Fonseca MS, Marques PT, Cunha MAA (2017) Obtenção e caracterização de lasiodiplodana fosforilada com trimetafosfato de sódio. Synerg scyentifica UTFPR 12:132–140

Smiderle FR, Alquini G, Tadra-Sfeir MZ, Iacomini M, Wichers HJ, Van Griensven LJLD (2013) *Agaricus bisporus* and *Agaricus brasiliensis* (1→6)-β-D-glucans show immunostimulatory activity on human THP-1 derived macrophages. Carbohydr Polym 94:91–99

Stier H, Ebbeskotte V, Gruenwald J (2014) Immune-modulatory effects of dietary yeast Beta-1, 3/1, 6-D-glucan. Nutr J 13:1–9

Sultan S, Sun L, Blunt JW, Cole ALJ, Munro MHG, Ramasamy K, Weber JFF (2014) Evolving trends in the dereplication of natural product extracts. 3: further lasiodiplodins from *Lasiodiplodia theobromae*, an endophyte from Mapania kurzii. Tetrahedron Lett 55:453–455

Sun Z, He Y, Liang Z, Zhou W, Niu T (2009) Sulfation of (1,3)-β-D-glucan from the fruiting bodies of *Russula virescens* and antitumor activities of the modifiers. Carbohydr Polym 77:628–633

Survase SA, Saudagar PS, Singhal RS (2007) Use of complex media for the production of scleroglucan by *Sclerotium rolfsii* MTCC 2156. Bioresour Technol 98:1509–1512

Theis TV (2018) Carboximetilação da (1,6)-β-D-glucana (lasiodiplodana): influência da concentração do agente derivatizante sobre o grau de substituição da molécula. Dissertation, Universidade Tecnológica Federal do Paraná, Pato Branco

Theis TV, Calegari GC, Santos VAQ, Zorel Junior HE, Barbosa AM, Dekker RFH, Cunha MAA (2017) Exocellular (1→6)-β-D-glucan (lasiodiplodan): Carboxymethylation, thermal behavior, antioxidant and antimicrobial activity. Am J Immunol 13:19–33

Treiman DM (2001) GABAergic mechanisms in epilepsy. Epilepsia 42:8–12

Túrmina JA, Carraro E, Cunha MAA, Dekker RFH, Barbosa AM, Santos FS, Silva LA, Malfatti CRM (2012) Toxicological assessment of β-(1→6)-glucan (lasiodiplodan) in mice during a 28-day feeding study by gavage. Molecules 17:14298–14309

Vasconcelos AFD, Monteiro NK, Dekker RFH, Barbosa AM, Carbonero ER, Silveira JLM, Sassaki GL, Da Silva R, Silva MLC (2008) Three exopolysaccharides of the β-(1→6)-D-glucan type and a β-(1→3;1→6)-D-glucan produced by strains of *Botryosphaeria rhodina* isolated from rotting tropical fruit. Carbohydr Res 343:2481–2485

Vasconcelos AFD, Dekker RFH, Barbosa AM, Carbonero ER, Silveira JLM, Glauser B, Pereira MS, Silva MLC (2013) Sulfonation and anticoagulant activity of fungal exocellular β-(1→6)-D-glucan (lasiodiplodan). Carbohydr Polym 92:1908–1914

Venkatesagowda B, Ponugupaty E, Barbosa-Dekker AM, Dekker RFH (2017) The purification and characterization of lipases from *Lasiodiplodia theobromae*, and their immobilization and use for biodiesel production from coconut oil. Appl Biochem Biotechnol 185:619–640

Vlaev SD, Pavlova K, Rusinova-Videva S, Georgieva K, Georgiev D (2016) Agitation effects and kinetic constants of exoglucomannan production by antarctic yeast strain in a stirred tank bioreactor. Chem Biochem Eng Q J 30:393–400

Vogel HJ (1956) A convenient growth medium for *Neurospora* (Medium N). Microb Genet Bull 13:42–43

Wang Y, Yu Y, Mao J (2009) Carboxymethylated β-glucan derived from *Poria cocos* with biological activities. J Agric Food Chem 57:10913–10915

Wang Y, Mo Q, Li Z, Lai H, Lou J, Liu S, Mao J (2012) Effects of degree of carboxymethylation on physicochemical and biological properties of pachyman. Int J Biol Macromol 51:1052–1056

Wang Q, Chen S, Han L, Lian M, Wen Z, Jiayinaguli T, Liu L, Sun R, Cao Y (2014) Antioxidant activity of carboxymethyl (1→3)-β-D-glucan (from the sclerotium of *Poria cocos*) sulfate (*in vitro*). Int J Biol Macromol 69:229–235

Wang Q, Sheng X, Shi A, Hu H, Yang Y, Liu L, Fei L, Liu H (2017) β-Glucans: relationships between modification, conformation and functional activities. Molecules 22:1–13

Wan-Mohtar WAAQI, Young L, Abbott GM, Clements C, Harvey LM, McNeil B (2016) Antimicrobial properties and cytotoxicity of sulfated (1,3)-β-D-glucan from the mycelium of the mushroom *Ganoderma lucidum*. J Microb Biotechnol 26:999–1010

Xu C, Leppänen AS, Eklund P, Holmlund P, Sjöholm R, Sundberg K, Willför S (2010) Acetylation and characterization of spruce (*Picea abies*) galactoglucomannans. Carbohydr Res 345:810–816

Ye M, Yuan RY, He YL, Du ZZ, Ma XJ (2013) Phosphorylation and anti-tumor activity of exopolysaccharide from *Lachnum* YM120. Carbohydr Polym 97:690–694

Zhang Y, Lu X, Fu Z, Wang Z, Zhang J (2011) Sulphated modification of a polysaccharide obtained from fresh persimmon (*Diospyros kaki* L.) fruit and antioxidant activities of the sulphated derivatives. Food Chem 127:1084–1090

Zhang Y, Kong H, Fang Y, Nishinari K, Phillips GO (2013) Schizophyllan: a review on its structure, properties, bioactivities and recent developments. Bioact Carbohydr Diet Fibre 1:53–71

Zhang J, Cao Y, Wang J, Guo X, Zheng Y, Zhao W, Mei X, Guo T, Yang Z (2016) Physicochemical characteristics and bioactivities of the exopolysaccharide and its sulphated polymer from *Streptococcus thermophilus* GST-6. Carbohydr Polym 146:368–375

Zhu F, Du B, Xu B (2016) A critical review on production and industrial applications of beta-glucans. Food Hydrocoll 52:275–288

Chapter 11
Botryosphaeran – A Fungal Exopolysaccharide of the (1→3)(1→6)-β-D-Glucan Kind: Structure and Biological Functions

Robert F. H. Dekker, Eveline A. I. F. Queiroz, Mario A. A. Cunha, and Aneli M. Barbosa-Dekker

Abstract A fungal isolate (MAMB-05) from a stem canker on a eucalypt tree, molecularly classified as *Botryosphaeria rhodina*, produced an exopolysaccharide (EPS) of the β-D-glucan type when cultivated on glucose by submerged fermentation. Isolation and elucidation of the chemical structure demonstrated that the β-glucan was of the (1→3)(1→6)-linked type and was named botryosphaeran. When cultivated on different carbohydrates, *B. rhodina* MAMB-05 produced a *family* of structurally related botryosphaerans sharing the same backbone chain of (1→3)-linked D-glucosidic residues, but varied in the degree of branching on C-6 with glucose and gentiobiose. A branch point occurred on every fifth glucose residue along the backbone chain for the botryosphaeran produced on glucose (EPS_{GLC}) and sucrose (EPS_{SUC}) and one in every three glucose residues when produced on fructose (EPS_{FRU}). Details of the chemical structures were resolved by methylation, Smith degradation, FT-IR, and ^{13}C NMR. Membrane-modifying agents (soybean oil, Tween 80) enhanced botryosphaeran production without altering its chemical structure. Sulfonylation of botryosphaeran increased water solubility and conferred new functions, anticoagulation and antiviral activity. Through extensive screening,

R. F. H. Dekker (✉)
Programa de Pós-graduação em Engenharia Ambiental, Universidade Tecnológica Federal do Paraná, Londrina, Paraná, Brazil
e-mail: xylanase@gmail.com

E. A. I. F. Queiroz
Núcleo de Pesquisa e Apoio Didático em Saúde (NUPADS), Instituto de Ciências da Saúde, Câmpus Universitário de Sinop, Universidade Federal de Mato Grosso, Sinop, MT, Brazil

M. A. A. Cunha
Departamento de Química, Universidade Tecnológica Federal do Paraná, Pato Branco, Paraná, Brazil

A. M. Barbosa-Dekker
Departamento de Química, Universidade Estadual de Londrina, Londrina, Paraná, Brazil

E. Cohen, H. Merzendorfer (eds.), *Extracellular Sugar-Based Biopolymers Matrices*, Biologically-Inspired Systems 12, https://doi.org/10.1007/978-3-030-12919-4_11

botryosphaeran was found to be non-mutagenic and non-genotoxic and is regarded as having Generally Recommended As Safe (GRAS) status. The biopolymer exhibited strong antimutagenic/anticlastogenic activity being chemoprotective against several cancer chemotherapy drugs. Botryosphaeran demonstrated hypoglycemia in diabetes-induced rats, and hypocholesterolemia in mice and rats conditioned on a high-lipid ration. Antiproliferative activity was demonstrated in breast cancer MCF-7 cells, was associated with apoptosis, necrosis, and oxidative stress, and mediated by AMP-activated protein kinase and forkhead transcription factor, FOXO3a. This chapter addresses the studies carried out with botryosphaeran.

11.1 Introduction

The English poet *John Milton* II (1608–1674) in 1645 was the first to give a description that defined "polysaccharides" when he wrote in his poem *L'Allegro*:

"*. . . . many a winding bout*
Of linked sweetness long drawn out . . . ."

This first mention perfectly described what today's knowledge constitutes of a description of the "polysaccharides" based upon the chemical and physical structures of these complex biomacromolecules composed of sugars. Yet in Milton's time "polysaccharides" were unknown and had not been described chemically. Polysaccharides are defined as naturally occurring biological macromolecules (*winding bout* and *long drawn out*) composed of sugar-linked building blocks (*linked sweetness*) that exert highly varied functions in all living organisms.

The term exopolysaccharide describes exocellular carbohydrate biomacromolecules secreted by microbial species (bacteria, fungi, microalgae) into the culture media (fermentation broth) when they are cultivated under conditions of submerged fermentation. These biopolymers are constituted of repeat units of various sugars linked by various glycosidic bonds of either α- or β-anomeric configuration that can be branched with single or multiple sugar residues also of different linkages and configurations. The sugars depending upon their biological source can be neutral (uncharged), acidic (uronic acids), or basic (amino sugars) and can exist in the pyranoside or furanoside form. Altogether, polysaccharides constitute biopolymers of complex heterogeneous structures that may be soluble or sparingly soluble in aqueous solutions and possess a high degree of polymerization being of large molecular mass. Knowledge on the chemical structures of polysaccharides is important in our understanding of their properties and functions. These carbohydrate biopolymers are formed enzymatically by condensation of various monosaccharides linked through specific glycosidic bonds producing compounds of high molecular weight with peculiar physicochemical and biological properties.

Microorganisms produce polysaccharides of three distinct types: intracellular (storage), extracellular (capsular and slime, biofilm), and structural forms (cell wall). The exopolysaccharides are exocellular in origin and are further classified as capsular, those integral with the exterior of the cell wall and those produced as loose slimes (biofilms) that accumulate in large quantities outside the cell wall and diffuse freely into the extracellular environment.

Many bacteria have been exploited for the commercial production of exopolysaccharides. Well-known examples include dextran, cellulose (insoluble), curdlan, gellan, and xanthan that have found applications in foods and cosmetic and pharmaceutical products (e.g., as blood plasma replacements, artificial skins in treating burn victims, hydrogels for drug delivery, viscosity enhancers, and gelling agents, among others). Other important industrial applications of microbial (and plant) polysaccharides are as emulsifying and foam-stabilizing agents, as food coating and thickening agents, and in pharmaceutical formulations as modified drug delivery systems.

Polysaccharides can present biological functions recognized for their medical and health benefits through modifying biological responses (Bohn and BeMiller 1995) that enhance the immune system systemically as immuno-potentiators (Savelkoul et al. 2013). Immunostimulatory polysaccharides such as the (1→3)-β-D-glucans are capable of interacting with the immune system and activate the innate and adaptive immune responses in the host (Ferreira et al. 2015; Snarr et al. 2017).

Chemical modification by adding functional groups along the polysaccharide chain, such as *O*-acetyl, carboxymethyl, phosphoryl, and sulfonyl groups (Cumpstey 2013; see chapter 3), changes the physicochemical properties of the modified polysaccharides, and this can impact on their biological functions (Kagimura et al. 2015; Li et al. 2015; Cunha et al. 2017; Chen and Huang 2018).

Many fungal polysaccharides present biological activities, and some in their in situ form as macro-fungi (macromycetes) such as mushrooms and fungal brackets have been used in traditional Chinese, Japanese, and Korean folkloric medicines for millennia to therapeutically treat human disease conditions including inflammation, diabetes, and cancer (Wasser 2002, 2014). The more common medicinal fungi are the basidiomycetes, for example, the bracket mushrooms that include *Ganoderma lucidum* (called reishi in Japan and ling zhi in China), *Lentinus edodes* (shiitake), and *Grifola frondosa* (maitake or keisho in Chinese). The ascomycete *Cordyceps militaris* is also an important medicinal mushroom.

One highly studied group of polysaccharides from the kingdom of Fungi is the noncellulosic β-D-glucans produced by the *Basidiomycota* (basidiomycetes), mostly ligninolytic white-rot fungi (Osińska-Jaroszuk et al. 2015). They can produce β-glucans exocellularly when cultivated under submerged fermentation conditions; for example, lentinan from *Lentinula edodes* (Nikitina et al. 2007), schizophyllan from *Schizophyllum commune* (Zhang et al. 2013), and scleroglucan from *Sclerotium rolfsii* (Castillo et al. 2015) are produced commercially. The ascomycetes, which is the largest phylum of fungi, also produce polysaccharides of the β-D-glucan kind, some of which can be produced exocellularly (Osińska-Jaroszuk et al. 2015), for example, botryosphaeran from *B. rhodina* (Barbosa et al. 2003; Selbmann et al. 2003) and lasiodiplodan from *Lasiodiplodia theobromae* (Cunha et al. 2017; see chapter 10).

The β-glucans are chemically heterogeneous in structure and are chiefly of the (1→3)-β-D-glucosidic type with branches containing D-glucose residues through β-(1→6)-linkages (Stone 2009). The chemistry and biology of the (1→3)-β-D-glucans have been much studied since the late 1950s, when first described, and have continued to attract interest globally because of their structure-function

relationships. An excellent book on the (1→3)-β-D-glucans was authored by Bruce A. Stone in 1992 (Stone and Clarke 1992) of *La Trobe University*, Melbourne, Australia: one of the *founding fathers* in the field. An updated book on the subject edited by Stone followed in 2009 (Bacic et al. 2009).

An uncommon and rarer group of fungal exocellular β-glucans that has attracted interest is the linear, unbranched (1→6)-β-D-glucans, e.g., lasiodiplodan produced by several strains of *Lasiodiplodia theobromae* (Vasconcelos et al. 2008; Oliveira et al. 2015) and pustulan from *Guignardia citricarpa* (Sassaki et al. 2002); see also chapter 10. Polysaccharides of this kind exist mainly as matrix constituents of the fungal cell wall and in yeasts can have highly complex structures that confer water insolubility (Aimanianda et al. 2009; Free 2013).

Both the (1→3)(1→6)- and (1→6)-linked β-D-glucan types also participate as structural elements in the cell wall of the fungi and can constitute from 65% to 90% of the total β-glucans present. They are found in a matrix with other cell wall constituents that includes other polysaccharides such as chitin, glucans of various linkages and of α- and β-configurations, and mannans, proteins and glycoproteins comprising oligomannoside chains, lipids, and melanins (Free 2013; Gow et al. 2017).

The β-glucans can vary in fine structure, molecular weight, extent of branching, and conformation (single and triple helices), all of which confer a crucial role on their biological activities (Leung et al. 2006; Wang et al. 2017). In fungal cells the (1→3)-β-D-glucans are synthesized within the cytoplasm by the enzyme β-(1→3)-glucan synthase. The biosynthesis of fungal β-glucans, which are mainly cell wall bound, was the subject of a comprehensive review by Papaspyridi et al. (2018). Briefly, fungal (1→3)-β-glucan chains of up to 1500 glucose monomers are synthesized in vivo in the cytoplasm from the glucosyl donor, uridine diphosphate glucose (UDPG), and catalyzed by β-glucan synthase (UDP-glucose, (1→3)-β-D-glucan 3-β-D-glucosyl transferase), a plasma membrane-associated enzyme. The polymer chain is then translocated to the periplasmic space of the cell wall by a transmembrane enzyme complex, where further modifications to the polysaccharide structure take place, specifically the addition of β-(1→6)-glucosidic side branches, and where (1→3)-β-glucan chains are connected to each other via (1→6)-linkages. A multistep enzymatic process involving chain initiation, chain elongation, and the addition of branched substituents along the biopolymer chain is involved to form a three-dimensional molecular network of the (1→3)-β-glucans integrated in the matrix of the fungal cell wall (Papaspyridi et al. 2018).

The β-glucans are known to possess strong antioxidant activity through scavenging of free radicals thereby avoiding damage by reactive oxygen species (Kogan et al. 2005). Botryosphaeran likewise exhibited free-radical scavenging properties and antioxidant activities (Giese et al. 2015a).

The fungal (1→3)-β-D-glucans are well-recognized in possessing medicinal properties effective in treating human disease conditions including microbial infections, inflammation, diabetes, cardiovascular diseases, dyslipidemia, and cancers (Chen and Seviour 2007; Chen and Raymond 2008; Vetvicka and Vetvickova 2012).

The varied biological functions of the (1→3)-β-D-glucans raise the question on the mechanisms behind the manifestation of the biological response events.

A possible mechanism to explain the action of β-glucans is through their recognition by immune cells via binding to pattern recognition receptors on the surface of these cells. The β-glucans are recognized as pathogen-associated molecular patterns and initiate the *innate* and *adaptive* immune response of the host. On binding to cell surface receptors on immune cells (e.g., macrophages, dendritic cells), they trigger an innate immune response signaling the secretion of cytokines (signaling proteins/peptides influencing cellular functions) and tumor necrosis factor-α (pro-inflammatory cytokine). Cytokines, in turn, activate an adaptive immune response (B and T lymphocytes) that results in the systemic activation of the whole immune system. The innate and adaptive immune responses can play important roles in preventing tumors (Vesely et al. 2011) and in treating cancers (Dougan and Dranoff 2009).

In cancer immunotherapy an attractive approach is by stimulating the immune system through targeting pattern recognition receptors on immune cells (Goutagny et al. 2012). The (1→3)-β-glucans bind specific receptor sites such as dectin-1, toll-like receptors (TLRs), and complement receptor 3 (CR-3) on the immune cells activating the innate and adaptive immune responses that contribute to antitumor activity (Albeituni and Yan 2013; Legentil et al. 2015). Once bound to their specific receptors, the (1→3)-β-glucans trigger gene expression and signal cytokine and chemokine secretion within immune cells that can have a direct antiproliferative effect on cancer cells, which is associated with cell cycle arrest, apoptosis, and oxidative stress (Malini et al. 2015; Queiroz et al. 2015).

This then in a "nutshell" provides some answers on how the (1→3)-β-glucans may elicit their biological activities!

In this chapter we highlight and discuss the developments of our research on the (1→3)(1→6)-β-D-glucan named botryosphaeran (see https://en.wikipedia.org/wiki/Botryosphaeran), an exopolysaccharide produced by the ascomycetous fungal isolate *Botryosphaeria rhodina* MAMB-05 when cultured on glucose. We describe our investigations of its chemical structure, chemical derivatization, production by submerged fermentation, mutagenicity and antimutagenicity, and various biological functions such as controlling glycaemia in diabetes, hypotriglyceridemia, and hypocholesterolaemia and present a mechanistic insight in its involvement in anticancer activity.

11.2 Historical Developments Leading to the Discovery of Botryosphaeran

Our studies on botryosphaeran, a (1→3)(1→6)-β-D-glucan, began in 1994 and arose quite by accident from a project investigating the *Bioremediation of Aromatic Compounds by Ligninolytic Fungi* initiated by one of us at *Murdoch University* (Perth, Western Australia) within the *School of Biological and Environmental Sciences*.

The project considered enzymes that could remediate aromatic and xenobiotic compounds through screening appropriate wood-decay fungi from various

biological niches. Fungi that were ligninolytic (those capable of utilizing lignin during growth) were being sought by screening ecological niches within the metropolitan area of the city of Perth and nearby rural areas.

Lignin is a natural aromatic biopolymer found in the plant cell wall and comprises 85% aromatic and 15% phenolic structures within the lignin molecule (Li et al. 2016). Lignin is recalcitrant to most microbial species but can be attacked by certain fungi (e.g., the white-rot basidiomycetes) that possess the biochemical metabolic machinery to utilize lignin by producing exocellular enzymes, mainly the peroxidases (lignin-, manganese-, and versatile-dependent types), polyphenol oxidases (laccases, multi-copper oxidases), cellobiose dehydrogenases, and others (Pollegioni et al. 2015; Janusz et al. 2017).

Another phylum of fungi, namely, the *Ascomycota* that include the ascomycetes, that inhabits the forest ecosystem including soils is responsible for decomposing forest and plant litter (leaf, branches, trunks, and dead trees). Since the 1990s, ascomycetes have increasingly been recognized as capable of attacking lignin producing a suite of enzymes similar to those produced by the *Basidiomycota* (Barbosa et al. 1996).

While searching for suitable fungi in a park near Murdoch University in May 1994, a sample of a fungus (black fruiting bodies or pycnidia) colonizing a canker on the stem of a eucalypt tree was collected and taken to the lab to isolate the microbes inhabiting this niche. On plating out the canker sample onto potato dextrose agar plates, one fungus stood out and grew profusely producing a white colony that was isolated and subsequently purified and selected for further study. This fungal isolate was designated MAMB-05 and was morphologically characterized as belonging to the genus *Botryosphaeria*. In our earlier publications on this fungus, we referred to the fungus simply as *Botryosphaeria* sp. MAMB-05. Later (2004), the isolate was characterized to the species level as *Botryosphaeria rhodina* (GenBank Accession Number: AY612337; Garcia et al. 2004) by molecular biology techniques – sequencing the internal transcribed spacer (ITS: ITS1, 5.8S and ITS2) regions of rDNA (Saldanha et al. 2007).

Dozens of fungal specimens collected in parks throughout the Perth metropolitan area, as well as those housed in the Plant Pathology Culture Collection at Murdoch University, were screened for their ability to decolorize the polymeric dye, Poly R-478, an indicator of the initial transformation of lignin (Barbosa et al. 1996). Laccases, enzymes that could be responsible for the bioremediation of aromatic and phenolic compounds, were sought and simultaneously screened. Among the collection of fungi evaluated, only *B. rhodina* MAMB-05 stood out as producing high laccase titers (units of enzyme per mL of culture fluid) when grown by submerged fermentation in flasks under shaking conditions on liquid basal medium (glucose and a minimum salt medium; Vogel 1956). Consequently, this fungal isolate was selected for further studies that have continued over the following 25 years evolving into two principal lines of research: enzymes and polysaccharides.

During the cultivation of *B. rhodina* MAMB-05 on basal medium, we noticed that the fermentation broth became viscous during laccase production, which indicated an exocellular biopolymer was secreted during the fermentation. To discover the chemical cause of the viscous nature, we contemplated that the biopolymer could

be carbohydrate in nature, i.e., a polysaccharide. The biopolymer was isolated on precipitating the cell-free fermentation broth with alcohol, and upon acid hydrolysis, glucose was found to be the only hydrolysis product, i.e., the biopolymer was a glucan. The isolated polysaccharide was treated with several different commercial crude enzyme preparations that included α- and β-glucanases to elucidate the nature of the glucosidic linkages of this biopolymer. Treatment with α-glucanases (amylase, glucoamylase) confirmed that the biopolymer was not starch nor glycogen-like in nature. Attack by cellulase (β-(1→4)-glucanase) and β-(1→3)-glucanase resulted in glucose and a series of gluco-oligosaccharides, as confirmed by the specific glucose oxidase assay and HPLC analysis. This finding led us to suspect that the biopolymer was an exopolysaccharide of the β-glucan type with both (1→3)- and (1→4)-glucosidic linkages due to the specificities of the β-glucanase preparations tested (Dekker and Barbosa 2001). Later studies (2003) on the detailed chemical structure of this exopolysaccharide confirmed us to be wrong. It was *unequivocally* demonstrated to be a β-D-glucan of mixed linkages of the (1→3)(1→6)-glucosidic type (Barbosa et al. 2003) and was named botryosphaeran in accordance with the convention in naming new polysaccharides after the microbial genus.

A new line of study initiated in 2004 evolved from our curiosity: *"What kind of biological activities would be presented by botryosphaeran?"*

Overall, our research group since 2003 has been associated with multidisciplinary studies on botryosphaeran, which were developed by some 70 students at different levels of study involving collaborations mostly within Brazil universities but also in Canada. Since 2008 our group also studied an associated fungal exopolysaccharide (a (1→6)-β-D-glucan) from several strains of *Lasiodiplodia theobromae* (the anamorphic form of *B. rhodina*) that we named lasiodiplodan, and this topic is discussed in Chap. 10.

11.3 Fungi Belonging to *Botryosphaeriaceae*

Botryosphaeria belongs to the taxa *Botryosphaeriaceae* that constitutes a family of "sac-like (ascus)" fungi representative of the order *Botryosphaeriales* (phylum, *Ascomycota*) and comprises endophytes, saprobes, and plant pathogens. The family contains 23 genera and 187 species of *Botryosphaeriaceae* (Dissanayake et al. 2016). This group of fungi is widely distributed geographically in temperate and tropical climatic regions at latitudes ranging from 40° north and south of the equator.

As phytopathogens, *Botryosphaeria* spp. are plurivorous that colonize a wide range of host plants in agriculture and forestry and are of ecological and economic importance, causing severe diseases that result in economic losses globally in the hundreds of millions of dollars annually. The fungus attacks woody angiosperms and coniferous tree species and can be destructive toward plants of horticultural importance such as fruit trees and ornamental shrubs. Infection and colonization by *Botryosphaeria* can be initiated through plant injury and environmental stress factors, and there are no effective fungicides for controlling and combating cankers and dieback diseases

caused by *Botryosphaeria* spp. One of the natural plant hosts of *Botryosphaeria* is eucalypt tree species and, in particular, those of native forests distributed throughout Australia, where the fungus can cause severe destruction resulting in branch and whole-tree dieback diseases that can decimate whole native forests.

Botryosphaeria species as plant pathogens primarily direct their attack on the plant cell wall by producing key enzymes such as cellulases, xylanases, pectinases, and laccases that are associated with the breakdown of the plant cell wall components (Dekker et al. 2001). The enzymatic hydrolysis of the carbohydrate biopolymers, cellulose, xylan, and pectin liberates fermentable sugars (glucose, xylose, and galacturonic acid, respectively) that provide the carbon sources (substrates) for the fermentative synthesis of exocellular botryosphaeran (Steluti et al. 2004). We hypothesize that botryosphaeran, which has a high molecular mass (>1 x 10^6 Da) and forms a viscous solution (gel-like), is responsible for blocking the phloem and xylem vessels in infected tree branches and trunks that carry nutrients and water, respectively, to aerial parts of the plant, causing dieback diseases in the hosts.

The natural host for our *B. rhodina* isolate MAMB-05 was a eucalypt tree, to which the fungus is a virulent pathogen. On its isolation in the lab, and our continued use of this fungal isolate in studies over a 25-year period, the fungus has been cultivated mainly on glucose and sucrose and has never been exposed to its natural host (eucalypt wood) during this time. After countless generations of isolate MAMB-05 grown on glucose-/sucrose-containing media, we conclude that our fungal strain is no longer virulent as exemplified by the health status of various tree species (eucalypts, mango, avocado, and others) grown around our lab, where studies were conducted on producing bio-products from *B. rhodina* MAMB-05.

11.4 Chemical and Structural Characterization of the Exopolysaccharides from *Botryosphaeria rhodina* MAMB-05

An exopolysaccharide from a *Botryosphaeria* sp. (isolate MAMB-05) was first reported in 2001 and was characterized as a β-glucan of mixed linkage on the basis of degradation by specific β-glucanases (Dekker and Barbosa 2001). In 2002, another strain of *Botryosphaeria rhodina*, viz., DABAC-P82, was reported to also produce an exopolysaccharide when cultured on cornstarch hydrolyzates, but its chemical structure was not determined (Selbmann et al. 2002). In a follow-up study, this group reported a yield of exopolysaccharide of 17 g/L within 24 h of fermentation when the fungus was cultivated at pH 3.7 under optimized conditions on starch hydrolyzates (Selbmann et al. 2003). After isolating the exopolysaccharide from the culture fluid by alcohol precipitation, total hydrolysis (acid) of the biopolymer produced only glucose, hence a glucan. Structural analysis was performed by methylation followed by acid hydrolysis of the permethylated polysaccharide. Analysis of the permethylated alditol acetates by gas chromatography-mass spectrometry (GC-MS) revealed the exopolysaccharide to

be a glucan with a repeat unit of (1→3)-linkages accompanied by (1→6)-linked branch points, but its fine structure was not further elucidated. Specific enzymatic hydrolysis of the exopolysaccharide by (1→3)-β-glucosidases and the separation of the hydrolysis products by TLC revealed the presence of glucose and gentiobiose. The results of this study indicated that the exopolysaccharide of *B. rhodina* strain DABAC-P82 is a mixed-linked (1→3)(1→6)-glucan, presumably of the β-configuration. Low-angle laser light scattering analysis revealed a high molecular mass (4.875 x 10^6 Da).

In this chapter, we elaborate on several homogeneous exopolysaccharides, (1→3)(1→6)-β-glucans, produced when *Botryosphaeria* sp. MAMB-05 was cultivated on medium containing different carbohydrate substrates. Each of the exopolysaccharides produced was isolated and characterized (HPLC analysis of the acid hydrolyzates and FTIR spectroscopy) and was found to be (1→3)(1→6)-β-glucans that constituted a *family* of *botryosphaerans* (see Sects. 11.4.2 and 11.6.1). Three substrates (glucose, sucrose, and fructose) were chosen for detailed studies on the chemical structures of the exopolysaccharides produced by *B. rhodina* MAMB-05, followed later by an examination of their biological functions (see Sects.11.7, 11.8, and 11.9). These botryosphaerans are denoted as EPS_{GLC}, EPS_{SUC}, and EPS_{FRU}, respectively, when discussed.

11.4.1 The Chemical Structure of the Exopolysaccharide Produced on Glucose

The chemical structure of the exopolysaccharide (**EPS_{GLC}**) from *Botryosphaeria* sp. MAMB-05 was determined after its isolation following the cultivation of the fungus on glucose (basal) medium by submerged fermentation for 4.5 days at 28°C. The exopolysaccharide was precipitated from the cell-free fermentation broth with ethanol, and the recovered precipitate was redissolved in deionized water, extensively dialyzed, and freeze-dried to obtain the crude botryosphaeran preparation (EPS_{GLC}). The exopolysaccharide was purified, and the chemical structure of EPS_{GLC} was determined through methylation analysis, Smith degradation, FTIR, and ^{13}C NMR spectroscopy to elucidate the precise chemical details of the sugar moiety and the nature and configuration of the glycosidic linkages and the biopolymer's side branches (Barbosa et al. 2003).

Methylation of EPS_{GLC} was performed (Hakomori 1964), and acid hydrolysis of the permethylated polysaccharide followed by reduction and acetylation resulted in partially methylated alditol acetates. Analysis by GC-MS revealed the presence of 2,3,4,6-tetra-*O*-methyl-glucose, 2,4,6-tri-*O*-methyl-glucose, 2,3,4-tri-*O*-methyl-glucose, and 2,4-di-*O*-methyl-glucose as the main methylated sugar derivatives in the relative molar proportion of 26:36:16:22, respectively (see Table 11.1). The findings of methylation analysis demonstrated that the exopolysaccharide (EPS_{GLC}) of *Botryosphaeria* sp. MAMB-05 was a glucan consisting of a (1→3)-linked glucosyl

Table 11.1 Comparative analysis of the methylation products and molar ratios following permethylation of the botryosphaerans obtained from *Botryosphaeria rhodina* MAMB-05 grown on fructose (EPS_{FRU}), sucrose (EPS_{SUC}), and glucose (EPS_{GLC}) as carbon sources

	Molar ratios (%)		
	Botryosphaerans		
Methylated derivatives (*linkage types*)	EPS_{FRU}	EPS_{SUC}	EPS_{GLC}
(**I**) 2,3,4,6-tetra-*O*-methyl-glucose (*nonreducing terminal units*)	34	23	26
(**II**) 2,4,6-tri-*O*-methyl-glucose (*3-O-substituted glucosyl residues*)	20	47	36
(**III**) 2,3,4-tri-*O*-methyl-glucose (*6-O-substituted glucosyl residues*)	15	9	16
(**IV**) 2,4-di-*O*-methyl glucose (*3,6-di-O-substituted units*)	31	21	22

backbone substituted with approximately 22% branch points on C-6 of the glucose moiety. Methylation of periodate-oxidized botryosphaeran showed almost total disappearance of terminal units, these being representative of branched glucose/di-glucose residues. Dimethylated units disappeared following Smith degradation, which removed the oxidized residues attached to the branching points. The linear (1→3)-β-glucan obtained from periodate oxidation and Smith degradation indicated that the side chains consisted of a single glucose residue and also of a short-chained (1→6)-β-linked glucosyl disaccharide. The latter constituent was confirmed by the presence of 1,5,6-tri-*O*-acetyl-2,3,4-tri-*O*-methylglucitol (Table 11.1).

^{13}C NMR studies on the purified botryosphaeran (EPS_{GLC}) and the periodate-oxidized polysaccharide revealed that all the carbon lines were well resolved, and the chemical shifts agreed with literature reports (Gorin et al. 1993). ^{13}C NMR analysis (see Table 11.2) revealed no peaks that resonated around δ 100.0 ppm, which correspond to the α-configuration of anomeric carbons (α-glucose). Anomeric β-glucose carbons, which resonate downfield and peaks between δ 103.3 and 102.9 ppm, provided evidence that only β-anomeric carbons were present. FTIR spectroscopy, an important tool in connection with the structural characterization of carbohydrate biopolymers, confirmed β-anomeric carbons in botryosphaeran (EPS_{GLC}) with bands at 890 cm^{-1} (typical of (1→3)-β-glucans) and 1370 cm^{-1} (characteristic of β-glucans).

The ^{13}C NMR signal at δ 102.9 for botryosphaeran is attributable to 3-*O*-substituted glucose units of the main chain containing branched residues (glucose and/or gentiobiose) at C-6. The signal at δ 103.1 (C-1) is due to 3-*O*-substituted β-glucose anomeric carbon, and this also agreed with the signal at C-1 of the residual linear polysaccharide following Smith degradation. The signal at δ 70.1 is from the C-6 carbons, which are *O*-substituted and disappear following Smith degradation, while unsubstituted C-6 carbons show signals at δ 61.1–60.7. The signal at δ 61.1 was attributable to the free C-6 from the principal region of the 3-*O*-substituted glucan and was also found in the spectrum after Smith degradation (Table 11.2). Signals at δ 60.9 and 60.7 (C-6) indicate adjacent glucose residues substituted with glucose and/or gentiobiose branches, respectively. The 3-*O*-substituted carbon

Table 11.2 ^{13}C NMR spectral assignments for the carbon lines of botryosphaerans (EPS_{GLC}, EPS_{SUC}, and EPS_{FRU}) and sulfonated botryosphaerans (EPS_{GLC}-S and EPS_{GLC}-RS) from *Botryosphaeria rhodina* MAMB-05

	Chemical shifts (δ, ppm)					
	Botryosphaerans (EPS_{GLC}, EPS_{SUC}, EPS_{FRU})					
Linked glucose residue	C-1	C-2	C-3	C-4	C-5	C-6
Glc*p*-(**1**→	103.3	73.5	75.5	68.8	76.7	61.1
→6)-Glc*p*-(1→	102.9	73.0	74.8	68.7	76.4	70.1
→**3**)-Glc*p*-(**1**→	103.1	73.0	86.6	68.7	76.7	61.1
						60.9
						60.7
→**3,6**)-Glc*p*-(**1**→	102.9	73.0	86.0	68.7	76.4	70.1
			85.5			
After Smith degradation						
→**3**)-Glc*p*-(**1**→	103.1	73.0	86.6	68.7	76.7	61.1
Sulfonated botryosphaerans (EPS_{GLC})						
EPS_{GLC}-S, EPS_{GLC}-RS[a]	101.3					
	100.9					~68.0
	100.6					

[a]Refers to once-sulfonated (S) and re-sulfonated (RS) botryosphaeran. Shifted signals appear at C-1, and the signal at C-6 was due to sulfonation

atoms from the main chain resonated between δ 85.5 and 86.3. In the ^{13}C NMR spectrum, the signal at δ 86.3 (C-3) resonated intensely and suggests that the (1→3)-β-glucan backbone chain contained a large number of regions with no substitutions. Signals at δ 86.0 and δ 85.5 (C-3) were attributed to →3,6-Glc*p*-1→ residues and were substituted with glucose and gentiobiose residues, respectively. The signal intensities found in substituted C-3, and free C-6 regions, suggest that the glucose substituents along the (1→3)-β-glucan backbone chain were distributed at random.

Fungal polysaccharides show irregular repeat structural features and differ from bacterial polysaccharides (e.g., capsular) that have regular and conserved structural domains (Raetz and Whitfield 2002). Bacterial exopolysaccharides (Nwodo et al. 2012) can be similar to those of fungi consisting of a backbone chain with appendages (e.g., dextran, xanthan) or without (e.g., curdlan, bacterial cellulose). The structural variations between microbial exopolysaccharides are determined during their synthesis by specific side-branching enzymes and/or through post-modification processes by specific enzymes that add sugar residues or trim the synthesized polysaccharides.

As the β-(1→3)-glucosidic linkages are more labile to acid hydrolysis than β-(1→6)-glucosidic linkages, it is possible to obtain gentiobiose and gentiotriose as hydrolysis products, which correspond, respectively, to glucose and gentiobiose linked at C-6 to the β-(1→3)-linked backbone chain. Partial acid hydrolyzates of botryosphaeran (EPS_{GLC}) and its fractionation resulted in a homologous series of

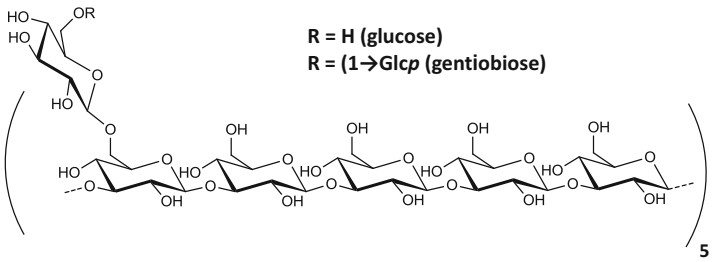

Fig. 11.1 Structure of botryosphaerans EPS_{GLC} and EPS_{SUC}; (1→3)(1→6)-β-glucans produced by *Botryosphaeria rhodina* MAMB-05 grown on glucose and sucrose, respectively. The degree of branching by glucose and/or gentiobiose units was 22% and 21%, respectively, indicating a branch point on every fifth glucose residue. Botryosphaeran produced on fructose (EPS_{FRU}) was more highly branched, 31%, with one branch point appearing at every three glucose residues along the (1→3)-β-glucan backbone chain (structure not shown)

β-(1→3)- and β-(1→6)-linked D-gluco-oligosaccharides identified by HPAEC/PAD (high-performance anion exchange chromatography with pulsed amperometric detection) analysis. The presence of gentiobiose in the hydrolyzate indicated a side branch composed of (1→6)-β-D-glucose, while gentiotriose presented evidence of a side branch consisting of a (1→6)-β-linked glucose disaccharide. The presence of laminaribiose and laminaritriose arise from cleavages of main-chain (1→3)-β-D-glucopyranosyl units upon acid hydrolysis.

From the foregoing discussion, the structural investigation concluded that botryosphaeran (EPS_{GLC}) from *B. rhodina* isolate MAMB-5 was a (1→3)-β-D-glucan with both single (1→6)-β-linked D-glucose and (1→6)-β-linked D-di-glucose (gentiobiose), side branches attached at random along the (1→3)-β-linked D-glucosyl backbone chain at a frequency of ~22%, i.e., one branch point (glucose or gentiobiose) to every five glucose residues along the chain (Barbosa et al. 2003) (see Fig. 11.1). Further evidence indicated that the proportion of glucose to gentiobiose along the backbone chain was 6:16 (Fonseca et al. 2011).

Soluble (1→3)-β-glucans are known to exist in several conformational forms that can include a single helix, triple helix, and random coil. Fungal branched-chain (1→3)(1→6)-β-D-glucans, e.g., scleroglucan and schizophyllan, adopt a triple-helix conformation that strongly influences biological activity (Yoshitomi et al. 2005). Similarly, botryosphaeran was found to exist in a triple-helix conformation (Giese et al. 2008). The conformation of polysaccharides can be determined by the Congo red dye inclusion method (Ogawa et al. 1972). Polysaccharides of the (1→3)(1→6)-β-D-glucan type exist in an ordered helical conformation and form a dye inclusion complex with Congo red in dilute aqueous NaOH solutions and undergo a shift in absorption maxima of the dye (λ_{max}) (Dong et al. 2006). The greater the λ_{max} shift, the higher the helical structure content (Fariña et al. 2001).

Botryosphaeran (EPS_{FRU}, see Sect. 11.4.3.), from *B. rhodina* MAMB-05 grown on fructose, presented more resistance than EPS_{GLC} to conformational transitions in

alkali medium, as indicated by a decrease in maximum wavelength (λ507 to λ495) between 0.25 and 0.35 M NaOH (Giese et al. 2008). EPS_{FRU} is more highly branched at C-6 than EPS_{GLC}. The presence of branched substituents at C-6 contributes to the enhancement of water solubility as the ramified chains of (1→3)(1→6)-β-D-glucans are outside the triple helix, thus avoiding the formation of insoluble aggregates (Bot et al. 2001).

11.4.2 A Family of Botryosphaerans

It was of interest to know whether *Botryosphaeria* sp. MAMB-05 grown on other carbohydrate substrates could also produce exopolysaccharides of the botryosphaeran kind (i.e., (1→3)(1→6)-β-D-glucans) and whether there would be variation in the chemical structures. Studies were conducted by growing *Botryosphaeria* sp. MAMB-05 on several carbohydrates as sole carbon source by submerged fermentation, followed by the isolation of the exopolysaccharides produced and later by determining their chemical composition (acid hydrolysis and analysis by HPLC) and constitution (FTIR spectroscopy). The influence of glucose concentration on the production of botryosphaeran by *Botryosphaeria* sp. MAMB-05 under submerged fermentation conditions revealed an optimal concentration of 50 g/L glucose with a concomitant viscosity reading of the cell-free fermentation broth of 12.3 centipoise.

When other carbohydrate substrates (galactose, mannose, fructose; lactose, sucrose, commercial sucrose, sugarcane molasses; sorbitol added at a concentration of 50 g/L) replaced glucose in the nutrient medium, they all produced exopolysaccharides, which, when isolated (ethanol precipitation) and hydrolyzed by acid, produced only glucose on analysis by HPLC. All of these exopolysaccharides, therefore, consisted exclusively of polymers comprising only D-glucose units, that is, they were β-glucans.

FTIR spectroscopy of the exopolysaccharides produced by *Botryosphaeria* sp. MAMB-05 presented bands at 882 and 1370 cm^{-1} characteristic of β-anomeric configuration of the main linkages of β-glucans indicating that all of the exopolysaccharides were of the β-glucan type. Further, FTIR bands at 1150, 1110, 1040, and 1000 cm^{-1} were due to (1→3)-di-*O*-substituted glucose residues, i.e., they all possessed a (1→3)-β-glucan backbone. Similar signals were reported for other β-glucans from several fungi.

Information gleaned from acid hydrolysis of each of the exopolysaccharides isolated (glucose being the only product), together with the analysis of the configuration (β-anomeric) of the glucosidic linkages of each exopolysaccharide by FTIR spectroscopy, demonstrated *unequivocally* that the exopolysaccharides from *Botryosphaeria* sp. MAMB-05 constituted a *family* of botryosphaerans (Steluti et al. 2004).

11.4.3 Influence of Carbohydrate Source on the Degree of Branching on Botryosphaeran

Botryosphaeria sp. MAMB-05 (molecularly classified in 2004 as *B. rhodina*; Garcia et al. 2004) when grown separately on fructose and sucrose as sole carbon sources secreted two exopolysaccharides (EPS_{FRU} and EPS_{SUC}, respectively) identified as botryosphaerans on the basis of glucose as the only acid hydrolysis product. FTIR spectroscopy established that these exopolysaccharides were of the β-anomeric configuration and contained (1→3)-di-*O*-substituted glucose residues (Steluti et al. 2004). They were of the (1→3)(1→6)-β-D-glucan type and members of the *family* of botryosphaerans as alluded to in Sect. 11.4.2 (Corradi da Silva et al. 2005).

Methylation of both purified exopolysaccharides (EPS_{FRU} and EPS_{SUC}) followed by GC-MS analysis of the alditol acetate permethylated sugar derivatives determined the nature of the glucosidic linkages as shown in Table 11.1. The results established that both botryosphaerans (EPS_{FRU} and EPS_{SUC}) constituted a (1→3)-linked glucosyl backbone substituted with branch points on C-6. The reduced content of 2,3,4-tri-*O*-methyl-glucose (III) of both exopolysaccharides indicated that the backbone consisted essentially of consecutive glucose residues linked by (1→3) bonds. The relatively low amount of 2,4,6-tri-*O*-methyl-glucose (II) in EPS_{FRU} by comparison to derivatives 2,3,4,6-tetra-*O*-methyl-glucose (I) and 2,4-di-*O*-methyl-glucose (IV) was in agreement with a highly branched structure (31% branching), while that for EPS_{SUC} was of somewhat lower degree of branching (21%). The results of methylation analysis compared with those of botryosphaeran (EPS_{GLC}) produced on glucose (Table 11.1), which showed a degree of branching of 22% (Barbosa et al. 2003). The proportion of glucose to gentiobiose along the backbone chain was 16:15 for EPS_{FRU} and for EPS_{SUC} 12:9, while that for EPS_{GLC} was 6:16 (Fonseca et al. 2011).

Both botryosphaerans (EPS_{FRU} and EPS_{SUC}) were subjected to Smith degradation. Partial acid hydrolysis followed by GC analysis of the alditol acetates indicated almost total disappearance of nonreducing terminal units. The linear (1→3)–βglucan obtained from periodate oxidation and Smith degradation of EPS_{FRU} and EPS_{SUC} indicated that the side chains constituted a single glucose residue and also a short-chained (1→6)-β-linked glucosyl disaccharide. The latter was confirmed by the presence of 1,5,6-tri-*O*-acetyl-2,3,4-tri-*O*-methylglucitol.

In accordance with the literature (Gorin et al. 1993), ^{13}C NMR spectra of the botryosphaerans (EPS_{FRU} and EPS_{SUC}) showed signals attributable to β(1→3)-glucans *O*-substituted on C-6, but did not reveal peaks resonating at δ 100.0 ppm indicative of the α-anomeric carbon configuration. Peaks between δ 103.3 and 102.9 ppm strongly indicated β-anomeric carbons. The chemical shift signals for each of the six carbons of EPS_{FRU} and EPS_{SUC} were identical to those found for EPS_{GLC} produced by *B. rhodina* MAMB-05 grown on glucose (see Table 11.2), and the glucose-linked residues corroborating to these are discussed in Sect. 11.4.1.

The ^{13}C NMR spectra of all three botryosphaerans (EPS_{GLC}, EPS_{FRU}, and EPS_{SUC}) were very similar (Table 11.2), differing only in the intensity of the signals.

In accordance with the results from methylation analysis, the most important difference was the higher amount of the 6-*O*-substituted derivative in EPS_{FRU}. This evidence was confirmed by the intensity of the signal at δ 70.1 and correlated to glucose residues with substitution on C-6 with glucose or gentiobiose, as found in similar ratios in the molecule in accordance with the methylation results.

The side-chain branching residues of EPS_{FRU} and EPS_{SUC} were determined by fragmenting botryosphaeran through partial acid hydrolysis and revealed a mixture of sugars comprising laminaribiose and laminaritriose (β-(1→3)-linked glucose residues) and gentiobiose and gentiotriose (β-(1→6)-linked glucose residues), as well as glucose. The detection of gentiotriose was confirmed through methylation analysis from the presence of the derivative 2,3,4-tri-*O*-methylglucitol.

In summary, the botryosphaeran EPS_{FRU} produced when the fungus was grown on fructose was more branched (31%) than the botryosphaerans produced on either glucose or sucrose, having a branch point to every three glucose units along the backbone chain with the proportion of glucose to gentiobiose of 16:15. Additionally, the relatively low amount of the 2,4,6-tri-*O*-methyl derivative of EPS_{FRU} in comparison to the tetra-*O*-methyl and the di-*O*-methyl derivatives agreed with a highly branched structure. Furthermore, the low value of the 2,3,4-tri-*O*-methyl derivative suggested that the backbone chain of this β-glucan consisted essentially of consecutive (1→3)-linked D-glucose residues with side branching on C-6 (Corradi da Silva et al. 2005). Our studies on botryosphaeran indicated that the extent of substitution of repetitive branching residues could be modified through the carbohydrate source of the nutrient medium in which the fungus was grown. Such manipulations, however, did not change the structure or molecular constitution of the botryosphaerans produced. Observations through manipulating the conditions of microbial culture have been reported in which it was possible to obtain appropriate polysaccharides for technical applications (Margaritis and Pace 1985).

11.5 Sulfonated Botryosphaerans: Structural Characterization, Properties, and Functions

Water solubility is a critical problem with most polysaccharides even those that are exocellularly secreted by microorganisms, and botryosphaeran is no exception, being limited in its solubility in water (3 g/L) after isolation from the cell-free fermentation broth and following lyophilization.

Certain physical structural features of the (1→3)-β-glucans include their high molecular weights, which are associated with the degree of polymerization, the chemical nature of the side-branch residues and their degree of ramification, and the conformation of the constituent chains in solution, all of which can lead to solubility problems of the polysaccharides in aqueous solutions (Wang et al. 2017). The problem of water solubility can be resolved either through fragmentation of the biopolymers into shorter chain lengths via hydrolysis, chemically (acids) or

enzymatically (glycan hydrolases), or through chemical modifications by adding particular functional groups to the hydroxyl positions along the polysaccharide chain. β-D-Glucans can be modified chemically through reactions involving *O*-acetylation, carboxymethylation, phosphorylation, and sulfonylation (Cumpstey 2013; see also chapter 3), which promote water solubility and result in solutions of decreased viscosity (Kagimura et al. 2015).

Chemical modification of polysaccharides by sulfonylation has been widely explored because of the ability to confer new functions such as anticoagulant, antioxidant, and antimicrobial activities. In this respect, sulfonated polysaccharides have been widely studied because of their biological functions that can mimic heparin activity, i.e., anticoagulation (Jiao et al. 2011). Chemical derivatization of polysaccharides by sulfonylation introduces a charged group (anionic sulfonate) onto the polymer chain that improves water solubility but can also change the biological functions of the modified polysaccharide (e.g., anticoagulation, antiviral, antiproliferative activities) compared to the unmodified parent polysaccharide. The biological activities of sulfonated (1→3)-β-D-glucans can be dependent upon both the degree of branching and the degree of substitution by sulfonate groups (Brandi et al. 2011; Kagimura et al. 2015). Botryosphaerans from *B. rhodina* MAMB-05 grown on glucose (EPS_{GLC}) and fructose (EPS_{FRU}) were sulfonylated using chlorosulfonic acid and pyridine (O'Neill 1955). In the sulfonylation reaction, solvent systems play an important role in dissolving polysaccharides, and formamide was found to dissolve botryosphaeran readily, facilitating the entrance of the sulfonation reagent (Mendes et al. 2009; Brandi et al. 2011). The water solubility of the sulfonated exopolysaccharide was dependent upon the molar ratio of chlorosulfonic acid to hydroxyl groups on the polysaccharide molecule. The sulfonation step can be repeated to obtain higher degrees of sulfonation (DS). The sulfur content and DS values of sulfonated botryosphaeran (EPS_{GLC}) were 15.4% and 1.54, respectively, for the once-sulfonated botryosphaeran (EPS_{GLC}-S), and upon re-sulfonylation (EPS_{GLC}-RS), the values increased slightly 15.9% and 1.64, respectively. The sulfur content and the DS of EPS_{FRU} were lower, for once-sulfonated 7.4% and 0.50 (EPS_{FRU}-S), and for re-sulfonylation, EPS_{FRU}-RS, was 10.5% and 0.80, respectively. The improved sulfur content and DS for the EPS_{GLC} were due to formamide that better dissolved botryosphaeran during the sulfonylation reaction. Dimethylformamide was used as solvent during the sulfonylation reaction of EPS_{FRU}, but botryosphaeran was poorly soluble in this aprotic polar solvent. Controlling the reaction conditions of time and temperature ensured relatively mild conditions that minimized possible degradation of the (1→3)-β-glucan chain during sulfonylation (Mendes et al. 2009). Both sulfonated botryosphaerans (EPS_{GLC}-S and EPS_{FRU}-S) were water-soluble, and this was due to the presence of the introduced anionic sulfonate groups along the polysaccharide chain that better interact with water molecules due to hydrogen bonding that promote water solubility. Purification of the sulfonated and re-sulfonated botryosphaerans of both types by gel filtration chromatography produced single peaks, indicating that the polysaccharides were not degraded during the sulfonylation reaction. In β-(1→3)-linked polysaccharides, the

primary OH groups on position C-6 is the more accessible site for sulfonation than the secondary OH groups at positions 2 and 4, which may be sterically hindered in introducing sulfonate groups at these positions. A reason for the less-efficient sulfonation of botryosphaeran might be due to the presence of the β-(1→6) glucosidic linkages of the side-chain appendages, which sterically reduce the number of primary OH groups available for sulfonation.

UV-Vis spectra of the sulfonated botryosphaerans (EPS_{GLC}-S and EPS_{FRU}-S) showed a new absorption band at 259 nm and were due to the n→π* transition of sulfonate and also to unsaturated bonds formed during the sulfonation process (Yang et al. 2003). FTIR spectra showed the presence of sulfonate groups in both botryosphaerans. The characteristic band at 1252 cm^{-1} indicated an asymmetrical stretching vibration, while that at 807 cm^{-1} indicated a symmetrical C-O-S vibration associated with a C-O-SO_3 group. The absorption band at 1623 cm^{-1} was related to the unsaturated bond formed in the sulfonation process (Mendes et al. 2009; Brandi et al. 2011).

The ^{13}C NMR chemical shift assignments for sulfonated botryosphaeran (EPS_{GLC}-S) and re-sulfonated (EPS_{GLC}-RS) are shown in Table 11.2. Compared with the original underivatized botryosphaeran (EPS_{GLC}), the ^{13}C NMR spectra of the sulfonated polysaccharides displayed broader signals due to sulfonation of the hydroxyl groups. In addition, the anomeric carbon (C-1) signals of EPS_{GLC}-S and EPS_{GLC}-RS were split upfield in bands at δ 101.4, 100.9, and 100.6, as a consequence of sulfonation; probably the anomeric region was influenced by an adjacent sulfonate substitution on C-2. The region at δ 60.7–61.1, attributable to the chemical shift of free C-6 for the un-sulfonated botryosphaeran (EPS_{GLC}), was almost absent from the ^{13}C NMR spectra for the sulfonated botryosphaeran, with new peaks appearing around 68.0 ppm in the spectra for EPS_{GLC}-S and EPS_{GLC}-RS. The shift of a carbon atom linked by a sulfonate group is 7 to 10 ppm downfield (Yang et al. 2005). The C-6-sulfonated signal shifted to ~68.0 ppm and indicated that most of the free (unlinked) C-6 was substituted by sulfonate groups. As botryosphaeran contains 22% side branching at C-6 with glucosyl and gentiobiosyl residues, sulfonate substitution on hydroxyls appeared to be absent at C-2 and C-4, due presumably to steric hindrance (Brandi et al. 2011).

Sulfonation of the hydroxyl groups on polysaccharides has been reported to occur in the order C-6>C-2>C-3>C-4 for pullulan (α-glucan), independent of the DS, with up to 48% of sulfonate groups occurring on C-6 (Alban et al. 2002). Pullulans are of low MW (50 to 200 kDa) and produced exocellularly by *Aureobasidium pullulans*. They are linear polysaccharides built of repeat units of maltotriose linked by (1→4)-α-glucosidic bonds and connected to consecutive maltotriose units through (1→6)-α-glucosidic bonds; hence the hydroxyls on mostly C-4, and some C-6, are bound through connecting linkages and are unavailable for sulfonation. Botryosphaeran is different in chemical constitution (β-glucan) and MW (>1 x 10^6 Da) than pullulan, and the hydroxyls on C-6 in the sulfonated botryosphaeran were primarily bound with sulfonate groups.

11.6 Production of Botryosphaeran by Submerged Fermentation

To produce exopolysaccharides, knowledge on the principles of microbial physiology is important in understanding the bioprocesses of cultivating microorganisms by submerged fermentation on nutrient medium. Many microorganisms producing exopolysaccharides respond to environmental factors directly, and for some, the carbon source (sugar) determines both the quantity of polysaccharide formed and the quality of the product synthesized (Mahapatra and Banerjee 2013; Osińska-Jaroszuk et al. 2015).

A study on the influence of the composition of the nutrient medium (nitrogen sources (organic and inorganic), phosphates, minerals, vitamins, supplements (e.g., plant seed oils and surfactants; see sect. 11.6.2), and the carbon source (e.g., sugars), as well as the parameters involving fermentation (aeration rate, agitation speed, initial pH, temperature, dissolved oxygen), is an important consideration to improve the microbial production of exopolysaccharide and cell biomass. Some biochemical conditions are critical and can limit the production of exopolysaccharides (β-glucan) through catabolite repression (Crognale et al. 2007) or through the presence of glycan-hydrolyzing enzymes that attack these polysaccharide substrates (Giese et al. 2011b). Fungal growth and mycelium production can also influence the production of the exopolysaccharides.

It is vitally important in producing microbial polysaccharides that they allow easy and economic extraction and recovery, whether this is by precipitation (exopolysaccharides) from fermentation broths or their extraction from microbial cell wall materials. The nature of the extraction procedure can have a pronounced effect on the structure and physical properties of the β-glucans isolated, with changes that may accompany aggregation and depolymerization as a consequence of the nature of the extraction steps (Zhu et al. 2016). Development of economically feasible biotechnological processes to produce and recover microbial exopolysaccharides is therefore necessary to open possibilities for their wider commercial applications. The most attractive feature of exopolysaccharides over extracted polysaccharides is the ease of their production by submerged fermentation and subsequent isolation. Commercial β-glucans have mostly been extracted from fungal fruiting bodies (mushroom, brackets), yeast cell walls (spent brewers' yeast, *Saccharomyces cerevisiae*), and cereal grains (oat, barley).

The extraction and isolation of β-glucans from fungal cell walls and cereals are rather complex and time-consuming processes that can involve multiple sequential extraction steps involving solvents (lipid removal), cold and hot water, acids and alkali, and enzyme treatments to facilitate their purification, which can accompany changes in the chemical structures of the extracted polysaccharides. This, in turn, can affect their properties and biological functions. In addition, the time taken to obtain the fungal fruiting bodies can take weeks to months compared with simple fermentation procedures (matter of days).

In the case of cereal β-glucans [(1→3)(1→4)-linked β-glucans], which have similar rheological properties and biological activities to their microbial (1→3)-β-glucan counterparts, their extracted yields are rather low (3–11%), but large amounts of cereal grain can be produced through agriculture from which β-glucans present in the brans can be isolated. The time taken, however, to grow cereals (oats, barley) in the field and the harvesting of the cereal grains prior to their extraction take several months on a timescale, and grain yields can be dependent upon climatic conditions. By contrast, microbial exocellular β-glucans are easily produced by simple submerged fermentation processes on low-cost nutrient media and are simply extracted from the cell-free fermentation broth through precipitation methods. This all takes place on a timescale of days compared to weeks to months for other extracted sources of β-glucans. Exopolysaccharides produced by microbial submerged fermentation are commonly quantified by gravimetry after their precipitation with ethanol (Selbmann et al. 2002; Barbosa et al. 2003). An alternative procedure to quantify exopolysaccharides is by measuring total sugars in the fermentation broth by the phenol-sulfuric acid method (Dubois et al. 1956). The latter method, however, is reliable only if the residual amount of sugar used as substrate in the fermentation broth (measured as reducing sugars or, in the case of glucose, by the glucose oxidase method) is subtracted from the amount of total sugars present. The result then represents exopolysaccharide. Reducing sugars can be measured by the cupro-arsenic method (Nelson 1944; Somogyi 1945), or the DNS method (Miller 1959), and glucose by the glucose oxidase method (Dekker and Richards 1971). Another method that has been used in relation to extracted β-glucans from mushrooms quantifies the β-glucans in the extracts (alkali and acid soluble fractions) by their reaction with a dye (Congo red) and measures the absorbance at 523 nm (López-Vázquez et al. 2017).

Selbmann et al. (2002, 2003) were the first to report on fermentation conditions for the production of an exopolysaccharide (a (1→3)(1→6)-linked β-glucan) by *B. rhodina* (DABAC P-82) using glucose, raw starch, and starch hydrolyzates as substrates, which resulted in high amounts of exopolysaccharide being produced (up to 17 g/L). As no previous study had been conducted on the influence of carbohydrate sources on the production of botryosphaeran by *Botryosphaeria* spp., we investigated the influence of glucose concentration and different carbohydrate substrates on botryosphaeran production (Steluti et al. 2004). This study compared the monosaccharide composition and the configuration of the glucosidic linkages of each of the exopolysaccharides produced by *Botryosphaeria* sp. MAMB-05 when grown on these carbohydrate sources.

11.6.1 Microbial Physiology of Botryosphaeran Production

Process steps in the production and isolation of botryosphaeran from *B. rhodina* isolate MAMB-05 are summarized in Fig. 11.2. Inoculum preparation typically involves using agar plugs (solid media comprising glucose and agar) colonized

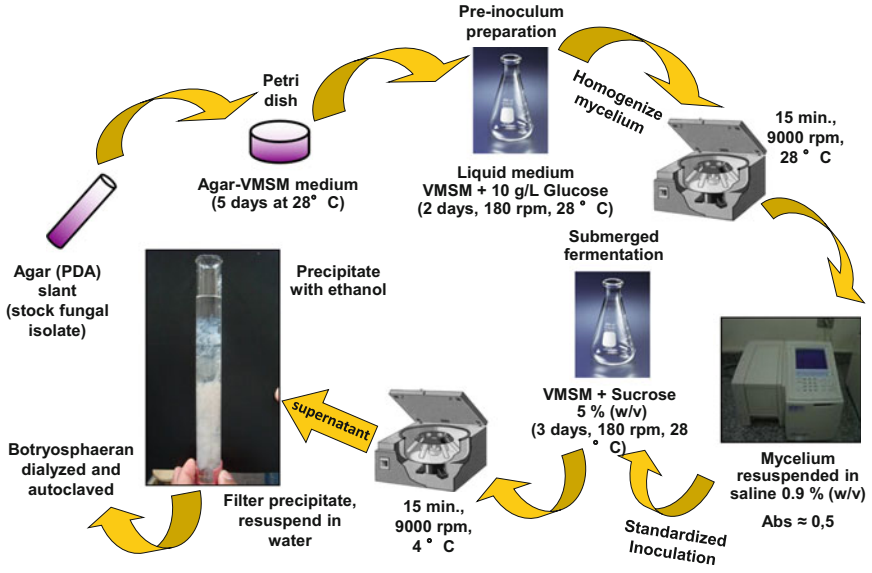

Fig. 11.2 Schematic showing the protocol for producing and standardizing inoculum for seeding cultures of *Botryosphaeria rhodina* MAMB-05 for the production of exocellular botryosphaeran

with a profuse cover of mycelial growth. However, when this type of inoculum is used for the production of botryosphaeran by *B. rhodina* MAMB-05, the exopolysaccharide secreted in the fermentation medium becomes attached to the mycelium-colonized agar plugs resulting in a solid mass making it impossible to quantify the exopolysaccharide produced. Consequently, the inoculum procedure was modified by homogenizing mycelia prepared in liquid culture as described by Barbosa et al. (2003) and Steluti et al. (2004) to produce a standardized mycelial homogenate that could be conveniently determined spectrophotometrically (absorbance at 400 nm between 0.4 and 0.5). Aliquots of the standardized inoculum could then be dispensed to inoculate nutrient medium containing sugars. By standardizing a blended liquid mycelial preparation obtained by growing the fungal precultures on low glucose concentration (5 g/L) for a short period (48 h), this step minimized the viscosity (low exopolysaccharide content) during the production of the pre-inoculum. A viscous medium (high glucose, e.g., 50 g/L), on the other hand, interfered with the standardization of mycelial homogenate as inoculum.

Fungal cultures grown on 25, 50, and 75 g/L glucose demonstrated that glucose (50 g/L) was optimal for the production of botryosphaeran. Highest viscosity values (12.3 centipoise at 50 g/L glucose) in the fermentation broth correlated with the amount of exopolysaccharide produced under the submerged fermentation conditions (Steluti et al. 2004). Profiles of fungal growth on 50 g/L glucose and botryosphaeran production showed that the fungus reached the exponential growth

phase within 24 h indicating that the inoculum concentration was adequate. The stationary phase was reached by 72 h and corresponded with optimal exopolysaccharide production. At this time point, glucose was almost totally consumed, but the total sugar content (quantified by the phenol-sulfuric acid method) in the fermentation broth had increased demonstrating the presence of exopolysaccharide, which could be detected until 144 h of fungal growth (Steluti et al. 2004).

In a related study on exopolysaccharide production by *B. rhodina* MAMB-05 cultivated on glucose, Giese et al. (2011b) observed that during the growth period from 108 h until 180 h, the exopolysaccharide concentration in the fermentation broth steadily decreased as a consequence of the fungus utilizing botryosphaeran as a growth substrate, since all glucose had been consumed. This resulted in secondary growth of the fungus and coincided with the induction and production of β-(1→3)-glucanases that enzymatically hydrolyzed botryosphaeran to provide substrate and energy to support continuing growth of the fungus. After all botryosphaeran had been consumed (180 h), the fungus obtained consumable substrate from cannibalization of its biomass constituents through the mobilization and action of β-(1→3)-glucanases, β-(1→6)-glucanases, and β-glucosidases to hydrolyze the mycelial cell wall components that are rich in β-glucans of both the (1→3)(1→6)- and (1→6)-linked types (see Corradi da Silva et al. 2008).

Exopolysaccharide production by *Botryosphaeria* sp. MAMB-05 on other carbohydrate substrates at 50 g/L (galactose, fructose, mannose, lactose, sucrose, commercial sucrose, sugarcane molasses, sorbitol) showed that all of these substrates produced botryosphaeran (Steluti et al. 2004). Sucrose, commercial sucrose, and sugarcane molasses were the best substrates resulting in respective exopolysaccharide yields of 3.1, 3.7, and 3.5 g/L, which compared to 2.8 g/L for glucose and 1.9 g/L for fructose, grown under similar fermentation conditions. Sorbitol, galactose, and lactose promoted least amounts of botryosphaeran. Highest mycelial biomass was produced on sugarcane molasses, a feedstock rich in sucrose, minerals, and vitamins. Glucose is biologically the most effective energy source; however, sucrose favored botryosphaeran formation by *Botryosphaeria* sp., as was also reported by Shingel (2004) for the synthesis of pullulan by *Aureobasidium pullulans*. All of the exopolysaccharides produced on the different carbohydrate sources were found to consist exclusively of glucose after total acid hydrolysis and analysis by HPLC. FTIR spectroscopy of each exopolysaccharide produced by *Botryosphaeria* sp. MAMB-05 showed they were of the β-glucan type and contained (1→3)-di-*O*-substituted glucose residues. Similar observations were reported for other fungal β-glucans (Krcmar et al. 1999).

In conclusion, *Botryosphaeria* sp. MAMB-05 produced more botryosphaeran on sucrose than glucose or fructose, and the botryosphaerans obtained on each of the different sugar sources were all found to be (1→3)-β-glucans and thus constituted a *family* of botryosphaerans (Steluti et al. 2004).

11.6.2 *Effect of Soybean Oil and Surfactants on Botryosphaeran Production*

In view that the β-glucans have important industrial and medical applications, and botryosphaeran is no exception, their inclusion as new materials in commercial applications is dependent upon the production scale (Zhu et al. 2016). In fermentation processes, an increase in the yield of exopolysaccharides requires strategies that control fermentation parameters and are influenced by the type of nutrients and supplements. Here we describe the influence of supplementary materials (plant seed oils and surfactants) on enhancing botryosphaeran production when grown on glucose.

While experimenting with Tween surfactants to increase laccase production by *B. rhodina* MAMB-05, Giese et al. (2004) found that the laccase titers were enhanced. This finding prompted examining other membrane-modifying agents, e.g., plant seed oils. Soybean oil was also found to enhance laccase activity (Dekker et al. 2007), but serendipitously, this also led to an increase in the amount of botryosphaeran produced. A range of different plant seed and palm (babassu) oils successfully increased botryosphaeran production above basal levels (Silva et al. 2007). Furthermore, emulsification of soybean oil with Tween 80 enhanced the production of higher amounts of botryosphaeran. Plant seed oils (triacylglycerols), fatty acids, and surfactants when added to nutrient medium are known to influence the growth of fungal mycelia and also the production of exopolysaccharides, including those of the β-glucan type. This phenomenon is first reported by Stasinopoulos and Seviour (1990), who found that adding olive or sunflower oil to nutrient medium enhanced β-glucan production by the fungus *Acremonium persicinum* under conditions of submerged fermentation. Other literature reports have similarly found that olive and soybean oils enhanced pullulan production by *Aureobasidium pullulans* when incorporated into nutrient media (West and Reed-Hamer 1995; Youssef et al. 1998). Some vegetable oils and fatty acids, however, also inhibited the biosynthesis of exopolysaccharides, and the extent of these effects was related to the type of fatty acids of the triacylglycerols (Hsieh et al. 2008). Yang et al. (2000) observed that while palmitic acid greatly enhanced the yields of a (1→3)-β-D-glucan in *Ganoderma lucidum*, linolenic acid was a strong inhibitor of both exopolysaccharide production and mycelial growth.

The surfactant, Tween 80 (polyoxyethylene sorbitan monooleate), also stimulated pullulan production in *Aureobasidium pullulans*, and depending upon the nitrogen source used in the nutrient medium, the addition of Tween 80 enhanced exopolysaccharide production (West and Reed-Hamer 1995). The stimulation of exopolysaccharide production by fungi, or its release into the extracellular medium, by a plant seed oil and surfactant, is most likely related to an interaction between the fatty acyl chains and the cell membrane phospholipids. Also, the activity of certain enzymes may be stimulated by surfactants. For example, Tween 80 promoted the activity of the enzyme glucosyltransferase, which is involved in the biosynthesis of pullulan, and this was accompanied by increased amounts of pullulan produced

(Sheng et al. 2013). Tween 80 correlated with glucosyltransferase activity and fatty acid composition. Vegetable seed oils are readily and abundantly available and are relatively cheap. As they are capable of enhancing exopolysaccharide production, this prompted an evaluation of the effects of soybean oil and Tween 80, and their combination, on the production of botryosphaeran when *B. rhodina* MAMB-05 was cultivated on glucose media by submerged fermentation. Statistical design was applied to optimize fermentation parameters to maximize the production of botryosphaeran. Assessment of various vegetable seed oils (canola, cotton, maize, olive, soybean, sunflower) and palm oil (babassu) for their ability to enhance botryosphaeran production indicated that soybean oil was superior, increasing the exopolysaccharide yields by up to 63% over controls without added oils. Different commercial soybean oils showed no significant difference on the amounts of exopolysaccharide produced among the different brands tested, regardless of the presence of the food preservative, *tert*-butylhydroquinone, added as an antioxidant to some edible seed oils.

The addition of Tween 80 to the nutrient medium increased botryosphaeran production by 68%, but had no effect on fungal biomass production indicating that under the conditions, Tween 80 did not serve as extra carbon source. When soybean oil and Tween 80 were combined and added to the nutrient medium, the production of botryosphaeran increased 2-fold and that of fungal biomass 1.2-fold (Silva et al. 2007). Box-Behnken statistical design factor screening demonstrated the most significant factors to enhance botryosphaeran production were the concentrations of glucose, soybean oil, and Tween 80. Experimental validation of the model was performed under the established conditions (40 g/L glucose, 10 mL/L soybean oil, and 4.5 g/L Tween 80) for 72 h and initial pH 5.7 and resulted in a predicted value of 8.22 ± 1.36 g/L. The observed experimental production of botryosphaeran under these conditions was 7.74 ± 0.13 g/L, which was within the confidence interval and consistent with the predicted values (Silva et al. 2007).

The structural characterization of the botryosphaeran produced was examined by FTIR spectroscopy and acid hydrolysis (HPLC analysis) to determine whether the addition of soybean oil and its emulsification by Tween 80 interfered with the synthesis of β-glucan when *B. rhodina* MAMB-05 was cultivated on glucose. FTIR spectral bands were characteristic of glucans with β-glucosidic linkages, consisting of (1→3)-di-*O*-substituted glucose residues. FTIR revealed no spectral differences for botryosphaeran arising from fungal growth in the combined presence of soybean oil and Tween 80 compared to the control (Silva et al. 2007). HPLC analysis of the monosaccharides resulting from acid hydrolysis of the botryosphaeran produced under the optimized conditions of growth in the combined presence of soybean oil and Tween 80 revealed three monosaccharides, with glucose as the major component (92.2%), and was consistent with botryosphaeran being comprised of glucose monomers. Two other monosaccharides occurred in relatively smaller amounts (galactose 6.2% and mannose 1.7%) and arise from glycoproteins that coprecipitate with ethanol and appear in the exopolysaccharide fraction recovered.

In conclusion, soybean oil and Tween 80 enhanced the production of the botryosphaeran by *B. rhodina* MAMB-05. Partial structural characterization of the

botryosphaeran produced revealed that the combined addition of soybean oil and Tween 80 did not present any unusual structural features and agreed with previous findings that this exopolysaccharide too belonged to the *family* of botryosphaerans (Barbosa et al. 2003; Steluti et al. 2004; Silva et al. 2007).

11.6.3 Optimization of Botryosphaeran Production Through Statistical Design (Response Surface Method)

A decisive factor to optimize microbial production of exopolysaccharides is through developing economically feasible fermentation processes that can be controlled using statistical methodologies (e.g., response surface method (RSM) (Box et al. 2005; Bruns et al. 2006), to maximize bio-product formation. Response surface methodology is an effective statistical technique to investigate complex processes and their interactions in optimizing metabolite production by microbial species.

The application of statistical factorial design methodologies associated with RSM assists to define the effects and interactions of the physiological factors that play a role in biotechnological processes in the production of microbial metabolites including exopolysaccharides. RSM consists of an empirical modeling system that evaluates the relationship between a group of variables (e.g., nutrient medium composition and fermentation parameters) that are controlled experimentally resulting in an enhanced response (e.g., exopolysaccharide production). The advantage of statistical factorial design is the reduced number of experiments required to provide sufficient information for statistically acceptable results. Moreover, RSM is a faster and less expensive approach for gathering data than the classical experimental methods analyzing *one factor at a time* and also minimizes possible errors of traditional techniques.

Some examples where RSM has been used to optimize production of microbial exopolysaccharides include gellan gum (an acidic bacterial polysaccharide with a tetrasaccharide repeat unit composed of →3)-β-D-Glcp-(1→4)-β-D-GlcpA-(1→4)-β-D-Glcp-(1→4)-α-L-Rhap-(1→ (Banik et al. 2007), two levan-type biopolymers from *Paenibacillus polymyxa* composed of a backbone (2→6)-linked β-D-fructofuranosyl residues with (2→1)-linked β-D-fructofuranosyl side branches (Liu et al. 2010), pullulan (Jiang 2010), and botryosphaeran (Giese et al. 2015b), as well as the influence of membrane-modifying agents (see Sect. 11.6.2) on botryosphaeran production (Silva et al. 2007).

The influence of different nitrogen sources on the production of botryosphaeran by *B. rhodina* MAMB-05 determined the best conditions that promoted production of this exopolysaccharide and fungal biomass. Highest botryosphaeran yields (4.39 g/L) were obtained using NH_4NO_3, which also favored highest mycelial growth (18.5 g biomass/L). Organic nitrogen sources produced lower botryosphaeran yields (e.g., L-asparagine, 2.5 g/L) but favored fungal growth (22 g biomass/L) over their inorganic nitrogen counterparts (Giese et al. 2015b).

The C/N ratio, an important factor in the biosynthesis of microbial metabolites, was assessed by RSM to establish whether C/N could influence microbial growth and exopolysaccharide production by *B. rhodina* MAMB-05. A Box-Behnken 2^3-factorial central-composite design matrix applied in two stages defined the best fermentation conditions for optimal production of botryosphaeran and fungal growth. In the first factorial design, the fungal cultures were grown on Vogel minimum salts medium that contained NH_4NO_3 as nitrogen source and were supplemented with different concentrations of glucose to confer C/N ratios in the culture medium ranging from 8 to 92 to evaluate some initial fermentation parameters (Giese et al. 2015b). Response surface analysis according to a first experimental matrix design established that the time of growth (88 h) and inoculum concentration (0.88 g mycelium/L) at a C/N of 30 were optimal for botryosphaeran production (5.2 g/L) by *B. rhodina* MAMB-05. Mycelial biomass was also optimal as a function of time of growth and inoculum concentration but, in this case, required a C/N of 92.

Based upon previous knowledge of the time-growth relationship of botryosphaeran production (Steluti et al. 2004), a shorter growing period was chosen (72 h), because when glucose was depleted in the nutrient medium, exopolysaccharide production declined thereafter. The reason for this was due to a combination of glucose limitation and derepression of synthesis of β-glucan hydrolases by the fungus that attack botryosphaeran, which acts as a carbon source especially during the stationary phase (Giese et al. 2011b). Furthermore, longer fermentation time results in the blackening of the fungal mycelium due to melanin, which, in turn, taints the botryosphaeran preparation produced, lowering its consumer acceptance. Longer periods of growth are therefore unfavorable.

According to the second factorial design, the most important variables for fungal biomass production by *B. rhodina* MAMB-05 at 72 h growth were the same as obtained for botryosphaeran production: time of growth and inoculum concentration. Highest mycelial biomass production (33.85 g/L) was achieved using an inoculum concentration of 0.72 g mycelium/L and a C/N ratio of 75 (Giese et al. 2015b).

The validation of the fermentation parameters by statistical factorial design improved botryosphaeran production by *B. rhodina* MAMB-05 over un-optimized conditions (3.2 g/L, Steluti et al. 2004). Even at lower C/N ratios, the fungus could produce botryosphaeran and biomass simultaneously, which are economically important in view of the fermentation process, and the potential of using cheaper raw materials, e.g., the mycelium of *B. rhodina* MAMB-05, which as a waste product is considered a cheap and rich source of β-glucans (Corradi da Silva et al. 2008).

11.6.4 Botryosphaeran Production: A Zero-Waste Concept

Contemplating a *zero-waste* technological process in the scaled-up production of botryosphaeran, a scheme outlining the steps proposed in the production of the exocellular β-glucan by *B. rhodina* MAMB-05 under submerged fermentation conditions and treatment of waste streams generated is shown in Fig. 11.3. Two

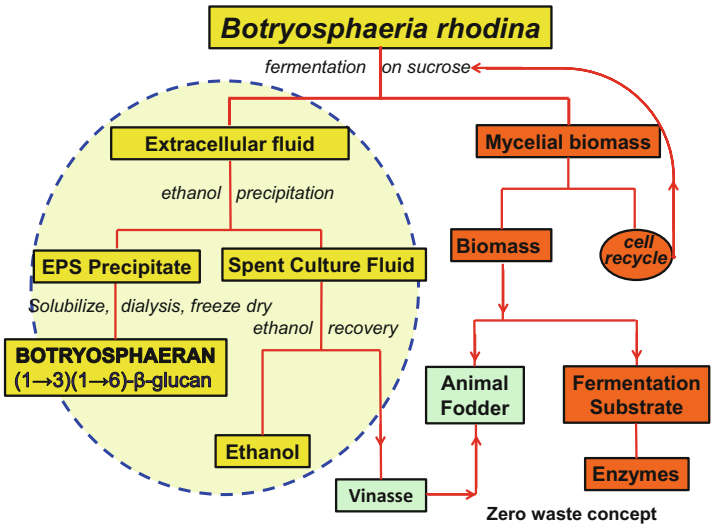

Fig. 11.3 Schematic of the process steps for the production of botryosphaeran by *Botryosphaeria rhodina* MAMB-05 based on a *zero-waste* concept

chief end products result (i) botryosphaeran and (ii) fungal biomass (mycelium). Scaling up the fermentation process will generate large amounts of fungal biomass, a portion (10%) of which can be reused for cell recycling for further fermentation batches. But the remainder can present waste disposal problems, unless the fungal biomass can be used for other purposes that add value to generate revenue, which will reduce the cost of botryosphaeran production.

The steps in producing botryosphaeran at different stages of the production process are shown in Fig. 11.4. Figure 11.5 shows a photograph of the gel form of botryosphaeran showing its firmness and transparency. The rheological properties of botryosphaeran have been described (Macedo Bongiovani et al. 2009; Fonseca et al. 2011). Botryosphaeran forms viscous solutions in water that are stable to heat as may occur during steam sterilization (autoclaving), and strong gels are formed when cooled (5 °C).

The fungal mycelium arising from the production of botryosphaeran is a rich source of β-glucans (mixture of (1→3)(1→6)- and (1→6)-linked β-glucosides), α-glucan (glycogen-like (1→4)(1→6)-linked α-glucoside), and chitin (polymer of β-(1→4)-linked 2-(acetylamino)-2-deoxy-glucose) that can be extracted (Corradi da Silva et al. 2008), and becomes another potential source of glucans and proteins present in mycelial biomass, and another revenue stream in business. Alternatively, the fungal mycelium per se can be used for other purposes, for example, as substrate for fermentation-derived bio-/chemical products including enzymes with commercial applications or as an animal feedstock (feed supplement); the cell wall β-glucans present would stimulate the immune system promoting the health benefits of farm animals and pets. The pet food industry is a huge market, globally. Defined value-

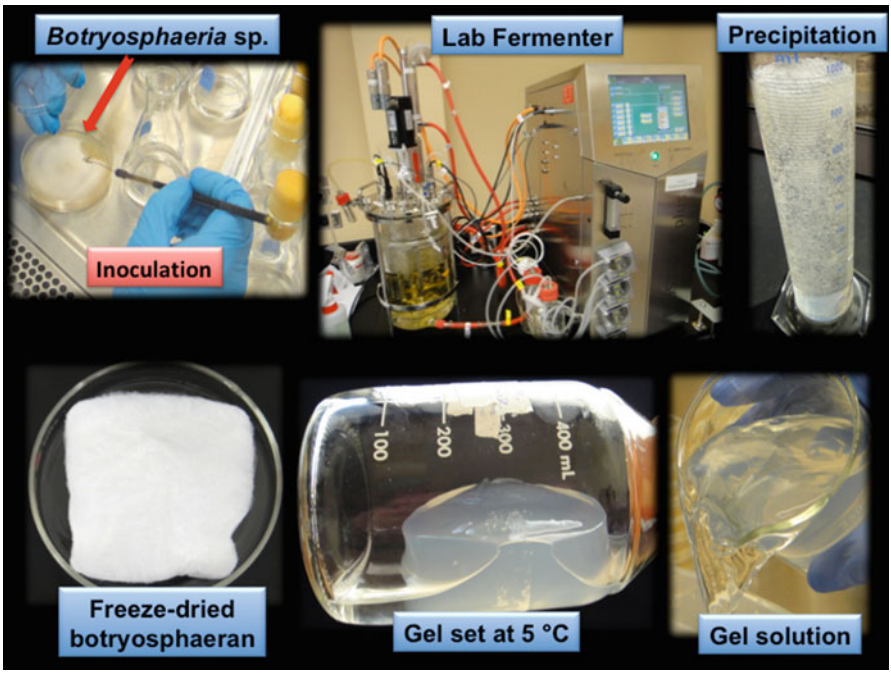

Fig. 11.4 Steps leading to the production of botryosphaeran by *Botryosphaeria rhodina* MAMB-05: from initial culture on solid agar to produce inoculum to seed the fermenter and cultivated for 72 h, followed by harvesting the contents and precipitation of the cell-free fermentation broth with ethanol, the recovery of the precipitate, its re-solubilization in water to produce a thick viscous slurry, that forms a gel upon refrigeration, and the dried fibrous product following lyophilization

Fig. 11.5 Photograph of botryosphaeran gel. Note the firmness and transparency of the gel

added products for utilizing fungal biomass have been considered in producing botryosphaeran, and a *zero-waste* concept can be achieved. Only the liquid streams arising from extraction and fermentation processes will require treatment. Alcohol used to precipitate botryosphaeran from the fermentation broth can be distilled off

and recycled, and the vinasse resulting can also be used as an animal feedstock. A vinasse can also be recovered from spent fermentation liquors that produce bio-based products (e.g., enzymes). Studies on the mutagenicity and genotoxicity of biomass (mycelium) from *B. rhodina* MAMB-05 have not yet been determined, nor for the vinasse resulting after removal of ethanol from the cell-free fermentation broth, to assess their safety for animal use. This will be a future direction.

Among the enzymes of interest that can be produced from the fungal biomass as fermentative feedstock are those that hydrolyze β-glucans, such as the β-glucanases of the (1→3)- and (1→6)- kinds, and β-glucosidases (Giese et al. 2005). These enzymes defragment botryosphaeran producing a series of (1→3)- and (1→6)-linked gluco-oligosaccharides, which can serve as prebiotics. Enzymes hydrolyzing botryosphaeran can be induced by *B. rhodina* MAMB-05 and *Trichoderma harzianum* Rifai when cultivated on nutrient medium containing botryosphaeran or on *B. rhodina* MAMB-05 biomass (Giese et al. 2005, 2006, 2011a, b). These enzymes hydrolyze botryosphaeran into a series of β-(1→3)-linked gluco-oligosaccharides of varying degrees of polymerization, as well as gentiobiose and gentiotriose (Giese et al. 2009, 2011a).

Prebiotics are nondigestible short-chain carbohydrates – oligosaccharides that pass undigested through the upper gastrointestinal tract to the large intestine (colon) where they are fermented by selective commensal bacteria (bifidobacteria) stimulating growth and enhancing activity to induce beneficial systematic effects within the host (Al-Sheraji et al. 2013). Within the group of prebiotics are the (1→3)-linked gluco-oligosaccharides, and botryosphaeran can serve as a source of generating these oligosaccharides through enzymatic hydrolysis as reported by Giese et al. (2009, 2011a). Oligosaccharides made up of fructose and galactose residues are commercially available and used as nutraceuticals in foods. Those constituted of (1→3)- and (1→6)-linked β-glucosides are emerging prebiotics.

11.7 Botryosphaeran: Presenting Non-mutagenicity, Non-genotoxicity, and Antimutagenic Activity

When assessing new compounds for potential nutraceutical and biomedical applications, they first need to be screened for mutagenic and genotoxic activities, as this property assesses cellular damage on the host. This can be conveniently performed by several tests, e.g., the micronucleus test (fluorescent staining method that identifies specific micronuclei, Hayashi 2016) and the comet assay (sensitive technique for measuring DNA damage (single-stranded breaks) in single cells (Tice et al. (2000)), using lab animals and/or mammalian cell lines. An alternative method to assess mutagenicity without the use of lab animals is the Ames test (uses strains of the bacterium *Salmonella typhimurium*, Maron and Ames 1983). Genotoxicity from mitotic index analysis can be assessed by the cytokinesis-block micronucleus assay (Fenech 1993). Taken together, these tests are considered biomarkers for assessing

mutagenic and genotoxic damage. New compounds can also affect cell viability and their proliferation, and this can be assessed by the MTT assay (uses a tetrazolium dye, Mosmann 1983) or by cell staining with acridine orange/ethidium bromide (Kasibhatla et al. 2006).

Another important factor assessing a new non-mutagenic compound is to discover whether it can exert a chemoprotective effect to reduce mutations induced by chemotherapeutic drugs commonly used to treat cancers (cyclophosphamide, doxorubicin, methyl methanesulfonate, bleomycin) or mutagens (benzo[a]pyrene). Our first priority was to determine whether botryosphaeran was mutagenic, and this was determined on adult mice by the micronucleus test. We also wanted to know if botryosphaeran could reduce the clastogenic (aneugenic) effect of cyclophosphamide-induced micronucleus formation in bone marrow (polychromatic erythrocytes, PCEs) and peripheral blood (reticulocytes, RETs) cells in vivo in mice. Cyclophosphamide, an alkylating agent used in chemotherapy to treat cancers, can be used experimentally as a cytostatic agent to induce cellular damage in micronucleus formation in bone marrow and peripheral blood cells of lab animals. Thus, in using cyclophosphamide it was possible to evaluate mutagenic and antimutagenic (anticlastogenic) activities of botryosphaeran (Miranda et al. 2008). Our study revealed that botryosphaeran administered by gavage at doses of up to 30 mg/kg body weight (b.w.) per day in Swiss adult mice over a 15-day period demonstrated no mutagenicity in bone marrow PCEs nor in peripheral blood RETs. Botryosphaeran did, however, exhibit strong antimutagenic activity (chemoprotective effect) against the in vivo DNA-damaging effect of cyclophosphamide leading to a reduction of cyclophosphamide-induced micronucleus frequencies in bone marrow (PCEs, 78%) and peripheral blood (RETs, 82%) of the mice (Miranda et al. 2008).

In a further study, Silva-Sena et al. (2018) supported the findings of Miranda et al. (2008) and confirmed that botryosphaeran was not mutagenic nor genotoxic in Swiss albino mice (young and adult of both genders). Botryosphaeran, furthermore, exhibited strong antimutagenic activity being able to reduce the number of micronucleated cells (100% in young and elderly male mice) formed by clastogenic cyclophosphamide. The finding that botryosphaeran did not present clastogenic or aneugenic damage in mice suggests that it should be safe for human use.

In similar studies using mammalian cell lines, Chinese hamster lung fibroblasts (V79) and rat hepatocarcinoma cells (HTC), botryosphaeran was found not to be mutagenic and genotoxic in either cell line by the micronucleus test and comet assay and exhibited protective effects against the clastogenic effects of doxorubicin, H_2O_2, and benzo[a]pyrene (Kerche-Silva et al. 2017). In another study, botryosphaeran again exhibited no mutagenicity and protected cultured human whole blood lymphocytes against DNA damage and cell death induced by bleomycin throughout the cell cycle. Malini et al. (2016) using cultured normal and tumor (leukaemic Jurkat cells) human T lymphocytes to evaluate the genotoxicity and antigenotoxicity of botryosphaeran alone and in combination with the alkylating mutagen, methyl methanesulfonate, found that botryosphaeran was not mutagenic as assessed by the Ames test on different *Salmonella typhimurium* strains nor induced genotoxicity (Comet assay).

Botryosphaeran again exerted a protective effect against genotoxic damage, in this case, by methyl methanesulfonate on lymphocyte DNA. The absence of mutagenicity and genotoxicity assessed by the micronucleus, Ames and MTT tests, and the comet assay established that botryosphaeran has GRAS (generally recommended as safe) status and is safe for use by humans and for veterinary medicine. Our studies also demonstrated strong antimutagenicity, and the chemoprotective nature of botryosphaeran against DNA damage and cell death induced by chemotherapeutic agents, and could find application as an adjuvant to lessen side effects in treating cancers. Another possible application for botryosphaeran could be as co-adjuvant in vaccines because of its immunopotentiation functions.

11.8 Glycemic and Lipidemic Studies on Botryosphaeran in Animals

Having established the safety of botryosphaeran in animal studies, our next foray into research (2005) was to assess the biological properties of botryosphaeran in lab animals: glycemic control in streptozotocin-induced diabetic rats and correcting dyslipidemia in rats preconditioned on a high-fat diet (Miranda-Nantes et al. 2011).

11.8.1 Antidiabetic Activities of Botryosphaeran

The incidence of obesity and diabetes is a growing health problem afflicting some 300 million people worldwide and is increasing at an alarming rate globally. Furthermore, the incidence of the comorbidities associated with these conditions, such as cardiovascular disease, dyslipidemia (abnormal blood lipid levels), hepatic steatosis (non-alcoholic fatty liver), and cancer, is also increasing significantly worldwide, as well as the mortality rate associated with these conditions. There is also epidemiological evidence of an increased risk of cancer linked to diabetes with the prevailing factor being the high glucose levels. Thus, the discovery of new drugs for the treatment or prevention of these diseases is primordial.

Obesity is a chronic metabolic disease characterized by the accumulation of adipose tissue in relation to lean mass (muscle tissue). The accumulation of adipose tissue increases the release of several factors, such as free fatty acids, leptin, resistin, interleukins, and tumor necrosis factor-*alpha* (TNF-α), and decreases the release of adiponectin, which can contribute to the development of insulin resistance, hyperinsulinemia, glucose intolerance, and hyperglycemia. These metabolic alterations, consequently, contribute to the development of many comorbidities associated with obesity, among them diabetes, dyslipidemia, hepatic steatosis, cardiovascular diseases, and cancer (Kopelman 2000; Calle and Kaaks 2004; Hursting and Hursting 2012; Kumar and Kelly 2017).

Diabetes mellitus is a debilitating chronic metabolic disorder featured by hyperglycemia due to defects in insulin secretion, insulin action, or both manifestations. There are two types of diabetes: *type-1*, an autoimmune disease in which the β-cells of the pancreas are selectively destroyed leading to severe deficiencies of insulin. The other diabetic disease is *type-2*, late-onset diabetes that can be manifested by obesity and afflicts the majority of diabetics. The symptom is due to two principal drivers: insulin resistance by the liver, muscle, and adipose tissue and insufficient amounts of insulin produced by the pancreatic β-cells to meet the metabolic demand. Insulin action is through a series of events initiated through its binding to its specific receptor that activates protein kinases leading to activation of multiple signaling pathways required for insulin's action to regulate glucose uptake and glycogen synthesis, among others (Pederson et al. 2001).

β-D-Glucans have attracted much attention for their medicinal properties. Consumption of macro-fungi fruiting bodies (e.g., mushrooms and brackets), which contain β-glucans, is known to reduce the risk of obesity and diabetes and has been used as folkloric medicines to treat disease conditions in humans (Wasser 2002, 2014). Fungal (1→3)-β-glucans and branched (1→3)(1→6)-β-glucans are effective in treating human hyperglycemia and hyperlipidemia including hypercholesterolemia that posit cardiovascular risks, and such treatments can alleviate dyslipidemia and reduce atherogenesis (Chen and Seviour 2007; Chen and Raymond 2008).

Studies by Cao et al. (2016) on a (1→3)-β-glucan isolated from yeast cell walls (MW 25 kDa and insoluble in water) have provided some mechanistic insights on the role of β-glucan in type 2 diabetic mice. They found that the yeast-derived β-glucan down-regulated blood glucose levels through suppressing the expression of sodium-glucose transporter-1 (SGT-1, a major glucose transporter in the small intestine) in type 2 diabetic mice. The yeast β-glucan ameliorated glucose and lipid metabolism through activation of the IRS/Akt pathway. β-Glucan enhanced the phosphorylation of Akt (at Ser473) and IRS (insulin receptor substrate) at Tyr612 (p-IRS) in the liver, which is down-regulated in insulin resistance, indicating the activation of the *insulin signaling pathway* by this β-glucan.

Research from our own group with botryosphaeran demonstrated that this fungal exopolysaccharide possessed hypoglycemic activity in rats (Miranda-Nantes et al. 2011) and mice (Silva-Sena et al. 2018), as well as in obese rats (Silva et al. 2018). Botryosphaeran presented significant hypoglycemic activity in rats in which diabetes was induced by streptozotocin through intramuscular injection. Streptozotocin selectively damages pancreatic insulin-secreting β-cells leading to type-1 diabetes. Adult male Wistar rats induced with diabetes and treated with 12 mg botryosphaeran/kg body weight/day by gavage over 15 days responded with lowered blood glucose levels by 52%. Treatment with botryosphaeran reduced the median ration intake by the diabetic animals, and this was accompanied by an increase in the median body weight gain, as well as in the efficiency of food conversion. This observation demonstrated that botryosphaeran exerted a protective effect by reducing the symptoms of cachexia (loss of body weight) in the type-1 diabetic rats (Miranda-Nantes et al. 2011).

In a similar study using a crude extracellular preparation (EPS, a mixture comprising two different heteropolysaccharides and two proteoglycans) from the medicinal mushroom *Phellinus baumii*, Hwang et al. (2005) reported that treatment of streptozotocin-induced diabetic rats with their EPS promoted a similar reduction (52.3%) in the plasma glucose level, but the dose was 17-fold higher (200 mg/kg b.w./day) than the botryosphaeran concentration (12 mg) used in the Miranda-Nantes et al. (2011) study. Similarly, Silva-Sena et al. (2018) demonstrated reduced plasma glucose levels (36%) in 18-month-old low-density lipoprotein receptor knockout ($LDLr^{-/-}$) male Swiss mice (genetic predisposition to hyperlipidemia (elevated plasma cholesterol levels and high atherogenesis) on feeding a lipid-rich diet) when treated with botryosphaeran (30 mg/kg mouse b.w./day) by gavage over 2 weeks.

Other studies of certain fungal polysaccharides have demonstrated these to be associated with increasing the production of insulin and its secretion by pancreatic β-cells, thus contributing to the beneficial effects of these polysaccharides on diabetes through control of the glycemic and lipidic profiles (Kiho et al. 2000; Lo et al. 2006; Rop et al. 2009; Ng et al. 2015).

In related work from our lab in which obesity in rats was induced by adding monosodium glutamate (MSG) to the ration, we found that botryosphaeran increased the food intake in female obese-MSG rats, decreased the perigonadal adipose tissue and the Lee (obesity) index, and improved significantly the insulin sensitivity in this group. These findings demonstrated that botryosphaeran can increase significantly the insulin sensitivity in female obese-MSG rats, and this reinforced the effect of botryosphaeran improving the metabolic parameters in these rats (E. Queiroz, unpublished data).

11.8.2 Cholesterol- and Lipid-Lowering Activities by Botryosphaeran

The development of the pathophysiology of obesity is associated with three factors – genetics, diet, and physical activity – that lead to cardiovascular and hepatic diseases, diabetes, and cancer. Obesity and cardiovascular diseases are often associated with dyslipidemia, esp., hypertriglyceridemia and hypercholesterolemia. Thus, the prevention of dyslipidemia decreases fat accumulation, and the management of obesity is a way to combat chronic diseases associated with this metabolic syndrome.

Lipids are transported in the blood packaged in lipoproteins that are differentiated because of their density (i.e., very low (VLDL)-, low (LDL)-, and high (HDL)-density lipoproteins). Abnormal levels in certain lipoproteins are linked to cardiovascular diseases, e.g., atherosclerosis. Cholesterol is synthesized in the liver from acetyl CoA. The initial step in the pathway leading to the formation of cholesterol (and the steroid hormones) is the synthesis of 3-hydroxy-3-methylglutaryl-CoA, which, in turn, is converted to mevalonate by the enzyme 3-hydroxy-3-

methylglutaryl-CoA reductase. This enzyme catalyzes the rate-limiting step to cholesterol synthesis and is regulated by a negative feedback mechanism mediated by sterols and metabolites derived from mevalonate.

Under normal conditions in mammalian cells, 3-hydroxy-3-methylglutaryl-CoA reductase is suppressed by cholesterol derived from the degradation of low-density lipoprotein (LDL) via the LDL receptor. Competitive inhibitors of this reductase induce the expression of LDL receptors in the liver, which in turn increases the catabolism of plasma LDL and lowers the plasma concentration of cholesterol. Low intracellular concentrations of cholesterol in the cell stimulates the expression of the low-density lipoprotein (LDL) receptor gene that leads to the synthesis of LDL receptors, which, in turn, promotes the uptake of LDL from the blood thereby lowering LDL cholesterol (Cohen and Armstrong 2014).

The control of cholesterol synthesis can be successfully targeted by *statins* (a class of lipid-lowering drugs – structural analogues of 3-hydroxy-3-methylglutaryl-CoA) through the competitive inhibition of 3-hydroxy-3-methylglutaryl-CoA reductase, thereby blocking the metabolic pathways leading to the synthesis of cholesterol. Statins are effective in reducing cardiovascular diseases and mortality in the category of those at high risk, but are not without their serious side effects, such as myopathy, fatigue, neuropathy, rhabdomyolysis, and memory loss (http://www.statinanswers.com/effects.htm).

On this pretext, it is advantageous to discover natural products that are safe (GRAS status) and can mimic the statin effect of lowering cholesterol without experiencing the serious side effects. In this respect, mushrooms containing various polysaccharides including the β-glucans have been demonstrated to be effective in lowering blood cholesterol levels (Wasser 2002, 2014), without inducing side effects (Babicek et al. 2007). In the category of the (1→3)-β-D-glucans, these macromolecules too have been demonstrated to be efficacious in treating hypercholesterolemic activity (Chen and Seviour 2007: Chen and Raymond 2008).

The cholesterol-lowering effect of oats (and barley) is well established and is attributable to the action of (1→3)(1→4)-linked β-D-glucans, which play roles in promoting health and preventing diseases (Daou and Zhang 2012). A *meta-analysis* performed on published randomized controlled trials in humans that compared the addition of ≥3 g of oat β-glucan/day to the diet was reported to reduce LDL cholesterol and total cholesterol without changing the levels of HDL cholesterol or triglycerides (Whitehead et al. 2014). A recent review by Sima et al. (2018) on β-glucans and cholesterol concluded that the β-glucans can serve as suitable therapeutic options to treat patients with dyslipidemia, and they do not induce any significant side effects.

In view of the observations discussed above, work from our research group on rats preconditioned on a high-fat diet containing cholesterol, saturated fats, and colic acid (HYPER diet, Reeves et al. 1993) and treated with botryosphaeran by gavage (12 mg/kg b.w./day) over 15 days reduced the plasma levels of total cholesterol and low-density lipoprotein cholesterol (LDL cholesterol) by 18% and 27%, respectively (Miranda-Nantes et al. 2011). In a related but independent study, Silva-Sena et al. (2018) demonstrated that botryosphaeran improved the lipidic profiles (reductions of

54% to 80%) and reduced LDL cholesterol by 86% in male knockout LDLr$^{-/-}$ mice that exhibited elevated plasma cholesterol levels and developed atherosclerosis on feeding a high-fat diet. Botryosphaeran furthermore decreased the aortic lipid deposition by 33% thus lowering the cardiovascular risk of atherosclerosis.

In another related study, Silva et al. (2018) demonstrated that obese rats induced on a high-fat and high-sugar diet showed significant increases in weight and adipose tissue (periepididymal, retroperitoneal, and mesenteric) and presented glucose intolerance, insulin resistance, dyslipidemia (hypertriglyceridemia, higher levels of VLDL cholesterol, and lower levels of HDL cholesterol), and hepatic steatosis. Treatment of the obese rats with botryosphaeran (12 mg/kg b.w.) over 15 days significantly reduced the feed intake, weight gain, and deposition of periepididymal and mesenteric fat and improved glucose tolerance, insulin sensitivity, and glucose levels. Furthermore, botryosphaeran corrected dyslipidemia, increased the amount of glycogen in the liver, and reduced total lipids, triglycerides, and cholesterol in the liver of the obese rats. These effects were mediated, at least in part, in adipose tissue, by AMPK activation and FOXO3a protein expression.

Several mechanisms have been proposed to explain the role of β-glucans in the treatment of dyslipidemia. The increased viscosity of these polysaccharides may reduce the absorption of cholesterol and triglycerides by the intestine, or the β-glucans may decrease the activity of digestive enzymes in the intestine thereby reducing lipid levels (Dong et al. 2011). Cao et al. (2016) excluded this hypothesis on observation that a yeast β-glucan did not inhibit intestinal α-glycosidase activity nor did their β-glucan decrease the intestinal absorption of glucose due to slow digestion. Furthermore, they demonstrated that the yeast-derived β-glucan promoted glycogen formation and reduced hepatic steatosis by decreasing the lipid vacuoles and suppressing the accumulation of lipids in the liver.

Galisteo et al. (2010) described another mechanistic insight of how polysaccharides could be involved in treating disorders of obesity and lipid metabolism. They demonstrated that a diet supplemented with psyllium (*Plantago ovata*, rich in a complex polysaccharide of the xylan type containing branches comprising arabinose, galacturonic acid, and rhamnose residues) over a 10-week period improved the obesity and lipid metabolism in obese Zucker rats. This finding was associated with a decrease in the production of TNF-α (a pro-inflammatory cytokine), reduced levels of insulin and leptin (*satiety* hormone released from adipose cells that sends signals to the hypothalamus to regulate long-term food intake and controls body energy homeostasis to promote or maintain obesity; Pan and Myers 2018), and increased activation of AMPK, which consequently inactivated the metabolic enzymes, acetyl CoA carboxylase and fatty acid synthase, in the liver. AMPK is an important enzyme that plays a key role in metabolism, especially in cellular energy homeostasis.

AMPK regulates several proteins and transcription factors including the FOXO forkhead transcription factors and signaling pathways in the liver, adipose tissue, skeletal muscle, and heart, thereby contributing to cellular metabolism of glucose and lipids (Kahn et al. 2005; Chiacchiera et al. 2009).

Other studies have suggested that β-glucans promote an increase in the conversion of cholesterol into bile acids by the up-regulation of cholesterol 7–αhydroxylase

activity, decreasing the quantity of these lipids in enterohepatic circulation (Brennan and Cleary 2005; Gunness and Gidley 2010; Chang et al. 2013). Further still, β-glucans may contribute to the formation of short-chain fatty acids arising from the degradation of dietary fibers by the intestinal microbiota that subsequently reduce cholesterol in the liver (Gunness and Gidley 2010). Recently, Cao et al. (2016) reported that type 2 diabetic mice fed a high-fat diet changed the gut microbiota greatly increasing the relative abundance of *Firmicutes* and decreasing the population of *Bacteroidetes* and that on treatment with yeast β-glucan decreased the relative abundance of *Firmicutes*. Alteration of the microbiota population may have promoted bile acids excreting cholesterol in the feces.

The effect of botryosphaeran in decreasing the body weight of obese rats induced on a high-fat and high-sugar diet compared with control rats could be attributed to the lower intake of food, water, and calories by this group of animals (Silva et al. 2018). Several factors, such as the dose, chemical structure, frequency, and degree of side branches, appear to influence the biological activities of β-glucans. In addition, El Khoury et al. (2012) in their review of the literature discussed that dose was a major factor influencing the efficacy of β-glucan on satiety. Botryosphaeran at a low dose (12 mg/kg b.w.) significantly decreased the feed intake in diet-induced obese rats and exhibited an important effect over feed intake and satiety, and consequently body weights and the accumulation of adipose tissue (Silva et al. 2018).

In conclusion, botryosphaeran presented important effects in the metabolism of carbohydrates and lipids, which contributed positively to the treatment of disorders in obesity and metabolic syndrome as indicated in Fig. 11.6.

11.9 Mechanistic Insights of Anticancer Activity Exhibited by Botryosphaeran in Breast Carcinoma MCF-7 Cells

Cancer is a multifactorial disease on the increase globally and is one of the principal causes of deaths among diseases in the world; ~8.2 million people die of cancer-related deaths per annum (INCA 2018). Surgery, chemotherapy, radiotherapy, and lately immunotherapy have been used to treat different types of cancers. Many of these treatments, however, promote side effects that can increase the morbidity and contribute to cancer mortality. Developing appropriate treatments that target cancer with minimal side effects and decrease tumor development is therefore of importance.

Many bioactive compounds contained in natural products of microbial and plant origin (non-prescription drugs) have been used as alternative and complementary medicines for millennia in practices to treat human disease conditions including cancers (Wasser 2002, 2014). They bear little of the side effects compared with the conventional treatments for cancer. Among these compounds are the group of polysaccharides of the (1→3)- and (1→3)(1→6)- β-glucan types produced by bacteria, fungi, and microalgae. They are recognized as possessing

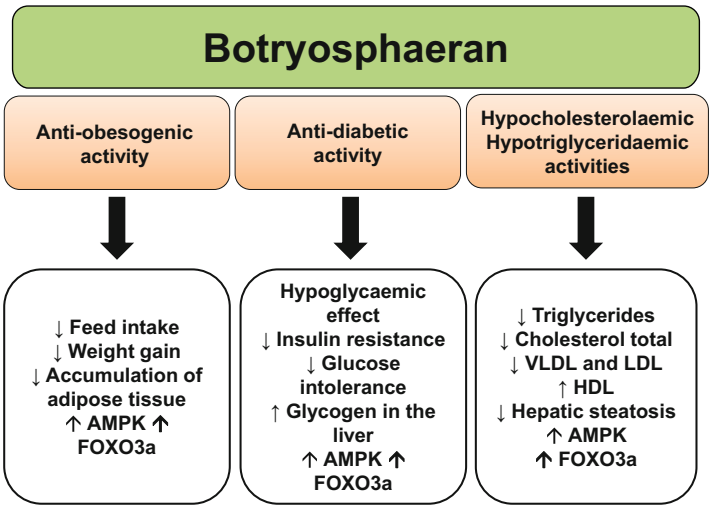

Fig. 11.6 Pharmacological effects of botryosphaeran in treating disorders associated with obesity and the metabolic syndrome

immunomodulatory and antitumor biological response-modifying activities (Albeituni and Yan 2013; Vetvicka and Vetvickova 2012) and can evoke the innate and adaptive immune responses of the host, an important role in preventing cancers and tumors (Vesely et al. 2011). The β-glucans stimulate the immune system by targeting pattern recognition receptors on immune cells, an attractive approach to immunotherapy of cancer (Goutagny et al. 2012).

β-Glucans have been described as possessing medicinal properties effective in treating cancers (Vetvicka and Vetvickova 2012). The antitumoral effect of β-glucans can be mediated directly against cancer cells via cytotoxicity and indirectly through immunomodulation (Chan et al. 2009; Batbayar et al. 2012). Some fungal polysaccharides (e.g., botryosphaeran) can exert a direct antiproliferative effect on cancer cells, promoting cell cycle arrest, apoptosis, necrosis, and oxidative stress (Malini et al. 2015; Queiroz et al. 2015). β-Glucans bind to specific cell surface receptors on immune cells (Albeituni and Yan 2013; Legentil et al. 2015) and modulate gene expression and signaling events leading to secretion of cytokines and chemokines that can manifest anticancer activity (Kerrigan and Brown 2010; Batbayar et al. 2012; Iliev et al. 2012).

Our group's studies on the effects of β-glucans on treating cancer cell lines (animal and human) – rat pancreas insulinoma (Kazak et al. 2014), human lymphocytes (Malini et al. 2015), and human breast cancer (Queiroz et al. 2015) – demonstrated that botryosphaeran manifested various biological responses. The action by which these occur in a mechanistic manner was advanced for breast cancer MCF-7 cells by Queiroz et al. (2015) and involved cell signaling pathways that suppressed tumorigenesis, decreased cancer cell proliferation, and promoted apoptosis, necrosis, and oxidative stress. Botryosphaeran-induced apoptosis was mediated by AMPK and the forkhead transcription factor, FOXO3a. In human tumorigenic lymphocytes (Jurkat

cells), botryosphaeran mediated the modulation of gene expression and the cell cycle (Malini et al. 2015). The biological activities of two exocellular β-glucans, botryosphaerans EPS_{GLC} and EPS_{FRU}, in the breast cancer MCF-7 cell line were studied in detail (Queiroz et al. 2015) and delineated the mechanism of action of these β-glucans as we discuss below.

11.9.1 Antiproliferation of Cancer Cells

β-Glucans are known to decrease cell proliferation in breast carcinoma MCF-7 cells by inducing cell cycle arrest (Zhang et al. 2006), apoptosis (Yang et al. 2006; Zhang et al. 2006), and oxidative stress (Thetsrimuang et al. 2011), and botryosphaeran is no exception in manifesting the same events (Malini et al. 2015; Queiroz et al. 2015).

Botryosphaerans EPS_{GLC} and EPS_{FRU} of different degrees of branching with glucose and gentiobiose residues (22 and 31%, respectively), demonstrated inhibition of cell proliferation in breast cancer MCF-7 cells in a time- and concentration-dependent manner with an IC_{50} (inhibitory concentration of 50%) of 100 μg/mL. The antiproliferative effect of EPS_{FRU} was greater than that for EPS_{GLC} as analyzed by the MTT assay described by Berridge et al. (2005), as only ~9% of MCF-7 cells remained viable after treatment with EPS_{FRU} compared to 22% for EPS_{GLC}. From our observations, we hypothesize that the higher degree of branching (31%) along the (1→3)-β-glucan chain in EPS_{FRU} compared to 22% in EPS_{GLC} influenced the antiproliferative effect. The influence of the degree of branching along the β-glucan chain on cell proliferation is the *first* report of this observation for β-glucans. The antiproliferative effect on MCF-7 cells by a water-soluble (1→3)(1→4)-β-glucan from *Poria cocos* was similarly time- and concentration-dependent and mediated by cell cycle arrest and cell apoptosis, but the IC_{50} value (400 μg/ml) was four-fold higher than the IC_{50} for botryosphaeran (Zhang et al. 2006).

The physicochemical properties of β-glucans are also known to correlate closely with the potency of their biological activity (Batbayar et al. 2012), and the association with a triple-helix conformation is known to enhance antitumor activity (Zhang et al. 2005). Both of the β-glucans (EPS_{GLC} and EPS_{FRU}) studied by our group exist in a triple-helix conformation (Giese et al. 2008), and since both polysaccharides exhibited antiproliferative activity in cancer MCF-7 cells, we assume that the triple-helix conformation of botryosphaeran also contributed to their antitumoral effect. This is an additional feature exhibited by these β-glucans.

11.9.2 Role of Oxidative Stress in Cancer

Oxidative stress generated by reactive oxygen species (ROSs) and subsequent redox signaling is implicated in the development of cancer. Some oxidants contribute to mutation and tumor growth, while excessive oxidative stress slows cell proliferation

and affects cell survival (Reuter et al. 2010; Sosa et al. 2013). It is well known that ROSs can promote cell apoptosis and consequently reduce cell viability (Queiroz et al. 2014; Schieber and Chandel 2014).

Botryosphaeran-treated breast cancer MCF-7 cells increased oxidative stress, and this effect was directly associated with a high degree of apoptosis and necrosis. Co-treatment of MCF-7 cells with botryosphaeran and the pro-oxidant hydrogen peroxide increased ROS levels confirming that oxidative stress was involved by the action of the two botryosphaerans. The combined treatment increased ROS levels relative to hydrogen peroxide alone, decreased cell viability of the MCF-7 cells, and confirmed the role of oxidative stress as part of the mechanism of action of botryosphaeran (Queiroz et al. 2015).

The precise mechanism of how β-glucans increase oxidative stress awaits further study. Literature findings suggest that β-glucans increase the production of ROS by activating the receptors, Dectin-1 and/or TLRs (Brown 2006; Batbayar et al. 2012). Binding of β-glucans to dectin-1 promoted the activation of spleen tyrosine kinase and NADPH oxidase and consequently increased the production of ROS. In this event, ROSs are the main product of the family of NADPH oxidases in a reaction that transfers electrons from NADPH to oxygen producing superoxide radical anion, a highly-reactive oxygen species (Paletta-Silva et al. 2013). Based on the scientific literature, we hypothesize that the increased production of ROS induced by the two β-glucans (EPS_{GLC} and EPS_{FRU}) may be associated with the activation of TLRs. Further studies, however, are required to substantiate this phenomenon. The exopolysaccharides from *Antrodia camphorata* were reported to induce cell death in a dose- and time-dependent manner in MCF-7 cells, and this effect was associated with an increase in the generation of ROS with consequent apoptosis (Yang et al. 2006). In a related study on the botryosphaeran (MW 1.82 x 10^6 Da) produced by a different strain of *B. rhodina* (RCYU 30101) grown on sucrose, Weng et al. (2011) demonstrated increased nitric oxide production in RAW 264.7 macrophage cells triggered by this β-glucan, which stimulated RAW 264.7 cells in producing TNF-α (an inflammatory cytokine responsible for signaling events within cells that lead to apoptosis and inhibit tumorigenesis) and contributed to antitumor activity. Nitric oxide (gaseous messenger molecule, or gasotransmitter) is a reactive nitrogen-oxygen species critical to a number of physiological and pathological events that act as signal transducers producing cytokines (Mocellin et al. 2007).

11.9.3 Botryosphaeran-Induced Apoptosis Mediated by AMP-Activated Protein Kinase and Forkhead Transcription Factor, FOXO3a

The LKB1/AMPK pathway (serine-threonine liver kinase B1, a tumor suppressor that functions by phosphorylating AMPK causing its activation to regulate cancer cell proliferation and metabolism) is an important pathway inhibiting cellular growth

and promoting apoptosis in cancer cells (Shackelford and Shaw 2009). It does this by inhibiting the activities of mTOR (mammalian target of rapamycin, a member of the phosphatidylinositol 3-kinase family of protein kinases) and p70S6K (ribosomal protein S6 kinase β-1, a serine/threonine kinase targeting S6 ribosomal protein through phosphorylation inducing protein synthesis), as well as through activating p53 protein (phosphorylated protein that regulates the cell cycle and functions as a tumor suppressor) (Feng et al. 2007; Zakikhani et al. 2008; Berstein et al. 2011). In addition, studies have shown that AMPK can activate the forkhead transcription factor, the FOXO proteins, under conditions of nutrient deprivation thereby increasing cell survival (Chiacchiera et al. 2009; Greer et al. 2009). The FOXO proteins, of which FOXO3a is a member, constitute a subfamily of transcription factors involved in regulating energy metabolism, angiogenesis, and stem cell proliferation (Calnan and Brunet 2008). FOXO proteins also promote tumor suppression by promoting cell cycle arrest, repairing damaged DNA, and promoting apoptosis (Brunet et al. 1999; Dijkers et al. 2000).

Cellular changes in the expression of FOXO proteins such as low expression of FOXO protein or phosphorylation of FOXO3a at Ser253 are linked to tumorigenesis and cancer (Hu et al. 2004; Yang and Hung 2011). Cytoplasmic localization of FOXO3a is correlated with poor survival in breast cancer patients (Hu et al. 2004). Through our studies, we demonstrated that EPS_{GLC} led to FOXO3a activity in MCF-7 cells and was due to increased expression of FOXO3a. Phosphorylation of FOXO3a at residue Ser253 was significantly lower as a consequence of treatment of MCF-7 cells by EPS_{GLC} that resulted in increasing FOXO3a activity (Queiroz et al. 2015). Phosphorylation at Ser253 of FOXO3a by Akt (serine-/threonine-specific protein kinase that plays a key role in multiple cellular processes) leads to the accumulation of FOXO3a in the cytoplasm, and subsequently the proteasome system may lead to its degradation by proteases (Calnan and Brunet 2008). Treatment of MCF-7 cells with EPS_{GLC} increased expression of p-AMPK (Thr172) and FOXO3a and reduced p-p70S6K (Thr389). This observation unequivocally demonstrated that the antiproliferative effect of botryosphaeran in MCF-7 cells was mediated by the actions of AMPK and FOXO3a (Queiroz et al. 2015).

How does this event occur? Activated FOXO3a binds to promoters and induces the transcription of certain target genes involved in cell cycle arrest that are involved in cell death and contributes to tumor suppression and apoptosis (Calnan and Brunet 2008; Ho et al. 2008; Chiacchiera et al. 2009). EPS_{GLC} increased the expression of mRNAs of p53 (*TP53* gene) and p27 (*CDKN1B* gene) that are involved in cell cycle arrest, increased the expression of Bax mRNA (*BAX* gene), and cleaved caspase-3 proteins that are involved in apoptotic pathways. The caspases constitute a family of cysteine proteases (up to 12 sub-families exist) that play essential roles in apoptosis (McIlwain et al. 2013). Intracellular targets of antiproliferation of MCF-7 cells mediated by EPS_{GLC} – p53, p27 (an inhibitor of cyclin-dependent kinases involved in the regulation of the cell cycle, Malumbres 2014), Bax, and caspase-3 – confirmed that this occurred via FOXO3a activity. EPS_{GLC} presented trends in protein expression, and increased the activity of AMPK and FOXO3a proteins. The higher

degree of branching of EPS_{FRU} influenced gene and protein expression differently without increasing FOXO3a activity compared to the lesser-branched EPS_{GLC} (Queiroz et al. 2015).

11.9.4 Cell Cycle Checkpoints

During cell proliferation, cells enter the cell cycle following stimulus by hormones and growth factors. The cell cycle is the series of events divided into four phases: G_1, S, G_2, and M. During this process the cellular components are doubled and then accurately segregated into two daughter cells. In eukaryotes, DNA replication occurs in the S phase (synthesis), and the chromosome segregation occurs at mitosis, or M phase. In addition, there are two Gap phases: one between the G_1 and S phase, and the other one between G_2 and M phase. Each phase of the cell cycle is regulated by certain cyclins and cyclin-dependent kinases (CDK), as well as regulated by CDK inhibitors such as p21, p27, and p53 (Barnum and O'Connell 2014). Cell proliferation is determined by the rate that the cell proceeds through the different cell cycle phases and checkpoints (Barnum and O'Connell 2014). Activation of these checkpoints induces cell cycle arrest through modulation of cyclin-dependent kinase activity (Malumbres and Barbacid 2009).

The two botryosphaerans increased the percentage of cells in the sub-G_1 phase (apoptotic cells) of the cell cycle of breast cancer MCF-7 cells. A higher pro-apoptotic effect was presented by EPS_{FRU} and was exhibited by a lower number of cells in the S phase that suggested cell cycle arrest in the G_0-G_1 phase. This feature is associated with a higher expression of p53 mRNA and Bax, and the cleaved caspase-3 proteins, and appears to be attributable to the higher degree of branching on EPS_{FRU} (Queiroz et al. 2015). Malini et al. (2015) also reported cell cycle arrest by EPS_{GLC} in human tumor T lymphocytes (Jurkat cells).

11.9.5 Apoptosis and Necrosis

Apoptosis, or *programmed* cell death, is generated by many physiological and pathological events and is highly regulated by different proteins that promote or block cell death at different stages (Portt et al. 2011). Apoptosis can be initiated by two pathways: extrinsic (cytoplasmic) or intrinsic (mitochondrial) (Hongmei 2012). Proteins of the Bcl-2 family and two groups of pro-apoptotic proteins (Bax and BH3) are important regulators of apoptosis. Bax may trigger apoptosis when it homodimerizes, or through heterodimerization with Bcl-2 and/or Bcl-xL, to inhibit apoptosis (Oltval et al. 1993; Reed 1997; Zamzami and Kroemer 2001). The expression of Bax and Bcl-2 proteins in MCF-7 cells by the two botryosphaerans (EPS_{GLC}, EPS_{FRU}) demonstrated that Bax expression was significantly higher in both, which might have contributed to the pro-apoptotic effects of these β-glucans. The Bax/Bcl-2 ratio was

increased in the botryosphaeran-treated groups. The Bax/Bcl-2 ratio determines the susceptibility of cells to apoptosis (Dijkers et al. 2000; Raisova et al. 2001). Bax cooperates to increase mitochondrial membrane permeability and releases pro-apoptotic cytochrome *c* and apoptosis-inducing factor, which in turn, activates the *executioner* caspases (3, 6, and 7) leading to apoptosis (Kroemer and Reed 2000; Youle and Strasser 2008). Botryosphaeran increased caspase-3/caspase-7 activity in breast cancer MCF-7 cells, as observed by the high numbers of caspase-3/caspase-7 positive cells measured by flow cytometry and high cleaved caspase-3 protein expression (active form of caspase-3) as detected by Western blotting, all of which contributed to apoptosis in MCF-7 cells (Queiroz et al. 2015). Long-term treatment (72 h) of MCF-7 cells with botryosphaeran increased necrosis, which can be associated with oxidative stress as observed in the treated cells.

Necrosis is a type of *un-programed* cell death triggered by a variety of factors (stimuli) external to the cell causing loss of membrane integrity, swelling of intracellular organelles, and intense depletion of ATP that leads to an influx of high levels of calcium and production of high levels of ROSs. The intensity of the stimulus can trigger apoptosis and necrosis, but beyond a certain threshold, oxidative stress-induced changes modify the mechanism of cell death from apoptosis to necrosis (Aki et al. 2015; McConkey 1998).

In conclusion, our studies have demonstrated the potential beneficial effects of botryosphaeran in cancer treatment, presenting for the *first* time a detailed mechanistic insight into the antiproliferative effect against cancer cells via activation by AMPK and FOXO3a expression in breast cancer MCF-7 cells. The pathways exhibiting the antiproliferative effects of botryosphaeran in breast cancer MCF-7 cells are schematically represented in Fig. 11.7.

11.9.6 Concluding Remarks: Insights into New Biological Functions and Applications of Botryosphaeran

Our research on botryosphaeran continues in collaborations with several groups throughout Brazil, and in Canada, examining new applications such as biological response-modifying activities of derivatized botryosphaerans, treatment of skin conditions (eczema and psoriasis), antimicrobial activities, antinociceptive activity, as a matrix for enzyme immobilization, as a platform for electrochemical sensors, and as a food additive (nutraceutical).

The botryosphaeran prepared by freeze-drying is sparingly soluble in water, but solubility can be enhanced through derivatization of the hydroxyl groups along the polysaccharide chain with functional groups (carboxymethyl, sulfonyl). We are eager to discover if this kind of modification will also improve its biological activity or create new biological functions. There are few studies on the biological properties of derivatized β-glucans, and this may open new opportunities and possibilities for creating further applications of botryosphaeran. Already we found that sulfonylation

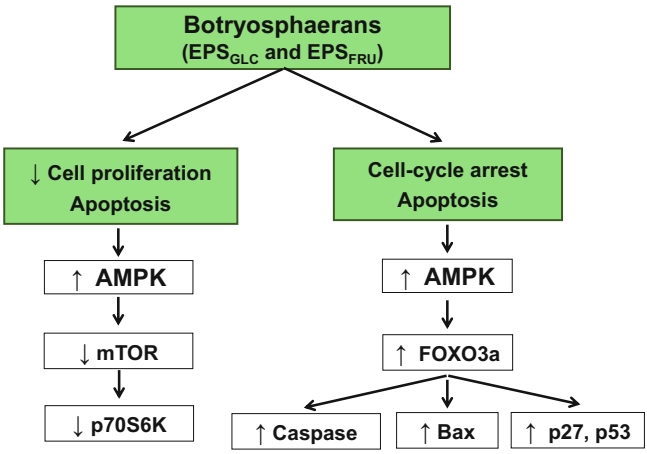

Fig. 11.7 Pathways exhibiting the antiproliferative and cell cycle effects of botryosphaeran in breast cancer MCF-7 cells

of botryosphaeran introduced a new biological function, anticoagulation (Mendes et al. 2009; Brandi et al. 2011). Studies in progress on sulfonated botryosphaeran have revealed strong antiviral activity against several enveloped viruses including *Herpes simplex* I and dengue (A. Orsato, unpublished results). Underivatized botryosphaeran, by contrast, only moderately inhibited viral infection. The presence of sulfonate groups and the degree of sulfonation were found important in manifesting this biological activity. Studies under development on the biological functions of carboxymethylated botryosphaeran in lab animals are assessing hypoglycemia, hypocholesterolemia, promotion of wound healing, and antiviral and anticancer activity.

The gel form of botryosphaeran is firm, and this property may lend a new possible application as a gel to replace silicone gels in breast implants. The gels may require cross-linking to enhance their strength. Botryosphaeran is immunostimulatory, and in the event of the implant leaking or breaking, would not pose the same dire consequences as exhibited by leaking silicone implants.

Encapsulation of the probiotic *Lactobacillus casei* in alginate microspheres together with botryosphaeran and mucilages from linseed and okra increased the encapsulation efficiency and improved the stability of the encapsulated probiotic bacteria during prolonged storage at 5 °C (Rodrigues et al. 2017). Gastrointestinal simulation studies on the microencapsulated *L. casei* cells demonstrated preservation of the viability of the probiotics against low pH and bile salts. The use of botryosphaeran in microencapsulating probiotic bacteria (and prebiotics) appears to be a promising application for this β-glucan.

It is well known that β-glucans have antinociceptive properties (Moreno et al. 2016). Botryosphaeran was found to effectively remove pain, decrease inflammation, and improve the healing process when a topical cosmetic crème containing this

β-glucan was applied to areas on the skin affected by hematomas, bruising, burns, superficial injuries, insect bites, and other irritations.

A future direction will be to assess the mutagenicity and genotoxicity of the biomass (mycelium) from *B. rhodina* MAMB-05 resulting from the fermentative production of botryosphaeran. The fungal biomass is rich in α- and β-glucans, chitin, and proteins and has potential as an animal feed supplement. Similarly, the vinasse resulting after removal of ethanol by distillation from the cell-free fermentation broth (Fig. 11.3) has potential as an animal feed material but needs to be to assessed for its safety on animal use. Studies in progress are also evaluating this biomass resource as a biosorbent to extract metallic species (lanthanides, lead, mercury, cadmium, and chromium) from effluents (Giese et al. 2019; and E. Castro, unpublished data).

Enzymes of the β-glucanase and β-glucosidase kinds that attack the β-(1→3)- and β-(1→6)-linkages of botryosphaeran defragment the biopolymer into a series of (1→3)- and (1→6)-linked gluco-oligosaccharides of varying degrees of polymerization that can serve as prebiotics. Such enzymes can easily be produced by submerged fermentation by *B. rhodina* MAMB-05, *Trichoderma harzianum* Rifai, and *Aureobasidium pullulans* (Giese et al. 2009, 2011a; Bauermeister et al. 2015). Gluco-oligosaccharides constituted of (1→3)- and (1→6)-linked β-glucosides are considered emerging prebiotics, and their use can be as nutraceuticals in food products.

Botryosphaeran has demonstrated strong antimutagenicity, and chemoprotective activity against DNA damage and cell death induced by chemotherapeutic agents such as used to treat cancer, and could find application as an adjuvant to lessen the side effects in treating cancers. Another possible application for botryosphaeran could be as co-adjuvant in vaccines because of its immunopotentiation functions.

Lastly, three formulated commercial cosmetic products have evolved from our years of studies on botryosphaeran: facial crème, body lotion and a serum containing botryosphaeran to promote skin health and treat skin conditions.

Acknowledgments The authors gratefully acknowledge the valuable contributions to the research on botryosphaeran made by Dr Ellen C Giese (whose work was instrumental in many of the early discoveries), Dr Maria de Lourdes Corradi da Silva (elucidation of chemical structures and physical properties), and Dr Ilce MS Cólus (mutagenic and cytotoxicity studies). We also acknowledge the valuable contributions and important roles played by a host of some 70 students (undergraduate, masters, doctoral, post-doc) in developing this line of research, and we gratefully thank them for their assiduous efforts.

References

Aimanianda V, Clavaud C, Simenel C, Fontaine T, Delepierre M, Latgé JP (2009) Cell wall β-(1,6)-glucan of *Saccharomyces cerevisiae*: structural characterization and in situ synthesis. J Biol Chem 284:13401–13412

Aki T, Funakoshi T, Uemura K (2015) Regulated necrosis and its implications in toxicology. Toxicology 333:118–126

Alban S, Schauerte A, Franz G (2002) Anticoagulant sulfated polysaccharides: Part I. Synthesis and structure-activity relationships of new pullulan sulfates. Carbohydr Polym 47:267–276

Albeituni SH, Yan J (2013) The effects of β-glucans on dendritic cells and implications for cancer therapy. Anticancer Agents Med Chem. 13:689–698

Al-Sheraji SH, Ismail A, Manap MY, Mustafa S, Yusof RM, Hassan FA (2013) Prebiotics as functional foods: a review. J Funct Foods 5:1542–1553

Babíček K, Čechová I, Simon RR, Harwood M, Cox DJ (2007) Toxicological assessment of a particulate yeast (1,3/1,6)-β-D-glucan in rats. Food Chem Toxicol. 45:1719–1730

Bacic A, Fincher G, Stone BA (eds) (2009) Chemistry, biochemistry and biology of (1→3)-β-glucans and related polysaccharides. Academic Press, Cambridge

Banik RM, Santhiagu A, Upadhyay SN (2007) Optimization of nutrients for gellan gum production by *Sphingomonas paucimobilis* ATCC-31461 in molasses based medium using response surface methodology. Bioresour Technol 98:792–797

Barbosa AM, Dekker RFH, St. Hardy GE (1996) Veratryl alcohol as an inducer of laccase by an ascomycete, *Botryosphaeria* sp., when screened on the polymeric dye Poly R-478. Lett Appl Microbiol 23:93–96

Barbosa AM, Steluti RM, Dekker RFH, Cardoso MS, Corradi da Silva ML (2003) Structural characterization of botryosphaeran: a (1→3;1→6)-β-D-glucan produced by the ascomyceteous fungus, *Botryosphaeria* sp. Carbohydr Res 338:1691–1698

Barnum KJ, O´connell MJ (2014) Cell cycle control. Methods Mol Biol 1170:29–40

Batbayar S, Lee DH, Kim HW (2012) Immunomodulation of fungal β-Glucan in host defense signaling by dectin-1. Biomol Ther 20:433–445

Bauermeister A, Amador IR, Pretti CP, Giese EC, Oliveira ALM, Borsato D, da Cunha MAA, Rezende MI, Dekker RFH, Barbosa AM (2015) β-(1→3)-Glucanolytic yeasts from Brazilian grape microbiota: Production and characterization of β-glucanolytic enzymes by *Aureobasidium pullulans* 1WA1 cultivated on fungal mycelium. J Agric Food Chem 63:269–278

Berridge MV, Herst PM, Tan AS (2005) Tetrazolium dyes as tools in cell biology: New insights into their cellular reduction. Biotechnol Annu Rev 11:127–152

Berstein LM, Yue W, Wang JP, Santen RJ (2011) Isolated and combined action of tamoxifen and metformin in wild-type, tamoxifen-resistant, and estrogen-deprived MCF-7 cells. Breast Cancer Res Treat 128:109–117

Bohn JA, BeMiller JN (1995) (1→3)-β-D-glucans as biological response modifiers: a review of structure-functional activity relationships. Carbohydr Polym 28:3–14

Bot A, Smorenburg HE, Vreeker R, Pâques M, Clark AH (2001) Melting behavior of schizophyllan extracellular polysaccharide gels in the temperature range between 5 and 20 °C. Carbohydr Polym 45:363–372

Box GEP, Hunter JS, Hunter WG (eds) (2005) Statistics for experimenters: design, innovation, and discovery, 2nd edn. Wiley-Interscience, Hoboken. ISBN: 978-0-471-71813-0

Brandi J, Oliveira EC, Monteiro NK, Vasconcelos AFD, Dekker RFH, Barbosa AM, Silveira JLM, Mourao PAS, Corradi da Silva ML (2011) Chemical modification of botryosphaeran: structural characterization and anticoagulant activity of a water-soluble sulfonated (1→3)(1→6)-β-D-glucan. J Microbiol Biotechnol 21:1036–1042

Brennan CS, Cleary LJ (2005) The potential use of cereal (1→3)(1→4)-β-D-glucans as functional food ingredients. J Cereal Sci 42:1–13

Brown GD (2006) Dectin-1: a signalling non-TLR pattern-recognition receptor. Nat Rev Immunol 6:33–43

Brunet A, Bonni A, Zigmond MJ, Lin MZ, Juo P, Hu LS, Anderson MJ, Arden KC, Blenis J, Greenberg ME (1999) Akt promotes cell survival by phosphorylating and inhibiting a forkhead transcription factor. Cell 96:857–868

Bruns RE, Scarminio IS, Barros Neto B (eds) (2006) Statistical design – chemometrics, Data handling in science and technology, 1st edn. Amsterdam, Elsevier

Calle EE, Kaaks R (2004) Overweight, obesity and cancer: epidemiological evidence and proposed mechanisms. Nat Rev Cancer 4:579–591

Calnan DR, Brunet A (2008) The FoxO code. Oncogene 27:2276–2288
Cao Y, Zou S, Xu H, Li M, Tong Z, Xu M, Xu X (2016) Hypoglycemic activity of the Baker's yeast β-glucan in obese/type 2 diabetic mice and the underlying mechanism. Mol Nutr Food Res 60:2678–2690
Castillo NA, Valdez AL, Fariña JI (2015) Microbial production of scleroglucan and downstream processing. Front Microbiol 6:1–19
Chan G, Chan W, Sze D (2009) The effects of β-glucan on human immune and cancer cells. J Hematol Oncol 2:25
Chang HC, Huang CN, Yeh DM, Wang SJ, Peng CH, Wang CJ (2013) Oat prevents obesity and abdominal fat distribution, and improves liver function in humans. Plant Foods Hum Nutr 68:18–23
Chen F, Huang G (2018) Preparation and immunological activity of polysaccharides and their derivatives. Int J Biol Macromol 112:211–216
Chen J, Raymond K (2008) Beta-glucans in the treatment of diabetes and associated cardiovascular risks. Vasc Health Risk Manag 4:1265–1272
Chen J, Seviour R (2007) Medicinal importance of fungal β-(1→3)(1→6)-glucans. Mycol Res 111:635–652
Chiacchiera F, Matrone A, Ferrari E, Ingravallo G, Lo Sasso G, Murzilli S, Petruzzelli M, Salvatore L, Moschetta A, Simone C (2009) p38α blockade inhibits colorectal cancer growth *in vivo* by inducing a switch from HIF1α- to FoxO-dependent transcription. Cell Death Differ 16:1203–1214
Cohen DE, Armstrong EJ (2014) Farmacologia do metabolismo do cholesterol e das lipoproteínas. In: Golan DE, Tashijian AH, Armstrong EJ, Armstrong AW (eds) Princípios de Farmacologia: a base fisiopatológica da farmacoterapia, 3rd edn. Editora Guanabara Koogan Ltda, Rio de Janeiro, pp 664–706
Corradi da Silva MDL, Izeli NL, Martinez PF, Silva IR, Constantino CJL, Cardoso MS, Barbosa AM, Dekker RFH, Silva GVJ (2005) Purification and structural characterisation of (1→3;1→6)-β-D-glucans (botryosphaerans) from *Botryosphaeria rhodina* grown on sucrose and fructose as carbon sources: a comparative study. Carbohydr Polym 61:10–17
Corradi da Silva M, Fukuda EK, Vasconcelos AFD, Dekker RFH, Matias AC, Monteiro NK, Cardoso MS, Barbosa AM, Silveira JLM, Sassaki GL, Carbonero ER (2008) Structural characterization of the cell wall D-glucans isolated from the mycelium of *Botryosphaeria rhodina* MAMB-05. Carbohydr Res 343:793–798
Crognale S, Bruno M, Moresi M, Petruccioli M (2007) Enhanced production of β-glucan from *Botryosphaeria rhodina* using emulsified media or fan impellers. Enzyme Microb Technol 41:111–120
Cumpstey I (2013) Chemical modification of polysaccharides. ISRN Org Chem 2013: Article ID 417672: 1–27
Cunha MAA, Albornoz SL, Santos VAQ, Sánchez WN, Barbosa-Dekker AM, Dekker RFH (2017) Structure and biological functions of D-glucans and their applications. In: Rahman AU (ed) Studies in natural products chemistry, 1st edn. Elsevier, Amterdã, pp 309–337
Daou C, Zhang H (2012) Oat beta-glucan: its role in health promotion and prevention of diseases. Compr Rev Food Sci Food Saf 11:355–365
Dekker RFH, Barbosa AM (2001) Effect of aeration and veratryl alcohol on the production of two laccases by the ascomycete *Botryosphaeria* sp. Enz Microb Technol 28:81–88
Dekker RFH, Richards GN (1971) Determination of starch in plant material. J Sci Food Agric 22:441–444
Dekker RFH, Vasconcelos AFD, Barbosa AM, Giese EC, Paccola-Meirelles L (2001) A new role for veratryl alcohol: regulation of synthesis of lignocellulose-degrading enzymes in the ligninolytic ascomyceteous fungus, *Botryosphaeria* sp.; influence of carbon source. Biotechnol Lett 23:1987–1993
Dekker RFH, Barbosa AM, Giese EC, Godoy SDS, Covizzi LG (2007) Influence of nutrients on enhancing laccase production by *Botryosphaeria rhodina* MAMB-05. Int Microbiol 10:177–185

Dijkers PF, Medema RH, Lammers JWJ, Koenderman L, Coffer PJ (2000) Expression of the pro-apoptotic Bcl-2 family member Bim is regulated by the forkhead transcription factor FKHR-L1. Curr Biol 10:1201–1204

Dissanayake AJ, Phillips AJL, Li XH, Hyde KD (2016) *Botryosphaeriaceae*: current status of genera and species. Mycosphere 7:1001–1073

Dong Q, Jia LM, Fang JN (2006) A β-D-glucan isolated from the fruiting bodies of *Hericium erinaceus* and its aqueous conformation. Carbohydr Res 341:791–795

Dong J, Cai F, Shen R, Liu Y (2011) Hypoglycaemic effects and inhibitory effect on intestinal disaccharidases of oat beta-glucan in streptozotocin-induced diabetic mice. Food Chem 129:1066–1071

Dougan M, Dranoff G (2009) Immune therapy for cancer. Annu Rev Immunol 27:83–117

Dubois M, Gilles K, Hamilton J, Rebers P, Smith F (1956) Colorimetric method for determination of sugars and related substances. Anal Chem 28:350–356

El Khoury D, Cuda C, Luhovyy BL, Anderson GH (2012) Beta-glucan: health benefits in obesity and metabolic syndrome. J Nutr Metabol Volume 2012: Article ID 851362: (pages 1–28)

Fariña JI, Siñeriz F, Molina OE, Perotti NI (2001) Isolation and physicochemical characterization of soluble scleroglucan from *Sclerotium rolfsii*. Rheological properties, molecular weight and conformational characteristics. Carbohydr Polym 44:41–50

Fenech M (1993) The cytokinesis-block micronucleus technique and its application to genotoxicity studies in human populations. Environ Health Perspect 101(Suppl 3):101–107

Feng Z, Hu W, Stanchina E, Teresky AK, Jin S, Lowe S, Levine AJ (2007) The regulation of AMPK β1, TSC2, and PTEN expression by p53: stress, cell and tissue specificity, and the role of these gene products in modulating the IGF-1-AKT-mTOR pathways. Cancer Res 67:3043–3053

Ferreira SS, Passos CP, Madureira P, Vilanova M, Coimbra MA (2015) Structure-function relationships of immunostimulatory polysaccharides: a review. Carbohydr Polym 132:378–396

Fonseca PRMS, Dekker RFH, Barbosa AM, Silveira JLM, Vasconcelos AFD, Monteiro NK, Aranda-Selverio G, Corradi da Silva ML (2011) Thermal and rheological properties of a family of botryosphaerans produced by *Botryosphaeria rhodina* MAMB-05. Molecules 16:7488–7501

Free SJ (2013) Fungal cell wall organization and biosynthesis. In: Friedmann T, Dunlap JC, Goodwin SF (eds) Advances in genetics, 1st edn. Academic Press, Burlington, pp 33–82

Galisteo M, Moro NR, Rivera L, Romero R, Anguera A, Zarzuelo A (2010) *Plantago ovata* husks-supplemented diet ameliorates metabolic alterations in obese Zucker rats through activation of AMP-activated protein kinase: comparative study with other dietary fibers. Clin Nutr 29:261–267

Garcia JE, Vilas-Boas LA, Dekker RFH, Fungaro MHP, Barbosa AM (2004) *Botryosphaeria rhodina* MAMB-05 isolated from eucalypt canker GenBank: AY612337

Giese EC, Covizzi LG, Dekker RFH, Barbosa ADM (2004) Influência de tween na produção de lacases constitutivas e indutivas pelo *Botryosphaeria* sp. Acta Sci Biol Sci 26:463–470

Giese EC, Covizzi LG, Borsato D, Dekker RFH, Silva MDLC, Barbosa AM (2005) Botryosphaeran, a new substrate for the production of β-1,3-glucanases by *Botryosphaeria rhodina* and *Trichoderma harzianum* Rifai. Process Biochem 40:3783–3788

Giese EC, Covizzi LG, Dekker RFH, Monteiro NK, Maria de Lourdes Corradi da Silva MDL, Barbosa AM (2006) Enzymatic hydrolysis of botryosphaeran and laminarin by β-1,3-glucanases produced by *Botryosphaeria rhodina* and *Trichoderma harzianum* Rifai. Process Biochem 41:1265–1271

Giese EC, Dekker RFH, Barbosa AM, da Silva R (2008) Triple helix conformation of botryosphaeran, a (1→3;1→6)-β-D-glucan produced by *Botryosphaeria rhodina* MAMB-05. Carbohydr Polym 74:953–956

Giese EC, Monteiro A, Dekker R, Barbosa AM, Corradi da Silva ML, Gomes E, Silva R (2009) Evaluation of the β-glucanolytic enzyme complex of *Trichoderma harzianum* Rifai for the production of gluco-oligosaccharide fragments by enzymatic hydrolysis of 1,3;1,6-β-D-glucans. In: Mendez-Vilas A (ed) Current research topics in applied microbiology and microbial biotechnology. World Scientific Publishing Co. Pte. Ltd., Singapore, pp 438–441

Giese EC, Dekker RFH, Barbosa AM, Corradi da Silva ML, da Silva R (2011a) Production of β-(1,3)-glucanases by *Trichoderma harzianum* Rifai: optimization and application to produce gluco-oligosaccharides from Paramylon and Pustulan. Ferment Technol 1:1–5

Giese EC, Dekker RFH, Scarminio IS, Barbosa AM, da Silva R (2011b) Comparison of β-1,3-glucanase production by *Botryosphaeria rhodina* MAMB-05 and *Trichoderma harzianum* Rifai and its optimization using a statistical mixture-design. Biochem Eng J 53:239–243

Giese EC, Gascon J, Anzelmo G, Barbosa AM, Alves da Cunha MA, Dekker RFH (2015a) Free-radical scavenging properties and antioxidant activities of the β-glucans: botryosphaeran, laminarin, curdlan and lasiodiplodan. Int J Biol Macromol 72:125–130

Giese EC, Sumiya AFG, Borsato D, Dekker RFH, Barbosa AM (2015b) Evaluation of fermentative parameters for the production of botryosphaeran (a (1→3;1→6)-β-D-glucan) and mycelial biomass by *Botryosphaeria rhodina* MAMB-05. Orbital – Electron J Chem 7:36–43

Giese EC, Dekker RFH, Barbosa-Dekker AM (2019) Biosorption of lanthanum and samarium by viable and autoclaved mycelium of *Botryosphaeria rhodina* MAMB-05. Biotechnol Prog: e2783. https://doi.org/10.1002/btpr.2783

Gorin PAJ, Corradi da Silva ML, Iacomini M, Jablonski E (1993) Carbohydrate, glycopeptide and protein components of the lichen *Sticta* sp. and effect of storage. Phytochemistry 33:547–552

Goutagny N, Estornes Y, Hasan U, Lebecque S, Caux C (2012) Targeting pattern recognition receptors in cancer immunotherapy. Target Oncol 7:29–54

Gow NAR, Latge J, Munro CA (2017) The fungal cell wall: structure, biosynthesis and function. Microbiol Spectr 5:1–25

Greer EL, Banko MR, Brunet A (2009) AMP-activated protein kinase and FoxO transcription factors in dietary restriction-induced longevity. Ann N Y Acad Sci 1170:688–692

Gunness P, Gidley MJ (2010) Mechanisms underlying the cholesterol-lowering properties of soluble dietary fibre polysaccharides. Food Funct 1:149–155

Hakomori S (1964) A rapid permethylation of glycolipid, and polysaccharide catalyzed by methylsulfinyl carbanion in dimethyl sulfoxide. J Biochem 55:205–208

Hayashi M (2016) The micronucleus test-most widely used in vivo genotoxicity test. Genes Environ 38:18. (pages 1–6)

Ho KK, Myatt SS, Lam EWF (2008) Many forks in the path: cycling with FoxO. Oncogene 27:2300–2311

Hongmei Z (2012) Extrinsic and intrinsic apoptosis signal pathway review. In: Ntuli T (ed) Apoptosis and medicine. IntechOpen Ltd, London, pp 3–22

Hsieh C, Wang HL, Chen CC, Hsu TH, Tseng MH (2008) Effect of plant oil and surfactant on the production of mycelial biomass and polysaccharides in submerged culture of *Grifola frondosa*. Biochem Eng J 38:198–205

Hu MCT, Lee DF, Xia W, Golfman LS, Ou-Yang F, Yang JY, Zou Y, Bao S, Hanada N, Saso H, Kobayashi R, Hung MC (2004) IκB kinase promotes tumorigenesis through inhibition of forkhead FOXO3a. Cell 117:225–237

Hursting SD, Hursting MJ (2012) Growth signals, inflammation, and vascular perturbations: mechanistic links between obesity, metabolic syndrome, and cancer. Arterioscler Thromb Vasc Biol 32:1766–1770

Hwang HJ, Kim SW, Lim JM, Joo JH, Kim HO, Kim HM, Yun JW (2005) Hypoglycemic effect of crude exopolysaccharides produced by a medicinal mushroom *Phellinus baumii* in streptozotocin-induced diabetic rats. Life Sci 76:3069–3080

Iliev ID, Funari VA, Taylor KD, Nguyen Q, Reyes CN, Strom SP, Brown J, Becker CA, Fleshner PR, Dubinsky M, Rotter JI, Wang HL, McGovern DPB, Brown GD, Underhill DM (2012) Interactions between commensal fungi and the C-type lectin receptor dectin-1 influence colitis. Science 336:1314–1317

INCA. – Ministério da Saúde: Instituto Nacional de Câncer José Alencar Gomes da Silva, http://www.inca.gov.br/wcm/dmdc/2016/numeros-cancer-brasil.asp. Accessed 4 Sept 2018

Janusz G, Pawlik A, Sulej J, Świderska-Burek U, Jarosz-Wilkolazka A, Paszczyński A (2017) Lignin degradation: microorganisms, enzymes involved, genomes analysis and evolution. FEMS Microbiol Rev 41:941–962

Jiang L (2010) Optimization of fermentation conditions for pullulan production by *Aureobasidium pullulan* using response surface methodology. Carbohydr Polym 79:414–417

Jiao G, Yu G, Zhang J, Ewart HS (2011) Chemical structures and bioactivities of sulfated polysaccharides from marine algae. Mar Drugs 9:196–233

Kagimura FY, Cunha MAA, Barbosa AM, Dekker RFH, Malfatti CRM (2015) Biological activities of derivatized D-glucans: a review. Int J Biol Macromol 72:588–598

Kahn BB, Alquier T, Carling D, Hardie DG (2005) AMP-activated protein kinase: ancient energy gauge provides clues to modern understanding of metabolism. Cell Metabol 1:15–25

Kasibhatla S, Amarante-Mendes GP, Finucane D, Brunner T, Bossy-Wetzel E, Green DR (2006) Acridine orange/ethidium bromide (ao/eb) staining to detect apoptosis. Cold Spring Harb Protoc 2006. https://doi.org/10.1101/pdb.prot4493

Kazak H, Barbosa AM, Baregzay B, Cunha MAA, Öner ET, Dekker RFH, Khaper N (2014) Biological activities of bacterial levan, and three fungal β-glucans, botryosphaeran and lasiodiplodan, under high glucose condition in the pancreatic β-cell line INS-1E. In: Popescu LM, Hargens AR, Singal PK (eds) Adaptation biology and medicine: new developments. Narosa Publishing House, New Delhi, Vol 7, Ch 8, pp 105–115

Kerche-Silva LE, Cólus IMS, Malini M, Mori MP, Dekker RFH, Barbosa-Dekker AM (2017) *In vitro* protective effects of botryosphaeran, a (1→ 3;1→ 6)-β-D-glucan, against mutagens in normal and tumor rodent cells. Mutat Res Gen Tox En Mut 814:29–36

Kerrigan AM, Brown GD (2010) Syk-coupled C-type lectin receptors that mediate cellular activation via single tyrosine based activation motifs. Immunol Rev 234:335–352

Kiho T, Kobayashi T, Morimoto H, Usui S, Ukai S, Hirano K, Aizawa K, Inakuma T (2000) Structural features of an anti-diabetic polysaccharide (TAP) from *Tremella aurantia*. Chem Pharm Bull 48:17931795

Kogan G, Staško A, Bauerová K, Polovka M, Šoltés L, Brezová V, Navarová J, Mihalová D (2005) Antioxidant properties of yeast (1→3)-β-D-glucan studied by electron paramagnetic resonance spectroscopy and its activity in the adjuvant arthritis. Carbohydr Polym 61:18–28

Kopelman PG (2000) Obesity as a medical problem. Nature 404:635–643

Krcmar P, Novotny C, Marais MF, Joseleau JP (1999) Structure of extracellular polysaccharide produced by lignin-degrading fungus Phlebia radiata in liquid culture. Int J Biol Macromol 24:61–64

Kroemer G, Reed JC (2000) Mitochondrial control of cell death. Nat Med 6:513–519

Kumar S, Kelly AS (2017) Review of childhood obesity: from epidemiology, etiology, and comorbidities to clinical assessment and treatment. Mayo Clin Proc 92:251–265

Legentil L, Paris F, Ballet C, Trouvelot S, Daire X, Vetvicka V, Ferrières V (2015) Molecular interactions of β-(1→3)-glucans with their receptors. Molecules 20:9745–9766

Leung MYK, Liu C, Koon JCM, Fung KP (2006) Polysaccharide biological response modifiers. Immunol Lett 105:101–114

Li S, Xiong Q, Lai X, Li X, Wan M, Zhang J, Yan Y, Cao M, Lu L, Guan J, Zhang D, Lin Y (2015) Molecular modification of polysaccharides and resulting bioactivities. Compr Rev Food Sci Food Saf 15:237–250

Li M, Pu Y, Ragauskas AJ (2016) Current understanding of the correlation of lignin structure with biomass recalcitrance. Front Chem 4:1–8

Liu J, Luo J, Ye H, Sun Y, Lu Z, Zeng X (2010) Medium optimization and structural characterization of exopolysaccharides from endophytic bacterium *Paenibacillus polymyxa* EJS-3. Carbohydr Polym 79:206–213

Lo HC, Tsai FA, Wasser SP, Yang JG, Huang BM (2006) Effects of ingested fruiting bodies, submerged culture biomass, and acidic polysaccharide glucuronoxylomannan of *Tremella mesenterica* Retz.:Fr. on glycemic responses in normal and diabetic rats. Life Sci 78:1957–1966

López-Vázquez E, Prieto-García F, Gayosso-Canales M, Otazo Sánchez EM, Villagómez Ibarra JR (2017) Phenolic acids, flavonoids, ascorbic acid, β-glucans and antioxidant activity in Mexican wild edible mushrooms. Ital J Food Sci 29:766–774

Macedo Bongiovani RA, Meira Silveira JL, Barretto Penna AL, Dekker RFH, Barbosa AM, Corradi da Silva ML (2009) Caracterização reológica dos botriosferanas produzidos pelo *Botryosphaeria rhodina* MAMB-05 em glucose, sacarose e frutose como fontes de carbon (*Rheological characterization of botryosphaerans produced by Botryosphaeria rhodina MAMB-05 in glucose, sucrose and fructose as carbon source*). Braz J Food Technol 12:53–59

Mahapatra S, Banerjee D (2013) Fungal exopolysaccharide: production, composition and applications. Microbiol Insights 6:1–16

Malini M, Souza MF, Oliveira MT, Antunes LMG, Figueiredo SG, Barbosa AM, Dekker RFH, Cólus IM (2015) Modulation of gene expression and cell cycle by botryosphaeran, a (1→3)(1→6)-β-d-glucan in human lymphocytes. Int J Biol Macromol 77:214–221

Malini M, Camargo MS, Hernandes LC, Vargas-Rechia CG, Varanda EA, Barbosa AM, Dekker RFH, Matsumoto ST, Antunes LMG, Cólus IMS (2016) Chemopreventive effect and lack of genotoxicity and mutagenicity of the exopolysaccharide botryosphaeran on human lymphocytes. Toxicol In Vitro 36:18–25

Malumbres M (2014) Cyclin-dependent kinases. Genome Biol 15:122

Malumbres M, Barbacid M (2009) Cell cycle, CDKs and cancer: a changing paradigm. Nat Rev Cancer 9:153–167

Margaritis A, Pace GW (1985) In: Blanch HW, Drew S, DIC W (eds) Comprehensive biotechnology: the principles, applications and regulations of biotechnology in industry, agriculture and medicine. Pergamon Press, New York, pp 1005–1044

Maron DM, Ames BN (1983) Revised methods for the *Salmonella mutagenicity* test. Mutat Res Environ Mutagen Relat Subj 113:173–215

McConkey DJ (1998) Biochemical determinants of apoptosis and necrosis. Toxicol Lett 99:157–168

McIlwain DR, Berger T, Mak TW (2013) Caspase functions in cell death and disease. Cold Spring Harb Perspect Biol 5:a008656. (pages 1-29)

Mendes SF, Santos O, Barbosa AM, Vasconcelos AFD, Aranda-Selverio G, Monteiro NK, Dekker RFH, Pereira MS, Tovar AMF, Mourão PAS, Corradi da Silva ML (2009) Sulfonation and anticoagulant activity of botryosphaeran from *Botryosphaeria rhodina* MAMB-05 grown on fructose. Int J Biol Macromol 45:305–309

Miller GL (1959) Use of dinitrosalicylic acid reagent for determination of reducing sugar. Anal Chem 31:426–428

Miranda CCBO, Dekker RFH, Serpeloni JM, Fonseca EAI, Cólus IMS, Barbosa AM (2008) Anticlastogenic activity exhibited by botryosphaeran, a new exopolysaccharide produced by *Botryosphaeria rhodina* MAMB-05. Int J Biol Macromol 42:172–177

Miranda-Nantes CCBO, Fonseca EAI, Zaia CTBV, Dekker RFH, Khaper N, Castro IA, Barbosa AM (2011) Hypoglycemic and hypocholesterolemic effects of botryosphaeran from *Botryosphaeria rhodina* MAMB-05 in diabetes-induced and hyperlipidemia conditions in rats. Mycobiology 39:187–193

Mocellin S, Bronte V, Nitti D (2007) Nitric oxide, a double edged sword in cancer biology: searching for therapeutic opportunities. Med Res Rev 27:317–352

Moreno RB, Ruthes AC, Baggio CH, Vilaplana F, Komura DL, Iacomini M (2016) Structure and antinociceptive effects of β-D-glucans from *Cookeina tricholoma*. Carbohydr Polym 141:220–228

Mosmann T (1983) Rapid colorimetric assay for cellular growth and survival: application to proliferation and cytotoxicity assays. J Immunol Methods 65:55–63

Nelson N (1944) A photometric adaptation of the Somogyi method for the determination of glucose. J Biol Chem 153:375–380

Ng SH, Mohd Zain MS, Zakaria F, Wan Ishak WR, Wan Ahmad WAN (2015) Hypoglycemic and antidiabetic effect of Pleurotus sajor-caju aqueous extract in normal and streptozotocin-induced diabetic rats. Biomed Res Int 2015: Article ID 214918: 1–8

Nikitina VE, Tsivileva OM, Pankratov AN, Bychkov NA (2007) *Lentinula edodes* biotechnology – from lentinan to lectins. Food Technol Biotechnol 45:230–237

Nwodo UU, Green E, Okoh AI (2012) Bacterial exopolysaccharides: functionality and prospects. Int J Mol Sci 13:14002–14015

O´Neil AN (1955) Sulphated derivatives of laminarin. Can J Chem 33:1097–1101
Ogawa K, Wanatabe T, Tsurugi J, Ono S (1972) Conformational behavior of a gel-forming (1→3)-β-D-glucan in alkaline solution. Carbohydr Res 23:399–405
Oliveira KSM, Di M, Cordeiro LMC, Costa MF, Toledo KA, Iacomini M, Babosa AM, Dekker RFH, Nascimento VMG (2015) (1→6)- and (1→3)(1→6)-β-glucans from *Lasiodiplodia theobromae* MMBJ : structural characterization and pro-inflammatory activity. Carbohydr Polym 133:539–546
Oltval ZN, Milliman CL, Korsmeyer SJ (1993) Bcl-2 heterodimerizes *in vivo* with a conserved homolog, Bax, that accelerates programed cell death. Cell 74:609–619
Osińska-Jaroszuk M, Jarosz-Wilkołazka A, Jaroszuk-Ściseł J, Szałapata K, Nowak A, Jaszek M, Ozimek E, Majewska M (2015) Extracellular polysaccharides from Ascomycota and Basidiomycota: production conditions, biochemical characteristics, and biological properties. World J Microbiol Biotechnol 31:1823–1844
Paletta-Silva R, Rocco-Machado N, Meyer-Fernandes JR (2013) NADPH oxidase biology and the regulation of tyrosine kinase receptor signaling and cancer drug cytotoxicity. Int J Mol Sci 14:3683–3704
Pan WW, Myers MG Jr (2018) Leptin and the maintenance of elevated body weight. Nature Rev Neurosci 19:95–105
Papaspyridi LM, Zerva A, Topakas E (2018) Biocatalytic synthesis of fungal β-Glucans. Catalysts 8:274. (pages 1–23)
Pederson TM, Kramer DL, Rondinone CM (2001) Serine/threonine phosphorylation of IRS-1 triggers its degradation: possible regulation by tyrosine phosphorylation. Diabetes 50:24–31
Pollegioni L, Tonin F, Rosini E (2015) Lignin-degrading enzymes. FEBS J 282:1190–1213
Portt L, Norman G, Clapp C, Greenwood M, Greenwood MT (2011) Anti-apoptosis and cell survival: a review. Biochim Biophys Acta Mol Cell Res 1813:238–259
Queiroz EAIF, Puukila S, Eichler R, Sampaio SC, Forsyth HL, Lees SJ, Barbosa AM, Dekker RFH, Fortes ZB, Khaper N (2014) Metformin induces apoptosis and cell cycle arrest mediated by oxidative stress, AMPK and FOXO3a in MCF-7 breast cancer cells. PLoS One 9:e98207
Queiroz EAIF, Fortes ZB, da Cunha MAA, Barbosa AM, Khaper N, Dekker RFH (2015) Antiproliferative and pro-apoptotic effects of three fungal exocellular β-glucans in MCF-7 breast cancer cells is mediated by oxidative stress, AMP-activated protein kinase (AMPK) and the Forkhead transcription factor, FOXO3a. Int J Biochem Cell Biol 67:14–24
Raetz CRH, Whitfield C (2002) Lipopolysaccharide endotoxins. Annu Rev Biochem 71:635–700
Raisova M, Hossini AM, Eberle J, Riebeling C, Wieder T, Sturm I, Daniel PT, Orfanos CE, Geilen CC (2001) The Bax/Bcl-2 ratio determines the susceptibility of human melanoma cells to CD95/Fas-mediated apoptosis. J Invest Dermatol 117:333–340
Reed JC (1997) Double identity for proteins of the bcl 2 family. Nature 387:773–776
Reeves PG, Nielsen FH, Fahey GC Jr (1993) AIN-93 purified diets for laboratory rodents: final report of the American Institute of Nutrition ad hoc writing committee on the reformulation of the AIN-76A rodent diet. J Nutr 123:1939–1951
Reuter S, Gupta SC, Chaturvedi MM, Aggarwal BB (2010) Oxidative stress, inflammation, and cancer: How are they linked? Free Radic Biol Med 49:1603–1616
Rodrigues FJ, Omura MH, Cedran MF, Dekker RFH, Barbosa-Dekker AM, Garcia S (2017) Effect of natural polymers on the survival of *Lactobacillus casei* encapsulated in alginate microspheres. J Microencapsulation 34:431–443
Rop O, Mlcek J, Jurikova T (2009) Beta-glucans in higher fungi and their health effects. Nutr Rev 67:624–631
Saldanha RL, Garcia JE, Dekker RFH, Vilas-Bôas LA, Barbosa AM (2007) Genetic diversity among *Botryosphaeria* species and their correlation with cell wall lytic enzyme production. Braz J Microbiol 38:259–264
Sassaki GL, Ferreira JC, Glienke-Blanco C, Torri G, De Toni F, Gorin PAJ, Iacomini M (2002) Pustulan and branched β-galactofuranan from the phytopathogenic fungus *Guignardia citricarpa*, excreted from media containing glucose and sucrose. Carbohydr Polym 48:385–389
Savelkoul HFJ, Chanput W, Wichers HJ (2013) Immunomodulatory effects of mushroom β-glucans. In: Calder PC, Yaqoob P (eds) Diet, immunity and inflammation, Woodhead

Publishing series in food science, technology and nutrition No. 232, pp 416–434. ISBN 9780857090379

Schieber M, Chandel NS (2014) ROS function in redoz signaling and oxidative stress. Curr Biol 24: R453–R462

Selbmann L, Crognale S, Petruccioli M (2002) Exopolysaccharide production from *Sclerotium glucanicum* NRRL 3006 and *Botryosphaeria rhodina* DABAC-P82 on raw and hydrolysed starchy materials. Lett Appl Microbiol 34:51–55

Selbmann L, Stingele F, Petruccioli M (2003) Exopolysaccharide production by filamentous fungi: the example of *Botryosphaeria rhodina*. Antonie Van Leeuwenhoek 84:135–145

Shackelford DB, Shaw RJ (2009) The LKB1-AMPK pathway: metabolism and growth control in tumor suppression. Nat Rev Cancer 9:563–575

Sheng L, Zhu G, Tong Q (2013) Mechanism study of Tween 80 enhancing the pullulan production by *Aureobasidium pullulans*. Carbohydr Polym 97:121–123

Shingel KI (2004) Current knowledge on biosynthesis, biological activity, and chemical modification of the exopolysaccharide, pullulan. Carbohydr Res. 339:447–460

Silva CC, Dekker RFH, Silva RSSF, Corradi da Silva ML, Barbosa AM (2007) Effect of soybean oil and Tween 80 on the production of botryosphaeran by *Botryosphaeria rhodina* MAMB-05. Process Biochem 42:1254–1258

Silva AZ, Costa FP, Souza IL, Ribeiro MC, Giordani M, Queiroz DA, Luvizotto RAM, Nascimento AF, Bomfim GF, Sugizaki MM, Dekker RFH, Barbosa-Dekker AM, Queiroz EAIF (2018) Botryosphaeran reduces obesity, hepatic steatosis, dyslipidaemia, insulin resistance and glucose intolerance in diet-induced obese rats. Life Sci 211:147–156

Silva-Sena GG, Malini M, Delarmelina JM, Dutra JCV, Gervásio SV, Leal MAS, Costa Pereira TM, Barbosa-Dekker AM, Dekker RFH, de Paula F, Batitucci MCP (2018) *In vivo* antimutagenic and antiatherogenic effects of the (1→3)(1→6)-β-D- glucan botryosphaeran. Mutat Res Gen Tox En 826:6–14

Sima P, Vannucci L, Vetvicka V (2018) β-glucans and cholesterol (Review). Int J Mol Med 41:1799–1808

Snarr B, Qureshi S, Sheppard D (2017) Immune recognition of fungal polysaccharides. J Fungi (Basel) 3:47

Somogyi M (1945) A new reagent for the determination of sugars. J Biol Chem 160:61–68

Sosa V, Moliné T, Somoza R, Paciucci R, Kondoh H, LLeonart ME (2013) Oxidative stress and cancer: an overview. Ageing Res Rev 12:376–390

Stasinopoulos SJ, Seviour RJ (1990) Stimulation of exopolysaccharide production in the fungus *Acremonium persicinum* with fatty acids. Biotechnol Bioeng 36:778–782

Steluti RM, Giese EC, Piggato MM, Sumiya AFG, Covizzi LG, Job AE, Cardoso MS, Corradi da Silva ML, Dekker RFH, Barbosa AM (2004) Comparison of Botryosphaeran production by the ascomyceteous fungus *Botryosphaeria* sp., grown on different carbohydrate carbon sources, and their partial structural features. J Basic Microbiol 44:480–486

Stone BA (2009) Chemistry of β-glucans. In: Stone BA, Clark AE, Fincher GB, Basic A (eds) Chemistry and biology of (1→3)-β-glucans and related polysaccharides. Elsevier Press, Amsterdam, pp 5–46

Stone BA, Clarke AE (1992) Chemistry and biology of (1→3)-β-glucans. La Trobe University Press, Bundoora

Thetsrimuang C, Khammuang S, Chiablaem K, Srisomsap C, Sarnthima R (2011) Antioxidant properties and cytotoxicity of crude polysaccharides from *Lentinus polychrous* Lév. Food Chem 128:634–639

Tice RR, Agurell E, Anderson D, Burlinson B, Hartmann A, Kobayashi H, Miyamae Y, Rojas E, Ryu JC, Sasaki YF (2000) Single cell gel/comet assay: guidelines for *in vitro* and *in vivo* genetic toxicology testing. Environ Mol Mutagen 35:206–221

Vasconcelos AFD, Monteiro NK, Dekker RFH, Barbosa AM, Carbonero ER, Silveira JLM, Sassaki GL, Silva R, Corradi da Silva ML (2008) Three exopolysaccharides of the β-(1→6)-d-glucan type and a β-(1→3,1→6)-d-glucan produced by strains of *Botryosphaeria rhodina* isolated from rotting tropical fruit. Carbohydr Res 343:2481–2485

Vesely MD, Kershaw MH, Schreiber RD, Smyth MJ (2011) Natural innate and adaptive immunity to cancer. Annu Rev Immunol 29:235–271

Vetvicka V, Vetvickova J (2012) β(1-3)-Glucan in cancer treatment. Am J Immunol 8:38–43

Vogel HJ (1956) A convenient growth medium for *Neurospora* (Medium N). Microb Genet Bull 13:42–43

Wang Q, Sheng X, Shi A, Hu H, Yang Y, Liu L, Fei L, Liu H (2017) β-Glucans: relationships between modification, conformation and functional activities. Molecules 22:257. (pages 1–12)

Wasser SP (2002) Medicinal mushrooms as a source of antitumor and immunomodulating polysaccharides. Appl Microbiol Biotechnol 60:258–274

Wasser SP (2014) Medicinal mushroom science: current perspectives, advances, evidences, and challenges. Biomed J 37:345–356

Weng BBC, Lin YC, Hu CW, Kao MY, Wang SH, Lo DY, Lai TY, Kan LS, Chiou RYY (2011) Toxicological and immunomodulatory assessments of botryosphaeran (β-glucan) produced by *Botryosphaeria rhodina* RCYU 30101. Food Chem Toxicol 49:910–916

West TP, Reed-Hamer B (1995) Effect of oils and surfactants on pullulan production relative to nitrogen source. Microbios 83:249–259

Whitehead A, Beck EJ, Tosh S, Wolever TMS (2014) Cholesterol-lowering effects of oat β-glucan: a meta-analysis of randomized controlled trials. Am J Clin Nutr 100:1413–1421

Yang FC, Ke YF, Kuo SS (2000) Effect of fatty acids on the mycelial growth and polysaccharide formation by *Ganoderma lucidum* in shake flask cultures. Enzyme Microb Technol 27:295–301

Yang J, Du Y, Wen Y, Li T, Hu L (2003) Sulfation of chinese lacquer polysaccharides in different solvents. Carbohydr Polym 52:397–403

Yang J, Du Y, Huang R, Wan Y, Wen Y (2005) The structure-anticoagulant activity relationships of sulfated lacquer polysaccharide: effect of carboxyl group and position of sulfation. Int J Biol Macromol 36:9–15

Yang HL, Chen CS, Chang WH, Lu FJ, Lai YC, Chen CC, Hseu TH, Kuo CT, Hseu YC (2006) Growth inhibition and induction of apoptosis in MCF-7 breast cancer cells by *Antrodia camphorata*. Cancer Lett 231:215–227

Yang JY, Hung MC (2011) Deciphering the role of forkhead transcription factorsin cancer therapy. Curr Drug Targets 2:1284–1290

Yoshitomi H, Sakaguchi N, Kobayashi K, Brown GD, Tagami T, Sakihama T, Hirota K, Tanaka S, Nomura T, Miki I, Gordon S, Akira S, Nakamura T, Sakaguchi S (2005) A role for fungal β-glucans and their receptor dectin-1 in the induction of autoimmune arthritis in genetically susceptible mice. J Exp Med 201:949–960

Youle RJ, Strasser A (2008) The BCL-2 protein family: opposing activities that mediate cell death. Nat Rev Mol Cell Biol 9:47–59

Youssef F, Biliaderis CG, Roukas T (1998) Enhancement of pullulan production by *Aureobasidium pullulans* in batch culture using olive oil and sucrose as carbon sources. Appl Biochem Biotechnol 74:13–30

Zakikhani M, Dowling RJO, Sonenberg N, Pollak MN (2008) The effects of adiponectin and metformin on prostate and colon neoplasia involve activation of AMP-activated protein kinase. Cancer Prev Res 1:369–375

Zamzami N, Kroemer G (2001) The mitochondrion in apoptosis: how Pandora's box opens. Nat Rev Mol Cell Biol 2:67–71

Zhang L, Li X, Xu X, Zeng F (2005) Correlation between antitumor activity, molecular weight, and conformation of lentinan. Carbohydr Res 340:1515–1521

Zhang M, Chiu LCM, Cheung PCK, Ooi VEC (2006) Growth-inhibitory effects of a beta-glucan from the mycelium of *Poria cocos* on human breast carcinoma MCF-7 cells: cell-cycle arrest and apoptosis induction. Oncol Rep 15:637–643

Zhang Y, Kong H, Fang Y, Nishinari K, Phillips GO (2013) Schizophyllan: a review on its structure, properties, bioactivities and recent developments. Bioact Carbohydr Diet Fibre 1:53–71

Zhu F, Du B, Xu B (2016) A critical review on production and industrial applications of beta-glucans. Food Hydrocoll 52:275–288

Part V
Galacturonic Acid and Xylolactan-Based Exopolysaccharide

Chapter 12
Pectic Polysaccharides in Plants: Structure, Biosynthesis, Functions, and Applications

Charles T. Anderson

Abstract Pectic polysaccharides, a broad class of exopolysaccharides that are made by plants and contain negatively charged sugars, are some of the most complex biomolecules in nature. They modulate the mechanics and adhesion of the extracellular cell walls of plants and require complex biosynthetic machinery to produce their array of structures. They are also post-synthetically modified by a large apparatus of enzymes. Recent advances in genomics and biochemistry have revealed some parts of this machinery, but many mysteries remain unsolved. Intermolecular cross-linking between pectins is thought to underlie cell adhesion and constrain cell expansibility in plants, and modulating this cross-linking, pectin hydration, and the interactions of pectins with other wall components is thought to be one of the drivers of key developmental processes, from wall assembly and growth through tissue maturation to the release of pollen and seeds. The large number of pectin-related genes in many plant taxa belies their fundamental importance in evolutionary innovations in plants. Finally, pectins can both facilitate and complicate the use of plant cell walls as feedstocks for useful products and might also possess unique applications in human health and medicine.

12.1 Introduction to Plant Cell Walls and Pectins

Plant cell walls are unique extracellular structures among living organisms in that they are composed largely of polysaccharides, adhere plant cells to one another and thus lock in place the relative locations of those cells during growth, and retain both high expansibility and high mechanical strength during growth. It is the strength of the plant cell wall that enables giant redwoods, *Sequoia sempervirens*, to achieve robust upright growth and tower up to 100 m, making them the tallest living organisms, and the plasticity of the cell wall allows plants to carry out indeterminate

C. T. Anderson (✉)
Department of Biology, Center for Lignocellulose Structure and Formation, The Pennsylvania State University, State College, PA, USA
e-mail: cta3@psu.edu

E. Cohen, H. Merzendorfer (eds.), *Extracellular Sugar-Based Biopolymers Matrices*, Biologically-Inspired Systems 12, https://doi.org/10.1007/978-3-030-12919-4_12

growth and development, allowing colonial plants, such as quaking aspens, *Populus tremuloides*, to survive for tens of thousands of years and become the heaviest living organisms, although both of these behemoths are currently under threat as a result of human-caused climate change and habitat alteration.

Sir Isaac Newton is said to have begun postulating the law of universal gravitation while observing the perpendicular fall of an apple from its tree to the ground in 1666, but he was unaware that the apple itself was largely composed of pectins! It was not until 1790 that pectins were isolated from apples by Louis Nicolas Vauquelin, and pectins were later named and found to be widespread among plants by Henri Braconnot in 1825. Because they were initially defined by the extraction methods used to isolate them, rather than by their chemical structures, pectins do not fit a strict chemical or structural definition and instead can be broadly defined as "acidic heteropolysaccharides" contained in the cell walls of plants. In this section, pectins are described and placed in the larger context of the extracellular matrices produced by plant cells, commonly called plant cell walls.

12.1.1 Overview of the Structure and Composition of Plant Cell Walls

The cell walls of plants are complex extracellular matrices that are composed primarily of interacting and intertwined networks of different types of polysaccharides (Somerville et al. 2004), with additional components that can include structural glycoproteins, a polyphenolic heteropolymer called lignin, cell wall-modifying enzymes, ions, reactive oxygen species, and water. Because they function as the interface between the protoplast, defined as the plant cell contained within its cell wall, and the extracellular environment, plant cell walls serve structural, protective, and sensory functions. The cell walls of plants constrain cellular growth and morphology, determining cell size and shape and thus affecting the developmental patterning of tissues and organs (Cosgrove 2018). Cell walls also protect plant cells from environmental and biotic stresses by acting as a barrier against cellular damage and pathogen invasion and are involved in sensing and responding to mechanical, biological, and abiotic stimuli (Houston et al. 2016; Hemant and Haswell 2017; Novakovic et al. 2018).

The structural framework of most plant cell walls is composed of cellulose, a cable-like polymer that is composed of hydrogen-bonded chains of β-1,4-linked glucose that are produced at the cell surface by mobile cellulose synthesis complexes and coalesce into long, thin, linear, multichain microfibrils that have a tensile strength that is higher than that of steel (Bledzki and Gassan 1999; Somerville 2006). Cellulose microfibrils interact with so-called matrix polymers, which include both hemicelluloses and pectins in the primary walls of growing plant cells and also include lignins in the secondary walls of cells that have ceased growth (Donaldson 2001; Cosgrove 2014) (see also Chap. 7). Hemicelluloses include linear and branched polysaccharides with

β-1,4-linked backbones with an equatorial configuration at C1 and C4 that are primarily composed of neutral sugars (Scheller and Ulvskov 2010). Xyloglucan, a branched polysaccharide with a β-1,4-linked glucan backbone and side chains consisting of xylose, galactose, and fucose residues, is the most abundant hemicellulose in the primary walls of eudicot and non-commelinoid monocot plants (Zabotina 2012; Park and Cosgrove 2015), whereas xylans, which have an α-1,4-linked backbone and can be decorated with arabinose-, xylose-, galactose-, glucuronic acid-, and ferulate-containing side chains, are the most abundant hemicellulose in the primary walls of commelinoid monocot species and the secondary walls of most plants (Rennie and Scheller 2014). Hemicelluloses also include mannans, glucomannans, and mixed-linkage glucans (Scheller and Ulvskov 2010).

Pectins are a unique class of matrix polysaccharides that are distinguished by possessing a large proportion of acidic sugars in the form of uronic acids, including predominantly galacturonic acid (GalA) and smaller amounts of glucuronic acid (GlcA). Pectins have recently undergone a renaissance in terms of scientific attention (Anderson 2016; Saffer 2018) due to several factors, including a growing appreciation of their intimate proximity to cellulose in the primary cell wall (Wang et al. 2015), their historically underappreciated mechanical importance in growth control (Peaucelle et al. 2012), and their structural and metabolic dynamics during plant growth and development (Saffer 2018). From one perspective, pectins can be thought of as "proto-polymers" that are capable of many of the functions of other wall polysaccharides, but have in some cases been at least partially functionally supplanted by cellulose and hemicellulose, especially with regard to the regulation of wall expansibility (Cosgrove 2018).

12.1.2 Overview of the Evolutionary Origins and Distribution of Pectins

Some types of pectins exist in charophycean green algae (Sorensen et al. 2011), which are proposed to be descendants of the last common ancestor of algal and embryophyte lineages (Harholt et al. 2016). Pectins can thus be hypothesized to be an ancestral wall component that might even predate the complex cellulose-hemicellulose networks that are mechanically predominant in the primary cell walls of land plants (Popper et al. 2011). Because of their ability to form gels in the presence of water and to sequester ions, pectins might have constituted an early buffer against the ionic and dilutive effects of life in an aqueous environment for marine algae, and their adhesion might have allowed both for cell-substrate adhesion and cell-cell adhesion, a precursor of multicellularity, to arise in the algal ancestors of land plants (Domozych and Domozych 2014; Domozych et al. 2014).

Pectins are widely distributed across plant taxa, although their abundance varies dramatically between taxa and developmental stages. Pectins are especially abundant in the primary cell walls of eudicots and non-commelinid monocots, where they

can comprise up to 35% of the dry mass of the wall, but are much less abundant in secondary walls and grass primary walls, where they make up around 5% of the dry mass of the wall (Vogel 2008). However, these estimates of pectin abundance must be viewed with caution because they are often based on extraction methods (Zablackis et al. 1995) that underestimate the insoluble fraction of pectin, which can be substantial and thus lead to underestimations of pectin content in the cell walls of different plant taxa (Atmodjo et al. 2013).

12.1.3 Overview of Pectin Functions in Plant Growth and Development

Pectins are essential for normal plant growth and development, since mutants with altered pectin content or modification patterns often show severe developmental defects that include stunting, loss of cell-cell adhesion, and aberrant organ initiation (Krupkova et al. 2007; Mouille et al. 2007; Peaucelle et al. 2008; Caffall et al. 2009). Pectins are one of the first wall polysaccharides to be laid down during the de novo formation of a new cell wall in cytokinesis (Samuels et al. 1995) and are enriched in the growing cell walls of eudicots (Knox et al. 1990; Derbyshire et al. 2007; Phyo et al. 2017a). Recent evidence has suggested that pectins function to establish anisotropic growth patterns in elongating cells that are later reinforced by cellulose-hemicellulose networks (Bou Daher et al. 2018; Peaucelle et al. 2015) and that pectin auto-degradation by plants is a key facilitator of cell expansion (Xiao et al. 2014; Xiao et al. 2017). Pectin networks are thought to cyclically soften and rigidify in growing cells to allow for wall expansion and resistance to turgor pressure (Boyer 2016).

By influencing wall mechanics (Abasolo et al. 2009) and possibly also wall integrity signaling (Feng et al. 2018), pectins are thought to drive developmental patterning, for example, in the shoot apical meristem, where altering the expression of pectin-modifying enzymes can either result in an absence of organ initiation or in ectopic organ formation (Peaucelle et al. 2011). Pectins have recently been shown to change in mobility and abundance along the developmental gradient of the *Arabidopsis thaliana* inflorescence stem (Phyo et al. 2017a), which implies that they are differentially synthesized, modified, and/or degraded along this gradient. Finally, pectin degradation is a key step in cell separation events in plants, which include abscission and dehiscence (Daher and Braybrook 2015). These separation events help optimize plant physiology, for instance, when leaves fall off of deciduous trees in the autumn to minimize metabolic costs during periods of low photosynthesis, and aid in gamete and seed dispersal, from the separation of pollen tetrads and release of pollen during anther dehiscence to seed pod dehiscence.

12.2 Structures, Classification, and Distribution of Pectic Polysaccharides

Pectin structures range from simple linear chains of GalA that form homogalacturonan (HG) to the highly branched pectic subtypes rhamnogalacturonan I (RG-I) and rhamnogalacturonan II (RG-II), and all three of these major classes of pectins can form intermolecular cross-links via ion coordination or diester bonding. Pectins are enriched in the walls of growing plant cells but can also be present in non-growing tissues. Their wide distribution across embryophyte (land plant) taxa strongly suggests that they are essential for plant survival.

12.2.1 Chemical Structures of Pectins

Pectins can be structurally divided into three major classes, or domains: HG and modified HG, RG-I, and RG-II. Although the structures of these heteropolysaccharide domains have been well defined biochemically and compositionally, the macromolecular structures and covalent and non-covalent interlinkages between different pectin domains have not been completely elucidated.

12.2.1.1 Methods for Structural and Compositional Analysis of Pectins

Due to their higher solubility relative to other wall polysaccharides, pectins can be extracted from plant cell walls by acid, hot water, and calcium chelators (Fry 1988), which was historically one of the ways in which they were defined. Extracted pectins can be compositionally analyzed by hydrolysis followed by chromatographic separation and quantification of their constituent monosaccharides (Yeats et al. 2016), although care must be taken that the hydrolysis step does not destroy the monosaccharides (De Ruiter et al. 1992). Monosaccharide composition can also be determined by producing alditol acetate derivatives followed by GC-MS (Pettolino et al. 2012), carbodiimide reduction of uronic acids followed by conversion to alditol acetates and GC-MS, and formation of trimethylsilyl (TMS) derivatives followed by GC-MS, with alditol acetate derivatization being assessed as a less sensitive method (Biswal et al. 2017). Pectin molecular mass can be estimated by size exclusion chromatography followed by detection of uronic acids (Ralet et al. 2008), although the diverse shapes and different electrostatic potentials of pectin subdomains are likely to make them difficult to precisely resolve using this method. Smaller, soluble fragments of homogalacturonan, called oligogalacturonides, can be generated by enzymatic degradation and detected using MALDI-TOF mass spectrometry (Guillaumie et al. 2003; Gunl et al. 2011).

Monoclonal antibodies targeting many different pectin epitopes provide useful tools for detecting specific subtypes of pectins, either in situ in plant cell walls (Willats et al. 2001) or after chemical extraction (Cornuault et al. 2014), although antibodies targeting some pectin subtypes, especially RG-II, are scarce (Zhou et al. 2018). To determine the structural diversity of an isolated pectin sample, linkage analysis using methylation is necessary (Pettolino et al. 2012), although this information does not translate directly into a complete macromolecular structure. Nuclear magnetic resonance (NMR) can also be used to determine the bonding patterns and interactions between pectic groups in isolated samples and between pectins and other polysaccharides in intact cell wall samples, but ^{13}C labeling of the cell walls is necessary for a full 2D NMR analysis (Wang and Hong 2016). Except for NMR, all of the above methods depend on isolating pectins from cell walls, which means that they are limited to analyzing pectins that can be solubilized or fractionated in some fashion. There is solid evidence for a significant fraction of pectin that remains insoluble during typical wall fractionation experiments (Atmodjo et al. 2013), and the structure of this pectic fraction is less well understood. Performing 2D NMR experiments on sequentially extracted wall fractions might reveal additional details regarding the structure of this insoluble population of pectins.

12.2.1.2 Structures of Homogalacturonan and Modified Homogalacturonans

Homogalacturonan is the structurally simplest and most abundant form of pectin in most types of plant cell walls (Zablackis et al. 1995; Sorensen et al. 2011). It is composed of a linear chain of α-1,4-linked GalA residues, each of which can be methyl-esterified at the C6 carboxyl group or acetylated at the *O*2 or *O*3 position (Fig. 12.1). The degree of polymerization of HG ranges widely but can exceed 100 residues (Yapo et al. 2007). HG molecules that contain stretches of de-methyl-esterified GalA totaling at least ten residues can form intermolecular cross-links that are coordinated by calcium ions (Ca^{2+}) and have been hypothesized to adopt an "egg-box" conformation, although molecular modeling has put the accuracy of this conformation into question (Braccini and Perez 2001), and it is not clear whether this structure actually exists in native cell walls (Hocq et al. 2017). HG can be modified with side chains containing xylose (forming xylogalacturonan) linked to the *O*3 position, or apiose (forming apiogalacturonan) linked to the *O*2 or *O*3 position. It is unknown what specific functions these sugar side chain modifications of HG serve, although they might interfere with HG cross-linking by Ca^{2+}. Methyl-esterified HG can also form helical structures in the cell wall (Goldberg et al. 1996).

12.2.1.3 Structure of Rhamnogalacturonan I

Rhamnogalacturonan I is a unique domain of pectin in that unlike HG and RG-II, its backbone is composed of alternating GalA and rhamnose (Rha) residues linked by

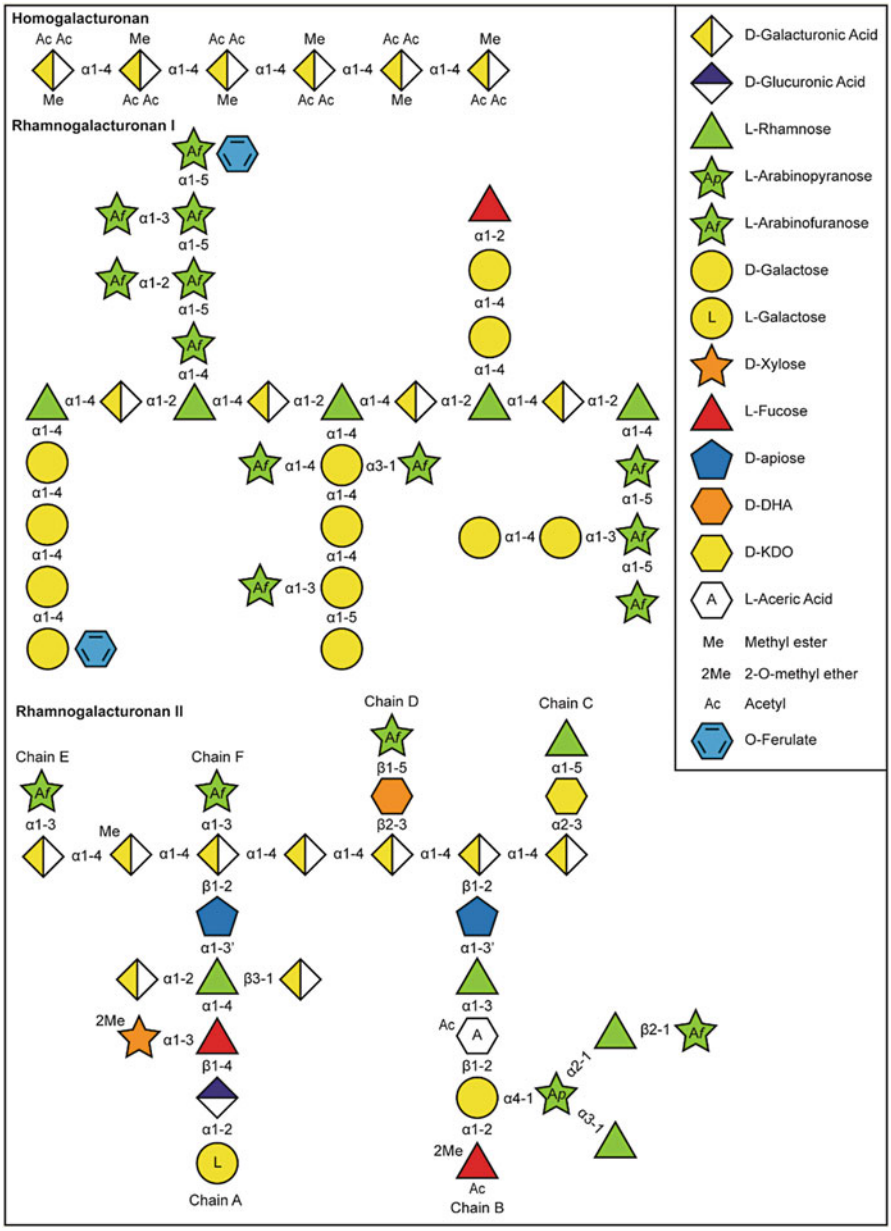

Fig. 12.1 Chemical structures of homogalacturonan, rhamnogalacturonan I, and rhamnogalacturonan II. Sugar symbols follow the Consortium for Functional Glycomics notation (Raman et al. 2006). Structures of RG-I side chains are not comprehensive; structure of RG-II is based on Ndeh et al. (2017)

α-1,2 and α-1,4 bonds, respectively (Fig. 12.1). Linear and branched side chains, which include arabinans, galactans, and arabinogalactans, decorate the RG-I backbone (Yapo 2011) (Fig. 12.1). Some galactan side chains on RG-I are thought to contain a terminal fucose (Nakamura et al. 2001), and both arabinan and galactan side chains can contain terminal ferulic acid moieties (Ishii 1997), which can potentially cross-link to form diferulate esters and generate RG-I dimers in the cell wall (Ralet et al. 2005) (Fig. 12.2). RG-I has been described as a "hairy" region of pectin with many side chains, with "smooth" regions with few or no side chains, potentially composed of HG, interspersed between hairy regions (Yapo 2011) (Fig. 12.2).

12.2.1.4 Structure of Rhamnogalacturonan II

Rhamnogalacturonan II is one of the most complex biomolecules in nature and is thought to be conserved, with some structural variation, across all vascular plants (Bar-Peled et al. 2012; O'Neill et al. 2004; Pabst et al. 2013). It comprises 13 different types of sugars that are linked by up to 22 unique glycosidic bonds to form 6 different unique side chains (Ndeh et al. 2017). RG-II molecules can be cross-linked via borate diesters that interconnect the apiose residues on side chain A, but not apparently on side chain B (Fig. 12.2), and the resulting RG-II dimers show unique migration patterns on size exclusion chromatographs (Ishii and Matsunaga 1996).

12.2.2 Taxonomic, Developmental, Tissue, and Cell Wall Distributions of Pectins

Pectins are ubiquitous among plants, although their abundance varies widely between different types of cell walls, tissues, developmental stages, and groups of species. Their abundance is typically negatively correlated with tissue age and differentiation. They are widespread across plant taxa and are highly abundant in the walls of eudicots and non-commelinid monocots, which also possess type I cell walls. Interestingly, RG-II is deeply conserved across almost all plant species, although its structure varies slightly in some taxa (O'Neill et al. 2004). Pectin-related genes are found in all land plants, with large families present for some pectin biosynthetic and modifying genes in angiosperms (McCarthy et al. 2014). However, these gene families likely arose from a limited set of genes in early land plants, as suggested by smaller numbers of genes in each family in bryophytes (McCarthy et al. 2014). Algal genomes also contain many putative pectin-related genes (Domozych et al. 2012; Sorensen et al. 2011), implying that pectins were abundant and functional in the ancestors of land plants.

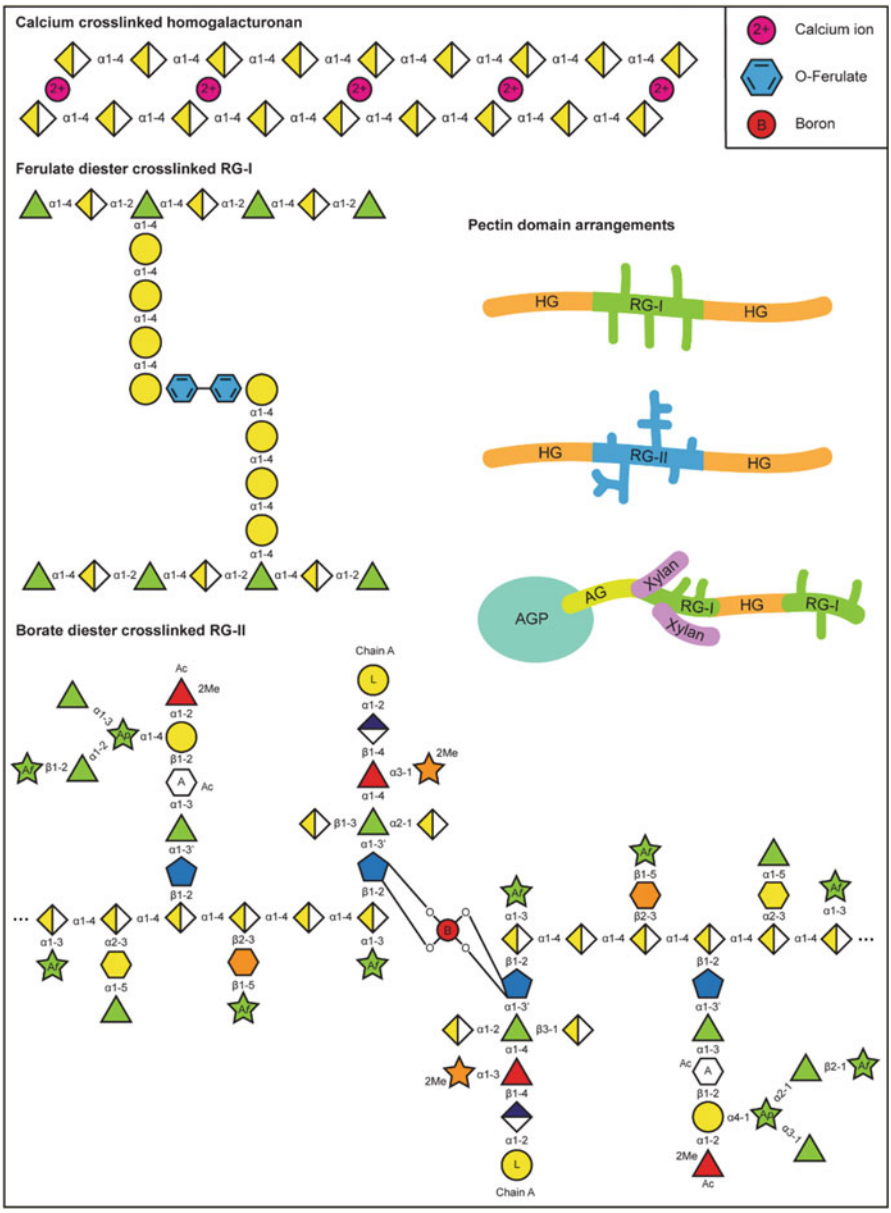

Fig. 12.2 Types of cross-links and domain arrangements for pectins. De-methyl-esterified GalA residues in HG can be cross-linked by calcium ions; arabinan and galactan side chains of RG-I can be cross-linked by ferulate diesters; apiose residues of side chain A in RG-II can cross-link via a borate diester linkage, which can be stabilized by a metal ion (not shown), to form RG-II dimers. Apiose residues of side chain B of RG-II do not appear to participate in RG-II dimerization. RG-I domains (aka "hairy regions") can be linked to HG (aka "smooth regions"), and RG-II domains can be linked to HG as well, but RG-I domains linked to RG-II domains have not been detected thus far (Atmodjo et al. 2013). Some pectins might initiate or exist in the wall as side chains of arabinogalactan proteins (AGPs) that are linked to RG-I, HG, and xylan chains by arabinogalactans (Tan et al. 2013)

12.2.2.1 Pectins in Primary and Secondary Plant Cell Walls

Pectins are abundant in the type I primary cell walls of eudicots and non-commelinid monocots, where they are intercalated throughout the wall and also are enriched in a specialized wall layer called the middle lamella that adjoins adjacent cells in plant tissues. The middle lamella contains high levels of HG but less RG-I or RG-II (Guillemin et al. 2005). Pectins might also serve as an interface between the cell wall and the cuticle in some epidermal cell types and have been detected in some cuticle layers (Guzman et al. 2014). Pectins are much less abundant in secondary cell walls and the so-called type II primary walls of commelinid monocots, which include grasses, although the limitations of traditional methods used to detect pectins (i.e., extraction and chemical composition analysis) might have led to underestimates of their abundance in these cell walls, if pectins in those walls are less extractable or soluble. Evidence for the functional importance of pectins in woody tissues comes from expression profiling of eucalyptus wood, in which pectin-modifying enzymes are upregulated during differentiation (Goulao et al. 2011; Sexton et al. 2012).

12.2.2.2 Pectins across Tissues and Developmental Gradients

Due to their enrichment in the primary walls of growing cells, pectins are most abundant in rapidly growing tissues, such as seedling hypocotyls, meristematic tissues, and organ primordia. Pectins are also highly enriched in the seed coats of some plant species, where they form a key component of the mucilage that is hypothesized to aid in seedling hydration during imbibition, and in the fleshy fruits of many eudicot species, where they protect the encased seeds and maintain the fruit in a hydrated state, making it appetizing to seed dispersers. However, pectins have not been hypothesized to be major storage polysaccharides, unlike starch and hemicelluloses in the seeds of some species (Opanowicz et al. 2011; Rodriguez-Gacio et al. 2012).

Because of their high abundance in rapidly growing tissues and low abundance in secondary walls, pectins can display a gradient in abundance across developmental age in tissues undergoing both growth and differentiation, such as inflorescence stems (Goldberg et al. 1986; Phyo et al. 2017a). This gradient has implications for overall hydration and polymer mobility in the wall, since certain subtypes of pectins show high hydration and mobility. It is likely that this gradient in abundance reflects two concurrent trends: increased synthesis of non-pectin polymers, such as xylans and lignins, in older tissues that are producing secondary walls, thus reducing the relative amount of pectin in the total wall mass; and pectin degradation over the course of development (Yang et al. 2018). The selective degradation of certain subtypes of pectin is also likely to change the relative composition of pectins over developmental time.

12.3 Pectin Biosynthesis

The site of pectin biosynthesis is the Golgi, a complex, mobile, multi-compartment organelle in plant cells that acts like a mobile factory for secreted molecules, including cell wall polysaccharides. Golgi-resident proteins are thus responsible for pectin biosynthesis, and proteomics analyses of isolated Golgi in plant cells have identified a large number of putative wall biosynthetic enzymes (Parsons et al. 2012), including nucleotide sugar transporters and nucleotide sugar interconversion enzymes, glycosyltransferases (GTs), methyltransferases, feruloyltransferases, and acetyltransferases. Altogether, at least 67 distinct types of enzymatic activities are posited to be required for pectin synthesis (Mohnen 2008), although only a subset of these activities have been characterized at the molecular level. Given the covalently linked domain structures of pectins (Fig. 12.2), it is likely that pectin synthesis occurs through a combination of (1) processive or non-processive backbone elongation (Amos et al. 2018), (2) elaboration of backbones with side chains (Ebert et al. 2018), and (3) domain linkage via uncharacterized transglycosylase activities (Atmodjo et al. 2013), to produce the completed pectin molecules that will be delivered to the apoplast.

12.3.1 Synthesis and Transport of NDP-Sugars as Substrates for Pectin Synthesis

Several branches of the central carbon metabolism pathway produce nucleotide sugars that are required for pectin biosynthesis (Bar-Peled and O'Neill 2011), but many pectin precursors can also be synthesized from sugar salvage pathways, in which free sugars are taken up by plant cells and upgraded to nucleotide sugar substrates for GTs. For instance, UDP-GalA can be interconverted from UDP-glucuronic acid, which is in turn derived from UDP-glucose, but UDP-GalA can also be generated from free GalA, which is phosphorylated and converted to UDP-GalA (Bar-Peled and O'Neill 2011). UDP-Rha is synthesized by members of the RHAMNOSE SYNTHASE (RHM) protein family (Diet et al. 2006). UDP-Gal is synthesized by UDP-Glc 4-epimerase (UGE) proteins (Rosti et al. 2007), whereas UDP-L-Ara is potentially synthesized by UGE and/or MURUS4 via UDP-Xyl (Atmodjo et al. 2013). The biosynthetic pathways for several of the sugars in RG-II are incompletely characterized, but UDP-apiose is thought to be generated by a UDP-D-apiose/UDP-D-xylose synthase (Molhoj et al. 2003).

To be incorporated into pectins, NDP-sugars must be transported to, or synthesized in, the Golgi lumen. The NDP-sugar transporter family is large and diverse and has recently been more fully characterized using functional assays in homologous and heterologous systems (Temple et al. 2016). The topology of these transporters must allow the biosynthetic and conversion activities of nucleotide sugar-metabolizing enzymes to dovetail with the activities of pectic glycosyltransferases, which are invariably located in the Golgi lumen.

12.3.2 Enzymes Involved in Pectin Biosynthesis

Given the structural complexity of pectins, it is perhaps not surprising that a large number of proteins are hypothesized to function in pectin biosynthesis. In total, it is estimated that at least 67 individual enzyme activities are required for pectin biosynthesis (Mohnen 2008). Many of these enzymes are likely to act in multimeric complexes that either synthesize pectin "modules," which can then be assembled into the final product molecules, or that act sequentially on nascent pectins to elaborate their structures. Given the difficulty in expression and purification, and the catalytic promiscuity of many glycosyltransferases in vitro, the identities of many of the enzymes responsible for pectin linkages are still unknown. Some of the enzyme families that have been functionally characterized are highlighted below.

12.3.2.1 GAUTs and Other Enzymes Involved in Homogalacturonan Synthesis

The major enzymes that are thought to function in HG biosynthesis are members of the GALACTURONOSYLTRANSFERASE (GAUT) family, which are glycosyltransferase 8 (GT8) family members that elongate GalA chains using UDP-GalA as a substrate (Atmodjo et al. 2013). *GAUT* genes, which exist as multigene families in most plant species (McCarthy et al. 2014), are accompanied in many plant genomes by GAUT-LIKE (GATL) genes that might also function in HG synthesis (Caffall et al. 2009; Kong et al. 2011). In *A. thaliana*, GAUT1 was the first GAUT that was biochemically confirmed to have bona fide galacturonosyltransferase (GalAT) activity, and additional GAUTs have more recently been demonstrated to have GalAT activity (Voiniciuc et al. 2018). However, some GAUTs, such as GAUT7, appear to lack enzymatic activity and are thought to act as scaffolding or anchoring proteins in GAUT-containing complexes (Atmodjo et al. 2011). Whether these complexes are responsible for assembly line-style HG synthesis has recently been put into question by a proposed two-phase, non-processive model of HG synthesis by GAUTs (Amos et al. 2018).

12.3.2.2 Putative HG Methyltransferases

HG is thought to be synthesized in a highly methyl-esterified form in the Golgi via the activity of HG methyltransferases that use S-adenosylmethionine (SAM) as a substrate. One putative HG methyltransferase is QUASIMODO2 (QUA2), mutants for which show aberrant HG extractability and cell adhesion defects (Krupkova et al. 2007; Mouille et al. 2007). A genetic suppressor of the cell adhesion defect of the *qua2* mutant of *A. thaliana*, named *esmeralda1*, encodes a putative *O*-fucosyltransferase and does not restore pectin levels to wild-type levels (Verger et al. 2016), but QUA2 has not been demonstrated to have HG methyltransferase activity in vitro, so its status as a bona fide HG methyltransferase is questionable. Two other proteins, COTTON GOLGI RELATED2 (CGR2) and CGR3, are also putative pectin methyltransferases, and microsomal membranes isolated from CGR overexpressors show enhanced HG methyltransferase activity, providing positive evidence to support their roles as bona fide HG methyltransferases (Kim et al. 2015). Whether QUA2, CGR2, and CGR3 work together to methyl-esterify identical HG substrates, or if they have specific targets that consist of HG subdomains, is unknown. It is also unclear whether HG is methyl-esterified simultaneously with its polymerization in the Golgi or if it is methyl-esterified after polymerization, although addition of SAM during in vitro HG synthesis does not enhance HG polymerization (Doong et al. 1995).

12.3.2.3 Putative Pectin Acetyltransferases

HG and RG-I acetyltransferases are likely to use acetyl-CoA as a substrate to transfer acetyl groups to GalA residues. Putative acetyltransferases include the REDUCED WALL ACETYLATION, ESKIMO, and TRICHOME BIREFRINGENCE-LIKE proteins (Stranne et al. 2018), although some of these proteins are likely to acetylate other wall polysaccharides, such as hemicelluloses (Lee et al. 2011; Manabe et al. 2011).

12.3.2.4 Patterning of Pectin Methyl-Esterification and Acetylation

Although the patterning of methyl-esterification is of critical importance for determining the susceptibility of a given HG molecule to Ca^{2+}-mediated cross-linking or degradation, it is currently unclear whether HG is synthesized with a stereotypical pattern of methyl-esterification or if its methyl-esterification pattern is random. Likewise, the acetylation patterning of pectins has not been fully defined. However, analogous to xylan, which shows differential binding to cellulose depending on whether it is acetylated every two or three residues (Grantham et al. 2017), pectic

molecules are likely to display differential conformations, solubilities, and/or interactions with other wall polymers that depend on their degrees of acetylation and acetylation patterns (Palmer and Ballantyne 1950).

12.3.3 RG-I Backbone and Side Chain Synthesizing Enzymes

Recently, rhamnosyltransferase enzymes for the RG-I backbone were characterized (Takenaka et al. 2018), and the GALACTAN SYNTASE (GALS) enzymes, which are members of the GT92 family, are thought to synthesize the galactan side chains of RG-I (Ebert et al. 2018). Arabinosyltransferases of the ARABINAN DEFICIENT (ARAD) family have been linked to the synthesis of the arabinan side chains of RG-I (Harholt et al. 2006; Harholt et al. 2012). However, how the full suite of arabinogalactan and galactoarabinan side chains are added to RG-I has not been completely worked out.

12.3.4 RG-II Biosynthetic Enzymes

A large suite of catalytic activities is putatively required to construct the complex side chains of RG-II (Mohnen 2008), just as a large number of glycosyl hydrolases are required to degrade RG-II (Ndeh et al. 2017), making it one of the most degradation-resistant pectin domains. Only a few of the enzymes required for RG-II synthesis have been identified, including a glucuronosyltransferase (Iwai et al. 2002) and two xylosyltransferases (Egelund et al. 2006).

12.4 Pectin Trafficking and Deposition in the Cell Wall

12.4.1 Intracellular Trafficking of Pectins from the Golgi to the Cell Surface

After synthesis in the Golgi, pectins are thought to be delivered to the cell surface by vesicles that bud from the medial or trans Golgi cisternae and are transported, either by active transport or diffusion, to the cell surface; this pathway might also be used for pectin-modifying enzymes, a few of which have been shown to be exocytose via a noncanonical secretory pathway (De Caroli et al. 2011; Wang et al. 2016). Recent work has implicated a kinesin, FRAGILE FIBER 1 (FRA1), in the delivery of pectins to the cell surface in a microtubule-dependent manner, although interestingly, *fra1* mutants do not show obvious defects in the trafficking of CELLULOSE SYNTHASEs or in cellulose organization, suggesting that the pathways that deliver

pectins and CELLULOSE SYNTHASEs might be distinct (Zhu et al. 2015; Zhu et al. 2018). Likewise, immunoelectron microscopy data have suggested that pectins and hemicelluloses, which are also produced in the Golgi lumen, bud off from different Golgi cisternae, suggesting that their trafficking pathways are at least partially independent.

12.4.2 Exocytosis of Pectins

Pectins are likely to be exocytosed via exocytic machinery that involves the TRAPPII complex (Rybak et al. 2014) and the exocyst complex (Zhu et al. 2018) including EXO84b (Rybak et al. 2014) and syntaxins. However, robust characterization of the entire exocytic machinery that is responsible for delivery pectins to the apoplast, especially along different developmental stages of the wall, has not yet been performed.

12.4.3 Pectins as Scaffolds for De Novo Wall Assembly

Pectins are one of the earliest detectable wall polysaccharides to be laid down in the developing cell plate during cytokinesis, as evinced by immunoelectron microscopy (Samuels et al. 1995), and might interact with networks of extensins (Cannon et al. 2008) via electrostatic attraction to help construct the initial scaffolding of the nascent cell wall. The ability of pectins to form gels in the absence or presence of calcium in vitro and affect the organization of bacterial cellulose synthesis (Lin et al. 2016; Lopez-Sanchez et al. 2017) suggests that pectins might influence how cellulose is initially laid down in the wall during later stages of cytokinesis in plant cells (Miart et al. 2014).

12.4.4 Initial Interactions between Pectins and Other Wall Polysaccharides

After delivery to the apoplast, pectins can begin to interact with cellulose. Despite a large amount of evidence suggesting that interactions between pectins and cellulose are of low affinity and/or reversible when established in vitro (Chanliaud and Gidley 1999; Zykwinska et al. 2008; Lin et al. 2015), recent NMR (Dick-Perez et al. 2012; Wang et al. 2015; Phyo et al. 2017b) and binding studies involving the synthesis of bacterial cellulose in the presence of pectins (Lin et al. 2015; Lin et al. 2016; Lopez-Sanchez et al. 2017) have suggested that pectins interact closely and extensively with cellulose in plant cell walls. These findings suggest that pectins might be "forced"

into interactions with cellulose due to simple proximity, although whether these interactions are initiated by electrostatic, hydrogen bonding, Van der Waals forces, or hydrophobicity/hydrophilicity interactions is unknown. It is also currently controversial which parts of pectin molecules are responsible for their interactions with cellulose; the neutral side chains of RG-I are thought to be major mediators of pectin-cellulose interactions in vitro (Zykwinska et al. 2005; Zykwinska et al. 2007; Lin et al. 2015), but GalA residues are also thought to reside in close proximity to cellulose, although whether these residues are charged or methyl-esterified remains unclear. The interactions between pectins, which are likely to be at least partially soluble, and cellulose, which is insoluble after its synthesis, might also resemble the deposition patterns of minerals that crystallize on insoluble substrates, although this idea is highly speculative.

Pectins are likely to interact to at least some extent with hemicelluloses, e.g., xyloglucans, en route to their exocytosis, although the extent to which these interactions are retained after delivery to the apoplast is unclear. Covalent linkages between pectins and hemicelluloses, either direct or indirect, have been detected (Popper and Fry 2005; Popper and Fry 2008), and in some cases both groups might be attached to proteoglycan cores (Tan et al. 2013). One unanswered question is the extent to which transglycosylation activity in the cell wall might be responsible for establishing these linkages, or whether they are established co-synthetically in the Golgi. Alternatively, it is possible that if pectins are delivered to the apoplast via trafficking pathways that are distinct from those of hemicelluloses, the first time pectins might encounter hemicelluloses would be after delivery to the apoplast, in which case these initial interactions might alter the solubility of one or both binding partners.

12.5 Pectin Organization and Dynamics in Plant Cell Walls

Upon their deposition into the wall, pectins likely adopt a mesh-like, reticulated organization at the innermost face of the wall (Zhang et al. 2016), which mirrors the patterning of isolated pectins as assessed by AFM (Round et al. 2010) (Fig. 12.3a). RG-II cross-linking is thought to modulate pore size in the cell wall, depending on boron abundance, which is required to maintain the physicochemical integrity of the wall (Fleischer et al. 1999). As pectins age in the wall and possibly are extruded into either the outer surface of the wall or the middle lamella, their conformation, degree of polymerization, degree of methyl-esterification, level of cross-linking, associations with other wall components, and organization change (Fig. 12.3a, b).

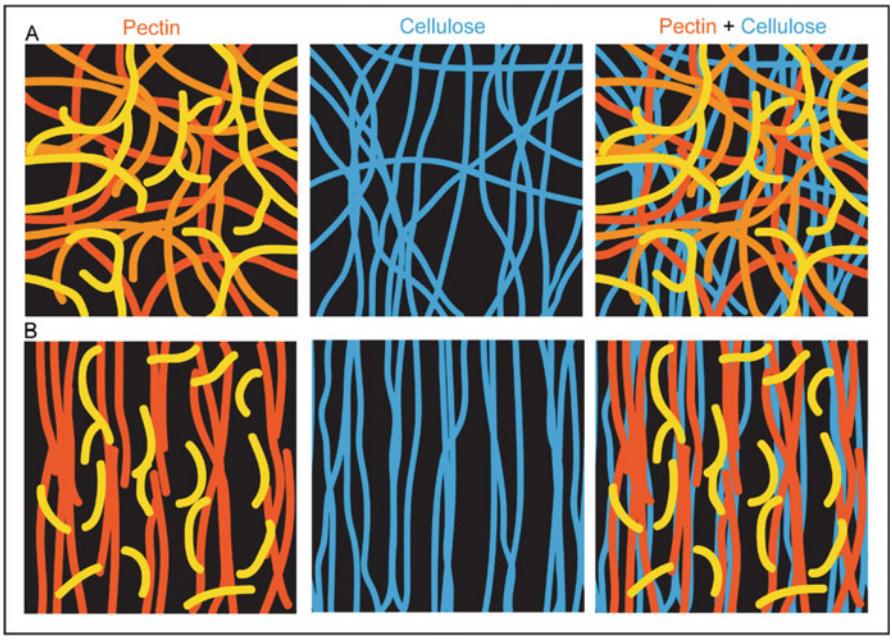

Fig. 12.3 A conception of what pectins (orange) might look like in the apoplast in relation to cellulose (blue) in newly deposited (**a**) and older (**b**) layers of the cell wall, based partly on FESEM (Zhang et al. 2016) and metabolic labeling (Anderson et al. 2012) studies. Each panel is 200 nm × 200 nm. In newly deposited walls (**a**), a gel-like pectin layer might serve as a scaffolding into which newly synthesized cellulose is laid down, preventing premature cellulose bundling during growth, whereas in older wall layers (**b**), cellulose is oriented and bundled after anisotropic cell expansion, resulting in pectin reorientation and consolidation into less mobile, cellulose-associated fractions (dark orange) and more mobile, non-associated fractions (light orange) that might differ in molecular weight due to pectinase activity and degree of cross-linking (Phyo et al. 2017a; Phyo et al. 2017b; Wang et al. 2015)

12.5.1 Pectin De-Methyl-Esterification and Deacetylation

After delivery to the cell wall, HG can be de-methyl-esterified by proteins of the PECTIN METHYLESTERASE (PME) family, which form large clades in many plant species and are differentially expressed in different tissues (Jolie et al. 2010). PMEs can be inhibited in the wall by PECTIN METHYLESTERASE INHIBITOR (PMEI) proteins (Wormit and Usadel 2018), which bind to and inactivate PMEs until a triggering event, such as a change in pH, causes dissociation between the PMEI and PME. Pectin acetylesterases remove the acetyl groups from pectin residues in the wall (Philippe et al. 2017).

12.5.2 Pectins and Wall Mechanics

In vitro, pectins form gels that have low compressive stiffness (Jarvis 1984). Because they are charged and can form hydrogen bonds with water, pectins are often highly hydrated in the cell wall and show a high degree of molecular mobility (Dick-Perez et al. 2012). In this sense, they might facilitate wall expansion by allowing for the reorientation or sliding of other wall polysaccharides, such as cellulose and hemicellulose, during wall yielding in response to turgor (Cosgrove 2018). Additionally, pectins might act as spacers that separate wall lamellae and allow them to deform independently of one another.

Stretches of de-methyl-esterified homogalacturonan can in theory be cross-linked by Ca^{2+} ions, forming an "egg-box" structure or some analogously cross-linked structure that stiffens the cell wall (Peaucelle et al. 2011). However, these non-covalent Ca cross-links can be remodeled over time as cell wall expansion proceeds, resulting in continuous breaking and formation of these cross-links (Boyer 2016). Pectin cross-linking can, at least in some cases, override the activity of expansins (Zhao et al. 2008), which are nonenzymatic proteins that facilitate wall creep by acting at cellulose-hemicellulose junctions (Wang et al. 2013). Interestingly, despite the low apparent compressive stiffness of pectins in vitro, the middle lamella in some cell types shows higher resistance to tensile force than the wall itself (Zamil et al. 2014), suggesting that pectins in the middle lamella confer high tensile strength.

The contributions of RG-I cross-linking by ferulate diesters and RG-II cross-linking by borate diesters to wall integrity have been hinted at by *Nicotiana plumbaginifolia* mutants in which RG-I arabinan and cell adhesion are both defective (Iwai et al. 2001), and experiments in which boron depletion affects wall thickness and therefore potentially tissue mechanics (Ishii et al. 2001), but the mechanical roles of these cross-links during normal plant growth are less well understood.

12.5.3 Pectin Auto-Degradation

Pectins can be degraded in the cell wall by several different classes of endogenous enzymes (Senechal et al. 2014; Yang et al. 2018). These include polygalacturonases, which hydrolyze the backbone of HG and can be categorized into endo- and exo-polygalacturonases; pectate lyases, which cleave HG backbones via β-elimination; and RG lyases, which cleave RG-I. Presumably, galactanases and arabinanases are able to degrade the side chains of RG-I, although the specific endogenous enzymes responsible for these activities have not yet been characterized. RG-II degradation requires an extensive suite of enzymes, many of which have been detected in enteric bacteria (Ndeh et al. 2017), but not all of which have been identified in plant genomes.

Polygalacturonases have been shown to function in two essential developmental processes: cell expansion and cell separation (Yang et al. 2018). During cell expansion, polygalacturonases are likely to reduce the ability of HG molecules to cross-link into mechanically limiting networks, and during cell separation, they are likely

to degrade HG in the middle lamella to facilitate a loss of intercellular adhesion. How PG activities are tuned to differentiate between these processes is not currently clear, although substrate specificity, pH dependence, or differential expression might all contribute to this tuning. Polygalacturonases have also been implicated in fruit ripening and softening.

Pectate lyases are less well characterized than polygalacturonases from a genetic perspective, but their enzymatic mechanism is distinct and depends on Ca^{2+} as a cofactor. It is interesting to consider whether the Ca^{2+} ions required for HG cross-linking and pectate lyase activity are identical or distinct; if the former is true, it is possible that de-cross-linking is a prerequisite for HG backbone cleavage by pectate lyases. The pH dependencies of pectate lyases also differ from that of polygalacturonases (Marin-Rodriguez et al. 2002).

12.5.4 Implications of Pectin Dynamics for Plant Growth and Development

Pectins have been implicated in the regulation of cell expansion, tissue elongation, organ initiation and patterning, fruit ripening, and many other developmental processes; this chapter does not go into detail on these topics, which have been nicely reviewed recently (Saffer 2018). For example, they are likely to function in stomatal guard cells, where their synthesis, deposition, and modification might modulate the flexibility and stiffness of the guard cell walls, enabling them both to develop a pore via partial separation of sister guard cells from one another and to elastically expand and contract (Jones et al. 2005; Rui et al. 2017; Rui et al. 2018).

12.6 Pectins in Food, Bioenergy, Materials, and Biomedical Applications

Given their prominence in many types of cell walls, pectins comprise a significant portion of the gigatons of biomass that plants produce each year via photosynthesis and are thus a potential source of energy, food, materials, and pharmaceuticals for human use.

12.6.1 Pectins in Food Applications

By providing soluble and insoluble fiber, pectins enhance the digestive quality of many foods (Lara-Espinoza et al. 2018). The utility of pectins as gelling agents has long been recognized in traditional cooking, where pectins, either those that are already present in the ingredients or those that have been extracted from other

sources, are used to make jellies, jams, and other gelatinous foods, sometimes via the addition of Ca^{2+} and sometimes due to the ability of HG to form gels even in the absence of Ca^{2+}. Pectins are sometimes intentionally removed by filtration or enzymatic degradation from fruit-based drinks to clarify them (Patidar et al. 2018), although the health impacts of this removal are questionable. Modern uses of pectins in food science include texture control, thickening, emulsification, and stabilization (Laurent and Boulenguer 2003; Leroux et al. 2003).

12.6.2 Pectins as Bioenergy Feedstocks

Although most bioenergy research involving plant cell walls is focused on the degradation of cellulose into fermentable glucose (Carroll and Somerville 2009), because they are abundant in certain food waste streams, such as fruit pulp and peels (Zema et al. 2018), pectins can also serve as a feedstock for bioenergy production (Edwards and Doran-Peterson 2012; Jordan et al. 2012). A key hurdle in this effort of pectin utilization is in the fermentation process, wherein the many different sugars present in pectins must be efficiently metabolized by fermentative microbes including bacteria (Ndeh et al. 2017) or yeast to produce platform chemicals, bioethanol, or other fuel molecules.

12.6.3 Pectins as Inhibitors of Plant Biomass Processing

Because they are negatively charged, interact with other wall polysaccharides, are distributed throughout the wall, and contain acetyl groups, pectins are considered to be inhibitors of biomass saccharification (Biswal et al. 2018b) during biomass processing due to their ability to bind to and/or block biomass-degrading enzymes. In addition, due to their role in cell-cell adhesion, pectins increase the energy requirements for biomass comminution during milling and pre-treatment (Xiao and Anderson 2013). The manipulation of pectin biosynthetic genes has recently been shown to enhance biomass saccharification in candidate eudicot and grass bioenergy crops (Biswal et al. 2018a; Biswal et al. 2015). Acetyl groups released from pectins in the form of acetate can inhibit the growth of fermentative microbes, although the primary source of acetate for biomass derived from wood or grasses is instead the acetylation present on hemicellulosic xylan. The secreted proteomes of many biomass-degrading microbes contain pectinases, implying that pectin degradation is a pre- or corequisite of the degradation of other wall polysaccharides, and pectinases can act synergistically with cellulase and hemicellulase enzymes during enzymatic saccharification (Benz et al. 2014). Despite this evidence, pectinases have not yet been extensively engineered for increased catalytic activity or mined for robustness across a range of temperatures and pH levels.

12.6.4 Pectins as Tunable Biogels and Biopharmaceuticals

The ability of pectins to form gels that can be reversibly formed and whose stiffness can be altered based on the molecular mass of the polymer, its chemical composition, and the degree of cross-linking induced in the gel makes them useful in materials applications where gels are required (Lara-Espinoza et al. 2018). For instance, combinations of chitosan and pectin have been used to fabricate functional films with applications in food packaging (see Chap. 14). Pectin gels have been combined with carbon nanotubes to make a bionic material with high temperature sensitivity (Di Giacomo et al. 2015). Due to their ability to dissolve slowly over time and form gels that trap larger molecules, pectins serve as useful time-release excipients for pharmaceuticals (Lara-Espinoza et al. 2018). Some pectin preparations, including modified citrus pectin, have been shown to have cytotoxic and anti-migration effects on cultured cancer cells (Leclere et al. 2013). However, the in vivo effectiveness of pectins alone on cancer progression in humans has not yet been demonstrated in clinical trials.

12.7 Concluding Remarks and Future Directions

Although pectins retain large swaths of mystery with respect to their native structure, synthesis, dynamics, interactions with other wall polymers, and degradation by plants, microbes, and humans, the "omics" age has ushered in a new perspective on these enigmatic but exciting heteropolysaccharides. Future work to deconstruct the structures of single pectin molecules, for example, by tandem mass spectrometry with single-molecule sensitivity, promises to reveal whether pectins represent a truly heterogeneous population in which every molecule is its own unique artifact of nature or whether pectins share commonalities that allow them to act in concert to perform their functions. These approaches, combined with advances in imaging at the nanoscale and the ability to manipulate plant genomes at the level of individual nucleotides, may finally help us unravel the complexity of pectins and engineer them for uses that will enhance the beauty and utility of the natural world, both for us and our coinhabitants on the planet.

Acknowledgments Thanks to Chaowen Xiao, Peter Dowd, Thomas McCarthy, Daniel McClosky, Melissa Ishler, Yue Rui, William Barnes, Yintong Chen, Deborah Petrik, Sydney Duncombe, Yang Yang, Anderson Lab rotation students and undergraduate researchers, and Daniel Cosgrove for stimulating discussions about pectins and plant cell walls. This work was supported as part of the Center for Lignocellulose Structure and Formation, an Energy Frontier Research Center funded by the US Department of Energy, Office of Science, Basic Energy Sciences under Award # DE-SC0001090.

References

Abasolo W et al (2009) Pectin may hinder the unfolding of xyloglucan chains during cell deformation: implications of the mechanical performance of *Arabidopsis* hypocotyls with pectin alterations. Mol Plant 2:990–999

Amos RA, Pattathil S, Yang JY, Atmodjo MA, Urbanowicz BR, Moremen KW, Mohnen D (2018) A two-phase model for the non-processive biosynthesis of homogalacturonan polysaccharides by the GAUT1:GAUT7 complex. J Biol Chem 293:19047–19063

Anderson CT (2016) We be jammin': an update on pectin biosynthesis, trafficking and dynamics. J Exp Bot 67:495–502

Anderson CT, Wallace IS, Somerville CR (2012) Metabolic click-labeling with a fucose analog reveals pectin delivery, architecture, and dynamics in *Arabidopsis* cell walls. Proc Natl Acad Sci USA 109:1329–1334

Atmodjo MA, Hao Z, Mohnen D (2013) Evolving views of pectin biosynthesis. Annu Rev Plant Biol 64:747–779

Atmodjo MA et al (2011) Galacturonosyltransferase (GAUT)1 and GAUT7 are the core of a plant cell wall pectin biosynthetic homogalacturonan: galacturonosyltransferase complex. Proc Natl Acad Sci USA 108:20225–20230

Bar-Peled M, O'Neill MA (2011) Plant nucleotide sugar formation, interconversion, and salvage by sugar recycling. Annu Rev Plant Biol 62:127–155

Bar-Peled M, Urbanowicz BR, O'Neill MA (2012) The synthesis and origin of the pectic polysaccharide rhamnogalacturonan II – insights from nucleotide sugar formation and diversity. Front Plant Sci 3:92. https://doi.org/10.3389/fpls.2012.00092

Benz JP, Chau BH, Zheng D, Bauer S, Glass NL, Somerville CR (2014) A comparative systems analysis of polysaccharide-elicited responses in *Neurospora crassa* reveals carbon source-specific cellular adaptations. Mol Microbiol 91:275–299

Biswal AK et al (2015) Downregulation of GAUT12 in *Populus deltoides* by RNA silencing results in reduced recalcitrance, increased growth and reduced xylan and pectin in a woody biofuel feedstock. Biotechnol Biofuels 8:41. https://doi.org/10.1186/s13068-015-0218-y

Biswal AK et al (2017) Comparison of four glycosyl residue composition methods for effectiveness in detecting sugars from cell walls of dicot and grass tissues. Biotechnol Biofuels 10:182. https://doi.org/10.1186/s13068-017-0866-1

Biswal AK et al (2018a) Sugar release and growth of biofuel crops are improved by downregulation of pectin biosynthesis. Nat Biotechnol 36:249–257

Biswal AK et al (2018b) Working towards recalcitrance mechanisms: increased xylan and homogalacturonan production by overexpression of GAlactUronosylTransferase12 (GAUT12) causes increased recalcitrance and decreased growth in *Populus*. Biotechnol Biofuels 11:9. https://doi.org/10.1186/s13068-017-1002-y

Bledzki AK, Gassan J (1999) Composites reinforced with cellulose based fibres. Prog Polym Sci 24:221–274

Bou Daher F, Chen Y, Bozorg B, Clough J, Jonsson H, Braybrook SA (2018) Anisotropic growth is achieved through the additive mechanical effect of material anisotropy and elastic asymmetry. Elife 7. https://doi.org/10.7554/eLife.38161

Boyer JS (2016) Enzyme-less growth in *Chara* and terrestrial plants. Front Plant Sci 7:866. https://doi.org/10.3389/fpls.2016.00866

Braccini I, Perez S (2001) Molecular basis of $Ca^{(2+)}$-induced gelation in alginates and pectins: the egg-box model revisited. Biomacromolecules 2:1089–1096

Caffall KH, Pattathil S, Phillips SE, Hahn MG, Mohnen D (2009) *Arabidopsis thaliana* T-DNA mutants implicate GAUT genes in the biosynthesis of pectin and xylan in cell walls and seed testa. Mol Plant 2:1000–1014

Cannon MC et al (2008) Self-assembly of the plant cell wall requires an extensin scaffold. Proc Natl Acad Sci USA 105:2226–2231

Carroll A, Somerville C (2009) Cellulosic biofuels. Annu Rev Plant Biol 60:165–182

Chanliaud E, Gidley MJ (1999) *In vitro* synthesis and properties of pectin/Acetobacter xylinus cellulose composites. Plant J 20:25–35

Cornuault V, Manfield IW, Ralet MC, Knox JP (2014) Epitope detection chromatography: a method to dissect the structural heterogeneity and inter-connections of plant cell-wall matrix glycans. Plant J 78:715–722

Cosgrove DJ (2014) Re-constructing our models of cellulose and primary cell wall assembly. Curr Opin Plant Biol 22:122–131

Cosgrove DJ (2018) Diffuse growth of plant cell walls. Plant Physiol 176:16–27

Daher FB, Braybrook SA (2015) How to let go: pectin and plant cell adhesion. Front Plant Sci 6:523

De Caroli M, Lenucci MS, Di Sansebastiano GP, Dalessandro G, De Lorenzo G, Piro G (2011) Protein trafficking to the cell wall occurs through mechanisms distinguishable from default sorting in tobacco. Plant J 65:295–308

De Ruiter GA, Schols HA, Voragen AG, Rombouts FM (1992) Carbohydrate analysis of water-soluble uronic acid-containing polysaccharides with high-performance anion-exchange chromatography using methanolysis combined with TFA hydrolysis is superior to four other methods. Anal Biochem 207:176–185

Derbyshire P, McCann MC, Roberts K (2007) Restricted cell elongation in *Arabidopsis* hypocotyls is associated with a reduced average pectin esterification level. BMC Plant Biol 7:31. https://doi.org/10.1186/1471-2229-7-31

Di Giacomo R, Daraio C, Maresca B (2015) Plant nanobionic materials with a giant temperature response mediated by pectin-Ca^{2+}. Proc Natl Acad Sci USA 112:4541–4545

Dick-Perez M, Wang T, Salazar A, Zabotina OA, Hong M (2012) Multidimensional solid-state NMR studies of the structure and dynamics of pectic polysaccharides in uniformly 13^{C}-labeled *Arabidopsis* primary cell walls. Magn Reson Chem MRC 50:539–550

Diet A et al (2006) The *Arabidopsis* root hair cell wall formation mutant *lrx1* is suppressed by mutations in the *RHM1* gene encoding a UDP-L-rhamnose synthase. Plant Cell 18:1630–1641

Domozych DS, Ciancia M, Fangel JU, Mikkelsen MD, Ulvskov P, Willats WG (2012) The cell walls of green algae: a journey through evolution and diversity. Front Plant Sci 3:82. https://doi.org/10.3389/fpls

Domozych DS, Domozych CE (2014) Multicellularity in green algae: upsizing in a walled complex. Front Plant Sci 5:649. https://doi.org/10.3389/fpls.2014.00649

Domozych DS et al (2014) Pectin metabolism and assembly in the cell wall of the charophyte green alga *Penium margaritaceum*. Plant Physiol 165:105–118

Donaldson LA (2001) Lignification and lignin topochemistry - an ultrastructural view. Phytochemistry 57:859–873

Doong RL, Liljebjelke K, Fralish G, Kumar A, Mohnen D (1995) Cell-free synthesis of pectin (identification and partial characterization of Polygalacturonate 4-[alpha]-Galacturonosyltransferase and its products from membrane preparations of tobacco cell-suspension cultures). Plant Physiol 109:141–152

Ebert B et al (2018) The three members of the *Arabidopsis* glycosyltransferase family 92 are functional beta-1,4-galactan synthases. Plant Cell Physiol 59:2624–2636

Edwards MC, Doran-Peterson J (2012) Pectin-rich biomass as feedstock for fuel ethanol production. Appl Microbiol Biotechnol 95:565–575

Egelund J et al (2006) *Arabidopsis thaliana* RGXT1 and RGXT2 encode Golgi-localized (1,3)-alpha-D-xylosyltransferases involved in the synthesis of pectic rhamnogalacturonan-II. Plant Cell 18:2593–2607

Feng W et al (2018) The FERONIA receptor kinase maintains cell-wall integrity during salt stress through $Ca^{(2+)}$ signaling. Curr Biol 28:666–675

Fleischer A, O'Neill MA, Ehwald R (1999) The pore size of non-graminaceous plant cell walls is rapidly decreased by borate ester cross-linking of the pectic polysaccharide rhamnogalacturonan II. Plant Physiol 121:829–838

Fry SC (1988) The growing plant cell wall: chemical and metabolic analysis. Monographs and surveys in the biosciences. Longman Scientific & Technical; Wiley, Harlow, Essex, England; New York

Goldberg R, Morvan C, Jauneau A, Jarvis MC (1996) Methyl-esterification, de-esterification and gelation of pectins in the primary cell wall. In: Visser J, Voragen AGJ (eds) Progress in biotechnology, vol 14. Elsevier, Amsterdam, pp 151–172

Goldberg R, Morvan C, Roland JC (1986) Composition, properties and localization of pectins in young and mature cells of the mung bean hypocotyl. Plant Cell Physiol 27:417–429

Goulao LF, Vieira-Silva S, Jackson PA (2011) Association of hemicellulose- and pectin-modifying gene expression with *Eucalyptus globulus* secondary growth. Plant Physiol Biochem: PPB / Societe francaise de physiologie vegetale 49:873–881

Grantham NJ et al (2017) An even pattern of xylan substitution is critical for interaction with cellulose in plant cell walls. Nat Plants 3:859–865

Guillaumie F, Sterling JD, Jensen KJ, Thomas ORT, Mohnen D (2003) Solid-supported enzymatic synthesis of pectic oligogalacturonides and their analysis by MALDI-TOF mass spectrometry. Carbohydr Res 338:1951–1960

Guillemin F et al (2005) Distribution of pectic epitopes in cell walls of the sugar beet root. Planta 222:355–371

Gunl M, Kraemer F, Pauly M (2011) Oligosaccharide mass profiling (OLIMP) of cell wall polysaccharides by MALDI-TOF/MS. Methods Mol Biol 715:43–54

Guzman P, Fernandez V, Garcia ML, Khayet M, Fernandez A, Gil L (2014) Localization of polysaccharides in isolated and intact cuticles of eucalypt, poplar and pear leaves by enzyme-gold labelling. Plant Physiol Biochem 76:1–6

Harholt J, Jensen JK, Sorensen SO, Orfila C, Pauly M, Scheller HV (2006) ARABINAN DEFICIENT 1 is a putative arabinosyltransferase involved in biosynthesis of pectic arabinan in *Arabidopsis*. Plant Physiol 140:49–58

Harholt J et al (2012) ARAD proteins associated with pectic Arabinan biosynthesis form complexes when transiently overexpressed *in planta*. Planta 236:115–128

Harholt J, Moestrup O, Ulvskov P (2016) Why plants were terrestrial from the beginning. Trends Plant Sci 21:96–101

Hemant O, Haswell ES (2017) Life behind the wall: sensing mechanical cues in plants. BMC Biol 15:59. https://doi.org/10.1186/s12915-017-0403-5

Hocq L, Pelloux J, Lefebvre V (2017) Connecting Homogalacturonan-type pectin remodeling to acid growth. Trends Plant Sci 22:20–29

Houston K, Tucker MR, Chowdhury J, Shirley N, Little A (2016) The plant cell wall: a complex and dynamic structure as revealed by the responses of genes under stress conditions. Front Plant Sci 7:984. https://doi.org/10.3389/fpls.2016.00984

Ishii T (1997) Structure and functions of feruloylated polysaccharides. Plant Sci 127:111–127

Ishii T, Matsunaga T (1996) Isolation and characterization of a boron-rhamnogalacturonan-II complex from cell walls of sugar beet pulp. Carbohydr Res 284:1–9

Ishii T, Matsunaga T, Hayashi N (2001) Formation of rhamnogalacturonan II-borate dimer in pectin determines cell wall thickness of pumpkin tissue. Plant Physiol 126:1698–1705

Iwai H, Ishii T, Satoh S (2001) Absence of arabinan in the side chains of the pectic polysaccharides strongly associated with cell walls of *Nicotiana plumbaginifolia* non-organogenic callus with loosely attached constituent cells. Planta 213:907–915

Iwai H, Masaoka N, Ishii T, Satoh S (2002) A pectin glucuronyltransferase gene is essential for intercellular attachment in the plant meristem. Proc Natl Acad Sci USA 99:16319–16324

Jarvis MC (1984) Structure and properties of pectin gels in plant-cell walls. Plant Cell Environ 7:153–164

Jolie RP, Duvetter T, Van Loey AM, Hendrickx ME (2010) Pectin methylesterase and its proteinaceous inhibitor: a review. Carbohydr Res 345:2583–2595

Jones L, Milne JL, Ashford D, McCann MC, McQueen-Mason SJ (2005) A conserved functional role of pectic polymers in stomatal guard cells from a range of plant species. Planta 221:255–264

Jordan DB et al (2012) Plant cell walls to ethanol. Biochem J 442:241–252

Kim SJ, Held MA, Zemelis S, Wilkerson C, Brandizzi F (2015) CGR2 and CGR3 have critical overlapping roles in pectin methylesterification and plant growth in *Arabidopsis thaliana*. Plant J 82:208–220

Knox JP, Linstead PJ, King J, Cooper C, Roberts K (1990) Pectin esterification is spatially regulated both within cell-walls and between developing-tissues of root apices. Planta 181:512–521

Kong Y, Zhou G, Yin Y, Xu Y, Pattathil S, Hahn MG (2011) Molecular analysis of a family of *Arabidopsis* genes related to galacturonosyltransferases. Plant Physiol 155:1791–1805

Krupkova E, Immerzeel P, Pauly M, Schmulling T (2007) The *TUMOROUS SHOOT DEVELOPMENT2* gene of *Arabidopsis* encoding a putative methyltransferase is required for cell adhesion and co-ordinated plant development. Plant J 50:735–750

Lara-Espinoza C, Carvajal-Millan E, Balandran-Quintana R, Lopez-Franco Y, Rascon-Chu A (2018) Pectin and pectin-based composite materials: beyond food texture. Molecules 23. https://doi.org/10.3390/molecules23040942

Laurent MA, Boulenguer P (2003) Stabilization mechanism of acid dairy drinks (ADD) induced by pectin. Food Hydrocoll 17:445–454

Leclere L, Cutsem PV, Michiels C (2013) Anti-cancer activities of pH- or heat-modified pectin. Front Pharmacol 4:128. https://doi.org/10.3389/fphar.2013.00128

Lee C, Teng Q, Zhong R, Ye ZH (2011) The four *Arabidopsis* reduced wall acetylation genes are expressed in secondary wall-containing cells and required for the acetylation of xylan. Plant Cell Physiol 52:1289–1301

Leroux J, Langendorff V, Schick G, Vaishnav V, Mazoyer J (2003) Emulsion stabilizing properties of pectin. Food Hydrocoll 17:455–462

Lin D, Lopez-Sanchez P, Gidley MJ (2015) Binding of arabinan or galactan during cellulose synthesis is extensive and reversible. Carbohydr Polym 126:108–121

Lin D, Lopez-Sanchez P, Gidley MJ (2016) Interactions of pectins with cellulose during its synthesis in the absence of calcium. Food Hydrocoll 52:57–68

Lopez-Sanchez P, Martinez-Sanz M, Bonilla MR, Wang D, Gilbert EP, Stokes JR, Gidley MJ (2017) Cellulose-pectin composite hydrogels: intermolecular interactions and material properties depend on order of assembly. Carbohydr Polym 162:71–81

Manabe Y et al (2011) Loss-of-function mutation of REDUCED WALL ACETYLATION2 in *Arabidopsis* leads to reduced cell wall acetylation and increased resistance to *Botrytis cinerea*. Plant Physiol 155:1068–1078

Marin-Rodriguez MC, Orchard J, Seymour GB (2002) Pectate lyases, cell wall degradation and fruit softening. J Exp Bot 53:2115–2119

McCarthy TW, Der JP, Honaas LA, dePamphilis CW, Anderson CT (2014) Phylogenetic analysis of pectin-related gene families in *Physcomitrella patens* and nine other plant species yields evolutionary insights into cell walls. BMC Plant Biol 14:79. https://doi.org/10.1186/1471-2229-14-79

Miart F et al (2014) Spatio-temporal analysis of cellulose synthesis during cell plate formation in Arabidopsis. Plant J 77:71–84

Mohnen D (2008) Pectin structure and biosynthesis. Curr Opin Plant Biol 11:266–277

Molhoj M, Verma R, Reiter WD (2003) The biosynthesis of the branched-chain sugar d-apiose in plants: functional cloning and characterization of a UDP-d-apiose/UDP-d-xylose synthase from *Arabidopsis*. Plant J 35:693–703

Mouille G et al (2007) Homogalacturonan synthesis in *Arabidopsis thaliana* requires a Golgi-localized protein with a putative methyltransferase domain. Plant J 50:605–614

Nakamura A, Furuta H, Maeda H, Nagamatsu Y, Yoshimoto A (2001) Analysis of structural components and molecular construction of soybean soluble polysaccharides by stepwise enzymatic degradation. Biosci Biotechnol Biochem 65:2249–2258

Ndeh D et al (2017) Complex pectin metabolism by gut bacteria reveals novel catalytic functions. Nature 544:65–70

Novakovic L, Guo T, Bacic A, Sampathkumar A, Johnson KL (2018) Hitting the wall-sensing and signaling pathways involved in plant Cell Wall remodeling in response to abiotic stress. Plants (Basel) 7. https://doi.org/10.3390/plants7040089

O'Neill MA, Ishii T, Albersheim P, Darvill AG (2004) Rhamnogalacturonan II: structure and function of a borate cross-linked cell wall pectic polysaccharide. Annu Rev Plant Biol 55:109–139

Opanowicz M et al (2011) Endosperm development in *Brachypodium distachyon*. J Exp Bot 62:735–748

Pabst M et al (2013) Rhamnogalacturonan II structure shows variation in the side chains monosaccharide composition and methylation status within and across different plant species. Plant J 76:61–72

Palmer KJ, Ballantyne M (1950) The structure of (I) some pectin esters and (ii) guar galactomannan. J Am Chem Soc 72:736–741

Park YB, Cosgrove DJ (2015) Xyloglucan and its interactions with other components of the growing cell wall. Plant Cell Physiol 56:180–194

Parsons HT et al (2012) Isolation and proteomic characterization of the *Arabidopsis* Golgi defines functional and novel components involved in plant cell wall biosynthesis. Plant Physiol 159:12–26

Patidar MK, Nighojkar S, Kumar A, Nighojkar A (2018) Pectinolytic enzymes-solid state fermentation, assay methods and applications in fruit juice industries: a review. 3 Biotech 8:199. https://doi.org/10.1007/s13205-018-1220-4

Peaucelle A, Louvet R, Johansen JN, Hofte H, Laufs P, Pelloux J, Mouille G (2008) Arabidopsis phyllotaxis is controlled by the methyl-esterification status of cell-wall pectins. Curr Biol 18:1943–1948

Peaucelle A, Braybrook SA, Le Guillou L, Bron E, Kuhlemeier C, Hofte H (2011) Pectin-induced changes in cell wall mechanics underlie organ initiation in *Arabidopsis*. Curr Biol 21:1720–1726

Peaucelle A, Braybrook S, Hofte H (2012) Cell wall mechanics and growth control in plants: the role of pectins revisited. Front Plant Sci 3:121. https://doi.org/10.3389/fpls.2012.00121

Peaucelle A, Wightman R, Höfte H (2015) The control of growth symmetry breaking in the *Arabidopsis* hypocotyl. Curr Biol 25:1746–1752

Pettolino FA, Walsh C, Fincher GB, Bacic A (2012) Determining the polysaccharide composition of plant cell walls. Nat Protoc 7:1590–1607

Philippe F, Pelloux J, Rayon C (2017) Plant pectin acetylesterase structure and function: new insights from bioinformatic analysis. BMC Genomics 18:456. https://doi.org/10.1186/s12864-017-3833-0

Phyo P, Wang T, Kiemle SN, O'Neill H, Pingali SV, Hong M, Cosgrove DJ (2017a) Gradients in wall mechanics and polysaccharides along growing inflorescence stems. Plant Physiol 175:1593–1607

Phyo P, Wang T, Xiao C, Anderson CT, Hong M (2017b) Effects of pectin molecular weight changes on the structure, dynamics, and polysaccharide interactions of primary cell walls of *Arabidopsis thaliana*: insights from solid-state NMR. Biomacromolecules 18:2937–2950

Popper ZA, Fry SC (2005) Widespread occurrence of a covalent linkage between xyloglucan and acidic polysaccharides in suspension-cultured angiosperm cells. Ann Bot 96:91–99

Popper ZA, Fry SC (2008) Xyloglucan-pectin linkages are formed intra-protoplasmically, contribute to wall-assembly, and remain stable in the cell wall. Planta 227:781–794

Popper ZA et al (2011) Evolution and diversity of plant cell walls: from algae to flowering plants. Annu Rev Plant Biol 62:567–590

Ralet MC, Andre-Leroux G, Quemener B, Thibault JF (2005) Sugar beet (*Beta vulgaris*) pectins are covalently cross-linked through diferulic bridges in the cell wall. Phytochemistry 66:2800–2814

Ralet MC, Crepeau MJ, Lefebvre J, Mouille G, Hofte H, Thibault JF (2008) Reduced number of homogalacturonan domains in pectins of an *Arabidopsis* mutant enhances the flexibility of the polymer. Biomacromolecules 9:1454–1460

Raman R, Venkataraman M, Ramakrishnan S, Lang W, Raguram S, Sasisekharan R (2006) Advancing glycomics: implementation strategies at the consortium for functional glycomics. Glycobiology 16:82R–90R

Rennie EA, Scheller HV (2014) Xylan biosynthesis. Curr Opin Biotechnol 26:100–107

Rodriguez-Gacio MD, Iglesias-Fernandez R, Carbonero P, Matilla AJ (2012) Softening-up mannan-rich cell walls. J Exp Bot 63:3976–3988
Rosti J et al (2007) UDP-glucose 4-epimerase isoforms UGE2 and UGE4 cooperate in providing UDP-galactose for cell wall biosynthesis and growth of *Arabidopsis thaliana*. Plant Cell 19:1565–1579
Round AN, Rigby NM, MacDougall AJ, Morris VJ (2010) A new view of pectin structure revealed by acid hydrolysis and atomic force microscopy. Carbohydr Res 345:487–497
Rui Y, Xiao C, Yi H, Kandemir B, Wang JZ, Puri VM, Anderson CT (2017) POLYGALACTURONASE INVOLVED IN EXPANSION3 functions in seedling development, rosette growth, and stomatal dynamics in *Arabidopsis thaliana*. Plant Cell 29:2413–2432
Rui Y, Chen Y, Kandemir B, Yi H, Wang JZ, Puri VM, Anderson CT (2018) Balancing strength and flexibility: how the synthesis, organization, and modification of guard cell walls govern stomatal development and dynamics. Front Plant Sci 9:1202. https://doi.org/10.3389/fpls.2018.01202
Rybak K et al (2014) Plant cytokinesis is orchestrated by the sequential action of the TRAPPII and exocyst tethering complexes. Dev Cell 29:607–620
Saffer AM (2018) Expanding roles for pectins in plant development. J Integr Plant Biol 60:910–923
Samuels AL, Giddings TH Jr, Staehelin LA (1995) Cytokinesis in tobacco BY-2 and root tip cells: a new model of cell plate formation in higher plants. J Cell Biol 130:1345–1357
Scheller HV, Ulvskov P (2010) Hemicelluloses. Annu Rev Plant Biol 61:263–289
Senechal F, Wattier C, Rusterucci C, Pelloux J (2014) Homogalacturonan-modifying enzymes: structure, expression, and roles in plants. J Exp Bot 65:5125–5160
Sexton TR et al (2012) Pectin Methylesterase genes influence solid wood properties of *Eucalyptus pilularis*. Plant Physiol 158:531–541
Somerville C (2006) Cellulose synthesis in higher plants. Annu Rev Cell Dev Biol 22:53–78
Somerville C et al (2004) Toward a systems approach to understanding plant cell walls. Science 306:2206–2211
Sorensen I et al (2011) The charophycean green algae provide insights into the early origins of plant cell walls. Plant J 68:201–211
Stranne M et al (2018) TBL10 is required for O-acetylation of pectic rhamnogalacturonan-I in *Arabidopsis thaliana*. Plant J 96:772–785
Takenaka Y et al (2018) Pectin RG-I rhamnosyltransferases represent a novel plant-specific glycosyltransferase family. Nat Plants 4:669–676
Tan L et al (2013) An *Arabidopsis* cell wall proteoglycan consists of pectin and arabinoxylan covalently linked to an arabinogalactan protein. Plant Cell 25:270–287
Temple H, Saez-Aguayo S, Reyes FC, Orellana A (2016) The inside and outside: topological issues in plant cell wall biosynthesis and the roles of nucleotide sugar transporters. Glycobiology 26:913–925
Verger S, Chabout S, Gineau E, Mouille G (2016) Cell adhesion in plants is under the control of putative O-fucosyltransferases. Development 143:2536–2540
Vogel J (2008) Unique aspects of the grass cell wall. Curr Opin Plant Biol 11:301–307
Voiniciuc C et al (2018) Identification of key enzymes for pectin synthesis in seed mucilage. Plant Physiol 178:1045–1064
Wang H et al (2016) A distinct pathway for polar exocytosis in plant cell wall formation. Plant Physiol 172:1003–1018
Wang T, Hong M (2016) Solid-state NMR investigations of cellulose structure and interactions with matrix polysaccharides in plant primary cell walls. J Exp Bot 67:503–514
Wang T, Park YB, Caporini MA, Rosay M, Zhong L, Cosgrove DJ, Hong M (2013) Sensitivity-enhanced solid-state NMR detection of expansin's target in plant cell walls. Proc Natl Acad Sci USA 110:16444–16449
Wang T, Park YB, Cosgrove DJ, Hong M (2015) Cellulose-pectin spatial contacts are inherent to never-dried *Arabidopsis* primary cell walls: evidence from solid-state nuclear magnetic resonance. Plant Physiol 168:871–884
Willats WG, McCartney L, Mackie W, Knox JP (2001) Pectin: cell biology and prospects for functional analysis. Plant Mol Biol 47:9–27

Wormit A, Usadel B (2018) The Multifaceted Role of Pectin Methylesterase Inhibitors (PMEIs). Int J Mol Sci 19

Xiao C, Anderson CT (2013) Roles of pectin in biomass yield and processing for biofuels. Front Plant Sci 4:67. https://doi.org/10.3389/fpls.2013.00067

Xiao C, Somerville C, Anderson CT (2014) POLYGALACTURONASE INVOLVED IN EXPANSION1 functions in cell elongation and flower development in *Arabidopsis*. Plant Cell 26:1018–1035

Xiao C, Barnes WJ, Zamil MS, Yi H, Puri VM, Anderson CT (2017) Activation tagging of *Arabidopsis* POLYGALACTURONASE INVOLVED IN EXPANSION2 promotes hypocotyl elongation, leaf expansion, stem lignification, mechanical stiffening, and lodging. Plant J 89:1159–1173

Yang Y, Yu Y, Liang Y, Anderson CT, Cao J (2018) A profusion of molecular scissors for pectins: classification, expression, and functions of plant polygalacturonases. Front Plant Sci 9:1208. https://doi.org/10.3389/fpls.2018.01208

Yapo BM (2011) Rhamnogalacturonan-I: a structurally puzzling and functionally versatile polysaccharide from plant cell walls and mucilages. Polym Rev 51:391–413

Yapo BM, Lerouge P, Thibault JF, Ralet MC (2007) Pectins from citrus peel cell walls contain homogalacturonans homogenous with respect to molar mass, rhamnogalacturonan I and rhamnogalacturonan II. Carbohydr Polym 69:426–435

Yeats T, Vellosillo T, Sorek N, Ibáñez AB, Bauer S (2016) Rapid determination of cellulose, neutral sugars, and Uronic acids from plant cell walls by one-step two-step hydrolysis and HPAEC-PAD. Bio-protocol 6:e1978

Zablackis E, Huang J, Muller B, Darvill AG, Albersheim P (1995) Characterization of the cell-wall polysaccharides of *Arabidopsis thaliana* leaves. Plant Physiol 107:1129–1138

Zabotina OA (2012) Xyloglucan and its biosynthesis. Front Plant Sci 3:134. https://doi.org/10.3389/fpls.2012.00134

Zamil MS, Yi H, Puri VM (2014) Mechanical characterization of outer epidermal middle lamella of onion under tensile loading. Am J Bot 101:778–787

Zema DA, Calabrò PS, Folino A, Tamburino V, Zappia G, Zimbone SM (2018) Valorisation of citrus processing waste: a review. Waste Manag 80:252–273

Zhang T, Zheng Y, Cosgrove DJ (2016) Spatial organization of cellulose microfibrils and matrix polysaccharides in primary plant cell walls as imaged by multichannel atomic force microscopy. Plant J 85:179–192

Zhao Q, Yuan S, Wang X, Zhang Y, Zhu H, Lu C (2008) Restoration of mature etiolated cucumber hypocotyl cell wall susceptibility to expansin by pretreatment with fungal pectinases and EGTA *in vitro*. Plant Physiol 147:1874–1885

Zhou Y, Kobayashi M, Awano T, Matoh T, Takabe K (2018) A new monoclonal antibody against rhamnogalacturonan II and its application to immunocytochemical detection of rhamnogalacturonan II in Arabidopsis roots. Biosci Biotechnol Biochem 82:1780–1789

Zhu C et al (2015) The Fragile Fiber1 kinesin contributes to cortical microtubule-mediated trafficking of cell wall components. Plant Physiol 167:780–792

Zhu X, Li S, Pan S, Xin X, Gu Y (2018) CSI1, PATROL1, and exocyst complex cooperate in delivery of cellulose synthase complexes to the plasma membrane. Proc Natl Acad Sci USA 115:E3578–E3587

Zykwinska A, Thibault JF, Ralet MC (2007) Organization of pectic arabinan and galactan side chains in association with cellulose microfibrils in primary cell walls and related models envisaged. J Exp Bot 58:1795–1802

Zykwinska A, Thibault JF, Ralet MC (2008) Competitive binding of pectin and xyloglucan with primary cell wall cellulose. Carbohydr Polym 74:957–961

Zykwinska AW, Ralet MC, Garnier CD, Thibault JF (2005) Evidence for *in vitro* binding of pectin side chains to cellulose. Plant Physiol 139:397–407

Part VI
Alginic Acid-Based Exopolysaccharides

Chapter 13
The Role of Alginate in Bacterial Biofilm Formation

M. Fata Moradali and Bernd H. A. Rehm

Abstract Alginates are natural exopolysaccharides produced by seaweeds and bacteria belonging to the genera *Pseudomonas* and *Azotobacter*. These natural polymers are important polymeric substances contributing to the formation and development of biofilm matrixes of numerous bacteria enhancing persistence under environmental stresses, antibiotic treatment, and the immune system. Studying bacterial alginates have gained substantial attentions not only for their importance in bacterial pathogenesis but also regarding their biotechnological production for various industrial purposes. The biosynthesis of alginate is unique and has been extensively studied in the opportunistic human pathogen *P. aeruginosa*. This chapter will present updated data about bacterial production of alginate, its biological function, biosynthesis pathway, and regulation.

13.1 An Overview of Bacterial Alginate Discovery

Alginates were first discovered and extracted from seaweeds by E.C.C. Stanford, an English chemist, in 1883 (Stanford 1883). Since this discovery, algal alginates have been extensively characterized for understanding their chemistry and properties, so they have been harnessed greatly for various industrial applications for more than a century. For the first time, Sonnenschein in 1927 reported encapsulated strains of *P. aeruginosa* (Sonnenschein 1927). Many years later in 1964, alginate production by encapsulated strains of *P. aeruginosa* was reported by Linker and Jones (Linker and Jones 1964). By analysis of sputum of cystic fibrosis (CF) patients, they found that *Pseudomonas* species formed unusually large mucoid colonies by producing polysaccharides, which chemically resembled alginic acids (Linker and Jones 1964).

M. F. Moradali
Department of Oral Biology, College of Dentistry, University of Florida, Gainesville, FL, USA

B. H. A. Rehm (✉)
Centre for Cell Factories and Biopolymers, Griffith Institute for Drug Discovery, Griffith University, Brisbane, Australia
e-mail: b.rehm@griffith.edu.au

E. Cohen, H. Merzendorfer (eds.), *Extracellular Sugar-Based Biopolymers Matrices*, Biologically-Inspired Systems 12, https://doi.org/10.1007/978-3-030-12919-4_13

Later in 1966, they reported that alginate from these isolates was acetylated contrary to algal alginates, while acetyl groups were removed during alkaline extraction (Linker and Jones 1966). Then, Gorin and Spencer reported that alginic acid was also produced by another bacterial species *Azotobacter vinelandii* (Gorin and Spencer 1966). In 1973, the slimy polysaccharide produced by *P. aeruginosa* was reported as consisting of β-1,4-linked D-mannuronic acid residues and variable amounts of its 5-epimer L-guluronic acid (Evans and Linker 1973). Between 1967 and 1976, multiple reports considered strong association of mucoid strains of *P. aeruginosa* with chronic pulmonary infections in CF patients (Reynolds et al. 1976; Wood et al. 1976; Elston and Hoffman 1967; Doggett 1969). In 1981, other *Pseudomonas* species including *P. fluorescens*, *P. putida*, and *P. mendocina* were introduced as other alginate-producing bacteria (Govan et al. 1981; Müller and Monte Alegre 2007). The first report of immunogenic properties of alginate from *P. aeruginosa* was reported in 1983 by Pier et al. (Pier et al. 1983). Later in 1984, Sherbrock-Cox et al. reported the chemical characterization of *P. aeruginosa* alginate (Sherbrock-Cox et al. 1984). According to this report, alginate produced by *P. aeruginosa* mainly consisted of random or poly(D-mannuronic acid) block structures while being highly acetylated (Sherbrock-Cox et al. 1984). Between 1985 and 1987, bacterial alginate was profoundly studied in the context of bacterial pathogenesis. In this regard, serial investigations demonstrated alginate binding to the surface of epithelial cells, and structural diversity in *P. aeruginosa* alginates was thought to be important for this binding (McEachran and Irvin 1985; Ramphal and Pier 1985; Doig et al. 1987).

Studies on the genetic background of alginate production and mucoid strains date back to 1966, when Doggett et al. understood that the mucoid phenotype of *P. aeruginosa* associated with the CF lung emerges from nonmucoid forms and becomes the predominant population during infection over time (Doggett et al. 1966). Later, others showed that mucoid and nonmucoid strains are the variants of the same strain (Diaz et al. 1970; Williams and Govan 1973). Between 1975 and 1978, various explanations were provided for genetic background of alginate production, and some suggested that the ability of alginate production is transferrable between strains of *P. aeruginosa* via conjugation (Govan 1976; Fyfe and Govan 1978). In 1980, Fyfe and Govan reported that at least one chromosomal locus is involved in alginate production by bacteria (Fyfe and Govan 1980) followed by introducing chromosomally clustered *Alg* loci (Ohman and Chakrabarty 1981).

13.2 Chemical Structure and Physiochemical Properties of the Alginates

Alginates are unbranched anionic polysaccharides produced by brown seaweeds and bacteria belonging to *Pseudomonas* and *Azotobacter* genera. Uronic acid residues including β-D-mannuronic acid (M) and its C5 epimer α-L-guluronic acid (G) build up alginate polymer via 1, 4-glycosidic bonds (Fig. 13.1). In nature, alginates are

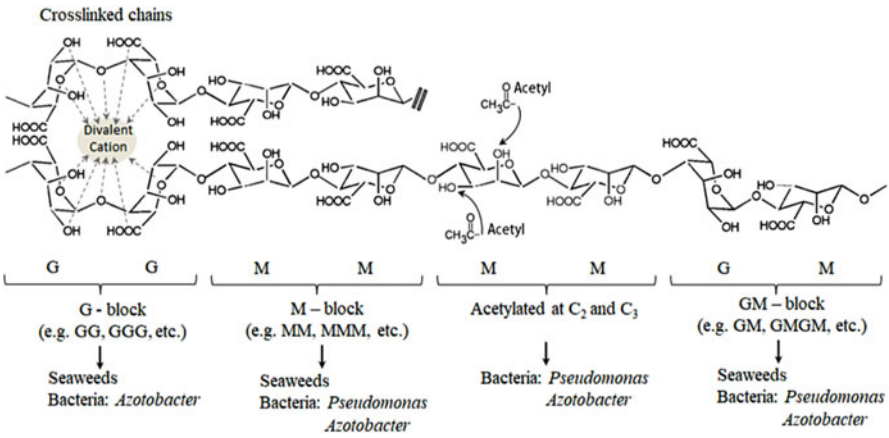

Fig. 13.1 Chemical composition and natural occurrence of various alginates produced by seaweeds and bacteria. Alginate chains efficiently and selectively bind different divalent cations resulting in cross-linked polymeric scaffold and hydrogel formation (Haug and Smidsrod 1970)

usually found in heteropolymeric forms containing variable numbers and lengths of M blocks, G blocks, MG blocks, and non-acetylated and acetylated residues (Rehm and Valla 1997; Douthit et al. 2005; Remminghorst and Rehm 2006b; Moradali et al. 2015) (Fig. 13.1). Algal alginates are non-acetylated chains, while bacterial alginates have been found highly acetylated (Skjåk-Bræk et al. 1989). The occurrence of G blocks in algal alginates is common, while *Pseudomonas* alginates lack G blocks contrary to *Azotobacter* alginates (Gimmestad et al. 2009; Hay et al. 2014; Peteiro 2018; Moradali et al. 2018).

Like other polymeric substances, physiochemical properties of the alginates are determined by their composition and molecular mass (Rehm 2010). Alginates were found to exhibit viscoelastic properties (Webber and Shull 2004; Moresi et al. 2004; Moradali et al. 2015). Furthermore, the most important feature of alginates is their ability to efficiently and selectively bind divalent cations, leading to the formation of hydrogels and cross-linked polymeric scaffolds (Mørch et al. 2006) (Fig. 13.1). The intrinsic flexibility of alginates depends on the frequency of constituting blocks as flexibility decreases in the order MG block > MM block > GG block (Meng and Liu 2013; Moradali et al. 2018). The affinity of alginates toward different divalent ions was found to increase in the order $Mg^{2+} << Mn^{2+} < Ca^{2+} < Sr^{2+} < Ba^{2+} < Cu^{2+} < Pb^{2+}$; however, the strength, dimension, stability, and mechanical properties of resulting hydrogels differ based on the type of interacting cation, the G content, and the variability of G blocks in polymers (Haug and Smidsrod 1967, 1970; Ouwerx et al. 1998; Sikorski et al. 2007).

The acetylation of alginates occurring as *O*-acetyl groups notably changes the properties of the alginates by impacting polymer conformation, chain expansion, solubility, water-binding capacity, viscoelasticity, and molecular mass (Moradali et al. 2015). An acetylated alginate absorbs more water due to the better interaction

of side chains with water molecules, leading to chain expansion and better solubility (Delben et al. 1982; Skjåk-Bræk et al. 1989; Straatmann et al. 2004).

13.3 Alginates in Bacterial Biofilms

Biofilms are defined as cellular aggregations surrounded by self-produced polymeric substances and exist as both monospecies and polyspecies cellular communities in a variety of habitats (Costerton et al. 1987; Høiby 2017) (Fig. 13.2). Indeed, adopting the biofilm lifestyle versus planktonic (freestyle) mode provides a survival advantage by which the microorganism can thrive in harsh conditions, stresses, antibiotic treatments, and the immune system (Costerton 1999; Mah and O'Toole 2001; Stewart and William Costerton 2001). Therefore, eradicating biofilms remains a challenge, and a much higher concentration of a killing agent is required to kill biofilm cells compared to planktonic cells (Lewis 2001; Mah and O'Toole 2001; Davies 2003).

P. aeruginosa is a well-known biofilm former as well as a well-studied alginate producer. It is an opportunistic human pathogen affecting immunocompromised patients and the leading cause of morbidity and mortality in CF patients (Moradali et al. 2017a). Extracellular polymeric substances including polysaccharides, proteins, extracellular DNA (eDNA), and lipids entangle within the biofilm matrix, which is a niche rendering bacteria for intense cell-cell interaction and communication, protecting cells from unfavorable conditions, as well as a reservoir of metabolic substances, nutrients, and energy for fostering growth (Flemming and Wingender 2010; Strempel et al. 2013; Moradali et al. 2017a).

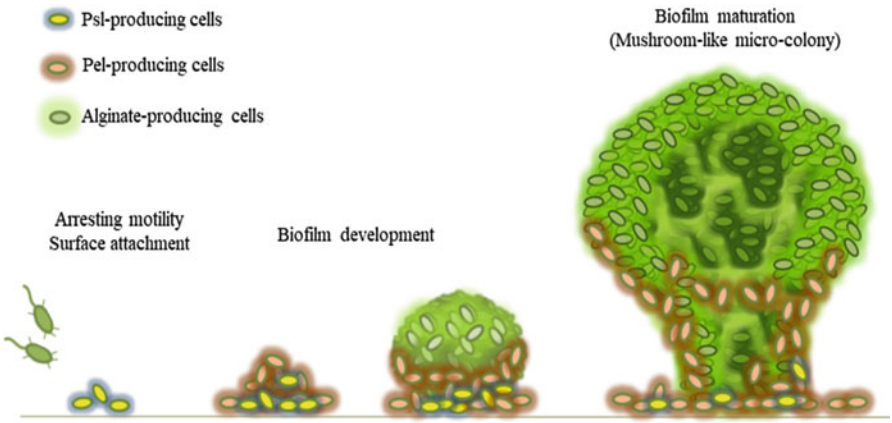

Fig. 13.2 Schematic process of biofilm formation by *P. aeruginosa* with temporal and spatial variation in production of Psl, Pel, and alginate exopolysaccharides (Ghafoor et al. 2011; Colvin et al. 2012; Jennings et al. 2015). To keep the figure simple, each polysaccharide is attributed to distinct cell population

The exopolysaccharides Psl, Pel, and alginate are major constituents of the *P. aeruginosa* biofilm matrix (Fig. 13.2). They are interacting with other small molecules and macromolecules such as rhamnolipid surfactants and eDNA, determining surface adhesion, biofilm initiation, maturation, and architecture (Davey et al. 2003; Ghafoor et al. 2011; Gellatly and Hancock 2013) (Fig. 13.2). While Pel and Psl are the primary structural polysaccharides in the biofilm of both nonmucoid and mucoid *P. aeruginosa* strains, alginate overproduction is responsible for the emerging excessive slimy or mucoid biofilm and predominantly occupies the bio-volume of biofilm matrix (Hentzer et al. 2001; Colvin et al. 2011, 2012; Ghafoor et al. 2011) (Fig. 13.2). The formation of mucoid biofilm by *P. aeruginosa* is the hallmark of chronic infections, and it is indicative of disease progression and long-term persistence (Boucher et al. 1997; Moradali et al. 2017a).

Indeed, the overproduction of alginate confers a highly structured architecture to the biofilms, which comprise microcolonies and so-called mushroom-like structures (Fig. 13.2), while it provides an effective protective layer against opsonophagocytosis, free radicals released from immune cells, and antibiotics used for treatment (Hentzer et al. 2001; Hay et al. 2009a; Strempel et al. 2013).

Likewise, *P. putida* colonizing the rhizosphere of a variety of plants harnesses alginate in combination with other exopolysaccharides in the structure of biofilm. It was demonstrated that alginate production by this species contributes to the formation of highly structured and developed biofilm mediating stress tolerance particularly under water-limiting conditions (Chang et al. 2007). Chang et al. suggested that alginate is produced by pseudomonads in response to water-limiting conditions to reduce the extent of water loss from biofilm residents (Chang et al. 2007). Alginate shields biofilm cells and maintains a hydrated microenvironment protecting cells from desiccation stress (Chang et al. 2007). Another study showed that alginate production by fluorescent pseudomonads was stimulated in response to high osmolarity and dehydration (Singh et al. 1992).

Recently, a study on the soil bacterium *P. alkylphenolia* demonstrated that an alginate-like exopolysaccharide biosynthesis gene cluster is necessary for the formation of biofilm aerial and multicellular structures (Lee et al. 2014). This species has the ability to grow in the presence of linear alkylphenols (C1–C5) (Mulet et al. 2015).

Alginate-like exopolysaccharides were also detected in the gel matrix of aerobic granular sludge and normal aerobic flocculent sludge which are complex microbial consortia. Lin et al. noticed that the granular or granular structures of these sludge particles were impacted by different compositions of the alginate-like exopolysaccharides (Lin et al. 2013). They found that aerobic granules contained significantly higher levels of G blocks and less MG blocks, while those derived from aerobic flocculent sludge had equal amounts of G and MG blocks (Lin et al. 2010, 2013). These sources of hydrogels and alginate-like materials have largely attracted researchers and companies to explore on how to recover and utilize these biopolymers from wastewater sludge (van der Hoek et al. 2016).

Our analysis and others showed that gene clusters homologous to *alg* gene cluster exist in the genomes of a few marine species of the genera *Alcanivorax* and *Marinobacter*, but if they are capable of producing alginates remains controversial (Manilla-Pérez et al. 2010; Lee et al. 2014).

13.4 Biosynthesis of Alginate

Our understanding of alginate biosynthesis is mainly based on the model organism *P. aeruginosa* and to less extend on *A. vinelandii*. For many years, understanding the biosynthesis of alginates has been of great importance for scientific community with regard to drug development for treatment of *P. aeruginosa* infections exacerbated by alginate overproduction as well as establishing the production of bacterial and tailor-made alginates.

Generally, alginate-producing bacteria have the same genetic elements in common for the biosynthesis of the alginates (Fig. 13.3), but they are mainly different at epimerization level and more likely controlling regulatory mechanisms. Genes required for alginate production are mainly clustered in bacterial genome. Except for *algC*, the genetic elements including *algD*, *alg8*, *alg44*, *algK*, *algE* (*algJ*), *algG*, *algX*, *algL*, *algI*, *algJ* (*algV*), *algF*, and *algA* are clustered within the alginate (*alg*) operon (Fig. 12.3).

13.5 Biosynthesis of Alginate Precursor

The best understood part of alginate biosynthesis is the formation of the activated precursor GDP-mannuronic acid. A series of cytosolic enzymatic steps catalyze the formation of precursor (Fig. 13.3). Synthesis starts with the entry of six carbon substrates to the Entner-Doudoroff pathway (KDPG pathway), resulting in pyruvate, which is channeled toward the tricarboxylic acid (TCA) cycle, while oxaloacetate from the TCA cycle can be converted to fructose-6-phosphate via gluconeogenesis. Three alginate-specific enzymes including AlgA (phosphomannose isomerase/GDP-mannose), AlgC (phosphomannomutase), and AlgD (GDP-mannose dehydrogenase) catalyze the four biosynthesis steps to convert fructose-6-phosphate to GDP-mannuronic acid (Chitnis and Ohman 1993; Rehm and Valla 1997; Hay et al. 2014). The final step catalyzed by AlgD is a key step in the control of the alginate pathway because GDP-D-mannose is channeled into this pathway and it is irreversibly converted to the precursor GDP-mannuronic acid, a step before alginate polymerization (Roychoudhury et al. 1989; Tavares et al. 1999) (Fig. 13.3).

13.6 Alginate Polymerization, Modification, and Secretion

In bacteria, alginate polymerization, modifications, and secretion are mediated by a membrane-spanning multiprotein complex in *P. aeruginosa* (Fig. 13.3). Briefly, this multiprotein complex involves (1) alginate-polymerizing unit (Alg8-Alg44); (2) a proposed periplasmic protein scaffold (Alg44-AlgG-AlgX-AlgK) protecting nascent alginate (polymannuronate) against lyase activity of periplasmic AlgL while

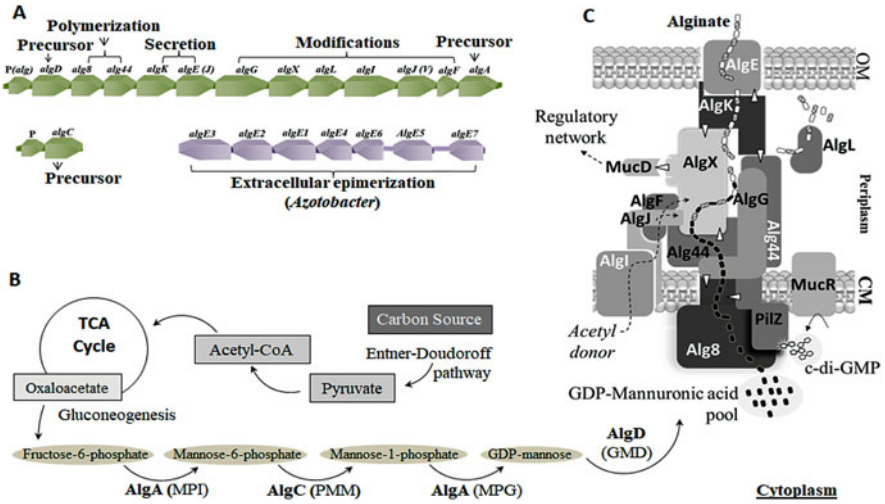

Fig. 13.3 Proposed model of alginate biosynthesis in bacteria. (**a**) Operonic organization of the genes encoding different proteins mediating different steps of alginate biosynthesis (Chitnis and Ohman 1993; Hay et al. 2014). (**b**) Sequential enzymatic events mediating the production of alginate precursor, GDP-mannuronic acid, from fructose-6-phosphate originating from TCA cycle (Narbad et al. 1988; Narbad A. et al. 1990; Rehm and Valla 1997). (**c**) Proposed model for the alginate biosynthesis/modification/secretion machinery complex and experimentally demonstrated protein-protein interactions (marked with white triangles) (Hay et al. 2012; Rehman et al. 2013; Moradali et al. 2015). This model shows alginate production is positively regulated by c-di-GMP binding to Alg44 which targets the catalytic site of Alg8 polymerase for activating the polymerization of alginate. MucR is proposed to specifically provide c-di-GMP pool in proximity of Alg44. Translocation of alginate across the periplasmic scaffold (AlgG/AlgX/AlgF/AlgI/AlgJ/AlgK) is coupled with modification events (i.e., acetylation and epimerization) (Jain et al. 2003; Robles-Price et al. 2004; Moradali et al. 2015). The alginate lyase, AlgL, is responsible for degrading misguided alginate accumulating in the periplasm (Bakkevig et al. 2005; Wang et al. 2016). Secretion of modified alginate is mediated by two interacting proteins AlgK and AlgE (Hay et al. 2010; Rehman et al. 2013). MucD protein links the complex with the posttranslational alginate regulatory network via an interaction with AlgX (Hay et al. 2012). *OM* outer membrane, *CM* cytoplasmic membrane, *P*(*alg*) promoter, *TCA cycle* the tricarboxylic acid cycle, *MPI* mannose-6-phosphate isomerase, *PMM* phosphomannomutase, *MPG* mannose-1-phosphate guanylyltransferase, *GMD* GDP-mannose 6-dehydrogenase

translocating polymer across the periplasm aligned with modifications (i.e., epimerization (AlgG)/acetylation (AlgX)); and (3) secretion unit (AlgK-AlgE) responsible for secreting modified alginate across the outer membrane of bacteria (Hay et al. 2012; Rehman et al. 2013; Moradali et al. 2015, 2018). Other subunits including AlgI, AlgJ, and AlgF have been proposed as taking part in the integrity of periplasmic scaffold, while they were found necessary for the acetylation of alginate probably by providing acetylation precursor for terminal acetyltransferase AlgX (Franklin et al. 2004) (Fig. 13.3).

13.6.1 Polymerization of Alginate

Two interacting membrane-anchored proteins Alg8 (polymerase) and Alg44 (co-polymerase) form the alginate synthase complex catalyzing the formation of polymannuronate chain from activated precursor GDP-mannuronic acid (Fig.13.3). Alg8 is a glycosyltransferase belonging to the glycosyltransferase family 2 that catalyzes the transfer of a sugar molecule from an activated donor, i.e., GDP-mannuronic acid, to an acceptor molecule which is a growing carbohydrate chain. Polymerization mechanism was understood as requiring conformational change of Alg44 upon binding to the second messenger bis-(3′, 5′)-cyclic dimeric guanosine monophosphate (c-di-GMP). In other words, the activation of alginate polymerization is essentially regulated through sensing c-di-GMP at posttranslational level (Remminghorst and Rehm 2006a; Merighi et al. 2007; Oglesby et al. 2008; Remminghorst et al. 2009). Alg44 consists of a cytoplasmic c-di-GMP-sensing PilZ domain, a transmembrane region extending into the periplasm of the bacteria while interacting with other periplasmic subunits (Remminghorst and Rehm 2006a; Oglesby et al. 2008) (Fig. 13.3). Studies based on protein-protein interaction, protein purification, and crystallization proposed that Alg44 is a dimer binding dimeric c-di-GMP toward activating polymerization (Whitney et al. 2015; Moradali et al. 2017b). Our attempt to understand the activation mechanism of alginate polymerization showed that the c-di-GMP binding to Alg44 targets the catalytic sites of Alg8 probably by inducing a conformational change via involving the engagement of some highly conserved amino acid residues of Alg8 at two predicted loops surrounding the catalytic site of Alg8 (Moradali et al. 2017b).

13.6.2 Modification of Alginate

Modification of polymers by producers aims at gaining physicochemical properties corresponding to their biological function in a given environment. Modification of alginate in bacteria comprises epimerization and acetylation of the polymannuronate chain. While enzymatic modifications occur, both AlgG and AlgX as well as likely AlgF/I/J constitute the proposed periplasmic scaffold, which translocates and guides alginate across the periplasm (Fig. 12.3). Upon epimerization of nascent alginate specifically mediated by the periplasmic AlgG epimerase, M residues are converted to G residues, leading to the formation of polyMG alginate (Jain et al. 2003; Gimmestad et al. 2003). Acetylation is mediated by terminal acetyltransferase AlgX by which *O*-acetyl ester linkages are added at the C2 or C3 position of M residues, resulting in acetylated alginates (Franklin and Ohman 2002; Baker et al. 2014) (Figs. 13.1 and 13.3).

Unmodified polymannuronate alginates are fairly a stiff polymer which is probably unfavorable for required flexibility in emerging matrix (Smidsrød et al. 1973). This is due to the nature of di-equatorial linkages of M blocks, while equatorial-axial

bond of MG block increases the flexibility of the chain (Smidsrød et al. 1973). On the other hand, alginate produced by *Pseudomonas* species was found lacking G blocks as AlgG cannot generate two consecutive G residues. The presence of G blocks increases cross-linked chains and gelling properties of alginates in the presence of divalent cations such as Ca^{2+} (Fig. 13.1). The formation of G blocks in *A. vinelandii* alginate is mediated by other types of mannuronan C-5-epimerases of the so-called Ca^{2+}-dependent AlgE-type, which act extracellularly in a Ca^{2+}-dependent manner (Haug and Larsen 1969; Campa et al. 2004; Gimmestad et al. 2006). The G blocks have been commonly found in algal alginates living in the oceans and coastal areas and also within the coat of dormant cysts of *A. vinelandii* known as a nitrogen-fixing and soil bacterium (Clementi 1997; Peteiro 2018). This indicates that this type of modification contributes to tolerating physical and mechanical stresses. The acetylation of bacterial alginate increases the interaction of polymers with water and causes chain expansion (Skjåk-Bræk et al. 1989; Moradali et al. 2015).

Furthermore, we found that alginate polymerization and modifications are linked processes. Using various mutants of *P. aeruginosa* complemented with different combinations of catalytically active and inactive variants of alginate-polymerizing and alginate-modifying genes (i.e., *alg8*, *alg44*, *algG*, and *algX*), we uncovered that AlgG and AlgX had mutually auxiliary role within the multiprotein complex and Alg44 regulates acetylation event beside its association with polymerization step (Moradali et al. 2015, 2017b). In addition, we noticed that the degree of alginate polymerization reflecting the molecular mass is determined by modification events, where the degree of polymerization showed a negative correlation with the degree of epimerization and a positive correlation with the degree of acetylation. Also, we noticed that the epimerization process did interfere with the processivity of alginate polymerization, leading to the formation of shorter chains, while acetylation did not (Moradali et al. 2015). This may explain why alginates produced by *P. aeruginosa* possess much higher molecular mass compared with algal alginates. Hence, this study resulted in the production of various alginates including those chemically characterized as acetylated polyMG, non-acetylated polyMG, acetylated polyM, and non-acetylated polyM.

The impact of resulting various alginates on the development of biofilms was also examined. We found that the biofilm architecture of *P. aeruginosa* and viscoelastic property of alginates were remarkably affected by the various alginates. Generally, viscoelastic property is a key physicochemical parameter to assess the behavior of materials under given condition, and it is determined by measuring solid-like elastic modulus (*G'*) and the liquid-like viscous modulus (*G"*). Our analysis showed that all resulting viscoelastic alginates displayed the solid-like elastic modulus (*G'*) greater than the liquid-like viscous modulus (*G"*), indicating they had greater elasticity than viscosity. We found out that while molecular mass is a key factor to determine viscoelastic property, the influence of the modification of alginates was also a striking determinant. Here, the presence of acetyl groups lowered viscoelasticity by possibly interfering with intermolecular alginate chain interactions. However increasing molar fractions of M blocks and resulting higher molecular masses increased viscoelasticity of the alginates (Moradali et al. 2015). Regarding biofilm

examination, genetically modified *P. aeruginosa* mutants producing merely acetylated alginates formed well-developed biofilms with highly organized heterogeneous architectures through promoted cell aggregations, when compared with those biofilms formed by the mutant producing non-acetylated alginate. As acetylated alginate displayed much lower viscoelasticity than non-acetylated alginate, we concluded that in the course of biofilm formation, acetyl groups of alginates may function as a signal for cell aggregation regardless of low viscoelastic property (Moradali et al. 2015).

Also, resultant alginates without G residues and acetyl groups (i.e., non-acetylated polyM) caused the formation of undeveloped and narrow microcolonies, which were supported by specific long trails or strips of cells emerging from stigmergic self-organization behavior (Moradali et al. 2015).

13.6.2.1 Alginate Lyases

The periplasmic alginate lyase AlgL is encoded within the alginate operon in *P. aeruginosa* (Jain and Ohman 2005) (Fig.13.3). This enzyme belongs to the family of alginate lyases or alginate degrading enzymes which act as either mannuronate or guluronate lyases, but due to their structural diversity, they have not been classified yet (Wong et al. 2000; Ertesvåg 2015). Interestingly, these alginate-modifying enzymes have a wide natural occurrence including in algae (but not brown algae), marine invertebrates, and terrestrial microorganisms (Wong et al. 2000; Ertesvåg 2015). Wide natural distribution of alginate lyases implicate their possible role in digesting alginates for utilizing them as carbon source, while no bacterial alginate producer has been found to be an alginate utilizer. Presumably, in bacteria, alginate lyases play other biological roles. Bacterial AlgL was demonstrated to be essential for degrading misguided alginate trapped in the periplasm, leading to releasing free uronic acid oligomers to avoid the lethal effect of accumulated alginate on cells (Bakkevig et al. 2005) (Fig. 13.3). We showed that AlgL in *P. aeruginosa* is functionally associated with existing alginate biosynthesis/modification/secretion multiprotein complex (Wang et al. 2016). Such a critical role in the biosynthesis of bacterial alginate is well-understood within various bacterial mutants defective in the production of proposed scaffold forming subunits, i.e., AlgK, AlgX, or AlgG, that destabilize the multiprotein complex. Subsequently, the translocation of alginate across bacterial envelope was supposed to be misguided into the periplasm, leading to AlgL-mediated alginate degradation and the production of unsaturated oligouronides (Jain and Ohman 1998; Jain et al. 2003; Gimmestad et al. 2003; Robles-Price et al. 2004) (Fig. 13.3). We demonstrated that chromosomal expression of *algL* in *P. aeruginosa* enhanced alginate *O*-acetylation and both attachment and dispersal stages of the bacterial biofilm lifecycle were sensitive to the level of *O*-acetylation (Wang et al. 2016). Alginate lyases have been attractive and promising to study for developing therapeutics in combination with antibiotics in order to eradicate alginate-based biofilms (Alkawash et al. 2006; Lamppa and Griswold 2013).

13.6.3 Secretion of Alginate

The mechanism of alginate secretion is well-understood in *P. aeruginosa*. Two interacting proteins AlgK and AlgE, respectively, localized in the periplasm and the outer membrane, mediate alginate secretion across the outer membrane (Whitney et al. 2011; Rehman et al. 2013) (Fig. 13.3). AlgE acts selectively for the secretion of the negatively charged alginate polymer upon possessing a highly electropositive pore constriction formed by an arginine-rich channel (Rehm et al. 1994; Hay et al. 2010; Whitney et al. 2011). On the other hand, the lipoprotein AlgK facilitates proper localization of AlgE at the outer membrane (Keiski et al. 2010). This protein possesses a tetratricopeptide repeat (TPR) protein-protein interaction motif possibly mediating the interaction of AlgK with other subunits of the multiprotein complex (Rehman et al. 2013; Moradali et al. 2015) (Fig. 13.3).

13.7 Multitier Regulation of Alginate Biosynthesis

The biosynthesis of bacterial alginate is under the control of a complex regulatory network acting at transcriptional, posttranscriptional, and posttranslational levels (Hay et al. 2014) (Fig. 13.4). At transcriptional level, the alternate sigma factor AlgU (previously called AlgT or σ22) plays as the master regulator of alginate biosynthesis, which positively acts on *algD* promoter. AlgU belongs to the extracytoplasmic function (ECF) family of sigma factors, which are known to be involved in conferring resistance to a wide range of envelope stresses. Recently, it is understood that stimulation of AlgU for cell envelope homeostasis overlaps with controlling pathways for biofilm formation (Wood and Ohman 2012). Under uninduced condition, the anti-sigma factor MucA protein binds to AlgU at the inner membrane and sequesters its activity (Fig. 13.4). The genes encoding AlgU and MucA are clustered with other important chromosomal genes including *mucB*, *mucC*, and *mucD*, and this operon is known as the switch locus for alginate biosynthesis. Multiple studies showed that mutations in this operon are frequent among clinical strains of *P. aeruginosa* leading to the inactivation of MucA. Consequently, AlgU activates the expression of the *alg* operon (Fig. 13.4) and its own operon (Boucher et al. 1997; Firoved et al. 2002). It also activates the expression of several other genes involved in alginate biosynthesis and regulation such as *algR*, *algB*, *algD*, *algC*, and *amrZ* (Boucher et al. 1997; Mathee et al. 1999; Firoved et al. 2002; Wozniak et al. 2003; Muhammadi and Ahmed 2007).

On the other hand, MucA is protected by the periplasmic protein MucB from proteolysis triggered via regulated intramembrane proteolysis (RIP). The RIP signaling cascade involves several proteases and proteolytic events activated by envelope stresses negatively affecting localization or folding of the membrane proteins. The degradation of periplasmic domain of MucA via the RIP cascade and the subsequent release of AlgU represent another regulatory layer of alginate

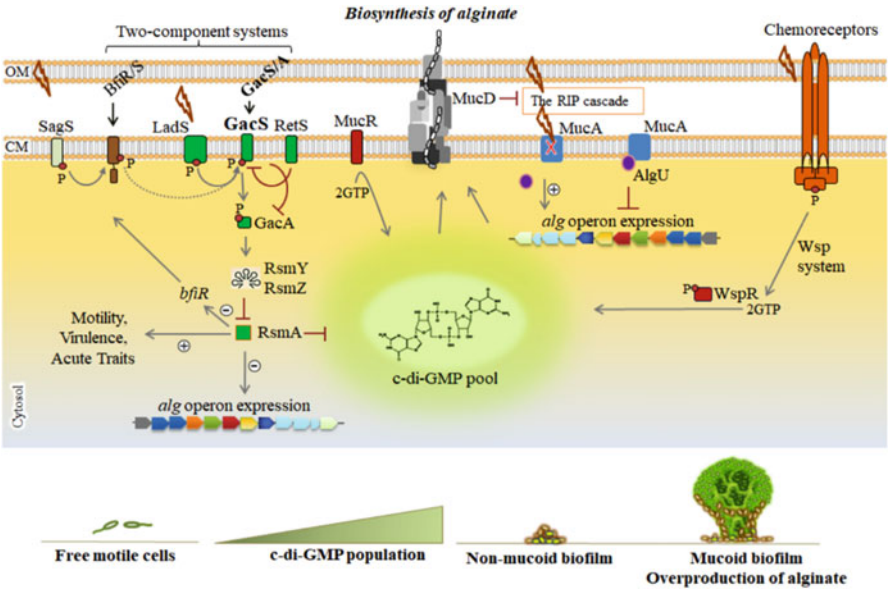

Fig. 13.4 Schematic major regulatory networks controlling the biosynthesis of alginate and biofilm formation by *P. aeruginosa*. Key determinants for alginate biosynthesis and overproduction of alginate include elevation of c-di-GMP and releasing AlgU sigma factor as a result of inactivation of MucA (blue rectangle with red cross) by either genetic mutation or proteolysis via the RIP cascade (Boucher et al. 1997; Firoved et al. 2002; Remminghorst and Rehm 2006a; Wood and Ohman 2012; Moradali et al. 2017b). The RIP cascade is thought to be negatively regulated by MucD which also interacts with the alginate biosynthesis multiprotein complex (Damron and Yu 2011). Various proteins localized in the envelope of the cells where these proteins form two-component systems (brown/green rectangles), chemoreceptor-like system (orange complex) and other protein networks sense environmental cues (Moradali et al. 2017a). Either triggered as phosphorylation cascades (small red circle labelled with "P") or protein-protein interactions, the signals induce diguanylate cyclases (containing GGDEF motif) such as WspR and MucR to synthesize c-di-GMP from two molecules of GTP (guanosine-5′-triphosphate) (Güvener and Harwood 2007; Hay et al. 2009b). Consequently, c-di-GMP-sensing proteins such as Alg44 act as receptor/effector for specific outputs such as induction of alginate and Pel polymerization, inhibition of motility and derepression of psl/pel expression via FleQ protein, induction of attachment, and biofilm formation/maturation (Lee et al. 2007; Baraquet et al. 2012; Li et al. 2012; Moradali et al. 2017b). Gray arrows indicate inductive effect of proteins or molecules, and red blunt headed arrows indicate suppressive effects. The two-component systems are interconnected, and the LadS/RetS/GacS/GacA/RsmA regulatory network (green rectangles) plays a key role in phenotypic switch from motility to biofilm (Brencic et al. 2009; Chambonnier et al. 2016). *RIP* regulated intramembrane proteolysis, *OM* outer membrane, *CM* cytoplasmic membrane

overproduction in response to inducing stresses (Alba et al. 2002; Qiu et al. 2007; Cezairliyan and Sauer 2009; Wood and Ohman 2009) (Fig. 13.4).

It was shown that the alginate biosynthesis multiprotein complex links to the RIP cascade via a periplasmic serine protease and chaperone-like protein called MucD which forms a complex with AlgX (Hay et al. 2012). MucD was proposed to

negatively regulate the RIP cascade by chaperoning and/or degrading misfolded membrane proteins that would otherwise activate the RIP cascade (Fig. 13.4). One study proposed that MucD may be sequestered by stable alginate biosynthesis multiprotein complex, while induced destabilization in the protein complex results in releasing MucD from it (Yorgey et al. 2001; Qiu et al. 2007; Damron and Yu 2011; Hay et al. 2012).

Studying clinical isolates of *P. aeruginosa* with mucoid phenotype unraveled another regulatory pathway for the overproduction of alginate via mutations in the *mucA* gene which seems frequently observed in these strains. Resulting defective MucA is readily prone to proteolytic degradation as its defective periplasmic domain cannot interact with MucB for being protected, leading to AlgU release (Reiling et al. 2005; Hay et al. 2014). The mutation of *mucA* is one of the key adaptive mutations in regulatory genes which occur during proposed adaptive radiation of *P. aeruginosa* over the course of persistent infections in CF patients. By definition, during adaptive radiation initial infecting strains diversify into a variety of genotypes and phenotypes over time until the most favorable and adapted descendants are selected for long-term persistence. Hence, biofilm formation, alginate overproduction, and mucoid phenotype are part of this phenotypic adaptation process (Higgins et al. 2003; Hogardt and Heesemann 2010, 2013; Rau et al. 2010; Winstanley et al. 2016).

The regulation of alginate biosynthesis at transcriptional level via AlgU activity and the regulation of *algD* promoter overlap or link with other regulatory pathways mainly based on other sigma factors. Hay et al. provided a comprehensive overview on these interconnected regulatory pathways at transcriptional level (Hay et al. 2014).

At posttranscriptional level, a complex regulatory system consists of RsmA/Y/Z complex controls alginate biosynthesis (Fig. 13.4). RsmA is considered as a global regulator acting upon binding to mRNAs and negatively controls biofilm formation pathways such as via inhibition of the elevation of c-di-GMP levels (Irie et al. 2010; Jimenez et al. 2012). Two noncoding RNAs, RsmY and RsmZ, bind to RsmA and counteract its translational repression activity, consequently derepressing the translation of the genes such as involved in biofilm formation, increasing c-di-GMP level, and exopolysaccharides production (Fig. 13.4). This signaling pathway is also under the control of the GacS/A two-component system where in response to external stimuli, a phosphorylated GacA directly induces the synthesis of RsmY and RsmZ noncoding RNAs (Bhagirath et al. 2017; Allsopp et al. 2017; Li et al. 2017) (Fig. 12.4). However, the regulation of alginate biosynthesis at posttranscriptional level is not limited to this RsmA/Y/Z and GacS/A pathways as recently it was shown that AlgU and also AlgR from the two-component transcriptional regulator AlgZ/R control RsmA synthesis, alginate biosynthesis, and several other genes (Stacey et al. 2017).

At posttranslational level, c-di-GMP is a key signal in the regulation of biofilm formation by which timely expression of many genes is controlled (Fig. 13.4). This ubiquitous second messenger present in a wide range of bacteria and principally controls motility-biofilm switch (Römling et al. 2013; Moradali et al. 2017a). Indeed, the cellular level of c-di-GMP is the major determinant for this substantial phenotypic alteration, so that its elevation triggers biofilm formation while inhibiting

motility. At least 40 enzymes directly synthesize and/or degrade c-di-GMP in *P. aeruginosa* which controls cellular level of this small molecule in response to perceived stimuli (Ryan et al. 2006). Previously, we demonstrated that alginate polymerization is impacted by cellular level of c-di-GMP via binding to Alg44 (Moradali et al. 2017b). One particular c-di-GMP-synthesizing protein, MucR, was demonstrated to specifically enhance the level of alginate production in *P. aeruginosa*, presumably by generating a localized c-di-GMP pool in proximity to the alginate polymerase (Hay et al. 2009b; Moradali et al. 2015, 2017b; Wang et al. 2015) (Fig. 12.4). Likewise, there are many other c-di-GMP receptor proteins which act as effectors for enhancing required pathways for biofilm formation including the production of alginate, Pel, and Psl while they inhibit the expression of motility-relevant genes such as those involved in flagella biosynthesis (Baraquet et al. 2012; Moradali et al. 2017a) (Fig. 13.4).

13.8 Concluding Remarks

Studying biopolymers constituting the biofilm matrix has gained substantial attention for many years. For more than a century, algal alginates have been of particular interests primarily for their unique physicochemical properties and wide industrial applications. However, the discovery of alginates in mucoid strains of *P. aeruginosa* and its direct impact on the development of chronic respiratory infections have further increased their importance for human affairs. In contrast to algal alginates, many aspects of the biosynthesis of bacterial alginates have now been unraveled. It is now well-known that microbial communities, either medically or environmentally relevant, harness specific material properties of alginates in response to their environment. Although much has been learned about physicochemical properties, applications, and the biosynthesis of alginates over the last few decades, there are still several key questions mainly about cognate multitier regulation and cross talks among various cellular regulators involved in alginate biosynthesis. In addition, persistent alginate-based biofilms in chronic respiratory infections are still a huge challenge for clinical settings and therapeutic development.

Reporting alginate-like polysaccharides surrounding microbial consortia in recent studies indicated that there are still many possibilities for discovering novel alginates and novel producers in different habitats. Studying novel alginate-producing bacteria from different habitats and comparing cognate regulatory networks would shed light on how environmental cues stimulate the production of various alginates by the bacterial community. On the other hand, understanding molecular mechanisms driving alginate biosynthesis in bacteria would establish a foundation for possible biotechnological production of tailor-made alginates as well as develop therapeutics to interfere with the formation of pathogenic alginate-based biofilms.

Acknowledgments The authors are grateful to the current and former member of the Rehm research group for their invaluable contributions providing insights into alginate biosynthesis in bacteria.

References

Alba BM, Leeds JA, Onufryk C, Lu CZ, Gross CA (2002) DegS and YaeL participate sequentially in the cleavage of RseA to activate the $\sigma^{(E)}$-dependent extracytoplasmic stress response. Genes Dev 16:2156–2168

Alkawash MA, Soothill JS, Schiller NL (2006) Alginate lyase enhances antibiotic killing of mucoid *Pseudomonas aeruginosa* in biofilms. APMIS 114:131–138

Allsopp LP, Wood TE, Howard SA, Maggiorelli F, Nolan LM, Wettstadt S, Filloux A (2017) RsmA and AmrZ orchestrate the assembly of all three type VI secretion systems in *Pseudomonas aeruginosa*. Proc Natl Acad Sci USA 114:7707–7712

Baker P, Ricer T, Moynihan PJ, Kitova EN, Walvoort MT, Little DJ, Whitney JC, Dawson K, Weadge JT, Robinson H, Ohman DE, Codée JD, Klassen JS, Clarke AJ, Howell PL (2014) *P. aeruginosa* SGNH hydrolase-like proteins AlgJ and AlgX have similar topology but separate and distinct roles in alginate acetylation. PLoS Pathog 10(8):e1004334

Bakkevig K, Sletta H, Gimmestad M, Aune R, Ertesvåg H, Degnes K, Christensen BE, Ellingsen TE, Valla S (2005) Role of the *Pseudomonas fluorescens* alginate lyase (AlgL) in clearing the periplasm of alginates not exported to the extracellular environment. J Bacteriol 187:8375–8384

Baraquet C, Murakami K, Parsek MR, Harwood CS (2012) The FleQ protein from *Pseudomonas aeruginosa* functions as both a repressor and an activator to control gene expression from the *pel* operon promoter in response to c-di-GMP. Nucleic Acids Res 40:7207–7218

Bhagirath AY, Somayajula D, Li Y, Duan K (2017) CmpX affects virulence in *Pseudomonas aeruginosa* through the Gac/Rsm signaling pathway and by modulating c-di-GMP levels. J Membr Biol 251(1):35–49

Boucher JC, Yu H, Mudd MH, Deretic V (1997) Mucoid *Pseudomonas aeruginosa* in cystic fibrosis: characterization of *muc* mutations in clinical isolates and analysis of clearance in a mouse model of respiratory infection. Infect Immun 65:3838–3846

Brencic A, McFarland KA, McManus HR, Castang S, Mogno I, Dove SL, Lory S (2009) The GacS/GacA signal transduction system of *Pseudomonas aeruginosa* acts exclusively through its control over the transcription of the RsmY and RsmZ regulatory small RNAs. Mol Microbiol 73:434–445

Campa C, Holtan S, Nilsen N, Bjerkan TM, Stokke BT, Skjåk-Braek G (2004) Biochemical analysis of the processive mechanism for epimerization of alginate by mannuronan C-5 epimerase AlgE4. Biochem J 381:155–164

Cezairliyan BO, Sauer RT (2009) Control of *P. aeruginosa* AlgW protease cleavage of MucA by peptide signals and MucB. Mol Microbiol 72:368–379

Chambonnier G, Roux L, Redelberger D, Fadel F, Filloux A, Sivaneson M, de Bentzmann S, Bordi C (2016) The hybrid histidine kinase LadS forms a multicomponent signal transduction system with the GacS/GacA two-component system in *Pseudomonas aeruginosa*. PLoS Genet 12(5): e1006032

Chang W-S, van de Mortel M, Nielsen L, Nino de Guzman G, Li X, Halverson LJ (2007) Alginate production by *Pseudomonas putida* creates a hydrated microenvironment and contributes to biofilm architecture and stress tolerance under water-limiting conditions. J Bacteriol 189:8290–8299

Chitnis CE, Ohman DE (1993) Genetic analysis of the alginate biosynthetic gene cluster of *Pseudomonas aeruginosa* shows evidence of an operonic structure. Mol Microbiol 8:583–593

Clementi F (1997) Alginate production by *Azotobacter Vinelandii*. Crit Rev Biotechnol 17:327–361

Colvin KM, Gordon VD, Murakami K, Borlee BR, Wozniak DJ, Wong GCL, Parsek MR (2011) The Pel polysaccharide can serve a structural and protective role in the biofilm matrix of *Pseudomonas aeruginosa*. PLoS Pathog 7(1):e1001264

Colvin KM, Irie Y, Tart CS, Urbano R, Whitney JC, Ryder C, Howell PL, Wozniak DJ, Parsek MR (2012) The Pel and Psl polysaccharides provide *Pseudomonas aeruginosa* structural redundancy within the biofilm matrix. Environ Microbiol 14:1913–1928

Costerton JW (1999) Introduction to biofilm. Int J Antimicrob Agents 11:217–221

Costerton JW, Cheng KJ, Geesey GG, Ladd TI, Nickel JC, Dasgupta M, Marrie TJ (1987) Bacterial biofilms in nature and disease. Annu Rev Microbiol 41:435–464

Damron FH, Yu HD (2011) *Pseudomonas aeruginosa* MucD regulates the alginate pathway through activation of MucA degradation via MucP proteolytic activity. J Bacteriol 193:286–291

Davey ME, Caiazza NC, O'Toole GA (2003) Rhamnolipid surfactant production affects biofilm architecture in *Pseudomonas aeruginosa* PAO1. J Bacteriol 185:1027–1036

Davies D (2003) Understanding biofilm resistance to antibacterial agents. Nat Rev Drug Discov 2:114

Delben F, Cesaro À, Paoletti S, Crescenzi V (1982) Monomer composition and acetyl content as main determinants of the ionization behavior of alginates. Carbohydr Res 100:C46–C50

Diaz E, Mosovich LL, Neter E (1970) Serogroups of *Pseudomonas aeruginosa* and the immune response of patients with cystic fibrosis. J Infect Dis 121:269–274

Doggett RG (1969) Incidence of mucoid *Pseudomonas aeruginosa* from clinical sources. Appl Microbiol 18:936–937

Doggett RG, Harrison GM, Stillwell NR, Wallis ES (1966) An atypical *Pseudomonas aeruginosa* associated with cystic fibrosis of the pancreas. J Pediatr 68:215–221

Doig P, Smith NR, Todd T, Irvin RT (1987) Characterization of the binding of *Pseudomonas aeruginosa* alginate to human epithelial cells. Infect Immun 55:1517–1522

Douthit SA, Dlakic M, Ohman DE, Franklin MJ (2005) Epimerase active domain of *Pseudomonas aeruginosa* AlgG, a protein that contains a right-handed beta-helix. J Bacteriol 187:4573–4583

Elston HR, Hoffman KC (1967) Increasing incidence of encapsulated *Pseudomonas aeruginosa* strains. Am J Clin Pathol 48:519–523

Ertesvåg H (2015) Alginate-modifying enzymes: biological roles and biotechnological uses. Front Microbiol 6:523. https://doi.org/10.3389/fmicb.2015.00523

Evans LR, Linker A (1973) Production and characterization of the slime polysaccharide of *Pseudomonas aeruginosa*. J Bacteriol 116:915–924

Firoved AM, Boucher JC, Deretic V (2002) Global genomic analysis of AlgU (ςsgr;(E))-dependent promoters (sigmulon) in *Pseudomonas aeruginosa* and implications for inflammatory processes in cystic fibrosis. J Bacteriol 184:1057–1064

Flemming H-C, Wingender J (2010) The biofilm matrix. Nat Rev Microbiol 8:623–633

Franklin MJ, Ohman DE (2002) Mutant analysis and cellular localization of the AlgI, AlgJ, and AlgF proteins required for O acetylation of alginate in *Pseudomonas aeruginosa*. J Bacteriol 184:3000–3007

Franklin MJ, Douthit SA, McClure MA (2004) Evidence that the algI/algJ gene cassette, required for O acetylation of *Pseudomonas aeruginosa* alginate, evolved by lateral gene transfer. J Bacteriol 186:4759–4773

Fyfe JAM, Govan JRW (1978) A genetic approach to the study of mucoid *Pseudomonas aeruginosa*. Proc Soc Gen Microbiol 5:54

Fyfe JA, Govan JR (1980) Alginate synthesis in mucoid *Pseudomonas aeruginosa*: a chromosomal locus involved in control. J Gen Microbiol 119:443–450

Gellatly SL, Hancock REW (2013) *Pseudomonas aeruginosa*: new insights into pathogenesis and host defenses. Pathog Dis 67:159–173

Ghafoor A, Hay ID, Rehm BHA (2011) Role of exopolysaccharides in *Pseudomonas aeruginosa* biofilm formation and architecture. Appl Environ Microbiol 77:5238–5246

Gimmestad M, Sletta H, Ertesvåg H, Bakkevig K, Jain S, Suh S-j, Skjåk-Bræk G, Ellingsen TE, Ohman DE, Valla S (2003) The *Pseudomonas fluorescens* AlgG protein, but not its mannuronan C-5-epimerase activity, is needed for alginate polymer formation. J Bacteriol 185:3515–3523

Gimmestad M, Steigedal M, Ertesvåg H, Moreno S, Christensen BE, Espín G, Valla S (2006) Identification and characterization of an *Azotobacter vinelandii* type I secretion system responsible for export of the AlgE-type mannuronan C-5-epimerases. J Bacteriol 188:5551–5560

Gimmestad M, Ertesvåg H, Heggeset TM, Aarstad O, Svanem BI, Valla S (2009) Characterization of three new *Azotobacter vinelandii* alginate lyases, one of which is involved in cyst germination. J Bacteriol 191:4845–4853

Gorin P, Spencer J (1966) Exocellular alginic acid from *Azotobacter vinelandii*. Can J Chem 44:993–998

Govan JRW (1976) Genetic studies on mucoid *Pseudomonas aeruginosa*. Proc Soc Gen Microbiol 3:187

Govan JR, Fyfe JA, Jarman TR (1981) Isolation of alginate-producing mutants of *Pseudomonas fluorescens*, *Pseudomonas putida* and *Pseudomonas mendocina*. J Gen Microbiol 125:217–220

Güvener ZT, Harwood CS (2007) Subcellular location characteristics of the *Pseudomonas aeruginosa* GGDEF protein, WspR, indicate that it produces cyclic-di-GMP in response to growth on surfaces. Mol Microbiol 66:1459–1473

Haug A, Smidsrod O (1967) Strontium–calcium selectivity of alginates. Nature 215:757

Haug A, Larsen B (1969) Biosynthesis of alginate. Epimerisation of D-mannuronic to L-guluronic acid residues in the polymer chain. Biochim Biophys Acta 192:557–559

Haug A, Smidsrod O (1970) Selectivity of some anionic polymers for divalent metal ions. Acta Chem Scand 24:843–854

Hay ID, Gatland K, Campisano A, Jordens JZ, Rehm BHA (2009a) Impact of alginate overproduction on attachment and biofilm architecture of a supermucoid *Pseudomonas aeruginosa* strain. Appl Environ Microbiol 75:6022–6025

Hay ID, Remminghorst U, Rehm BH (2009b) MucR, a novel membrane-associated regulator of alginate biosynthesis in *Pseudomonas aeruginosa*. Appl Environ Microbiol 75:1110–1120

Hay ID, Rehman ZU, Rehm BH (2010) Membrane topology of outer membrane protein AlgE, which is required for alginate production in *Pseudomonas aeruginosa*. Appl Environ Microbiol 76:1806–1812

Hay ID, Schmidt O, Filitcheva J, Rehm BH (2012) Identification of a periplasmic AlgK-AlgX-MucD multiprotein complex in *Pseudomonas aeruginosa* involved in biosynthesis and regulation of alginate. Appl Microbiol Biotechnol 93:215–227

Hay ID, Wang Y, Moradali MF, Rehman ZU, Rehm BH (2014) Genetics and regulation of bacterial alginate production. Environ Microbiol 16:2997–3011

Hentzer M, Teitzel GM, Balzer GJ, Heydorn A, Molin S, Givskov M, Parsek MR (2001) Alginate overproduction affects *Pseudomonas aeruginosa* biofilm structure and function. J Bacteriol 183:5395–5401

Higgins PG, Fluit AC, Milatovic D, Verhoef J, Schmitz FJ (2003) Mutations in GyrA, ParC, MexR and NfxB in clinical isolates of *Pseudomonas aeruginosa*. Int J Antimicrob Agents 21:409–413

Hogardt M, Heesemann J (2010) Adaptation of *Pseudomonas aeruginosa* during persistence in the cystic fibrosis lung. Int J Med Microbiol 300:557–562

Hogardt M, Heesemann J (2013) Microevolution of *Pseudomonas aeruginosa* to a chronic pathogen of the cystic fibrosis lung. Curr Top Microbiol Immunol 358:91–118

Høiby N (2017) A short history of microbial biofilms and biofilm infections. APMIS 125:272–275

Irie Y, Starkey M, Edwards AN, Wozniak DJ, Romeo T, Parsek MR (2010) *Pseudomonas aeruginosa* biofilm matrix polysaccharide Psl is regulated transcriptionally by RpoS and post-transcriptionally by RsmA. Mol Microbiol 78:158–172

Jain S, Ohman DE (1998) Deletion of *algK* in mucoid *Pseudomonas aeruginosa* blocks alginate polymer formation and results in uronic acid secretion. J Bacteriol 180:634–641

Jain S, Ohman DE (2005) Role of an alginate lyase for alginate transport in mucoid *Pseudomonas aeruginosa*. Infect Immun 73:6429–6436

Jain S, Franklin MJ, Ertesvåg H, Valla S, Ohman DE (2003) The dual roles of AlgG in C-5-epimerization and secretion of alginate polymers in *Pseudomonas aeruginosa*. Mol Microbiol 47:1123–1133

Jennings LK, Storek KM, Ledvina HE, Coulon C, Marmont LS, Sadovskaya I, Secor PR, Tseng BS, Scian M, Filloux A, Wozniak DJ, Howell PL, Parsek MR (2015) Pel is a cationic exopolysaccharide that cross-links extracellular DNA in the *Pseudomonas aeruginosa* biofilm matrix. Proc Natl Acad Sci USA 112:11353–11358

Jimenez PN, Koch G, Thompson JA, Xavier KB, Cool RH, Quax WJ (2012) The multiple signaling systems regulating virulence in *Pseudomonas aeruginosa*. Microbiol Mol Biol Rev 76:46–65

Keiski CL, Harwich M, Jain S, Neculai AM, Yip P, Robinson H, Whitney JC, Riley L, Burrows LL, Ohman DE, Howell PL (2010) AlgK is a TPR-containing protein and the periplasmic component of a novel exopolysaccharide secretin. Structure 18:265–273

Lamppa JW, Griswold KE (2013) Alginate lyase exhibits catalysis-independent biofilm dispersion and antibiotic synergy. Antimicrob Agents Chemother 57:137–145

Lee VT, Matewish JM, Kessler JL, Hyodo M, Hayakawa Y, Lory S (2007) A cyclic-di-GMP receptor required for bacterial exopolysaccharide production. Mol Microbiol 65:1474–1484

Lee K, Lim EJ, Kim KS, Huang S-L, Veeranagouda Y, Rehm BHA (2014) An alginate-like exopolysaccharide biosynthesis gene cluster involved in biofilm aerial structure formation by *Pseudomonas alkylphenolia*. Appl Microbiol Biotechnol 98:4137–4148

Lewis K (2001) Riddle of biofilm resistance. Antimicrob Agents Chemother 45:999–1007

Li K, Yang G, Debru AB, Li P, Zong L, Xu T, Wu W, Jin S, Bao Q (2017) SuhB regulates the motile-sessile switch in *Pseudomonas aeruginosa* through the Gac/Rsm pathway and c-di-GMP signaling. Front Microbiol 8:1045. https://doi.org/10.3389/fmicb.2017.01045

Li Z, Chen JH, Hao Y, Nair SK (2012) Structures of the PelD cyclic diguanylate effector involved in pellicle formation in *Pseudomonas aeruginosa* PAO1. J Biol Chem 287:30191–30204

Lin Y, de Kreuk M, van Loosdrecht MCM, Adin A (2010) Characterization of alginate-like exopolysaccharides isolated from aerobic granular sludge in pilot-plant. Water Res 44:3355–3364

Lin YM, Sharma PK, van Loosdrecht MCM (2013) The chemical and mechanical differences between alginate-like exopolysaccharides isolated from aerobic flocculent sludge and aerobic granular sludge. Water Res 47:57–65

Linker A, Jones RS (1964) A polysaccharide resembling alginic acid from a *Pseudomonas* microorganism. Nature 204:187–188

Linker A, Jones RS (1966) A new polysaccharide resembling alginic acid isolated from pseudomonads. J Biol Chem 241:3845–3851

Mah T-FC, O'Toole GA (2001) Mechanisms of biofilm resistance to antimicrobial agents. Trends Microbiol 9:34–39

Manilla-Pérez E, Reers C, Baumgart M, Hetzler S, Reichelt R, Malkus U, Kalscheuer R, Wältermann M, Steinbüchel A (2010) Analysis of lipid export in hydrocarbonoclastic bacteria of the genus *Alcanivorax*: identification of lipid export-negative mutants of *Alcanivorax borkumensis* SK2 and *Alcanivorax jadensis* T9. J Bacteriol 192:643–656

Mathee K, Ciofu O, Sternberg C, Lindum PW, Campbell JI, Jensen P, Johnsen AH, Givskov M, Ohman DE, Molin S, Høiby N, Kharazmi A (1999) Mucoid conversion of *Pseudomonas aeruginosa* by hydrogen peroxide: a mechanism for virulence activation in the cystic fibrosis lung. Microbiology 145:1349–1357

McEachran DW, Irvin RT (1985) Adhesion of *Pseudomonas aeruginosa* to human buccal epithelial cells: evidence for two classes of receptors. Can J Microbiol 31:563–569

Meng S, Liu Y (2013) Alginate block fractions and their effects on membrane fouling. Water Res 47:6618–6627

Merighi MT, Lee V, Hyodo M, Hayakawa Y, Lory S (2007) The second messenger bis-(3′-5′)-cyclic-GMP and its PilZ domain-containing receptor Alg44 are required for alginate biosynthesis in *Pseudomonas aeruginosa*. Mol Microbiol 65:876–895

Moradali FM, Donati I, Sims IM, Ghods S, Rehm BH (2015) Alginate polymerization and modification are linked in *Pseudomonas aeruginosa*. MBio 6(3):e00453–e00415

Moradali MF, Ghods S, Rehm BH (2017a) *Pseudomonas aeruginosa* lifestyle: a paradigm for adaptation, survival, and persistence. Front Cell Infect Microbiol 7:39. https://doi.org/10.3389

Moradali MF, Ghods S, Rehm BHA (2017b) Activation mechanism and cellular localization of membrane-anchored alginate polymerase in *Pseudomonas aeruginosa*. Appl Environ Microbiol 83(9):e03499–e03416

Moradali MF, Ghods S, Rehm BHA (2018) Alginate biosynthesis and biotechnological production. In: Rehm BHA, Moradali MF (eds) Alginates and their biomedical applications. Springer series in biomaterials science and engineering, vol 11. Springer, Singapore

Moresi M, Bruno M, Parente E (2004) Viscoelastic properties of microbial alginate gels by oscillatory dynamic tests. J Food Eng 64:179–186

Muhammadi, Ahmed N (2007) Genetics of bacterial alginate: alginate genes distribution, organization and biosynthesis in bacteria. Curr Genomics 8:191–202

Mulet M, Sánchez D, Lalucat J, Lee K, García-Valdés E (2015) *Pseudomonas alkylphenolica* sp. Nov., a bacterial species able to form special aerial structures when grown on *p*-cresol. Int J Syst Evol Microbiol 65:4013–4018

Mørch ÝA, Donati I, Strand BL (2006) Effect of Ca^{2+}, Ba^{2+}, and Sr^{2+} on alginate microbeads. Biomacromolecules 7:1471–1480

Müller JM, Monte Alegre R (2007) Alginate production by *Pseudomonas mendocina* in a stirred draft fermenter. World J Microbiol Biotechnol 23:691–695

Narbad A, Russell NJ, Gacesa P (1988) Radiolabelling patterns in alginate of *Pseudomonas aeruginosa* synthesized from specifically-labelled ^{14}C-monosaccharide precursors. Microbios 54:171–179

Narbad A, Gacesa P, Russell NJ (1990) Biosynthesis of alginate. In: Gacesa P, Russell NJ (eds) Pseudomonas infection and alginates. Springer, Dordrecht

Oglesby LL, Jain S, Ohman DE (2008) Membrane topology and roles of *Pseudomonas aeruginosa* Alg8 and Alg44 in alginate polymerization. Microbiology 154:1605–1615

Ohman DE, Chakrabarty AM (1981) Genetic mapping of chromosomal determinants for the production of the exopolysaccharide alginate in a *Pseudomonas aeruginosa* cystic fibrosis isolate. Infect Immun 33:142–148

Ouwerx C, Velings N, Mestdagh MM, Axelos MAV (1998) Physico-chemical properties and rheology of alginate gel beads formed with various divalent cations. Polym Gels Netw 6:393–408

Peteiro C (2018) Alginate production from marine macroalgae, with emphasis on kelp farming. In: Rehm BHA, Moradali MF (eds) Alginates and their biomedical applications. Springer series in biomaterials science and engineering, vol 11. Springer, Singapore

Pier GB, Matthews WJ, Eardley DD (1983) Immunochemical characterization of the mucoid exopolysaccharide of *Pseudomonas aeruginosa*. J Infect Dis 147:494–503

Qiu D, Eisinger VM, Rowen DW, Yu HD (2007) Regulated proteolysis controls mucoid conversion in *Pseudomonas aeruginosa*. Proc Natl Acad Sci USA 104:8107–8112

Ramphal R, Pier GB (1985) Role of *Pseudomonas aeruginosa* mucoid exopolysaccharide in adherence to tracheal cells. Infect Immun 47:1–4

Rau MH, Hansen SK, Johansen HK, Thomsen LE, Workman CT, Nielsen KF, Jelsbak L, Høiby N, Yang L, Molin S (2010) Early adaptive developments of *Pseudomonas aeruginosa* after the transition from life in the environment to persistent colonization in the airways of human cystic fibrosis hosts. Environ Microbiol 12:1643–1658

Rehm BH (2010) Bacterial polymers: biosynthesis, modifications and applications. Nat Rev Microbiol 8:578–592

Rehm BH, Valla S (1997) Bacterial alginates: biosynthesis and applications. Appl Microbiol Biotechnol 48:281–288

Rehm BH, Boheim G, Tommassen J, Winkler UK (1994) Overexpression of *algE* in *Escherichia coli*: subcellular localization, purification, and ion channel properties. J Bacteriol 176:5639–5647

Rehman ZU, Wang Y, Moradali MF, Hay ID, Rehm BH (2013) Insights into the assembly of the alginate biosynthesis machinery in *Pseudomonas aeruginosa*. Appl Environ Microbiol 79:3264–3272

Reiling SA, Jansen JA, Henley BJ, Singh S, Chattin C, Chandler M, Rowen DW (2005) Prc protease promotes mucoidy in *mucA* mutants of *Pseudomonas aeruginosa*. Microbiology 151:2251–2261

Remminghorst U, Rehm BH (2006a) Alg44, a unique protein required for alginate biosynthesis in *Pseudomonas aeruginosa*. FEBS Lett 580:3883–3888

Remminghorst U, Rehm BH (2006b) Bacterial alginates: from biosynthesis to applications. Biotechnol Lett 28:1701–1712

Remminghorst U, Hay ID, Rehm BH (2009) Molecular characterization of Alg8, a putative glycosyltransferase, involved in alginate polymerisation. J Biotechnol 140:176–183

Reynolds HY, Di Sant'Agnese PA, Zierdt CH (1976) Mucoid *Pseudomonas aeruginosa*. A sign of cystic fibrosis in young adults with chronic pulmonary disease? JAMA 236:2190–2192

Robles-Price A, Wong TY, Sletta H, Valla S, Schiller NL (2004) AlgX is a periplasmic protein required for alginate biosynthesis in *Pseudomonas aeruginosa*. J Bacteriol 186:7369–7377

Roychoudhury S, May TB, Gill JF, Singh SK, Feingold DS, Chakrabarty AM (1989) Purification and characterization of guanosine diphospho-D-mannose dehydrogenase. A key enzyme in the biosynthesis of alginate by *Pseudomonas aeruginosa*. J Biol Chem 264:9380–9385

Ryan RP, Fouhy Y, Lucey JF, Dow JM (2006) Cyclic di-GMP signaling in bacteria: recent advances and new puzzles. J Bacteriol 188:8327–8334

Römling U, Galperin MY, Gomelsky M (2013) Cyclic di-GMP: the first 25 years of a universal bacterial second messenger. Microbiol Mol Biol Rev 77:1–52

Sherbrock-Cox V, Russell NJ, Gacesa P (1984) The purification and chemical characterisation of the alginate present in extracellular material produced by mucoid strains of *Pseudomonas aeruginosa*. Carbohydr Res 135:147–154

Sikorski P, Mo F, Skjåk-Bræk G, Stokke BT (2007) Evidence for egg-box-compatible interactions in calcium−alginate gels from fiber X-ray diffraction. Biomacromolecules 8:2098–2103

Singh S, Koehler B, Fett WF (1992) Effect of osmolarity and dehydration on alginate production by fluorescent pseudomonads. Curr Microbiol 25:335–339

Skjåk-Bræk G, Paoletti S, Gianferrara T (1989) Selective acetylation of mannuronic acid residues in calcium alginate gels. Carbohydr Res 185:119–129

Smidsrød O, Glover RM, Whittington SG (1973) The relative extension of alginates having different chemical composition. Carbohydr Res 27:107–118

Sonnenschein C (1927) Die mucosus form des Pyocyaneus-Bakteriums, bacterium pyocyaneum mucosum. Zentralblatt für Bakteriologie [Naturwiss] 104:365–373

Stacey SD, Williams DA, Pritchett CL (2017) The *Pseudomonas aeruginosa* two-component regulator AlgR directly activates *rsmA* expression in a phosphorylation independent manner. J Bacteriol 199(18):e00048–e00017

Stanford E (1883) On align: a new substance obtained from some of the commoner species of marine algae. Chem News 47:254–257

Stewart PS, William Costerton J (2001) Antibiotic resistance of bacteria in biofilms. Lancet 358:135–138

Straatmann A, Windhues T, Borchard W (2004) Effects of acetylation on thermodynamic properties of seaweed alginate in sodium chloride solutions. In: Lechner MD, Börger L (eds) Analytical ultracentrifugation VII. Springer, Berlin/Heidelberg, pp 26–30

Strempel N, Neidig A, Nusser M, Geffers R, Vieillard J, Lesouhaitier O, Brenner-Weiss G, Overhage J (2013) Human host defense peptide LL-37 stimulates virulence factor production and adaptive resistance in *Pseudomonas aeruginosa*. PLoS One 8(12):e82240

Tavares IM, Leitão JH, Fialho AM, Sá-Correia I (1999) Pattern of changes in the activity of enzymes of GDP-D-mannuronic acid synthesis and in the level of transcription of *algA*, *algC* and *algD* genes accompanying the loss and emergence of mucoidy in *Pseudomonas aeruginosa*. Res Microbiol 150:105–116

van der Hoek JP, de Fooij H, Struker A (2016) Wastewater as a resource: strategies to recover resources from Amsterdam's wastewater. Resour Conserv Recycl 113(Suppl C):53–64

Wang Y, Hay ID, Rehman ZU, Rehm BH (2015) Membrane-anchored MucR mediates nitrate-dependent regulation of alginate production in *Pseudomonas aeruginosa*. Appl Microbiol Biotechnol 99:7253–7265

Wang Y, Moradali MF, Goudarztalejerdi A, Sims IM, Rehm BH (2016) Biological function of a polysaccharide degrading enzyme in the periplasm. Sci Rep 6:31249. https://doi.org/10.1038/srep31249

Webber RE, Shull KR (2004) Strain dependence of the viscoelastic properties of alginate hydrogels. Macromolecules 37:6153–6160

Whitney JC, Hay ID, Li C, Eckford PD, Robinson H, Amaya MF, Wood LF, Ohman DE, Bear CE, Rehm BH, Howell PL (2011) Structural basis for alginate secretion across the bacterial outer membrane. Proc Natl Acad Sci USA 108:13083–13088

Whitney JC, Whitfield GB, Marmont LS, Yip P, Neculai AM, Lobsanov YD, Robinson H, Ohman DE, Howell PL (2015) Dimeric c-di-GMP is required for post-translational regulation of alginate production in *Pseudomonas aeruginosa*. J Biol Chem 290:12451–12462

Williams RJ, Govan JR (1973) Pyocine typing of mucoid strains of *Pseudomonas aeruginosa* isolated from children with cystic fibrosis. J Med Microbiol 6:409–412

Winstanley C, O'Brien S, Brockhurst MA (2016) *Pseudomonas aeruginosa* evolutionary adaptation and diversification in cystic fibrosis chronic lung infections. Trends Microbiol 24:327–337

Wong TY, Preston LA, Schiller NL (2000) Alginate lyase: review of major sources and enzyme characteristics, structure-function analysis, biological roles, and applications. Annu Rev Microbiol 54:289–340

Wood LF, Ohman DE (2009) Use of cell wall stress to characterize sigma 22 (AlgT/U) activation by regulated proteolysis and its regulon in *Pseudomonas aeruginosa*. Mol Microbiol 72:183–201

Wood LF, Ohman DE (2012) Identification of genes in the $\sigma^{(22)}$ regulon of *Pseudomonas aeruginosa* required for cell envelope homeostasis in either the planktonic or the sessile mode of growth. MBio 3(3):e00094–e00012

Wood RE, Boat TF, Doershuk CF (1976) Cystic fibrosis. Am Rev Respir Dis 113:833–878

Wozniak DJ, Sprinkle AB, Baynham PJ (2003) Control of *Pseudomonas aeruginosa algZ* expression by the alternative sigma factor AlgT. J Bacteriol 185:7297–7300

Yorgey P, Rahme L, Tan MW, Ausubel F (2001) The roles of *mucD* and alginate in the virulence of *Pseudomonas aeruginosa* in plants, nematodes and mice. Mol Microbiol 41:1063–1076

Part VII
Industrial and Biomedical Applications of Biopolysaccharides

Chapter 14
Chitin/Chitosan: Versatile Ecological, Industrial, and Biomedical Applications

Hans Merzendorfer and Ephraim Cohen

Abstract Chitin is a linear polysaccharide of N-acetylglucosamine, which is highly abundant in nature and mainly produced by marine crustaceans. Chitosan is obtained by hydrolytic deacetylation. Both polysaccharides are renewable resources, simply and cost-effectively extracted from waste material of fish industry, mainly crab and shrimp shells. Research over the past five decades has revealed that chitosan, in particular, possesses unique and useful characteristics such as chemical versatility, polyelectrolyte properties, gel- and film-forming ability, high adsorption capacity, antimicrobial and antioxidative properties, low toxicity, and biocompatibility and biodegradability features. A plethora of chemical chitosan derivatives have been synthesized yielding improved materials with suggested or effective applications in water treatment, biosensor engineering, agriculture, food processing and storage, textile additives, cosmetics fabrication, and in veterinary and human medicine. The number of studies in this research field has exploded particularly during the last two decades. Here, we review recent advances in utilizing chitosan and chitosan derivatives in different technical, agricultural, and biomedical fields.

14.1 Introduction

Chitosan, a polymer of β(1-4)-linked glucosamine (2-amino-2-deoxy-O-glucose) units, is a biopolymer with unique characteristics due to the presence of free amino groups on its backbone. It is obtained by partial deacetylation of chitin, which is found in the cell walls of unicellular and filamenous fungi and in

H. Merzendorfer (✉)
School of Science and Technology, Institute of Biology – Molecular Biology, University of Siegen, Siegen, Germany
e-mail: merzendorfer@chemie-bio.uni-siegen.de

E. Cohen
Department of Entomology, The Robert H. Smith Faculty of Agriculture Food and Environment, The Hebrew University of Jerusalem, Rehovot, Israel
e-mail: ephraim.cohen@mail.huji.ac.il

E. Cohen, H. Merzendorfer (eds.), *Extracellular Sugar-Based Biopolymers Matrices*, Biologically-Inspired Systems 12, https://doi.org/10.1007/978-3-030-12919-4_14

extracellular matrices and skeletal deposits of many protozoan and metazoan organisms including algae, choanoflagellates, sponges, corals, cephalopods, and arthropods. Commercially, chitin is extracted from the waste shells of marine crustaceans such as shrimp and crab. A significant proportion is used to produce chitosan, which, in contrast to chitin, is soluble in water at a slightly acidic pH and is easy to modify chemically to increase solubility at neutral pH and to add new functionalities. Chitosan and its derivatives have many desirable properties such as antioxidative and antimicrobial effects, mucoadhesiveness, biodegradability, and biocompatibility and can be manufactured in various formulations including hydrogels, films, membranes, porous sponges, nanoparticles, and nanofibers. Moreover, chitosan is considered a harmless compound, as it has received the generally recognized as safe (GRAS) status by the US Food and Drug Administration (FDA), and it has been approved as a food additive in several Asian countries (No et al. 2007). In the European Union, chitosan is registered as a basic substance, and the use of chitosan hydrochloride is considered by the European Food Safety Authority (EFSA) as having neither harmful effects on human or animal health nor any negative effects on the environment (European Commission 2014). Therefore, chitosan-based materials have been adopted worldwide in numerous applications in water treatment; food, cosmetic, and textile industry; biosensor engineering; plant protection; pharmaceutical industry; and regenerative medicine. They are used as flocculants, ion exchangers, chelating agents, coating materials, drug carriers, and scaffolds for tissue engineering. During the past years, many companies have started to develop chitosan-based products, and some have already successfully launched them for commercial purposes. This review is intended to summarize recent developments in the use of chitosan-based materials for potential and effective applications in different technical, environmental, agricultural, and biomedical fields.

14.2 Chitosan-Based Flocculants and Hydrogels Used in Water Treatment

Pollutants in water, industrial wastewater, and reclaimed wastewater for crop irrigation have presented severe environmental and medical problems all over the world. Such contaminants include various heavy metal ions (copper, cobalt, manganese, chromium, mercury, lead, arsenic, cadmium, and nickel), dyes (mainly azo dyes like malachite green, methyl violet, or methylene blue), oil spills, and a variety of pharmaceuticals and endocrine-disrupting compounds. Among the various methods used as remedial measures to treat polluted water and wastewater, the potential of chitosan-based composites as efficient adsorbent, flocculating and chelating agents has been widely investigated.

The presence of free hydroxyls and amino groups in many structural forms of chitosan-derived composites facilitates adsorption of pollutants such as dyes, metals, and organic compounds. Chitosan derivatives like carboxymethyl chitosan and graft

polymerization are a prevalent strategy to add a variety of functional groups to the composite. Magnetic particles are embedded usually as nanoparticles in the complex core to facilitate regeneration and reuse of adsorbent composites by applying external magnetic field.

14.2.1 Removal of Heavy Metal Ions

A large number of chitosan-based composites were investigated for removal of metal ions from aqueous solutions. They include chitosan-polymer macromolecular complexes (as cellulose, cellulosic matrix like cotton fibers, alginate, polyvinyl alcohol, polyvinyl chloride), chitosan ceramics, as well as clay and silicate composites (bentonite, montmorillonite, perlite, and zeolite) (Wan Ngah et al. 2011). Due to the vast number of scientific publications on chitosan-based adsorption that have been published, only a representative sample is depicted for Cr(VI) and Cu(II). Cognate composites were devised as adsorbents of other metal ions (Cd, As, Fe, Pb, Co, Pb, Hg, Ni, Zn, U) that can be found in the detailed reviews of Reddy and Lee (2013), Liu and Bai (2014), Wang and Chen (2014), Kyzas and Bikiaris (2015), Salehi et al. (2016), and Wang and Wang (2016).

Chromium (VI) The mutagenic and carcinogenic Cr(VI) is considered as a dangerous pollutant for humans and marine ecosystems. Composites of chitin and chitosan nano-hydroxyapatite hybrids removed Cr(VI) from aqueous solution by electrostatic interactions and reduction to Cr(III) via electron-donating groups present in the scaffold (Kousalya et al. 2010). A nanocomposite cross-linked hybrid of chitosan-alginate was able to remove Cr(VI) from water waste (Gokila et al. 2017). A more complex scaffold resin, where chitosan was mixed with magnetic particles (Fe_3O_4), modified by ethylenediamine and stabilized by glutaraldehyde as cross-linker, was established as an effective adsorbent of Cr(VI) (Hu et al. 2011). Reducing toxic Cr(VI) to nontoxic Cr(III) was accomplished by zero-valent iron [Fe(0)] embedded in chitosan beads (Geng et al. 2009). The oxidized iron Fe(III) formed a precipitately complex with Cr(III), thus enabling the regeneration of the adsorbing complex. Another method used ceramic aluminum coated with chitosan to remove Cr(VI) by electrostatic attraction of the hydrogen chromate ions to the positively charged amino groups of chitosan (Boddu et al. 2003).

Copper(II) Like chromium, Cu^{2+} ions found particularly in industrial wastewater are hazardous to human health and the ecosystems. Ingenious absorbance methods using a variety of organic and inorganic compounds have been devised to adsorb and remove the toxic ions. Among them are promising measures based on chitosan composite supra-macromolecular structures. Chitosan-based composites with various organic and inorganic compounds were examined as Cu(II) adsorbents. A recyclable complex composed of L-arginine-chitosan-Fe_3O_4 for removal of Cu (II) ions (Wu et al. 2016) and magnetic cellulose-chitosan composite microspheres

was capable to adsorb heavy metals like Cu(II) but also Cd(II) and Pb(II) from aqueous solutions (Peng et al. 2014). Chitosan-algal biomass composite microbeads (Sargın et al. 2016b), a binary chitosan/silk fibroin composite (Ramya and Sudha 2013), and cotton fibers functionalized by triethylenetetramine (TETA) and carboxymethyl chitosan form composites and hybrids for adsorption of Cu (II) from water (Niu et al. 2017). Microcapsules composed of phytopathogenic (*Ustilago* sp.) fungal spores immobilized in cross-linked chitosan matrix (Sargın et al. 2016a) and a binary complex of chitosan and emu egg shells (Anantha and Kota 2016) were shown to remove copper ions from aqueous solutions.

Chitosan complexed with clays, ceramic minerals, and carbon-based materials was used to enhance absorbance of heavy metals from aqueous solutions. A nanocomposite that consisted of chitosan-montmorillonite (Pereira et al. 2013) and silica gel/chitin and chitosan with nano-hydroxyapatite was used as adsorbents for Cu(II) (Rajiv Gandhi et al. 2011). Nanocomposites containing chitosan-poly (vinyl alcohol)-attapulgite were also used for removal of Cu(II) from aqueous solutions (Wang and Wang 2016). Furthermore, a recyclable magnetic microsphere composed of cross-linked chitosan-rectorite (a clay mineral) and Fe_3O_4 was studied for adsorption of Cu(II) and Cd(II) (Xie et al. 2015), and chitosan-zeolite composite hydrogel beads were examined for Cu(II) sorption (Djelad et al. 2016).

A particular interesting recyclable composite with chelating capacity consists of core magnetic (Fe_3O_4)-silica particles combined with cross-linked chitosan. Its porous and highly specific surface area contributed by activated carbon carrier showed an excellent adsorption capability for Cu^{2+} ions (Li et al. 2017). A recyclable nanocomposite with a core xanthated Fe_3O_4 chitosan grafted on graphene oxide introduced sulfur groups to the composite using carbon disulfide (Liu et al. 2016a).

Other sorbent composites that were prepared and studied are a recyclable composites containing chitosan grafted on a core of Fe_3O_4-hexadecyl trimethoxysilane (Liu et al. 2016b), a flocculant composed of poly(acrylic acid) grafted on chitosan (Saleh et al. 2017) or beads containing chitosan-poly(vinyl alcohol) and ZnO (Xu et al. 2017a). A sophisticated composite was prepared by using magnetic nanoparticles on the surface of polystyrene as core, coated with chitosan cross-linked by glutaraldehyde followed by grafting polyethylenimine on the complex surface (Xiao et al. 2017). This submicron composite is recyclable and exhibits good adsorption capacity for Cu(II) ions.

Highly selective adsorption of copper ions from aqueous solutions was achieved by the ion-imprinting polymer method (Kong et al. 2017). Microspheres of magnetic cores of Fe_3O_4 with a shell of cross-linked chitosan and graphene oxide were used to imprint Cu^{2+} ions. Zarghami et al. (2014) prepared Cu(II) ion-imprinted membranes composed of cross-linked chitosan/poly(vinyl alcohol) for adsorption of the metal from aqueous solutions. A similar ion-imprinted technique was reported for selective adsorption of Pb(II) from a recycling wastewater unit (Hande et al. 2016).

14.2.2 Removal of Man-Made Environmental Pollutants

14.2.2.1 Industrial Dyes

Textile, leather, paper, and food industries discharge a plethora of environmental pollutants such as synthetic dyes. A variety of chitosan-based composites was examined as promising adsorbents of hard to remove industrial dyes. Chitosan per se contains functional groups for interaction with pollutants including dyes. Adding more functional groups by modifying chitosan (cross-linking of chitosan layers, direct chemical modification, or graft polymerization – see Chapter 3) improves adsorption capability. Molecular imprinting technique was devised as selective adsorbent of pollutants. Composites' core of iron oxide magnetic nanoparticles like maghemite (γ-Fe_2O_3) and magnetite (Fe_3O_4) offers a way to recover the adsorbent scaffolds for reuse. Again, since the published articles are enormous in number, only essential parameters and basic blocks of adsorbing chitosan-based composites are included.

Methyl orange as a model anionic azo dye was adsorbed by films of cross-linked chitosan/nanonized maghemite from aqueous solution (Jiang et al. 2012). Improved adsorption of the same anionic dye was achieved by preparing a magnetic chitosan grafted with multi-walled carbon nanotubes (Zhu et al. 2010), and magnetic chitosan grafted with graphite oxide nanocomposite was able to adsorb the toxic azo dye, Reactive Black 5 (Travlou et al. 2013). Chitosan modified by ethylenediamine (Zhou et al. 2011) or polyaniline (Abbasian et al. 2017) grafting was able to adsorb other anionic azo dyes like Orange 7, Acid Orange 10 acid and red 4 and direct red 23, respectively. A magnetic complex of chitosan and zirconium oxide was a potent adsorbent of food anionic azo dyes like amaranth and tetrazine (Jiang et al. 2013a). Moreover, a complex composite adsorbent was prepared by grafting chitosan with poly[poly(ethylene glycol) methyl ether methacrylate] (Tsai et al. 2017). The functionalized groups added to chitosan contributed to improved removal of the azo dye Reactive Orange 16 from water.

Recyclable composite microspheres composed of cross-linked chitosan grafted with glutamic acid and having a core of Fe_3O_4 nanoparticles coated with silica adsorb cationic dyes like methylene blue, crystal violet, and light yellow 7GL (Yan et al. 2013). Similarly, an amphiphilic *N*-benzyl-*O*-carboxymethyl chitosan composite with a core of iron oxide nanoparticles was prepared for adsorption of methylene blue, crystal violet, and malachite green (Debrassi et al. 2012). The cyclic oligosaccharide β-cyclodextrin (β-CD) was added to chitosan-based composites as it provides a hydrophobic inner cavity and a hydrophilic exterior. Magnetic chitosan-β-CD with grafted graphene oxide to enlarge surface area exhibited an improved adsorption of methylene blue as a model dye from water (Fan et al. 2013). Molecular imprinting technique is of interest to selectively remove dyes from aqueous solutions. The molecule or ion used as templates will be subsequently removed, and a recognition site is generated. Alizarin red served as template molecule, and imprinted magnetic chitosan nanoparticles showed improved adsorption of the dye (Fan et al. 2012).

14.2.2.2 Removal of Micropollutants (Pharmaceuticals, Endocrine Disruptors)

Pharmaceutical, endocrine-disrupting compounds and personal care products have become a new class of hazardous environmental pollutants (Grassi et al. 2013) and have emerged as an extensive global concern. They are discharged as municipal and hospital effluents, from manufacturing industries, and found in water, reclaimed wastewater, and even in crops irrigated by reclaimed water (Paltiel et al. 2016). Pharmaceuticals, endocrine disruptors, and personal care products and their chemical transformation derivatives are characterized as stable, persistent compounds that are biologically active at very low concentrations.

The challenging goal has been to completely remove the above micropollutants from wastewater following conventional cleaning methods. Laboratory research including adsorption by chitosan-based composites has been high on the agenda (Amouzgar and Salamatinia 2015). Zhang et al. (2014) used a rather simple cross-linked magnetic chitosan-Fe_3O_4 composite to examine the sorption of three pharmaceutical compounds from contaminated water. The absorbance analysis showed effective sorption of diclofenac (a nonsteroidal anti-inflammatory drug) and clofibric acid (an antilipemic agent) but not of carbamazepine (an antiepileptic medication). Pharmaceuticals in water can be present as cationic, anionic, and neutral forms at different pH values. Thus, Zhang et al. (2016) in a more recent study devised an innovative, more complex three-dimensional chitosan-based scaffold. A magnetic core of chitosan-Fe_3O_4 was grafted with polymeric arms of either the polycation [poly(2-methyl acryoxyethyl trimethyl ammonium chloride], the polyanion poly (acrylic acid), or the neutral polymer poly(methylmethacrylate). The polycationic extension was cost-effective in removal of diclofenac from water due to charge attraction (Zhang et al. 2016). Further, magnetic composite pellets with grafted clay (bentonite) and activated carbon were prepared to examine possible cost-effective removal of cationic and anionic pharmaceuticals (Arya and Philip 2016). The composite was effective as a sorbent for the beta-blocker (atenolol), the antibiotic (ciprofloxacin), and the lipid regulator (gemfibrozil).

A variety of chitosan composites have been tested for the removal of other drugs. Cross-linked chitosan grafted with sulfonate or *N*-(2-carboxymethyl) groups was used as a sorbent to remove the dopamine agonist pramipexole dihydrochloride from polluted water (Kyzas et al. 2013). Chitosan-poly(acrylic acid)-graphite oxide nanocomposite showed adsorption of dorsolamide, a carbonic anhydrase inhibitor for eye treatment (Kyzas et al. 2014). Adsorption of nonsteroidal anti-inflammatory drugs ibuprofen and ketoprofen was studied using porous composite beads prepared of Chitosan-MIL 101 (Cr) (Zhuo et al. 2017). Using the antiepilectic carbamazepine as template, the magnetic molecular imprinted technique, based on chitosan-Fe_3O_4 nanoparticles, was applied for selective sorption of the drug (Zhang et al. 2013c).

Chlorophenols are endocrine-disrupting chemicals, used inter alia in manufacturing pharmaceuticals that are found in wastewaters (Sin et al. 2012). Excellent adsorbing capability was demonstrated using a cross-linked chitosan-salicylic

acid-β-CD composite. Composites of chitosan-γ-CD were capable of adsorbing the endocrine disruptors, polychlorophenols, and bisphenol A (Duri and Tran 2013). Composite films prepared by blending microporous carbon fibers with cross-linked chitosan/polyvinyl alcohol were examined as sorbents of bisphenol A from water (Bilgin Simsek et al. 2017).

Finally, Soares et al. (2017b) proposed an interesting and unusual concept of using low-cost magnetic chitosan-based scaffold for absorbing and removing oil spills following initial skimming from water. In addition, the composite, which had a core of magnetic nanoparticles with a shell of chitosan-silica hybrid, effectively adsorbs nonpolar organic solvents.

14.3 Biosensors

Biosensors are essentially analytical devices that convert biological reactions or interactions into measurable signals. Basically, the biosensors' constructs consist of a biological sensing element associated and intimately interfaced with a transducer that converts a signal in one form of energy to a signal of another form. Such signals should be proportional to the amount of analyte within a certain concentration range. Electrochemical biosensor devices, for example, possess advantages as being simple and relatively cheap while offering rapid detection and high sensitivity and further being amenable to miniaturization. Biosensors have been developed not only as analytical tools for medical purposes of clinical detection but also for applications in food industry and environmental monitoring.

Chitosan, and to a much lesser extent chitin, has several advantageous qualities in the design of biosensors. The polysaccharides are biocompatible, have functional groups pliable to chemical modification, and can be easily deposited on the surface of the transducer as adhesive thin films for the immobilization of recognition elements (enzymes, antibodies, DNA, whole cells, and cell organelles). Addition of carbon tubes, graphite, and graphene oxide to the composite increases electron transfer to the transducer and enhanced mechanical strength as well as water permeability and retention. Since there is a vast array of biosensors based on chitosan in their constructs, the following provide only representative devices.

Glucose detection and monitoring is of paramount importance in the medical field. A variety of biosensors, constructed with chitosan and using immobilized glucose oxidase for the detection of glucose levels, were reported. A glucose electrochemical sensor was prepared with glucose oxidase immobilized on the composite of chitosan-carbon nanotubes (Liu et al. 2005). An amperometric glucose biosensor composed of multilayered chitosan biofilms-gold nanoparticles-glucose oxidase on platinum (Pt) electrode was devised (Wu et al. 2007). The biocompatible gold nanoparticles helped in directing the transfer of electrons to the transducer. Yang et al. (2009) devised a different glucose biosensor composed of Pt electrode-glucose oxidase-Fe_3O_4-chitosan-nafion. Zhang et al. (2015c) prepared an electrochemical biosensor for glucose with chitosan-graphite composite and the

addition of magnetic Fe_3O_4 nanoparticles on Pt-coated indium tin oxide (ITO) glass electrode. Shrestha et al. (2016) devised a glucose biosensor with a glassy carbon electrode on which a nanocomposite film of glucose oxidase immobilized on chitosan and on which a graft of polypyrrole-nafion and multi-walled carbon nanotubes was deposited.

Electrochemical biosensors using other oxidases and various constructs were fabricated to monitor food and medically important compounds. For instance, a lactate biosensor was generated using lactate oxidase and a nanocomposite structure of chitosan-polyvinylimidazole-Os-carbon nanotubes (Cui et al. 2007). Glutamate and xanthine oxidases as recognition elements immobilized on chitosan/graphene oxide-polymerized riboflavin were constructed as glutamate and hypoxanthine biosensors (Celiesiute et al. 2017). In addition, a xanthine biosensor based on immobilization of xanthine oxidase on chitosan-polypyrrole-gold nanoparticles was fabricated by Dervisevic et al. (2017). Tkac et al. (2007) developed a selective galactose biosensor with a rather simple configuration of chitosan-single-walled carbon nanotubes and immobilized galactose oxidase. A sensitive amperometric nanocomposite biosensor for cholesterol detection was constructed using a matrix of Pt nanoparticles deposited on multi-walled chitosan-carbon nanotubes complexes with immobilized cholesterol oxidase (Tsai et al. 2008). A similar construct was proposed by Medyantseva et al. (2014) for the detection of antidepressant monoamine drugs using immobilized monoamine oxidase. Dai et al. (2010) developed an electro-chemiluminiscent biosensor to detect choline by immobilizing choline oxidase on a chitosan/titanate nanotubes composite film. Finally, a biosensor for measuring ethanol was prepared using alcohol oxidase immobilized on chitosan-eggshell film (Wen et al. 2007). The biosensor monitored the decrease in oxygen level vs ethanol concentration.

A number of electrochemical biosensors were similarly constructed to immobilize various dehydrogenase enzymes (Zhang et al. 2004). The nanocomposite scaffold film, attached predominantly to glassy carbon electrodes, consists of chitosan, multi-walled carbon nanotubes, and NAD^+ as cofactor. The signal current is based essentially on electrooxidation of the formed NADH. Among the large list of enzymes suffice it to mention NAD-dependent alcohol (Lee and Tsai 2009; Zhang and Gorski 2011), lactate (Tsai et al. 2007) and glutamate (Hughes et al. 2015) dehydrogenases, and FAD-dependent glucose dehydrogenase (Monosik et al. 2012).

In contrast to the above enzyme-based biosensors, a nonenzymatic electrochemical device for monitoring glucose was formulated (Al-Mokaram et al. 2017). The construct, which was based on a nanocomposite film composed of polypyrrole-chitosan-titanium dioxide nanoparticles on ITO glass electrodes, involved redox reactions and exhibited improved glucose oxidation and high electron transfer kinetics.

Other biosensors detecting and measuring diverse compounds were formulated, for example, nitrite biosensor based on Cu-containing nitrite reductase immobilized on viologen-chitosan that catalyzes the reduction of nitrite (Quan and Shin 2010). Horseradish peroxidase immobilized on alumina nanoparticles-chitosan composite was devised to detect phenolic compounds (Liu et al. 2011). Wang et al. (2003) developed a biosensor to detect and measure glucose, galactose, and glutamate in

human blood by using their corresponding oxidases immobilized on chitosan-Prussian blue composite film. The biosensor used Prussian blue as a good catalyst to form hydrogen peroxide by electroreduction. Biosensors to detect catechol as well as other phenolic compounds were based on immobilized tyrosinase on a film of chitosan-nickel nanoparticles (Yang et al. 2012a). A biosensor for detection of chlorophenol that includes immobilized laccase on ZnO-chitosan nanocomposite was prepared by Mendes et al. (2017). Nanocomposite of functionalized graphene oxide (enriched with carboxylic moieties)-polypyrrole-chitosan film was constructed to detect hydrogen peroxide using screen-printed carbon electrodes (Akhtar et al. 2017). Such a device was able to electro-catalyze the reduction of hydrogen peroxide. Teepoo et al. (2017) constructed an electrochemical biosensor to detect and monitor hydrogen peroxide by using horseradish peroxidase immobilized on a chitin-gelatin nanofiber composite. Another biosensor for hydrogen peroxide that used immobilized catalase on chitosan-β-cyclodextrin (with ferrocene in its cavity) was fabricated by Dong et al. (2017). It was based on chitosan-functionalized graphene oxide (enriched with carboxylic moieties)-polypyrrole nanocomposite able to electrocatalytically reduce hydrogen peroxide.

Detection and quantification of trace amounts of carcinogenic and toxic metallic ions are of great challenge and importance. A cross-linked chitosan-carbon nanotube sensor was developed for the determination of Cd(II) and Hg(II) (Janegitz et al. 2011). Sugunan et al. (2005) prepared a biosensor made of chitosan-gold nanoparticles to detect Cu(II) and Zn(II), and Ahmed and Fekry (2013) used a construct of chitosan-α-Fe_3O_4 nanoparticles sensor to detect Ni(II), As(II), and Pb (II). Biosensors were developed to detect and determine organophosphorus (OP) pesticides as well. For instance, Stoytcheva et al. (2018) prepared a device based on OP hydrolase immobilization on a chitosan-carbon-nanoparticles-hydroxyapatite nanocomposite. A nanocomposite immunosensor to monitor the OP compound, chlorpyriphos, is based on immobilized anti-chloropyriphos monoclonal antibody on multi-walled carbon nanotubes-chitosan-thionine (as electronic mediator) (Sun et al. 2012b). An intricate electrochemical immunosensor for the detection and monitoring of the fungal hepatocarcinogen, aflatoxin B1, as model antigen was developed by Masoomi et al. (2013). The construct scaffold involved chitosan-gold nanoparticles, immobilized polyclonal anti-aflatoxin B1, and a magnetite core that can enable regeneration of the immunosensor.

Biosensors based on chitosan/multi-walled carbon nanotubes hybrid films were developed largely by Babaei and colleagues to determine and quantitate drugs and neurotransmitters: acetaminophen and mefenamic acid (Babaei et al. 2010), dopamine and morphine (Babaei et al. 2011a), paracetamol (Babaei et al. 2011b), L-DOPA (Babaei and Babazadeh 2011), and 5-hydroxytryptamine and dopamine (Xu et al. 2015).

The polycationic nature of chitosan films in immunobiosensors is also exploited to immobilize polyanionic polymers such as nucleic acid sequences and proteins. Singh et al. (2013) devised an electrochemical DNA biosensor to detect typhoid which was constructed by surface immobilizing *Salmonella typhi* single-stranded (ss) DNA on graphene oxide/chitosan/ITO nanocomposite as a bioelectrode. The biosensor was

capable of distinguishing between complementary, noncomplementary, and one base mismatch sequences. A similar electrochemical DNA biosensor was developed for the detection of *Escherichia coli* 0157:H7 (Xu et al. 2017b). It was prepared with immobilized *E. coli* ss-DNA using a graphene oxide/chitosan hybrid nanocomposite. An electrochemical immunobiosensor to detect botulism neurotoxin A was reported by Afkhami et al. (2017). The sensor consisted of a gold nanoparticles/chitosan/graphene nanocomposite with immobilized antibodies to quantify the bound neurotoxin. To detect α-fetoprotein in human serum, an immunosensor was fabricated in which the α-fetoprotein antigen was immobilized on a film of a gold nanoparticles/carbon nanotubes/chitosan nanocomplex to quantify protein levels using a competitive immunoassay format (Lin et al. 2009). Giannetto et al. (2017) fabricated a competitive electrochemical immunosensor to detect HIV1-related capsid protein p24 in human serum. The p24 antigen was immobilized on gold-free single-walled carbon nanotube-chitosan complex for the interaction with a mouse monoclonal anti-p24, which was used for competitive immunodetection. Liu et al. (2009) developed an immunosensor to detect carcinoembryonic antigen, which is based on corresponding antibodies immobilized on chitosan-gold nanoparticles. Finally, Qiu et al. (2009) reported an immunosensor to detect hepatitis B surface antigen, which was constructed on the basis of a gold nanoparticles/chitosan/ferrocene biofilm with immobilized hepatitis B antibodies.

14.4 Beneficial Properties of Chitosan for Possible Use in Agriculture, Food, and Textile Industry

The wide-ranging antimicrobial, antiviral, and antioxidant activities, induction of defense systems in plants, and stimulation of plant growth by chitosan, chitosan oligomers, chemically modified chitosan and their composites have indicated their potential use in agricultural practices (El Hadrami et al. 2010; Malerba and Cerana 2016). Pre- and postharvest treatment of coating seeds, fruits, and vegetables by edible chitosan-based films effectively improve germination and plant vigor and prolonged shelf life and storage quality of food products (No et al. 2007). Preservation by chitosan-based coating also expanded to include meat, eggs, dairy products, and seafood (Friedman and Juneja 2010). Other promising practices such as delivery and slow and sustained release of chitosan-based encapsulated agrochemicals (fertilizers, micronutrients, pest control agents, and genetic materials) have been widely investigated (Malerba and Cerana 2016).

14.4.1 Antimicrobial and Antioxidant Activities

There are several comprehensive reviews that summarize the potential use of chitosan, its derivatives, and chitooligosaccharides in agriculture as related to their

broad-spectrum antimicrobial and antioxidant activities (Aider 2010; Cota-Arriola et al. 2013; Li et al. 2013a; Xing et al. 2015; Liaqat and Eltem 2018). Such beneficial activities were demonstrated in a variety of agricultural products like preservation of vegetables, fruits, cereals, dairy products, eggs, meat, and seafood (No et al. 2007; Friedman and Juneja 2010). Chitosan per se has antimicrobial activity that depends on higher degree of deacetylation, low molecular weight (its oligosaccharides), increased protonation at low pH, and the type of microorganisms (Katiyar et al. 2014). The antimicrobial efficiency is enhanced by adding essential oils (extracted from lemon, lemon grass, cinnamon, or rosemary) (Duan and Zhang 2013; Xing et al. 2016; Yuan et al. 2016) or by adding metal ions like silver or copper (An et al. 2011; Brunel et al. 2013; Kumar-Krishnan et al. 2015; Choudhary et al. 2017a; Sharma 2017) particularly to chitosan-based nanoparticles (Friedman and Juneja 2010; Cota-Arriola et al. 2013). The mode of action is mainly attributed to electrochemical interactions between the positively charged chitosan and the negative surface charge of bacterial cells leading to membranes disruption (Xing et al. 2015). In addition, penetration and binding of nanochitosan with microbial DNA that impact mRNA and protein synthesis were proposed (Rabea et al. 2003, Malerba and Cerana 2016).

Scavenging of free radical and reactive oxygen species by chitosan and its derivatives is responsible for its antioxidative effects (Guo et al. 2005; Ngo and Kim 2014). Scavenging of superoxide and hydroxyl radicals by chitosan and its derivatives was demonstrated by several studies (Xie et al. 2001; Guo et al. 2005; Yen et al. 2008; Wan et al. 2013). Furthermore, chitosan acts as a biogenic elicitor of various enzymes that detoxify reactive oxygen species (Malerba and Cerana 2016) and induces the formation of antioxidant and fungicidal phytoalexins (Yamada et al. 1993; Hadwiger 2013; Xing et al. 2015).

14.4.2 Eliciting Defense Responses in Plants

Chitosan and its derivatives were shown to activate plant immunity enzymes (catalase, peroxidase, superoxide dismutase, phenyl oxidase, phenylalanine ammonia lyase) that are capable of detoxifying reactive oxygen species (Hadwiger 2013; Xing et al. 2015; Malerba and Cerana 2016). Such activation engages different signal transduction pathways that involve a variety of second messengers. Other defense responses include pathogenesis-related proteins, phytoalexins, proteinase inhibitors, lignin synthesis, or callose formation (El Hadrami et al. 2010; Hadwiger 2013). Induction of programmed cell death and hypersensitivity-associated responses by chitosan and chitooligosaccharides was documented (Zuppini et al. 2004; Vasilêv et al. 2009; Zhang et al. 2012), as well as activation of plant defense genes via the octadecanoid pathway leading to jasmonate synthesis (Doares et al. 1995; Rakwal et al. 2002). Chitosan induces hydrolase enzymes such as chitinase and β-1,3 glucanase able to destroy chitin/glucan-containing fungal cell walls (Ma et al. 2013b; Xing et al. 2015).

14.4.3 Plant Protection and Food Preservation

Controlled and sustained release of chitosan-encapsulated agrochemical such as fertilizers, micronutrient, pesticides, and genetic materials was demonstrated by a plethora of investigations (Kashyap et al. 2015). Food products coating by films of edible chitosan derivatives (plus a variety of additives) prolong their shelf life with concomitant improvements in storage quality (Xing et al. 2016; Yuan et al. 2016).

14.4.3.1 Pesticides

A number of examples linked to chitosan-coated pesticides given below indicate the potential of the eco-friendly techniques in plant protection against phytopathogens, insects, and weeds: controlled release of insecticides like the botanicals azadirachtin being encapsulated in the complex carboxymethyl chitosan-ricinoleic acid (Feng and Peng 2012) and rotenone wrapped in oleoyl carboxymethyl chitosan (Kamari and Aljafree 2017); nanoparticulate chitosan-β-cyclodextrin, which encapsulated carvacrol and exhibited high acaricidal and repellency activities (Campos et al. 2018); and controlled release of avermectin conjugated to *N*,*O*-carboxymethyl chitosan (Li et al. 2016) or avermectin coated by silica cross-linked chitosan composite (He et al. 2013). Encapsulation of the neonicotinoids imidacloprid (Li et al. 2012a; Lim and Ahmad 2017) and acetamiprid (Yan et al. 2014), malathion, and spinosad (El Badawy et al. 2016) by chitosan-alginate capsules exhibited prolonged release of the insecticides. Slow release of the fungicide carbendazim against the phytopathogens *Sclerotinia sclerotiorum* using chitosan/β-CD-epichlorohydrin (Wang et al. 2017a) and hexaconazole encapsulated by chitosan nanoparticles against *Rhizoctonia solani* (Chauhan et al. 2017) was demonstrated. Ilk et al. (2017) reported the antifungal and antioxidant activities of kaempferol encapsulated in lecithin-chitosan nanoparticles against *Fusarium oxysporum*.

In addition to their slow release property, chitosan composites also protect pesticides from photodegradation. Nanoparticles of chitosan-beeswax protected deltamethrin from photodegradation (Nguyen et al. 2012), and a similar protective effect of avermectin was demonstrated for a silica/chitosan copolymer (He et al. 2013). Likewise, composites of chitosan with a variety of clays (montmorillonite, attapulgite, bentonite, and kaolinite), safe anionic dyes (Fast Green and Naphthol Yellow S), and photo-stabilized fungal conidia of the insect biocontrol agent *Aschersonia* spp. were reported (Cohen et al. 2003). Chitosan composites were found to be useful carriers of herbicides facilitating soil sorption as in the case of paraquat associated with chitosan-alginate nanoparticles (Silva Mdos et al. 2011) or slow release of paraquat encapsulated in tripolyphosphate-generated chitosan nanoparticles (Grillo et al. 2014). Moreover, encapsulation of metolachlor in blended gel beads of cross-linked carboxymethyl cellulose and carboxymethyl chitosan was effective in slow release of the herbicide as a model compound (Dong et al. 2012). Finally, slow release of atrazine encapsulated in carboxymethyl chitosan/bentonite gel was demonstrated (Li et al. 2012a).

14.4.3.2 Fertilizers

The modulated release of encapsulated fertilizers is important for enhanced growth of plants while reducing environmental problems of their excessive use. Experiments were accompanied by swelling rates of composites, fertilizer loads, and kinetics of release. Examples are chitosan-xanthan tablets (Melaj and Daraio 2013) or chitosan-starch beads (Perez and Francois 2016) as carriers of potassium nitrate that serve as model fertilizer; slow release of NPK fertilizers aggregated on chitosan nanoparticles (Corradini et al. 2010) and application on leaf surfaces enables translocation via stomata into the phloem (Abdel-Aziz et al. 2016); efficient controlled slow release of water soluble NPK fertilizers coated by chitosan with an additional outer coating by poly (acrylic acid–co-acrylamide) (Wu and Liu 2008). This composite also exhibited improved water absorption and retention. Noppakundilograt et al. (2015) examined the controlled release of NPK fertilizer granules embedded in a hydrogel composed of poly(vinyl alcohol) and then chitosan and a third layer of acrylamide and acrylic acid following cross-linking of chitosan by glutaraldehyde. Controlled release of urea by a variety of chitosan-based composites was established. Urea dispersed with humic substances in chitosan (Araújo et al. 2017), urea encapsulated in chitosan-acryamide (Siafu 2017), urea release from adduct of silk fibroin-gelatin-chitosan hydrogels (Rattanamanee et al. 2015), urea smectite clay chitosan composite (Puspita et al. 2017), and urea-kaolinite mixed with chitosan (Roshanravan et al. 2015) were tested for controlled release of the fertilizer.

14.4.3.3 Chitosan-Coated Plant Materials

14.4.3.3.1 Preharvest

Beneficial effects of preharvest chitosan-based seed coating and foliar treatment were reported by El Hadrami et al. (2010). Chitosan-coated artichoke seeds, for example, induced better germination, stimulated root system growth, and were effective against a number of pathogenic fungi (Ziani et al. 2010). Bhaskara Reddy et al. (1999) demonstrated induced resistance to seed-borne *Fusarium graminearum* followed by improved germination and vigor in wheat seeds coated with chitosan. Soybean seeds coated by chitosan had anti-feeding effects and protected against several insect pests (Zeng et al. 2012), and coating rice seeds increased antifungal effect, stimulated seeding growth, improved root system, and increased crop yield (Zeng and Shi 2009). Tomato seeds coated with chitosan resulted in resistance to infection by inducing plant defense mechanisms (Benhamou et al. 1994). Chickpea seeds treated with chitosan-silver nanoparticles promoted germination and increased biomass, chlorophyll, carotenoids, and protein contents as well as amylase activity and defense enzyme activities (Anusuya and Banu 2016). Similar effects were demonstrated in maize seeds coated with Cu/chitosan nanoparticles (Saharan et al. 2016; Choudhary et al. 2017b).

14.4.3.3.2 Postharvest

The antimicrobial activity of chitosan was targeted for use to improve preservation of a large variety of vegetable and fruit crops as well as of eggs, meat, and dairy products (Devlieghere et al. 2004; Friedman and Juneja 2010; Yuan et al. 2016). Chitosan with added compounds such as plant materials and animal proteins (formulations of chitosan with additions of tapioca starch, hydroxypropyl cellulose, pectin, and fish gelatin) was used to develop edible films. Such films in addition to their antimicrobial and antioxidant activities also keep food products from loss of moisture and oxygen penetration (Aider 2010; Duan and Zhang 2013). Postharvest coating of vegetables and fruits with chitosan and additional essential oils (extracts from lemon, rosemary, lemon grass, bergamont, cinnamon, oregano, and thymine), which by themselves exert antimicrobial and antioxidant activities, improved storage quality and prolonged the shelf life of products (Xing et al. 2016). Controlling postharvest decay during storage was reported also for additives such as olive oil, glacial acetic acid, green tea extract, and lactic acid (Xing et al. 2016; Yuan et al. 2016).

14.4.3.4 Technical Applications in Food Packaging

Microbial contaminations are a serious problem in food industry, because food-borne bacteria and fungi are associated with food spoilage and food poisoning leading to economic losses and human health risks. Using appropriate food packaging materials with antimicrobial properties may prevent or at least slow down bacterial and fungal growth. For this reason, a variety of biopolymers has been tested to identify alternative materials to the classical nondegradable plastic packaging materials, which have caused serious environmental issues due to their inappropriate disposal. Optimal alternative materials should be environmentally safe due to biodegradability and biocompatibility. As chitosan-based material combine antimicrobial properties with biodegradability and biocompatibility, they are the focus of research in food packaging. Moreover, chitosan-based materials have food-preserving antioxidant activity and film-forming ability, which allows the production of transparent foils and bags. Different methods have been established during the past decades to fabricate chitosan films including casting, coating, extrusion, and layer-by-layer synthesis, and the resulting materials have been evaluated for their antimicrobial and antioxidant activity and for their optical, mechanical, barrier, and thermal characteristics. Chitosan has also been combined with other functional materials resulting in composite films with tremendous preservative properties that can be utilized for the packaging of different foods such as vegetables, fruit, and meat. For a comprehensive overview on this topic, the reader is referred to an excellent review article published recently by Wang et al. (2018).

Pure chitosan films are frequently based on dispersions of chitosan nanoparticles (Ali et al. 2014), to which plasticizers, such as glycol (Leceta et al. 2013), and/or surfactants, such as Tween 80 (Martins et al. 2012), are added to modify the mechanical properties and to emulsify auxiliary compounds. In addition, chitosan nanofibers have been fabricated as a packaging material and tested for their antimicrobial activity. For instance, Arkoun et al. (2017) examined the antimicrobial activity of chitosan/polyethylene oxide nanofibers produced by an electrospinning process. They showed that the chitosan nanofibers were efficient in inhibiting growth of *E. coli*, *Staphylococcus aureus*, *Lysteria innocua*, and *S. typhimurium*, however at pH 5.8, which was below the pKa of chitosan, limiting the applicability to slightly acidic food. Importantly, the authors demonstrated that the antibacterial effects were irreversible, suggesting a bactericidal rather than bacteriostatic mechanism.

Combinations of chitosan and other natural polysaccharides have been frequently used to fabricate functional films with applications in food packaging. These biopolymers comprise of cellulose and various cellulose derivatives, alginate, cyclodextrin, glucan, mannan, pectin, starch, and xylan. Chitosan/cellulose films revealed improved mechanical properties while maintaining excellent antimicrobial properties (Xiao et al. 2013). Also chitosan/hydroxypropyl methylcellulose (HMPC) films exhibit significant antimicrobial activity. For instance, Möller et al. (2004) examined the antimicrobial effects of chitosan/HPMC films against *Listeria monocytogenes* and found that bacterial growth was completely inhibited on the film. Similarly, chitosan/carboxymethyl cellulose films showed superb food preservation properties when tested on packaged cheese (Youssef et al. 2016). Antimicrobial chitosan-alginate films have a great potential for food packaging as well, particularly because they show improved gas exchange and water vapor permeability properties when prepared by a layer-by-layer electrostatic deposition approach (Poverenov et al. 2014a). Martiñon et al. (2014) studied the effectiveness of antimicrobial multilayered coatings consisting of chitosan, pectin, and *trans*-cinnamaldehyde at different concentrations to extend the shelf life of fresh-cut cantaloupe and found that certain compositions were effective in preventing bacterial growth and spoilage. Lorevice et al. (2016) produced chitosan nanoparticles and combined them with different methyl pectin matrices to generate nanocomposite films and tested the mechanical, thermal, and barrier properties. The results showed that the nanocomposite film improved mechanical characteristics when compared with conventionally produced pectin films, making these novel materials promising for food packaging production. Similarly, chitosan/cyclodextrin films with inclusions of essential oil have been reported to possess desirable mechanical properties for food packaging (Sun et al. 2014). Moreover, this material showed significant antimicrobial activities against a variety of pathogenic bacteria.

Chitosan films have been also combined with a variety of proteins including casein (Khwaldia et al. 2014), gelatin (Poverenov et al. 2014b; Noorbakhsh-Soltani et al. 2018), collagen (Ahmad et al. 2016), kidney bean protein (Ma et al. 2013a), lactoferrin (Brown et al. 2008), and lysozyme (Yuceer and Caner 2014), as well as with antibacterial peptides such as nisin (Wang et al. 2015). In addition, chitosan was

blended with antimicrobial and antioxidant extracts from bee wax (Velickova et al. 2013) and plants, such as citrus (Iturriaga et al. 2014), thyme (Talon et al. 2017), and maqui berry (Genskowsky et al. 2015), as well as with essential oils including clove bud oil, cinnamon oil, and star anise oil (Wang et al. 2011).

Other approaches in fabricating chitosan-based films employed grafts, blends, or casts using synthetic polymers such as poly(vinyl alcohol) (Wang et al. 2015), poly (lactic acid) (Pal and Katiyar 2016), poly(ethylene) (Reesha et al. 2015), poly(ethylene oxide) (Kohsari et al. 2016), poly(styrene) (Lopez-Carballo et al. 2013), poly(propylene) (Cavallo et al. 2014), poly(caprolactone) (Alix et al. 2013), and poly(acrylonitrile-co-acrylamide) (Kumar et al. 2018) that led to improved mechanical and thermal properties. However, these synthetic polymers are not readily degraded in nature; hence concerns regarding the environmental safety have been raised. Guo et al. (2015) developed new edible antimicrobial films using microemulsions in combination with high-pressure homogenization processing. The films were made of chitosan, allyl isothiocyanide, and barley straw arabinoxylan, which were used as film-forming, antimicrobial, and emulsifying agents, respectively. The material was tested to be efficient in preventing growth of *L. innocua*.

To improve antibacterial activity, chitosan-based films were synthesized as composites with metals, minerals, and other inorganic compounds. Youssef et al. (2014) produced chitosan-silver and chitosan-gold (CS-Au) nanocomposites films, which showed enhanced antimicrobial activity against Gram-positive (*S. aureus*) and Gram-negative bacteria (*Pseudomonas aerugenosa*), fungi (*Aspergillus niger*), and yeast (*Candida albicans*). In another study published by Al-Naamani et al. (2016), poly(ethylene) films were coated with zinc oxide/chitosan nanocomposite, which completely inactivated and prevented the growth of food pathogens. In an approach based on a solution cast method, Sanuja et al. (2015) fabricated a chitosan-based nanocomposite film using nano zinc oxide and neem essential oil, which improved mechanical, physical, barrier, and optical properties. Moreover, Zhang et al. (2017) prepared chitosan/titanium dioxide composite films, which were found to possess significant antimicrobial activity against *E. coli*, *S. aureus*, *C. albicans*, *and A. niger*. Xu et al. (2017c) employed a different strategy by synthesizing chitosan/graphene oxide nanocomposites with titanium dioxide and analyzed their antimicrobial and food-preserving efficacies. They showed that the material effectively prevented *Bacillus subtilis* and *A. niger* biofilm formation presumably by disrupting cellular membranes. In addition, they demonstrated that the nano-coating could be applied as a cling film, which delays loss of moisture in fruits and vegetables and inhibits polyphenol oxidase activity and thus enzymatic browning but increases superoxide dismutase activity, which protects against reactive oxygen species. Next to these materials, chitosan-montmorillonite composites, chitosan/nanosilica films, and manifold combinations of chitin, metals, and minerals have been tested. In addition, numerous chemical chitosan derivatives have been explored for their properties to screen for new films suitable in food packaging. These derivatives include carboxymethyl chitosan and quaternized chitosan such as (2-*N*-Hydroxypropyl-3-trimethylammonium chloride) chitosan (Hu et al. 2016).

14.4.4 The Use of Chitosan in the Textile Sector

Due to their versatile and unique physicochemical and biological properties, chitosan, its multiple derivatives, and their adjunct complexes (addition of functional groups) have attracted considerable attention for possible use of eco-friendly materials in the textile industry. They are relatively inexpensive, biocompatible, biodegradable, and nontoxic and readily adhere to textile fabrics and usually demonstrate antibacterial activity. Certain formulations retain moisture as well as impart thermal stability and UV protection.

Chitosan per se or blends of chitosan-based composites deposited onto textiles fabrics were mostly tested for durable antibacterial activity (nearly all antibacterial studies include *E. coli* and *S. aureus* that represent correspondingly Gram-negative and Gram-positive bacteria). Coated Thai silk fabric with chitosan using radio frequencies plasma treatment exhibited antibacterial effects (Wongsawaeng et al. 2017), and polyester/cotton fabric treated with chitosan can be used as an alternative to the antibacterial triclosan (Ranganath and Sarkar 2014). Chitosan grafted on cotton (Ferrero et al. 2015) or on wool (Periolatto and Ferrero 2013) fabrics using UV irradiation bestowed antibacterial activity after many washing cycles. Chitosan reduced to nanoparticles and applied onto wool fabric imparted durable antibacterial and bestowed shrink proofing (Yang et al. 2010). Nanonized chitosan applied onto cotton exhibited, in addition to antibacterial activity, also thermal stability, UV protection, as well as improved dye-binding ability (Hebeish et al. 2013). Periolatto et al. (2012) demonstrated antibacterial effects and laundry durability of cotton and silk fabrics by UV curing with 2-hydroxy-2-methylpropylpropane-1-one as photoinitiator of the photochemical reaction.

Chitosan possesses abundant potential, in particular, for use in medical textiles and sportswear. For example, a blend of chitosan (short fibers) with cotton (long fibers) yarn by spinning technology is desirable for medical applications (Lam et al. 2017). Gauze bandages for wound dressing were prepared by electrospinning of chitosan nanofibers and cotton fabric (Nawalakhe et al. 2015). Plasma treatment was applied to improve adhesion by increased cross-linking between the two fiber systems imparting subsequent durability (Nawalakhe et al. 2015). Pure chitosan microfibers produced by wet spinning process was aimed for possible stable 3-D scaffold woven or nonwoven textile fabrics to be used in regenerative medicine such as bone and cartilage engineering (Toskas et al. 2013). Lam et al. (2018) examined a blend of chitin fibrils with cotton jersey fabric and showed reduced rigidity that may provide comfort to patients with epidermolysis bullosa skin disease. Likewise, chitosan-coated textile fabrics improved atopic dermatitis disease by restraining skin microbiome (Lopes et al. 2015). Sonochemical deposition was used by Petkova et al. (2014) to coat cotton fabrics with a hybrid of chitosan and ZnO nanoparticles. This complex showed improved antibacterial activity, slow release of the metal and washing stability, and postulated as effective treatment for hospital textiles to prevent transfer of pathogens. Similarly, the hybrid of chitosan and silver nanoparticles deposited onto cotton fabric

demonstrated antibacterial effects and laundry durability befitting their possible use for medical textiles and sportswear (Xu et al. 2016). Ali et al. (2011) proposed to use chitosan nanoparticles that are able to pick and retain silver ions in medical textile applications. A polyester fabric coated with this complex hybrid imparted enhanced antibacterial activity. Nanonized chitosan applied onto cotton exhibited in addition to antibacterial activity, also thermal stability, UV protection as well as improved dye-ability (Hebeish et al. 2013).

A large number of publications signified and reported beneficial properties of chitosan and chitosan-based formulations with possibly great potential to treat textile fabrics. Such valuable features include protecting a variety of fabrics with emphasis on medical textiles, production of aromatic and flame-retarding fabrics, as well as dye removal and treatment of textile wastewater. Table 14.1 summarizes inter alia nanochitosan, chitosan nanometal complexes, or chitosan derivative composites with metals and other substances, which were treated onto textile fabrics (notably cotton), and depicts their conceivable potential for the textile industry.

14.5 Utilization of Chitosan in Cosmetics

Chitin and, in particular, chitosan and its derivatives provide advantageous properties in the cosmetic area. They are biocompatible and adhere to surface components of the skin and hair, forming elastic films with moisturizing and water retention capabilities. They can serve as vehicles for encapsulated cosmetic ingredients and their controlled delivery and release and formation of gels in mixtures with water and alcohol and have some antimicrobial, antioxidant, and anti-inflammatory activities, with the additional important benefit of low cytotoxicity (Lee et al. 2013; Jimtaisong and Saewan 2014; Aranaz et al. 2018).

Chitosan and its derivatives are included in cosmetic formulations and products for mainly care and protection of the skin and hair but inter alia in tooth enamel and tooth lacquer, nail lacquer, lipsticks, cleansing and bath materials, toothpaste, mouthwash, chewing gum, deodorants, and breath refresheners (Dutta et al. 2004). Aging of the skin, viewed as wrinkling, dryness, loss of elasticity, dehydration, and hyperpigmentation, is the result of long-term exposure to sunlight UV, which mainly forms reactive oxygen species. Protection from photoaging is a major drive in the cosmetic industry. For example, chitooligosaccharides per se were able to protect UV-irradiated hairless mouse skin from photoaging damage (Kong et al. 2018). Gel formulation of chitosan microparticles served as a delivery system for the sustained release of the hydrophilic sunscreen, phenylbenzimidazole sulphonic acid (Gomaa et al. 2010). The cosmetic gel formulation of blended chitosan, collagen, and *Aloe vera*, with antibacterial and antioxidant effects, proved useful in the regeneration and rejuvenation of the skin using cultured mouse fibroblast (Rajashree and Rose 2017). Microspheres composed of carboxymethyl chitosan/collagen peptides-calcium chloride protected mice skin and thymus lymphocytes from UV-B radiation damage

Table 14.1 Possible applications of chitosan and chitosan-based composites in the textile industry

Textile fabric	Chitosan-based composite	Property	Reference
Chitosan derivatives			
Cotton, silk	CS-2-hydroxy-2-methylpropylpropane-1-one[a]	AB, laundry durability	Periolatto et al. (2012)
Cotton	CS nanoparticles-copper	AB, thermal stability, UV protection	Hebeish et al. (2013)
Polyester	CS nanoparticles-silver	AB, sustained release of silver	Ali et al. (2011)
Cotton	CS-silver nanoparticles	AB, laundry durability	Xu et al. (2016)
Cotton	CS-ZnO	AB, slow release of metal, washing stability	Petkova et al. (2014)
Cotton	CS-ZnO nanoparticles	AB, UV blocking	Raza et al. (2016)
Cotton	CS-CuO nanoparticles	AB	Dhineshbabu and Rajendran (2016)
Cotton/ polyester	CS-ZnO, RiO_2, SiO_2 (nanoparticles)	AB, UV protection, self-cleaning, washing durability	Ibrahim et al. (2017b)
Cotton	CS-silver nanoparticles, montmorillonite	AB, thermal stability, flame-retarding activity, UV protection, water retention	Rehan et al. (2018)
Cotton	CS-poly (N-isopropylacrylamide) –silver nanoparticles	AB, controlled release of silver	Štular et al. (2017)
Cotton	CS-silver-zeolite film	Antimicrobial	Scacchetti et al. (2017)
Cotton	LBL CS and graphene oxide	UV protection, laundering durability	Tian et al. (2016)
Cotton	CS-poly(2-acrylamide-2-methylpropane sulfonic acid salt). LBL film	AB	Cheng et al. (2016)
Cotton	CS-(N,N,N-three methyloxirane methylammonium chloride)	Antimicrobial wound dressing, moisture retention	Yin et al. (2018)
Cotton	CS-poly (N-isopropylacrylamide)	AB, thermosensitivity	Wang et al. (2016a)
Cotton	CS-N-benzyl-N,N diethyl quaternary ammonium salt	AB	Feng et al. (2016)
Wool	CS-poly(propylene) imine	AB, durable washings	Sadeghi-Kiakhani et al. (2013)
Silk (Antheraea pernyi)	CS-(N-[(2-hydroxy-3-trimethylammonium)propyl] chloride nanoparticles	AB, durable wrinkle and shrinkage resistant, laundry durability	Lu et al. (2014)
Polyester (polylactic acid)	CS-poly(vinyl alcohol)	Thermally stable blend	Grande et al. (2018)

(continued)

Table 14.1 (continued)

Textile fabric	Chitosan-based composite	Property	Reference
Cotton	CS-coating pyrazole compounds	AB	Nada et al. (2018)
Wool	CS-cyanuric acid	AB, improved dyeing performance	Zargarkazemi et al. (2015)
Polyester	CS covered by nanonized polyaniline	Electrical conductivity, water repellency, stable laundry	Tang et al. (2014)
Plant extracts and aromatic textiles			
Cotton	CS-neem seed extract	AB, antiviral	Revathi and Thambidurai (2017)
Cotton	CS-beeswax are impregnated with essential oils (*Eucalyptus*, tea tree, sage)	AB, slow release of fragrant	Cerempei et al. (2015)
Cotton	CS microcapsules containing essential oils (*Eucalyptus*, sandal wood)	AB	Javid et al. (2014)
Cotton	CS-β-CD, inclusion of cinnamon oil	AB, slow release of fragrant	Bashari et al. (2017)
Cotton	CS β-CD, inclusion of lavender oil	AB, slow release of fragrant	Singh et al. (2017)
Cotton	CS-vanillin microcapsules	AB, slow release and retained fragrant after wash cycles	Yang et al. (2014)
Flame retardation			
Cotton	CS-diammonium hydrogen phosphate	Durable flame retardation	El-Tahlawy (2008)
Cotton	LBL CS and ammonium polyphosphate	Itumescent flame effect	Fang et al. (2015)
Cotton	CS phosphate-TiO_2 nanoparticles-1,2,3,4-butane tetracarboxylic acid, hypophosphite	AB, flame retardation	El-Shafei et al. (2015)
Cotton/ polyester	LBL CS and melamine polyphosphate	Flame retardation	Leistner et al. (2015)
Cotton	LBL CS and ammonium polyphosphate	Flame retardation	Jimenez et al. (2016)
Polyamide 66 fabric	CS-phytic acid, oxidized sodium alginate	Flame retardation	Kundu et al. (2017)
Acrylic fabric	LBL CS and montmorillonite	Flame retardant	Carosio and Alongi (2018)
Textile wastewater and dye removal			
Cotton	UV-grafted CS	Absorbance and removal of excess dyes	Periolatto and Ferrero (2013)
Textile fabrics	CS beads impregnated with ZnO	Photodecolorization of Rhodamine B & Methylene Blue dyes	Farzana and Meenakshi (2015)

(continued)

Table 14.1 (continued)

Textile fabric	Chitosan-based composite	Property	Reference
Textile fabrics	Laccase immobilized on CS-cerium (VI) dioxide microspheres	Decolorization of methyl red and orange II reactive dyes	Lin et al. (2015)
Textile fabrics	CS plus ferrous sulfate	Decolorization	Kos (2016)
Textile fabrics	CS-coating ZnO nanoparticles-Fe_3O_4 nanoparticles	Removal of azo dye (reactive blue 198), recyclable composite	Nguyen et al. (2015)
Textile fabrics	CS-coating Fe_3O_4 nanoparticles	Removal of azo dye (Acid Red 2)	Kadam and Lee (2015)
Textile fabrics	Acrylic acid grafted on Jute fibers followed by immobilization of CS	Desorption of anthraquinone dye	Hassan (2015)
Textile fabrics	Manganese peroxidase immobilized on CS beads	Degradation and detoxification of dyes	Bilal et al. (2016)
Textile fabrics	Manganese doped in CS-ZnO	Photocatalytic degradation of azo dye	Nguyen et al. (2016)
Textile fabrics	CS-poly(methacrylic acid)-TiO_2 microparticles	Removal and degradation of anionic azo dyes	Škorić et al. (2016)

AB antibacterial effects, *CS* chitosan, *LBL* layer by layer deposition, *β-CD* β-cyclodextrin
[a]Photochemical reaction by UV generating cross-linked polymers

(Liu et al. 2015b). A cosmetic cream formulation composed of quaternized carboxymethyl chitosan-montmorillonite nanocomposite bestowed good UV protection and additional moisturizing and water retention effects (Chen et al. 2017). There is a possible cosmetic use of neutralized chitosan in citrate buffer film for skin exfoliation (Libio et al. 2016).

Chitosan and various chitosan derivatives, as active ingredients, were examined in cosmetic hair care products like shampoos, permanent wave agents, hair conditioner, styling lotions, rinses, hair colorant, hair sprays, and hair tonics (Dutta et al. 2004; Aranaz et al. 2018). They can adhere to the negatively charged hair keratin forming a transparent elastic film that covers hair fibers endowing smoothness, softness, and also mechanical strength (Dutta et al. 2004). A blend of chitosan and two other biopolymers like collagen and hyaluronic acid that forms a thin film over hair surface provides enhanced mechanical strength and improved conditioning of the treated hair (Sionkowska et al. 2017). Chitosan as a targeting vehicle to hair follicles in the skin was demonstrated with entrapped minoxidil, a medication to treat hair loss (Gelfuso et al. 2011; Matos et al. 2015). Microparticles and nanoparticles of chitosan-encapsulating minoxidil enabled its controlled release.

A large number of possible applications of cosmetic formulations containing chitosan and its derivatives have been patented. It is noteworthy that formulations containing chitosan are already in the busy cosmetic market.

14.6 Biomedical Applications of Chitosan Derivatives

Because chitosan and many of its derivatives are nontoxic, biocompatible, biodegradable, and highly versatile polymers, a large assortment of possible biomedical applications have been explored, of which some were implemented into therapeutic strategies by the pharmaceutical industry. To obtain optimal materials for the delivery of drugs, several factors have to be considered including the stability of the bioactive agents, absorption properties and mucoadhesiveness, gelling properties, particle sizes, permeation and transfection-enhancing properties, efflux pump inhibition, tissue targeting, residual toxicity of the final products, as well as release kinetic profiles. Chitosan derivatives have been developed into different kinds of pharmaceutical excipients used for the production of tablets and capsules (Illum 1998; Werle and Bernkop-Schnurch 2008), suppositories (Caramella et al. 2015), sprays (Osman et al. 2013), ointments (Kang et al. 2016), eye drops (Basaran and Yazan 2012), and wound dressings (Bano et al. 2017). The drugs are usually encapsulated by ionotropic gelation, spray drying, emulsion solvent evaporation, and coacervation (Panos et al. 2008). Chitosan-based excipients have been found useful in tablet disintegration and drug dissolution (Illum 1998) and in enhancing penetration and absorption properties (Thanou et al. 2001; van der Merwe et al. 2004; Sahni et al. 2008). Most importantly, certain dosage forms allow the controlled release of drugs (Jennings et al. 2015; Fonseca-Santos and Chorilli 2017). These include chitosan-based hydrogels (Knapczyk 1993; Kristl et al. 1993; Berger et al. 2004; Ishihara et al. 2006; Elviri et al. 2017) and micro-/nanoparticles for drug delivery (Hamman 2010). Here, we will focus on the applications of chitosan-based matrices in drug delivery for cancer, immune, and gene therapy, and we will summarize some recent advances in tissue engineering (Fig. 14.1).

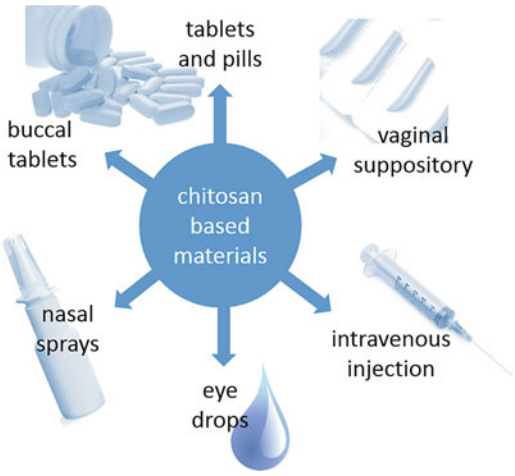

Fig. 14.1 Overview on biomedical applications of chitosan-based materials in cancer therapy and tissue engineering

14.6.1 Chitosan-Based Drug Carrier Systems

Chitosan-based materials can be used in various forms as drug delivery system (Fig. 14.2). Tablets are probably the most favorable and accurate dosage form, which are moreover easy to fabricate and handle. A simple method for their production is homogenization of the drug and chitosan and compressing the resulting mixture to tablets. However, it has to be considered that due to the alkaline conditions in the distal intestine, drug absorption is restricted to the more proximal regions of the gastrointestinal tract when pure chitosan is used which precipitates at an alkaline pH (Sakkinen et al. 2004; Dhaliwal et al. 2008). Therefore, more pH-insensitive formulations using higher-charged chitosan derivatives such as trimethylated chitosans or thiolated chitosan conjugates have improved absorption properties along the gastrointestinal tract. Although there is still a lack of robust data in human volunteers, some studies indicate that tablet formulations using higher-charged chitosan derivatives increase bioavailability due to improved mucoadhesiveness and better protection of the drug from degrading enzymes (van der Merwe et al. 2004). Chitosan-based tablets have been also examined for their use in vaginal drug delivery, mainly as carriers for antiviral and antifungal therapeutics (El-Kamel et al. 2002; Senyigit et al. 2014; Frank et al. 2017). However, the antimicrobial properties of chitosan may negatively affect the vaginal microflora, and hence long-term treatment should be critically evaluated (Raafat and Sahl 2009).

As chitosan-based hydrogels facilitate equal distribution and increase mucoadhesiveness, permeation, and bioavailability, they are effective formulations for eye drops to administer therapeutic drugs in ophthalmology (Krishnaswami et al. 2018). Chitosan-based formulations used in eye care include hydrogels, nanoparticles, and liposomal and colloidal systems (De Campos et al. 2001; De

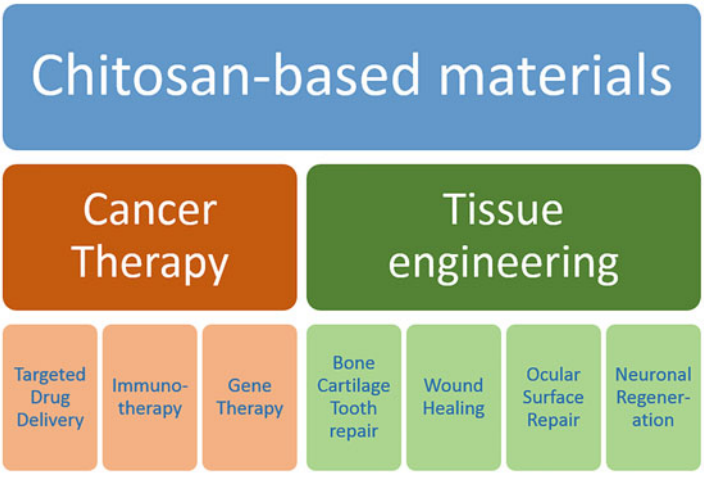

Fig. 14.2 Chitosan-based drug delivery systems

Campos et al. 2003; Diebold et al. 2007; Gupta et al. 2010). For similar reasons, they are also in use for nasal drug delivery, which is impaired by high turnover and secretion rates (Illum 2003). Notably, chitosan-coated lipid micro- and nanoparticles have been developed for nose-to-brain delivery of a variety of therapeutic drugs (Casettari and Illum 2014; Sarvaiya and Agrawal 2015). Chitosan-based nanoparticles are also a promising carrier for buccal drug delivery, which has the advantage of avoiding the hepatic first-pass metabolism and degradation in the gastrointestinal system (Sandri et al. 2005). Polymeric carriers generally have the potential advantage of prolonged release times of low-molecular-weight drugs. Because chitosan is additionally susceptible to hydrolysis by lysozyme in the blood serum, which facilitates drug release, and exhibits no toxic or hemolytic effects when applied parenteral (Nordtveit et al. 1994; Richardson et al. 1999), chitosan-based formulations are also suitable carriers for controlled drug release when administered by intravenous injection (Thanoo et al. 1992).

14.6.2 Chitosan-Based Drug Delivery Systems in Chemotherapy

Conventional chemotherapeutics are frequently not very effective in reaching the tumor cells, as solid tumors are not well supplied with blood, and lack lymphatic vessels, which results in and decreased convective flow in the interstitial fluid. To overcome these problems, novel drug delivery systems have been designed. These carriers are capable of encapsulating high concentrations of the cytotoxic compound within a macromolecular matrix that specifically targets the cargo to the tumor cells where the drugs are finally released in a controlled manner. This concept profits from the EPR (enhanced permeability and retention) effect, the phenomenon that macromolecules preferentially accumulate in solid tumors, probably because they have a defective vasculature and lack effective lymphatic drainage (Matsumura and Maeda 1986). Chitosan-based nanoparticles have many properties that make them suitable carriers for anticancer drugs. Next to their great chemical flexibility, allowing the design of selective carriers, chitosan-based materials evidently exhibit also the EPR effect depending on the tumor microenvironment (Yhee et al. 2017). Moreover, they are degraded inside the body into fragments which can be cleared by the kidney (Kean and Thanou 2010), and several studies suggested that chitosan itself has antitumor effects (Qi and Xu 2006; Yao et al. 2013a), making this polymer a highly suitable supplementary antitumor drug and drug carrier. Indeed, chitosan-based nanocomposites can be used to deliver hydrophilic and hydrophobic drugs such as doxorubicin hydrochloride and paclitaxel, respectively (Kim et al. 2006; Yousefpour et al. 2011). Studies analyzing chitosan-based drug delivery systems for cancer treatment are summarized in Table 14.2.

To target tumor cells by the EPR effect passively, Mitra et al. (2001) fabricated chitosan-based nanoparticles of about 100 nm carrying a dextran-doxorubicin

Table 14.2 In vitro and in vivo studies using chitosan-based nanoparticles in various cancer treatments

Drug/ targeting	Chitosan-based composite	Experimental system, effects	Reference
Chemotherapeutic drug delivery			
Doxorubicin	CS-dextrane conjugate	Mice, AT, prolonged circulation	Mitra et al. (2001)
Doxorubicin/ trastuzumab	CS cross-linked by succinic anhydrate, Lys thiolation	SKOV-3 cells, AT, targets HER2+ receptors, enhanced uptake	Hebeish et al. (2013)
Doxorubicin	CS-pluronic F127 micelles	MCF7 cells, AT, high drug loading capacity	Naruphontjirakul and Viravaidya-Pasuwat (2011)
Doxorubicin/ luteinizing hormone RH	CS-/poly(methyl vinyl ether maleic acid, magnetic nanoparticles	MCF7 cells, AT, increased cytotoxicity, targeting LHRH receptors	Varshosaz et al. (2016)
Doxorubicin/ folate	CS-coated magnetic nanoparticles	U87 cells in athymic mice, AT, guide by magnetic field, decreased tumor growth	Yang et al. (2017)
Doxorubicin	Aluminosilicate zeolite (ZSM-5) CS core-shell nanodisks	Mice, AT, pH-dependent drug release, reduced Tu growth and increased apoptosis	Yang et al. (2018)
Doxorubicin	CS-cobalt-ferrite-titanium oxide nanofibers	B16F10 cells, AT, fast drug release at low pH and alternating magnetic field	Radmansouri et al. (2018)
Doxorubicin, verapamil/ cRGD	Magnetic CS-poly(lactic acid-co-glycolic acid) nanoparticles	HepG2 and S-180 cells, Tu-bearing mice, AT, accumulation in tumor tissue	Shen et al. (2013a)
Paclitaxel	Glycol-CS-β-cholanic acid nanoparticles	Tu-bearing mice, AT, impaired tumor growth after injection	Kim et al. (2006)
Paclitaxel	CS-glyceryl monooleate core-shell nanopoparticles	MDA-MB-231cells, AT, 1000-fold reduction in IC50	Trickler et al. (2008)
Cisplatin	Glycol-CS-β-cholanic acid nanoparticles	Tu-bearing mice, AT, impaired tumor growth after injection, EPR	Kim et al. (2008)
5-Fluorouracil	CS-polyaspartic acid sodium salt	Mice, sustained drug release in vitro and in vivo	Zheng et al. (2007)
5-Fluorouracil/ hyaluronidase	CS-polyethylenglycol-gelatin copolymer	COLO-205 and HT-29 cells, AT, increased cytotoxicity by uptake and controlled drug release	Rajan et al. (2013)
5-Fluorouracil	N-succinyl-CS-*g*-poly (acrylamide-co-acrylic acid)	Simulated gastric and intestinal fluids, efficient drug loading pH-dependent drug release	Bashir et al. (2017)
5-Fluorouracil/folic acid	cystamine conjugated CS-methoxy poly(ethylene glycol)	MCF7 cells, AT, improved hemocompatibility, high cytotoxicity to cancer cells	Antoniraj et al. (2018)

(continued)

Table 14.2 (continued)

Drug/ targeting	Chitosan-based composite	Experimental system, effects	Reference
TNF-α/anti-EGFR-2	CS-silica hollow nanospheres	MCF-7 cells, AT, pH-dependent TNF-α release inside tumor	Deng et al. (2011b)
Oxaliplatin/ hyaluronic acid	CS nanoparticles encapsulated in Eudragit S100 coated pellets	Mice, HT-29 cells, AT, specific drug delivery in the colon	Jain et al. (2010)
Trans-resveratrol/Biotin, avidin	CS nanoparticles	HepG2 cells, cytotoxicity highest when both, avidin and biotin, were coupled	Bu et al. (2013)
Gemcitabine/ anti-EGFR, anti-chitosan	Glycol-CS nanobioconjugate	SW1990 cells, effective inhibition of cell proliferation, colony formation, migration, and invasion	Xiao and Yu (2017)
Cancer gene therapy			
Survivin-siRNA/ baclofen	*N*-trimethyl CS-TPP developed for pulmonary delivery	A549 cells, bronchoalveolar lavage fluid, effective gene silencing of the survivin gene resulting in apoptosis	Ni et al. (2018)
Midkine-siRNA	CS combined with 2-chloroethylamine and N, N-dimethyl-2-chloroethylamine hydrochloride	HepG2 cells, efficient transfection, significant decrease of cell proliferation	Zhong et al. (2015)
psiRNA-hBCL2/ dendrimeric RGD	Polyethyleneimine-*g*-CS	Tu-bearing mice, AT, efficient and specific transfection of tumor cells and silencing of anti-apoptotic hBcl2	Kim et al. (2017)
Cancer immunotherapy			
Ovalbumin	CS nanoparticles	Mice, AT, increased cytokine levels and stimulation of natural killer cells, deacreased tumor growth, detection of ovalalbumin specific cytotoxic T cells	Wen et al. (2011), Highton et al. (2016)
IL-12	CS nanoparticles	Mice, AT, activcation of cytotoxic T cells and natural killer cells, tumor regression, nor recurrence	Zaharoff et al. (2009)
GRP	Mannosylated CS nanoparticles	Mice, intranasal application, AT, enhanced tumor regression paralleled by anti-GRP antibody production	Yao et al. (2013b)
IP-10 plasmid/folate	CS nanoparticles	Mice, AT, inhibition of cell proliferation, induction of apoptosis, suppression of angiogenesis, and inactivation of regulatory T cells	Lai et al. (2014)

AT anti-tumor effects, *CS* chitosan, *Tu* tumor

conjugate and examined the antitumor effects in vivo in macrophage tumor cells implanted into BALB/c mice. The authors observed an improved therapeutic efficacy of dextran-doxorubicin loaded chitosan nanoparticles, which is probably due to the prolonged circulation time and/or drug accumulation at the tumor sites. In another study published by Yousefpour et al. (2011), doxorubicin was conjugated to chitosan using succinic anhydride as a cross-linker. In a second step, the resulting self-assembled chitosan-doxorubicin conjugate nanoparticles were conjugated with trastuzumab, a monoclonal antibody to the human epidermal growth factor receptor 2+ (Her2+), via lysine thiolation and subsequent linking of the derived thiols to chitosan. The Trastuzumab conjugated chitosan-doxorubicin nanoparticles selectively targeted Her2+ cancer cells resulting in enhanced uptake when compared to chitosan-doxorubicin particles and the free drugs. In another study, pluronic F127, a block copolymer of hydrophobic polyoxypropylene flanked by two chains of hydrophilic polyoxyethylene, was grafted onto chitosan to generate a copolymer micelle that can encapsulate doxorubicin (Naruphontjirakul and Viravaidya-Pasuwat 2011). The resulting chitosan-pluronic micelles carrying doxorubicin showed a high drug loading capacity and revealed a higher cytotoxic activity to MCF7 breast cancer cell lines in vitro than the free drug. Another approach to deliver doxorubicin specifically to cancer cells was reported by Varshosaz et al. (2016). The research team fabricated dual targeted nanoparticles loaded with doxorubicin and magnetic nanoparticles to treat breast cancer. For this purpose, the nanoparticles were produced via a layer-by-layer technique and functionalized with a bioconjugate of chitosan/poly(methyl vinyl ether maleic acid) and luteinizing hormone-releasing hormone (LHRH) to target corresponding receptors on the surface of MCF7 breast cancer cells, which presumably take up the particles by endocytosis. The targeted nanoparticles increased the cytotoxicity of doxorubicin about twofold in LHRH-positive cancer cells. In a similar approach, folate-grafted chitosan-coated magnetic nanoparticles were loaded with doxorubicin to target human glioblastoma U87 cells in athymic BALB/c nude mice in a subcutaneous tumor model system (Yang et al. 2017). Guiding the injected nanoparticles to the tumor by a magnetic field significantly decreased tumor growth by controlled delivery of doxorubicin to the cancer cells and demonstrated the feasibility of magnetic nanoparticles to direct the localization of drug release. Mesoporous aluminosilicate zeolite (ZSM-5) chitosan core-shell nanodisks loaded with doxorubicin were used as pH-responsive drug delivery systems against osteosarcoma that release the drug after upon endosomal acidification (Yang et al. 2018). Recently, Radmansouri et al. (2018) showed that doxorubicin-loaded electrospun chitosan/cobalt ferrite/titanium oxide nanofibers could be used for localized melanoma cancer therapy. The fastest release of doxorubicin from prepared magnetic nanofibers was observed at acidic pH when an alternating magnetic field was applied. As mentioned above, chitosan-based nanoparticles can also be modified to carry hydrophobic drugs such as paclitaxel. For this purpose, hydrophobic side chains are grafted onto chitosan. For instance, Kim et al. (2006) used glycol chitosan nanoparticles that were hydrophobically modified with β-cholanic acid and incorporated paclitaxel. The resulting nanoparticles showed sustained drug release, and following injection into the tail

vein of tumor-bearing mice, tumor growth was impaired. In a subsequent study, the same research team used this system as carrier for cisplatin, which is also poorly soluble in water. The hydrophobically modified glycol chitosan nanoparticles loaded with cisplatin exhibited the EPR effect, as they accumulated in solid tumors, and was proven to have a high antitumor efficacy in a tumor-bearing mice model (Kim et al. 2008). Paclitaxel was also encapsulated in chitosan-containing glyceryl monooleate core-shell nanoparticles, which were generated by the emulsification/evaporation technique (Trickler et al. 2008). Using this drug delivery system, the authors observed a 1000-fold increase in cytotoxicity, when determining the IC_{50} values in a human breast cancer cell line. Another common hydrophobic anticancer drug is 5-fluorouracil, which has been widely used to treat different kinds of solid tumors. In a study by Zheng et al. (2007), polyelectrolyte nanoparticles based on chitosan and polyaspartic acid sodium salt were used to encapsulate 5-fluorouracil testing various conditions for nanoparticle preparation such as temperature, ionic strength, pH and cross-linker concentration, and different loading methods. The optimized nanoparticles showed sustained drug release in vitro and in vivo. Rajan et al. (2013) prepared hyaluronidase-5-fluoruracil-loaded chitosan-polyethylenglycol-gelatin copolymers as a targeted drug delivery system and examined particle size, distribution, morphology, and drug loading capacity. The nanoparticles showed less cytotoxicity than free 5-fluorouracil when applied to colon cancer cells for a few hours. Another approach for controlled drug delivery used molecular surface imprinted graft copolymer of chitosan with methyl methacrylate, which was prepared by free-radical polymerization with 5-fluorouracil as template molecule (Zheng et al. 2016). The pH dependency and the kinetics of drug release suggested that this chitosan-based carrier is optimal for orally applied colon-specific drug delivery. A similar strategy to achieve colon specificity was used recently by Bashir et al. (2017). They synthesized pH-responsive semi-interpenetrating network hydrogels of *N*-succinyl-chitosan via Schiff base mechanism using glutaraldehyde as a cross-linking agent and embedded poly(acrylamide-co-acrylic acid). The hydrogel exhibited a porous structure and pH-dependent swelling properties. The hydrogel was effectively loaded with 5-fluorouracil, and the determined drug release was pH-dependent as well, with high release rates at pH 7.4 and low rates at pH 1.2.

In many cases, chitosan nanoparticles have been conjugated with tumor-specific ligands to mediate active targeting of cancer cells, which is expected to increase therapeutic efficacy, accelerate drug release to selected sites, prevent unwanted drug release before arrival at the target sites, and diminish adverse side effects of chemotherapeutic drugs. Active targeting can be accomplished by functionalizing chitosan-based nanoparticles and hydrogels using tumor-targeting ligands, which bind to specific receptors that are specifically present on the surface of cancer cells. Proper ligands of such kind include cytokines, peptides, folic acid, hyaluronic acid, biotin or avidin, and antibodies (Prabaharan 2015). Here, we will discuss only a one example for each of these ligands to illustrate active targeting.

Deng et al. (2011b) synthesized monodispersed and pH-sensitive chitosan-silica hollow nanospheres, loaded them with antitumorigenic tumor necrosis factor α (TNF-α), and conjugated them with an antibody to epidermal growth factor receptor

2, which is overexpressed in about 20% of all women suffering from breast cancer (Owens et al. 2004). Subsequent drug release studies demonstrated that the nanospheres delivered cytotoxic TNF-α to MCF-7 breast cancer cells and suppressed tumor with high therapeutic efficacy. Due to the acidic microenvironment inside solid tumors, TNF-α is gradually released from the nanospheres, binds to the TNF-α receptor, and activates a signaling cascade which induces programed cell death.

In a study published by Shen et al. (2013a), doxorubicin and verapamil were combined in chitosan nanoparticles to achieve an integrated treatment for cancer and doxorubicin-induced cardiomyopathy in the process of cancer therapy. For this purpose, chitosan shells coated on magnetic nanoparticles were loaded with both drugs and entrapped into poly(lactic acid-co-glycolic acid) nanoparticles conjugated with a cyclo(Arg-Gly-Asp-D-Phe-Lys) (cRGD) peptide targeting $\alpha_v\beta_3$ integrin, which is highly expressed on activated endothelial cells of newborn vessels during tumor angiogenesis as well as in some tumor cells (Liu et al. 2008). Near-infrared laser irradiation was sufficient to trigger drug release within an acidic microenvironment. Cytotoxicity assays performed in vitro suggested that cRGD-conjugated nanoparticles exhibited a greater growth inhibitory potential in cancer cell lines than the free drug or control nanoparticles likely due to cRGD-mediated targeting of tumor cells. In vivo imaging and biodistribution studies further showed that the nanoparticles preferentially accumulated in the tumor tissue under magnetic guidance. Finally, in vivo data for tumor regression along with electrocardiogram recordings and histopathology observations indicated that the cRGD-conjugated polymer-coated magnetic nanoparticles could have a high therapeutic potential as a dual-drug delivery system for the treatment of both cancer and doxorubicin-mediated cardiotoxicity.

Recently, a novel disulfide-linked chitosan-g-methoxy poly(ethylene glycol) copolymer was successfully synthesized, which was suggested to have excellent properties for redox-responsive drug delivery (Antoniraj et al. 2018). Redox-responsive 5-fluorouracil-loaded nanoparticles were synthesized by ionic gelation method, and folic acid was used to functionalize the nanoparticles for receptor-targeted drug delivery, as cancer cells commonly express high-affinity folate receptors on their surface. The 5-fluorouracil-free nanoparticles showed improved hemocompatibility, and the 5-fluorouracil-loaded nanoparticles conjugated with folic acid had a high cytotoxicity to MCF7 breast cancer cells, presumably due to intracellular internalization because of folic acid conjugation, which is expected to enhance the cellular uptake of the nanoparticles.

Many types of cancer cells overexpress different isoforms of hyaluronic acid receptors, which leads to enhanced binding and internalization of hyaluronic acid, as reported for instance in breast tumor cells (Bourguignon et al. 2000). To exploit this fact for targeting tumor cells, Jain et al. (2010) prepared hyaluronic acid-conjugated chitosan nanoparticles loaded with oxaliplatin and encapsulated in Eudragit S100-coated pellets for effective delivery to colorectal tumors. In immunodeficient C57BL mice model with HT-29 cancer cells injected into the ascending colon, relatively high local drug concentrations were found in the colon tumors after oral administration of the oxaliplatin nanoparticles, and the concentrations increased with

prolonged exposure time. Coupling of hyaluronic acid onto the surface of chitosan nanoparticles was found to make them more specific for delivery of the anticancer drug to the tumor of the colon.

Several studies revealed that also biotin and avidin possess tumor-targeting properties. Biotin receptors are overexpressed in many tumor types characterized by rapid division rates and aggressive growth (Russell-Jones et al. 2004), and avidin (a highly glycosylated protein) is recognized by lectins expressed on the surface of tumor cells (Yao et al. 1998). For this reason, Bu et al. (2013) prepared chitosan nanoparticles conjugated with either biotin or both biotin and avidin as tumor-targeted carrier system for the delivery of *trans*-resveratrol. Pharmacokinetic experiments revealed that avidin-biotin-loaded nanoparticles rapidly accumulated in the liver after injection, while the delivery nanoparticles conjugated only with biotin was attenuated. Cytotoxicity assays using HepG2 cells further uncovered that compared to *trans*-resveratrol solution and unconjugated chitosan nanoparticles, both biotin and avidin-biotin loaded nanoparticles significantly improved anticancer activity, but the latter combination exhibited a higher cytotoxicity. Thus, it was proposed that the synthesized nanoparticles conjugated with avidin and biotin may be a potent drug delivery system particularly to targeting hepatic carcinoma.

Finally, Xiao and Yu (2017) developed a glycol/chitosan nanobioconjugate loaded with gemcitabine and conjugated with anti-EGFR and anti-chitosan antibodies to target pancreatic cancer cells and cause aggregation. Administration of the chitosan conjugates efficiently blocked tumor growth and metastatic spread in human pancreatic cancer cells.

14.6.3 Chitosan-Based Vectors for Gene Therapy

Gene therapy requires the transmission of nucleic acids (DNA or RNA) into the target cell to mediate expression of therapeutic genes or to silence gene expression by RNA interference. However, negatively charged phosphates of nucleic acids impair permeation through the plasma membrane, which is negatively charged as well. In addition, unprotected nucleic acids are highly susceptible to degradation by nucleases. Hence, delivery of nucleic acids into cells relies on non-viral or viral vectors, which drastically improves transfection and protects from enzymatic degradation (Wivel and Wilson 1998). As viral vectors have the risk of causing adverse side effects such as immune reactions and malignant transformation, many efforts have been made to develop non-viral vectors for gene delivery, among them are ample examples of different chitosan-based nanoparticles.

Actually, unmodified chitosan is not an effective carrier for the transfer of nucleic acids due to its low solubility in water and instability of DNA/RNA chitosan complexes at physiological pH. Thus, chitosan requires chemical modification or grafting to convey appropriate physicochemical properties to the resulting complex. Chitosan modifications that have been used to design chitosan-based carriers for gene or siRNA delivery include quaternization by alkylation of tertiary amines,

reaction with 2-chloroethylamine hydrochloride and *N*,*N*-dimethyl-2-chloroethylamine hydrochloride, conjugation with polyethylene glycol, poly (amidoamine) or RGD dendrimer grafting, modification with phosphatidylcholine, or combinations of these modifications.

Among the quaternized chitosan derivatives, *N*-trimethyl chitosan and its derivatives have been extensively studied for their suitability in gene delivery, because they are reasonably soluble in water, have comparably little tendency to form aggregates, and exhibit a high loading capacity for nucleic acid under physiological conditions. In a systematic study published by Germershaus et al. (2008), the physicochemical properties of chitosan, *N*-trimethyl chitosan, and poly (ethylenglycol)-*N*-trimethyl chitosan were analyzed and compared. Using cell lines derived from mouse embryonic fibroblasts as a transfection system for plasmid DNA, the authors observed a significant increase in transfection efficiency when *N*-trimethyl chitosan nanoparticles were used to deliver plasmid DNA instead of chitosan nanoparticles. In addition, grafting poly(ethylenglycol) onto *N*-trimethyl chitosan further improved transfection efficiency, stabilized the particles, decreased particle size, and reduced cytotoxicity when compared to unmodified *N*-trimethyl chitosan nanoparticles. Zheng et al. (2009) prepared folate-conjugated *N*-trimethyl chitosan nanoparticles and compared cellular uptake and transfection of plasmid DNA (pDNA) in vitro with non-conjugated *N*-trimethyl chitosan nanoparticles using folate overexpressing KB and SKOV3 cells and folate receptor-deficient A549 and NIH/3T3 cells. The folate-*N*-trimethyl chitosan/pDNA complex showed a decrease in cytotoxicity in comparison to pDNA complexes made of polyethylenimine. Moreover, folate conjugation increased transfection efficiency and folate receptor-mediated endocytosis by KB cells and SKOV3 cells when compared to non-conjugated *N*-trimethyl chitosan nanoparticles.

Exploring further possible improvements of *N*-trimethyl chitosan-based gene delivery systems, Zheng et al. (2015) synthesized arginine, cysteine, and histidine-modified trimethyl chitosan nanoparticles to form complexes with pDNA. Using HEK 239 cells, they evaluated stability, cellular uptake, endosomal escape, release behavior, nuclear localization, and in vitro and in vivo transfection efficiencies. The cysteine-modified *N*-trimethyl chitosan nanoparticles turned out to be the most promising candidates for gene delivery due to sufficient stability, high cellular uptake, and glutathione-responsive release-favoring mechanism in combination with preferable nuclear distribution. Addition of sodium tripolyphosphate to the cysteine-modified nanoparticles was further effective to compromise certain disadvantageous attributes for pDNA delivery. *N*-trimethyl chitosan nanoparticles were also employed in drug-siRNA co-delivery using a metastatic breast cancer cell line (Eivazy et al. 2017). In this study, the authors tested simultaneous delivery of siRNA to silence the gene encoding the high mobility antigen (HMGA-2) and the anticancer drug doxorubicin to boost therapeutic anticancer effects. They found that dual delivery of HMGA-2 siRNA and doxorubicin by trimethyl chitosan nanoparticles significantly inhibited breast cancer cells growth.

A very recent study developed novel strategies in fighting lung cancer by RNA interference mediated gene silencing of the gene encoding the anti-apoptotic protein,

Survivin. For this purpose, Ni et al. (2018) designed nanoparticles consisting of baclofen functionalized *N*-trimethyl chitosan as polymeric carriers, TPP as ionic cross-linker, and siRNA to Survivin. Baclofen was used to target the nanoparticles to non-small lung cancer cells that overexpress the $GABA_B$ receptor, which specifically binds baclofen (Zhang et al. 2013b). The siRNA-loaded nanoparticles increased the uptake of Survivin-siRNA through the interaction with $GABA_B$ receptor and efficiently induced apoptosis and gene silencing. The authors further encapsulated the siRNA-loaded nanoparticles into mannitol microparticles for dispersion in the HFA-134a aerosol to allow administration by pressurized metered-dose inhalers. Pulmonary delivery of siRNA is expected to avoid serum-induced degradation, reduce systemic side effects, and improve therapeutic efficacy.

Zhong et al. (2015) hypothesized that the addition of amino residues to chitosan could improve stable complex formation with negatively charged siRNA enhancing transfection and gene silencing efficiency. For this purpose, they prepared a novel chitosan derivative (MixNCH) combining 2-chloroethylamine hydrochloride and *N*, *N*-dimethyl-2-chloroethylamine hydrochloride with chitosan and examined the physicochemical properties of the resulting nanoparticles. Using a hepatocellular carcinoma cell line (HepG2), gene transfection efficiency of MixNCH/midkine-siRNA nanoparticles and inhibition of HepG2 cell proliferation were analyzed. They found that midkine-siRNA delivered by MixNCH nanoparticles was able to significantly reduce both mRNA and protein levels of the midkine growth factor, resulting in a significant decrease of cell proliferation in HepG2 cells.

Guzman-Villanueva et al. (2014) evaluated the capability of different-sized chitosan derivative-based polyplexes to carry, internalize, and release siRNA in human adenocarcinomic epithelial cells. For this purpose, they first prepared *N*-phthaloyl-chitosan or *N*-phthaloyl-oligochitosan, reacted them with polyethylene glycol and hydroxybenzotriazole in DMF, and then cross-linked the polymers using ECD. Finally, the *N*-phthalimido groups were removed by the reaction with hydrazine monohydrate, and the products were purified by dialysis against water and ethanol. Both the chitosan- and oligochitosan-based polyplexes exhibited biodegradability, low cytotoxicity, and resistance to enzymatic degradation up to 24 h. When loaded with siRNA, the oligochitosan-based polyplexes drastically increased cellular internalization of the siRNA and gene silencing compared to naked siRNA. To improve the transfection efficiency of chitosan-based gene delivery systems, Deng et al. (2011a) fabricated a dendronized chitosan derivative using a copper-catalyzed azide alkyne cyclization reaction of propargyl focal point poly (amidoamine) dendron with 6-azido-6-deoxy-chitosan. The resulting dendronized chitosan nanoparticles exhibited higher water solubility and buffering capacity than native chitosan and showed lower cytotoxicity and enhanced transfection efficiency in transformed human embryonic kidney and nasophyryngeal carcinoma cell lines than commonly used polyethyeneimine.

As already mentioned above, the RGD motif can be used for targeting chitosan-based nanoparticles to tumor sites via the interaction with integrin $\alpha_v\beta_3$. Utilizing this fact, Kim et al. (2017) produced a dendrimeric RGD peptide/polyethyleneimine grafted chitosan copolymer, which was soluble in water. The copolymer was

nontoxic to mammalian cells and erythrocytes in the absence and presence of plasmid DNA. Moreover, it was found to transfect cells involving microtubule-dependent macropinocytosis and clathrin-mediated endocytosis. Finally, injecting copolymers complexed with psiRNA-hBCL2 to silence the gene for the human anti-apoptotic Bcl2 protein into BALB/c-nu mice carrying a PC3 prostate tumor xenografts, markedly inhibited tumor growth. Thus, the copolymer was suggested to be a good candidate to develop a specific targeted gene delivery system.

To confer membrane-like properties to chitosan-based gene delivery systems, Li et al. (2015) grafted phosphorylcholine and macrocyclic polyamine onto chitosan to obtain water-soluble nanoparticles. Chitosan grafted with both compounds were more efficient in binding and protecting plasmid DNA than chitosan grafted only with phosphorylcholine or macrocyclic polyamine. The authors also demonstrated that phosphorylcholine and macrocyclic, polyamine-grafted chitosan had a positive net charge and can, therefore, wrap DNA to yield nanoparticles of about 100 nm in diameter. Finally, the DNA-loaded nanoparticles significantly increased cellular uptake and transfection rates in transformed human embryonic kidney cells when compared to chitosan/DNA complexes. A similar transfection strategy was published by Picola et al. (2016), who inserted phosphorylcholine and increasing numbers of diethylaminoethyl (DEAE) groups into the polymer. The resulting chitosan nanoparticles were water soluble at physiological pH and less cytotoxic than lipofectamine, a commonly used transfection reagent. They further could form complexes with plasmid DNA, and the transfection efficiencies of the nanoparticles with high DEAE substitution rates tested in HeLa cells were in the same range as determined for lipofectamine. When the nanoparticles were loaded with siRNA, they were able to induce gene silencing, with efficiencies highly dependent on the N/P ratio.

14.6.4 Chitosan-Based Adjuvants for Vaccine in Immunotherapy

Chitosan-based materials have been recognized to be potent adjuvants for immunotherapy, because they non-specifically stimulate immune responses in the host organism and therefore have antiviral, antimicrobial, and antitumor properties (Li et al. 2013b). The adjuvant potency of chitosan is comparable to incomplete Freund's adjuvant, and it has stronger immune-stimulatory effect than aluminum hydroxide, which is frequently used in vaccines though it shows adverse side effects such as neurotoxicity (Zaharoff et al. 2007). The mechanism of how chitosan triggers immune responses involves phagocytosis-dependent activation of the NOD-like receptor family, pyrin domain containing 3 (NLRP3) inflammasome, which finally induces a robust interleukin-1β response (Bueter et al. 2011, 2014). Carroll et al. (2016) described another mechanism by which chitosan stimulates the activation of dendritic cells inducing cellular immunity. They found that chitosan

promotes the intracellular release of DNA, which involves the cGAS-STING pathway. As a result, type I interferon is secreted activating the expression of interferon-controlled genes. Due to the release of the cytokines that stimulate dendritic cells, the cellular immune system is elicited.

Due to its mucoadhesiveness, chitosan and its derivatives are considered effective for mucosal administration, which includes oral, nasal, as well as ocular antigen-delivery routes. However, other routes are also anticipated to be effective in provoking immune response including subcutaneous (Borges et al. 2008; Scherliess et al. 2013), intraperitoneal (Chang et al. 2010), intravenous (Shi et al. 2011), and intratumoral injections (Zaharoff et al. 2010). Evidently, innate immune responses are stimulated by chitin, chitosan, or derivatives (Peluso et al. 1994; Tokura et al. 1999; Lee et al. 2008; Lee 2009). This includes the activation of alveolar macrophages with the release of cytokines such as interleukin (IL)-12, tumor necrosis factor-α, or IL-18, leading to INF-γ production predominantly released by natural killer cells (Shibata et al. 1997a, b). However, also humoral and cellular adaptive immune responses are triggered by some antigens when co-administered or encapsulated in chitosan-containing micro- and nanoparticles (Tokura et al. 1999; van der Lubben et al. 2001; Arca et al. 2009; Mori et al. 2012). In particular, Wen et al. (2011) found that the stimulatory effect on the humoral and cellular immune system by chitosan results in a balanced Th1/Th2 response. However, care has to be taken in assessing the properties of chitosan-based adjuvants, as many studies do not provide sufficient data on the chemical and physical characteristics, preparation and formulation procedures, as well as potential impurities (Vasiliev 2015). This is particularly critical, as immune responses appear to depend on these parameters as uncovered by Scherliess et al. (2013), who reported that the degree of immune response varied when chitosans of different qualities were used. The immune-stimulatory effect of chitosan is affected by the combination of molecular weight, solubility, particle size, and viscosity as well as deacetylation degree.

Preclinical studies performed predominantly in mice models suggested that chitosan-containing antigen-delivery systems are promising adjuvant platforms for mucosal vaccination against human pathogenic viruses such as influenza (Read et al. 2005; Svindland et al. 2012; Sawaengsak et al. 2014; Liu et al. 2015a); hepatitis A, B, and E (Jiang et al. 2007; Tao et al. 2017a; Tao et al. 2017b; Soares et al. 2018); human papilloma virus (Ma et al. 2015); and poliovirus (Ghendon et al. 2011). Combinations of chitosan and heat-inactivated human herpes viruses (HSV) were further tested as an immunomodulating adjuvant in T cells and antigen-presenting cells in HSV-infected mice (Choi et al. 2016). Using chitosan nanoparticles targeted to dendritic cells via antibodies to the DEC-205 surface receptor, Raghuwanshi et al. (2012) successfully delivered plasmid DNA carrying the cDNA for the N protein to trigger immunization against the severe acute respiratory syndrome coronavirus (SARS-CoV). Simultaneous comparison of targeted formulations using intramuscular and intranasal routes revealed that intramuscular administration induced a more potent systemic IgG response compared to intranasal administration. Solid evidence substantiating the advantages of chitosan as an efficient adjuvant for nasal vaccination originates from clinical examinations on a norovirus vaccine, which

demonstrated the ability of a chitosan/monophosphoryl lipid-based antigen delivery system (ChiSys®) to induce immunity against the gastroenteric norovirus infections after immunization (Smith et al. 2014).

Chitosan-derived adjuvants were also used in combination with antigens derived from bacterial toxins, such as diphtheria toxoids (McNeela et al. 2000; Schipper et al. 2017), tetanus toxoids (Ahire et al. 2007; Pirouzmand et al. 2017), and dermonecrotoxin (Jiang et al. 2004). In addition, the potential of various vaccine formulations against anthrax were evaluated in female BALB/c mice (Malik et al. 2018). Encapsulating protective antigens (PA) in trimethyl-chitosan nanoparticles and administering them by subcutaneous, intramuscular, and intraperitoneal injections resulted in a strong IgG antibody response (Th1-biased) when combined with immune-stimulatory CpG oligodeoxynucleotides or polyinosinic-polycytidylic acids. Interestingly, without the immune-stimulatory nucleic acids, the PA-loaded trimethyl-chitosan nanoparticles led to a Th2-biased immune response.

Many studies have explored the adjuvant properties of chitosan in vaccines against cancer. In a study published by Wen et al. (2011), the effects of chitosan nanoparticles on the immune response triggered by an ovalbumin antigen in mice were analyzed. As the administration of the chitosan nanoparticles did not only increase cytokine levels of Th1 (IL-2 and IFN-γ) and Th2 (Il-10) cells, but also stimulated natural killer cells, the authors suggested that chitosan is a promising adjuvant for cancer immunotherapy by promoting both humoral and cellular immune responses. This hypothesis was confirmed by Highton et al. (2016), who demonstrated that immunization with an ovalbumin/chitosan hydrogel had antitumor effects in an intracaecal mice cancer model. After subcutaneous injection of the ovalbumin/chitosan vaccine, the authors detected $CD8^+$ T memory cells specific for ovalbumin and observed decreased tumor growth in contrast to unvaccinated control mice or mice that were vaccinated with dendritic cells and ovalbumin.

Zaharoff et al. (2009) analyzed antitumor effects in mice using a bioluminescent orthotopic bladder cancer model, after repeatedly administering chitosan/IL-12 into the bladder and comparing the antitumor efficacy of this treatment with that of an established adjuvant therapy applied to treat bladder cancer based on attenuated mycobacteria (bacillus Calmette-Guerin therapy). Determination of the urinary cytokine spectrum and immunohistochemical analysis resulted in the identification of cytotoxic T cells and natural killer cells as effector cells responsible for tumor regression. In contrast to the *Bacillus* Calmette-Guerin therapy, chitosan/IL-12 treatment utterly prevented recurrence of the disease.

More recently, Yao et al. (2013b) prepared mannosylated chitosan nanoparticles and loaded it with a plasmid to produce a vaccine against gastrin-releasing peptide (GRP), whose receptor is overexpressed in various cancer cells. The nanoparticles were intranasally administered in a subcutaneous mice prostate carcinoma model to evaluate the efficacy on inhibition of the growth of tumor cells. Cell binding and cellular uptake assays revealed that the mannosylated chitosan nanoparticles facilitate targeting to antigen-presenting cells, promoting receptor-mediated endocytosis

via the mannose receptor. Due to antigen representation, enhanced tumor regression was observed as a result of the production of high titers of anti-GRP antibodies. A similar strategy was finally used by Lai et al. (2014) to test an immune therapy against hepatocellular carcinoma in a H22 tumor-bearing mice model. They synthesized folate-conjugated chitosan nanoparticles and loaded them with a plasmid-encoding mouse interferon-γ-inducible protein-10 (IP-10). They found that IP-10 plasmid exhibited efficient antitumor activity, prolonging the survival time in H22 tumor-bearing mice. The antitumor effects were likely due to different effects. Next to the secretion of IFN-γ and IP-10, inhibition of regulatory T cells, suppression of angiogenesis, inhibition of cancer cell proliferation, and activation of apoptosis contributed to tumor growth inhibition.

14.6.5 Tissue Engineering

Tissue engineering is an increasingly important interdisciplinary field in regenerative medicine, which aims to create replacements for damaged tissues based on the combined knowledge provided by physicians, biologists, and engineers. Most approaches employ scaffolds made from biocompatible polymers, which are colonized by cells of the respective tissue. Ideally, the scaffold increases adherence, proliferation, and differentiation of colonizing cells. Chitosan and its derivatives offer ample benefits to generate cell and tissue supporting matrices, which include chemical versatility, antimicrobial activity, biocompatibility, biodegradability, and neglible toxicity (Ahsan et al. 2018). Chitosan can be produced to form sponge-like scaffolds using rather simple phase separation techniques including freeze-drying (Aranaz et al. 2014), gas foaming (Kaynak Bayrak et al. 2017), and electrospinning procedures (Qasim et al. 2018). The presence of a system of interconnected pores with appropriate diameters facilitates vascularization and tissue integration. Moreover, chitosan-based scaffolds can be synthesized in combinations with ample natural and synthetic polymers resulting in matrices exhibiting special characteristics. Due to their positive surface charges they open the possibility to fabricate polyelectrolyte complexes with anionic polymers such as glutamic acid (Fang et al. 2014), hyaluronic acid (Lalevee et al. 2016), dextrane sulfate (Kulkarni et al. 2016), heparin (Almodovar and Kipper 2011), dermatan sulfate (Rasente et al. 2016), and chondroitin sulfate (Tsai et al. 2011). Particularly the presence of glycosaminoglycans, which are naturally found in extracellular matrices, is known to modulate the activity of cytokines and growth factors by binding to the polymers (Zaman et al. 2016). Otherwise, chitosan-based scaffolds can be loaded with cytokines and growth factors to attract cells and stimulate tissue regeneration (Sun et al. 2012a; Bader et al. 2015; Choi et al. 2015). Finally, they further open the possibility of controlled degradation and resorption in physiological environments, designing mechanical properties that match the conditions found in the respective tissue, and determination of desired sizes and shape by easy fabrication procedures. Therefore,

chitosan-based scaffolds have numerous applications in tissue engineering, and we will review recent progress in using these materials for tissue regeneration and wound healing.

14.6.5.1 Bone, Cartilage, and Tooth Repair

Bone defects can either be congenital or result from trauma, infection, cancer, or failed orthopedic surgical procedures (Venkatesan and Kim 2010). The grafts used to bridge bone defects can be autografts (bone material from other body regions of the same patient) or allografts (bone material from decedents). However, both materials have disadvantages: autografts require bone harvesting from healthy tissues and may cause complications of wound healing and pain, and allografts may result in immunogenic rejection and have the risk of transmitting viral diseases from the donor to the recipient. Due to these concerns, scientists around the world are searching for alternative materials as bone graft substitutes. As described before, chitosan-based materials have valuable properties for orthopedic applications. Chitosan itself has the capacity to increase bone regeneration rates (Muzzarelli et al. 1993b); however, it cannot fully substitute natural bone material. Therefore, different composite scaffolds have been developed to assure porosity for vascularization and nutrition, facilitate the formation of new bone material (osteoconductivity), guarantee structural integrity during ingrowth at the site of implantation, and orchestrate biodegradation with bone regeneration (Venkatesan and Kim 2010). In addition, chitosan-based composites can be loaded with cells and growth factors that promote osteoconductivity and hence facilitate bone regeneration. One of the most important chitosan grafting that has been used in bone tissue engineering is hydroxyapatite, which by itself stimulates bone regeneration, provided that the scaffold has a microporous structure (Woodard et al. 2007). Hydroxyapatite grafting of chitosan can be easily achieved by coprecipitation from homogeneous mixtures of precursor (Deepthi et al. 2016, and references therein). One of the first researchers who tested combinations of chitosan and hydroxyapatite was Michio Ito, who examined the use of chitosan-bonded hydroxyapatite paste for treatment of periodontal defects (Ito 1991). In 2004, Ge et al. (2004) published a remarkable study, in which they tested different combinations of air- and freeze-dried chitosan/hydroxyapatite materials that were colonized by osteoblasts and implanted into rats. The material was found to be nontoxic and biodegradable and to stimulate mineralization. The explanted material that was colonized by osteoblasts before implantation showed newly formed bone material containing proliferating osteoblasts that recruited surrounding tissue to grow in. In another study published by Oliveira et al. (2006), three-dimensional macroporous hydroxyapatite/chitosan bilayered scaffolds of inorganic and organic deposits were produced in a stepwise procedure and examined with regard to their mechanical properties and cytotoxicity to mouse fibroblast-like cells. Moreover, in vitro cell culture studies using goat marrow stromal cells revealed that the macroporous hydroxyapatite/chitosan

composite is a suitable material that promotes attachment, proliferation, and differentiation into osteoblasts and chondrocytes. Additionally, three-layered porous materials of collagen, hydroxyapatite, and chitosan were produced and characterized as an artificial bone matrix (Wang et al. 2008b). When testing murine pre-osteoblast cell line (MC3T3-E1) grown on this matrix, the cells proliferated significantly more rapidly than cells grown on a pure chitosan matrix (Teng et al. 2008). In addition, higher levels of alkaline phosphatase (secreted by osteoblasts) were determined, which is indicative for bone regeneration. Similar results were obtained when osteoblasts were cultured on hydroxyapatite/chitosan nanocomposites and osteocalcin as a marker for late osteoblastic differentiation, and mineralized bone matrix formation was determined (Chesnutt et al. 2009). Further studies characterized hydroxyapatite/chitosan hybrids with additional blend materials such as montmorillonite (Katti et al. 2008), polylactic acid (Cai et al. 2009), cellulose and carboxymethyl cellulose (Liuyun et al. 2009; Jiang et al. 2013b), gelatin (Sellgren and Ma 2012; Maji et al. 2015; Lee et al. 2017), nylon 66 (Huang et al. 2011), polygalacturonic acid (Khanna et al. 2011), marine sponge collagen (Pallela et al. 2012), collagen (Wang et al. 2009), alginate (Jin et al. 2012; Kim et al. 2015; Liao et al. 2018), chondroitin sulfate (Venkatesan et al. 2012a; Hu et al. 2017), hyaluronic acid (Hu et al. 2017), fibroin (Lima et al. 2013; Ran et al. 2016; Ye et al. 2017), poly-3-hydroxybutyrate-co-3-hydroxyvalerate (Zhang et al. 2015b), fucoidan (Lowe et al. 2016), β-tricalcium phosphate (Shavandi et al. 2015; Oryan et al. 2017), graphene oxide (Yu et al. 2017), β-cyclodextrin (Shakir et al. 2016), β-1,3-glucan (Przekora and Ginalska 2017; Przekora et al. 2017), whitlockite (Zhou et al. 2017a), zoledronic acid (Lu et al. 2018), and zirconium dioxide (Balagangadharan et al. 2018). Also, three-dimensional hydroxyapatite/chitosan-carbon nanotube scaffolds were shown to be promising materials for bone regeneration (Im et al. 2012). Naturally, many of these combinations have been tested also in the absence of hydroxyapatite (Park et al. 2000a; Li et al. 2005; Jiang et al. 2006; Arpornmaeklong et al. 2008; Venkatesan et al. 2012b; Deng et al. 2013; Azevedo et al. 2014; Dinescu et al. 2014; Listoni et al. 2015; Georgopoulou et al. 2018; Koç Demir et al. 2018).

Several studies showed that various growth factors such as transforming growth factors (TGFs), vascular endothelial growth factors (VGEFs), bone morphogenic proteins (BMPs), insulin-like growth factors (IGFs), and platelet-derived growth factors (PDGFs) have major impacts on vascularization and osteoblast activities and thus have been employed to stimulate bone regeneration (Yun et al. 2012). However, there are limitations in maintaining therapeutic concentrations due to the short half-life of the growth factors in vivo. This can be effectively prevented by the controlled release of the growth factors from porous chitosan composite matrices, which have been demonstrated to stimulate bone formation. For instance, PDGF-BB is an important osteogenic growth factor in the process of bone regeneration, as it stimulates mesenchymal cell proliferation and differentiation and mediates chemotaxis of osteoblast. Park et al. (2000a, b) produced a porous chitosan or chondroitin-4-sulfate/chitosan sponges releasing PDGF-BB to stimulate bone regeneration. The release rate of PDGF-BB increased proportionally with increasing concentrations loaded onto the sponge, and PDGF-BB retained its chemotactic activity regardless of

being loaded onto the sponge or added freely to test solution (Park et al. 2000a). Finally, osteoblast proliferation was found to be stimulated in PDGF-BB-loaded chondroitin-4-sulfate/chitosan sponge compared with that of the unloaded sponge. PGFs have also been used in combination with other growth factors. As VEGF is known to prolong cell survival, osteoblast proliferation, differentiation, and migration next to its effects on angiogenesis, it has been suggested that the combined action of VEGF and PDGF can accelerate the bone healing process even more efficiently. De la Riva et al. (2010) established a system based on brushite-chitosan capable of controlling release kinetics for these two growth factors. After implanting the chitosan scaffolds loaded with the growth factors into rabbits with femur defects, release kinetics and tissue distribution of radiolabeled VEGF and PDGF were determined. Analyzing bone repair histologically revealed that the combined use of VEGF and PDGF promoted bone regeneration most effectively.

Also, the controlled release of IGF-1 and BMP-2 by the enzymatic degradation of the porous chitosan scaffold stimulates bone healing and regeneration in rabbits considerably (Nandi et al. 2013). When the chitosan particles were loaded only with one of the two growth factors, the effect was found to be more pronounced for IGF-1 than for BMP-2 infiltrated matrices. In a very recent study, chitosan/biphasic calcium phosphate scaffolds functionalized with BMP-2-encapsulated nanoparticles and the RGD tripeptide were produced using a desolvation technique (Gan et al. 2018). In vitro cell culture and in vivo implantation tests demonstrated that RGD and BMP-2 synergistically increased cell adhesion and spreading via integrin binding triggering differentiation of osteoblasts. Increased bone healing was also observed, when porous chitosan scaffolds were loaded with resolvin D1, a potent lipid immune modulator derived from both eicosapentaenoic acid, and implanted into rats with a femur defect (Vasconcelos et al. 2018). Obviously, resolving D1 administration in the acute phase of the innate immune response to the bio-implant had beneficial effects during bone tissue repair.

Impairment of the articular cartilage is frequently due to sport-related injury, disease, trauma, and tumor. If not treated successfully, it may result in osteoarthritis, which increasingly affects also younger individuals (Muzzarelli et al. 2012). In contrast to bone regeneration, cartilage healing is limited by the lack of vascularization and poor proliferation rates of chondrocytes. Injection of hyaluronan into the joints of arthritic patients is known to improve their function, as it restores viscoelasticity and flow of the synovial fluid, helps to normalize hyaluronan production, and finally reduces pain and inflammation. Chitosan easily forms polyelectrolyte complexes with hyaluronan and chondroitin sulfate, which are important building blocks particularly of the hyaline cartilage found on the surface of joints. Therefore, combinations of chitosan and hyaluronan and/or chondroitin sulfate may be useful in cartilage healing. In a first attempt to realize this idea, Kuo et al. (2015) synthesized a highly elastic, macroporous, and chitosan-containing gelatin/chondoitin-6-sulfate/hyaluronan (GCH) cryogel scaffold, which mimics the extracellular matrix composition of the cartilage. Furthermore, in vitro cell culture studies suggest that chondrocytes proliferate and redifferentiate within the porous matrix of the cryogels. Although chitosan reduces cell proliferation, it stimulates the secretion of sulfated

glycosaminoglycans and type II collagen. In addition, they performed in vivo studies culturing chondrocytes on the GCH chitosan cryogel and implanting the material into rabbits with an articular cartilage defect (Kuo et al. 2015). After 3 months, the defect in the chondrocytes/cryogel group was completely covered with semitransparent tissue, which had similar characteristics as the native cartilage. A large variety of other chitosan-based materials lacking glycosaminoglycans have been suggested as suitable scaffolds for cartilage tissue engineering and some of them have been tested as mesenchymal stem cell carriers. Such materials include scaffolds containing *N*,*N*-dicarboxymethyl chitosan (Mattioli-Belmonte et al. 1999), chitosan/gelatin and/or alginate complex (Xia et al. 2004; Li and Zhang 2005; Bhat et al. 2011), poly(L-lactide)/chitosan microspheres (Lao et al. 2008; Haaparanta et al. 2014), polyethylene oxide/chitin/chitosan scaffolds (Kuo and Ku 2008), genipin-cross-linked chitosan/silk fibroin sponges (Silva et al. 2008; Vishwanath et al. 2016), chitosan/polyester-based scaffolds (Alves da Silva et al. 2010), chitosan/collagen type I scaffolds (Gong et al. 2010), chitosan/poly(epsilon-caprolactone) blend scaffolds (Neves et al. 2011; Filova et al. 2016), chitosan/poly(l-glutamic acid) scaffolds (Zhang et al. 2013a, 2015a), polyvinyl alcohol/chitosan composite hydrogels (Dashtdar et al. 2015), poly(*N*-isopropylacrylamide)/chitosan hydrogels (Mellati et al. 2016), viscoelastic silk/chitosan microcomposite scaffolds (Chameettachal et al. 2017), and chitosan/graphene oxide polymer nanofibers (Cao et al. 2017).

As in the case of bone repair, strategies using various chitosan-based scaffolds loaded with growth factors such as TGFs (Kim et al. 2003; Choi et al. 2015), IGFs (Zhao et al. 2010), BMPs (Mattioli-Belmonte et al. 1999), and basic fibroblast growth factor (bFGF) (Tan et al. 2007) have been tested for cartilage repair. In an interesting pilot study, Qi et al. (2013) produced an injectable chitosan/polyvinyl alcohol gel and examined its structure and physicochemical properties. The resulting material exhibited low cytotoxicity and good biocompatibility. Next, the gel was mixed with rabbit bone marrow stromal cells (BMSCs) that were transfected with an adenovirus to produce TGF-b1, and rabbits with cartilage defects were injected with this mixture. After 16 weeks, the defects appeared to be fully repaired. The regenerated tissue was almost indistinguishable from the native cartilage. In another study, a demineralized bone matrix was conjugated with mesenchymal stem cell (MSC) E7 affinity peptide (EPLQLKM) and combined with a chitosan hydrogel for cartilage engineering. Cell culture and implantation experiments demonstrated that the developed material has a high chondrogenic capacity facilitating tissue repair of cartilage defects (Meng et al. 2015). In a more recently published study, the proliferation and differentiation of multipotent dental pulp stem cells into chondrocytes were investigated to generate cartilage-like material. In this case, a porous chitosan-xanthan gum matrix was employed as a scaffold and loaded with kartogenin to promote chondrogenic differentiation (Westin et al. 2017). The manufactured scaffold exhibited favorable characteristics for cartilage tissue engineering, such as high porosity, low cytotoxicity, and mechanical properties compatible with those characteristic of cartilage.

Very recently, Agrawal et al. (2018) reported the in vitro generation of cartilage-like material by seeding human mesenchymal stem cells on freeze-dried porous silk fibroin/chitosan scaffolds and culturing them in a spinner flask bioreactor under dynamic conditions. The team was successful in preparing a cartilage construct of 5 mm thickness, which roughly corresponds to the thickness of a native articular cartilage.

Due to its unique properties, chitosan has also emerged as a scaffold for potential applications in dental medicine. Chitosan-based hydrogels and nanocomposites have been used as anti-erosive and enamel-repairing additives in dentifrices and chewing gums (Shibasaki et al. 1994; Arnaud et al. 2010; Ganss et al. 2011; Ruan et al. 2014), for reduction of dental bacterial biofilm formation (Jahanizadeh et al. 2017), for guided tissue regeneration to treat periodontal diseases such as periodontitis (Ma et al. 2014; Lotfi et al. 2016), as dentin-bonding agent (Fawzy et al. 2013), as modification of dental restorative materials and implants (Petri et al. 2007; Ali et al. 2017; Ibrahim et al. 2017a), and as scaffold for stem cell-based tissue regeneration (Yang et al. 2012b; Asghari Sana et al. 2017; Soares et al. 2017a). Periodontitis is a chronic inflammation of the gum, which ultimately may lead to the loss of periodontal tissues and teeth (Pihlstrom et al. 2005). Current therapeutic strategies mainly rely on good oral hygiene (brushing and flossing), plaque removal, and in more severe cases local application of antibiotics and surgical intervention including open flap debridement, osseous surgery, as well as guided tissue and bone regeneration. Chitosan-based materials turned out to be very useful for periodontal tissue regeneration. Such materials comprise methylpyrrolidinone chitosan (Muzzarelli et al. 1993a), chitosan scaffolds coated with a bioactive hydroxyapatite (Ang et al. 2002; Coimbra et al. 2011; Fraga et al. 2011; Miranda et al. 2016), injectable thermosensitive chitosan/β-glycerophosphate/hydroxyapatite hydrogels (Chen et al. 2016), chitosan-based risedronate/zinc-hydroxyapatite intrapocket dental films (Khajuria et al. 2018), asymmetric chitosan/tripolyphosphate cross-linked membranes (Ma et al. 2014), porous chitosan/collagen scaffolds (Yang et al. 2012b), mucoadhesive electrospun chitosan and thiolated chitosan nanofibers (Samprasit et al. 2015), chitosan-coated titanium surfaces (Campos et al. 2015), chitosan modified glass ionomer restoratives (Petri et al. 2007), chitosan-intercalated montmorillonite/poly(vinyl alcohol) nanofibers (Ghasemi Hamidabadi et al. 2017), and polyhydroxybutyrate/chitosan/nano-bioglass nanofiber scaffolds (Hashemi-Beni et al. 2018).

In one of the first studies that used growth factors to promote dental pulp stem cell differentiation, porous chitosan/collagen scaffolds prepared by freeze-drying were used and loaded with a plasmid vector encoding the human BMP-7 gene (Yang et al. 2012b). The stem cells grown in this scaffold were successfully transfected by the plasmid vector, which led to the formation of BMP-7 triggering odontoblastic differentiation as indicated by the activation of specific marker genes encoding steocalcin, bone sialoprotein, dentin sialophosphoprotein, and dentin matrix protein 1. The chitosan/collagen scaffolds with stem cells were subcutaneously implanted into the back of BALB/c mice. After 4 weeks, the material was explanted and evaluated by immunohistochemistry. In the gene-activated scaffold group, there were still transfected cells detectable showing the upregulated gene expression when compared to pure scaffold groups.

14.6.5.2 Cutaneous Wound Healing

Cutaneous wound healing is a complex process in which the skin repairs itself. The process is divided into different stages, which include blood clotting (hemostasis), inflammation, cell migration and proliferation, and tissue remodeling (maturation). The wound healing process may be delayed or completely fail leading to non-healing chronic wounds, which are frequently found in patients with diabetes, venous or arterial diseases, infections, and age-related metabolic deficiencies. Bedsore and burns behave differently, as the healing process is complicated by coagulation, necrosis, and infections. Small, non-severe wounds may be treated with chitosan-containing ointments (Kweon et al. 2003), topical gels (Alsarra 2009), and/or wound dressings (Jayakumar et al. 2011). For instance, Kang et al. (2016) reported the synthesis of silver chloride nanoparticles stabilized with chitosan oligomer for an ointment that was tested on burn wound healing in a rat model. Burn wound healing of rats treated with this ointment was superior to rats treated with pure Vaseline or chitosan ointments. More severe wounds may require removal of necrotic tissue and surgical wound closure using suturing techniques. If the defects are too large to be covered in this way, autologous avascular mesh grafts, microvascular flap grafts, mikroskin grafts, and/or cultured epithelial grafts are transplanted to the wound site (Chua et al. 2016). However, surgical intervention is only possible up to a critical size. To cover large-sized skin defects, artificial grafts produced by tissue engineering techniques are required. This type of wound dressings must protect from infections, absorb excess exudates, and facilitate oxygen and nutrient exchange. In addition, the material must be nontoxic, non-allergenic, non-adherent, and biocompatible.

Chitosan-based materials are a good choice for wound dressings, as they fullfil most of the criteria mentioned above, and they are known to promote wound healing by activating platelets when getting into contact with blood (Periayah et al. 2013). Moreover, chitosan-based scaffolds can be loaded with growth factors to facilitate skin repair by promoting cell adhesion and proliferation (Lu et al. 2016). Several in vitro, preclinical and clinical studies actually demonstrated that chitosan-based hydrogels films, powders, and dressings, as well as artificial skins, accelerate wound healing and reepithelialization (Patrulea et al. 2015). However, the precise mechanism of action in promoting wound healing is still under debate. Next to chitosan-mediated immunomodulation, the type of functionalization contributes to wound healing.

Chitosan-based scaffolds used to promote wound healing comprise hydrogels, films, micro- and nanoparticles, nanocomposite materials, and micelles, and many biocompatible chitosan derivatives have been tested including N-carboxybutyl chitosan (Dias et al. 2010), hydroxybutyl chitosan (Hu et al. 2018), fluorinated methacrylamide chitosan (Wijekoon et al. 2013; Patil et al. 2016; Akula et al. 2017), and chitosan/polyvinyl alcohol materials (Charernsriwilaiwat et al. 2014; Wang et al. 2016b).

In addition, numerous chitosan hybrid materials have been synthesized for wound healing, which comprise chitosan or carboxymethyl chitosan/gelatin hydrogels (Huang et al. 2013; Patel et al. 2018), chitosan/heparin/poly(γ-glutamic acid) composite hydrogels (Zhang et al. 2018), chitosan-hyaluronan composite sponge scaffolds (Sanad and Abdel-Bar 2017; Tamer et al. 2018), heparin-chitosan complexes (Kratz et al. 1997; Kweon et al. 2003), chitosan-fibrin nanocomposites (Vedakumari et al. 2015), polyvinyl alcohol/chitosan/fibroin-blended sponges (Yeo et al. 2000), polyvinyl alcohol/starch/chitosan hydrogels with nano zinc oxide (Baghaie et al. 2017), poly(caprolactone)/chitosan/poly(vinyl alcohol) nanofibrous sponges (Gholipour-Kanani et al. 2014), chitosan/poly(ethylene glycol)-tyramine hydrogels (Lih et al. 2012), chitosan-alginate polyelectrolyte complexes (Wang et al. 2002; Hong et al. 2008; Caetano et al. 2015; Kong et al. 2016), porous keratin/chitosan scaffolds without and with zinc oxide (Tan et al. 2015; Zhai et al. 2018), nano-titanium oxide/chitosan complexes (Peng et al. 2008), chitosan/collagen hydrogels and sponges (Wang et al. 2008a; Cui et al. 2011; Ti et al. 2015), chitosan green tea polyphenol complexes (Qin et al. 2010, 2013), dextran hydrogels loaded with chitosan microparticles (Ribeiro et al. 2013), chitosan/polycaprolactone scaffolds (Bai et al. 2014; Zhou et al. 2017b), chitosan oleate ionic micelles (Dellera et al. 2014), castor oil polymeric films reinforced with chitosan/zinc oxide nanoparticles (Diez-Pascual and Diez-Vicente 2015), sponge-like nano-silver/zinc oxide-loaded chitosan composites (Lu et al. 2017), gellan gum-chitosan hydrogels (Shukla et al. 2016), chitosan-silica hybrid dressing materials (Park et al. 2017), chitosan/bentonite or tourmaline nanocomposites (Devi and Dutta 2017; Zou et al. 2017), chitosan/gelatin/chondroitin-4-sulfate films with and without zinc oxide (Cahu et al. 2017), chitosan/polyvinylpyrrolidone/cellulose nanowhiskers nanocomposites (Hasan et al. 2017), α-tocopherol-loaded chitosan oleate nanoemulsions (Bonferoni et al. 2018), chitosan-based liposome formulations (Mengoni et al. 2017), and electrospun chitosan/polyethylene oxide/fibrinogen biocomposites (Yuan et al. 2018).

Topical application of anti-inflammatory and antioxidant curcumin, which is a component of many curry powders, has been shown to promote wound healing, significantly preventing oxidative damage in tissues (Gopinath et al. 2004). Chitosan-alginate sponges have been used to deliver curcumin for dermal wound healing in rat. Loading curcumin onto the chitosan sponge enhanced the therapeutic healing effect when compared to other carriers like cotton gauze. Similarly, injectable nanocomposite hydrogels composed of curcumin, N,O-carboxymethyl chitosan, and oxidized alginate possess many characteristics that promote wound healing including exudate absorption and immobilization and activation of growth factors. Nano-curcumin, which is released slowly from the hydrogel in a sustained manner, evidently stimulates fibroblast proliferation, angiogenesis, and collagen production, supporting the healing process when tested in a mice model (Li et al. 2012b). Wound dressings made of chitosan/poly-γ-glutamic acid/pluronic/curcumin nanoparticles also promoted collagen formation and tissue regeneration (Lin et al. 2017), and collagen-alginate scaffolds impregnated with curcumin-loaded chitosan nanoparticles proved promising in the treatment of various pathological manifestations of diabetic wounds (Karri et al. 2016). Most recently, Zhao et al. (2018)

prepared a thermosensitive chitosan/β-glycerophosphate hydrogel loaded with β-cyclodextrin-curcumin and demonstrated improved healing of infected cutaneous wounds in rats, which may be due to the combination of antioxidative, antimicrobial, and anti-NF-κB signaling effects.

As silver has been demonstrated to have potent antimicrobial activities with no reports on bacterial resistances, several laboratories prepared chitosan wound dressings impregnated with silver to prevent wound infections and promote wound healing (Graham 2005). Indeed, a wound dressing composed of nano-silver and chitosan improved wound healing in rats better than a silver sulfadiazine dressing, which led to unwanted higher silver levels in the blood than the chitosan-silver dressing (Lu et al. 2008). In another study, Abdelgawad et al. (2014) combined silver nanoparticles that were embedded in chitosan with polyvinyl alcohol to produce antimicrobial nanofibrous material for wound dressing. The material with the highest chitosan-silver nanoparticle content was tested against *E. coli* and showed significant antibacterial activity. A combined antibacterial/tissue regeneration response triggered by functional chitosan-silver nanocomposites was also reported for thermal burns (Luna-Hernandez et al. 2017). To increase antibacterial activity wound dressings, several groups combined chitosan-silver-based materials with sulfadiazine, a sulfonamide antibiotic. Topical administration of chitosan-based hydrogels containing silver sulfadiazine improved burn and wound healing capacities in different studies (Nascimento et al. 2009; Chakavala et al. 2012; Aguzzi et al. 2014; Lee et al. 2014; El-Feky et al. 2017a). Besides inhibiting Gram-negative bacteria such as *E. coli*, chitosan-based dressings carrying silver sulfadiazine also inhibited the growth of Gram-positive bacteria as well as fungi such as *C. albicans* on an infected wound (El-Feky et al. 2017b).

Several studies reported that wound healing is accelerated when chitosan hydrogels are combined with adipose-derived or mesenchymal stem cells. Altman et al. (2009) grew human adipose-derived stem cells onto a chitosan/silk fibroin scaffolds and used it in a cutaneous wound healing model. They found that this regimen significantly enhanced wound healing, increasing micro-vascularization and differentiation into epidermal epithelial cells. In another study, an artificial dermis was fabricated by culturing human adipose-derived stem cells on a poly (L-glutamic acid)/chitosan scaffold (Shen et al. 2013b). Notably, the seeded stem cells maintained their capability to proliferate, produce extracellular matrix, and secrete cytokines including transforming growth factor β1 and vascular endothelial growth factor. The artificial dermis was used to cover wounds that have been generated before in streptozotocin-induced diabetic mice. The artificial dermis significantly accelerated wound closure and healing in diabetic mice. Tong et al. (2016) used a different stem cell-based strategy to generate a skin substitute promoting wound healing. They manufactured a collagen-chitosan sponge scaffold to culture bone marrow-derived stem cells, which were pre-treated by hypoxia to induce the expression of pro-angiogenic cytokines. When the skin substitute was used to treat wounds generated in diabetic rats with hindlimb ischemia, wound healing was enhanced in comparison to scaffold-only controls or skin substitutes that were generated with normoxic stem cells.

A novel strategy for wound healing involving exosomes was reported recently. Exosomes are small secretory membrane vesicles that are involved in cell-to-cell communication. Stem cell-derived exosomes can improve wound healing and promote skin regeneration by stimulating cell proliferation and migration, angiogenesis, and reepithelization and modulating immune responses (Phinney and Pittenger 2017). Based on these observations, Shi et al. (2017b) isolated exosomes derived from gingival mesenchymal stem cells and encapsulated them in chitosan/silk hydrogel sponge. The combination of the exosomes and hydrogel was effective in promoting skin wound healing in a diabetic rat model by inducing reepithelialization, vascularization, and neuronalization paralleled by the remodeling of the extracellular matrix.

14.6.5.3 Ocular Surface Reconstruction

Corneal damage can be the result of different diseases and injuries and may lead to a reduction or even loss of vision. Currently, the only therapy to cure vision loss after irreversible corneal damage is a surgical procedure where the cornea is replaced by donated corneal tissue. Frequently, the entire cornea is replaced in a surgical intervention called penetrating keratoplasty. As there is a shortage of corneal donors and there is a certain risk associated with the surgery and graft rejection, new types of corneal replacements are examined including materials containing chitosan. Actually, topical application of chitosan or chitosan/*N*-acetylcysteine to the eye is known to enhance corneal epithelial proliferation and migration during the wound healing in rabbits (Fischak et al. 2017). This process appears to involve the activation of the extracellular signal-regulated kinases (ERK) pathway (Cui et al. 2017). Another study evaluated the effects on corneal epithelium regeneration by combination of exogenous recombinant human serum-derived factor-1α (rhSDF-1α) with a thermosensitive chitosan/gelatin hydrogel and analyzed the underlying mechanism (Tang et al. 2017). Conducting in vitro experiments, the team showed that rhSDF-1α enhanced stem cell proliferation, chemotaxis, and migration, as well as the expression of related genes in limbal epithelial and mesenchymal stem cells (LESCs and MSCs). In vivo experiment using an alkali burn-injury rat model further revealed enhanced corneal epithelium regeneration and increased local expression of growth factors known to be essential for corneal epithelium repair. The underlying mechanism by which rhSDF-1α released from the chitosan/gelatin hydrogel stimulates corneal regeneration may involve activation of C-X-C chemokine receptor type 4 (CXCR4) expressing cells (LESCs and MSCs) and chemotactic attraction of these cells to the sites of lesion via the binding of rhSDF-1α to the CXCR4 receptor.

Chen et al. (2005) had considered a tissue-engineering scaffold made of collagen, chitosan, and hyaluronic acid as a potential replacement for corneal tissue. To study cytocompatibility in vitro, they cultured rabbit limbal corneal epithelial cells, corneal endothelial cells, and keratocytes on the polymer complexes and demonstrated that the corneal cells were able to attach, migrate, and proliferate. To evaluate

biocompatibility in vivo, they implanted the polymer complex into the corneal stroma of rabbit eyes and inspected ocular reactions. Overall, the polymer complexes exhibited transparency and good biocompatibility, as they were degraded and absorbed within the corneal tissue while maintaining transparency. In another study, poly(ethylene glycol)-stabilized carbodiimide-cross-linked collagen-chitosan hydrogels were tested for biocompatibility and host-graft integration. For this purpose, Rafat et al. (2008) performed in vitro and in vivo studies demonstrating excellent biocompatibility when analyzing human corneal cells, dorsal root ganglia from chick embryos, or subcutaneous implants. The hydrogel scaffold was also studied as corneal substitute by implanting it into the cornea of pig eyes and monitoring them for 12 months. The substitute was seamlessly integrated into the cornea with regeneration of host corneal epithelium, stroma, and nerves. Liang et al. (2011) prepared a blend membrane composed of hydroxyethyl-chitosan, gelatin, and chondroitin sulfate. The membrane exhibited good transparency, ion and glucose permeability, and cytocompatibility for corneal endothelial cells, which formed a monolayer on the membrane in cell culture. In vivo animal experiments revealed that the membranes were characterized by biodegradability and a good histocompatibility suggesting that the membranes may be employed as carriers for corneal endothelial cell transplantation. Similar results were obtained for chitosan/polycaprolactone, chitosan/poly(ethylene glycol), silk fibroin/chitosan, carboxymethyl chitosan/gelatin/hyaluronic acid, as well as hydroxyethyl-chitosan blend membranes, which were tested as potential scaffolds and carriers for bovine, ovine, and rabbit corneal endothelial cells, respectively (Wang et al. 2012b; Guan et al. 2013; Ozcelik et al. 2013; Liang et al. 2014; Xu et al. 2018).

Using an allogeneic rabbit model of stromal destruction caused by bacterial keratitis, Chou et al. (2018) tested the hypothesis that intra-stromal injection of keratocyte spheroids manufactured on chitosan coatings has higher therapeutic efficacies than eye drop instillations or isolated cell injections. The results of clinical observations and histological studies performed 2 weeks after the surgical intervention showed that, in comparison to a treatment relying only on antibiotics, intra-stromal grafting of keratocytes provides additional benefits due to improved preservation of cellular phenotypes, secretion of collagen matrix, and retention of the graft.

In a stem cell therapeutic approach published by Chien et al. (2012), human corneal fibroblasts (keratocytes) were reprogrammed into human-induced pluripotent stem cells (iPSC) using a feeder cell-free culturing system. To increase iPSC delivery and engraftment, the researchers generated an injectable thermogelling carboxymethyl-hexanoyl chitosan nanogel with seeded iPSCs and showed that viability and pluripotent properties of the reprogrammed iPSCs were maintained in the hydrogel system. They further demonstrated that the reprogrammed iPSCs grown on the hydrogel could be used to enhance corneal wound healing efficiently. This strategy opens the possibility for a personalized therapy for human corneal damage when iPSCs are reprogrammed from cells derived from corneal surgical residues.

14.6.5.4 Neuronal Regeneration

The plethora of favorable characteristics of chitosan outlined in this chapter prompted many researchers around the world to employ chitosan-based materials also in the reconstruction of peripheral nerves to improve healing of nerve damage caused by accidents or diseases. Although therapeutic interventions to peripheral nerve repair have yielded some progress during the past years, a full recovery of nerve function is usually not achieved. Current therapies mostly rely on microsurgical techniques, which either try to directly establish a tension-free connection between the ends of severed nerves (epineural, fascicular, and grouped fascicular repair) or bridge larger nerve defects by autologous grafts (cable grafts, trunk grafts, and vascularized nerve grafts) (Matsuyama et al. 2000; Houschyar et al. 2016). The various neurosurgical techniques used to connect nerve ends are challenging, and the therapeutic results are frequently not satisfactory. Many studies have provided evidence that various types of conduits, such as veins, pseudo-sheaths, and bioabsorbable tubes, are helpful in bridging shorter gaps by promoting nerve regeneration. After bridging nerve gaps with hollow conduits, the lumen between the nerve ends becomes filled with fibrin, and macrophages and other cells are attracted, which create a favorable microenvironment for vascularization and neuronalization.

Chitosan-based conduits have been extensively analyzed for this purpose. An early electrophysiological and histological study on nerve regeneration using rat sciatic nerve defects demonstrated that pure chitosan/collagen conduits were superior in bridging 1 cm nerve defects to that of control groups (Wei et al. 2003). The chitosan/collagen film was found to be degraded about 3 months after the surgery. In a methodologically similar study, Wang et al. (2005) generated an artificial nerve graft composed of a chitosan conduit and tested them to bridge a 3 cm dog sciatic nerve defect. In contrast to the previous study, the conduit was filled with longitudinally arranged filaments of polyglcyolic acid. The team found that the sciatic nerve trunk was successfully reconstructed in dogs treated with the chitosan/polyglycolic acid graft with reinnervation of the target skeletal muscle. In a case report on a 55-year-old man with a 3 cm median nerve defect in the distal forearm, implantation of chitosan/polyglycolic acid graft promoted nerve regeneration and functional reconstruction, so that the patient was able after 36 months to fully use the injured hand during daily activities (Gu et al. 2012). Other chitosan-based conduits have been successfully used to guide and promote nerve generation in various in vitro and in vivo models. These materials include chitosan/gelatin and chitosan/poly(L-lysine) polyelectrolyte-based scaffolds (Martin-Lopez et al. 2012), chitosan-gold nanocomposites (Lin et al. 2008), chitosan/polylactic acid films (Xie et al. 2008), chitosan/poly(3-hydroxybutyrate-co-3-hydroxyvalerate) nanofibers (Biazar and Heidari Keshel 2014), porous chitosan-poly(p-dioxanone)/silk fibroin copolymers (Wu et al. 2015), poly(D,L-lactide-co-glycolide) sleeves with multifilament chitosan yarn or a microcrystalline chitosan sponge core (Wlaszczuk et al. 2016), chitosan/hyaluronic acid hybrid materials (Li et al. 2018a), porous

chitosan-γ-glycidoxypropyltrimethoxysilane hybrid membranes (Shirosaki et al. 2014), hydroxyapatite-coated tendon chitosan tubes with adsorbed laminin peptides (Itoh et al. 2003), and hyaluronic acid doped-poly(3,4-ethylenedioxythiophene) nanoparticles in a chitosan/gelatin matrix (Wang et al. 2017b).

An evident upgrade of chitosan-based conduits is lumenal loading with neurotrophic factors such as nerve growth factor (NGF), ciliary neurotrophic factor (CNF), or brain-derived neurotrophic factor (BDNF), which are all secreted by Schwann cells that support growth of neuronal cells (Houschyar et al. 2016). In addition, fibroblast growth factor (FGF), glial growth factor (GGF), and vascular endothelial growth factor (VEGF) were reported to have positive effects on nerve regeneration.

Yang et al. (2011) immobilized NGF on genipin-cross-linked chitosan and tested the material for cytotoxicity using primary cultured Schwann cells and for neuronal differentiation of PC12 cells in response to NGF release. Subsequently, Wang et al. (2012a) demonstrated that genipin-cross-linked chitosan conduits loaded with NGF can be successfully used to bridge 1-cm-long sciatic nerve defects in rats as revealed by electrophysiological assessment, behavioral analysis, and histological examination 24 weeks after the surgery. Similar results were obtained, when NGF-containing microspheres were implanted into chitosan conduits to repair a 1 cm defect of the facial nerve in rabbits (Liu et al. 2013). In another NGF-based approach, Chao et al. (2016) combined an autologous vein conduit with a chitosan-β-glycerophosphate-NGF hydrogel. The researchers surgically reconstructed a 5-mm-long defect of a rat facial nerve with an autologous vein and then injected the chitosan-β-glycerophosphate-NGF hydrogel into the lumen of the conduit. Facial nerve regeneration was as efficient as in control groups, which were transplanted with an autologous nerve, but significantly better than in control groups where the vein conduit was injected with NGF only.

Shen et al. (2010) used a polylactic/polyglycolic acid chitosan nerve conduit loaded with CNF to repair larger canine tibial nerve defects in crossbred dogs and evaluated nerve regeneration by general inspection, electrophysiological, immunological, and histological analyses 3 months after the surgery. Nerve regeneration was significantly improved in animals that were treated with CNF-loaded polylactic/polyglycolic acid chitosan conduits when compared to groups treated with the polylactic/polyglycolic acid chitosan conduits. The results were similar to controls groups that were treated with autologous nerve grafts, suggesting that the artificial nerve conduit is a promising alternative for bridging nerve defects.

Furthermore, Zhao et al. (2014) hypothesized that tacrolismus-loaded chitosan enhances peripheral nerve regeneration through modulation of the expression profiles of neurotrophic factors. To test this hypothesis, they loaded tacrolismus onto chitosan conduits and examined nerve regeneration of sciatic nerve injury in a rat model. They found significant regeneration of sciatic nerves with normal morphology but higher density of myelinated nerve fibers in rats treated with tacrolismus-loaded chitosan. The underlying mechanism seems to involve BDNF signaling, because nerve regeneration was paralleled by an increased expression of BDNF and its corresponding receptor (TrkB) in the motor neurons in the spinal cord.

The membrane-bound cell adhesion molecule L1 is known to promote neurite growth and prevent neuronal apoptosis, a function which can be mimicked by a recombinant chimeric version of this molecule called L1-Fc (Roonprapunt et al. 2003). Loading L1-Fc to an artificial chitosan/polyglycolic acid conduit, Xu et al. (2004) studied guided regeneration of rat optic nerves. They found that the implanted chitosan/polyglycolic acid conduit was degraded and absorbed. When L1-Fc loaded conduits were implanted to bridge a defect caused by surgical intervention, axonal regeneration and remyelination were significantly improved when compared to control groups that were treated with conduits lacking L1-Fc.

Nerve regeneration can be additionally promoted using chitosan-based scaffolds as conduits seeded with stem cells that express neurotrophic factors and can differentiate into nerve cells. Zheng and Cui (2010) tested chitosan conduits of such kind combined with rat bone marrow mesenchymal stem cells to evaluate their potential for the reconstruction of 8-mm-long rat sciatic nerve defects. They demonstrated that the combination of chitosan and mesenchymal stem cells alone was sufficient to improve nerve regeneration and functional recovery. Moreover, some of the mesenchymal stem cells were found to have differentiated into neural stem cells. Similar results were obtained when injured rat sciatic nerves were treated in this way, and the nerve repair was monitored electrophysiologically and histomorphologically (Moattari et al. 2018) or by noninvasive magnetic resonance neurographic imaging (Liao et al. 2012). In addition, chitosan-coated poly-3-hydroxybutyrate conduits combined with human bone marrow mesenchymal stem cells were recently shown to be efficient in promoting nerve regeneration in this rat model of sciatic nerve injury (Ozer et al. 2018). Improved nerve regeneration was also reported for chitosan/poly(lactic-co-glycolic acid) scaffolds seeded with autologous bone marrow mesenchymal stem cells to treat injuries of dog sciatic nerves and rhesus monkey median nerves (Xue et al. 2012; Hu et al. 2013). In another approach, Zhu et al. (2015) used chitosan conduits filled with bone marrow mesenchymal stem cells and evaluated nerve regeneration and neuronal survival when injured lumbosacral nerves were bridged with this material. They found that this treatment enhanced sacral nerve regeneration and motor function 6 and 12 weeks after the surgery. Moreover, the mesenchymal stem cells prevented cell death of motor neurons in the anterior horn of the spinal cord, thereby improving the motor function in rats treated with the mesenchymal stem cell-seeded chitosan conduit. Finally, a clinical study performed with 14 patients suggests that defects in chronic spinal cord injury can be successfully bridged with peripheral nerve grafts combined with a chitosan-laminin scaffold and co-transplanted bone marrow-derived mesenchymal stem cells, which enhanced recovery (Amr et al. 2014).

Using chitosan/silk fibroin scaffolds grafts seeded with adipose-derived stem cells, Wei et al. (2011) examined regeneration of surgically injured rat sciatic nerves. Implantation of this conduit significantly improved axonal regeneration and functional recovery in comparison to control groups. The positive effect was partially attributed to the differentiation of adipose-derived stem cells into Schwann cells, which additionally secrete neurotrophic factors and prevent apoptosis. Nie et al. (2014) investigated axonal regeneration and remyelination using a chitosan/gelatin-

based conduit combined with TGF-β1 and Schwann cells. For this purpose, they bridged a 10-mm defect of a rat sciatic nerve and examined nerve regeneration based on functional recovery, electrophysiological measurements, retrograde labeling, and immunohistochemical analysis. The obtained data indicate satisfactory functional recovery of the injured sciatic nerve.

Meyer et al. (2016) filled chitosan (5% degree of acetylation) conduits with a gel containing hyaluronic acid and laminin (NVR-gel) and added genetically modified neonatal rat Schwann cells as cellular delivery system for neurotrophic factors. Testing the chitosan conduits in the rat sciatic nerve model revealed that the chitosan conduit, which only is filled with the NVR-gel, was insufficient to promote nerve regeneration in contrast to autologous nerve grafts. Notably, delivery of FGF by seeded Schwann cells genetically modified to overexpress this factor improved nerve regeneration significantly. Unexpectedly, Schwann cells expressing GDNF did not show positive effects in this experimental setup. Recently, Zhu et al. (2017) used skin-derived precursor Schwann cells to seed chitosan/silk scaffolds for bridging a 10-mm-long rat sciatic nerve gap. The artificial graft exhibited significant promoting effects on peripheral nerve repair and hence constitutes an alternative to other stem cell-based approach promoting nerve regeneration.

14.7 Concluding Remarks

Numerous studies reported favorable effects of chitosan-based materials for a wide range of applications. Doubtless, the controlled and targeted delivery of drugs to specific tissues has a great potential in biomedicine, and first clinical trials with chitosan-based drug carrier systems revealed promising results for the therapy of a variety of diseases including diabetes and cancer and also mainly because adverse side effects are reduced. The antimicrobial activity of chitosan and its derivatives is particularly important when the polymer is used for textile fabrication, food packaging, wound dressings, and tissue engineering. However, the underlying mechanism of antimicrobial activity is not fully understood. One prominent explanation is the assumed interaction of chitosan's positively charged amine groups with the negatively charged surface of bacteria and fungi, which might impair the movement of ions across membranes and hence disrupt cellular integrity. Although the proposed mechanisms seem plausible, there is a clear lack of experimental data that would provide evidence at a molecular level reminding us to continue basic research on the mode of actions. The studies conducted so far indicate that the antimicrobial activity of pure chitosan is not sufficient to prevent microbial infections completely in vivo. However, chitosan and its derivatives can be combined with other antimicrobial compounds including essential oils (Krausz et al. 2015), polyphenols (Madureira et al. 2015), tretinoin (Ridolfi et al. 2012), metal ions (Sanpui et al. 2008; Tran et al. 2010), lysozyme (Wu et al. 2017), or antibodies (Jamil et al. 2016), to prevent bacterial of fungal infections. Thus, chitosan appears to be an ideal

adjuvant polymer for design and production of new materials exhibiting intrinsic antimicrobial properties for a large variety of potential applications in the chemical, pharmaceutical, food, and textile industry. Similarly, the observed immune-stimulatory effects of chitosan need further investigation, as there may be a certain risk to develop allergic or even anaphylactic reactions after oral ingestion (Kato et al. 2005). However, it has to be noted that overall the beneficial characteristics exceed possible side effects due to some allergic potential. Finally, the antitumor activity of chitosan also needs to be analyzed in more detail. Recently, Li et al. (2018b) provided some evidence indicating that chitosan activates dendritic cells, which subsequently secrete pro-inflammatory cytokines and thereby enhance immune surveillance by natural killer cells. Accordingly, the antitumor effects of chitosan can be enhanced by specifically targeting dendritic cells by attaching mannose to the surface of chitosan nanoparticles (Shi et al. 2017a). Different pattern recognition receptors that are expressed on the surface of dendritic cells are potential receptors for chitosan. This includes Toll-like receptors, C-type lectin receptors, and other molecules, which are known to recognize specific molecular patterns, particularly those associated with pathogens. However, currently it is not known how dendritic cells recognize chitosan. In summary, it has to be noted that chitosan is a highly promising material for a variety of applications in industry and medicine. While chitosan-based materials have been commercially launched as packaging and coating material in food industry, as an ingredient in cosmetics, and as ion exchanger in water treatment and are approved for human dietary use and wound dressing, their commercial applications in medicine as drug delivery systems or scaffold for tissue engineering are pending. Nevertheless, there are clinical phase 2/3 trials, and depending on their outcome, some products may reach first approval by the health authorities in near future.

Acknowledgment The authors are grateful to Subbaratnam Muthukrishnan for critically reading the manuscript.

References

Abbasian M, Jaymand M, Niroomand P, Farnoudian-Habibi A, Karaj-Abad SG (2017) Grafting of aniline derivatives onto chitosan and their applications for removal of reactive dyes from industrial effluents. Int J Biol Macromol 95:393–403

Abdel-Aziz HMM, Hasaneen MNA, Omer AM (2016) Nano chitosan-NPK fertilizer enhances the growth and productivity of wheat plants grown in sandy soil. Span J Agric Res 14:e0902. https://doi.org/10.5424/Sjar/2016141-8205

Abdelgawad AM, Hudson SM, Rojas OJ (2014) Antimicrobial wound dressing nanofiber mats from multicomponent (chitosan/silver-NPs/polyvinyl alcohol) systems. Carbohydr Polym 100:166–178

Afkhami A, Hashemi P, Bagheri H, Salimian J, Ahmadi A, Madrakian T (2017) Impedimetic immunosensor for the label-free and direct detection of botulinum neurotoxin serotype A using Au nanoparticles/graphene-chitosan composite. Biosens Bioelectron 93:124–131

Agrawal P, Pramanik K, Biswas A, Ku Patra R (2018) *In vitro* cartilage construct generation from silk fibroin- chitosan porous scaffold and umbilical cord blood derived human mesenchymal stem cells in dynamic culture condition. J Biomed Mater Res A 106:397–407

Aguzzi C, Sandri G, Bonferoni C, Cerezo P, Rossi S, Ferrari F, Caramella C, Viseras C (2014) Solid state characterisation of silver sulfadiazine loaded on montmorillonite/chitosan nanocomposite for wound healing. Colloid Surf B 113:152–157

Ahire VJ, Sawant KK, Doshi JB, Ravetkar SD (2007) Chitosan microparticles as oral delivery system for tetanus toxoid. Drug Dev Ind Pharm 33:1112–1124

Ahmad M, Nirmal NP, Danish M, Chuprom J, Jafarzedeh S (2016) Characterisation of composite films fabricated from collagen/chitosan and collagen/soy protein isolate for food packaging applications. RSC Adv 6:82191–82204

Ahmed RA, Fekry AM (2013) Preparation and characterization of a nanoparticles modified chitosan sensor and its application for the determination of heavy metals from different aqueous media. Int J Electrochem Sci 8:6692–6708

Ahsan SM, Thomas M, Reddy KK, Sooraparaju SG, Asthana A, Bhatnagar I (2018) Chitosan as biomaterial in drug delivery and tissue engineering. Int Biol Macromol 110:97–109

Aider M (2010) Chitosan application for active bio-based films production and potential in the food industry: review. LWT – Food Sci Technol 43:837–842

Akhtar MA, Hayat A, Iqbal N, Marty JL, Nawaz MH (2017) Functionalized graphene oxide-polypyrrole-chitosan (fGO-PPy-CS) modified screen-printed electrodes for non-enzymatic hydrogen peroxide detection. J Nanopart Res 19:334. https://doi.org/10.1007/S11051-017-4029-X

Akula S, Brosch IK, Leipzig ND (2017) Fluorinated methacrylamide chitosan hydrogels enhance cellular wound healing processes. Ann Biomed Eng 45:2693–2702

Ali SW, Rajendran S, Joshi M (2011) Synthesis and characterization of chitosan and silver loaded chitosan nanoparticles for bioactive polyester. Carbohydr Polym 83:438–446. https://doi.org/10.1016/j.carbpol.2010.08.004

Ali A, Zahid N, Manickam S, Siddiqui Y, Alderson PG (2014) Double layer coatings: a new technique for maintaining physico-chemical characteristics and antioxidant properties of dragon fruit during storage. Food Bioprocess Technol 7:2366–2374

Ali S, Sangi L, Kumar N (2017) Exploring antibacterial activity and hydrolytic stability of resin dental composite restorative materials containing chitosan. Technol Health Care 25:11–18

Alix S et al (2013) Active pseudo-multilayered films from polycaprolactone and starch based matrix for food-packaging applications. Eur Polym J 49:1234–1242

Almodovar J, Kipper MJ (2011) Coating electrospun chitosan nanofibers with polyelectrolyte multilayers using the polysaccharides heparin and *N,N,N*-trimethyl chitosan. Macromol Biosci 11:72–76

Al-Mokaram AMAAA, Yahya R, Abdi MM, Mahmud HNME (2017) The development of non-enzymatic glucose biosensors based on electrochemically prepared polypyrrole-chitosan-titanium dioxide nanocomposite films. Nanomaterials 7:129. https://doi.org/10.3390/Nano7060129

Al-Naamani L, Dobretsov S, Dutta J (2016) Chitosan-zinc oxide nanoparticle composite coating for active food packaging applications. Innovative Food Sci Emerg Technol 38:231–237

Alsarra IA (2009) Chitosan topical gel formulation in the management of burn wounds. Int Biol Macromol 45:16–21

Altman AM, Yan Y, Matthias N, Bai X, Rios C, Mathur AB, Song YH, Alt EU (2009) IFATS collection: Human adipose-derived stem cells seeded on a silk fibroin-chitosan scaffold enhance wound repair in a murine soft tissue injury model. Stem Cells 27:250–258

Alves da Silva ML, Crawford A, Mundy JM, Correlo VM, Sol P, Bhattacharya M, Hatton PV, Reis RL, Neves NM (2010) Chitosan/polyester-based scaffolds for cartilage tissue engineering: assessment of extracellular matrix formation. Acta Biomater 6:1149–1157

Amouzgar P, Salamatinia B (2015) A short review on presence of pharmaceuticals in water bodies and the potential of chitosan and chitosan derivatives for elimination of pharmaceuticals. J Mol Genet Med S4:001. https://doi.org/10.4172/1747-0862.S4-001

Amr SM, Gouda A, Koptan WT, Galal AA, Abdel-Fattah DS, Rashed LA, Atta HM, Abdel-Aziz MT (2014) Bridging defects in chronic spinal cord injury using peripheral nerve grafts combined with a chitosan-laminin scaffold and enhancing regeneration through them by co-transplantation with bone-marrow-derived mesenchymal stem cells: case series of 14 patients. J Spinal Cord Med 37:54–71

An J, Luo Q, Yuan X, Wang D, Li X (2011) Preparation and characterization of silver-chitosan nanocomposite particles with antimicrobial activity. J Appl Polymer Sci 120:3180–3189

Anantha RK, Kota S (2016) An evaluation of the major factors influencing the removal of copper ions using the egg shell (*Dromaius novaehollandiae*): chitosan (*Agaricus bisporus*) composite. 3 Biotech 6:83. https://doi.org/10.1007/s13205-016-0381-2

Ang TH, Sultana FSA, Hutmacher DW, Wong YS, Fuh JYH, Mo XM, Loh HT, Burdet E, Teoh SH (2002) Fabrication of 3D chitosan–hydroxyapatite scaffolds using a robotic dispensing system. Mater Sci Eng C 20:35–42

Antoniraj MG, Tisha SA, Mahesh A, Shanmugarathinam A, Kandasamy R (2018) Synthesis and characterization of cystamine-conjugated chitosan-SS-mPEG based 5-Fluorouracil loaded polymeric nanoparticles for redox responsive drug release. Eur J Pharm Sci 116:37–47

Anusuya S, Banu KN (2016) Silver-chitosan nanoparticles induced biochemical variations of chickpea (*Cicer arietinum* L.). Biocatal Agric Biotechnol 8:39–44

Aranaz I, Gutierrez MC, Ferrer ML, del Monte F (2014) Preparation of chitosan nanocomposites with a macroporous structure by unidirectional freezing and subsequent freeze-drying. Mar Drugs 12:5619–5642

Aranaz I, Acosta N, Civera C, Elorza B, Mingo J, Castro C, Gandía DM, Heras Caballero A (2018) Cosmetics and cosmeceutical applications of chitin, chitosan and their derivatives. Polymers 10:213. https://doi.org/10.3390/polym10020213

Araújo BR, Romao LPC, Doumer ME, Mangrich AS (2017) Evaluation of the interactions between chitosan and humics in media for the controlled release of nitrogen fertilizer. J Environ Manage 190:122–131

Arca HC, Gunbeyaz M, Senel S (2009) Chitosan-based systems for the delivery of vaccine antigens. Expert Rev Vaccines 8:937–953

Arkoun M, Daigle F, Heuzey MC, Ajji A (2017) Mechanism of action of electrospun chitosan-based nanofibers against meat spoilage and pathogenic bacteria. Molecules 22:585. https://doi.org/10.3390/molecules22040585

Arnaud TM, de Barros Neto B, Diniz FB (2010) Chitosan effect on dental enamel de-remineralization: an *in vitro* evaluation. J Dent 38:848–852

Arpornmaeklong P, Pripatnanont P, Suwatwirote N (2008) Properties of chitosan-collagen sponges and osteogenic differentiation of rat-bone-marrow stromal cells. Int J Oral Max Surg 37:357–366

Arya V, Philip L (2016) Adsorption of pharmaceuticals in water using Fe_3O_4 coated polymer clay composite. Microporous Mesoporous Mater 232:273–280

Asghari Sana F, Capkin Yurtsever M, Kaynak Bayrak G, Tuncay EO, Kiremitci AS, Gumusderelioglu M (2017) Spreading, proliferation and differentiation of human dental pulp stem cells on chitosan scaffolds immobilized with RGD or fibronectin. Cytotechnology 69:617–630

Azevedo AS, Sá MJ, Fook MV, Neto PI, Sousa OB, Azevedo SS, Teixeira MW, Costa FS, Araújo AL (2014) Use of chitosan and beta-tricalcium phosphate, alone and in combination, for bone healing in rabbits. J Mater Sci Mater Med 25:481–486

Babaei A, Babazadeh M (2011) Multi-walled carbon nanotubes/chitosan polymer composite modified glassy carbon electrode for sensitive simultaneous determination of levodopa and morphine. Anal Methods 3:2400–2405

Babaei A, Afrasiabi M, Babazadeh M (2010) A glassy carbon electrode modified with multiwalled carbon nanotube/chitosan composite as a new sensor for simultaneous determination of acetaminophen and mefenamic acid in pharmaceutical preparations and biological samples. Electroanal 22:1743–1749

Babaei A, Babazadeh M, Momeni HR (2011a) A sensor for simultaneous determination of dopamine and morphine in biological samples using a multi-walled carbon nanotube/chitosan composite modified glassy carbon electrode. Int J Electrochem Sci 6:1382–1395

Babaei A, Garrett DJ, Downard AJ (2011b) Selective simultaneous determination of paracetamol and uric acid using a glassy carbon electrode modified with multiwalled carbon nanotube/chitosan composite. Electroanal 23:417–423

Bader AR, Li T, Wang W, Kohane DS, Loscalzo J, Zhang YY (2015) Preparation and characterization of SDF-1alpha-chitosan-dextran sulfate nanoparticles. J Vis Exp:52323. https://doi.org/10.3791/52323

Baghaie S, Khorasani MT, Zarrabi A, Moshtaghian J (2017) Wound healing properties of PVA/starch/chitosan hydrogel membranes with nano Zinc oxide as antibacterial wound dressing material. J Biomater Sci Polym Ed 28:2220–2241

Bai MY, Chou TC, Tsai JC, Yu WC (2014) The effect of active ingredient-containing chitosan/polycaprolactone nonwoven mat on wound healing: *in vitro* and *in vivo* studies. J Biomed Mater Res A 102:2324–2333

Balagangadharan K, Viji Chandran S, Arumugam B, Saravanan S, Devanand Venkatasubbu G, Selvamurugan N (2018) Chitosan/nano-hydroxyapatite/nano-zirconium dioxide scaffolds with miR-590-5p for bone regeneration. Int Biol Macromol 111:953–958

Bano I, Arshad M, Yasin T, Ghauri MA, Younus M (2017) Chitosan: A potential biopolymer for wound management. Int Biol Macromol 102:380–383

Basaran E, Yazan Y (2012) Ocular application of chitosan. Expert Opin Drug Deliv 9:701–712

Bashari A, Hemmatinejad N, Pourjavadi A (2017) Smart and fragrant garment via surface modification of cotton fabric with cinnamon oil/stimuli responsive PNIPAAm/chitosan nano hydrogels. IEEE Trans Nanobiosci 16:455–462

Bashir S, Teo YY, Naeem S, Ramesh S, Ramesh K (2017) pH responsive N-succinyl chitosan/Poly (acrylamide-co-acrylic acid) hydrogels and *in vitro* release of 5-fluorouracil. PloS One 12: e0179250. https://doi.org/10.1371/journal.pone.0179250

Benhamou N, Lafontaine PJ, Nicole M (1994) Induction of systemic resistance to *Fusarium* crown and root-rot in tomato plants by seed treatment with chitosan. Phytopathology 84:1432–1444

Berger J, Reist M, Mayer JM, Felt O, Peppas NA, Gurny R (2004) Structure and interactions in covalently and ionically crosslinked chitosan hydrogels for biomedical applications. Eur J Pharm Biopharm 57:19–34

Bhaskara Reddy MV, Arul J, Angers P, Couture L (1999) Chitosan treatment of wheat seeds induces resistance *to Fusarium graminearum* and improves seed quality. J Agric Food Chem 47:1208–1216

Bhat S, Tripathi A, Kumar A (2011) Supermacroprous chitosan-agarose-gelatin cryogels: *in vitro* characterization and *in vivo* assessment for cartilage tissue engineering. J R Soc Interface 8:540–554

Biazar E, Heidari Keshel S (2014) Development of chitosan-crosslinked nanofibrous PHBV guide for repair of nerve defects. Artif Cells Nanomed Biotechnol 42:385–391

Bilal M, Asgher M, Iqbal M, Hu H, Zhang X (2016) Chitosan beads immobilized manganese peroxidase catalytic potential for detoxification and decolorization of textile effluent. Int Biol Macromol 89:181–189

Bilgin Simsek E, Saloglu D, Ozcan N, Novak I, Berek D (2017) Carbon fiber embedded chitosan/PVA composites for decontamination of endocrine disruptor bisphenol-A from water. J Taiwan Inst Chem E 70:291–301

Boddu VM, Abburi K, Talbott JL, Smith ED (2003) Removal of hexavalent chromium from wastewater using a new composite chitosan biosorbent. Environ Sci Technol 37:4449–4456

Bonferoni MC et al (2018) Alpha tocopherol loaded chitosan oleate nanoemulsions for wound healing. Evaluation on cell lines and *ex vivo* human biopsies, and stabilization in spray dried Trojan microparticles. Eur J Pharm Biopharm 123:31–41

Borges O, Silva M, de Sousa A, Borchard G, Junginger HE, Cordeiro-da-Silva A (2008) Alginate coated chitosan nanoparticles are an effective subcutaneous adjuvant for hepatitis B surface antigen. Int Immunopharmacol 8:1773–1780

Bourguignon LYW, Zhu H, Shao L, Chen YW (2000) CD44 Interaction with Tiam1 promotes Rac1 signaling and hyaluronic acid-mediated breast tumor cell migration. J Biol Chem 275:1829–1838

Brown CA, Wang B, Oh JH (2008) Antimicrobial activity of lactoferrin against foodborne pathogenic bacteria incorporated into edible chitosan film. J Food Prot 71:319–324

Brunel F, El Gueddari NE, Moerschbacher BM (2013) Complexation of copper(II) with chitosan nanogels: toward control of microbial growth. Carbohydr Polym 92:1348–1356

Bu L, Gan LC, Guo XQ, Chen FZ, Song Q, Qi-Zhao GXJ, Hou SX, Yao Q (2013) Trans-resveratrol loaded chitosan nanoparticles modified with biotin and avidin to target hepatic carcinoma. Int J Pharm 452:355–362

Bueter CL, Lee CK, Rathinam VA, Healy GJ, Taron CH, Specht CA, Levitz SM (2011) Chitosan but not chitin activates the inflammasome by a mechanism dependent upon phagocytosis. J Biol Chem 286:35447–35455

Bueter CL, Lee CK, Wang JP, Ostroff GR, Specht CA, Levitz SM (2014) Spectrum and mechanisms of inflammasome activation by chitosan. J Immunol 92:5943–5951

Caetano GF, Frade MA, Andrade TA, Leite MN, Bueno CZ, Moraes AM, Ribeiro-Paes JT (2015) Chitosan-alginate membranes accelerate wound healing. J Biomed Mater Res B 103:1013–1022

Cahu TB et al (2017) Evaluation of chitosan-based films containing gelatin, chondroitin 4-sulfate and ZnO for wound healing. Appl Biochem Biotechnol 183:765–777

Cai X, Tong H, Shen X, Chen W, Yan J, Hu J (2009) Preparation and characterization of homogeneous chitosan-polylactic acid/hydroxyapatite nanocomposite for bone tissue engineering and evaluation of its mechanical properties. Acta Biomater 5:2693–2703

Campos DM, Toury B, D'Almeida M, Attik GN, Ferrand A, Renoud P, Grosgogeat B (2015) Acidic pH resistance of grafted chitosan on dental implant. Odontology 103:210–217

Campos EVR, Proença PLF, Oliveira JL, Melville CC, Della Vechia JF, de Andrade DJ, Fraceto LF (2018) Chitosan nanoparticles functionalized with β-cyclodextrin: a promising carrier for botanical pesticides. Sci Rep 8:2067. https://doi.org/10.1038/s41598-018-20602-y

Cao L, Zhang F, Wang Q, Wu X (2017) Fabrication of chitosan/graphene oxide polymer nanofiber and its biocompatibility for cartilage tissue engineering. Mater Sci Eng C Mater Biol Appl 79:697–701

Caramella CM, Rossi S, Ferrari F, Bonferoni MC, Sandri G (2015) Mucoadhesive and thermogelling systems for vaginal drug delivery. Adv Drug Deliv Rev 92:39–52

Carosio F, Alongi J (2018) Flame retardant multilayered coatings on acrylic fabrics prepared by one-step deposition of chitosan/montmorillonite complexes. Fibers 6:36. https://doi.org/10.3390/fib6020036

Carroll EC et al (2016) The vaccine adjuvant chitosan promotes cellular immunity via DNA sensor cGAS-STING-dependent induction of Type I interferons. Immunity 44:597–608

Casettari L, Illum L (2014) Chitosan in nasal delivery systems for therapeutic drugs. J Control Release 190:189–200

Cavallo JA, Strumia MC, Gomez CG (2014) Preparation of a milk spoilage indicator adsorbed to a modified polypropylene film as an attempt to build a smart packaging. J Food Eng 136:48–55

Celiesiute R, Radzevic A, Zukauskas A, Vaitekonis S, Pauliukaite R (2017) A strategy to employ polymerised riboflavin in the development of electrochemical biosensors. Electroanal 29:2071–2082

Cerempei A, Guguianu E, Muresan EI, Horhogea C, Rîmbu C, Borhan O (2015) Antimicrobial controlled release systems for the knitted cotton fabrics based on natural substances. Fiber Polym 16:1688–1695

Chakavala SR, Patel NG, Pate NV, Thakkar VT, Patel KV, Gandhi TR (2012) Development and *in vivo* evaluation of silver sulfadiazine loaded hydrogel consisting polyvinyl alcohol and chitosan for severe burns. J Pharm Bioallied Sci 4:S54–S56

Chameettachal S, Murab S, Vaid R, Midha S, Ghosh S (2017) Effect of visco-elastic silk-chitosan microcomposite scaffolds on matrix deposition and biomechanical functionality for cartilage tissue engineering. J Tissue Eng Regen Med 11:1212–1229

Chang H, Li X, Teng Y, Liang Y, Peng B, Fang F, Chen Z (2010) Comparison of adjuvant efficacy of chitosan and aluminum hydroxide for intraperitoneally administered inactivated influenza H5N1 vaccine. DNA Cell Biol 29:563–568

Chao X, Xu L, Li J, Han Y, Li X, Mao Y, Shang H, Fan Z, Wang H (2016) Facilitation of facial nerve regeneration using chitosan-beta-glycerophosphate-nerve growth factor hydrogel. Acta Otolaryngol 136:585–591

Charernsriwilaiwat N, Rojanarata T, Ngawhirunpat T, Opanasopit P (2014) Electrospun chitosan/polyvinyl alcohol nanofibre mats for wound healing. Int Wound J 11:215–222

Chauhan N, Dilbaghi N, Gopal M, Kumar R, Kim KH, Kumar S (2017) Development of chitosan nanocapsules for the controlled release of hexaconazole. Int Biol Macromol 97:616–624

Chen J, Li Q, Xu J, Huang Y, Ding Y, Deng H, Zhao S, Chen R (2005) Study on biocompatibility of complexes of collagen-chitosan-sodium hyaluronate and cornea. Artif Organs 29:104–113

Chen Y, Zhang F, Fu Q, Liu Y, Wang Z, Qi N (2016) *In vitro* proliferation and osteogenic differentiation of human dental pulp stem cells in injectable thermo-sensitive chitosan/beta-glycerophosphate/hydroxyapatite hydrogel. J Biomater Appl 31:317–327

Chen K, Guo B, Luo J (2017) Quaternized carboxymethyl chitosan/organic montmorillonite nanocomposite as a novel cosmetic ingredient against skin aging. Carbohydr Polym 173:100–106

Cheng X, Li R, Li X, Umair MM, Ren X, Huang T (2016) Preparation and characterization of antimicrobial cotton fabrics via *N*-halamine chitosan derivative/poly(2-acrylamide-2-methylpropane sulfonic acid sodium salt) self-assembled composite films. J Ind Text 46:1039–1052

Chesnutt BM, Yuan Y, Buddington K, Haggard WO, Bumgardner JD (2009) Composite chitosan/nano-hydroxyapatite scaffolds induce osteocalcin production by osteoblasts *in vitro* and support bone formation *in vivo*. Tissue Eng Part A 15:2571–2579

Chien Y et al (2012) Corneal repair by human corneal keratocyte-reprogrammed iPSCs and amphiphatic carboxymethyl-hexanoyl chitosan hydrogel. Biomaterials 33:8003–8016

Choi B, Kim S, Fan J, Kowalski T, Petrigliano F, Evseenko D, Lee M (2015) Covalently conjugated transforming growth factor-beta1 in modular chitosan hydrogels for the effective treatment of articular cartilage defects. Biomater Sci 3:742–752

Choi B, Jo DH, Anower AK, Islam SM, Sohn S (2016) Chitosan as an immunomodulating adjuvant on T-cells and antigen-presenting cells in Herpes Simplex virus type 1 infection. Mediat Inflamm 2016:4374375. https://doi.org/10.1155/2016/4374375

Chou SF, Lee CH, Lai JY (2018) Bioengineered keratocyte spheroids fabricated on chitosan coatings enhance tissue repair in a rabbit corneal stromal defect model. J Tissue Eng Regen Med 12:316–320

Choudhary RC, Kumaraswamy RV, Kumari S, Sharma SS, Pal A, Raliya R, Biswas P, Saharan V (2017a) Cu-chitosan nanoparticle boost defense responses and plant growth in maize (*Zea mays* L.). Sci Rep 7:9754. https://doi.org/10.1038/s41598-017-08571-0

Choudhary SMJ, Joshi A, Saharan V (2017b) Assessment of Cu-chitosan nanoparticles for its antibacterial activity against *Pseudomonas syringae* pv. *Glycinea*. Int J Curr Microbiol App Sci 6:1335–1350

Chua AWC, Khoo YC, Tan BK, Tan KC, Foo CL, Chong SJ (2016) Skin tissue engineering advances in severe burns: review and therapeutic applications. Burns Trauma 4:3. https://doi.org/10.1186/s41038-016-0027-y

Cohen E, Joseph T, Kahana F, Magdassi S (2003) Photostabilization of an entomopathogenic fungus using composite clay matrices. Photochem Photobiol 77:180–185

Coimbra P, Alves P, Valente TA, Santos R, Correia IJ, Ferreira P (2011) Sodium hyaluronate/chitosan polyelectrolyte complex scaffolds for dental pulp regeneration: synthesis and characterization. Int Biol Macromol 49:573–579

Corradini E, de Moura MR, Mattoso LHC (2010) A preliminary study of the incorporation of NPK fertilizer into chitosan nanoparticles. Express Polym Lett 4:509–515

Cota-Arriola O, Cortez-Rocha MO, Burgos-Hernandez A, Ezquerra-Brauer JM, Plascencia-Jatomea M (2013) Controlled release matrices and micro/nanoparticles of chitosan with antimicrobial potential: development of new strategies for microbial control in agriculture. J Sci Food Agric 93:1525–1536

Cui XQ, Li CM, Zang JF, Yu SC (2007) Highly sensitive lactate biosensor by engineering chitosan/PVI-Os/CNT/LOD network nanocomposite. Biosens Bioelectron 22:3288–3292

Cui F, Li G, Huang J, Zhang J, Lu M, Lu W, Huan J, Huang Q (2011) Development of chitosan-collagen hydrogel incorporated with lysostaphin (CCHL) burn dressing with anti-methicillin-resistant *Staphylococcus aureus* and promotion wound healing properties. Drug Deliv 18:173–180

Cui R, Lu Q, Teng Y, Li K, Li N (2017) Chitosan promoted the corneal epithelial wound healing via activation of erk pathway. Curr Eye Res 42:21–27

Dai H, Chi YW, Wu XP, Wang YM, Wei MD, Chen GN (2010) Biocompatible electrochemiluminescent biosensor for choline based on enzyme/titanate nanotubes/chitosan composite modified electrode. Biosens Bioelectron 25:1414–1419

Dashtdar H, Murali MR, Abbas AA, Suhaeb AM, Selvaratnam L, Tay LX, Kamarul T (2015) PVA-chitosan composite hydrogel versus alginate beads as a potential mesenchymal stem cell carrier for the treatment of focal cartilage defects. Knee Surg Sports Traumatol Arthrosc 23:1368–1377

De Campos AM, Sanchez A, Alonso MJ (2001) Chitosan nanoparticles: a new vehicle for the improvement of the delivery of drugs to the ocular surface. Application to cyclosporine A. Int J Pharm 224:159–168

De Campos AM, Sanchez A, Gref R, Calvo P, Alonso MJ (2003) The effect of a PEG versus a chitosan coating on the interaction of drug colloidal carriers with the ocular mucosa. Eur J Pharm Sci 20:73–81

De la Riva B et al (2010) Local controlled release of VEGF and PDGF from a combined brushite–chitosan system enhances bone regeneration. J Control Release 143:45–52

Debrassi A, Corrêa AF, Baccarin T, Nedelko N, Ślawska-Waniewska A, Sobczak K, Dłużewski P, Greneche J-M, Rodrigues CA (2012) Removal of cationic dyes from aqueous solutions using *N*-benzyl-*O*-carboxymethylchitosan magnetic nanoparticles. Chem Eng J 183:284–293

Deepthi S, Venkatesan J, Kim S-K, Bumgardner JD, Jayakumar R (2016) An overview of chitin or chitosan/nano ceramic composite scaffolds for bone tissue engineering. Int Biol Macromol 93:1338–1353

Dellera E, Bonferoni MC, Sandri G, Rossi S, Ferrari F, Del Fante C, Perotti C, Grisoli P, Caramella C (2014) Development of chitosan oleate ionic micelles loaded with silver sulfadiazine to be associated with platelet lysate for application in wound healing. Eur J Pharm Biopharm 88:643–650

Deng J, Zhou Y, Xu B, Mai K, Deng Y, Zhang LM (2011a) Dendronized chitosan derivative as a biocompatible gene delivery carrier. Biomacromolecules 12:642–649

Deng Z, Zhen Z, Hu X, Wu S, Xu Z, Chu PK (2011b) Hollow chitosan–silica nanospheres as pH-sensitive targeted delivery carriers in breast cancer therapy. Biomaterials 32:4976–4986

Deng J, She R, Huang W, Dong Z, Mo G, Liu B (2013) A silk fibroin/chitosan scaffold in combination with bone marrow-derived mesenchymal stem cells to repair cartilage defects in the rabbit knee. J Mater Sci Mater Med 24:2037–2046

Dervisevic M, Dervisevic E, Cevik E, Senel M (2017) Novel electrochemical xanthine biosensor based on chitosan-polypyrrole-gold nanoparticles hybrid bio-nanocomposite platform. J Food Drug Anal 25:510–519

Devi N, Dutta J (2017) Preparation and characterization of chitosan-bentonite nanocomposite films for wound healing application. Int Biol Macromol 104:1897–1904

Devlieghere F, Vermeulen A, Debevere J (2004) Chitosan: antimicrobial activity, interactions with food components and applicability as a coating on fruit and vegetables. Food Microbiol 21:703–714

Dhaliwal S, Jain S, Singh HP, Tiwary AK (2008) Mucoadhesive microspheres for gastroretentive delivery of acyclovir: *in vitro* and *in vivo* evaluation. AAPS J 10:322–330

Dhineshbabu NR, Rajendran V (2016) Antibacterial activity of hybrid chitosan-cupric oxide nanoparticles on cotton fabric. IET Nanobiotechnol 10:13–19

Dias AM, Seabra IJ, Braga MM, Gil MH, de Sousa HC (2010) Supercritical solvent impregnation of natural bioactive compounds in *N*-carboxybutyl chitosan membranes for the development of topical wound healing applications. J Control Release 148:e33–e35

Diebold Y, Jarrín M, Sáez V, Carvalho EL, Orea M, Calonge M, Seijo B, Alonso MJ (2007) Ocular drug delivery by liposome-chitosan nanoparticle complexes (LCS-NP). Biomaterials 28:1553–1564

Diez-Pascual AM, Diez-Vicente AL (2015) Wound healing bionanocomposites based on castor oil polymeric films reinforced with chitosan-modified ZnO nanoparticles. Biomacromolecules 16:2631–2644

Dinescu S, Ionita M, Pandele AM, Galateanu B, Iovu H, Ardelean A, Costache M, Hermenean A (2014) *In vitro* cytocompatibility evaluation of chitosan/graphene oxide 3D scaffold composites designed for bone tissue engineering. Biomed Mater Eng 24:2249–2256

Djelad A, Morsli A, Robitzer M, Bengueddach A, di Renzo F, Quignard F (2016) Sorption of Cu (II) ions on chitosan-Zeolite x composites: impact of gelling and drying conditions. Molecules 21:E109. https://doi.org/10.3390/molecules21010109

Doares SH, Syrovets T, Weiler EW, Ryan CA (1995) Oligogalacturonides and chitosan activate plant defensive genes through the octadecanoid pathway. Proc Natl Acad Sci USA 92:4095–4098

Dong H, Li F, Li J, Li Y (2012) Characterizations of blend gels of carboxymethylated polysaccharides and their use for the controlled release of herbicide. J Macromol Sci A 49:235–241

Dong WB, Wang KY, Chen Y, Li WP, Ye YC, Jin SH (2017) Construction and characterization of a chitosan-immobilized-enzyme and beta-cyclodextrin-included-ferrocene-based electrochemical biosensor for H2O2 detection. Materials 10:868. https://doi.org/10.3390/Ma10080868

Duan J, Zhang S (2013) Application of chitosan based coating in fruit and vegetable preservation: a review. J Food Process Technol 4:227. https://doi.org/10.4172/2157-7110.1000227

Duri S, Tran CD (2013) Supramolecular composite materials from cellulose, chitosan and cyclodextrin: facile preparation and their selective inclusion complex formation with endocrine disruptors. Langmuir 29:5037–5049

Dutta PK, Dutta J, Tripathi VS (2004) Chitin and chitosan: Chemistry, properties and applications. J Sci Ind Res 63:20–31

Eivazy P, Atyabi F, Jadidi-Niaragh F, Aghebati Maleki L, Miahipour A, Abdolalizadeh J, Yousefi M (2017) The impact of the codelivery of drug-siRNA by trimethyl chitosan nanoparticles on the efficacy of chemotherapy for metastatic breast cancer cell line (MDA-MB-231). Artif Cells Nanomed Biotechnol 45:889–896

El Badawy M, Taktak NEM, Awad OM, Elfiki SA, Abou El-Ela NE (2016) Evaluation of released malathion and spinosad from chitosan/alginate/gelatin capsules against *Culex pipiens* larvae. Res Rep Trop Med 7:23–38

El Hadrami A, Adam LR, El Hadrami I, Daayf F (2010) Chitosan in plant protection. Mar Drugs 8:968–987

El-Feky GS, El-Banna ST, El-Bahy GS, Abdelrazek EM, Kamal M (2017a) Alginate coated chitosan nanogel for the controlled topical delivery of Silver sulfadiazine. Carbohydr Polym 177:194–202

El-Feky GS, Sharaf SS, El Shafei A, Hegazy AA (2017b) Using chitosan nanoparticles as drug carriers for the development of a silver sulfadiazine wound dressing. Carbohydr Polym 158:11–19

El-Kamel A, Sokar M, Naggar V, Al Gamal S (2002) Chitosan and sodium alginate-based bioadhesive vaginal tablets. AAPS PharmSci 4:E44. https://doi.org/10.1208/ps040444

El-Shafei A, ElShemy M, Abou-Okeil A (2015) Eco-friendly finishing agent for cotton fabrics to improve flame retardant and antibacterial properties. Carbohydr Polym 118:83–90

El-Tahlawy K (2008) Chitosan phosphate: a new way for production of eco-friendly flame-retardant cotton textiles. J Text Inst 99:185–191
Elviri L, Bianchera A, Bergonzi C, Bettini R (2017) Controlled local drug delivery strategies from chitosan hydrogels for wound healing. Expert Opin Drug Deliv 14:897–908
European Commission SCotFCaAH (2014) Chitosan hydrochloride SANCO 12388:rev. 2
Fan L, Zhang Y, Li X, Luo C, Lu F, Qiu H (2012) Removal of alizarin red from water environment using magnetic chitosan with Alizarin Red as imprinted molecules. Colloids Surf B Biointerfaces 91:250–257
Fan L, Luo C, Sun M, Qiu H, Li X (2013) Synthesis of magnetic β-cyclodextrin–chitosan/graphene oxide as nanoadsorbent and its application in dye adsorption and removal. Colloids Surf B Biointerfaces 103:601–607
Fang J, Zhang Y, Yan S, Liu Z, He S, Cui L, Yin J (2014) Poly(L-glutamic acid)/chitosan polyelectrolyte complex porous microspheres as cell microcarriers for cartilage regeneration. Acta Biomater 10:276–288
Fang F, Zhang X, Meng Y, Gu Z, Bao C, Ding X, Li S, Chen X, Tian X (2015) Intumescent flame retardant coatings on cotton fabric of chitosan and ammonium polyphosphate via layer-by-layer assembly. Surf Coat Technol 262:9–14
Farzana MH, Meenakshi S (2015) Visible light-driven photoactivity of zinc oxide impregnated chitosan beads for the detoxification of textile dyes. Appl Catal A 503:124–134
Fawzy AS, Nitisusanta LI, Iqbal K, Daood U, Beng LT, Neo J (2013) Chitosan/Riboflavin-modified demineralized dentin as a potential substrate for bonding. J Mech Behav Biomed Mater 17:278–289
Feng B-H, Peng L-F (2012) Synthesis and characterization of carboxymethyl chitosan carrying ricinoleic functions as an emulsifier for azadirachtin. Carbohydr Polym 88:576–582
Feng X, Zheng K, Wang C, Chu F, Chen Y (2016) Durable antibacterial cotton fabrics with chitosan based quaternary ammonium salt. Fiber Polym 17:371–379
Ferrero F, Periolatto M, Ferrario S (2015) Sustainable antimicrobial finishing of cotton fabrics by chitosan UV-grafting: from laboratory experiments to semi industrial scale-up. J Clean Prod 96:244–252
Filova E et al (2016) Polycaprolactone foam functionalized with chitosan microparticles – a suitable scaffold for cartilage regeneration. Physiol Res 65:121–131
Fischak C, Klaus R, Werkmeister RM, Hohenadl C, Prinz M, Schmetterer L, Garhofer G (2017) Effect of topically administered chitosan-*N*-acetylcysteine on corneal wound healing in a rabbit model. J Ophthalmol 2017:5192924. https://doi.org/10.1155/2017/5192924
Fonseca-Santos B, Chorilli M (2017) An overview of carboxymethyl derivatives of chitosan: Their use as biomaterials and drug delivery systems. Mater Sci Eng C Mater Biol Appl 77:1349–1362
Fraga AF, Filho EA, Rigo ECS, Boschi AO (2011) Synthesis of chitosan/hydroxyapatite membranes coated with hydroxycarbonate apatite for guided tissue regeneration purposes. Appl Surf Sci 257:3888–3892
Frank LA, Chaves PS, D'Amore CM, Contri RV, Frank AG, Beck RC, Pohlmann AR, Buffon A, Guterres SS (2017) The use of chitosan as cationic coating or gel vehicle for polymeric nanocapsules: increasing penetration and adhesion of imiquimod in vaginal tissue. Eur J Pharm Biopharm 114:202–212
Friedman M, Juneja VK (2010) Review of antimicrobial and antioxidative activities of chitosans in food. J Food Prot 73:1737–1761
Gan D, Liu M, Xu T, Wang K, Tan H, Lu X (2018) Chitosan/biphasic calcium phosphate scaffolds functionalized with BMP-2-encapsulated nanoparticles and RGD for bone regeneration. J Biomed Mater Res A. https://doi.org/10.1002/jbm.a.36453
Ganss C, Lussi A, Grunau O, Klimek J, Schlueter N (2011) Conventional and anti-erosion fluoride toothpastes: effect on enamel erosion and erosion-abrasion. Caries Res 45:581–589
Ge Z, Baguenard S, Lim LY, Wee A, Khor E (2004) Hydroxyapatite–chitin materials as potential tissue engineered bone substitutes. Biomaterials 25:1049–1058

Gelfuso GM, Gratieri T, Simao PS, de Freitas LA, Lopez RF (2011) Chitosan microparticles for sustaining the topical delivery of minoxidil sulphate. J Microencapsul 28:650–658
Geng B, Jin Z, Li T, Qi X (2009) Kinetics of hexavalent chromium removal from water by chitosan-Fe0 nanoparticles. Chemosphere 75:825–830
Genskowsky E, Puente LA, Pérez-Álvarez JA, Fernandez-Lopez J, Muñoz LA, Viuda-Martos M (2015) Assessment of antibacterial and antioxidant properties of chitosan edible films incorporated with maqui berry (*Aristotelia chilensis*). LWT – Food Sci Technol 64:1057–1062
Georgopoulou A, Papadogiannis F, Batsali A, Marakis J, Alpantaki K, Eliopoulos AG, Pontikoglou C, Chatzinikolaidou M (2018) Chitosan/gelatin scaffolds support bone regeneration. J Mater Sci Mater Med 29:59
Germershaus O, Mao S, Sitterberg J, Bakowsky U, Kissel T (2008) Gene delivery using chitosan, trimethyl chitosan or polyethylenglycol-graft-trimethyl chitosan block copolymers: establishment of structure-activity relationships *in vitro*. J Control Release 125:145–154
Ghasemi Hamidabadi H et al (2017) Chitosan-intercalated montmorillonite/poly(vinyl alcohol) nanofibers as a platform to guide neuronlike differentiation of human dental pulp stem cells. ACS Appl Mater Interfaces 9:11392–11404
Ghendon Y, Markushin S, Akopova I, Koptiaeva I, Krivtsov G (2011) Chitosan as an adjuvant for poliovaccine. J Med Virol 83:847–852
Gholipour-Kanani A, Bahrami SH, Joghataie MT, Samadikuchaksaraei A, Ahmadi-Taftie H, Rabbani S, Kororian A, Erfani E (2014) Tissue engineered poly(caprolactone)-chitosan-poly (vinyl alcohol) nanofibrous scaffolds for burn and cutting wound healing. IET Nanobiotechnol 8:123–131
Giannetto M, Costantini M, Mattarozzi M, Careri M (2017) Innovative gold-free carbon nanotube/chitosan-based competitive immunosensor for determination of HIV-related p24 capsid protein in serum. RSC Adv 7:39970–39976
Gokila S, Gomathi T, Sudha PN, Anil S (2017) Removal of the heavy metal ion chromiuim (VI) using Chitosan and Alginate nanocomposites. Int Biol Macromol 104:1459–1468
Gomaa YA, El-Khordagui LK, Boraei NA, Darwish IA (2010) Chitosan microparticles incorporating a hydrophilic sunscreen agent. Carbohydr Polym 81:234–242
Gong Z, Xiong H, Long X, Wei L, Li J, Wu Y, Lin Z (2010) Use of synovium-derived stromal cells and chitosan/collagen type I scaffolds for cartilage tissue engineering. Biomed Mater 5:055005. https://doi.org/10.1088/1748-6041/5/5/055005
Gopinath D, Ahmed MR, Gomathi K, Chitra K, Sehgal PK, Jayakumar R (2004) Dermal wound healing processes with curcumin incorporated collagen films. Biomaterials 25:1911–1917
Graham C (2005) The role of silver in wound healing. Br J Nurs 14:S22, S24, S26 passim. https://doi.org/10.12968/bjon.2005.14.Sup5.19954
Grande R, Pessan LA, Carvalho AJF (2018) Thermoplastic blends of chitosan: A method for the preparation of high thermally stable blends with polyesters. Carbohydr Polym 191:44–52
Grassi M, Rizzo L, Farina A (2013) Endocrine disruptors compounds, pharmaceuticals and personal care products in urban wastewater: implications for agricultural reuse and their removal by adsorption process. Environ Sci Pollut Res 20:3616–3628
Grillo R, Pereira AE, Nishisaka CS, de Lima R, Oehlke K, Greiner R, Fraceto LF (2014) Chitosan/tripolyphosphate nanoparticles loaded with paraquat herbicide: an environmentally safer alternative for weed control. J Hazard Mater 278:163–171
Gu J, Hu W, Deng A, Zhao Q, Lu S, Gu X (2012) Surgical repair of a 30 mm long human median nerve defect in the distal forearm by implantation of a chitosan-PGA nerve guidance conduit. J Tissue Eng Regen Med 6:163–168
Guan L, Ge H, Tang X, Su S, Tian P, Xiao N, Zhang H, Zhang L, Liu P (2013) Use of a silk fibroin-chitosan scaffold to construct a tissue-engineered corneal stroma. Cells Tissues Organs 198:190–197
Guo Z, Xing R, Liu S, Yu H, Wang P, Li C, Li P (2005) The synthesis and antioxidant activity of the Schiff bases of chitosan and carboxymethyl chitosan. Bioorganic Med Chem Lett 15:4600–4603

Guo M, Jin TZ, Yadav MP, Yang R (2015) Antimicrobial property and microstructure of micro-emulsion edible composite films against *Listeria*. Int J Food Microbiol 208:58–64

Gupta H, Velpandian T, Jain S (2010) Ion- and pH-activated novel in-situ gel system for sustained ocular drug delivery. J Drug Target 18:499–505

Guzman-Villanueva D, El-Sherbiny IM, Vlassov AV, Herrera-Ruiz D, Smyth HD (2014) Enhanced cellular uptake and gene silencing activity of siRNA molecules mediated by chitosan-derivative nanocomplexes. Int J Pharm 473:579–590

Haaparanta AM, Jarvinen E, Cengiz IF, Ella V, Kokkonen HT, Kiviranta I, Kellomaki M (2014) Preparation and characterization of collagen/PLA, chitosan/PLA, and collagen/chitosan/PLA hybrid scaffolds for cartilage tissue engineering. J Mater Sci Mater Med 25:1129–1136

Hadwiger LA (2013) Multiple effects of chitosan on plant systems: solid science or hype Plant science: an international. J Exp Plant Biol 208:42–49

Hamman JH (2010) Chitosan based polyelectrolyte complexes as potential carrier materials in drug delivery systems. Mar Drugs 8:1305–1322

Hande PE, Kamble S, Samui AB, Kulkarni PS (2016) Chitosan-based lead ion-imprinted interpenetrating polymer network by simultaneous polymerization for selective extraction of lead(II). Ind Eng Chem Res 55:3668–3678

Hasan A, Waibhaw G, Tiwari S, Dharmalingam K, Shukla I, Pandey LM (2017) Fabrication and characterization of chitosan, polyvinylpyrrolidone, and cellulose nanowhiskers nanocomposite films for wound healing drug delivery application. J Biomed Mater Res A 105:2391–2404

Hashemi-Beni B, Khoroushi M, Foroughi MR, Karbasi S, Khademi AA (2018) Cytotoxicity assessment of polyhydroxybutyrate/chitosan/nano- bioglass nanofiber scaffolds by stem cells from human exfoliated deciduous teeth stem cells from dental pulp of exfoliated deciduous tooth. Dent Res J 15:136–145

Hassan MS (2015) Removal of reactive dyes from textile wastewater by immobilized chitosan upon grafted Jute fibers with acrylic acid by gamma irradiation. Radiat Phys Chem 115:55–61

He S, Zhang W, Li D, Li P, Zhu Y, Ao M, Lia J, Cao Y (2013) Preparation and characterization of double-shelled avermectin microcapsules based on copolymer matrix of silica-glutaraldehyde-chitosan. J Mater Chem B 1:1270–1278

Hebeish A, Sharaf S, Farouk A (2013) Utilization of chitosan nanoparticles as a green finish in multifunctionalization of cotton textile. Int Biol Macromol 60:10–17

Highton AJ, Girardin A, Bell GM, Hook SM, Kemp RA (2016) Chitosan gel vaccine protects against tumour growth in an intracaecal mouse model of cancer by modulating systemic immune responses. BMC Immunol 17:39. https://doi.org/10.1186/s12865-016-0178-4

Hong HJ, Jin SE, Park JS, Ahn WS, Kim CK (2008) Accelerated wound healing by smad3 antisense oligonucleotides-impregnated chitosan/alginate polyelectrolyte complex. Biomaterials 29:4831–4837

Houschyar KS, Momeni A, Pyles MN, Cha JY, Maan ZN, Duscher D, Jew OS, Siemers F, van Schoonhoven J (2016) The role of current techniques and concepts in peripheral nerve repair. Plast Surg Int 2016:4175293. https://doi.org/10.1155/2016/4175293

Hu X-, Wang JS, Liu YG, Li X, Zeng GM, Bao ZL, Zeng XX, Chen AW, Long F (2011) Adsorption of chromium (VI) by ethylenediamine-modified cross-linked magnetic chitosan resin: Isotherms, kinetics and thermodynamics. J Hazard Mater 185:306-314.

Hu N, Wu H, Xue C, Gong Y, Wu J, Xiao Z, Yang Y, Ding F, Gu X (2013) Long-term outcome of the repair of 50 mm long median nerve defects in rhesus monkeys with marrow mesenchymal stem cells-containing, chitosan-based tissue engineered nerve grafts. Biomaterials 34:100–111

Hu D, Wang H, Wang L (2016) Physical properties and antibacterial activity of quaternized chitosan/carboxymethyl cellulose blend films. LWT – Food Sci Technol 65:398–405

Hu Y, Chen J, Fan T, Zhang Y, Zhao Y, Shi X, Zhang Q (2017) Biomimetic mineralized hierarchical hybrid scaffolds based on *in situ* synthesis of nano-hydroxyapatite/chitosan/chondroitin sulfate/hyaluronic acid for bone tissue engineering. Colloid Surf B 157:93–100

Hu S, Bi S, Yan D, Zhou Z, Sun G, Cheng X, Chen X (2018) Preparation of composite hydroxybutyl chitosan sponge and its role in promoting wound healing. Carbohydr Polym 184:154–163

Huang D, Zuo Y, Zou Q, Zhang L, Li J, Cheng L, Shen J, Li Y (2011) Antibacterial chitosan coating on nano-hydroxyapatite/polyamide66 porous bone scaffold for drug delivery. J Biomater Sci Polym Ed 22:931–944

Huang X, Zhang Y, Zhang X, Xu L, Chen X, Wei S (2013) Influence of radiation crosslinked carboxymethyl-chitosan/gelatin hydrogel on cutaneous wound healing. Mater Sci Eng C Mater Biol Appl 33:4816–4824

Hughes G, Pemberton RM, Fielden PR, Hart JP (2015) Development of a novel reagentless, screen-printed amperometric biosensor based on glutamate dehydrogenase and NAD(+), integrated with multi-walled carbon nanotubes for the determination of glutamate in food and clinical applications. Sensor Actuat B-Chem 216:614–621

Ibrahim MA, Meera Priyadarshini B, Neo J, Fawzy AS (2017a) Characterization of chitosan/TiO_2 cano-powder modified glass-ionomer cement for restorative dental applications. J Esthet Restor Dent 29:146–156

Ibrahim NA, Eid BM, El-Aziz EA, Elmaaty TMA, Ramadan SM (2017b) Loading of chitosan – nano metal oxide hybrids onto cotton/polyester fabrics to impart permanent and effective multifunctions. Int Biol Macromol 105:769–776

Ilk S, Saglam N, Ozgen M (2017) Kaempferol loaded lecithin/chitosan nanoparticles: preparation, characterization, and their potential applications as a sustainable antifungal agent. Artif Cells Nanomed Biotechnol 45:907–916. https://doi.org/10.1080/21691401.2016.1192040

Illum L (1998) Chitosan and its use as a pharmaceutical excipient. Pharm Res 15:1326–1331

Illum L (2003) Nasal drug delivery-possibilities, problems and solutions. J Control Release 87:187–198

Im O, Li J, Wang M, Zhang LG, Keidar M (2012) Biomimetic three-dimensional nanocrystalline hydroxyapatite and magnetically synthesized single-walled carbon nanotube chitosan nanocomposite for bone regeneration. Int J Nanomedicine 7:2087–2099

Ishihara M et al (2006) Chitosan hydrogel as a drug delivery carrier to control angiogenesis. J Artif Organs 9:8–16

Ito M (1991) *In vitro* properties of a chitosan-bonded hydroxyapatite bone-filling paste. Biomaterials 12:41–45

Itoh S, Yamaguchi I, Suzuki M, Ichinose S, Takakuda K, Kobayashi H, Shinomiya K, Tanaka J (2003) Hydroxyapatite-coated tendon chitosan tubes with adsorbed laminin peptides facilitate nerve regeneration *in vivo*. Brain Res 993:111–123

Iturriaga L, Olabarrieta I, Castellan A, Gardrat C, Coma V (2014) Active naringin-chitosan films: impact of UV irradiation. Carbohydr Polym 110:374–381

Jahanizadeh S, Yazdian F, Marjani A, Omidi M, Rashedi H (2017) Curcumin-loaded chitosan/carboxymethyl starch/montmorillonite bio-nanocomposite for reduction of dental bacterial biofilm formation. Int Biol Macromol 105:757–763

Jain A, Jain SK, Ganesh N, Barve J, Beg AM (2010) Design and development of ligand-appended polysaccharidic nanoparticles for the delivery of oxaliplatin in colorectal cancer. Nanomedicine 6:179–190

Jamil B, Habib H, Abbasi S, Nasir H, Rahman A, Rehman A, Bokhari H, Imran M (2016) Cefazolin loaded chitosan nanoparticles to cure multi drug resistant Gram-negative pathogens. Carbohydr Polym 136:682–691

Janegitz BC, Figueiredo LCS, Marcolino LH, Souza SPN, Pereira ER, Fatibello O (2011) Development of a carbon nanotubes paste electrode modified with crosslinked chitosan for cadmium (II) and mercury(II) determination. J Electroanal Chem 660:209–216

Javid A, Raza ZA, Hussain T, Rehman A (2014) Chitosan microencapsulation of various essential oils to enhance the functional properties of cotton fabric. J Microencapsul 31:461–468

Jayakumar R, Prabaharan M, Sudheesh Kumar PT, Nair SV, Tamura H (2011) Biomaterials based on chitin and chitosan in wound dressing applications. Biotechnol Adv 29:322–337

Jennings JA, Wells CM, McGraw GS, Velasquez Pulgarin DA, Whitaker MD, Pruitt RL, Bumgardner JD (2015) Chitosan coatings to control release and target tissues for therapeutic delivery. Ther Deliv 6:855–871

Jiang HL, Park IK, Shin NR, Yoo HS, Akaike T, Cho CS (2004) Controlled release of *Bordetella* bronchiseptica dermonecrotoxin (BBD) vaccine from BBD-loaded chitosan microspheres *in vitro*. Arch Pharm Res 27:346–350

Jiang T, Abdel-Fattah WI, Laurencin CT (2006) *In vitro* evaluation of chitosan/poly(lactic acid-glycolic acid) sintered microsphere scaffolds for bone tissue engineering. Biomaterials 27:4894–4903

Jiang L, Qian F, He X, Wang F, Ren D, He Y, Li K, Sun S, Yin C (2007) Novel chitosan derivative nanoparticles enhance the immunogenicity of a DNA vaccine encoding hepatitis B virus core antigen in mice. J Gene Med 9:253–264

Jiang R, Fu YQ, Zhu HY, Yao J, Xiao L (2012) Removal of methyl orange from aqueous solutions by magnetic maghemite/chitosan nanocomposite films: Adsorption kinetics and equilibrium. J Appl Polymer Sci 125:E540–E549

Jiang H, Chen P, Luo S, Luo X, Tu X, Cao Q, Zhou Y, Zhang W (2013a) Synthesis of novel biocompatible composite Fe_3O_4/ZrO_2/chitosan and its application for dye removal. J Inorg Organomet Polym Mater 23:393–400

Jiang H, Zuo Y, Zou Q, Wang H, Du J, Li Y, Yang X (2013b) Biomimetic spiral-cylindrical scaffold based on hybrid chitosan/cellulose/nano-hydroxyapatite membrane for bone regeneration. ACS Appl Mater Interfaces 5:12036–12044

Jimenez M, Guin T, Bellayer S, Dupretz R, Bourbigot S, Grunlan JC (2016) Microintumescent mechanism of flame-retardant water-based chitosan–ammonium polyphosphate multilayer nanocoating on cotton fabric. J Appl Polymer Sci 133. https://doi.org/10.1002/app.43783

Jimtaisong A, Saewan N (2014) Utilization of carboxymethyl chitosan in cosmetics. Int J Cosmet Sci 36:12–21

Jin HH, Kim DH, Kim TW, Shin KK, Jung JS, Park HC, Yoon SY (2012) *In vivo* evaluation of porous hydroxyapatite/chitosan-alginate composite scaffolds for bone tissue engineering. Int Biol Macromol 51:1079–1085

Kadam AA, Lee DS (2015) Glutaraldehyde cross-linked magnetic chitosan nanocomposites: Reduction precipitation synthesis, characterization, and application for removal of hazardous textile dyes. Bioresour Technol 193:563–567

Kamari A, Aljafree NFA (2017) Amphiphilic chitosan derivatives as carrier agents for rotenone. AIP Conf Proc 1868:020001. https://doi.org/10.1063/1.4995087

Kang YO, Jung JY, Cho D, Kwon OH, Cheon JY, Park WH (2016) Antimicrobial silver chloride nanoparticles stabilized with chitosan oligomer for the healing of burns. Materials 9. https://doi.org/10.3390/ma9040215

Karri VV, Kuppusamy G, Talluri SV, Mannemala SS, Kollipara R, Wadhwani AD, Mulukutla S, Raju KR, Malayandi R (2016) Curcumin loaded chitosan nanoparticles impregnated into collagen-alginate scaffolds for diabetic wound healing. Int Biol Macromol 93:1519–1529

Kashyap PL, Xiang X, Heiden P (2015) Chitosan nanoparticle based delivery systems for sustainable agriculture. Int Biol Macromol 77:36–51

Katiyar D, Hemantaranjan A, Singh B, Bhanu AN (2014) A future perspective in crop protection: chitosan and its oligosaccharides. Adv Plants Agric Res 1:23–30

Kato Y, Yagami A, Matsunaga K (2005) A case of anaphylaxis caused by the health food chitosan. Arerugi 54:1427–1429

Katti KS, Katti DR, Dash R (2008) Synthesis and characterization of a novel chitosan/montmorillonite/hydroxyapatite nanocomposite for bone tissue engineering. Biomed Mater 3:034122. https://doi.org/10.1088/1748-6041/3/3/034122

Kaynak Bayrak G, Demirtas TT, Gumusderelioglu M (2017) Microwave-induced biomimetic approach for hydroxyapatite coatings of chitosan scaffolds. Carbohydr Polym 157:803–813

Kean T, Thanou M (2010) Biodegradation, biodistribution and toxicity of chitosan. Adv Drug Deliv Rev 62:3–11

Khajuria DK, Zahra SF, Razdan R (2018) Effect of locally administered novel biodegradable chitosan based risedronate/zinc-hydroxyapatite intra-pocket dental film on alveolar bone density in rat model of periodontitis. J Biomater Sci Polym Ed 29:74–91

Khanna R, Katti KS, Katti DR (2011) Bone nodules on chitosan-polygalacturonic acid-hydroxyapatite nanocomposite films mimic hierarchy of natural bone. Acta Biomater 7:1173–1183

Khwaldia K, Basta AH, Aloui H, El-Saied H (2014) Chitosan-caseinate bilayer coatings for paper packaging materials. Carbohydr Polym 99:508–516

Kim SE, Park JH, Cho YW, Chung H, Jeong SY, Lee EB, Kwon IC (2003) Porous chitosan scaffold containing microspheres loaded with transforming growth factor-beta1: implications for cartilage tissue engineering. J Control Release 91:365–374

Kim JH et al (2006) Hydrophobically modified glycol chitosan nanoparticles as carriers for paclitaxel. J Control Release 111:228–234

Kim JH et al (2008) Antitumor efficacy of cisplatin-loaded glycol chitosan nanoparticles in tumor-bearing mice. J Control Release 127:41–49

Kim HL, Jung GY, Yoon JH, Han JS, Park YJ, Kim DG, Zhang M, Kim DJ (2015) Preparation and characterization of nano-sized hydroxyapatite/alginate/chitosan composite scaffolds for bone tissue engineering. Mater Sci Eng C Mater Biol Appl 54:20–25

Kim Y-M, Park S-C, Jang M-K (2017) Targeted gene delivery of polyethyleneimine-grafted chitosan with RGD dendrimer peptide in αvβ3 integrin-overexpressing tumor cells. Carbohydr Polym 174:1059–1068

Knapczyk J (1993) Chitosan hydrogel as a base for semisolid drug forms. Int J Pharm 93:233–237

Koç Demir A, Elçin AE, Elçin YM (2018) Strontium-modified chitosan/montmorillonite composites as bone tissue engineering scaffold. Mater Sci Eng C 89:8–14

Kohsari I, Shariatinia Z, Pourmortazavi SM (2016) Antibacterial electrospun chitosan-polyethylene oxide nanocomposite mats containing ZIF-8 nanoparticles. Int Biol Macromol 91:778–788

Kong Y, Xu R, Darabi MA, Zhong W, Luo G, Xing MM, Wu J (2016) Fast and safe fabrication of a free-standing chitosan/alginate nanomembrane to promote stem cell delivery and wound healing. Int J Nanomedicine 11:2543–2555

Kong D, Wang N, Qiao N, Wang Q, Wang Z, Zhou Z, Ren Z (2017) Facile preparation of ion-imprinted chitosan microspheres enwrapping Fe3O4 and graphene oxide by inverse suspension cross-linking for highly selective removal of copper(II). ACS Sustain Chem Eng 5:7401–7409

Kong SZ et al (2018) Anti-photoaging effects of chitosan oligosaccharide in ultraviolet-irradiated hairless mouse skin. Exp Gerontol 103:27–34

Kos L (2016) Use of chitosan for textile wastewater decolourization fibres. Text East Eur 24:130–135

Kousalya GN, Gandhi MR, Meenakshi S (2010) Removal of toxic Cr(VI) ions from aqueous solution using nano-hydroxyapatite-based chitin and chitosan hybrid composites. Adsorpt Sci Technol 28:49–64

Kratz G, Arnander C, Swedenborg J, Back M, Falk C, Gouda I, Larm O (1997) Heparin-chitosan complexes stimulate wound healing in human skin. Scand J Plastic Reconstructi Surg Hand Surg 31:119–123

Krausz AE et al (2015) Curcumin-encapsulated nanoparticles as innovative antimicrobial and wound healing agent. Nanomedicine 11:195–206

Krishnaswami V, Kandasamy R, Alagarsamy S, Palanisamy R, Natesan S (2018) Biological macromolecules for ophthalmic drug delivery to treat ocular diseases. Int Biol Macromol 110:7–16

Kristl J, Šmid-Korbar J, Štruc E, Schara M, Rupprecht H (1993) Hydrocolloids and gels of chitosan as drug carriers. Int J Pharm 99:13–19

Kulkarni AD, Vanjari YH, Sancheti KH, Patel HM, Belgamwar VS, Surana SJ, Pardeshi CV (2016) New nasal nanocomplex self-assembled from charged biomacromolecules: *N,N,N*-Trimethyl chitosan and dextran sulfate. Int Biol Macromol 88:476–490

Kumar D, Kumar P, Pandey J (2018) Binary grafted chitosan film: synthesis, characterization, antibacterial activity and prospects for food packaging. Int Biol Macromol 115:341–348

Kumar-Krishnan S, Prokhorov E, Hernández-Iturriaga M, Mota-Morales JD, Vázquez-Lepe M, Kovalenko Y, Sanchez IC, Luna-Bárcenas G (2015) Chitosan/silver nanocomposites: Synergistic antibacterial action of silver nanoparticles and silver ions. Eur Polym J 67:242–251

Kundu CK, Wang W, Zhou S, Wang X, Sheng H, Pan Y, Song L, Hu Y (2017) A green approach to constructing multilayered nanocoating for flame retardant treatment of polyamide 66 fabric from chitosan and sodium alginate. Carbohydr Polym 166:131–138

Kuo YC, Ku IN (2008) Cartilage regeneration by novel polyethylene oxide/chitin/chitosan scaffolds. Biomacromolecules 9:2662–2669

Kuo CY, Chen CH, Hsiao CY, Chen JP (2015) Incorporation of chitosan in biomimetic gelatin/chondroitin-6-sulfate/hyaluronan cryogel for cartilage tissue engineering. Carbohydr Polym 117:722–730

Kweon DK, Song SB, Park YY (2003) Preparation of water-soluble chitosan/heparin complex and its application as wound healing accelerator. Biomaterials 24:1595–1601

Kyzas GZ, Bikiaris DN (2015) Recent modifications of chitosan for adsorption applications: a critical and systematic review. Mar Drugs 13:312–337

Kyzas GZ, Kostoglou M, Lazaridis NK, Lambropoulou DA, Bikiaris DN (2013) Environmental friendly technology for the removal of pharmaceutical contaminants from wastewaters using modified chitosan adsorbents. Chem Eng J 222:248–258

Kyzas GZ, Bikiaris DN, Seredych M, Bandosz TJ, Deliyanni EA (2014) Removal of dorzolamide from biomedical wastewaters with adsorption onto graphite oxide/poly(acrylic acid) grafted chitosan nanocomposite. Bioresour Technol 152:399–406

Lai C et al (2014) Anti-tumor immune response of folate-conjugated chitosan nanoparticles containing the IP-10 gene in mice with hepatocellular carcinoma. J Biomed Nanotechnol 10:3576–3589

Lalevee G, Sudre G, Montembault A, Meadows J, Malaise S, Crépet A, David L, Delair T (2016) Polyelectrolyte complexes via desalting mixtures of hyaluronic acid and chitosan-Physicochemical study and structural analysis. Carbohydr Polym 154:86–95

Lam NYK, Zhang M, Guo H-f, Ho CP, Li L (2017) Effect of fiber length and blending method on the tensile properties of ring spun chitosan–cotton blend yarns. Text Res J 87:244–257

Lam NYK, Zhang M, Yang CX, Ho CP, Li L (2018) A pilot intervention with chitosan/cotton knitted jersey fabric to provide comfort for epidermolysis bullosa patients. Text Res J 88:704–716

Lao L, Tan H, Wang Y, Gao C (2008) Chitosan modified poly(L-lactide) microspheres as cell microcarriers for cartilage tissue engineering. Colloid Surf B 66:218–225

Leceta I, Guerrero P, Ibarburu I, Dueñas MT, de la Caba K (2013) Characterization and antimicrobial analysis of chitosan-based films. J Food Eng 116:889–899

Lee CG (2009) Chitin, chitinases and chitinase-like proteins in allergic inflammation and tissue remodeling. Yonsei Med J 50:22–30

Lee CA, Tsai YC (2009) Preparation of multiwalled carbon nanotube-chitosan-alcohol dehydrogenase nanobiocomposite for amperometric detection of ethanol. Sensor Actuators B-Chem 138:518–523

Lee CG, Da Silva CA, Lee J-Y, Hartl D, Elias JA (2008) Chitin regulation of immune responses: an old molecule with new roles. Curr Opin Immunol 20:684–689

Lee SM, Liu KH, Liu YY, Chang YP, Lin CC, Chen YS (2013) Chitosonic((R)) acid as a novel cosmetic ingredient: evaluation of its antimicrobial, antioxidant and hydration activities. Materials 6:1391–1402

Lee SJ et al (2014) Chitosan/polyurethane blended fiber sheets containing silver sulfadiazine for use as an antimicrobial wound dressing. J Nanosci Nanotechnol 14:7488–7494

Lee CM, Yang SW, Jung SC, Kim BH (2017) Oxygen plasma treatment on 3D-printed chitosan/gelatin/hydroxyapatite scaffolds for bone tissue engineering. J Nanosci Nanotechnol 17:2747–2750

Leistner M, Abu-Odeh AA, Rohmer SC, Grunlan JC (2015) Water-based chitosan/melamine polyphosphate multilayer nanocoating that extinguishes fire on polyester-cotton fabric. Carbohydr Polym 130:227–232

Li Z, Zhang M (2005) Chitosan-alginate as scaffolding material for cartilage tissue engineering. J Biomed Mater Res A 75:485–493

Li Z, Ramay HR, Hauch KD, Xiao D, Zhang M (2005) Chitosan-alginate hybrid scaffolds for bone tissue engineering. Biomaterials 26:3919–3928

Li J, Yao J, Li Y, Shao Y (2012a) Controlled release and retarded leaching of pesticides by encapsulating in carboxymethyl chitosan/bentonite composite gel. J Environ Sci Health B 47:795–803

Li X, Chen S, Zhang B, Li M, Diao K, Zhang Z, Li J, Xu Y, Wang X, Chen H (2012b) *In situ* injectable nano-composite hydrogel composed of curcumin, *N,O*-carboxymethyl chitosan and oxidized alginate for wound healing application. Int J Pharm 437:110–119

Li B, Shan CL, Ge MY, Wang L, Fang Y, Wang YL, Xie GL, Sun GC (2013a) Antibacterial mechanism of chitosan and its applications in protection of plant from bacterial disease. Asian J Chem 25:10033–10036

Li X, Min M, Du N, Gu Y, Hode T, Naylor M, Chen D, Nordquist RE, Chen WR (2013b) Chitin, chitosan, and glycated chitosan regulate immune responses: the novel adjuvants for cancer vaccine. Clin Dev Immunol 2013:387023. https://doi.org/10.1155/2013/387023

Li L, Zhao F, Zhao B, Zhang J, Li C, Qiao R (2015) Chitosan grafted with phosphorylcholine and macrocyclic polyamine as an effective gene delivery vector: Preparation, characterization and *in vitro* transfection. Macromol Biosci 15:912–926

Li Y, Qin Y, Liu S, Xing R, Yu H, Li K, Li P (2016) Preparation, characterization, and insecticidal activity of avermectin-grafted-carboxymethyl chitosan. BioMed Res Int 2016:9805675. https://doi.org/10.1155/2016/9805675

Li J, Jiang B, Liu Y, Qiu C, Hu J, Qian G, Guo W, Ngo HH (2017) Preparation and adsorption properties of magnetic chitosan composite adsorbent for Cu^{2+} removal. J Clean Prod 158:51–58

Li R et al (2018a) Chitosan conduit combined with hyaluronic acid prevent sciatic nerve scar in a rat model of peripheral nerve crush injury. Mol Med Rep 17:4360–4368

Li X et al (2018b) The natural product chitosan enhances the anti-tumor activity of natural killer cells by activating dendritic cells. Oncoimmunology 7:e1431085. https://doi.org/10.1080/2162402x.2018.1431085

Liang Y, Liu W, Han B, Yang C, Ma Q, Zhao W, Rong M, Li H (2011) Fabrication and characters of a corneal endothelial cells scaffold based on chitosan. J Mater Sci Mater Med 22:175–183

Liang Y, Xu W, Han B, Li N, Zhao W, Liu W (2014) Tissue-engineered membrane based on chitosan for repair of mechanically damaged corneal epithelium. J Mater Sci Mater Med 25:2163–2171

Liao CD, Zhang F, Guo RM, Zhong XM, Zhu J, Wen XH, Shen J (2012) Peripheral nerve repair: monitoring by using gadofluorine M-enhanced MR imaging with chitosan nerve conduits with cultured mesenchymal stem cells in rat model of neurotmesis. Radiology 262:161–171

Liao J, Li Y, Li H, Liu J, Xie Y, Wang J, Zhang Y (2018) Preparation, bioactivity and mechanism of nano-hydroxyapatite/sodium alginate/chitosan bone repair material. J Appl Biomater Funct Mater 16:28–35

Liaqat F, Eltem R (2018) Chitooligosaccharides and their biological activities: a comprehensive review. Carbohydr Polym 184:243–259

Libio IC, Demori R, Ferrao MF, Lionzo MIZ, da Silveira NP (2016) Films based on neutralized chitosan citrate as innovative composition for cosmetic application. Mater Sci Eng C Mater Biol Appl 67:115–124

Lih E, Lee JS, Park KM, Park KD (2012) Rapidly curable chitosan-PEG hydrogels as tissue adhesives for hemostasis and wound healing. Acta Biomater 8:3261–3269

Lim G-P, Ahmad MS (2017) Development of Ca-alginate-chitosan microcapsules for encapsulation and controlled release of imidacloprid to control dengue outbreaks. J Ind Eng Chem 56:382–393

Lima PA, Resende CX, Soares GD, Anselme K, Almeida LE (2013) Preparation, characterization and biological test of 3D-scaffolds based on chitosan, fibroin and hydroxyapatite for bone tissue engineering. Mater Sci Eng C Mater Biol Appl 33:3389–3395

Lin YL, Jen JC, Hsu SH, Chiu IM (2008) Sciatic nerve repair by microgrooved nerve conduits made of chitosan-gold nanocomposites. Surg Neurol 70(S1):9–18

Lin JH, He CY, Zhang LJ, Zhang SS (2009) Sensitive amperometric immunosensor for alpha-fetoprotein based on carbon nanotube/gold nanoparticle doped chitosan film. Anal Biochem 384:130–135

Lin J, Fan L, Miao R, Le X, Chen S, Zhou X (2015) Enhancing catalytic performance of laccase via immobilization on chitosan/CeO2 microspheres. Int Biol Macromol 78:1–8

Lin YH, Lin JH, Hong YS (2017) Development of chitosan/poly-gamma-glutamic acid/pluronic/curcumin nanoparticles in chitosan dressings for wound regeneration. J Biomed Mater Res B 105:81–90

Listoni AJ, Arruda I, Maia L, Barberini DJ, Martins I, Vasconcellos FC, Landim-Alvarenga FC (2015) Differentiation potential of mesenchymal stem cells from equine bone marrow cultured on hyaluronic acid-chitosan polyelectrolyte multilayer biofilm. J Stem Cells 10:69–77

Liu C, Bai R (2014) Recent advances in chitosan and its derivatives as adsorbents for removal of pollutants from water and wastewater. Curr Opin Chem Eng 4:62–70

Liu Y, Wang MK, Zhao F, Xu ZA, Dong SJ (2005) The direct electron transfer of glucose oxidase and glucose biosensor based on carbon nanotubes/chitosan matrix. Biosens Bioelectron 21:984–988

Liu Z, Wang F, Chen X (2008) Integrin α(v)β(3)-targeted cancer therapy. Drug Dev Res 69:329–339

Liu YX, Yuan R, Chai YQ, Hong CL, Liu KG, Guan S (2009) Ultrasensitive amperometric immunosensor for the determination of carcinoembryonic antigen based on a porous chitosan and gold nanoparticles functionalized interface. Microchim Acta 167:217–224

Liu XJ, Luo LQ, Ding YP, Xu YH (2011) Amperometric biosensors based on alumina nanoparticles-chitosan-horseradish peroxidase nanobiocomposites for the determination of phenolic compounds. Analyst 136:696–701

Liu H, Wen W, Hu M, Bi W, Chen L, Liu S, Chen P, Tan X (2013) Chitosan conduits combined with nerve growth factor microspheres repair facial nerve defects. Neural Regen Res 8:3139–3147

Liu Q, Zheng X, Zhang C, Shao X, Zhang X, Zhang Q, Jiang X (2015a) Conjugating influenza a (H1N1) antigen to *N*-trimethylaminoethylmethacrylate chitosan nanoparticles improves the immunogenicity of the antigen after nasal administration. J Med Virol 87:1807–1815

Liu X-Y, Gohi BFCA, Zeng H-Y, Liao M-C, Sun J-W (2015b) Effect of collagen peptides-carboxymethyl chitosan microspheres on ultraviolet induced damages. Mater Express 5:497–504

Liu J, Liu W, Wang Y, Xu M, Wang B (2016a) A novel reusable nanocomposite adsorbent, xanthated Fe_3O_4-chitosan grafted onto graphene oxide, for removing Cu(II) from aqueous solutions. Appl Surf Sci 367:327–334

Liu Y, Chen L, Yang Y, Li M, Li Y, Dong Y (2016b) The efficient removal of Cu(II) from aqueous solutions by Fe_3O_4@hexadecyl trimethoxysilane@chitosan composites. J Mol Liq 219:341–349

Liuyun J, Yubao L, Chengdong X (2009) Preparation and biological properties of a novel composite scaffold of nano-hydroxyapatite/chitosan/carboxymethyl cellulose for bone tissue engineering. J Biomed Sci 16:65. https://doi.org/10.1186/1423-0127-16-65

Lopes C et al (2015) Chitosan coated textiles may improve atopic dermatitis severity by modulating skin staphylococcal profile: a randomized controlled trial. PloS One 10:e0142844. https://doi.org/10.1371/journal.pone.0142844

Lopez-Carballo G, Higueras L, Gavara R, Hernandez-Munoz P (2013) Silver ions release from antibacterial chitosan films containing *in situ* generated silver nanoparticles. J Agric Food Chem 61:260–267

Lorevice MV, Otoni CG, MRd M, Mattoso LHC (2016) Chitosan nanoparticles on the improvement of thermal, barrier, and mechanical properties of high- and low-methyl pectin films. Food Hydrocolloid 52:732–740

Lotfi G, Shokrgozar MA, Mofid R, Abbas FM, Ghanavati F, Baghban AA, Yavari SK, Pajoumshariati S (2016) Biological evaluation (*in vitro and in vivo*) of bilayered collagenous coated (nano electrospun and solid wall) chitosan membrane for periodontal guided bone regeneration. Ann Biomed Eng 44:2132–2144

Lowe B, Venkatesan J, Anil S, Shim MS, Kim SK (2016) Preparation and characterization of chitosan-natural nano hydroxyapatite-fucoidan nanocomposites for bone tissue engineering. Int Biol Macromol 93:1479–1487

Lu S, Gao W, Gu HY (2008) Construction, application and biosafety of silver nanocrystalline chitosan wound dressing. Burns 34:623–628

Lu Y, Cheng D, Lu S, Huang F, Li G (2014) Preparation of quaternary ammonium salt of chitosan nanoparticles and their textile properties on Antheraea pernyi silk modification. Text Res J 84:2115–2124

Lu B, Wang T, Li Z, Dai F, Lv L, Tang F, Yu K, Liu J, Lan G (2016) Healing of skin wounds with a chitosan–gelatin sponge loaded with tannins and platelet-rich plasma. Int Biol Macromol 82:884–891

Lu Z, Gao J, He Q, Wu J, Liang D, Yang H, Chen R (2017) Enhanced antibacterial and wound healing activities of microporous chitosan-Ag/ZnO composite dressing. Carbohydr Polym 156:460–469

Lu Y et al (2018) High-activity chitosan/nano hydroxyapatite/zoledronic acid scaffolds for simultaneous tumor inhibition, bone repair and infection eradication. Mater Sci Eng C Mater Biol Appl 82:225–233

Luna-Hernandez E et al (2017) Combined antibacterial/tissue regeneration response in thermal burns promoted by functional chitosan/silver nanocomposites. Int Biol Macromol 105:1241–1249

Ma W, Tang C-H, Yang X-Q, Yin S-W (2013a) Fabrication and characterization of kidney bean (*Phaseolus vulgaris* L.) protein isolate–chitosan composite films at acidic pH. Food Hydrocolloid 31:237–247

Ma Z, Yang L, Yan H, Kennedy JF, Meng X (2013b) Chitosan and oligochitosan enhance the resistance of peach fruit to brown rot. Carbohydr Polym 94:272–277

Ma S et al (2014) Guided bone regeneration with tripolyphosphate cross-linked asymmetric chitosan membrane. J Dent 42:1603–1612

Ma F, Zhang Q, Zheng L (2015) Interleukin/chitosan (JY) adjuvant enhances the mucosal immunity of human papillomavirus 16 L1 virus-like particles in mice. Biotechnol Lett 37:773–777

Madureira AR, Pereira A, Pintado M (2015) Current state on the development of nanoparticles for use against bacterial gastrointestinal pathogens. Focus on chitosan nanoparticles loaded with phenolic compounds. Carbohydr Polym 130:429–439

Maji K, Dasgupta S, Kundu B, Bissoyi A (2015) Development of gelatin-chitosan-hydroxyapatite based bioactive bone scaffold with controlled pore size and mechanical strength. J Biomater Sci Polym Ed 26:1190–1209

Malerba M, Cerana R (2016) Chitosan effects on plant systems. Int J Mol Sci 17. https://doi.org/10.3390/ijms17070996

Malik A, Gupta M, Mani R, Gogoi H, Bhatnagar R (2018) Trimethyl chitosan nanoparticles encapsulated protective antigen protects the mice against anthrax. Front Immunol 9:562. https://doi.org/10.3389/fimmu.2018.00562

Martin-Lopez E, Alonso FR, Nieto-Diaz M, Nieto-Sampedro M (2012) Chitosan, gelatin and poly (L-lysine) polyelectrolyte-based scaffolds and films for neural tissue engineering. J Biomater Sci Polym Ed 23:207–232

Martiñon ME, Moreira RG, Castell-Perez ME, Gomes C (2014) Development of a multilayered antimicrobial edible coating for shelf-life extension of fresh-cut cantaloupe (*Cucumis melo* L.) stored at 4 °C. LWT – Food Sci Technol 56:341–350

Martins JT, Cerqueira MA, Vicente AA (2012) Influence of α-tocopherol on physicochemical properties of chitosan-based films. Food Hydrocolloid 27:220–227

Masoomi L, Sadeghi O, Banitaba MH, Shahrjerdi A, Davarani SSH (2013) A non-enzymatic nanomagnetic electro-immunosensor for determination of Aflatoxin B-1 as a model antigen. Sensor Actuat B-Chem 177:1122–1127

Matos BN, Reis TA, Gratieri T, Gelfuso GM (2015) Chitosan nanoparticles for targeting and sustaining minoxidil sulphate delivery to hair follicles. Int Biol Macromol 75:225–229

Matsumura Y, Maeda H (1986) A new concept for macromolecular therapeutics in cancer chemotherapy: mechanism of tumoritropic accumulation of proteins and the antitumor agent smancs. Cancer Res 46:6387–6392

Matsuyama T, Mackay M, Midha R (2000) Peripheral nerve repair and grafting techniques: a review. Neurol Med Chir 40:187–199

Mattioli-Belmonte M, Gigante A, Muzzarelli RA, Politano R, De Benedittis A, Specchia N, Buffa A, Biagini G, Greco F (1999) *N,N*-dicarboxymethyl chitosan as delivery agent for bone morphogenetic protein in the repair of articular cartilage. Med Biol Eng Comput 37:130–134

McNeela EA, O'Connor D, Jabbal-Gill I, Illum L, Davis SS, Pizza M, Peppoloni S, Rappuoli R, Mills KH (2000) A mucosal vaccine against diphtheria: formulation of cross reacting material (CRM(197)) of diphtheria toxin with chitosan enhances local and systemic antibody and Th2 responses following nasal delivery. Vaccine 19:1188–1198

Medyantseva EP, Brusnitsyn DV, Varlamova RM, Baibatarova MA, Budnikov GK, Fattakhova AN (2014) determination of antidepressants using monoamine oxidase amperometric biosensors based on screen-printed graphite electrodes modified with multi-walled carbon nanotubes. Pharm Chem J 48:478–482

Melaj MA, Daraio ME (2013) Preparation and characterization of potassium nitrate controlled-release fertilizers based on chitosan and xanthan layered tablets. J Appl Polymer Sci 130:2422–2428

Mellati A, Kiamahalleh MV, Madani SH, Dai S, Bi J, Jin B, Zhang H (2016) Poly(*N*-isopropylacrylamide) hydrogel/chitosan scaffold hybrid for three-dimensional stem cell culture and cartilage tissue engineering. J Biomed Mater Res A 104:2764–2774

Mendes RK, Arruda BS, de Souza EF, Nogueira AB, Teschke O, Bonugli LO, Etchegaray A (2017) Determination of chlorophenol in environmental samples using a voltammetric biosensor based on hybrid nanocomposite. J Brazil Chem Soc 28:1212–1219

Meng Q et al (2015) A composite scaffold of MSC affinity peptide-modified demineralized bone matrix particles and chitosan hydrogel for cartilage regeneration. Sci Rep 5:17802. https://doi.org/10.1038/srep17802

Mengoni T, Adrian M, Pereira S, Santos-Carballal B, Kaiser M, Goycoolea FM (2017) A Chitosan-based liposome formulation enhances the *in vitro* wound healing efficacy of substance P. Neuropeptide 9. https://doi.org/10.3390/pharmaceutics9040056

Meyer C et al (2016) Peripheral nerve regeneration through hydrogel-enriched chitosan conduits containing engineered Schwann cells for drug delivery. Cell Transplant 25:159–182

Miranda DG, Malmonge SM, Campos DM, Attik NG, Grosgogeat B, Gritsch K (2016) A chitosan-hyaluronic acid hydrogel scaffold for periodontal tissue engineering. J Biomed Mater Res B 104:1691–1702

Mitra S, Gaur U, Ghosh PC, Maitra AN (2001) Tumour targeted delivery of encapsulated dextran–doxorubicin conjugate using chitosan nanoparticles as carrier. J Control Release 74:317–323

Moattari M, Kouchesfehani HM, Kaka G, Sadraie SH, Naghdi M, Mansouri K (2018) Chitosan-film associated with mesenchymal stem cells enhanced regeneration of peripheral nerves: a rat sciatic nerve model. J Chem Neuroanat 88:46–54

Möller H, Grelier S, Pardon P, Coma V (2004) Antimicrobial and physicochemical properties of chitosan−HPMC-based films. J Agric Food Chem 52:6585–6591

Monosik R, Stred'ansky M, Luspai K, Magdolen P, Sturdik E (2012) Amperometric glucose biosensor utilizing FAD-dependent glucose dehydrogenase immobilized on nanocomposite electrode. Enzym Microb Technol 50:227–232

Mori A et al (2012) The vaccine adjuvant alum inhibits IL-12 by promoting PI3 kinase signaling while chitosan does not inhibit IL-12 and enhances Th1 and Th17 responses. Eur J Immunol 42:2709–2719

Muzzarelli RA, Biagini G, Bellardini M, Simonelli L, Castaldini C, Fratto G (1993a) Osteoconduction exerted by methylpyrrolidinone chitosan used in dental surgery. Biomaterials 14:39–43

Muzzarelli RAA, Zucchini C, Ilari P, Pugnaloni A, Mattioli Belmonte M, Biagini G, Castaldini C (1993b) Osteoconductive properties of methylpyrrolidinone chitosan in an animal model. Biomaterials 14:925–929

Muzzarelli RA, Greco F, Busilacchi A, Sollazzo V, Gigante A (2012) Chitosan, hyaluronan and chondroitin sulfate in tissue engineering for cartilage regeneration: a review. Carbohydr Polym 89:723–739

Nada A, Al-Moghazy M, Soliman AAF, Rashwan GMT, Eldawy THA, Hassan AAE, Sayed GH (2018) Pyrazole-based compounds in chitosan liposomal emulsion for antimicrobial cotton fabrics. Int Biol Macromol 107:585–594

Nandi SK, Kundu B, Basu D (2013) Protein growth factors loaded highly porous chitosan scaffold: a comparison of bone healing properties. Mater Sci Eng C 33:1267–1275

Naruphontjirakul P, Viravaidya-Pasuwat K (2011) Development of doxorubicin – core shell chitosan nanoparticles to treat cancer. Int Conf Biomed Eng Technol, IPCBEE, 11, Singapore

Nascimento EG, Sampaio TB, Medeiros AC, Azevedo EP (2009) Evaluation of chitosan gel with 1% silver sulfadiazine as an alternative for burn wound treatment in rats. Acta Cir Bras 24:460–465

Nawalakhe R, Shi Q, Vitchuli N, Bourham MA, Zhang X, McCord MG (2015) Plasma-assisted preparation of high-performance chitosan nanofibers/gauze composite bandages. Int J Polym Mater Polym 64:709–717

Neves SC, Moreira Teixeira LS, Moroni L, Reis RL, Van Blitterswijk CA, Alves NM, Karperien M, Mano JF (2011) Chitosan/poly(epsilon-caprolactone) blend scaffolds for cartilage repair. Biomaterials 32:1068–1079

Ngo DH, Kim SK (2014) Antioxidant effects of chitin, chitosan, and their derivatives. Adv Food Nutr Res 73:15–31

Nguyen HM, Hwang IC, Park JW, Park HJ (2012) Photoprotection for deltamethrin using chitosan-coated beeswax solid lipid nanoparticles. Pest Manag Sci 68:1062–1068

Nguyen VC, Nguyen NLG, Pho QH (2015) Preparation of magnetic composite based on zinc oxide nanoparticles and chitosan as a photocatalyst for removal of reactive blue 198. Adv Nat Sci Nanosci Nanotechnol 6:035001. https://doi.org/10.1088/2043-6262/6/3/035001

Nguyen NLG, Pho Q-H, Nguyen V-C (2016) A high photo-catalytic activity of magnetic composite based on chitosan and manganese-doped zinc oxide nanoparticles for removal of dyeing wastewater. J Nanosci Nanotechnol 16:7959–7967

Ni S, Liu Y, Tang Y, Chen J, Li S, Pu J, Han L (2018) GABAB receptor ligand-directed trimethyl chitosan/tripolyphosphate nanoparticles and their pMDI formulation for survivin siRNA pulmonary delivery. Carbohydr Polym 179:135–144

Nie X, Deng M, Yang M, Liu L, Zhang Y, Wen X (2014) Axonal regeneration and remyelination evaluation of chitosan/gelatin-based nerve guide combined with transforming growth factor-beta1 and Schwann cells. Cell Biochem Biophys 68:163–172

Niu Y, Li K, Ying D, Wang Y, Jia J (2017) Novel recyclable adsorbent for the removal of copper (II) and lead(II) from aqueous solution. Bioresour Technol 229:63–68

No HK, Meyers SP, Prinyawiwatkul W, Xu Z (2007) Applications of chitosan for improvement of quality and shelf life of foods: a review. J Food Sci 72:R87–R100

Noorbakhsh-Soltani SM, Zerafat MM, Sabbaghi S (2018) A comparative study of gelatin and starch-based nano-composite films modified by nano-cellulose and chitosan for food packaging applications. Carbohydr Polym 189:48–55

Noppakundilograt S, Pheatcharat N, Kiatkamjornwong S (2015) Multilayer-coated NPK compound fertilizer hydrogel with controlled nutrient release and water absorbency. J Appl Polymer Sci 132. https://doi.org/10.1002/App.41249

Nordtveit RJ, Varum KM, Smidsrod O (1994) Degradation of fully water-soluble, partially N-acetylated chitosans with lysozyme. Carbohydr Polym 23:253–260

Oliveira JM et al (2006) Novel hydroxyapatite/chitosan bilayered scaffold for osteochondral tissue-engineering applications: Scaffold design and its performance when seeded with goat bone marrow stromal cells. Biomaterials 27:6123–6137

Oryan A, Alidadi S, Bigham-Sadegh A, Meimandi-Parizi A (2017) Chitosan/gelatin/platelet gel enriched by a combination of hydroxyapatite and beta-tricalcium phosphate in healing of a radial bone defect model in rat. Int Biol Macromol 101:630–637

Osman R, Kan PL, Awad G, Mortada N, El-Shamy AE, Alpar O (2013) Spray dried inhalable ciprofloxacin powder with improved aerosolisation and antimicrobial activity. Int J Pharm 449:44–58

Owens MA, Horten BC, Da Silva MM (2004) HER2 amplification ratios by fluorescence *in situ* hybridization and correlation with immunohistochemistry in a cohort of 6556 breast cancer tissues. Clin Breast Cancer 5:63–69

Ozcelik B, Brown KD, Blencowe A, Daniell M, Stevens GW, Qiao GG (2013) Ultrathin chitosan-poly(ethylene glycol) hydrogel films for corneal tissue engineering. Acta Biomater 9:6594–6605

Ozer H, Bozkurt H, Bozkurt G, Demirbilek M (2018) Regenerative potential of chitosan-coated poly-3-hydroxybutyrate conduits seeded with mesenchymal stem cells in a rat sciatic nerve injury model. Int J Neurosci 128:828–834

Pal AK, Katiyar V (2016) Nanoamphiphilic chitosan dispersed poly(lactic acid) bionanocomposite films with improved thermal, mechanical, and gas barrier properties. Biomacromolecules 17:2603–2618

Pallela R, Venkatesan J, Janapala VR, Kim SK (2012) Biophysicochemical evaluation of chitosan-hydroxyapatite-marine sponge collagen composite for bone tissue engineering. J Biomed Mater Res A 100:486–495

Paltiel O, Fedorova G, Tadmor G, Kleinstern G, Maor Y, Chefetz B (2016) Human exposure to wastewater-derived pharmaceuticals in fresh produce: a randomized controlled trial focusing on carbamazepine. Environ Sci Technol 50:4476–4482

Panos I, Acosta N, Heras A (2008) New drug delivery systems based on chitosan. Curr Drug Discov Technol 5:333–341

Park YJ, Lee YM, Lee JY, Seol YJ, Chung CP, Lee SJ (2000a) Controlled release of platelet-derived growth factor-BB from chondroitin sulfate–chitosan sponge for guided bone regeneration. J Control Release 67:385–394

Park YJ, Lee YM, Park SN, Sheen SY, Chung CB, Lee SJ (2000b) Platelet derived growth factor releasing chitosan sponge for periodontal bone regeneration. Biomaterials 21:153–159

Park JU, Jung HD, Song EH, Choi TH, Kim HE, Song J, Kim S (2017) The accelerating effect of chitosan-silica hybrid dressing materials on the early phase of wound healing. J Biomed Mater Res B 105:1828–1839

Patel S, Srivastava S, Singh MR, Singh D (2018) Preparation and optimization of chitosan-gelatin films for sustained delivery of lupeol for wound healing. Int Biol Macromol 107:1888–1897

Patil PS, Fountas-Davis N, Huang H, Michelle Evancho-Chapman M, Fulton JA, Shriver LP, Leipzig ND (2016) Fluorinated methacrylamide chitosan hydrogels enhance collagen synthesis in wound healing through increased oxygen availability. Acta Biomater 36:164–174

Patrulea V, Ostafe V, Borchard G, Jordan O (2015) Chitosan as a starting material for wound healing applications. Eur J Pharm Biopharm 97:417–426

Peluso G, Petillo O, Ranieri M, Santin M, Ambrosio L, Calabró D, Avallone B, Balsamo G (1994) Chitosan-mediated stimulation of macrophage function. Biomaterials 15:1215–1220

Peng CC, Yang MH, Chiu WT, Chiu CH, Yang CS, Chen YW, Chen KC, Peng RY (2008) Composite nano-titanium oxide-chitosan artificial skin exhibits strong wound-healing effect-an approach with anti-inflammatory and bactericidal kinetics. Macromol Biosci 8:316–327

Peng S, Meng H, Ouyang Y, Chang J (2014) Nanoporous magnetic cellulose–chitosan composite microspheres: preparation, characterization, and application for Cu(II) adsorption. Ind Eng Chem Res 53:2106–2113

Pereira FAR, Sousa KS, Cavalcanti GRS, Fonseca MG, de Souza AG, Alves APM (2013) Chitosan-montmorillonite biocomposite as an adsorbent for copper (II) cations from aqueous solutions. Int Biol Macromol 61:471–478

Perez JJ, Francois NJ (2016) Chitosan-starch beads prepared by ionotropic gelation as potential matrices for controlled release of fertilizers. Carbohydr Polym 148:134–142

Periayah MH, Halim AS, Hussein AR, Saad AZ, Rashid AH, Noorsal K (2013) *In vitro* capacity of different grades of chitosan derivatives to induce platelet adhesion and aggregation. Int J Biol Macromol 52:244–249

Periolatto M, Ferrero F (2013) Cotton filter fabrics functionalization by chitosan UV-grafting for removal of dyes. Chem Eng Trans 32:85–90

Periolatto M, Ferrero F, Vineis C (2012) Antimicrobial chitosan finish of cotton and silk fabrics by UV-curing with 2-hydroxy-2-methylphenylpropane-1-one. Carbohydr Polym 88:201–205

Petkova P, Francesko A, Fernandes MM, Mendoza E, Perelshtein I, Gedanken A, Tzanov T (2014) Sonochemical coating of textiles with hybrid ZnO/chitosan antimicrobial nanoparticles. ACS Appl Mater Interfaces 6:1164–1172

Petri DF, Donega J, Benassi AM, Bocangel JA (2007) Preliminary study on chitosan modified glass ionomer restoratives. Dent Mater 23:1004–1010

Phinney DG, Pittenger MF (2017) Concise review: msc-derived exosomes for cell-free therapy. Stem Cells 35:851–858

Picola IP, Shi Q, Fernandes JC, Petronio MS, Lima AM, de Oliveira Tiera VA, Tiera MJ (2016) Chitosan derivatives for gene transfer: effect of phosphorylcholine and diethylaminoethyl grafts on the *in vitro* transfection efficiency. J Biomater Sci Polym Ed 27:1611–1630

Pihlstrom BL, Michalowicz BS, Johnson NW (2005) Periodontal diseases. Lancet 366:1809–1820

Pirouzmand H, Khameneh B, Tafaghodi M (2017) Immunoadjuvant potential of cross-linked dextran microspheres mixed with chitosan nanospheres encapsulated with tetanus toxoid. Pharm Biol 55:212–217

Poverenov E, Danino S, Horev B, Granit R, Vinokur Y, Rodov V (2014a) Layer-by-layer electrostatic deposition of edible coating on fresh cut melon model: anticipated and unexpected effects of alginate–chitosan combination. Food Bioprocess Technol 7:1424–1432

Poverenov E, Zaitsev Y, Arnon H, Granit R, Alkalai-Tuvia S, Perzelan Y, Weinberg T, Fallik E (2014b) Effects of a composite chitosan–gelatin edible coating on postharvest quality and storability of red bell peppers. Postharvest Biol Technol 96:106–109

Prabaharan M (2015) Chitosan-based nanoparticles for tumor-targeted drug delivery. Int Biol Macromol 72:1313–1322

Przekora A, Ginalska G (2017) Chitosan/beta-1,3-glucan/hydroxyapatite bone scaffold enhances osteogenic differentiation through TNF-alpha-mediated mechanism. Mater Sci Eng C Mater Biol Appl 73:225–233

Przekora A, Vandrovcova M, Travnickova M, Pajorova J, Molitor M, Ginalska G, Bacakova L (2017) Evaluation of the potential of chitosan/beta-1,3-glucan/hydroxyapatite material as a scaffold for living bone graft production *in vitro* by comparison of ADSC and BMDSC behaviour on its surface. Biomed Mater 12:015030

Puspita A, Prawati G, Fatimah I (2017) Chitosan-modified smectite clay and study on adsorption-desorption of urea. Chem Eng Trans 56:1645–1650

Qasim SB, Zafar MS, Najeeb S, Khurshid Z, Shah AH, Husain S, Rehman IU (2018) Electrospinning of chitosan-based solutions for tissue engineering and regenerative medicine. Int J Mol Sci 19:407

Qi L, Xu Z (2006) *In vivo* antitumor activity of chitosan nanoparticles. Bioorg Med Chem Lett 16:4243–4245

Qi BW, Yu AX, Zhu SB, Zhou M, Wu G (2013) Chitosan/poly(vinyl alcohol) hydrogel combined with Ad-hTGF-beta1 transfected mesenchymal stem cells to repair rabbit articular cartilage defects. Exp Biol Med 238:23–30

Qin Y, Wang HW, Karuppanapandian T, Kim W (2010) Chitosan green tea polyphenol complex as a released control compound for wound healing. Chin J Traumatol 13:91–95

Qin Y, Guo XW, Li L, Wang HW, Kim W (2013) The antioxidant property of chitosan green tea polyphenols complex induces transglutaminase activation in wound healing. J Med Food 16:487–498

Qiu JD, Liang RP, Wang R, Fan LX, Chen YW, Xia XH (2009) A label-free amperometric immunosensor based on biocompatible conductive redox chitosan-ferrocene/gold nanoparticles matrix. Biosens Bioelectron 25:852–857

Quan D, Shin W (2010) A nitrite biosensor based on co-immobilization of nitrite reductase and viologen-modified chitosan on a glassy carbon electrode. Sensors 10:6241–6256

Raafat D, Sahl HG (2009) Chitosan and its antimicrobial potential-a critical literature survey. Microb Biotechnol 2:186–201

Rabea EI, Badawy MET, Stevens CV, Smagghe G, Steurbaut W (2003) Chitosan as antimicrobial agent: applications and mode of action. Biomacromolecules 4:1457–1465

Radmansouri M, Bahmani E, Sarikhani E, Rahmani K, Sharifianjazi F, Irani M (2018) Doxorubicin hydrochloride – Loaded electrospun chitosan/cobalt ferrite/titanium oxide nanofibers for hyperthermic tumor cell treatment and controlled drug release. Int Biol Macromol. 116:378–384

Rafat M, Li F, Fagerholm P, Lagali NS, Watsky MA, Munger R, Matsuura T, Griffith M (2008) PEG-stabilized carbodiimide crosslinked collagen-chitosan hydrogels for corneal tissue engineering. Biomaterials 29:3960–3972

Raghuwanshi D, Mishra V, Das D, Kaur K, Suresh MR (2012) Dendritic cell targeted chitosan nanoparticles for nasal DNA immunization against SARS CoV nucleocapsid protein. Mol Pharm 9:946–956

Rajan M, Raj V, Al-Arfaj AA, Murugan AM (2013) Hyaluronidase enzyme core-5-fluorouracil-loaded chitosan-PEG-gelatin polymer nanocomposites as targeted and controlled drug delivery vehicles. Int J Pharm 453:514–522

Rajashree S, Rose C (2017) Studies on an anti-aging formulation prepared using Aloe vera blended collagen and chitosan. Intl J Pharm Sci Res 19:582–588

Rajiv Gandhi M, Kousalya GN, Meenakshi S (2011) Removal of copper(II) using chitin/chitosan nano-hydroxyapatite composite. Int Biol Macromol 48:119–124

Rakwal R, Tamogami S, Agrawal GK, Iwahashi H (2002) Octadecanoid signaling component "burst" in rice (*Oryza sativa* L.) seedling leaves upon wounding by cut and treatment with fungal elicitor chitosan. Biochem Biophys Res Commun 295:1041–1045

Ramya R, Sudha PN (2013) Adsorption of cadmium (II) and copper (II) ions from aqueous solution using chitosan composite. Polym Compos 34:233–240

Ran J, Hu J, Sun G, Chen S, Jiang P, Shen X, Tong H (2016) A novel chitosan-tussah silk fibroin/nano-hydroxyapatite composite bone scaffold platform with tunable mechanical strength in a wide range. Int Biol Macromol 93:87–97

Ranganath AS, Sarkar AK (2014) Evaluation of durability to laundering of triclosan and chitosan on a textile substrate. J Text 2014:5. https://doi.org/10.1155/2014/812303

Rasente RY, Imperiale JC, Lazaro-Martinez JM, Gualco L, Oberkersch R, Sosnik A, Calabrese GC (2016) Dermatan sulfate/chitosan polyelectrolyte complex with potential application in the treatment and diagnosis of vascular disease. Carbohydr Polym 144:362–370

Rattanamanee A, Niamsup H, L-o S, Punyodom W, Watanesk R, Watanesk S (2015) Role of chitosan on some physical properties and the urea controlled release of the silk fibroin/gelatin hydrogel. J Polym Environ 23:334–340

Raza ZA, Anwar F, Ahmad S, Aslam M (2016) Fabrication of ZnO incorporated chitosan nanocomposites for enhanced functional properties of cellulosic fabric. Mater Res Express 3:115001. https://doi.org/10.1088/2053-1591/3/11/115001

Read RC, Naylor SC, Potter CW, Bond J, Jabbal-Gill I, Fisher A, Illum L, Jennings R (2005) Effective nasal influenza vaccine delivery using chitosan. Vaccine 23:4367–4374

Reddy DHK, Lee S-M (2013) Application of magnetic chitosan composites for the removal of toxic metal and dyes from aqueous solutions. Adv Colloid Interface Sci 201-202:68–93

Reesha KV, Panda SK, Bindu J, Varghese TO (2015) Development and characterization of an LDPE/chitosan composite antimicrobial film for chilled fish storage. Int Biol Macromol 79:934–942

Rehan M, El-Naggar ME, Mashaly HM, Wilken R (2018) Nanocomposites based on chitosan/silver/clay for durable multi-functional properties of cotton fabrics. Carbohydr Polym 182:29–41

Revathi T, Thambidurai S (2017) Synthesis of chitosan incorporated neem seed extract (*Azadirachta indica*) for medical textiles. Int Biol Macromol 104:1890–1896

Ribeiro MP, Morgado PI, Miguel SP, Coutinho P, Correia IJ (2013) Dextran-based hydrogel containing chitosan microparticles loaded with growth factors to be used in wound healing. Mater Sci Eng C Mater Biol Appl 33:2958–2966

Richardson SC, Kolbe HV, Duncan R (1999) Potential of low molecular mass chitosan as a DNA delivery system: biocompatibility, body distribution and ability to complex and protect DNA. Int J Pharm 178:231–243

Ridolfi DM, Marcato PD, Justo GZ, Cordi L, Machado D, Duran N (2012) Chitosan-solid lipid nanoparticles as carriers for topical delivery of tretinoin. Colloid Surf B 93:36–40

Roonprapunt C, Huang W, Grill R, Friedlander D, Grumet M, Chen S, Schachner M, Young W (2003) Soluble cell adhesion molecule L1-Fc promotes locomotor recovery in rats after spinal cord injury. J Neurotrauma 20:871–882

Roshanravan B, Soltani SM, Rashid SA, Mahdavi F, Yusop MK (2015) Enhancement of nitrogen release properties of urea-kaolinite fertilizer with chitosan binder. Chem Spec Bioavailab 27:43–50

Ruan Q, Siddiqah N, Li X, Nutt S, Moradian-Oldak J (2014) Amelogenin-chitosan matrix for human enamel regrowth: effects of viscosity and supersaturation degree. Connect Tissue Res 55 (Suppl 1):150–154

Russell-Jones G, McTavish K, McEwan J, Rice J, Nowotnik D (2004) Vitamin-mediated targeting as a potential mechanism to increase drug uptake by tumours. J Inorg Biochem 98:1625–1633

Sadeghi-Kiakhani M, Arami M, Gharanjig K (2013) Application of a biopolymer chitosan-poly (propylene)imine dendrimer hybrid as an antimicrobial agent on the wool fabrics. Iran Polym J 22:931–940

Saharan V, Kumaraswamy RV, Choudhary RC, Kumari S, Pal A, Raliya R, Biswas P (2016) Cu-chitosan nanoparticle mediated sustainable approach to enhance seedling growth in maize by mobilizing reserved food. J Agric Food Chem 64:6148–6155

Sahni JK, Chopra S, Ahmad FJ, Khar RK (2008) Potential prospects of chitosan derivative trimethyl chitosan chloride (TMC) as a polymeric absorption enhancer: synthesis, characterization and applications. J Pharm Pharmacol 60:1111–1119

Sakkinen M, Marvola J, Kanerva H, Lindevall K, Ahonen A, Marvola M (2004) Scintigraphic verification of adherence of a chitosan formulation to the human oesophagus. Eur J Pharm Biopharm 57:145–147

Saleh AS, Ibrahim AG, Abdelhai F, Elsharma EM, Metwally E, Siyam T (2017) Preparation of poly (chitosan-acrylamide) flocculant using gamma radiation for adsorption of Cu(II) and Ni(II) ions. Radiat Phys Chem 134:33–39

Salehi E, Daraei P, Arabi Shamsabadi A (2016) A review on chitosan-based adsorptive membranes. Carbohydr Polym 152:419–432

Samprasit W, Kaomongkolgit R, Sukma M, Rojanarata T, Ngawhirunpat T, Opanasopit P (2015) Mucoadhesive electrospun chitosan-based nanofibre mats for dental caries prevention. Carbohydr Polym 117:933–940

Sanad RA, Abdel-Bar HM (2017) Chitosan-hyaluronic acid composite sponge scaffold enriched with Andrographolide-loaded lipid nanoparticles for enhanced wound healing. Carbohydr Polym 173:441–450

Sandri G, Rossi S, Bonferoni MC, Ferrari F, Zambito Y, Di Colo G, Caramella C (2005) Buccal penetration enhancement properties of *N*-trimethyl chitosan: Influence of quaternization degree on absorption of a high molecular weight molecule. Int J Pharm 297:146–155

Sanpui P, Murugadoss A, Prasad PV, Ghosh SS, Chattopadhyay A (2008) The antibacterial properties of a novel chitosan-Ag-nanoparticle composite. Int J Food Microbiol 124:142–146

Sanuja S, Agalya A, Umapathy MJ (2015) Synthesis and characterization of zinc oxide–neem oil–chitosan bionanocomposite for food packaging application. Int Biol Macromol 74:76–84

Sargın İ, Arslan G, Kaya M (2016a) Efficiency of chitosan–algal biomass composite microbeads at heavy metal removal. React Funct Polym 98:38–47

Sargın İ, Arslan G, Kaya M (2016b) Microfungal spores (*Ustilago maydis* and *U. digitariae*) immobilised chitosan microcapsules for heavy metal removal. Carbohydr Polym 138:201–209

Sarvaiya J, Agrawal YK (2015) Chitosan as a suitable nanocarrier material for anti-Alzheimer drug delivery. Int Biol Macromol 72:454–465

Sawaengsak C, Mori Y, Yamanishi K, Srimanote P, Chaicumpa W, Mitrevej A, Sinchaipanid N (2014) Intranasal chitosan-DNA vaccines that protect across influenza virus subtypes. Int J Pharm 473:113–125

Scacchetti FAP, Pinto E, Soares GMB (2017) Preparation and characterization of cotton fabrics with antimicrobial properties through the application of chitosan/silver-zeolite film. Procedia Eng 200:276–282

Scherliess R, Buske S, Young K, Weber B, Rades T, Hook S (2013) *In vivo* evaluation of chitosan as an adjuvant in subcutaneous vaccine formulations. Vaccine 31:4812–4819

Schipper P et al (2017) *Diphtheria* toxoid and *N*-trimethyl chitosan layer-by-layer coated pH-sensitive microneedles induce potent immune responses upon dermal vaccination in mice. J Control Release 262:28–36

Sellgren KL, Ma T (2012) Perfusion conditioning of hydroxyapatite-chitosan-gelatin scaffolds for bone tissue regeneration from human mesenchymal stem cells. J Tissue Eng Regen Med 6:49–59

Senyigit ZA, Karavana SY, Erac B, Gursel O, Limoncu MH, Baloglu E (2014) Evaluation of chitosan based vaginal bioadhesive gel formulations for antifungal drugs. Acta Pharm 64:139–156

Shakir M, Jolly R, Khan MS, Rauf A, Kazmi S (2016) Nano-hydroxyapatite/beta-CD/chitosan nanocomposite for potential applications in bone tissue engineering. Int Biol Macromol 93:276–289

Sharma S (2017) Enhanced antibacterial efficacy of silver nanoparticles immobilized in a chitosan nanocarrier. Int Biol Macromol 104:1740–1745

Shavandi A, Bekhit Ael D, Sun Z, Ali A, Gould M (2015) A novel squid pen chitosan/hydroxyapatite/beta-tricalcium phosphate composite for bone tissue engineering. Mater Sci Eng C Mater Biol Appl 55:373–383

Shen H, Shen ZL, Zhang PH, Chen NL, Wang YC, Zhang ZF, Jin YQ (2010) Ciliary neurotrophic factor-coated polylactic-polyglycolic acid chitosan nerve conduit promotes peripheral nerve regeneration in canine tibial nerve defect repair. J Biomed Mater Res B 95:161–170

Shen J-M, Gao F-Y, Yin T, Zhang H-X, Ma M, Yang Y-J, Yue F (2013a) cRGD-functionalized polymeric magnetic nanoparticles as a dual-drug delivery system for safe targeted cancer therapy. Pharmacol Res 70:102–115

Shen T, Pan ZG, Zhou X, Hong CY (2013b) Accelerated healing of diabetic wound using artificial dermis constructed with adipose stem cells and poly (L-glutamic acid)/chitosan scaffold. Chin Med J 126:1498–1503

Shi Q, Wang H, Tran C, Qiu X, Winnik FM, Zhang X, Dai K, Benderdour M, Fernandes JC (2011) Hydrodynamic delivery of chitosan-folate-DNA nanoparticles in rats with adjuvant-induced arthritis. J Biomed Biotechnol 2011:148763. https://doi.org/10.1155/2011/148763

Shi GN et al (2017a) Enhanced antitumor immunity by targeting dendritic cells with tumor cell lysate-loaded chitosan nanoparticles vaccine. Biomaterials 113:191–202

Shi Q, Qian Z, Liu D, Sun J, Wang X, Liu H, Xu J, Guo X (2017b) GMSC-derived exosomes combined with a chitosan/silk hydrogel sponge accelerates wound healing in a diabetic rat skin defect model. Front Physiol 8:904. https://doi.org/10.3389/fphys.2017.00904

Shibasaki K, Sano H, Matsukubo T, Takaesu Y (1994) pH response of human dental plaque to chewing gum supplemented with low molecular chitosan. Bull Tokyo Dent College 35:61–66

Shibata Y, Foster LA, Metzger WJ, Myrvik QN (1997a) Alveolar macrophage priming by intravenous administration of chitin particles, polymers of *N*-acetyl-D-glucosamine, in mice. Inf Immun 65:1734–1741

Shibata Y, Metzger WJ, Myrvik QN (1997b) Chitin particle-induced cell-mediated immunity is inhibited by soluble mannan: mannose receptor-mediated phagocytosis initiates IL-12 production. J Immunol 159:2462–2467

Shirosaki Y, Hayakawa S, Osaka A, Lopes MA, Santos JD, Geuna S, Mauricio AC (2014) Challenges for nerve repair using chitosan-siloxane hybrid porous scaffolds. BioMed Res Int 2014:153808. https://doi.org/10.1155/2014/153808

Shrestha BK, Ahmad R, Mousa HM, Kim IG, Kim JI, Neupane MP, Park CH, Kim CS (2016) High-performance glucose biosensor based on chitosan-glucose oxidase immobilized polypyrrole/Nafion/functionalized multi-walled carbon nanotubes bio-nanohybrid film. J Colloid Interface Sci 482:39–47

Shukla R, Kashaw SK, Jain AP, Lodhi S (2016) Fabrication of Apigenin loaded gellan gum-chitosan hydrogels (GGCH-HGs) for effective diabetic wound healing. Int Biol Macromol 91:1110–1119

Siafu SI (2017) Silicone doped chitosan-acrylamide coencapsulated urea fertilizer: an approach to controlled release fertilizers. J Nanotechnol 8490730. https://doi.org/10.1155/2017/8490730

Silva Mdos S, Cocenza DS, Grillo R, de Melo NF, Tonello PS, de Oliveira LC, Cassimiro DL, Rosa AH, Fraceto LF (2011) Paraquat-loaded alginate/chitosan nanoparticles: preparation, characterization and soil sorption studies. J Hazard Mater 190:366–374

Silva SS, Motta A, Rodrigues MT, Pinheiro AF, Gomes ME, Mano JF, Reis RL, Migliaresi C (2008) Novel genipin-cross-linked chitosan/silk fibroin sponges for cartilage engineering strategies. Biomacromolecules 9:2764–2774

Sin J-C, Lam S-M, Mohamed AR, Lee K-T (2012) Degrading endocrine disrupting chemicals from wastewater by TiO_2 photocatalysis: a review. Int J Photoenergy:185159. https://doi.org/10.1155/2012/185159

Singh A, Sinsinbar G, Choudhary M, Kumar V, Pasricha R, Verma HN, Singh SP, Arora K (2013) Graphene oxide-chitosan nanocomposite based electrochemical DNA biosensor for detection of typhoid. Sensor Actuat B-Chem 185:675–684

Singh N, Yadav M, Khanna S, Sahu O (2017) Sustainable fragrance cum antimicrobial finishing on cotton: indigenous essential oil. Sustain Chem Pharm 5:22–29

Sionkowska A, Kaczmarek B, Michalska M, Lewandowska K, Grabska S (2017) Preparation and characterization of collagen/chitosan/hyaluronic acid thin films for application in hair care. Cosmetics 89. https://doi.org/10.1515/pac-2017-0314

Škorić ML, Terzić I, Milosavljević N, Radetić M, Šaponjić Z, Radoičić M, Krušić MK (2016) Chitosan-based microparticles for immobilization of TiO_2 nanoparticles and their application for photodegradation of textile dyes. Eur Polym J 82:57–70

Smith A, Perelman M, Hinchcliffe M (2014) Chitosan: a promising safe and immune-enhancing adjuvant for intranasal vaccines. Hum Vaccin Immunother 10:797–807

Soares DG, Rosseto HL, Scheffel DS, Basso FG, Huck C, Hebling J, de Souza Costa CA (2017a) Odontogenic differentiation potential of human dental pulp cells cultured on a calcium-aluminate enriched chitosan-collagen scaffold. Clin Oral Invest 21:2827–2839

Soares SF, Rodrigues MI, Trindade T, Daniel-da-Silva AL (2017b) Chitosan-silica hybrid nanosorbents for oil removal from water. Colloids Surf A 532:305–313

Soares E, Jesus S, Borges O (2018) Oral hepatitis B vaccine: chitosan or glucan based delivery systems for efficient HBsAg immunization following subcutaneous priming. Int J Pharm 535:261–271

Stoytcheva M, Zlatev R, Montero G, Velkova Z, Gochev V (2018) A nanotechnological approach to biosensors sensitivity improvement: application to organophosphorus pesticides determination. Biotechnol Biotechnol Equip 32:213–220

Štular D, Jerman I, Naglič I, Simončič B, Tomšič B (2017) Embedment of silver into temperature- and pH-responsive microgel for the development of smart textiles with simultaneous moisture management and controlled antimicrobial activities. Carbohydr Polym 159:161–170

Sugunan A, Thanachayanont C, Dutta J, Hilborn JG (2005) Heavy-metal ion sensors using chitosan-capped gold nanoparticles. Sci Technol Adv Mater 6:335–340

Sun H, Wang X, Hu X, Yu W, You C, Hu H, Han C (2012a) Promotion of angiogenesis by sustained release of rhGM-CSF from heparinized collagen/chitosan scaffolds. J Biomed Mater Res B 100:788–798

Sun X, Cao YY, Gong ZL, Wang XY, Zhang Y, Gao JM (2012b) An amperometric immunosensor based on multi-walled carbon nanotubes-thionine-chitosan nanocomposite film for chlorpyrifos detection. Sensors 12:17247–17261

Sun X, Sui S, Ference C, Zhang Y, Sun S, Zhou N, Zhu W, Zhou K (2014) Antimicrobial and mechanical properties of beta-cyclodextrin inclusion with essential oils in chitosan films. J Agric Food Chem 62:8914–8918

Svindland SC, Jul-Larsen Å, Pathirana R, Andersen S, Madhun A, Montomoli E, Jabbal-Gill I, Cox RJ (2012) The mucosal and systemic immune responses elicited by a chitosan-adjuvanted intranasal influenza H5N1 vaccine. Influenza Other Respir Viruses 6:90–100

Talon E, Trifkovic KT, Nedovic VA, Bugarski BM, Vargas M, Chiralt A, Gonzalez-Martinez C (2017) Antioxidant edible films based on chitosan and starch containing polyphenols from thyme extracts. Carbohydr Polym 157:1153–1161

Tamer TM et al (2018) MitoQ loaded chitosan-hyaluronan composite membranes for wound healing. Materials 11. https://doi.org/10.3390/ma11040569

Tan H, Gong Y, Lao L, Mao Z, Gao C (2007) Gelatin/chitosan/hyaluronan ternary complex scaffold containing basic fibroblast growth factor for cartilage tissue engineering. J Mater Sci Mater Med 18:1961–1968

Tan HB, Wang FY, Ding W, Zhang Y, Ding J, Cai DX, Yu KF, Yang J, Yang L, Xu YQ (2015) Fabrication and evaluation of porous keratin/chitosan (KCS) scaffolds for effectively accelerating wound healing. Biomed Environ Sci 28:178–189

Tang X, Tian M, Qu L, Zhu S, Guo X, Han G, Sun K, Hu X, Wang Y, Xu X (2014) A facile fabrication of multifunctional knit polyester fabric based on chitosan and polyaniline polymer nanocomposite. Appl Surf Sci 317:505–510

Tang Q, Luo C, Lu B, Fu Q, Yin H, Qin Z, Lyu D, Zhang L, Fang Z, Zhu Y, Yao K (2017) Thermosensitive chitosan-based hydrogels releasing stromal cell derived factor-1 alpha recruit MSC for corneal epithelium regeneration. Acta Biomater 61:101–113

Tao W, Fu T, He Z, Hu R, Jia L, Hong Y (2017a) Evaluation of immunostimulatory effects of *N*-(2-hydroxy) propyl-3-trimethylammonium chitosan chloride for improving live attenuated hepatitis a virus vaccine efficacy. Viral Immunol 30:120–126

Tao W, Zheng HQ, Fu T, He ZJ, Hong Y (2017b) N-(2-hydroxy) propyl-3-trimethylammonium chitosan chloride: An immune-enhancing adjuvant for hepatitis E virus recombinant polypeptide vaccine in mice. Hum Vaccin Immunotherap 13:1818–1822

Teepoo S, Dawan P, Barnthip N (2017) electrospun chitosan-gelatin biopolymer composite nanofibers for horseradish peroxidase immobilization in a hydrogen peroxide biosensor. Biosensors 7:47. https://doi.org/10.3390/Bios7040047

Teng SH, Lee EJ, Wang P, Shin DS, Kim HE (2008) Three-layered membranes of collagen/hydroxyapatite and chitosan for guided bone regeneration. J Biomed Mater Res B 87:132–138

Thanoo BC, Sunny MC, Jayakrishnan A (1992) Cross-linked chitosan microspheres: preparation and evaluation as a matrix for the controlled release of pharmaceuticals. J Pharm Pharmacol 44:283–286

Thanou M, Verhoef JC, Junginger HE (2001) Oral drug absorption enhancement by chitosan and its derivatives. Adv Drug Deliv Rev 52:117–126

Ti D et al (2015) Controlled release of thymosin beta 4 using a collagen-chitosan sponge scaffold augments cutaneous wound healing and increases angiogenesis in diabetic rats with hindlimb ischemia. Tissue Eng Part A 21:541–549

Tian M, Hu X, Qu L, Du M, Zhu S, Sun Y, Han G (2016) Ultraviolet protection cotton fabric achieved via layer-by-layer self-assembly of graphene oxide and chitosan. Appl Surf Sci 377:141–148

Tkac J, Whittaker JW, Ruzgas T (2007) The use of single walled carbon nanotubes dispersed in a chitosan matrix for preparation of a galactose biosensor. Biosens Bioelectron 22:1820–1824
Tokura S, Tamura H, Azuma I (1999) Immunological aspects of chitin and chitin derivatives administered to animals. EXS 87:279–292
Tong C et al (2016) Hypoxia pretreatment of bone marrow-derived mesenchymal stem cells seeded in a collagen-chitosan sponge scaffold promotes skin wound healing in diabetic rats with hindlimb ischemia. Wound Repair Regen 24:45–56
Toskas G, Brünler R, Hund H, Hund R-D, Hild M, Aibibu D, Cherif C (2013) Pure chitosan microfibres for biomedical applications. Autex Res J 13:134. https://doi.org/10.2478/v10304-012-0041-5
Tran N, Mir A, Mallik D, Sinha A, Nayar S, Webster TJ (2010) Bactericidal effect of iron oxide nanoparticles on *Staphylococcus aureus*. Int J Nanomedicine 5:277–283
Travlou NA, Kyzas GZ, Lazaridis NK, Deliyanni EA (2013) Graphite oxide/chitosan composite for reactive dye removal. Chem Eng J 217:256–265
Trickler WJ, Nagvekar AA, Dash AK (2008) A novel nanoparticle formulation for sustained paclitaxel delivery. AAPS PharmSciTech 9:486–493
Tsai YC, Chen SY, Liaw HW (2007) Immobilization of lactate dehydrogenase within multiwalled carbon nanotube-chitos anhanocompo site for application to lactate biosensors. Sensor Actuators B-Chem 125:474–481
Tsai YC, Chen SY, Lee CA (2008) Amperometric cholesterol biosensors based on carbon nanotube-chitosan-platinum-cholesterol oxidase nanobiocomposite. Sensor Actuators B-Chem 135:96–101
Tsai HY, Chiu CC, Lin PC, Chen SH, Huang SJ, Wang LF (2011) Antitumor efficacy of doxorubicin released from crosslinked nanoparticulate chondroitin sulfate/chitosan polyelectrolyte complexes. Macromol Biosci 11:680–688
Tsai B, Garcia-Valdez O, Champagne P, Cunningham M (2017) Poly(poly(ethylene glycol) methyl ether methacrylate) grafted chitosan for dye removal from water. Processes 5:12. https://doi.org/10.3390/pr5010012
van der Lubben IM, Verhoef JC, Borchard G, Junginger HE (2001) Chitosan for mucosal vaccination. Adv Drug Deliv Rev 52:139–144
van der Merwe SM, Verhoef JC, Verheijden JH, Kotze AF, Junginger HE (2004) Trimethylated chitosan as polymeric absorption enhancer for improved peroral delivery of peptide drugs. Eur J Pharm Biopharm 58:225–235
Varshosaz J, Hassanzadeh F, Aliabadi HS, Khoraskani FR, Mirian M, Behdadfar B (2016) Targeted delivery of doxorubicin to breast cancer cells by magnetic LHRH chitosan bioconjugated nanoparticles. Int Biol Macromol 93:1192–1205
Vasconcelos DP, Costa M, Neves N, Teixeira JH, Vasconcelos DM, Santos SG, Águas AP, Barbosa MA, Barbosa JN (2018) Chitosan porous 3D scaffolds embedded with resolvin D1 to improve *in vivo* bone healing. J Biomed Mater Res A 106:1626–1633
Vasilêv LA, Dzyubinskaya EV, Zinovkin RA, Kiselevsky DB, Lobysheva NV, Samuilov VD (2009) Chitosan-induced programmed cell death in plants. Biochemistry (Mosc) 74:1035–1043
Vasiliev YM (2015) Chitosan-based vaccine adjuvants: incomplete characterization complicates preclinical and clinical evaluation. Expert Rev Vaccines 14:37–53
Vedakumari WS, Prabu P, Sastry TP (2015) Chitosan-fibrin nanocomposites as drug delivering and wound healing materials. J Biomed Nanotechnol 11:657–667
Velickova E, Winkelhausen E, Kuzmanova S, Alves VD, Moldão-Martins M (2013) Impact of chitosan-beeswax edible coatings on the quality of fresh strawberries (*Fragaria ananassa* cv *Camarosa*) under commercial storage conditions. LWT – Food Sci Technol 52:80–92
Venkatesan J, Kim S-K (2010) Chitosan composites for bone tissue engineering—an overview. Mar Drugs 8:2252–2266
Venkatesan J, Pallela R, Bhatnagar I, Kim SK (2012a) Chitosan-amylopectin/hydroxyapatite and chitosan-chondroitin sulphate/hydroxyapatite composite scaffolds for bone tissue engineering. Int Biol Macromol 51:1033–1042

Venkatesan J, Ryu B, Sudha PN, Kim SK (2012b) Preparation and characterization of chitosan-carbon nanotube scaffolds for bone tissue engineering. Int Biol Macromol 50:393–402
Vishwanath V, Pramanik K, Biswas A (2016) Optimization and evaluation of silk fibroin-chitosan freeze-dried porous scaffolds for cartilage tissue engineering application. J Biomater Sci Polym Ed 27:657–674
Wan Ngah WS, Teong LC, Hanafiah MAKM (2011) Adsorption of dyes and heavy metal ions by chitosan composites: a review. Carbohydr Polym 83:1446–1456
Wan A, Xu Q, Sun Y, Li H (2013) Antioxidant activity of high molecular weight chitosan and *N,O*-quaternized chitosans. J Agric Food Chem 61:6921–6928
Wang J, Chen C (2014) Chitosan-based biosorbents: Modification and application for biosorption of heavy metals and radionuclides. Bioresour Technol 160:129–141
Wang X, Wang C (2016) Chitosan-poly(vinyl alcohol)/attapulgite nanocomposites for copper (II) ions removal: pH dependence and adsorption mechanisms. Colloids and Surfaces A 500:186–194
Wang L, Khor E, Wee A, Lim LY (2002) Chitosan-alginate PEC membrane as a wound dressing: assessment of incisional wound healing. J Biomed Mater Res 63:610–618
Wang YT, Zhu JZ, Zhu RJ, Zhu ZQ, Lai ZS, Chen ZY (2003) Chitosan/Prussian blue-based biosensors. Meas Sci Technol 14:831–836
Wang X, Hu W, Cao Y, Yao J, Wu J, Gu X (2005) Dog sciatic nerve regeneration across a 30-mm defect bridged by a chitosan/PGA artificial nerve graft. Brain 128:1897–1910
Wang W, Lin S, Xiao Y, Huang Y, Tan Y, Cai L, Li X (2008a) Acceleration of diabetic wound healing with chitosan-crosslinked collagen sponge containing recombinant human acidic fibroblast growth factor in healing-impaired STZ diabetic rats. Life Sci 82:190–204
Wang Y, Zhang L, Hu M, Liu H, Wen W, Xiao H, Niu Y (2008b) Synthesis and characterization of collagen-chitosan-hydroxyapatite artificial bone matrix. J Biomed Mater Res A 86:244–252
Wang X, Wang X, Tan Y, Zhang B, Gu Z, Li X (2009) Synthesis and evaluation of collagen-chitosan-hydroxyapatite nanocomposites for bone grafting. J Biomed Mater Res A 89:1079–1087
Wang L, Liu F, Jiang Y, Chai Z, Li P, Cheng Y, Jing H, Leng X (2011) Synergistic antimicrobial activities of natural essential oils with chitosan films. J Agric Food Chem 59:12411–12419
Wang H, Zhao Q, Zhao W, Liu Q, Gu X, Yang Y (2012a) Repairing rat sciatic nerve injury by a nerve-growth-factor-loaded, chitosan-based nerve conduit. Biotechnol Appl Biochem 59:388–394
Wang TJ, Wang IJ, Lu JN, Young TH (2012b) Novel chitosan-polycaprolactone blends as potential scaffold and carrier for corneal endothelial transplantation. Mol Vis 18:255–264
Wang H, Zhang R, Zhang H, Jiang S, Liu H, Sun M, Jiang S (2015) Kinetics and functional effectiveness of nisin loaded antimicrobial packaging film based on chitosan/poly(vinyl alcohol). Carbohydr Polym 127:64–71
Wang B, Wu X, Li J, Hao X, Lin J, Cheng D, Lu Y (2016a) Thermosensitive behavior and antibacterial activity of cotton fabric modified with a chitosan-poly(n-isopropylacrylamide) interpenetrating polymer network hydrogel. Polymers 8:110
Wang M, Roy AK, Webster TJ (2016b) Development of chitosan/poly(vinyl alcohol) electrospun nanofibers for infection related wound healing. Front Physiol 7:683. https://doi.org/10.3389/fphys.2016.00683
Wang D, Jia M, Wang L, Song S, Feng J, Zhang X (2017a) Chitosan and β-cyclodextrin-epichlorohydrin polymer composite film as a plant healthcare material for carbendazim-controlled release to protect rape against *Sclerotinia sclerotiorum* (Lib.) de Bary. Materials 10:343. https://doi.org/10.3390/ma10040343
Wang S, Guan S, Zhu Z, Li W, Liu T, Ma X (2017b) Hyaluronic acid doped-poly(3,4-ethylenedioxythiophene)/chitosan/gelatin (PEDOT-HA/Cs/Gel) porous conductive scaffold for nerve regeneration. Mater Sci Eng C Mater Biol Appl 71:308–316
Wang H, Qian J, Ding F (2018) Emerging chitosan-based films for food packaging applications. J Agric Food Chem 66:395–413

Wei X, Lao J, Gu YD (2003) Bridging peripheral nerve defect with chitosan-collagen film. Chin J Traumatol 6:131–134
Wei Y, Gong K, Zheng Z, Wang A, Ao Q, Gong Y, Zhang X (2011) Chitosan/silk fibroin-based tissue-engineered graft seeded with adipose-derived stem cells enhances nerve regeneration in a rat model. J Mater Sci Mater Med 22:1947–1964
Wen GM, Zhang Y, Shuang SM, Dong C, Choi MMF (2007) Application of a biosensor for monitoring of ethanol. Biosens Bioelectron 23:121–129
Wen Z-S, Xu Y-L, Zou X-T, Xu Z-R (2011) Chitosan nanoparticles act as an adjuvant to promote both Th1 and Th2 immune responses induced by ovalbumin in mice. Mar Drugs 9:1038–1055
Werle M, Bernkop-Schnurch A (2008) Thiolated chitosans: useful excipients for oral drug delivery. J Pharm Pharmacol 60:273–281
Westin CB, Trinca RB, Zuliani C, Coimbra IB, Moraes AM (2017) Differentiation of dental pulp stem cells into chondrocytes upon culture on porous chitosan-xanthan scaffolds in the presence of kartogenin. Mater Sci Eng C Mater Biol Appl 80:594–602
Wijekoon A, Fountas-Davis N, Leipzig ND (2013) Fluorinated methacrylamide chitosan hydrogel systems as adaptable oxygen carriers for wound healing. Acta Biomater 9:5653–5664
Wivel NA, Wilson JM (1998) Methods of gene delivery. Hematol Oncol Clinics North Am 12:483–501
Wlaszczuk A, Marcol W, Kucharska M, Wawro D, Palen P, Lewin-Kowalik J (2016) Poly(D, L-lactide-co-glycolide) tubes with multifilament chitosan yarn or chitosan sponge core in nerve regeneration. J Oral Maxillofac Surg 74:2327.e1–2327.e12
Wongsawaeng D, Khemngern S, Somboonna NEJVI (2017) Environmentally-friendly RF plasma treatment of Thai silk fabrics with chitosan for durable antibacterial property. Eng J 21:29–43
Woodard JR et al (2007) The mechanical properties and osteoconductivity of hydroxyapatite bone scaffolds with multi-scale porosity. Biomaterials 28:45–54
Wu L, Liu M (2008) Preparation and properties of chitosan-coated NPK compound fertilizer with controlled-release and water-retention. Carbohydr Polym 72:240–247
Wu BY, Hou SH, Yin F, Li J, Zhao ZX, Huang JD, Chen Q (2007) Amperometric glucose biosensor based on layer-by-layer assembly of multilayer films composed of chitosan, gold nanoparticles and glucose oxidase modified Pt electrode. Biosens Bioelectron 22:838–844
Wu H, Zhang J, Luo Y, Wan Y, Sun S (2015) Mechanical properties and permeability of porous chitosan-poly(p-dioxanone)/silk fibroin conduits used for peripheral nerve repair. J Mech Behav Biomed Mater 50:192–205
Wu Z-C, Wang Z-Z, Liu J, Yin J-H, Kuang S-P (2016) Removal of Cu(II) ions from aqueous water by l-arginine modifying magnetic chitosan. Colloids Surf A 499:141–149
Wu T, Wu C, Fu S, Wang L, Yuan C, Chen S, Hu Y (2017) Integration of lysozyme into chitosan nanoparticles for improving antibacterial activity. Carbohydr Polym 155:192–200
Xia W, Liu W, Cui L, Liu Y, Zhong W, Liu D, Wu J, Chua K, Cao Y (2004) Tissue engineering of cartilage with the use of chitosan-gelatin complex scaffolds. J Biomed Mater Res B 71:373–380
Xiao J, Yu H (2017) Gemcitabine conjugated chitosan and double antibodies (Abc-GC-gemcitabine nanoparticles) enhanced cytoplasmic uptake of gemcitabine and inhibit proliferation and metastasis in human SW1990 pancreatic cancer cells. Med Sci Monit 23:1613–1620
Xiao W, Xu J, Liu X, Hu Q, Huang J (2013) Antibacterial hybrid materials fabricated by nanocoating of microfibril bundles of cellulose substance with titania/chitosan/silver-nanoparticle composite films. J Mater Chem B 1:3477–3485
Xiao C, Liu X, Mao S, Zhang L, Lu J (2017) Sub-micron-sized polyethylenimine-modified polystyrene/Fe3O4/chitosan magnetic composites for the efficient and recyclable adsorption of Cu(II) ions. Appl Surf Sci 394:378–385
Xie W, Xu P, Liu Q (2001) Antioxidant activity of water-soluble chitosan derivatives. Bioorg Med Chem Lett 11:1699–1701
Xie F, Li QF, Gu B, Liu K, Shen GX (2008) *In vitro* and *in vivo* evaluation of a biodegradable chitosan-PLA composite peripheral nerve guide conduit material. Microsurgery 28:471–479

Xie M, Zeng L, Zhang Q, Kang Y, Xiao H, Peng Y, Chen X, Luo J (2015) Synthesis and adsorption behavior of magnetic microspheres based on chitosan/organic rectorite for low-concentration heavy metal removal. J Alloys Compd 647:892–905

Xing K, Zhu X, Peng X, Qin S (2015) Chitosan antimicrobial and eliciting properties for pest control in agriculture: a review. Agron Sustain Dev 35:569–588

Xing Y, Xu Q, Li X, Chen C, Ma L, Li S, Che Z, Lin H (2016) Chitosan-based coating with antimicrobial agents: preparation, property, mechanism, and application effectiveness on fruits and vegetables international. J Polym Sci 2016:24

Xu G et al (2004) Optic nerve regeneration in polyglycolic acid-chitosan conduits coated with recombinant L1-Fc. Neuroreport 15:2167–2172

Xu HR, Wang L, Luo JP, Song YL, Liu JT, Zhang S, Cai XX (2015) Selective recognition of 5-hydroxytryptamine and dopamine on a multi-walled carbon nanotube-chitosan hybrid film-modified microelectrode array. Sensors 15:1008–1021

Xu Q, Wu Y, Zhang Y, Fu F, Liu X (2016) Durable antibacterial cotton modified by silver nanoparticles and chitosan derivative binder. Fiber Polym 17:1782–1789

Xu J, Zhang Y, Gutha Y, Zhang W (2017a) Antibacterial property and biocompatibility of Chitosan/Poly(vinyl alcohol)/ZnO (CS/PVA/ZnO) beads as an efficient adsorbent for Cu (II) removal from aqueous solution. Colloid Surf B: Biointerfaces 156:340–348

Xu SC, Zhang YY, Dong K, Wen JN, Zheng CM, Zhao SH (2017b) Electrochemical DNA biosensor based on graphene oxide-chitosan hybrid nanocomposites for detection of *Escherichia coli* O157:H7. Int J Electrochem Sc 12:3443–3458

Xu W, Xie W, Huang X, Chen X, Huang N, Wang X, Liu J (2017c) The graphene oxide and chitosan biopolymer loads TiO_2 for antibacterial and preservative research. Food Chem 221:267–277

Xu W, Wang Z, Liu Y, Wang L, Jiang Z, Li T, Zhang W, Liang Y (2018) Carboxymethyl chitosan/gelatin/hyaluronic acid blended-membranes as epithelia transplanting scaffold for corneal wound healing. Carbohydr Polym 192:240–250

Xue C, Hu N, Gu Y, Yang Y, Liu Y, Liu J, Ding F, Gu X (2012) Joint use of a chitosan/PLGA scaffold and MSCs to bridge an extra large gap in dog sciatic nerve. Neurorehab Neural Repair 26:96–106

Yamada A, Shibuya N, Kodama O, Akatsuka T (1993) Induction of phytoalexin formation in suspension-cultured rice cells by *N*-acetyl-chitooligosaccharides. Biosci Biotechnol Biochem 57:405–409

Yan H, Li H, Yang H, Li A, Cheng R (2013) Removal of various cationic dyes from aqueous solutions using a kind of fully biodegradable magnetic composite microsphere. Chem Eng J 223:402–411

Yan H, Chen X, Wu T, Feng Y, Wang C, Li J, Lin Q (2014) Mechanochemical modification of kaolin surfaces for immobilization and delivery of pesticides in alginate-chitosan composite beads. Polym Bull 71:2923–2944

Yang LQ, Ren XL, Tang FQ, Zhang L (2009) A practical glucose biosensor based on Fe_3O_4 nanoparticles and chitosan/nafion composite film. Biosens Bioelectron 25:889–895

Yang H-C, Wang W-H, Huang K-S, Hon M-H (2010) Preparation and application of nanochitosan to finishing treatment with anti-microbial and anti-shrinking properties. Carbohydr Polym 79:176–179

Yang Y, Zhao W, He J, Zhao Y, Ding F, Gu X (2011) Nerve conduits based on immobilization of nerve growth factor onto modified chitosan by using genipin as a crosslinking agent. Eur J Pharm Biopharm 79:519–525

Yang L, Xiong H, Zhang X, Wang S (2012a) A novel tyrosinase biosensor based on chitosan-carbon-coated nickel nanocomposite film. Bioelectrochemistry 84:44–48

Yang X, Han G, Pang X, Fan M (2012b) Chitosan/collagen scaffold containing bone morphogenetic protein-7 DNA supports dental pulp stem cell differentiation *in vitro* and *in vivo*. J Biomed Mater Res A. https://doi.org/10.1002/jbm.a.34064

Yang Z, Zeng Z, Xiao Z, Ji H (2014) Preparation and controllable release of chitosan/vanillin microcapsules and their application to cotton fabric. Flavour Fragr J 29:114–120

Yang CL, Chen JP, Wei KC, Chen JY, Huang CW, Liao ZX (2017) Release of doxorubicin by a folate-grafted, chitosan-coated magnetic nanoparticle. Nanomaterials 7:85. https://doi.org/10.3390/nano7040085

Yang F, Wen X, Ke QF, Xie XT, Guo YP (2018) pH-responsive mesoporous ZSM-5 zeolites/chitosan core-shell nanodisks loaded with doxorubicin against osteosarcoma. Mater Sci Eng C Mater Biol Appl 85:142–153

Yao Z, Zhang M, Sakahara H, Saga T, Arano Y, Konishi J (1998) Avidin targeting of intraperitoneal tumor xenografts. J Natl Cancer Inst 90:25–29

Yao Q et al (2013a) Preparation, characterization, and cytotoxicity of various chitosan nanoparticles. J Nanomaterials 2013:6. https://doi.org/10.1155/2013/183871

Yao W, Peng Y, Du M, Luo J, Zong L (2013b) Preventative vaccine-loaded mannosylated chitosan nanoparticles intended for nasal mucosal delivery enhance immune responses and potent tumor immunity. Mol Pharm 10:2904–2914

Ye P, Yu B, Deng J, She RF, Huang WL (2017) Application of silk fibroin/chitosan/nano-hydroxyapatite composite scaffold in the repair of rabbit radial bone defect. Exp Therapeut Med 14:5547–5553

Yen M-T, Yang J-H, Mau J-L (2008) Antioxidant properties of chitosan from crab shells. Carbohydr Polym 74:840–844

Yeo JH, Lee KG, Kim HC, Oh HYL, Kim AJ, Kim SY (2000) The effects of Pva/chitosan/fibroin (PCF)-blended spongy sheets on wound healing in rats. Biol Pharm Bull 23:1220–1223

Yhee JY et al (2017) Effects of tumor microenvironments on targeted delivery of glycol chitosan nanoparticles. J Control Release 267:223–231

Yin X et al (2018) Enhanced wettability and moisture retention of cotton fabrics coated with self-suspended chitosan derivative. Cellulose 25:2721–2732

Yousefpour P, Atyabi F, Vasheghani-Farahani E, Movahedi A-AM, Dinarvand R (2011) Targeted delivery of doxorubicin-utilizing chitosan nanoparticles surface-functionalized with anti-Her2 trastuzumab. Int J Nanomedicine 6:1977–1990

Youssef AM, Abdel-Aziz MS, El-Sayed SM (2014) Chitosan nanocomposite films based on Ag-NP and Au-NP biosynthesis by *Bacillus subtilis* as packaging materials. Int Biol Macromol 69:185–191

Youssef AM, El-Sayed SM, El-Sayed HS, Salama HH, Dufresne A (2016) Enhancement of Egyptian soft white cheese shelf life using a novel chitosan/carboxymethyl cellulose/zinc oxide bionanocomposite film. Carbohydr Polym 151:9–19

Yu P, Bao RY, Shi XJ, Yang W, Yang MB (2017) Self-assembled high-strength hydroxyapatite/graphene oxide/chitosan composite hydrogel for bone tissue engineering. Carbohydr Polym 155:507–515

Yuan G, Chen X, Li D (2016) Chitosan films and coatings containing essential oils: The antioxidant and antimicrobial activity, and application in food systems. Food Res Int 89:117–128

Yuan TT, DiGeorge Foushee AM, Johnson MC, Jockheck-Clark AR, Stahl JM (2018) Development of Electrospun chitosan-polyethylene oxide/fibrinogen biocomposite for potential wound healing applications. Nanoscale Res Lett 13:88. https://doi.org/10.1186/s11671-018-2491-8

Yuceer M, Caner C (2014) Antimicrobial lysozyme-chitosan coatings affect functional properties and shelf life of chicken eggs during storage. J Sci Food Agric 94:153–162

Yun YR, Jang JH, Jeon E, Kang W, Lee S, Won JE, Kim HW, Wall I (2012) Administration of growth factors for bone regeneration. Regen Med 7:369–385

Zaharoff DA, Rogers CJ, Hance KW, Schlom J, Greiner JW (2007) Chitosan solution enhances both humoral and cell-mediated immune responses to subcutaneous vaccination. Vaccine 25:2085–2094

Zaharoff DA et al (2009) Intravesical immunotherapy of superficial bladder cancer with chitosan/interleukin-12. Cancer Res 69:6192–6199

Zaharoff DA, Hance KW, Rogers CJ, Schlom J, Greiner JW (2010) Intratumoral immunotherapy of established solid tumors with chitosan/IL-12. J Immunother 33:697–705
Zaman P, Wang J, Blau A, Wang W, Li T, Kohane DS, Loscalzo J, Zhang YY (2016) Incorporation of heparin-binding proteins into preformed dextran sulfate-chitosan nanoparticles. Int J Nanomedicine 11:6149–6159
Zargarkazemi A, Sadeghi-Kiakhani M, Arami M, Bahrami SH (2015) Modification of wool fabric using prepared chitosan-cyanuric chloride hybrid. J Text Inst 106:80–89
Zarghami S, Kazemimoghadam M, Mohammadi T (2014) Cu(II) removal enhancement from aqueous solutions using ion-imprinted membrane technique. Chem Pap 68:809–815
Zeng D, Shi Y (2009) Preparation and application of a novel environmentally friendly organic seed coating for rice. J Sci Food Agric 89:2181–2185
Zeng D, Luo X, Tu R (2012) Application of bioactive coatings based on chitosan for soybean seed protection international. J Carbohydr Chem 2012:5. https://doi.org/10.1155/2012/104565
Zhai M, Xu Y, Zhou B, Jing W (2018) Keratin-chitosan/n-ZnO nanocomposite hydrogel for antimicrobial treatment of burn wound healing: characterization and biomedical application. J Photochem Photobiol B 180:253–258
Zhang MG, Gorski W (2011) Amperometric Ethanol biosensors based on chitosan-NAD(+)-alcohol dehydrogenase films. Electroanal 23:1856–1862
Zhang MG, Smith A, Gorski W (2004) Carbon nanotube-chitosan system for electrochemical sensing based on dehydrogenase enzymes. Anal Chem 76:5045–5050
Zhang H, Wang W, Yin H, Zhao X, Du Y (2012) Oligochitosan induces programmed cell death in tobacco suspension cells. Carbohydr Polym 87:2270–2278
Zhang K, Zhang Y, Yan S, Gong L, Wang J, Chen X, Cui L, Yin J (2013a) Repair of an articular cartilage defect using adipose-derived stem cells loaded on a polyelectrolyte complex scaffold based on poly(l-glutamic acid) and chitosan. Acta Biomater 9:7276–7288
Zhang X et al (2013b) Expression of gamma-aminobutyric acid receptors on neoplastic growth and prediction of prognosis in non-small cell lung cancer. J Translat Med 11:102
Zhang Y-L, Zhang J, Dai C-M, Zhou X-F, Liu S-G (2013c) Sorption of carbamazepine from water by magnetic molecularly imprinted polymers based on chitosan-Fe_3O_4. Carbohydr Polym 97:809–816
Zhang Y, Shen Z, Dai C, Zhou X (2014) Removal of selected pharmaceuticals from aqueous solution using magnetic chitosan: sorption behavior and mechanism. Environ Sci Pollut R 21:12780–12789
Zhang K, Yan S, Li G, Cui L, Yin J (2015a) *In-situ* birth of MSCs multicellular spheroids in poly (L-glutamic acid)/chitosan scaffold for hyaline-like cartilage regeneration. Biomaterials 71:24–34
Zhang S, Prabhakaran MP, Qin X, Ramakrishna S (2015b) Biocomposite scaffolds for bone regeneration: role of chitosan and hydroxyapatite within poly-3-hydroxybutyrate-co-3-hydroxyvalerate on mechanical properties and *in vitro* evaluation. J Mech Behav Biomed Mater 51:88–98
Zhang WJ, Li XJ, Zou RT, Wu HZ, Shi HY, Yu SS, Liu Y (2015c) Multifunctional glucose biosensors from Fe3O4 nanoparticles modified chitosan/graphene nanocomposites. Sci Rep 5. https://doi.org/10.1038/Srep11129
Zhang S, Dong Y, Yang Z, Yang W, Wu J, Dong C (2016) Adsorption of pharmaceuticals on chitosan-based magnetic composite particles with core-brush topology. Chem Eng J 304:325–334
Zhang X, Xiao G, Wang Y, Zhao Y, Su H, Tan T (2017) Preparation of chitosan-TiO_2 composite film with efficient antimicrobial activities under visible light for food packaging applications. Carbohydr Polym 169:101–107
Zhang L, Ma Y, Pan X, Chen S, Zhuang H, Wang S (2018) A composite hydrogel of chitosan/heparin/poly (gamma-glutamic acid) loaded with superoxide dismutase for wound healing. Carbohydr Polym 180:168–174

Zhao R, Ren Y, Sun B, Zhang R, Liang D (2010) Experimental study on chitosan mediated insulin-like growth factor gene transfection repairing injured articular cartilage in rabbits. Chin J Reparat Reconstr Surg 24:1372–1375

Zhao J, Zheng X, Fu C, Qu W, Wei G, Zhang W (2014) FK506-loaded chitosan conduit promotes the regeneration of injured sciatic nerves in the rat through the upregulation of brain-derived neurotrophic factor and TrkB. J Neurol Sci 344:20–26

Zhao Y, Liu JG, Chen WM, Yu AX (2018) Efficacy of thermosensitive chitosan/beta-glycerophosphate hydrogel loaded with beta-cyclodextrin-curcumin for the treatment of cutaneous wound infection in rats. Exp Therapeut Med 15:1304–1313

Zheng L, Cui HF (2010) Use of chitosan conduit combined with bone marrow mesenchymal stem cells for promoting peripheral nerve regeneration. J Mater Sci Mater Med 21:1713–1720

Zheng Y, Yang W, Wang C, Hu J, Fu S, Dong L, Wu L, Shen X (2007) Nanoparticles based on the complex of chitosan and polyaspartic acid sodium salt: preparation, characterization and the use for 5-fluorouracil delivery. Eur J Pharm Biopharm 67:621–631

Zheng Y, Cai Z, Song X, Yu B, Bi Y, Chen Q, Zhao D, Xu J, Hou S (2009) Receptor mediated gene delivery by folate conjugated *N*-trimethyl chitosan *in vitro*. Int J Pharm 382:262–269

Zheng H, Tang C, Yin C (2015) Exploring advantages/disadvantages and improvements in overcoming gene delivery barriers of amino acid modified trimethylated chitosan. Pharm Res 32:2038–2050

Zheng XF, Lian Q, Yang H, Wang X (2016) Surface molecularly imprinted polymer of chitosan grafted poly(methyl methacrylate) for 5-fluorouracil and controlled release. Sci Rep 6:21409. https://doi.org/10.1038/srep21409

Zhong J, Huang HL, Li J, Qian FC, Li LQ, Niu PP, Dai LC (2015) Development of hybrid-type modified chitosan derivative nanoparticles for the intracellular delivery of midkine-siRNA in hepatocellular carcinoma cells. Hepatobiliary Pancreat Dis Int 14:82–89

Zhou L, Jin J, Liu Z, Liang X, Shang C (2011) Adsorption of acid dyes from aqueous solutions by the ethylenediamine-modified magnetic chitosan nanoparticles. J Hazard Mater 185:1045–1052

Zhou D, Qi C, Chen YX, Zhu YJ, Sun TW, Chen F, Zhang CQ (2017a) Comparative study of porous hydroxyapatite/chitosan and whitlockite/chitosan scaffolds for bone regeneration in calvarial defects. Int J Nanomedicine 12:2673–2687

Zhou X, Wang H, Zhang J, Li X, Wu Y, Wei Y, Ji S, Kong D, Zhao Q (2017b) Functional poly (epsilon-caprolactone)/chitosan dressings with nitric oxide-releasing property improve wound healing. Acta Biomater 54:128–137

Zhu HY, Jiang R, Xiao L, Zeng GM (2010) Preparation, characterization, adsorption kinetics and thermodynamics of novel magnetic chitosan enwrapping nanosized γ-Fe2O3 and multi-walled carbon nanotubes with enhanced adsorption properties for methyl orange. Bioresour Technol 101:5063–5069

Zhu L, Liu T, Cai J, Ma J, Chen AM (2015) Repair and regeneration of lumbosacral nerve defects in rats with chitosan conduits containing bone marrow mesenchymal stem cells. Injury 46:2156–2163

Zhu C, Huang J, Xue C, Wang Y, Wang S, Bao S, Chen R, Li Y, Gu Y (2017) Skin derived precursor Schwann cell-generated acellular matrix modified chitosan/silk scaffolds for bridging rat sciatic nerve gap. Neurosci Res pii S0168-0102(17):30584–30589. https://doi.org/10.1016/j.neures.2017.12.007

Zhuo N, Lan Y, Yang W, Yang Z, Li X, Zhou X, Liu Y, Shen J, Zhang X (2017) Adsorption of three selected pharmaceuticals and personal care products (PPCPs) onto MIL-101(Cr)/natural polymer composite beads. Sep Purif Technol 177:272–280

Ziani K, Ursua B, Mate JI (2010) Application of bioactive coatings based on chitosan for artichoke seed protection. Crop Prot 29:853–859

Zou Q, Cai B, Li J, Li J, Li Y (2017) *In vitro* and *in vivo* evaluation of the chitosan/Tur composite film for wound healing applications. J Biomater Sci Polym Ed 28:601–615

Zuppini A, Baldan B, Millioni R, Favaron F, Navazio L, Mariani P (2004) Chitosan induces Ca^{2+}-mediated programmed cell death in soybean cells. New Phytol 161:557–568

Chapter 15
Marine Glycosaminoglycans (GAGs) and GAG-Mimetics: Applications in Medicine and Tissue Engineering

Sylvia Colliec-Jouault and Agata Zykwinska

Abstract Glycosaminoglycans or GAGs are fundamental constituents of both cell surface and extracellular matrix (ECM), and through their localization they participate in many biological processes by playing a key role in cell-cell and cell-matrix interactions. Therefore, they present a great potential for the design and preparation of therapeutic drugs to treat major diseases such as ischemic heart disease, stroke, cancers, infectious diseases, and degenerative diseases. With the demand of both animal-free molecules and clean environmentally friendly processes, the production of GAG-mimetics or GAG-like molecules from other sources than mammalian tissues is flourishing. Glycans, carbohydrates, or polysaccharides from marine resources are unique in terms both of function and structure, and they differ considerably from those of terrestrial origin. With the simultaneous development of both glycoscience and marine biotechnologies, the potential of marine polysaccharides as an innovative source for new pharmaceuticals has emerged and gained considerable attention. Algal and microbial polysaccharides offer a tremendous structural diversity for drug discovery. With the recent progress in genetic engineering, the bacterial production of tailor-made polysaccharides will provide very competitive molecules with properties of interest especially to treat major diseases and to elaborate new applications in tissue engineering.

15.1 Introduction

15.1.1 Glycosaminoglycans (GAGs) in Health

With the breakthrough of both glycobiology and glycochemistry, the major biological role of GAGs in health and disease has been highlighted. GAGs are highly evolutionary conserved complex anionic linear carbohydrates in a broad range of

S. Colliec-Jouault (✉) · A. Zykwinska
Laboratoire Ecosystèmes Microbiens et Molécules Marines pour les Biotechnologies, Ifremer, Nantes, France
e-mail: Sylvia.Colliec.Jouault@ifremer.fr

E. Cohen, H. Merzendorfer (eds.), *Extracellular Sugar-Based Biopolymers Matrices*, Biologically-Inspired Systems 12, https://doi.org/10.1007/978-3-030-12919-4_15

vertebrates and invertebrates. They are fundamental constituents of both cell surface and extracellular matrix (ECM), and through their localization they participate in many biological processes by playing a key role in cell-cell and cell-matrix interactions. Thus their presence and also their structural integrity are crucial for cell growth, tissue maturation, and restoration to maintain the physiological state of living tissues and so to prevent organ dysfunction. GAGs present a high diversity, they are unique for each cell type, and consequently they provide a cell- and tissue-specific identity (Praillet et al. 1998a; Praillet et al. 1998b; DeAngelis 2012). The most common GAGs are hyaluronan/hyaluronic acid, heparin/heparan sulfate, chondroitin sulfate, and dermatan sulfate. Heparin, hyaluronic acid, and chondroitin sulfate are the most used in medicine to treat thrombosis, inflammation, and osteoarthritis/osteoarthrosis, respectively. The biological effects of GAGs are mainly due to their interaction with various proteins present in their environment such as chemokines, cytokines, growth factors, morphogens, enzymes and their natural inhibitors, and adhesion molecules. The binding between GAGs and proteins requires specific structural features (conformational flexibility, sulfation pattern, chain length, counterions, etc.) that determine the level of affinity (Gandhi and Mancera 2008). These structural requirements are essential to design compounds that mimic the bioactive function of GAGs and to fine-tune their benefit/risk ratio (Schnabelrauch et al. 2013). With the demand of both animal-free molecules and clean environmentally friendly processes, the production of GAG-mimetics or GAG-like molecules from other sources than mammalian tissues is flourishing. So the road to animal-free GAG production is now open to future developments to avoid a risk of contamination by harmful substances and/or unconventional pathogens. The production of GAG-mimetics with specific biological targets can be performed by organic synthesis, by chemo-enzymatic approaches, or by recombinant bacteria. Synthetic route has its limits because only small oligosaccharides can be produced (not above 10 sugar units). Some research groups synthesize oligosaccharide library from heparin or heparan sulfate, and some others design heparan sulfate mimics by chemically substituting anionic polyelectrolytes, copolylactic or polysaccharides such as dextran with sulfates and carboxyl groups (Ikeda et al. 2011; Miura et al. 2016; Barritault et al. 2017). Some bacteria can synthesize polysaccharides with structure really close or even apparently identical to mammalian GAGs. *Escherichia coli* serotype K5 can produce a precursor of heparin, a desulfatoheparin, whereas *E. coli* K4 produces a desulfatochondroitin (Oreste and Zoppetti 2012; Badri et al. 2018). Group A and group C Streptococci produce hyaluronan similar to that obtained from mammalian tissues (Murano et al. 2011). These bacterial GAGs are already produced through medium- to large-scale fermentation at good yield. The fermentation process offers innovative approaches by providing the perfect tools to identify the key enzymes involved in the biosynthesis and useful to design or produce tailor-made polysaccharides (Rehm 2010; DeAngelis 2012).

15.1.2 Marine GAGs

Marine habitats present a very huge diversity and offer enormous possibilities for the discovery of new species that could be considered as bioactive compound producers. Some habitats can be extreme environments in which species survive and grow being well adapted to unusual physical and chemical conditions and consequently develop original biological systems such as unique biosynthetic pathways (Mayer et al. 2011; Imhoff et al. 2011; Martins et al. 2014). Polysaccharides are ubiquitous and can be extracted or produced by a wide range of marine species such as animals, plants, or algae from both macro- and micro-resources. Glycans, carbohydrates, or polysaccharides from marine resources are unique in terms both of function and structure, and they differ considerably from those of terrestrial origin. They are often highly branched anionic heteropolysaccharides with complex repeating units (above 4 sugar units) (Roger et al. 2004). Traditionally, marine macro-resource (e.g., animals, invertebrates, macro-algae) has been exploited mainly to produce polysaccharides. Nowadays, advances in molecular techniques and microbial research are creating significant opportunities to exploit the biological resource of the marine microorganisms (e.g., microalgae, cyanobacteria, bacteria) (Deming 1998; Colliec-Jouault et al. 2012; Raposo et al. 2013).

The exoskeleton of marine organisms, mainly crabs and shrimps, is widely used to produce chitin (Laurienzo 2010). In addition, marine macro-resource is an alternative supplier of GAGs, commonly extracted from terrestrial mammalian tissues. Chondroitin sulfate and hyaluronan can be extracted from fish wastes (e.g., cartilage, skin, eyes) (Nandini et al. 2005; Alonso et al. 2010). Heparin-like glycans, oversulfated dermatans, can be isolated from ascidian tissues and fucosylated chondroitin sulfate from sea cucumbers (Pavao 2014). Polysaccharides from macro-algae are frequently anionic and sometimes highly sulfated heteropolysaccharides and are naturally endowed with biological properties described for GAGs. Biological properties of the macro-algal polysaccharides have been largely studied to explore their potential as animal-free GAG-mimetics. The most studied are carrageenans from red algae, alginates and fucoidans from brown seaweeds, and ulvans from green algae (Tseng 2001; Wijesinghe and Jeon 2012; de Jesus Raposo et al. 2015). Despite their great interest, polysaccharides from macro-resource present some disadvantages: difficult physical access to certain areas (e.g., political conflicts), low reproducibility mainly due to the seasonal variations, and dependence on ecological hazards (e.g., oil spills, heavy metals, germs, viruses) (Rioux et al. 2009). More recently the polysaccharides from micro-resource have been considered as an advantageous alternative over those isolated from marine macro-resource. With the advances in biotechnology, now marine microorganisms such as bacteria, cyanobacteria, microalgae, and even fungi are increasingly studied. They can grow under fully controlled culture conditions compatible with current safety standards (e.g., traceability, containment), with shorter production times and in completely automatizable

high-capacity systems (Wang et al. 2007; Finore et al. 2014). The diversity of these microorganisms is almost unlimited that suggests numerous polysaccharides presenting original complex structures still have to be discovered. With increased knowledge of both genome and gene expression, there is reason to believe that the production of tailored polysaccharides with the required purity degree by genetically modified strains is achievable (Raja et al. 2008; Nicolaus et al. 2010; Schmid et al. 2015; Freitas et al. 2017).

15.1.3 Marine GAG-Mimetic Design

Marine resources provide polysaccharides with peculiar chemical features as a consequence of their adaptation to various environments. Marine polysaccharides with their reactive groups allow the design of targeted bioactive structures by adding functional groups (e.g., methyl, sulfate, phosphate) that enhance initial properties or even create novel functions (Jiao et al. 2011). The distribution of functional groups and also the length of the polysaccharide chains are indispensable physicochemical parameters to tailor structure-function relationships. Marine macro-algae present a rich source of sulfated polysaccharides (e.g., carrageenans, ulvans, and fucans) that can present naturally GAG-like properties; consequently the most often conducted modifications for pharmaceutical applications are desulfation, oversulfation, acetylation, benzoylation, and molecular size modification. Oversulfated fucans have been produced to generate derivatives with different degrees of anticoagulant activity (Nishino and Nagumo 1992). Ulvans have been acetylated and benzoylated in order to produce derivatives with antioxidant activities (Qi et al. 2006). Concerning the alginate that is an anionic copolymer composed of mannuronic and guluronic acid units, its abundant free hydroxyl groups can be sulfated to generate GAG-like properties (Yang et al. 2011). More recently, microalgal bioactive derivatives have been developed to offer a promising and innovative alternative to the existing macroalgal polysaccharides despite their current low productivity value (Geresh et al. 2002; Martins et al. 2014; Freitas et al. 2017). However, although the marine fungal polysaccharides present a large chemical and structural diversity, at present their very low productivity does not promote their biotechnological applications. Biological properties such as antioxidant, antitumor, immunostimulating, and antimicrobial properties have been reported on several native polysaccharides (Chen et al. 2011; Chen et al. 2012; Chen et al. 2015) and very few on modified fungal polysaccharides (Yang et al. 2005a; Yang et al. 2005b).

Low molecular weight (LMW) polysaccharides from marine high molecular weight (HMW) polysaccharides can be prepared by chemical (e.g., acidic hydrolysis, radical process) or physical (e.g., ultrasonic irradiation) or even enzymatic (e.g., glycoside hydrolases, algal polysaccharidases, alginate lyases, bacterial glycoside hydrolases, and lyases) processes (Colliec et al. 1994; Nardella et al. 1996; Chen et al. 1997; Petit et al. 2007; Martin et al. 2014; Zykwinska et al. 2018). The depolymerization allows to reduce the heterogeneity of the polysaccharides, to

increase their solubility, and to have a better control of their pharmacokinetic parameters. Consequently, purified LMW derivatives are most often safer and can be administrated intravenously or subcutaneously with a predictable relationship between drug concentration and drug efficacy (Sabourel et al. 2014).

15.2 Applications of Marine GAGs and GAG-Mimetics in Medicine

15.2.1 Vascular and Ischemic Diseases

Marine macro-algae are a rich source of naturally sulfated polysaccharides. They can be extracted from green (Chlorophyta), red (Rhodophyta), or brown (Phaeophyta) algae. Sulfated galactans and sulfated fucoidans extracted from red and brown algae, respectively, are the most studied for their therapeutic effects and can be considered as marine non-GAGs (or GAG-mimetics) sulfated glycans (Pomin 2015).

In Chlorophyta, sulfated polysaccharides are polydisperse and highly branched heteropolysaccharides rich in rhamnose, galactose, and arabinose units. The green algae represent an important biomass that is still little used but needs to be exploited to eliminate overabundant algae on beach and coastal areas that damage marine ecosystems and impair local tourism. HMW highly sulfated arabinan and arabinogalactan extracted from *Codium dwarkense* Boergs. (Bryopsidales) exhibited an anticoagulant activity around threefold lower than heparin (Siddhanta et al. 1999). Arabinogalactans extracted from *C. vermilara* (Bryopsidales) presented a higher anticoagulant activity than the one from *C. fragile*. This greater activity was mainly due to their sulfate content (30 and 20% of sulfate groups, respectively) and also to their molecular weight (66×10^3 and 11×10^3 g/mol, respectively) (Jurd et al. 1995; Ciancia et al. 2007).

The sulfated polysaccharides extracted from red algae are mainly galactans (linear homopolysaccharide composed of galactose units) such as agars and carrageenans. Sulfated mannans or neutral xylans can be also found in several red algae. The most active are the highly sulfated lambda-carrageenans that are also the most water soluble. They present a proportion of sulfate groups close to that found in GAGs and especially heparin (35% of sulfate groups). *In vitro* anticoagulant assays showed an anticoagulant activity tenfold lower for lambda-carrageenans than heparin (Shanmugam and Mody 2000; Barabanova et al. 2008). Homogeneous LMW derivatives have been isolated by chemical depolymerization from different carrageenans and sulfated galactans in order to improve their specificity. A decrease of the anticoagulant activity was observed with the decrease of the molecular weight (Yamada et al. 1997; Zuniga et al. 2006). Both anticoagulant and antithrombotic properties of sulfated galactans extracted from the red alga *Botryocladia occidentalis* have been deeply analyzed. A LMW derivative (5×10^3 g/mol) was very potent in a rat model of venous thrombosis accompanied by a weak anticoagulant effect. In

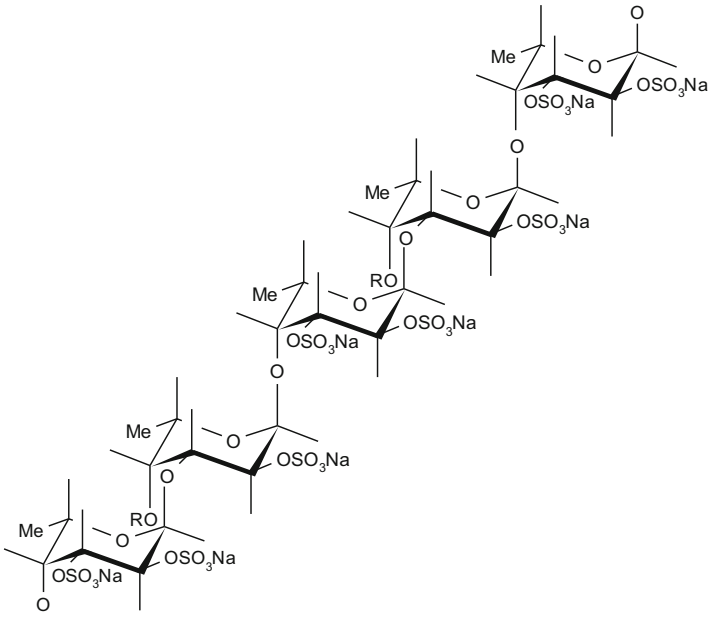

Fig. 15.1 Structure of the major repeating unit of the fucoidan extracted from *Ascophyllum nodosum* (Chevolot et al. 2001). R = H or SO_3Na or sulfated fucose

contrast, it presented a weak activity in a rat model of arterial thrombosis (Fonseca et al. 2008). The toxicity of LMW carrageenans was reported (Yu et al. 2002). *Porphyridium haitanensis* (rhodophyte) secreted a sulfated linear galactan named porphyran (20% sulfate groups). Porphyran was oversulfated in order to evaluate its antioxidant and anticoagulant activities using in vitro assays testing different derivatives. Their activities were clearly linked to both degree of sulfation and position of sulfate groups. The anticoagulant activity mainly depends on the position of sulfate groups, and the most anticoagulant derivative was tenfold less potent than heparin. The oversulfated spirulan probably exerts its anticoagulant activity via the inhibition of thrombin, an enzyme that catalyzes the conversion of fibrinogen to fibrin, the last step of the blood clotting process (Zhang et al. 2010).

The fucoidan family from brown algae has been studied extensively for its anticoagulant and antithrombotic properties. According to the algal species (*Laminaria digitata*, *Fucus vesiculosus*, *Pelvetia canaliculata*, *Ecklonia kurome*, *Ascophyllum nodosum*), fucoidans are more or less complex; they are highly branched sulfated polysaccharides primarily composed of fucose units and various amounts of xylose, galactose, mannose, and uronic acid units. Like heparin, they are highly sulfated bearing 25–35% of sulfate groups (Fig. 15.1).

Their biological activities depend on starting material, purification processes, structural heterogeneity, and molecular weight dispersion (Deniaud-Bouet et al. 2017). Fucoidans present a wide spectrum of biological activities (Berteau and

Mulloy 2003). Since 1957, anticoagulant activity of heterogeneous HMW extracts has been reported without investigating their anticoagulation mechanism. In 1989 and 1991, three studies performed on homogeneous LMW fucoidans ($< 30 \times 10^3$ g/mol) rich in both fucose units ($\geq 20\%$) and sulfate groups ($> 20\%$) showed that they enhance the inhibition of thrombin in the presence of its natural inhibitors (two serpins, antithrombin and heparin cofactor II); and the rate of thrombin inhibition depends on both their molecular weight and sulfate content (Church et al. 1989; Colliec et al. 1991; Nishino et al. 1991).The antithrombotic activity of fucoidans has been widely described in various animal models. Injected intravenously or subcutaneously, a LMW fucoidan extracted from *A. nodosum* was a potent antithrombotic agent in rabbit venous thrombosis model. This venous antithrombotic effect was accompanied with a weaker hemorrhagic effect than heparin (Mauray et al. 1995; Millet et al. 1999). This LMW fucoidan from *A. nodosum* injected both intravenously and subcutaneously in rat and rabbit models of arterial thrombosis appeared to be more potent than heparin for preventing arterial thrombosis with a lower hemorrhagic risk than LMW heparin (Colliec-Jouault et al. 2003; Durand et al. 2008). Fucoidans according to their structural characteristics can act as pro- or anti-angiogenic agents (Ustyuzhanina et al. 2014). By modulating the proangiogenic properties of heparin-binding growth factors such as FGF-2 (fibroblast growth factor) and VEGF (vascular endothelial growth factor), fucoidans can induce or inhibit new blood vessel formation. Anti-angiogenic activity was observed for HMW fucoidans, whereas LMW fucoidans were proangiogenic agent (Matou et al. 2002; Cumashi et al. 2007). In vitro and in vivo, LMW fucoidans were able to enhance both proliferation and migration of endothelial cells and also to inhibit smooth muscle cells. This dual effect suggests a real therapeutic potential of LMW fucoidans in ischemic diseases by favoring revascularization and thereby preventing necrosis (Deux et al. 2002; Luyt et al. 2003; Boisson-Vidal et al. 2007).

Soluble exocellular (found attached outside the cell wall) or extracellular (excreted into the extracellular environment) polysaccharides (EPS) from cyanobacteria are often anionic heteropolysaccharides due to the presence of uronic acids, pyruvyl, or sulfate groups. They have a great variety of structures and are very attractive of isolating innovative GAG-mimetics (De Philippis and Vincenzini 1998). As described above for fucoidans, a sulfated heteropolysaccharide rich in rhamnose, uronic acids, and calcium named calcium spirulan, isolated from the cyanobacterial strain *Arthrospira* (formerly, *Spirulina) platensis*, was potent to enhance the rate of inhibition of thrombin by its natural inhibitor heparin cofactor II, so it could be an innovative antithrombotic agent similar to heparin and dermatan sulfate (Hayakawa et al. 2000). The red microalgae *Porphyridium* sp. produce sulfated anionic heteropolysaccharides that have been described to exert biological activities such as anti-inflammatory, antitumor, and antiviral. A sulfated polysaccharide from *Porphyridium* sp. exhibited anti-inflammatory effect on endothelial cells that could suggest its use as potential therapeutic agent to treat endothelial dysfunction or endothelial cell injury-related diseases (Levy-Ontman et al. 2017).

Few studies have been conducted on both anticoagulant and antithrombotic properties of bacterial EPS. In fact, it is extremely rare to isolate marine bacteria

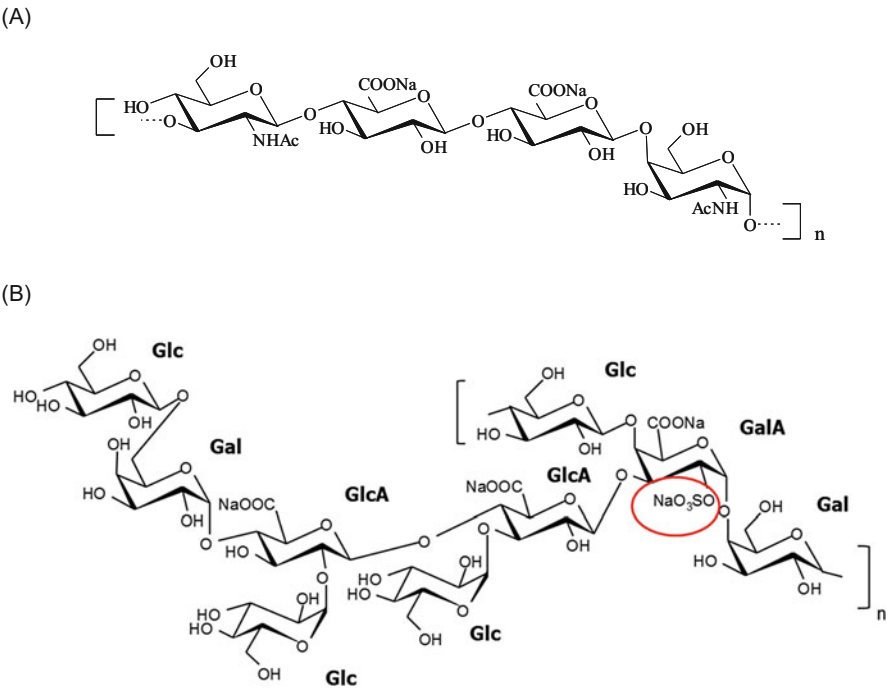

Fig. 15.2 (**a**) Tetrasaccharidic repeating unit of the EPS secreted by *Vibrio diabolicus*. (**b**) Nonasaccharidic repeating unit of the EPS secreted by *Alteromonas infernus*

that can produce naturally EPS with a GAG-mimetic structure; that means heteropolysaccharides composed of uronic acids or hexosamine sugars with or without sulfate groups. As noticed recently by Casillo and co-workers "Strikingly, marine bacteria seem to have chosen carboxyl groups, instead of sulfates of seaweeds, to make their polysaccharides negatively charged, as it results by the common presence of uronic acids in marine EPS" (Casillo et al. 2018). EPS isolated from two marine bacteria collected in deep-sea hydrothermal vents present unusual structures that can be considered as GAG-like molecules. *Vibrio diabolicus* can produce a very innovative EPS (Fig. 15.2a), presenting a chemical resemblance to hyaluronic acid: a linear HMW unsulfated heteropolysaccharide with a tetrasaccharide repeating unit composed of glucuronic acid and hexosamine residues (Rougeaux et al. 1999). *Alteromonas infernus* secretes a HMW slightly sulfated (10% of sulfate groups) branched heteropolysaccharide (Fig. 15.2b), with a nonasaccharide repeating unit composed of neutral sugars (glucose and galactose) and acidic sugars (glucuronic acid and galacturonic acid) bearing one sulfate group (Roger et al. 2004). These two EPS have been modified in order to design GAG-mimetic derivatives with a reduced molecular weight ($< 30 \times 10^3$ g/mol) and a high content of sulfate groups (30%).

The LMW highly sulfated EPS derivatives were less efficient than heparin to prolong plasma clotting. They were in vitro tenfold less anticoagulant than heparin, and they present affinity to both serpins antithrombin and heparin cofactor II (Colliec-Jouault et al. 2001). The same derivatives were studied to explore their capacity to promote angiogenesis in ischemic diseases. The LMW highly sulfated derivatives promoted in vitro angiogenesis thanks to their positive effects on vascular tube formation by both proliferation and migration of endothelial cells via the two angiogenic growth factors such as FGF-2 and VEGF. The LMW slightly sulfated derivatives had no effect, underlying again the importance of sulfate groups in the angiogenic effect as described for the anticoagulant effect (Matou et al. 2005).

A HMW polysaccharide (>10^6 g/mol) was isolated from a marine filamentous fungus *Keissleriella* sp. and is a linear glucan, and its chemically sulfated derivatives showed anticoagulant and antiplatelet aggregation activities in in vitro assays (the highest sulfated derivative imparted the highest anticoagulant activity) (Han et al. 2005).

15.2.2 Cancer Therapy and Immunomodulation Activity

For more than 30 years, the antitumoral activity of sulfated polysaccharides extracted from macro-algae has been extensively studied, using mainly carrageenans and fucoidans either unmodified (HMW polysaccharides) or depolymerized (LMW derivatives) (Fedorov et al. 2013; Moussavou et al. 2014). A LMW iota-carrageenan could induce in vitro and in vivo apoptosis in human osteosarcoma cells and reduce the tumor growth in an established xenograft tumor model performed in mice. The survival rate of treated animals was improved, and the analysis of their tumor showed a reduction of the intratumoral microvessels (Jin et al. 2013). Other studies performed on different tumor models (adenocarcinoma, leukemia, colon cancer) showed that undegraded kappa- and lambda-carrageenans and LMW lambda-carrageenans significantly inhibited the tumor growth of transplanted sarcoma in mice by the way of the immunomodulation of the immune system. The highest activity was observed with lambda-carrageenans whose molecular weight is equal or below 15×10^3 g/mol (Zhou et al. 2004; Khotimchenko 2010).

Native and LMW fucoidans isolated from several brown algae (*Sargassum* sp., *Fucus* sp., *F. vesiculosus* Sigma product, *A. nodosum*) have been studied in several in vitro and in vivo tumor models (lymphoma, melanoma, lung carcinoma, colon, and breast cancers). Unlike heparin, the observed inhibition of both in vitro cancer cell line proliferation and in vivo tumor growth involves different mechanisms. The antitumor activity is mainly due to the induction of apoptosis (Foley et al. 2011; Wijesinghe and Jeon 2012; Zhang et al. 2013). The inhibition of cancer cell adhesion was also observed by blocking the cell surface receptors (integrin family) involved in both invasion and metastasis (Liu et al. 2005). The activation of the immune response in vitro and in vivo was shown by stimulating immune cell activity such as macrophages and natural killer cells (Ale et al. 2011; Khil'chenko et al. 2011; Nakano et al.

2012; Kwak 2014). Additionally, the fucoidans could exert their antitumor activity via their anti-angiogenic activity, but this latter activity was only observed with HMW highly sulfated fucoidans (see above) (Koyanagi et al. 2003).

Sulfated calcium spirulan, composed mainly of rhamnose and fructose, presented in vitro an inhibitory effect on tumor invasion and metastasis. In a lung metastasis model induced by melanoma cells performed in mice, calcium spirulan injected intravenously after tumor inoculation could strongly reduce lung tumor colonies but had no effect on the primary tumor growth. This therapeutic effect could be due to its anti-heparanase activity, enzyme that digests and alters heparan sulfate on cell surface and participates in cancer progression (Mishima et al. 1998). Another study showed that a sulfated EPS (composed of galactose and uronic acids) from *Gyrodinium impudicum* dinoflagellate could induce secretory and cellular responses in murine peritoneal macrophages and augment their tumoricidal activity. This EPS has a potential therapeutic use to treat cancers as well as inflammatory diseases (Bae et al. 2006). A galactan sulfate from *Gymnodinium* sp., which is very close to *Gyrodinium* sp. (both are dinoflagellate of the same family of Gymnodiniaceae), presented an inhibitory effect on several human leukemic cell lines by inducing apoptotic cell death (Sogawa et al. 2000). An extract from *Chlorella pyrenoidosa* (Chlorophyta) rich in polysaccharide also revealed immunostimulatory effect and could activate macrophages (Kralovec et al. 2007). A purified polysaccharide from *C. pyrenoidosa* (composed of rhamnose, mannose, glucose, and galactose) presented an in vitro antitumor effect against human lung adenocarcinoma cells (Sheng et al. 2007). The red microalgae *Porphyridium* sp., *P. cruentum*, and *P. griseum* (regarded as synonym of *Dixioniella grisea*) produce hydrosoluble sulfated anionic heteropolysaccharides (6% sulfate groups and $\geq$ 10% uronic acids). Highly cytotoxic and apoptogenic activities on primary tumor cells have been observed in the presence of these sulfated polysaccharides (Gardeva et al. 2012). Different fractions of EPS from *P. cruentum* with various molecular weights were evaluated in vivo in a mouse tumor-bearing model. The molecular weight had a notable effect on the inhibitory activity; the fraction with the lowest molecular weight (6×10^3 g/mol) exhibited the strongest inhibitory activity without showing cytotoxic effect, suggesting an antitumor effect by improving the immune response (Sun et al. 2012). More recently, Sun and co-workers found the same activity and mechanism with a sulfated acidic polysaccharide extracted from *Pavlova viridis* (haptophyte) with a molecular weight of 55×10^3 g/mol (Sun et al. 2016). With oversulfated and LMW polysaccharides of *Porphyridium* sp. and *Rhodella reticulata* prepared chemically, a correlation between their inhibitory effects on myeloid and lymphoma cell lines and their molecular weight was evidenced (Geresh et al. 2002). A highly branched glucan extracted from *Isochrysis galbana* (haptophyte) presented an antitumor activity against myeloid cancer without causing an apoptotic effect and inducing cell mortality. Its effect was probably due to a direct inhibition of cell proliferation (Sadovskaya et al. 2014).

Few marine bacterial EPS have been tested as antitumoral agents. The therapeutic interest of LMW highly sulfated EPS derivatives from *A. infernus* (described above) was evaluated in vitro and in vivo against osteosarcoma, a rare malignant bone

tumor. In vitro study showed that only a sulfated derivative with a molecular weight of 15×10^3 g/mol was able to inhibit both invasiveness and migration of osteosarcoma cells. The derivative had no significant effect on the osteosarcoma cell cycle and highly increased the expression of the physiological specific tissue inhibitor TIMP-1. In vivo in a mouse model of lung metastases induced by injection of osteosarcoma cells, the same derivative was very efficient in inhibiting the establishment of lung metastases, but had no effect on the growth of the primary osteosarcoma tumor. Moreover, the survival rate of treated animal was improved (Heymann et al. 2016). An unsulfated heteropolysaccharide (70% glucose, 20% mannose, and 10% fucose), produced by the *Flavobacterium uliginosum* isolated from marine algae and called marinactan, had antitumor effect against mouse mammary tumor and S-180 tumor. A complete regression of the tumor was observed in treated mice with prolonged survival rate (Okami 1986; Austin 1989).

15.2.3 Antiviral Activities

The antiviral activities have been described for algal sulfated polysaccharides extracted either macro-algae (extending 30 meters) or microscopic unicellular algae. Since 1987, anti-human immunodeficiency virus (HIV) activity of different algal sulfated polysaccharides such as carrageenan, fucoidan, and calcium spirulan have been studied (Schaeffer and Krylov 2000; Smit 2004; Vo and Kim 2010; Wang et al. 2012). Several studies have been conducted on the antiviral properties of carrageenans against a broad spectrum of viruses (HIV, yellow fever virus, herpes simplex virus (HSV)). As described above for other activities, their antiviral efficacy was linked to both their sulfate content and their molecular weight. A decrease of the antiviral activity was observed with the decrease of the polysaccharide molecular weight. Different carrageenan structural types have been depolymerized by chemical (free-radical reaction and mild acid hydrolysis) or enzymatic (carrageenase) processes, yielding very LMW derivatives ($< 4 \times 10^3$ g/mol). The highest activity was shown for LMW derivatives isolated by mild acid hydrolysis but lower than HMW carrageenans and the lowest for derivatives obtained by enzymatic degradation (Kalitnik et al. 2013). In the case of HSV-1, the specific inhibitory effect of a lambda-type carrageenan was mainly due to its interaction with the virus leading to virus inactivation by disturbing the interaction between virus and host cells (Carlucci et al. 1999). The antiviral effect of carrageenans depends on the carrageenan structural type, the virus serotypes, and the host cells (Wang et al. 2012).

Sulfated polysaccharides from brown algae such as the fucoidan family (galactofucans, fucans) are also very attractive for their antiviral effects. Fucoidans extracted from various brown algal species have been reported as very potent antiviral agents (Hayashi et al. 2008). The most active fucoidans are often the ones with the higher levels of sulfate groups and lower levels of uronic acids (Hemmingson et al. 2006). A defensive effect against HSV infection has been shown in mice by oral administration of fucoidan. In this model, oral intake of

fucoidan was probably effective through direct inhibition of viral replication and stimulation (Hayashi et al. 2008). A recent clinical study showed that fucoidan given orally daily for 12 months was safe and effective in the treatment of patients with chronic hepatitis C virus infection (Mori et al. 2012).

The calcium spirulan already described above for its antithrombin activity via heparin cofactor II has shown in vitro and ex vivo antiviral activities against several enveloped viruses such as herpes simplex virus (HSV) and HIV (Hayashi et al. 1996). The spirulan was potent in inhibiting the viral replication in vitro without being cytotoxic, and its mechanism of action differed with the type of virus, targeting more or less the virus entry step (Rechter et al. 2006). The halophilous cyanobacterium *Aphanothece halophytica* secreted a single type sulfated acidic EPS (35% of sulfate groups and composed of arabinose, rhamnose, fucose, mannose, glucose, galactose, and glucuronic acid). This EPS was very effective in inhibiting influenza virus-induced pneumonia in mouse model, and its effect was mediated by a modulation of the host immune system. The marine microalgal sulfated EPS from *G. impudicum* inhibited the replication of encephalomyocarditis virus and imparted immunostimulatory effect (Yim et al. 2004; Yim et al. 2005). This EPS could also inhibit the influenza type A but not the type B viruses (Kim et al. 2012). A diatom collected from deep-sea water *Navicula directa* can produce a sulfated heteropolysaccharide named naviculan (composed of fucose, xylose, galactose, mannose, rhamnose, and small amount of uronic acids). Naviculan had a broad antiviral spectrum against enveloped viruses such as HSV, HIV, and influenza A virus (Lee et al. 2006). Naviculan affects both viral adhesion and penetration into host cells.

Both immunomodulatory and antiviral activities against HSV-2 have been demonstrated with an EPS produced by *Geobacillus thermodenitrificans* isolated from a shallow marine vent in Vulcano Island (Italy). The EPS is a HMW heteropolysaccharide composed of mannose and glucose (Arena et al. 2009). An EPS mainly composed of glucose produced by *Pseudoalteromonas* sp. isolated from a marine sponge sample in the Red Sea (Egypt) exhibited a strong antiviral activity against HSV-1 (Al-Nahas et al. 2011). A sulfated EPS produced by a marine *Pseudomonas* sp. isolated from the brown seaweed *Undaria pinnatifida* composed of galactosamine and glucuronic acid bearing both pyruvate and sulfate groups was oversulfated. Strong antiviral activity against HSV-1 was obtained with the native compound and against influenza virus type A for oversulfated derivatives (Matsuda et al. 1999).

15.3 Applications of Marine GAG-Mimetics in Tissue Engineering

Defects of tissues such as cartilage, bone, or skin, arising from trauma, progressive degenerative diseases (e.g., osteoarthritis, periodontitis), or oncological resection and the necessity for their reconstruction, led to the development of an alternative strategy to surgical treatment, namely, tissue engineering. Tissue engineering aims to

create a functional tissue through an appropriate combination between cells, scaffolds that provide the cells three-dimensional (3D) environment, and biological signaling molecules, such as growth factors necessary for stimulation of cellular processes (Langer and Vacanti 1993). An ideal scaffold for tissue reconstruction needs to respond to several requirements, including biocompatibility to prevent the inflammatory reactions against foreign body, 3D shape to allow proliferation of cells and their differentiation, and appropriate porosity, enabling cell migration and diffusion of molecules, nutriments, and oxygen. Such a matrix should also mimic the mechanical properties of the tissue to be reconstructed; however after implantation, it should progressively be degraded to allow the new tissue to settle down. Bioactive properties of the scaffold are also important since they may enhance adhesion of cells, thus facilitating their implantation in the lesion to be repaired. Bioactive matrix may also exert protecting and stabilizing properties toward the growth factors, in a similar manner to GAGs from the extracellular matrix (ECM). Indeed, by interacting with growth factors, GAGs protect these signaling molecules from undesired proteolytic degradation and enhance both their local concentration up to levels required for signaling and their stability, allowing the growth factor binding to their receptors (Ruoslahti and Yamaguchi 1991; Ramirez and Rifkin 2003; Gandhi and Mancera 2008). Although it seems particularly complex to establish a scaffold joining all the requirements necessary for successful repair of the tissue, several advanced matrices have already been engineered. Some of them were elaborated using marine GAG-mimetics, which were used to form an entire scaffold or applied as bioactive molecules incorporated into the matrix with the aim to enhance its properties.

15.4 Marine GAG-Mimetics as Bioactive Molecules

Marine polysaccharides exhibiting GAG-mimetic properties can also be explored for tissue engineering as bioactive molecules with the aim to enrich the properties of the basic scaffold. The addition of fucoidan to chitosan scaffold prompted the mesenchymal stem cells (MSC) differentiation into osteogenic-like cells for bone regeneration applications (Puvaneswary et al. 2016). Porphyran isolated from *Porphyra yezoensis* could suppress in vitro osteoclastogenesis without any cytotoxic effect. This result suggests that porphyran can be a promising therapeutic agent in regulating bone growth and remodeling in bone diseases (Ueno et al. 2018).

Native HMW EPS from *V. diabolicus* (as described above with a hyaluronic acid-like structure) could enhance in vivo bone repair in a rat model of critical size defect technique (defined as the smallest size intraosseous wound that will not heal spontaneously) (Zanchetta et al. 2003). This HMW EPS incorporated within collagen hydrogel containing dermal fibroblasts was shown to favor collagen fibrillogenesis as well as cell migration and proliferation (Senni et al. 2011; Senni et al. 2013). Marine bacterial EPS can thus be exploited as GAG-mimetic compound for skin regeneration. In another study, silanized-hydroxypropyl methylcellulose

(Si-HPMC) hydrogel enriched in marine HMW EPS from *A. infernus* (see above) was cytocompatible and competent for the 3D culture of chondrocytes, which were able to produce cartilage ECM proteins in vitro. This complex Si-HPMC/GY785 EPS hydrogel enabled the chondrocytes to produce a cartilage-like ECM in an in vivo experiment (Rederstorff et al. 2017). As described for porphyran and GAGs, oversulfated LMW derivatives obtained from the EPS secreted by *A. infernus* inhibited osteoclastogenesis in cell models and regulated different levels of bone resorption. These derivatives could play an important role in bone metabolism (Ruiz Velasco et al. 2011).

15.5 Marine GAG-Mimetics as Bioactive Scaffolds

Bioactive scaffolds for tissue engineering are mainly elaborated as hydrogels or porous matrices at macro-, micro-, and nanoscales. Hydrogels are highly hydrophilic 3D polymer networks presenting some structural and functional similarities with the ECM. They are obtained through physical or chemical cross-linking, allowing the control of the gelation kinetics and the subsequent hydrogel mechanical properties. When freeze-dried, hydrogels form highly porous scaffolds. Two major marine polysaccharides, namely, alginate and chitosan, have extensively been studied as matrices for tissue engineering (Lee and Mooney 2012; Muzzarelli et al. 2012; Croisier and Jérôme 2013; Bidarra et al. 2014). The ability of alginate to form physical gels in the presence of divalent ions, and in particular calcium ions, has largely been explored to develop cell and growth factor delivery systems. Indeed, mild conditions offered by physical gelation with the use of nontoxic reactants are particularly well-suited for such applications. In the case of hydrogels, cells can directly be suspended in alginate solution, and gelation is then induced by adding calcium-based cross-linking agents (Kuo and Ma 2001; Aguado et al. 2012; Follin et al. 2015). To obtain more uniform and mechanically stronger gels, gelation rate can be controlled by replacing calcium chloride ($CaCl_2$), inducing rapid and heterogeneous alginate cross-linking, by calcium sulfate ($CaSO_4$) or calcium carbonate ($CaCO_3$), displaying lower solubilities (Kuo and Ma 2001). Alginate gelation rate can also be modulated by decreasing alginate molecular weight leading to low-viscosity solutions appropriate for injectable hydrogels (Aguado et al. 2012). Because alginate lacks cell adhesion properties, it is frequently functionalized with cell recognition arginine-glycine-aspartic acid (RGD) peptide motif to promote cell adhesion (Rowley et al. 1999). RGD-modified alginate was also explored to form hydrogels through cell-cross-linking (Lee et al. 2003). The interaction between cell receptors and adhesion ligands leads to formation of reversible gel systems, allowing the cells to play a double role of therapeutic materials and cross-linkers. To reduce the number of cells required for alginate gelation, cell cross-linking was further combined with calcium cross-linking (Park et al. 2009). The resulting shear-

reversible hydrogel was shown to be efficient to regenerate new cartilage tissues in vivo and could then be used as an injectable delivery system for minimally invasive surgeries. RGD-functionalized alginate was calcium cross-linked to prepare after freeze-drying a macroporous scaffold, which favored the chondrogenic differentiation of mesenchymal stem cells (MSCs) in the presence of transforming growth factor-β1 (TGF-β1) (Re'em et al. 2010). To increase TGF-β1 binding to the matrix, alginate is devoid of sulfate groups and was chemically sulfated to mimic the structural and functional features of the ECM and in particular high sulfate content (Freeman and Cohen 2009; Re'em et al. 2012). In vitro and in vivo studies performed on affinity bound TGF-β1 to alginate/alginate sulfate scaffold indicated that the efficient capture and sustained presentation of the growth factor ensured the appropriate MSC differentiation, up to the appearance of committed chondrocytes specific of the hyaline cartilage type (Re'em et al. 2012).

In contrast to alginate, chitosan in aqueous solutions below pH 6 is a positively charged polysaccharide with the ability to form physical gels by itself through hydrogen bonding and hydrophobic interactions and also in the presence of anions such as phosphates, sulfates, or citrates (Croisier and Jérôme 2013). Chitosan may be regarded as a structural analog of GAG molecules due to the presence of D-glucosamine and *N*-acetyl D-glucosamine residues. Chitosan was successfully formulated as an injectable hydrogel, supporting survival, proliferation, and MSC chondrogenic differentiation (Naderi-Meshkin et al. 2014), while a macroporous scaffold favors osteoblastic differentiation of seeded cells for bone regeneration (Seol et al. 2004).

To overcome limitations arising from the direct incorporation of cells or growth factors within macroscale matrices, microscale scaffolds have been developed. Indeed, microencapsulation of cells enhances their retention at the targeted tissue and protects them from the mechanical forces during hydrogel injection, whereas microencapsulation of growth factors enables their protection from undesired degradation and their sustained release (Chen et al. 2010; Lee et al. 2011; Aguado et al. 2012). Successful encapsulation of cells or growth factors or both within alginate and chitosan microgels for tissue engineering was reported in several studies (Sun and Tan 2013; Croisier and Jérôme 2013). Gelled microparticles based on RGD-modified alginate encapsulating both MSCs and TGF-β1 were shown to constitute an appropriate microenvironment supporting viability, metabolic activity, and chondrogenic differentiation of cells in vitro and in vivo (Moshaverinia et al. 2013). Cells were also encapsulated inside alginate calcium-cross-linked microfibers that can further be used as vehicles for cells or therapeutic molecules for the regeneration of damaged tissues or used as a 3D-line scaffold to create nerve or muscle fibers (Shin et al. 2007; Daniele et al. 2015). Recently, a marine EPS produced by *V. diabolicus* displaying biological activities in bone and skin regeneration (Zanchetta et al. 2003; Senni et al. 2013) was structured into gelled microparticles and microfibers for protein delivery applications (Zykwinska et al. 2016). Both physicochemical (gelling) and biological (GAG-like) properties of the EPS from *V. diabolicus* could be explored to formulate new microcarriers for biological molecule delivery that can further be used in tissue engineering.

15.6 Concluding Remarks

The ocean has not yet revealed all its treasures and its potential. In combining conservation and exploitation to preserve biodiversity, marine resource should be for many long years a vast field of investigation for the discovery of novel bioactive compounds with biomedical potential. In fact, marine bio-resource, including animals (e.g., fish,), invertebrates (e.g., crustaceans, worms, sea cucumbers, sea urchins, corals, starfish), macro-algae, microalgae, bacteria, and fungi, offers a great potential to highlight unknown or atypical species that can produce a wide range of molecules.

Polysaccharides and especially anionic polysaccharides endowed with GAG-like or GAG-mimetic properties present a great potential for pharmaceutical and biotechnological applications such as drugs and biomaterials. In the biotechnological challenge for the discovery of safer, biocompatible, biodegradable, valuable renewable, and animal-free molecules, the marine habitats and particularly their micro-resources are an endless treasure for the production of original polysaccharides. These marine polysaccharides can be modified to design derivatives with specific functional groups and defined molecular weight in order to improve both their bioactivities and their benefit/risk ratio. With the breakthrough of biotechnology based on specific bio-tools (e.g., molecular biology, bioinformatics, culture systems), the fine-tuning of the production of GAG-mimetics with promising biological properties should accelerate both development and applications of marine polysaccharides.

Acknowledgments This work was supported by the CNRS in the framework of the GDR GAG (GDR 3739).

References

Aguado BA, Mulyasasmita W, Su J, Lampe KJ, Heilshorn SC (2012) Improving viability of stem cells during syringe needle flow through the design of hydrogel cell carriers. Tissue Eng 18:806–815

Ale MT, Maruyama H, Tamauchi H, Mikkelsen JD, Meyer AS (2011) Fucoidan from *Sargassum* sp. and *Fucus vesiculosus* reduces cell viability of lung carcinoma and melanoma cells in vitro and activates natural killer cells in mice in vivo. Int J Biol Macromol 49:331–336

Al-Nahas MO, Darwish MM, Ali AE, Amin MA (2011) Characterization of an exopolysaccharide-producing marine bacterium, isolate *Pseudoalteromonas* sp AM. Afr J Microbiol Res 5:3823–3831

Alonso AA, Antelo LT, Otero-Muras I, Pérez-Gálvez R (2010) Contributing to fisheries sustainability by making the best possible use of their resources: the BEFAIR initiative. Trends Food Sci Technol 21:569–578

Arena A, Gugliandolo C, Stassi G, Pavone B, Iannello D, Bisignano G, Maugeri TL (2009) An exopolysaccharide produced by *Geobacillus thermodenitrificans* strain B3-72: antiviral activity on immunocompetent cells. Immunol Lett 123:132–137

Austin B (1989) Novel pharmaceutical compounds from marine bacteria. J Appl Bacteriol 67:461–470

Badri A, Williams A, Linhardt RJ, Koffas MAG (2018) The road to animal-free glycosaminoglycan production: current efforts and bottlenecks. Curr Opin Biotechnol 53:85–92

Bae S-Y, Yim JH, Lee HK, Pyo S (2006) Activation of murine peritoneal macrophages by sulfated exopolysaccharide from marine microalga *Gyrodinium impudicum* (strain KG03): involvement of the NF-[kappa]B and JNK pathway. Int Immunopharmacol 6:473–484

Barabanova A, Shashkov A, Glazunov V, Isakov V, Nebylovskaya T, Helbert W, Solov'eva T, Yermak I (2008) Structure and properties of carrageenan-like polysaccharide from the red alga *Tichocarpus crinitus* (Gmel.) Rupr. (Rhodophyta, Tichocarpaceae). J Appl Phycol 20:1013–1020

Barritault D, Gilbert-Sirieix M, Rice KL, Siñeriz F, Papy-Garcia D, Baudouin C, Desgranges P, Zakine G, Saffar J-L, van Neck J (2017) RGTA® or ReGeneraTing agents mimic heparan sulfate in regenerative medicine: from concept to curing patients. Glycoconj J 34:325–338

Berteau O, Mulloy B (2003) Sulfated fucans, fresh perspectives: structures, functions, and biological properties of sulfated fucans and an overview of enzymes active toward this class of polysaccharide. Glycobiology 13:29R–40R

Bidarra SJ, Barrias CC, Granja PL (2014) Injectable alginate hydrogels for cell delivery in tissue engineering. Acta Biomater 10:1646–1662

Boisson-Vidal C, Zemani F, Caligiuri G, Galy-Fauroux I, Colliec-Jouault S, Helley D, Fischer AM (2007) Neoangiogenesis induced by progenitor endothelial cells: effect of fucoidan from marine algae. Cardiovasc Hematol Agents Med Chem 5:67–77

Carlucci MJ, Ciancia M, Matulewicz MC, Cerezo AS, Damonte EB (1999) Antiherpetic activity and mode of action of natural carrageenans of diverse structural types. Antivir Res 43:93–102

Casillo A, Lanzetta R, Parrilli M, Corsaro M (2018) Exopolysaccharides from marine and marine extremophilic bacteria: structures, properties, ecological roles and applications. Mar Drugs 16:69. https://doi.org/10.3390/md16020069

Chen RH, Chang JR, Shyur JS (1997) Effects of ultrasonic conditions and storage in acidic solutions on changes in molecular weight and polydispersity of treated chitosan. Carbohydr Res 299:287–294

Chen HM, Ouyang W, Martoni C, Afkhami F, Lawuyi B, Lim T, Prakash S (2010) Investigation of genipin cross-linked microcapsule for oral delivery of live bacterial cells and other biotherapeutics: preparation and in vitro analysis in simulated human gastrointestinal model. Int J Polym Sci 2010:1–10

Chen Y, Mao W, Tao H, Zhu W, Qi X, Chen Y, Li H, Zhao C, Yang Y, Hou Y, Wang C, Li N (2011) Structural characterization and antioxidant properties of an exopolysaccharide produced by the mangrove endophytic fungus *Aspergillus* sp. Y16. Bioresour Technol 102:8179–8184

Chen Y, Mao WJ, Yang YP, Teng XC, Zhu WM, Qi XH, Chen YL, Zhao CQ, Hou YJ, Wang CY, Li N (2012) Structure and antioxidant activity of an extracellular polysaccharide from coral-associated fungus, *Aspergillus versicolor* LCJ-5-4. Carbohydr Polym 87:218–226

Chen YL, Mao WJ, Tao HW, Zhu WM, Yan MX, Liu X, Guo TT, Guo T (2015) Preparation and characterization of a novel extracellular polysaccharide with antioxidant activity, from the mangrove-associated fungus *Fusarium oxysporum*. Mar Biotechnol 17:219–228

Chevolot L, Mulloy B, Ratiskol J, Foucault A, Colliec-Jouault S (2001) A disaccharide repeat unit is the major structure in fucoidans from two species of brown algae. Carbohydr Res 330:529–535

Church FC, Meade JB, Treanor RE, Whinna HC (1989) Antithrombin activity of fucoidan. The interaction of fucoidan with heparin cofactor II, antithrombin III, and thrombin. J Biol Chem 264:3618–3623

Ciancia M, Quintana I, Vizcarguenaga MI, Kasulin L, de Dios A, Estevez JM, Cerezo AS (2007) Polysaccharides from the green seaweeds *Codium fragile* and *C. vermilara* with controversial effects on hemostasis. Int J Biol Macromol 41:641–649

Colliec S, Fischer AM, Taponbretaudiere J, Boisson C, Durand P, Jozefonvicz J (1991) Anticoagulant properties of a fucoidan fraction. Thromb Res 64:143–154

Colliec S, Boisson-Vidal C, Jozefonvicz J (1994) A low molecular weight fucoidan fraction from the brown seaweed *Pelvetia canaliculata*. Phytochemistry 35:697–700

Colliec-Jouault S, Chevolot L, Helley D, Ratiskol J, Bros A, Sinquin C, Roger O, Fischer AM (2001) Characterization, chemical modifications and in vitro anticoagulant properties of an exopolysaccharide produced by *Alteromonas infernus*. Biochim Biophys Acta 1528:141–151

Colliec-Jouault S, Millet J, Helley D, Sinquin C, Fischer AM (2003) Effect of low-molecular-weight fucoidan on experimental arterial thrombosis in the rabbit and rat. J Thromb Haemost 1:1114–1115

Colliec-Jouault S, Bavington C, Delbarre-Ladrat C (2012) Heparin-like entities from marine organisms. Handb Exp Pharmacol 207:423–449

Croisier F, Jérôme C (2013) Chitosan-based biomaterials for tissue engineering. Eur Polym J 49:780–792

Cumashi A, Ushakova NA, Preobrazhenskaya ME, D'Incecco A, Piccoli A, Totani L, Tinari N, Morozevich GE, Berman AE, Bilan MI, Usov AI, Ustyuzhanina NE, Grachev AA, Sanderson CJ, Kelly M, Rabinovich GA, Iacobelli S, Nifantiev NE, Nazio CI (2007) A comparative study of the anti-inflammatory, anticoagulant, antiangiogenic, and antiadhesive activities of nine different fucoidans from brown seaweeds. Glycobiology 17:541–552

Daniele MA, Boyd DA, Adams AA, Ligler FS (2015) Microfluidic strategies for design and assembly of microfibers and nanofibers with tissue engineering and regenerative medicine applications. Adv Healthc Mater 4:11–28

de Jesus Raposo MF, de Morais AMB, de Morais RMSC (2015) Marine polysaccharides from algae with potential biomedical applications. Mar Drugs 13:2967–3028

De Philippis R, Vincenzini M (1998) Exocellular polysaccharides from cyanobacteria and their possible applications. FEMS Microbiol Rev 22:151–175

DeAngelis PL (2012) Glycosaminoglycan polysaccharide biosynthesis and production: today and tomorrow. Appl Microbiol Biotechnol 94:295–305

Deming J (1998) Deep ocean environmental biotechnology. Curr Opin Biotechnol 9:283–287

Deniaud-Bouet E, Hardouin K, Potin P, Kloareg B, Herve C (2017) A review about brown algal cell walls and fucose-containing sulfated polysaccharides: cell wall context, biomedical properties and key research challenges. Carbohydr Polym 175:395–408

Deux JF, Meddahi-Pelle A, Le Blanche AF, Feldman LJ, Colliec-Jouault S, Bree F, Boudghene F, Michel JB, Letourneur D (2002) Low molecular weight fucoidan prevents neointimal hyperplasia in rabbit iliac artery in-stent restenosis model. Arterioscler ThrombVasc Biol 22:1604–1609

Durand E, Helley D, Zen AAH, Dujols C, Bruneval P, Colliec-Jouault S, Fischer AM, Lafont A (2008) Effect of low molecular weight fucoidan and low molecular weight heparin in a rabbit model of arterial thrombosis. J Vasc Res 45:529–537

Fedorov SN, Ermakova SP, Zvyagintseva TN, Stonik VA (2013) Anticancer and cancer preventive properties of marine polysaccharides: some results and prospects. Mar Drugs 11:4876–4901

Finore I, Di Donato P, Mastascusa V, Nicolaus B, Poli A (2014) Fermentation technologies for the optimization of marine microbial exopolysaccharide production. Mar Drugs 12:3005–3024

Foley SA, Szegezdi E, Mulloy B, Samali A, Tuohy MG (2011) An unfractionated fucoidan from *ascophyllum nodosum*: extraction, characterization, and apoptotic effects in vitro. J Nat Prod 74:1851–1861

Follin B, Juhl M, Cohen S, Pedersen AE, Gad M, Kastrup J, Ekblond A (2015) Human adipose-derived stromal cells in a clinically applicable injectable alginate hydrogel: phenotypic and immunomodulatory evaluation. Cytotherapy 17:1104–1118

Fonseca RJ, Oliveira SN, Melo FR, Pereira MG, Benevides NM, Mourao PA (2008) Slight differences in sulfation of algal galactans account for differences in their anticoagulant and venous antithrombotic activities. Thromb Haemost 99:539–545

Freeman I, Cohen S (2009) The influence of the sequential delivery of angiogenic factors from affinity-binding alginate scaffolds on vascularization. Biomaterials 30:2122–2131

Freitas F, Torres CAV, Reis MAM (2017) Engineering aspects of microbial exopolysaccharide production. Bioresour Technol 245:1674–1683

Gandhi NS, Mancera RL (2008) The structure of glycosaminoglycans and their interactions with proteins. Chem Biol Drug Des 72:455–482

Gardeva E, Toshkova R, Yossifova L, Minkova K, Gigova L (2012) Cytotoxic and apoptogenic potential of red microalgal polysaccharides. Biotechnol Biotechnol Equip 26:3167–3172

Geresh S, Mamontov A, Weinstein J (2002) Sulfation of extracellular polysaccharides of red microalgae: preparation, characterization and properties. J Biochem Biophys Methods 50:179–187

Han F, Yao W, Yang X, Liu X, Gao X (2005) Experimental study on anticoagulant and antiplatelet aggregation activity of a chemically sulfated marine polysaccharide YCP. Int J Biol Macromol 36:201–207

Hayakawa Y, Hayashi T, Lee JB, Ozawa T, Sakuragawa N (2000) Activation of heparin cofactor II by calcium spirulan. J Biol Chem 275:11379–11382

Hayashi K, Hayashi T, Kojima I (1996) A natural sulfated polysaccharide, calcium spirulan, isolated from Spirulina platensis: in vitro and ex vivo evaluation of anti-herpes simplex virus and anti-human immunodeficiency virus activities. AIDS Res Hum Retrovir 12:1463–1471

Hayashi K, Nakano T, Hashimoto M, Kanekiyo K, Hayashi T (2008) Defensive effects of a fucoidan from brown alga *Undaria pinnatifida* against herpes simplex virus infection. Int Immunopharmacol 8:109–116

Hemmingson JA, Falshaw R, Furneaux RH, Thompson K (2006) Structure and antiviral activity of the galactofucan sulfates extracted from *Undaria Pinnatifida* (Phaeophyta). J Appl Phycol 18:185–193

Heymann D, Ruiz-Velasco C, Chesneau J, Ratiskol J, Sinquin C, Colliec-Jouault S (2016) Anti-metastatic properties of a marine bacterial exopolysaccharide-based derivative designed to mimic glycosaminoglycans. Molecules 21:309. https://doi.org/10.3390/molecules21030309

Ikeda Y, Charef S, Ouidja M-O, Barbier-Chassefiere V, Sineriz F, Duchesnay A, Narasimprakash H, Martelly I, Kern P, Barritault D, Petit E, Papy-Garcia D (2011) Synthesis and biological activities of a library of glycosaminoglycans mimetic oligosaccharides. Biomaterials 32:769–776

Imhoff JF, Labes A, Wieses J (2011) Bio-mining the microbial treasures of the ocean : new natural products. Biotechnol Adv 29:468–482

Jiao GL, Yu GL, Zhang JZ, Ewart HS (2011) Chemical structures and bioactivities of sulfated polysaccharides from marine algae. Mar Drugs 9:196–223

Jin Z, Han YX, Han XR (2013) Degraded iota-carrageenan can induce apoptosis in human osteosarcoma cells via the Wnt/-Catenin signaling pathway. Nutr Cancer 65:126–131

Jurd KM, Rogers DJ, Blunden G, McLellan DS (1995) Anticoagulant properties of sulphated polysaccharides and a proteoglycan from *Codium fragile ssp. atlanticum*. J Appl Phycol 7:339–345

Kalitnik AA, Barabanova AOB, Nagorskaya VP, Reunov AV, Glazunov VP, Solov'eva TF, Yermak IM (2013) Low molecular weight derivatives of different carrageenan types and their antiviral activity. J Appl Phycol 25:65–72

Khil'chenko SR, Zaporozhets TS, Shevchenko NM, Zvyagintseva TN, Vogel U, Seeberger P, Lepenies B (2011) Immunostimulatory activity of fucoidan from the brown alga *fucus evanescens*: role of sulfates and acetates. J Carbohydr Chem 30:291–305

Khotimchenko YS (2010) The antitumor properties of nonstarch polysaccharides: carrageenans, alginates, and pectins. Russ J Mar Biol 36:401–412

Kim M, Yim JH, Kim SY, Kim HS, Lee WG, Kim SJ, Kang PS, Lee CK (2012) In vitro inhibition of influenza A virus infection by marine microalga-derived sulfated polysaccharide p-KG03. Antivir Res 93:253–259

Koyanagi S, Tanigawa N, Nakagawa H, Soeda S, Shimeno H (2003) Oversulfation of fucoidan enhances its anti-angiogenic and antitumor activities. Biochem Pharmacol 65:173–179

Kralovec JA, Metera KL, Kumar JR, Watson LV, Girouard GS, Guan Y, Carr RI, Barrow CJ, Ewart HS (2007) Immunostimulatory principles from *Chlorella pyrenoidosa* – Part 1: isolation and biological assessment in vitro. Phytomedicine 14:57–64

Kuo CK, Ma PX (2001) Ionically crosslinked alginate hydrogels as scaffolds for tissue engineering: Part 1. Structure, gelation rate and mechanical properties. Biomaterials 22:511–521

Kwak JY (2014) Fucoidan as a marine anticancer agent in preclinical development. Mar Drugs 12:851–870

Langer R, Vacanti JP (1993) Tissue engineering. Science 260:920–926

Laurienzo P (2010) Marine polysaccharides in pharmaceutical applications: an overview. Mar Drugs 8:2435–2465

Lee KY, Mooney DJ (2012) Alginate: properties and biomedical applications. Prog Polym Sci 37:106–126

Lee KY, Kong HJ, Larson RG, Mooney DJ (2003) Hydrogel formation via cell crosslinking. Adv Mater 15:1828–1832

Lee J-B, Hayashi K, Hirata M, Kuroda E, Suzuki E, Kubo Y, Hayashi T (2006) Antiviral sulfated polysaccharide from *navicula directa*, a diatom collected from deep-sea water in Toyama Bay. Biol Pharm Bull 29:2135–2139

Lee K, Silva EA, Mooney DJ (2011) Growth factor delivery-based tissue engineering: general approaches and a review of recent developments. J R Soc Interface 8:153–170

Levy-Ontman O, Huleihel M, Hamias R, Wolak T, Paran E (2017) An anti-inflammatory effect of red microalga polysaccharides in coronary artery endothelial cells. Atherosclerosis 264:11–18

Liu RM, Bignon J, Haroun-Bouhedja F, Bittoun P, Vassy J, Fermandjian S, Wdzieczak-Bakala J, Boisson-Vidal C (2005) Inhibitory effect of fucoidan on the adhesion of adenocarcinoma cells to fibronectin. Anticancer Res 25:2129–2133

Luyt CE, Meddahi-Pelle A, Ho-Tin-Noe B, Colliec-Jouault S, Guezennec J, Louedec L, Prats HE, Jacob MP, Osborne-Pellegrin M, Letourneur D, Michel JB (2003) Low-molecular-weight fucoidan promotes therapeutic revascularization in a rat model of critical hindlimb ischemia. J Pharmacol Exp Ther 305:24–30

Martin M, Portetelle D, Michel G, Vandenbol M (2014) Microorganisms living on macroalgae: diversity, interactions, and biotechnological applications. Appl Microbiol Biotechnol 98:2917–2935

Martins A, Vieira H, Gaspar H, Santos S (2014) Marketed marine natural products in the pharmaceutical and cosmeceutical industries: tips for success. Mar Drugs 12:1066–1101

Matou S, Helley D, Chabut D, Bros A, Fischer A-M (2002) Effect of fucoidan on fibroblast growth factor-2-induced angiogenesis *in vitro*. Thromb Res 106:213–221

Matou S, Colliec-Jouault S, Galy-Fauroux I, Ratiskol J, Sinquin C, Guezennec J, Fischer A-M, Helley D (2005) Effect of an oversulfated exopolysaccharide on angiogenesis induced by fibroblast growth factor-2 or vascular endothelial growth factor *in vitro*. Biochem Pharmacol 69:751–759

Matsuda M, Shigeta S, Okutani K (1999) Antiviral activities of marine *Pseudomonas* polysaccharides and their oversulfated derivatives. Mar Biotechnol 1:68–73

Mauray S, Sternberg C, Theveniaux J, Millet J, Sinquin C, Taponbretaudiere J, Fischer AM (1995) Venous antithrombotic and anticoagulant activities of a fucoidan fraction. Thromb Haemost 74:1280–1285

Mayer AMS, Rodriguez AD, Berlinck RGS, Fusetani N (2011) Marine pharmacology in 2007–2008: marine compounds with antibacterial, anticoagulant, antifungal, anti-inflammatory, antimalarial, antiprotozoal, antituberculosis, and antiviral activities; affecting the immune and nervous system, and other miscellaneous mechanisms of action. Comp Biochem Physiol C Toxicol Pharmacol 153:191–222

Millet J, Jouault SC, Mauray S, Theveniaux J, Sternberg C, Boisson Vidal C, Fischer AM (1999) Antithrombotic and anticoagulant activities of a low molecular weight fucoidan by the subcutaneous route. J Thromb Haemost 81:391–395

Mishima T, Murata J, Toyoshima M, Fujii H, Nakajima M, Hayashi T, Kato T, Saiki I (1998) Inhibition of tumor invasion and metastasis by calcium spirulan (Ca-SP), a novel sulfated polysaccharide derived from a blue-green alga, *Spirulina platensis*. Clin Exp Metastasis 16:541–550

Miura Y, Fukuda T, Seto H, Hoshino Y (2016) Development of glycosaminoglycan mimetics using glycopolymers. Polym J 48:229–237

Mori N, Nakasone K, Tomimori K, Ishikawa C (2012) Beneficial effects of fucoidan in patients with chronic hepatitis C virus infection. World J Gastroenterol 18:2225–2230

Moshaverinia A, Xu XT, Chen C, Akiyama K, Snead ML, Shi ST (2013) Dental mesenchymal stem cells encapsulated in an alginate hydrogel co-delivery microencapsulation system for cartilage regeneration. Acta Biomater 9:9343–9350

Moussavou G, Kwak DH, Obiang-Obonou BW, Maranguy CAO, Dinzouna-Boutamba SD, Lee DH, Pissibanganga OGM, Ko K, Seo JI, Choo YK (2014) Anticancer effects of different seaweeds on human colon and breast cancers. Mar Drugs 12:4898–4911

Murano E, Perin D, Khan R, Bergamin M (2011) Hyaluronan: from biomimetic to industrial business strategy. Nat Prod Commun 6:555–572

Muzzarelli RAA, Greco F, Busilacchi A, Sollazzo V, Gigante A (2012) Chitosan, hyaluronan and chondroitin sulfate in tissue engineering for cartilage regeneration: a review. Carbohydr Polym 89:723–739

Naderi-Meshkin H, Andreas K, Matin MM, Sittinger M, Bidkhori HR, Ahmadiankia N, Bahrami AR, Ringe J (2014) Chitosan-based injectable hydrogel as a promising in situ forming scaffold for cartilage tissue engineering. Cell Biol Int 38:72–84

Nakano K, Kim D, Jiang ZD, Ueno M, Okimura T, Yamaguchi K, Oda T (2012) Immunostimulatory activities of the sulfated polysaccharide ascophyllan from *Ascophyllum nodosum* in *in vivo* and *in vitro* systems. Biosci Biotechnol Biochem 76:1573–1576

Nandini CD, Itoh N, Sugahara K (2005) Novel 70-kDa chondroitin Sulfate/Dermatan sulfate hybrid chains with a unique heterogenous sulfation pattern from shark skin, which exhibit neuritogenic activity and binding activities for growth factors and neurotrophic factors. J Biol Chem 280:4058–4069

Nardella A, Chaubet F, Boisson Vidal C, Blondin C, Durand P, Jozefonvicz J (1996) Anticoagulant low molecular weight fucans produced by radical process and ion exchange chromatography of high molecular weight fucans extracted from the brown seaweed *Ascophyllum nodosum*. Carbohydr Res 289:201–208

Nicolaus B, Kambourova M, Oner ET (2010) Exopolysaccharides from extremophiles: from fundamentals to biotechnology. Environ Technol 31:1145–1158

Nishino T, Nagumo T (1992) Anticoagulant and antithrombin activities of oversulfated fucans. Carbohydr Res 229:355–362

Nishino T, Aizu Y, Nagumo T (1991) The influence of sulfate content and molecular weight of a fucan sulfate from the brown seaweed *Ecklonia kurome* on its antithrombin activity. Thromb Res 64:723–731

Okami Y (1986) Marine microorganisms as a source of bioactive agents. Microb Ecol 12:65–78

Oreste P, Zoppetti G (2012) Semi-synthetic heparinoids. Handb Exp Pharmacol 207:403–422

Park H, Kang SW, Kim BS, Mooney DJ, Lee KY (2009) Shear-reversibly crosslinked alginate hydrogels for tissue engineering. Macromol Biosci 9:895–901

Pavao MSG (2014) Glycosaminoglycans analogs from marine invertebrates: structure, biological effects, and potential as new therapeutics. Front Cell Infect Microbiol 4:123. https://doi.org/10.3389/fcimb.2014.00123

Petit AC, Noiret N, Guezennec J, Gondrexon N, Colliec-Jouault S (2007) Ultrasonic depolymerization of an exopolysaccharide produced by a bacterium isolated from a deep-sea hydrothermal vent polychaete annelid. Ultrason Sonochem 14:107–112

Pomin VH (2015) Marine non-glycosaminoglycan sulfated glycans as potential pharmaceuticals. Pharmaceuticals (Basel) 8:848–864

Praillet C, Grimaud JA, Lortat-Jacob H (1998a) Proteoglycans as therapeutic agents (I). M S-Med Sci 14:412–420

Praillet C, Lortat-Jacob H, Grimaud JA (1998b) Proteoglycans and pathology (ll). M S-Med Sci 14:421–428

Puvaneswary S, Raghavendran HB, Talebian S, Murali MR, Mahmod SA, Singh S, Kamarul T (2016) Incorporation of Fucoidan in β-Tricalcium phosphate-Chitosan scaffold prompts the differentiation of human bone marrow stromal cells into osteogenic lineage. Sci Rep-UK 6:24202. https://doi.org/10.1038/srep24202

Qi HM, Zhang QB, Zhao TT, Hu RG, Zhang K, Li Z (2006) *In vitro* antioxidant activity of acetylated and benzoylated derivatives of polysaccharide extracted from *Ulva pertusa* (Chlorophyta). Bioorg Med Chem Lett 16:2441–2445

Raja R, Hemaiswarya S, Kumar NA, Sridhar S, Rengasamy R (2008) A perspective on the biotechnological potential of microalgae. Crit Rev Microbiol 34:77–88

Ramirez F, Rifkin DB (2003) Cell signaling events: a view from the matrix. Matrix Biol 22:101–107

Raposo MFD, de Morais R, de Morais A (2013) Bioactivity and applications of sulphated polysaccharides from marine microalgae. Mar Drugs 11:233–252

Rechter S, Konig T, Auerochs S, Thulke S, Walter H, Dornenburg H, Walter C, Marschall M (2006) Antiviral activity of Arthrospira-derived spirulan-like substances. Antivir Res 72:197–206

Rederstorff E, Rethore G, Weiss P, Sourice S, Beck-Cormier S, Mathieu E, Maillasson M, Jacques Y, Colliec-Jouault S, Fellah BH, Guicheux J, Vinatier C (2017) Enriching a cellulose hydrogel with a biologically active marine exopolysaccharide for cell-based cartilage engineering. J Tissue Eng Regen Med 11:1152–1164

Re'em T, Tsur-Gang O, Cohen S (2010) The effect of immobilized RGD peptide in macroporous alginate scaffolds on TGF beta 1-induced chondrogenesis of human mesenchymal stem cells. Biomaterials 31:6746–6755

Re'em T, Kaminer-Israeli Y, Ruvinov E, Cohen S (2012) Chondrogenesis of hMSC in affinity-bound TGF-beta scaffolds. Biomaterials 33:751–761

Rehm BHA (2010) Bacterial polymers: biosynthesis, modifications and applications. Nat Rev Microbiol 8:578–592

Rioux LE, Turgeon SL, Beaulieu M (2009) Effect of season on the composition of bioactive polysaccharides from the brown seaweed *Saccharina longicruris*. Phytochemistry 70:1069–1075

Roger O, Kervarec N, Ratiskol J, Colliec-Jouault S, Chevolot L (2004) Structural studies of the main exopolysaccharide produced by the deep-sea bacterium *Alteromonas infernus*. Carbohydr Res 339:2371–2380

Rougeaux H, Kervarec N, Pichon R, Guezennec J (1999) Structure of the exopolysaccharide of *Vibrio diabolicus* isolated from a deep-sea hydrothermal vent. Carbohydr Res 322:40–45

Rowley JA, Madlambayan G, Mooney DJ (1999) Alginate hydrogels as synthetic extracellular matrix materials. Biomaterials 20:45–53

Ruiz Velasco C, Baud'huin M, Sinquin C, Maillasson M, Heymann D, Colliec-Jouault S, Padrines M (2011) Effects of a sulfated exopolysaccharide produced by *Altermonas infernus* on bone biology. Glycobiology 21:781–795

Ruoslahti E, Yamaguchi Y (1991) Proteoglycans as modulators of growth factors activities. Cell 64:867–869

Sabourel P, Chaubet F, Rouzet F, Al-Shoukr F, Ben Azzouna R, Bouchemal N, Picton L, Louedec L, Maire M, Rolland L, Potier G, Le Guludec D, Letourneur D, Chauvierre C (2014) Purification of a low molecular weight fucoidan for SPECT molecular imaging of myocardial infarction. Mar Drugs 12:4851–4867

Sadovskaya I, Souissi A, Souissi S, Grard T, Lencel P, Greene CM, Duin S, Dmitrenok PS, Chizhov AO, Shashkov AS, Usov AI (2014) Chemical structure and biological activity of a highly branched (1 -> 3,1 -> 6)-beta-D-glucan from *Isochrysis galbana*. Carbohydr Polym 111:139–148

Schaeffer DJ, Krylov VS (2000) Anti-HIV activity of extracts and compounds from algae and cyanobacteria. Ecotoxicol Environ Saf 45:208–227

Schmid J, Sieber V, Rehm B (2015) Bacterial exopolysaccharides: biosynthesis pathways and engineering strategies. Front Microbiol 6:496. https://doi.org/10.3389/fmicb.2015.00496

Schnabelrauch M, Scharnweber D, Schiller J (2013) Sulfated glycosaminoglycans as promising artificial extracellular matrix components to improve the regeneration of tissues. Curr Med Chem 20:2501–2523

Senni K, Pereira J, Gueniche F, Delbarre-Ladrat C, Sinquin C, Ratiskol J, Godeau G, Fischer A-M, Helley D, Colliec-Jouault S (2011) Marine polysaccharides: a source of bioactive molecules for cell therapy and tissue engineering. Mar Drugs 9:1664–1681

Senni K, Gueniche F, Changotade S, Septier D, Sinquin C, Ratiskol J, Lutomski D, Godeau G, Guezennec J, Colliec-Jouault S (2013) Unusual glycosaminoglycans from a deep sea hydrothermal bacterium improve fibrillar collagen structuring and fibroblast activities in engineered connective tissues. Mar Drugs 11:1351–1369

Seol YJ, Lee JY, Park YJ, Lee YM, Young K, Rhyu IC, Lee SJ, Han SB, Chung CP (2004) Chitosan sponges as tissue engineering scaffolds for bone formation. Biotechnol Lett 26:1037–1041

Shanmugam M, Mody KH (2000) Heparinoid-active sulphated polysaccharides from marine algae as potential blood anticoagulant agents. Curr Sci 79:1672–1683

Sheng J, Yu F, Xin Z, Zhao L, Zhu X, Hu Q (2007) Preparation, identification and their antitumor activities in vitro of polysaccharides from *Chlorella pyrenoidosa*. Food Chem 105:533–539

Shin S, Park JY, Lee JY, Park H, Park YD, Lee KB, Whang CM, Lee SH (2007) "On the fly" continuous generation of alginate fibers using a microfluidic device. Langmuir 23:9104–9108

Siddhanta AK, Shanmugam M, Mody KH, Goswami AM, Ramavat BK (1999) Sulphated polysaccharides of Codium dwarkense Boergs. from the west coast of India: chemical composition and blood anticoagulant activity. Int J Biol Macromol 26:151–154

Smit A (2004) Medicinal and pharmaceutical uses of seaweed natural products: a review. J Appl Phycol 16:245–262

Sogawa K, Yamada T, Sumida T, Hamakawa H, Kuwabara H, Matsuda M, Muramatsu Y, Kose H, Matsumoto K, Sasaki Y, Okutani K, Kondo K, Monden Y (2000) Induction of apoptosis and inhibition of DNA topoisomerase-I in K-562 cells by a marine microalgal polysaccharide. Life Sci 66:PL227–PL231

Sun JC, Tan HP (2013) Alginate-based biomaterials for regenerative medicine applications. Materials 6:1285–1309

Sun L, Wang L, Zhou Y (2012) Immunomodulation and antitumor activities of different-molecular-weight polysaccharides from *Porphyridium cruentum*. Carbohydr Polym 87:1206–1210

Sun LQ, Chu JL, Sun ZL, Chen LH (2016) Physicochemical properties, immunomodulation and antitumor activities of polysaccharide from *Pavlova viridis*. Life Sci 144:156–161

Tseng CK (2001) Algal biotechnology industries and research activities in China. J Appl Phycol 13:375–380

Ueno M, Cho K, Isaka S, Nishiguchi T, Yamaguchi K, Kim D, Oda T (2018) Inhibitory effect of sulphated polysaccharide porphyran (isolated from *Porphyra yezoensis*) on RANKL-induced differentiation of RAW264.7 cells into osteoclasts. Phytother Res 32:452–458

Ustyuzhanina NE, Bilan MI, Ushakova NA, Usov AI, Kiselevskiy MV, Nifantiev NE (2014) Fucoidans: pro- or antiangiogenic agents? Glycobiology 24:1265–1274

Vo T-S, Kim S-K (2010) Potential anti-HIV agents from marine resources: an overview. Mar Drugs 8:2871–2892

Wang J, Chen B, Rao X, Huang J, Li M (2007) Optimization of culturing conditions of *Porphyridium cruentum* using uniform design. World J Microbiol Biotechnol 23:1345–1350

Wang W, Wang S-X, Guan H-S (2012) The antiviral activities and mechanisms of marine polysaccharides: an overview. Mar Drugs 10:2795–2816

Wijesinghe W, Jeon YJ (2012) Biological activities and potential industrial applications of fucose rich sulfated polysaccharides and fucoidans isolated from brown seaweeds: a review. Carbohydr Polym 88:13–20

Yamada T, Ogamo A, Saito T, Watanabe J, Uchiyama H, Nakagawa Y (1997) Preparation and anti-HIV activity of low-molecular-weight carrageenans and their sulfated derivatives. Carbohydr Polym 32:51–55

Yang XB, Gao XD, Han F, Tan RX (2005a) Sulfation of a polysaccharide produced by a marine filamentous fungus *Phoma herbarum* YS4108 alters its antioxidant properties in vitro. Biochim Biophys Acta Gen Subj 1725:120–127

Yang XB, Gao XD, Han F, Xu BS, Song YC, Tan RX (2005b) Purification, characterization and enzymatic degradation of YCP, a polysaccharide from marine filamentous fungus *Phoma herbarum* YS4108. Biochimie 87:747–754

Yang J-S, Xie Y-J, He W (2011) Research progress on chemical modification of alginate: a review. Carbohydr Polym 84:33–39

Yim JH, Kim SJ, Ahn SH, Lee CK, Rhie KT, Lee HK (2004) Antiviral effects of sulfated exopolysaccharide from the marine microalga *Gyrodinium impudicum* strain KG03. Mar Biotechnol 6:17–25

Yim JH, Son E, Pyo S, Lee HK (2005) Novel sulfated polysaccharide derived from red-tide microalga *Gyrodinium impudicum* strain KG03 with immunostimulating activity in vivo. Mar Biotechnol 7:331–338

Yu G, Guan H, Ioanoviciu AS, Sikkander SA, Thanawiroon C, Tobacman JK, Toida T, Linhardt RJ (2002) Structural studies on kappa-carrageenan derived oligosaccharides. Carbohydr Res 337:433–440

Zanchetta P, Lagarde N, Guezennec J (2003) A new bone-healing material: a hyaluronic acid-like bacterial exopolysaccharide. Calcif Tissue Int 72:74–79

Zhang ZS, Zhang QB, Wang J, Song HF, Zhang H, Niu XZ (2010) Regioselective syntheses of sulfated porphyrans from porphyra haitanensis and their antioxidant and anticoagulant activities *in vitro*. Carbohydr Polym 79:1124–1129

Zhang ZY, Teruya K, Eto H, Shirahata S (2013) Induction of apoptosis by low-molecular-weight fucoidan through calcium- and caspase-dependent mitochondrial pathways in MDA-MB-231 breast cancer cells. Biosci Biotechnol Biochem 77:235–242

Zhou G, Sun Y, Xin H, Zhang Y, Li Z, Xu Z (2004) *In vivo* antitumor and immunomodulation activities of different molecular weight lambda-carrageenans from *Chondrus ocellatus*. Pharmacol Res 50:47–53

Zuniga EA, Matsuhiro B, Mejias E (2006) Preparation of a low-molecular weight fraction by free radical depolymerization of the sulfated galactan from *Schizymenia binderi* (Gigartinales, Rhodophyta) and its anticoagulant activity. Carbohydr Polym 66:208–215

Zykwinska A, Marquis M, Sinquin C, Cuenot S, Colliec-Jouault S (2016) Assembly of HE800 exopolysaccharide produced by a deep-sea hydrothermal bacterium into microgels for protein delivery applications. Carbohydr Polym 142:213–221

Zykwinska A, Berre LT-L, Sinquin C, Ropartz D, Rogniaux H, Colliec-Jouault S, Delbarre-Ladrat C (2018) Enzymatic depolymerization of the GY785 exopolysaccharide produced by the deep-sea hydrothermal bacterium Alteromonas infernus: structural study and enzyme activity assessment. Carbohydr Polym 188:101–107

Chapter 16
Alginate: Pharmaceutical and Medical Applications

Patrícia Sofia Pinhanços Batista, Alcina Maria Miranda Bernardo de Morais, Maria Manuela Estevez Pintado, and Rui Manuel Santos Costa de Morais

Abstract Due to their outstanding properties in terms of mild gelation conditions and simple functionalization, biocompatibility, low toxicity, biodegradability, non-antigenicity and chelating ability, as well as relatively low cost, alginates have been widely used in a variety of biomedical applications including tissue engineering and drug delivery systems. Smart alginate hydrogels for on-demand drug release in response to environmental stimuli and 3D bioprinting will play an important role in the future. These and the introduction of appropriate cell interactive features will be crucial for many tissue engineering applications. The focus of the present chapter is to highlight the great potential of the alginates as biomaterial for biomedical applications and to discuss the role that alginate-based materials are likely to play in biomedical applications in the future.

16.1 Introduction

Alginate is a naturally occurring anionic and hydrophilic polysaccharide. It is one of the most abundant biosynthesized materials (Narayanan et al. 2012; Skjåk-Bræk et al. 1989a), and it is derived primarily from brown seaweed (Fucophyceae, previously Phaeophyceae), mainly *Laminaria* (*L. hyperborea, L. digitata, L. japonica*) and other species, such as *Ascophyllum nodosum* and *Macrocystis pyrifera* (Smidsrød and Skja 1990). Bacteria (*Pseudomonas aeruginosa, Azotobacter* sp.) are other sources of alginate. In this case, alginate is an exopolysaccharide (EPS) secreted by the bacteria into the surrounding environment by cell wall-anchored enzymes, and it is composed of sugar residues.

Alginate is the most common encapsulating agent and it is a linear polysaccharide consisting of 1 → 4 linked α-L-guluronic (**G**) and β-D-mannuronic (**M**) acids (Davis et al. 2003). Alginates from bacteria have a slightly different composition.

P. S. P. Batista · A. M. M. B. de Morais · M. M. E. Pintado · R. M. S. C. de Morais (✉)
Universidade Católica Portuguesa, Porto, Portugal
e-mail: rcmorais@porto.ucp.pt

E. Cohen, H. Merzendorfer (eds.), *Extracellular Sugar-Based Biopolymers Matrices*,
Biologically-Inspired Systems 12, https://doi.org/10.1007/978-3-030-12919-4_16

In general, alginates show high water absorption and may be used as low-viscosity emulsifiers and shear-thinning thickeners. They can be used to stabilize phase separation in low-fat products or as fat substitutes, for example, as alginate/caseinate blends in three-phase starch systems. The roles of alginates in health have been reviewed (Dettmar et al. 2011; Szekalska et al. 2016). Due to their outstanding properties in terms of biocompatibility, low toxicity, biodegradability, non-antigenicity, and chelating ability, as well as relatively low cost (Table 16.1), alginates have been widely used in a variety of biomedical applications, including tissue engineering, drug delivery and in some formulations, for prevention of gastric reflux, and medical surgical dressings (Buwalda et al. 2017; McSwain et al. 2005; Park et al. 2017; Sun and Tan 2013; Vijayabaskar et al. 2011; Zhang and Khademhosseini 2017).

Besides being a Food and Drug Administration (FDA)-approved polymer, alginate has become one of the most important biomaterials for diverse applications in

Table 16.1 Advantages and drawbacks of alginate hydrogels

Advantages	Drawbacks	Applications
Low toxicity		Oral or injectable in vivo delivery systems
Biocompatibility		Structural similarity to living tissues, allows wide range of biomedical applications (wound healing, scaffold, etc.)
Versatility		Deliver drugs and cells, scaffold for tissue formation, and control the structure and function of the engineered tissue
Hydrophilicity		Aqueous environment can protect cells and fragile drugs (peptides, proteins, oligonucleotides, DNA)
Porosity and stiffness		Micro- and nanostructure of the surfaces and stiffness of the gel are important signals (together with the chemicals signals) for cell polarization, differentiation, metabolism, and organization
		Porosity allows good transport of nutrients and bioactive to cells and products from cells
Functionalization		May be easily modified with cell adhesion ligands
Low cost and easy to manipulate		Available in large amounts
Degradable		Allow cell migration and growth while the matrix degenerates
	Can be hard to handle Not so adhesive Mechanically weak Syneresis and inhibition Reproducibility Difficult to sterilize	

Chirani et al. (2015) and Lee and Mooney (2012)

regenerative medicine (Balakrishnan and Jayakrishnan 2005; Bouhadir et al. 2001; Gåserød et al. 1998; Kong et al. 2004; Rowley et al. 1999). In fact, alginates may act as scaffold materials and as cell-supporting matrices in regenerative medicine, mainly due to their similarities with extracellular matrix (ECM) as well as their chemical versatility and biological performance.

16.2 Properties of Alginates

16.2.1 Chemical Structure

Alginates constitute a family of linear binary unbranched and not random copolymers, consisting of blocks with β-(1,4)-linked D-mannuronic acid (**M**) and α-(1,4)-linked L-guluronic acid (**G**) residues. These residues are epimers (D-mannuronic acid residues being enzymatically converted to L-guluronic after polymerization) and only differ at C-5. However, they possess very different conformations—D-mannuronic acid is $^4C_1$ with di-equatorial links between units, and L-guluronic acid is $^1C_4$ with diaxial links between units. Each block in the polymer is composed of consecutive G residues (e.g., GGGGGG), consecutive M residues (e.g., MMMMMM), or alternating M and G residues (e.g., GMGMGM) (Fig. 16.1a, b). Each block has different conformation preferences and behavior. The chemical composition and sequence of the different blocks may vary among algae species and even among different parts of the algae and the time of year when it is harvested. Alginates from different sources differ in M and G contents as well as in the length of each block, and more than 200 different alginates are currently on the market (Tønnesen and Karlsen 2002). The G-block content is 60% in *Laminaria hyperborea* stems, and, for other commercially available alginates, it is in the range of 14–31% (Qin 2008). Alginates from bacterial biosynthesis may present more defined chemical structures and physical properties than those obtained from seaweed-derived alginate. Bacterial alginates are O-acetylated on the second and/or third positions of the D-mannuronic acid residues. The bacterial O-acetylase may be used to O-acetylate also the algal alginates, increasing in this way their water binding.

16.2.2 Physicochemical Properties

The alginate bead matrix (porosity, swelling, mechanical and chemical stability) can, at least in part, be controlled by carefully choosing the alginates (selection, purification) and gel ions and handling gelling kinetics and interaction with other polymers (Draget and Taylor 2011).

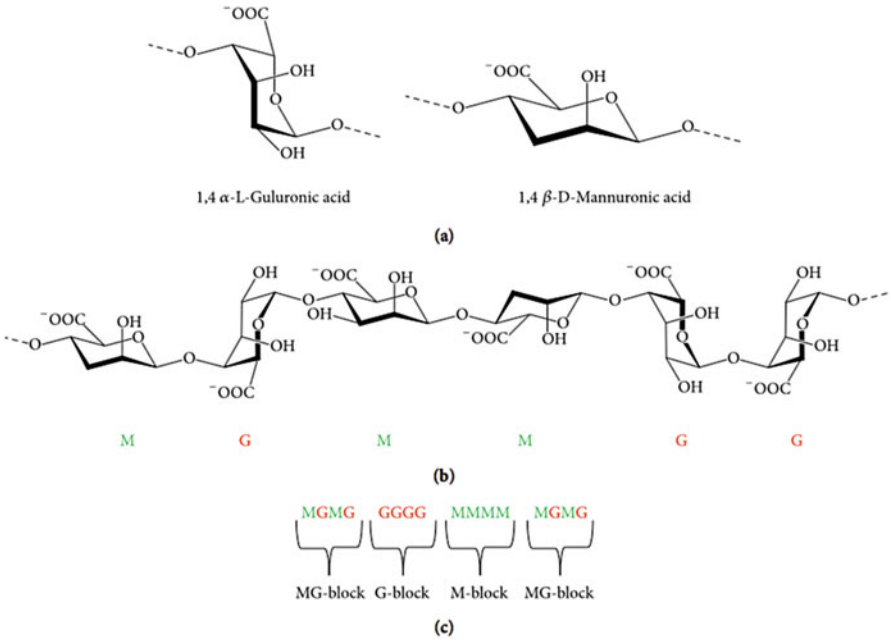

Fig. 16.1 Structural characteristics of alginates: (**a**) alginate monomers conformation, (**b**) chain blocks of β-D-mannuronate (M) and α-L-guluronate (G), (**c**) variation in composition and sequential arrangements. (Caption modified. Copyright © 2016 Szekalska et al. 2016)

16.2.2.1 Molecular Weight and Solubility

Commercially available sodium alginates have a molecular weight (MW) between 32,000 and 400,000 Da. For sodium alginate in 0.1 M NaCl solution at 25 °C, Mark-Houwink's parameters ($[\eta] = KMva$) are $K = 2 \times 10^{-3}$ and $a = 0.97$, where $[\eta]$ is intrinsic viscosity (mL/g) and Mv is the viscosity-average molecular weight (g/mol) (Rinaudo 1992). The viscosity of alginate solutions increases as pH decreases and reaches a maximum around pH = 3–3.5, as carboxylate groups in the alginate backbone become protonated and form hydrogen bonds.

The manipulation of the MW and its distribution can independently control the pre-gel solution viscosity and post-gelling stiffness. The elastic modulus of gels can be increased significantly, while the viscosity of the solution minimally rises when a combination of high and low MW alginate polymers is used (Kong et al. 2002; Lee and Mooney 2012). The increase of alginate MW can improve the physical properties of the resultant gels. However, an alginate solution with high MW polymer becomes highly viscous, which is often undesirable during processing (LeRoux et al. 1999). For example, proteins or cells mixed with an alginate solution of high viscosity risk damage due to the high shear forces developed during mixing and injection into the body (Kong et al. 2003).

The solubility of alginate and water-holding capacity depend on the pH (it precipitates below ca. pH 3.5), MW (low MW calcium alginate chains with less than 500 residues presenting increasing water binding with increasing size), ionic strength, and nature of the ions present and alginate concentration (Costa et al. 2018; Kopeček 2002).

16.2.2.2 Gelling Capacity

Alginate hydrogels have been particularly attractive in wound healing, drug delivery, and tissue engineering applications, as these gels are able to present structures similar to the extracellular matrix (ECM) in tissues, and can be manipulated to play different roles (Lee and Mooney 2012). Alginates are capable of forming hydrogels that swell but do not dissolve, at least not immediately, in water (Kopeček 2002). The term hydrogel was originally used by Wichterle and Lim (Wichterle and Lim 1960). This class of materials present a high thermodynamic affinity for the solvent, revealing swelling properties (Chirani et al. 2015).

In fact, the most important feature of alginate is the selective binding of multivalent cations, which is the basis of gel formation. The sol/gel transition of alginates is not particularly influenced by temperature (Draget and Taylor 2011). Hydrogels may be chemically stable, or they may degrade and, eventually, disintegrate and dissolve. In the latter case, they are called "reversible" or "physical" gels because the networks are held by weak molecular interactions through secondary forces (Chirani et al. 2015).

Hydrogels are unique polymeric matrices, consisting of a self-supporting, water-swollen three-dimensional viscoelastic network, which allows the diffusion and attachment of molecules and cells. The two main disadvantages of natural hydrogels in relation to synthetic polymers are the difficulty to control and reproduce the microstructure and properties and the possibility of a variable composition from batch to batch (Chirani et al. 2015). This is specifically critical in the case of the algae, due to the location in the polymer from where it is obtained, as mentioned above, and also because of a higher difficulty in controlling the culture growth.

Alginate hydrogels can be prepared by various cross-linking methods, and their structural similarity to ECM of living tissues makes them suitable for several applications, namely, in wound healing; delivery of bioactive agents, such as small chemical drugs and proteins; and cell transplantation (Lee and Mooney 2012). In addition, alginate can form two types of hydrogel, an acid gel, depending on pH, and an ionotropic gel, which gives the polymer unique properties compared to neutral macromolecules. These gels can, therefore, be tailor-made in order to allow desirable applications (Tønnesen and Karlsen 2002).

Alginates rapidly form heat-stable gels at low temperature. In fact, their primary function is as thermally stable cold-setting gelling agents in the presence of specific ions. Gelling depends on the ion binding ($Mg^{2+} \ll Ca^{2+} < Sr^{2+} < Ba^{2+}$) (Huynh et al. 2016), the control of the method of addition being important for the production of homogeneous gels (e.g., by ionic diffusion or controlled acidification of $CaCO_3$).

These gels can be heat-treated without melting, although they may eventually degrade. Only the G-blocks of alginate are believed to participate in intermolecular cross-linking with divalent cations (e.g., Ca^{2+}) to form hydrogels. Besides MW already mentioned above, the composition (i.e., M/G ratio; see Fig 16.1c), sequence, and G-block length are critical factors affecting the physical properties of alginates and, consequently, its resultant hydrogels (George and Abraham 2006). A high G content produces strong brittle gels thermally stable (except if present in low MW alginates). However, they may present water seepage (syneresis) in freezing-thawing processes. Some chelation of multivalent cations takes place as a result of structural features in the G-blocks, with the so-called "egg-box" model (Grant et al. 1973). While a high M content produces weaker and more elastic gels with a good freezing-thawing behavior, high MGMG content zips with Ca^{2+} ions to reduce shear (Donati et al. 2005). However, at low or very high Ca^{2+} concentrations, high M content alginates produce the strongest gels. So, when the average chain is not particularly short, the gelling properties correlate with the average G-block length (optimum block size ~12, with similarity with pectin gelling) and not necessarily with the M/G ratio, which may be primarily due to alternating MGMG chains.

Physical properties significantly control the stability of the gels, the rate of drug release from gels, and the phenotype and function of cells encapsulated in alginate gels. Different alginate sources provide polymers with a range of chemical structures and properties, e.g., bacterial alginate produced from *Azotobacter* has a high content of G-blocks, and its gels present a relatively high stiffness (Hay et al. 2010).

Progress in the regulation of alginate biosynthesis in bacteria and in modifying bacteria will allow the production of alginate with suitable characteristics, which enable several applications in biomedical area.

The future prospects are excellent as recombinant epimerases with different specificities may be used to produce novel alginates (Tøndervik et al. 2013).

16.2.2.3 Conventional Methods of Gelation

Lee and Mooney (2012) produced a comprehensive review of the alginate gelling techniques. Some chemical and physical methods have been reported to form alginate gels namely (Lee and Mooney 2012):

16.2.2.3.1 Ionic Cross-Linking

The most common method to prepare hydrogels from an aqueous alginate solution consists of mixing the solution with ionic cross-linking agents, such as divalent cations (e.g., Ca^{2+}). These cations are believed to bind solely to guluronate blocks (G-blocks) of the alginate chains, as the structure of the guluronate blocks allows a high degree of coordination of the divalent ions. Junctions are formed among the guluronate blocks of two adjacent polymer chains, resulting in a gel structure according to the so called egg-box model of cross-linking (Grant et al. 1973). A controlled introduction of cross-

linking ions is possible by two methods of preparation of an alginate gel: the "diffusion" method and the "internal setting" one (Smidsrød and Draget 1997). In the first method, the cross-linking ions diffuse into the alginate solution from an outside reservoir leading to an ion gradient across the thickness of the gel. A direct mixing of alginate and multivalent cations rarely produces homogeneous gels due to the quick and irreversible binding of such ions. By the internal setting method, the ion source is located in the alginate solution, and the cross-link is set off by a trigger (usually pH or ion solubility). This method produces a more uniform ion concentration throughout the gel matrix (Skjåk-Bræk et al. 1989a).

16.2.2.3.2 Covalent Cross-Linking

Covalent cross-linking has been widely investigated in an effort to improve the physical properties of gels for many applications, including tissue engineering. However, some covalent cross-linking reagents may be toxic, and the excess used need to be removed. One of the first methods to be investigated was the covalent cross-linking of alginate with poly(ethylene glycol)-diamines of various molecular weights (Eiselt et al. 1999). More recently, other techniques have been developed, such as oxidation or photocross-linking methods for the preparation of hydrogels for tissue engineering applications (Balakrishnan and Jayakrishnan 2005; Dahlmann et al. 2013; Jeon et al. 2009). However, while allowing the preparation of hydrogels with tailored-made properties, most of these methods use toxic compounds, which may compromise the biocompatibility of the materials produced. Thus, the use of less hazardous chemical strategies seems essential in biomaterials design (García-Astrain and Avérous 2018).

16.2.2.3.3 Thermal Gelation

Thermosensitive gels undergo a reversible phase transition near body temperature in aqueous media. The transition temperature can be modulated by copolymerization with monomers, such as acrylic acid and acrylamide (Rzaev et al. 2007). This type of hydrogels has been investigated as drug delivery systems due to their adjustable swelling properties in response to temperature changes (Roy et al. 2010). Despite the potential of thermosensitive hydrogels in biomedical applications, there are a few systems using alginates, due to the fact that these are not naturally thermosensitive polymers. However, there are some thermosensitive hydrogels involving alginates, such as the semi-interpenetrating polymer network semi-IPN (Zhao et al. 2010b) and the graft copolymerization of N-isopropylacrylamide (NIPAAm) onto the alginate backbone (Lee and Mooney 2012). Shao et al. (2018) reported a novel dual responsive polysaccharide-based aerogel with thermo- and pH-sensitive properties as a drug-controlled release system. In this case, alginate was grafted successfully with *N*-isopropylacryamide (NIPAM) and *N*-(hydroxymethyl)acrylamide (NHMAM), in order to obtain a new responsive copolymer, alginate-g-P(NIPAM-co-NHMAM) (Shao et al. 2018).

16.2.2.3.4 Cell Cross-Linking

Alginates modified with cell adhesion ligands may form a gel due to the ability of cells to bind to multiple polymer chains, forming a reversible network even in the absence of chemical cross-linking agents. This system generates the cross-linked network structure via specific-ligand interactions. In contrast, cells added to non-modified alginate solutions aggregate and form a nonuniform matrix, due to the dominance of cell-to-cell interaction in the so formed system (Lee et al. 2003).

16.2.2.4 Nonconventional Methods of Gelation

Recently, a critical review was performed on advances in nonconventional gelation methods of native alginates and also in the subsequent drying step, specially focusing three methods: cryotropic gelation (or cryogelation), non-solvent-induced phase separation, and carbon dioxide-induced gelation (Gurikov and Smirnova 2018). These new techniques are being evaluated at both molecular and engineering levels, and it is foreseen that these techniques will be powerful additions and alternatives to the existing methods in materials science.

16.2.3 Biological Properties

Alginate is a Food and Drug Administration (FDA)-approved natural polymer; it is widely used in food, biomedical, and pharmaceutical applications because of its biological properties (Patel et al. 2017). Alginate is considered low or nontoxic, non-immunogenic, biocompatible, and biodegradable (Abdellatif et al. 2016; Cardoso et al. 2016; Dalheim et al. 2016; Patel et al. 2017; Petchsomrit et al. 2017; Sumayya and Muraleedhara Kurup 2017; Szekalska et al. 2016).

16.2.3.1 Biocompatibility

Various alginate salts (calcium, sodium, ammonium, potassium) and propylene glycol alginate derivative were generally recognized as safe (GRAS) ingredients, for oral administration by the FDA (FDA 2016; George and Abraham 2006). Although there has been a polemic in the past over the alginate biocompatibility (Orive et al. 2006), today, several studies are confirmed in vitro with different cells (Kumar et al. 2017; Lee and Mooney 2012; Orive et al. 2005; Venkatesan et al. 2015) and in vivo after ocular (Lin et al. 2004), nasal (Sarei et al. 2013), topical (Coşkun et al. 2014), local (Chang et al. 2012), and oral administration (Sosnik 2014).

The alginate composition, the amount of alginic acid content, and purity determine the biocompatibility of the alginate (Shilpa et al. 2003). Sometimes, bioactive molecules, such as proteins, have been associated with a reduced biocompatibility of the alginate (Agüero et al. 2017; Orive et al. 2006). Therefore, for implantation purposes, it is important to validate and monitor the purification process and to remove all its contaminants, allowing a very-high-purity alginate for biomedical applications (Agüero et al. 2017).

16.2.3.2 Toxicity

Alginate is considered low or nontoxic (Abdellatif et al. 2016; Patel et al. 2017; Petchsomrit et al. 2017; Shilpa et al. 2003; Szekalska et al. 2016). In studies where the alginate was administrated by the intravenous route, the low-molecular-weight fraction appeared in the urine, and the larger polymer fraction stayed in the circulation (not accumulating in any tissues) (Liberski 2016). It should be remarked that the renal clearance threshold only allows the excretion of small alginate molecules. In order to completely eliminate alginate molecules from the body, partial oxidation of the polymer backbone is required (Lee and Mooney 2012; Szekalska et al. 2016). Due to the alginate chelating capacity, the polymer is able to bind toxins and heavy metals in the gut, thus, protecting cells from the carcinogenesis process (Maciel et al. 2013; Szekalska et al. 2016).

16.2.3.3 Immunogenicity

Alginate immunogenicity is affected by a number of variables, such as the chemical composition (particularly the guluronic/mannuronic ratio), the purification process, the nature and quantity of residual contaminants, and their respective impact (Ménard et al. 2010; Shilpa et al. 2003). For example, studies showed that mannuronate-rich fragments leached out of the alginate biomaterials and lead to an immune response (Draget and Taylor 2011). Otterlei et al. reported that alginate with high G-block content is much less potent in inducing cytokine production in comparison with alginate with high M-block content (Otterlei et al. 1991). Moreover, a potentially immunogenic response could be related to several impurities in alginates, such as bioactive molecules and heavy metals (Ménard et al. 2010; Szekalska et al. 2016). Therefore, it is important that the decontamination processes should be applied during the extraction, in order to remove all of the potentially immunogenic contaminants and purify the alginate (Szekalska et al. 2016). Some studies support the opinion that hydrophilicity is indeed important for minimizing biomaterial immunogenicity (Orive et al. 2006; Tam et al. 2011). Even so, only the results of in vivo implantations can supply correct knowledge about the immunogenicity of alginates (Orive et al. 2006).

16.2.3.4 Antioxidant and Anti-inflammatory

Several authors (Falkeborg et al. 2014; Maciel et al. 2013; Szekalska et al. 2016; Zhou et al. 2015) reported that alginates have excellent antioxidant, anti-inflammatory, and potential prebiotic activities. The antioxidant activity might be explained because some alginate oligosaccharides reduce the production of reactive oxygen species.

Alginate showed a beneficial effect on promoting the growth of *Bifidobacterium* sp. with simultaneous inhibition of *Salmonella enteritidis* colonization in the large intestine, demonstrating its effect as a prebiotic agent (Chaluvadi et al. 2012). In addition, the immune stimulatory activity of alginates through the ability to upregulate the production of anti-inflammatory factors could be attributed to the balance of commensal bacteria (Szekalska et al. 2016; Xu et al. 2014). The anti-inflammatory property has been proven in several studies. For example, alginate-based dressings are attractive for their capability to release bioactive compounds and to maintain a moist environment around the wound, promoting tissue granulation and new epithelialization, because of the release of Ca^{2+} ions from the dressing to the wound site stimulates the production of pro-inflammatory cytokines, such as interleukin-6 (IL-6), interleukin-1β (IL-1β), tumor necrosis factor-α (TNF-α), and the chemotactic cytokine IL-8 (Hajiali et al. 2016). In another study, microspheres with sulfated alginates were found to attenuate the inflammatory response, by lowering the expression of several inflammatory cytokines. Human chondrocytes were encapsulated in alginate gels, prior to inflammatory induction with IL-1, and the chondrocytes demonstrated lowered expression of inflammatory and catabolic markers (Arlov and Skjåk-Bræk 2017).

16.2.3.5 Antibacterial

Different studies emphasize the use of alginate derivatives as antibacterial, antiviral, and antifungal agents (Lee et al. 2011; Szekalska et al. 2016; Xu et al. 2014). Some authors justify the alginate antimicrobial activity based on the negatively charged alginate interact with the outer bacterial cellular surface, leading to its disruption and leakage of intracellular substances (Benavides et al. 2012; Yan et al. 2011); or the alginate chelation capacity could be responsible for modulating the production of toxins, microbial growth, and factors crucial for microorganism stability, providing the antibacterial efficacy. Bacteriostatic activity of alginate was proved against a wide variety of species, including *Pseudomonas*, *Escherichia*, *Proteus*, and *Acinetobacter* (Szekalska et al. 2016).

16.2.3.6 Bioadhesion

Alginate is classified as a good mucoadhesive agent, important in delivery systems, because it helps in prolonged adhesion of the drug, increases the drug residence time

at the site of activity or resorption, and increases the efficiency and the bioavailability of drugs to mucosal tissues (Agüero et al. 2017; George and Abraham 2006; Shilpa et al. 2003; Szekalska et al. 2017).

The good mucoadhesive properties of alginate can be explained based on the presence of free carboxyl and hydroxyl groups and the electrostatic repulsive forces between alginate and mucin (Agüero et al. 2017). Studies have shown that an anionic polymer (alginate) with carboxyl end group and polymers with charge density can serve as good mucoadhesive agents because an increased charge density will give better adhesion (George and Abraham 2006). Some studies have expressed that alginate has the highest mucoadhesive strength as compared to polymers (such as polystyrene, chitosan, carboxymethylcellulose, and poly(lactic acid)), because polyanion polymers are more effective bioadhesives than polycation or nonionic polymers (George and Abraham 2006; Shilpa et al. 2003). This alginate bioadhesive property has a potential advantage in mucosal drug delivery (i.e., to the gastrointestinal tract and nasopharynx), protein transit time is delayed, and the drug is localized to the absorptive surfaces. So, alginate biomaterials improve drug bioavailability and effectiveness.

16.2.3.7 Biodegradability

Alginate is not degraded in mammals due to the lack of the alginase enzyme, which would be responsible for the cleavage of the polymer chains (Lee and Mooney 2012). Although due to exchange reactions with monovalent cations, alginate biomaterials with ionically cross-linked alginate can be dissolved by the release of the divalent ions cross-linking the gel into the surrounding media. However, the average molecular weights of many commercially available alginates are high, making it difficult for the kidneys to filter, and, therefore, they will not be completely removed from the body (Lee and Mooney 2012; Szekalska et al. 2016). So, an attractive approach to make alginate degradable include the partial oxidation of alginate chains in aqueous solution (Szekalska et al. 2016).

16.3 Functionalization of Alginates

Pawar and Edgar published a review on alginate derivatives (Pawar and Edgar 2012). Alginates are a very versatile family of polysaccharides, allowing the preparation of hydrogels in mild conditions (pH, temperature), which are suitable for sensitive biomolecules (proteins and nucleic acids). In addition to that, in recent years, the development of chemical and biochemical techniques that allow the creation of modified alginic acid derivatives, with specific properties (solubility, hydrophobicity, affinity for specific proteins, etc.), has taken place. Such properties are of special importance for biomedical applications.

The physical properties of alginate, including swelling, permeation, mechanical strength, and surface characteristics, can be modulated through the structure modification. The chemical modification of alginates may have two objectives: (i) to enhance existing properties (ionic strength, hydrophobicity, biodegradation) and (ii) to introduce completely new properties in native alginates (anticoagulant properties, chemical/biochemical anchors to interact with cell surfaces, modifying the temperature dependence). These modifications may also be used to produce "smart" hydrogels, which are able to change the gel structure in response to environmental *stimuli*.

In addition to the enhancement of cellular interactions, functionalization may also play a role in controlling the growth, differentiation, and behavior of cells in culture. As biomaterials, alginates offer several advantages including hydrophilicity, biocompatibility, and non-immunogenicity (Shapiro and Cohen 1997). The ability of alginates to form gels capable of encapsulating cells, drugs, and other biological compounds is another important advantage for biological applications. However, cells may not adhere to alginates naturally, and it is for that reason that Lee and Mooney (2012) described alginates as "blank slates." Chemical functionalization with cell signaling moieties becomes crucial in order to overcome the low affinity of alginates to cell surfaces.

16.3.1 Acetylation

Chamberlain et al. published the first chemical modification of alginates by acetylation of the hydroxyl groups of alginic acid with a mixture of benzene, acetic anhydride, and sulfuric acid catalyst (Chamberlain et al. 1946). Two years later, Wasserman reported the acetylation of alginic acid through a less aggressive procedure using the gaseous reagent ketene in order to avoid alginate degradation (Wassermann 1948). Later on, Schweiger (1962a) developed an acid-catalyzed esterification procedure that allows the synthesis of both partially and fully acetylated alginic acid derivatives, confirming that the availability of hydroxyl groups was essential for acetylation, according to what was reported by Chamberlain et al. (Chamberlain et al. 1946; Schweiger 1962a). These derivatives were useful as tools to comprehend the chelate structure of ionically cross-linked gels (Schweiger 1962b).

Skjåk-Bræk et al. reported the effects of the acetylation on alginate properties (Skjåk-Bræk et al. 1989b). They showed that during the gel acetylation, the polymer did not undergo a significant degradation. However, the addition of the acetyl group to the alginate backbone caused a noticeable extension at 0.11 M ionic strength. Alginates biosynthesized by bacteria are partially acetylated (Franklin et al. 2004; Franklin and Ohman 1993, 2002).

16.3.2 Phosphorylation

Coleman et al. introduced the synthesis of phosphorylated alginate derivatives for evaluating their ability to induce hydroxyapatite nucleation and growth (Coleman et al. 2011). The urea/phosphoric acid used leads to some molecular weight degradation, which, along with the conformational changes induced by the phosphorylation reaction, seems to be responsible for the inability of these derivatives to form gels. However, Ca-crosslinked gels resulting from the blend of phosphorylated with unreacted alginates presented higher resistance to calcium extraction. The regioselectivity of phosphorylation was studied by using a combination of NMR techniques.

16.3.3 Sulfation

It is known that most biological functions (among others, blood compatibility and anticoagulant activity, e.g., in heparin (Alban et al. 2002; Linhardt 2003)) are related to their sulfation pattern and sequence (Gama et al. 2006; Raposo et al. 2013; Rogers et al. 2011). Therefore, the introduction of sulfate groups into polysaccharides, both enzymatically and by chemical methods, is of great interest. The anticoagulant activity of alginate sulfate was found to be comparable to the one of heparin. Sulfation of alginates, first reported by Ronghua et al., may be beneficial in many cases (Ronghua et al. 2003). However, oversulfation is not desired, and it must be controlled as it can cause side effects (e.g., increase of the anticoagulation activity). Freeman et al. reported another method of alginate sulfation, by using carbodiimide coupling chemistry (Freeman et al. 2008). These authors studied the ability of alginate sulfates to provide protection of growth factors and to sustain their release. Fan et al. reported another sulfation method in an attempt to overcome the alginate degradation induced by the traditional sulfation agents (Fan et al. 2011). The placement of sulfate groups along the alginate backbone cannot yet be controlled (Pawar and Edgar 2012). This would be essential to understand and perhaps control structure-property relationships in alginate sulfates. Recently, the reasons and mechanism leading to the bleeding side effect of propylene glycol alginate sodium sulfate (PSS) were clarified (Xue et al. 2018).

Sulfated polysaccharides of marine origin became popular among the scientific community for several applications, as they are biocompatible and less cytotoxic and possess low immunogenicity. Significant research needs to be carried out to find out clinically relevant solutions and to be able to use these sulfated polysaccharide-based hydrogels as novel tissue engineering scaffolds in humans (Popa et al. 2015). Very recently, a US patent (Zenobi-Wong et al. 2018) was granted on the use of sulfated alginate hydrogels and their use in tissue engineering and regenerative medicine.

16.3.4 Hydrophobic Modification

Alginates are hydrophilic polysaccharides, due to the presence of hydroxyl groups. In addition, the carboxylate ion enhances water solubility at pH equal to or higher than 5. In order to extend the applications of alginate derivatives, the hydrophobic assembly of amphiphilic copolymers has drawn researchers' attention (Zhao et al. 2018). Hydrophobic modification of alginates turns the polysaccharide, with predominantly hydrophilic nature, into a molecule with amphiphilic or hydrophobic characteristics. The most straightforward way to achieve this transformation is by covalent attachment of hydrophobic moieties, such as long alkyl chains or aromatic groups to the polymer backbone (Yao et al. 2010). Hydrophobically modified alginate hydrogels have great potential in drug delivery, as they are biologically compatible and cost-efficient. Choudhary et al. investigated the impact of the cross-linker density and hydrophobic degree of replacement within modified alginate gels and solutions on the release kinetics using sulindac as a model hydrophobic drug (Choudhary et al. 2018).

16.3.5 Covalent Cross-Linking

Although physical alginate gels have a large number of applications in very diverse fields, such as biomedical, food, pharmaceutical, paper, and textile industries (Draget et al. 2005; Lee and Mooney 2012), they show limited long-term stability. Their mechanical strength is considerably reduced along time due to ion release from the matrix in physiological conditions (Lee and Mooney 2012; Sun and Tan 2013). To overcome these drawbacks and to enhance the stability of alginate networks, covalent cross-linking methods have been developed. Alginate, as most of the polysaccharides, can be easily modified via the hydroxyl and carboxyl groups available in their backbone structure (Yang et al. 2011).

16.3.6 Graft Copolymerization

Alginates are important biomaterials in the area of bioengineering (Augst et al. 2006). A critical requirement of such biomaterials is their ability to provide an environment that is both physically and chemically favorable to the presence of biological species, like living cells. In order to enhance the chemical interactions of alginate matrices with cells, they are functionalized with cell-specific ligands or extracellular signaling molecules.

Graft copolymerization allows the modification of the physical and chemical properties of alginates. Grafting synthetic polymers to the alginate backbone provides it with hydrophobicity and steric bulkiness, which help to protect it from rapid

dissolution and erosion. This polysaccharide backbone becomes a sustained release of active molecules from alginate matrices. Shah et al. reported the ceric ammonium nitrate (CAN)-induced grafting of poly(acrylonitrile) (PAN), poly(methyl acrylate) (PMA), or poly(methyl methacrylate) (PMMA) into alginates (Shah et al. 1995). Tripathy and coworkers also described the grafting of polyacrylamide (PAAm) into alginates using a ceric-induced system (Tripathy et al. 1999; Tripathy and Singh 2001). Mandal et al. reported the preparation of alginate-based sustained release interpenetrating polymer network (IPN) tablets (Mandal et al. 2010). IPNs are formed when one polymer is cross-linked in the presence of another one. Such networks impart additional rigidity to simple cross-linked polymer matrices.

16.4 Alginate Biomaterials

Alginate can be used as biomaterial due to its unique properties. This biopolymer is versatile and can be used in a wide range of forms, hydrogels, films, fibers, and beads and virtually in any shape and in a variety of sizes, for different applications (Fig. 16.2) (Abdellatif et al. 2016; Ching et al. 2017; da Silva et al. 2017; Dalheim et al. 2016; Petchsomrit et al. 2017; Sun and Tan 2013; Szekalska et al. 2016).

It can be easily modified and, by cross-link, copolymerize and blend with other polymers due to its polar side chain made of hydroxyl and carboxyl groups, and the combination of favorable properties of each constituent polymer results in a biomaterial with the properties that are often significantly improved or substantially different from those of the individual polymers (da Silva et al. 2017; Sumayya and Muraleedhara Kurup 2017). The alginate modifications (including the incorporation with other polymers) have been investigated to improve drug encapsulation, swelling, mucoadhesion, and drug release and can increase the applications of alginate in various fields such as tissue engineering, drug delivery, environment, and others (Ching et al. 2017; da Silva et al. 2017).

16.4.1 Particles

Alginate particles can be prepared easily through simple and economic procedures (da Silva et al. 2017; Sumayya and Muraleedhara Kurup 2017). There are different methods of producing alginate particles (macro-, micro-, and nano-sized), such as dripping/extrusion, coaxial laminar airflow, electrostatic potential, vibrating nozzle, jetcutting, spinning disk, spinning nozzle, spray nozzle, atomization, impinging, emulsification and microfluidics, and spray-dryer (Agüero et al. 2017; Bagheri et al. 2014; Ching et al. 2017; Gamboa et al. 2015; Guo et al. 2018; Hanga and Holdich 2014; Istenič et al. 2015; Kavoosi et al. 2018; Mori et al. 2014; Paques et al. 2014;

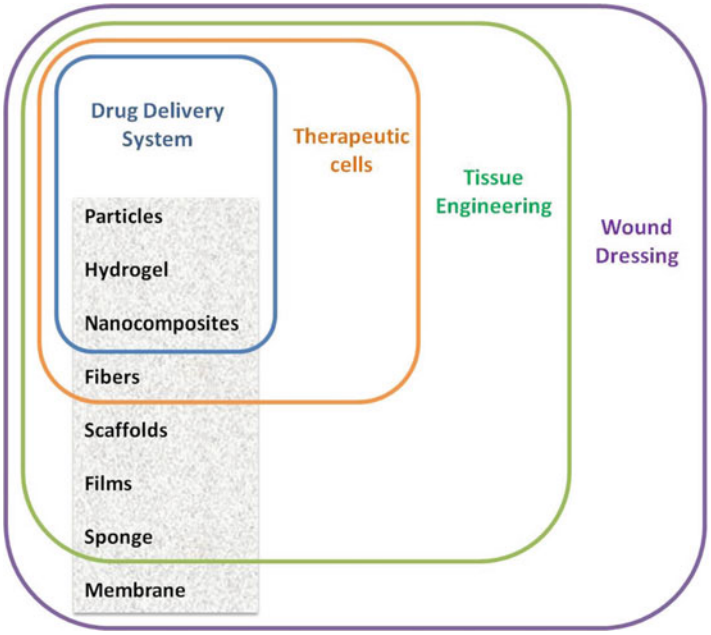

Fig. 16.2 Alginate-based materials and their applications in various fields

Sosnik 2014; Tzankova et al. 2017; Unagolla and Jayasuriya 2018). The processing method used will condition the particle size, which may vary between 2000 μm and 600 nm (Mazzitelli et al. 2011).

The alginate particle production is increasing for the targeted delivery and controlled release of bioactive molecules and drugs (Mazzitelli et al. 2011; Sosnik 2014). Alginate particles are already widely used in pharmaceutical, cosmetic, chemical, and food industries, but their use in the food industry is still comparatively limited (Ching et al. 2017). Alginate particles present advantages, such as slow and reproducible degradation rates, incorporation of hydrophilic and hydrophobic materials, effective protection of the drug/biomolecule against enzymatic degradation, and high oral bioavailability of encapsulated drugs (Mukhopadhyay et al. 2018). The bioavailability is an important property because it avoids the administration frequency, minimizing the adverse side effects and the preservation of cellular metabolism.

The alginate particles can be modified with other constituents (e.g., natural polysaccharide) to improve drug encapsulation, swelling, mucoadhesion, and drug release (da Silva et al. 2017; Mukhopadhyay et al. 2018; Sumayya and Muraleedhara Kurup 2017). For example, the chitosan and alginate combination is mostly used (Mukhopadhyay et al. 2018; Tzankova et al. 2017; Unagolla and Jayasuriya 2018), but other natural and synthetic polymers are used too (such as pectin, poly-L-lysine) (Guo et al. 2018).

16.4.2 Hydrogels

The alginates with gelling characteristics have the ability to form hydrogels (with water) in situ, and the gelling process can use non-toxic solvents and mild temperature and pH conditions (Abdelghany et al. 2017; Bidarra et al. 2014; Ching et al. 2017; Liberski 2016; Passemard et al. 2017). Hydrogels are water-insoluble, two- and three-dimensional (2D/3D) networks of cross-linked hydrophilic polymers, with a high degree of swelling in aqueous environments (that facilitate the transport of nutrients into and cellular wastes away from the hydrogels). Moreover, their biodegradability and nontoxicity and their 3D structure can provide space and mechanical stability for new tissue formation; they can be used to encapsulate drugs, growth factors, and cells to engineer tissues and develop promising hydrogel biomaterials for tissue engineering (Augst et al. 2006; Jeon et al. 2009; Joddar et al. 2016; Lewandowska-Łańcucka et al. 2017; Nieto-Suárez et al. 2016). The formation of alginate gels can be achieved by two methods: ionic cross-linking with cations (ionic gels) and acid precipitation (acidic gels) (Bidarra et al. 2014; Ching et al. 2017; Dalheim et al. 2016; Passemard et al. 2017; Patel et al. 2017).

To date, applications of particulate alginate gels can be used in pharmaceutical, biomedical, agriculture, and food encapsulation areas. They have been studied substantially in tissue engineering as biomaterials for skin, cartilage, bone, and cardiac tissue regeneration and as drug delivery systems (Bidarra et al. 2014).

Hydrogels have an important role in wound healing applications, because their mechanical and structural properties are similar to many tissues and the synthetic extracellular matrix (ECM), and can be delivered to the body in a minimally invasive process (Bidarra et al. 2014; Joddar et al. 2016; Lewandowska-Łańcucka et al. 2017). Sometimes, to enhance the mechanical, physical, and biological properties, the alginate hydrogels can be conjugated with other constituents (poly(vinyl alcohol) (PVA), gelatin, chitosan) (Balakrishnan et al. 2005; Bidarra et al. 2014; Duan et al. 2013; Nieto-Suárez et al. 2016). For example, there are PVA-ALG hydrogels developed for wound healing application, which give proper swelling and degradation ratio with enhanced mechanical properties and blood coagulation activity (Golafshan et al. 2017). Another interesting mixture is the gelatin and alginate, due to their chemical similarity to the ECM, their flexibility ensuring fast diffusion of hydrophilic nutrients and metabolites, as well as the low content of dry mass, which reduced irrigation and lowers the number of degradation products (Yan et al. 2005).These hydrogels can be applied to bone/cartilage regeneration, too (Lewandowska-Łańcucka et al. 2017).

16.4.2.1 Smart Hydrogels

Smart hydrogel systems with various chemical and structural compositions respond to external stimuli, such as temperature, pH, ionic concentration, light, and magnetic and electrical fields. Polymers with multiple-responsive properties have also been

developed with two or more stimuli-responsive mechanism combinations. Smart polymer hydrogels change their structural and volume phase transition as a response to external stimuli, presenting an enormous potential for scientific studies and advanced technological applications (Chirani et al. 2015; Dai et al. 2017; García-Astrain and Avérous 2018).

16.4.3 Beads

Alginate gel beads have been widely used for various encapsulation (bioactive molecules/drugs) applications due to their abundant availability, biocompatibility, and nontoxic properties. Alginate beads are similar to the ECM with particular characteristics of porosity and mechanical properties (Li et al. 2017). Alginate can be solidified easily with the presence of multivalent cations, and alginate gel beads can be formed using external or internal gelation (the resultant beads have different characteristics) or electrospraying (Al Dalaty et al. 2016; Amiri et al. 2017; Lee et al. 2018; Pankongadisak et al. 2015). Alginate gel beads are commonly formed by dripping sodium or potassium alginate solution into an aqueous solution of calcium ions typically using calcium chloride. These beads comprised a simple core structure, and it is being used with encapsulation method (Amiri et al. 2017; Chen et al. 2016; Focaroli et al. 2016; Jain and Bar-Shalom 2014; Lin et al. 2016; Ma et al. 2003). The cell encapsulation into hydrogel beads had shown a promise as a fabrication method for 3D tissue constructs (Al Dalaty et al. 2016; Jain and Bar-Shalom 2014; Li et al. 2017; Yu et al. 2015).

Alginate can be combined with other polymers to improve biomaterial properties. An example is the hybrid beads based on alginate and guar gum succinate, developed as pH-sensitive carriers for colon-targeted drug delivery. These beads may have an improved water-absorbing capacity, susceptibility to microbial degradation, and controlled drug release properties due to the presence of guar gum, as well as pH-sensitive character due to the presence of alginate (Seeli et al. 2016).

16.4.4 Films/Membranes

Films, membranes, or coatings with alginate show promise because this natural polysaccharide is not only mucoadhesive due to the formation of hydrogen bonds with mucin-type glycoproteins but also biocompatible and biodegradable (Kessler et al. 2016). Alginate films, with flexible and hydrophilic properties, have the potential to be used as wound dressings (Kaygusuz et al. 2017; Kessler et al. 2016). Many hydrogel films are prepared by chemical or physical cross-linking method to obtain the ideal hydrogel film properties (thickness, water-swollen polymer networks) (Wathoni et al. 2016). These hydrogel films can potentially be used in several biomedical applications, outstandingly in wound dressing application

(Wathoni et al. 2016). Also, alginates produce hydrogel membranes, whose characteristics (gel thickness, volume, mechanical resistance, and porosity) can be modified (Villani et al. 2008).

Blends of natural polymers, based on alginate and other polymers (gelatin, chitosan, carboxymethyl cellulose, pectin, collagen), were prepared in the form of films and characterized to test the possibility of using them as biomaterials (Gregurec et al. 2016; Kumar and Kumar 2017; Nešić et al. 2017; Rezvanian et al. 2017; Rosellini et al. 2009). These biocomposites are extensively found in nature and present structures with distinct mechanical properties and reinforcing properties comparatively to composites alone (de Moraes and Beppu 2013). The conjugation of chitosan and alginate offers advantages, forming a cross-linked polyelectrolyte complex (PEC) that increases physical properties and can be applied in several biomedical applications, such as wound dressings and pharmaceutical technology (Alsharabasy et al. 2016; Caetano et al. 2015; Meng et al. 2010; Wang et al. 2002). This biocomposite when compared with the isolated compounds improves some properties such as swelling and mechanical strength (Alsharabasy et al. 2016; Caetano et al. 2015; Shaari and Kamarudin 2015; Sibaja et al. 2015). So, there has been an increasing interest in the application of biocomposites with chitosan and alginate for wound dressings and tissue engineering. This PEC presents adequate 3D biological support to enhance the migration, proliferation, and organization of cells in the physiological environment. For example, Caetano et al. showed that chitosan/alginate membrane modulated the inflammatory process and stimulated the proliferation of fibroblasts and collagen production, accelerating the wound healing (Caetano et al. 2015). So, it is indeed a promising biomaterial as a therapeutic application for the treatment of tissue injuries by incorporating a drug/bioactive molecules to repair wounds (Caetano et al. 2015; Meng et al. 2010). Also, different combinations of chitosan, alginate, and other constituents were developed. Kumar and Kumar prepared films using different combinations of chitosan, alginate, carboxymethylcellulose, and polyvinyl alcohol (Kumar and Kumar 2017). These composites films could be used as drug delivery systems and wound dressing (Kumar and Kumar 2017). Tarusha et al. (2018) developed a wound dressing biomaterial, membrane, constituted by alginate, chitosan, and hyaluronan. This biomaterial is of particular interest for use in chronic non-healing wounds, enhancing skin regeneration (Tarusha et al. 2018).

Gelatin is another polysaccharide that results in appropriate conjugation with alginate. Rosellini et al. (2009) used the alginate/gelatin blend to develop a biomaterial for myocardial tissue engineering (Rosellini et al. 2009). Alemdar developed biomaterials composed of gelatin, sodium alginate, hyaluronic acid, and bio-ceramic reinforced polymer composite materials (such as hydroxyapatite and bioglass particles), with a potential for use as a pH-sensitive carrier for the colon-specific drug delivery (Alemdar 2016). The biocomposites can be developed for use in bone applications, too (Beherei et al. 2018).

Also, sodium alginate and pectin are two natural biopolymers (derived from renewable resources), which together are responsible for enhanced synergic physicochemical properties (capacity to produce water-insoluble films, gels, and beads, in

presence of cations) (Nešić et al. 2017). Their biodegradability, biocompatibility, and good film-forming characteristics increase their potential for wound dressing applications (Rezvanian et al. 2017). Also, collagen is another polymer that combined with alginate has already shown high stability and biocompatibility, which also lead to improved cell proliferation (Gregurec et al. 2016).

The combination of alginate (hydrophilic) and poly(lactide) (PLA) or poly (vinyl pyrrolidone) (PVP) is appropriate for drug delivery system. Summa et al. developed alginate composite films with incorporated PVP that facilitated its controlled release at the wound surface (Summa et al. 2018). They demonstrated that these films have antimicrobial and antifungal activities against *Escherichia coli* and *Candida albicans*. Kessler and collaborators developed promising barrier membranes for the prevention of postsurgical adhesions with alginate and PLA, too (Kessler et al. 2016).

The abovementioned biomaterials have great acceptability for various biomedical applications like drug delivery (transdermal or transbuccal route), cardiac tissue engineering, wound healing therapy, and cell regenerative therapy (Kaygusuz et al. 2017; Kumar and Kumar 2017; Rezvanian et al. 2017; Rosellini et al. 2009; Villani et al. 2008; Wathoni et al. 2016).

16.4.5 Fibers

Fabricating fibers (micro or nano) using biocompatible and biodegradable materials, such as alginate, is becoming of great interest in the biomedical field of tissue engineering due to their structures, flexible composites, biological functions, and capability to mimic the in vivo-like ECM (Anderson et al. 2011; Cheng et al. 2017). Fibers are advantageous in biomedical applications, due to the diversity of polymers available with physico-chemically agents (such as, alginate, pectin, chitosan); a high drug loading, encapsulation efficiency and the ability to control drug/bioactive molecule delivery (Zhang et al. 2017).

Electrospinning and microfluidic spinning are two promising techniques to create fibers (micro and nanofibers), and the selected technique is crucial for the specific application (Cheng et al. 2017). Nanofibers from electrospinning of biopolymers such as polysaccharides and proteins are high interest in biological and medical applications by their specific surface, flexibility, porosity, and similarity to natural extracellular microenvironment (Lin et al. 2017; Shen and Hsieh 2014; Zhang et al. 2017). In addition to choosing the type of processing, it is important to choose the constituent, or the composites to be used, with different properties for a particular applications (Lin et al. 2017). For example, Shen and Hsieh developed alginate/PVA fibers that are biologically compatible and ingestible for potential biomedical, food, and other applications (Shen and Hsieh 2014). Zhang and collaborators (2017)

developed a novel fiber composite with nano-silica or hydroxyapatite with alginate, which showed higher surface area and porosity, as well as increased cell proliferation and delayed degradation, higher mechanical performance, and bioactivity, due to the presence of alginate fibers (Zhang et al. 2017). This biomaterial has particular interest for wound dressing applications.

Alginate fibers produced by wet spinning technology are formulated into nanocapsules that can incorporate drugs/bioactive molecules for faster delivery, wound repair, and tissue reconstruction (Anderson et al. 2011; Lin et al. 2017; Liu et al. 2014; Shin et al. 2007; Zhang et al. 2017). Cells or other bioactive molecules can be incorporated into alginates during the fiber fabrication process while maintaining their viability, for example, the incorporation of endothelial or glial cells into microfibers in order to engineer capillary-like networks (strategy for nerve repair) (Anderson et al. 2011; Lin et al. 2017; Shin et al. 2007).

16.4.6 Sponges

Sponges are 3D porous structures, which generally involve relatively few components and simple procedures. These sponges can be produced by the freeze-drying method (Petchsomrit et al. 2017). They have been used as scaffolds for culturing chondrocytes, osteoblasts for bone formation, wound dressings, and other applications (Miralles et al. 2001; Petchsomrit et al. 2017; Reddy et al. 2015). Alginate sponges were developed for controlled release of drugs, as potential matrix for wound dressings or tissue engineering (Kumbhar and Pawar 2017; Petchsomrit et al. 2017).

16.4.7 Bioink-Based Alginates for 3D Bioprinting

The applications of bioinks for 3D printing were recently reviewed (Gungor-Ozkerim et al. 2018; Hölzl et al. 2016). Bioprinting is an innovative technology based on additive manufacturing from materials containing living cells, for several applications in the development of functional tissue to repair or substitute tissues. The bioprinting process consists of cell encapsulation into biomaterials (solution with one constitute or a mixture) in the hydrogel form, called the bioink, to repair/substitute a tissue. This bioink can be cross-linked or stabilized during or immediately after bioprinting to generate the final structure and design. Bioinks are based on biocompatible hydrogel with natural composition, such as alginates (Horch et al. 2018; Kingsley et al. 2013; Williams et al. 2013), collagen (Duarte Campos et al. 2014), and silk (Das et al. 2015), among others, or synthetic biomaterials (Ng et al.

2017) alone or in combination. In certain cases, cell aggregates without any additional biomaterial can also be adopted as a bioink for bioprinting processes.

16.5 Biomedical and Pharmaceutical Applications

Alginate has been studied extensively in tissue engineering as biomaterial for the regeneration of skin, cartilage, bone, and cardiac tissue (Liberski 2016; Sumayya and Muraleedhara Kurup 2017; Szekalska et al. 2016; Venkatesan et al. 2015). Also, there is a broad scope for the application of alginate in the field of biomedicine and pharmaceutical industry, including wound healing; cell transplantation, immobilization, and matrix for living cell; delivery of bioactive agents, such as chemical drugs and proteins; and manufacture of tablets, to promote greater protection, stabilization of the drug, and extended drug release (da Silva et al. 2017; Liberski 2016). Alginates also have extensive uses in several industrial fields, including textiles, food, and cosmetics. It is noteworthy that there are several commercial products based on alginates (Table 16.2) (da Silva et al. 2017; Szekalska et al. 2016).

16.5.1 Drug Delivery Systems

Alginates have attracted much attention as a potential device for controlling drug release (hydrophilic and hydrophobic). Alginate has been successfully used as a matrix for entrapment and/or delivery of drugs (Sachan et al. 2009) and bioactive molecules such as proteins or growth factors (d'Ayala et al. 2008; Goh et al. 2012; Liberski 2016; Sosnik 2014). The encapsulation and release of proteins from alginate gels can increase their efficacy and release (Augst et al. 2006). The molecules are encapsulated into the polymers, for their protection and controlled release (d'Ayala et al. 2008). They have many advantages such as the following: they protect the stomach mucosa from the aggressive drug effect or protect acid-sensitive drugs from gastric juice, they offer a controlled drug delivery, and they are non-toxic when orally administered (Abdellatif et al. 2016; Al-Otoum et al. 2014; Liakos et al. 2013). Drugs with non-favorable solid-state properties (e.g., low solubility) benefit from encapsulation, too.

Nowadays, solid preparations, which are based on alginates such as oral tablets, microcapsules, implants, and topical delivery systems, are available (d'Ayala et al. 2008). The excellent properties of alginate have resulted in their use in a wide variety of pharmaceutical applications. Alginate has been used as a biomaterial for drug delivery in the form of microcapsules, microparticles, gel particles, pellets, and

Table 16.2 Commercial products based on alginate

Application	Product	References
Drug delivery system	Gastrotuss®	Chellini et al. (2015) and Ummarino et al. (2015)
	Algicid®	Jakaria et al. (2015)
	Gaviscon Double Action®	De Ruigh et al. (2014) and Thomas et al. (2014)
Tissue engineering	Progenix putty™	Thomas et al. (2014)
	Emdogain®	Esposito et al. (2009) and Yan et al. (2014)
	Algisyl™	Liberski et al. (2016)
Wound dressing	Flaminal Forte®	Rashaan et al. (2016)
	Purilon Gel®	Szekalska et al. (2016)
	Saf-Gel®	Duncan et al. (2002) and Szekalska et al. (2016)
	Hyalogran®	Carella et al. (2013)
	SeaSorb®	Ausili et al. (2013), Bale et al. (2001) and Szymonowicz et al. (2017)
	Tromboguard®	Szymonowicz et al. (2017)
	Fibracol Plus®	Rangaraj et al. (2011)
	Algivon®	Hajská et al. (2017)
	Guardix-SG®	Park et al. (2013)
	AlgiCell®	Newsom et al. (2015)
	AlgiSite®	Angspatt et al. (2010), Dhivya et al. (2015) and Knill et al. (2004)
	Algosteril®	Knill et al. (2004)
	Comfeel®	Knill et al. (2004)
	Kaltocarb®	Knill et al. (2004)
	Kaltostat®	Dhivya et al. (2015) and Knill et al. (2004)
	Melgisorb®	Knill et al. (2004)
	Sorbalgon®	Knill et al. (2004)
	Sorbsan®	Dhivya et al. (2015) and Knill et al. (2004)
Therapeutic cell	AlgiMatrix®	Andersen et al. (2015), Godugu et al. (2013) and Godugu and Singh (2016)
	NovaMatrix®-3D	Andersen et al. (2015)
	ALG-encapsulation Technology Immupel™	Szekalska et al. (2016)
	DIABECELL®	Hillberg et al. (2013)
	NTCELL®	Irving et al. (2014)

beads. Alginate can be used to modify drug release profiles during oral controlled drug delivery or the targeted delivery and controlled release of bioactive compounds (Table 16.3) (Ching et al. 2017; Mukhopadhyay et al. 2018; Petchsomrit et al. 2017; Szekalska et al. 2016).

Table 16.3 Alginate-based materials and their applications in delivery systems

Composites	Type of biomaterial	Application	References
Alginate/chitosan	Nanoparticles	Delivery system	Li et al. (2008) and Mukhopadhyay et al. (2015)
Alginate/chitosan	Beads	Delivery system	Anal and Stevens (2005) and Shi et al. (2008)
Alginate/chitosan	Hydrogel	Delivery system	Yang et al. (2013)
Alginate/chitosan	Gel beads	Delivery system	Xu et al. (2017)
Alginate (sodium)/chitosan/ hydroxyapatite nanocomposite	Hydrogel	Delivery system	Taleb et al. (2015)
Alginate/chitosan/poly(lactide) (PLA)	Sponges	Delivery system	De la Riva et al. (2009)
Alginate/N-α-glutaric acid chitosan	Hydrogel	Delivery system	Gong et al. (2011)
Alginate/carboxymethyl chitosan	Hydrogel	Delivery system	Yang et al. (2013)
Alginate/carboxymethyl chitosan	Beads	Delivery system	Mukhopadhyay et al. (2013)
Alginate/N,O-carboxymethyl chitosan	Hydrogel	Delivery system	Chen et al. (2004) and Lin et al. (2005)
Alginate (oxidized)/N,O-carboxymethyl chitosan	Hydrogel	Delivery system	Li et al. (2012)
Alginate/low methoxyl pectin/ hydroxypropylmethylcellulose	Beads	Delivery system	Awasthi and Kulkarni (2014)
Alginate/poly(acrylic acid)	Hydrogels	Delivery system	d'Ayala et al. (2008)
Alginate/poly(lactic-co-glycolic acid) (PLGA)/RGD	Microparticles	Delivery system	Mata et al. (2011)
Alginate (sodium)/g*raft*-PNIPAM	Micelles	Delivery system	Yu et al. (2016)
Alginate (sodium)/g*raft*-PNIPAM	Beads	Delivery system	Işıklan and Küçükbalcı (2012)
Alginate/polyacrylamide	Hydrogel	Delivery system	Samanta and Ray (2014)
Alginate-G-poly(*N*-vinylpyrrolidone) (PVP)	Beads	Delivery system	Yiğitoğlu et al. (2014)
Alginate-G-poly(sodium acrylate)/PVP	Hydrogel	Delivery system	Tally and Atassi (2015) and Wang and Wang (2010)
Alginate/starch	Beads	Delivery system	Malakar et al. (2013)
Alginate/resistant starch	Microparticles	Delivery system	Hosseini et al. (2014)
Alginate/silica	Nanoparticle	Delivery system	Boissière et al. (2007)

16.5.2 Tissue Engineering

16.5.2.1 Bone and Cartilage

Alginate biomaterials have been used in the treatment of bone injuries as delivery systems to osteoinductive factors, drugs, bone-forming cells, or a combination of both. Alginate gels have advantages for bone and cartilage regeneration, as compared to other materials, because they can be introduced into the body in a minimally invasive process, have the ability to fill defects (with regular or irregular shapes), can be easily modified chemically with adhesive ligands (e.g., RGD), and can control the release of drug/bioactive molecules into tissues (e.g., BMP, TGF). However, alginate gels do not have sufficient mechanical strength, but this property can be overcome when combined with other constituents such as hydroxyapatite, calcium phosphate, or chitosan (Table 16.4) (Kumbhar and Pawar 2017; Sumayya and Muraleedhara Kurup 2017). For example, the combination of alginate gels with collagen type I and tricalcium phosphate allowed to improve cell adhesion and proliferation that do not readily attach or proliferate on pure alginate gels (Nahar et al. 2017). Alginate/chitosan gels entrapping mesenchymal stem cells and growth factors (BMP-2, BMP-7, and VEGF) also showed potential for trabecular bone formation in animal models (Kanczler et al. 2010).

Alginate gels are potential biomaterials that have proved to be useful for transplanting chondrogenic cells to restore damaged cartilage in animal models, too. For example, some studies used a suspension of chondrocytes in an alginate solution mixed with calcium sulfate and injected into molds of facial implants in order to produce cartilage (Nahar et al. 2017).

16.5.3 Cardiac Applications

Alginate-based biomaterials have been developed to be used in cardiac applications too (Liberski 2016; Tallawi et al. 2015). Alginate was described as a material of non-thrombotic nature, which is confirmed by several biomedical applications and clinical assays (Hasan et al. 2015; Liberski et al. 2016; Liberski 2016; Ruvinov and Cohen 2016). So it can be an attractive candidate for cardiac applications such as heart valve tissue engineering (Table 16.4). For example, Bai et al. (2011) demonstrated that the alginate/collagen composite microbeads can provide a physiologic microenvironment for cardiomyocytes that can be appropriate to heart-like tissues development (Bai et al. 2011). Other biomaterials, such as injectable hydrogels, were tried for application in cardiac repair. They have the potential to deliver bioactive molecules, therapeutic agents, and cells in situ in damaged tissue in order to regenerate a functional cardiac tissue (Hasan et al. 2015). The hydrogel is injected into the damaged heart muscle and polymerizes in situ between the cells and fibers of

Table 16.4 Alginate-based materials and their applications in tissue engineering

Composites	Type of biomaterial	Application	References
Alginate/Ag	Nanoparticles	Tissue engineering Wound dressing	Jovanović et al. (2012)
Alginate/calcium phosphate	Hydrogel	Tissue engineering (bone)	Zhao et al. (2010a)
Alginate (sodium)/calcium phosphate	Scaffold	Tissue engineering (bone)	Egorov et al. (2016)
Alginate/chitosan/gelatin	Hydrogel	Tissue engineering	Naghizadeh et al. (2018)
Alginate/chitosan/nanosilica	Scaffold	Tissue engineering (bone)	Sowjanya et al. (2013)
Alginate/chitosan/poly(ethylene glycol) (PEG)	Hydrogel	Tissue engineering	Radhakrishnan et al. (2015)
Alginate/chitosan/titanium	Scaffolds	Tissue engineering	Wang et al. (2014)
Alginate/*O*-carboxymethyl chitosan/fibrin	Hydrogels	Tissue engineering	Jaikumar et al. (2015)
Alginate/PVA/fibrin			
Alginate (polypyrrole)/chitosan	Scaffold	Tissue engineering (bone)	Sajesh et al. (2013)
Alginate/collagen	Microbeads	Tissue engineering (cardiac)	Bai et al. (2011)
Alginate/collagen/titanium	Films	Tissue engineering (bone)	Gregurec et al. (2016)
Alginate/glass ceramics	Injectable biocomposite	Tissue engineering (bone)	Gabbai-Armelin et al. (2014)
Alginate/gelatin	Hydrogel	Tissue engineering (bone)	Lewandowska-Łańcucka et al. (2017)
Alginate/gelatin	Hydrogel	Tissue engineering (cardiac)	Duan et al. (2013)
Alginate(oxidized)/gelatin/biphasic calcium phosphate	Hydrogel	Tissue engineering (bone)	Paul et al. (2015) and Sarker et al. (2015)
Alginate/gelatin/nanocrystalline cellulose	Hydrogel	Tissue engineering (bone)	Wang et al. (2016)
Alginate/halloysite	Beads	Tissue engineering	Chiew et al. (2014)
Alginate/hyaluronan	Sponge	Tissue engineering	Catanzano et al. (2018)
Alginate-lignin	Aerogels	Tissue engineering	Quraishi et al. (2015)
Alginate/PLGA	Gel with nanoparticles	Tissue engineering	Wang et al. (2011)
Alginate/starch	Aerogels	Tissue engineering (bone)	Martins et al. (2015)
Calcium-cobalt alginate	Beads	Tissue engineering (cartilage)	Focaroli et al. (2016)
Alginate-thiol-terminated peptides	Gel	Tissue engineering	Bubenikova et al. (2012)

the damaged tissue. This biomaterial supplies the needful physical support to the heart muscle during repair process (Liberski 2016). Sometimes, 3D alginate scaffolds can be modified with RGD peptide to improve cell attachment and growth and increased angiogenic growth factor expression (Yu et al. 2010). Also, immobilization of alginate biomaterials with RGD peptide has been presented as an important parameter in functional cardiac muscle tissue repair and in improving the protection of the regenerated tissue in culture (Shachar et al. 2011).

16.5.4 Wound Dressing

Alginate wound dressings have a high projection in the management of exudative wounds and treatment of acute and chronic wounds and offer many advantageous features when compared with traditional wound dressings (Coşkun et al. 2014; Dhivya et al. 2015; Nahar et al. 2017; Sun and Tan 2013). Alginate wound dressings maintain a moist environment in situ, retain the wound exudates, potentiate fibroblast proliferation and keratinocyte migration, improve wound healing, and minimize bacterial infection at the skin tissue damage (Caló and Khutoryanskiy 2015; Golafshan et al. 2017; Lee and Mooney 2012; Nahar et al. 2017; Wathoni et al. 2016). Alginate wound dressings are typically produced by ionic cross-linking (to form a gel), freeze-dried (i.e., foam) and fibrous non-woven dressings (Lee and Mooney 2012). These wound dressings can have different functions, for example, the dry form absorbs wound fluid to re-gel, and the gels then can supply water to a dry wound, maintaining moisture of the physiological environment, and decrease the bacterial infection in situ. These properties can also promote granulation tissue formation and increase epithelialization and healing. Alginate dressings are still used as a delivery system in order to provide controlled release of therapeutic substances (e.g., pain-relieving, antibacterial, and anti-inflammatory agents) and bioactive molecules to wound healing (Table 16.5) (Wathoni et al. 2016).

There are several commercial alginate wound dressings, such as Algicell™ (Derma Sciences), AlgiSite M™ (Smith & Nephew), Comfeel Plus™ (Coloplast), Kaltostat™ (ConvaTec), Sorbsan™ (UDL Laboratories), and Tegagen™ (3 M Healthcare) (Coşkun et al. 2014; Dhivya et al. 2015; Knill et al. 2004; Lee and Mooney 2012; Nahar et al. 2017; Newsom et al. 2015).

16.5.5 Therapeutic Cell

Alginate biological properties like its interactions with cells by bioadhesive bonds make it as a promising biomaterial for cell and tissue cultures. Alginates have been used as 3D systems with the capacity to mimic the native ECM and are very useful

Table 16.5 Alginate-based materials and their applications in wound dressing

Composites	Type of biomaterial	Application	References
Alginate/chitosan	Fibers	Wound dressing	Knill et al. (2004)
Alginate/chitosan	Membranes	Wound dressing	Meng et al. (2010)
Alginate/chitosan	Hydrogel	Wound dressing	Straccia et al. (2015)
Alginate/chitosan	Fibers	Wound dressing	Sweeney et al. (2014)
Alginate/chitosan	Fibers	Wound dressing	Knill et al. (2004)
Alginate/chitosan/fucoidan	Hydrogel	Wound dressing	Murakami et al. (2010)
Alginate/chitosan/pectin	Nanofibers	Wound dressing	Chen et al. (2017)
Alginate (sodium)/ carboxymethyl chitosan/collagen	Microspheres	Wound dressing	Xie et al. (2018)
Alginate/collagen-I	Gel	Wound dressing	da Cunha et al. (2014)
Alginate/gelatin	Hydrogel	Wound dressing	Balakrishnan et al. (2005)
Alginate/halloysite	Gel	Wound dressing	Pasbakhsh et al. (2016)
Alginate/hyaluronic acid	Particles	Wound dressing	Rossi et al. (2018)
Alginate/hyaluronic acid/ chitosan-silver nanoparticles	Membranes	Wound dressing	Tarusha et al. (2018)
Alginate/PEG	Hydrogel	Wound dressing	Koehler et al. (2017)
Alginate/ poly(lactic-co-glycolic acid (PLGA)	Microspheres	Wound healing	Gainza et al. (2013)
Alginate (sodium)/PLGA/ ciprofloxacin	Scaffolds	Wound dressing	Liu et al. (2018)
Alginate/PVA	Membrane	Wound dressing	Kamoun et al. (2015)
Alginate/PVA	Hydrogel	Wound dressing	George et al. (2017) and Golafshan et al. (2017)
Alginate/PVA	Hydrogel	Wound dressing	George et al. (2017)
Alginate (sodium)/PVA/ moxifloxacin hydrochloride	Membrane	Wound dressing	Fu et al. (2016)
Alginate (sodium)/povidone iodine	Film	Wound dressing	Summa et al. (2018)
Alginate/sago starch	Film	Wound dressing	Arockianathan et al. (2012)

for evaluating and understanding the complex cellular physiology, drug evaluation, and tissue engineering (Andersen et al. 2015; Cardoso et al. 2016; Dalheim et al. 2016; Sun and Tan 2013; Szekalska et al. 2016). The biomaterials used in cellular therapeutics should have suitable porosity, sufficient pore size, and interconnected pore structure for transporting cells, metabolites, nutrients, and signal molecules. The alginate biomaterials with macroporous structures develop propitious conditions for cell attachment, proliferation, and differentiation, for cell encapsulation with the ability to mimic natural physiological environment. These 3D alginate constructs increase the seeding efficiency of cells (Liberski 2016; Szekalska et al. 2017).

Considering the above, alginate is widely established as the most suitable polymer for cell encapsulation (Simó et al. 2017). The production of alginate scaffolds for cell encapsulation can be accomplished by inkjet-based and extrusion-based systems. Cell encapsulation is a technique that involves immobilization of the cells within a polymeric gel, preserving cellular metabolic activity. The encapsulated cells grow within the alginate biomaterials and secrete new ECM, restoring the injured tissue. This advanced technology is important to increase the knowledge about cellular physiology, drug delivery, and tissue engineering and regenerative medicine (Szekalska et al. 2017).

Also, alginate modifications with bioactive peptides have been frequently used as in vitro cell culture substrates. These biomaterials mimic the adhesive properties of ECM and stimulate cellular responses such as differentiation and proliferation (Dalheim et al. 2016). The presence of RGD peptides in alginate gels allows to control the cellular phenotype of interacting myoblasts, chondrocytes, osteoblasts, as well as bone marrow stromal cells (BMSCs). For example, the adhesion and proliferation of myoblasts cultured on alginate gels were increased when RGD peptides are combined with alginate (Lee and Mooney 2012).

In the past 10 years, research has been conducted on the development of cell transplantation therapy by using alginate-encapsulation technology Immupel™ (LCT, Living Cell Technologies Limited, Australia), and commercial alginate-based 3D products for cell culture, such as AlgiMatrix (Thermo Fisher Scientific/Life Technologies, USA) and NovaMatrix_3D (NovaMatrix, Norway), were developed (Hillberg et al. 2013; Irving et al. 2014; Szekalska et al. 2016, 2017).

16.6 Conclusions

Alginates have demonstrated great potential as biomaterials for biomedical applications, especially in wound healing, drug delivery, in vitro cell culture, and tissue engineering. They present features, such as biocompatibility, mild gelation conditions, and simple functionalization, which enable to prepare alginate derivatives with new properties.

Advances in the biochemistry of the complex alginate polysaccharides have provided several opportunities (Pawar and Edgar 2012):

1. To be able to control monosaccharides sequences, an area unique in polysaccharide chemistry (Mørch et al. 2007).
2. To provide insight into the structure-properties relationship of alginates in structural gels and in bacterial biofilms (Ramsey and Wozniak 2005).
3. To tailor-make alginate materials for particular applications.
4. Chemical derivatization allows to create the next-generation alginate biomaterials with enhanced or altogether new properties.
5. New organic solvents systems may provide enhanced exploration of chemoselectivity (e.g., OH vs. COOH reaction) and regioselectivity (M vs G, 2-OH vs. 3-OH within each monosaccharide).

Alginate-based materials are likely to evolve in the future and play an even more active role in biomedical applications, in which the precise control over the delivery can potentially improve the safety and effectiveness of drugs and provide new therapies (Lee and Mooney 2012). Likewise, smart alginate hydrogels for on-demand drug release in response to, for example, mechanical signals (Lee and Mooney 2012) and magnetic field (Zhao et al. 2011) among other stimuli, will play an important future role. These and the introduction of appropriate cell interactive features will be crucial in many tissue engineering applications.

Acknowledgments This work was supported by the National Funds from FCT through project PEst-OE/EQB/LA0016/2013.

References

Abdelghany S, Alkhawaldeh M, AlKhatib HS (2017) Carrageenan-stabilized chitosan alginate nanoparticles loaded with ethionamide for the treatment of tuberculosis. J Drug Deliv Sci Technol 39:442–449

Abdellatif A, El Hamd M, Saleh K (2016) A formulation, optimization and evaluation of controlled released alginate beads loaded-flurbiprofen. J Nanomed Nanotechnol 7:357–364

Agüero L, Zaldivar-Silva D, Peña L, Dias ML (2017) Alginate microparticles as oral colon drug delivery device: a review. Carbohydr Polym 168:32–43

Al Dalaty A, Karam A, Najlah M, Alany RG, Khoder M (2016) Effect of non-cross-linked calcium on characteristics, swelling behaviour, drug release and mucoadhesiveness of calcium alginate beads. Carbohydr Polym 140:163–170

Alban S, Schauerte A, Franz G (2002) Anticoagulant sulfated polysaccharides: Part I. Synthesis and structure–activity relationships of new pullulan sulfates. Carbohydr Polym 47:267–276

Alemdar N (2016) Fabrication of a novel bone ash-reinforced gelatin/alginate/hyaluronic acid composite film for controlled drug delivery. Carbohydr Polym 151:1019–1026

Al-Otoum R, Abulateefeh S, Taha M (2014) Preparation of novel ionotropically crosslinked beads based on alginate-terephthalic acid composites as potential controlled release matrices. Pharmazie 69:10–18

Alsharabasy AM, Moghannem SA, El-Mazny WN (2016) Physical preparation of alginate/chitosan polyelectrolyte complexes for biomedical applications. J Biomater Appl 30:1071–1079

Amiri M, Salavati-Niasari M, Pardakhty A, Ahmadi M, Akbari A (2017) Caffeine: a novel green precursor for synthesis of magnetic $CoFe_2O_4$ nanoparticles and pH-sensitive magnetic alginate beads for drug delivery. Mater Sci Eng C 76:1085–1093

Anal AK, Stevens WF (2005) Chitosan–alginate multilayer beads for controlled release of ampicillin. Int J Pharm 290:45–54

Andersen T, Auk-Emblem P, Dornish M (2015) 3D cell culture in alginate hydrogels. Microarrays 4:133–161

Anderson T, Strand BL, Formo K, Alsberg E, Christensen B (2011) Alginates as biomaterials in tissue engineering. In: Rauter AP (ed) Carbohydrate chemistry: chemical and biological approaches, vol 37. Royal Society of Chemistry, London, pp 227–258

Angspatt A, Tanvatcharaphan P, Channasanon S, Tanodekaew S, Chokrungvaranont P, Sirimaharaj W (2010) Comparative study between chitin/polyacrylic acid (PAA) dressing, lipido-colloid absorbent dressing and alginate wound dressing: a pilot study in the treatment of partial thickness wound. J Med Assoc Thail 93:694–697

Arlov Ø, Skjåk-Bræk G (2017) Sulfated alginates as heparin analogues: a review of chemical and functional properties. Molecules 22:71–75

Arockianathan PM, Sekar S, Sankar S, Kumaran B, Sastry T (2012) Evaluation of biocomposite films containing alginate and sago starch impregnated with silver nano particles. Carbohydr Polym 90:717–724

Augst AD, Kong HJ, Mooney DJ (2006) Alginate hydrogels as biomaterials. Macromol Biosci 6:623–633

Ausili E, Paolucci V, Triarico S et al (2013) Treatment of pressure sores in spina bifida patients with calcium alginate and foam dressings. Eur Rev Med Pharmacol Sci 17:1642–1647

Awasthi R, Kulkarni GT (2014) Development of novel gastroretentive drug delivery system of gliclazide: hollow beads. Drug Dev Ind Pharm 40:398–408

Bagheri L, Madadlou A, Yarmand M, Mousavi ME (2014) Spray-dried alginate microparticles carrying caffeine-loaded and potentially bioactive nanoparticles. Food Res Int 62:1113–1119

Bai X, Zheng H, Fang R et al (2011) Fabrication of engineered heart tissue grafts from alginate/collagen barium composite microbeads. Biomed Mater 6(4):045002–045011. https://doi.org/10.1088/1748-6041/6/4/045002

Balakrishnan B, Jayakrishnan A (2005) Self-cross-linking biopolymers as injectable *in situ* forming biodegradable scaffolds. Biomaterials 26:3941–3951

Balakrishnan B, Mohanty M, Umashankar P, Jayakrishnan A (2005) Evaluation of an *in situ* forming hydrogel wound dressing based on oxidized alginate and gelatin. Biomaterials 26:6335–6342

Bale S, Baker N, Crook H, Rayman A, Rayman G, Harding K (2001) Exploring the use of an alginate dressing for diabetic foot ulcers. J Wound Care 10:81–84

Beherei HH, Shaltout AA, Mobrouk M, Abdelwahed NAM, Das DB (2018) Influence of niobium pentoxide particulates on the properties of brushite/gelatin/alginate membranes. J Pharm Sci 107:1361–1371

Benavides S, Villalobos-Carvajal R, Reyes J (2012) Physical, mechanical and antibacterial properties of alginate film: effect of the crosslinking degree and oregano essential oil concentration. J Food Eng 110:232–239

Bidarra SJ, Barrias CC, Granja PL (2014) Injectable alginate hydrogels for cell delivery in tissue engineering. Acta Biomater 10:1646–1662

Boissière M, Allouche J, Chanéac C et al (2007) Potentialities of silica/alginate nanoparticles as hybrid magnetic carriers. Int J Pharm 344:128–134

Bouhadir KH, Lee KY, Alsberg E, Damm KL, Anderson KW, Mooney DJ (2001) Degradation of partially oxidized alginate and its potential application for tissue engineering. Biotechnol Prog 17:945–950

Bubenikova S, Stancu I-C, Kalinovska L et al (2012) Chemoselective cross-linking of alginate with thiol-terminated peptides for tissue engineering applications. Carbohydr Polym 88:1239–1250

Buwalda SJ, Vermonden T, Hennink WE (2017) Hydrogels for therapeutic delivery: current developments and future directions. Biomacromolecules 18:316–330

Caetano GF, Frade MAC, Andrade TAM et al (2015) Chitosan-alginate membranes accelerate wound healing. J Biomed Mater Res B Appl Biomater 103:1013–1022

Caló E, Khutoryanskiy VV (2015) Biomedical applications of hydrogels: a review of patents and commercial products. Eur Polym J 65:252–267

Cardoso MJ, Costa RR, Mano JF (2016) Marine origin polysaccharides in drug delivery systems. Mar Drugs 14:34–60

Carella S, Maruccia M, Fino P, Onesti MG (2013) An atypical case of Henoch-Shönlein purpura in a young patient: treatment of the skin lesions with hyaluronic acid-based dressings. In Vivo 27:147–151

Catanzano O, D'Esposito V, Formisano P, Boateng JS, Quaglia F (2018) Composite alginate-hyaluronan sponges for the delivery of tranexamic acid in postextractive alveolar wounds. J Pharm Sci 107:654–661

Chaluvadi S, Hotchkiss A Jr, Call J et al (2012) Protection of probiotic bacteria in a synbiotic matrix following aerobic storage at 4 C. Benefic Microbes 3:175–187

Chamberlain N, Cunningham G, Speakman J (1946) Alginic acid diacetate. Nature 158:553–554

Chang AA, Reuther MS, Briggs KK et al (2012) In vivo implantation of tissue-engineered human nasal septal neocartilage constructs: a pilot study. Otolaryngol Head Neck Surg 146:46–52

Chellini E, Lavorini F, Campi G, Mannini C, Fontana GA (2015) Effect of an anti-reflux medical device in the control of deflation cough: a placebo-controlled comparative study with an antacid drug in chronic coughers. Pulm Pharmacol Ther 33:11–14

Chen S-C, Wu Y-C, Mi F-L, Lin Y-H, Yu L-C, Sung H-W (2004) A novel pH-sensitive hydrogel composed of N, O-carboxymethyl chitosan and alginate cross-linked by genipin for protein drug delivery. J Control Release 96:285–300

Chen K, Ling Y, Cao C, Li X, Chen X, Wang X (2016) Chitosan derivatives/reduced graphene oxide/alginate beads for small-molecule drug delivery. Mater Sci Eng C 69:1222–1228

Chen S, Cui S, Hu J, Zhou Y, Liu Y (2017) Pectinate nanofiber mat with high absorbency and antibacterial activity: a potential superior wound dressing to alginate and chitosan nanofiber mats. Carbohydr Polym 174:591–600

Cheng J, Jun Y, Qin J, Lee S-H (2017) Electrospinning versus microfluidic spinning of functional fibers for biomedical applications. Biomaterials 114:121–143

Chiew CSC, Poh PE, Pasbakhsh P, Tey BT, Yeoh HK, Chan ES (2014) Physicochemical characterization of halloysite/alginate bionanocomposite hydrogel. Appl Clay Sci 101:444–454

Ching SH, Bansal N, Bhandari B (2017) Alginate gel particles–a review of production techniques and physical properties. Crit Rev Food Sci Nutr 57:1133–1152

Chirani N, Yahia L, Gritsch L, Motta FL, Chirani S, Fare S (2015) History and applications of hydrogels. J Biomed Sci 4:13–35

Choudhary S, Reck JM, Carr AJ, Bhatia SR (2018) Hydrophobically modified alginate for extended release of pharmaceuticals. Polym Adv Technol 29:198–204

Coleman RJ, Lawrie G, Lambert LK, Whittaker M, Jack KS, Grøndahl L (2011) Phosphorylation of alginate: synthesis, characterization, and evaluation of *in vitro* mineralization capacity. Biomacromolecules 12:889–897

Coşkun G, Karaca E, Ozyurtlu M, Özbek S, Yermezler A, Çavuşoğlu İ (2014) Histological evaluation of wound healing performance of electrospun poly (vinyl alcohol)/sodium alginate as wound dressing *in vivo*. Biomed Mater Eng 24:1527–1536

Costa MJ, Marques AM, Pastrana LM, Teixeira JA, Sillankorva SM, Cerqueira MA (2018) Physicochemical properties of alginate-based films: effect of ionic crosslinking and mannuronic and guluronic acid ratio. Food Hydrocoll 81:442–448

d'Ayala GG, Malinconico M, Laurienzo P (2008) Marine derived polysaccharides for biomedical applications: chemical modification approaches. Molecules 13:2069–2106

da Cunha CB, Klumpers DD, Li WA et al (2014) Influence of the stiffness of three-dimensional alginate/collagen-I interpenetrating networks on fibroblast biology. Biomaterials 35:8927–8936

da Silva TL, Vidart JMM, da Silva MGC, Gimenes ML, Vieira MGA (2017) Alginate and sericin: environmental and pharmaceutical applications. In: Shalaby EA (ed) Biological activities and application of marine polysaccharides. InTech, London, pp 57–85
Dahlmann J, Krause A, Möller L et al (2013) Fully defined *in situ* cross-linkable alginate and hyaluronic acid hydrogels for myocardial tissue engineering. Biomaterials 34:940–951
Dai H, Ou S, Huang Y, Liu Z, Huang H (2017) Enhanced swelling and multiple-responsive properties of gelatin/sodium alginate hydrogels by the addition of carboxymethyl cellulose isolated from pineapple peel. Cellulose 25:593–606
Dalheim MØ, Vanacker J, Najmi MA, Aachmann FL, Strand BL, Christensen BE (2016) Efficient functionalization of alginate biomaterials. Biomaterials 80:146–156
Das S, Pati F, Choi Y-J et al (2015) Bioprintable, cell-laden silk fibroin–gelatin hydrogel supporting multilineage differentiation of stem cells for fabrication of three-dimensional tissue constructs. Acta Biomater 11:233–246
Davis TA, Volesky B, Mucci A (2003) A review of the biochemistry of heavy metal biosorption by brown algae. Water Res 37:4311–4330
De la Riva B, Nowak C, Sánchez E et al (2009) VEGF-controlled release within a bone defect from alginate/chitosan/PLA-H scaffolds. Eur J Pharm Biopharm 73:50–58
de Moraes MA, Beppu MM (2013) Biocomposite membranes of sodium alginate and silk fibroin fibers for biomedical applications. J Appl Polym Sci 130:3451–3457
De Ruigh A, Roman S, Chen J, Pandolfino JE, Kahrilas PJ (2014) Gaviscon double action liquid (antacid & alginate) is more effective than antacid in controlling post-prandial oesophageal acid exposure in GERD patients: a double-blind crossover study. Aliment Pharmacol Ther 40:531–537
Dettmar PW, Strugala V, Richardson JC (2011) The key role alginates play in health. Food Hydrocoll 25:263–266
Dhivya S, Padma VV, Santhini E (2015) Wound dressings–a review. Biomedicine 5:24–28
Donati I, Holtan S, Mørch YA, Borgogna M, Dentini M, Skjåk-Bræk G (2005) New hypothesis on the role of alternating sequences in calcium−alginate gels. Biomacromolecules 6:1031–1040
Draget KI, Taylor C (2011) Chemical, physical and biological properties of alginates and their biomedical implications. Food Hydrocoll 25:251–256
Draget KI, Smidsrød O, Skjåk-Bræk G (2005) Alginates from algae. In: Steinbüchel A (ed) Biopolymers online. Wiley, New York, pp 215–224
Duan B, Hockaday LA, Kang KH, Butcher JT (2013) 3D bioprinting of heterogeneous aortic valve conduits with alginate/gelatin hydrogels. J Biomed Mater Res A 101:1255–1264
Duarte Campos DF, Blaeser A, Korsten A et al (2014) The stiffness and structure of three-dimensional printed hydrogels direct the differentiation of mesenchymal stromal cells toward adipogenic and osteogenic lineages. J Tissue Eng Part A 21:740–756
Duncan G, Andrews S, McCulloch W (2002) Issues in clinical practice: dressings. Prim Intention Aust J Wound Manage 10:29–35
Egorov AA, Fedotov AY, Mironov AV, Komlev VS, Popov VK, Zobkov YV (2016) 3D printing of mineral–polymer bone substitutes based on sodium alginate and calcium phosphate. Beilstein J Nanotechnol 21:1794–1799
Eiselt P, Lee KY, Mooney DJ (1999) Rigidity of two-component hydrogels prepared from alginate and poly (ethylene glycol)− diamines. Macromolecules 32:5561–5566
Esposito M, Grusovin MG, Coulthard P, Worthington HV (2009) Enamel matrix derivative (Emdogain) for periodontal tissue regeneration in intrabony defects. A Cochrane systematic review. Eur J Oral Implantol 2:247–266
Falkeborg M, Cheong L-Z, Gianfico C et al (2014) Alginate oligosaccharides: enzymatic preparation and antioxidant property evaluation. Food Chem 164:185–194
Fan L, Jiang L, Xu Y et al (2011) Synthesis and anticoagulant activity of sodium alginate sulfates. Carbohydr Polym 83:1797–1803
FDA USFaDA (2016) Generally recognized as safe (Internet) In. http://www.fda.gov/Food/IngredientsPackagingLabeling/GRAS/SCOGS/ucm260857.htm.2016

Focaroli S, Teti G, Salvatore V, Orienti I, Falconi M (2016) Calcium/cobalt alginate beads as functional scaffolds for cartilage tissue engineering. Stem Cells Int 2016:2030478–2030489. https://doi.org/10.1155/2016/2030478

Franklin MJ, Ohman DE (1993) Identification of algF in the alginate biosynthetic gene cluster of *Pseudomonas aeruginosa* which is required for alginate acetylation. J Bacteriol 175:5057–5065

Franklin MJ, Ohman DE (2002) Mutant analysis and cellular localization of the AlgI, AlgJ, and AlgF proteins required for O acetylation of alginate in *Pseudomonas aeruginosa*. J Bacteriol 184:3000–3007

Franklin MJ, Douthit SA, McClure MA (2004) Evidence that the algI/algJ gene cassette, required for O acetylation of *Pseudomonas aeruginosa* alginate, evolved by lateral gene transfer. J Bacteriol 186:4759–4773

Freeman I, Kedem A, Cohen S (2008) The effect of sulfation of alginate hydrogels on the specific binding and controlled release of heparin-binding proteins. Biomaterials 29:3260–3268

Fu R, Li C, Yu C et al (2016) A novel electrospun membrane based on moxifloxacin hydrochloride/poly (vinyl alcohol)/sodium alginate for antibacterial wound dressings in practical application. Drug Deliv 23:818–829

Gabbai-Armelin P, Cardoso DA, Zanotto E et al (2014) Injectable composites based on biosilicate® and alginate: handling and *in vitro* characterization. RSC Adv 4:45778–45785

Gainza G, Aguirre JJ, Pedraz JL, Hernández RM, Igartua M (2013) rhEGF-loaded PLGA-Alginate microspheres enhance the healing of full-thickness excisional wounds in diabetised Wistar rats. Eur J Pharm Sci 50:243–252

Gama CI, Tully SE, Sotogaku N et al (2006) Sulfation patterns of glycosaminoglycans encode molecular recognition and activity. Nat Chem Biol 2:467–473

Gamboa A, Araujo V, Caro N, Gotteland M, Abugoch L, Tapia C (2015) Spray freeze-drying as an alternative to the ionic gelation method to produce chitosan and alginate nano-particles targeted to the colon. J Pharm Sci 104:4373–4385

García-Astrain C, Avérous L (2018) Synthesis and evaluation of functional alginate hydrogels based on click chemistry for drug delivery applications. Carbohydr Polym 190:271–280

Gåserød O, Smidsrød O, Skjåk-Bræk G (1998) Microcapsules of alginate-chitosan–I: a quantitative study of the interaction between alginate and chitosan. Biomaterials 19:1815–1825

George M, Abraham TE (2006) Polyionic hydrocolloids for the intestinal delivery of protein drugs: alginate and chitosan – a review. J Control Release 114:1–14

George L, Bavya MC, Rohan KV, Srivastava R (2017) A therapeutic polyelectrolyte–vitamin C nanoparticulate system in polyvinyl alcohol–alginate hydrogel: an approach to treat skin and soft tissue infections caused by *Staphylococcus aureus*. Colloids Surf B: Biointerfaces 160:315–324

Godugu C, Singh M (2016) AlgiMatrix™-based 3D cell culture system as an *in vitro* tumor model: an important tool in cancer research. In: Strano S (ed) Cancer chemoprevention. Springer, New York, pp 117–128

Godugu C, Patel AR, Desai U, Andey T, Sams A, Singh M (2013) AlgiMatrix™ based 3D cell culture system as an in-vitro tumor model for anticancer studies. PLoS One 8(1):e53708–e53720

Goh CH, Heng PWS, Chan LW (2012) Alginates as a useful natural polymer for microencapsulation and therapeutic applications. Carbohydr Polym 88:1–12

Golafshan N, Rezahasani R, Tarkesh Esfahani M, Kharaziha M, Khorasani SN (2017) Nanohybrid hydrogels of laponite: PVA-alginate as a potential wound healing material. Carbohydr Polym 176:392–401

Gong R, Li C, Zhu S, Zhang Y, Du Y, Jiang J (2011) A novel pH-sensitive hydrogel based on dual crosslinked alginate/N-α-glutaric acid chitosan for oral delivery of protein. Carbohydr Polym 85:869–874

Grant GT, Morris ER, Rees DA, Smith PJ, Thom D (1973) Biological interactions between polysaccharides and divalent cations: the egg-box model. FEBS Lett 32:195–198

Gregurec D, Wang G, Pires RH et al (2016) Bioinspired titanium coatings: self-assembly of collagen–alginate films for enhanced osseointegration. J Mater Chem B 4:1978–1986
Gungor-Ozkerim PS, Inci I, Zhang YS, Khademhosseini A, Dokmeci MR (2018) Bioinks for 3D bioprinting: an overview. Biomater Sci 6:915–946
Guo J, Monica Giusti M, Kaletunç G (2018) Encapsulation of purple corn and blueberry extracts in alginate-pectin hydrogel particles: impact of processing and storage parameters on encapsulation efficiency. Food Res Int 107:414–422
Gurikov P, Smirnova I (2018) Non-conventional methods for gelation of alginate. Gels 4:14–28
Hajiali H, Summa M, Russo D et al (2016) Alginate-lavender nanofibers with antibacterial and anti-inflammatory activity to effectively promote burn healing. J Mater Chem B 4:1686–1695
Hajská M, Dragúňová J, Koller J (2017) Cytotoxicity testing of burn wound dressings: first results. Cell Tissue Bank 18:143–151
Hanga MP, Holdich RG (2014) Membrane emulsification for the production of uniform poly-N-isopropylacrylamide-coated alginate particles using internal gelation. Chem Eng Res Des 92:1664–1673
Hasan A, Khattab A, Islam MA et al (2015) Injectable hydrogels for cardiac tissue repair after myocardial infarction. Adv Sci 2(11):1500122–1500140. https://doi.org/10.1002/advs.201500122
Hay ID, Ur Rehman Z, Ghafoor A, Rehm BH (2010) Bacterial biosynthesis of alginates. J Chem Technol Biotechnol 85:752–759
Hillberg AL, Kathirgamanathan K, Lam JB, Law LY, Garkavenko O, Elliott RB (2013) Improving alginate-poly-L-ornithine-alginate capsule biocompatibility through genipin crosslinking. J Biomed Mater Res B Appl Biomater 101:258–268
Hölzl K, Lin S, Tytgat L, Van Vlierberghe S, Gu L, Ovsianikov A (2016) Bioink properties before, during and after 3D bioprinting. Biofabrication 8(3):032002–032010. https://doi.org/10.1088/1758-5090/8/3/032002
Horch RE, Weigand A, Wajant H, Groll J, Boccaccini AR, Arkudas A (2018) Biofabrikation–neue Ansätze für den artifiziellen Gewebeersatz. In: Giunta M (ed) Handchirurgie·Mikrochirurgie·Plastische Chirurgie 50:93–100
Hosseini SM, Hosseini H, Mohammadifar MA et al (2014) Preparation and characterization of alginate and alginate-resistant starch microparticles containing nisin. Carbohydr Polym 103:573–580
Huynh UT, Lerbret A, Neiers F, Chambin O, Assifaoui A (2016) Binding of divalent cations to polygalacturonate: a mechanism driven by the hydration water. J Phys Chem B 120:1021–1032
Irving S, Gillespie L, Richardson R, Rowe D, Fallon J, Wise A (2014) Electroacoustic stimulation: now and into the future. Biomed Res Int 2014:350504–350521. https://doi.org/10.1155/2014/350504
Işıklan N, Küçükbalcı G (2012) Microwave-induced synthesis of alginate–graft-poly (N-isopropylacrylamide) and drug release properties of dual pH-and temperature-responsive beads. Eur J Pharm Biopharm 82:316–331
Istenič K, Balanč BD, Djordjević VB et al (2015) Encapsulation of resveratrol into Ca-alginate submicron particles. J Food Eng 167:196–203
Jaikumar D, Sajesh K, Soumya S et al (2015) Injectable alginate-O-carboxymethyl chitosan/nano fibrin composite hydrogels for adipose tissue engineering. Int J Biol Macromol 74:318–326
Jain D, Bar-Shalom D (2014) Alginate drug delivery systems: application in context of pharmaceutical and biomedical research. Drug Dev Ind Pharm 40:1576–1584
Jakaria M, Zaman R, Parvez M et al (2015) Comparative study among the different formulation of antacid tablets by using acid-base neutralization reaction. Glob J Pharmacol 9:278–281
Jeon O, Bouhadir KH, Mansour JM, Alsberg E (2009) Photocrosslinked alginate hydrogels with tunable biodegradation rates and mechanical properties. Biomaterials 30:2724–2734
Joddar B, Garcia E, Casas A, Stewart CM (2016) Development of functionalized multi-walled carbon-nanotube-based alginate hydrogels for enabling biomimetic technologies. Sci Rep 6:32456–32467

Jovanović Ž, Stojkovska J, Obradović B, Mišković-Stanković V (2012) Alginate hydrogel microbeads incorporated with Ag nanoparticles obtained by electrochemical method. Mater Chem Phys 133:182–189

Kamoun EA, Kenawy E-RS, Tamer TM, El-Meligy MA, Eldin MSM (2015) Poly (vinyl alcohol)-alginate physically crosslinked hydrogel membranes for wound dressing applications: characterization and bio-evaluation. Arab J Chem 8:38–47

Kanczler JM, Ginty PJ, White L et al (2010) The effect of the delivery of vascular endothelial growth factor and bone morphogenic protein-2 to osteoprogenitor cell populations on bone formation. Biomaterials 31:1242–1250

Kavoosi G, Derakhshan M, Salehi M, Rahmati L (2018) Microencapsulation of zataria essential oil in agar, alginate and carrageenan. Innov Food Sci Emerg Technol 45:418–425

Kaygusuz H, Torlak E, Akın-Evingür G, Özen İ, von Klitzing R, Erim FB (2017) Antimicrobial cerium ion-chitosan crosslinked alginate biopolymer films: a novel and potential wound dressing. Int J Biol Macromol 105:1161–1165

Kessler M, Esser E, Groll J, Tessmar J (2016) Bilateral PLA/alginate membranes for the prevention of postsurgical adhesions. J Biomed Mater Res B Appl Biomater 104:1563–1570

Kingsley D, Dias A, Chrisey D, Corr D (2013) Single-step laser-based fabrication and patterning of cell-encapsulated alginate microbeads. Biofabrication 5(4):045006–045027. https://doi.org/10.1088/1758-5082/5/4/045006

Knill C, Kennedy J, Mistry J et al (2004) Alginate fibres modified with unhydrolysed and hydrolysed chitosans for wound dressings. Carbohydr Polym 55:65–76

Koehler J, Wallmeyer L, Hedtrich S, Goepferich AM, Brandl FP (2017) pH-modulating poly (ethylene glycol)/alginate hydrogel dressings for the treatment of chronic wounds. Macromol Biosci 17:1600369–1600370

Kong H-J, Lee KY, Mooney DJ (2002) Decoupling the dependence of rheological/mechanical properties of hydrogels from solids concentration. Polym J 43:6239–6246

Kong HJ, Smith MK, Mooney DJ (2003) Designing alginate hydrogels to maintain viability of immobilized cells. Biomaterials 24:4023–4029

Kong HJ, Alsberg E, Kaigler D, Lee KY, Mooney DJ (2004) Controlling degradation of hydrogels via the size of crosslinked junctions. Adv Mater 16:1917–1921

Kopeček J (2002) Polymer chemistry: swell gels. Nature 417:388–391

Kumar A, Kumar A (2017) Development and characterization of tripolymeric and bipolymeric composite films using glyoxal as a potent crosslinker for biomedical application. Mater Sci Eng C 73:333–339

Kumar A, Lee Y, Kim D et al (2017) Effect of crosslinking functionality on microstructure, mechanical properties, and in vitro cytocompatibility of cellulose nanocrystals reinforced poly (vinyl alcohol)/sodium alginate hybrid scaffolds. Int J Biol Macromol 95:962–973

Kumbhar S, Pawar S (2017) Self-functionalized, oppositely charged chitosan-alginate scaffolds for biomedical applications. Biotechnol Indian J 13:130–144

Lee KY, Mooney DJ (2012) Alginate: properties and biomedical applications. Prog Polym Sci 37:106–126

Lee KY, Kong HJ, Larson RG, Mooney DJ (2003) Hydrogel formation via cell crosslinking. Adv Mater 15:1828–1832

Lee J-B, Takeshita A, Hayashi K, Hayashi T (2011) Structures and antiviral activities of polysaccharides from Sargassum trichophyllum. Carbohydr Polym 86:995–999

Lee B-B, Bhandari BR, Howes T (2018) Gelation of an alginate film via spraying of calcium chloride droplets. Chem Eng Sci 183:1–12

LeRoux MA, Guilak F, Setton LA (1999) Compressive and shear properties of alginate gel: effects of sodium ions and alginate concentration. J Biomed Mater Res 47:46–53

Lewandowska-Łańcucka J, Mystek K, Mignon A, Van Vlierberghe S, Łatkiewicz A, Nowakowska M (2017) Alginate- and gelatin-based bioactive photocross-linkable hybrid materials for bone tissue engineering. Carbohydr Polym 157:1714–1722

Li P, Dai Y-N, Zhang J-P, Wang A-Q, Wei Q (2008) Chitosan-alginate nanoparticles as a novel drug delivery system for nifedipine. Int J Biomed Sci 4:221–228
Li X, Kong X, Zhang Z et al (2012) Cytotoxicity and biocompatibility evaluation of N, O-carboxymethyl chitosan/oxidized alginate hydrogel for drug delivery application. Int J Biol Macromol 50:1299–1305
Li N, Sun G, Wang S et al (2017) Engineering islet for improved performance by optimized reaggregation in alginate gel beads. Biotechnol Appl Biochem 64:400–405
Liakos I, Rizzello L, Bayer IS, Pompa PP, Cingolani R, Athanassiou A (2013) Controlled antiseptic release by alginate polymer films and beads. Carbohydr Polym 92:176–183
Liberski AR (2016) Three-dimensional printing of alginate: from seaweeds to heart valve scaffolds. QSCI Connect 2016(2):3. https://doi.org/10.5339/connect.2016.3
Liberski A, Latif N, Raynaud C, Bollensdorff C, Yacoub M (2016) Alginate for cardiac regeneration: from seaweed to clinical trials. Glob Cardiol Sci Pract 1:e201604–e201628. https://doi.org/10.21542/gcsp.2016.4
Lin H-R, Sung K, Vong W-J (2004) In situ gelling of alginate/pluronic solutions for ophthalmic delivery of pilocarpine. Biomacromolecules 5:2358–2365. https://doi.org/10.1021/bm0496965
Lin Y-H, Liang H-F, Chung C-K, Chen M-C, Sung H-W (2005) Physically crosslinked alginate/N, O-carboxymethyl chitosan hydrogels with calcium for oral delivery of protein drugs. Biomaterials 26:2105–2113
Lin S-F, Chen Y-C, Chen R-N et al (2016) Improving the stability of astaxanthin by microencapsulation in calcium alginate beads. PLoS One 11(4):e0153685–e0153694
Lin SC-Y, Wang Y, Wertheim DF, Coombes AGA (2017) Production and in vitro evaluation of macroporous, cell-encapsulating alginate fibres for nerve repair. Mater Sci Eng C 73:653–664
Linhardt RJ (2003) 2003 Claude S. Hudson award address in carbohydrate chemistry. Heparin: structure and activity. J Med Chem 46:2551–2564
Liu L, Jiang L, Xu G, Ma C, Yang X, Yao J (2014) Potential of alginate fibers incorporated with drug-loaded nanocapsules as drug delivery systems. J Mater Chem B 2:7596–7604
Liu X, Nielsen LH, Kłodzińska SN et al (2018) Ciprofloxacin-loaded sodium alginate/poly (lactic-co-glycolic acid) electrospun fibrous mats for wound healing. Eur J Pharm Biopharm 123:42–49
Ma HL, Hung SC, Lin SY, Chen YL, Lo WH (2003) Chondrogenesis of human mesenchymal stem cells encapsulated in alginate beads. J Biomed Mater Res A 64:273–281
Maciel D, Figueira P, Xiao S et al (2013) Redox-responsive alginate nanogels with enhanced anticancer cytotoxicity. Biomacromolecules 14:3140–3146
Malakar J, Nayak AK, Das A (2013) Modified starch (cationized)–alginate beads containing aceclofenac: formulation optimization using central composite design. Starch-Stärke 65:603–612
Mandal S, Basu SK, Sa B (2010) Ca^{2+} ion cross-linked interpenetrating network matrix tablets of polyacrylamide-grafted-sodium alginate and sodium alginate for sustained release of diltiazem hydrochloride. Carbohydr Polym 82:867–873
Martins M, Barros AA, Quraishi S et al (2015) Preparation of macroporous alginate-based aerogels for biomedical applications. J Supercrit Fluids 106:152–159
Mata E, Igartua M, Patarroyo ME, Pedraz JL, Hernández RM (2011) Enhancing immunogenicity to PLGA microparticulate systems by incorporation of alginate and RGD-modified alginate. Eur J Pharm Sci 44:32–40
Mazzitelli S, Luca G, Mancuso F et al (2011) Production and characterization of engineered alginate-based microparticles containing ECM powder for cell/tissue engineering applications. Acta Biomater 7:1050–1062
McSwain B, Irvine R, Hausner M, Wilderer P (2005) Composition and distribution of extracellular polymeric substances in aerobic flocs and granular sludge. Appl Environ Microbiol 71:1051–1057
Ménard M, Dusseault J, Langlois G et al (2010) Role of protein contaminants in the immunogenicity of alginates. J Biomed Mater Res B Appl Biomater 93:333–340

Meng X, Tian F, Yang J, He C-N, Xing N, Li F (2010) Chitosan and alginate polyelectrolyte complex membranes and their properties for wound dressing application. J Mater Sci Mater Med 21:1751–1759

Miralles G, Baudoin R, Dumas D et al (2001) Sodium alginate sponges with or without sodium hyaluronate: in vitro engineering of cartilage. J Biomed Mater Res A 57:268–278

Mørch Ý, Donati I, Strand B, Skjåk-Bræk G (2007) Molecular engineering as an approach to design new functional properties of alginate. Biomacromolecules 8:2809–2814

Mori M, Rossi S, Bonferoni MC et al (2014) Calcium alginate particles for the combined delivery of platelet lysate and vancomycin hydrochloride in chronic skin ulcers. Int J Pharm 461:505–513

Mukhopadhyay P, Sarkar K, Soam S, Kundu P (2013) Formulation of pH-responsive carboxymethyl chitosan and alginate beads for the oral delivery of insulin. J Appl Polym Sci 129:835–845

Mukhopadhyay P, Chakraborty S, Bhattacharya S, Mishra R, Kundu P (2015) pH-sensitive chitosan/alginate core-shell nanoparticles for efficient and safe oral insulin delivery. Int J Biol Macromol 72:640–648

Mukhopadhyay P, Maity S, Mandal S, Chakraborti AS, Prajapati AK, Kundu PP (2018) Preparation, characterization and in vivo evaluation of pH sensitive, safe quercetin-succinylated chitosan-alginate core-shell-corona nanoparticle for diabetes treatment. Carbohydr Polym 182:42–51

Murakami K, Aoki H, Nakamura S et al (2010) Hydrogel blends of chitin/chitosan, fucoidan and alginate as healing-impaired wound dressings. Biomaterials 31:83–90

Naghizadeh Z, Karkhaneh A, Khojasteh A (2018) Self-crosslinking effect of chitosan and gelatin on alginate based hydrogels: injectable in situ forming scaffolds. Mater Sci Eng C 89:256–264

Nahar K, Hossain MK, Khan TA (2017) Alginate and its versatile application in drug delivery. J Pharm Sci Res 9:606–617

Narayanan RP, Melman G, Letourneau NJ, Mendelson NL, Melman A (2012) Photodegradable iron (III) cross-linked alginate gels. Biomacromolecules 13:2465–2471

Nešić A, Onjia A, Davidović S et al (2017) Design of pectin-sodium alginate based films for potential healthcare application: study of chemico-physical interactions between the components of films and assessment of their antimicrobial activity. Carbohydr Polym 157:981–990

Newsom EC, Connolly KL, Nehal KS (2015) Facilitating healing of granulating wounds: dressings, dermal substitutes, and other methods. Curr Dermatol Rep 4:125–133

Ng WL, Yeong WY, Naing MW (2017) Polyvinylpyrrolidone-based bio-ink improves cell viability and homogeneity during drop-on-demand printing. Materials 10:190–201

Nieto-Suárez M, López-Quintela MA, Lazzari M (2016) Preparation and characterization of crosslinked chitosan/gelatin scaffolds by ice segregation induced self-assembly. Carbohydr Polym 141:175–183

Orive G, Carcaboso A, Hernandez R, Gascon A, Pedraz J (2005) Biocompatibility evaluation of different alginates and alginate-based microcapsules. Biomacromolecules 6:927–931

Orive G, Tam SK, Pedraz JL, Hallé J-P (2006) Biocompatibility of alginate–poly-l-lysine microcapsules for cell therapy. Biomaterials 27:3691–3700

Otterlei M, Ostgaard K, Skjåk-Bræk G, Smidsrød O, Soon-Shiong P, Espevik T (1991) Induction of cytokine production from human monocytes stimulated with alginate. J Immunother 10:286–291

Pankongadisak P, Ruktanonchai UR, Supaphol P, Suwantong O (2015) Development of silver nanoparticles-loaded calcium alginate beads embedded in gelatin scaffolds for use as wound dressings. Polym Int 64:275–283

Paques JP, van der Linden E, van Rijn CJM, Sagis LMC (2014) Preparation methods of alginate nanoparticles. Adv Colloid Interf Sci 209:163–171

Park SO, Han J, Minn KW, Jin US (2013) Prevention of capsular contracture with Guardix-SG® after silicone implant insertion. Aesthet Surg J 37:543–548

Park H, Lee HJ, An H, Lee KY (2017) Alginate hydrogels modified with low molecular weight hyaluronate for cartilage regeneration. Carbohydr Polym 162:100–107

Pasbakhsh P, De Silva R, Vahedi V, Churchman GJ (2016) Halloysite nanotubes: prospects and challenges of their use as additives and carriers–a focused review. Clay Miner 51:479–487

Passemard S, Szabó L, Noverraz F et al (2017) Synthesis strategies to extend the variety of alginate-based hybrid hydrogels for cell microencapsulation. Biomacromolecules 18:2747–2755

Patel MA, AbouGhaly MH, Schryer-Praga JV, Chadwick K (2017) The effect of ionotropic gelation residence time on alginate cross-linking and properties. Carbohydr Polym 155:362–371

Paul K, Linh NTB, B-r K et al (2015) Effect of rat bone marrow derived–stem cell delivery from serum-loaded oxidized alginate–gelatin–biphasic calcium phosphate hydrogel for bone tissue regeneration using a nude mouse critical-sized calvarial defect model. J Bioact Compat Polym 30:188–208

Pawar SN, Edgar KJ (2012) Alginate derivatization: a review of chemistry, properties and applications. Biomaterials 33:3279–3305

Petchsomrit A, Sermkaew N, Wiwattanapatapee R (2017) Alginate-based composite sponges as gastroretentive carriers for Curcumin-loaded self-microemulsifying drug delivery systems. Sci Pharm 85:11–26

Popa EG, Reis RL, Gomes ME (2015) Seaweed polysaccharide-based hydrogels used for the regeneration of articular cartilage. Crit Rev Biotechnol 35:410–424

Qin Y (2008) Alginate fibres: an overview of the production processes and applications in wound management. Polym Int 57:171–180

Quraishi S, Martins M, Barros AA et al (2015) Novel non-cytotoxic alginate–lignin hybrid aerogels as scaffolds for tissue engineering. J Supercrit Fluids 105:1–8

Radhakrishnan A, Jose GM, Kurup M (2015) PEG-penetrated chitosan–alginate co-polysaccharide-based partially and fully cross-linked hydrogels as ECM mimic for tissue engineering applications. Prog Biomater 4:101–112

Ramsey DM, Wozniak DJ (2005) Understanding the control of *Pseudomonas aeruginosa* alginate synthesis and the prospects for management of chronic infections in cystic fibrosis. Mol Microbiol 56:309–322

Rangaraj A, Harding K, Leaper D (2011) Role of collagen in wound management. Wounds UK 7:54–63

Raposo MF dJ, de Morais RMSC, Bernardo de Morais AMM (2013) Bioactivity and applications of sulphated polysaccharides from marine microalgae. Mar Drugs 11:233–252

Rashaan ZM, Krijnen P, van den Akker-van ME et al (2016) Clinical effectiveness, quality of life and cost-effectiveness of Flaminal® versus Flamazine® in the treatment of partial thickness burns: study protocol for a randomized controlled trial. Trials 17:122–130

Reddy N, Reddy R, Jiang Q (2015) Crosslinking biopolymers for biomedical applications. Trends Biotechnol 33:362–369

Rezvanian M, Ahmad N, Amin MCIM, Ng S-F (2017) Optimization, characterization, and in vitro assessment of alginate-pectin ionic cross-linked hydrogel film for wound dressing applications. Int J Biol Macromol 97:131–140

Rinaudo M (1992) On the abnormal exponents a ν and a D in Mark Houwink type equations for wormlike chain polysaccharides. Polym Bull 27:585–589

Rogers CJ, Clark PM, Tully SE et al (2011) Elucidating glycosaminoglycan–protein–protein interactions using carbohydrate microarray and computational approaches. Proc Natl Acad Sci USA 108:9747–9752

Ronghua H, Yumin D, Jianhong Y (2003) Preparation and in vitro anticoagulant activities of alginate sulfate and its quaterized derivatives. Carbohydr Polym 52:19–24

Rosellini E, Cristallini C, Barbani N, Vozzi G, Giusti P (2009) Preparation and characterization of alginate/gelatin blend films for cardiac tissue engineering. J Biomed Mater Res A 91:447–453

Rossi S, Mori M, Vigani B et al (2018) A novel dressing for the combined delivery of platelet lysate and vancomycin hydrochloride to chronic skin ulcers: hyaluronic acid particles in alginate matrices. Eur J Pharm Sci 118:87–95

Rowley JA, Madlambayan G, Mooney DJ (1999) Alginate hydrogels as synthetic extracellular matrix materials. Biomaterials 20:45–53

Roy D, Cambre JN, Sumerlin BS (2010) Future perspectives and recent advances in stimuli-responsive materials. Prog Polym Sci 35:278–301

Ruvinov E, Cohen S (2016) Alginate biomaterial for the treatment of myocardial infarction: progress, translational strategies, and clinical outlook: from ocean algae to patient bedside. Adv Drug Deliv Rev 96:54–76

Rzaev ZM, Dincer S, Pişkin E (2007) Functional copolymers of N-isopropylacrylamide for bioengineering applications. Prog Polym Sci 32:534–595

Sachan NK, Pushkar S, Jha A, Bhattcharya A (2009) Sodium alginate: the wonder polymer for controlled drug delivery. J Pharm Res 2:1191–1199

Sajesh K, Jayakumar R, Nair SV, Chennazhi K (2013) Biocompatible conducting chitosan/polypyrrole–alginate composite scaffold for bone tissue engineering. Int J Biol Macromol 62:465–471

Samanta HS, Ray SK (2014) Synthesis, characterization, swelling and drug release behavior of semi-interpenetrating network hydrogels of sodium alginate and polyacrylamide. Carbohydr Polym 99:666–678

Sarei F, Dounighi NM, Zolfagharian H, Khaki P, Bidhendi SM (2013) Alginate nanoparticles as a promising adjuvant and vaccine delivery system. Indian J Pharm Sci 75:442–449

Sarker A, Amirian J, Min YK, Lee BT (2015) HAp granules encapsulated oxidized alginate–gelatin–biphasic calcium phosphate hydrogel for bone regeneration. Int J Biol Macromol 81:898–911

Schweiger RG (1962a) Acetylation of alginic acid. I. Preparation and viscosities of algin acetates. J Organomet Chem 27:1786–1789

Schweiger RG (1962b) Acetylation of alginic acid. II. Reaction of algin acetates with calcium and other divalent ions. J Organomet Chem 27:1789–1791

Seeli DS, Dhivya S, Selvamurugan N, Prabaharan M (2016) Guar gum succinate-sodium alginate beads as a pH-sensitive carrier for colon-specific drug delivery. Int J Biol Macromol 91:45–50

Shaari N, Kamarudin SK (2015) Chitosan and alginate types of bio-membrane in fuel cell application: an overview. J Power Sources 289:71–80

Shachar M, Tsur-Gang O, Dvir T, Leor J, Cohen S (2011) The effect of immobilized RGD peptide in alginate scaffolds on cardiac tissue engineering. Acta Biomater 7:152–162

Shah S, Patel C, Trivedi H (1995) Ceric-induced grafting of acrylate monomers onto sodium alginate. Carbohydr Polym 26:61–67

Shao L, Cao Y, Li Z, Hu W, Li S, Lu L (2018) Dual responsive aerogel made from thermo/pH sensitive graft copolymer alginate-gP (NIPAM-co-NHMAM) for drug controlled release. Int J Biol Macromol 114:1338–1344

Shapiro L, Cohen S (1997) Novel alginate sponges for cell culture and transplantation. Biomaterials 18:583–590

Shen W, Hsieh Y-L (2014) Biocompatible sodium alginate fibers by aqueous processing and physical crosslinking. Carbohydr Polym 102:893–900

Shi J, Alves NM, Mano JF (2008) Chitosan coated alginate beads containing poly (N-isopropylacrylamide) for dual-stimuli-responsive drug release. J Biomed Mater Res B Appl Biomater 84:595–603

Shilpa A, Agrawal S, Ray AR (2003) Controlled delivery of drugs from alginate matrix. J Macromol Sci Polym Rev 43:187–221

Shin S-J, Park J-Y, Lee J-Y et al (2007) "On the fly" continuous generation of alginate fibers using a microfluidic device. Langmuir 23:9104–9108

Sibaja B, Culbertson E, Marshall P et al (2015) Preparation of alginate–chitosan fibers with potential biomedical applications. Carbohydr Polym 134:598–608

Simó G, Fernández-Fernández E, Vila-Crespo J, Ruipérez V, Rodríguez-Nogales JM (2017) Research progress in coating techniques of alginate gel polymer for cell encapsulation. Carbohydr Polym 170:1–14

Skjåk-Bræk G, Grasdalen H, Smidsrød O (1989a) Inhomogeneous polysaccharide ionic gels. Carbohydr Polym 10:31–54

Skjåk-Bræk G, Zanetti F, Paoletti S (1989b) Effect of acetylation on some solution and gelling properties of alginates. Carbohydr Res 185:131–138
Smidsrød O, Draget KI (1997) Alginate gelation technologies. In: Dickinson E, Bergenstahl B (eds) Food colloids: proteins, lipids and polysaccharides. Woodhead Publishing Limited, Cambridge, pp 279–293
Smidsrød O, Skja G (1990) Alginate as immobilization matrix for cells. Trends Biotechnol 8:71–78
Sosnik A (2014) Alginate particles as platform for drug delivery by the oral route: state-of-the-art. ISRN Pharm 2014:926157–926164
Sowjanya J, Singh J, Mohita T et al (2013) Biocomposite scaffolds containing chitosan/alginate/nano-silica for bone tissue engineering. Colloids Surf B: Biointerfaces 109:294–300
Straccia MC, d'Ayala GG, Romano I, Oliva A, Laurienzo P (2015) Alginate hydrogels coated with chitosan for wound dressing. Mar Drugs 13:2890–2908
Sumayya A, Muraleedhara Kurup G (2017) Marine macromolecules cross-linked hydrogel scaffolds as physiochemically and biologically favorable entities for tissue engineering applications. J Biomater Sci Polym Ed 28:807–825
Summa M, Russo D, Penna I et al (2018) A biocompatible sodium alginate/povidone iodine film enhances wound healing. Eur J Pharm Biopharm 122:17–24
Sun J, Tan H (2013) Alginate-based biomaterials for regenerative medicine applications. Materials 6:1285–1309
Sweeney I, Miraftab M, Collyer G (2014) Absorbent alginate fibres modified with hydrolysed chitosan for wound care dressings–II. Pilot scale development. Carbohydr Polym 102:920–927
Szekalska M, Puciłowska A, Szymańska E, Ciosek P, Winnicka K (2016) Alginate: current use and future perspectives in pharmaceutical and biomedical applications. Int J Polym Sci 2016:171–175
Szekalska M, Sosnowska K, Zakrzeska A, Kasacka I, Lewandowska A, Winnicka K (2017) The influence of chitosan cross-linking on the properties of alginate microparticles with metformin hydrochloride—*in vitro* and *in vivo* evaluation. Molecules 22:182–202
Szymonowicz M, Kucharska M, Wiśniewska-Wrona M, Dobrzyński M, Kołodziejczyk K, Rybak Z (2017) The evaluation of resorbable haemostatic wound dressings in contact with blood *in vitro*. Acta Bioeng Biomech 19:151–165
Taleb MFA, Alkahtani A, Mohamed SK (2015) Radiation synthesis and characterization of sodium alginate/chitosan/hydroxyapatite nanocomposite hydrogels: a drug delivery system for liver cancer. Polym Bull 72:725–742
Tallawi M, Rosellini E, Barbani N et al (2015) Strategies for the chemical and biological functionalization of scaffolds for cardiac tissue engineering: a review. J R Soc Interface 12 (108):20150254–20150278. https://doi.org/10.1098/rsif.2015.0254
Tally M, Atassi Y (2015) Optimized synthesis and swelling properties of a pH-sensitive semi-IPN superabsorbent polymer based on sodium alginate-g-poly (acrylic acid-co-acrylamide) and polyvinylpyrrolidone and obtained via microwave irradiation. J Polym Res 22:181–193
Tam S, Bilodeau S, Dusseault J, Langlois G, Hallé J-P, Yahia L (2011) Biocompatibility and physicochemical characteristics of alginate–polycation microcapsules. Acta Biomater 7:1683–1692
Tarusha L, Paoletti S, Travan A, Marsich E (2018) Alginate membranes loaded with hyaluronic acid and silver nanoparticles to foster tissue healing and to control bacterial contamination of non-healing wounds. J Mater Sci Mater Med 29:22–35
Thomas E, Wade A, Crawford G, Jenner B, Levinson N, Wilkinson J (2014) Randomised clinical trial: relief of upper gastrointestinal symptoms by an acid pocket-targeting alginate–antacid (Gaviscon Double Action)–a double-blind, placebo-controlled, pilot study in gastro-oesophageal reflux disease. Aliment Pharmacol Ther 39:595–602
Tøndervik A, Klinkenberg G, Aachmann FL et al (2013) Mannuronan C-5 epimerases suited for tailoring of specific alginate structures obtained by high-throughput screening of an epimerase mutant library. Biomacromolecules 14:2657–2666

Tønnesen HH, Karlsen J (2002) Alginate in drug delivery systems. Drug Dev Ind Pharm 28:621–630
Tripathy T, Singh R (2001) Characterization of polyacrylamide-grafted sodium alginate: a novel polymeric flocculant. J Appl Polym Sci 81:3296–3308
Tripathy T, Pandey S, Karmakar N, Bhagat R, Singh R (1999) Novel flocculating agent based on sodium alginate and acrylamide. Eur Polym J 35:2057–2072
Tzankova V, Aluani D, Kondeva-Burdina M et al (2017) Hepatoprotective and antioxidant activity of quercetin loaded chitosan/alginate particles *in vitro* and *in vivo* in a model of paracetamol-induced toxicity. Biomed Pharmacother 92:569–579
Ummarino D, Miele E, Martinelli M et al (2015) Effect of magnesium alginate plus simethicone on gastroesophageal reflux in infants. J Pediatr Gastroenterol Nutr 60:230–235
Unagolla JM, Jayasuriya AC (2018) Drug transport mechanisms and *in vitro* release kinetics of vancomycin encapsulated chitosan-alginate polyelectrolyte microparticles as a controlled drug delivery system. Eur J Pharm Sci 114:199–209
Venkatesan J, Bhatnagar I, Manivasagan P, Kang K-H, Kim S-K (2015) Alginate composites for bone tissue engineering: a review. Int J Biol Macromol 72:269–281
Vijayabaskar P, Babinastarlin S, Shankar T, Sivakumar T, Anandapandian K (2011) Quantification and characterization of exopolysaccharides from *Bacillus subtilis* (MTCC 121). Adv Biol Res 5:71–76
Villani S, Marazzi M, Bucco M et al (2008) Statistical approach in alginate membrane formulation for cell encapsulation in a GMP-based cell factory. Acta Biomater 4:943–949
Wang W, Wang A (2010) Synthesis and swelling properties of pH-sensitive semi-IPN superabsorbent hydrogels based on sodium alginate-g-poly (sodium acrylate) and polyvinylpyrrolidone. Carbohydr Polym 80:1028–1036
Wang L, Khor E, Wee A, Lim LY (2002) Chitosan-alginate PEC membrane as a wound dressing: assessment of incisional wound healing. J Biomed Mater Res A 63:610–618
Wang Q, Jamal S, Detamore MS, Berkland C (2011) PLGA-chitosan/PLGA-alginate nanoparticle blends as biodegradable colloidal gels for seeding human umbilical cord mesenchymal stem cells. J Biomed Mater Res A 96:520–527
Wang Z, Zhang X, Gu J, Yang H, Nie J, Ma G (2014) Electrodeposition of alginate/chitosan layer-by-layer composite coatings on titanium substrates. Carbohydr Polym 103:38–45
Wang K, Nune K, Misra R (2016) The functional response of alginate-gelatin-nanocrystalline cellulose injectable hydrogels toward delivery of cells and bioactive molecules. Acta Biomater 36:143–151
Wassermann A (1948) Alginic acid acetate. Nature 158:197–198
Wathoni N, Motoyama K, Higashi T, Okajima M, Kaneko T, Arima H (2016) Physically crosslinked-sacran hydrogel films for wound dressing application. Int J Biol Macromol 89:465–470
Wichterle O, Lim D (1960) Hydrophilic gels for biological use. Nature 185:117–118
Williams SK, Touroo JS, Church KH, Hoying JB (2013) Encapsulation of adipose stromal vascular fraction cells in alginate hydrogel spheroids using a direct-write three-dimensional printing system. BioRes Open Access 2:448–454
Xie H, Chen X, Shen X et al (2018) Preparation of chitosan-collagen-alginate composite dressing and its promoting effects on wound healing. Int J Biol Macromol 107:93–104
Xu X, Bi D, Wu X et al (2014) Unsaturated guluronate oligosaccharide enhances the antibacterial activities of macrophages. FASEB J 28:2645–2654
Xu W, Shen R, Yan Y, Gao J (2017) Preparation and characterization of electrospun alginate/PLA nanofibers as tissue engineering material by emulsion eletrospinning. J Mech Behav Biomed Mater 65:428–438
Xue Y-T, Li S, Liu W-J et al (2018) The mechanisms of sulfated polysaccharide drug of propylene glycol alginate sodium sulfate (PSS) on bleeding side effect. Carbohydr Polym 194:365–374
Yan Y, Wang X, Xiong Z et al (2005) Direct construction of a three-dimensional structure with cells and hydrogel. J Bioact Compat Polym 20:259–269

Yan G, Guo Y, Yuan J, Liu D, Zhang B (2011) Sodium alginate oligosaccharides from brown algae inhibit *Salmonella Enteritidis* colonization in broiler chickens. Poult Sci 90:1441–1448

Yan X, Rathe F, Gilissen C et al (2014) The effect of enamel matrix derivative (emdogain®) on gene expression profiles of human primary alveolar bone cells. J Tissue Eng Regen Med 8:463–472

Yang J-S, Xie Y-J, He W (2011) Research progress on chemical modification of alginate: a review. Carbohydr Polym 84:33–39

Yang J, Chen J, Pan D, Wan Y, Wang Z (2013) pH-sensitive interpenetrating network hydrogels based on chitosan derivatives and alginate for oral drug delivery. Carbohydr Polym 92:719–725

Yao B, Ni C, Xiong C, Zhu C, Huang B (2010) Hydrophobic modification of sodium alginate and its application in drug controlled release. Bioprocess Biosyst Eng 33:457–463

Yiğitoğlu M, Aydın G, Işıklan N (2014) Microwave-assisted synthesis of alginate-g-polyvinylpyrrolidone copolymer and its application in controlled drug release. Polym Bull 71:385–414

Yu J, Du KT, Fang Q et al (2010) The use of human mesenchymal stem cells encapsulated in RGD modified alginate microspheres in the repair of myocardial infarction in the rat. Biomaterials 31:7012–7020

Yu L, Ni C, Grist SM, Bayly C, Cheung KC (2015) Alginate core-shell beads for simplified three-dimensional tumor spheroid culture and drug screening. Biomed Microdevices 17:33–41

Yu N, Li G, Gao Y, Jiang H, Tao Q (2016) Thermo-sensitive complex micelles from sodium alginate-graft-poly (N-isopropylacrylamide) for drug release. Int J Biol Macromol 86:296–301

Zenobi-Wong M, Palazzolo G, Mhanna R, Becher J, Moller S, Schnabelrauch M (2018) Sulfated alginate hydrogels for cell culture and therapy. Google Patents

Zhang YS, Khademhosseini A (2017) Advances in engineering hydrogels. Science 356:3627–3653

Zhang X, Huang C, Zhao Y, Jin X (2017) Preparation and characterization of nanoparticle reinforced alginate fibers with high porosity for potential wound dressing application. RSC Adv 7:39349–39358

Zhao L, Weir MD, Xu HH (2010a) An injectable calcium phosphate-alginate hydrogel-umbilical cord mesenchymal stem cell paste for bone tissue engineering. Biomaterials 31:6502–6510

Zhao S, Cao M, Li H, Li L, Xu W (2010b) Synthesis and characterization of thermo-sensitive semi-IPN hydrogels based on poly (ethylene glycol)-co-poly (ε-caprolactone) macromer, N-isopropylacrylamide, and sodium alginate. Carbohydr Res 345:425–431

Zhao X, Kim J, Cezar CA et al (2011) Active scaffolds for on-demand drug and cell delivery. Proc Natl Acad Sci USA 108:67–72

Zhao X, Li J, Feng Y et al (2018) Self-aggregation behavior of hydrophobic sodium alginate derivatives in aqueous solution and their application in the nanoencapsulation of acetamiprid. Int J Biol Macromol 106:418–424

Zhou R, Shi X, Gao Y, Cai N, Jiang Z, Xu X (2015) Anti-inflammatory activity of guluronate oligosaccharides obtained by oxidative degradation from alginate in lipopolysaccharide-activated murine macrophage RAW 264.7 cells. J Agric Food Chem 63:160–168

Chapter 17
Nanocellulose Composite Biomaterials in Industry and Medicine

Oded Shoseyov, Doron Kam, Tal Ben Shalom, Zvi Shtein, Sapir Vinkler, and Yehudit Posen

Abstract Cellulose, the most abundant polymer on earth, has merited a remarkable wave of attention, largely revolving around its nanocellulose derivative, a green, easily extractable, high-performance nanomaterial. Its widespread availability, high abundance, renewable nature, biocompatibility, low toxicity, unique structure, and easily tailorable mechanical and physical properties render it an attractive reagent in various sectors. While free of biological activity, nanocellulose presents a versatile platform for fabrication of composite, clinically relevant materials with healing and regeneration capacities. Similarly, its tunable characteristics enable design of smart drug delivery systems and biomimetics. It has also proven a transformative agent in the food packaging and 3D printing industries. The vast potential of nanocellulose continues to emerge and promises to bring to further exciting and novel applications. This chapter provides an overview of the various sources, production, and processing methods of nanocellulose, as well as the chemical modifications used to modify its properties and functions. In addition, its vast applications in the worlds of printing, wound healing, pharmaceutics, and tissue engineering are extensively reviewed.

17.1 Introduction

The availability, easy handling, and good mechanical properties of tree-derived materials have made them a basic material in a variety of disciplines. Their complex hierarchical, composite, multilayered architecture provides them with the ability to withstand nature's harshest conditions. Despite its wide use as a traditional material for furniture and construction, wood is minimally exploited as a bulk material in

O. Shoseyov (✉) · D. Kam · T. Ben Shalom · Z. Shtein · S. Vinkler
Institute of Plant Science and Genetics, The Robert H. Smith Faculty of Agriculture, Food and Environment, The Hebrew University of Jerusalem, Rehovot, Israel
e-mail: Oded.Shoseyov@collplant.com

Y. Posen
PSW Ltd., Rehovot, Israel

E. Cohen, H. Merzendorfer (eds.), *Extracellular Sugar-Based Biopolymers Matrices*, Biologically-Inspired Systems 12, https://doi.org/10.1007/978-3-030-12919-4_17

fields of advanced functional and structural materials, which make extensive use of synthetic polymers and metals. The use of wood as bulk material in industrial fields is limited due to concerns regarding durability, natural heterogeneity, and limitations in functionalization and shape design. Recent works have proposed processes that involve delignification, densification, or hot press transformation to transform wood into high-performance, low-weight bulk material (Nilsson and Rowell 2012; Frey et al. 2018; Li et al. 2018b; Song et al. 2018; Yang and Berglund 2018). The use of and interest in wood design and structure have expanded to encompass nanoscale building blocks fabricated from wood-derived materials.

Nanocellulose is one of the most exciting biomaterials recently made available on a commercial scale. Nanocellulose can be produced from cellulosic raw materials, such as wood pulp, paper waste, flax, cotton, and others (Brinchi et al. 2013; Wang et al. 2013; Tang et al. 2015c). Its green nature and characteristic physical and chemical properties, including a large surface area and high aspect ratio, unique self-assembly capacities and rheological behavior, and nontoxicity and biocompatibility, render it suitable for a wide range of applications. The considerable need for high-performance, biocompatible materials, with relevant mechanical and physical properties, and the growing demand for bio-based substitutes for synthetic petrochemical source materials (Lapidot et al. 2012), have brought nanocellulose center stage, as an attractive renewable material, suitable for many applications in a variety of fields, including food packaging, flexible electronic devices, nanocomposites, thermoplastics polymers, wound healing, tissue engineering, drug delivery, 3D printing, optical devices, smart actuators and sensors, biomedical devices, transparent and flexible materials, surface-sized paper, textile, superadsorbents, and more (Csoka et al. 2012; Li et al. 2013; Nasseri and Mohammadi 2014; Rivkin et al. 2015; Hokkanen et al. 2016; Kaushik and Moores 2016; Meirovitch et al. 2016; Kargarzadeh et al. 2017; Gotta et al. 2018).

The term "nanocellulose" refers to raw cellulosic extracts or processed cellulosic materials, bearing at least one external dimension in the nanoscale range (between 1 and 100 nm). Nanoscale cellulosic materials usually refer to cellulose nanofibrils (CNFs), also referred to as nanofibrillated cellulose (NFC), cellulose nanocrystals (CNCs), also referred to as nanocrystalline cellulose (NCC) or cellulose nanowhiskers (CNWs), and bacterial cellulose (BC) or bacterial nanocellulose (BNC).

Various principles and methods can be applied to extract nanocellulose from a variety of cellulose sources, with CNFs and CNCs usually extracted from a plant cellulose source. The source and production methods dictate the unique structure of each type of nanocellulose, which, in turn, determines functionality, compatibility with other materials, and applicability. For example, exploitation of the ability of *Gluconacetobacter xylinus* to produce composites in situ can be leveraged to generate composite scaffolds for medical devices. The high tensile strength, Young's modulus and gas barrier properties, and the self-assembling behavior of CNCs render them suitable for cosmetics, as a packaging barrier material and as a reinforcement agent for composite materials. The combination of high tensile strength, stiffness and elasticity, gel-forming capacities at low concentrations, and the

thixotropic behavior of CNFs, opens new opportunities for its use as a rheological modifier in coating materials and in the food and printing ink (2D or 3D) industries. The main industrial uses and current and potential applications are detailed later in the chapter.

17.2 Production and Surface Chemistries of Nanocellulose Fibers

17.2.1 Production

In nature, during cellulose synthesis, single cellulose chains assemble to form a composite structure called microfibrils (Delmer and Amor 1995). The long polymeric chains of glucose form a network held together by hydrogen and van der Waals bonds, eventually leading to crystallization of the cellulose in certain areas of the microfibril. These highly organized crystalline domains are linked together by less crystalline "amorphous" regions. The cellulose crystalline areas form tight arrays which protect the glycoside bonds from enzymatic decomposition and, together with the other cell wall components, make the cell wall a very compact and inaccessible material (Young and Rowell 1986; Rose and Bennett 1999; Brett 2000).

In 1949, Rånby described acid hydrolysis/heat-controlled techniques for production of cellulose fibers, which result in degradation of the "amorphous" regions, yielding highly crystalline cellulose micelles (Rånby 1949). In 1959, Marchessault was the first to identify the rod-like shaped nanoparticles (Marchessault et al. 1959). CNC particle dimensions depend on the cellulose source from which they were generated. For example, plant-derived CNCs exhibit a particle dimension range between 5–20 nm in width and 100–500 nm in length. In terms of mechanical properties, the estimated modulus of CNC particles is approximately 150 GPa, and the tensile strength is estimated at ~10 GPa, similar to superstrong materials, such as aramid fibers (Kevlar) and carbon fibers (Šturcová et al. 2005).

Indeed, CNC can be produced either by hydrochloric acid (HCl) (Araki et al. 1999), hydrobromic acid (HBr) (Sadeghifar et al. 2011), or sulfuric acid cellulose fiber hydrolysis, yielding products with different physical and chemical characteristics. More specifically, sulfuric acid grafts negatively charge sulfate half-ester groups on CNC particle surfaces, which prevent aggregation in aqueous suspensions and form concentration-dependent, stable, semitransparent liquid crystals with unique self-assembly behavior (Abitbol et al. 2018). In contrast, CNCs derived from HCl- or HBr-based fiber hydrolysis are uncharged and aggregate over time in aqueous suspensions. Currently, sulfuric acid is the most frequently utilized and beneficial hydrolyzing agent in CNC production processes.

CNFs are nanocellulosic fibers, first discovered in the early 1980s following high-shear grinding of cellulose pulp (Turbak et al. 1983). Since then, the extraction process has been optimized by enzymatic and chemical pretreatment of cellulosic

raw materials to loosen the intrafibril hydrogen bonds, thereby lowering the energy required for their production (Pääkko et al. 2007; Wågberg et al. 2008). Saito and Isogai presented a low-energy method for CNF isolation utilizing TEMPO-based oxidation of cellulose pulps, while other methods combine chemical treatments and mechanical grinding (Saito and Isogai 2004, 2006; Saito et al. 2006, 2007; Chen et al. 2011). Mechanical methods, such as cryocrushing, homogenization, grinding, and microfluidization methods (Moon et al. 2011; Zhou et al. 2012, 2013b), have also been developed.

Unlike CNCs, CNFs contain both amorphous and crystalline cellulose regions, forming 10–40-nm-wide and 10–40-micrometer-long fibers, depending on the production methods used. However, their mechanical properties are different, due to the amorphous domains. Due to their length, CNFs form viscous aqueous suspensions, even at relatively low concentrations.

BCs are produced extracellularly by bacteria, such as *Acetobacter xylinum* (or *Gluconacetobacter xylinum*), or sea creatures, such as *Microcosmus sulcatus*, and form near-perfect mesh-like structures (Favier et al. 1995; Klemm et al. 2005). The Gram-negative *G. xylinum* bacterium is the most efficient cellulose-producing microorganisms. *G. xylinum* is an obligate aerobe that secretes cellulose nanofibers from its terminal complexes that contain cellulose synthase enzymes. Each complex produces 1.5-nm-thick fibers that organize into 3.5–4-nm-thick microfibrils and subsequently assemble into nanofibers. The bacterium produces the BC 3D structure on top of the liquid media surface. This 3D surface, termed a pellicle or nata de coco, serves as a floating surface for the bacteria and has many historical uses in the food industry, as a traditional candy in Asian countries or as thickener and stabilizing agent.

BC is exceptionally pure and metabolically inert, with no traces of lignin, hemicellulose, or other substances. Unlike CNCs and CNFs, BCs do not require pretreatment to remove lignin or hemicellulose before hydrolysis or grinding. BCs are primarily used for a variety of medical applications, including wound healing devices. *G. xylinum*, under exact conditions, extrude fine, non-woven, and 10–100-nm-thick and 10–100-micrometer-long 3D network of nanofibrils (Shpigel et al. 1998; Eichhorn et al. 2010). The fibers have moduli in the range 78–114 GPa (Guhados et al. 2005; Hsieh et al. 2008) and a tensile strength of 2 GPa (Iguchi et al. 2000; Yano 2005).

17.2.2 Surface Chemistries

The uniqueness of nanocellulose compared to micro- or macrocellulose derives mainly from its nanoscale dimension, associated with an extremely high specific surface area, and from its surface reactivity, arising from the relative abundance of free hydroxyl groups, providing a vast surface for surface chemistry modifications (Lin et al. 2012a, b).

Efforts are being invested to improve compatibility of CNFs and CNCs in nonpolar solvents and hydrophobic polymers resins, especially due to the hydrophilic nature of the hydroxyl groups, which interferes with nanocellulose dispersion in hydrophobic matrices (Kovalenko 2014; Abraham et al. 2016b). Redispersion of nanocellulose in nonpolar solvents upon drying can often be achieved using nanocellulose surface functionalization. Various covalent modification options will be discussed in this section, but there are also many possibilities for noncovalent binding (Villares et al. 2015).

The 2,2,6,6-tetramethylpiperidine-1-oxyl (TEMPO)-mediated oxidation method, which selectively modifies hydroxyl groups to carboxylic acids, is a common covalent chemical modification of CNFs and CNCs. This modification leads to more stable nanocellulose suspensions in water and improves redispersion (Carlsson et al. 2014b; Sun et al. 2015; Karim et al. 2017). Periodate oxidation methods introduce aldehydes on the nanocellulose surface. Aldehyde and carboxylic functional groups can form covalent bonds with other functional groups and can be exploited to cross-link between protein or polymer functional groups and CNC (Singla et al. 2017b).

Nanocellulose acetylation, commonly achieved by adding acetic anhydride and acetic acid, in the presence of sulfuric or perchloric acid as a catalyst, is a common nanocellulose hydrophobization method, which improves nanocellulose dispersibility and distribution in organic solvents and in polymer matrices (Rodionova et al. 2011; Habibi 2014; Cheng et al. 2018). Silylation is used to enable nanocellulose dispersion in nonpolar solvents. CNF surfaces are silylated using isopropyl dimethylchlorosilane; fibrils show no damage, and the CNFs easily disperse in organic solvents in a non-flocculating manner (Goussé et al. 2004). Recently, silylated CNF aerogels designed for selective oil removal in water purification processes were developed using hexadecyltrimethoxysilane (HDTMS) and methyltrimethoxysilane (MTMS). The CNF aerogels exhibited solvent absorption capacities and successfully absorbed oil, diesel, kerosene, gasoline (Laitinen et al. 2017).

Click chemistry can also be used to modify nanocellulose. In 2010, Filpponen and Argyropoulos successfully formed CNC nanoplatelet gels via click chemistry using TEMPO-oxidized CNC and carbodiimide mediation (Filpponen and Argyropoulos 2015). Recently, Zhou et al. reported using click chemistry methods to enhance the thermal stability and hydrophobic properties of CNC, via grafting polycaprolactone diol (PCL diol) onto CNC surfaces (Zhou et al. 2018).

Cationization of nanocellulose promises to give rise to innovative applications, particularly in drug delivery, vaccine adjuvants, tissue engineering, and many other bio-applications (Sunasee and Hemraz 2018). Etherification via (2,3-epoxypropyl) trimethylammonium chloride (EPTMAC) can serve as a CNC cationization agent in the presence of sodium hydroxide (Hasani et al. 2008). Non-covalent methods also allow for surface cationization via physical adsorption of cationic polyethylenimine polymer to CNC (Lin et al. 2016). Recently, injectable cationic CNC-based hydrogels were designed via etherification of CNCs with 3-chloro-2-hydroxypropyl-trimethylammonium chloride (CHPTAC) (You et al. 2016). Polymer grafting techniques, which can be classified as "grafting onto" and "grafting from,"

can also be used for cationic modification (Hemraz et al. 2014, 2015). Polymer grafting is an efficient means of producing nanocellulose-polymer composites, as the graft chains improve both inter-chain associations and associations between the polymer chains and nanocellulose, which enhance the strength and stress transfer of the composite material (Abitbol et al. 2016; Pickering et al. 2016; Kargarzadeh et al. 2017). Nanocellulose grafting with polystyrene, via surface-initiated atom transfer radical polymerization (SI-ATRP), and its successful dispersion in the PMMA matrix, improve the thermal and mechanical properties of the polymer (Yin et al. 2016), as well as of poly(n-butyl acrylate) and poly(2-(dimethylamino) ethyl methacrylate) brushes on CNF surface (Morits et al. 2017).

Urethanization is an efficient means of enhancing nanocellulose hydrophobicity; isocyanate (n-octadecyl isocyanate) reacts with available hydroxyl groups on the nanocellulose surface, to form a strong urethane linkage (Siqueira et al. 2010; Habibi 2014; Liu et al. 2015). Recently, BNC was used to synthesize polyurethane foams and was shown to react with isocyanate, which improved the thermomechanical properties of polyurethane nanocomposite foams (Gimenez et al. 2017).

Amidation using 4-amino-TEMPO (Follain et al. 2010), benzylamine, hexylamine, dodecylamine, and Jeffamine (Lasseuguette 2008) or 1-Ethyl-3-(3-dimethylaminopropyl) carbodiimide (EDAC) hydrochloride is a less common approach for nanocellulose functionalization (Habibi 2014). CNF surface modification with amine groups using 4-(Boc-aminomethyl)phenyl isothiocyanate can be applied to graft a wide range of commercially available molecules that contain carboxylic acid groups (Wang et al. 2010a).

17.3 Processing of Cellulose into Nanocomposite Materials

17.3.1 Solvent Casting

Solvent casting is the method most commonly used to produce cellulose nanocomposites. Nanocellulose-polymer nanocomposites can be processed in both aqueous and nonaqueous solutions. CNCs disperse well in aqueous solutions, which allows for extensive use of aqueous media, primarily in film casting and fiber wet spinning processes (El Miri et al. 2015; El Achaby et al. 2017; Vollick et al. 2017). Nanocellulose-polymer processing in nonaqueous polar solutions can be achieved with DMF, DMSO, NMP, or a mixture of solvents. This approach usually involves intermediate steps, such as solvent exchange or the use of solvents with good interaction with water THF (tetrahydrofuran). In such media, cellulose surface modification or coating with surfactant is necessary to avoid agglomeration (Mariano et al. 2014). The modified cellulose nanomaterials can then be effectively dispersed in nonpolar liquid media and mixed with the corresponding polymer solution prior to casting and evaporation (Girouard et al. 2016; Dufresne 2018). Casting and evaporation of PVA-CNC composite films have been reported to increase thermal stabilities and improve modulus compared to neat PVA films.

Tanpichai and Oksman described increased tensile strength and modulus (111.4 MPa and 3.9 GPa, compared to 94.7 and 3.2 GPa, respectively) of borax-cross-linked PVA films upon addition of 3 wt % CNCs. In addition, the crystallization temperature of the cross-linked PVA with CNCs increased considerably from 152 °C to 187 °C (Tanpichai and Oksman 2018). Popescu showed H-bond interactions between PVA chains and CNC in composite matrices, resulting in conformational changes, as well as increased crystallite size and decreased crystallinity, indicating a reinforcing effect of CNC (Popescu 2017).

17.3.2 Melt Processing

Extrusion, compression molding, and injection molding are the methods most commonly used to design and process polymer-based material. Processes involve high temperatures and do not involve solvents. To overcome self-aggregation upon drying, as well as the temperature limitations of cellulose nanoparticles, pretreatment, e.g., the use of surfactants, chemical modifications, and freeze-drying, is required.

Amphiphilic molecule, containing both hydrophobic and hydrophilic ends, can be added as a surfactant material in aqueous cellulose dispersions to coat the cellulose nanoparticles. Such coatings prevent irreversible aggregation, improve thermal stability, and allow for dispersion and extrusion of polymer-cellulose composites, e.g., polystyrene PLA and (polypropylene) PP, at 190–200 °C. A more stable approach for melt processing of such composite materials involves physical coating that can prevent surfactant detachment from the nanoparticles during the melt processing, which occurs due to the extreme shear force of the process. Freeze-dried PEO-coated CNC successfully formed nanocomposites with LDPE, polystyrene (PS), and PLA in the melt process. The nanocellulose is coated with polar polymers with affinity for hydroxyl end groups of the composite polymer and allows interaction and dispersion within the composite (Pereda et al. 2014; Dufresne 2017, 2018). However, weak interactions between CNC and the coating polymer cause movement and separation of the polymer from the nanoparticles during the melt processing, which can induce CNC self-aggregation (Lin and Dufresne 2013; Pereda et al. 2014). Recently, stronger surface interactions between the surface –OH groups of the CNC and epoxide-terminated PEO, under highly alkaline conditions, were reported to improve stress transfer in the CNC-epoxide composite (Kargarzadeh et al. 2017; Inai et al. 2018).

Overall, many works have demonstrated the potential in incorporating nanocellulose in composite with polymers. Solvent casting and evaporation result in improved properties when forming nanocellulose composite. Melt processing is the most widely used method in industry but still remains with several challenges (Aitomäki and Oksman 2014).

17.4 Nanocellulose as a Reinforcing Agent in Polymer Composites

Incorporation of nanocellulose in matrix materials can affect mechanical, thermal, crystalline, optical, and other properties. Cellulose-polymer composites can be prepared from a variety of polymers, including rubber, thermoset polymers, such as epoxy resins, and unsaturated polyester (Abraham et al. 2016a; Bayer et al. 2016; Fan and Fu 2017). Well-established methods of polymer molding, solvent casting, melt processing, and resin impregnation with nanocellulose are the most common processes used in the polymer industry and in formation of cellulose-polymer nanocomposites (Oksman et al. 2016). Many works have described integration of CNC and CNF in polymer composites (Yuan Lu et al. 2003; Chen et al. 2018). For example, Sinclair et al. showed that nanofiber-based reinforcement of poly(ethylene oxide) polymer matrices significantly increased the tensile modulus and yield strength of the nanocomposites, by up to 154% and 103%, respectively (Sinclair et al. 2018). Aitomäki and Oksman presented a theoretical model for evaluation of the reinforcement efficiency of cellulose nanoparticles in composites (Aitomäki and Oksman 2014). According to the theoretical model and literature, they showed that the presence of nanocellulose in the polymer matrix is advantageous to soft matrices, but suggested that composites with stiffer matrices benefit less from the effect of nanocellulose reinforcement. Their work suggested that much of the stress transfer in strong nanocellulose composites heavily depends on the presence of a strong nanocellulose-polymer network and underscored the importance of plastic deformation in the nanocellulose composites. Koon-Yang Lee et al. also showed that better dispersion of individual cellulose nanoparticle in the polymer matrix can improve composite properties, including tensile modulus and strength (Lee et al. 2014).

17.4.1 Challenges in Use of Nanocellulose as an Industrial Reinforcing Material

The highly hydrophilic nature of nanocellulose, limiting its adhesiveness and dispersion in nonpolar matrices, alongside its high moisture absorption capacities and low thermal stability, requires low processing temperatures that limit industrial processing and polymer melting (Dufresne 2018). Moreover, owing to the large number of H-bonds formed by surface hydroxyl groups and the high specific surface area, during drying processes, the cellulose CNC and CNF particles agglomerate and reorganize into structures which are irreversible without external force. Dry cellulose materials required in melt processing techniques, present dispersing problems and suffer from low mechanical properties of the resulting composites (Siqueira et al. 2009). In order to use nanocellulose as a reinforcing agent, it is crucial to avoid agglomeration. Drying can be minimized by using water soluble matrices or performing solvent exchange to an organic solvent. Alternatively, chemical modifications or addition of small amounts of a judiciously selected polymeric dispersant

that also serves as a binder between the CNCs, such as PVA, can prevent agglomeration and increase the distances between CNC/CNF particles (Khoshkava and Kamal 2014; Meesorn et al. 2017).

17.5 3D Printing

Additive manufacturing (AM) is a bottom-up process that constructs 3D objects by adding layer by layer of materials. In this rapidly growing field, biomaterials have inspired the scientific community to replicate and reverse-engineer naturally occurring elements, in both their composition and 3D architecture. As mentioned, cellulose is the most abundant mechanical "brick" in the plant kingdom, where its three-dimensional architecture plays a key role in the remarkable properties of plants. Thus, various attempts have been made to apply cellulose in AM.

AM is generally performed using one of four central techniques: material extrusion, vat polymerization, material jetting, and laminated object manufacturing. Laminated object manufacturing is a well-known process in the wood industry and dates back to the late nineteenth century. Nanocellulose in its various forms is used in the preparation of glue-laminated and cross-laminated timber or in other newly developed lamination techniques. The four main AM processes can be divided into two sub-processes: 3D printing and lamination. This section will focus on AM in the context of 3D printing, and readers interested in further details on lamination are referred to an extensive review on the topic (Ansell 2015).

17.5.1 Material Extrusion

Extrusion-based 3D printing extrudes a material through a nozzle, where each printed layer is the substrate of the one printed above it. The printed ink must be rapidly fixated so it can withstand the printed material deposited above it, eventually yielding a 3D structure. Currently, this form of 3D printing is common, due to its simplicity and cost-effectiveness. The extrusion can be in the form of direct ink writing (DIW), where material is driven out by a controlled syringe, or by fused deposition molding (FDM), where solid filament material is heated to liquefaction and then rapidly fixated by cooling (thermoplastic behavior).

17.5.2 Direct Ink Writing (DIW)

The ability to extrude material in a DIW process relies on the shear thinning property of the applied suspension. In shear thinning, stress is applied by the piston of a syringe, which decreases viscosity of the suspension and allows the material to flow

out of the nozzle. As the suspension exits the nozzle, no stress is applied and viscosity increases. In DIW, meeting these rheological property requirements is essential to enable printing of subsequent layers without structure collapse during printing. These rheological requirements explain the extensive use of CNC and CNF in DIW-based printing.

As CNC particles suspend well in aqueous environments, interparticle cross-linking is necessary to preserve the 3D structure of materials printed with CNC-based inks. Chi-Fung et al. demonstrated DIW with pure, high-concentration (>11.8 wt.%) CNC, which fully gelled and maintained its shape (Chi-Fung et al. 2017). The group used a freeze-casting technique to physically cross-link the particles, which led to sublimation of water, enabling transformation of the hydrogel into an aerogel. Khabibullin et al. achieved DIW by physically cross-linking the surface hydroxyl and sulfate half-ester groups of CNC to carboxylic graphene quantum dots (GQDs), yielding a hydrogel (Khabibullin et al. 2017). The described approach took advantage of the dual function of the cross-linker. The GQDs served as a cross-linker, stabilizing the CNC hydrogel, and introduced GQD photoluminescence, resulting in a fluorescent hydrogel. In another approach, CNC served as a reinforcing agent in calcium-alginate-gelatin hydrogels (Sultan and Mathew 2018), acting as a rheological modifier during extrusion and as an agent that preserved the printed structure throughout the printing process. Then, posttreatment with calcium and glutaraldehyde physically cross-links the printed product to preserve the structure.

In addition to printing with high-concentration, pure CNC, Siqueira et al. overcame cross-linking challenges by modifying CNC surfaces with methacrylic anhydride that provides vinyl functionality and the possibility of interactions between monomers and oligomers via photopolymerization (Siqueira et al. 2017). Such use of organic solvents then required solvent exchange of DMF to ethanol/isopropanol. CNF, as opposed to CNC, is highly viscous at low concentrations, which limits its printability to solutions of up ~2.5 wt%. As with CNC inks, the addition of different materials to CNF may preserve CNF shear thinning properties, enabling previously unprintable materials to be printed. For example, mixing different ratios of CNF/alginate increases CNF shear thinning rheology, which can be DIW intro structures that can then be cross-linked with calcium chloride to yield alginate hydrogel properties (Markstedt et al. 2015). Before cross-linking, the rheology of aqueous alginate solutions is not sufficient to preserve shape fidelity during printing, although viscosity can be controlled over a wide range by tuning the alginate concentration.

Hydrogels can be preserved in the aqueous state or post-processed (or solidified) for dry applications. Håkansson et al. investigated four post-processing techniques for 2 wt.% CNF DIW-printed structures (Håkansson et al. 2016). Air-drying the structure led to uneven shrinkage and shape loss, while the addition of surfactants also led to uneven shrinkage but preserved some features of the printed structure. Solvent exchange to ethanol-acetone-hexane provided no benefit over the original water phase, while freezing and lyophilizing the printed structure resulted in a porous structure without loss of its external dimensions.

Gladman et al. printed plant-inspired structures using a mixture of 0.73% CNF with clay and a UV-cross-linkable *N*,*N*-dimethylacrylamide (DMAm) or *N*-isopropylacrylamide (NIPAm) monomers (Gladman et al. 2016). In their work, CNFs were aligned by the printing nozzle to obtain a 3D structure, and then immersed in water to allow swelling and shaping. The group demonstrated the ability to fuse a precise macrodesign with nanomaterial "bricks," exploiting the full potential of the 3D printing technology.

Markstedt et al. printed a hydrogel structure by mixing CNF with modified xylan functionalized with tyramine (Markstedt et al. 2017). Tyramine-driven functionalization enables cross-linking of the structure upon its submergence in a 1% hydrogen peroxide bath for 10 min. In this work, 2.5–3.5 wt.% CNF concentration exhibited printability, while cross-linking occurred at >5 wt.% xylan.

17.5.3 Fused Deposition Molding (FDM)

Thermoplastic filaments are in wide use in 3D printing, in general, and in the extrusion-based technique, in particular. Currently, the extensive filament lifetime and the simple printing concept of heating and cooling are the main reasons for the extensive use of this technique. FDM-oriented research efforts primarily seek to improve the mechanical properties of printed structures and to enlarge filament material variety. Although CNC is not a polymer, two attempts have been made to manufacture CNC-reinforced filaments and to apply them to print a 3D structure via FDM. Acrylonitrile butadiene styrene (ABS) is one of the most abundant filaments in the field of 3D printing and was the first to be reinforced by lignin-coated CNC (Feng et al. 2017). To manufacture a thermoplastic filament, ABS and lignin-coated CNC were extruded separately at 180 °C and then cut and extruded together at 200 °C, while the FDM printing was executed at 210 °C. The printed filament showed a foaming effect, resulting in lighter objects and preferable mechanical properties as compared to bare ABS. Later, Rigotti et al. used CNC to reinforce PVA (Rigotti et al. 2018). In their work, the dried (a key factor to obtaining a good printable filament) CNC-PVA suspension was extruded at 175 °C and printed at 230 °C. The addition of CNC improved the thermal stability and stress at break of PVA.

17.5.4 Vat Polymerization

In the vat polymerization technique, photopolymer resin in a vat is selectively cured (polymerized) by a light source. In this technique, a reservoir of ink is placed in a bath with a transparent bottom to allow entrance of UV light. A platform is lowered to the bottom of the bath, leaving a layer height space. Then, light is shone to cure selected points according to the 3D design. The platform is elevated after each layer is polymerized, allowing the unpolymerized ink to settle again before the next layer

is printed. In this technique, the 3D model is printed upside down on a platform. This technique requires UV-curable and, therefore, UV-transparent ink. Stereolithography (SLA) and digital light processing (DLP) are among the lead methods of vat polymerization printing. The two techniques differ by their light-emitting device, with a laser used in SLA and a projected image with DLP.

For CNC-based, UV-curable ink, there are two main straightforward strategies to print via vat polymerization: modification of the CNC particle so that it can play an active role in the polymerization reaction or suspension of CNC in water-soluble photopolymerized polymers which can then interact with the CNC particle. CNC has low solubility in solvents in which the majority of UV functional modifications occur, limiting modification of CNC. Usually, freeze-dried CNC is modified by suspending it in DMF, followed by solvent exchange to toluene-acetone-ethanol. The final rod might then loose its ability to be suspended back in water, depending on the number of modified chemical groups and the reaction.

To apply aqueous CNC suspensions in 3D printing via vat polymerization, monomers, cross-linkers, and photoinitiators (PIs), must also be soluble in water, where the solubility of the latter currently presents one of the greatest limitations in water-based inks. Currently, the most water-soluble PI is Irgacure 2959, which has an absorption peak at 275 nm, incompatible with the 356 nm UV light source of common 3D printers, subsequently reducing Irgacure 2959 efficiency and extending printing time. Lithium phenyl-2,4,6-trimethylbenzoylphosphinate (LAP) is a recently available PI, while new approaches for synthesizing other water-soluble PIs are being investigated (Pawar et al. 2016). The new PIs remain to be fully tested but provide early solutions for 3D photopolymerization printing using water-based suspensions.

Palaganas et al. suspended CNC (1.2 wt%) with PEGDA, which served as a monomer and cross-linker, and LAP, which served as a PI, to print a 3D structure using the SLA technique (Palaganas et al. 2017). CNC was loaded up to 1.2 wt.% and provided neither any mechanical nor any significant structural improvement, but set the stage for SLA-printed cellulose. Wang et al. used the DLP technique to print with ink comprised of modified CNC rods, cross-linked to a hydrogel net via bis (acyl)phosphane oxides (BAPOs), PEGMEM as a monomer and Irgacure 2959 as a PI (Wang et al. 2018a). Young's modulus increased as more CNC was added, similar to the effect of reinforced hydrogel with CNC.

17.5.5 Material Jetting

Material jetting or powder bed 3D printers use a dry, solid material to print 3D structures. The printing can be achieved by combining "glue" from an ink-jet head or by selectively heating the solid particle. Currently, there are no works describing integration of cellulose nanomaterials in the printing process, but this technique has recently attracted much attention after HP announced its multi-jet fusion 3D printer.

While heating wood material is a challenging process, ink jetting is a simple process that can easily be applied to CNC. The ability to ink jet material lies in the ability to tune viscosity to low viscosities (<15 cP), so the ink can be fully suspended and flow through a micron-sized nozzle in response to pulse pressure build from the ink chamber.

17.5.6 Exotic Printing Technique

Because of the vast open-source software and the large industry of 3D printers, custom 3D printers can be designed to address new and interesting printing concepts that do not fall into standard categories. Prince et al. combined a microfluidic head with a controlled stage to print a gelatin-CNC hydrogel (Prince et al. 2018). Aldehyde-modified CNCs are pumped with gelatin into a microfluidic device on a moving substrate, resulting in an imine-cross-linked hydrogel film. The direction of the extrusion aligns the particles, while manipulation of the CNC-gelatin ratio results in different morphology states, pore sizes, and mechanical properties. Although this technique is not officially considered 3D printing, the 2D printing approach enables controllable hydrogel mixing that could result in a new 3D printing methodology.

17.6 Nanocellulose in Medical Devices

17.6.1 Wound Healing

Wound healing is a dynamic process that involves the complex interaction of various cell types, extracellular matrix (ECM) molecules, and soluble compounds. Typically, normal wound healing progresses through a series of processes including homeostasis, inflammation, tissue granulation, and tissue remodeling (Eming et al. 2002).Wound dressings are an essential component in the clinical treatment of burns, ulcers, and wounds, playing a central role in accelerating the re-epithelization rate, reducing pain, and preventing contaminations. The ideal wound dressing must (1) maintain a moist environment at the wound surface and thus enhance re-epithelialization and reduce scar formation; (2) serve as a physical barrier against bacterial infections; (3) demonstrate a high exudate absorbance capacity, hence shortening the inflammatory phase; (4) be simple to use, (5) inexpensive, (6) sterile, and (7) available in a variety of shapes and sizes; (8) allow for easy and painless removal; (9) reduce pain during treatment via specific interaction with nerve endings; (10) be a porous structure for gaseous and fluid exchange; (11) be non-toxic, non-pyrogenic, and biocompatible; and (12) be highly conformable, elastic, and mechanically stable (Czaja et al. 2007).

17.6.1.1 Bacterial Cellulose

BC presents ideal properties for wound dressing applications, including hydrophilicity, hydrogel properties, eternal hydration, high elasticity and conformability, and a high water vapor transmission rate. Wet BC membranes provide wound beds with moisture levels ideal for wound healing and tissue regeneration and, at the same time, absorb exudates from the wound. In addition, the BC membrane is a highly nano-porous material, which can support transfer of antibiotics or other materials directly into the wound. BC membranes serve as a barrier, protect the wound/burn from contaminations, and are nontoxic, non-pyrogenic, biocompatible, and inexpensive (Czaja et al. 2006). BC dressing films have been shown to reduce inflammation and accelerate cell adhesion and proliferation, thereby promoting tissue regeneration (Fu et al. 2013). A clinical study in Poland demonstrated that second-degree burns treated with hydrated BC membranes healed faster than those treated with conventional wound dressings (Czaja et al. 2006, 2007). Another study concluded that BC dressing-treated wounds showed a reduced degree of inflammation, enhanced collagen deposition and neovascularization, and an accelerated healing process, as compared to those treated with Vaseline gauze (Park et al. 2012). Full-thickness skin wounds in mice treated with BC films demonstrated biocompatibility and good proliferation of human adipose-derived stem cells (hASCs). In addition, significantly more fresh tissue regeneration and capillary formation, which correlated with accelerated healing and a reduced inflammatory response in the wound area, were shown in the BC group compared to the groups treated with cotton gauze (Fu et al. 2012).

BC is being investigated worldwide in an array of wound dressing applications, and several commercial BC-based wound dressings have been approved and are commercially available. Studies assessing the utility of Biofil® as a temporary human skin substitute in over 300 patients, demonstrated that it brings to immediate pain reduction, diminishes post-surgery discomfort, demonstrates water vapor permeability, adheres well to wounds, protects wounds against infections, is easy to handle, provides for easy inspection of wounds, due to its transparency, accelerates healing, improves exudate retention, and reduces treatment time and costs (Fontana et al. 1990; Czaja et al. 2007). Nanocell® is a commercially available BC wound dressing that acts as a barrier against bacterial contamination without inducing irritation or allergic reactions during treatment (Muangman et al. 2011). Bionext® and Membracell® are two additional commercially available BC-based wound dressings that mimic the extracellular matrix, leading to enhanced epithelialization (Fadel Picheth et al. 2017).

Recently developed nanocomposites for wound healing applications demonstrated improved properties and functionalities as compared to neat BC. These include BC/collagen (Zhijiang and Guang 2011; Moraes et al. 2016), a composite shown to feature better mechanical properties, to enable cell adhesion and proliferation and markedly higher cytocompatibility than pure BC (Zhijiang and Guang 2011). The composite was shown to significantly reduce the levels of several proteases and interleukins, as well as reactive oxygen species (ROS) activity in the

wound environment, and possess distinct antioxidant capacities as well, which is particularly advantageous in chronic wound management (Wiegand et al. 2006). BC/chitosan composites demonstrate properties which are beneficial in comparison to pure BC wound dressings, including improved dry- and wet-state mechanical properties, a higher water-holding capacity, a slower water release rate, improved biocompatibility, and broad antimicrobial activity. These properties are particularly beneficial in treating burns, skin ulcers, hard-to-heal wounds, and wounds requiring frequent dressing changes (Ciechańska 2004; Ul-Islam et al. 2011). BC/chitosan composites elicited no cytotoxicity in vivo, and treated wounds showed faster epithelization and regeneration as compared to those treated with unmodified BC (Lin et al. 2013a). When the BC/chitosan composite was incubated with lysozyme solution, the composite chitosan degraded to mono- and oligosaccharides, which stimulate angiogenesis and tissue regeneration (Ciechańska 2004). Microporous oxidized BC (MOBC) in situ grafted with arginine, formed a novel biocomposite which exhibited better biocompatibility and promoted proliferation, migration, and expression of collagen I in human dermal fibroblasts and human umbilical vein endothelial cells, as compared to pure BC. In addition, the composite was more effective than non-modified BC (Qiao et al. 2018).

Owing to their reactive and large surface area and nano-porous structure that enables absorption, interaction, and later release of a variety of active molecules, BC wound dressings can also act as drug delivery system (Chen and Huang 2015; Sulaeva et al. 2015). For improved wound dressing applications, BC can bind and release (1) analgesic drugs, (2) healing-promoting growth factors, stem cells, and ECM components, and (3) antimicrobial and antiseptic agents. The BC membrane has been applied as a drug delivery system for analgesics, such as diclofenac, lidocaine HCl, and ibuprofen (Trovatti et al. 2012). BC membranes can be easily loaded with diclofenac sodium, using glycerol as plasticizer, yielding a system that demonstrates higher swelling behavior when compared to pure BC, a feature fundamental in rehydration when in contact with the skin, in the rate of diclofenac release, and in their ability to absorb exudates when applied to injured skin. The drug permeation rate from the impregnated BC membrane was similar to that of a commercial patch of diclofenac sodium salt patch (Olfen® 0.5% (w/w) diclofenac (Mepha Lda, Porto Salvo, Portugal) (Silva et al. 2014b)). Delivery of wound healing-promoting drugs, such as growth factors and stem cells, has also been shown with BC-based materials. In uninfected wounds, oxidized BC membranes coated with chitosan and alginate layers and incorporating epidermal growth factor (EGF) exhibited sustained release of EGF, a factor required for normal wound repair. The nanopolymeric layers can rapidly undergo architectural transitions triggered by infection stimuli, which allow for burst release of EGF to the wound. Thus, the system serves as both a wound dressing and local delivery platform, responsive to infection status (Picheth et al. 2014).

A variety of growth and extracellular matrix (ECM) factors, mixed with alginate and incubated with a BC membrane, have been shown to form semi-penetrate hydrogels that allowed for diffusion of the impregnated components under physiological conditions. h-EGF (growth factor)-modified BC and collagen-modified BC

hydrogels have been shown to support the growth of human skin fibroblasts, were biocompatible and degradable under the tested physiological conditions, and demonstrated a gradual release profile, indicating the potential of using this composite as a vehicle for delivery of therapeutic compounds during wound healing (Lin et al. 2011a).

Stem cell therapy has proven to be an effective option in the treatment of skin injuries. A novel healing-enhancing approach combines BC membranes with mesenchymal stem cells. A recent study demonstrated that loading adipose-derived stem cells on a BC membrane in the presence of gellan gum with fluconazole, to treat a murine model skin burn, allowed for cell expansion and migration to the injury site and enhanced tissue repair (Souza et al. 2014). BC/acrylic acid (AA) composite films embedded with human epidermal keratinocytes and dermal fibroblasts supported cell attachment, allowed for cell transfer, and maintained cell viability in vitro. In an in vivo study of athymic mice bearing a full-thickness skin wound treated with this composite, accelerated healing was shown, indicating that this composite has a potential for dual application as a cell carrier and wound dressing material (Loh et al. 2018).

BC-based antibacterial dressings can be impregnated with several types of materials which display antibacterial activity: (1) inorganic compounds (Wu et al. 2014b; Shao et al. 2015a, c), (2) peptides (Basmaji et al. 2014), (3) biological and synthetic polymers (Ul-Islam et al. 2011; Jiang et al. 2014; Figueiredo et al. 2015), (4) antibiotics (Rouabhia et al. 2014; Türkoglu 2014; Ye et al. 2018), and (5) cationic antiseptics (Wei et al. 2011; Barud et al. 2013; Kukharenko et al. 2014; Moritz et al. 2014). In light of its effective antibacterial, antifungal, and antiviral properties, integration of silver (Ag) in wound dressings bears great healing-promoting potential. BC/Ag films are the most promising and investigated BC/inorganic metal-based composite and can be generated by several techniques, using various chemical and molecular modifications. Several works have reported its broad antimicrobial activity and low cytotoxicity, as well as adherence and proliferation of fibroblasts, reduced inflammation, and accelerated wound healing (Maneerung et al. 2008; Maria et al. 2010; Wu et al. 2014a, 2018; Tabaii and Emtiazi 2018). When prepared in a composite with BC, silver sulfadiazine, the gold standard agent used in topical burn treatment, induced significant epithelialization, antimicrobial activity, and biocompatibility (Luan et al. 2012). Other inorganic materials, such as zinc oxide (Katepetch et al. 2013; Khalid et al. 2017a), titanium dioxide (Khan et al. 2015; Khalid et al. 2017b), copper (Araújo et al. 2018), gold (Li et al. 2017), and montmorillonite (clay mineral) (Ul-islam et al. 2013), showed antibacterial behavior when incorporated with BC membranes and, hence, are promising composites for treatment of infected wounds. Zinc oxide nanoparticles dispersed in BC sheets also demonstrated antimicrobial activity, significant burn healing, and accelerated epithelization. In addition, new hair follicles and new blood vessels were seen near the wound area (Khalid et al. 2017a). A recent work reported that a BC-titanium dioxide composite exhibited beneficial wound healing properties in a rat burn wound model, as measured by high antimicrobial activity, good wound contraction, enhanced re-epithelization, and formation of healthy granulation tissue, as compared to pure BC (Khalid et al. 2017b). Similarly, natural polymers, such as

chitosan and chitin, exhibit antimicrobial activity and, when mixed with BC, form an effective antimicrobial wound dressing (Ul-Islam et al. 2011; Jiang et al. 2014; Figueiredo et al. 2015).

Many studies have investigated integration of antibiotics in BC wound dressings and have demonstrated promising outcomes. For example, loading chloramphenicol, a broad-range antibiotic, onto oxidized BC membranes, provided a prolonged antimicrobial effect and improved adhesion and proliferation of fibroblasts (Türkoglu 2014). Gentamycin loaded onto BC films by chemical grafting, using a coupling agent that covalently binds gentamycin, exhibited bactericidal activity and was nontoxic to human dermal fibroblasts (Rouabhia et al. 2014). A recent study demonstrated that regenerated BC grafted with amoxicillin had antibacterial activity, accelerated wound healing in vivo, and was nontoxic (Ye et al. 2018).

BC films immersed in benzalkonium chloride solution, which is a cationic surfactant that has antimicrobial properties, showed high water-absorbing capacity and at least 24 h of antimicrobial activity, especially against *Staphylococcus aureus* and *Bacillus subtilis*, which are general Gram-positive bacteria that are found on contaminated wounds (Wei et al. 2011). BNC composites loaded with antiseptic materials, such as povidone-iodine (PI) and polyhexanide, showed antimicrobial activity, with the BC/PI composite demonstrating slow release, a property that can be beneficial in chronic wound management (Wiegand et al. 2015). CELMAT® Wound/Eye/Face P is a commercially available hydrated, antiseptic wound dressing loaded with polyhexanide, indicated for treatment of chronic wounds and burns (Ludwicka et al. 2016). Octenidine-loaded BNC dressings showed a time-dependent biphasic release profile of octenidine, with a rapid release in the first 8 h, followed by a slower release rate up to 96 h. In a long-term storage test, the octenidine loaded in BNC was found to be stable, releasable, and biologically active over a period of 6 months without changes, rendering it a suitable, ready-to-use wound dressing for the treatment of infected wounds that can be stored over 6 months without losing its antibacterial activity (Barud et al. 2013; Moritz et al. 2014).

Chemical modification of BC surfaces has also been proven an effective means of ensuring prolonged antimicrobial activity and preventing wound contamination by dead bacterial cells and endotoxins (Sulaeva et al. 2015). For example, introduction of nitrogen-containing groups on the BC surface can mimic the antimicrobial activity of chitosan, whose intrinsic antimicrobial activity arises from the amino groups along its polymer chains (Fernandes et al. 2013; Jiang et al. 2014). Various other chemical modification approaches are being researched, including introduction of triazine derivatives containing quaternary ammonium and multi-cationic benzyl groups (Hou et al. 2009) or addition of N-containing functional groups to the BC surface (Jampala et al. 2008; Hou et al. 2009). The most novel and promising method generates functional hydrophobic sites on the BC surface, which capture bacterial cells. The microorganisms are removed during dressing exchange, reducing risk of colonization, without enhancing inflammation arising from dead cell debris (Butcher M 2011).

Dressing biodegradability is of critical importance, as it gives way to ingrowth of natural tissue (Petersen and Gatenholm 2011). Several modifications aiming to enhance biodegradation have been tested, including oxidation of BC membranes

(Li et al. 2009; Luo et al. 2013), incorporation of cellulose enzymes into BC films (Hu and Catchmark 2011a, b), and incorporation of *N*-acetyl glucosamine (NAcG) into BC, through genetically engineered bacterial strains, which decreased crystallinity and improved degradability of BC membranes compared to unmodified BC (Yadav et al. 2010). Addition of cellulose enzymes yielded a biodegradable BC, with a tensile strength and extensibility similar to those of human skin, suggesting its potential application in wound dressings (Hu and Catchmark 2011a, b).

17.6.1.2 Cellulose Nanocrystals

CNC is an emerging material in the wound healing field and has attracted much interest in recent years. Its application in wound dressings is generally in combination with other materials. Upon addition of CNC, chitosan-polyethylene oxide composites showed increased tensile strength, tensile modulus, and O_2/CO_2 transmission and had no cytotoxic impact on adipose-derived stem cells and, hence, have been flagged as promising candidates for wound healing (Naseri et al. 2015). CNC dressings can also promote coagulation processes in bleeding wounds (Cheng et al. 2017a). Oxidized CNC/alginate composite films and sponges demonstrated excellent hemostatic efficiency and are fully biodegraded within 3 weeks, without eliciting an inflammatory reaction. The hemostatic effect was ascribed to the carboxyl functionalization on the CNC surface, which contributed to significant absorption of blood plasma on the material surface, rendering it more effective in promoting platelet aggregation and in inducing erythrocytes to accelerate blood clotting (Cheng et al. 2017a).

CNC can be loaded with antibacterial materials for advanced dressing applications. CNC films incorporating curcumin and applied to diabetic wounds showed stable curcumin release, which plateaued after 36 h. The dressing demonstrated antibacterial activity, accelerated healing, and improved the regeneration of hair follicles and sebaceous glands (Tong et al. 2018). Complexes of porous collagen (Coll)-CNC composite scaffolds loaded with both curcumin and gelatin microspheres (GMs) demonstrated sustained curcumin release and antibacterial activity in vitro and accelerated dermis regeneration and prevented local inflammation when applied to full-thickness burn infections (Guo et al. 2017). A CNC-Ag composite tested as a wound dressing for diabetic or full-thickness wounds, led to reduced pro-inflammatory cytokine levels, full wound recovery, elevated collagen and growth factor expression, improved re-epithelization and vasculogenesis, and measurable antimicrobial activity and water absorption capacities (Singla et al. 2017c). CNC dispersed in chitosan films with Ag nanoparticles/curcumin demonstrated accelerated complete healing of excision wounds in albino rats, with no reports of skin irritation (Bajpai et al. 2017). A recent study described antibacterial collagen (Coll)/CNC scaffolds, doped with gentamycin sulfate (GS), which was absorbed in gelatin microspheres (GMs). Release tests showed sustained GS release, low cellular cytotoxicity, and antibacterial activity (Zhu et al. 2018). CNC-reinforced hydrogels containing poly(N-isopropylacrylamide) (PNIPAAm) exhibited properties that were

dependent on the amount of incorporated CNC; the thermal stability decreased, and the mechanical properties improved as CNC content rose. The thermo-responsive gel featured a volume phase transition temperature (VPTT) in the range of 36–39 °C, which is close to normal human body temperature. Metronidazole loaded on the hydrogel underwent burst release at room temperature, and slow and sustained release at 37 °C. This composite is a promising wound dressing with antibacterial activity (Zubik et al. 2017). CNC/alginate hydrogel consisting of a double-membrane system of cationic CNC (CCNC) and anionic alginate, was designed to incorporate different drugs in each hydrogel membranes: ceftazidime hydrate (CH) antibiotics in the external membrane (pure alginate) and EGF in the internal membrane (CCNC and alginate). The system enabled different release rates, with rapid drug release from the outer hydrogel, and prolonged drug release from the inner hydrogel, and complex drug co-delivery, i.e., rapid release of antibiotic and then sustained release of growth factor. This hydrogel is suitable as a wound dressing and for oral drug delivery applications (Lin et al. 2016).

A recent work reported on a novel drug and plasmid DNA (pDNA) dual delivery system, fabricated, by electrospinning, a dispersion composed of polyethyleneimine-carboxymethyl chitosan/pDNA-angiogenin (ANG) nanoparticles, curcumin (Cur), poly (D, L-lactic-co-glycolic acid) (PLGA), and CNCs. The composite was designed to provide antioxidant, antitumor, anti-inflammatory, and antibacterial activity (Cur) and to stimulate blood vessel formation (ANG), thereby promoting wound repair. An initial release burst of Cur (24 h) was followed by a slower release rate that lasted for up to 144 h, while ANG showed prolonged and sustained release. The composite stimulated tissue ANG expression, improved mature vessels density, and significantly enhanced healing of infected full-thickness burn wounds (Mo et al. 2017).

Recent development of an intelligent wound dressing integrated a protease sensor, to target chronic wounds which characteristically present high levels of proteolytic enzymes, such as neutrophil elastase. The biosensor dressing was composed of a nanocellulosic transducer surface, to which a fluorescent elastase tripeptide or tetrapeptide biomolecule was immobilized, to selectively act upon human neutrophil elastase present in fluid of chronic wounds. The detected neutrophil elastase levels can serve as an early predictor of outcome and to gauge the healing process (Fontenot et al. 2017).

17.6.1.3 Cellulose Nanofibers

CNF has also benefited from increasing popularity in wound healing studies conducted in recent years. CNF is biodegradable, absorbs and retains moisture, and can form three-dimensional structures (hydrogels, aerogels, or films). In addition, CNF films are smooth and translucent and have been shown to successfully reduce bacterial growth (Powell et al. 2016; Jack et al. 2017). A CNF-based wound dressing was shown to shorten healing time and accelerate epithelization, as compared to the commercial lactocapromer-based Suprathel® wound dressing, without eliciting allergic or inflammatory responses. The CNF dressings attached easily to

wound beds, remained in place until the wound healed, and also detached from the skin by itself after wound healing (Hakkarainen et al. 2016).

Composites and modified CNF exhibit properties which can further enhance wound dressing applications. TEMPO-CNF can form films, which demonstrate biocompatibility, marked fluid-absorbing capacities, and translucency (Rogstad Nordli et al. 2016). Addition of PEG to CNF improved the mechanical properties of the dressing in wet conditions mimicking the wound environment, rendering the dressing more flexible, ductile, and comfortable (Sun et al. 2017). CNF films cross-linked by calcium or copper ions demonstrated antimicrobial activity and barrier properties (Basu et al. 2018). In addition, calcium ion-cross-linked CNF demonstrated solid-like behavior, a moist environment suitable for a variety of wound types, non-cytotoxicity, and biocompatibility, suggesting its great potential in healing advanced wounds (Basu et al. 2017). Another device mixed CNF with calcium peroxide (CPO), with or without catalase, to release oxygen or hydrogen peroxide, respectively. While the catalase-free CNF/CPO composite reduced L-929 fibroblast attachment and proliferation, CNF/CPO composites prepared with catalase, which converts hydrogen peroxide to oxygen, accelerated cell proliferation. These findings indicate that hydrogen peroxide and oxygen release from CNF-based materials can be modulated and applied for wound sterilization and wound healing acceleration (Chang and Wang 2013). Alternatively, chemical modification of CNF surfaces can trigger antimicrobial activity. Amino-modified CNF (6-deoxy-6-trisaminoethyl-amino (TEAE) CNF) showed antimicrobial activity when integrated with PVA nanofibers (Roemhild et al. 2013).

CNF can also serve as a drug delivery system, releasing drugs directly to the wound to advance the healing process. Oxidized CNF features a polyanionic surface and thus exhibits pH-responsiveness, swelling to a significantly higher degree in neutral and alkaline conditions, compared to acidic environments (pH 3). This feature can be of utility for controlled and intelligent release of antibacterial components into chronic wounds, which are characterized by alkaline environments (pH, 7.15–8.9) (Chinga-Carrasco and Syverud 2014). A recent report demonstrated that tetracycline HCl loaded on polydopamine in composite with TEMPO-oxidized CNF, can be released on demand upon near-infrared (NIR) exposure or at low pH. In addition, the study showed that this composite has a positive synergistic effect on wound healing in vivo, an extended drug release profile, antibacterial properties, biodegradability, and biocompatibility, marking it a promising composite for wound healing and drug delivery (Liu et al. 2018b). CNF threads applied to suture wounds can serve as a stem cell carrier, releasing cells to the wound and accelerating the healing process. Glutaraldehyde-driven chemical modification of CNF threads containing human adipose mesenchymal stem cells (HASCs) applied to suture wounds demonstrated high mechanical strength in both wet cell cultures and under surgical conditions. In addition, HASCs adhered, migrated, and proliferated on the CNF while preserving their bioactivity, providing a xenogeneic-free tool for delivering stem cells into injured areas in a precise manner that might be useful to reduce postoperative inflammation and help in the treatment of chronic wounds (Mertaniemi et al. 2016). Venlafaxine (an analgesic drug used to treat neuropathic

pain) and tetracycline (antibiotic) were loaded on CNF films for simultaneous delivery to diabetic foot ulcers. The CNF film proved an appropriate carrier for co-delivery of the two drugs (Cheginia and Meamar 2018).

17.6.2 Dental/Oral

BC is the leading nanocellulose family member used for dental applications. One of its earliest applications was in the form of Gengiflex®, a membrane applied to stimulate guided tissue regeneration, a surgical process performed in order to prevent soft fibrous tissues from infiltrating the healing wound and to accelerate healing rates (Czaja et al. 2007). Gengiflex® is composed of an internal layer of a pure BC network and an external, chemically modified alkali-cellulose layer. Owing to the unique properties of BC, the membrane is strong, rigid, and biocompatible (Novaes et al. 1993). When integrated in osseointegrated implants, the non-reabsorbing Gengiflex® membrane serves as a physical barrier and contributes to regeneration of damaged periodontal tissues (Jonas and Farah 1998). More specifically, Gengiflex® prevents fibroblast cell growth inside the defect and isolates incised oral epithelial cells and gingival connective tissue from the treated root canal while allowing bone and osseous cells to proliferate and to create new bone (Macedo et al. 2004; Czaja et al. 2007). Dogs with periodontal disease that were treated with Gengiflex® showed faster and complete healing compared to non-treated dogs (Novaes et al. 1993). Two studies demonstrated that Gengiflex® has lower efficacy than expanded polytetrafluoroethylene (ePTFE) membranes in guided bone tissue regeneration. In vitro tests revealed that both materials supported the attachment, migration, and differentiation of osteoblast-like cells. However, while in vivo tests in rats showed a similar amount of new bone formation in both groups, Gengiflex® membranes induced a significantly greater inflammatory response, and bone regeneration was predominantly endochondral, in contrast to ePTFE, which induced direct bone formation (intramembranous ossification) (Salata et al. 2001). Similarly, osseous, 8-mm-diameter defects in the hind foot of adult rabbits treated with PTFE barriers, were completely repaired, within 3 months, while incomplete lamellar bone formation and inflammation were detected in defects treated with the Gengiflex® membrane (Macedo et al. 2004).

A BC/alginate sponge composite developed as a temporary bandage for, and to accelerate wound healing of oral mucosa wounds, contains a dense outer layer which prevents bacterial infection and dehydration of the wound, while the inner porous layer is supportive, providing mechanical strength and allowing for wound exudate drainage. In vivo biocompatibility tests demonstrated that this composite enhanced cell proliferation and was nontoxic (Chiaoprakobkij et al. 2011).

When tested as a scaffold for dental tissue regeneration, BC, brought to increased cell viability and adhesion over time (Olyveira et al. 2013). A bilayered polylactic-co-glycolic acid (PLGA)/multiwall carbon nanotube (MWNT)-BC composite membrane tested for its efficacy in repairing maxillary canine periodontal defects in

beagle dogs, was associated with histologically identified periodontal tissue regeneration, indicating its potential applications in periodontal disease (Zhang et al. 2018). BC proved superior to paper point, a plant cellulose conventionally used to dry and sterilize the dental root canal. More specifically, BC allowed for higher solution and residue absorption, maintained its tensile strength after absorption of root canal fluid or blood, and showed higher expansion, higher compatibility, and higher cumulative release of impregnated drugs (Yoshino et al. 2013).

Addition of BC nanowhiskers to commercial mineral trioxide aggregates (MTA) accelerated the hardening processes of MTA cement and demonstrated good biocompatibility (Jinga et al. 2014). A recent study concluded that addition of small amounts of CNC to commercial dental glass ionomer cement (GIC) notably improved the mechanical properties of GIC, as manifested by higher elastic modulus and compressive strength and lower mass. In contrast, addition of cellulose microfibers to GIC had little impact on mechanical properties (Silva et al. 2016). BC powder mixed with silicate cement powders sustained cell survival and promoted cell proliferation in vitro, demonstrating its applicative potential in dentistry (Voicu et al. 2017).

17.6.3 Drug Delivery

Cellulose and its derivatives are frequently used in drug delivery systems as thickeners, binding agents, emulsifiers, film formers, surfactants, stabilizers, lubricants, and suspending agents (Onofrei and Filimon 2016). Nanocellulose and its derivatives are also used as drug excipients and drug delivery matrices, yielding advanced drug-loaded systems, which enable administration of insoluble drugs in nanoparticle formulation (Fakes et al. 2009; Valo et al. 2013). The surface charge and modifications of nanocellulose largely dictate its interactions with drug nanoparticles, while the drug release rate is controlled by the structure and interactions between the drug nanoparticles and the cellulose matrix (Valo et al. 2013).

17.6.3.1 Bacterial Cellulose

The high purity, biocompatibility, and unique structure and mechanical properties of BC, alongside its ability to adhere to irregular skin surfaces, proven efficacy in wound healing, high skin tolerance, and swelling capacity following chemical modification, stand as significant advantages in topical drug delivery systems. For example, BC membranes loaded with caffeine showed extended and predictable caffeine release over time, indicating its potential as a transdermal drug delivery systems for treating cellulite (Silva et al. 2014a). BC can also be used for oral drug administration. When applied as a carrier of berberine hydrochloride and berberine sulfate, BC significantly extended drug release time compared to commercial carriers. This effect was ascribed to the structure of BC, the dissolution media, and the

solubility of the drug. The system demonstrated pH-responsiveness, with the lowest release rate observed in simulated gastric fluid solution, and the highest release rate in simulated intestinal fluid (Huang et al. 2013).

BC hydrogel can bind and release macromolecules, such as proteins. A study demonstrated controlled uptake and release of albumin by BNC, a profile which can be modified with pretreatment, such as freeze-drying, which lowers albumin uptake (Müller et al. 2013). Proteins loaded on BNC films preserved their bioactivity both after loading and release, indicating the ability of BNC to stabilize and protect immobilized drugs and proteins. For example, the activity and structure of luciferase were preserved during binding and upon release from BC hydrogels (Müller et al. 2013).

A study testing BC as a single excipient-based oral drug delivery system for famotidine or tizanidine, exhibited immediate drug release irrespective of the drug's aqueous solubility and concentration and drying method of BC. In conventional formulations, similar release profiles were only achieved upon addition of a number of excipients, multiprocessing steps, more labor, and utilization of time, expensive machinery, and energy (Badshah et al. 2017). BC matrices loaded with poorly water-soluble famotidine or highly water-soluble tizanidine, followed by modification with acetic anhydride and drying in oven (simple operation and low cost), released most of the drug (despite difference in aqueous solubility) in the initial 0.25 h, without showing any drug retention effect. In contrast, freeze-dried famotidine-loaded BC matrices demonstrated a slower release rate. It was observed that freeze-dried formulations have shown a superior drug-sustaining effect as compared to oven drying for relatively low aqueous soluble drug, i.e., famotidine, indicating that the surface modification and processing procedures effectively control the drug release properties of BC (Badshah et al. 2018).

BNC powder showed a higher bulk density, better flowability, easy fragmentation of particles and rearrangement at a lower compression load, less elastic recovery and a higher tensile strength than microcrystalline cellulose (e.g., Avicel® 101), and overall improved BNC processability in tablet and capsule formulations (Kulkarni et al. 2012). BC aerogels maintain a steady structure, feature a high surface area for binding active molecules, prevent drug nanoparticle aggregation, and provide for controlled drug release. BC aerogel can be prepared by drying BC with supercritical CO_2, rendering the pore network fully accessible for drug loading. This system can by fully rewetted without collapsing. Dexpanthenol and L-ascorbic acid loaded on BC aerogels demonstrated loading release kinetics controlled by the thickness of the gel and the solute concentration in the loading bath (Haimer et al. 2010).

BC can act as a film-coating agent on tablets, being applied using a spray-drying technique. It was found that BC exhibits excellent ability to form soft, flexible, and foldable films and is associated with better mechanical properties, lower cost, and better film-forming properties than existing film-coating agents (Mohd Amin et al. 2012a). Application of BC in the preparation of capsule shells was associated with an immediate release drug profile. However, addition of cellulosic polymers as a release retardant led to sustained release, with the capsule shells remaining buoyant for up to 12 h in a pH 1.2 solution (Ullah et al. 2017).

BC composites can also serve as a platform for advanced drug delivery systems. pH-sensitive drug release of ibuprofen loaded onto composite films of poly(vinyl alcohol)-chitosan-bacterial cellulose (PVA-chitosan-BC) was reported, with drug release rate decreasing with increasing BC content (Pavaloiu et al. 2014). A novel graphene oxide/BC nanocomposite demonstrated better biocompatibility and ibuprofen-carrying capacities than neat BC. In addition, the drug release was pH-sensitive, with the release behavior being more sustainable for graphene oxide/BC as compared to BC (Luo et al. 2017). Poly(*N*-methacryloyl glycine)/BNC composites demonstrated good thermal stability and mechanical properties and high uptake capacities, as well as nontoxic behavior. When loaded with diclofenac sodium (DCF), the composite demonstrated pH-responsiveness; DCF was retained in the nanocomposites at pH 2.1 and released at pH 7.4 (Saïdi et al. 2017). BC/alginate films exhibited three-fold higher doxorubicin-loading capacity, as well as higher surface area, pore volume, and pore size as compared to BC. When compared to the free doxorubicin, doxorubicin loaded on BC-alginate scaffolds more effectively decreased the cell viability of HT-29 human colorectal adenocarcinoma cells and exhibited stable release for 14 days (Cacicedo et al. 2016).

Stimuli-responsiveness tests found bacterial cellulose-g-poly-(acrylic acid) hydrogels both cytocompatible and nontoxic upon oral administration. Bovine serum albumin (BSA) loaded on the hydrogels underwent cumulative release of less than 10% in acidic environments, indicating that this hydrogel can protect BSA against degradation in the stomach. In addition, the hydrogel maintained and preserved BSA structure and bioactivity and enabled increased BSA penetration across the intestinal mucosa (Ahmad et al. 2014). Electron beam radiation was applied to control release of drugs carried by BC/acrylic acid hydrogels and demonstrated higher swelling at lower doses of electron beam radiation, with maximal release achieved at pH 7 (Halib et al. 2010). The same behavior was observed for tetracycline encapsulated in electron beam-irradiated BC matrices, which showed a slower drug release rate compared to non-irradiated membranes (Stoica-Guzun et al. 2007)

Controlled pore functionalization of a BC membrane using a molecularly imprinted polymer (MIP) layer synthesized with a specific binding site for *S*-propranolol, enabled enantioselective loading and release of *S*-propranolol, indicating its potential for chiral applications (Bodhibukkana et al. 2006). In addition, when formulated in conjunction with a conducting polymer (e.g., polyaniline) and a drug entity, BC can act as an electrically stimulated drug delivery device (Lin et al. 2013b). A novel microfiber consisting of a hydrogel core of BC and a conductive polymer shell layer of poly(3,4-ethylenedioxythiophene) (PEDOT), with diclofenac sodium (DCF) loaded in the core layer, demonstrated effective control of DCF release by an external electric field. The hybrid was successfully cultured with PC12 neural cells and provided a cell growth-supportive environment. The electrical stimulation can also be applied to mediate cell orientation, suggesting a flexible template for the reconstruction of electrically responsive tissues mimicking muscle fibers or nerve networks (Chen et al. 2017). BC/sodium alginate hybrid hydrogels loaded with ibuprofen exhibited dual-stimuli release responsiveness, with the swelling ratio shifting in accordance with the electric field, or pH, with alkaline conditions

allowing for faster and acidic conditions for slower release. Electro-responsive hydrogels may offer unique advantages for on-demand release of drug molecules from implants or transdermal drug delivery systems (Shi et al. 2014).

17.6.3.2 Cellulose Nanocrystals

While CNC exhibits mechanical properties, high surface area, reactive surface, porosity, and biocompatibility appropriate for formulation of drug delivery systems, its surface charge impacts the stability of loaded drugs (Carlsson et al. 2014a). A study demonstrated that CNC can bind significant amounts of water-soluble, ionizable drugs, such as tetracycline and doxorubicin, which were subsequently released within 1 day. Surface modifications of CNCs with cetyltrimethylammonium bromide (CTAB), to increase the zeta potential, enabled loading of significant amounts of hydrophobic drugs, e.g., docetaxel, paclitaxel, and etoposide, which then underwent controlled release over a 2-day period; cell uptake was also observed (Jackson et al. 2011). The "grafting to" method was used to modify CNC with the biodegradable polymer propargyl-terminated poly(ethyl ethylene phosphate), resulting in a high negative charge, which allowed for doxorubicin (DOX) binding via electrostatic interactions. These DOX-loaded nanocrystals were successfully internalized into HeLa cells, and DOX was released due to the disruption of the electrostatic interaction in the acidic environment inside the tumor cells. The CNC-based carrier showed good biocompatibility toward both HeLa cells and L929 cells, with average cell viabilities above 90%, even at high carrier concentrations (Wang et al. 2015b). Polyethylenimine (PEI) covalently bound to CNC and subsequently loaded with siRNA elicited no cytotoxicity, protected siRNA from degradation, and enhanced its delivery into the cells. The delivered siRNA (siRNA killer) successfully silenced the expression of cell cycle genes and induced apoptotic cell death, indicating its potential as an antitumor drug delivery system (Ndong Ntoutoume et al. 2017). Poly-(propylene imine) (PPI)-grafted CNC conjugated to folic acid (FA) demonstrated higher doxorubicin-loading capacity, as compared to FA-free complexes. Both FA-conjugated and nonconjugated nanostructures showed more rapid release of doxorubicin when media pH was lowered. Yet, nonconjugated structures showed higher cumulative drug release as compared to FA-conjugated systems (Golshan et al. 2017). Folate receptor-positive cancer cells demonstrated significantly higher uptake of folic acid-conjugated CNC, as compared to folic acid-free CNC, indicating its potential as a drug targeting platform (Dong et al. 2014). An intelligent antitumor gene delivery system consisting of modified CNC with cleavable poly(2-(dimethylamino)ethyl methacrylate) (PDMAEMA) side chains, can bind plasmid DNA (pDNA) via electrostatic interactions and interact well with the negatively charged cell membrane, bringing to internalization of the complex into target cells. Upon reduction, PDMAEMA is cleaved and pDNA is released, subsequently initiating death of transformed cells (Hu et al. 2015, 2016a). CNC can also be used as a reinforcing agent. PLA nanofibers mixed with CNC, as a reinforcing agent, and PEG, as a compatibilizer, exhibited a high drug-loading capacity and

biocompatibility and improved mechanical strength; the loaded tetracycline hydrochloride underwent sustained release (Yu et al. 2017). Supramolecular cyclodextrin/triblock polymer EPE hydrogels incorporating CNC demonstrated higher modulus, increased stability, and no additional cytotoxicity compared to the hydrogel without CNC. BSA proteins loaded on the hydrogel exhibited sustained release, with CNC reducing the diffusion rate of BSA proteins, hence acting as both a reinforcing agent as well as a controlled release excipient (Zhang et al. 2010). A CNC/sodium alginate microsphere-based controlled drug release system improved the mechanical properties of sodium alginate and resulted in more consistent swelling patterns, higher encapsulation efficiency, pH-responsiveness, and a promising sustained release profile for theophylline, the model drug (Lin et al. 2011a). CNC and chitosan layer-by-layer-assembled films loaded with doxorubicin hydrochloride and the water-insoluble curcumin showed sustained release of both drugs at physiological conditions. However, at acidic pH, higher curcumin concentrations were released, which can be advantageous in the low-pH tumor environment (Mohanta et al. 2014).

A recent study tested the applicability of a CNC delivery system in ocular procedures. The system, which incorporated chitosan-poly(acrylic acid) nanoparticles and CNC in PVA lenses, and a fluorescent marker as a drug model, demonstrated extended drug release and nanoparticle disintegration in the presence of physiological concentrations of lysozyme, which triggered chitosan hydrolysis (Åhlén et al. 2018).

CNC can serve as a co-stabilizer to improve flow properties, stability, and physicochemical properties of polymeric excipients. Acrylic beads, synthesized by suspension polymerization using CNC as a co-stabilizer, demonstrated a narrower size distribution, smaller bead sizes, higher flow rate, and nontoxic activity, indicating CNC potential as an excipient in tablet matrices (Villanova et al. 2011). In addition, the good fluidity, good absorbance abilities, and consistently rapid disintegration and dissolution of CNC render it an effective disintegrator at low concentrations in tablet formulations. Carbonate calcium tablets containing CNC exhibited faster disintegration compared to tablets formulated with other known disintegrators (Wang et al. 2015a). CNC can also be applied to modulate hard capsule properties and degradation time (Hamdan et al. 2018).

17.6.3.3 Cellulose Nanofibers

CNF can act as a matrix, providing for sustained drug release over several weeks, and as a film, with immediate release of poorly soluble drugs (Löbmann and Svagan 2017). Furthermore, the use of structured nanofibrillar cellulose (CNF) from various sources and subjected to various modifications, can improve the control of drug release. In addition, the porous structure and large reactive surface area of CNF enable it to interact efficiently with a variety of active molecules and prevent drug nanoparticle aggregation (Valo et al. 2013). Beclomethasone dipropionate (BDP) nanoparticles coated with amphiphilic/hydrophobic proteins (used to facilitate drug nanoparticle binding to CNF) and integrated into aerogels prepared from CNF of

different origins showed that although the aerogels were chemically similar, the release profiles varied with CNF origin, ranging from immediate to sustained release (Valo et al. 2013). CNF aerogels loaded with bendamustine hydrochloride showed tensile strength and swelling tendency suitable for oral drug delivery and a pH-responsive release profile, with higher drug release at pH 7.4 as compared to pH 1.2. In addition, an in vivo assessment demonstrated a 3.25-fold increase in drug bioavailability compared to the oral bioavailability of the pure drug solution (Bhandari et al. 2017).

Anionic CNF (ACNF) hydrogels loaded with small molecules, including metronidazole, nadolol, or ketoprofen, or with FITC-dextran, lysozyme, or BSA (high molecular weight compounds), demonstrated sustained drug release, with kinetics varying between the drugs. For large molecules, the diffusion coefficients were significantly smaller when ACNF content was increased, while for small molecules, ACNF content only moderately impacted diffusion coefficients. In addition, freeze-drying did not affect the drug release properties from redispersed ACNF hydrogels, indicating that these systems can be stored in the dry form and only redispersed when needed (Paukkonen et al. 2017a).

Spray-dried CNF microparticles loaded with indomethacin, metoprolol tartrate, or verapamil demonstrated sustained drug release over a period of 2 months, with kinetics varying in accordance with drug solubility in the medium and their affinity to the CNF matrix (Kolakovic et al. 2012a). In another study, itraconazole nanoparticles coated with hydrophobin infusion proteins coupled to CNF demonstrated that the CNF matrix provided protection of the drug nanoparticles during the formulation process and storage. In addition, the matrix increased the storage stability and the dissolution rate of itraconazole, due to the formation of an immobilized nano-dispersion, which enhanced the in vivo performance of the drug (Valo et al. 2011).

Porous sponges were obtained by cross-linking TEMPO-oxidized CNF with branched polyethylenimine (bPEI) in the presence of different amounts of citric acid. When tested for its potential as a carrier of amoxicillin (AM) and ibuprofen (IB), the sponge effectively absorbed both drugs. Interestingly, samples cross-linked in the presence of citric acid showed slower release kinetics in aqueous environments than materials cross-linked without citric acid (Fiorati et al. 2017).

Metastases pose a significant challenge to successful treatment in cancer. Nanofibers can mimic the structure of extracellular matrices and limit cancer cell migration when implanted in and around tumors. Moreover, they can be designed to locally release anti-metastatic drugs such as metformin. Metformin loaded on CNF surfaces exhibited fast release within the first hour, followed by slower and sustained release. In a migration assay using transwell plates, CNF gels loaded with metformin significantly suppressed the migration and invasion of melanoma cells (Nurani et al. 2017). Alternatively, DOX-loaded CNF gels can be injected for localized chemotherapy of melanoma and for physical prevention of melanoma cell migration across the CNF barrier. CNF-DOX demonstrated sustained release and proved more cytotoxic against melanoma cancer cells than free DOX (Alizadeh et al. 2018). A novel hydrogel formulated for anticancer drug delivery relies on the self-assembly of

positively charged, partially deacetylated α-chitin nanofibers (α-DECHN) and negatively charged 2,2,6,6-tetramethylpiperidine-1-oxyl (TEMPO)-oxidized cellulose nanofibers (TOCNF). The hydrogel showed the highest degree of physical cross-linking when composed of a α-DECHN/TOCNF ratio of 40%/60%, which also demonstrated the highest 5-fluorouracil loading efficiency when compared to other tested ratios (Xu et al. 2018).

CNF can also act as a coating material. Paper samples immersed in caffeine and then coated with CNF allowed for sustained and prolonged release of caffeine as compared to non-coated paper samples, marking it a potential agent for smart packing and drug delivery devices (Lavoine et al. 2014).

Comparative assessments of the tableting potential of spray-dried CNF versus commercial microcrystalline cellulose (MCC) (Avicel) showed that CNF has better packing qualities, which can be attributed to the smaller particle size of CNF powder and its spherical shape and lower powder porosity than MCC. CNF demonstrated good flow properties, and tableting with CNF was achieved by both wet granulation and direct compression (Kolakovic et al. 2011).

CNF is suitable for pharmaceutical emulsion formulations, as shown in a recent study investigating a novel biopolymer-based, oil-in-water emulsion formulation for encapsulation and release of the poorly water-soluble model compounds, naproxen and ibuprofen. The group used a surfactant (Class II hydrophobin protein) to stabilize the oil/water interface and CNF as a viscosity modifier to further stabilize the emulsions and encapsulate protein-coated oil droplets in a CNF network. In vitro drug release studies demonstrated that when integrating oxidized CNF, sustained release was obtained, while native CNF provided for immediate drug release (Paukkonen et al. 2017a, b).

Additional studies assessing the applicability of NC in drug delivery systems will be necessary to further characterize its influence on and regulation of drug release, interactions with drugs (Kolakovic et al. 2013), and the stability and functionality of drugs (Tables 17.1, 17.2 and 17.3).

17.7 Tissue Engineering

Tissue engineering techniques harnessed to rectify damaged tissue and organs are proving to be a viable alternative to transplantation, prosthetics, and surgical intervention. The scaffold, a 3D cell culture system that provides geometrical and biological conditions for cell attachment and growth, is an essential component in tissue engineering. Therefore, scaffolds must be designed to provide the microenvironment that cells require to proliferate, migrate, and differentiate (Salgado et al. 2013). Scaffolds must be biocompatible and bear a structure that closely resembles the natural extracellular structure. In addition, they must have a highly porous microstructure with interconnected pore networks to allow for cell ingrowth and reorganization, appropriate surface chemistry, and controlled degradation. It has been found that when the scaffold has a nanoscale morphology, cell attachment,

Table 17.1 Commercially available nanocellulose-based products

Commercial product name	Medical indication
Bacterial cellulose	
Wound dressing	
Biofill®	Temporary substitute for human skin
Bioprocess®	Dressing for burns and ulcers
Gengiflex®	Dressing for dental ulcers and implants
Xcell®	Wound dressing
Xcell® + PHMB	Antimicrobial wound dressing
Nanocell®	Wound dressing
Dermafill™	Translucent cellulose membrane dressing
NexFill®	Wound and burns dressing
Suprasorb® Xb	Wound dressing for non-infected wounds
Suprasorb® Xb + PHMB	Antimicrobial wound dressing for infected, or at risk of infection, wounds
CELMAT®Wound/Eye/Face	Hydrated wound dressing
CELMAT®Wound/Eye/Face H	Hydrated wound dressing with sodium hyaluronate
CELMAT®Wound/Eye/Face P	Antiseptic hydrated wound dressing with polyhexamine
Bionext®	Wound dressing
Membracell®	Wound dressing
Cardiovascular implants	
BASYC®	Artificial blood vessel
XYLOS™ Vessel Guard	Cover for vessels during anterior vertebral surgery
Surgical mesh	
Xylos ® Macro-porous surgical mesh	Implantation to reinforce and protect soft tissue
Securian ™ Tissue Reinforcement Matrix	Management and protection of soft tissues and tendon injuries
MTA ™ Surgical Sheet	Management and protection of tendon injuries
BioCelltrix	Surgical mesh for hernia repair and pelvic floor reconstruction
Dura replacement	
SyntheCel®	Dura replacement device
Cellulose nanofibers	
GrowDex	Hydrogel for advanced cell culture studies

proliferation, and matrix component expression are increased (Pattison et al. 2005). In addition, nanoscale scaffolds possess a larger surface area for the attachment of proteins and present many more binding sites for cell membrane receptors compared to microscale scaffolds. The nanoscale topography, porosity, pore size, pore interconnectivity, surface area to volume ratio, and composites can influence the phenotype, orientation, behavior, motility, and surface antigen display of embedded cells (Stevens 2005). Engineered scaffolds have been designed to bear mechanical properties similar to those of native tissue, for example, hard scaffolds for application in the bone and elastic for use in the bladder, veins, and arteries (Stevens 2005). The

Table 17.2 Nanocellulose-based composites for wound dressing

Composite	Preparation method	Properties	References
Bacterial cellulose			
Wound dressing			
Collagen	Immersion, mixing, addition of collagen to the culture medium	Good mechanical properties, enables cell adhesion and proliferation, reduces inflammation, and exhibits faster healing time and skin repair compared to collagen only	Wiegand et al. (2006), Zhijiang and Guang (2011) and Moraes et al. (2016)
Chitosan	Immersion	Improved mechanical properties, higher water-holding capacity, slower water release rate, and shorter healing time compared to pure BC	Ul-Islam et al. (2011)
Alginate	Mixing	Biocompatible, relatively low-cost, nontoxic, demonstrates improved mechanical properties, thermal stability, and higher swelling ability compared to neat alginate	Lin et al. (2014)
Arginine	Immersion	More effective in promoting wound healing as compared to BC alone	Qiao et al. (2018)
Hyaluronic (HA)	Impregnation	Reduces scar formation, demonstrates improved water retention and water vapor transmission rates, facilitates the growth of primary human fibroblast cells, exhibits higher cell viability and shorter healing time in vivo as compared to pure BC	Li et al. (2015b)
Polyacrylamide	Mixing	Nontoxic, non-irritant to the skin, has a significant effect on wound contraction, accelerates epithelization and	Pandey et al. (2017)

(continued)

Table 17.2 (continued)

Composite	Preparation method	Properties	References
		fibroblast proliferation in vivo	
Poly(2-hydroxyethyl methacrylate) (PHEMA)	Impregnation	Better thermal stability and mechanical performance compared to PHEMA alone. Nontoxic and demonstrates cell attachment and proliferation	Figueiredo et al. (2013)
Dextran	Immersion	Nontoxic, enhances cell proliferation, accelerates wound healing, and facilitates skin maturation in vivo	Lin et al. (2017)
Vaccarin	Immersion	Non-cytotoxic, biocompatible, promotes cell proliferation, and accelerates healing process	Qiu et al. (2016)
Polyethylene glycol	Immersion	Good thermal stability, biocompatibility, and provides a microenvironment for cell proliferation, migration, and differentiation	Cai and Kim (2010)
Acrylic acid	Mixing	High swelling ratio, high water vapor transmission rate, and no toxicity. Promotes wound healing, accelerates epithelization, and enhances fibroblast proliferation	Mohamad et al. (2014)
	Adding aloe vera to the culture medium	Better water swelling ability, crystallinity, mechanical strength, and water vapor permeability than pure BC	Saibuatong and Phisalaphong (2010)
Superoxide dismutase (antioxidant)	Impregnation	Pronounced anti-inflammatory effect, shortens wound healing phases, promotes connective tissue proliferation, and wound epithelialization	Legeza et al. (2004)
Antibacterial wound dressing			
Inorganic compounds (silver, silver		Effective antibacterial, antifungal, and antiviral	Luan et al. (2012), Katepetch et al. (2013),

(continued)

Table 17.2 (continued)

Composite	Preparation method	Properties	References
sulfadiazine, zinc oxide, titanium dioxide, copper, gold, graphene oxide, and montmorillonite)	Immersion, impregnation, mixing	properties. Reduces inflammation, is biocompatible, demonstrates significant epithelialization, and accelerates wound healing	Ul-islam et al. (2013), Wu et al. (2014a, b), Khan et al. (2015), Shao et al. (2015b), Di et al. (2017), Khalid et al. (2017a, b), Li et al. (2017), Liu et al. (2017), Araújo et al. (2018), Mohammadnejad et al. (2018) and Tabaii and Emtiazi (2018)
Natural polymers with antibacterial activity (chitosan, chitin, or deacetylate chitin)	Immersion, addition to the culture medium	Antimicrobial activity and shorter healing time than pure BC	Mihaela Jipa et al. (2012), Butchosa et al. (2013), Lin et al. (2013a) and Wang et al. (2018b)
Antibiotic (chloramphenicol, gentamycin, amoxicillin, amikacin, ceftriaxone, tetracycline HCl, fusidic acid, metronidazole, levofloxacin)	Immersion, mixing, impregnation	Antimicrobial and bactericidal effect. Improved adhesion and proliferation of fibroblasts, nontoxic, and accelerates the healing process	Stoica-Guzun et al. (2007), Rouabhia et al. (2014), Türkoglu (2014), Shao et al. (2016), Liyaskina et al. (2017), Ma et al. (2017), Cacicedo et al. (2018), Volova et al. (2018) and Ye et al. (2018)
Antiseptics (benzalkonium chloride, povidone-iodine (PI), polihexanide (PHMA), octenidine)	Immersion	Antimicrobial activity, high water-absorbing capacity, biocompatibility	Wei et al. (2011), Moritz et al. (2014), Wiegand et al. (2015), Alkhatib et al. (2017) and Foong et al. (2018)
Catalytic enzymes (laccase, bromelain)	Immersion	Antimicrobial effect and cytotoxicity acceptable for wound dressing applications	Sampaio et al. (2016) and Ataide et al. (2017)
Natural antibacterial materials (propolis, silymarin, *Tridax procumbens* leaf extract)	Immersion	Antimicrobial activity, accelerate healing, and prevent/treat infections	Barud et al. (2013), Rangaswamy and Vanitha (2017) and Tsai et al. (2018)
Therapeutic wound dressing			
Analgesic drugs (diclofenac sodium, lidocaine HCl, ibuprofen)	Impregnation, immersion	Good swelling behavior, drugs penetrate the skin	Trovatti et al. (2011, 2012), Silva et al. (2014b) and Saïdi et al. (2017)
Growth factors (epidermal growth factor		Biocompatible, supports the growth of	Lin et al. (2011b)

(continued)

Table 17.2 (continued)

Composite	Preparation method	Properties	References
(EGF)) or ECM (collagen)	Impregnation with alginate gel	human skin fibroblasts, gradual growth factor release profile	
Active proteins (macrophage-stimulating protein (MSP))	Impregnation	Induces keratinocyte proliferation, prevents epithelial cell apoptosis, promotes proliferation and migration of fibroblasts, and enhances collagen synthesis and remodeling. Accelerates wound closure and collagen synthesis in vivo	Zhao et al. (2015a)
Stem cells (adipose-derived stem cells)	Immersion	Facilitates cell expansion and migration to the injury site, enhances tissue repair, good adhesion and proliferation of cells	Souza et al. (2014)
Human epidermal keratinocytes and dermal fibroblasts	Immersion with BC/acrylic acid films	Excellent cell attachment, maintains cell viability with limited migration, and allows for cell transfer in vitro. Accelerates wound healing in vivo	Loh et al. (2018)
Kaolin (a blood clotting agent)	Mixing	Exhibits dual potential as both a short-term (due to the kaolin) and a long-term (BC) wound healing agent	Wanna et al. (2013)
Cellulose nanocrystals			
Wound dressing			
PVA	Mixing	Good thermal stability, good mechanical properties, and water vapor transmission rate. Acts as a good barrier against microorganisms	Gonzalez et al. (2014)
Chitosan-polyethylene oxide	Electrospinning	Increased tensile strength, tensile modulus, and O_2/CO_2 transmission with the addition of CNC. Nontoxic	Naseri et al. (2015)

(continued)

Table 17.2 (continued)

Composite	Preparation method	Properties	References
Antibacterial wound dressing			
Curcumin	Mixing	Sustained release profile, good antibacterial activity, accelerated dermis regeneration, improves the regeneration of hair follicles and sebaceous glands, and prevents inflammation in vivo	Bajpai et al. (2017), Guo et al. (2017) and Tong et al. (2018)
Inorganic compounds (silver, zinc oxide)	Impregnation, precipitation	Reduce pro-inflammatory cytokine levels, induce full wound recovery, elevate collagen and growth factor expression, improve re-epithelization and vasculogenesis, exhibit antimicrobial activity and water absorption capacity	Yu et al. (2015), Bajpai et al. (2017) and Singla et al. (2017a, c)
Antibiotics (gentamycin sulfate, metronidazole, ceftazidime)	Impregnation, immersion	Sustained release, antibacterial activity	Lin et al. (2016), Zubik et al. (2017) and Zhu et al. (2018)
Polyrhodanine	Mixing and heating	Sustained antimicrobial activity, low toxicity	Tang et al. (2015b)
Chitosan/poly(vinyl pyrrolidone)	Solution casting method	Blood compatibility, enhanced swelling, antibacterial activity and maintains moist environment	Poonguzhali et al. (2017)
Therapeutic wound dressing			
Plasmid DNA (polyethyleneimine-carboxymethyl chitosan/pDNA-angiogenin (ANG) nanoparticles, curcumin (Cur), poly(D, L-lactic-co-glycolic acid) (PLGA), and CNCs)	Electrospinning	Antioxidant, antitumor, anti-inflammatory, and antibacterial activity (Cur) and stimulates blood vessel formation	Mo et al. (2017)
Cellulose nanofibers			
Wound dressing			
PEG	Mixing	More flexible, ductile, and comfortable as compared to CNF alone	Sun et al. (2017)
Hemicellulose			Liu et al. (2016)

(continued)

Table 17.2 (continued)

Composite	Preparation method	Properties	References
	Mixing, simultaneous impregnation	Supports cell growth and proliferation	
Antibacterial wound dressing			
Copper-coper oxide	Mixing	Antimicrobial activity, biocompatibility	Barua et al. (2013)
Tetracycline-HCl	Mixing, immersion	Accelerates wound healing, extended drug release, good antibacterial properties, biodegradability, and biocompatibility	Cheginia and Meamar (2018) and Liu et al. (2018b)
Therapeutic wound dressing			
Human adipose-derived mesenchymal stem cells (hASC)	Extrusion and seeding	hASCs adhere, migrate, and proliferate on CNF while preserving their bioactivity	Mertaniemi et al. (2016)
Analgesic drug (venlafaxine)	Immersion	Wound dressing for diabetic ulcers	Cheginia and Meamar (2018)

three leading approaches to improve cell adhesion to the scaffold involve (a) alteration of the scaffold's physical properties, e.g., pore size and wettability, (b) chemical modifications to change the scaffold surface properties, e.g., charge, and (c) impregnation of the scaffold with cell-specific adhesion molecules or with a secondary component, to form a composite that improves cell affinity and attachment to the scaffold.

17.7.1 Bacterial Cellulose

Due to its unique properties and biocompatibility, BC is the most investigated nanocellulose material for tissue engineering applications. The BC network can be synthesized to any desired shape or with any given porosity, by controlling the fermentation process of BC-generating bacteria (Backdahl et al. 2008; Rambo et al. 2008). In addition, BNC networks demonstrate a very high affinity to water and exhibit hydrogel-like properties, resulting in an ideal environment for host cells (Petersen and Gatenholm 2011). Its high porosity enables diffusion of nutrients, growth factors, and adhesion proteins inside the growing cell mass (Watanabe et al. 1993). Studies have demonstrated that human embryonic kidney (HEK) cells (Grande et al. 2009), bone-forming osteoblast (OB) cells, infinite culture cell line L929 fibroblasts (Chen et al. 2009), and human smooth muscle cells (SMC) (Bäckdahl et al. 2006) can proliferate on BC scaffolds. Nevertheless, the BC surface is associated with poor cell

Table 17.3 Nanocellulose-based composites for drug carrier systems

Carrier form	Matrix	Active material	Properties	References
Bacterial cellulose				
Film or membrane	Sodium carboxymethyl cellulose	Ibuprofen	BC concentration and drug release rate show negative correlation	Juncu et al. (2016)
	Poly(vinyl alcohol)-chitosan			Pavaloiu et al. (2014)
	Alginate	Doxorubicin	Three-fold higher doxorubicin-loading capacity, higher surface area, pore volume, and pore size compared to BC. Stable drug release for 14 days, decreased cancer cell viability	Cacicedo et al. (2016)
	Highly methoxylated pectin	Human serum albumin	Sustained drug release profile, nontoxic	Cacicedo et al. (2018)
	–	Lidocaine	>90% of the drug was released within 20 min, slower drug permeation rate compared to conventional systems	Trovatti et al. (2011, 2012)
	–	Diclofenac	Rapid release, good skin penetration	Silva et al. (2014b)
	–	Ibuprofen	Good skin permeability	Trovatti et al. (2012)
	Carboxymethylcelullose	Methotrexate	Immediate release profile	De Lima Fontes et al. (2018)
	Starch/pectin	Methotrexate	Enhanced the drug dissolution rates compared to raw methotrexate	Meneguin et al. (2017)
	–	Caffeine	Low caffeine permeability into the epidermis. Extended and predictable caffeine release over time	Silva et al. (2014a)
	–	Berberine hydrochloride, berberine sulfate	Extended, pH-dependent drug release	Huang et al. (2013)
	Poly(*N*-methacryloyl glycine)	Diclofenac sodium (DCF)	Good thermal stability, good mechanical properties, good uptake capacities, biocompatibility, nontoxic, pH-responsiveness release	Saïdi et al. (2017)

Microfibers or nanofibers	Poly(3,4-ethylenedioxythiophene) (PEDOT)	Diclofenac sodium	DCF release controlled by external electric field. The hybrid provided a cell growth-supportive environment	Chen et al. (2017)
Hydrogel or gel	Graphene oxide	Ibuprofen	Improved cell viability, drug carrying capacity, sustainable and pH-dependent release behavior as compared to BC	Luo et al. (2017)
	Poly-(acrylic acid)	Bovine serum albumin (BSA)	pH- and thermo-responsive release profile. Released BSA was bioactive and preserved	Mohd Amin et al. (2012b) and Ahmad et al. (2014)
	Poly(ethylene oxide)-*b*-poly (caprolactone) (PEO-b-PCL)	Retinol	Slow release system	Numata et al. (2015)
	Polyacrylamide	Theophylline	pH- and ion-responsive swelling behavior, high drug release	Pandey et al. (2013)
	Sodium alginate	Ibuprofen	pH- and electric stimuli-responsive release	Shi et al. (2014)
	Gelatin-coated magnetic nanoparticles	Methylene blue	Excellent thermal stability, chemical resistance, and mechanical properties. Temperature-, pH-, and magnetic field-responsive properties	Treesuppharat et al. (2017) and Siangsanoh et al. (2018)
Aerogel	–	Dexpanthenol	Loading and release control by varying the thickness of the gel and the solute concentration in the loading bath	Haimer et al. (2010)
		L-ascorbic acid		
Xerogel	–	Azorubine	A rapid release in the initial 1–2 h that was followed by a slower release rate up to 168 h	Müller et al. (2014)
Tablet	–	Famotidine	Immediate drug release	Badshah et al. (2017)
		Tizanidine		

(continued)

Table 17.3 (continued)

Carrier form	Matrix	Active material	Properties	References
Cellulose nanocrystals				
Film or membrane	Oxidized C	Procaine hydrochloride or imipramine hydrochloride	Oxidized CNC: rapid drug release; oxidized CNC modified by chitosan oligosaccharide: more sustained release. pH-responsiveness	Akhlaghi et al. (2013, 2014)
	NC			
	Oxidized CNC modified by chitosan oligosaccharide			
	Poly(3- hydroxybutyrate-co-3-hydroxyvalerate) (PHBV)	Tetracycline	High loading capacity, sustained release, and cytocompatibility	Cheng et al. (2017b)
	Polyelectrolyte complex (PEC)	Diltiazem hydrochloride	Transparent, nontoxic, and nonirritant, adheres well to the skin, resistant to microbial growth. Good skin penetration	Anirudhan et al. (2017)
	Chitosan	Doxorubicin hydrochloride or curcumin	Sustained release of both drugs at physiological conditions	Mohanta et al. (2014)
Microfibers or nanofibers	Poly(lactic acid) (PLA), PEG	Tetracycline	High drug-loading capacity, sustained release, biocompatibility	Yu et al. (2017)
	PLA	Columbia blue	Degradation-controlled release. 10% CNC content accelerates drug release, while 1% exhibits slower drug release	Xiang et al. (2013)
	Prolamin	Riboflavin	Controlled release profile	Wang and Chen (2014)
Hydrogel or gel	Cyclodextrin/triblock polymer EPE	Bovine serum albumin	Sustained release profile	Zhang et al. (2010)
	Gelatin	Theophylline	pH-sensitive swelling capacities, controlled drug delivery	Ooi et al. (2016)
	Regenerated cellulose	BSA	Well-organized porous inner structure. Steady release of BSA in simulated body fluid	Wang and Chen (2011)
	Poly(acrylic acid-co-acrylamide-co22-acrylamido-2-methyl-1-	Amoxicillin	pH-sensitive swelling capacities and release rate	Anirudhan and Rejeena (2014)

	propanesulfonic acid)-grafted CNC-PVA			
	Quaternized cellulose (QC) dispersed with cationic CNCs	Doxorubicin	Sustained release, no inflammatory response, non-cytotoxic, and slows liver cancer tumor growth in vivo	You et al. (2016)
	Starch	B12	Addition of CNC slowed the release rate	Mauricio et al. (2015)
	Poly-(acrylamidoglycolic acid)	Diclofenac sodium	pH-sensitive swelling and release properties	Rao et al. (2017a)
	Xanthan and chitosan	5-flurouracil	Controlled release profile, excellent cytocompatibility	Rao et al. (2017b)
Micro particles or nanoparticles or microspheres	–	Tetracycline	pH-sensitive release	Wijaya et al. (2017)
	–	Hydroquinone	Sustained drug release rate	Taheri and Mohammadi (2015)
	Chitosan	Repaglinide	High encapsulation efficacy. Diffusion-controlled release mechanism. Sustained and controlled release profile. Oxidized CNC/chitosan/repaglinide demonstrated a slower release rate	Abo-elseoud et al. (2018)
	Polyethylenimine	siRNA	No cytotoxicity, protected siRNA from degradation, and enhanced its delivery into the cell	Ndong Ntoutoume et al. (2017)
	Sodium alginate	Theophylline	Consistent swelling patterns, high encapsulation efficiency, pH-responsiveness, and sustained release profile	Lin et al. (2011a)
	Poly-(methyl methacrylate) (PMMA)	Curcumin	Long-term stability, good curcumin encapsulating capacities, and controlled drug release	Liu et al. (2018a)
Suspension	Cetyltrimethylammonium bromide	Docetaxel	Controlled release rate. High loading efficacy	Jackson et al. (2011) and Qing et al. (2016)
		Paclitaxel		

(continued)

Table 17.3 (continued)

Carrier form	Matrix	Active material	Properties	References
		Etoposide		
		Luteolin		
		Luteoloside		
	Propargyl-terminated poly(ethyl ethylene phosphate)	Doxorubicin	Drug release in tumor cells, biocompatibility, and anticancer activity	Wang et al. (2015b)
	Poly(2-oxazoline)	Indocyanine green	Effective in photothermal cancer therapy	Hou et al. (2017)
	Poly-(propylene imine) (PPI) conjugated with folic acid (FA)	Doxorubicin	Higher doxorubicin-loading capacity, as compared to FA-free complexes	Golshan et al. (2017)
Complex	Cyclodextrin	Curcumin	Slow release profile. Good anticancer activity	Ntoutoume et al. (2016)
	Poly(2-(dimethylamino)ethyl methacrylate)	Plasmid DNA (pDNA)	Complex internalization into target cells, followed by pDNA release, subsequently initiating death of transformed cells	Hu et al. (2015, 2016b)
Cellulose nanofibers				
Membrane or film	–	Itraconazole	Sustained drug release with kinetics varying between the drugs	Kolakovic et al. (2012b) and Gao et al. (2014)
		Beclomethasone		
		Indomethacin		
	Hydroxypropyl methylcellulose	Ketorolac tromethamine (KT)	The cumulative drug release percentage and release rate are decreased with the increase of CNF concentration in the nanocomposites	Orasugh et al. (2018)
	Starch/pectin	Methotrexate	Enhanced the drug dissolution rates compared to raw methotrexate	Meneguin et al. (2017)
Microfibers or nanofibers	Titania	Diclofenac sodium	Slow and controlled release, depending on drug	Galkina et al. (2015)
		D-penicillamine		
		Phosphomycin		
	Fe_3O_4-Ag_2O quantum dot	Etoposide		Fakhri et al. (2017)

		Methotrexate	Constant drug release, pharmacologic efficacy	
Gel or hydrogel	–	Doxorubicin	Sustained release profile	Alizadeh et al. (2018)
	–	Metformin	Fast release within 1 h, followed by a slower but sustained release	Nurani et al. (2017)
	Anionic CNF	Metronidazole	Sustained drug release, with kinetics varying between the drugs	Paukkonen et al. (2017a)
		Nadolol		
		Ketoprofen		
		FITC-dextran		
		Lysozyme		
		Bovine serum albumin		
	Partially deacetylated α-chitin nanofibers	5-fluorouracil	High drug-loading efficiency and cumulative release percentage	Xu et al. (2018)
Aerogel	–	Beclomethasone dipropionate	Release profiles varied with CNF origin, ranging from immediate to sustained release	Valo et al. (2013)
	–	Bendamustine hydrochloride	pH-responsive release profile, increased oral bioavailability compared to the bioavailability of the pure drug solution	Bhandari et al. (2017)
	Polyethylenimine	Sodium salicylate	High drug-loading capacity, sustained and controlled release, depending on pH and temperature	Zhao et al. (2015b)
Cryogel	Polyethylene oxide (PEO)/curdlan	Diclofenac sodium	Controlled and slower release of diclofenac compared to PEO/curdlan composite without CNF	El-naggar et al. (2017)
Microparticles or nanoparticles or microspheres		Indomethacin	Sustained drug release, with kinetics varying between the drugs	Kolakovic et al. (2012a)
		Metoprolol tartrate		
		Verapamil		

(continued)

Table 17.3 (continued)

Carrier form	Matrix	Active material	Properties	References
	Hydrophobin fusion protein	Itraconazole	Dissolution rate and in vivo bioavailability of itraconazole was increased significantly	Valo et al. (2011)
	PNIPAM (poly(*N*-isopropylacrylamide))	5-Fluorouracil	High drug-loading capacity and controlled release of 5-FU	Zhang et al. (2016)
Sponge	Polyethyleneimine	Amoxicillin	Effectively absorbs both drugs. Slow release rate	Fiorati et al. (2017)
		Ibuprofen		

attachment/adhesion because cellulose is biochemically inert. The BC surface can be modified to optimize cell adhesion and interactions, as well as the growth and viability of and selectivity for different cell types (Angelova and Hunkeler 1999).

Plasma surface modifications are an effective and economical means of selectively changing surface properties, thereby improving biocompatibility and mimicking the local tissue environment without altering the main attributes of the starting material (Chu et al. 2002). Nitrogen plasma is used to introduce amino groups in polymers, metals, and membrane surfaces, resulting in modified polarity, reactivity, and wettability (Charpentier et al. 2006). One study modifying BC membranes with nitrogen plasma reported increased porosity and positive surface charge of the membrane. In addition, significantly improved adhesion and proliferation of human endothelial cells (HMEC-1) and rat neuroblasts (N1E-115), but not of 3T3 cells, were observed, demonstrating a cell-specific effect (Pertile et al. 2010). BC sheets chemically modified with glycidyltrimethylammonium chloride to introduce a positive charge (cationic cellulose) showed a 70% increase in human osteoblast cancer cell attachment as compared to unmodified cellulose. In contrast, when modified by oxidation, the resulting anionic cellulose showed low levels of cell attachment comparable to those seen for unmodified cellulose. Only a minimal level of cationic surface derivatization (~3% degree of substitution) was required for increased cell attachment, and no mediating proteins were required. In addition, the modification did not impair the mechanical properties of the film (Courtenay et al. 2017).

BC pores exhibit nanometric dimensions, while human fibroblasts, one of the smallest cells in the body, fall within the range of 10–15 μm. The upper surface of BC is more dense and compact, which prevents cell migration into the network, while the porous lower surface of bacterial cellulose enables human chondrocyte ingrowth to a depth of up to 70 μm (Gama et al. 2012). Therefore, various methods are in regular use to improve BNC porosity. The leading approach adds porogens (e.g., starch (Backdahl et al. 2008), polyethylene glycol (Heßler and Klemm 2009), simple paraffin microspheres (Backdahl et al. 2008), or just pins immersed in the culture liquid (Rambo et al. 2008) to the bacteria culture media, which act as removable auxiliaries that are not incorporated into the BNC membranes. A 3D BC scaffold with controlled microporosity was fabricated by adding paraffin wax and starch particles to the bacteria culture medium. After successful removal of the porogens, the scaffolds were seeded with smooth muscle cells (SMCs), which showed improved attachment and proliferation on and partially in the scaffolds as compared to their behavior on pure BC (Backdahl et al. 2008). The nutrients in and the viscosity of the culture medium can affect BC membrane porosity and biological performance as well (Stumpf et al. 2013; Yang et al. 2014). BC/potato starch (PS) composites fabricated by addition of potato starch to the bacteria culture medium, exploit the gelatinization properties of PS to interfere with cellulose assembly during static culture, to generate more free spaces within the fibrous network. The composite was associated with higher cell ingrowth as the starch content increased, due to the larger pore sizes (Yang et al. 2014). Another means of enlarging pore sizes involves formation of composites or modifications following BC production. For example, addition of acrylic acid to BC suspensions created

hydrogels with a pore diameter in the range 10–100 μm (Halib et al. 2014). Other techniques include post-processing 3D laser perforation (Ahrem et al. 2014) or freeze-drying cycles (Gao et al. 2011; Xiong et al. 2014).

Combining BC with different polymers and molecules can improve biocompatibility, cell attachment, proliferation, and viability on the scaffold, as well as the mechanical properties of the scaffold. Incorporation of keratin to BC enhanced dermal fibroblast attachment and proliferation profiles and preserved keratinocytes epithelial morphology, indicating the potential of the novel BC/keratin nanocomposites for use in skin tissue engineering and wound healing applications (Keskin et al. 2017). Early studies demonstrated that modifications of the ionic charge of the BC membrane and absorption of collagen to the membrane promoted cell adhesion to the membrane surface. In addition, cell viability and bioactivity were maintained for about 1 month, while cultures on plastic dishes survived for only 12 days, likely related to the ultrastructure of BNC membrane (Watanabe et al. 1993). A recent report described the development of a homogeneous alginate/bacterial cellulose nanocrystals/collagen composite (ALG/BCNs/COL) scaffold, which maintained MC3T3-E1 and h-AMS cell viability and supported attachment and proliferation. In addition, the alginate composite hydrogel exhibited a stable and defined 3D architecture, with improved compressive strength, swelling, and biodegradation behaviors compared to pure alginate (Yan et al. 2018). Similarly, layer-by-layer assembly of a 3D alginate-chitosan-gelatin composite scaffold incorporating BNCs exhibited a good 3D architecture, with a well-defined, porous structure, regulated biodegradation and improved compressive strength compared to the alginate-chitosan-gelatin composite without BC. In particular, the excellent biocompatibility and the reinforcing effect of BCNs, and the outer gelatin chains containing repetitive motifs of arginine-glycine-aspartic (RGD) sequences, favored the attachment, proliferation, and differentiation of osteoblastic MC3T3-E1 cells (Yan et al. 2017). Nanocomposite sponges based on BC and silk fibroin (SF) proved non-cytotoxic and non-genotoxic and enhanced fibroblast attachment as compared to pure BC, likely due to the SF amino acid sequence that facilitates cell adhesion and growth (Oliveira Barud et al. 2015).

Small signaling peptides found in extracellular matrix proteins can incorporate into scaffolds and promote cell adhesion and proliferation. For example, fusion of the integrin-ligand sequences isoleucine-lysine-valine-alanine-valine (IKVAV) peptide to a carbohydrate-binding module (CBM3) to modify BC surfaces significantly improved the adhesion of both neuronal and mesenchymal cells, with BC fibers acting as a scaffold which maintained a continuous path that promoted infiltration of cells. In addition, MSCs adhering to the BC scaffold proliferated and secreted neurotrophin to the culture medium, creating a microenvironment supportive of neuronal regeneration (Pertile et al. 2012). The attachment of cells to biomaterials can also be improved by utilizing cell-binding amino acid sequences, such as Arg-Gly-Asp (RGD), found in several ECM proteins. One work coated BC fibers with bifunctional recombinant proteins, bearing both a cellulose-binding module (CBM) and Arg-Gly-Asp (RGD). Fibroblasts exhibited improved interaction with the CBM-RGD-coated BC sheets as compared to those treated with CMB only (Andrade et al.

2009). BC films incorporating xyloglucan extracted from tamarind seeds demonstrated improved Young's modulus and thermal stability compared to pure BC (De Souza et al. 2013). In addition, BC modified with xyloglucan and bearing the adhesion peptide RGD was associated with enhanced adhesion and proliferation of endothelial cells (Bodin et al. 2007a; Fink et al. 2011). Active molecules and growth factors can be incorporated into the scaffold to enhance various aspects of the tissue regeneration process. For example, porous BC/gelatin scaffolds loaded with vascular endothelial growth factor (VEGF)-loaded silk fibroin nanoparticles (VEGF-NPs) were prepared to enhance vascularization. VEGF underwent sustained release from the scaffold over a 28-day period, and the scaffold led to enhanced endothelial cell proliferation and viability in vitro. Upon implantation in a dog skin defect, the scaffold significantly promoted blood vessel formation as compared to the BC/gelatin scaffolds (Wang et al. 2017).

One of the requirements for a good scaffold is biodegradability (Hutmacher 2001), a property which is difficult to achieve with BC, due to the lack of cellulose enzymes in mammals. Periodate oxidation of BC maintained the original 3D nanonetwork structure of unmodified BC, preserved the BC mechanical properties suitable for tissue engineering applications, and improved BC biodegradability in water, phosphate-buffered saline, and simulated body fluid (Li et al. 2009). C2, 3-oxidized aldehyde BC (DBC) exhibited a characteristic nonlinear elasticity and promoted the adhesion and proliferation of cells (epidermal cells and fibroblast) within the DBC networks (Wu et al. 2014a, b, c).

17.7.2 Cellulose Nanocrystals

CNC has been extensively investigated for its use in tissue engineering due to its low cost, biocompatibility, high surface area to volume ratio, mechanical properties, and nanometric structure (Abraham et al. 2017). Studies demonstrated that CNC is nontoxic to a variety of cell lines, including human embryonic kidney 293 (HEK 293), *Spodoptera frugiperda* (Sf9) cells (Mahmoud et al. 2010), Chinese hamster lung fibroblast V79 (Male et al. 2012), and human fibroblasts (Liebert et al. 2011).

CNC has been proven a potent reinforcing agent, improving the mechanical properties and stability of scaffolds comprised of silk fibroin (Noishiki et al. 2002), poly(3-hydroxybutyrate-co-3-hydroxyvalerate) (PHBV) (Ten et al. 2010), polyhydroxybutyrate (PHB) (Kampeerapappun 2016), poly(lactic acid) (PLA) (Hossain et al. 2012), poly(vinyl alcohol) (PVA) (Fortunati et al. 2013a, b; Rescignano et al. 2014), poly(vinyl acetate) (Fox et al. 2013), hyaluronic acid (Domingues et al. 2015), poly(ε-caprolactone) (Zoppe et al. 2009), polyethylene oxide (Zhou et al. 2011), PEG (Yang et al. 2013a), polyurethane (Rueda et al. 2013), gelatin (Dash et al. 2013), *N*-isopropyl acrylamide (Cha et al. 2012), poly(acrylic acid) (Yang et al. 2012), alginate (Lin et al. 2012a), chitosan (Ko et al. 2018), collagen (Li et al. 2014), or keratin (Song et al. 2017). When deployed as a reinforcing agent in collagen films, CNC enhanced the mechanical properties of

the film, without imparting any negative effect on cell morphology, viability, or proliferation or on film biocompatibility (Li et al. 2014). Carboxymethyl cellulose and dextran reinforced with rigid, rod-like CNCs or aldehyde-functionalized CNCs (CHO-CNCs) were more structurally stable in extended (60-day) swelling experiments, remaining coherent, while unfilled hydrogels degraded over the same time period. The CHO-CNCs acted as both filler and a chemical cross-linker and yielded more elastic hydrogels which exhibited higher nanoparticle-loading capacities compared to hydrogels with unmodified CNCs. No significant cytotoxicity to NIH 3 T3 fibroblast cells was observed for the hydrogels or their individual components, indicating their potential use as tissue engineering matrices (Yang et al. 2013b).

CNC can improve biodegradability, biocompatibility, and cell adhesion and proliferation when added to other materials. For example, PLA fibers coated with a blend of CNC and polyvinyl acetate demonstrated enhanced mechanical properties and NIH-3T3 mouse fibroblast cell adhesion compared with the uncoated PLA (Hossain et al. 2014). When integrated in the fabrication of different chitosan-g-D, L-lactic acid (CgLA) scaffolds, CNC content positively correlated with degradability, porosity, and cell viability, likely due to the increased surface area (Ko et al. 2018). Poly(butylene adipate-co-terephthalate) (PBAT) chemically modified with maleic anhydride (MA) and reinforced by CNC yielded a composite with viscoelastic properties, thermal stability, and mechanical properties that improved with increasing concentrations of CNC content. In vitro biocompatibility and L929 fibroblast cell adhesion testing revealed no cytotoxic effect of CNCs, and the composite enabled better cell attachment compared to MA-g-PBAT matrix (Kashani Rahimi et al. 2017).

In order to enhance tissue regeneration and vascularization, biodegradable gelatin microspheres (GMs) containing basic fibroblast growth factor (bFGF) were fabricated and incorporated into a porous collagen/CNCs scaffold, as a platform for long-term release and consequent angiogenic boosting. When incubating the scaffolds with human umbilical vein endothelial cells, significantly augmented cell proliferation, excellent biocompatibility and no cytotoxicity were noted. Upon subcutaneous implantation into rats, a significantly higher number of newly formed and mature blood vessels were observed in bFGF-GM scaffolds as compared to the controls. In addition, they demonstrated a faster degradation rate (Li et al. 2015a).

CNC can be used to fabricate advanced and intelligent scaffolds. For example, CNCs functionalized with allyl moieties were embedded within a poly(vinyl acetate) and cross-linked through a photoinduced cross-linking procedure. By controlling photo-irradiation exposure time of different parts of the film, a gradient of the degree of covalent cross-linking was created. When the films were exposed to water, which "switches off" the noncovalent CNC interactions, significant mechanical contrasts were observed within the same film. This technique can enable formation of scaffolds for regeneration of the interface of different tissue types bearing contrasting mechanical properties, for example, ligament to bone, tendon to bone, and cartilage to bone (Fox et al. 2013).

CNC can also be applied to guide cell orientation and location. Oriented surfaces of adsorbed CNCs with particularly small diameters (a few nanometers) were prepared using a flexible and facile spin-coating method. Oriented CNCs induced C2C12 myoblast fusion, terminal differentiation, and adoption of similarly oriented morphologies. Highly oriented multinuclear myotubes were formed, and fibrillar fibronectin deposition was observed on the surfaces of the oriented CNCs, indicating the potential of nanoscale materials in engineering-oriented tissues. With a mean height of only 5–6 nm, CNC surfaces presented the smallest reported features capable of inducing contact guidance in skeletal muscle myoblasts (Dugan et al. 2013). Injectable nanocomposite hydrogels based on hydrazone-cross-linked poly (oligoethylene glycol methacrylate) and magnetically aligned CNCs successfully encapsulated skeletal muscle myoblasts and promoted their differentiation into highly oriented myotubes in situ. CNC alignment occurred on the same time scale as network gelation and remained fixed even after removal of the magnetic field, enabling concurrent CNC orientation and hydrogel injection. The aligned hydrogels showed mechanical and swelling profiles that can be rationally modulated by the degree of CNC alignment and can direct myotube alignment both in two and three dimensions following co-injection of the myoblasts with the gel precursor components. As such, these hydrogels represent a critical advancement in anisotropic biomimetic scaffolds that can be noninvasively generated in vivo following simple injection (De France et al. 2017).

Bioprinting is a promising and advancing technology, which can be used in fabrication of bioscaffolds. CNCs demonstrate rheological properties favorable for 3D printing, as shown with a hydrogel ink comprised of sodium alginate and gelatin (SA/G) reinforced with CNCs used to print 3D scaffolds. 3D bio-based scaffolds with uniform pore sizes, gradient pore structures, nanoscaled pore wall roughness, and orientation of the nanostructures for optimal cell attachment and tissue regeneration can be developed (Sultan and Mathew 2018). A high-strength hydrogel system based on dialdehyde cellulose nanocrystals (DAC) and gelatin (GEL) was investigated as a new bioink for 3D scaffold printing. Cross-linked scaffolds with adjustable porosity and good fidelity were obtained and showed good biocompatibility (Jiang et al. 2018).

17.7.3 Cellulose Nanofibers

CNF exhibits good biocompatibility and mechanical properties and supports cell attachment, characteristics that are important and suitable for tissue engineering applications. *GrowDex* is a commercially available CNF hydrogel, suitable for in vitro applications in advanced cell culture studies. It is biocompatible with human cells and tissues, maintaining viability and functionality of different types of cells, such as WA07 and iPS(IMR90)-4 stem cell lines and HepG2, HepaRG, and ARPE-19 cell lines (UPM Biochemicals 2018).

CNF hydrogels cultured with hepatic progenitor cells exhibited biocompatibility, supported differentiation of human hepatic cell lines HepaRG and HepG2, and featured rheological properties that enabled in situ formation of a 3D scaffold after facile injection. In addition, at high shear stress, the aqueous CNF had low viscosity, rendering it injectable, while under low shear stress conditions (e.g., after injection), the material was converted to an elastic gel, which provided the required mechanical support for cell growth and differentiation (Bhattacharya et al. 2012). CNF can also serve as a reinforcing agent for several scaffold materials, improving their stability and mechanical properties. For example, CNF dispersed in PVA yielded nanocomposites with a higher modulus and tensile strength compared to PVA alone (Zimmermann et al. 2004). Thermoplastic polyurethane (TPU) nanofibers immersed in CNF and subjected to ultrasonication showed increased hydrophilicity and higher Young's modulus and tensile strength at break. In addition, the adhesion and proliferation of human umbilical vein endothelial cells cultured on the CNF-absorbed TPU scaffold were prominently enhanced in comparison with those of cells cultured on a non-modified TPU scaffold (Ye et al. 2017). A novel scaffold composed of pectin, carboxymethyl cellulose (CMC), and microfibrillated cellulose (MFC) were associated with higher NIH3T3 fibroblast cell viability and exhibited excellent thermal stability, higher compression modulus, and slower biodegradation as compared to the composite without MFC (Ninan et al. 2013). Oxidized CNF offers active sites for introduction of collagen. When cross-linking with collagen, the collagen grew along the oxidized CNF and formed composite aerogels, which demonstrated high porosity, strong water absorption, good biocompatibility, and high levels of L929 cell activity and proliferation, indicating that this composite may be suitable as a tissue engineering scaffold and wound dressing (Lu et al. 2014). TEMPO-modified cellulose nanofiber (T-CNF) was printed, using the direct-ink-writing (DIW) technique, into customizable 3D structures. The resulting aerogel exhibited sustainability, biocompatibility, ultralight weight with high porosity, and deformability, indicating its potential in tissue engineering (Li et al. 2018a).

17.7.4 Cardiovascular Implants

Vascular failure is commonly treated by bypass surgery, which involves replacement of blood vessels with either autologous vessels or synthetic materials. Commonly used synthetic vascular grafts perform satisfactorily in large caliber blood vessels but are prone to fail in small-diameter (<5 mm) vessels due to intimal hyperplasia, poor blood flow, and surface thrombogenicity (Esguerra et al. 2010). Artificial valves and small-diameter vascular graft implants must be hemocompatible and biocompatible, provide long-term blood flow, and exhibit mechanical properties that can withstand the pressures of blood circulation. In addition, the implant has to be stable and permeable to water and electrolytes, enable cell attachment and ingrowth, and be non-thrombotic as well as non-immunogenic.

17.7.4.1 Bacterial Cellulose

BC has been extensively investigated as a scaffold and implant material for cardiovascular-related applications. BC carries a low risk of blood clot formation, does not degrade in the human body, and supports the growth and proliferation of smooth muscle, endothelial, and fibroblast cells that ultimately create a viable artificial blood vessel. In addition, BC possesses mechanical features enabling it to withstand the high pressure generated by the circulatory system, as well as dynamic compliance similar to those of arteries and the saphenous vein. BC is also hemocompatible and permeable to water, ions, and small molecules. When comparing between induced coagulation on the surface of BC and graft materials in clinical use, i.e., expanded polytetrafluoroethylene (ePTFE) and poly(ethyleneterephtalat) (PET), BC demonstrated least and slowest activation of the coagulation cascade (Fink et al. 2010). In addition, BC is highly biocompatible and enables greater incorporation of biomaterial into the host tissue as compared with materials commonly used in vascular surgery (polyglycolic acid and ePTFE) (Esguerra et al. 2010). BASYC® tubes are BC tubes synthesized directly in the culture medium, using a patented matrix technique during fermentation, and are available in a range of inner diameters, wall thicknesses, and lengths. The BC tubes demonstrate high mechanical strength in the wet state, considerable water retention capacities, low inner surface roughness, and complete vitalization of BASYC® (Klemm et al. 2001). The stored water stabilizes the cellulose network and contributes to the hemocompatibility of BASYC®. The hollow spaces of the BASYC® material transport water, monovalent ions, and small molecules, but exclude biopolymers or corpuscular blood constituents. Additional BASYC® features advantageous in microvessel replacement applications include constant shape, stability against internal and external pressures, flexibility and elasticity, and capacity to handle a tight microsurgical suture (Klemm et al. 2005). Application of BASYC® as a microvessel endoprosthesis was investigated in the case of a typical end-to-end anastomosis of the carotid artery of the rat. Four weeks after the procedure, the carotid artery-BASYC® complex was wrapped with connective tissue, pervaded with small vessels without any rejection reaction, and all interpositioned BASYC® tubes maintained 100% patency throughout the observation period. In addition, the internal surface became completely covered with well-oriented endogenous cells, forming a regular vascular wall inside the BASYC® tubes (Klemm et al. 2001, 2005). Long-term incorporation (1 year) in rats demonstrated that branches of fibroblasts and cellular compounds of the newly built vessel penetrated the cellulosic network and anchored themselves in the artificial vessel prosthesis. The fibroblasts were active, as confirmed by detection of collagen, which further advanced integration of BASYC® without degradation. In addition, no thrombosis was noted (Klemm 2006).

BC tubes can be fabricated, using several techniques, and customized to the desired length, inner diameter, thickness, and mechanical properties (Bodin et al. 2007b; Putra et al. 2008; Zang et al. 2015). For example, the use of the highly oxygen-permeable PDMS (polydimethylsiloxane), as a tubular template material,

allowed for fabrication of BC tubes with elaborate nanofiber architectures, mechanical properties comparable to porcine carotid artery, and high thermal stability. The tubes were biocompatible and supported endothelial cell, smooth muscle cell, and fibroblast attachment, proliferation, and ingrowth, with no toxic or adverse effects on vessel-related cells cultured on their surface. Moreover, complete endothelialization was achieved, and no signs of inflammation were observed around the implants placed in the rabbit femoral artery (Zang et al. 2015).

Several studies combined BC with other materials to improve mechanical properties. For example, BC/PVA nanoparticles are biocompatible and possess mechanical properties determined by material ratios and processing parameters. The composite was shown to exhibit mechanical properties, including anisotropy, similar to cardiovascular tissues, such as aorta and heart valve leaflets (Millon and Wan 2006; Millon et al. 2008; Mohammadi 2011). For artificial blood vessel applications, PVA was impregnated into BC tubes, yielding a composite with significantly improved water permeability and mechanical properties compared to BC tubes and PVA tubes separately, rendering the composite a more suitable artificial blood vessel (Tang et al. 2015a). The BC/PVA composite exhibited good hemocompatibility, eliciting only low activation of platelets and Factor XII, thus bearing potential for applications in cardiac prostheses (Leitao et al. 2013). BC/fibrin composites treated with glutaraldehyde to cross-link the polymer showed tensile strength, modulus, stress-strain response, and time-dependent viscoelastic behavior that better matched those of native small-diameter blood vessels (Brown et al. 2012).

To improve the adhesion of human microvascular endothelial cells (HMEC) to BC, chimeric proteins containing a cellulose-binding module (CBM) and an adhesion peptide (RGD or GRGDY) were produced. The modified BC was associated with significantly increased HMEC attachment, which formed a confluent cell layer on the BC surfaces, induced angiogenesis, and inhibited platelet adhesion (Andrade et al. 2010, 2011). Another study hybridized BC and heparin to mimic the natural ECM and to promote blood compatibility. This was achieved by introducing anticoagulant sulfate groups into the BC nanofiber, as a means of improving anticoagulant properties of tissue-engineered vessels as an alternative to coating with heparin (Wan et al. 2011).

To treat obstructive coronary artery disease (CAD), a stent is placed to widen and support the narrowed artery. While conventional metallic stents are extensively used, their main disadvantage is the incidence of in-stent restenosis (ISR) and release of endothelium fragments into the blood stream. A BC-based coating of the stent prevented migration of smooth muscle cells toward the vessel lumen (Loures 2004). Currently used stents also require prolonged anti-platelet therapy to prevent stent thrombosis. Poly(3-hydroxyoctanoate) [P(3HO)] fabricated as a composite with acetylated BC exhibited improved mechanical properties as compared to neat P(3HO), was biodegradable, and supported the proliferation of human microvascular endothelial tissue culture cells (HMEC-1), suggesting its utility in fabrication of biodegradable stents (Basnett et al. 2012).

17.7.4.2 Cellulose Nanocrystals

CNC and its composites can potentially function as structural materials for prosthetic vascular conduits, given their moldability, mechanical strength in the wet state, stability, biocompatibility, and durability. A CNC and fibrin nanocomposite was tested for its potential as a small-diameter replacement vascular graft (SDRVG). Periodate oxidation of CNC facilitated its cross-linking with fibrin. The resulting oxidized CNC (o-CNC) was homogeneously dispersed in the fibrin matrix, with fibrin providing elasticity and o-CNC providing strength. Modifying the degree of CNC oxidation and the CNC-to-fibrin ratio resulted in variation of nanocomposite strength and elongation, indicating that the nanocomposite can be tailored to conform to the diverse mechanical properties of native blood vessels. For example, CNC oxidized for 4 h and integrated in nanocomposites with an o-CNC/fibrin ratio of 1:1 possessed the same strength and elasticity as porcine coronary arteries (Brown et al. 2013). CNWs embedded in a matrix of cellulose acetate propionate (CAP) exhibited excellent mechanical performance at body temperature due to the fact that CNWs impart significant strength and directional rigidity even at concentrations as low as 0.2% wt. This fibrous and porous microstructure scaffold can withstand the physiological pressure within and mimic the features of the native extracellular matrix in a human vessel (Pooyan et al. 2012). A later work aligned the CNCs embedded within the CAP matrix by using a relatively weak external magnetic field. Magnetically induced alignment not only improved the directionality and percolation limits of the nanoparticles within the medium but also drastically lowered the amount of CNWs required to obtain optimal composite performance (Pooyan et al. 2013).

17.7.5 Bone and Connective Tissue Regeneration

Bone consists of 50–70% mineral (calcium hydroxyapatite), 20–40% organic components (collagen and non-collagenous proteins) and 5–10% water and demonstrates limited healing capacities. A variety of artificial grafts have been used to treat extensive bone lesions. As an alternative, scaffolds for bone regeneration can be used. The scaffold must possess strong mechanical properties, a microscopic pore structure to facilitate osteoblast ingrowth and formation of a mineralized tissue, biocompatibility, and slow degradability to maintain structural support during the initial stages of bone formation. Composite scaffolds can best mimic the native bone composition, for example, hydroxyapatite-based scaffold seeded with osteoblasts can generate bone segments for implantation (Stevens et al. 2008).

17.7.5.1 Bacterial Cellulose

BC features good mechanical properties, porosity, and biocompatibility and forms fine web-like network structures. In addition, BC exhibits a collagen-like structure, is not toxic to stem cells and osteoblast cells and enables cell attachment, proliferation, differentiation, and activation (Chen et al. 2009; Favi et al. 2013). For example, human adipose-derived mesenchymal stem cells seeded on a BC membrane proliferated, differentiated into osteoblasts, deposited significant mineral material, and were activated in the presence of osteogenic medium (Zang et al. 2014). In order to improve BC porosity, a microporous BC scaffold was prepared by incorporating 300–500 μm paraffin wax microspheres during the fermentation process, which were later removed. When seeding the scaffold with MC3T3-E1 osteoprogenitor cells, cells clustered within the pores, forming denser mineral deposits than cells grown on nano-porous BC scaffolds (Zaborowska et al. 2010).

Combining BC with other materials and active ingredients (growth peptides) can improve bone regeneration processes. Biopolymer-based membranes fabricated from BC and collagen (COL) adsorbed osteogenic growth peptide (OGP(10–14)) and promoted cell proliferation and alkaline phosphatase activity in osteoblastic cell cultures. In vivo tests in rats demonstrated that BC-COL OGP(10–14) membranes induced a higher percentage of bone tissue as well as higher radiographic density in the repaired bone than in the other tested groups (BC, BC(OGP(10–14), BC/COL) (Saska et al. 2018). Another study coated BC scaffolds with bone morphogenetic protein-2 (BMP-2), to obtain a composite that induced differentiation of mouse fibroblast-like C2C12 cells into osteoblasts in vitro. In vivo subcutaneous implantation studies demonstrated that BC scaffolds carrying BMP-2 showed more bone formation and higher calcium concentrations than the BC scaffolds alone (Shi et al. 2012a). Otoliths/collagen/BC composites stimulated bone regeneration and enhanced migration of cells required for formation of new bone. This was ascribed to the addition of nano-otholits, osteoinducers, which are rich in minerals considered essential to the bone mineralization process. In vivo histological experiments showed bone tissue formation with regular appearance, high osteoblast activity, and areas with osteo-reabsorption activity (De Olyveira et al. 2011).

Nanometer-sized, poorly crystalline hydroxyapatite (HA) is distributed in and along collagen fibers in bones. It is the most abundant mineral in bones and can promote cell differentiation and activation. A study group cultured *Acetobacter xylinum* in medium supplemented with HA, to form BC/HA membranes, which were associated with increased osteoblast adhesion and growth, as compared to BC alone, as well as greater nodule formation and mineralization (Tazi et al. 2012). Alternatively, BC can be soaked in $CaCl_2$ solution, followed by biomimetic mineralization, to yield the same BC/HA membranes (Wan et al. 2006). When seeded with stromal cells derived from human bone marrow (hBMSC), the cells exhibited better adhesion and activity, faster proliferation and differentiation, and higher expression of osteopontin, osteocalcin, and bone sialoprotein as compared to hBMSC loaded on pure BC membranes (Fang et al. 2009). Four weeks after implanting BC/HA membranes into noncritical bone defects in rat tibiae, defects were completely filled

with new bone tissue, indicating that the membranes accelerated new bone formation at the defect sites (Saska et al. 2011). Graphene oxide/hydroxyapatite (GOHA) composites support the adhesion of osteoblast cells, which maintain their viability. Upon addition of BC, GOHA-BC composites demonstrated enhanced cell adhesion, proliferation, and viability, exhibited good biocompatibility, and induced alkaline phosphatase activity (Ramani and Sastry 2014). A recent study explored the use of BC in combination with functionalized multiwall carbon nanotubes (MWNTs), a 3D scaffold suitable for osteoblastic cell culture. This composite scaffold was associated with higher osteoblast viability, adhesion, and proliferation as compared to pure BC (Gutiérrez-hernández et al. 2017).

As neat BC does not degrade in the human body, modifications are necessary to improve its biodegradation. Electron beam-irradiated BC membranes (EI-BCMs) are resorbable and demonstrate better bioactivity, higher NIH3T3 cell viability, adhesion, and proliferation as compared to non-irradiated BC. In vivo implantation of EI-BCMs in a rat calvarial defect model resulted in significantly more new bone areas as compared to those treated with non-irradiated membranes. These properties suggest that resorbable EI-BCMs can be used as an alternative biomaterial to existing resorbable barrier membranes in guided bone regeneration (GBR) (An et al. 2017; Lee et al. 2017) Alternatively, cellulose enzymes can be added to increase biodegradability. A BC-calcium phosphate composite incorporating cellulose enzymes underwent nearly complete in vitro bioabsorption, suggesting that it can act as a biodegradable carrier of calcium phosphate to bone defect sites. The BC membrane is highly biocompatible and metabolizes mainly to glucose, thus providing nutrition for osteoblast growth and function (Hu et al. 2016b). Periodate oxidation of BC yields dialdehyde cellulose, which breaks down at physiological pH. Oxidized BC retains the natural BC structure and therefore maintains its ability to initiate the mineralization of calcium-deficient hydroxyapatite (CdHAP) via a biomimetic mineralization process. CdHAP produced in oxidized BC has identical properties to that produced in native BC, both being similar to natural bone apatite. By entrapping CdHAP in a degradable hydrogel carrier, this composite should elicit bone regeneration and then resorb over time and be replaced by new osseous tissue (Hutchens et al. 2009).

17.7.5.2 Cellulose Nanocrystals

CNCs have been used to synthesize hybrid materials by the biomimetic growth of HAp in SBF medium. The CNC/Hap composite showed improved mechanical properties, due to the inherent mechanical strength of CNCs, while maintaining Haps biological activities that are similar to or superior to those of pure Hap (Fragal et al. 2016). A novel hydroxyapatite/cellulose nanocrystal/silk fibroin (HA/CNC/SF) scaffold, fabricated by mixing a solution of SF with HA and CNC nanoparticles, was tested for its efficacy in repairing critical-size calvarial defects. The thermostability and mechanical properties of the composite scaffolds were significantly better than those of either SF, CNC/SF, or HA/SF scaffolds, due to the smaller pore

sizes, more uniform pore size distribution, and embedding of the HA and CNC nanoparticles in the SF scaffold. Additionally, the composite scaffold exhibited excellent biocompatibility and superior osteoconductivity and promoted the proliferation of MC3T3-E1 cells. The rat calvarial defect healed and presented newly formed and dense bone within 12 weeks of implantation; the degradation rate of the scaffold was a good match to the bone regeneration rate (Chen et al. 2016). Electrospun fibrous bio-nanocomposite scaffolds reinforced with CNCs were fabricated by using maleic anhydride (MAH)-grafted poly(lactic acid) (PLA) as matrix, yielding MPLA/CNC. The addition of CNC improved the mechanical properties and thermal stability of the scaffold, which exhibited excellent stability during in vitro degradation compared to the pure MPLA. Moreover, the fibrous MPLA/CNC composite scaffolds were nontoxic to human adult adipose-derived mesenchymal stem cells (hASCs), were capable of supporting cell proliferation, and possessed useful mechanical properties for bone tissue engineering (Zhou et al. 2013a). Sodium alginate (Alg) and xanthan gum (XG)-based nanocomposite scaffolds reinforced with various amounts of CNCs showed high porosity and pore interconnectivity, good thermal stability, cytocompatibility, and improved compressive strengths compared to free CNC composites, indicating its potential in bone tissue engineering (Kumar et al. 2017).

17.7.5.3 Cellulose Nanofibers

CNF-enriched gelatine (GEL) scaffolds were fabricated with various forms of surface-unionized CNFs (carboxylated/CNF-COOH/, and phosphonated with 3-aminopropyl phosphonic acid/CNF-COOH-ApA), yielding composites that all exhibited osteoid-like compressive strength and elasticity and supported the growth of MSCs, resulting in more extensive Ca^{2+} deposition compared to the pure GEL scaffold. The scaffold prepared with the 50% v/v CNF-COOH-ApA showed significantly increased mineralization kinetics, as well as bone-like patterning capacities (Gorgieva et al. 2017).

A simvastatin-loaded gelatin-nanofibrillar cellulose-beta tricalcium phosphate (GNTS) hydrogel scaffold was prepared using the freeze-drying method. The gelatin and beta tricalcium phosphate provide osteoconductivity, while simvastatin is an osteoinductive molecule. CNF contributed to the slower degradation rate of the scaffold, which, in turn, favored the sustainable release of simvastatin, which, following an initial burst release, was constant for up to 30 days. When incorporating 0.5 mM simvastatin, alkaline phosphatase (ALP), osteopontin (OPN), and osteocalcin (OCN) mRNAs, three proteins involved in the osteoblastic differentiation of rat bone marrow mesenchymal stem cells (RBMSCs), were expressed in higher amounts. In addition, after implanting scaffolds into critical-sized rat calvarial defects, a greater extent of bone formation, with a higher amount of collagen matrix deposition, was observed in scaffolds with 0.5 mM simvastatin, indicating its potential in bone regeneration applications (Sukul et al. 2015).

17.7.6 Cartilage and Meniscus Scaffolds and Implants

Cartilage is a smooth elastic tissue that exhibits viscoelastic behavior and absorbs shocks and loading. In addition, it has a limited regeneration capacity. As the currently available solutions for damaged cartilage provide unsatisfactory outcomes, there exists a great demand for development of cartilage scaffolds and implants. The artificial implant must feature properties that are similar to those of native cartilage, and hence, it must be biocompatible and resistant to wear, support native ECM and biopolymer production, withstand various loads, and show degradation rates that commensurate with the rate of the new tissue formation (Svensson et al. 2005; Huey et al. 2012).

17.7.6.1 Bacterial Cellulose

Chondrocytes seeded on BC membranes demonstrated BC membrane porosity-dependent viability and proliferated and expressed collagen type II RNA, without inducing any inflammatory reactions during in vitro macrophage screening. The Young's modulus of BC was in the same range as articular cartilage, indicating its suitability as a bio-mimicking scaffold for cartilage replacement (Svensson et al. 2005). A study comparing a BC gel with real pig meniscus and a collagen meniscal implant, an implant in clinical use for regeneration of meniscal tissue after partial meniscectomy, showed that the Young's modulus of BC gel and pig meniscus were similar in magnitude under a compression load of 2 kPa and had five-fold better mechanical properties than the collagen-based implant. At higher compression strains, however, the pig meniscus was clearly stronger (Bodin et al. 2007c). Another study synthesized a BC scaffold which was perforated by micro-channels and seeded with 3T6 fibroblasts. The micro-channels facilitated the alignment of cells and collagen fibers. In addition, collagen production was enhanced by mechanical stimulation of the scaffold, which resulted in high-content and parallel orientation of collagen fibers, mimicking the ultrastructure of the knee meniscus (Martínez et al. 2012). BNC can also act as implant material for auricular cartilage reconstruction due to its excellent mechanical properties, biocompatibility, and good tissue integration. BNC samples containing varying concentrations of cellulose were tested as a possible ear cartilage replacement material. At 14–17% effective cellulose content, the samples demonstrated mechanical properties which were equivalent to ear cartilage, were non-cytotoxic, induced a minimal foreign body response, and exhibited non-resorbable behavior. In addition, BNC can be tailored to a patient-specific auricular shape, using 3T MRI scanning (Nimeskern et al. 2013; Martínez Ávila et al. 2014). Yet, the proposed implants are dense with low porosity, rendering chondrocyte ingrowth and migration impossible. Microporous BC scaffolds were prepared by fermentation of *Acetobacter xylinum* in the presence of slightly fused wax particles (150–300 μm diameter), which were then removed by extrusion. Articular chondrocytes from young adult patients as well as neonatal articular

chondrocytes seeded onto the porous BC scaffolds infiltrated the pores of the scaffolds and filled in the pores with increasing incubation times. In addition, chondrocytes proliferated and glycosaminoglycan production was observed in areas containing cell clusters, indicating the promising potential of this material for cartilage regeneration applications (Andersson et al. 2010). A novel bilayer BNC scaffold developed as an auricular cartilage tissue substitute was composed of a dense nanocellulose layer that resembled the structure of collagen fibrils found in extracellular matrix, joined with a macroporous composite layer of nanocellulose and alginate. When seeded with human nasoseptal chondrocytes (NC), the composite proved non-cytotoxic, and NCs effectively produced and accumulated cartilage-specific ECM components in the scaffold. The porous layer supported NC ingrowth and facilitated homogeneous cell distribution. The subcutaneously implanted cell-seeded bilayer BC scaffold offered good mechanical stability and maintained its structural integrity while providing a porous architecture that supported cell ingrowth and neocartilage formation (Martínez Ávila et al. 2015). 3D laser perforation of never-dried BNC hydrogels also proved effective in controlling BC porosity. The modified BNC allowed for and supported ingrowth and movement of vital bovine/human chondrocytes throughout the BNC nanofiber network. Human chondrocytes seeded on the surface/channels of laser-perforated BNC expressed cartilage-specific matrix products, suggesting chondrocyte differentiation. In addition, 3D-perforated BNC exhibited high biocompatibility and provided for short diffusion distances for nutrients and extracellular matrix components. The modified BC showed compressive strength comparable to that of unmodified samples, indicating its potential as a cartilage replacement material (Ahrem et al. 2014). Poly (3-hydroxybutyrate) (PHB)/microfibrillated bacterial cellulose (MFC) 3D scaffolds exhibited improved mechanical properties compared to PHB, and both mouse chondrogenic ATDC5 cell attachment and proliferation were found to be optimal. The large pore sizes (60–83 μm) allowed for the infiltration and migration of ATDC5 cells deep into the porous network of the scaffold material (Akaraonye et al. 2016).

BC exhibits high crystallinity and is nondegradable in vivo, a characteristic that limits its application in tissue engineering. In order to overcome this limitation, a novel lysozyme-degradable BC was generated from metabolically engineered *Gluconacetobacter xylinus*. The modified BC (MBC) possessed glucosaminoglycan-like chemistry combined with in vivo degradability, supported adult human mesenchymal stem cell (hMSC) attachment and proliferation, and demonstrated chondrogenesis and collagen type 2 production (Yadav et al. 2015).

17.7.6.2 Cellulose Nanocrystals

Poly(2-hydroxyethylmethacrylate) (PHEMA) matrices reinforced with CNC form a composite hydrogel with enhanced toughness, increased viscoelasticity, and improved recovery behavior. The hydrogel's water-holding capacity, mechanical properties, and viscoelasticity appeared to be similar to those of natural load-bearing

tissue featuring hydrogel-like characteristics. Therefore, such hydrogels present a potential replacement materials for articular cartilage (Karaaslan et al. 2011).

Tendon and ligament functions are intrinsically related, largely as a result of their unique hierarchically and anisotropically organized extracellular matrix. As their intrinsic healing ability is very limited, nanofibrous 3D scaffolds combining the slow degradation and mechanical behavior of polycaprolactone (PCL) and chitosan (CHT), with improved mechanical properties by reinforcement with small amounts of CNC, have been developed to mimic tendon and ligament nano-to-macro architecture and nonlinear biomechanical behavior. Scaffold nanotopography and microstructure supported extensive cytoskeleton elongation and anisotropic organization typical of tendon tissues. The scaffolds exhibited tensile strength and Young's modulus in the range of tendon tissues, preserved the phenotype of seeded human-tendon-derived cells (hTDCs) and also favored induction of tenogenic-like differentiation of adipose stem cells, without any supplementation with biochemical factors (Laranjeira et al. 2017).

17.7.6.3 Cellulose Nanofibers

Fully bio-based, three-dimensional porous scaffolds prepared from freeze-dried cellulose nanofibers (70–90 wt%) and stabilized using a genipin-cross-linked matrix of gelatin and chitosan demonstrated interconnected pore diameters and nanoscale pore wall roughness favorable for cell interactions required during cartilage repair. The compression moduli of the scaffolds in dry conditions, at 37 °C, were approximately 1 MPa, comparable to natural cartilaginous tissue. When immersed in PBS, the scaffolds proved as viscoelastic as natural cartilage but showed a lower compression modulus (18–32 kPa), which was considered favorable for chondrogenesis and soft tissue regeneration. Furthermore, the high porosity (95%), high PBS uptake, and good cytocompatibility toward chondrocytes were considered beneficial for cell attachment and ECM production (Naseri et al. 2016). Nanocomposites of CNF and collagen cross-linked with genipin, a bio-based cross-linker that introduces flexible cross-links, demonstrated mechanical performance close to that of natural ligament and tendon, in simulated body conditions after sterilization. In addition, these nanocomposites allowed for human endothelial cell and human ligament cell adhesion, growth, differentiation, and phenotype expression and are, therefore, very good candidates for supporting ligament repair through angiogenesis and ECM synthesis (Mathew et al. 2013).

CNF was used to synthesize fibrous cellulose nanocomposites, with dissolved cellulose nanofibers forming the matrix phase and undissolved or partially dissolved nanofibers forming the reinforcing phase. The mechanical properties in simulated body conditions were comparable to those of natural ligaments and tendons. The nanocomposite was able to withstand cyclic loading and unloading and exhibited in vitro biocompatibility, as shown by adhesion/proliferation and differentiation of both human ligament and endothelial cells (Mathew et al. 2012).

For 3D bioprinting applications, bioink, combining the outstanding shear thinning properties of CNF with the fast cross-linking ability of alginate, was formulated to print living soft tissue with cells. Anatomically shaped cartilage structures, such as a human ear and sheep meniscus, were 3D-printed with high fidelity and stability, using MRI and CT images as blueprints. The rheological properties of the bioink provided excellent printability at room temperature and low pressure, two essential conditions when 3D bioprinting with living cells. The tested bioink was biocompatible, with 73% and 86% of bioprinted human chondrocytes remaining viable after 1 and 7 days of 3D culture, respectively (Markstedt et al. 2015). In another study, CNF/alginate bioink was embedded with human bone marrow-derived stem cells (hBMSCs) and human nasal chondrocytes (hNC). In order to evaluate neocartilage formation and the stability of the bioprinted constructs in vivo, a $5 \times 5 \times 1$ mm piece of bioprinted cell-laden CNF/alginate construct was implanted into a subcutaneous pocket in 36 nude mice. The constructs exhibited preserved mechanical properties and structural integrity after 60 days of implantation. On day 60 postimplantation, the formed tissue showed all the qualitative features of proper cartilage: human collagen II and glycosaminoglycans deposition and formation of chondrocyte cell clusters, clear evidence that the embedded cells can proliferate. These observations suggest the potential of 3D bioprinting of human cartilage for future application in reconstructive surgery (Möller et al. 2017).

17.7.7 Urinary Conduits

Bladder cancer is a common urologic malignancy and sometimes demands surgical resection of the tumor, followed by the creation of a urinary reservoir using segments of the small or large intestine, a procedure associated with complications. In vitro construction of a neobladder (or bladder tissue) using autologous cells harvested from the patient and biomaterials as a scaffold, is currently being investigated as a means of urinary diversion (de Oliveira Barud et al. 2016).

17.7.7.1 Bacterial Cellulose

BC was tested as scaffold material for the proposed neobladder and was seeded with human urine-derived stem cells that were induced to differentiate into urothelial and smooth muscle cells. The cells formed multilayers on the BC scaffold surface, and some cells infiltrated into the scaffold. In addition, urothelial markers as well as smooth muscle markers were expressed. Upon implantation in athymic mice, the cells differentiated and expressed urothelial and smooth muscle markers. In addition, BC did not elicit any fibrotic capsule formation (Bodin et al. 2010). Another study developed a 3D porous BC scaffold with gelatin sponge, which was seeded with lingual keratinocytes and applied to repair rabbit ventral urethral defects. Postoperation examinations revealed that all urethras maintained wide calibers and showed an intact epithelium. In addition, the implant enhanced epithelial and

urethral tissue regeneration without inducing inflammatory reactions (Huang et al. 2015). A bilayer scaffold comprising a microporous network of silk fibroin (SF) and a nano-porous BC scaffold was tested for long-segment urethral regeneration. When seeded with lingual keratinocytes and lingual muscle cells, adhesion and proliferation and no cytotoxicity were observed. In vivo implantation of the scaffold with seeded cells in dogs led to epithelium regeneration, which showed intact epithelial cellular layers and organized muscle bundles (Lv et al. 2018).

17.7.8 Artificial Cornea/Contact Lens

17.7.8.1 Bacterial Cellulose

Due to its biocompatibility, light transmittance, and mechanical properties, BC is a suitable material for artificial cornea replacement or as a scaffold for cornea regeneration. Human corneal stromal cells grown on BC proliferated and successfully filled the scaffold (Jia et al. 2009). A patented technology using BC to create contact lenses for cornea regeneration enables tailoring into correct angles and shapes necessary for the correction of presbyopia, astigmatism, hyperopia, and myopia (Messaddeq et al. 2008). BC/PVA composites exhibited high water content, high visible light transmittance, suitable UV absorbance, increased mechanical strength (compared to neat PVA), biocompatibility, and thermal properties appropriate for artificial cornea replacement (Wang et al. 2010b). BC membranes in the shape of a contact lens can bind active materials and release them locally in the eye in a controlled manner. BC membranes impregnated with ciprofloxacin (CPX), with 2-hydroxypropyl-gamma-cyclodextrin (gamma-CD), demonstrated a slower release rate as compared to BC-CPX without gamma-CD. BC, BC/gamma-CD, BC/gamma-CD/CPX composites showed no cytotoxicity, genotoxicity, or mutagenicity, while BC/CPX showed a cytotoxic effect (Cavicchioli et al. 2015).

Age-related macular degeneration (AMD) can be treated by transplanted retinal pigment epithelial (RPE) cells (Booij et al. 2010). The unique BC properties, including permeability to gas and fluid transport and stability, ease of manipulation (mechanical stability), biocompatibility, and limited swelling, render it a potential substrate for RPE transplantation. Surface modifications made on BC to improve RPE-material interactions included acetylation or polysaccharide adsorption, using either chitosan or carboxymethyl cellulose, both of which enhanced RPE cell adhesion and proliferation (Gonçalves et al. 2015). An acetylated BC substrate coated with urinary bladder matrix enabled RPE cells to form a monolayer configuration with the desire phenotype, in which cells were polygonal shaped, with microvilli, and expressed proteins essential for their cytoskeletal organization and metabolic function (ZO-1 and RPE65). In addition, the coated substrate showed a low degree of swelling and no signs of hydrolytic degradation, was easily manipulable, and displayed high mechanical strength, indicating their potential as a cell carrier in RPE transplantation procedures (Gonçalves et al. 2016).

17.7.8.2 Cellulose Nanocrystals

PVA hydrogel reinforced by carboxylated CNC exhibited oxygen permeability, high water content, biocompatibility, and transparency above 95% in the visible range. The hydrogel had a higher water content than commercial contact lenses and possessed a mechanical profile that resembled that of natural cornea, combining the softness and elasticity with remarkable mechanical strength. Thus, this hydrogel can be integrated in a range of ophthalmic applications, including disposable contact lenses and cornea regeneration implants (Tummala et al. 2016).

17.7.9 Neural Implants/Dura Mater

Regeneration and reconstruction of nervous tissue is a complicated and challenging task, where the self-regeneration capacities of nervous tissue are limited. Dural implants are used either to complete a dural gap or to reinforce primary closure.

17.7.9.1 Bacterial Cellulose

BC is compatible with Schwann cells and facilitates their survival and growth. In vivo tests showed that BC neural implantation caused no adverse hematological and histological effects and no cytotoxicity (Zhu et al. 2014).

A BC membrane seeded with human dural fibroblasts showed dural fibroblast ingrowth and cell viability. The biomechanics of this material, the capacity to customize its shape, its biocompatibility, and its documented dural fibroblastic ingrowth, implies that BC can be a candidate reagent in perioperative dural repair (Goldschmidt et al. 2016). When tested as dura matter substitute in dogs, BC grafts were well accepted, with few and moderate extradural fibroses, which caused adherence of the implants to the bone fragment. Neither adherence to the cortex nor foreign body reactions were observed. Microscopic examinations revealed that the cellulose was enveloped by two layers of connective tissue, the external layer being thicker than the internal one. The external membrane consisted of collagen (neodura), whereas the inner layer was comprised of a layer of fibroblasts, which are the most important cells of the dura mater (Mello et al. 1997). In addition, in vivo implantation of BC membranes to repair a dura defect in rats did not induce any immune reaction, chronic inflammatory response, or neurotoxicity (Lima et al. 2017).

BC-based BASYC® tubes can be used as protective cuffs during nerve surgery. Upon dissection of the rat nervus ischiadicus and subsequent reconnection by a typical microsurgical suture, a protective cuff of BASYC® prevented connective tissue from growing into the nerve gap and favored the adhesion of the fascicles, which facilitated early regeneration of the nerve and a rapid return of muscle function (Klemm et al. 2005). Twenty-six weeks after the procedure, the BASYC® tube was covered with connective tissue and had small vessels within; no inflammatory

reaction or encapsulation of the implant was observed. The regeneration of nerve function improved after 10 weeks, compared to an uncovered anastomosed nerve (Klemm 2006). When applied to reconstruct damaged peripheral nerves in rats, BC nanotubes covering the two sides of a stumped femoral nerve, and then stabilized with four single sutures (called cellulosic guidance channels), prevented the formation of neuromas, exhibited very good biocompatibility, enabled proper guidance of the growing axons, and were conducive to accumulation of neurotrophic factors within, thus facilitating nerve regeneration (Kowalska-Ludwicka et al. 2013).

BC composites developed for advanced nerve tissue regeneration applications included the conductive polypyrrole (PPy), in situ polymerized onto the surface of BC. When seeded with PC12 rat neuronal cells, the neural cells adhered and underwent significantly more proliferation on BNC/PPy as compared to BNC. The PPy acts as an active interface and may be used to regulate cell activity through electrical stimulations. The composite's topographical features and electrical activity may be advantageous in tissue engineering applications that require electrical conductivity, such as nerve tissue reconstruction (Muller et al. 2013).

Biodegradable oxidized BC scaffolds proved cell- and blood-compatible, were highly porous, with interconnecting pores, were biodegradable, and featured suitable mechanical properties relevant for peripheral nerve repair applications (Hou et al. 2018).

17.7.9.2 Cellulose Nanocrystals

Neural interfaces can record neural signals from individual neurons or small groups of neurons in the brain, and, thus, neural interface implants hold great potential for restoring neural functions to persons with paralysis (Jorfi and Foster 2015). The ideal electrode should initially be stiff to facilitate minimal trauma during its insertion into the cortex, yet become mechanically compliant to match the stiffness of the brain tissue and minimize forces exerted on the tissue. Mechanically adaptive materials were designed using poly(vinyl acetate) (PVAc) and CNCs, with the controllable structural scaffold of rigid CNC embedded within the soft polymeric matrix. PVAc/CNC composites were inserted through the pia mater into the cerebral cortex of a rat, without requiring assistive devices. The initially stiff microprobe harnessed the in vivo environment to rapidly become compliant to more closely match the surrounding cortical tissue. Initial histological examination suggested cellular integration at the microprobe-tissue interface (Harris et al. 2011). At 2, 8, and 16 weeks postimplantation in the rat cortex, the compliant implants demonstrated a significantly reduced neuroinflammatory response when compared to stiff reference materials. In addition, no appreciable neuron loss was observed around the PVAc/CNC implants (Nguyen et al. 2014). Another composite based on PVA and CNC, whose initial stiffness was higher than the PVAc/CNC composite, was applied to ensure the reliable insertion of the cortical microelectrodes. The mechanical properties of the composite significantly changed upon exposure to simulated physiological conditions (Jorfi et al. 2013).

17.7.10 Other Tissue Engineering Applications

17.7.10.1 Bacterial Cellulose

Tympanic membrane (TM) perforation is a very common clinical problem resulting in conductive hearing loss and chronic perforations. In order to avoid surgical interventions, regeneration of the TM is needed. A nanofibrillar BC patch proved biocompatible, transparent and with tensile strength and Young's modulus satisfying the requirements of an ideal wound healing platform for TM regeneration. In vitro studies showed that TM cells adhered well and proliferated on the BC patch. In vivo tests demonstrated that the BC patch increased the TM healing rate and contributed to TM function recovery (Kim et al. 2013). In a recent study, BC membranes placed directly on the TM induced no complications such as ear pain, bleeding, and hematomas. In addition, the treatment with BC was significantly cheaper and was as effective as treatment with autologous temporal fascia (Silveira et al. 2016).

Severe infection and mechanical injury of the uterus may lead to infertility and miscarriage. Currently, there is a paucity of effective treatment modalities for functional repair of uterine injury. To address this challenge, a novel scaffold composed of recombinant human stromal cell-derived factor-1α (rhSDF-1α) incorporated into a silk fibroin-bacterial cellulose (SF-BC) membrane carrier, was developed and implanted in a rat uterine injury model. The SF-BC loaded with rhSDF-1α significantly enhanced endometrial regeneration and arteriogenesis of the injured rat uterus. One month post-injury, embryos were implanted, and improved pregnancy outcomes were observed in SF-BC-/rhSDF-1α-treated rats (Cai et al. 2018).

BC and its composites can be used for many other applications, such as adipose tissue engineering (Krontiras et al. 2015), laryngeal medialization (De Souza et al. 2011), vascular embolization (Wu et al. 2013), closure of ventricular septal defects (Lang et al. 2015), esophageal defect repair (Zhu et al. 2015), and artificial intervertebral discs (Yang et al. 2018).

17.7.10.2 Cellulose Nanofibers (CNFs)

Biocomposite hydrogels with carboxymethylated CNF (c-CNF) powder, prepared by UV polymerization of *N*-vinyl-2-pyrrolidone with Tween 20, were evaluated for replacement of the native, human nucleus pulposus (NP) in IVDs. The biocomposite hydrogels successfully mimicked the mechanical and swelling behavior of the NP, and the presence of c-CNF improved material relaxation properties as compared with neat hydrogels (Borges et al. 2011; Eyholzer et al. 2011) (Table 17.4).

Table 17.4 Nanocellulose in tissue engineering applications

Treatment/modification	Properties	References
Bacterial cellulose		
Surface modifications		
Nitrogen plasma	Significantly improves adhesion and proliferation of human endothelial cells (HMEC-1) and rat neuroblasts (N1E-115)	Pertile et al. (2010)
CF4 plasma	Improves L-929 fibroblasts and Chinese hamster ovary cell line adhesion and proliferation	Kurniawan et al. (2012)
Glycidyl trimethyl ammonium chloride	Better growth of L929 fibroblasts compared to pure BC	Watanabe et al. (1993)
Beta-dimethyl hydrochloride		
2-chloroethylamine hydrochloride		
Monochloro acetic acid sodium		
Amine-terminated 3-aminopropyltriethoxysilane	Improves human dermal fibroblast (NHDF) attachment, spreading and growth	Taokaew et al. (2015)
Fibronectin	Supports attachment of human umbilical vein endothelial cells and of mouse mesenchymal stem cells	Kuzmenko et al. (2013)
Collagen type I		
Lecithin	Improves proliferation of breast cancer cells as compared to pure BC	Nakaya and Li (1999) and Zhang et al. (2015)
Composites		
Collagen	Maintains cell viability and bioactivity for about 1 month, promotes cell adhesion	Watanabe et al. (1993)
Alginate	Stable structure, 90–160 μm pore size, supports attachment, spreading, and proliferation of human gingival fibroblast, limited ingrowth, biocompatible	Kirdponpattara et al. (2015)
Alginate/collagen	Maintains MC3T3-E1 and h-AMS cell viability and proliferation, good 3D architecture	Yan et al. (2018)
Gelatin	High porosity, good swelling properties, good structural stability in water, nontoxic, supports fibroblast adhesion and proliferation, better biocompatibility than pure BC	Kim et al. (2010), Wang et al. (2012) and Kirdponpattara et al. (2017)
Alginate-chitosan-gelatin	Good 3D architecture, porous structure, regulated biodegradation, supports attachment, proliferation and differentiation of osteoblastic MC3T3-E1 cells	Yan et al. (2017)

(continued)

Table 17.4 (continued)

Treatment/modification	Properties	References
Silk fibroin	Non-cytotoxic, non-genotoxic, supports fibroblast attachment and growth	Oliveira Barud et al. (2015)
PEG	Improves thermal stability, biocompatibility, and 3T3 fibroblast adhesion and proliferation as compared to pure BC	Cai and Kim (2010)
Chitosan	Bioactive, suitable for cell adhesion and proliferation, better biocompatibility compared to pure BC	Kim et al. (2011)
Potato starch	Higher cell ingrowth tendency with increasing starch content	Yang et al. (2014) and Lv et al. (2016)
PVA	Cell viability >90%, supports cell adhesion and proliferation	Palaninathan et al. (2018)
Keratin	Enhances dermal fibroblast attachment and proliferation profiles	Keskin et al. (2017)
Poly-3-hydroxybutyrate (PHB), polyhydroxyalkanoate (PHA)	Good L929 attachment and proliferation, biocompatible	Chiulan et al. (2016)
Poly(3-hydroxybutyrate-co-4-hydroxybutyrate)	Supports Chinese hamster lung (CHL) fibroblast cell adhesion and proliferation, better biocompatibility than pure P(3HB-co-4HB) scaffold	Zhijiang et al. (2012)
Cellulose nanocrystals		
Composites		
Poly(lactic acid)	Degrades more rapidly and exhibits higher tensile stress and Young's modulus compared to neat PLA	Shi et al. (2012b)
Collagen	Biocompatible, higher tensile strength, and Young's modulus compared to neat collagen	Li et al. (2014)
Polyurethane	Higher Young's modulus with increasing CNC content, biocompatible, good substrate for L-929 fibroblast adhesion and proliferation	Rueda et al. (2013)
Starch/PVA	Size, shape, and homogeneity of the pores controlled by the addition of CNCs, cytocompatible, COS-7 cells adhere and spread	Wang et al. (2010c)
Chitosan-g-D,L-lactic acid	Increased porosity, degradability, and cell viability with increasing CNC content	Ko et al. (2018)
Polyhydroxybutyrate (PHB)	Nontoxic to L-929, supports cell proliferation. An optimal CNC concentration improves the tensile strength and Young's modulus	Kampeerapappun (2016)

(continued)

Table 17.4 (continued)

Treatment/modification	Properties	References
Hyaluronic acid	Pronounced proliferative activity and spreading of human adipose-derived stem cells (hASCs). An optimal CNC concentration improves the storage modulus	Domingues et al. (2015)
Carboxymethyl cellulose and dextran	Biocompatible, stable, elastic	Yang et al. (2013b)
Cellulose	Enhanced mechanical properties, nontoxic, strong effect on directing cellular organization, cells proliferate fast on and inside matrix	He et al. (2014)
MA-g-PBAT	Biocompatible, enhanced cell adhesion and proliferation	Kashani Rahimi et al. (2017)
Cellulose nanofibers		
Composites		
PVA	Higher modulus and tensile strength compared to PVA alone	Zimmermann et al. (2004)
Collagen	High porosities, strong water absorption, good biocompatibility, high level of L929 cell activity and proliferation	Lu et al. (2014)
Pectin and carboxymethyl cellulose	Optimal CNF concentration (0.1%) exhibits the highest compression modulus, excellent thermal stability, and the lowest degradation rate. Biocompatible	Ninan et al. (2013)
Thermoplastic polyurethane (TPU)	Improved cell adhesion and proliferation compared to TPU alone	Ye et al. (2017)

17.8 Concluding Remarks

The recent revival of wood biomass resources has been largely enabled by contemporary technological, primarily nanotechnological, advances. The remarkable features of nanocellulose, including its physical properties, unique and modifiable surface chemistry, biocompatibility, biodegradability, and low toxicity, render it a high-quality, low-cost, and renewable raw material, which has proven advantageous in a range of sectors, including biomedical devices, pharmaceuticals, and 3D printing. Intensified streaming of nature's most abundant polymer to high tech and biotechnology promises to fully unleash its immense potential and to provide for greener alternatives, with a more desirable environment-resources balance. More specifically, further works assessing the distinct qualities of each nanocellulose subfamily will allow for optimization of materials, rational micro−/macrostructural manipulation, improved regulation of their interactions with proximal materials, and formulation of composites with novel functionalities.

References

Abitbol T, Rivkin A, Cao Y, Nevo Y, Abraham E, Ben-Shalom T, Lapidot S, Shoseyov O (2016) Nanocellulose, a tiny fiber with huge applications. Curr Opin Biotechnol 39:76–88

Abitbol T, Kam D, Levi-Kalisman Y, Gray DG, Shoseyov O (2018) Surface charge influence on the phase separation and viscosity of cellulose nanocrystals. Langmuir. https://doi.org/10.1021/acs.langmuir.7b04127

Abo-elseoud WS, Hassan ML, Sabaa MW, Basha M, Hassan EA, Fadel SM (2018) Chitosan nanoparticles/cellulose nanocrystals nanocomposites as a carrier system for the controlled release of repaglinide. Int J Biol Macromol 111:604–613

Abraham E, Kam D, Nevo Y, Slattegard R, Rivkin A, Lapidot S, Shoseyov O (2016a) Highly modified cellulose nanocrystals and formation of Epoxy-Nanocrystalline Cellulose (CNC) nanocomposites. ACS Appl Mater Interfaces 8:28086–28095

Abraham E, Nevo Y, Slattegard R, Attias N, Sharon S, Lapidot S, Shoseyov O (2016b) Highly hydrophobic thermally stable liquid crystalline cellulosic nanomaterials. ACS Sustain Chem Eng 4:1338–1346

Abraham E, Weber DE, Sharon S, Lapidot S, Shoseyov O (2017) Multifunctional cellulosic scaffolds from modified cellulose nanocrystals. ACS Appl Mater Interfaces 9:2010–2015

Åhlén M, Tummala GK, Mihranyan A (2018) Nanoparticle-loaded hydrogels as a pathway for enzyme-triggered drug release in ophthalmic applications. Int J Pharm 536:73–81

Ahmad N, Mohd Amin MCI, Mahali SM, Ismail I, Giam Chuang VT (2014) Biocompatible and mucoadhesive bacterial cellulose-g-poly(acrylic acid) hydrogels for oral protein delivery. Mol Pharm 11:4130–4142

Ahrem H, Pretzel D, Endres M, Conrad D, Courseau J, Müller H, Jaeger R, Kaps C, Klemm DO, Kinne RW (2014) Laser-structured bacterial nanocellulose hydrogels support ingrowth and differentiation of chondrocytes and show potential as cartilage implants. Acta Biomater 10:1341–1353

Aitomäki Y, Oksman K (2014) Reinforcing efficiency of nanocellulose in polymers. React Funct Polym 85:151–156

Akaraonye E, Filip J, Safarikova M, Salih V, Keshavarz T, Knowles JC, Roy I (2016) Composite scaffolds for cartilage tissue engineering based on natural polymers of bacterial origin, thermoplastic poly(3-hydroxybutyrate) and micro-fibrillated bacterial cellulose. Polym Int 65:780–791

Akhlaghi SP, Berry RC, Tam KC (2013) Surface modification of cellulose nanocrystal with chitosan oligosaccharide for drug delivery applications. Cellulose 20:1747–1764

Akhlaghi SP, Tiong D, Berry RM, Tam KC (2014) Comparative release studies of two cationic model drugs from different cellulose nanocrystal derivatives. Eur J Pharm Biopharm 88:207–215

Alizadeh N, Akbari V, Nurani M, Taheri A (2018) Preparation of an injectable doxorubicin surface modified cellulose nanofiber gel and evaluation of its anti-tumor and anti-metastasis activity in melanoma. Biotechnol Prog 34:537–545

Alkhatib Y, Dewaldt M, Moritz S, Nitzsche R, Kralisch D, Fischer D (2017) Controlled extended octenidine release from a bacterial nanocellulose/Poloxamer hybrid system. Eur J Pharm Biopharm 112:164–176

An SJ, Lee SH, Huh JB, Jeong SI, Park JS, Gwon HJ, Kang ES, Jeong CM, Lim YM (2017) Preparation and characterization of resorbable bacterial cellulose membranes treated by electron beam irradiation for guided bone regeneration. Int J Mol Sci 18:2236

Andersson J, Stenhamre H, Bäckdahl H, Gatenholm P (2010) Behavior of human chondrocytes in engineered porous bacterial cellulose scaffolds. J Biomed Mater Res Part A 94A:1124–1132

Andrade FK, Moreira SMG, Domingues L, Gama FMP (2009) Improving the affinity of fibroblasts for bacterial cellulose using carbohydrate-binding modules fused to RGD. J Biomed Mater Res Part A 92:9–17

Andrade FK, Costa R, Domingues L, Soares R, Gama M (2010) Improving bacterial cellulose for blood vessel replacement: functionalization with a chimeric protein containing a cellulose-binding module and an adhesion peptide. Acta Biomater 6:4034–4041

Andrade FK, Silva JP, Carvalho M, Castanheira EMS, Soares R, Gama M (2011) Studies on the hemocompatibility of bacterial cellulose. J Biomed Mater Res Part A 98(A):554–566

Angelova N, Hunkeler D (1999) Rationalizing the design of polymeric biomaterials. Trends Biotechnol 17:409–421

Anirudhan TS, Rejeena SR (2014) Poly(acrylic acid-co-acrylamide-co-2-acrylamido-2-methyl-1-propanesulfonic acid)-grafted nanocellulose/poly(vinyl alcohol) composite for the in vitro gastrointestinal release of amoxicillin. Appl Polym 131:40699

Anirudhan TS, Nair SS, Chithra Sekhar V (2017) Deposition of gold-cellulose hybrid nanofiller on a polyelectrolyte membrane constructed using guar gum and poly(vinyl alcohol) for transdermal drug delivery. J Membr Sci 539:344–357

Ansell MP (2015) Wood composites. Elsevier Ltd, New York City

Araki J, Wada M, Kuga S, Okano T (1999) Influence of surface charge on viscosity behavior of cellulose microcrystal suspension. J Wood Sci 45:258–261

Araújo IMS, Silva RR, Pacheco G, Lustri WR, Tercjak A, Gutierrez J, Júnior JRS, Azevedo FHC, Figuêredo GS, Vega ML, Ribeiro SJL, Barud HS (2018) Hydrothermal synthesis of bacterial cellulose–copper oxide nanocomposites and evaluation of their antimicrobial activity. Carbohydr Polym 179:341–349

Ataide JA, De Carvalho NM, Rebelo MDA, Chaud MV, Grotto D, Gerenutti M, Rai M, Mazzola PG, Jozala AF (2017) Bacterial nanocellulose loaded with bromelain: assessment of antimicrobial, antioxidant and physical-chemical properties. Sci Rep 7:18031

Bäckdahl H, Helenius G, Bodin A, Nannmark U, Johansson BR, Risberg B, Gatenholm P (2006) Mechanical properties of bacterial cellulose and interactions with smooth muscle cells. Biomaterials 27:2141–2149

Backdahl H, Esguerra M, Delbro D, Risberg B, Gatenholm P (2008) Engineering microporosity in bacterial cellulose scaffolds. J Tissue Eng Regen Med 2:320–330

Badshah M, Ullah H, Khan SA, Joong K, Park JK, Khan T (2017) Preparation, characterization and in-vitro evaluation of bacterial cellulose matrices for oral drug delivery. Cellulose 24:5041–5052

Badshah M, Ullah H, Khan AR, Khan S, Park JK, Khan T (2018) Surface modification and evaluation of bacterial cellulose for drug delivery. Int J Biol Macromol 113:526–533

Bajpai SK, Ahuja S, Chand N, Bajpai M (2017) Nano cellulose dispersed chitosan film with Ag NPs/Curcumin: an in vivo study on Albino Rats for wound dressing. Int J Biol Macromol 104:1012–1019

Barua S, Das G, Aidew L, Buragohain AK, Karak N (2013) Copper–copper oxide coated nanofibrillar cellulose: a promising biomaterial. RSC Adv 3:14997–15004

Barud HDS, de Araújo Júnior AM, Saska S, Mestieri LB, Campos JADB, de Freitas RM, Ferreira NU, Nascimento AP, Miguel FG, Vaz MMDOLL, Barizon EA, Marquele-Oliveira F, Gaspar AMM, Ribeiro SJL, Berretta AA (2013) Antimicrobial Brazilian propolis (EPP-AF) eontaining biocellulose membranes as promising biomaterial for skin wound healing. Evid Based Complement Alternat Med 2013:1–10

Basmaji P, De Olyveira GM, Marcio Luiz dos S, Guastaldi AC (2014) Novel antimicrobial peptides bacterial cellulose obtained by symbioses culture between polyhexanide biguanide (PHMB) and green tea. J Biomater Tissue Eng 4:59–64

Basnett P, Knowles JC, Pishbin F, Smith C, Keshavarz T, Boccaccini AR, Roy I (2012) Novel biodegradable and biocompatible poly(3-hydroxyoctanoate)/bacterial cellulose composites. Adv Eng Mater 14:330–343

Basu A, Lindh J, Ålander E, Strømme M, Ferraz N (2017) On the use of ion-crosslinked nanocellulose hydrogels for wound healing solutions: physicochemical properties and application-oriented biocompatibility studies. Carbohydr Polym 174:299–308

Basu A, Heitz K, Strømme M, Welch K, Ferraz N (2018) Ion-crosslinked wood-derived nanocellulose hydrogels with tunable antibacterial properties: candidate materials for advanced wound care applications. Carbohydr Polym 181:345–350

Bayer J, Granda LA, Méndez JA, Pèlach MA, Vilaseca F, Mutjé P (2016) Cellulose polymer composites (WPC). In: Advanced high strength natural fibre composites in construction. Elsevier Science, Kent, pp 115–139

Bhandari J, Mishra H, Mishra PK, Wimmer R, Ahmad FJ, Talegaonkar S (2017) Cellulose nanofiber aerogel as a promising biomaterial for customized oral drug delivery. Int J Nanomedicine 12:2021–2031

Bhattacharya M, Malinen MM, Lauren P, Lou YR, Kuisma SW, Kanninen L, Lille M, Corlu A, Guguen-Guillouzo C, Ikkala O, Laukkanen A, Urtti A, Yliperttula M (2012) Nanofibrillar cellulose hydrogel promotes three-dimensional liver cell culture. J Control Release 164:291–298

Bodhibukkana C, Srichana T, Kaewnopparat S, Tangthong N, Bouking P, Martin GP, Suedee R (2006) Composite membrane of bacterially-derived cellulose and molecularly imprinted polymer for use as a transdermal enantioselective controlled-release system of racemic propranolol. J Control Release 113:43–56

Bodin A, Ahrenstedt L, Fink H, Brumer H, Risberg B, Gatenholm P (2007a) Modification of nanocellulose with a xyloglucan – RGD conjugate enhances adhesion and proliferation of endothelial cells: implications for tissue engineering. Biomacromolecules 8:3697–3704

Bodin A, Backdahl H, Fink H, Gustafsson L, Risberg B, Gatenholm P (2007b) Influence of cultivation conditions on mechanical and morphological properties of bacterial cellulose tubes. Biotechnol Bioeng 97:425–434

Bodin A, Concaro S, Brittberg M, Gatenholm P (2007c) Bacterial cellulose as a potential meniscus implant. J Tissue Eng Regen Med 1:406–408

Bodin A, Bharadwaj S, Wu S, Gatenholm P, Atala A, Zhang Y (2010) Tissue-engineered conduit using urine-derived stem cells seeded bacterial cellulose polymer in urinary reconstruction and diversion. Biomaterials 31:8889–8901

Booij JC, Baas DC, Beisekeeva J, Gorgels TGMF, Bergen AAB (2010) The dynamic nature of Bruch's membrane. Prog Retin Eye Res 29:1–18

Borges AC, Eyholzer C, Duc F, Bourban PE, Tingaut P, Zimmermann T, Pioletti DP, Månson JAE (2011) Nanofibrillated cellulose composite hydrogel for the replacement of the nucleus pulposus. Acta Biomater 7:3412–3421

Brett CT (2000) Cellulose microfibrils in plants: biosynthesis, deposition, and integration into the cell wall. Int Rev Cytol 199:161–199

Brinchi L, Cotana F, Fortunati E, Kenny JM (2013) Production of nanocrystalline cellulose from lignocellulosic biomass: technology and applications. Carbohydr Polym 94:154–169

Brown EE, Laborie MPG, Zhang J (2012) Glutaraldehyde treatment of bacterial cellulose/fibrin composites: impact on morphology, tensile and viscoelastic properties. Cellulose 19:127–137

Brown EE, Hu D, Abu Lail N, Zhang X (2013) Potential of nanocrystalline cellulose-fibrin nanocomposites for artificial vascular graft applications. Biomacromolecules 14:1063–1071

Butcher M (2011) Catch or kill? How DACC technology redefines antimicrobial management. Br J Nurs/Br J Community Nurs 13:S15–S16

Butchosa N, Brown C, Larsson PT, Berglund LA, Bulone V, Zhou Q (2013) Nanocomposites of bacterial cellulose nanofibers and chitin nanocrystals: fabrication, characterization and bactericidal activity. Green Chem 15:3404–3413

Cacicedo ML, León IE, Gonzalez JS, Porto LM, Alvarez VA, Castro GR (2016) Modified bacterial cellulose scaffolds for localized doxorubicin release in human colorectal HT-29 cells. Colloids Surf B Biointerfaces 140:421–429

Cacicedo ML, Islan GA, Drachemberg MF, Alvarez VA, Bartel L, Bolzán AD, Castro GR (2018) Hybrid bacterial cellulose – pectin films for delivery of bioactive molecules. New J Chem 42:7457–7467

Cai Z, Kim J (2010) Bacterial cellulose/poly (ethylene glycol) composite: characterization and first evaluation of biocompatibility. Cellulose 17:83–91

Cai H, Wu B, Liu Y, Li Y, Shi L, Gong L, Xia Y, Heng B, Wu H, Ouyang H, Zhu Z, Zou X (2018) Local delivery of stromal cell-derived factor-1α improves the pregnancy rate of injured uterus through the promotion of endometrial and vascular regeneration. In: bioRvix https://doi.org/10.1101/251579

Carlsson DO, Hua K, Forsgren J, Mihranyan A (2014a) Aspirin degradation in surface-charged TEMPO-oxidized mesoporous crystalline nanocellulose. Int J Pharm 461:74–81

Carlsson L, Fall A, Chaduc I, Wågberg L, Charleux B, Malmström E, D'Agosto F, Lansalot M, Carlmark A (2014b) Modification of cellulose model surfaces by cationic polymer latexes prepared by RAFT-mediated surfactant-free emulsion polymerization. Polym Chem 5:6076–6086

Cavicchioli M, Corso CT, Coelho F, Mendes L, Saska S, Soares CP, Souza FO, Franchi LP, Capote TSO, Scarel-Caminaga RM, Messaddeq Y, Ribeiro SJL (2015) Characterization and cytotoxic, genotoxic and mutagenic evaluations of bacterial cellulose membranes incorporated with ciprofloxacin: a potential material for use as therapeutic contact lens. World J Pharm Pharm Sci 4:1626–1647

Cha R, He Z, Ni Y (2012) Preparation and characterization of thermal/pH-sensitive hydrogel from carboxylated nanocrystalline cellulose. Carbohydr Polym 88:713–718

Chang C, Wang M (2013) Preparation of microfibrillated cellulose composites for sustained release of H2O2 or O2 for biomedical applications. ACS Sustain Chem Eng 1:1129–1134

Charpentier PA, Maguire A, Wan W k. (2006) Surface modification of polyester to produce a bacterial cellulose-based vascular prosthetic device. Appl Surf Sci 252:6360–6367

Cheginia SP, Meamar R (2018) Varshosaz J (2018) Co- delivery of Venlafaxine and Doxycycline by films of cellulose nanofibers for diabetic foot ulcers. Pharm Updat 1:36–37

Chen S, Huang Y (2015) Bacterial cellulose nanofibers decorated with phthalocyanine: preparation, characterization and dye removal performance. Mater Lett 142:235–237

Chen YM, Xi T, Zheng Y, Guo T, Hou J, Wan Y, Gao C (2009) In vitro cytotoxicity of bacterial cellulose scaffolds used for tissue-engineered bone. J Bioact Compat Polym 24:137–145

Chen W, Yu H, Liu Y, Chen P, Zhang M, Hai Y (2011) Individualization of cellulose nanofibers from wood using high-intensity ultrasonication combined with chemical pretreatments. Carbohydr Polym 83:1804–1811

Chen X, Zhou R, Chen B, Chen J (2016) Nanohydroxyapatite/cellulose nanocrystals/silk fibroin ternary scaffolds for rat calvarial defect regeneration. RSC Adv 6:35684–35691

Chen C, Chen X, Zhang H, Zhang Q, Wang L, Li C, Dai B, Yang J, Liu J, Sun D (2017) Electrically-responsive core-shell hybrid microfibers for controlled drug release and cell culture. Acta Biomater 55:434–442

Chen W, Yu H, Lee SY, Wei T, Li J, Fan Z (2018) Nanocellulose: a promising nanomaterial for advanced electrochemical energy storage. Chem Soc Rev 47:2837–2872

Cheng F, Liu C, Wei X, Yan T, Li H, He J, Huang Y (2017a) Preparation and characterization of 2,2,6,6-tetramethylpiperidine-1- oxyl (TEMPO)-oxidized cellulose nanocrystal/alginate biodegradable composite dressing for hemostasis applications. ACS Sustain Chem Eng 5:3819–3828

Cheng M, Qin Z, Hu S, Dong S, Ren Z, Yu H (2017b) Achieving long-term sustained drug delivery for electrospun biopolyester nanofibrous membranes by introducing cellulose nanocrystals. ACS Biomater Sci Eng 3:1666–1676

Cheng L, Zhang D, Gu Z, Li Z, Hong Y, Li C (2018) Preparation of acetylated nanofibrillated cellulose from corn stalk microcrystalline cellulose and its reinforcing effect on starch films. Int J Biol Macromol 111:959–966

Chiaoprakobkij N, Sanchavanakit N, Subbalekha K, Pavasant P, Phisalaphong M (2011) Characterization and biocompatibility of bacterial cellulose/alginate composite sponges with human keratinocytes and gingival fibroblasts. Carbohydr Polym 85:548–553

Chi-Fung LV, Dunn CK, Zhang Z, Deng Y, Qi HJ (2017) Direct Ink Write (DIW) 3D printed cellulose nanocrystal aerogel structures. Sci Rep 7:1–8

Chinga-Carrasco G, Syverud K (2014) Pretreatment-dependent surface chemistry of wood nanocellulose for pH-sensitive hydrogels. J Biomater Appl 29:423–432

Chiulan I, Mihaela Panaitescu D, Nicoleta Frone A, Teodorescu M, Andi Nicolae C, Căşărică A, Tofan V, Sălăgeanu A (2016) Biocompatible polyhydroxyalkanoates/bacterial cellulose composites: preparation, characterization, and in vitro evaluation. J Biomed Mater Res Part A 104A:2576–2584

Chu PK, Chen JY, Wang LP, Huang N (2002) Plasma-surface modification of biomaterials. Mater Sci Eng R Rep 36:143–206

Ciechańska D (2004) Multifunctional bacterial cellulose/chitosan composite materials for medical applications. Fibres Text East Eur 12:69–72

Courtenay JC, Johns MA, Galembeck F, Deneke C, Lanzoni EM, Costa CA, Scott JL, Sharma RI (2017) Surface modified cellulose scaffolds for tissue engineering. Cellulose 24:253–267

Csoka L, Hoeger IC, Rojas OJ, Peszlen I, Pawlak JJ, Peralta PN (2012) Piezoelectric effect of cellulose nanocrystals thin films. ACS Macro Lett 1:867–870

Czaja W, Krystynowicz A, Bielecki S, Brown RM (2006) Microbial cellulose – the natural power to heal wounds. Biomaterials 27:145–151

Czaja WK, Young DJ, Kawecki M, Brown RM (2007) The future prospects of microbial cellulose in biomedical applications. Biomacromolecules 8:1–12

Dash R, Foston M, Ragauskas AJ (2013) Improving the mechanical and thermal properties of gelatin hydrogels cross-linked by cellulose nanowhiskers. Carbohydr Polym 91:638–645

De France KJ, Yager KG, Chan KJW, Corbett B, Cranston ED, Hoare T (2017) Injectable anisotropic nanocomposite hydrogels direct in situ growth and alignment of myotubes. Nano Lett 17:6487–6495

De Lima Fontes M, Meneguin AB, Tercjak A, Gutierrez J, Cury BSF, Dos Santos AM, Ribeiro SJL, Barud HS (2018) Effect of in situ modification of bacterial cellulose with carboxymethylcellulose on its nano/microstructure and methotrexate release properties. Carbohydr Polym 179:126–134

De Macedo NL, Silva Matuda F da, Macedo LGS de, Monteiro ASF, Valera MC, Carvalho YR (2004) Evaluation of two membranes in guided bone tissue regeneration: histological study in rabbits. Braz J Oral Sci 3:395–400

de MT de Lima F, Pinto FCM, Andrade-da-Costa BL da S, Silva JGM da, Campos Júnior O, Aguiar JL de A (2017) Biocompatible bacterial cellulose membrane in dural defect repair of rat. J Mater Sci Mater Med 28:37

de Oliveira Barud HG, da Silva RR, da Silva Barud H, Tercjak A, Gutierrez J, Lustri WR, de Oliveira Junior OB, Ribeiro SJL (2016) A multipurpose natural and renewable polymer in medical applications: bacterial cellulose. Carbohydr Polym 153:406–420

De Olyveira GM, Valido DP, Costa LMM, Gois PBP, Filho LX, Basmaji P (2011) First otoliths/collagen/bacterial cellulose nanocomposites as a potential scaffold for bone tissue regeneration. J Biomater Nanobiotechnol 2:239–243

De Souza FC, Olival-Costa H, Da Silva L, Pontes PA, Lancellotti CLP (2011) Bacterial cellulose as laryngeal medialization material: an experimental study. J Voice 25:765–769

De Souza CF, Lucyszyn N, Woehl MA, Riegel-Vidotti IC, Borsali R, Sierakowski MR (2013) Property evaluations of dry-cast reconstituted bacterial cellulose/tamarind xyloglucan biocomposites. Carbohydr Polym 93:144–153

Delmer DP, Amor Y (1995) Cellulose biosynthesis. Am Soc Plant Physiol 7:987–1000

Di Z, Shi Z, Wajid Ullah M, Li S, Yang G (2017) A transparent wound dressing based on bacterial cellulose whisker and poly(2-hydroxyethyl methacrylate). Int J Biol Macromol 105:638–644

Domingues RMA, Silva M, Gershovich P, Betta S, Babo P, Caridade SG, Mano JF, Motta A, Reis RL, Gomes ME (2015) Development of injectable hyaluronic acid/cellulose nanocrystals bionanocomposite hydrogels for tissue engineering applications. Bioconjug Chem 26:1571–1581

Dong S, Cho HJ, Lee YW, Roman M (2014) Synthesis and cellular uptake of folic acid-conjugated cellulose nanocrystals for cancer targeting. Biomacromolecules 15:1560–1567

Dufresne A (2017) Current opinion in colloid & interface science cellulose nanomaterial reinforced polymer nanocomposites. Curr Opin Colloid Interface Sci 29:1–8

Dufresne A (2018) Cellulose nanomaterials as green nanoreinforcements for polymer nanocomposites. Philos Trans R Soc A Math Phys Eng Sci 376:20170040

Dugan JM, Collins RF, Gough JE, Eichhorn SJ (2013) Oriented surfaces of adsorbed cellulose nanowhiskers promote skeletal muscle myogenesis. Acta Biomater 9:4707–4715

Eichhorn SJ, Dufresne A, Aranguren M, Marcovich NE, Capadona JR, Rowan SJ, Weder C, Thielemans W, Roman M, Renneckar S, Gindl W, Veigel S, Keckes J, Yano H, Abe K, Nogi M, Nakagaito AN, Mangalam A, Simonsen J, Benight AS, Bismarck A, Berglund LA, Peijs T (2010) Review: current international research into cellulose nanofibres and nanocomposites. J Mater Sci 45(1):1–33

El Achaby M, El Miri N, Aboulkas A, Zahouily M, Bilal E, Barakat A, Solhy A (2017) Processing and properties of eco-friendly bio-nanocomposite films filled with cellulose nanocrystals from sugarcane bagasse. Int J Biol Macromol 96:340–352

El Miri N, Abdelouahdi K, Barakat A, Zahouily M, Fihri A, Solhy A, El Achaby M (2015) Bio-nanocomposite films reinforced with cellulose nanocrystals: rheology of film-forming solutions, transparency, water vapor barrier and tensile properties of films. Carbohydr Polym 129:156–167

El-naggar ME, Abdelgawad AM, Tripathi A, Rojas OJ (2017) Curdlan cryogels reinforced with cellulose nanofibrils for controlled release. J Environ Chem Eng 5:5754–5761

Eming SA, Smola H, Krieg T (2002) Treatment of chronic wounds: state of the art and future concepts. Cells Tissues Organs 172:105–117

Esguerra M, Fink H, Laschke MW, Jeppsson A, Delbro D, Gatenholm P, Menger MD, Risberg B (2010) Intravital fluorescent microscopic evaluation of bacterial cellulose as scaffold for vascular grafts. J Biomed Mater Res Part A 93:140–149

Eyholzer C, Borges De Couraça A, Duc F, Bourban PE, Tingaut P, Zimmermann T, Månson JAE, Oksman K (2011) Biocomposite hydrogels with carboxymethylated, nanofibrillated cellulose powder for replacement of the nucleus pulposus. Biomacromolecules 12:1419–1427

Fadel Picheth G, Luiz Pirich C, Rita Sierakowski M, Aurélio Woehl M, Novak Sakakibara C, Fernandes C, De Souza CF, Amado Martin A, da Silva R, De Freitas RA (2017) Bacterial cellulose in biomedical applications: a review. Int J Biol Macromol 104:97–106

Fakes MG, Vakkalagadda BJ, Qian F, Desikan S, Gandhi RB, Lai C, Hsieh A, Franchini MK, Toale H, Brown J (2009) Enhancement of oral bioavailability of an HIV-attachment inhibitor by nanosizing and amorphous formulation approaches. Int J Pharm 370:167–174

Fakhri A, Tahami S, Nejad PA (2017) Preparation and characterization of Fe3O4 -Ag 2O quantum dots decorated cellulose nano fibers as a carrier of anticancer drugs for skin cancer. J Photochem Photobiol B Biol 175:83–88

Fan M, Fu F (2017) Advanced high strength natural fibre composites in construction, 1st edn. Elsevier Ltd, Duxford

Fang B, Wan YZ, Tang TT, Gao C, Dai KR (2009) Proliferation and osteoblastic differentiation of human bone marrow stromal cells on hydroxyapatite/bacterial cellulose nanocomposite scaffolds. Tissue Eng Part A 15:1091–1098

Favi PM, Benson RS, Neilsen NR, Hammonds RL, Bates CC, Stephens CP, Dhar MS (2013) Cell proliferation, viability, and in vitro differentiation of equine mesenchymal stem cells seeded on bacterial cellulose hydrogel scaffolds. Mater Sci Eng C 33:1935–1944

Favier V, Chanzy H, Cavaillé JY (1995) Polymer nanocomposites reinforced by cellulose whiskers. Macromolecules 28:6365–6367

Feng X, Yang Z, Rostom SSH, Dadmun M, Xie Y, Wang S (2017) Structural, mechanical, and thermal properties of 3D printed L-CNC/acrylonitrile butadiene styrene nanocomposites. J Appl Polym Sci 134:45082

Fernandes SCM, Sadocco P, Alonso-Varona A, Palomares T, Eceiza A, Silvestre AJD, Mondragon I, Freire CSR (2013) Bioinspired antimicrobial and biocompatible bacterial cellulose membranes obtained by surface functionalization with aminoalkyl groups. ACS Appl Mater Interfaces 5:3290–3297

Figueiredo AGPR, Figueiredo ARP, Alonso-varona A, Fernandes SCM, Palomares T, Rubio-azpeitia E, Barros-timmons A, Silvestre AJD, Neto CP, Freire CSR (2013) Biocompatible bacterial cellulose-Poly(2-hydroxyethyl methacrylate) nanocomposite films. Biomed Res Int 2013:1–14

Figueiredo ARP, Figueiredo AGPR, Silva NHCS, Barros-timmons A, Almeida A, Silvestre AJD, Freire CSR (2015) Antimicrobial bacterial cellulose nanocomposites prepared by in situ polymerization of 2-aminoethyl methacrylate. Carbohydr Polym 123:443–453

Filpponen I, Argyropoulos DS (2015) Regular linking of cellulose nanocrystals via click chemistry: synthesis and formation of cellulose nanoplatelet gels. Biomacromolecules 11(4):1060–1066

Fink H, Faxälv L, Molnár GF, Drotz K, Risberg B, Lindahl TL, Sellborn A (2010) Real-time measurements of coagulation on bacterial cellulose and conventional vascular graft materials. Acta Biomater 6:1125–1130

Fink H, Ahrenstedt L, Bodin A, Brumer H, Gatenholm P, Krettek A, Risberg B (2011) Bacterial cellulose modified with xyloglucan bearing the adhesion peptide RGD promotes endothelial cell adhesion and metabolism – a promising modification for vascular grafts. J Tissue Eng Regen Med 5:454–463

Fiorati A, Turco G, Travan A, Caneva E, Pastori N, Cametti M, Punta C, Melone L (2017) Mechanical and drug release properties of sponges from cross-linked cellulose nanofibers. ChemPlusChem 82:848–858

Follain N, Marais MF, Montanari S, Vignon MR (2010) Coupling onto surface carboxylated cellulose nanocrystals. Polymer (Guildf) 51:5332–5344

Fontana JD, De Souza AM, Fontana CK, Torriani IL, Moreschi JC, Gallotti BJ, De Souza SJ, Narcisco GP, Bichara JA, Farah LFX (1990) Acetobacter cellulose pellicle as a temporary skin substitute. Appl Biochem Biotechnol 24–25:253–264

Fontenot KR, Edwards JV, Haldane D, Pircher N, Liebner F, Condon BD, Qureshi H, Yager D (2017) Designing cellulosic and nanocellulosic sensors for interface with a protease sequestrant wound-dressing prototype: implications of material selection for dressing and protease sensor design. J Biomater Appl 32:622–637

Foong CY, Hamzah MSA, Razak SIA, Saidin S, Nayan NHM (2018) Influence of poly(lactic acid) layer on the physical and antibacterial properties of dry bacterial cellulose sheet for potential acute wound healing materials. Fibers Polym 19:263–271

Fortunati E, Puglia D, Luzi F, Santulli C, Kenny JM, Torre L (2013a) Binary PVA bio-nanocomposites containing cellulose nanocrystals extracted from different natural sources: part I. Carbohydr Polym 97:825–836

Fortunati E, Puglia D, Monti M, Santulli C, Maniruzzaman M, Kenny JM (2013b) Cellulose nanocrystals extracted from okra fibers in PVA nanocomposites. J Appl Polym Sci 128:3220–3230

Fox JD, Capadona JR, Marasco PD, Rowan SJ (2013) Bioinspired water-enhanced mechanical gradient nanocomposite films that mimic the architecture and properties of the squid beak. J Am Chem Soc 135:5167–5174

Fragal EH, Cellet TSP, Fragal VH, Companhoni MVP, Ueda-Nakamura T, Muniz EC, Silva R, Rubira AF (2016) Hybrid materials for bone tissue engineering from biomimetic growth of hydroxiapatite on cellulose nanowhiskers. Carbohydr Polym 152:734–746

Frey M, Widner D, Segmehl JS, Casdorff K, Keplinger T, Burgert I (2018) Delignified and densified cellulose bulk materials with excellent tensile properties for sustainable engineering. ACS Appl Mater Interfaces 10:5030–5037

Fu L, Zhang Y, Li C, Wu Z, Zhuo Q, Huang X, Qiu G, Zhou P, Yang G (2012) Skin tissue repair materials from bacterial cellulose by a multilayer fermentation method. J Mater Chem 22:12349–12357

Fu L, Zhou P, Zhang S, Yang G (2013) Evaluation of bacterial nanocellulose-based uniform wound dressing for large area skin transplantation. Mater Sci Eng C 33:2995–3000

Galkina OL, Ivanov VK, Agafonov AV, Seisenbaeva GA, Kessler VG (2015) Cellulose nanofiber–titania nanocomposites as potential drug delivery systems for dermal applications. J Mater Chem B 3:1688–1698

Gama M, Gatenholm P, Klemm D (2012) Bacterial nanocellulose: a sophisticated multifunctional material. CRC Press, Taylor & Francis Group, Boca Raton

Gao C, Wan Y, Yang C, Dai K, Tang T, Luo H, Wang J (2011) Preparation and characterization of bacterial cellulose sponge with hierarchical pore structure as tissue engineering scaffold. J Porous Mater 18:139–145

Gao J, Li Q, Chen W, Liu Y, Yu H (2014) Self-assembly of nanocellulose and indomethacin into hierarchically ordered structures with high encapsulation efficiency for sustained release applications. ChemPlusChem 79:725–731

Gimenez RB, Leonardi L, Cerrutti P, Amalvy J, Chiacchiarelli LM (2017) Improved specific thermomechanical properties of polyurethane nanocomposite foams based on castor oil and bacterial nanocellulose. J Appl Polym Sci 134:44982

Girouard NM, Xu S, Schueneman GT, Shofner ML, Meredith JC (2016) Site-selective modification of cellulose nanocrystals with isophorone diisocyanate and formation of polyurethane-CNC composites. ACS Appl Mater Interfaces 8:1458–1467

Goldschmidt E, Cacicedo M, Kornfeld S, Valinoti M, Ielpi M, Ajler PM, Yampolsky C, Rasmussen J, Castro GR, Argibay P (2016) Construction and in vitro testing of a cellulose dura mater graft. Neurol Res 38:25–31

Golshan M, Salami-Kalajahi M, Roghani-Mamaqani H, Mohammadi M (2017) Poly(propylene imine) dendrimer-grafted nanocrystalline cellulose: doxorubicin loading and release behavior. Polym (UK) 117:287–294

Gonçalves S, Padrão J, Rodrigues IP, Silva JP, Sencadas V, Lanceros-Mendez S, Girão H, Dourado F, Rodrigues LR (2015) Bacterial cellulose as a support for the growth of retinal pigment epithelium. Biomacromolecules 16:1341–1351

Gonçalves S, Rodrigues IP, Padrão J, Silva JP, Sencadas V, Lanceros-Mendez S, Girão H, Gama FM, Dourado F, Rodrigues LR (2016) Acetylated bacterial cellulose coated with urinary bladder matrix as a substrate for retinal pigment epithelium. Colloids Surf B Biointerfaces 139:1–9

Gonzalez JS, Ludueña LN, Ponce A, Alvarez VA (2014) Poly(vinyl alcohol)/cellulose nanowhiskers nanocomposite hydrogels for potential wound dressings. Mater Sci Eng C 34:54–61

Gorgieva S, Girandon L, Kokol V (2017) Mineralization potential of cellulose-nanofibrils reinforced gelatine scaffolds for promoted calcium deposition by mesenchymal stem cells. Mater Sci Eng C 73:478–489

Gotta J, Shalom TB, Aslanoglou S, Cifuentes-Rius A, Voelcker NH, Elnathan R, Shoseyov O, Richter S (2018) Stable white light-emitting biocomposite films. Adv Funct Mater 28:1706967

Goussé C, Chanzy H, Cerrada ML, Fleury E (2004) Surface silylation of cellulose microfibrils: preparation and rheological properties. Polymer (Guildf) 45:1569–1575

Grande CJ, Torres FG, Gomez CM, Bañó MC (2009) Nanocomposites of bacterial cellulose/hydroxyapatite for biomedical applications. Acta Biomater 5:1605–1615

Guhados G, Wan W, Hutter JL (2005) Measurement of the elastic modulus of single bacterial cellulose fibers using atomic force microscopy. Langmuir 21:6642–6646

Guo R, Lan Y, Xue W, Cheng B, Zhang Y, Wang C, Ramakrishna S (2017) Collagen-cellulose nanocrystal scaffolds containing curcumin-loaded microspheres on infected full-thickness burns repair. J Tissue Eng Regen Med 11:3544–3555

Gutiérrez-hernández JM, Escobar-garcía DM, Escalante A, Flores H, González FJ, Gatenholm P, Toriz G (2017) In vitro evaluation of osteoblastic cells on bacterial cellulose modified with multi-walled carbon nanotubes as scaffold for bone regeneration. Mater Sci Eng C 75:445–453

Habibi Y (2014) Key advances in the chemical modification of nanocelluloses. Chem Soc Rev 43:1519–1542

Haimer E, Wendland M, Schlufter K, Frankenfeld K, Miethe P, Potthast A, Rosenau T, Liebner F (2010) Loading of bacterial cellulose aerogels with bioactive compounds by antisolvent precipitation with supercritical carbon dioxide. Macromol Symp 294:64–74

Håkansson KMO, Henriksson IC, de la Peña Vázquez C, Kuzmenko V, Markstedt K, Enoksson P, Gatenholm P (2016) Solidification of 3D printed nanofibril hydrogels into functional 3D cellulose structures. Adv Mater Technol 1:1600096

Hakkarainen T, Koivuniemi R, Kosonen M, Escobedo-lucea C, Sanz-garcia A, Vuola J, Valtonen J, Tammela P, Mäkitie A, Luukko K, Yliperttula M, Kavola H (2016) Nanofibrillar cellulose wound dressing in skin graft donor site treatment. J Control Release 244:292–301

Halib N, Mohd Amin MCI, Ahmad I (2010) Unique stimuli responsive characteristics of electron beam synthesized bacterial cellulose/acrylic acid composite. J Appl Polym Sci 116:2920–2929

Halib N, Mohd Amin MCI, Ahmad I, Abrami M, Fiorentino S, Farra R, Grassi G, Musiani F, Lapasin R, Grassi M (2014) Topological characterization of a bacterial cellulose-acrylic acid polymeric matrix. Eur J Pharm Sci 62:326–333

Hamdan MA, Adam F, Amin KNM (2018) Investigation of mixing time on carrageenan- cellulose nanocrystals(CNC) hard capsule for drug delivery carrier. Int J Innov Sci Res Technol 3:457–461

Harris JP, Hess AE, Rowan SJ, Weder C, Zorman CA, Tyler DJ, Capadona JR (2011) In vivo deployment of mechanically adaptive nanocomposites for intracortical microelectrodes. J Neural Eng 8:046010

Hasani M, Cranston ED, Westman G, Gray DG (2008) Cationic surface functionalization of cellulose nanocrystals. Soft Matter 4:2238–2244

He X, Xiao Q, Lu C, Wang Y, Zhang X, Zhao J, Zhang W, Zhang X, Deng Y (2014) Uniaxially aligned electrospun all-cellulose nanocomposite nanofibers reinforced with cellulose nanocrystals: scaffold for tissue engineering. Biomacromolecules 15:618–627

Hemraz UD, Lu A, Sunasee R, Boluk Y (2014) Structure of poly(N-isopropylacrylamide) brushes and steric stability of their grafted cellulose nanocrystal dispersions. J Colloid Interface Sci 430:157–165

Hemraz UD, Campbell K a, Burdick JS, Ckless K, Boluk Y, Sunasee R (2015) Cationic poly (2-aminoethylmethacrylate) and poly (N- (2- aminoethylmethacrylamide)) modified cellulose nanocrystals: synthesis, characterization, and cytotoxicity. Biomacromolecules 16:319–325

Heßler N, Klemm D (2009) Alteration of bacterial nanocellulose structure by in situ modification using polyethylene glycol and carbohydrate additives. Cellulose 16:899–910

Hokkanen S, Bhatnagar A, Sillanpää M (2016) A review on modification methods to cellulose-based adsorbents to improve adsorption capacity. Water Res 91:156–173

Hossain KMZ, Ahmed I, Parsons AJ, Scotchford CA, Walker GS, Thielemans W, Rudd CD (2012) Physico-chemical and mechanical properties of nanocomposites prepared using cellulose nanowhiskers and poly(lactic acid). J Mater Sci 47:2675–2686

Hossain KMZ, Hasan MS, Boyd D, Rudd CD, Ahmed I, Thielemans W (2014) Effect of cellulose nanowhiskers on surface morphology, mechanical properties, and cell adhesion of melt-drawn polylactic acid fibers. Biomacromolecules 15:1498–1506

Hou A, Zhou M, Wang X (2009) Preparation and characterization of durable antibacterial cellulose biomaterials modified with triazine derivatives. Carbohydr Polym 75:328–332

Hou L, Fang J, Wang W, Xie Z, Dong D, Zhang N (2017) Indocyanine green-functionalized bottle brushes of poly(2-oxazoline) on cellulose nanocrystals for photothermal cancer therapy. J Mater Chem B 5:3348–3354

Hou Y, Wang X, Yang J, Zhu R, Zhang Z, Li Y (2018) Development and biocompatibility evaluation of biodegradable bacterial cellulose as a novel peripheral nerve scaffold. J Biomed Mater Res Part A 106A:1288–1298

Hsieh YC, Yano H, Nogi M, Eichhorn SJ (2008) An estimation of the Young's modulus of bacterial cellulose filaments. Cellulose 15:507–513

Hu Y, Catchmark JM (2011a) In vitro biodegradability and mechanical properties of bioabsorbable bacterial cellulose incorporating cellulases. Acta Biomater 7:2835–2845

Hu Y, Catchmark JM (2011b) Integration of cellulases into bacterial cellulose: toward bioabsorbable cellulose composites. J Biomed Mater Res Part B 97:114–123
Hu H, Yuan W, Liu FS, Cheng G, Xu FJ, Ma J (2015) Redox-responsive polycation-functionalized cotton cellulose nanocrystals for effective cancer treatment. ACS Appl Mater Interfaces 7:8942–8951
Hu H, Hou X, Wang X, Nie J, Cai Q, Xu F (2016a) Gold nanoparticle-conjugated heterogeneous polymer brush-wrapped cellulose nanocrystals prepared by combining different controllable polymerization techniques for theranostic applications. Polym Chem 7:3107–3116
Hu Y, Zhu Y, Zhou X, Ruan C, Pan H, Catchmark JM (2016b) Bioabsorbable cellulose composites prepared by an improved mineral-binding process for bone defect repair. J Mater Chem B 4:1235–1246
Huang L, Chen X, Nguyen TX, Tang H, Zhang L, Yang G (2013) Nano-cellulose 3D-networks as controlled-release drug carriers. J Mater Chem B 1:2976–2984
Huang J-W, Lv X-G, Li Z, Song L-J, Feng C, Xie M-K, Li C, Li H-B, Wang J-H, Zhu W-D, Chen S-Y, Wang H-P, Xu Y-M (2015) Urethral reconstruction with a 3D porous bacterial cellulose scaffold seeded with lingual keratinocytes in a rabbit model. Biomed Mater 10:055005
Huey DJ, Hu JC, Athanasiou K a (2012) Unlike Bone, cartilage regeneration remains elusive. Science (80-) 338:917–921
Hutchens SA, Benson RS, Evans BR, Rawn CJ, O'Neill H (2009) A resorbable calcium-deficient hydroxyapatite hydrogel composite for osseous regeneration. Cellulose 16:887–898
Hutmacher DW (2001) Scaffold design and fabrication technologies for engineering tissues – state of the art and future perspectives. J Biomater Sci Polym Ed 12:107–124
Iguchi M, Yamanaka S, Budhiono a. (2000) Bacterial cellulose – a masterpiece of nature's arts. J Mater Sci 35:261–270
Inai NH, Lewandowska AE, Ghita OR, Eichhorn SJ (2018) Interfaces in polyethylene oxide modified cellulose nanocrystal – polyethylene matrix composites. Compos Sci Technol 154:128–135
Jack AA, Nordli HR, Powell LC, Powell KA, Kishnani H, Olav Johnsen P, Pukstad B, Thomas DW, Chinga-carrasco G, Hill KE (2017) The interaction of wood nanocellulose dressings and the wound pathogen *P. aeruginosa*. Carbohydr Polym 157:1955–1962
Jackson JK, Letchford K, Wasserman BZ, Ye L, Hamad WY, Burt HM (2011) The use of nanocrystalline cellulose for the binding and controlled release of drugs. Int J Nanomedicine 6:321–330
Jampala SN, Sarmadi M, Somers EB, Wong ACL, Denes FC (2008) Plasma-enhanced synthesis of bactericidal quaternary ammonium thin layers on stainless steel and cellulose surfaces. Langmuir 24:8583–8591
Jia H, Jia Y, Wang J, Hu Y, Zhang Y, Jia S (2009) Potentiality of bacterial cellulose as the scaffold of tissue engineering of cornea. In: 2009 2nd international conference on biomedical engineering and informatics. IEEE, Tianjin, pp 1–5
Jiang T, James R, Kumbar SG, Laurencin CT (2014) Chitosan as a biomaterial. In: Natural and synthetic biomedical polymers, 1st edn. Elsevier, Burlington, pp 91–113
Jiang Y, Zhou J, Yang Z, Liu D, Xv X, Zhao G, Shi H, Zhang Q (2018) Dialdehyde cellulose nanocrystal/gelatin hydrogel optimized for 3D printing applications. J Mater Sci 53:11883–11900
Jinga SI, Voicu G, Stoica-Guzun A, Stroescu M, Grumezescu AM, Bleotu C (2014) Biocellulose nanowhiskers cement composites for endodontic use. Dig J Nanomater Biostructures 9:543–550
Jonas R, Farah LF (1998) Production and application of microbial cellulose. Polym Degrad Stab 59:101–106
Jorfi M, Foster EJ (2015) Recent advances in nanocellulose for biomedical applications. J Appl Polym Sci 132:41719
Jorfi M, Roberts MN, Foster EJ, Weder C (2013) Physiologically responsive, mechanically adaptive bio-nanocomposites for biomedical applications. ACS Appl Mater Interfaces 5:1517–1526

Juncu G, Stoica-Guzun A, Stroescu M, Isopencu G, Jinga SI (2016) Drug release kinetics from carboxymethylcellulose-bacterial cellulose composite films. Int J Pharm 510:485–492
Kampeerapappun P (2016) The electrospun polyhydroxybutyrate fibers reinforced with cellulose nanocrystals: morphology and properties. J Appl Polym Sci 133:43273
Karaaslan MA, Tshabalala MA, Yelle DJ, Buschle-Diller G (2011) Nanoreinforced biocompatible hydrogels from wood hemicelluloses and cellulose whiskers. Carbohydr Polym 86:192–201
Kargarzadeh H, Mariano M, Huang J, Lin N, Ahmad I, Dufresne A, Thomas S (2017) Recent developments on nanocellulose reinforced polymer nanocomposites: a review. Polym (UK) 132:368–393
Karim Z, Hakalahti M, Tammelin T, Mathew AP (2017) In situ TEMPO surface functionalization of nanocellulose membranes for enhanced adsorption of metal ions from aqueous medium. RSC Adv 7:5232–5241
Kashani Rahimi S, Aeinehvand R, Kim K, Otaigbe JU (2017) Structure and biocompatibility of bioabsorbable nanocomposites of aliphatic-aromatic copolyester and cellulose nanocrystals. Biomacromolecules 18:2179–2194
Katepetch C, Rujiravanit R, Tamura H (2013) Formation of nanocrystalline ZnO particles into bacterial cellulose pellicle by ultrasonic-assisted in situ synthesis. Cellulose 20:1275–1292
Kaushik M, Moores A (2016) Review: nanocelluloses as versatile supports for metal nanoparticles and their applications in catalysis. Green Chem 18:622–637
Keskin Z, Urkmez AS, Hames EE (2017) Novel keratin modified bacterial cellulose nanocomposite production and characterization for skin tissue engineering. Mater Sci Eng C 75:1144–1153
Khabibullin A, Alizadehgiashi M, Khuu N, Prince E, Tebbe M, Kumacheva E (2017) Injectable shear-thinning fluorescent hydrogel formed by cellulose nanocrystals and graphene quantum dots. Langmuir 33:12344–12350
Khalid A, Khan R, Ul-islam M, Khan T, Wahid F (2017a) Bacterial cellulose-zinc oxide nanocomposites as a novel dressing system for burn wounds. Carbohydr Polym 164:214–221
Khalid A, Ullah H, Ul-islam M, Khan R, Khan S, Ahmad F, Khan T, Wahid F (2017b) Bacterial cellulose–TiO2 nanocomposites promote healing and tissue regeneration in burn mice model. RSC Adv 7:47662–47668
Khan S, UI-Islam M, Khattak WA, Ullah MW, Park JK (2015) Bacterial cellulose-titanium dioxide nanocomposites: nanostructural characteristics, antibacterial mechanism, and biocompatibility. Cellulose 22:565–579
Khoshkava V, Kamal MR (2014) Effect of drying conditions on cellulose nanocrystal (CNC) agglomerate porosity and dispersibility in polymer nanocomposites. Powder Technol 261:288–298
Kim J, Cai Z, Chen Y (2010) Biocompatible bacterial cellulose composites for biomedical application. J Nanotechnol Eng Med 1:011006
Kim J, Cai Z, Lee HS, Choi GS, Lee DH, Jo C (2011) Preparation and characterization of a bacterial cellulose/chitosan composite for potential biomedical application. J Polym Res 18:739–744
Kim J, Kim SW, Park S, Lim KT, Seonwoo H, Kim Y, Hong BH, Choung YH, Chung JH (2013) Bacterial cellulose nanofibrillar patch as a wound healing platform of tympanic membrane perforation. Adv Healthc Mater 2:1525–1531
Kirdponpattara S, Khamkeaw A, Sanchavanakit N, Pavasant P, Phisalaphong M (2015) Structural modification and characterization of bacterial cellulose-alginate composite scaffolds for tissue engineering. Carbohydr Polym 132:146–155
Kirdponpattara S, Phisalaphong M, Kongruang S (2017) Gelatin-bacterial cellulose composite sponges thermally cross-linked with glucose for tissue engineering applications. Carbohydr Polym 177:361–368
Klemm D (2006) Polysaccharides II, advances in polymer science. Springer US, New York
Klemm D, Schumann D, Udhardt U, Marsch S (2001) Bacterial synthesized cellulose – artificial blood vessels for microsurgery. Prog Polym Sci 26:1561–1603
Klemm D, Heublein B, Fink HP, Bohn A (2005) Cellulose: fascinating biopolymer and sustainable raw material. Angew Chem Int Ed 44:3358–3393

Ko SW, Soriano JPE, Lee JY, Unnithan AR, Park CH, Kim CS (2018) Nature derived scaffolds for tissue engineering applications: design and fabrication of a composite scaffold incorporating chitosan-g-D,L-lactic acid and cellulose nanocrystals from *Lactuca sativa* L. cv green leaf. Int J Biol Macromol 110:504–513

Kolakovic R, Peltonen L, Laaksonen T, Putkisto K, Laukkanen A, Hirvonen J (2011) Spray-dried cellulose nanofibers as novel tablet excipient. AAPS PharmSciTech 12:1366–1373

Kolakovic R, Laaksonen T, Peltonen L, Laukkanen A, Hirvonen J (2012a) Spray-dried nanofibrillar cellulose microparticles for sustained drug release. Int J Pharm 430:47–55

Kolakovic R, Peltonen L, Laukkanen A, Hirvonen J, Laaksonen T (2012b) Nanofibrillar cellulose films for controlled drug delivery. Eur J Pharm Biopharm 82:308–315

Kolakovic R, Peltonen L, Laukkanen A, Hellman M, Laaksonen P, Linder MB, Hirvonen J, Laaksonen T (2013) Evaluation of drug interactions with nanofibrillar cellulose. Eur J Pharm Biopharm 85:1238–1244

Kovalenko A (2014) Predictive multiscale modeling of nanocellulose based materials and systems. IOP Conf Ser Mater Sci Eng 64:012040

Kowalska-Ludwicka K, Cala J, Grobelski B, Sygut D, Jesionek-Kupnicka D, Kolodziejczyk M, Bielecki S, Pasieka Z (2013) Modified bacterial cellulose tubes for regeneration of damaged peripheral nerves. Arch Med Sci 9:527–534

Krontiras P, Gatenholm P, Hagg DA (2015) Adipogenic differentiation of stem cells in three-dimensional porous bacterial nanocellulose scaffolds. J Biomed Mater Res Part B Appl Biomater 103B:195–203

Kukharenko O, Bardeau J, Zaets I, Ovcharenko L, Tarasyuk O, Porhyn S, Mischenko I, Vovk A, Rogalsky S, Kozyrovska N (2014) Promising low cost antimicrobial composite material based on bacterial cellulose and polyhexamethylene guanidine hydrochloride. Eur Polym J 60:247–254

Kulkarni PK, Anil Dixit S, Singh UB (2012) Evaluation of bacterial cellulose produced fron Acetobacter xylinum as pharmacutical excipient. Am J Drug Discov Dev 2:72–86

Kumar A, Rao KM, Han SS (2017) Development of sodium alginate-xanthan gum based nanocomposite scaffolds reinforced with cellulose nanocrystals and halloysite nanotubes. Polym Test 63:214–225

Kurniawan H, Lai JT, Wang MJ (2012) Biofunctionalized bacterial cellulose membranes by cold plasmas. Cellulose 19:1975–1988

Kuzmenko V, Sämfors S, Hägg D, Gatenholm P (2013) Universal method for protein bioconjugation with nanocellulose scaffolds for increased cell adhesion. Mater Sci Eng C 33:4599–4607

Laitinen O, Suopajärvi T, Österberg M, Liimatainen H (2017) Hydrophobic, superabsorbing aerogels from choline chloride-based deep eutectic solvent pretreated and silylated cellulose nanofibrils for selective oil removal. ACS Appl Mater Interfaces 9:25029–25037

Lang N, Merkel E, Fuchs F, Schumann D, Klemm D, Kramer F, Mayer-Wagner S, Schroeder C, Freudenthal F, Netz H, Kozlik-Feldmann R, Sigler M (2015) Bacterial nanocellulose as a new patch material for closure of ventricular septal defects in a pig model. Eur J Cardio-Thoracic Surg 47:1013–1021

Lapidot S, Meirovitch S, Sharon S, Heyman A, Kaplan DL, Shoseyov O (2012) Clues for biomimetics from natural composite materials. Nanomedicine 7:1409–1423

Laranjeira M, Domingues RMA, Costa-Almeida R, Reis RL, Gomes ME (2017) 3D mimicry of native-tissue-fiber architecture guides tendon-derived cells and adipose stem cells into artificial tendon constructs. Small 13:1700689

Lasseuguette E (2008) Grafting onto microfibrils of native cellulose. Cellulose 15:571–580

Lavoine N, Desloges I, Bras J (2014) Microfibrillated cellulose coatings as new release systems for active packaging. Carbohydr Polym 103:528–537

Lee KY, Aitomäki Y, Berglund LA, Oksman K, Bismarck A (2014) On the use of nanocellulose as reinforcement in polymer matrix composites. Compos Sci Technol 105:15–27

Lee S, An S, Lim Y, Huh J (2017) The efficacy of electron beam irradiated bacterial cellulose membranes as compared with collagen membranes on guided bone regeneration in peri-implant bone defects. Materials (Basel) 10:1018

Legeza VI, Galenko-Yaroshevskii VP, Zinov'ev EV, Paramonov BA, Kreichman GS, Turkovskii II, Gumenyuk ES, Karnovich AG, Khripunov AK (2004) Effects of new wound dressings on healing of thermal burns of the skin in acute radiation disease. Bull Exp Biol Med 138:311–315

Leitao AF, Gupta S, Silva JP, Reviakine I, Gama M (2013) Hemocompatibility study of a bacterial cellulose/polyvinyl alcohol nanocomposite. Colloids Surf B Biointerfaces 111:493–502

Li J, Wan Y, Li L, Liang H, Wang J (2009) Preparation and characterization of 2,3-dialdehyde bacterial cellulose for potential biodegradable tissue engineering scaffolds. Mater Sci Eng C 29:1635–1642

Li F, Biagioni P, Bollani M, Maccagnan A, Piergiovanni L (2013) Multi-functional coating of cellulose nanocrystals for flexible packaging applications. Cellulose 20:2491–2504

Li W, Guo R, Lan Y, Zhang Y, Xue W, Zhang Y (2014) Preparation and properties of cellulose nanocrystals reinforced collagen composite films. J Biomed Mater Res Part A 102:1131–1139

Li W, Lan Y, Guo R, Zhang Y, Xue W, Zhang Y (2015a) In vitro and in vivo evaluation of a novel collagen/cellulose nanocrystals scaffold for achieving the sustained release of basic fibroblast growth factor. J Biomater Appl 29:882–893

Li Y, Jiang H, Zheng W, Gong N, Chen L, Jiang X, Yang G (2015b) Bacterial cellulose–hyaluronan nanocomposite biomaterials as wound dressings for severe skin injury repair. J Mater Chem B 3:3498–3507

Li Y, Tian Y, Zheng W, Feng Y, Huang R, Shao J, Tang R, Wang P, Jia Y, Zhang J, Zheng W, Yang G, Jiang X (2017) Composites of bacterial cellulose and small molecule-decorated gold nanoparticles for treating gram-negative bacteria-infected wounds. Small 13:1–10

Li VCF, Mulyadi A, Dunn CK, Deng Y, Qi HJ (2018a) Direct ink write 3D printed cellulose nanofiber aerogel structures with highly deformable, shape recoverable, and functionalizable properties. ACS Sustain Chem Eng 6:2011–2022

Li Y, Fu Q, Yang X, Berglund L (2018b) Transparent wood for functional and structural applications. Philos Trans R Soc A Math Phys Eng Sci 376:pii: 20170182

Liebert T, Kostag M, Wotschadlo J, Heinze T (2011) Stable cellulose nanospheres for cellular uptake. Macromol Biosci 11:1387–1392

Lin N, Dufresne A (2013) Physical and/or chemical compatibilization of extruded cellulose nanocrystal reinforced polystyrene nanocomposites. Macromolecules 46:5570–5583

Lin N, Huang J, Chang PR, Feng L, Yu J (2011a) Effect of polysaccharide nanocrystals on structure, properties, and drug release kinetics of alginate-based microspheres. Colloids Surf B Biointerfaces 85:270–279

Lin YK, Chen KH, Ou KL, Liu M (2011b) Effects of different extracellular matrices and growth factor immobilization on biodegradability and biocompatibility of macroporous bacterial cellulose. J Bioact Compat Polym 26:508–518

Lin N, Bruzzese C, Dufresne A (2012a) TEMPO-oxidized nanocellulose participating as crosslinking aid for alginate-based sponges. ACS Appl Mater Interfaces 4:4948–4959

Lin N, Huang J, Dufresne A (2012b) Preparation, properties and applications of polysaccharide nanocrystals in advanced functional nanomaterials: a review. Nanoscale 4:3274

Lin WC, Lien CC, Yeh HJ, Yu CM, Hsu SH (2013a) Bacterial cellulose and bacterial cellulose-chitosan membranes for wound dressing applications. Carbohydr Polym 94:603–611

Lin Z, Guan Z, Huang Z (2013b) New bacterial cellulose/polyaniline nanocomposite film with one conductive side through constrained interfacial polymerization. Ind Eng Chem Res 52:2869–2874

Lin Q, Zheng Y, Ren L, Wu J, Wang H, An J, Fan W (2014) Preparation and characteristic of a sodium alginate/carboxymethylated bacterial cellulose composite with a crosslinking Semi-interpenetrating network. J Appl Polym Sci 131:1–9

Lin N, Gèze A, Wouessidjewe D, Huang J, Dufresne A (2016) Biocompatible double-membrane hydrogels from cationic cellulose nanocrystals and anionic alginate as complexing drugs codelivery. ACS Appl Mater Interfaces 8:6880–6889

Lin S-P, Kung H-N, Tsai Y-S, Tseng T-N, Hsu K-D, Cheng KC (2017) Novel dextran modified bacterial cellulose hydrogel accelerating cutaneous wound healing. Cellulose 24:4927–4937

Liu P, Borrell PF, Božič M, Kokol V, Oksman K, Mathew AP (2015) Nanocelluloses and their phosphorylated derivatives for selective adsorption of Ag^{+}, Cu^{2+} and Fe^{3+} from industrial effluents. J Hazard Mater 294:177–185

Liu J, Chinga-Carrasco G, Cheng F, Xu W, Willför S, Syverud K, Xu C (2016) Hemicellulose-reinforced nanocellulose hydrogels for wound healing application. Cellulose 23:3129–3143

Liu L, Yang X, Ye L, Xue D, Liu M, Jia S, Hou Y, Chu L-Q, Zhong C (2017) Preparation and characterization of a photocatalytic antibacterial material: graphene oxide/TiO2/bacterial cellulose nanocomposite. Carbohydr Polym 174:1078–1086

Liu H, Zhou C, Liu X, Xu Y, Geng S, Chen Y, Wei C, Yu C (2018a) PMMA@SCNC composite microspheres prepared from pickering emulsion template as curcumin delivery carriers. J Appl Polym Sci 135:46127

Liu Y, Sui Y, Liu C, Liu C, Wu M, Li B, Li Y (2018b) A physically crosslinked polydopamine/nanocellulose hydrogel as potential versatile vehicles for drug delivery and wound healing. Carbohydr Polym 188:27–36

Liyaskina E, Revin V, Paramonova E, Nazarkina M, Pestov N, Revina N, Kolesnikova S (2017) Nanomaterials from bacterial cellulose for antimicrobial wound dressing. J Phys Conf Ser 784:1–7

Löbmann K, Svagan AJ (2017) Cellulose nanofibers as excipient for the delivery of poorly soluble drugs. Int J Pharm 533:285–297

Loh EYX, Mohamad N, Fauzi MB, Ng MH, Ng SF, Mohd Amin MCI (2018) Development of a bacterial cellulose-based hydrogel cell carrier containing keratinocytes and fibroblasts for full-thickness wound healing. Sci Rep 8:2875

Loures BR (2004) Endoprosthesis process to obtain and methods used. Google patents

Lu T, Li Q, Chen W, Yu H (2014) Composite aerogels based on dialdehyde nanocellulose and collagen for potential applications as wound dressing and tissue engineering scaffold. Compos Sci Technol 94:132–138

Luan J, Wu J, Zheng Y, Song W, Wang G, Guo J, Ding X (2012) Impregnation of silver sulfadiazine into bacterial cellulose for antimicrobial and biocompatible wound dressing. Biomed Mater 7:1–11

Ludwicka K, Jedrzejczak-Krzepkowska M, Kubiak K, Kolodziejczyk M, Pankiewicz T, Bielecki S (2016) Medical and cosmetic applications of bacterial nanocellulose. In: Bacterial nanocellulose. Elsevier, Amsterdam, pp 145–165

Luo H, Xiong G, Hu D, Ren K, Yao F, Zhu Y, Gao C, Wan Y (2013) Characterization of TEMPO-oxidized bacterial cellulose scaffolds for tissue engineering applications. Mater Chem Phys 143:373–379

Luo H, Ao H, Li G, Li W, Xiong G, Zhu Y (2017) Bacterial cellulose/graphene oxide nanocomposite as a novel drug delivery system. Curr Appl Phys 17:249–254

Lv X, Yang J, Feng C, Li Z, Chen S, Xie M, Huang J, Li H, Wang H, Xu Y (2016) Bacterial cellulose-based biomimetic nanofibrous scaffold with muscle cells for hollow organ tissue engineering. ACS Biomater Sci Eng 2:19–29

Lv X, Feng C, Liu Y, Peng X, Chen S, Xiao D, Wang ZL, Xu Y, Lu M (2018) A smart bilayered scaffold supporting keratinocytes and muscle cells in micro/nano-scale for urethral reconstruction. Theranostics 8:3153–3163

Ma S, Akbari M, Jahani-kadosarai M (2017) Assessing the loading and release of metronidazole from bacterial cellulose film as a pharmaceutical dressing. J Kashan Univ Med Sci 21:240–246

Mahmoud KA, Mena JA, Male KB, Hrapovic S, Kamen A, Luong JHT (2010) Effect of surface charge on the cellular uptake and cytotoxicity of fluorescent labeled cellulose nanocrystals. ACS Appl Mater Interfaces 2:2924–2932

Male KB, Leung ACW, Montes J, Kamen A, Luong JHT (2012) Probing inhibitory effects of nanocrystalline cellulose: inhibition versus surface charge. Nanoscale 4:1373

Maneerung T, Tokura S, Rujiravanit R (2008) Impregnation of silver nanoparticles into bacterial cellulose for antimicrobial wound dressing. Carbohydr Polym 72:43–51
Marchessault RH, Morehead FF, Walter NM (1959) Liquid crystal systems from fibrillar polysaccharides. Nature 184:632–633
Maria LCS, Santos ALC, Oliveira PC, Valle ASS, Barud HS, Messaddeq Y, Ribeiro SJL (2010) Preparation and antibacterial activity of silver nanoparticles impregnated in bacterial cellulose. Polímeros 20:72–77
Mariano M, El Kissi N, Dufresne A (2014) Cellulose nanocrystals and related nanocomposites: review of some properties and challenges. J Polym Sci Part B Polym Phys 52:791–806
Markstedt K, Mantas A, Tournier I, Martínez Ávila H, Hägg D, Gatenholm P (2015) 3D bioprinting human chondrocytes with nanocellulose-alginate bioink for cartilage tissue engineering applications. Biomacromolecules 16:1489–1496
Markstedt K, Escalante A, Toriz G, Gatenholm P (2017) Biomimetic inks based on cellulose nanofibrils and cross-linkable xylans for 3D printing. ACS Appl Mater Interfaces 9:40878–40886
Martínez Ávila H, Schwarz S, Feldmann EM, Mantas A, Von Bomhard A, Gatenholm P, Rotter N (2014) Biocompatibility evaluation of densified bacterial nanocellulose hydrogel as an implant material for auricular cartilage regeneration. Appl Microbiol Biotechnol 98:7423–7435
Martínez Ávila H, Feldmann EM, Pleumeekers MM, Nimeskern L, Kuo W, de Jong WC, Schwarz S, Müller R, Hendriks J, Rotter N, van Osch GJVM, Stok KS, Gatenholm P (2015) Novel bilayer bacterial nanocellulose scaffold supports neocartilage formation in vitro and in vivo. Biomaterials 44:122–133
Martínez H, Brackmann C, Enejder A, Gatenholm P (2012) Mechanical stimulation of fibroblasts in micro-channeled bacterial cellulose scaffolds enhances production of oriented collagen fibers. J Biomed Mater Res Part A 100(A):948–957
Mathew AP, Oksman K, Pierron D, Harmand MF (2012) Fibrous cellulose nanocomposite scaffolds prepared by partial dissolution for potential use as ligament or tendon substitutes. Carbohydr Polym 87:2291–2298
Mathew AP, Oksman K, Pierron D, Harmand MF (2013) Biocompatible fibrous networks of cellulose nanofibres and collagen crosslinked using genipin: potential as artificial ligament/tendons. Macromol Biosci 13:289–298
Mauricio MR, da Costa PG, Haraguchi SK, Guilherme MR, Muniz EC, Rubira AF (2015) Synthesis of a microhydrogel composite from cellulose nanowhiskers and starch for drug delivery. Carbohydr Polym 115:715–722
Meesorn W, Shirole A, Vanhecke D, De Espinosa LM, Weder C (2017) A simple and versatile strategy to improve the mechanical properties of polymer nanocomposites with cellulose nanocrystals. Macromolecules 50:2364–2374
Meirovitch S, Shtein Z, Ben-Shalom T, Lapidot S, Tamburu C, Hu X, Kluge JA, Raviv U, Kaplan DL, Shoseyov O (2016) Spider silk-CBD-cellulose nanocrystal composites: mechanism of assembly. Int J Mol Sci 17:1573
Mello LR, Feltrin LT, Fontes Neto PT, Ferraz FAP (1997) Duraplasty with biosynthetic cellulose: an experimental study. J Neurosurg 86:143–150
Meneguin AB, Cury BSF, Dos Santos AM, Faza Franco D, Barud HS, Da Silva Filho EC (2017) Resistant starch/pectin free-standing films reinforced with nanocellulose intended for colonic methotrexate release. Carbohydr Polym 157:1013–1023
Mertaniemi H, Escobedo-Lucea C, Sanz-Garcia A, Gandía C, Mäkitie A, Partanen J, Ikkala O, Yliperttula M (2016) Human stem cell decorated nanocellulose threads for biomedical applications. Biomaterials 82:208–220
Messaddeq Y, Ribeiro SJL, Thomazini W (2008) Contact lens for therapy, method and apparatus for their production and use. Brazil patent BR, PI0603704-6
Mihaela Jipa I, Dobre L, Stroescu M, Stoica-Guzun A, Jinga S, Dobre T (2012) Preparation and characterization of bacterial cellulose-poly(vinyl alcohol) films with antimicrobial properties. Mater Lett 66:125–127

Millon LE, Wan WK (2006) The polyvinyl alcohol–bacterial cellulose system as a new nanocomposite for biomedical applications. J Biomed Mater Res B Appl Biomater 79:245–253
Millon LE, Guhados G, Wan W (2008) Anisotropic polyvinyl alcohol-bacterial cellulose nanocomposite for biomedical applications. J Biomed Mater Res Part B Appl Biomater 86:444–452
Mo Y, Guo R, Zhang Y, Xue W, Cheng B, Zhang Y (2017) Controlled dual delivery of angiogenin and curcumin by electrospun nanofibers for skin regeneration. Tissue Eng Part A 23:597–608
Mohamad N, Mohd Amin MCI, Pandey M, Ahmad N, Fadilah N (2014) Bacterial cellulose/acrylic acid hydrogel synthesized via electron beam irradiation: accelerated burn wound healing in an animal model. Carbohydr Polym 114:312–320
Mohammadi H (2011) Nanocomposite biomaterial mimicking aortic heart valve leaflet mechanical behaviour. Proc Inst Mech Eng Part H J Eng Med 225:718–722
Mohammadnejad J, Yazdian F, Omidi M, Rostami AD, Rasekh B, Fathinia A (2018) Graphene oxide/silver nanohybrid: optimization, antibacterial activity and its impregnation on bacterial cellulose as a potential wound dressing based on GO-Ag nanocomposite-coated BC. Eng Life Sci 18:298–307
Mohanta V, Madras G, Patil S (2014) Layer-by-layer assembled thin films and microcapsules of nanocrystalline cellulose for hydrophobic drug delivery. ACS Appl Mater Interfaces 6:20093–20101
Mohd Amin MCI, Abadi AG, Ahmad N, Katas H, Jamal JA (2012a) Bacterial cellulose film coating as drug delivery system: physicochemical, thermal and drug release properties. Sains Malaysiana 41:561–568
Mohd Amin MCI, Ahmad N, Halib N, Ahmad I (2012b) Synthesis and characterization of thermo- and pH-responsive bacterial cellulose/acrylic acid hydrogels for drug delivery. Carbohydr Polym 88:465–473
Möller T, Amoroso M, Hägg D, Brantsing C, Rotter N, Apelgren P, Lindahl A, Kölby L, Gatenholm P (2017) In vivo chondrogenesis in 3D bioprinted human cell-laden hydrogel constructs. Plast Reconstr Surg Glob Open 5:e1227
Moon RJ, Martini A, Nairn J, Simonsen J, Youngblood J (2011) Cellulose nanomaterials review: structure, properties and nanocomposites. Chem Soc Rev 40(7):3941–3994
Moraes PRF de S, Saska S, Barud H, Lima LR de, Martins V da CA, Plepis AM de G, Ribeiro SJL, Gaspar AMM (2016) Bacterial cellulose/collagen hydrogel for wound healing. Mater Res 19:106–116
Morits M, McKee JR, Majoinen J, Malho JM, Houbenov N, Seitsonen J, Laine J, Gröschel AH, Ikkala O (2017) Polymer brushes on cellulose nanofibers: modification, SI-ATRP, and unexpected degradation processes. ACS Sustain Chem Eng 5:7642–7650
Moritz S, Wiegand C, Wesarg F, Hessler N, Müller FA, Kralisch D, Hipler U, Fischer D (2014) Active wound dressings based on bacterial nanocellulose as drug delivery system for octenidine. Int J Pharm 471:45–55
Muangman P, Opasanon S, Suwanchot S, Thangthed O (2011) Efficiency of microbial cellulose dressing in partial-thickness burn wounds. J Am Col Certif Wound Spec 3:16–19
Müller A, Ni Z, Hessler N, Wesarg F, Müller FA, Kralisch D, Fischer D (2013) The biopolymer bacterial nanocellulose as drug delivery system: investigation of drug loading and release using the model protein albumin. J Pharm Sci 102:579–592
Muller D, Silva JP, Rambo CR, GMO B, Dourado F, Gama FM (2013) Neuronal cells behavior on polypyrrole coated bacterial nanocellulose three-dimensional (3D) scaffolds. J Biomater Sci Polym Ed 24:1368–1377
Müller A, Zink M, Hessler N, Wesarg F, Müller FA, Kralisch D, Fischer D (2014) Bacterial nanocellulose with a shape-memory effect as potential drug delivery system. RSC Adv 4:57173–57184
Nakaya T, Li YJ (1999) Phospholipid polymers. Prog Polym Sci 24:143–181
Naseri N, Mathew AP, Girandon L, Frohlich M, Oksman K (2015) Porous electrospun nanocomposite mats based on chitosan – cellulose nanocrystals for wound dressing: effect of surface characteristics of nanocrystals. Cellulose 22:521–534

Naseri N, Poirier J-M, Girandon L, Fröhlich M, Oksman K, Mathew AP (2016) 3-Dimensional porous nanocomposite scaffolds based on cellulose nanofibers for cartilage tissue engineering: tailoring of porosity and mechanical performance. RSC Adv 6:5999–6007

Nasseri R, Mohammadi N (2014) Starch-based nanocomposites: a comparative performance study of cellulose whiskers and starch nanoparticles. Carbohydr Polym 106:432–439

Ndong Ntoutoume GMA, Grassot V, Brégier F, Chabanais J, Petit J, Granet R, Sol V (2017) PEI-cellulose nanocrystal hybrids as efficient siRNA delivery agents – synthesis, physicochemical characterization and in vitro evaluation. Carbohydr Polym 164:258–267

Nguyen JK, Park DJ, Skousen JL, Hess-Dunning AE, Tyler DJ, Rowan SJ, Weder C, Capadona JR (2014) Mechanically-compliant intracortical implants reduce the neuroinflammatory response. J Neural Eng 11:056014

Nilsson T, Rowell R (2012) Historical wood – structure and properties. J Cult Herit 13:S5–S9

Nimeskern L, Martínez Ávila H, Sundberg J, Gatenholm P, Müller R, Stok KS (2013) Mechanical evaluation of bacterial nanocellulose as an implant material for ear cartilage replacement. J Mech Behav Biomed Mater 22:12–21

Ninan N, Muthiah M, Park IK, Elain A, Thomas S, Grohens Y (2013) Pectin/carboxymethyl cellulose/microfibrillated cellulose composite scaffolds for tissue engineering. Carbohydr Polym 98:877–885

Noishiki Y, Nishiyama Y, Wada M, Kuga S, Magoshi J (2002) Mechanical properties of silk fibroin-microcrystalline cellulose composite films. J Appl Polym Sci 86:3425–3429

Novaes AB Jr, Novaes AB, Grisi MF, Soares UN, Gabarra F (1993) Genfiflex, an alkali-cellulose membrane for GTR: histologic observations. Braz Dent J 4:65–71

Ntoutoume GMAN, Granet R, Mbakidi JP, Brégier F, Léger DY, Fidanzi-Dugas C, Lequart V, Joly N, Liagre B, Chaleix V, Sol V (2016) Development of curcumin-cyclodextrin/cellulose nanocrystals complexes: new anticancer drug delivery systems. Bioorg Med Chem Lett 26:941–945

Numata Y, Mazzarino L, Borsali R (2015) A slow-release system of bacterial cellulose gel and nanoparticles for hydrophobic active ingredients. Int J Pharm 486:217–225

Nurani M, Akbari V, Taheri A (2017) Preparation and characterization of metformin surface modified cellulose nanofiber gel and evaluation of its anti-metastatic potentials. Carbohydr Polym 165:322–333

Oksman K, Aitomäki Y, Mathew AP, Siqueira G, Zhou Q, Butylina S, Tanpichai S, Zhou X, Hooshmand S (2016) Composites: part A review of the recent developments in cellulose nanocomposite processing. Compos Part A 83:2–18

Oliveira Barud HG, HDS B, Cavicchioli M, Do Amaral TS, De Oliveira Junior OB, Santos DM, De Oliveira Almeida Petersen AL, Celes F, Borges VM, De Oliveira CI, De Oliveira PF, Furtado RA, Tavares DC, Ribeiro SJL (2015) Preparation and characterization of a bacterial cellulose/silk fibroin sponge scaffold for tissue regeneration. Carbohydr Polym 128:41–51

Olyveira GM, Acasigua GAX, Costa LMM, Scher CR, Filho LX, Pranke PHL, Basmaji P (2013) Human dental pulp stem cell behavior using natural nanotolith/bacterial cellulose scaffolds for regenerative medicine. J Biomed Nanotechnol 9:1370–1377

Onofrei M, Filimon A (2016) Cellulose-based hydrogels: designing concepts, properties, and perspectives for biomedical and environmental applications. In: Méndez-Vilas A, Solano A (eds) Polymer science: research advances, practical applications, and educational aspects. Formatex Research Center, Badajoz, pp 108–120

Ooi SY, Ahmad I, Mohd Amin MCI (2016) Cellulose nanocrystals extracted from rice husks as a reinforcing material in gelatin hydrogels for use in controlled drug delivery systems. Ind Crop Prod 93:227–234

Orasugh JT, Saha NR, Rana D, Sarkar G, Mollick MMR, Chattoapadhyay A, Mitra BC, Mondal D, Ghosh SK, Chattopadhyay D (2018) Jute cellulose nano- fibrils/hydroxypropylmethylcellulose nanocomposite: a novel material with potential for application in packaging and transdermal drug delivery system. Ind Crop Prod 112:633–643

Pääkko M, Ankerfors M, Kosonen H, Nykänen A, Ahola S, Österberg M, Ruokolainen J, Laine J, Larsson PT, Ikkala O, Lindström T (2007) Enzymatic hydrolysis combined with mechanical shearing and high-pressure homogenization for nanoscale cellulose fibrils and strong gels. Biomacromolecules 8:1934–1941

Palaganas NB, Mangadlao JD, De Leon ACC, Palaganas JO, Pangilinan KD, Lee YJ, Advincula RC (2017) 3D printing of photocurable cellulose nanocrystal composite for fabrication of complex architectures via stereolithography. ACS Appl Mater Interfaces 9:34314–34324

Palaninathan V, Raveendran S, Rochani AK, Chauhan N, Sakamoto Y, Ukai T, Maekawa T, Sakthi Kumar D (2018) Bioactive bacterial cellulose sulfate electrospun nanofibers for tissue engineering applications. J Tissue Eng Regen Med 12:1634–1645

Pandey M, Mohd Amin MCI, Ahmad N, Abeer MM (2013) Rapid synthesis of superabsorbent smart-swelling bacterial cellulose/acrylamide-based hydrogels for drug delivery. Int J Polym Sci 2013:905471

Pandey M, Mohamad N, Low W, Martin C, Mohd Amin MCI (2017) Microwaved bacterial cellulose-based hydrogel microparticles for the healing of partial thickness burn wounds. Drug Deliv Transl Res 7:89–99

Park SU, Lee BK, Kim MS, Park KK, Sung WJ, Kim HY, Han DG, Shim JS, Lee YJ, Kim SH, Kim IH, Park DH (2012) The possibility of microbial cellulose for dressing and scaffold materials. Int Wound J 11:35–43

Pattison MA, Wurster S, Webster TJ, Haberstroh KM (2005) Three-dimensional, nano-structured PLGA scaffolds for bladder tissue replacement applications. Biomaterials 26:2491–2500

Paukkonen H, Kunnari M, Laurén P, Hakkarainen T, Auvinen V, Oksanen T, Koivuniemi R, Yliperttula M, Laaksonen T (2017a) Nanofibrillar cellulose hydrogels and reconstructed hydrogels as matrices for controlled drug release. Int J Pharm 532:269–280

Paukkonen H, Ukkonen A, Szilvay G, Yliperttula M, Laaksonen T (2017b) Hydrophobin-nanofibrillated cellulose stabilized emulsions for encapsulation and release of BCS class II drugs. Eur J Pharm Sci 100:238–248

Pavaloiu R, Stoica-guzun A, Stroescu M, Jinga SI, Dobre T (2014) Composite films of poly(vinyl alcohol)– chitosan – bacterial cellulose for drug controlled release. Int J Biol Macromol 68:117–124

Pawar AA, Saada G, Cooperstein I, Larush L, Jackman JA, Tabaei SR, Cho NJ, Magdassi S (2016) High-performance 3D printing of hydrogels by water-dispersible photoinitiator nanoparticles. Sci Adv 2:1–8

Pereda M, Kissi N El, Dufresne A (2014) Extrusion of polysaccharide nanocrystal reinforced polymer nanocomposites through compatibilization with poly(ethylene oxide). ACS Appl Mater Interfaces 6:9365–9375

Pertile RAN, Andrade FK, Alves C Jr, Gama M (2010) Surface modification of bacterial cellulose by nitrogen-containing plasma for improved interaction with cells. Carbohydr Polym 82:692–698

Pertile R, Moreira S, Andrade F, Domingues L, Gama M (2012) Bacterial cellulose modified using recombinant proteins to improve neuronal and mesenchymal cell adhesion. Biotechnol Prog 28:526–532

Petersen N, Gatenholm P (2011) Bacterial cellulose-based materials and medical devices: current state and perspectives. Appl Microbiol Biotechnol 91:1277–1286

Picheth GF, Sierakowski MR, Woehl MA, Ono L, Cofré AR, Vanin LP, Pontarolo R, De Freitas RA (2014) Lysozyme-triggered epidermal growth factor release from bacterial cellulose membranes controlled by smart nanostructured films. J Pharm Sci 103:3958–3965

Pickering KL, Efendy MGA, Le TM (2016) A review of recent developments in natural fibre composites and their mechanical performance. Compos Part A Appl Sci Manuf 83:98–112

Poonguzhali R, Basha SK, Kumari VS (2017) Synthesis and characterization of chitosan-PVP-nanocellulose composites for in-vitro wound dressing application. Int J Biol Macromol 105:111–120

Pooyan P, Tannenbaum R, Garmestani H (2012) Mechanical behavior of a cellulose-reinforced scaffold in vascular tissue engineering. J Mech Behav Biomed Mater 7:50–59

Pooyan P, Kim IT, Jacob KI, Tannenbaum R, Garmestani H (2013) Design of a cellulose-based nanocomposite as a potential polymeric scaffold in tissue engineering. Polym (United Kingdom) 54:2105–2114

Popescu MC (2017) Structure and sorption properties of CNC reinforced PVA films. Int J Biol Macromol 101:783–790

Powell LC, Khan S, Chinga-Carrasco G, Wright CJ, Hill KE, Thomas DW (2016) An investigation of *Pseudomonas aeruginosa* biofilm growth on novel nanocellulose fibre dressings. Carbohydr Polym 137:191–197

Prince E, Alizadehgiashi M, Campbell M, Khuu N, Albulescu A, De France K, Ratkov D, Li Y, Hoare T, Kumacheva E (2018) Patterning of structurally anisotropic composite hydrogel sheets. Biomacromolecules 19:1276–1284

Putra A, Kakugo A, Furukawa H, Gong JP, Osada Y (2008) Tubular bacterial cellulose gel with oriented fibrils on the curved surface. Polymer (Guildf) 49:1885–1891

Qiao H, Guo T, Zheng Y, Zhao L, Sun Y, Liu Y, Xie Y (2018) A novel microporous oxidized bacterial cellulose/arginine composite and its effect on behavior of fibroblast/endothelial cell. Carbohydr Polym 184:323–332

Qing W, Wang Y, Wang Y, Zhao D, Liu X, Zhu J (2016) The modified nanocrystalline cellulose for hydrophobic drug delivery. Appl Surf Sci 366:404–409

Qiu Y, Qiu L, Cui J, Wei Q (2016) Bacterial cellulose and bacterial cellulose-vaccarin membranes for wound healing. Mater Sci Eng C 59:303–309

Ramani D, Sastry TP (2014) Bacterial cellulose-reinforced hydroxyapatite functionalized graphene oxide: a potential osteoinductive composite. Cellulose 21:3585–3595

Rambo CR, Recouvreux DOS, Carminatti CA, Pitlovanciv AK, Antônio RV, Porto LM (2008) Template assisted synthesis of porous nanofibrous cellulose membranes for tissue engineering. Mater Sci Eng C 28:549–554

Rånby BG (1949) Aqueous colloidal solutions of cellulose micelles. Acta Chem Scand 3:649–650

Rangaswamy BE, Vanitha KP (2017) Tridax procumbens leaf extracted based bacterial cellulose for wound healing. Asian J Microbiol Biotechnol 2:9–14

Rao KM, Kumar A, Han SS (2017a) Poly(acrylamidoglycolic acid) nanocomposite hydrogels reinforced with cellulose nanocrystals for pH-sensitive controlled release of diclofenac sodium. Polym Test 64:175–182

Rao KM, Kumar A, Han SS (2017b) Polysaccharide based bionanocomposite hydrogels reinforced with cellulose nanocrystals: drug release and biocompatibility analyses. Int J Biol Macromol 101:165–171

Rescignano N, Fortunati E, Montesano S, Emiliani C, Kenny JM, Martino S, Armentano I (2014) PVA bio-nanocomposites: a new take-off using cellulose nanocrystals and PLGA nanoparticles. Carbohydr Polym 99:47–58

Rigotti D, Duc V, Nguyen H, Cataldi A, Pegoretti A (2018) Polyvinyl alcohol reinforced crystalline nanocellulose in 3D printing application. Mater Today Commun 15:1–8

Rivkin A, Abitbol T, Nevo Y, Verker R, Lapidot S, Komarov A, Veldhuis SC, Zilberman G, Reches M, Cranston ED, Shoseyov O (2015) Bionanocomposite films from resilin-CBD bound to cellulose nanocrystals. Ind Biotechnol 11:44–58

Rodionova G, Lenes M, Eriksen Ø, Gregersen Ø (2011) Surface chemical modification of microfibrillated cellulose: improvement of barrier properties for packaging applications. Cellulose 18:127–134

Roemhild K, Wiegand C, Hipler U, Heinze T (2013) Novel bioactive amino-functionalized cellulose nanofibers. Macromol Rapid Commun 34:1767–1771

Rogstad Nordli H, Chinga-carrasco G, Mari Rokstad A, Pukstad B (2016) Producing ultrapure wood cellulose nanofibrils and evaluating the cytotoxicity using human skin cells. Carbohydr Polym 150:65–73

Rose JKC, Bennett AB (1999) Cooperative disassembly of the cellulose-xyloglucan network of plant cell walls: parallels between cell expansion and fruit ripening. Trends Plant Sci 4:176–183

Rouabhia M, Asselin J, Tazi N, Messaddeq Y, Levinson D, Zhang Z (2014) Production of biocompatible and antimicrobial bacterial cellulose polymers functionalized by RGDC grafting groups and gentamicin. ACS Appl Mater Interfaces 6:1439–1446

Rueda L, Saralegi A, Fernández-d'Arlas B, Zhou Q, Alonso-Varona A, Berglund LA, Mondragon I, Corcuera MA, Eceiza A (2013) In situ polymerization and characterization of elastomeric polyurethane-cellulose nanocrystal nanocomposites. Cell response evaluation. Cellulose 20:1819–1828

Sadeghifar H, Filpponen I, Clarke SP, Brougham DF, Argyropoulos DS (2011) Production of cellulose nanocrystals using hydrobromic acid and click reactions on their surface. J Mater Sci 46:7344–7355

Saibuatong O ard, Phisalaphong M (2010) Novo aloe vera-bacterial cellulose composite film from biosynthesis. Carbohydr Polym 79:455–460

Saïdi L, Vilela C, Oliveira H, Silvestre AJD, Freire CSR (2017) Poly(N-methacryloyl glycine)/nanocellulose composites as pH-sensitive systems for controlled release of diclofenac. Carbohydr Polym 169:357–365

Saito T, Isogai A (2004) TEMPO-mediated oxidation of native cellulose. The effect of oxidation conditions on chemical and crystal structures of the water-insoluble fractions. Biomacromolecules 5:1983–1989

Saito T, Isogai A (2006) Introduction of aldehyde groups on surfaces of native cellulose fibers by TEMPO-mediated oxidation. Colloids Surf A Physicochem Eng Asp 289:219–225

Saito T, Nishiyama Y, Putaux JL, Vignon M, Isogai A (2006) Homogeneous suspensions of individualized microfibrils from TEMPO-catalyzed oxidation of native cellulose. Biomacromolecules 7:1687–1691

Saito T, Kimura S, Nishiyama Y, Isogai A (2007) Cellulose nanofibers prepared by TEMPO-mediated oxidation of native cellulose. Biomacromolecules 8:2485–2491

Salata LA, Hatton PV, Devlin AJ, Craig GT, Brook IM (2001) In vitro and in vivo evaluation of e-PTFE and alkali-cellulose membranes for guided bone regeneration. Clin Oral Implants Res 12:62–68

Salgado AJ, Oliveira JM, Martins A, Teixeira FG, Silva NA, Neves NM, Sousa N, Reis RL (2013) Tissue engineering and regenerative medicine. In: Elsevier. Elsevier Inc., London, pp 1–33

Sampaio LMP, Padrão J, Faria J, Silva JP, Silva CJ, Dourado F, Zille A (2016) Laccase immobilization on bacterial nanocellulose membranes: antimicrobial, kinetic and stability properties. Carbohydr Polym 145:1–12

Saska S, Barud HS, Gaspar AMM, Marchetto R, Ribeiro SJL, Messaddeq Y (2011) Bacterial cellulose-hydroxyapatite nanocomposites for bone regeneration. Int J Biomater 2011:175362

Saska S, Pigossi SC, Oliveira GJPL, Teixeira LN, Capela MV, Gonçalves A, de Oliveira PT, Messaddeq Y, Ribeiro SJL, Gaspar AMM, Marchetto R (2018) Biopolymer-based membranes associated with osteogenic growth peptide for guided bone regeneration. Biomed Mater 13:035009

Shao W, Liu H, Liu X, Sun H, Wang S, Zhang R (2015a) pH-responsive release behavior and anti-bacterial activity of bacterial cellulose-silver nanocomposites. Int J Biol Macromol 76:209–217

Shao W, Liu H, Liu X, Wang S, Wu J, Zhang R, Min H, Huang M (2015b) Development of silver sulfadiazine loaded bacterial cellulose/sodium alginate composite films with enhanced antibacterial property. Carbohydr Polym 132:351–358

Shao W, Liu H, Liu X, Wang S, Zhang R (2015c) Anti-bacterial performances and biocompatibility of bacterial cellulose/graphene oxide composites. RSC Adv 5:4795–4803

Shao W, Liu H, Wang S, Wu J, Huang M, Min H, Liu X (2016) Controlled release and antibacterial activity of tetracycline hydrochloride-loaded bacterial cellulose composite membranes. Carbohydr Polym 145:114–120

Shi Q, Li Y, Sun J, Zhang H, Chen L, Chen B, Yang H, Wang Z (2012a) The osteogenesis of bacterial cellulose scaffold loaded with bone morphogenetic protein-2. Biomaterials 33:6644–6649

Shi Q, Zhou C, Yue Y, Guo W, Wu Y, Wu Q (2012b) Mechanical properties and in vitro degradation of electrospun bio-nanocomposite mats from PLA and cellulose nanocrystals. Carbohydr Polym 90:301–308

Shi X, Zheng Y, Wang G, Lin Q, Fan J (2014) pH- and electro-response characteristics of bacterial cellulose nanofibersodium alginate hybrid hydrogels for dual controlled drug delivery. RSC Adv 4:47056–47065

Shpigel E, Roiz L, Goren R, Shoseyov O (1998) Bacterial cellulose-binding domain modulates in vitro elongation of different plant cells. Plant Physiol 117:1185–1194

Siangsanoh C, Ummartyotin S, Sathirakul K, Rojanapanthu P, Treesuppharat W (2018) Fabrication and characterization of triple-responsive composite hydrogel for targeted and controlled drug delivery system. J Mol Liq 256:90–99

Silva NHCS, Drumond I ˆs, Almeida IF, Costa P, Rosado CF, Neto CP, Freire CSR, Silvestre AJD (2014a) Topical caffeine delivery using biocellulose membranes: a potential innovative system for cellulite treatment. Cellulose 21:665–674

Silva NHCS, Filipe Rodrigues A, Almeida IF, Costa PC, Rosado C, Pascoal Neto C, Silvestre AJD, Freire CSR (2014b) Bacterial cellulose membranes as transdermal delivery systems for diclofenac: in vitro dissolution and permeation studies. Carbohydr Polym 106:264–269

Silva RM, Pereira FV, Mota FAP, Watanabe E, Soares SMCS, Santos MH (2016) Dental glass ionomer cement reinforced by cellulose microfibers and cellulose nanocrystals. Mater Sci Eng C 58:389–395

Silveira FCA, Pinto FCM, Caldas Neto S da S, Leal M de C, Cesário J, Aguiar JL de A (2016) Treatment of tympanic membrane perforation using bacterial cellulose: a randomized controlled trial. Braz J Otorhinolaryngol 82:203–208

Sinclair A, Jiang L, Bajwa D, Bajwa S, Tangpong S, Wang X (2018) Cellulose nanofibers produced from various agricultural residues and their reinforcement effects in polymer nanocomposites. J Appl Polym Sci 135:9–11

Singla R, Soni S, Markand Kulurkar P, Kumari A, Mahesh S, Patial V, Padwad YS, Kumar Yadav S (2017a) In situ functionalized nanobiocomposites dressings of bamboo cellulose nanocrystals and silver nanoparticles for accelerated wound healing. Carbohydr Polym 155:152–162

Singla R, Soni S, Padwad YS, Acharya A, Yadav SK (2017b) Sustained delivery of BSA/HSA from biocompatible plant cellulose nanocrystals for in vitro cholesterol release from endothelial cells. Int J Biol Macromol 104:748–757

Singla R, Soni S, Patial V, Markand Kulurkar P, Kumari A, Mahesh S, Padwad YS, Kumar Yadav S (2017c) In vivo diabetic wound healing potential of nanobiocomposites containing bamboo cellulose nanocrystals impregnated with silver nanoparticles. Int J Biol Macromol 105:45–55

Siqueira G, Bras J, Dufresne A (2009) Cellulose whiskers versus microfibrils: influence of the nature of the nanoparticle and its surface functionalization on the thermal and mechanical properties of nanocomposites. Biomacromolecules 10:425–432

Siqueira G, Bras J, Dufresne A (2010) New process of chemical grafting of cellulose nanoparticles with a long chain isocyanate. Langmuir 26:402–411

Siqueira G, Kokkinis D, Libanori R, Hausmann MK, Gladman AS, Neels A, Tingaut P, Zimmermann T, Lewis JA, Studart AR (2017) Cellulose nanocrystal inks for 3D printing of textured cellular architectures. Adv Funct Mater 27(12):1604619

Song K, Xu H, Xie K, Yang Y (2017) Keratin-based biocomposites reinforced and cross-linked with dual-functional cellulose nanocrystals. ACS Sustain Chem Eng 5:5669–5678

Song J, Chen C, Zhu S, Zhu M, Dai J, Ray U, Li Y, Kuang Y, Li Y, Quispe N, Yao Y, Gong A, Leiste UH, Bruck HA, Zhu JY, Vellore A, Li H, Minus ML, Jia Z, Martini A, Li T, Hu L (2018) Processing bulk natural wood into a high-performance structural material. Nature 554:224–228

Souza CMCO, Mesquita LAF, Souza D, Irioda AC, Francisco JC, Souza CF, Guarita-Souza LC, Sierakowski M, Carvalho KAT (2014) Regeneration of skin tissue promoted by mesenchymal stem cells seeded in nanostructured membrane. Transplant Proc 46:1882–1886

Stevens MM (2005) Exploring and engineering the cell surface interface. Science (80-) 310:1135–1138

Stevens B, Yang Y, Mohandas A, Stucker B, Nguyen KT (2008) A review of materials, fabrication methods, and strategies used to enhance bone regeneration in engineered bone tissues. J Biomed Mater Res Part B Appl Biomater 85B:573–582

Stoica-Guzun A, Stroescu M, Tache F, Zaharescu T, Grosu E (2007) Effect of electron beam irradiation on bacterial cellulose membranes used as transdermal drug delivery systems. Nucl Instruments Methods Phys Res Sect B Beam Interact With Mater Atoms 265:434–438

Stumpf TR, Pértile RAN, Rambo CR, Porto LM (2013) Enriched glucose and dextrin mannitol-based media modulates fibroblast behavior on bacterial cellulose membranes. Mater Sci Eng C 33:4739–4745

Šturcová A, Davies GR, Eichhorn SJ (2005) Elastic modulus and stress-transfer properties of tunicate cellulose whiskers. Biomacromolecules 6:1055–1061

Sukul M, Min Y, Lee S, Lee B (2015) Osteogenic potential of simvastatin loaded gelatin-nanofibrillar cellulose- b tricalcium phosphate hydrogel scaffold in critical-sized rat calvarial defect. Eur Polym J 73:308–323

Sulaeva I, Henniges U, Rosenau T, Potthast A (2015) Bacterial cellulose as a material for wound treatment: properties and modifications: a review. Biotechnol Adv 33:1547–1571

Sultan S, Mathew A (2018) 3D printed scaffolds with gradient porosity based on cellulose nanocrystal hydrogel. Nanoscale 4421–4431

Sun B, Hou Q, Liu Z, Ni Y (2015) Sodium periodate oxidation of cellulose nanocrystal and its application as a paper wet strength additive. Cellulose 22:1135–1146

Sun F, Nordli HR, Pukstad B, Gamstedt EK, Chinga-carrasco G (2017) Mechanical characteristics of nanocellulose-PEG bionanocomposite wound dressings in wet conditions. J Mech Behav Biomed Mater 69:377–384

Sunasee R, Hemraz U (2018) Synthetic strategies for the fabrication of cationic surface-modified cellulose nanocrystals. Fibers 6:15

Svensson A, Nicklasson E, Harrah T, Panilaitis B, Kaplan DL, Brittberg M, Gatenholm P (2005) Bacterial cellulose as a potential scaffold for tissue engineering of cartilage. Biomaterials 26:419–431

Sydney Gladman A, Matsumoto EA, Nuzzo RG, Mahadevan L, Lewis JA (2016) Biomimetic 4D printing. Nat Mater 15:413–418

Tabaii MJ, Emtiazi G (2018) Transparent nontoxic antibacterial wound dressing based on silver nano particle/bacterial cellulose nano composite synthesized in the presence of tripolyphosphate. J Drug Deliv Sci Technol 44:244–253

Taheri A, Mohammadi M (2015) The use of cellulose nanocrystals for potential application in topical delivery of hydroquinone. Chem Biol Drug Des 86:102–106

Tang J, Bao L, Li X, Chen L, Hong FF (2015a) Potential of PVA-doped bacterial nano-cellulose tubular composites for artificial blood vessels. J Mater Chem B 3:8537–8547

Tang J, Song Y, Tanvir S, Anderson WA, Berry RM, Tam KC (2015b) Polyrhodanine coated cellulose nanocrystals: a sustainable antimicrobial agent. ACS Sustain Chem Eng 3:1801–1809

Tang Y, Shen X, Zhang J, Guo D, Kong F, Zhang N (2015c) Extraction of cellulose nano-crystals from old corrugated container fiber using phosphoric acid and enzymatic hydrolysis followed by sonication. Carbohydr Polym 125:360–366

Tanpichai S, Oksman K (2018) Crosslinked poly(vinyl alcohol) composite films with cellulose nanocrystals: mechanical and thermal properties. J Appl Polym Sci 135:1–11

Taokaew S, Phisalaphong M, Newby BZ (2015) Modification of bacterial cellulose with organosilanes to improve attachment and spreading of human fibroblasts. Cellulose 22:2311–2324

Tazi N, Zhang Z, Messaddeq Y, Almeida-Lopes L, Zanardi LM, Levinson D, Rouabhia M (2012) Hydroxyapatite bioactivated bacterial cellulose promotes osteoblast growth and the formation of bone nodules. AMB Express 2:61

Ten E, Turtle J, Bahr D, Jiang L, Wolcott M (2010) Thermal and mechanical properties of poly (3-hydroxybutyrate-co-3-hydroxyvalerate)/cellulose nanowhiskers composites. Polymer (Guildf) 51:2652–2660

Tong WY, bin Abdullah AYK, binti Rozman NAS, bin Wahid MIA, Hossain MS, Ring LC, Lazim Y, Tan W-N (2018) Antimicrobial wound dressing film utilizing cellulose nanocrystal as drug delivery system for curcumin. Cellulose 25:631–638

Treesuppharat W, Rojanapanthu P, Siangsanoh C, Manuspiya H, Ummartyotin S (2017) Synthesis and characterization of bacterial cellulose and gelatin-based hydrogel composites for drug-delivery systems. Biotechnol Rep 15:84–91

Trovatti E, Silva NHCS, Duarte IF, Rosado CF, Almeida IF, Costa P, Freire CSR, Silvestre AJD, Neto CP (2011) Biocellulose membranes as supports for dermal release of lidocaine. Biomacromolecules 12:4162–4168

Trovatti E, Freire CSR, Pinto PC, Almeida IF, Costa P, Silvestre AJD, Pascoal Neto C, Rosado C (2012) Bacterial cellulose membranes applied in topical and transdermal delivery of lidocaine hydrochloride and ibuprofen: in vitro diffusion studies. Int J Pharm 435:83–87

Tsai Y, Yang Y, Ho Y, Tsai M, Mi F-L (2018) Drug release and antioxidant/antibacterial activities of silymarin-zein nanoparticle/bacterial cellulose nanofiber composite films. Carbohydr Polym 180:286–296

Tummala GK, Joffre T, Lopes VR, Liszka A, Buznyk O, Ferraz N, Persson C, Griffith M, Mihranyan A (2016) Hyperelastic nanocellulose-reinforced hydrogel of high water content for ophthalmic applications. ACS Biomater Sci Eng 2:2072–2079

Turbak A, Snyder F, Sandberg KR (1983) Microfibrillated cellulose, a new cellulose product: properties, uses, and commercial potential. Appl Polym 37:815–827

Türkoglu N (2014) Development of biodegradable antibacterial cellulose based hydrogel membranes for wound healing. Int J Biol Macromol 67:22–27

Ul-Islam M, Shah N, Ha JH, Park JK (2011) Effect of chitosan penetration on physico-chemical and mechanical properties of bacterial cellulose. Korean J Chem Eng 28:1736–1743

Ul-islam M, Khan T, Khattak WA, Park JK (2013) Bacterial cellulose-MMTs nanoreinforced composite films: novel wound dressing material with antibacterial properties. Cellulose 20:589–596

Ullah H, Badshah M, Makila E, Salonen J, Shahbazi M, Santos HA, Khan T (2017) Fabrication, characterization and evaluation of bacterial cellulose-based capsule shells for oral drug delivery. Cellulose 24:1445–1454

UPM Biochemicals (2018) Growdex the natural choice for cell culture. http://www.upmbiochemicals.com/growdex/Pages/Default.aspx

Valo H, Kovalainen M, Laaksonen P, Häkkinen M, Auriola S, Peltonen L, Linder M, Järvinen K, Hirvonen J, Laaksonen T (2011) Immobilization of protein-coated drug nanoparticles in nanofibrillar cellulose matrices – enhanced stability and release. J Control Release 156:390–397

Valo H, Arola S, Laaksonen P, Torkkeli M, Peltonen L, Linder MB, Serimaa R, Kuga S, Hirvonen J, Laaksonen T (2013) Drug release from nanoparticles embedded in four different nanofibrillar cellulose aerogels. Eur J Pharm Sci 50:69–77

Villanova JCO, Ayres E, Carvalho SM, Patrício PS, Pereira FV, Oréfice RL (2011) Pharmaceutical acrylic beads obtained by suspension polymerization containing cellulose nanowhiskers as excipient for drug delivery. Eur J Pharm Sci 42:406–415

Villares A, Moreau C, Dammak A, Capron I, Cathala B (2015) Kinetic aspects of the adsorption of xyloglucan onto cellulose nanocrystals. Soft Matter 11:6472–6481

Voicu G, Jinga S, Drosu B, Busuioc C (2017) Improvement of silicate cement properties with bacterial cellulose powder addition for applications in dentistry. Carbohydr Polym 174:160–170

Vollick B, Kuo P-Y, Alizadehgiashi M, Yan N, Kumacheva E (2017) From structure to properties of composite films derived from cellulose nanocrystals. ACS Omega 2:5928–5934

Volova TG, Shumilova AA, Shidlovskiy IP, Nikolaeva ED, Sukovatiy AG, Vasiliev AD, Shishatskaya EI (2018) Antibacterial properties of films of cellulose composites with silver nanoparticles and antibiotics. Polym Test 65:54–68

Wågberg L, Decher G, Norgren M, Lindström T, Ankerfors M, Axnäs K (2008) The build-up of polyelectrolyte multilayers of microfibrillated cellulose and cationic polyelectrolytes. Langmuir 24:784–795

Wan YZ, Hong L, Jia SR, Huang Y, Zhu Y, Wang YL, Jiang HJ (2006) Synthesis and characterization of hydroxyapatite-bacterial cellulose nanocomposites. Compos Sci Technol 66:1825–1832

Wan Y, Gao C, Han M, Liang H, Ren K, Wang Y, Luo H (2011) Preparation and characterization of bacterial cellulose/heparin hybrid nanofiber for potential vascular tissue engineering scaffolds. Polym Adv Technol 22:2643–2648

Wang Y, Chen L (2011) Impacts of nanowhisker on formation kinetics and properties of all-cellulose composite gels. Carbohydr Polym 83:1937–1946

Wang Y, Chen L (2014) Cellulose nanowhiskers and fiber alignment greatly improve mechanical properties of electrospun prolamin protein fibers. ACS Appl Mater Interfaces 6:1709–1718

Wang H, Liu Y, Li M, Huang H, Xu HM, Hong RJ, Shen H (2010a) Multifunctional TiO2nanowires-modified nanoparticles bilayer film for 3D dye-sensitized solar cells. Optoelectron Adv Mater Rapid Commun 4:1166–1169

Wang J, Gao C, Zhang Y, Wan Y (2010b) Preparation and in vitro characterization of BC/PVA hydrogel composite for its potential use as artificial cornea biomaterial. Mater Sci Eng C 30:214–218

Wang Y, Chang C, Zhang L (2010c) Effects of freezing/thawing cycles and cellulose nanowhiskers on structure and properties of biocompatible starch/PVA sponges. Macromol Mater Eng 295:137–145

Wang J, Wan YZ, Luo HL, Gao C, Huang Y (2012) Immobilization of gelatin on bacterial cellulose nanofibers surface via crosslinking technique. Mater Sci Eng C 32:536–541

Wang Q, Zhu JY, Considine JM (2013) Strong and optically transparent films prepared using cellulosic solid residue recovered from cellulose nanocrystals production waste stream. ACS Appl Mater Interfaces 5:2527–2534

Wang C, Huang H, Jia M, Jin S, Zhao W, Cha R (2015a) Formulation and evaluation of nanocrystalline cellulose as a potential disintegrant. Carbohydr Polym 130:275–279

Wang H, He J, Zhang M, Tam KC, Ni P (2015b) A new pathway towards polymer modified cellulose nanocrystals via a "grafting onto" process for drug delivery. Polym Chem 6:4206–4209

Wang B, Lv X, Chen S, Li Z, Yao J, Peng X, Feng C, Xu Y, Wang H (2017) Bacterial cellulose/gelatin scaffold loaded with VEGF-silk fibroin nanoparticles for improving angiogenesis in tissue regeneration. Cellulose 24:5013–5024

Wang J, Chiappone A, Roppolo I, Shao F, Fantino E, Lorusso M, Rentsch D, Dietliker K, Pirri CF, Grützmacher H (2018a) All-in-one cellulose nanocrystals for 3D printing of nanocomposite hydrogels. Angew Chem Int Ed 57:2353–2356

Wang X, Xie Y, Ge H, Chen L, Wang J, Zhang S, Guo Y, Li Z, Feng X (2018b) Physical properties and antioxidant capacity of chitosan/epigallocatechin-3- gallate films reinforced with nano-bacterial cellulose. Carbohydr Polym 179:207–220

Wanna D, Alam C, Toivola DM, Alam P (2013) Bacterial cellulose–kaolin nanocomposites for application as biomedical wound healing materials. Adv Nat Sci Nanosci Nanotechnol 4:045002

Watanabe K, Eto Y, Takano S, Nakamori S, Shibai H, Yamanaka S (1993) A new bacterial cellulose substrate for mammalian cell culture – a new bacterial cellulose substrate. Cytotechnology 13:107–114

Wei B, Yang G, Hong F (2011) Preparation and evaluation of a kind of bacterial cellulose dry films with antibacterial properties. Carbohydr Polym 84:533–538

Wiegand C, Elsner P, Hipler UC, Klemm D (2006) Protease and ROS activities influenced by a composite of bacterial cellulose and collagen type I in vitro. Cellulose 13:689–696

Wiegand C, Moritz S, Hessler N, Kralisch D, Wesarg F, Müller FA, Fischer D, Hipler U (2015) Antimicrobial functionalization of bacterial nanocellulose by loading with polihexanide and povidone-iodine. J Mater Sci Mater Med 26:245

Wijaya CJ, Saputra SN, Soetaredjo FE, Putro JN, Lin CX, Kurniawan A, Ju Y, Ismadji S (2017) Cellulose nanocrystals from passion fruit peels waste as antibiotic drug carrier. Carbohydr Polym 175:370–376

Wu L, Zhou H, Sun H-J, Zhao Y, Yang X, Cheng SZD, Yang G (2013) Thermoresponsive bacterial cellulose whisker/poly(NIPAM- co -BMA) nanogel complexes: synthesis, characterization, and biological evaluation. Biomacromolecules 14:1078–1084

Wu J, Zheng Y, Song W, Luan J, Wen X, Wu Z, Chen X, Wang Q, Guo S (2014a) In situ synthesis of silver-nanoparticles/bacterial cellulose composites for slow-released antimicrobial wound dressing. Carbohydr Polym 102:762–771

Wu J, Zheng Y, Wen X, Lin Q, Chen X, Wu Z (2014b) Silver nanoparticle/bacterial cellulose gel membranes for antibacterial wound dressing: investigation in vitro and in vivo. Biomed Mater 9:1–12

Wu J, Zheng Y, Yang Z, Lin Q, Qiao K, Chen X, Peng Y (2014c) Influence of dialdehyde bacterial cellulose with the nonlinear elasticity and topology structure of ECM on cell adhesion and proliferation. RSC Adv 4:3998–4009

Wu CN, Fuh SC, Lin SP, Lin YY, Chen HY, Liu JM, Cheng KC (2018) TEMPO-Oxidized bacterial cellulose pellicle with silver nanoparticles for wound dressing. Biomacromolecules 19:544–554

Xiang C, Taylor AG, Hinestroza JP, Frey MW (2013) Controlled release of nonionic compounds from poly(lactic acid)/cellulose nanocrystal nanocomposite fibers. J Appl Polym Sci 127:79–86

Xiong G, Luo H, Zhu Y, Raman S, Wan Y (2014) Creation of macropores in three-dimensional bacterial cellulose scaffold for potential cancer cell culture. Carbohydr Polym 114:553–557

Xu J, Liu S, Chen G, Chen T, Song T, Wu J, Shi C, He M, Tian J (2018) Engineering biocompatible hydrogels from bicomponent natural nanofibers for anticancer drug delivery. Agric Food Chem 66:935–942

Yadav V, Paniliatis BJ, Shi H, Lee K, Cebe P, Kaplan DL (2010) Novel in vivo -degradable cellulose-chitin copolymer from metabolically engineered Gluconacetobacter xylinus. Appl Environ Microbiol 76:6257–6265

Yadav V, Sun L, Panilaitis B, Kaplan DL (2015) In vitro chondrogenesis with lysozyme susceptible bacterial cellulose as a scaffold. J Tissue Eng Regen Med 9:E276–E288

Yan H, Chen X, Feng M, Shi Z, Zhang D, Lin Q (2017) Layer-by-layer assembly of 3D alginate-chitosan-gelatin composite scaffold incorporating bacterial cellulose nanocrystals for bone tissue engineering. Mater Lett 209:492–496

Yan H, Huang D, Chen X, Liu H, Feng Y, Zhao Z, Dai Z, Zhang X, Lin Q (2018) A novel and homogeneous scaffold material: preparation and evaluation of alginate/bacterial cellulose nanocrystals/collagen composite hydrogel for tissue engineering. Polym Bull 75:985–1000

Yang X, Berglund LA (2018) Water-based approach to high-strength all-cellulose material with optical transparency. ACS Sustain Chem Eng 6:501–510

Yang J, Han C-R, Duan J-F, Ma M-G, Zhang X-M, Xu F, Sun R-C, Xie X-M (2012) Studies on the properties and formation mechanism of flexible nanocomposite hydrogels from cellulose nanocrystals and poly(acrylic acid). J Mater Chem 22:22467–22480

Yang J, Han CR, Duan JF, Xu F, Sun RC (2013a) Mechanical and viscoelastic properties of cellulose nanocrystals reinforced poly(ethylene glycol) nanocomposite hydrogels. ACS Appl Mater Interfaces 5:3199–3207

Yang X, Bakaic E, Hoare T, Cranston ED (2013b) Injectable polysaccharide hydrogels reinforced with cellulose nanocrystals: morphology, rheology, degradation, and cytotoxicity. Biomacromolecules 14:4447–4455

Yang J, Lv X, Chen S, Li Z, Feng C, Wang H, Xu Y (2014) In situ fabrication of a microporous bacterial cellulose/potato starch composite scaffold with enhanced cell compatibility. Cellulose 21:1823–1835

Yang J, Wang L, Zhang W, Sun Z, Li Y, Yang M, Zeng D, Peng B, Zheng W, Jiang X, Yang G (2018) Reverse reconstruction and bioprinting of bacterial cellulose-based functional total intervertebral disc for therapeutic implantation. Small 14:1702582

Yano H (2005) Optically transparent composites reinforced with networks of bacterial nanofibers. Sustain Humanosph 1:11

Ye J, Si J, Cui Z, Wang Q, Peng K, Chen W, Peng X, Chen SC (2017) Surface modification of electrospun TPU nanofiber scaffold with CNF particles by ultrasound-assisted technique for tissue engineering. Macromol Mater Eng 302:1700277

Ye S, Jiang L, Wu J, Su C, Huang C, Liu X, Shao W (2018) Flexible amoxicillin grafted bacterial cellulose sponges for wound dressing: in vitro and in vivo evaluation. ACS Appl Mater Interfaces 10:5862–5870

Yin Y, Tian X, Jiang X, Wang H, Gao W (2016) Modification of cellulose nanocrystal via SI-ATRP of styrene and the mechanism of its reinforcement of polymethylmethacrylate. Carbohydr Polym 142:206–212

Yoshino A, Tabuchi M, Uo M, Tatsumi H, Hideshima K, Kondo S, Sekine J (2013) Applicability of bacterial cellulose as an alternative to paper points in endodontic treatment. Acta Biomater 9:6116–6122

You J, Cao J, Zhao Y, Zhang L, Zhou J, Chen Y (2016) Improved mechanical properties and sustained release behavior of cationic cellulose nanocrystals reinforeced cationic cellulose injectable hydrogels. Biomacromolecules 17:2839–2848

Young R, Rowell R (1986) Cellulose: structure, modification, and hydrolysis. Wiley, New York

Yu HY, Chen GY, Wang YB, Yao JM (2015) A facile one-pot route for preparing cellulose nanocrystal/zinc oxide nanohybrids with high antibacterial and photocatalytic activity. Cellulose 22:261–273

Yu H, Wang C, Abdalkarim SYH (2017) Cellulose nanocrystals/polyethylene glycol as bifunctional reinforcing/compatibilizing agents in poly (lactic acid) nanofibers for controlling long-term in vitro drug release. Cellulose 24:4461–4477

Yuan Lu ASO, Levent Tekinalp H, Eberle CC, Peter W, Kumar Naskar A (2003) Nanocellulose in polymer composites and biomedical applications. TAPPI J 13:10–12

Zaborowska M, Bodin A, Bäckdahl H, Popp J, Goldstein A, Gatenholm P (2010) Microporous bacterial cellulose as a potential scaffold for bone regeneration. Acta Biomater 6:2540–2547

Zang S, Zhuo Q, Chang X, Qiu G, Wu Z, Yang G (2014) Study of osteogenic differentiation of human adipose-derived stem cells (HASCs) on bacterial cellulose. Carbohydr Polym 104:158–165

Zang S, Zhang R, Chen H, Lu Y, Zhou J, Chang X, Qiu G, Wu Z, Yang G (2015) Investigation on artificial blood vessels prepared from bacterial cellulose. Mater Sci Eng C 46:111–117

Zhang X, Huang J, Chang PR, Li J, Chen Y, Wang D, Yu J, Chen J (2010) Structure and properties of polysaccharide nanocrystal-doped supramolecular hydrogels based on Cyclodextrin inclusion. Polymer (Guildf) 51:4398–4407

Zhang J, Chang P, Zhang C, Xiong G, Luo H, Zhu Y, Ren K, Yao F, Wan Y (2015) Immobilization of lecithin on bacterial cellulose nanofibers for improved biological functions. React Funct Polym 91–92:100–107

Zhang F, Wu W, Zhang X, Meng X, Tong G, Deng Y (2016) Temperature-sensitive poly-NIPAm modified cellulose nanofibril cryogel microspheres for controlled drug release. Cellulose 23:415–425

Zhang H, Wang J, Wang K, Xu L (2018) A bilayered PLGA/multiwall carbon nanotubes/bacterial cellulose composite membrane for tissue regeneration of maxillary canine periodontal bone defects. Mater Lett 212:118–121

Zhao J, Hu L, Gong N, Tang Q, Du L, Chen L (2015a) The effects of macrophage-stimulating protein on the migration, proliferation, and collagen synthesis of skin fibroblasts in vitro and in vivo. Tissue Eng Part A 21:982–991

Zhao J, Lu C, He X, Zhang X, Zhang W, Zhang X (2015b) Polyethylenimine-grafted cellulose nanofibril aerogels as versatile vehicles for drug delivery. ACS Appl Mater Interfaces 7:2607–2615

Zhijiang C, Guang Y (2011) Bacterial cellulose/collagen composite: chatacterization and first evaluation of cytocomptability. J Appl Polym Sci 120:2938–2944

Zhijiang C, Chengwei H, Guang Y (2012) Poly(3-hydroxubutyrate-co-4-hydroxubutyrate)/bacterial cellulose composite porous scaffold: preparation, characterization and biocompatibility evaluation. Carbohydr Polym 87:1073–1080

Zhou C, Chu R, Wu R, Wu Q (2011) Electrospun polyethylene oxide/cellulose nanocrystal composite nanofibrous mats with homogeneous and heterogeneous microstructures. Biomacromolecules 12:2617–2625

Zhou Y, Fuentes-Hernandez C, Shim J, Meyer J, Giordano AJ, Li H, Winget P, Papadopoulos T, Cheun H, Kim J, Fenoll M, Dindar A, Haske W, Najafabadi E, Khan TM, Sojoudi H, Barlow S, Graham S, Brédas JL, Marder SR, Kahn A, Kippelen B (2012) A universal method to produce low-work function electrodes for organic electronics. Science 336:327–332

Zhou C, Shi Q, Guo W, Terrell L, Qureshi AT, Hayes DJ, Wu Q (2013a) Electrospun bio-nanocomposite scaffolds for bone tissue engineering by cellulose nanocrystals reinforcing maleic anhydride grafted PLA. ACS Appl Mater Interfaces 5:3847–3854

Zhou Y, Fuentes-Hernandez C, Khan TM, Liu JC, Hsu J, Shim JW, Dindar A, Youngblood JP, Moon RJ, Kippelen B (2013b) Recyclable organic solar cells on cellulose nanocrystal substrates. Sci Rep 3:24–26

Zhou L, He H, Li MC, Huang S, Mei C, Wu Q (2018) Grafting polycaprolactone diol onto cellulose nanocrystals via click chemistry: enhancing thermal stability and hydrophobic property. Carbohydr Polym 189:331–341

Zhu C, Li F, Zhou X, Lin L, Zhang T (2014) Kombucha-synthesized bacterial cellulose: preparation, characterization, and biocompatibility evaluation. J Biomed Mater Res Part A 102A:1548–1557

Zhu C, Liu F, Qian W, Wang Y, You Q, Zhang T, Li F (2015) Esophageal replacement by hydroxylated bacterial cellulose patch in a rabbit model. Turk J Med Sci 45:762–770

Zhu Q, Teng J, Liu X, Lan Y, Guo R (2018) Preparation and characterization of gentamycin sulfate-impregnated gelatin microspheres/collagen–cellulose/nanocrystal scaffolds. Polym Bull 75:77–91

Zimmermann T, Pöhler E, Geiger T (2004) Cellulose fibrils for polymer reinforcement. Adv Eng Mater 6:754–761

Zoppe JO, Peresin MS, Habibi Y, Venditti RA, Rojas OJ (2009) Reinforcing poly(ε-caprolactone) nanofibers with cellulose nanocrystals. ACS Appl Mater Interfaces 1:1996–2004

Zubik K, Singhsa P, Wang Y, Manuspiya H, Narain R (2017) Thermo-responsive poly (n-isopropylacrylamide)- cellulose nanocrystals hybrid hydrogels for wound dressing. Polymers (Basel) 9:119

Index

E. Cohen, H. Merzendorfer (eds.), *Extracellular Sugar-Based Biopolymers Matrices*,
Biologically-Inspired Systems 12, https://doi.org/10.1007/978-3-030-12919-4